CHE 332: INORGANIC CHEMISTRY



Karin Young
Centre College

LibreTexts™

Centre College

CHE 332: Inorganic Chemistry

Karin Young

This text is disseminated via the Open Education Resource (OER) LibreTexts Project (https://LibreTexts.org) and like the thousands of other texts available within this powerful platform, it is freely available for reading, printing, and "consuming."

The LibreTexts mission is to bring together students, faculty, and scholars in a collaborative effort to provide an accessible, and comprehensive platform that empowers our community to develop, curate, adapt, and adopt openly licensed resources and technologies; through these efforts we can reduce the financial burden born from traditional educational resource costs, ensuring education is more accessible for students and communities worldwide.

Most, but not all, pages in the library have licenses that may allow individuals to make changes, save, and print this book. Carefully consult the applicable license(s) before pursuing such effects. Instructors can adopt existing LibreTexts texts or Remix them to quickly build course-specific resources to meet the needs of their students. Unlike traditional textbooks, LibreTexts' web based origins allow powerful integration of advanced features and new technologies to support learning.



LibreTexts is the adaptable, user-friendly non-profit open education resource platform that educators trust for creating, customizing, and sharing accessible, interactive textbooks, adaptive homework, and ancillary materials. We collaborate with individuals and organizations to champion open education initiatives, support institutional publishing programs, drive curriculum development projects, and more.

The LibreTexts libraries are Powered by NICE CXone Expert and was supported by the Department of Education Open Textbook Pilot Project, the California Education Learning Lab, the UC Davis Office of the Provost, the UC Davis Library, the California State University Affordable Learning Solutions Program, and Merlot. This material is based upon work supported by the National Science Foundation under Grant No. 1246120, 1525057, and 1413739.

Any opinions, findings, and conclusions or recommendations expressed in this material are those of the author(s) and do not necessarily reflect the views of the National Science Foundation nor the US Department of Education.

Have questions or comments? For information about adoptions or adaptions contact info@LibreTexts.org or visit our main website at https://LibreTexts.org.

This text was compiled on 03/11/2026

TABLE OF CONTENTS

Licensing

Chapter 1: Introduction to Inorganic Chemistry

- Section 1.1: What is Inorganic Chemistry?
- Section 1.2: Inorganic vs Organic Chemistry
- Section 1.3: History of Inorganic Chemistry

Chapter 2: Atomic Theory

- Section 2.1: Quantum Numbers and Atomic Wavefunctions
- Section 2.2: Aufbau Principle
- Section 2.3: Shielding
- Section 2.4: Periodic Properties of Atoms

Chapter 3: Molecular Symmetry and Point Groups

- Section 3.1: Symmetry Operations and Elements
- Section 3.2: Point Groups
- Section 3.3: Properties and Representations of Groups
  - Section 3.3.1: Representations of Symmetry Operations
  - Section 3.3.2: Matrices
  - Section 3.3.3: Mathematical Notation of Representations
  - Section 3.3.4: Character Tables
- Section 3.4: Examples and Applications of Symmetry
  - Section 3.4.1: Chirality
  - Section 3.4.2: Molecular Vibrations

Chapter 4: Molecular Orbitals

- Section 4.1: Formation of Molecular Orbitals from Atomic Orbitals
  - Section 4.1.1: Molecular Orbitals from s Orbitals
  - Section 4.1.2: Molecular Orbitals from p Orbitals
  - Section 4.1.3: Molecular orbitals from d orbitals
  - Section 4.1.4: Nonbonding Orbitals and Other Factors
- Section 4.2: Molecular Orbital Theory of Diatomic Molecules
  - Section 4.2.1: Orbital Overlap
  - Section 4.2.2: Homonuclear Diatomic Molecules
  - Section 4.2.3: Heteronuclear Diatomic Molecules
  - Section 4.2.4: Orbital Mixing
  - Section 4.2.5: Diatomic Molecules of the First and Second Periods
  - Section 4.2.6: Photoelectron Spectroscopy
- Section 4.3: Larger (Polyatomic) Molecules
  - Section 4.3.1: Bifluoride anion
  - Section 4.3.2: Carbon Dioxide
  - Section 4.3.3: H_2O
  - Section 4.3.4: NH_3

- Section 4.3.5: CO_2 (Revisted with Projection Operators)
- Section 4.3.6: BF_3
- Section 4.4: Problems

Chapter 5: Coordination Chemistry- Structure and Isomers

- Section 5.1: History
- Section 5.2: Nomenclature and Ligands
- Section 5.3: Acid-Base and Donor-Acceptor Chemistry
  - Section 5.3.1: Acid-Base Models as Organizing Concepts
  - Section 5.3.2: Lewis Concept and Frontier Orbitals
    - Section 5.3.2.1: The frontier orbital approach considers Lewis acid-base reactions in terms of the donation of electrons from the base's highest occupied orbital into the acid's lowest unoccupied orbital.
    - Section 5.3.2.2: All other things being equal, electron withdrawing groups tend to make Lewis acids stronger and bases weaker while electron donating groups tend to make Lewis bases stronger and acids weaker
    - Section 5.3.2.3: The electronic spectra of charge transfer complexes illustrate the impact of frontier orbital interactions on the electronic structure of Lewis acid-base adducts
    - Section 5.3.2.4: Substances' solution phase Lewis basicity towards a given acid may be estimated using the enthalphy change for dissociation of its adduct with a reference acid of similar hardness.
    - Section 5.3.2.5: In the boron trifluoride affinity scale, the enthalphy change on formation of an adduct between the base and boron trifluoride is taken as a measure of Lewis basicity.
    - Section 5.3.2.6: Lewis base strength may also be estimated by measuring structural or energy changes upon formation of a Lewis acid-base complex, as illustrated by efforts to spectroscopically assess the strengths of halogen bonds
    - Section 5.3.2.7: Bulky groups weaken the strength of Lewis acids and bases because they introduce steric strain into the resulting acid-base adduct.
    - Section 5.3.2.8: Frustrated Lewis pair chemistry uses Lewis acid and base sites within a molecule that are sterically restricted from forming an adduct with each other.
  - Section 5.3.3: Hard and Soft Acids and Bases
    - Section 5.3.3.1: Hard-Hard and Soft-Soft preferences may be explained and quantified in terms of electrostatic and covalent and electronic stabilization on the stability of Lewis acid-base adducts
    - Section 5.3.3.2: Quantitative Measures of Hardness, Softness, and Acid-Base Interactions from a Hard Soft Acid-Base Principle Perspective Involve Orbital Energies and/or Apportioning Acid-Base Bonding in Terms of Electrostatic and Covalent Factors
  - Section 5.3.4: Problems
- Section 5.4: Coordination Numbers and Structures
- Section 5.5: Isomerism

Chapter 6: Coordination Chemistry- Bonding

- Section 6.1: Crystal Field Theory
- Section 6.2: Crystal Field Stabilization Energy
- Section 6.3: Factors That Affect Crystal Field Splitting
- Section 6.4: Ligand Field Theory
- Section 6.5: Metal-Metal Bonds
  - Section 6.5.1: Metal-Metal Multiple Bonds
- Section 6.6: Jahn-Teller Distortions

Chapter 7: Coordination Chemistry- Reactions and Mechanisms

- Section 7.1: Thermodynamic Stability of Metal Complexes
- Section 7.2: Trends in Kinetic Lability
- Section 7.3: Ligand Substitution Mechanisms
- Section 7.4: The Trans Effect Observation
- Section 7.5: The Trans Effect Explanation
- Section 7.6: Electron Transfer Reactions

Chapter 8: Coordination Chemistry - Electronic Spectra

- Section 8.1: Absorption of Light
  - Section 8.1.1: Beer-Lambert Absorption Law
- Section 8.2: Quantum Numbers of Multielectron Atoms
  - Section 8.2.1: Finding Microstates and Term Symbols
  - Section 8.2.2: Spin-Orbit Coupling
- Section 8.3: Electronic Spectra of Coordination Compounds
  - Section 8.3.1: Tanabe-Sugano Diagrams
  - Section 8.3.2: Symmetry labels for split terms
  - Section 8.3.3: Selection Rules
  - Section 8.3.4: Correlation Diagrams
  - Section 8.3.5: Applications of Tanabe-Sugano Diagrams
  - Section 8.3.6: Tetrahedral Complexes
  - Section 8.3.7: Charge-Transfer Spectra
  - Section 8.3.8: Applications of Charge-Transfer

Chapter 9: Structure and Energetics of Solids

- Section 9.1: Crystal Structures and Unit Cells
- Section 9.2: Energetics of Ionic Solids- Lattice Energy
- Section 9.3: Lattice Enthalpies and Born Haber Cycles
- Section 9.4: Lattice Energy and Solubility
- Section 9.5: Bonding in Metals and Semicondoctors
- Section 9.6: Nanomaterials
- Section 9.1b: Ionic Radii and Radius Ratios

Chapter 10: Organometallic Chemistry

- Section 10.1: The 18 Electron Rule
- Section 10.2: Organometallic Ligands
- Section 10.3: Characterization of Organometallic Complexes

Chapter 11: Organometallic Reactions and Catalysis

- Section 11.1: Reactions Involving Gain or Loss of Ligands
  - Section 11.1.1: Ligand Dissociation and Substitution
  - Section 11.1.2: Oxidative Addition
  - Section 11.1.3: Reductive Elimination
  - Section 11.1.4: Sigma Bond Metathasis
  - Section 11.1.5: Application of Pincer Ligands
- Section 11.2: Reactions Invloving Modification of Unsaturated Ligands

- Section 11.2.1: Introduction to Insertion
- Section 11.2.2: CO Insertions (Alkyl Migration)
- Section 11.2.3: Migratory Insertion-1,2-Insertions
- Section 11.2.4: β-Elimination Reactions
- Section 11.2.5: Abstraction and Addition
- Section 11.3: Organometallic Catalysts
  - Section 11.3.1: Catalytic Deuteration
  - Section 11.3.2: Hydroformylation
  - Section 11.3.3: Monsanto Acetic Acid Process
  - Section 11.3.4: Wacker (Smidt) Process
  - Section 11.3.5: Hydrogenation by Wilkinson's Catalyst
  - Section 11.3.6: Olefin Metathesis
- Section 11.4: Heterogeneous Catalysts
  - Section 11.4.1: Ziegler-Natta Polymerizations
  - Section 11.4.2: Water-Gas Shift Reaction
- Section 11.5: Problems
  - Section 11.5.1: Concept Review Questions Chapter 12
  - Section 11.5.2: Homework Problems Chapter 12

Chapter 12: Bioinorganic Chemistry

- Section 12.1: Biological Significance of Metals
- Section 12.2: Introduction to Amino Acids and Proteins
- Section 12.3: Biological Dioxygen Transport and Storage
- Section 12.4: Biological Metal Storage
- Section 12.5: Zinc as Lewis Acid and Template
- Section 12.6: Electron Transfer

Index

Glossary

Detailed Licensing

Licensing

*A detailed breakdown of this resource's licensing can be found in **Back Matter/Detailed Licensing**.*

CHAPTER OVERVIEW

Chapter 1: Introduction to Inorganic Chemistry

This chapter will introduce the breadth of the field of inorganic chemistry

Learning Objectives

- Identify different subfields of inorganic chemistry
- Recognize the historical and modern distinction between the fields of inorganic and organic chemistry

Section 1.1: What is Inorganic Chemistry?
Section 1.2: Inorganic vs Organic Chemistry
Section 1.3: History of Inorganic Chemistry

Chapter 1: Introduction to Inorganic Chemistry is shared under a CC BY-NC-SA 4.0 license and was authored, remixed, and/or curated by LibreTexts.

Section 1.1: What is Inorganic Chemistry?

Where did the name "Inorganic Chemistry" come from? Well, the term "Organic Chemistry" literally means the *chemistry of life*. Organic chemistry is the study of carbon-based molecules because the first molecules that were isolated from living organisms contained carbon. On the other hand, minerals and other non-living things seemed to be made of other elements. For some time in our history, scientists believed that the chemical difference between living and non-living things was carbon. So, if "organic" molecules are the molecules of life, then is "inorganic chemistry" the "chemistry of death"? Almost? "Inorganic" chemistry historically meant the chemistry of "non-living" things; and these were non-carbon based molecules and ions.

The names "organic" and "inorganic" come from science history, and still today a generally-accepted definition of *Inorganic Chemistry is the study of non-carbon molecules, or all the elements on the periodic table except carbon (*Figure ***Section*1.1.1**. But, this definition is not completely correct because the field of Inorganic Chemistry also includes organometallic compounds and the study of some carbon-based molecules that have properties that are familiar to metals (like conduction of electricity). This makes the field of inorganic chemistry very broad, and practically limitless. A great way to understand the breadth of the field is to take a look at the abstracts in the latest article of Inorganic Chemistry. Or, check out the 20 most-read articles from this past year using the links below.

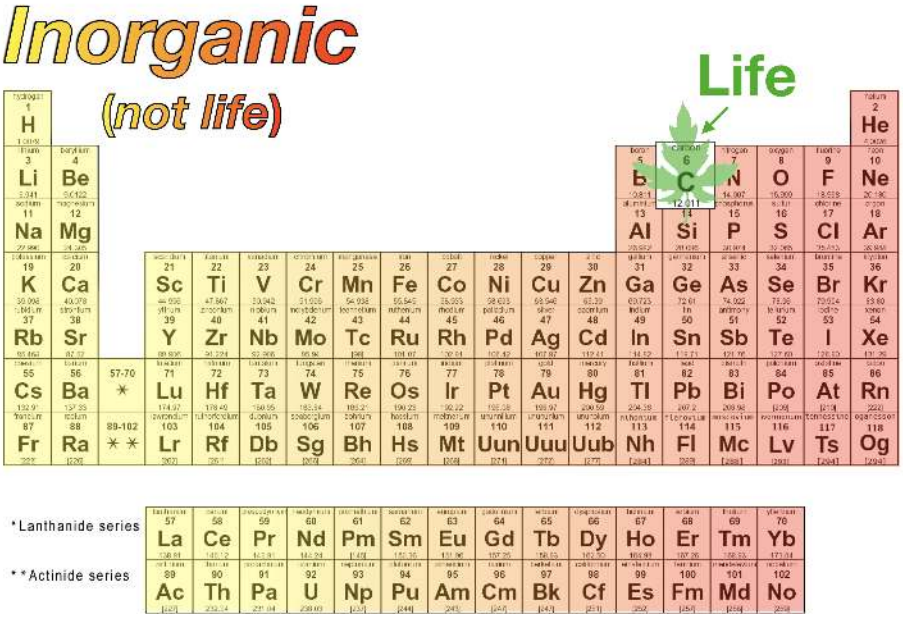


Figure ***Section*1.1.1**. An illustration of the historic meaning of "organic" and "inorganic". The modern understanding of organic and inorganic chemistry is not consistent with these historical meanings. (Kathryn Haas; CC-NC-BY-SA)

External links:

- The journal, Inorganic Chemistry: https://pubs.acs.org/journal/inocaj
- The latest issue of Inorganic chemistry: https://pubs.acs.org/toc/inocaj/current
- The most popular Inorganic Chemistry articles from the past month and the past year: https://pubs.acs.org/action/showMostReadArticles?journalCode=inocaj

Practice

? What are the Sub-Fields of Inorganic Chemistry?

To appreciate the breadth of Inorganic Chemistry, go to the most recent issue of Inorganic Chemistry and look at the titles and visual abstracts. Identify at least 4 sub-fields of Inorganic Chemistry.

Answer

There are a lot of correct answers here! The point here is that you notice that Inorganic Chemistry is a very broad field. It has something for almost everyone because many other fields overlap with Inorganic Chemistry. You might notice that some of the sub-fields you identified are also interdisciplinary fields between inorganic chemistry and another discipline. For a list of some of the subfields of Inorganic Chemistry, check this Wikipedia article.

Section 1.1: What is Inorganic Chemistry? is shared under a CC BY-NC-SA 4.0 license and was authored, remixed, and/or curated by LibreTexts.

- **1.1: What is Inorganic Chemistry?** by Kathryn Haas is licensed CC BY-NC-SA 4.0.

Section 1.2: Inorganic vs Organic Chemistry

The division between the fields of Inorganic and Organic chemistry has become blurred. For example, let's look at one of the major classes of catalysts used for organic synthesis reactions: organometalic catalysts (Figure ***Section*1.2.1**). Organometallic catalysts like these, and all organometallic compounds, contain metals that are bonded to carbon or carbon-containing molecules. So, are they "inorganic" because they contain metals, or "organic" because they contain carbon? These illustrate that clear divisions between organic and inorganic chemistry do not exist. Further, metal ions are common in biology and so the idea that metals are "inorganic" and thus classed as "non-living or non-biological" is incorrect. A canonical example is the organometallic catalyst adenosylcobalbumin, which is an important biological cofactor containing a cobalt (Co) ion (Figure ***Section*1.2.1**, right) and a cobalt-carbon bond.

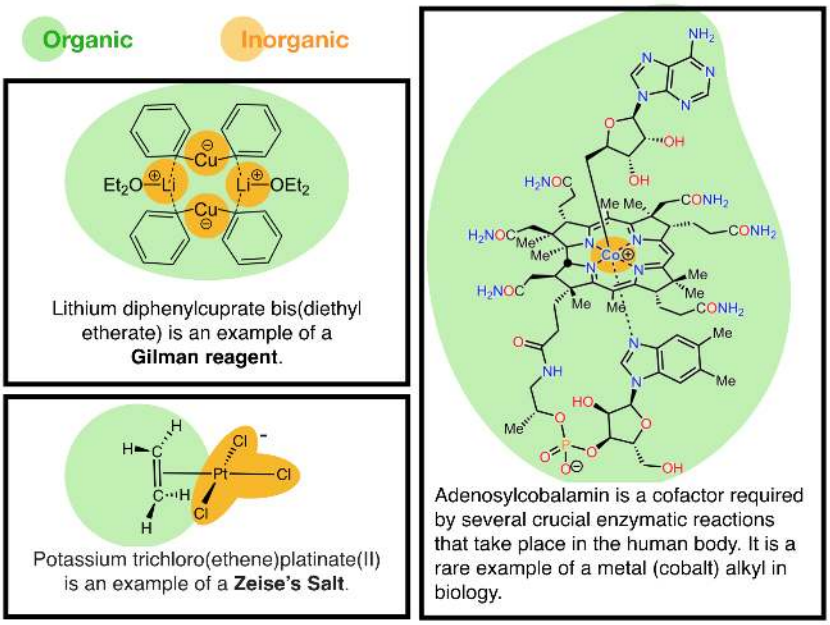


Figure ***Section*1.2.1**: Some examples of organometallic catalysts. These compounds catalyze organic reactions or biochemical reactions and they are compounds that contain both carbon and metals. These compounds are examples of molecules that cannot be defined only as organic molecules or only as inorganic molecules. Adenosylcobalbumin is an example of an organometallic catalyst that is present in biology, further illustrating that "inorganic" metals are important cofactors in biology. This image is based on information on the Wikipedia article on Organometallic Chemistry and is created from images found there; attribution to images created by Alsosaid1987, AdoCbl-ColorCoded, CC BY-SA 4.0 and Smokefoot, Zeise'sSalt, CC BY-SA 3.0. (Kathryn Haas; CC-BY-SA)

Some of the subfields of Inorganic Chemistry focus on electrical conductivity of inorganic materials (i.e., conduction, superconduction, and semiconduction) and on the study of optical and electronic properties of inorganic nanomaterials. Electrical conductivity is a canonical property of metals, but carbon-based materials also demonstrate electrical conductivity. For example, carbon nanotubes conduct electricity through their extended conjugated π systems. Fullerenes, of which the most famous is Buckminsterfullerene, or Buckeyball (C_{60}), demonstrate interesting properties that are similar to nanoparticles, and when combined with metals and crystallized can demonstrate superconductivity.

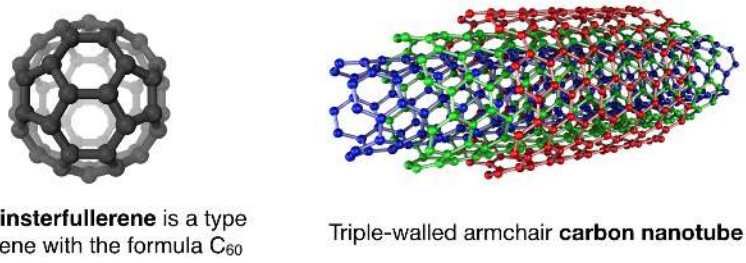


Figure *Section*1.2.2: This figure is created from information found on the Wikipedia articles for Buckmisterfullerene and carbon nanotubes. Attribution Eric Wieser, Multi-walled Carbon Nanotube, CC BY-SA 3.0. (Kathryn Haas; CC-BY-SA)

Although carbon nanotubes and fullerenes are allotropes of carbon, their material properties are somewhat foreign to many organic chemists, who traditionally have focused on smaller organic molecules having very different properties. However, these properties are familiar to inorganic chemists. Thus, inorganic chemists have embraced these molecules as "inorganic" due to the fact that they behave more like inorganic materials than smaller organic molecules. This class of carbon-based molecules serves as another example of molecules that are not perfectly matched to the traditional definitions of "organic" and "inorganic" chemistry. Certainly, the future will hold more and more examples of molecules that do not fit into the traditional disciplines of chemistry.

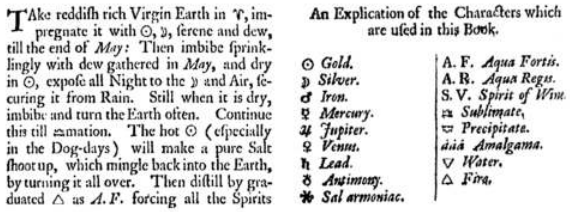
This page titled Section 1.2: Inorganic vs Organic Chemistry is shared under a CC BY-NC-SA 4.0 license and was authored, remixed, and/or curated by Kathryn Haas.

- **1.2: Inorganic vs Organic Chemistry** by Kathryn Haas is licensed CC BY-NC-SA 4.0.

Section 1.3: History of Inorganic Chemistry

Metals serve an essential role in many aspects of human civilization and have defined Ages of human history. The period of time from about 3300 BC to 1200 BC is often referred to as the Bronze Age. During this period our ancestors first started using metal and learned to mix various elements with copper to make a strong alloy, called bronze. This Age yielded significant advancement in crafting of sharper knives and stronger weapons out of metal instead of rock, wood and bone. Around 1200 BC the human race found an even harder metal and discovered a much stronger alloy called steel. This period is known as the Iron Age. More recently, periods of time known as Gold Rushes have caused huge changes in population distributions and wealth in some countries. Metal has obvious importance in our modern way of life. Today, iron and steel are used for making buildings, machines, automobiles, jewelry, cooking pots, tools, weapons, vehicles, electronics, surgical instruments and symbolic structures like the Eiffel Tower. Gold, silver, and copper still serve as currency for trade and exchange of goods and services.

The existence of Chemistry as a field of study owes much to the fact that gold was a valuable commodity throughout our history. In both the ancient Egyptian society and during the Roman Empire, the gold mines were the property of the state, not an individual or group. So there were few ways for most people to legally get any gold for themselves. The Alchemists were a varied group of scholars and charlatans who aimed to solve this problem by creating the **Philosopher's Stone** (which caused the transmutation of lead into gold). Three major streams of alchemy are known, Chinese, Indian, and European, with all three streams having some factors in common. Techniques developed in the European stream ultimately influenced the development of the science of chemistry.



TAke reddiſh rich Virgin Earth in ♈, impregnate it with ☉, ☽, ſerene and dew, till the end of *May*: Then imbibe ſprinklingly with dew gathered in *May*, and dry in ☉, expoſe all Night to the ☽ and Air, ſecuring it from Rain. Still when it is dry, imbibe and turn the Earth often. Continue this till ſ. mation. The hot ☉ (eſpecially in the Dog-days) will make a pure Salt ſhoot up, which mingle back into the Earth, by turning it all over. Then diſtill by graduated △ as *A. F.* forcing all the Spirits

An Explication of the Characters which are uſed in this Book.

☉ *Gold.*
☽ *Silver.*
♂ *Iron.*
☿ *Mercury.*
♃ *Jupiter.*
♀ *Venus.*
♄ *Lead.*
♁ *Antimony.*
✻ *Sal armoniac.*

A. F. *Aqua Fortis.*
A. R. *Aqua Regis.*
S. V. *Spirit of Wine.*
♎ *Sublimate.*
♍ *Precipitate.*
ȧȧȧ *Amalgama.*
▽ *Water.*
△ *Fire.*

Figure ***Section*1.3.1**. Alchemist recipe. Many of the specific approaches that alchemists used when they tried changing lead into gold are vague and unclear. Each alchemist had his own code for recording his data. The processes were kept secret so others could not profit from them. Different scholars developed their own set of symbols as they recorded the information they came up with. Many alchemists were not very honest, taking money from a nobleman by claiming to be able to make gold from lead, then leaving town in the middle of the night. Sometimes the nobleman would detect the fraud and have the alchemist hung. By the 1300's, several European rulers had declared alchemy to be illegal and set out strict punishments for those practicing the alchemical arts.

Although alchemists were never successful in changing lead into gold, they made several contributions to modern-day chemistry. Strong acids and bases were discovered, including nitric acid (H_2NO_3), sulfuric acid (H_3SO_4), and hydrochloric acid (HCl), and sodium hydroxide (NaOH). Glassware for running chemical reactions were developed, as well as methods for distillation, crystallization, sublimation. Alchemy helped improve the study of metallurgy and the extraction of metals from ores. More systematic approaches to research were developed that allowed the discovery of atoms and laid the groundwork for development of the periodic table. For more about the History of Chemistry in general, try the LibreText page History of Chemistry.

Inorganic compounds have been known and used since antiquity; probably the oldest is the deep blue pigment called Prussian blue, $Fe_4[Fe(CN)_6]$. However, the chemical nature of these substances was unknown until the late nineteenth and early twentieth century when the modern field of Coordination Chemistry emerged. Much of what we know about inorganic chemistry is based largely on the work of and debates between of Alfred Werner (1866–1919; Nobel Prize in Chemistry in 1913) and Sophus Mads Jørgensen (1837 –1914). After Werner succeeded in these debates, the field of Inorganic Chemistry declined in popularity until the mid twentieth century when the second world war stimulated renewed interest. During the post-war era, several important discoveries and theories were developed. For example, important theories of bonding in coordination compounds were developed. Soon after World War II, Crystal Field Theory (CFT) and Ligand Field Theory (LFT) were developed. These are two critical and complimentary theories that provide explanation of spectroscopic, chemical, and structural properties of inorganic coordination compounds; CFT being more simple, and LFT more accurate. In the 1950's, organometallic catalysts were discovered that catalyzed important organic reactions.

$$N_2(g) + 3H_2(g) \rightleftharpoons 2NH_3(g) \qquad \text{(Section 1.3.1)}$$

The Haber-Bosch Process is catalyzed by an inorganic oxide catalyst and is one of the world's most important industrial reactions. It provides for the synthesis of ammonia directly from elemental nitrogen, N_2, and hydrogen, H_2. Since its development in the early twentieth century, it has led to the production of an enormous quantity of fertilizer, vastly increasing global food production. As a result, it is estimated that a significant fraction of the nitrogen content in the typical human body is ultimately derived from this process. Yet while the reaction must be run at high temperatures and pressures in the industrial setting, the nitrogenase enzyme on the roots of plants can carry out this reaction at the mild conditions within soil. Intense investigations were then aimed to improve inorganic catalysts through understanding the metal cofactors in enzymes. The link between the Haber-Bosch industrial process and the nitrogenase enzyme was an early bridge between the fields of organometallic chemistry and biochemistry.

Contributions

Part of this page is adapted from K.Haas Ph.D. dissertation

Part of this page is adapted from the following LibreTexts pages

- Alchemy contributed by CK-12 Foundation by Sharon Bewick, Richard Parsons, Therese Forsythe, Shonna Robinson, and Jean Dupon.
- Werner's Theory of Coordination Compounds
- The Haber-Bosch Process Worksheet

Section 1.3: History of Inorganic Chemistry is shared under a CC BY-NC-SA 4.0 license and was authored, remixed, and/or curated by LibreTexts.

- **1.3: History of Inorganic Chemistry** by Kathryn Haas is licensed CC BY-NC-SA 4.0.
- **1.3: History of Inorganic Chemistry** is licensed CC BY-NC-SA 4.0.

CHAPTER OVERVIEW

Chapter 2: Atomic Theory

This chapter reviews atomic orbitals and the periodic properties of atoms.

Learning Objectives

- Understand the sizes, shapes, and relative energies of atomic orbitals and how they depend on quantum numbers
- Identify the number of radial and angular nodes in an atomic orbital
- Determine the ground state electron configuration and number of unpaired electrons for a given atom
- Explain periodic trends and their physical origins

Section 2.1: Quantum Numbers and Atomic Wavefunctions
Section 2.2: Aufbau Principle
Section 2.3: Shielding
Section 2.4: Periodic Properties of Atoms

Chapter 2: Atomic Theory is shared under a CC BY-NC-SA 4.0 license and was authored, remixed, and/or curated by LibreTexts.

Section 2.1: Quantum Numbers and Atomic Wavefunctions

Considering the failures of the Bohr model in systems with more than one electron, Erwin Schrödinger and Werner Heisenberg proposed a major change in the paradigm regarding the electron. In several breakthrough papers (1925-1927) they attributed wave properties to electrons and they each received Nobel prizes for developing the theories of Wave Mechanics (or the "New Quantum Mechanics"). This approach treated electrons as having "dual" nature: posessing properties of *both* waves and particles.

Schrödinger's Equation describes the behavior of the electron (in a hydrogen atom) in three dimensions. It is a mathematical equation that defines the electron's position, mass, total energy, and potential energy. The simplest form of the Schrödinger Equation is as follows:

$$\hat{H}\psi = E\psi \tag{Section 2.1.1}$$

where $\hat{H}$ is the Hamiltonian operator, **E** is the energy of the electron, and ψ is the wavefunction.

The Hamiltonian, $\hat{H}$

The Hamiltonian operator is like a set of instructions that tells us what to do with the function that follows it. A Hamiltonian operator is a function over three-dimensional space that corresponds to the sum of kinetic energies and potential energies of the particles in a system, one electron and its nucleus in this case. The Hamiltonian operator for a one-electron system is:

$$\hat{H} = \frac{-h^2}{8\pi^2 m_e}\left(\frac{\partial^2}{\partial x^2} + \frac{\partial^2}{\partial y^2} + \frac{\partial^2}{\partial z^2}\right) - \frac{Ze^2}{4\pi\epsilon_0 r} \tag{Section 2.1.2}$$

Where h is Planc's constant, m_e is the mass of the electron, e is the charge of the electron, r is the distance from the nucleus ($r = \sqrt{x^2+y^2+z^2}$), Z is the charge of the nucleus, and $4\pi\epsilon_0$ is permittivity of a vacuum.

Kinetic Energy

The first part of the Hamiltonian written above, $\frac{-h^2}{8\pi^2 m_e}\left(\frac{\partial^2}{\partial x^2} + \frac{\partial^2}{\partial y^2} + \frac{\partial^2}{\partial z^2}\right)$ describes the kinetic energy of the electron. This is the energy due to motion of the electron.

Potential energy

The second part written above, $\frac{-Ze^2}{4\pi\epsilon_0 r}$ describes the potential energy of the electron, and is commonly written as $V(r)$ or $V(x,y,z)$.

$$V(x,y,x) = \frac{-Ze^2}{4\pi\epsilon_0 r} = \frac{-Ze^2}{4\pi\epsilon_0\sqrt{x^2+y^2+z^2}} \tag{Section 2.1.3}$$

The potential energy depends on the attractive electrostatic force between the electron and the nucleus. You might notice that this attraction is essentially the same as the electrostatic force defined by Coulomb's law. And, just as in Coulomb's law, when two opposite charges are attracted to one another, the potential energy of the force is negative. Thus, when an electron is close to the nucleus, the potential energy is a large negative number corresponding to a strong attractive force. When an electron is farther from the nucleus, the potential energy is still negative but with a smaller magnitude, corresponding to a weaker attractive force. If the electron is very far from the nucleus ($r = \infty$) then the attractive force, and the potential energy, is zero.

The Wavefunction, ψ

In simple terms, the wavefunction (ψ) of an electron describes the electron's position in space, relative to the nucleus. The square of the ψ describes an atomic orbital. We can't define the position too exactly because we would violate the Heisenberg Uncertainty principle, but we can define its wave. Here, we will describe the ψ in general terms. Generally, in a one-electron atom, the electron ψ is defined by the wave's distance from the nucleus and its angle with respect to x, y, and z axes of the atom's Cartesian coordinates (nucleus is at the origin). The general form of the (ψ) for an electron in a hydrogen atom can be written as follows:

$$\psi_{n,l,m_l} = R_{n,l}(r) + Y_{l,m_l}(\theta,\phi) \tag{Section 2.1.4}$$

Quantum numbers

In one dimension, the wavefunction requires only one quantum number, n. A full explanation of the three-dimensional wavefunction for an electron is outside of the scope of this course. Instead, we will focus on gaining a conceptual understanding by extending knowledge of the one-dimensional wavefunction to a three-dimensional space. Extending the wavefunction to three dimensions requires a total of three quantum numbers. In addition to n, which we saw in the one-dimensional case, we also need l and m_l to express the wavefunction in three dimensions. A complete solution to the Schrödinger equation, both the three-dimensional wavefunction and energy, includes a set of three quantum numbers (n, l, m_l). The wavefunction describes what we know as an atomic orbital; it defines the region in space where the electron is located. Additionally, there is a fourth quantum number, m_s. The m_s quantum number accounts for the observed interaction of electrons with an applied magnetic field; it is an additional postulate that is not part of the wavefunction. These four quantum numbers are described below.

The quantum number, n: This is the principle quantum number. This number represents the shell, including both the overall energy of the electron in that shell and the size of that shell. An allowed value for n is any non-zero, positive integer (1, 2, 3, 4, ... etc are allowed, but 4.1 is not allowed).

The quantum number, l: This is the angular momentum quantum number that corresponds to the subshell and its shape. It represents the angular dependence of the subshell, or the "shape" of the orbitals within a subshell. The allowed values of$l$ depends on n. The allowed values of l for an electron in shell n are integer values between 0 to $(n-1)$, or $l = 0 \rightarrow (n-1)$. These values correspond to the orbital shape where $l = 0$ is an s-orbital, $l = 1$ is a p-orbital, $l = 2$ is a d-orbital, $l = 3$ is an f-orbital.

The quantum number m_l: This is the magnetic quantum number. Its possible values give the the number of orbitals within a subshell and its specific value gives the orbital's orientation in space. The allowed values of m_l depend on the value of l. The value of m_l is allowed to be any positive or negative integer between $+l$ and $-l$. In other terms, $m_l = (0, \pm 1 ... \pm l)$. For example, if the electron is in a 3-p-orbital, then $n = 3, l = 1$, and the possible values of m_l are $-1, 0$, and $+1$. Since there are three possible values of m_l there are three orbitals in the p subshell. The specific m_l value defines in which of the three possible p-orbitals (p_x, p_y, or p_z) the electron exists. In the case of the s subshell, there is only one value, $m_l = 0$ because $l = 0$. The one value corresponds to the fact that there is only one s orbital in any shell.

The quantum number m_s: This quantum number accounts for the electron's "spin". In short, electrons interact with magnetic fields in a way that is similar to how a tiny bar magnet would interact with a magnetic field. The allowed values for m_s are $+\frac{1}{2}$ and $-\frac{1}{2}$.

Table *Section*2.1.1. Quantum Numbers

SYMBOL	NAME	VALUES	MEANING
n	principle	$1, 2, 3$...(any integer)	energy level, orbital size
l	angular momentum	$0 \rightarrow (n-1)$	subshell, $0 = s, 1 = p, 2 = d, 3 = f$... this is the angular dependence of the orbital, shape of the orbital *letters have historical meaning, sharp, principle, diffuse, fundamental
m_l	magnetic	$0, \pm 1 ... \pm l$	orientation of angular momentum in space, orbital orientation
m_s	spin	$+\frac{1}{2}, -\frac{1}{2}$	orientation of the electron's magnetic field "spin up" or "spin down"

Atomic orbitals (one electron wavefunctions)

One simplified representation of the three-dimensional wavefunction is shown below. This representation breaks the wavefunction into two parts: the **radial contribution** ($R_{n,l}(r)$) and the **angular contribution** ($Y_{l,m_l}(\theta,\phi)$).

$$\psi_{(n,l,m_l)} = R_{n,l}(r) \times Y_{l,m_l}(\theta,\phi) \qquad \text{(Section 2.1.5)}$$

Radial contribution, $R_{n,l}(r)$

The radial part of the wavefunction, $R_{n,l}(r)$ gives the radial variation of ψ. In other words, $R_{n,l}(r)$ defines how the wavefunction depends on the distance of the electron from the nucleus (the radius). The principle quantum number n is derived from the radial part of the wavefunction, and determines the size (radial extent) of an orbital. The $R_{n,l}(r)$ parts of the wavefunction for a hydrogenic atom are plotted in Figure *Section*2.1.1. Notice that the $R_{n,l}(r)$ of all s-orbitals (solid lines) reaches a maximum at $r = 0$. This is unique to the s-orbitals' $R_{n,l}(r)$. The $R_{n,l}(r)$ of p- and d-orbitals orbitals approaches zero as r approaches zero. This has important consequences for how closely an electron in these orbitals can approach the nucleus.

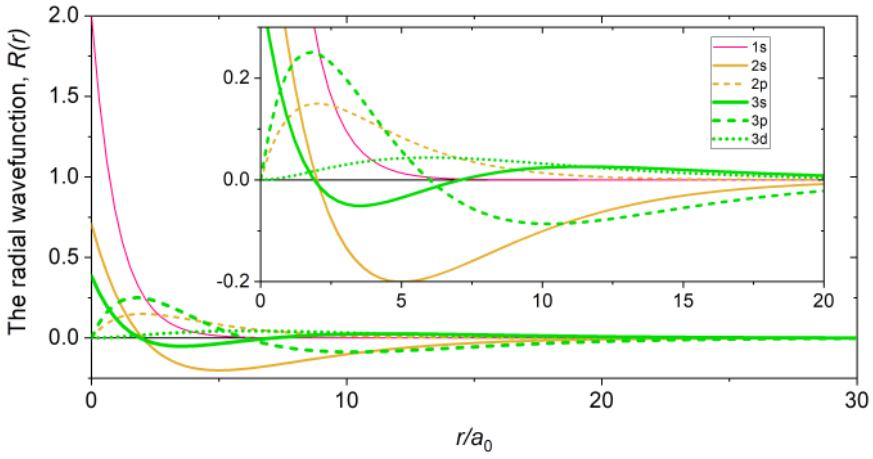


Figure *Section*2.1.1: Plots of the radial wavefunction, $R_{n,l}(r)$, for the first three shells. The wavefunctions are plotted relative to $\frac{r}{a_0}$, where $a_0 = 52.9pm = 0.529\mathring{A}$ is the Bohr Radius (the radius of a hydrogen 1s orbital). The expressions for these radial wavefunctions ($R_{n,l}(r)$) are shown in Table *Section*2.1.2.

Radial probability function, $4\pi r^2(R_{n,l}(r))^2$

The square of the wavefunction is proportional to the probability of finding a particle (electron) at some point in space. The square of the radial part of the wavefuction is called the radial distribution function $4\pi r^2(R_{n,l}(r))^2$, and it describes the probability of locating the electron at some distance r away from the nucleus. When we normalize the probability functions by dividing the function by its integral over all space, we get the plots shown in Figure *Section*2.1.2. The normalized probability functions are compared to the original radial part of the wavefunctions in Figure *Section*2.1.3. The most probable distance for finding an electron is shown by the maximum value of the function. For an electron in the 1s orbital of H, the most probable distance from the nucleus occurs at $r = 1a_0$. This is the Bohr Radius, and it has a value of ($a_0 = 52.9pm = 0.529\mathring{A}$). It is convenient to plot the functions of the hydrogen atomic orbitals relative to the size of its smallest orbital, the 1s orbital; this is the reason we plot $R_{n,l}(r)$ and $4\pi r^2(R_{n,l}(r))^2$ relative to $\frac{r}{a_0}$.

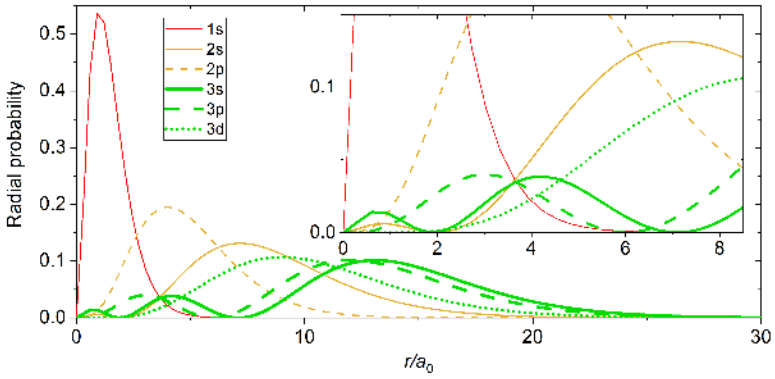


Figure *Section*2.1.2: Plots of the normalized radial probability functions for the first three shells.

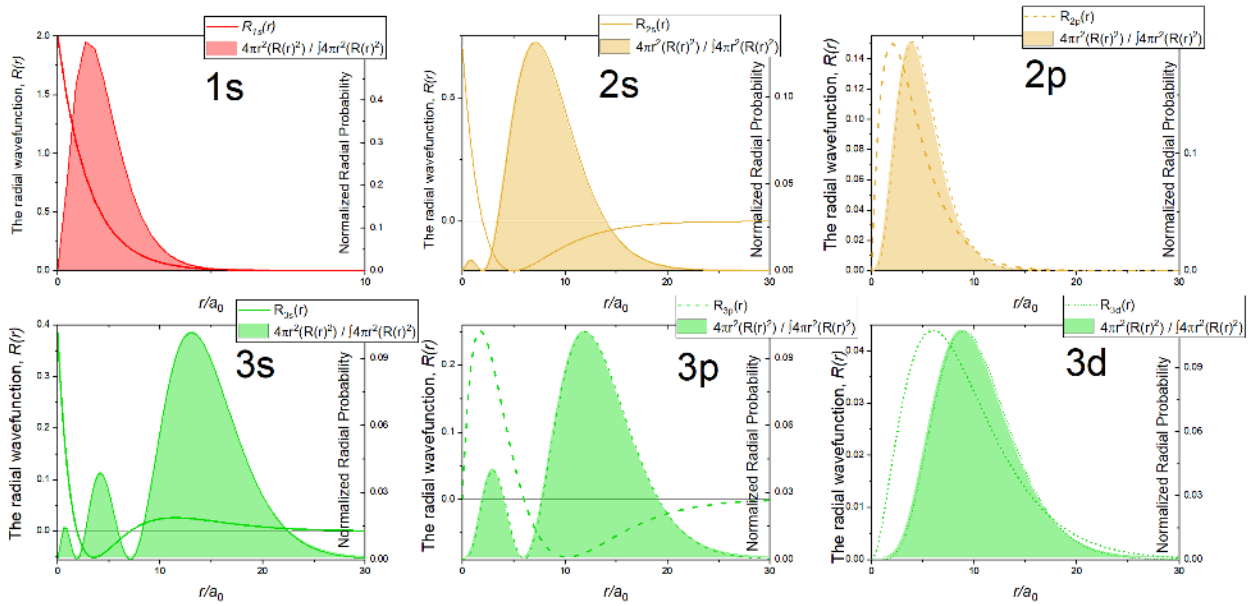


Figure *Section*2.1.3. Plots of the normalized radial probability function for each orbital in the first three shells (shaded curves). The y-axis on the left of each plot corresponds to the radial wavefunction (line); the y-axis on the right of each plot corresponds to radial probability function (shaded).

Radial nodes

In the case of the 3-dimensional wavefunction, there are two different types of nodes: radial nodes and angular nodes. **Radial nodes occur where the radial part of the wavefunction is zero ($R(x) = 0$).** These are easy to see by plotting the radial part of the wavefunction and finding where the radial part of the wavefunction (and the radial probability function) is zero as seen in Figures *Section*2.1.2 and *Section*2.1.3. These nodes are spherical in shape and depend on the energy level and subshell (the values of n and l). **The number of radial nodes is $n - l - 1$.** An example of a radial node is the single node that occurs in the **2*s*** orbital ($2 - 0 - 1 = 1$ node). In contrast, the 1s orbital has zero radial nodes ($1 - 0 - 1 = 0$ nodes). Where there is a node, there is zero probability of finding an electron.

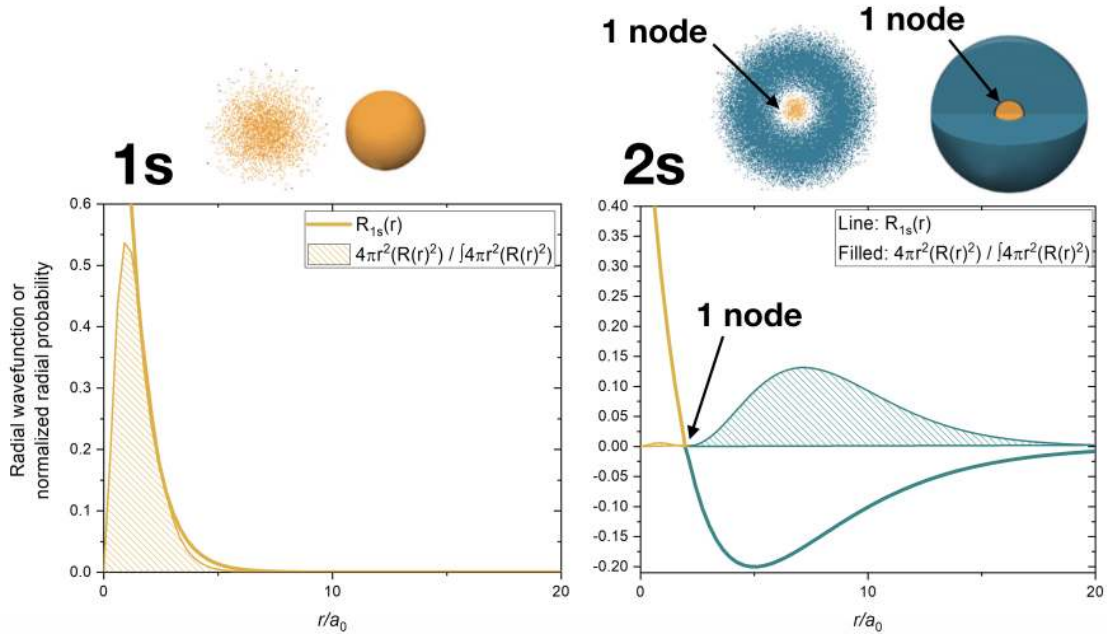


Figure *Section*2.1.4: Visualization of the 1s and 2s atomic orbitals. Each orbital is shown as both an electron probability density plot and a contour plot above its wavefunction and probability density function. The 1s orbital has zero radial nodes. The 2s orbital has one radial node where its wavefunction changes sign and its radial probability function is zero. Modified by K. Haas (CC-BY-NC-SA; Libretexts)

Boundary surfaces

A true node occurs where the probability of finding an electron is zero. Nodes occur where $\psi = \psi^2 = 0$. Far from the nucleus, the probability of finding the electron rapidly approaches zero, but is never *exactly* zero. What this means is that it is rather improbable to find the electron at far distances from the nucleus, but its not impossible. The rapid fall of probability creates a boundary surface rather than a node. The boundary surface represents the area around the nucleus where the electron exists most of the time.

Exercise *Section*2.1.1

How many radial nodes are in the s, p, d, and f orbitals in the first four shells? $n = 1, 2, 3, 4$?

Answer

You can approach this answer by using the mathematical relationship between the number of radial nodes and the values of n and l: **number of radial nodes is** $n - 1 - l$. You could also notice the pattern that the first orbital of any type (1s, 2p, 3d...) has zero radial nodes, the second orbital of a type (2s, 3p, 4d...) has one radial node, the third orbital of a type has two radial nodes (3s, 4p, 5d...)...etc.

A full list of all of the orbitals in the first four shells and their number of radial nodes is below. Its a good idea to prove to yourself that the numbers given below are consistent with the plots of the orbitals wavefunctions for those orbitals in the first three shells:

s-orbitals:

1s: $n - 1 - l = 1 - 1 - 0 = 0$, zero radial nodes

2s: $n - 1 - l = 2 - 1 - 0 = 1$, one radial node

3s: $n - 1 - l = 3 - 1 - 0 = 2$, two radial nodes

4s: $n - 1 - l = 4 - 1 - 0 = 3$, three radial nodes

p-orbitals

2p: $n - 1 - l = 2 - 1 - 1 = 0$, zero radial nodes

3p: $n-1-l=3-1-1=1$, one radial node

4p: $n-1-l=4-1-1=2$, two radial nodes

d-orbitals

3d: $n-1-l=3-1-2=0$, zero radial nodes

4d: $n-1-l=4-1-2=1$, one radial nodes

f-orbital

4f: $n-1-l=4-1-3=0$, zero radial nodes

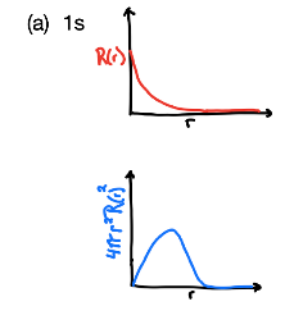
Exercise *Section*2.1.2

Draw a rough plot of the following:

a. The radial wavefunction, $R_{n,l}(r)$ and the probability density function, $4\pi r^2(R_{n,l}(r))^2$, for the 1s orbital.
b. The radial wavefunction, $R_{n,l}(r)$ and the probability density function, $4\pi r^2(R_{n,l}(r))^2$, for the 4s orbital.

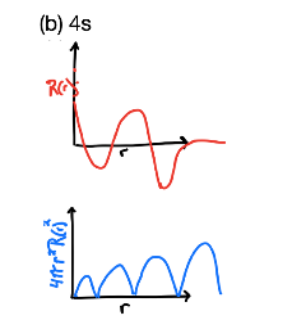
Answer, 1s

The 1s orbital's $R_{n,l}(r)$ reaches a maximum near the origin and approaches zero far from the nucleus. The $4\pi r^2(R_{n,l}(r))^2$ approaches zero at the origin, has a maximum intensity at the Bohr radius, and approaches zero far from the nucleus (its boundary surface).



Answer, 4s

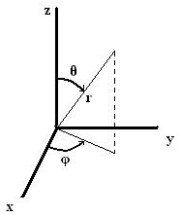
Like all s orbitals, the 4s orbital's $R_{n,l}(r)$ reaches a maximum near X=0, but it would be less intense than the function of the 1s, 2s, and 3s orbitals. It should have three radial nodes and so its wavefunction would change sign three times. This would give four regions of electron density in the probability function while the function would approach zero (boundary surface) far from the nucleus.



Angular contribution, $Y_{l,m_l}(\theta,\phi)$, and angular probability function, $(Y_{l,m_l}(\theta,\phi))^2$

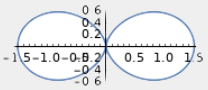
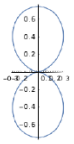
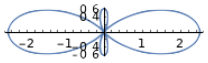
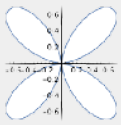
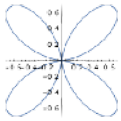
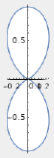
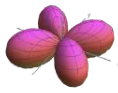
The angular contribution to the wavefunction, $Y_{l,m_l}(\theta,\phi)$, describes the wavefunction's shape, or the angle with respect to a coordinate system. To describe the direction in space, we use spherical coordinates that tell us distance *and* orientation in 3-

dimensional space. There are three spherical coordinates: r, ϕ, and θ. r is the radius, or the actual distance from the origin. ϕ and θ are angles. ϕ is measured from the positive x axis in the xy plane and may be between 0 and 2π. θ is measured from the positive z axis towards the xy plane and may be between 0 and π. $Y_{l,m_l}(\theta,\phi)$, is slightly more difficult to describe than the radial contribution was. This is partly because $Y_{l,m_l}(\theta,\phi)$ contains imaginary numbers, which have no real, physical meaning. However, the angular part of the wavefunction becomes more "real" when you square it to get angular probability density, a more tangible concept described as the **shapes of orbitals**.



The values of θ, ϕ, and $y(\theta,\phi)$ for orbitals in the hydrogen atom are listed in Table *Section* 2.1.2, but $Y_{l,m_l}(\theta,\phi)$ is only a mathematical function and has not real physical meaning. The square of the radial wavefunction, $Y_{l,m_l}(\theta,\phi)^2$ gives the probability of finding the electron at a point in space on a ray described by (ϕ,θ). Thus $Y_{l,m_l}(\theta,\phi)^2$ describes the shape of the orbital.

Table *Section* 2.1.2. Components of the angular wavefunction and the resulting orbital shapes. The plots in the two right hand columns were created using Desmos and Mathematica: specifically "Spherical Harmonics" from the Wolfram Demonstrations Project, http://demonstrations.wolfram.com/SphericalHarmonics/ and "Visualizing Atomic Orbitals", https://demonstrations.wolfram.com/VisualizingAtomicOrbitals/.

subshell	m_l (orbital)	θ	ϕ	Plots of θ^2	orbital shapes
$l = 0$, s	$m_l = 0$	$\frac{1}{\sqrt{2}}$	$\frac{1}{\sqrt{2\pi}}$		
$l = 1$, p	$m_l = 0$	$\frac{\sqrt{6}}{2}\cos\theta$	$\frac{1}{\sqrt{2\pi}}$		
$l = 1$, p	$m_l = +1$	$\frac{\sqrt{3}}{2}\sin\theta$	$\frac{1}{\sqrt{2\pi}}e^{i\phi}$		
$l = 1$, p	$m_l = -1$	$\frac{\sqrt{3}}{2}\sin\theta$	$\frac{1}{\sqrt{2\pi}}e^{-i\phi}$		
$l = 2$, d	0	$\frac{\sqrt{10}}{4}\left(3\cos^2\theta - 1\right)$	$\frac{1}{\sqrt{2\pi}}$		
$l = 2$, d	$m_l = +1$	$\frac{\sqrt{15}}{2}\sin\theta\cos\theta$	$\frac{1}{\sqrt{2\pi}}e^{i\phi}$		
$l = 2$, d	$m_l = -1$	$\frac{\sqrt{15}}{2}\sin\theta\cos\theta$	$\frac{1}{\sqrt{2\pi}}e^{-i\phi}$		
$l = 2$, d	$m_l = +2$	$\frac{\sqrt{15}}{4}\sin^2\theta$	$\frac{1}{\sqrt{2\pi}}e^{i2\phi}$		
$l = 2$, d	$m_l = -2$	$\frac{\sqrt{15}}{4}\sin^2\theta$	$\frac{1}{\sqrt{2\pi}}e^{-i2\phi}$		

Angular nodes

Angular nodes exist where $(Y_{l,m_l}(\theta,\phi))^2 = 0$. These nodes are planar in shape, and they depend on the value of l. The number of angular nodes in any orbital is equal to l. This means that s-orbitals ($l = 0$) have zero angular nodes, p-orbitals ($l = 1$) have one angular node, d-orbitals ($l = 2$) have two angular nodes, and so on. Planar nodes can be flat planes (like the nodes in all p orbitals) or they can have a conical shape, like the two angular nodes in the d_{Z^2} orbital. Angular nodes in some p and d orbitals are shown in Figure *Section* 2.1.5.

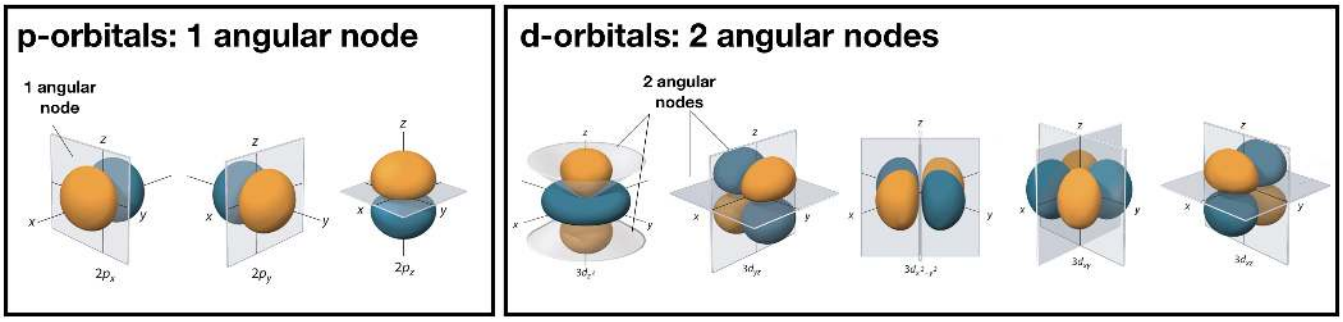
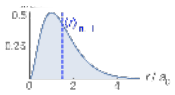
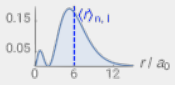
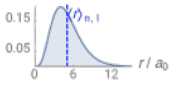
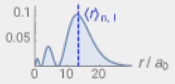
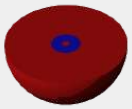
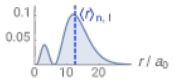
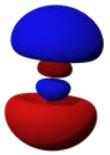
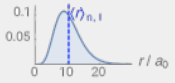
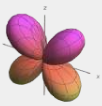


Figure *Section* 2.1.5: The angular nodes in p-orbitals and d-orbitals are shown. Every p orbital has one angular node, and every d orbital has two angular nodes. The number of angular nodes in any orbital is equal to the value of the quantum number, l. (CC BY-NC-SA; anonymous by request)

Atomic Orbitals

Atomic orbitals result from a combination of both the radial and angular contributions of the wavefunction. Atomic orbitals can have both angular nodes and radial nodes, depending on the values of n and l.

The chart below compares the radial variation, angular variation, and their combinations (orbitals).

Orbital	Radial Probability	Radial Nodes	Angular Probability	Angular Nodes	Combination (Orbital)	Total Nodes
1s		0		0		0
2s		1		0		1
2p		0		1		1
3s		2		0		2
3p		1		1		2
3d		0		2		2

This page titled Section 2.1: Quantum Numbers and Atomic Wavefunctions is shared under a CC BY-NC-SA 4.0 license and was authored, remixed, and/or curated by Kathryn Haas.

- **2.2: The Schrödinger equation, particle in a box, and atomic wavefunctions** by Kathryn Haas is licensed CC BY-NC-SA 4.0.
- **2.1: Quantum Numbers and Atomic Wavefunctions** by Kathryn Haas is licensed CC BY-NC-SA 4.0.
- **2.2.2: Quantum Numbers and Atomic Wave Functions** by Kathryn Haas is licensed CC BY-NC-SA 4.0.

Section 2.2: Aufbau Principle

Introduction

The **Aufbau Principle** (also called the **building-up principle** or the **Aufbau rule**) states that, in the ground state of an atom or ion, electrons fill atomic orbitals of the lowest available energy level before occupying higher-energy levels. In general, an electron will occupy an atomic orbital with the lowest value of n, l, m_l, in that order of priority. The value of m_s for an unpaired electron is conventionally assigned a value of $+\frac{1}{2}$. Each electron in an atom/ion must have a unique set of values for all four quantum numbers.

The Ground State of Hydrogenic Atoms/Ions

In a hydrogenic atom/ion, there is only one electron. In this case, the *only factor determining energy is the value of* n. The ground state will always be the 1s orbital ($n = 1, l = 0, m_l = 0, m_s = +\frac{1}{2}$).

The Ground State of Multi-electron Atoms/Ions

In atoms/ions with two or more electrons, the ground state electron configuration (1) minimizes the total energy of the electrons, (2) obeys the Pauli exclusion principle, (3) obeys Hunds rule of maximum multiplicity, and (4) considers the exchange interaction. These "rules" are described below.

(1) Electrons will occupy the lowest energy orbitals in order to minimize the total energy. The two quantum numbers that are related to energy in multi-electron atoms are n, and l. Thus, orbitals with the lowest values of n and l will fill first.

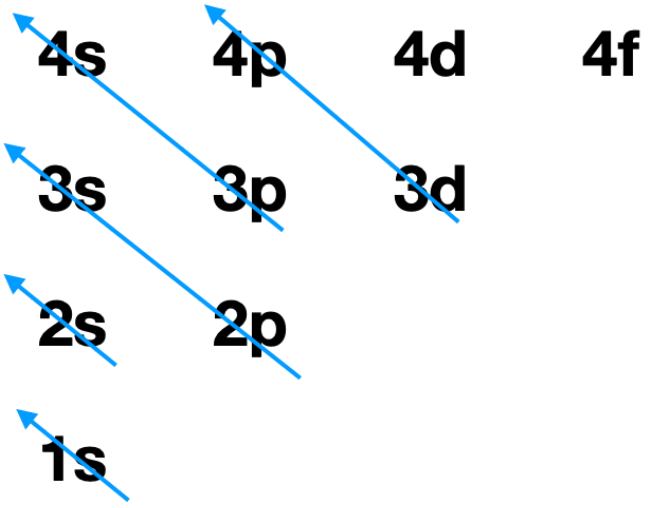


Figure *Section*2.2.1. The order of filling of ground state electron orbitals is 1s, 2s, 2p, 3s, 3p, 4s, 3d, 4p, etc... (CC-BY-NC-SA; Kathryn Haas)

(2) Hund's rule of maximum multiplicity states that for a given electron configuration, the lowest energy arrangement of electrons in degenerate orbitals is the one with the greatest "multiplicity," where multiplicity is the number of unpaired electrons (n) plus 1 (multiplicity = n + 1). This rule is used to predict the ground state of an atom or molecule with one or more open electronic shells.

Hund's rule is based on empirical observation of atomic spectra, and it is a consequence of the energy required to pair two electrons in the same orbital. This energy of repulsion between two electrons in the same orbitals is a Coulombic energy of repulsion, Π_c, caused by two electrons with like charge sharing the same area of space (an orbital). When more than one electron occupies a set of degenerate orbitals, the most favorable arrangement is one where the number of paired electrons is minimized.

A simplified definition of Hund's rule is that **the lowest energy arrangement is the one with the greatest number of unpaired electrons**. This implies that if two or more orbitals of equal energy are available, electrons will occupy them singly before filling them in pairs. Examples of ground

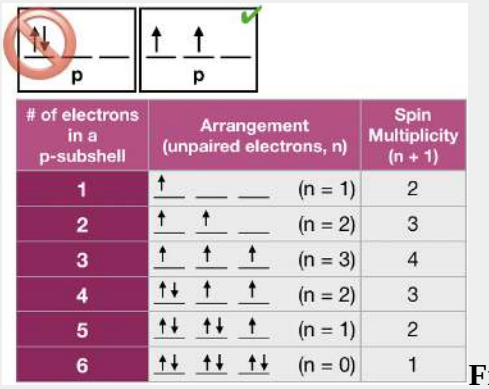


Figure *Section*2.2.2. Hund's rule is that spin multiplicity must be maximized in the ground state. (CC-BY-NC-SA; Libretexts)

state arrangements of electrons in three degenerate p-orbitals is given in the figure shown here.

(3) The Pauli exclusion principle states that it is impossible for two electrons of a multi-electron atom to have the same set of values for the four quantum numbers. Two electrons in different orbitals will have a different set of n, l, and m_l values. When two electrons reside in the same orbital, they posses the same n, l, and m_l values, therefore their m_s must be different. Thus, two electrons in the same orbital must have opposite half-integer spin projections of $+\frac{1}{2}$ and $-\frac{1}{2}$.

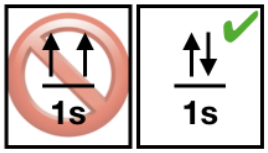


Figure *Section*2.2.3. Pauli's principle tells us that paired electrons must have opposite spin. CC-BY-NC-SA; Libretexts)

(4) The exchange interaction is sometimes called the *exchange energy* or *exchange force*, however it is not a true energy or force. Rather, it is a quantum mechanical effect that takes place between identical particles. The exchange interaction results in a ground state electron configuration with unpaired electrons all being of the same spin. Unpaired electrons are conventionally written in the "spin up" direction.

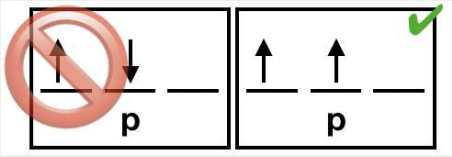


Figure *Section*2.2.4. Unpaired electrons should have identical spins according due to the exchange interaction. CC-BY-NC-SA; Libretexts)

Trends in Expected Electron Configuration

The four "rules" above can be used as guidelines to predict the ground state electron configuration of atoms, the filling of subshells, and the configuration of electrons in degenerate orbitals. However, the utility of these guidelines for predicting actual electron configurations requires more nuanced knowledge of the relative energy levels of orbitals.

Generally, orbital energy levels directly correspond to their shell number. Additionally, orbitals within a shell generally follow the energetic trend where s<p<d<f. Although these general trends for relative orbital energy levels hold true for most of the main block elements (the s - and p-blocks), there are important exceptions in the orbital energy levels of transition metal atoms and ions of the d- and f-blocks.

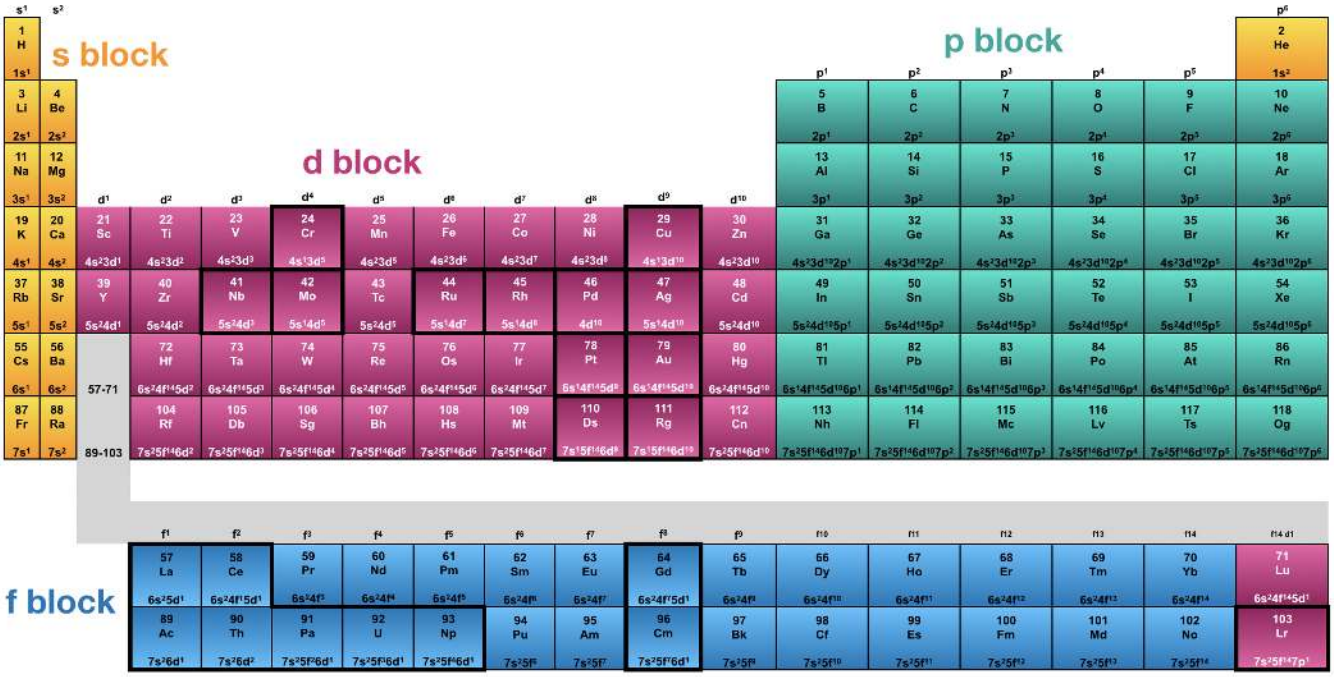


Figure *Section*2.2.5. This is a depiction of the periodic table that highlights the s-, p-, d-, and f- blocks in different colors. Violations of the expected trend in electron configurations are outlined in a heavy black line. Several elements of the d block and f block violate the general trends in electron configuration because their orbital energy levels do not follow *general* trends. (CC-BY-NC-SA; Kathryn Haas)

Elements that violate general trends in electron configuration are outlined with a dark line in Figure *Section*2.2.5. All of the exceptions are within the d- and f- blocks, and the violations are caused by an unexpected order of the orbital energy levels.

In the next section you will learn why the orbital energy levels correlate with shell number and why subshells within a shell usually follow the trend that s<p<d<f. You will also learn why there are occasional exceptions to this trend and how these exceptions influence elemental properties.

References

1. Miessler, Gary L., and Donald A. Tarr. *Inorganic Chemistry*. Upper Saddle River, NJ: Pearson Prentice Hall, 2010. Print.
2. Brown, Ian David. *The Chemical Bond in Inorganic Chemistry the Bond Valence Model*. Oxford: Oxford UP, 2006. Print.

This page titled Section 2.2: Aufbau Principle is shared under a CC BY-NC-SA 4.0 license and was authored, remixed, and/or curated by Kathryn Haas.

- **2.2.3: Aufbau Principle** by Kathryn Haas is licensed CC BY-NC-SA 4.0.
- **2.3: Aufbau Principle** by Kathryn Haas is licensed CC BY-NC-SA 4.0.

Section 2.3: Shielding

Introduction

Coulomb's Law is from classical physics; it tells us that particles with opposite electrostatic charge are attracted to each other; and the larger the charge on either particle or the closer the distance between them, the stronger the attraction. Coulomb's law explains why atomic size decreases as the charge on the nucleus increases, but it can't explain the nuances and variations in size as we go across the periodic table. Coulomb's Law also explains why electrons in different shells (*n*), at different distances from the nucleus, have different energies. But on its own, Coulomb's law doesn't quite explain why electron subshells within a shell (like 2s vs 2p) would have different energies. To explain these things, we need to consider how both electron **shielding** and **penetration** result in variations in effective nuclear charge (Z*) that depend on shell and subshell.

Effective Nuclear Charge (Z*)

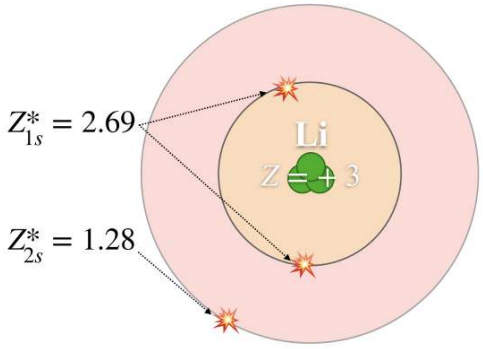


Figure **Section2.3.1**. In a lithium atom, the nuclear charge (Z) is +3. 1s electrons experience an effective nuclear charge (Z*) of +2.69, and 2s electrons experience an Z* of +1.28. (CC-BY-NC-SA; Kathryn Haas)

Coulombs' law works well for predicting the energy of an electron in a hydrogen atom (because H has only one electron). It also works for hydrogen-like atoms: any nucleus with exactly one electron (a He^+ ion, for example, has one electron). However, Coulomb's law is insufficient for predicting the energies of electrons in multi-electron atoms and ions.

Electrons within a multi-electron atom interact with the nucleus and with all other electrons. Each electron in a multi-electron atom experiences both attraction to the nucleus and repulsion from interactions with other electrons. The presence of multiple electrons decreases the nuclear attraction to some extent. Each electron in a multi-electron atom experiences a different magnitude of (and attraction to) the nuclear charge depending on what specific shell and subshell the electron occupies. The amount of positive nuclear charge experienced by any individual electron is the **effective nuclear charge (Z*)**.

For example, in lithium (Li), none of the three electrons "feel" the full +3 charge from the nucleus (see Figure **Section2.3.1**). Rather, each electron "feels" a Z* that is less than the actual Z and that depends on the electron's orbital. The actual nuclear charge in Li is $Z = +3$; the 1s electrons experience a $Z^* = +2.69$, and the 2s electron experiences a $Z^* = +1.28$. In general, core electrons (or the electrons closest to the nucleus), "feel" a Z* that is close to, but less than, Z. On the other hand, outer valence electrons experience a Z* that is much less than Z.

In summary:

- Core electrons: $Z^* \lessapprox Z$
- Valence electrons: $Z^* \ll Z$

Shielding:

Shielding is the reduction of true nuclear charge (Z) to the effective nuclear charge (Z*) by other electrons in a multi-electron atom or ion. Shielding occurs in all atoms and ions that have more than one electron. H is the only atom in which shielding does not occur.

Explanation of shielding: Electrons in a multi-electron atom interact with the nucleus and all other electrons in the atom. To describe shielding, we can use a simplified model of the atom: we will choose an electron-of-interest in a multi-electron atom and treat all the "other" electrons as a group of spherically-distributed negative charge. Classical electrostatics allows us to treat spherical distribution of charge as a point of charge at the center of the distribution. Thus, we consider all the "other" electrons in our atom as a point of negative charge in the center of the atom. While the positive charge of the nucleus provides an attractive force toward our electron, the negative charge distribution at the center of the atom would provide a repulsive force. The attractive and repulsive forces would partially cancel each other; but since there are less "other" electrons than there are protons in our atom, the nuclear charge is never completely canceled. The "other" electrons partially block, or shield, part of the nuclear charge so that our electron-of-interest experiences a partially-reduced nuclear charge, the Z*.

In reality, there is not a one-for-one "canceling" of the nuclear charge by each electron. Partly due to *penetration*, no single electron can completely shield a full unit of positive charge. Core electrons shield valence electrons, but valence electrons have little effect on the Z* of core electrons. The ability to shield, and be shielded by, other electrons strongly depends the electron orbital's average distance from the nucleus and its *penetration*; thus shielding depends on both shell (n) and subshell (l).

Shielding depends on electron penetration

Coulomb's law shows us that distance of an electron from its nucleus is important in determining the electron's energy (its attraction to the nucleus). The shell number (n) determines approximately how far an electron is from the nucleus *on average*. Thus, all orbitals in the same shell (s,p,d) have similar sizes and similar average distance of their electrons from the nucleus. But there is another distance-related factor that plays a critical role in determining orbital energy levels: *penetration*. **Penetration** describes the ability of an electron in a given subshell to penetrate into other shells and subshells to get close to the nucleus. Penetration is the **extent to which an electron can approach the nucleus**. Penetration depends on both the shell (n) and subshell (l).

The penetration of individual orbitals can be visualized using the radial probability functions. For example, Figure ***Section*2.3.2** below shows plots of the radial probability function of the 1s, 2s, and 2p orbitals. From these plots, we can see that the 1s orbital is able to approach the closest to the nucleus; thus it is the most penetrating. While the 2s and 2p have most of their probability at a farther distance from the nucleus (compared to 1s), the 2s orbital and the 2p orbital have different extents of penetration. Notice that the 2s orbital is able to penetrate the 1s orbital because of the central 2s lobe. The 2p orbital penetrates somewhat into the 1s, but it cannot approach the nucleus as closely as the 2s orbital can. While the 2s orbital penetrates more than 2p (2s orbital can approach closer to the nucleus), the 2p is slightly *closer on average* than 2s. The order of Z* in 2s and 2p subshells depends on which factor (average distance or penetration) is more important. In the first two rows of the periodic table, penetration is the dominant factor that results in 2s having a lower energy compared to 2p (see Figure ***Section*2.3.4** for values).

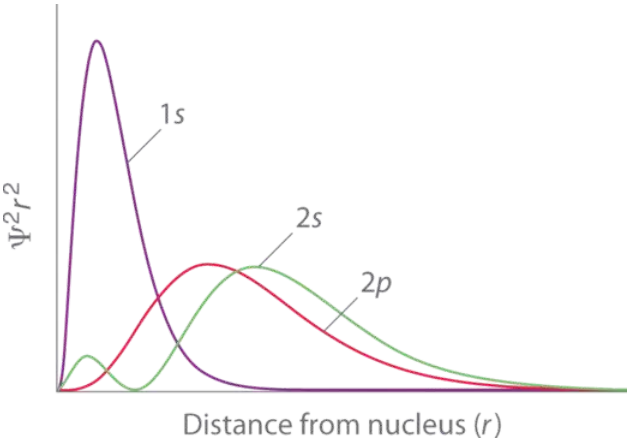


Figure *Section*2.3.2. Orbital Penetration. A comparison of the radial probability distribution of the 2s and 2p orbitals for various states of the hydrogen atom shows that the 2s orbital penetrates inside the 1s orbital more than the 2p orbital does. Consequently, when an electron is in the small inner lobe of the 2s orbital, it experiences a relatively large value of Z*, which causes the energy of the 2s orbital to be lower than the energy of the 2p orbital.

An electron orbital's penetration effects its ability to shield other electrons and effects the extent to which it is shielded by other electrons. In general, electron orbitals that have greater penetration experience stronger attraction to the nucleus and less shielding by other electrons; these electrons thus experience a larger (Z*). Electrons in orbitals that have greater penetration also shield other electrons to a greater extent.

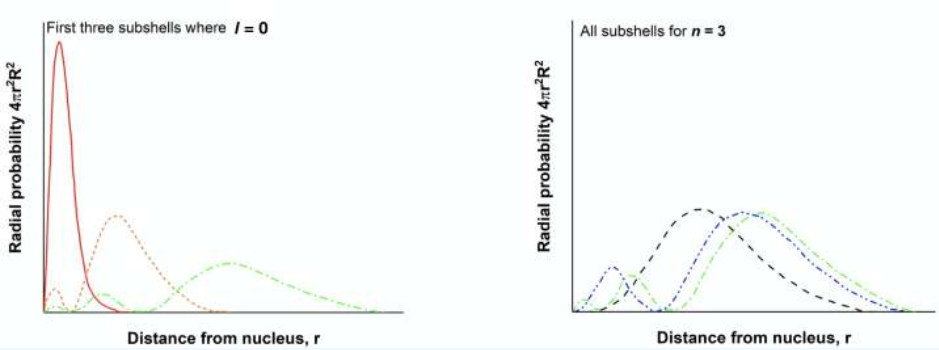
Within the same shell value (n), the penetrating power of an electron follows this trend in subshells (l):

s>p>d>f

Exercises

Exercises

1. Compare the 2s and 2p orbitals:
   (a) Which is closer to the nucleus on average?
   (b) Which is more penetrating?
   (c) Which orbital experiences a stronger Z* and is thus lower in energy (consider your experience, but also inspect Figure *Section*2.3.5)? Please explain.
2. Visit the Orbitron and peruse the radial distribution functions for different orbitals. Compare the 2p and 3s orbitals:
   (a) Which is farther from the nucleus on average?
   (b) Which is more penetrating?
   (c) Which orbital is lower in energy?
3. Which atom, Li, or N, has a stronger valence Z*? Explain why.
4. Explain why 2s and 2p subshells are completely degenerate in a hydrogen atom.
5. Which atom has a smaller radii: Be or F? Explain.
6. Which electrons shield others more effectively: 3p or 3d?
7. Use the clues given in the figures below to label the radial distribution functions shown.



8. Explain why the ground state (most energetically favorable) electron configuration of Be is $1s^2 2s^2$ rather than alternative configurations like $1s^2 2s^1 2p^1$ or $1s^2 2p^2$.

Answer 1

(a) The 2s orbital is closer to the nucleus on average.

(b) The 2s orbital is more penetrating than 2p.

(c) You might "know" that the 2s orbital is lower in energy than 2p because 2s fills first. But a close inspection of Figures 1.1.2.3 and 1.1.2.4 from the previous page indicates that while the 2s and 2p elements are degenerate in Ne (element 10), for elements with atomic number 11 and greater 2p has a higher Z* than 2s! This example illustrates that both average distance and penetration are factors in determining Z*, and the factor that is more important may change as we increase in atomic number.

Answer 2

(a) The 3s orbital reaches farther away from the nucleus and is on average farther from the nucleus than 2p.

(b) The 3s orbital is more penetrating than 2p, even though 3s is farther on average!

(c) The 2p orbital is lower in energy than 3s; this is because 2p is still significantly closer to the nucleus on average and experiences a stronger Z*. (Penetration is not the only consideration!)

Answer 3

A nitrogen atom has a stronger effective nuclear charge (Z*) than lithium due to its greater number of protons; even though N also has more electrons that would shield the nuclear charge, each electron only partially shields each proton. This means that atoms with greater atomic number always have greater Z* for any given electron.

Answer 4

The hydrogen atom has only one electron; thus there is no shielding to consider. When there are not other electrons to shield the nucleus, penetration and shielding are irrelevant, and subshells within a shell are degenerate.

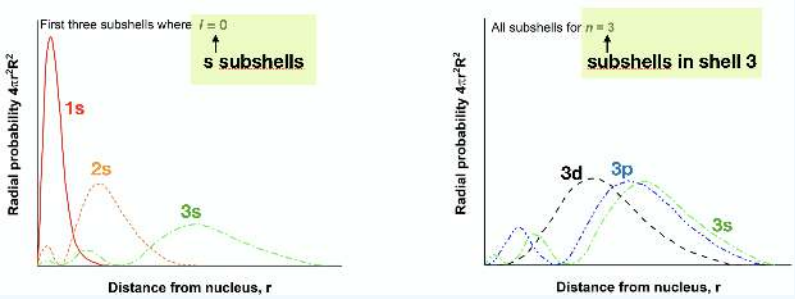
Answer 5

Fluorine has a smaller radii than Beryllium due to F having a greater valence Z* and therefore pulling the valence electrons close to the nucleus and providing a smaller atomic radii.

Answer 6

3p shields better than 3d because p orbitals penetrate more than d orbitals within the same shell.

Answer 7

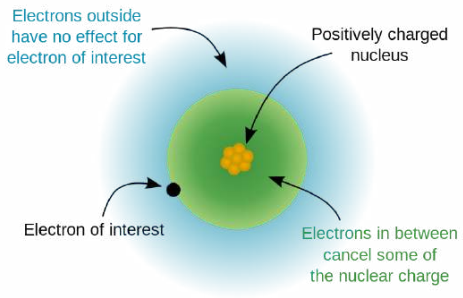


Answer 8

This question is asking why the 2s orbital fills in Be before 2p is occupied. This is a multi-electron atom, therefore core electrons shield the 2s and 2p orbitals to different extents. In Be we expect the 2s orbital to fill before 2p because 2s penetrates more and experiences a higher Z*.

Slater's rules for estimating Z*

Figure *Section*2.3.3. Diagram illustrating effective nuclear charge according to Slater's rules.



The Z* can be estimated using a number of different methods; probably the best known and most commonly used method is known as **Slater's Rules**. Slater developed a set of rules to estimate Z* based on how many other electrons exist in the atom and on the orbital location of the electron-of-interest. These two factors are important determinants in shielding, and they are used to calculate a **shielding constant (S)** used in Slater's formula:

$$Z* = Z - S \qquad \text{(Section 2.3.1)}$$

where Z is the actual nuclear charge (the atomic number) and Z* is the effective nuclear charge.

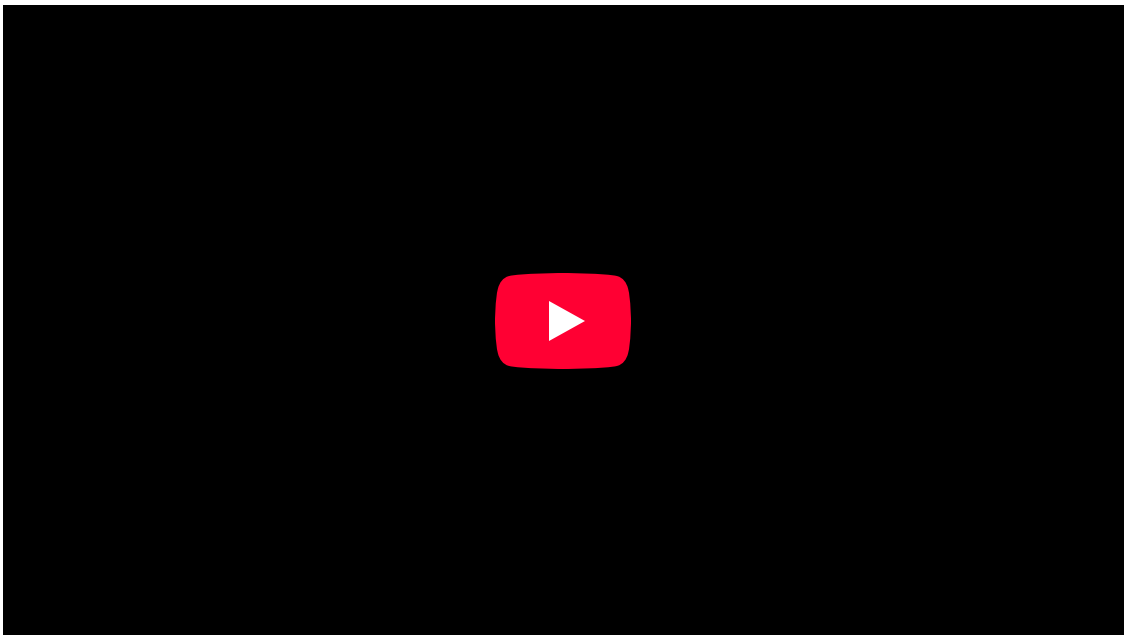
In the calculation of S, it is assumed that electrons closer to the nucleus than our electron-of-interest cancel some of the nuclear charge; those farther from the nucleus have no effect. To calculate S, all the relevant orbitals in an atom are written out in order of increasing energy, separating them into in "groups". Each change in shell number is a new group; s and p subshells are in the same group but d and f orbitals are their own group. You write out all the orbitals using parentheses until you get to the group of the electron-of-interest, like this:

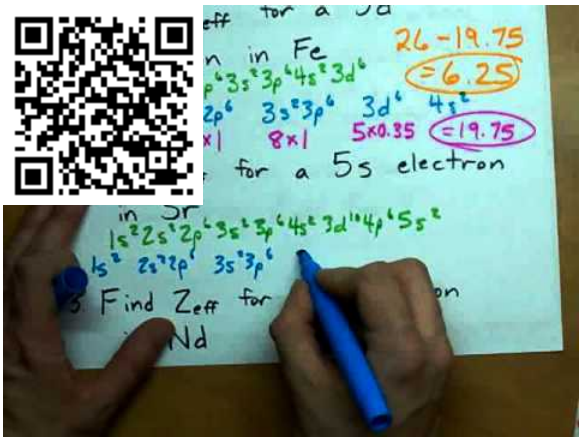
(1s)(2s,2p)(3s,3p)(3d)(4s,4p)(4d)(4f)(5s,5p) etc.

**Critical: The orbitals must be written in order of increasing energy!

1. **Electrons in the same Group():**
   - Each other electron (not counting the electron-of-interest) in the same group () as the chosen electron, contributes 0.35 to S.
   - Each 1s electron contributes 0.30 to S.
     Conceptually, this means electrons in the same group shield each other 30-35%.
2. **Electrons in Groups() to the left:**
   - If the electron-of-interest is in a d or f subshell, every electron in groups () to the left contributes 1.00 to S.
     Conceptually, this means that d and f electrons are shielded 100% by all electrons in the same shell with a smaller value of l, as well as all electrons in lower shells (n).
   - If the electron-of-interest is in an s or p subshell, all electrons in the next lower shell (n - 1) contribute 0.85 to S. And all the electrons in even lower shells contribute 1.00 to S.
     Conceptually, this means that s and p electrons are shielded 85% by the electrons one shell lower, and 100% by all electrons in shells n - 2 or lower.
3. **Electrons in Groups() to the right:**
   - Electrons to the right contribute 0 to S.
     Conceptually, this means electrons in higher energy groups don't contribute to shielding.

A video explaining how to use Slater's Rules





Example *Section*2.3.1: Fluorine, Neon, and Sodium

What is the Z* experienced by the valence electrons in the three isoelectronic species: fluorine anion (F^-), neutral neon atom (Ne), and sodium cation (Na^+)?

Solution

Each species has 10 electrons, and the number of core electrons is 2 (10 total electrons - 8 valence), but the effective nuclear charge varies because each has a different atomic number (Z). The approximate Z* can be found with Slater's Rules. For all of these species, we would calculate the same sigma value:

Calculating S: (1s)(2s,2p), $S = 2(0.85) + 7(0.35) = 1.7 + 2.45 = 4.15$

Fluorine anion: $Z* = 9 - S = 9 - 4.15 = 4.85$

Neon atom: $Z* = 10 - S = 10 - 4.15 = 5.85$

Sodium Cation: $Z* = 11 - S = 11 - 4.15 = 6.85$

So, the sodium cation has the greatest effective nuclear charge.

Exercise *Section*2.3.1

Calculate Z* for a 3d-electron in a zinc (Zn) atom.

Answer

Write out the relevant orbitals: (1s)(2s,2p)(3s,3p)(3d) ~~(4s)~~

Notice that although 4s is fully occupied, we don't include it because in Zn, 4s is higher in energy than 3d. Therefore, 4s is to the right of the d electrons we are considering. The electron-of-interest is in 3d, so the other nine electrons in 3d each contribute 0.35 to the value of S. The other 18 electrons each contribute 1 to the value of S.

$S = 18(1) + 9(0.35) = 21.15$

$Z* = 30 - 21.15 = 8.85$

So, although the nuclear charge of Zn is 30, the 3d electrons only experience a $Z* \approx 8.85$!

"Best" values for Z*

Slater's rules are a set of simple rules for predicting S and Z* based on empirical evidence from quantum mechanical calculations. In other words, the Z* calculated from Slater's rules are approximate values. The values considered to be the most accurate are derived from quantum mechanical calculations directly. You can find these values in a nice chart on the Wikipedia article of Effective Nuclear Charge. The chart is recreated here in Figure *Section*2.3.4 for convenience:

Z or Z_{eff}	H																	He
Z	1.00																	2.00
1s	1.00																	1.69
	Li	Be											B	C	N	O	F	Ne
Z	3.00	4.00											5.00	6.00	7.00	8.00	9.00	10.00
1s	2.69	3.69											4.68	5.67	6.67	7.66	8.65	9.64
2s	1.28	1.91											2.58	3.22	3.85	4.49	5.13	5.76
2p													2.42	3.14	3.83	4.45	5.10	5.76
	Na	Mg											Al	Si	P	S	Cl	Ar
Z	11.00	12.00											13.00	14.00	15.00	16.00	17.00	18.00
1s	10.63	11.61											12.59	13.58	14.56	15.54	16.52	17.51
2s	6.57	7.39											8.21	9.02	9.83	10.63	11.43	12.23
2p	6.80	7.83											8.96	9.95	10.96	11.98	12.99	14.01
3s	2.51	3.31											4.12	4.90	5.64	6.37	7.07	7.76
3p													4.07	4.29	4.89	5.48	6.12	6.76
	K	Ca	Sc	Ti	V	Cr	Mn	Fe	Co	Ni	Cu	Zn	Ga	Ge	As	Se	Br	Kr
Z	19.00	20.00	21.00	22.00	23.00	24.00	25.00	26.00	27.00	28.00	29.00	30.00	31.00	32.00	33.00	34.00	35.00	36.00
1s	18.49	19.47	20.46	21.44	22.43	23.41	24.40	25.38	26.37	27.35	28.34	29.33	30.31	31.29	32.28	33.26	34.25	35.23
2s	13.01	13.78	14.57	15.38	16.18	16.98	17.79	18.60	19.41	20.21	21.02	21.83	22.60	23.37	24.13	24.89	25.64	26.40
2p	15.03	16.04	17.06	18.07	19.07	20.08	21.08	22.09	23.09	24.10	25.10	26.10	27.09	28.08	29.07	30.07	31.06	32.05
3s	8.68	9.60	10.34	11.03	11.71	12.37	13.02	13.68	14.32	14.96	15.59	16.22	17.00	17.79	18.60	19.40	20.22	21.03
3p	7.73	8.66	9.41	10.10	10.79	11.47	12.11	12.78	13.44	14.09	14.73	15.37	16.20	17.01	17.85	18.71	19.57	20.43
4s	3.50	4.40	4.63	4.82	4.98	5.13	5.28	5.43	5.58	5.71	5.84	5.97	7.07	8.04	8.94	9.76	10.55	11.32
3d			7.12	8.14	8.98	9.76	10.53	11.18	11.86	12.53	13.20	13.88	15.09	16.25	17.38	18.48	19.56	20.63
4p													6.22	6.78	7.45	8.29	9.03	9.34
	Rb	Sr	Y	Zr	Nb	Mo	Tc	Ru	Rh	Pd	Ag	Cd	In	Sn	Sb	Te	I	Xe
Z	37.00	38.00	39.00	40.00	41.00	42.00	43.00	44.00	45.00	46.00	47.00	48.00	49.00	50.00	51.00	52.00	53.00	54.00
1s	36.21	37.19	38.18	39.16	40.14	41.13	42.11	43.09	44.08	45.06	46.04	47.03	48.01	48.99	49.97	50.96	51.94	52.92
2s	27.16	27.90	28.62	29.37	30.13	30.88	31.63	32.38	33.16	33.88	34.63	35.39	36.12	36.86	37.60	38.33	39.07	39.80
2p	33.04	34.03	35.00	35.99	36.98	37.97	38.94	39.95	40.94	41.93	42.92	43.91	44.90	45.89	46.87	47.86	48.85	49.84
3s	21.84	22.66	23.55	24.36	25.17	25.98	26.79	27.60	28.44	29.22	30.03	30.84	31.63	32.42	33.21	34.00	34.79	35.58
3p	21.30	22.17	23.09	23.85	24.62	25.47	26.38	27.22	28.15	29.02	29.81	30.69	31.52	32.35	33.18	34.01	34.84	35.67
4s	12.39	13.44	14.26	14.90	15.28	16.10	17.20	17.66	18.58	18.99	19.87	20.87	21.76	22.66	23.54	24.41	25.30	26.17
3d	21.68	22.73	25.40	25.57	26.25	27.23	28.35	29.36	30.41	31.45	32.54	33.61	34.68	35.74	36.80	37.84	38.90	39.95
4p	10.88	11.93	12.75	13.46	14.08	14.98	15.81	16.44	17.14	17.72	18.56	19.41	20.37	21.27	22.18	23.12	24.03	24.96
5s	4.99	6.07	6.26	6.45	5.92	6.11	7.23	6.49	6.64	(empty)	6.76	8.19	9.51	10.63	11.62	12.54	13.40	14.22
4d			15.96	13.07	11.24	11.39	12.88	12.81	13.44	13.62	14.76	15.88	16.94	17.97	18.97	19.96	20.93	21.89
5p													8.47	9.10	10.00	10.81	11.61	12.43

Figure *Section*2.3.4. This chart shows Z* values calculated by Clementi et. al. in 1963 and 1967 that are consistent with SCF Calculations. This chart was created using data from the Wikipedia article on Effective Nuclear Charge.

Z* modulates attraction

When valence electrons experience less nuclear charge than core electrons, different electrons experience different magnitudes of attraction to the nucleus. A modified form of Coulomb's Law is written below, where e is the charge of an electron, Z* is the effective nuclear charge experienced by that electron, and r is the radius (distance of the electron from the nucleus).

$$F_{eff} = k\frac{Z * e^2}{r^2} \qquad \text{(Section 2.3.2)}$$

This formula suggests that if we can estimate Z*, then we can predict the attractive force experienced by, and the energy of, an electron in a multi-electron atom (ex. Li).

The attraction of the nucleus to valence electrons determines the atomic or ionic size, ionization energy, electron affinity, and electronegativity. The stronger the attraction, and the stronger Z*, the closer the electrons are pulled toward the nucleus. This in turn results in a smaller size, higher ionization energy, higher electron affinity, and stronger electronegativity.

General Periodic Trends in Z*

Close inspection of Figure *Section*2.3.4 and analysis of Slater's rules indicate that there are some predictable trends in Z*. The data from Figure *Section*2.3.4 is plotted below in Figure *Section*2.3.5 to provide a visual aid to the discussion below.

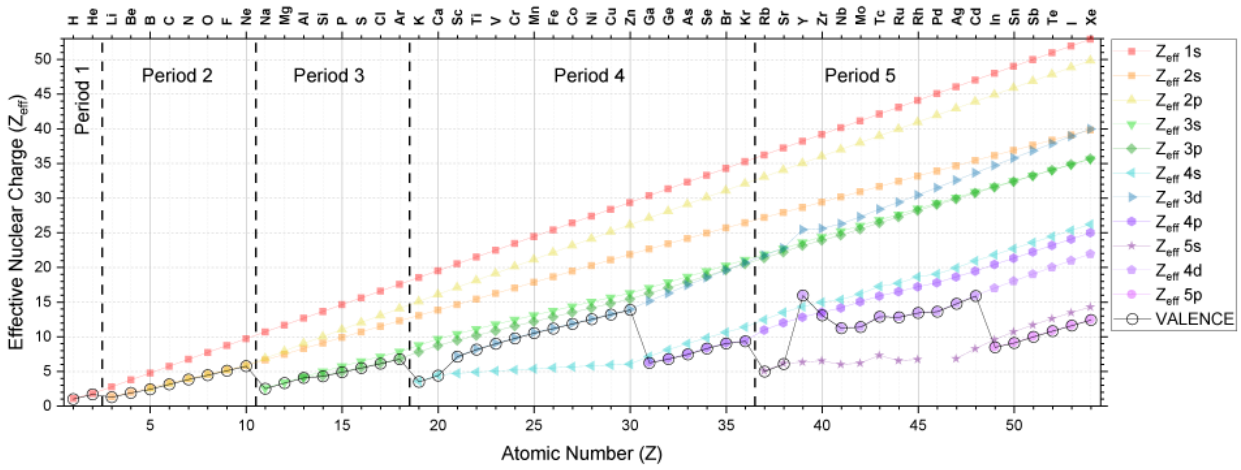


Figure *Section*2.3.5: The Z* values for electrons in each subshell of the first 54 elements (H to Xe) are plotted. Each subshell is plotted as a different series (see legend) and the valence shell is highlighted by a solid black line with open circles. (CC-BY-NC-SA; Kathryn Haas)

Trends in Z* for electrons in a specific shell and subshell

The Z* for electrons in a given shell and subshell generally increases as atomic number increases; this trend holds true going across the periodic table and down the periodic table. Convince yourself that this is true for any subshell by examining Figure *Section*2.3.5.

Do you notice any exceptions to this general trend?

Inspection of Figure *Section*2.3.5 should confirm for you that the Z* increases as Z increases for electrons in any subshell (like the 1s subshell for example, which is plotted above as a red line with square points). You can see this trend as the positive slope in each series. There is one obvious exception in Period 5 in elements 39 (Y) to 41 (Nb; the Z* of 4s actually decreases across these three elements as atomic number increases. There is also an exception between Y and Zr in the 3d subshell, and between Tc and Ru in the 5s subshell.

For valence electrons:

It is useful to understand trends in valence Z* because the valence Z* determines atomic/ionic properties and chemical reactivity. The trends in the valence Z* are not simple because as atomic number increases, the valence shell and/or subshell also changes. The valence Z* is indicated in Figure *Section*2.3.5 as a black line with open circles.

Down the table: As we go down a column of the periodic table, the valence Z* increases. This is a simple trend because type of subshell is consistent and there is an increase only in shell and in atomic number, Z. This trend is best illustrated by inspection of Figure *Section*2.3.4.

Across the table: the trend depends on shell and subshell, but generally Z* increases across a period.

Periods 1-3 (s and p only): As we go across the table in periods 1-3, the shell stays constant as Z increases and the subshell changes from s to p. In these periods, there is a gradual increase in valence Z* as we move across any of the first three periods.

Periods 4 and 5 (s, p, and d): Now we have some more complex trends because valence subshell and shell are changing as we increase in atomic number. Notice that the valence Z* generally increases going across a period as long as subshell isn't changing; the exception is within the 4d subshell (elements 39-44 or Y-Ru). In general, going from $(n)s$ subshell to $(n-1)d$ subshell, there a relatively large increase in valence Z*. And in going from $(n-1$d\) subshell to $(n)p$ subshell, there is a relatively large decrease in Z*.

From one period to another: From Figure *Section*2.3.5, we can see that as we increase Z by one proton, going from one period to the next, there is a relatively large decrease in Z* (from Ne to Na, for example). This is because as Z increases by a

small interval, the shell number increases, and so the electrons in the valence shell are much farther from the nucleus and are more shielded by all the electrons in the lower shell numbers.

Exercises

Exercise *Section2.3.2*

1. Compare trends in Z* and atomic size. Explain how and why atomic size depends on Z*.
2. Compare trends in Z* and ionization energy. Explain how and why ionization energy depends on Z*.

Answer

1. On the periodic table, atomic radius generally decreases across the periods (left to right) and increases down the groups. As atomic number increases across the periodic table, nuclear charge (Z) increases and Z* increases. In turn, the atomic radius decreases because the higher nuclear charge (and thus higher Z*) pulls electrons closer to the nucleus. Atomic radius increases down the periodic table because the shell number increases. Despite an increase in Z* going down the periodic table, larger atomic radii results from electrons occupying higher shells.

2. Ionization energies (IE) are inversely related to atomic radius; IE increases across the periods and decreases down the groups. Since the nucleus holds valence electrons more strongly (due to higher Z*) across the periods, IE increases because valence electrons are harder to remove. Down the periodic table, larger atomic radius causes electrons in valence orbitals to be shielded by core electrons. Recall that shielding reduces the nuclear charge available to electrons in higher orbital levels, resulting in a lower Z*. With more shielding and lower Z*, the valence electrons are held less tightly by the nucleus such that ionization energy decreases (i.e. valence electrons are easier to remove).

References

1. Petrucci, Ralph H., William S. Harwood, F. Geoffrey Herring, and Jeffry D. Madura. General Chemistry: Principles and Modern Applications, Ninth Edition. Pearson Education Inc. Upper Saddle River, New Jersey: 2007.
2. Raymond Chang. Physical Chemistry for Biological Sciences. Sausalito, California: University Science Books, 2005
3. R. S. Mulliken, Electronic Structures of Molecules and Valence. II General Considerations, Physical Review, vol. 41, pp. 49-71 (1932)
4. Anastopoulos, Charis (2008). *Particle Or Wave: The Evolution of the Concept of Matter in Modern Physics*. Princeton University Press. pp. 236–237. ISBN 0691135126. http://books.google.com/?id=rDEvQZhpltEC&pg=PA236.

Contributors and Attributions

- Sidra Ayub (UCD), Alan Chu (UCD)
- Emily V Eames (City College of San Francisco)
- Curated or created by Kathryn Haas

Section 2.3: Shielding is shared under a CC BY-NC-SA 4.0 license and was authored, remixed, and/or curated by LibreTexts.

- **2.2.4: Shielding** by Kathryn Haas is licensed CC BY-NC-SA 4.0.
- **2.2: Shielding** is licensed CC BY-NC-SA 4.0.

Section 2.4: Periodic Properties of Atoms

Introduction

General periodic trends are specific patterns that are present within the periodic table; these are patterns in properties like electronegativity, ionization energy, electron affinity, atomic radius, melting point, and metallic character. General periodic trends provide chemists with an invaluable tool to quickly predict an element's properties. These trends exist because of the similar atomic structure of the elements within their respective group families or periods, and because of the periodic nature of the elements. Some of the general periodic trends are described in this section.

Ionization Energy

Ionization energy (IE) is the energy required to **remove an electron from a neutral atom or cation in its gaseous phase**. IE is also known as *ionization potential*.

$$A^{n+}_{(g)} \longrightarrow A^{(n+1)+}_{(g)} + e^- \qquad IE = \Delta U \tag{Section 2.4.1}$$

Conceptually, ionization energy is the affinity of an element for its outermost electron (an electron it already has in its valence shell).

1st, 2nd, and 3rd Ionization Energies

The symbol IE_1 stands for the ***first ionization energy*** (energy required to take away an electron from a neutral atom, where $n = 0$). The symbol IE_2 stands for the ***second ionization energy*** (energy required to take away an electron from an atom with a +1 charge, $n = 2$.)

First Ionization Energy, IE_1 (general element, A): $A_{(g)} \rightarrow A^{1+}_{(g)} + e^-$

Second Ionization Energy, IE_2 (general element, A): $A^{1+}_{(g)} \rightarrow A^{2+}_{(g)} + e^-$

Third Ionization Energy, IE_3 (general element, A): $A^{2+}_{(g)} \rightarrow A^{3+}_{(g)} + e^-$

Each succeeding ionization energy is larger than the preceding energy. This means that $IE_1 < IE_2 < IE_3 < ... < IE_n$ will always be true. For example, ionization energy increases as succeeding electrons are taken away from Mg.

$$Mg_{(g)} \rightarrow Mg^+_{(g)} + e^- \quad IE_1 = 738\,kJ/mol \tag{Section 2.4.2}$$

$$Mg^+_{(g)} \rightarrow Mg^{2+}_{(g)} + e^- \quad IE_2 = 1451\,kJ/mol \tag{Section 2.4.3}$$

Ionization energy is correlated with the strength of attraction between the positively-charged nucleus and the negatively-charged valence electrons, and therefore the effective nuclear charge Z_eff. The higher the ionization energy, the stronger the attractive force between nucleus and valence electrons, and the more energy is required to remove a valence electron. The lower the ionization energy, the weaker the attractive force between nucleus and valence electrons, and the less energy required to remove a valence electron.

General periodic trends in ionization energy

In general, ionization energies increase from left to right and decrease down a group; however there are variations in these trends that would be expected from the effects of penetration and shielding. The trends in **first ionization energy** are shown in Figure $Section 2.4.1$ and are summarized below.

- **Across a period:** As Z* increases across a period, the ionization energy of the elements generally increases from left to right. However there are breaks or variation in the trends in the following cases:
  - IE is especially low when removal of an electron creates a newly empty p subshell (examples include IE_1 of B, Al, Sc)
  - IE energy is especially low where removal of an electron results in a half-filled p or d subshell (examples include IE_1 of O, S)

- IE increases more gradually across the d- and f-subshells compared to s- and p- subshells. This is because d- and f-electrons are weakly penetrating and experience especially low Z*.

- **From one period to the next:** There is an especially large decrease in IE with the start of every new period (from He to Li or from Ne to Na for example). This is consistent with the idea that IE is especially low when removal of an electron creates a newly empty s-subshell.
- **Nobel gases:** The noble gases posses very high ionization energies. Note that helium has the highest ionization energy of all the elements.
- **Down a group:** Although Z* increases going down a group, there is no reliable trend in IE going down any group; in some cases IE increases going down a group, while in other cases IE decreases going down a group.

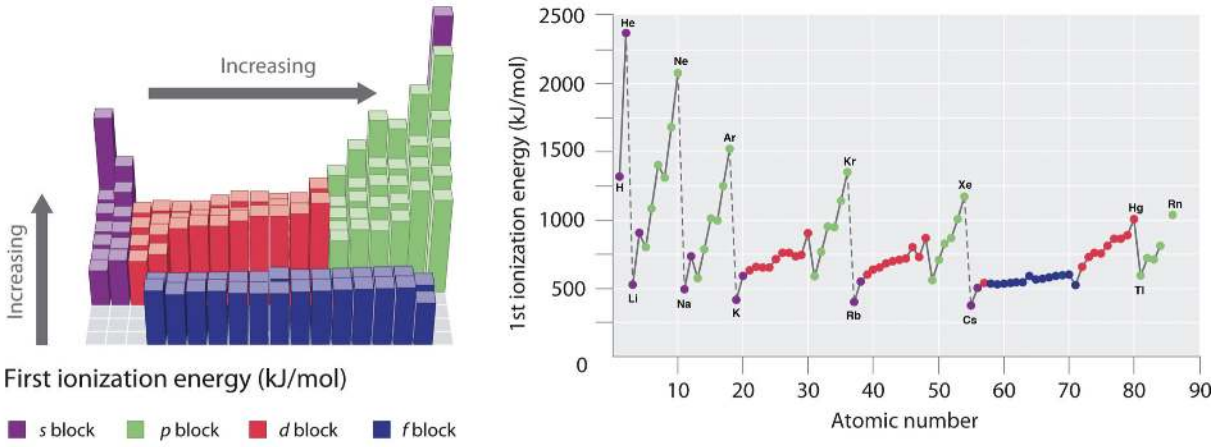


Figure *Section*2.4.1: Graph showing the First Ionization Energy of the Elements. Left: ionization energies are mapped onto the periodic table, where the magnitude of ionization energy is depicted as a bar graph. Right: the first ionization energy is plotted against atomic number. In both panels the elements of the s-block are shown in purple, p-block are shown in green, d-block are shown in red, and f-block are shown in blue.

Plots of the $IE_1, IE_2,$ and IE_3 of elements from hydrogen to krypton (first four periods) are shown in Figure *Section*2.4.2. Notice that $IE_3 > IE_2 > IE_1$. Also notice that trends mentioned above for IE_1 hold true for subsequent ionizations when electron configurations are considered!

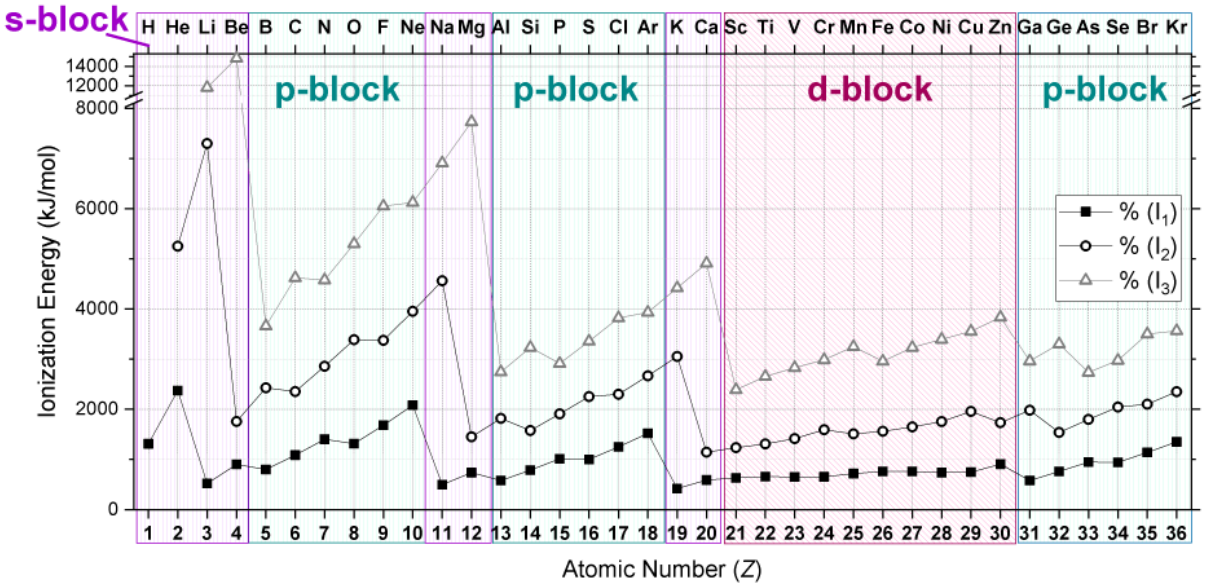


Figure *Section*2.4.2. The first (I_1), second (I_2), and third (I_3) ionization energies are plotted for elements with Z = 1 to 36 (H to Kr). The position of each element in its atomic form is indicated as s- p- or d-block. (CC-BY-NC-SA; Kathryn Haas)

Electron Affinity

According to IUPAC, there are two different, but equivalent, definitions of **electron affinity (EA)**.[6]

EA defined as removal of an electron

Electron affinity can be defined as the energy *required* when an electron is removed from a gaseous anion. The reaction as shown in equation Section 2.4.4 is *endothermic* (positive ΔU) for elements except noble gases and alkaline earth metals. Under this definition, the more positive the EA value, the higher an atom's affinity for electrons.

$$A^-_{(g)} \longrightarrow A_{(g)} + e^- \qquad EA = \Delta U \tag{Section 2.4.4}$$

The reaction shown in equation Section 2.4.4 is similar those that define ionization energy. For this reason, the EA is also described as the *zeroth ionization energy*.

EA defined as addition of an electron

An alternate and more common definition is the microscopic reverse of equation Section 2.4.4. This more common definition states that electron affinity is the energy *released* when an electron is added to a gaseous atom, as shown in equation Section 2.4.5. The reaction as shown in equation Section 2.4.5 is *exothermic* (negative ΔU) for elements except noble gases and alkaline earth metals. The more negative this EA value, the higher an atom's affinity for electrons.

$$A_{(g)} + e^- \longrightarrow A^-_{(g)} \qquad EA = \Delta U \tag{Section 2.4.5}$$

Conceptually, this second definition is quite similar to the concept of electronegativity; but unlike electronegativity, EA is a well-defined quantitative measurement.

Trends in Electron Affinity

For this discussion, we will use the first definition of EA: a more positive (larger) value means that the EA is higher (meaning stronger affinity toward an electron).

Across a period: Similar to ionization energy, EA generally increases across a row of the periodic table; this observation is consistent with the increase in effective nuclear charge (Z*) from left to right across a period. However, there are variations across

a period that are similar to variations in ionization energy and that can be explained by shielding, penetration, and electron configuration.

Down a group: Like the case of ionization energy trends, EA does not consistently decrease going down a column of the periodic table despite the fact that Z^* increases down a group.

The trend in EA follows a similar zig-zag pattern as the one seen with ionization energies, except that it is displaced by one unit from the trend in IE_1, two units from IE_2, and so on. For example, EA peaks at F, while IE_1 peaks at Ne, IE_2 peaks at Na, and IE_3 peaks at Mg. A plot of EA for the first 13 elements is shown overlaid on plots of IE_1, IE_2 and IE_3 in Figure *Section*2.4.3., where the shifts in the peaks and valleys within each zig-zag trend are indicated.

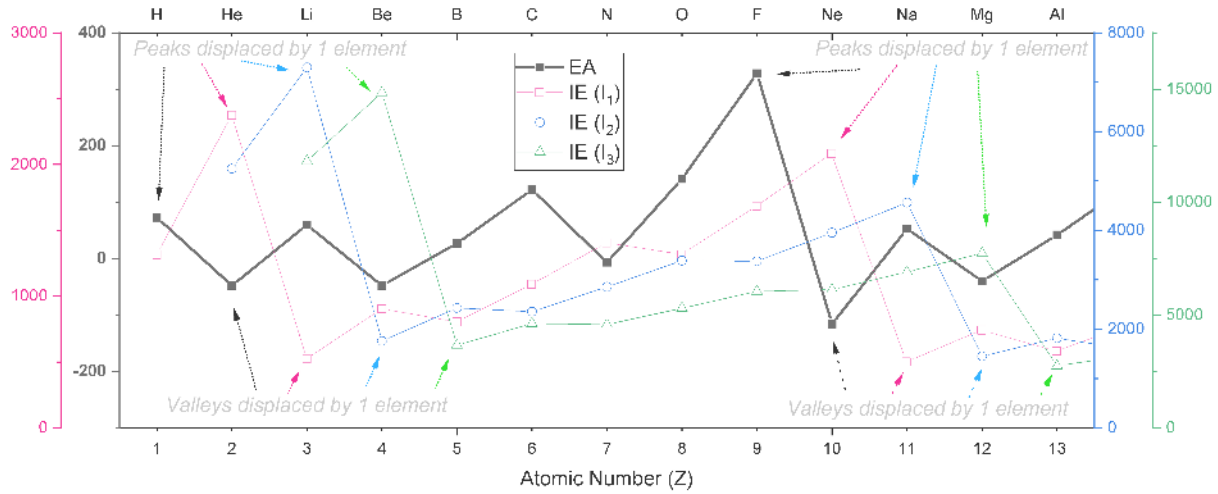


Figure *Section*2.4.3. A plot of electron affinity (the zeroth ionization energy) is overlaid on plots of the first (I_1), second (I_2), and third (I_3) ionization energies. Each plot is shown using separate y-axes. Trends in EA are similar to those in ionization energies, except the peaks and valleys of the trends are shifted by one unit, as indicated. These plots are shown in units of kJ/mole. (CC-BY-NC-SA; Kathryn Haas)

Atomic and Ionic Radii

There are several methods that can be used to determine radii of atoms and ions:

- **Nonpolar atomic radii:** The radius of an atom is derived from the bond lengths within nonpolar molecules; one-half the distance between the nuclei of two atoms within a covalent bond.
- **van der Waals radius:** The radius of an atom is determined by collision with other atoms.
- **Crystal Radii**: The atomic or ionic radius is determined using electron density maps from X-ray data.

The measurement of atomic or ionic size will depend on a number of factors, including the covalent character of bonding in any particular molecule, coordination number, physical state (liquid, solid, gas), the identity of nearby atoms/ions, variation in crystal structure, and distortions within regular crystal structures. You should keep in mind that the size of an atom or ion is a "fuzzy" measure, and the radius under a different set of conditions will probably change slightly.

Regardless, measured atomic and ionic radii reveal obvious trends across the periodic table and between atoms and ions. The relative atomic sizes shown in Figure *Section*2.4.4 were derived from crystallographic data.[9]

Trends in Atomic Radius

Atomic size generally decreases gradually from left to right across a period of elements. As nuclear charge (Z) increases, we expect the effective nuclear charge (Z*) of the valence electrons to also increase. Increasing Z pulls electrons closer to the nucleus. However, with each additional unit of Z, there is also an additional electron. The change in size is a balance of a compression caused by increasing Z and an expansion in the number of electrons. As a result, the atomic radius decreases *gradually* across a period.

Atomic size generally increases going down a group. As valence electrons occupying higher level shells due to the increasing quantum number (n), size increases despite the fact that Z and Z* are increasing going down the group.

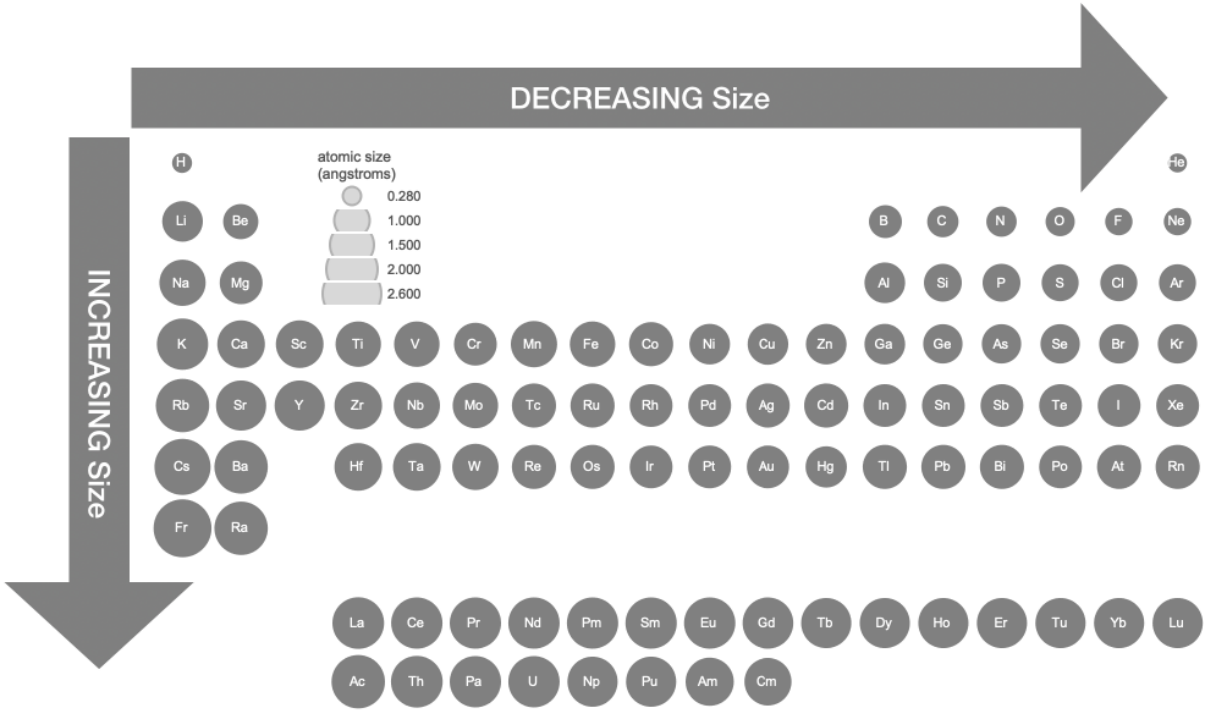


Figure ***Section*2.4.4.** *Atomic Radii Calculated from Crystalographic Data. Data from Cordero, Beatriz, Veronica Gomez, Ana E. Platero-Prats, Marc Reves, Jorge Echeverria, Eduard Cremades, Flavia Barragan, and Santiago Alvarez. "Covalent Radii Revisited." Dalton Transactions, no. 21 (2008): 2832–38. doi:10.1039/b801115j.*

Trends in Ionic Radius

Trends in ionic radius follow general trends in atomic radius for ions of the same charge. Ionic radius varies with charge of the ion (and number of electrons) and the electron configuration (e.g. high spin or low spin).

Cations

Compared to their atoms, cations have the same Z but fewer electrons. Removal of electrons from an atom to form a cation results in a significant increase in effective nuclear charge, resulting in all other electrons being more strongly attracted to the nucleus, and having a lower energy level. The result is a contraction in size from the atom to cation. Figure ***Section*2.4.5** visually illustrates the relative size of atoms and some cations of the first four periods; the data is available in tabular format in Figure ***Section*2.4.6**.

Anions

Compared to their atoms, anions have the same Z but more electrons. Addition of electrons to an atom to form an anion results in a decrease in effective nuclear charge, which corresponds to a decrease in attractive force between the nucleus and electrons. Lower attractive force leads to expansion, where the size of the atom becomes larger in the formation of an anion. Figure ***Section*2.4.5** visually illustrates the relative size of atoms and some anions of the first four periods, while the data is available in tabular format in Figure ***Section*2.4.6**.

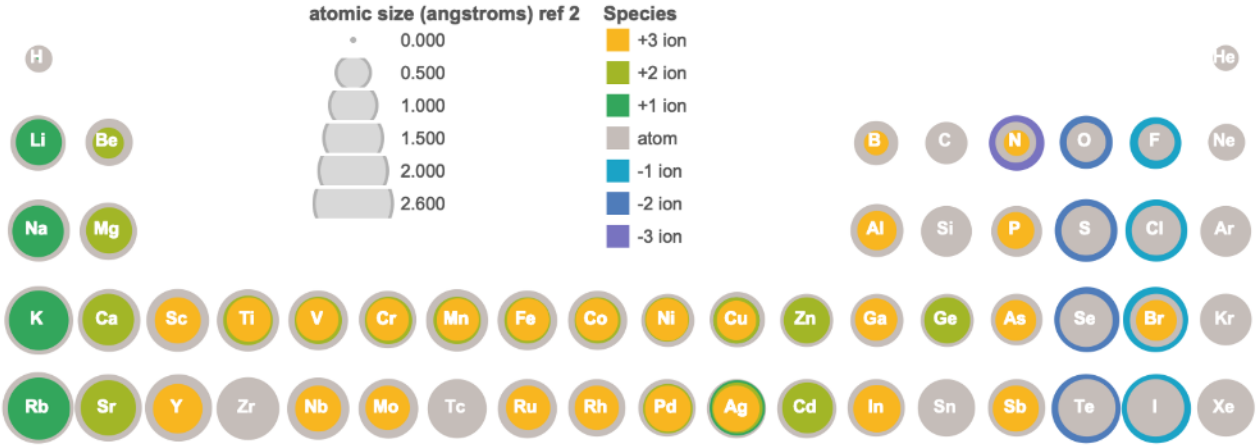


Figure *Section*2.4.5. This figure illustrates relative size of atoms and ions of the first four periods of the periodic table. Atomic radius is indicated by grey circles. Radius of cations is shown in green (+1), lime (+2), and yellow (+3) circles. Radius of anions are shown as aqua (-1), blue (-2), and purple (-3) circles. Data from sources 1-3

H 0.31 (atom) 0 (+1)																	He 0.28 (atom)
Li 1.28 (atom) 0.9 (+1) -	Be 0.96 (atom) 0.41 (+2) -											B 0.84 (atom) 0.25 (+1)	C 0.76 (atom) 0.29 (+4)	N 1.32 (-3) 0.71 (atom) 0.3 (+3) 0.27 (+5)	O 1.21 (-2) 0.66 (atom)	F 1.145 (-1) 0.57 (atom)	Ne 0.58 (atom)
Na 1.66 (atom) 1.16 (+1)	Mg 1.41 (atom) 0.86 (+2)											Al 1.21 (atom) 0.675 (+3)	Si 1.11 (atom) 0.4 (+4)	P 1.07 (atom) 0.58 (+3) 0.31 (+5)	S 1.7 (-2) 1.05 (atom) 0.51 (+4) 0.26 (+6)	Cl 1.67 (-1) 1.02 (atom)	Ar 1.06 (atom)
K 2.03 (atom) 1.52 (+1)	Ca 1.76 (atom) 1.14 (+2)	Sc 1.7 (atom) 0.885 (+3)	Ti 1.6 (atom) 1 (+2) 0.81 (+3) 0.745 (+4)	V 1.53 (atom) 0.93 (+2) 0.78 (+3) 0.72 (+4)	Cr 1.39 (atom) 0.94 (+2 hs) 0.87 (+2 ls) 0.7555 (+3) 0.69 (+4) 0.63 (+5) 0.58 (+6)	Mn 1.61 (atom) 0.97 (+2 hs) 0.81 (+2 ls) 0.785 (+3 hs) 0.72 (+3 ls) 0.67 (+4) 0.47 (+5) 0.395 (+6) 0.39 (+7)	Fe 1.52 (atom) 0.92 (+2 hs) 0.765 (+3 hs) 0.75 (+2 ls) 0.725 (+4) 0.69 (+3 ls) 0.39 (+6)	Co 1.5 (atom) 0.885 (+2 hs) 0.79 (+2 ls) 0.75 (+3 hs) 0.685 (+3 ls) 0.67 (+4 hs)	Ni 1.24 (atom) 0.83 (+2) 0.74 (+3 hs) 0.7 (+3 ls) 0.62 (+4)	Cu 1.32 (atom) 0.91 (+1, cn6) 0.87 (+2, cn6) 0.68 (+3, cn6)	Zn 1.22 (atom) 0.88 (+2)	Ga 1.22 (atom) 0.76 (+3)	Ge 1.2 (atom) 0.87 (+2) 0.67 (+4)	As 1.19 (atom) 0.72 (+3) 0.6 (+5)	Se 1.84 (-2) 1.2 (atom) 0.64 (+4) 0.56 (+6)	Br 1.82 (-1) 1.2 (atom) 0.73 (+3) 0.53 (+7) 0.45 (+5)	Kr 1.16 (atom)
Rb 2.2 (atom) 1.66 (+1)	Sr 1.95 (atom) 1.32 (+2)	Y 1.9 (atom) 1.04 (+3)	Zr 1.75 (atom) 0.86 (+4)	Nb 1.64 (atom) 0.86 (+3) 0.82 (+4) 0.78 (+5)	Mo 1.54 (atom) 0.83 (+3) 0.79 (+4) 0.75 (+5) 0.73 (+6)	Tc 1.47 (atom) 0.785 (+4) 0.74 (+5) 0.7 (+7)	Ru 1.46 (atom) 0.82 (+3) 0.76 (+4) 0.705 (+5) 0.52 (+7) 0.5 (+8)	Rh 1.42 (atom) 0.805 (+3) 0.74 (+4) 0.69 (+5)	Pd 1.39 (atom) 0.73 (+1) 1 (+2) 0.9 (+3) 0.755 (+4)	Ag 1.45 (atom) 1.29 (+1) 1.08 (+2) 0.89 (+3)	Cd 1.44 (atom) 1.09 (+2)	In 1.42 (atom) 0.94 (+3)	Sn 1.39 (atom) 0.83 (+4)	Sb 1.39 (atom) 0.9 (+3) 0.74 (+5)	Te 2.07 (-2) 1.38 (atom) 1.1 (+4) 0.7 (+6)	I 2.06 (-1) 1.39 (atom) 1.09 (+5) 0.67 (+7)	Xe 1.4 (atom) 0.62 (+8)

Figure *Section*2.4.6.

This figure shows radii (in Angstroms) of atoms and ions of the first four periods of the periodic table. Radii from each element are listed from largest to smallest, ionic charge indicated in parentheses (); hs = high spin, ls = low spin, cn6 = coordination number is 6. Data from sources 9-11.

Contributors and Attributions

- Swetha Ramireddy (UCD), Bingyao Zheng (UCD), Emily Nguyen (UCD)
- Curated or created by Kathryn Haas

References

1. Russo, Steve, and Mike Silver. Introductory Chemistry. San Francisco: Pearson, 2007.
2. Petrucci, Ralph H, et al. General Chemistry: Principles and Modern Applications. 9th Ed. New Jersey: Pearson, 2007.
3. Atkins, Peter et. al, *Physical Chemistry*, 7th Edition, 2002, W.H Freeman and Company, New York, pg. 390.
4. Alberty, Robert A. et. al, *Physical Chemistry*, 3rd Edition, 2001, John Wiley & Sons, Inc, pg. 380.
5. Kots, John C. et. al, *Chemistry & Chemical Reactivity*, 5th Edition, 2003, Thomson Learning Inc, pg. 305-309.
6. *IUPAC. Compendium of Chemical Terminology, 2nd ed. (the "Gold Book"). Compiled by A. D. McNaught and A. Wilkinson. Blackwell Scientific Publications, Oxford (1997). Online version (2019-) created by S. J. Chalk. ISBN 0-9678550-9-8. doi.org/10.1351/goldbook.*
7. *Electron Affinity (data page), Wikipedia. en.Wikipedia.org/wiki/Electron_affinity_(data_page) Accessed 12/3/19.*

8. Cordero, Beatriz, Veronica Gomez, Ana E. Platero-Prats, Marc Reves, Jorge Echeverria, Eduard Cremades, Flavia Barragan, and Santiago Alvarez. *"Covalent Radii Revisited." Dalton Transactions, no. 21 (2008): 2832–38. doi:10.1039/b801115j.*
9. R. D. Shannon (1976). "Revised effective ionic radii and systematic studies of interatomic distances in halides and chalcogenides". *Acta Crystallogr A.* **32** (5): 751–767. Bibcode:1976AcCrA..32..751S. doi:10.1107/S0567739476001551.
10. *Atomic Radius, Wikipedia.* https://en.Wikipedia.org/wiki/Atomic_radius
11. *Ionic Radius, Wikipedia.* https://en.Wikipedia.org/wiki/Ionic_radius

---

Section 2.4: Periodic Properties of Atoms is shared under a CC BY-NC-SA 4.0 license and was authored, remixed, and/or curated by LibreTexts.

- **2.3: Periodic Properties of Atoms** by Kathryn Haas is licensed CC BY-NC-SA 4.0.
- **2.4: Periodic Properties of Atoms** is licensed CC BY-NC-SA 4.0.
- **2.3.1: Ionization energy** by Bingyao Zheng, Emily Nguyen, Kathryn Haas, Swetha Ramireddy is licensed CC BY-NC-SA 3.0.
- **2.3.2: Electron Affinity** by Kathryn Haas is licensed CC BY-NC-SA 4.0.
- **2.3.3: Covalent and Ionic Radii** by Bingyao Zheng, Emily Nguyen, Kathryn Haas, Swetha Ramireddy is licensed CC BY-NC-SA 4.0.

CHAPTER OVERVIEW

Chapter 3: Molecular Symmetry and Point Groups

Symmetry in Chemistry

Symmetry is actually a concept of mathematics and not of chemistry. However, symmetry, and the underlying mathematical theory for symmetry, group theory, are of tremendous importance in chemistry because they can be applied to many chemistry problems. For example it helps us to classify the structures of molecules and crystals, understand chemical bonding, predict vibrational spectra, and determine the optical activity of compounds. We will therefore first discuss the general foundations of symmetry and group theory, and then how they can be applied to chemical problems.

Let us first find a definition for symmetry. The human brain innately recognizes symmetry and patterns and we associate symmetry with beauty, but very familiar things are not necessarily easy to define scientifically. One common definition is that symmetry is the self-similarity of an object. The more similar parts it has the more symmetric it appears. For example, we would argue that the two wings of the butterfly depicted look similar. If the left wing was very different from the right wing the butterfly would look less symmetric.



Figure *Chapter*3.1: Symmetry depicted through an image of a butterfly (Photo by Alfred Schrock on Unsplash)

In other classes you have learned different ways to describe symmetry, radial and bilateral symmetry in biology; R and S enantiomers or cis and trans isomers in organic chemistry. Group theory gives us a universal language and tools to define and describe the symmetry of any object or molecule.

This TED talk explains symmetry from a mathematical and artistic perspective.

Learning Objectives

- Identify symmetry elements and operations in molecules and objects
- Use flowchart to assign a molecule to a point group
- Recognize the components of a character table
- Determine whether a vibrational mode is infrared allowed

Section 3.1: Symmetry Operations and Elements
Section 3.2: Point Groups

Section 3.3: Properties and Representations of Groups
Section 3.3.1: Representations of Symmetry Operations
Section 3.3.2: Matrices
Section 3.3.3: Mathematical Notation of Representations
Section 3.3.4: Character Tables
Section 3.4: Examples and Applications of Symmetry
Section 3.4.1: Chirality
Section 3.4.2: Molecular Vibrations

Chapter 3: Molecular Symmetry and Point Groups is shared under a CC BY-NC-SA license and was authored, remixed, and/or curated by LibreTexts.

Section 3.1: Symmetry Operations and Elements

Introduction

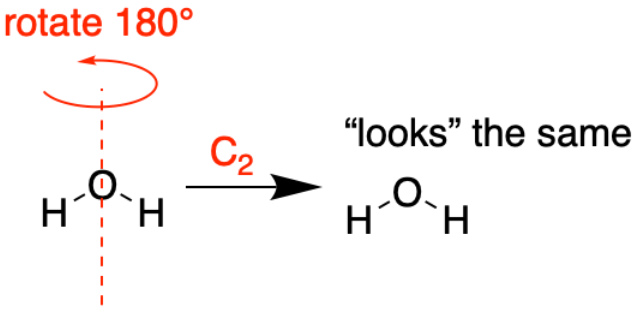


Figure ***Section*3.1.1**: An example of a symmetry operation is a 180° rotation where the resulting position is indistinguishable from the original. A 180° rotation is called a C_2 operation; the axis of rotation is the symmetry element. (CC-BY-NC-SA; Kathryn Haas)

The symmetry of a molecule consists of symmetry operations and symmetry elements. A symmetry operation is an operation that is performed to a molecule which leaves it indistinguishable and superimposable on the original position. Symmetry operations are performed with respect to symmetry elements (points, lines, or planes).

Definition: Symmetry Operation

Manipulation of an object around a symmetry element. The object must be indistinguishable before and after the operation.

Definition: Symmetry Element

A geometric entity (point, axis, or plane) around which a symmetry operation is performed

An example of a symmetry operation is a 180° rotation of a water molecule in which the resulting position of the molecule is indistinguishable from the original position (see Figure ***Section*3.1.1**). In this example, the symmetry operation is the rotation and the symmetry element is the axis of rotation.

There are five types of symmetry operations including **identity**, **reflection**, **inversion**, **proper rotation**, and **improper rotation**. The improper rotation is the sum of a rotation followed by a reflection. The symmetry elements that correspond to the five types of symmetry operations are listed in Table ***Section*3.1.1**.

Table ***Section*3.1.1**: Table of elements and operations

Element	Operation	Symbol
Identity	identity	E
Proper axis	rotation by (360/n)°	C_n
Symmetry plane	reflection in the plane	σ
Inversion center	inversion of a point at (x,y,z) to (-x,-y,-z)	*i*
Improper axis	rotation by (360/n)°, followed by reflection in the plane perpendicular to the rotation axis	S_n

Symmetry Operations and Elements

Identity (E)

All molecules have the identity element. The identity operation is a 360° rotation, essentially doing nothing to the molecule. It is included to fulfill the mathematical requirements of a group.

Proper Rotation and Proper Axis (C_n)

A "proper" rotation is just a simple rotation operation about an axis. The symbol for any proper rotation or proper axis is $C_{(360/n)}$, where n is the degree of rotation. Thus, a 180° rotation is a C_2 rotation around a C_2 axis, and a 120° rotation is a C_3 rotation about a C_3 axis. Figure \(\PageIndex{2}\) shows both the C_3 principal rotation axis and one of the C_2 rotation axes in BF_3.

Definition: Principal Rotation Axis

The principal axis of a molecule is the highest order proper rotation axis. For example, if a molecule had C_2 and C_4 axes, the C_4 is the principal axis.

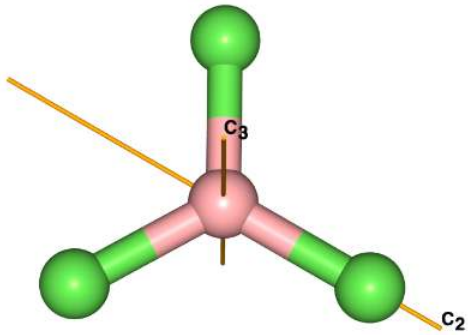


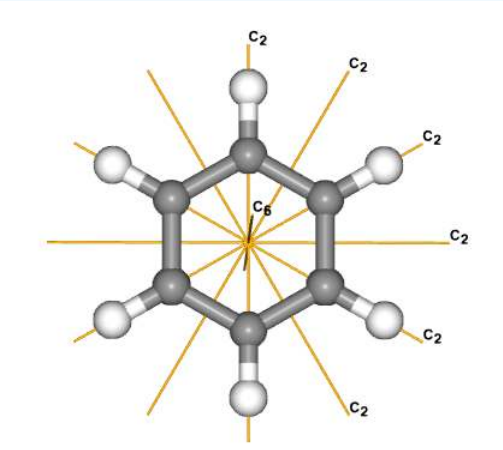
Figure *Section*3.1.2:The C_3 and one of the C_2 rotation axes in BF_3. C_3 is the principal rotation axis. (Image source: https://symotter.org/gallery)

Exercise *Section*3.1.1

What is the principal rotation axis in benzene (C_6H_6)?

Answer

Benzene is a planar molecule. It has one C_6 axis and 6 C_2 axes. The principal rotation axis is the C_6 as it has the highest order.



Reflection and Mirror Planes (σ)

A reflection operation occurs with respect to a mirror plane. Mirror planes can be classified based on their relationship to the principal rotation axis:

1. σ_h (horizontal): horizontal reflection planes are perpendicular to principal rotation axis
2. σ_v (vertical): vertical reflection planes contain the principal rotation axis
    - σ_d (dihedral): dihedral reflection planes are vertical reflection planes that bisect two C_2 rotation axes

Figure ***Section*3.1.3** shows the three types of mirror planes in the square planar $PtCl_4$. The horizontal reflection plane, shown in red, is in the plane of the molecule, and bisects the C_4 principal rotation axis. The vertical reflection planes, shown in orange, are along the Pt-Cl bonds and contain the C_4 principal rotation axis. The dihedral reflection planes, shown in yellow, bisect the Pt-Cl bonds (and the C_2 rotation axes along those bonds) and also contain the C_4 principal rotation axis.

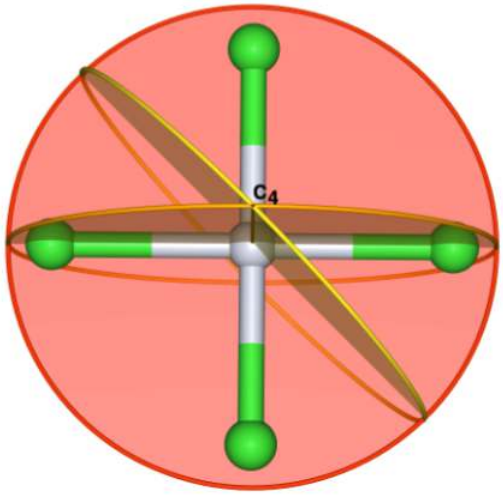


Figure ***Section*3.1.3**: The horizontal reflection plane (red), one of the vertical reflection planes (orange) and one of the dihedral reflection planes (yellow) in $PtCl_4$. (Image source: https://symotter.org/gallery)

Inversion and Inversion Center (i)

The inversion operation takes any point through the inversion center to an equidistant point on the opposite side of the inversion center. In other words, a point at the center of the molecule that can transform (x,y,z) into (-x,-y,-z) coordinates. The inversion center may be on the central atom or it may be at a point in space in the center of a molecule (Figure ***Section*3.1.4**).

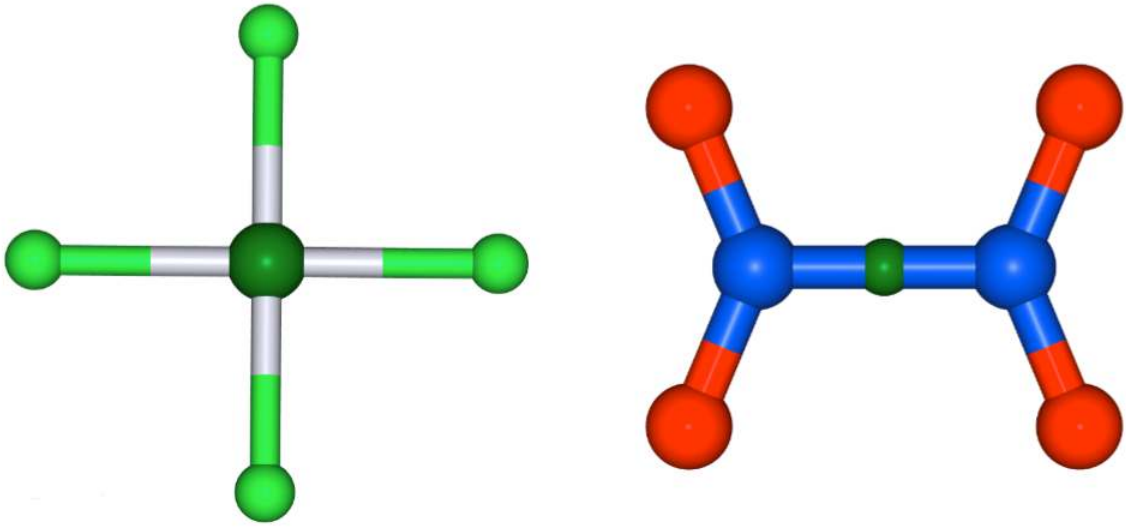


Figure ***Section*3.1.4**: The inversion center (dark green) in $PtCl_4$ and in N_2O_4. (Image source: https://symotter.org/gallery)

Improper Rotation and Improper Rotation Axis (S_n)

Improper rotation is by far the most difficult symmetry operation to visualize. It is a combination of a rotation with respect to an axis of rotation (C_n), followed by a reflection through a plane perpendicular to that C_n axis. The rotation and reflection may or may not be valid symmetry operations on their own. In short, an S_n operation is equivalent to C_n followed by σ_h. In methane (Figure *Section*3.1.5), the S_4 improper rotation axis will rotate 90° and rotate the in plane H's out of plane and vice versa. The perpendicular reflection then exchanges the in and out of plane H's, returning them to the original confirmation. In this example, neither the C_4 rotation or the perpendicular reflection are symmetry operations on their own.

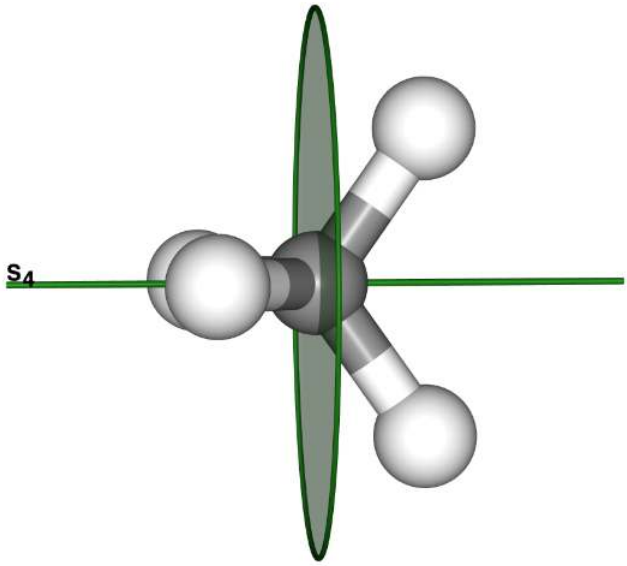


Figure *Section*3.1.5: The improper rotation axis and reflection plane in methane. (Image source: https://symotter.org/gallery)

Successive Operations

Sometimes, new symmetry operations form by carrying out two or more simpler operations successively to result in an indistinguishable configuration. For example, the improper rotation axis above results from rotation about an axis of rotation (C_n) followed by reflection about a plane perpendicular to that axis (σ_h).

$$S_n = C_n \times \sigma_h \qquad \text{(Section 3.1.1)}$$

Note also that C_n in this case need not be a symmetry element for the molecule. For example, staggered ethane has an S_6 symmetry element although it does not have a C_6. Another example of a symmetry element that results from a combination of two different elements is the inversion center (i), which results from a C_2 rotation followed by a reflection about a plane perpendicular to that axis (σ_h).

$$i = C_2 \times \sigma_h \qquad \text{(Section 3.1.2)}$$

Note that an inversion center is a special case of an improper rotation axis because it results when, in the first equation, $n = 2$. That is,

$$i = S_2 \qquad \text{(Section 3.1.3)}$$

In fact, any symmetry operation can be carried out multiple time in a row. For example, when BH_3 is rotated twice by 120°, the two-step operation can be symboled by C_3^2. When the C_3 operation is performed a third time, the molecule returns to its original configuration; i.e,

$$C_3^3 = E \qquad \text{(Section 3.1.4)}$$

In general,

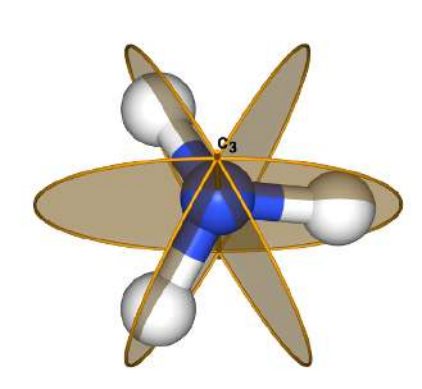
$$C_n^n = E \qquad \text{(Section 3.1.5)}$$

Exercise *Section*3.1.1

List all of the symmetry elements in ammonia (NH_3).

Answer

Ammonia has a trigonal pyramidal geometry. It has one C_3 rotation axis (the principal rotation axis) which will exchange the three H atoms. It also has three vertical reflection planes, one along each N-H bond.



Sources:

1. Introduction to Molecular Symmetry by J. S Ogden
2. Inorganic Chemistry by Catherine Housecroft And Alan G. Sharpe.
3. Symmetry@Otterbien: https://symotter.org/

Section 3.1: Symmetry Operations and Elements is shared under a CC BY-NC-SA 4.0 license and was authored, remixed, and/or curated by LibreTexts.

- **3.2: Symmetry Operations and Elements** is licensed CC BY-NC-SA 4.0.
- **4.1: Symmetry Operations and Elements** is licensed CC BY-NC-SA 4.0.
- **3.3: Successive Operations** is licensed CC BY-NC-SA 4.0.

Section 3.2: Point Groups

Introduction

In group theory, molecules or other objects can be organized into point groups based on the type and number of symmetry operations they possess. Every molecule in a point group will have all of the same symmetry operations as any other molecule in that same point group. The most common, and chemically relevant point groups are described below.

The Low Symmetry Point Groups

C_1 Point Group

Overall, we divide point groups into three major categories: High symmetry point groups, low symmetry point groups, dihedral point groups, and rotational point groups. Let us begin with the low symmetry point groups. As the name says, these point groups only have few symmetry elements and operations. The point group C_1 is the point group with the lowest symmetry. Molecules that belong to this point group only have the identity as symmetry element.

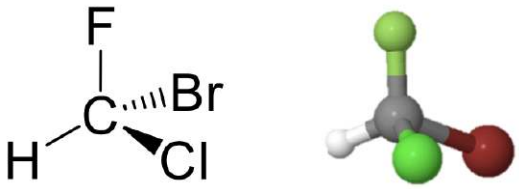


Figure ***Section*3.2.1** C_1 point group of bromochlorofluromethane (Attribution: symotter.org/gallery)

An example is the bromochlorofluromethane molecule (Figure ***Section*3.2.1**). It has no symmetry element except the identity (E). The name C_1 comes from the symmetry element C_1. A C_1 operation is the same as the identity.

C_s Point Group

The point group C_s has a mirror plane in a addition to the identity. An example is the 1,2-bromochloroethene molecule (Figure ***Section*3.2.2**).

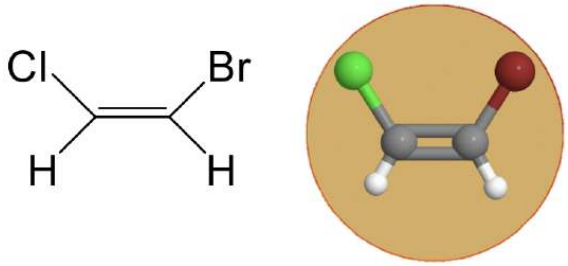


Figure ***Section*3.2.2** C_s point group of 1, 2-bromochloroethene (Attribution: symotter.org/gallery)

This is a planar molecule and the mirror plane is within the plane of the molecule. This mirror plane does not move any atoms when the reflection operation is carried out, nonetheless it exists because any point of the molecule above the mirror plane will be found below the mirror plane after the execution of the operation. Vice versa, any point below the mirror plane will be above the mirror plane. This mirror plane does not have a vertical or horizontal mirror plane designation because no proper rotational axes exist.

C_i Point Group

The point group C_i has the inversion as the only symmetry element besides the identity. The point group C_i is sometimes also called S_2 because an S_2 improper rotation-reflection is the same as an inversion. An example is the 1,2-dibromo 1,2-dichloro ethane (Figure ***Section*3.2.3**).

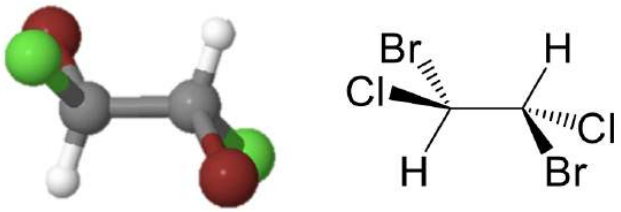


Figure ***Section*3.2.3** The C_i point group: 1,2-dibromo-1,2-dichloroethane (Attribution: symotter.org/gallery)

This molecule looks quite symmetric, but it has inversion center in the middle of the carbon-carbon bond as the only symmetry element. Upon execution of the inversion operation, the two carbons swap up their positions, and so do the two bromine, the two chorine, and the two hydrogen atoms.

The High Symmetry Point Groups

The symmetry elements of the high symmetry point groups can be more easily understood when the properties of platonic solids are understood first. Platonic solids are polyhedra made of regular polygons. In a platonic solid all faces, edges, and vertices (corners) are symmetry-equivalent. We will see that this is a property that can be used to understand the symmetry elements in high symmetry point groups. There are only five possibilities to make platonic solids from regular polygons (Figure ***Section*3.2.4**).

File:Platonic Solids Transparent.svgFigure ***Section*3.2.4** The platonic solids (Attribution: Drummyfish [CC0] https://commons.wikimedia.org/wiki/F...ransparent.svg)

The first possibility is to construct a tetrahedron from four regular triangles. The second platonic solid is the octahedron made of eight regular triangles. The third possibility is the icosahedron made of twenty triangles. In addition, six squares can be connected to form a cube, and twelve pentagons can be connected to form a dodecahedron. There are no possibilities to connect other regular polygons like hexagons to make a platonic solid.

The T_d Point Group

The tetrahedron, as well as tetrahedral molecules and anions such as CH_4 and BF_4- belong to the high symmetry point group T_d (Note that only tetrahedral molecules where all four outer atoms/groups are the same will be in the T_d point group). Let us find the symmetry elements and symmetry operations that belong to the point group T_d. First, we should not forget the identity operation, E. Next, it is useful to look for the principal axes.

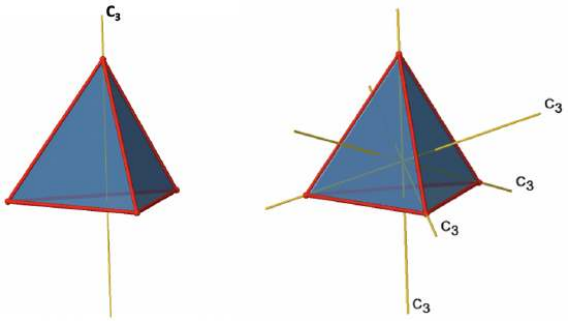


Figure ***Section*3.2.5** The C_3 axes in a tetrahedron (Attribution: symotter.org/gallery)

The tetrahedron has four principal C_3 axes (Figure ***Section*3.2.5**). It is a property of the high-symmetry point groups that they have more than one principal axis. The C_3 axes go through the vertices of the tetrahedron. Because each C_3 axis goes through one vertex, there are four vertices, and we know that in a platonic solid all vertices are symmetry-equivalent, we can understand that there are four C_3 axes. How many unique C_3 operations are associated with these axes? After three rotations around 120° we reach the identity. Therefore C_3^3=E, and we only need to consider the C_3^1 and the C_3^2 rotation about 120 and 240° respectively. Because

there are four C_3 axes, there are four C_3^1 and four C_3^2 operations and eight C_3 operations overall. In addition to the C_3 axes there are C_2 axes (Figure ***Section*3.2.6**).

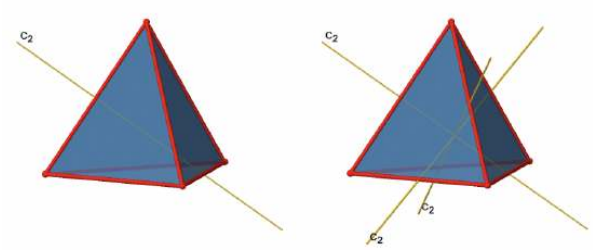


Figure ***Section*3.2.6** The C_2 axes in a tetrahedron belonging to the point group T_d (Attribution: symotter.org/gallery)

You can see that a C_2 axis goes through two opposite edges in the tetrahedron. Because a tetrahedron has six edges, and each C_2 axis go through two edges there are 6/2=3 C_2 axes. There is only one C_2 symmetry operation per C_2 axis because we produce the identity already after two rotations. Therefore there are three C_2^1 operations overall.

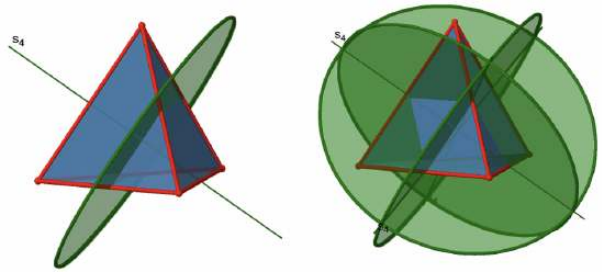


Figure ***Section*3.2.7** The S_4 axes in a tetrahedron (Attribution: symotter.org/gallery)

In addition, the T_d point group has S_4 improper rotation reflections. Like the C_2 axes, they pass through the middle of two opposite edges. This also means that they are superimposing the C_2 axes. Because there are six edges, and two S_4 axes per edge there are 6/2=3 S_4 axes (Figure ***Section*3.2.7**). How many operations are associated with these S_4 axes? The order of the axes are even, and therefore we need four S_4 operations to produce the identity. The S_4^2 operation is the same as a C_2^1 operation because reflecting two times is equivalent to not reflecting at all, and rotating two times by 90° is the same as rotating about 180°. Therefore overall, only S_4^1 and S_4^3 operations are unique operations. S_4^2 and S_4^4 can be expressed by the simpler operations C_2^1 and E respectively. Because there are 3 S_4 axes, there are three S_4^1 and three S_4^3 operations. Overall there are six S_4 operations.

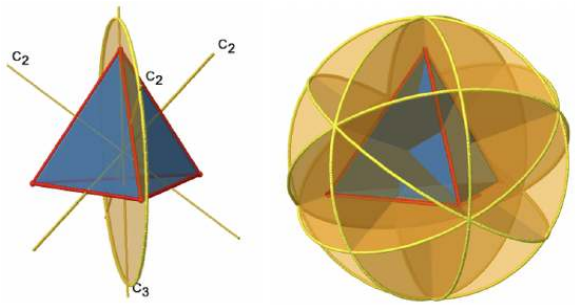


Figure ***Section*3.2.8** The mirror planes and C_2 axes in a tetrahedron belonging to the point group T_d (Attribution: symotter.org/gallery)

There are also mirror planes (Figure ***Section*3.2.8**). The planes contain a single edge of the tetrahedron, thereby bisecting the tetrahedron. There a six edges in a tetrahedron, and therefore there are 6/1=6 mirror planes.These planes are dihedral planes because each plane contains a C_3 principal axis and is bisects the angle between two C_2 axes. Overall, there are three C_2 axes and three C_2 operations. There is one reflection operation per mirror plane because reflecting two times produces the identity. Therefore, there are six σ_d reflection operations.

Symmetry Operations in the T_d Point Group

Every molecule or object in the T_d point group has the following symmetry operations:

- E, 8 C_3, 3 C_2, 6 S_4, and 6 σ_d

The Octahedral Point Group O_h

Another high symmetry point group is the point group O_h. Both the octahedron as well as the cube belong to this point group despite their very different shape Figure ***Section*3.2.9**. Because they belong to the same point group they must have the same symmetry elements and operations. There are many octahedrally shaped molecules, such as the SF_6.

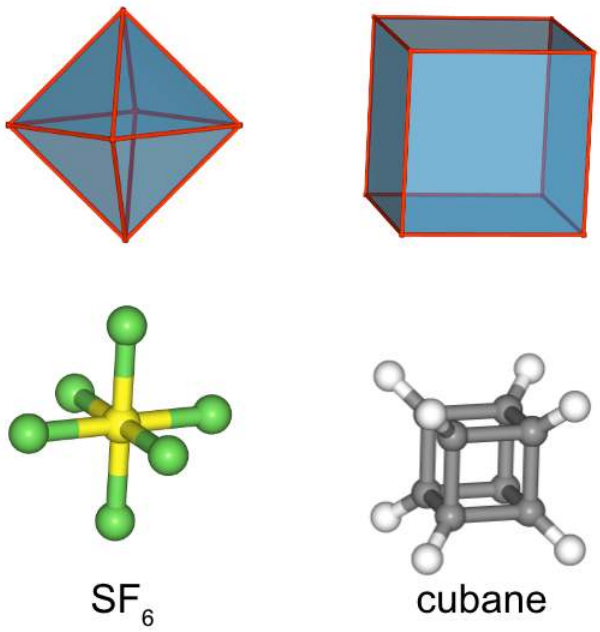


Figure ***Section*3.2.9**: SF_6 and cubane with cubic and octahedral shape, respectively, belong to the point group O_h (Attribution: symotter.org/gallery)

Molecules with cubic shapes are far less common, because a cubic shape often leads to significant strain in the molecule. An example is cubane C_8H_8. Let us determine the symmetry elements and operations for the point group O_h using the example of the octahedron. If we used the cube, we would get exactly the same results.

There are three C_4 principal axes in the octahedron. They go through two opposite vertices of the octahedron (Figure ***Section*3.2.10**). There are three C_4 axes because an octahedron has six vertices which are all symmetry-equivalent because the octahedron is a platonic solid.

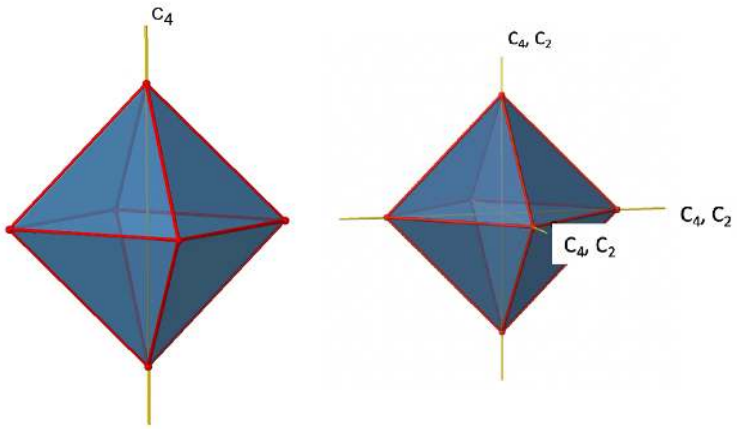


Figure ***Section*3.2.10**: The C_4 and C_2 axes in the octahedral point group O_h (Attribution: symotter.org/gallery)

We can see that there are also C_2 axes where the C_4 axes run. This is because rotating two times around 90° is the same as rotating around 180°. What are the symmetry operations associated with these symmetry elements? Rotating four times around 90° using the C_4 axes produces the identity. So we have to consider the operations C_4^1, C_4^2, C_4^3 and C_4^4. How many of these are unique? C_4^4 is the same as the identity, so it is not unique, In addition a C_4^2 is identical to a C_2^1, and thus C_4^2 is also not unique, and can be expressed by the simpler operation C_2^1. That leaves the C_4^1 and the C_4^3 as the only unique symmetry operations. Because we have three C_4 axes, there are 2x3=6 C_4 operations, in detail there are $3C_4^1$ and three C_4^3 operations. In addition, there are the three C_2^1 operations belonging the the three C_2 axes.

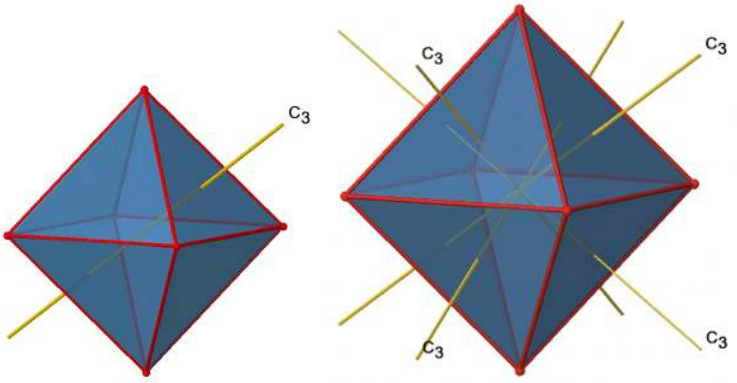


Figure ***Section*3.2.11**: The C_3 axes in the octahedral point group O_h (Attribution: symotter.org/gallery)

In addition, there are four C_3 axes (Figure ***Section*3.2.11**:). They are going through the center of two opposite triangular faces of the octahedron.You see above a single C_3 axis, and on the right hand side all four of these axes. How can we understand that there are four axes? An octahedron has overall eight triangular faces, and each C_3 axis goes through two opposite faces, so there are 8/2=4 C_3 axes. Each C_3 axis has the C_3^1 and the C_3^2 as unique symmetry operations. The C_3^3 is the same as the identity. So overall we have 4x2=8 operations, four of them are C_3^1, and four of them are C_3^2.

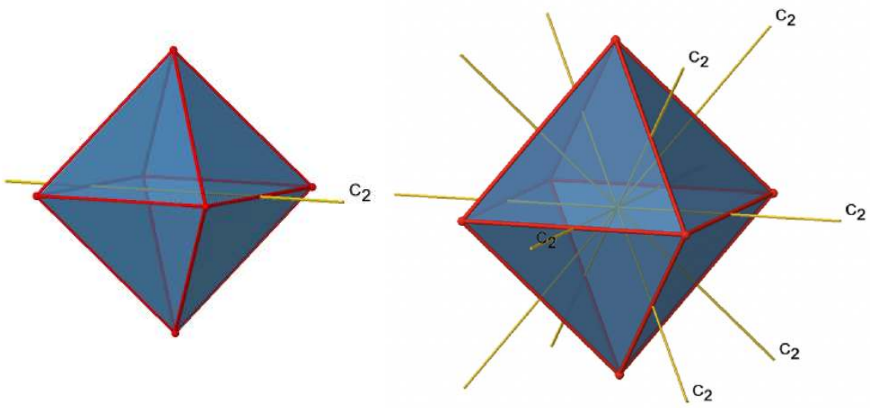


Figure ***Section*3.2.12**: The C_2' axes in the octahedral point group O_h (Attribution: symotter.org/gallery)

In addition to the C_2 axes that superimpose the C_4 axes, there are C_2' axes which go though two opposite edges of the octahedron (Figure ***Section*3.2.12**:). How many of them are there? An octahedron has twelve edges, and because each C_2' passes through two edges, there must be 12/2=6 C_2' axes. These axes have primes because they are not conjugate to the C_2 axes that superimpose the C_4 axes. For each C_2' axis there is only the C_2' ^{1} as the unique symmetry operation, and therefore there are overall 6 C_2'^{1} symmetry operations.

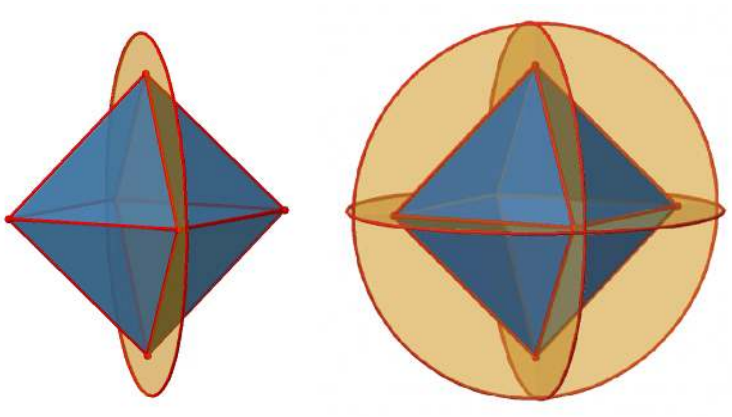


Figure ***Section*3.2.13**: The horizontal mirror planes in the octahedral point group O_h (Attribution: symotter.org/gallery)

Let us look at the horzontal mirror planes next (Figure ***Section*3.2.13**). There are horizontal mirror planes that stand perpendicular to the C_4 principal axes. Note that this mirror plane also contains two axes, in addition to the one to which it stands perpendicular. Because it contains two principal C_4 axes, it has also properties of a vertical mirror plane. Nonetheless, we call it a horizontal mirror plane because it stands perpendicular to the third C_4. The horizontal properties trump the vertical ones, so to say. You can see that a single mirror plane contains four edges of the octahedron. Because there are twelve edges, there are 12/4=3 horizontal mirror planes. There is one mirror plane per principal C_4 axis. There are three horizontal reflection operations because there is always only one reflection operation per mirror plane

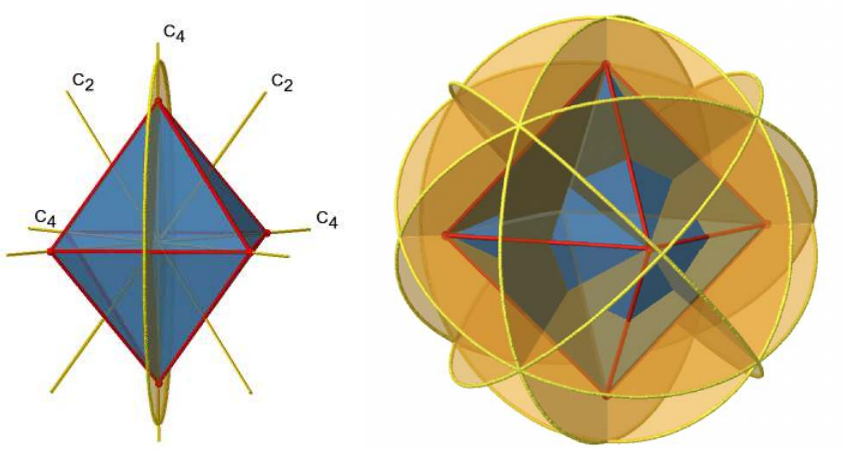


Figure *Section*3.2.14: The vertical mirror planes in the octahedral point group O_h (Attribution: symotter.org/gallery)

Next let us look for vertical mirror planes (Figure *Section*3.2.14). You can see that - contrast to the horizontal mirror planes - it does not contain any edges. Rather, it cuts through two opposite edges. You can see that this plane contains a C_4 axis, but it does not stand perpendicular to the other two C_4 axes. Therefore it has only the properties of a vertical mirror plane. You can see however, that the mirror plane bisects the angle between two C_2' axes which also depicted. This makes the vertical mirror planes dihedral mirror planes, σ_d. How may of them do we have? As previously mentioned, each mirror plane cuts through two opposite edges. There are twelve edges in an octahedron, and thus there are 12/2=6 dihedral mirror planes. You can see all of them on the right side of Figure *Section*3.2.14. Each mirror plane is associated with one reflection operation, therefore there are six dihedral reflection operations.

Next we can ask if the point group O_h has an inversion center? Yes, there is one in the center of the octahedron (Figure *Section*3.2.15)!

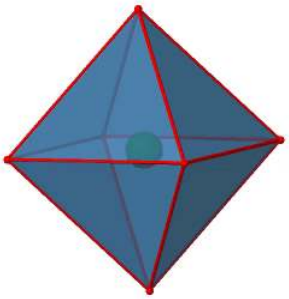


Figure *Section*3.2.15: The inversion center of the octahedral point group O_h (Attribution: symotter.org/gallery)

Each point in the octahedron can be moved through the inversion center to the other side, and the produced octahedron will superimpose the original one. There is always one inversion operation associated with an inversion center.

Next, let us look for improper rotations. You can see an S_6 improper rotation operation below (Figure *Section*3.2.16, left).

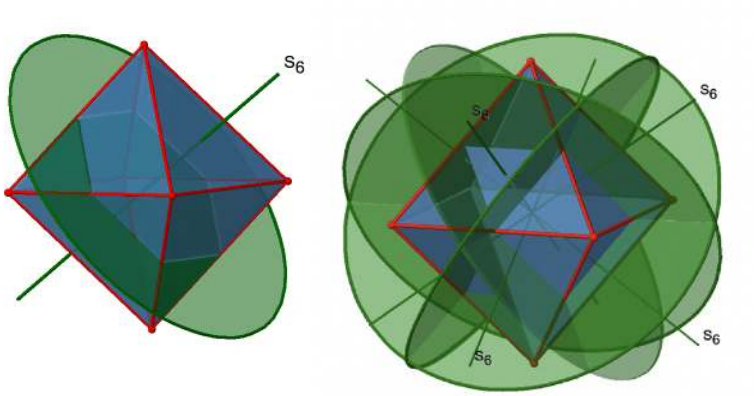


Figure ***Section*3.2.16**: The S_6 improper rotation element of the octahedral point group O_h (Attribution: symotter.org/gallery)

The improper S_6 axis passes though the centers of two opposite triangular faces. One can see that rotation about 60° alone does not make the octahedron superimpose. The reflection at a plane perpendicular to the improper axis is required to achieve superposition. Overall, the rotation-reflection swaps up the position of the two opposite triangular faces. How many S_6 improper axes are there? Since each S_6 passes through two faces, and an octahedron has 8 faces there must be 8/2=4 S_4 axes. You can see all of them above (Fig. 2.2.31, right). Note that they are in the same position as the $4C_3$ axes we previously discussed. How many unique operations are associated with them? For an S_6 axis we need to consider operations from S_6^1 to S_6^6. S_6^6 is the same as the identity so it is not unique. The S_6^2 is the same as a C_3^1 because rotating two times round 60° is the same as rotating around 120°, and reflecting twice is the same as not reflecting at all. Similarly, an S_6^4 is the same as an C_3^2. Rotating four time by 60° is the same as rotating two times by 120° and reflecting four times is the same as not reflecting at all. Further, an S_6^3 is the same as an inversion. After three 60° rotations we have rotated by 180°. If we reflect after that, then this is the same as an S_2^1 operation which is the same as an inversion. Therefore, only the S_6^1 and the S_6^5 operations are unique, all other operations can be expressed by simpler operations.

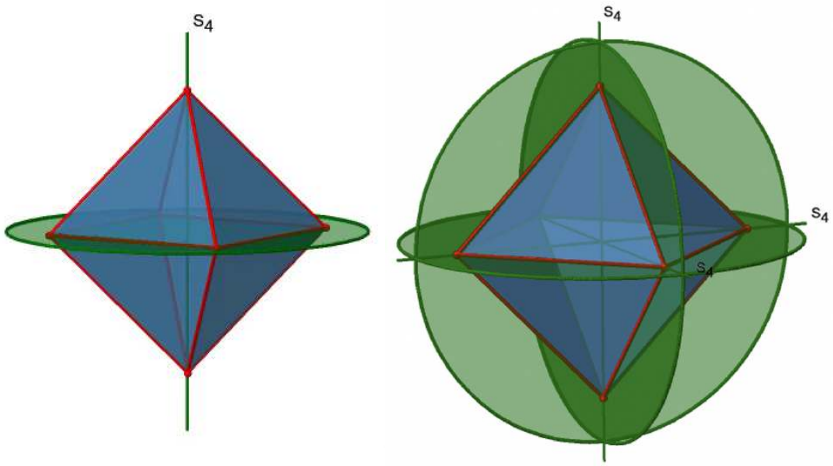


Figure ***Section*3.2.17**: The S_4 improper axis of the octahedral point group O_h (Attribution: symotter.org/gallery)

The octahedron also has S_4 improper axes, and you can see one of them in Figure ***Section*3.2.17**, right). It goes through two opposite corners of the octahedron. The S_4 improper axis seemingly does the same as the C_4 axis that goes through the same two opposite vertices, but actually does not. While rotating around 90° already makes the octahedron superimpose with its original form, executing the reflection operation after the rotation swaps up the position of the two vertices, and generally all points of the octahedron above and below the plane, respectively. Overall the S_4 moves the points within the object differently compared to the C_4 which makes it an additional, unique symmetry element. There are overall three S_4 improper axes because the octahedron has six vertices and one S_4 passes through two vertices.

Symmetry Operations in the O_h Point Group

Every molecule or object in the O_h point group has the following 48 symmetry operations:

- E, 8 C_3, 6 C_2, 6 C_4, 3 C_2 (C_4^2), i, 6 S_4, 8 S_6, 3 σ_h, and 6 σ_d

The I_h Point Group

The two remaining platonic solids, the icosahedron and the dodecahedron, belong both to the icosahedral point group I_h. This is despite they are made of different polygons. Because they belong to the same point group, they have exactly the same symmetry operations. An example for a molecule with icosahedral shape is the molecular anion $B_{12}H_{12}^{2-}$. Examples of molecules with dodecahedral shape include dodecahedrane ($C_{20}H_{20}$) and buckminsterfullerene (C_{60}). Let us determine the symmetry elements and symmetry operations for the example of the icosahedron. We could also use the dodecahedron, and the results would be the same. The principal axes of the icosahedron are the C_5 axes. You can see one of them, going through the center of the pentagon comprised of five triangular faces below (Figure ***Section*3.2.18**).

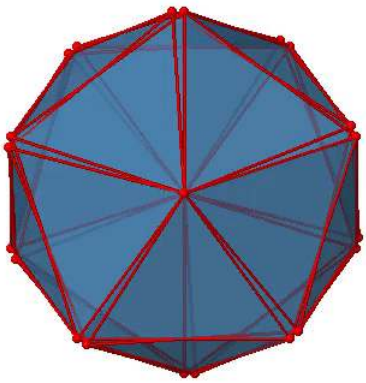


Figure ***Section*3.2.18**: One of the C_5 axes of the icosahedron stands perpendicular to the paper plane going through the center of a pentagon of the icosahedron (Attribution: symotter.org/gallery)

You can understand that there is a C_5 when considering that there are five triangular faces making a pentagon. The C_5 axis sits in the center of the pentagon. We can see that when we rotate around this C_5 axis, then the produced icosahedron superimposes the original one. The C_5 axis goes through two opposite vertices of the icosahedron. Because an icosahedron has 12 vertices, there must be six C_5 axes overall. You can see all of them below (Figure ***Section*3.2.19**). There are four unique symmetry operations associated with a single C_5 axis, namely the C_5^1, the C_5^2, the C_5^3, and the C_5^4. The C_5^5 is the same as the identity. Because there are six C_5 axes, there are overall 6x4=24 C_5 symmetry operations.

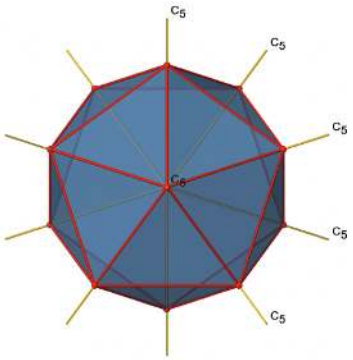


Figure ***Section*3.2.19**: The C_5 axes of the icosahedron (Attribution: symotter.org/gallery)



Figure ***Section*3.2.20**: One of the C_3 axes of the icosahedral point group (Attribution: symotter.org/gallery)

In addition, there are C_3 axes. One of them is shown below, and you can see that it passes through the centers of two opposite triangular faces (Figure ***Section*3.2.20**). As one rotates by 120° the atoms on the triangular faces change their position, and the resulting icosahedron superimposes the original one. As the name icosahedron says, there are twenty faces overall.

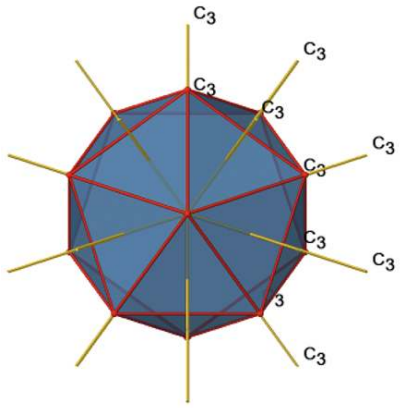


Figure ***Section*3.2.21**: The C_3 axes of the icosahedral point group (Attribution: symotter.org/gallery)

Because one C_3 passes through two opposite axes, there are 20/2=10 C_3 axes overall (Figure ***Section*3.2.21**:). Each C_3 axis is associated with two symmetry operations, namely C_3^1, and C_3^2. Thus, there are overall 10x2=20 C_3 symmetry operations.

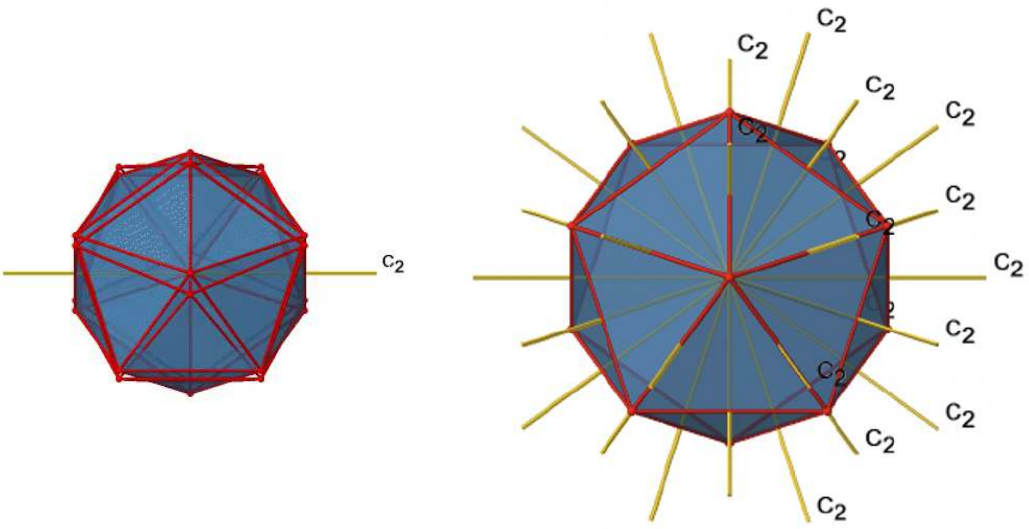


Figure *Section*3.2.22: The C_2 axes of the icosahedral point group (Attribution: symotter.org/gallery)

There are also C_2 axes (Figure *Section*3.2.21). They pass through the centers of two opposite edges of the icosahedron. Rotating around the C_2 axis shown makes the icosahedron superimpose. An icosoahedron has overall 30 edges. Because one C_2 axis passes through the centers of two opposite edges, we can understand that there are 30/2=15 C_2 axes. There is one unique C_2 operation per axis, and therefore there are 15 C_2 operations.

We have now found all proper rotations. Let us look for mirror planes, next. You can see a mirror plane below (Figure *Section*3.2.22).

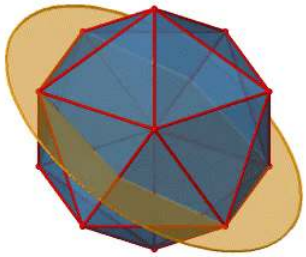


Figure *Section*3.2.22: A mirror plane in the icosahedral point group (Attribution: symotter.org/gallery)

It contains two opposite edges. It also bisects two other edges. An icosahedron has overall 30 edges, therefore there are 30/2=15 mirror planes. You can see all of them below (Figure *Section*3.2.23)).

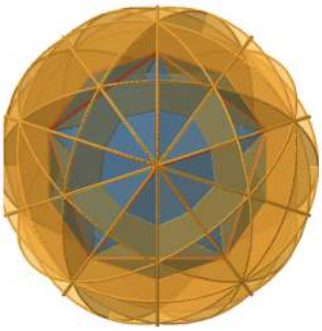


Figure *Section*3.2.23: All the mirror planes in the icosahedral point group (Attribution: symotter.org/gallery)

The icosahedron also has an inversion center in the center of the icosahedron (Figure *Section*3.2.24). As we carry out the associated symmetry operation, all points in the icosahedron move through the inversion center to the other side.



Figure *Section*3.2.24: The inversion center in the icosahedron (Attribution: symotter.org/gallery)

Let us now look for improper rotations. The improper rotational axes with the highest order are S_{10} axes. They are located in the same position as the C_5 axes, and go through two opposite corners (Figure *Section*3.2.25).

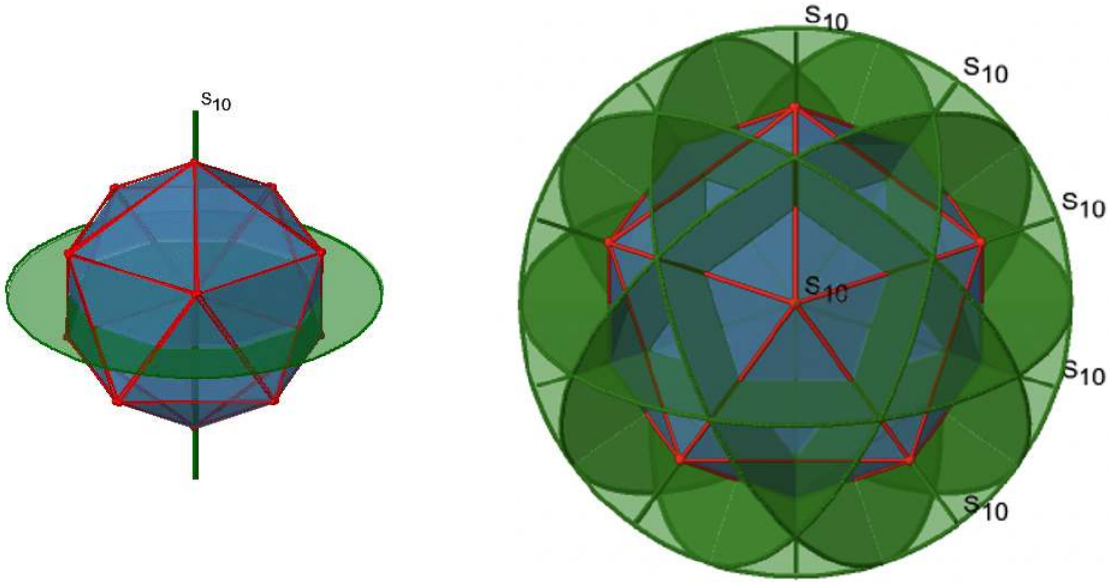


Figure *Section*3.2.25: The S_{10} improper rotational axes in the icosahedral point group (Attribution: symotter.org/gallery)

The S_{10} exists because in an icosahedron there are pairs of co-planar pentagons that are oriented staggered relative to each other. The rotation around 36° brings one pentagon in eclipsed position relative to the other, but superposition is only achieved after the reflection at the mirror plane perpendicular to the rotational axis. Because one S_{10} passes through two opposite vertices, and there are 12 vertices there are 6 S_{10} improper axes. For each axis there are four unique symmetry operations, the S_{10}^1, the S_{10}^3, the S_{10}^7, and the S_{10}^9. Therefore, there are overall 4x6=24 operations possible.

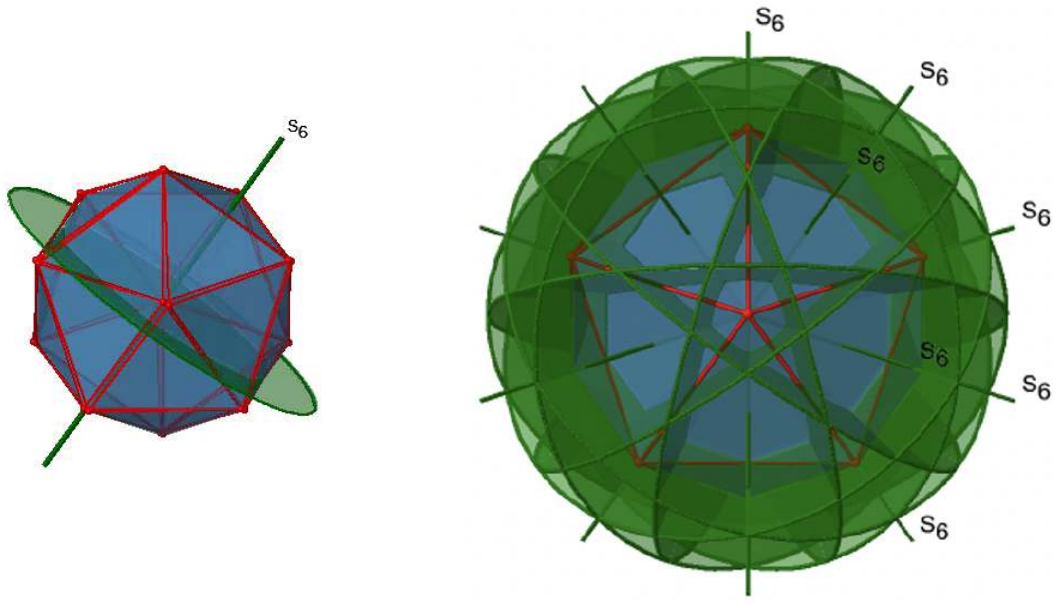


Figure *Section*3.2.26: The S_6 rotation-reflections in the icosahedral point group (Attribution: symotter.org/gallery)

Are the lower order improper rotational axes? Yes, there are S_6 axes that pass through the centers of two opposite triangular faces (Figure *Section*3.2.26). This symmetry element exists because the two triangular faces are in staggered orientation to each other. Rotation alone brings one face in eclipsed orientation relative to the other, but reflection at a mirror plane perpendicular to the axis is required to achieve superposition. The S_6 axes are in the same location as the C_3 axes. There are 10 S_6 axes because there are twenty faces and one axis passes through two opposite faces. Only the S_6^1 and the S_6^5 operations are unique S_6 operations, all others can be expressed by simpler operations. Therefore there are overall 10 S_6^1+10 S_6^5 = 20 S_6 operations.

We have now found all symmetry operations for the I_h symmetry. There are overall 120 operations making the point group I_h the point group with the highest symmetry.

Symmetry Operations in the I_h Point Group

Every molecule or object in the I_h point group has the following 120 symmetry operations:

- E, 24 C_5, 20 C_3, 15 C_2, i, 24 S_{10}, 20 S_6, and 15 σ

Rotational Point Groups

After having discussed high and low symmetry point groups, let us next look at rotational point groups. Unlike the high symmetry point groups, these only have a single proper rotational axis. The presence or absence of reflection planes further defines this class of point groups

C_n Point Groups

In the most simple case the point groups do not have any additional symmetry element such as mirror planes or improper rotations. These point groups are called pure rotation groups and denoted C_n whereby n is the order of the proper rotation axis. An example is the hydrogen peroxide molecule H_2O_2 (Figure ***Section*3.2.27**). It has a so-called roof-structure due to its non-planarity. One hydrogen atom points toward us, and the other points away from us. This structure is due to the two electron-lone pairs at each sp^3-hybridized oxygen atom. These electron-lone pairs consume somewhat more space than the H atoms, and there is electrostatic repulsion between the electron lone pairs. Therefore, the electron lone pairs at the different oxygen atoms try to achieve the greatest distance from each other. This forces the H-atoms out of the plane, leading to the roof-structure of the hydrogen peroxide. Because the H_2O_2 molecule is not planar, it only has a single C_2 axis, but no other symmetry element besides the identity. The C_2 axis passes through the center of the O-O bond. Execution of the C_2 operation swaps up both the O and the H atoms.

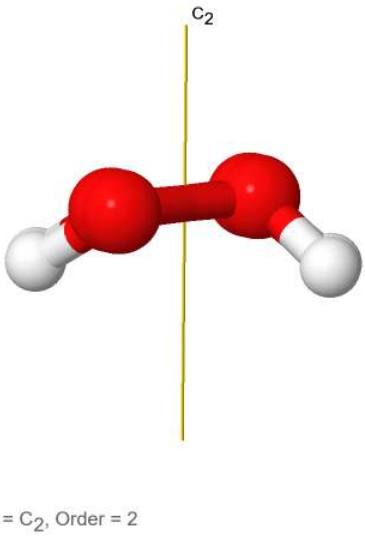


Figure ***Section*3.2.27**: The C_2 rotational axis of hydrogen peroxide (Attribution: symotter.org/gallery)

C_{nv} Point Groups

Another class of groups are the pyramidal groups, denoted C_{nv}. They have n vertical mirror planes containing the principal axis C_n in addition to the principal axis C_n. Generally molecules belonging to pyramidal groups are derived from an n-gonal pyramid. An n-gonal pyramid has an n-gonal polygon as the basis which is capped. For example a trigonal pyramid has a triangular basis which is capped, a tetragonal pyramid has a square which is capped, and so on. The proper axis associated with a specific pyramid has the order n and goes through the tip of the pyramid and the center of the polygon. An example of a molecule with a trigonal pyramidal shape is the NH_3 (Figure ***Section*3.2.28**).

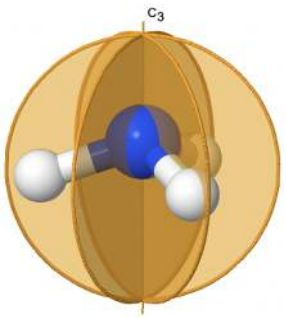


Figure *Section*3.2.28: C_3 axis and vertical mirror planes in NH_3 (Attribution: symotter.org/gallery)

The three H atoms form the triangular basis of the pyramid, which is capped by the N atom. The NH_3 molecule belongs to the point group C_{3v}. The C_3 axis goes though the N atom which is the tip of the pyramid, and the center of the triangle defined by the H atoms. There are three vertical mirror planes that contain the C_3 axis. Each of them goes through an N-H bond.

C_{nh} Point Groups

If we add a horizontal mirror plane instead of n vertical mirror planes to a proper rotational axis C_n we arrive at the point group type C_{nh}. The presence of the horizontal mirror planes also generates an improper axis of the order n. This is because when one can rotate and reflect perpendicular to the rotational axes independently, then it must also be possible to do it in combination. An example of a molecule belong to a C_{nh} group is the trans-difluorodiazene N_2F_2 (Figure *Section*3.2.29). It is a planar molecule with a C_2 axis going through the middle of the N-N double bond, and standing perpendicular to the plane of the molecule. The horizontal mirror plane stands perpendicular to the C_2 axis, and is within the plane of the molecule. There is an additional inversion center because an S_2 must exist which is the same as an inversion center. The inversion center is in the middle of the N-N bonds. Overall, the molecule has the symmetry C_{2h}.

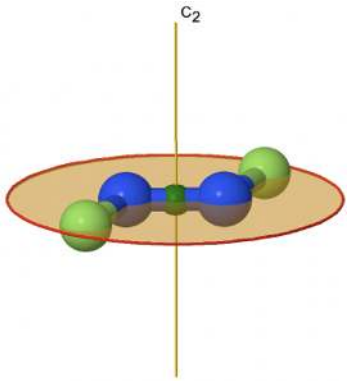


Figure *Section*3.2.29: C_2 axis and horizontal mirror plane in trans-N_2F_2 (Attribution: symotter.org/gallery)

S_{2n} Point Groups

The category of rotational point groups to be discussed are the improper rotation point groups. The only have one proper rotational axis, and an improper rotational axis that has twice the order of the proper rotational axis (Figure *Section*3.2.30). There may be an inversion center present depending on the order of the proper and improper axes. Molecules that fall into these point groups are rare. An example the tetramethylcycloocta-tetraene molecule (Figure *Section*3.2.30).

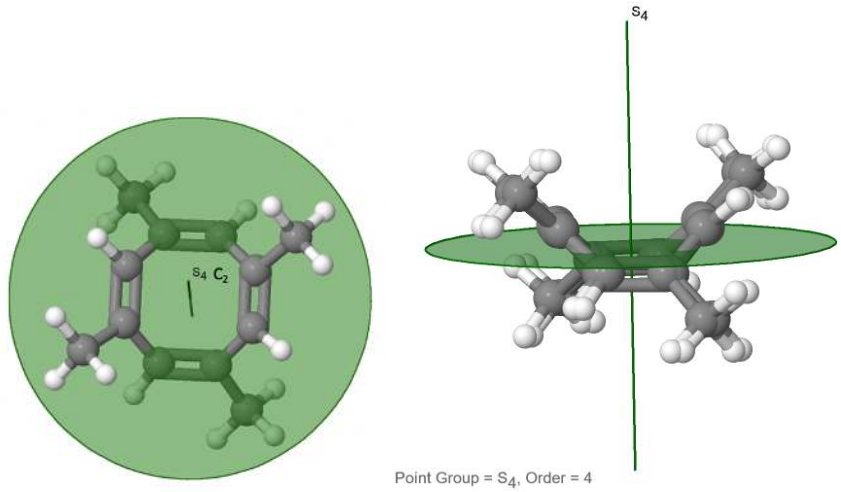


Figure ***Section*3.2.30**: The S_4 and an C_2 axes of tetramethyl cycloocta-tetraene

It has an S_4 and an C_2 axis as the only symmetry elements besides the identity. Rotating by 90° alone does not superimpose the molecule because two C-C double bonds lie above the plane and two below the plane. In addition, two opposite methyl groups lie above and below the plane respectively. Therefore it needs the additional reflection to achieve superposition. There is also a C_2 axis which is in the same locations as the S_4 axis.

Dihedral Groups

D_n Point Groups

Dihedral groups are point groups that have n additional C_2 axes that stand perpendicular to the principal axis of the order n. If there are no other symmetry elements, then the point group is of the type D_n. For example in the point group D_3 there is a C_3 principal axis, and three additional C_2 axes, but no other symmetry element (Fig. 2.2.75). The tris-oxolatoferrate(III) ion belongs to this point group (Figure ***Section*3.2.31**). You can see that the C_3 axis stands perpendicular to the paper plane, and there are three C_2 axes in the paper plane.

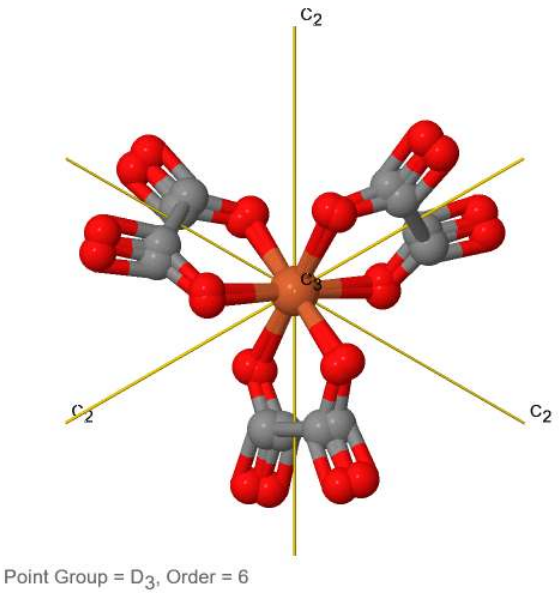


Figure ***Section*3.2.31**: The tris-oxolatoferrate(III) ion and its symmetry elements. (Attribution: symotter.org/gallery)

D_{nh} Point Groups

If a horizontal mirror plane is added to the C_n axis and the n C_2 axes we arrive at the D_{nh} point groups. The addition of the horizontal mirror plane generates further symmetry elements namely an S_n and n vertical mirror planes. An example for a molecule belonging to this class of point group is PF_5 (Figure ***Section*3.2.32**). It has a trigonal bipyramidal shape. The C_3 axis goes through the axial F atoms of the molecule, and the three C_2 axes go through the three equatorial F atom. The horizontal mirror plane stands perpendicular to the principal C_3 axis and is located within the equatorial plane of the molecule. In addition, there are the vertical mirror planes that contain the C_3 axis, and go through the three equatorial P-F bonds. There is also an S_3 axis which superimposes the C_3 axis.

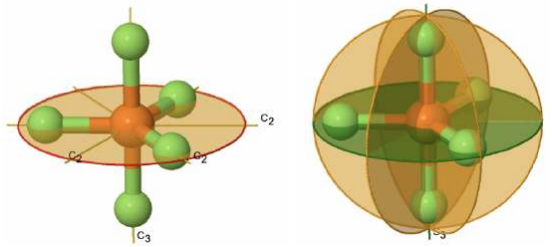


Figure ***Section*3.2.32**: The PF_5 molecule belonging to the point group D_{3h} and its symmetry elements. (Attribution: symotter.org/gallery)

D_{nd} Point Groups

If we add n vertical mirror planes to the principal axis and the n C_2 axes, we arrive at the point group D_{nd}. The vertical mirror planes are dihedral mirror planes because they bisect the angle between the C_2 axes. An example is the ethane molecule in staggered conformation which has the symmetry D_{3d} (Figure ***Section*3.2.33**:). The C_3 axis goes along the C-C bond, and the $3C_2$ axes pass through the middle of the carbon-carbon bond, and bisect the angle between two hydrogens and one carbon atom. The three dihedral mirror planes pass through the C-H bonds. In addition, the ethane molecule has an S_6 axis, and an inversion center.

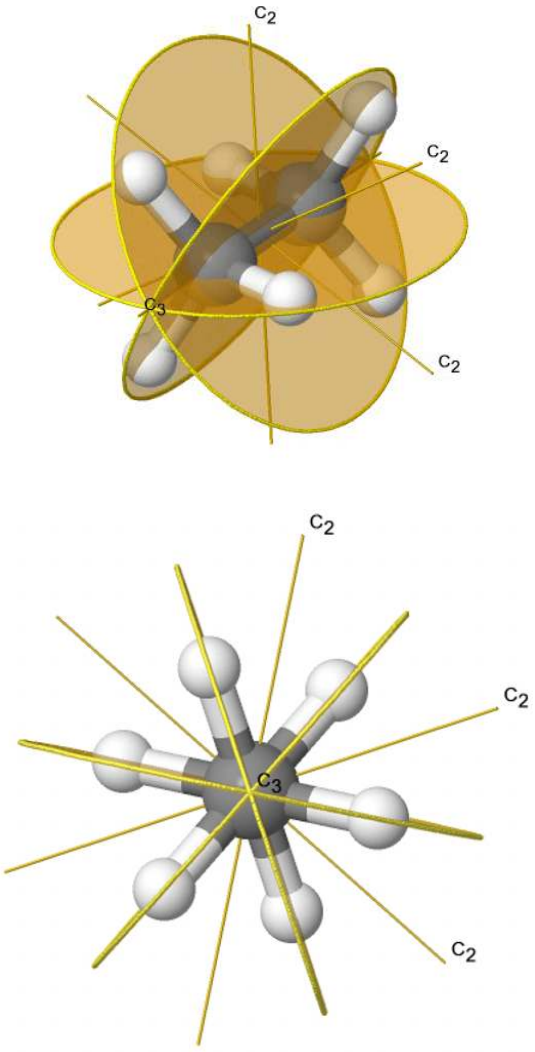


Figure *Section*3.2.33: The ethane molecule in the staggered conformation belongs to the point group type D_{nd} (Attribution: symotter.org/gallery)

Linear Point Groups

The principal rotation axis in a linear molecule is a C_∞ axis, meaning the molecule can be rotated along its bond axis an infinitely small amount and remain unchanged. Linear molecules can be subdivided based on the presence or absence of a horizontal reflection plane and inversion center.

$C_{\infty v}$ point groups

A special n-gonal polygon is the cone. A cone can be conceived as an n-gonal pyramid with an infinite number *n* of corners at the base (Figure *Section*3.2.34).

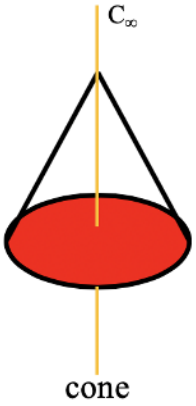


Figure *Section*3.2.34: Cone having a proper rotational axis with infinite order.

In this case the order of the rotational axis that passes through the tip of the cone and the center of the circular basis is infinite. This also means that there is an infinite number of vertical mirror planes that contain the C_∞ axis. The point group describing the symmetry of a cone is called the linear point group $C_{\infty v}$. Polar, linear molecules such as CO, HF, N_2O, and HCN belong to this point group. You can see the HCN molecule with its C_∞ axis and its infinite number of vertical mirror planes below (Figure *Section*3.2.35). The infinite number of mirror planes, shown in blue are forming a cylinder that surround the molecule.

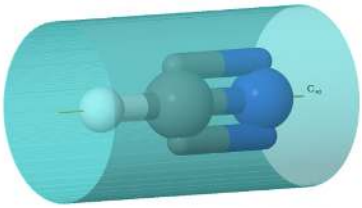


Figure *Section*3.2.35: C_∞ axis of the HCN molecule.

$D_{\infty h}$ point groups

A special case of a D_{nh} group is the linear group $D_{\infty h}$. An object that has this symmetry is a cylinder. A cylinder can be conceived as a prism with an infinite number of vertices. Thus, the principal axis that passes through a cylinder has infinite order. Because of the infinite order of the principal axis, there is an infinite number of C_2 axes that stand perpendicular to the principal axis. You can see one such C_2 going though the cylinder (Figure *Section*3.2.36:).

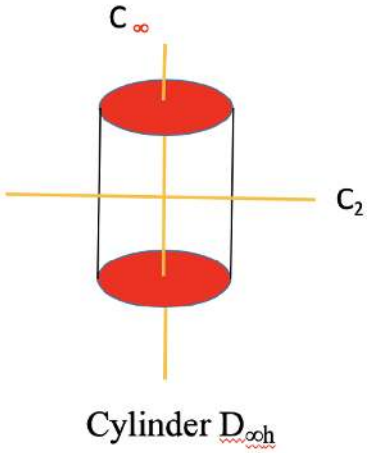
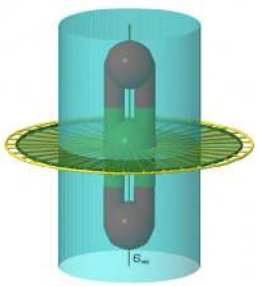


Figure *Section*3.2.36: Cylinder as an example of linear group $D_{\infty h}$.

There is now also an improper axis of infinite order, as well as an infinite number of vertical mirror planes. Non-polar linear molecules like H_2, CO_2, and acetylene C_2H_2 belong to the point group $D_{\infty h}$. You can see the C_∞ axis passing through a CO_2 molecule below (Figure *Section*3.2.37). You can see the infinite number of vertical mirror planes as a blue cylinder. The infinite number of C_2 axes is shown a yellow lines going around the molecule.



CO_2

Figure *Section*3.2.37: C_∞ in a CO_2 molecule.

Guide for the Determination of Point Groups

The symmetry operations a molecule possesses will determine which point group the molecule is in. The key to success is that you are able to see the symmetry elements in the molecule which takes practice. Luckily, especially for high symmetry point groups, you don't need to identify every single symmetry operation to correctly assign a point group. You can use a flow chart to identify a point group more easily. These flow charts ask systematic questions about the presence or absence of key symmetry elements. Eventually, after having answered enough questions the guide will lead you to the respective point group. You can see an example flow chart below (Figure *Section*3.2.38:).

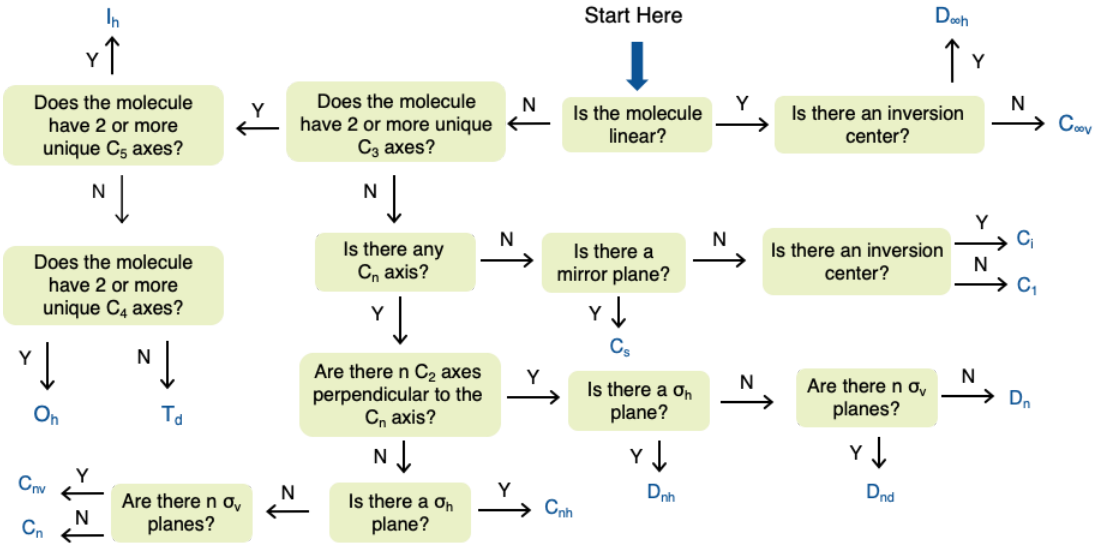


Figure *Section*3.2.38: Flow chart for the determination of point groups. (CC BY-NC-SA; Catherine McCusker)

You can first ask if the molecule is linear (has a C_∞ rotation axis). Then we can ask next, if there is a high symmetry point group. This is the case when there are either $4C_3$, $3C_4$, or $6C_5$ rotational axes present, standing for tetrahedral, octahedral, and icosahedral symmetry, respectively. If there is are no C_n axes of any type present the molecule must be in a low symmetry point group. We ask if there are n $\perp C_2$ axes in addition to the C_n principal axis. If this is so, then we must have a dihedral group of the D type. If there are no $\perp$ C_2 axes in addition to the C_n, the group must be a rotational (C) group.

Example: Dibromonaphtalene

Let us practice the point group flow chart by example. Let us look at the dibromonaphtalene molecule (Figure *Section*3.2.39).

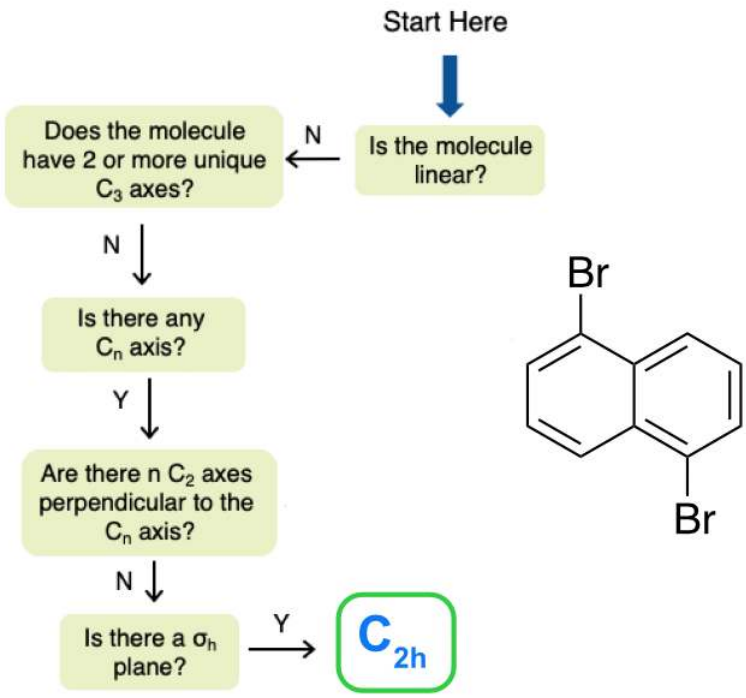


Figure *Section*3.2.39: Guide for determining the point group of dibromonaphtalene

After determining that the molecule is not linear or in a high symmetry group (having 2 or more C_3 rotation axes), the first question we ask is: Can you see at least one proper rotational axis? The answer is yes. There is a C_2 proper rotational axis that stands perpendicular to the plane of the molecule and goes through the center of the C-C bond that is shared by the two aromatic rings. Next we can think about if the there are $2C_2$ axes in addition to the C_2 axes we already found. The answer is no, so the point group cannot be a dihedral (D) group. Next, we would ask: Is there a horizontal mirror plane. This is indeed the case. There is a horizontal mirror plane in the plane of the molecule. It does not move any atoms around, but as we discussed before, a mirror does not need to do this to exist. This identifies the point group as C_{2h}.

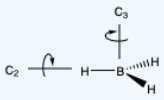
The Symmetry Challenge at Otterbein University is a great way to practice assigning molecules to point groups!

Exercise *Section*3.2.1

Use the flow chart to assign the point group for (a) BH_3 and (b) H_2O.

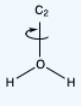
Answer

(a) BH_3 has a trigonal planar geometry.



- It has a C_3 principal rotation axis
- It doesn't have C_5, C_4, or multiple C_3 axes
- It has 3 $\perp$ C_2 axes
- It has a σ_h (the plane of the molecule)
- The point group is $\mathbf{D_{3h}}$

(b) H_2O has a bent geometry.



- It has a C_2 principal rotation axis
- It doesn't have any C_5, C_4, or C_3 axes
- It doesn't have $\perp$ C_2 axes
- It doesn't have a σ_h reflection plane
- It does have 2 σ_v reflection planes

- The point group is $\mathbf{C_{2v}}$

Dr. Kai Landskron (Lehigh University). If you like this textbook, please consider to make a donation to support the author's research at Lehigh University: Click Here to Donate.

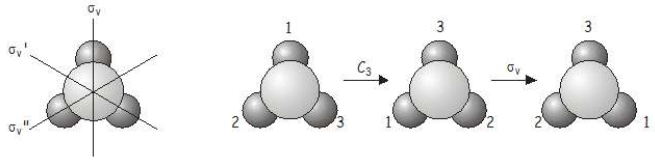
This page titled Section 3.2: Point Groups is shared under a CC BY-NC-SA 4.0 license and was authored, remixed, and/or curated by Kai Landskron.

- **2.2: Point Groups** by Kai Landskron is licensed CC BY 4.0.
- **4.2: Point Groups** by Kai Landskron is licensed CC BY-NC-SA 4.0.

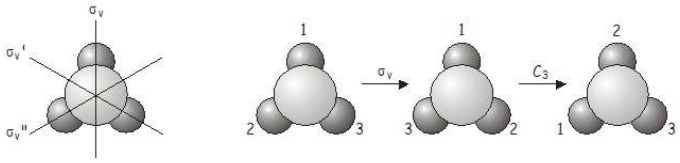
Section 3.3: Properties and Representations of Groups

Group Multiplication

Now we will investigate what happens when we apply two symmetry operations in sequence. As an example, consider the NH_3 molecule, which belongs to the C_{3v} point group. Consider what happens if we apply a C_3rotation (120˚ counter-clockwise) followed by a σ_v reflection (reflection over the σ_v axis). We write this combined operation $\sigma_v C_3$ (when written, symmetry operations operate on the thing directly to their right, just as operators do in quantum mechanics – we therefore have to work backwards from right to left from the notation to get the correct order in which the operators are applied). As we shall soon see, the order in which the operations are applied is important.



The combined operation $\sigma_v C_3$ is equivalent to σ_v'' (note the double prime on σ_v''!), which is also a symmetry operation of the C_{3v} point group. Now let's see what happens if we apply the operators in the reverse order, i.e., $C_3\sigma_v$ is (σ_v followed by C_3).



Again, the combined operation $C_3\sigma_v$ is equivalent to another operation of the point group, this time σ_v' (note the single prime on σ_v'!).

There are two important points that are illustrated by this example:

1. The order in which two operations are applied is important. For two symmetry operations A and B, AB is not necessarily the same as BA, i.e. symmetry operations do not in general ***commute***. In some groups the symmetry elements do commute; such groups are said to be ***Abelian***.
2. If two operations from the same point group are applied in sequence, the result will be equivalent to another operation from the point group. Symmetry operations that are related to each other by other symmetry operations of the group are said to belong to the same ***class***. In NH_3, the three mirror planes σ_v, σ_v' and σ_v'' belong to the same class (related to each other through a C_3 rotation), as do the rotations C_3^+ and C_3^- (anticlockwise and clockwise rotations about the principal axis, related to each other by a vertical mirror plane).

Four Properties of Mathematical Groups

Now that we have explored some of the properties of symmetry operations and elements and their behavior within point groups, we are ready to introduce the formal mathematical definition of a group. The definitions below will be put into the context of *molecular* symmetry.

A mathematical group is defined as a set of elements (A_1, A_2, A_3...) together with a rule for forming combinations A_i,A_j... For our purposes, A_1, A_2, A_3, etc. are symmetry elements and A_i, A_j, etc. are symmetry operations described in a previous section. The elements of the group and the rule for combining them must satisfy the following four criteria.

1. The group must include the **identity** E, which commutes with other members of the group. In other terms, $EA_i = A_i$ for all the elements of the group. Application of the identity operation before or after another operation, A_i, results in the same outcome as A_i alone.
2. The elements must satisfy the group property that the combination of any pair of elements is also an element of the group. For example, in the C_{3v} point group, a C_3 rotation followed by a σ_v gives another operation that is already part of the group: a σ_v''.

3. Each symmetry operation A_i must have an inverse A_i^{-1}, which is also an element of the group, such that

$$A_i A_i^{-1} = A_i^{-1} A_i = E$$

   The inverse g_i^{-1} effectively 'undoes' the effect of the symmetry operation g_i. For example, in the C_{3v} point group, the inverse of C_3^+ is C_3^-.
4. The rule of combination must be associative

$$(A_i A_j)(A_k) = A_i(A_j A_k)$$

   Or $A(BC) = (AB)C$. In other words, the order of operations should not matter.

Group theory is an important area in mathematics, and luckily for chemists the mathematicians have already done most of the work for us. Along with the formal definition of a group comes a comprehensive mathematical framework that allows us to carry out a rigorous treatment of symmetry in molecular systems and learn about its consequences.

Many problems involving operators or operations (such as those found in quantum mechanics or group theory) may be reformulated in terms of matrices. Any of you who have come across transformation matrices before will know that symmetry operations such as rotations and reflections may be represented by matrices. It turns out that the set of matrices representing the symmetry operations in a group obey all the conditions laid out above in the mathematical definition of a group, and using matrix representations of symmetry operations simplifies carrying out calculations in group theory. Before we learn how to use matrices in group theory, it will probably be helpful to review some basic definitions and properties of matrices.

*This page was adapted from here (click).

Contributors and Attributions

- Claire Vallance (University of Oxford)
- Curated or created by Kathryn Haas

Section 3.3: Properties and Representations of Groups is shared under a not declared license and was authored, remixed, and/or curated by LibreTexts.

- **4.3: Properties and Representations of Groups** by Kathryn Haas is licensed CC BY-NC-SA 4.0.

Section 3.3.1: Representations of Symmetry Operations

Symmetry Operations: Matrix Representations

A **symmetry operation**, such as a rotation around a symmetry axis or a reflection through a plane, is an operation that, when performed on an object, results in a new orientation of the object that is indistinguishable from the original. For example, if we rotate a square in the plane by $\pi/2$ or π, the new orientation of the square is superimposable on the original one (Figure ***Section*3.3.1.1**).

If rotation by an angle θ of a molecule (or object) about some axis results in an orientation of the molecule (or object) that is superimposable on the original, the axis is called a rotation axis. The molecule (or object) is said to have an n-fold rotational axis, where n is $2\pi/\theta$. The axis is denoted as C_n. The square of Figure ***Section*3.3.1.1** has a C_4 axis perpendicular to the plane because a $90°$ rotation leaves the figure indistinguishable from the initial orientation. This axis is also a C_2 axis because a $180°$ degree rotation leaves the square indistinguishable from the original square. In addition, the figure has several other C_2 axis that lie on the same plane as the square:

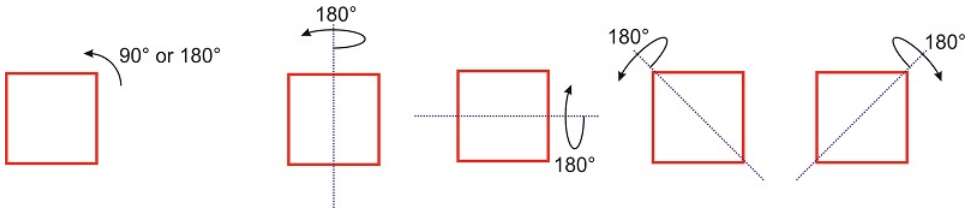


Figure ***Section*3.3.1.1**: Symmetry operations performed on a square

A symmetry operation moves all the points of the object from one initial position to a final position, and that means that symmetry operators are 3×3 square matrices (or 2×2 in two dimensions). Each symmetry operation can be expressed as a **transformation matrix** where the vector (x', y', z') represents the new coordinates of the point (x, y, z) after the symmetry operation.

$$[\text{New Coordinates}(x', y', z')] = [\text{Transformation Matrix}] \times [\text{Old Coordinates}(x, y, z)]$$

We will use the example of water, which is in the C_{2v} point group, to illustrate how transformation matrices can be used to represent the symmetry of a group.

Figure ***Section*3.3.1.2** shows the three symmetry elements of the molecule of water (H_2O). This molecule has only one rotation axis, which is 2-fold, and therefore we call it a "C_2 axis." It also has two mirror planes, one that contains the two hydrogen atoms (σ_{yz}), and another one perpendicular to it (σ_{xz}). Both planes contain the C_2 axis.

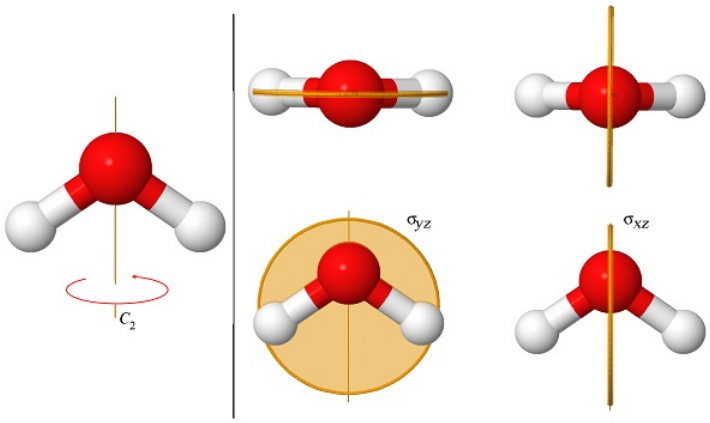


Figure ***Section*3.3.1.2**: The symmetry elements of the molecule of water

Transformation Matrix of C_2 rotation

A 2-fold rotation around the z–axis changes the location of a point (x, y, z) to $(-x, -y, z)$ (see Figure ***Section*3.3.1.3**). By convention, rotations are always taken in the counterclockwise direction.

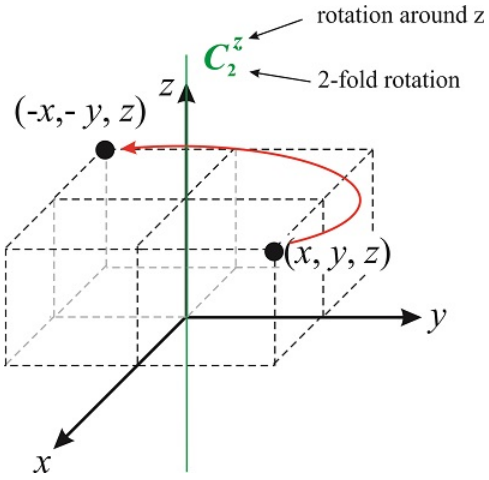


Figure *Section*3.3.1.3: A 2-fold rotation around the z-axis

What is the matrix that represents the C_2 rotation? The matrix transforms the vector (x, y, z) into $(-x, -y, z)$, so

$$C_2(x, y, z) = (-x, -y, z)$$

$$\begin{pmatrix} a_{11} & a_{12} & a_{13} \\ a_{21} & a_{22} & a_{23} \\ a_{31} & a_{32} & a_{33} \end{pmatrix} \begin{pmatrix} x \\ y \\ z \end{pmatrix} = \begin{pmatrix} -x \\ -y \\ z \end{pmatrix}$$

We know the matrix is a 3×3 square matrix because it needs to multiply a 3-dimensional vector. In addition, we write the vector as a vertical column to satisfy the requirements of matrix multiplication.

$$\begin{pmatrix} a_{11} & a_{12} & a_{13} \\ a_{21} & a_{22} & a_{23} \\ a_{31} & a_{32} & a_{33} \end{pmatrix} \begin{pmatrix} x \\ y \\ z \end{pmatrix}$$

$$a_{11}x + a_{12}y + a_{13}z = -x$$

$$a_{21}x + a_{22}y + a_{23}z = -y$$

$$a_{31}x + a_{32}y + a_{33}z = z$$

and we conclude that $a_{11} = -1$, $a_{12} = a_{13} = 0$, $a_{22} = -1$, $a_{21} = a_{23} = 0$ and $a_{33} = 1$, $a_{31} = a_{32} = 0$. The transformation matrix of the C_2 operation of the C_{2v} point group is:

$$C_2 = \begin{pmatrix} -1 & 0 & 0 \\ 0 & -1 & 0 \\ 0 & 0 & 1 \end{pmatrix}$$

Transformation Matrix of σ_{xz} reflection

Rotations are not the only symmetry operations we can perform on a molecule. Figure *Section*3.3.1.4 illustrates the reflection of a point through the xz plane. This operation transforms the vector (x, y, z) into the vector $(x, -y, z)$. Symmetry operators involving reflections through a plane are usually denoted with the letter σ, so the operator that reflects a point through the xz plane is $\hat{\sigma}_{xz}$:

$$\sigma_{xz}(x, y, z) = (x, -y, z)$$

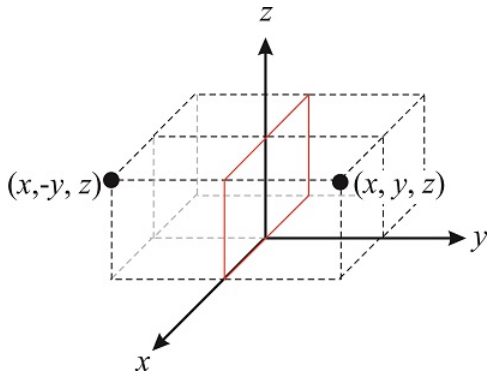


Figure **Section3.3.1.3**: A reflection through the xz plane

Following the same logic we used for the rotation matrix, we can write the σ_{xz} transformation matrix as:

$$\sigma_{x,z} = \begin{pmatrix} 1 & 0 & 0 \\ 0 & -1 & 0 \\ 0 & 0 & 1 \end{pmatrix}$$

This is true because

$$\begin{pmatrix} 1 & 0 & 0 \\ 0 & -1 & 0 \\ 0 & 0 & 1 \end{pmatrix} \begin{pmatrix} x \\ y \\ z \end{pmatrix} = \begin{pmatrix} x \\ -y \\ z \end{pmatrix}$$

? Exercise *Section*3.3.1.1

Find the transformation matrix of the identity (E) and the $\sigma_{y,z}$ operations under the C_{2v} point group.

Answer

The transformation matrix for E is $\begin{pmatrix} 1 & 0 & 0 \\ 0 & 1 & 0 \\ 0 & 0 & 1 \end{pmatrix}$.

The transformation matrix for $\sigma_{v(yz)''}$ is $\begin{pmatrix} -1 & 0 & 0 \\ 0 & 1 & 0 \\ 0 & 0 & 1 \end{pmatrix}$.

Characters

For a square matrix, the ***character*** is the trace of the matrix. For the C_2 operation, with the transformation matrix

$$\begin{pmatrix} -1 & 0 & 0 \\ 0 & -1 & 0 \\ 0 & 0 & 1 \end{pmatrix},$$

the trace is $(-1) + (-1) + 1 = -1$.

The set of characters for a point group is called a **reducible representation (Γ)**. The reducible representation for the C_{2v} point group is:

C_{2v}	E	C_2	σ_v	σ'_v
Γ	3	−1	1	1

? Exercise *Section*3.3.1.1

Prove that the characters in the reducible representation for C_{2v} are correct:

C_{2v}	E	C_2	σ_v	σ'_v
Γ	3	−1	1	1

Answer

For the E operation, with the transformation matrix $\begin{pmatrix}1&0&0\\0&1&0\\0&0&1\end{pmatrix}$, the trace is $1+1+1=3$.

For the C_2^z operation, with the transformation matrix $\begin{pmatrix}-1&0&0\\0&-1&0\\0&0&1\end{pmatrix}$, the trace is $(-1)+(-1)+1=-1$.

For the $\sigma_{v(xz)'}$ operation, with the transformation matrix $\begin{pmatrix}1&0&0\\0&-1&0\\0&0&1\end{pmatrix}$, the trace is $1+(-1)+1=1$.

For the $\sigma_{v(yz)''}$ operation, with the transformation matrix $\begin{pmatrix}-1&0&0\\0&1&0\\0&0&1\end{pmatrix}$, the trace is $-1+1+1=1$.

This gives the reducible representation

C_{2v}	E	C_2	σ_v	σ_v'
Γ	3	−1	1	1

Reducible and Irreducible Representations

Let us now go back and look in more detail at the transformation matrices of the C_{2v} point group that we derived above. If we look at the matrices carefully we see that they all take the same block diagonal form (a square matrix is said to be **block diagonal** if all the elements are zero except for a set of submatrices lying along the diagonal).

$$E=\begin{pmatrix}[1]&0&0\\0&[1]&0\\0&0&[1]\end{pmatrix},\ C_2=\begin{pmatrix}[-1]&0&0\\0&[-1]&0\\0&0&[1]\end{pmatrix},$$
$$\sigma'_{v(xz)}=\begin{pmatrix}[1]&0&0\\0&[-1]&0\\0&0&[1]\end{pmatrix},\ \sigma_{v(yz)''}=\begin{pmatrix}[-1]&0&0\\0&[1]&0\\0&0&[1]\end{pmatrix}$$

All the non-zero elements become 1x1 matrices that each represent individual x, y, z coordinates. In other words, the element a_{11} represents x, a_{22} represents y, and a_{33} represents z. The matrix elements for x from each transformation matrix combine to form an irreducible representation of the C_{2v} point group. Likewise, the matrix elements for y combine to form a second irreducible representation, and the same is true for z elements. These irreducible representations are shown below:

C_{2v}	E	C_2	σ_v	σ_v'	Coordinate Used
	1	−1	1	−1	x
	1	−1	−1	1	y
	1	1	1	1	z
Γ	3	−1	1	1	

The irreducible representations add to form the reducible representation, Γ. This Γ, which is the set of 3x3 matrices, can be reduced to the set of 1x1 matrices of the irreducible representations. The irreducible representations cannot be reduced further, hence their name.

Sources & Attribution

- Parts of this page was adapted from Matrices (click here) (Symmetry Operators), contributed by Marcia Levitus, Associate Professor (Biodesign Institute) at Arizona State University.
- Parts of this page were adapted from Reductions of Representations, contributed by

  Claire Vallance (University of Oxford)
- Curated or created by Kathryn Haas

Section 3.3.1: Representations of Symmetry Operations is shared under a not declared license and was authored, remixed, and/or curated by LibreTexts.

- **4.3.2: Representations of Point Groups** by Kathryn Haas is licensed CC BY-NC-SA 4.0.

Section 3.3.2: Matrices

The symmetry of molecules is essential for understanding the structures and properties of organic and inorganic compounds. The properties of chemical compounds are often easily explained by consideration of symmetry. For example, the symmetry of a molecule determines whether the molecule has a permanent dipole moment or not. The theories that describe optical activity, infrared and ultraviolet spectroscopy, and crystal structure involve the application of symmetry considerations. Matrix algebra is the most important mathematical tool in the description of symmetry.

The properties of symmetry groups are organized in character tables (discussed later in this chapter). Character tables are constructed based on matrices. This page is a brief description of matrices and matrix multiplication.

What is a matrix?

An $m \times n$ matrix $\mathbf{A}$ is a rectangular array of numbers with m rows and n columns. The numbers m and n are the dimensions of $\mathbf{A}$. The numbers in the matrix are called its entries. The entry in row i and column j is called a_{ij}.

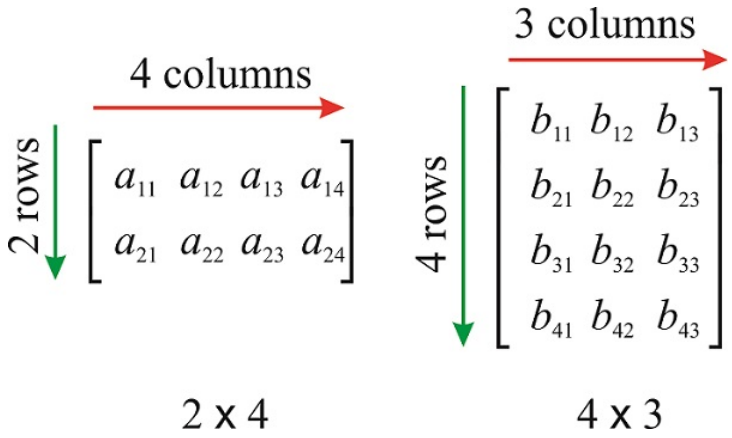


Figure *Section*3.3.2.1: Matrices of different dimensions

Some types of matrices have special names:

- A square matrix:

$$\begin{pmatrix} 3 & -2 & 4 \\ 5 & 3i & 3 \\ -i & 1/2 & 9 \end{pmatrix}$$

  with $m = n$
- A rectangular matrix:

$$\begin{pmatrix} 3 & -2 & 4 \\ 5 & 3i & 3 \end{pmatrix}$$

  with $m \neq n$
- A column vector:

$$\begin{pmatrix} 3 \\ 5 \\ -i \end{pmatrix}$$

  with $n = 1$
- A row vector:

$$\begin{pmatrix} 3 & -2 & 4 \end{pmatrix}$$

  with $m = 1$
- The identity matrix:

$$\begin{pmatrix} 1 & 0 & 0 \\ 0 & 1 & 0 \\ 0 & 0 & 1 \end{pmatrix}$$

with $a_{ij} = \delta_{i,j}$, where $\delta_{i,j}$ is a function defined as $\delta_{i,j} = 1$ if $i = j$ and $\delta_{i,j} = 0$ if $i \neq j$.

- A diagonal matrix:

$$\begin{pmatrix} a & 0 & 0 \\ 0 & b & 0 \\ 0 & 0 & c \end{pmatrix}$$

with $a_{ij} = c_i \delta_{i,j}$.

- An upper triangular matrix:

$$\begin{pmatrix} a & b & c \\ 0 & d & e \\ 0 & 0 & f \end{pmatrix}$$

All the entries below the main diagonal are zero.

- A lower triangular matrix:

$$\begin{pmatrix} a & 0 & 0 \\ b & c & 0 \\ d & e & f \end{pmatrix}$$

All the entries above the main diagonal are zero.

- A triangular matrix is one that is either lower triangular or upper triangular.

The Trace of a Matrix

The trace of an $n \times n$ square matrix $\mathbf{A}$ is the sum of the diagonal elements, and formally defined as $Tr(\mathbf{A}) = \sum_{i=1}^{n} a_{ii}$.

For example,

$$\mathbf{A} = \begin{pmatrix} 3 & -2 & 4 \\ 5 & 3i & 3 \\ -i & 1/2 & 9 \end{pmatrix} ; Tr(\mathbf{A}) = 12 + 3i$$

Singular and Nonsingular Matrices

A square matrix with nonzero determinant is called *nonsingular*. A matrix whose determinant is zero is called *singular*. (Note that you cannot calculate the determinant of a non-square matrix).

For a 2x2 matrix,

$$\mathbf{B} = \begin{pmatrix} a & b \\ c & d \end{pmatrix} ; det(\mathbf{B}) = ad - cb$$

For a 3x3 matrix,

$$\mathbf{C} = \begin{pmatrix} a & b & c \\ d & e & f \\ g & h & i \end{pmatrix}$$

$$det(\mathbf{C}) = a \begin{pmatrix} e & f \\ h & i \end{pmatrix} - b \begin{pmatrix} d & f \\ g & i \end{pmatrix} + c \begin{pmatrix} d & e \\ g & h \end{pmatrix}$$

$$det(\mathbf{C}) = aei - ahf - bdi + bgf + cdh - cge$$

The Matrix Transpose

The matrix transpose, most commonly written $\mathbf{A}^T$, is the matrix obtained by exchanging $\mathbf{A}$'s rows and columns. It is obtained by replacing all elements a_{ij} with a_{ji}. For example:

$$\mathbf{A} = \begin{pmatrix} 3 & -2 & 4 \\ 5 & 3i & 3 \end{pmatrix} \rightarrow \mathbf{A}^T = \begin{pmatrix} 3 & 5 \\ -2 & 3i \\ 4 & 3 \end{pmatrix}$$

Matrix Multiplication

To multiply two matrices, the number of vertical columns in the first matrix must be the same as the number of rows in the second matrix. If $\mathbf{A}$ has dimensions $m \times n$ and $\mathbf{B}$ has dimensions $n \times p$, then the product $\mathbf{AB}$ is defined, and has dimensions $m \times p$.

$$c_{ij} = \sum a_{ij} \times b_{ij}$$

The entry $a_{ij} \times b_{ij}$ is obtained by multiplying row i of $\mathbf{A}$ by column j of $\mathbf{B}$, which is done by multiplying corresponding entries together and then adding the results:

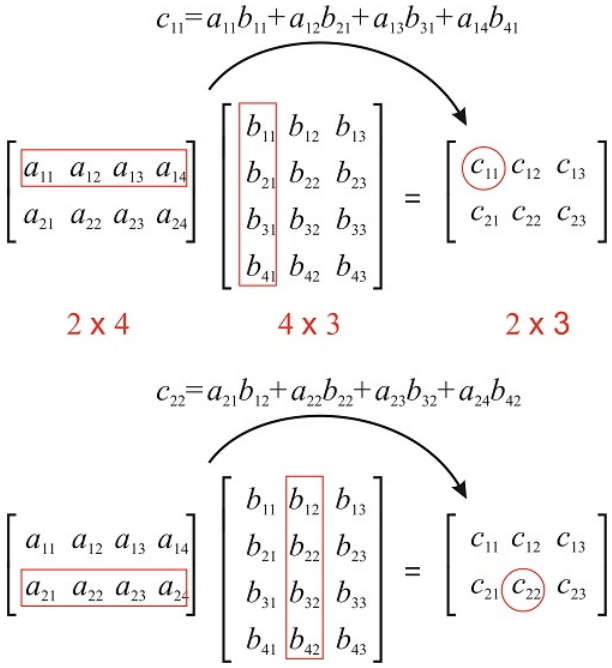


Figure *Section*3.3.2.1: Matrix multiplication

Example *Section*3.3.2.1

Calculate the product

$$\begin{pmatrix} 1 & -2 & 4 \\ 5 & 0 & 3 \\ 0 & 1/2 & 9 \end{pmatrix} \begin{pmatrix} 1 & 0 \\ 5 & 3 \\ -1 & 0 \end{pmatrix}$$

Solution

We need to multiply a 3×3 matrix by a 3×2 matrix, so we expect a 3×2 matrix as a result.

$$\begin{pmatrix} 1 & -2 & 4 \\ 5 & 0 & 3 \\ 0 & 1/2 & 9 \end{pmatrix} \begin{pmatrix} 1 & 0 \\ 5 & 3 \\ -1 & 0 \end{pmatrix} = \begin{pmatrix} a & b \\ c & d \\ e & f \end{pmatrix}$$

To calculate a, which is entry (1,1), we use row 1 of the matrix on the left and column 1 of the matrix on the right:

$$\begin{pmatrix} 1 & -2 & 4 \\ 5 & 0 & 3 \\ 0 & 1/2 & 9 \end{pmatrix} \begin{pmatrix} 1 & 0 \\ 5 & 3 \\ -1 & 0 \end{pmatrix} = \begin{pmatrix} a & b \\ c & d \\ e & f \end{pmatrix} \rightarrow a = 1 \times 1 + (-2) \times 5 + 4 \times (-1) = -13$$

To calculate b, which is entry (1,2), we use row 1 of the matrix on the left and column 2 of the matrix on the right:

$$\begin{pmatrix}1 & -2 & 4\\ 5 & 0 & 3\\ 0 & 1/2 & 9\end{pmatrix}\begin{pmatrix}1 & 0\\ 5 & 3\\ -1 & 0\end{pmatrix}=\begin{pmatrix}a & b\\ c & d\\ e & f\end{pmatrix}\rightarrow b=1\times 0+(-2)\times 3+4\times 0=-6$$

To calculate c, which is entry (2,1), we use row 2 of the matrix on the left and column 1 of the matrix on the right:

$$\begin{pmatrix}1 & -2 & 4\\ 5 & 0 & 3\\ 0 & 1/2 & 9\end{pmatrix}\begin{pmatrix}1 & 0\\ 5 & 3\\ -1 & 0\end{pmatrix}=\begin{pmatrix}a & b\\ c & d\\ e & f\end{pmatrix}\rightarrow c=5\times 1+0\times 5+3\times(-1)=2$$

To calculate d, which is entry (2,2), we use row 2 of the matrix on the left and column 2 of the matrix on the right:

$$\begin{pmatrix}1 & -2 & 4\\ 5 & 0 & 3\\ 0 & 1/2 & 9\end{pmatrix}\begin{pmatrix}1 & 0\\ 5 & 3\\ -1 & 0\end{pmatrix}=\begin{pmatrix}a & b\\ c & d\\ e & f\end{pmatrix}\rightarrow d=5\times 0+0\times 3+3\times 0=0$$

To calculate e, which is entry (3,1), we use row 3 of the matrix on the left and column 1 of the matrix on the right:

$$\begin{pmatrix}1 & -2 & 4\\ 5 & 0 & 3\\ 0 & 1/2 & 9\end{pmatrix}\begin{pmatrix}1 & 0\\ 5 & 3\\ -1 & 0\end{pmatrix}=\begin{pmatrix}a & b\\ c & d\\ e & f\end{pmatrix}\rightarrow e=0\times 1+1/2\times 5+9\times(-1)=-13/2$$

To calculate f, which is entry (3,2), we use row 3 of the matrix on the left and column 2 of the matrix on the right:

$$\begin{pmatrix}1 & -2 & 4\\ 5 & 0 & 3\\ 0 & 1/2 & 9\end{pmatrix}\begin{pmatrix}1 & 0\\ 5 & 3\\ -1 & 0\end{pmatrix}=\begin{pmatrix}a & b\\ c & d\\ e & f\end{pmatrix}\rightarrow f=0\times 0+1/2\times 3+9\times 0=3/2$$

The result is:

$$\begin{pmatrix}1 & -2 & 4\\ 5 & 0 & 3\\ 0 & 1/2 & 9\end{pmatrix}\begin{pmatrix}1 & 0\\ 5 & 3\\ -1 & 0\end{pmatrix}=\begin{pmatrix}-13 & -6\\ 2 & 0\\ -13/2 & 3/2\end{pmatrix}$$

✔ Example *Section*3.3.2.2

Calculate

$$\begin{pmatrix}1 & -2 & 4\\ 5 & 0 & 3\end{pmatrix}\begin{pmatrix}1\\ 5\\ -1\end{pmatrix}$$

Solution

We are asked to multiply a 2×3 matrix by a 3×1 matrix (a column vector). The result will be a 2×1 matrix (a vector).

$$\begin{pmatrix}1 & -2 & 4\\ 5 & 0 & 3\end{pmatrix}\begin{pmatrix}1\\ 5\\ -1\end{pmatrix}=\begin{pmatrix}a\\ b\end{pmatrix}$$

$$a=1\times 1+(-2)\times 5+4\times(-1)=-13$$

$$b=5\times 1+0\times 5+3\times(-1)=2$$

The solution is:

$$\begin{pmatrix}1 & -2 & 4\\ 5 & 0 & 3\end{pmatrix}\begin{pmatrix}1\\ 5\\ -1\end{pmatrix}=\begin{pmatrix}-13\\ 2\end{pmatrix}$$

Need help? The link below contains solved examples: Multiplying matrices of different shapes (three examples): http://tinyurl.com/kn8ysqq

External links:

- Multiplying matrices, example 1: http://patrickjmt.com/matrices-multiplying-a-matrix-by-another-matrix/
- Multiplying matrices, example 2: http://patrickjmt.com/multiplying-matrices-example-2/
- Multiplying matrices, example 3: http://patrickjmt.com/multiplying-matrices-example-3/

The Commutator

Matrix multiplication is not, in general, commutative. For example, we can perform

$$\begin{pmatrix} 1 & -2 & 4 \\ 5 & 0 & 3 \end{pmatrix} \begin{pmatrix} 1 \\ 5 \\ -1 \end{pmatrix} = \begin{pmatrix} -13 \\ 2 \end{pmatrix}$$

but cannot perform

$$\begin{pmatrix} 1 \\ 5 \\ -1 \end{pmatrix} \begin{pmatrix} 1 & -2 & 4 \\ 5 & 0 & 3 \end{pmatrix}$$

Even with square matrices, that can be multiplied both ways, multiplication is not commutative. In this case, it is useful to define the **commutator**, defined as:

$$[\mathbf{A}, \mathbf{B}] = \mathbf{AB} - \mathbf{BA}$$

Example *Section*3.3.2.3

Given $\mathbf{A} = \begin{pmatrix} 3 & 1 \\ 2 & 0 \end{pmatrix}$ and $\mathbf{B} = \begin{pmatrix} 1 & 0 \\ -1 & 2 \end{pmatrix}$

Calculate the commutator $[\mathbf{A}, \mathbf{B}]$

Solution

$$[\mathbf{A}, \mathbf{B}] = \mathbf{AB} - \mathbf{BA}$$

$$\mathbf{AB} = \begin{pmatrix} 3 & 1 \\ 2 & 0 \end{pmatrix} \begin{pmatrix} 1 & 0 \\ -1 & 2 \end{pmatrix} = \begin{pmatrix} 3 \times 1 + 1 \times (-1) & 3 \times 0 + 1 \times 2 \\ 2 \times 1 + 0 \times (-1) & 2 \times 0 + 0 \times 2 \end{pmatrix} = \begin{pmatrix} 2 & 2 \\ 2 & 0 \end{pmatrix}$$

$$\mathbf{BA} = \begin{pmatrix} 1 & 0 \\ -1 & 2 \end{pmatrix} \begin{pmatrix} 3 & 1 \\ 2 & 0 \end{pmatrix} = \begin{pmatrix} 1 \times 3 + 0 \times 2 & 1 \times 1 + 0 \times 0 \\ -1 \times 3 + 2 \times 2 & -1 \times 1 + 2 \times 0 \end{pmatrix} = \begin{pmatrix} 3 & 1 \\ 1 & -1 \end{pmatrix}$$

$$[\mathbf{A}, \mathbf{B}] = \mathbf{AB} - \mathbf{BA} = \begin{pmatrix} 2 & 2 \\ 2 & 0 \end{pmatrix} - \begin{pmatrix} 3 & 1 \\ 1 & -1 \end{pmatrix} = \begin{pmatrix} -1 & 1 \\ 1 & 1 \end{pmatrix}$$

$$[\mathbf{A}, \mathbf{B}] = \begin{pmatrix} -1 & 1 \\ 1 & 1 \end{pmatrix}$$

Multiplication of a vector by a scalar

The multiplication of a vector $\vec{v}_1$ by a scalar n produces another vector of the same dimensions that lies in the same direction as $\vec{v}_1$;

$$n \begin{pmatrix} x \\ y \end{pmatrix} = \begin{pmatrix} nx \\ ny \end{pmatrix}$$

The scalar can stretch or compress the length of the vector, but cannot rotate it (figure [fig:vector_by_scalar]).

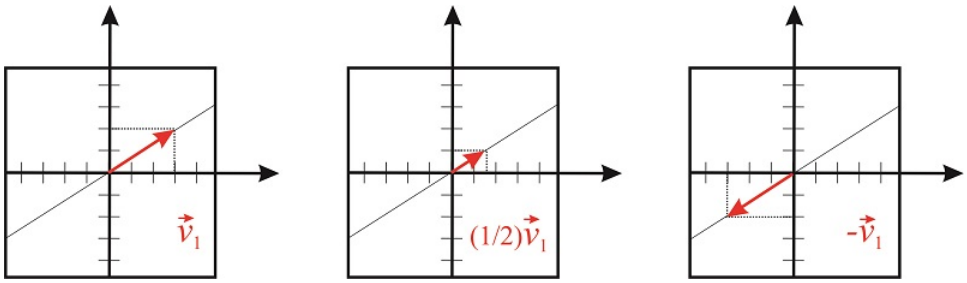


Figure *Section*3.3.2.2: Multiplication of a vector by a scalar

Multiplication of a square matrix by a vector

The multiplication of a vector $\vec{v_1}$ by a square matrix produces another vector of the same dimensions of $\vec{v_1}$. For example, we can multiply a 2×2 matrix and a 2-dimensional vector:

$$\begin{pmatrix} a & b \\ c & d \end{pmatrix} \begin{pmatrix} x \\ y \end{pmatrix} = \begin{pmatrix} ax + by \\ cx + dy \end{pmatrix}$$

For example, consider the matrix

$$\mathbf{A} = \begin{pmatrix} -2 & 0 \\ 0 & 1 \end{pmatrix}$$

The product

$$\begin{pmatrix} -2 & 0 \\ 0 & 1 \end{pmatrix} \begin{pmatrix} x \\ y \end{pmatrix}$$

is

$$\begin{pmatrix} -2x \\ y \end{pmatrix}$$

We see that 2×2 matrices act as operators that transform one 2-dimensional vector into another 2-dimensional vector. This particular matrix keeps the value of y constant and multiplies the value of x by -2 (Figure *Section*3.3.2.3).

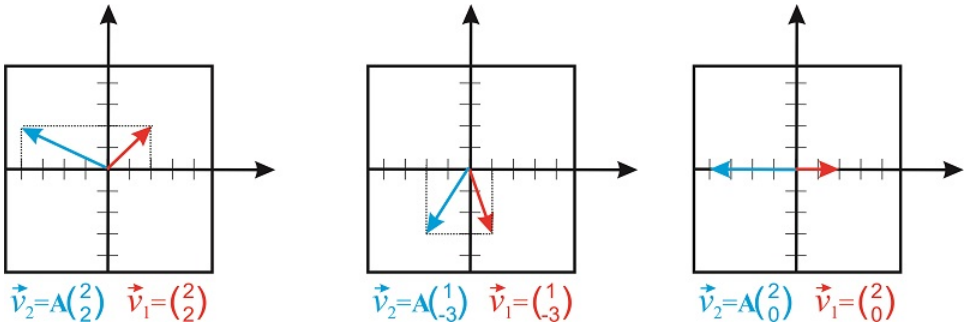


Figure *Section*3.3.2.3: Multiplication of a vector by a square matrix

Notice that matrices are useful ways of representing operators that change the orientation and size of a vector. An important class of operators that are of particular interest to chemists are the so-called symmetry operators.

Attribution

This page was adapted from Matrices (click here), contributed by Marcia Levitus, Associate Professor (Biodesign Institute) at Arizona State University.

Curated or created by Kathryn Haas

Section 3.3.2: Matrices is shared under a not declared license and was authored, remixed, and/or curated by LibreTexts.

- **4.3.1: Matrices** by Kathryn Haas is licensed CC BY-NC-SA 4.0.

Section 3.3.3: Mathematical Notation of Representations

A **representation** is a set of matrices, each of which corresponds to a symmetry operation and combine in the same way that the symmetry operators in the group combine.[1] Symmetry operators can be presented in matrices, this allows us to understand the relationship between symmetry operators through calculation from matrices. In order to understand representations, knowing matrix notions for symmetry operations is essential.

Here is some examples of symmetry operations in matrix form:

$$\text{a point in space} = \begin{bmatrix} x \\ y \\ z \end{bmatrix}$$

$$E = \begin{bmatrix} 1 & 0 & 0 \\ 0 & 1 & 0 \\ 0 & 0 & 1 \end{bmatrix}$$

$$i = \begin{bmatrix} -1 & 0 & 0 \\ 0 & -1 & 0 \\ 0 & 0 & -1 \end{bmatrix}$$

$$\sigma_{xy} = \begin{bmatrix} 1 & 0 & 0 \\ 0 & 1 & 0 \\ 0 & 0 & -1 \end{bmatrix}$$

$$\mathrm{C_n} = \begin{bmatrix} \cos\theta & -\sin\theta & 0 \\ \sin\theta & \cos\theta & 0 \\ 0 & 0 & 1 \end{bmatrix}$$

$$S_n = \begin{bmatrix} \cos\theta & -\sin\theta & 0 \\ \sin\theta & \cos\theta & 0 \\ 0 & 0 & -1 \end{bmatrix}$$

Both C_n and S_n have z set as the principal axis.

For C_n operation, θ depends on n with the relationship of $\theta = \frac{360}{n}$. If the symmetry is C_2, then θ would be 180° because the molecule is rotated 180°. For C_3, θ would be 120°, C_4 θ would be 90°, etc.

To apply a symmetry operation on an atom of a molecule, matrices can be combined to produce another operation in the group. For a C_{2v} symmetry compound such as water shown in Figure ***Section*3.3.3.1**, the operations (E, C_2, σ_{v1}, σ_{v2}) can be applied on the vector (x, y, z) to find the representation. To simplify the math, a 1x1 matrix can be done by block diagonalizing for individual vector.

Example *Section*3.3.3.1

E(y) = [1] [y] = y

C_2(y) = [-1] [y] = -y

$\sigma_{v1}(y) = \sigma_{xz}$ = [-1] [y] = -y

$\sigma_{v2}(y) = \sigma_{yz}$ = [1] [y] = y

In this example, if you apply identity (E) on vector y shown in Figure ***Section*3.3.3.2**, you would obtain y. If you apply C_2 rotation along the principal axis on y, then you would obtain -y, etc. These obtained results show the position of the vector after the symmetry operation. The coefficient of each vector after symmetry operation can be represented as Γ_y in character table ***Section*3.3.3.1**. This set of matrices each of which corresponds to the character of a matrix a **representation**[1]. The same symmetry operation can be applied on x and z to obtain a representation for Γ_x and Γ_z.

Table ***Section*3.3.3.1**: xyz representations in C_{2v}.

C_{2v}	E	C_2	σ_{v1}	σ_{v2}
Γ_z	[1]	[1]	[1]	[1]
Γ_y	[1]	[-1]	[-1]	[1]
Γ_x	[1]	[-1]	[1]	[-1]

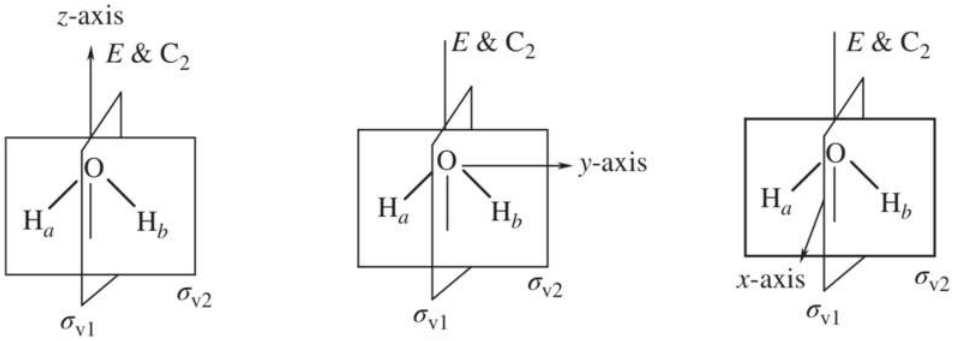


Figure *Section*3.3.3.1. Water molecule a) z-axis b) y-axis c) x-axis.

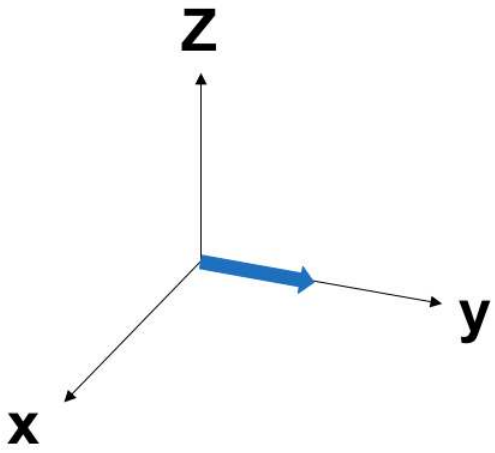


Figure *Section*3.3.3.2: y vector on a Cartesian coordinate.

A **representation** can combine in the same way that the symmetry operators in the group combine, thus, the multiplication table for the matrices that represent each symmetry operation must also multiply together in the same way that the symmetry operators themselves multiply.[1] Refer to the following tables.

Table *Section*3.3.3.1: Multiplication tables for the C_{2v} point group, showing how the 1 × 1 matrix representations multiply together in the same way that the symmetry operations do.

C_{2v}	E	C_2	σ_{v1}	σ_{v2}
E	E	C_2	σ_{v1}	σ_{v2}
C_2	C_2	E	σ_{v2}	σ_{v1}
σ_{v1}	σ_{v1}	σ_{v2}	E	C_2
σ_{v2}	σ_{v2}	σ_{v1}	C_2	E

Γ_z	[1]	[1]	[1]	[1]
[1]	[1]	[1]	[1]	[1]
[1]	[1]	[1]	[1]	[1]
[1]	[1]	[1]	[1]	[1]
[1]	[1]	[1]	[1]	[1]

Γ_y	[1]	[-1]	[-1]	[1]
[1]	[1]	[-1]	[-1]	[1]
[-1]	[-1]	[1]	[1]	[-1]
[-1]	[-1]	[1]	[1]	[-1]
[1]	[1]	[-1]	[-1]	[1]

Γ_x	[1]	[-1]	[1]	[-1]
[1]	[1]	[-1]	[1]	[-1]
[-1]	[-1]	[1]	[-1]	[1]
[1]	[1]	[-1]	[1]	[-1]
[-1]	[-1]	[1]	[-1]	[1]

Irreducible Representation and Reducible Representations

A **representation** can be categorized as **irreducible representation** and **reducible representations**. A character table is given with **irreducible representations**, which are the blue shaded part in Figure 5. There are 5 rules to irreducible representations, shown in the following box.

5 Rules to Irreducible Representations

1. The sum of the squares of the dimensions of the irreducible representations of a group is equal to the order of the group.

$$h = \sum_i l_i^2$$

2. The sum of the squares of the characters in any irreducible representation equals h.

$$h = \sum_i [\chi_i(R)^2]$$

3. The vectors whose components are the characters of two different irreducible representations are orthogonal.

$$\sum_R [\chi_i R \times \chi_j R] = 0$$

   if $i \neq j$.
4. In a given representation (reducible or irreducible), the characters of all matrices belonging to symmetry operations in the same class are identical.
5. The number of irreducible representations of a group is equal to the number of classes in the group.

The classes correspond directly to the sets of equivalent operations. Two operations belong to the same class when one may be replaced by the other in a new coordinate system that is accessible by a symmetry operation. For example, a C_7 point group would have C_7^1, C_7^2, C_7^3, C_7^4, C_7^5, C_7^6, C_7^7. Since cos(θ) = cos(θ), the characters associated with these matrices are the same. In this

case, C_7^1=C_7^6, C_7^2 = C_7^5, C_7^3 = C_7^4, and C_7^7 = E because they belong to the same class. We can simplify the C_7 point group's symmetry into 2 C_7^1, 2C_7^2, 2C_7^3, and E because there are two operations belonging to the same class.

C_{2v}	E	C_2	$\sigma_v(xz)$	$\sigma_v'(yz)$		
A_1	1	1	1	1	z	x^2, y^2, z^2
A_2	1	1	-1	-1	R_z	xy
B_1	1	-1	1	-1	x, R_y	xz
B_2	1	-1	-1	1	y, R_x	yz
Γ_σ	2	0	0	2		

$\Gamma_\sigma = A_1 + B_2$

Figure ***Section*3.3.3.3**: a) Blue shaded part: irreducible representation b) Green shaded part: reducible representation c) Yellow shaded part: Reducing reducible representations into irreducible representation

The green shaded part in Figure ***Section*3.3.3.3** is a the **reducible representation** that is found based on number of unmoved molecule after a symmetry operation. For example, if we are looking at Γ_σ of C_{2v} symmetry molecule such as water from Figure ***Section*3.3.3.3**, we would focus on the number of unmoved σ bonds after the symmetry operation. In a water molecule, there are two s bonds which are the two O-H bonds. If we apply E, both of the bonds don't move, so the reducible representation would be 2 because each unmoved σ bonds contribute to 1 reducible representation. If we apply C_2 operation on it, both bonds would move, where the O-H bonds would switch places. This means that there are zero unmoved σ bonds, so the reducible representation would be zero as shown in Figure ***Section*3.3.3.3*b***.

The yellow shaded part in Figure ***Section*3.3.3.3** is the **reduction of reducible representations** into irreducible representations. This can be done by using the formula,

$$n_i = \frac{1}{h}\sum_N \chi_R \chi_L$$

where

- n_i is the number of times the irreducible representation occurs in the reducible representation,
- N is the coefficient in front of each symmetry element symbol (shown on the top row of the character table),
- h is the order of the group (sum of the coefficients N),
- χ_R and χ_I are the characters of the reducible and irreducible representations.

Reference

1. Pfennig, Brian (2015). *Principles of Inorganic Chemistry*. Hoboken, New Jersey: John Wiley & Sons, Inc.. pp. 195–202. ISBN 978-1-118-85910-0.

Section 3.3.3: Mathematical Notation of Representations is shared under a CC BY-SA license and was authored, remixed, and/or curated by LibreTexts.

- **1.4: Representations** by Wikipedia is licensed CC BY-SA 4.0. Original source: https://en.wikibooks.org/wiki/Advanced_Inorganic_Chemistry.

Section 3.3.4: Character Tables

Definition of a Character Table

A character table is a 2 dimensional chart associated with a point group that contains the irreducible representations of each point group along with their corresponding matrix characters. It also contains the Mulliken symbols used to describe the dimensions of the irreducible representations, and the functions for symmetry symbols for the Cartesian coordinates as well as rotations about the Cartesian coordinates.

Components of a Character Table

A character table can be separated into 6 different parts, namely:

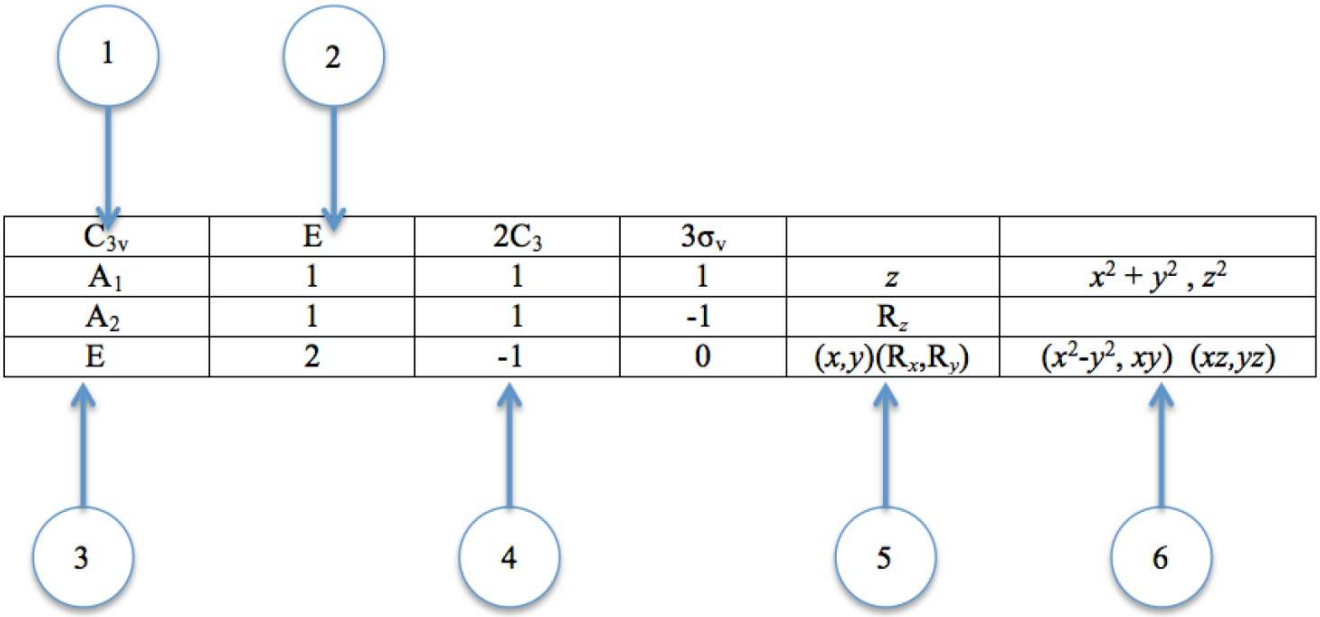


Figure *Section*3.3.4.1: An example of a character table with different parts labelled

1. The Point Group
2. The Symmetry Operation
3. The Mulliken Symbols
4. The Characters for the Irreducible Representations
5. The Functions for Symmetry Symbols for Cartesian Coordinates and Rotations
6. The Function for Symmetry Symbols for Square and Binary Products

1. The Point Group

The symbol for the point group is found on the uppermost left corner of the character table. It denotes a collection of symmetry operations that are present in a molecule. It is called a point group because all the symmetry elements will intersect at one point[1].

2. The Symmetry Operations/Elements

A symmetry operation is “a geometrical operation that moves an object about some symmetry element in a way that brings the object into an arrangement that is indistinguishable from the original”(Pfennig, 199)[2]. The symmetry operations are at the first row at the top of the table. They are organized into classes, with each class having an order number in front of it. For example, $2S_4$ represents the operation S_4 with order number 2. Operations can belong to the same class when one operation may be replaced by another in a new coordinate system that is accessible by a similar symmetry operation.

Common symmetry operations that are present in character tables are:

E	C_n	C'_n
σ_d	σ_v	σ_d
I	S_n	C''_n

3. The Mulliken Symbols

These are symbols that occur under the first column of the character table. They are named after Robert S. Mulliken, who suggested using the symbols to describe the irreducible representations. The meanings of the symbols are as follows:

- The dimensions/degeneracy of characters are denoted by the letters A,B,E,T,G and H with each letter representing degeneracy 1,1,2,3,4 and 5 respectively i.e.

Mulliken Symbol	Number of Dimensions
A,B	1
E	2
T	3
G	4
H	5

For example, the Mulliken symbol A is singly degenerate and symmetric with respect to the rotation about the principal axis whereas the symbol B is anti-symmetric with respect to rotation about the principal axis even though it is also singly degenerate[3].

- The subscripts featured with each Mulliken symbol also represent different aspects of symmetry i.e.

4. The Characters for Irreducible Representations[4]

These are the rows of numbers at the center of the character table. They represent the irreducible representations of each Mulliken symbol under the point group. A representation is “a set of matrices, each corresponding to a single operation in the group, which can be combined amongst themselves similarly to how the group elements (symmetry operations) combine” .

These characters correspond to the characters of individual symmetry operations that can be described matrices, themselves. Each character can adopt a +1 or -1 or multiple of this numerical value depending on the symmetric or anti-symmetric behavior of the object undergoing a specific symmetry operation. If the object is symmetric with respect to itself after undergoing the operation, then the character is +1. If the object is anti-symmetric, then the character is -1[5].

5. The Functions for Symmetry Symbols for Cartesian Coordinates and Rotations

These are the symbols that correspond to the symmetry of the Cartesian coordinates (x, y, z) and the symmetry of the rotations about the Cartesian coordinates (R_x, R_y, R_z). They form basis representations for the group and are related to the transformation properties of the group.

For example, for the C_{3v} point group, it can be said that z forms a basis for the A_1 representation, x forms a basis for the E representation, and R_z forms a basis for the A_2 representation.

6. The Functions for Symmetry Symbols for Square and Binary Products

These are the symbols for the functions that correspond to the square (x^2+y^2, z^2, x^2-y^2) and binary products (xy, xy, yz) of the Cartesian Coordinates with respect to their transformation properties.

For example, for the C_{3v} point group, it can be said that z^2 forms a basis for the A_1 representation, (xz,yz) forms a basis for the E representation, and there is no function for the A_2 representation.

Mathematics of Character Tables

Each character table follows some main set of mathematical operations that allow for the calculation of important characteristics of the table. These operations are as follows:

a. The order of the group (h) can be calculated by taking the sum of the order of individual symmetry operations in a character table. For example, the order of the C_{3v} point group is 6.
b. The sum of the squares of the dimensions of the irreducible representations of a group is equal to the order of the group.
c. The sum of the squares of the characters in any irreducible representation equals h.
d. The vectors whose components are the characters of two different irreducible representations are orthogonal.
e. In a given representation (reducible or irreducible) the characters of all matrices belonging to symmetry operations in the same class are identical.
f. The number of irreducible representations of a group is equal to the number of classes in the group.

Examples of Character Tables

The Character Table for the C2 Point Group

C_2	E	C_2	Linear Functions, Rotations	Quadratic Functions	Cubic Functions
A	+1	+1	z, R_z	x^2, y^2, z^2, xy	z^3, xyz, y^2z, x^2z
B	+1	-1	x, y, R_x, R_y	yz, xz	xz^2, yz^2, x^2y, xy^2, x^3, y^3

The Character Table for the Td Point Group

T_d	E	$8C_3$	$3C_2$	$6S_4$	$6\sigma_d$	Linear Functions, Rotations	Quadratic Functions	Cubic Functions
A_1	+1	+1	+1	+1	+1	-	$x^2+y^2+z^2$	xyz
A_2	+1	+1	+1	-1	-1	-	-	-
E	+2	-1	+2	0	0	-	$(2z^2-x^2-y^2, x^2-y^2)$	-
T_1	+3	0	-1	+1	-1	(R_x, R_y, R_z)	-	$[x(z^2-y^2), y(z^2-x^2), z(x^2-y^2)]$
T_2	+3	0	-1	-1	+1	x, y, z	xy, xz, yz	(x^3, y^3, z^3), $[x(z^2+y^2), y(z^2+x^2), z(x^2+y^2)]$

The Character Table for the D2d Point Group

D_{2d}	E	$2S_4$	$C_2(z)$	$2C'_2$	$2\sigma_d$	Linear Functions, Rotations	Quadratic Functions	Cubic Functions
A_1	+1	+1	+1	+1	+1	-	x^2+y^2, z^2	xyz
A_2	+1	+1	+1	-1	-1	R_z	-	$z(x^2-y^2)$
B_1	+1	-1	+1	+1	-1	-	x^2-y^2	-
B_2	+1	-1	+1	-1	+1	z	xy	z^3, $z(x^2+y^2)$
E	+2	0	-2	0	0	(x, y),(R_x, R_y)	(xz, yz)	(xz^2, yz^2), (xy^2, x^2y), (x^3, y^3)

References

1. Johnston, Dean H. "Symmetry @ Otterbein". http://symmetry.otterbein.edu/index.html
2. Pfennig, Brian W. Principles of Inorganic Chemistry. , 2015. Internet resource.
3. “Understanding Character Tables of Symmetry Groups". https://chem.libretexts.org/Core/Phy...ymmetry_Groups
4. Rowland, Todd; Weisstein, Eric W. "Character Table". http://mathworld.wolfram.com/CharacterTable.html
5. Jones, Richard. “Character Tables”. University of Texas, Austin. 2015. https://sites.cns.utexas.edu/jones_c...aracter-tables

Section 3.3.4: Character Tables is shared under a CC BY-SA license and was authored, remixed, and/or curated by LibreTexts.

- **1.5: Character Tables** by Wikipedia is licensed CC BY-SA 4.0. Original source: https://en.wikibooks.org/wiki/Advanced_Inorganic_Chemistry.

SECTION OVERVIEW

Section 3.4: Examples and Applications of Symmetry

The purpose of learning group theory is that molecular symmetry can be applied to understand the properties of molecules. This chapter introduces two applications of symmetry: chirality and molecular vibrations (in the context of analyzing IR and Raman spectra). An additional application of symmetry, to understand molecular bonding, deserves its own chapter and will be explored in Chapter 5.

Section 3.4.1: Chirality

Section 3.4.2: Molecular Vibrations

Section 3.4: Examples and Applications of Symmetry is shared under a not declared license and was authored, remixed, and/or curated by LibreTexts.

Section 3.4.1: Chirality

Introduction

Around the year 1847, the French scientist Louis Pasteur provided an explanation for the optical activity of tartaric acid salts. When he carried out a particular reaction, Pasteur observed that two types of crystals precipitated. Patiently and carefully using tweezers, Pasteur was able to separate the two types of crystals. Pasteur noticed that the types rotated plane-polarized light by the same amount but in different directions. These two compounds are called enantiomers.

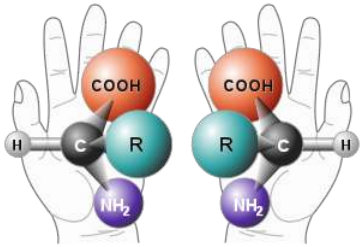


Figure *Section*3.4.1.1: Two enantiomers of an amino acid (with side chain R).

What is chirality?

A molecule is **chiral** (or **dissymetric**) if it is non-superimposable on its mirror image. The two mirror images of a chiral molecule are called enantiomers. Enantiomers have the same physical properties (e.g., melting point, etc.). They differ in their ability to rotate plane polarized light and in their reactivity with other chiral molecules. Due to their ability to rotate plane polarized light, they are referred to as being *optically active*.

Using Symmetry to Determine Chirality

There are some general rules of thumb that help determine whether a molecule is chiral or achiral. The point group of the molecule, and the symmetry operations within that point group, can give clues as to whether the molecule is chiral.

Symmetry operations of chiral molecules

A chiral molecule cannot possess a plane of symmetry (σ), a center of inversion (i), or an improper rotation (S_n). Due to the fact that all groups that lack both σ and i also lack S_n, **a molecule that belongs to any group that lacks S_n is chiral**.

An example of an inorganic coordination complex is tris(ethylenediamine)cobalt(III) (Figure *Section*3.4.1.1). Figure *Section*3.4.1.1 shows the two enantiomers of tris(ethylenediamine)cobalt(III): the **Δ** and **Λ** isomers.

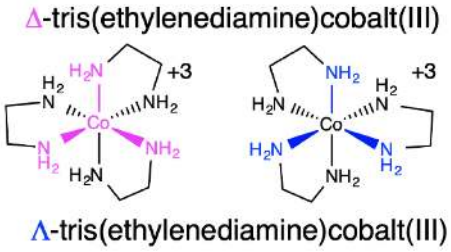


Figure *Section*3.4.1.2: Two chiral enantiomers of tris(ethylenediamine)coalt(III).

You can visualize the **Λ** and **Δ** isomers by imagining that the ligands around the metal centers are blades of a fan. To push the air toward you, you would need to rotate the **Δ** isomer clockwise, and the **Λ** isomer counter-clockwise.

Exercise *Section*3.4.1.1

Which point groups are possible for chiral molecules?

Answer

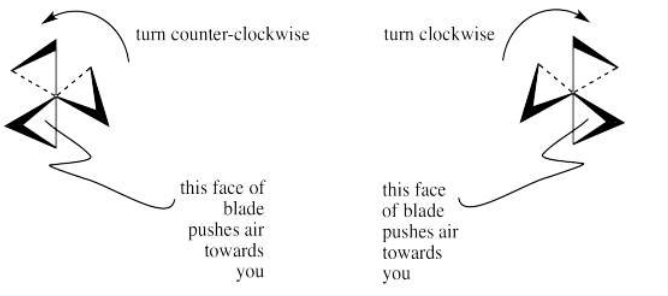


Figure ***Section*3.4.1.3**: Another way of thinking about the chirality of the two chiral enantiomers of tris(ethylenediamine)coalt(III) shown in Figure ***Section*3.4.1.2**. This figure was taken from Structure and Reactivity in Organic, Biological, and Inorganic Chemistry.

As a result of the previous discussion, there are a few classes of point groups that lack an improper axis. Those classes are C_1, C_n, and D_n.

Section 3.4.1: Chirality is shared under a CC BY-NC 4.0 license and was authored, remixed, and/or curated by LibreTexts.

- **4.4.1: Chirality** by Kathryn Haas is licensed CC BY-NC 4.0.

Section 3.4.2: Molecular Vibrations

Symmetry and group theory can be applied to understand molecular vibrations. This is particularly useful in the context of predicting the number of peaks expected in the infrared (IR) and Raman spectra of a given compound.

We will use water as a case study to illustrate how group theory is used to predict the number of peaks in IR and Raman spectra.

How many IR and Raman peaks would we expect for H_2O?

To answer this question with group theory, a pre-requisite is that you **assign the molecule's point group and assign an axis system** to the entire molecule. By convention, the z axis is collinear with the principle axis, the x axis is in-plane with the molecule or the most number of atoms. It is a good idea to stick with this convention (see Figure $Section 3.4.2.1$).

What is the point group for H_2O? (click to see answer)

H_2O has the following operations: E, C_2, σ_v, σ_v'. The point group is C_{2v}.

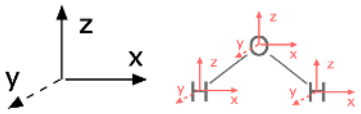


Figure $Section 3.4.2.1$: The first step to finding normal modes is to assign a consistent axis system to the entire molecule and to each atom. (CC-BY-SA; Kathryn Haas)

Now that we know the molecule's point group, we can use group theory to determine the symmetry of all motions in the molecule, or the symmetry of each of its degrees of freedom. Then we will subtract rotational and translational degrees of freedom to find the vibrational degrees of freedom. The number of degrees of freedom depends on the number of atoms (N) in a molecule. Each atom in the molecule can move in three dimensions (x, y, z), and so the number of degrees of freedom is three dimensions times N number of atoms, or $3N$. The total degrees of freedom include a number of vibrations, three translations (in x, y, and z), and either two or three rotations. Linear molecules have two rotational degrees of freedom, while non-linear molecules have three. The vibrational modes are represented by the following expressions:

$$\begin{aligned} \text{Linear Molecule Degrees of Freedom} &= 3N-5 \\ \text{Non-Linear Molecule Degrees of Freedom} &= 3N-6 \end{aligned}$$

Our goal is to find the symmetry of all degrees of freedom, and then determine which are vibrations that are IR- and Raman-active.

STEP 1: Find the reducible representation for all normal modes Γ_{modes}.

The first major step is to **find a reducible representation (Γ)** for the movement of all atoms in the molecule (including rotational, translational, and vibrational degrees of freedom). We'll refer to this as Γ_{modes}. To find normal modes using group theory, **assign an axis system** to each individual atom to represent the three dimensions in which each atom can move. Each axis on each atom should be consistent with the conventional axis system you previously assigned to the entire molecule (see Figure $Section 3.4.2.1$).

Γ_{modes} is the sum of the characters (trace) of the transformation matrix for the entire molecule (in the case of water, there are 9 degrees of freedom and this is now a 9x9 matrix). Let's walk through this step-by-step. The transformation matrix of E and C_2 are shown below:

$$E = \begin{pmatrix} 1 & 0 & 0 & 0 & 0 & 0 & 0 & 0 & 0 \\ 0 & 1 & 0 & 0 & 0 & 0 & 0 & 0 & 0 \\ 0 & 0 & 1 & 0 & 0 & 0 & 0 & 0 & 0 \\ 0 & 0 & 0 & 1 & 0 & 0 & 0 & 0 & 0 \\ 0 & 0 & 0 & 0 & 1 & 0 & 0 & 0 & 0 \\ 0 & 0 & 0 & 0 & 0 & 1 & 0 & 0 & 0 \\ 0 & 0 & 0 & 0 & 0 & 0 & 1 & 0 & 0 \\ 0 & 0 & 0 & 0 & 0 & 0 & 0 & 1 & 0 \\ 0 & 0 & 0 & 0 & 0 & 0 & 0 & 0 & 1 \end{pmatrix} \begin{pmatrix} x_{oxygen} \\ y_{oxygen} \\ z_{oxygen} \\ x_{hydrogen-a} \\ y_{hydrogen-a} \\ z_{hydrogen-a} \\ x_{hydrogen-b} \\ y_{hydrogen-b} \\ z_{hydrogen-b} \end{pmatrix} = \begin{pmatrix} x'_{oxygen} \\ y'_{oxygen} \\ z'_{oxygen} \\ x'_{hydrogen-a} \\ y'_{hydrogen-a} \\ z'_{hydrogen-a} \\ x'_{hydrogen-b} \\ y'_{hydrogen-b} \\ z'_{hydrogen-b} \end{pmatrix}, \chi = 9$$

$$C_2 = \begin{pmatrix} -1 & 0 & 0 & 0 & 0 & 0 & 0 & 0 & 0 \\ 0 & -1 & 0 & 0 & 0 & 0 & 0 & 0 & 0 \\ 0 & 0 & 1 & 0 & 0 & 0 & 0 & 0 & 0 \\ 0 & 0 & 0 & 0 & 0 & 0 & -1 & 0 & 0 \\ 0 & 0 & 0 & 0 & 0 & 0 & 0 & -1 & 0 \\ 0 & 0 & 0 & 0 & 0 & 0 & 0 & 0 & 1 \\ 0 & 0 & 0 & -1 & 0 & 0 & 0 & 0 & 0 \\ 0 & 0 & 0 & 0 & -1 & 0 & 0 & 0 & 0 \\ 0 & 0 & 0 & 0 & 0 & 1 & 0 & 0 & 0 \end{pmatrix} \begin{pmatrix} x_{oxygen} \\ y_{oxygen} \\ z_{oxygen} \\ x_{hydrogen-a} \\ y_{hydrogen-a} \\ z_{hydrogen-a} \\ x_{hydrogen-b} \\ y_{hydrogen-b} \\ z_{hydrogen-b} \end{pmatrix} = \begin{pmatrix} x'_{oxygen} \\ y'_{oxygen} \\ z'_{oxygen} \\ x'_{hydrogen-a} \\ y'_{hydrogen-a} \\ z'_{hydrogen-a} \\ x'_{hydrogen-b} \\ y'_{hydrogen-b} \\ z'_{hydrogen-b} \end{pmatrix}, \chi = 1$$

It is unnecessary to find the transformation matrix for each operation since it is only the TRACE that gives us the character, and any off-diagonal entries do not contribute to Γ_{modes}. The values that contribute to the trace can be found simply by performing each operation in the point group and assigning a value to each individual atom to represent how it is changed by that operation. If the atom moves away from itself, that atom gets a character of zero (this is because any non-zero characters of the transformation matrix are off of the diagonal). If the atom remains in place, each of its three dimensions is assigned a value of $\cos\theta$. For the example of H_2O under the C_{2v} point group, the axes that remain unchanged ($\theta = 0°$) are assigned a value of $\cos(0°) = 1$, while those that are moved into the negative of themselves (rotated or reflected to $\theta = 180°$) are assigned $\cos(180°) = -1$. The character for Γ is the sum of the values for each transformation.

Let's walk through the steps to assign characters of Γ_{modes} for H_2O to illustrate how this works:

For the operation E, performed on H_2O, all three atoms remain in place. The three axes x, y, z on each atom remain unchanged. Thus, each of the three axes on each of three atom (nine axes) is assigned the value $\cos(0°) = 1$, resulting in a sum of $\chi = 9$ for the Γ_{modes}.

For the operation C_2, the two hydrogen atoms are moved away from their original position, and so the hydrogens are assigned a value of zero. The oxygen remains in place; the z-axis on oxygen is unchanged ($\cos(0°) = 1$), while the x and y axes are inverted ($\cos(180°)$). The sum of these characters gives $\chi = -1$ in the Γ_{modes}.

Now you try! Find the characters of $\sigma_{v(xz)}$ and $\sigma_{v(yz)}$ under the C_{2v} point group. Compare what you find to the Γ_{modes} for all normal modes given below.

C_{2v}	E	C_2	σ_v	σ'_v
Γ_{modes}	9	−1	3	1

(Section 3.4.2.1)

STEP 2: Break Γ_{modes} into its component irreducible representations.

Now that we've found the Γ_{modes} (Section 3.4.2.1), we need to break it down into the individual irreducible representations (i, j, k...) for the point group. We can do this systematically using the following formula:

Misplaced '#'

In other words, the number of irreducible representations of type i is equal to the sum of the number of operations in the class × the character of the Γ_{modes} × the character of i, and that sum is divided by the order of the group (h).

Using equation ???, we find that for all normal modes of H_2O:

$$\Gamma_{modes} = 3A_1 + 1A_2 + 3B_1 + 2B_2 \qquad \text{(Section 3.4.2.2)}$$

.

Notice there are 9 irreducible representations in Equation Section 3.4.2.2. These irreducible representations represent the symmetries of all 9 motions of the molecule: vibrations, rotations, and translations.

? Exercise *Section*3.4.2.1: Derive the irreducible representation in equation Section 3.4.2.2.

Derive the nine irreducible representations of Γ_{modes} for H_2O, expression Section 3.4.2.2.

Hint

To find the number of each kind of irreducible representation that combine to form the Γ_{modes}, we need the characters of Γ_{modes} that we found above (Section 3.4.2.1), the C_{2v} character table (below), and equation ???.

C_{2v}	$1E$	$1C_2$	$1\sigma_v$	$1\sigma_v'$	$h=4$	
A_1	1	1	1	1	z	x^2, y^2, z^2
A_2	1	1	−1	−1	R_z	xy
B_1	1	−1	1	−1	x, R_y	xz
B_2	1	−1	−1	1	y, R_x	yz

In the C_{2v} point group, each class has only one operation, so the number of operations in each class (from equation ???) is 1 for each class. This has been explicitly added to the character table above for emphasis.

Answer

The number of $A_1 = \frac{1}{4}[(1\times 9\times 1) + (1\times(-1)\times 1) + (1\times 3\times 1) + (1\times 1\times 1)] = 3A_1$

The number of $A_2 = \frac{1}{4}[(1\times 9\times 1) + (1\times(-1)\times 1) + ((-1)\times 3\times 1) + ((-1)\times 1\times 1)] = 1A_2$

The number of $B_1 = \frac{1}{4}[(1\times 9\times 1) + ((-1)\times(-1)\times 1) + (1\times 3\times 1) + ((-1)\times 1\times 1)] = 3B_1$

The number of $B_2 = \frac{1}{4}[(1\times 9\times 1) + ((-1)\times(-1)\times 1) + ((-1)\times 3\times 1) + (1\times 1\times 1)] = 2B_2$

STEP 3: Subtract rotations and translations to find vibrational modes.

Because we are interested in molecular vibrations, we need to subtract the rotations and translations from the total degrees of freedom.

$$\text{Vibrations} = \Gamma_{modes} - \text{Rotations} - \text{Translations}$$

In the example of H_2O, the total degrees of freedom are given above in equation Section 3.4.2.2, and therefore the vibrational degrees of freedom can be found by:

$$\begin{aligned} &H_2O \text{ vibrations} \\ &= (3A_1 + 1A_2 + 3B_1 + 2B_2) - \text{Rotations} - \text{Translations} \end{aligned} \qquad \text{(Section 3.4.2.3)}$$

But which of the irreducible representations are ones that represent rotations and translations? The symmetry of rotational and translational degree modes can be found by inspecting the right-hand columns of any character table. Rotational modes correspond to irreducible representations that include R_x, R_y, and R_z in the table, while each of the three translational modes has the same symmetry as the x, y and z axes. For a non-linear molecule, subtract three rotational irreducible representations and three translational irreducible representations from the total Γ_{modes}.

In the specific case of water, we refer to the C_{2v} character table:

C_{2v}	E	C_2	σ_v	σ_v'	$h=4$	
A_1	1	1	1	1	z	x^2, y^2, z^2
A_2	1	1	−1	−1	R_z	xy
B_1	1	−1	1	−1	x, R_y	xz
B_2	1	−1	−1	1	y, R_x	yz

In C_{2v}, translations correspond to B_1, B_2, and A_1 (respectively for x, yz), and rotations correspond to B_2, B_1, and A_1 (respectively for R_x, R_y, R_z). Subtracting these six irreducible representations from Γ_{modes} will leave us with the irreducible representations for vibrations.

$$\begin{aligned} H_2O \text{ vibrations} &= \Gamma_{modes} - \text{Rotations} - \text{Translations} \\ &= (3A_1 + 1A_2 + 3B_1 + 2B_2) - (A_1 + B_1 + B_2) - (A_2 + B_1 + B_2) \\ &= 2A_1 + 1B_1 \end{aligned}$$

The three vibrational modes for H_2O are $2A_1 + 1B_1$. Note that we have the correct number of vibrational modes based on the expectation of $3N - 6$ vibrations for a non-linear molecule.

STEP 4: Determine which of the vibrational modes are IR-active and Raman-active.

The next step is to determine which of the vibrational modes is IR-active and Raman-active. To do this, we apply the IR and Raman Selection Rules below:

IR and Raman Selection Rules

Infrared selection rules:

If a vibration results in the change in the molecular dipole moment, it is IR-active. In the character table, we can recognize the vibrational modes that are IR-active by those with symmetry of the x, y, and z axes.

In C_{2v}, any vibrations with A_1, B_1 or B_2 symmetry would be IR-active.

Raman selection rules:

If a vibration results in a change in the molecular polarizability, it will be Raman-active. In the character table, we can recognize the vibrational modes that are Raman-active by those with symmetry of any of the binary products (xy, xz, yz, x^2, y^2, and z^2) or a linear combination of binary products (e.g. $x^2 - y^2$).

In C_{2v}, any vibrations with A_1, A_2, B_1 or B_2 symmetry would be Raman-active.

In our H_2O example, we found that of the three vibrational modes, two have A_1 and one has B_1 symmetry. Both A_1 and B_1 are IR-active, and both are also Raman-active. ***There are two possible IR peaks and three possible Raman peaks expected for water***.*

*It is important to note that this prediction tells only what is possible, but not what we might actually see in the IR and Raman spectra. For example, if the two IR peaks overlap, we might actually notice only one peak in the spectrum. Or, if one or more peaks is off-scale, we wouldn't see it in actual data. Group theory tells us what is *possible and allows us to make predictions or interpretations of spectra*.

Summary of Analysis for Water

Each molecular motion for water, or any molecule, can be assigned a symmetry under the molecule's point group. For water, we found that there are a total of 9 molecular motions; $3A_1 + A_2 + 3B_1 + 2B_2$. Six of these motions are not the translations and rotations. The remaining motions are vibrations; two with A_1 symmetry and one with B_1 symmetry.

We can tell what these vibrations would look like based on their symmetries. The two A_1 vibrations must be completely symmetric, while the B_1 vibration is antisymmetric with respect to the principal C_2 axis.

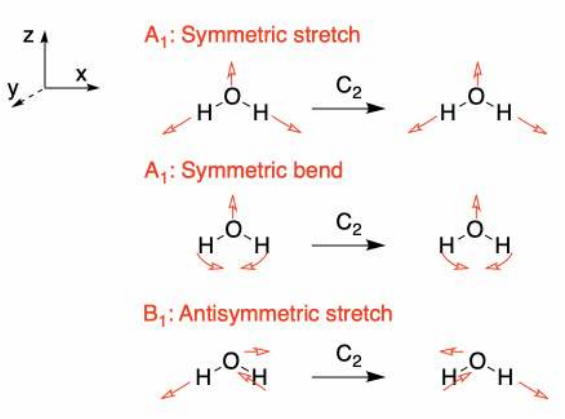


Figure *Section*3.4.2.2: Illustration of the vibrational motions of water. The antisymmetric stretch has B_1 symmetry, while the symmetric stretch and symmetric bend both have A_1 symmetry. (Click here to see animation) (CC-BY-NC-SA; Kathryn Haas)

Table *Section*3.4.2.1: Summary of the Symmetry of Molecular Motions for Water

All Motions (step 2 above)	Translations (x,y,z)	Rotations (R_x, R_y, R_z)	**Remaining Vibrations**	Description of Vibration
$3A_1$	$1A_1$		$2A_1$	One is a symmetric stretch. The other is a symmetric bend. Both are *IR-active* and *Raman-active*
A_2		$1A_2$		
$3B_1$	$1B_1$	$1B_1$	$1B_1$	Antisymmetric stretch that is *IR-active* and *Raman-active*.
$2B_2$	$1B_2$	$1B_2$		

? Exercise *Section*3.4.2.2

Find the symmetries of all motions of the square planar complex, tetrachloroplatinate (II). Determine which are rotations, translations, and vibrations. Determine which vibrations are IR and Raman active.

Answer

The point group of $[PtCl_4]^{2-}$ is D_{4h} (refer to its character table). There are five atoms and 15 vectors (x, y, z for each atom × 5 atoms).

STEP 1: The first major step is to **find a reducible representation (Γ)** for the movement of all atoms in the molecule.

C_{2v}	E	$2C_4$	C_2	$2C_2'$	$2C_2''$	i	$2S_4$	σ_h	$2\sigma_v$	$2\sigma_d$
Γ_{modes}	15	1	−1	−3	−1	−3	−1	5	3	1

(Section 3.4.2.4)

.

STEP 2: Break Γ_{modes} into its component irreducible representations.

Following the process described earlier, we come to $A_{1g} + A_{2g} + B_{1g} + B_{2g} + E_g + 2A_{2u} + B_{2u} + 3E_u$. This accounts for all modes of movement, including rotations and translations.

STEP 3: Subtract rotations and translations to find vibrational modes.

The translations are $A_{2u} + E_u$ and the rotations are $A_{2g} + E_g$.
The remaining normal modes are: $A_{1g} + B_{1g} + B_{2g} + A_{2u} + B_{2u} + 2E_u$

STEP 4: Determine which of the vibrational modes are IR-active and Raman-active:

$A_{2u} + E_u$ are IR-active. Since A_{2u} is singly degenerate and E_u is doubly degenerate, we expect three possible IR bands.
$A_{1g} + B_{1g} + B_{2g}$ are Raman-Active. Each of these is singly degenerate, so we expect three possible Raman bands.

Selected Vibrational Modes

The interpretation of CO stretching vibrations in an IR spectrum is particularly useful. Symmetry and group theory can be applied to predict the number of CO stretching bands that appear in a vibrational spectrum for a given metal coordination complex. A classic example of this application is in distinguishing isomers of metal-carbonyl complexes. For example, the *cis*- and *trans*-isomers of square planar metal dicarbonyl complexes ($ML_2(CO)_2$) have a different number of IR stretches that can be predicted and interpreted using symmetry and group theory. Another example is the case of *mer*- and *fac*- isomers of octahedral metal tricarbonyl complexes ($ML_3(CO)_3$). Structures of the two types of metal carbonyl configurations and their isomers are shown in Figure ***Section*3.4.2.1**. The isomers in each case can be distinguished using vibrational spectroscopy.

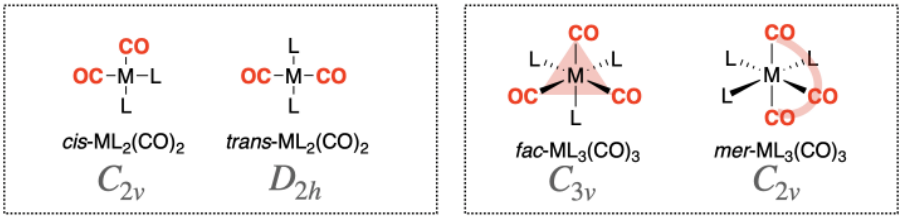


Figure ***Section*3.4.2.3**: Cis- and *trans*- isomers of square planar metal dicarbonyl complexes ($ML_2(CO)_2$) are shown in the left box. *Mer*- and *fac*- isomers of octahedral metal tricarbonyl complexes ($ML_3(CO)_3$) are shown in the right box. The point group for each of the general structures is also shown. (CC-BY-NC-SA; Kathryn Haas)

EXAMPLE 1: Distinguishing *cis*- and *trans*- isomers of square planar metal dicarbonyl complexes

General structures of the *cis*- and *trans*- isomers of square planar metal dicarbonyl complexes ($ML_2(CO)_2$) are shown in the left box in Figure ***Section*3.4.2.1**. We can use symmetry and group theory to predict how many carbonyl stretches we should expect for each isomer following the steps below.

Step 1: Assign the point group and Cartesian coordinates for each isomer.

The *cis*-isomer has C_{2v} symmetry and the *trans*-isomer has D_{2h} symmetry. We assign the Cartesian coordinates so that z is colinear with the principle axis in each case. For the D_2h isomer, there are several orientations of the z axis possible. The axes shown in Figure ***Section*3.4.2.2** will be used here.



Figure ***Section*3.4.2.4**: Cis- and *trans*- isomers of square planar metal dicarbonyl complexes ($ML_2(CO)_2$) are shown and oriented with respect to the Cartesian coordinates shown at the left so that the highest-order rotation axis is colinear with z and the molecule is co-planar with the xz plane. The vector along each C—O bond is shown using a red arrow (→). These vectors represent the direction of C—O stretching motions. (CC-BY-NC-SA; Kathryn Haas)

Step 2: Produce a reducible representation (Γ) for CO stretches in each isomer

First, assign a vector along each C—O bond in the molecule to represent the direction of C—O stretching motions, as shown in Figure ***Section*3.4.2.2** (red arrows →). These vectors are used to produce a reducible representation (Γ) for the C—O stretching motions in each molecule. Using the symmetry operations under the appropriate character table, assign a value of 1 to each vector that remains in place during the operation, and a value of 0 if the vector moves out of place. There will be no occasion where a vector remains in place but is inverted, so a value of -1 will not occur.

https://chem.libretexts.org/@go/page/456652

cis- $ML_2(CO)_2$:

For *cis*- $ML_2(CO)_2$, the point group is C_{2v} and so we use the operations under the C_{2v} character table to create the Γ_{cis-CO}.

$\mathbf{C_{2v}}$	E	C_2	$\sigma_v(xz)$	$\sigma'_v(yz)$
$\mathbf{\Gamma_{cis-CO}}$	2	0	2	0

trans- $ML_2(CO)_2$:

For trans- $ML_2(CO)_2$, the point group is D_{2h} and so we use the operations under the D_{2h} character table to create the $\Gamma_{trans-CO}$.

$\mathbf{D_{2h}}$	E	$C_2(z)$	$C_2(y)$	$C_2(x)$	i	$\sigma(xy)$	$\sigma(xz)$	$\sigma(yz)$
$\mathbf{\Gamma_{trans-CO}}$	2	0	0	2	0	2	2	0

Step 3: Break each Γ into its component irreducible representations

Each Γ can be reduced using inspection or by the systematic method described previously.

In the case of the *cis*- $ML_2(CO)_2$, the CO stretching vibrations are represented by A_1 and B_1 irreducible representations:

$\mathbf{C_{2v}}$	E	C_2	$\sigma_v(xz)$	$\sigma'_v(yz)$		
$\mathbf{\Gamma_{cis-CO}}$	2	0	2	0		
A_1	1	1	1	1	z	x^2, y^2, z^2
B_1	1	−1	1	−1	x, R_y	xz

(Section 3.4.2.5)

In the case of *trans*- $ML_2(CO)_2$, the CO stretching vibrations are represented by A_1 and B_{3u} irreducible representations:

$\mathbf{D_{2h}}$	E	$C_2(z)$	$C_2(y)$	$C_2(x)$	i	$\sigma(xy)$	$\sigma(xz)$	$\sigma(yz)$	
$\mathbf{\Gamma_{trans-CO}}$	2	0	0	2	0	2	2	0	
A_g	1	1	1	1	1	1	1	1	$x^2,\ y^2,\ z^2$
B_{3u}	1	−1	−1	1	−1	1	1	−1	x

These irreducible representations correspond to the symmetries of only the selected C—O vibrations. Since these motions are isolated to the C—O group, they do not include any rotations or translations of the entire molecule, and so we do not need to find and subtract rotationals or translations (unlike the previous cases where all motions were considered).

Step 4: Determine which vibrational modes are IR-active and/or Raman-active

Apply the infrared selection rules described previously to determine which of the CO vibrational motions are IR-active and Raman-active. The two isomers of $ML_2(CO)_2$ are described below.

In the case of the *cis*- $ML_2(CO)_2$, the CO stretching vibrations are represented by A_1 and B_1 irreducible representations. The characters of both representations and their functions are shown above, in Section 3.4.2.5 (and can be found in the C_{2v} character table). Under C_{2v}, both the A_1 and B_1 CO vibrational modes are IR-active and Raman-active. Therefore, two bands in the IR spectrum and two bands in the Raman spectrum are possible.

In the case of the trans- $ML_2(CO)_2$, the CO stretching vibrations are represented by A_g and B_{3u} irreducible representations. The characters of both representations and their functions are shown above, in Section 3.4.2.5 (and can be found in the D_{2h} character table). Under D_{2h}, the A_g vibrational mode is is Raman-active only, while the B_{3u} vibrational mode is IR-active only. Therefore, only one IR band and one Raman band are possible for this isomer.

Summary

It is possible to distinguish between the two isomers of square planar $ML_2(CO)_2$ using either IR or Raman vibrational spectroscopy. The *cis*- $ML_2(CO)_2$ can produce two CO stretches in an IR or Raman spectrum, while the *trans*- $ML_2(CO)_2$ isomer can produce only one band in either type of vibrational spectrum. If a sample of $ML_2(CO)_2$ produced two CO stretching bands, we could rule out the possibility of a pure sample of *trans*-$ML_2(CO)_2$.

? Exercise *Section*3.4.2.3

Repeat the steps outlined above to determine how many CO vibrations are possible for *mer*-$ML_3(CO)_3$ and *fac*-$ML_3(CO)_3$ isomers (see Figure ***Section*3.4.2.1**) in both IR and Raman spectra. Could either of these vibrational spectroscopies be used to distinguish the two isomers?

Answer

Step 1: Assign the point group and Cartesian coordinates for each isomer.
The *fac*-isomer is C_{3v}. The *mer*-isomer is C_{2v}.

Step 2: Produce a reducible representation for CO stretches in each isomer.

Step 3: Break each into its component irreducible representations.

Step 4: Determine which vibrational modes are IR-active and/or Raman-active.

***For fac*-$ML_3(CO)_3$**, the point group is C_{3v} and so we use the operations under the C_{3v} character table to create the Γ_{fac-CO}. Then break it into its irreducible representations and determine which are IR and Raman active:

C_{3v}	E	$2C_2$	$3\sigma_v$
Γ_{fac-CO}	3	0	1

This reduces to $A_1 + E$. Both of these are IR active, and since one is singly degenerate while the other is doubly degenerate, we expect three possible IR bands from this isomer. Both vibrational modes are also Raman active, and again we would expect three possible bands in the Raman spectrum.

For mer-$ML_3(CO)_3$, the point group is C_{2v} and so we use the operations under the C_{2v} character table to create the Γ_{mer-CO}. Then break it into its irreducible representations and determine which are IR and Raman active:

C_{2v}	E	C_2	$\sigma_v(xz)$	$\sigma'_v(yz)$
Γ_{mer-CO}	3	1	3	1

This reduces to $2A_1 + B_1$; both A_1 and B_1 are IR and Raman active. So this isomer would have three possible IR bands and three possible Raman Bands.

These two isomers have the same number of possible bands in both IR and Raman spectroscopy. It would not be straightforward to distinguish them from each other based on the number of possible bands in the vibrational spectrum.

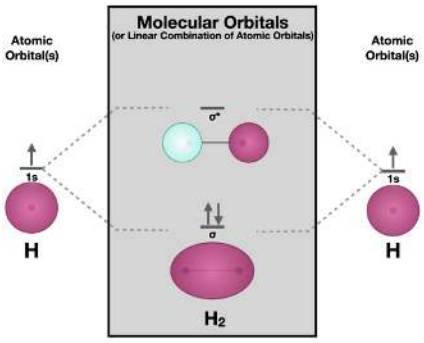
This page titled Section 3.4.2: Molecular Vibrations is shared under a CC BY-NC 4.0 license and was authored, remixed, and/or curated by Kathryn Haas.

- **4.4.2: Molecular Vibrations** by Kathryn Haas is licensed CC BY-NC 4.0.

CHAPTER OVERVIEW

Chapter 4: Molecular Orbitals

Molecular Orbital Theory



Molecular Orbital (MO) Theory is a sophisticated bonding model. It is generally considered to be more powerful than *Lewis* and *Valence Bond Theories* for predicting molecular properties; however, this power comes at the price of complexity. In its full development, MO Theory requires complex mathematics, though the ideas behind it are simple. Atomic orbitals (AOs) that are localized on individual atoms combine to make molecular orbitals (MOs) that are distributed over the molecule. The simplest example is the molecule dihydrogen (H_2), in which two independent hydrogen 1s orbitals combine to form the σ bonding MO and the σ antibonding MO of the dihydrogen molecule (see figure). The MO's are also called Linear Combinations of Atomic Orbitals (LCAO).

Section 4.1: Formation of Molecular Orbitals from Atomic Orbitals

Section 4.1.1: Molecular Orbitals from s Orbitals

Section 4.1.2: Molecular Orbitals from p Orbitals

Section 4.1.3: Molecular orbitals from d orbitals

Section 4.1.4: Nonbonding Orbitals and Other Factors

Section 4.2: Molecular Orbital Theory of Diatomic Molecules

Section 4.2.1: Orbital Overlap

Section 4.2.2: Homonuclear Diatomic Molecules

Section 4.2.3: Heteronuclear Diatomic Molecules

Section 4.2.4: Orbital Mixing

Section 4.2.5: Diatomic Molecules of the First and Second Periods

Section 4.2.6: Photoelectron Spectroscopy

Section 4.3: Larger (Polyatomic) Molecules

Section 4.3.1: Bifluoride anion

Section 4.3.2: Carbon Dioxide

Section 4.3.3: H_2O

Section 4.3.4: NH_3

Section 4.3.5: CO_2 (Revisted with Projection Operators)

Section 4.3.6: BF_3

Section 4.4: Problems

This page titled Chapter 4: Molecular Orbitals is shared under a CC BY-NC-SA 4.0 license and was authored, remixed, and/or curated by Kathryn Haas.

Section 4.1: Formation of Molecular Orbitals from Atomic Orbitals

Molecular orbital theory extends from quantum theory and the atomic orbital wavefunctions (ψ) described by the Schrödinger equation. While the Schrödinger equation defines a Ψ for electrons in individual atoms, we can approximate the molecular wavefunction (what Ψ would look like if we combined the ψ of individual atoms). The addition or subtraction of wavefunctions is termed **linear combination of atomic orbitals** (LCAO). Molecular orbital theory is applied to LCAO to describe bonding.

The LCAO for the wavefunction of two atoms (ψ_a and ψ_b) is represented by the general expression below. The coefficients c_a and c_b quantify the contribution of each atomic ψ to the molecular Ψ.

$$\Psi = c_a\psi_a + c_b\psi_b$$

For two atomic ψs to form a bond, three conditions must be satisfied:

- First, the **distance between the atoms** must be small enough to provide good overlap. This is because the two orbitals must be able to overlap using regions of ψ^2 where the probability of finding electrons is significant. If atoms are not close enough, ψ_a and ψ_b cannot interact productively. At the same time, the atoms must be far enough apart that their nuclei do not repel each other.
- The **symmetry of the orbitals** must be compatible such that regions of ψ_a and ψ_b with the same sign constructively interfere more than regions with opposite sign destructively interfere. In other words, for a productive interaction, there must be a relatively high probability of finding an electron between the two nuclei, and this depends on the symmetry (and sign of the ψ) of the atomic orbitals.
- Third, the **energies of the atomic orbitals** must be similar. Orbitals with similar energy combine to make the most stable bonding molecular orbitals. Atomic orbitals with very different energies form less stable bonding interactions, and the larger the difference in the atomic orbitals, the weaker the bonding interaction will be.

Atomic orbitals combine to form molecular orbitals when these three conditions are met. The result is a set of bonding molecular orbitals that are lower in energy than the original atomic orbital energies.

This page titled Section 4.1: Formation of Molecular Orbitals from Atomic Orbitals is shared under a CC BY-NC-SA 4.0 license and was authored, remixed, and/or curated by Kathryn Haas.

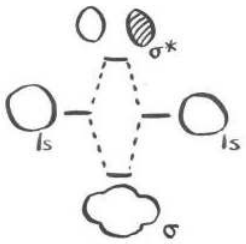
- **5.1: Formation of Molecular Orbitals from Atomic Orbitals** by Kathryn Haas is licensed CC BY-SA 4.0.

Section 4.1.1: Molecular Orbitals from s Orbitals

In the case of the hydrogen molecule, we took two atomic orbitals and combined them to form two molecular orbitals. These new molecular orbitals had different wavelengths than the two atomic orbitals: one had a longer wavelength and was a little lower in energy, while the other had a shorter wavelength and was a little higher in energy. If we take into account the energy of the two original atomic wavefunctions, and compare them to the total energy of the two new molecular wavefunctions, there is no change overall.

We started with two atomic orbitals, and by combining them we produced two molecular orbitals. Both of these ideas are useful in considering the formation of more complex molecules from individual atoms.

- The average energy of the orbitals has remained almost constant.
- Also, the number of wavefunctions has remained constant.



Of course, from the point of view of the two real electrons, some remarkable changes have occurred. Both of these electrons have adopted a longer wavelength and a lower energy and that has made all the difference. There is an occupied molecular orbital and an unoccupied molecular orbital; only the occupied orbital makes a real energetic contribution to the overall stability of the molecule. The unoccupied orbital is completely imaginary.

A bonding picture of He_2 would look exactly the same, because it would also involve the overlap of 1s electrons on one atom with 1s electrons on the other atom. There would be a different electronic energy, however. That difference would affect the prospects of helium-helium bond formation.

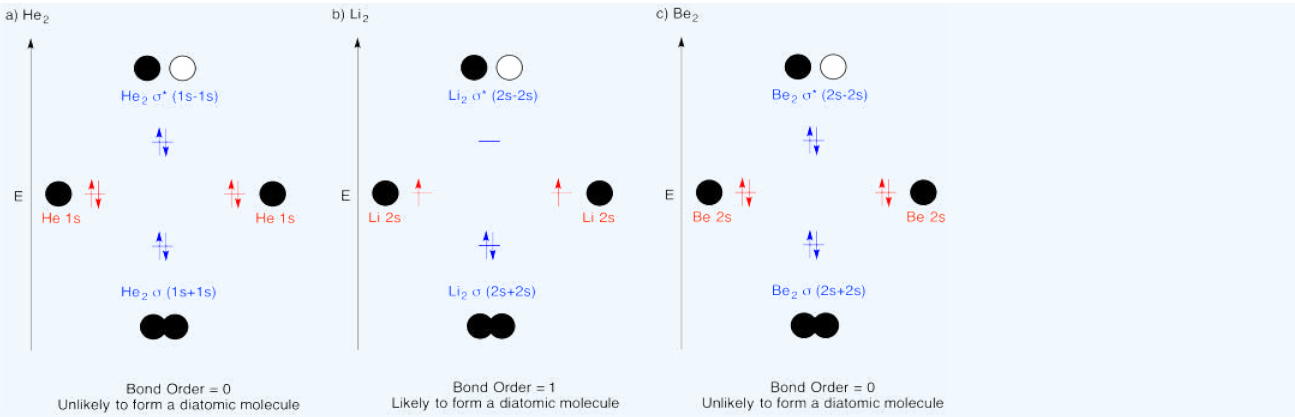
- The electrons have lower kinetic energy in the bond than they had before bonding.
- Electronic energy has decreased. A stable bond has formed.

? Exercise *Section*4.1.1.1

Construct molecular orbital diagrams for the following diatomic species and discuss the likelihood of bond formation in each case.

a. He_2.
b. Li_2.
c. Be_2.

Answer



This page titled Section 4.1.1: Molecular Orbitals from s Orbitals is shared under a CC BY-NC-SA 3.0 license and was authored, remixed, and/or curated by Chris Schaller & Kathryn Haas.

Section 4.1.2: Molecular Orbitals from p Orbitals

Bonding with P-orbitals

Sigma bonding with p-orbitals

Other diatomic molecules in the upper right corner of the periodic table can be constructed in a similar way. Look at dinitrogen, N_2.

We can think about how dinitrogen would form if two nitrogen atoms were placed close enough together to share electrons. Nitrogen has more electrons than hydrogen, so this interaction is more complicated.

In our qualitative examination of bonding in main group diatomics, we will take the approach used in Lewis structures and just look at the valence electrons. A quantitative molecular orbital calculation with a computer would not take this shortcut, but would include all of the electrons in the atoms that are bonding together.

Nitrogen has five valence electrons, and these electrons are found in the 2s and 2p levels. There are three possible atomic orbitals in the 2p level where some of these electrons could be found: p_x, p_y and p_z. We need to look at the interaction between the s and p_x, p_y and p_z orbitals on one nitrogen atom with the s and p_x, p_y and p_z orbitals on the other nitrogen. That process could be extremely complicated, but:

- Orbital interactions are governed by symmetry.

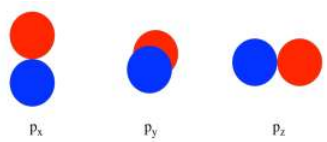
Orbitals interact most easily with other orbitals that have the same element of symmetry. For now, we can simplify and say that orbitals on one atom only interact with the same type of orbitals on the other atom.

- s orbitals interact with s orbitals. We can already see how that will work out in dinitrogen, because that is what happened in dihydrogen.
- p_x orbitals interact with p_x orbitals.
- p_y orbitals interact with p_y orbitals.
- p_z orbitals interact with p_z orbitals.

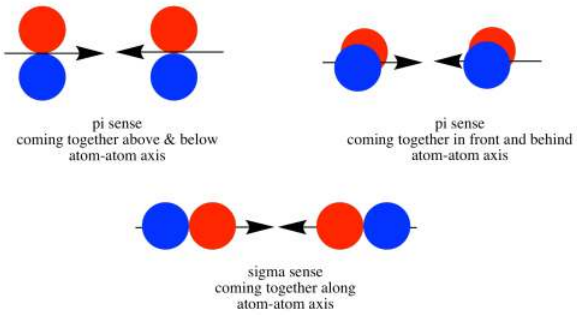
Another complication here is that the s and p orbitals do not start out at the same energy level. When the orbitals mix, one combination goes up in energy and one goes down. Does the s antibonding combination go higher in energy than the combinations from p orbitals? Do the p bonding combinations go lower in energy than the combinations from s orbitals? We will **simplify** and **assume** that the s and p levels remain completely separate from each other. This is not always true, but the situation varies depending on what atoms we are dealing with.

- The combination of one s orbital with another is just like in hydrogen. Two original orbitals will combine and rearrange to produce two new orbitals.
- There is a bonding combination in which the orbitals are in phase. The new orbital produced has a longer wavelength than the original orbital. It is lower in energy.
- There is an antibonding combination in which the orbitals are out of phase. The new orbital produced has a shorter wavelength than the original orbital. It is higher in energy.

In considering the interaction of two p orbitals, we have to keep in mind that p orbitals are directional. A p orbital lies along a particular axis: x, y or z. The three p orbitals on nitrogen are all mutually perpendicular (or orthogonal) to each other. That situation is in contrast to s orbitals, which are spherical and thus look the same from any direction.

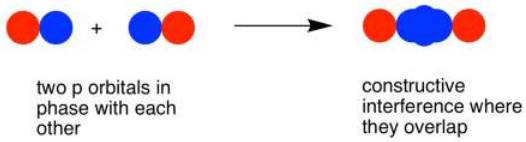


We first need to define one axis as lying along the N-N bond. It does not really matter which one. We arbitrarily say the N-N bond lies along the z axis. The p_z orbitals have a different spatial relationship to each other compared to the p_y and p_x. The p_z orbitals lie along the bond axis, whereas the p_y and p_x are orthogonal to it.

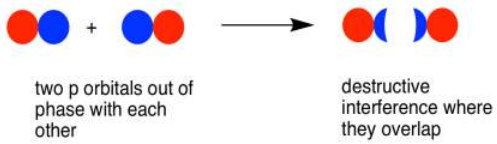


As the nitrogen atoms are brought together, one lobe on one p_z orbital overlaps strongly with one lobe on the other p_z orbital. The other lobes point away from each other and do not interact in any obvious way.

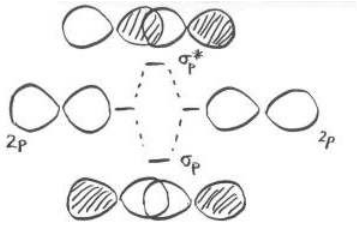
As with the s orbital, the p_z orbitals can be in-phase or out-of-phase. The in-phase combination results in constructive interference. (Here, "in-phase" means the lobes that overlap are in-phase; for that to happen the two p orbitals are actually completely out-of-phase with each other mathematically, so that one orbital is the mirror image of the other.) This combination is at a longer wavelength than the original orbital. It is a lower energy combination.



The out-of-phase combination (meaning in this case that the overlapping lobes are out-of-phase) results in destructive interference. This combination is at shorter wavelength than the original orbital. It is a higher energy combination.



As a result, we have two different combinations stemming from two different p orbitals coming together in two different ways. We get a low-energy, in-phase, bonding combination and a high-energy, out-of-phase, antibonding combination.

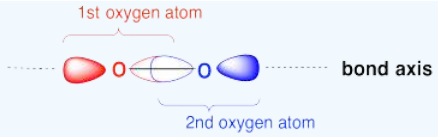


What about those other p orbitals, the ones that do not lie along the bond axis? We'll take a look at that problem on the next page.

? Exercise *Section*4.1.2.2

Draw an MO cartoon of a sigma bonding orbital formed by the overlap of two p orbitals between two oxygen atoms. Label the positions of the oxygen nuclei with the symbol "O". Label the O-O bond axis.

Answer



Exercise *Section*4.1.2.3

Chemical reactions can be described by MO diagrams too! Consider the following reaction in which a new sigma bond is formed.



Draw an MO diagram for the reaction above. In other words, start from the one frontier MO on each reactant to build the MO's of the new sigma bond in the product.

o Draw the orbital from the base (hydroxide) that is likely to donate its electrons.

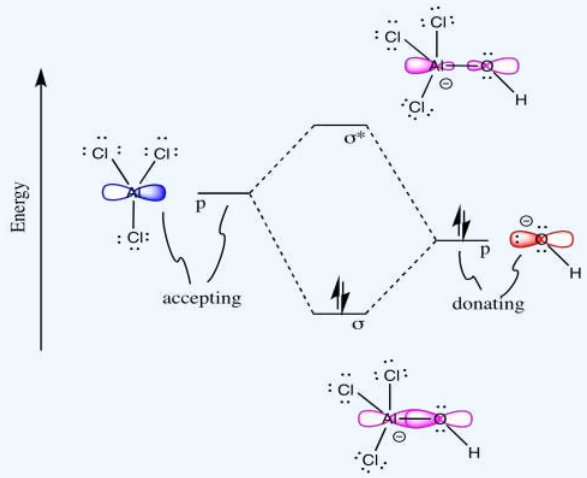
o Draw the orbital from the acid (aluminum chloride) that is likely to accept electrons.

o Complete the MO mixing diagram of these two orbitals:

- Label the electron donating orbital
- Label the electron accepting orbital
- Populate the MO mixing diagram with electrons

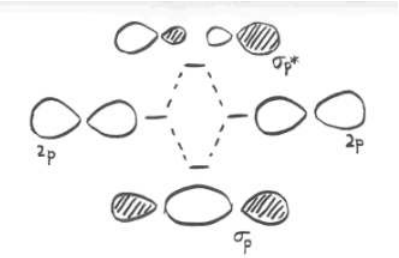
o Draw a cartoon showing each reactant and product MO that contributes to the bonding interaction.

Answer



Pi-bonding with p-orbitals

Earlier, we saw that p orbitals that lie along the same axis can interact to form bonds.



Parallel, but not collinear, p orbitals can also interact with each other. They would approach each other side by side, above and below the bond axis between the two atoms. They can be close enough to each other to overlap, although they do not overlap as strongly as orbitals lying along the bond axis. They can make an in-phase combination, as shown below.

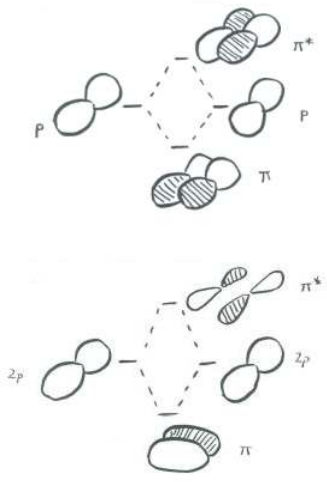


They could also make an out-of-phase combination, as shown below.



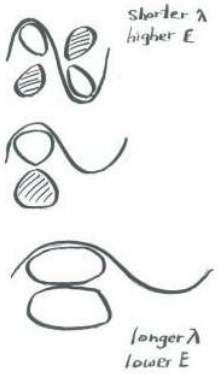
- parallel p orbitals can overlap to produce bonding and antibonding combinations.
- the resulting orbitals contain nodes along the bond axis.
- the electron density is found above and below the bond axis.
- this is called a p (pi) bond.

The illustration above is for one set of p orbitals that are orthogonal to the bond axis. The second picture shows the result of the constructive (or destructive) interference. A similar picture could be shown for the other set of p orbitals.

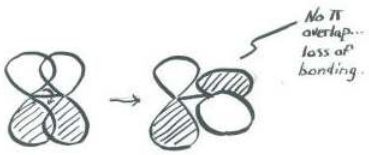


In a main group diatomic species like dinitrogen, one p orbital lying along the bond axis can engage in s bonding. The two p orbitals orthogonal to the bond axis can engage in p bonding. There will be both bonding and antibonding combinations.

Just as the sigma-bonding orbitals display progressively shorter wavelengths along the bonding axis as they go to higher energy, so do the pi bonding orbitals. In other words, there are more nodes in the higher-energy orbitals than in the lower-energy ones.



An important consequence of the spatial distribution or "shape" of a p orbital is that it is not symmetric with respect to the bond axis. An s orbital is not affected when the atom at one end of the bond is rotated with respect to the other. A p orbital is affected by such a rotation. If one atom turns with respect to the other, the p orbital would have to stretch to maintain the connection. The orbitals would not be able to overlap, so the connection between the atoms would be lost.



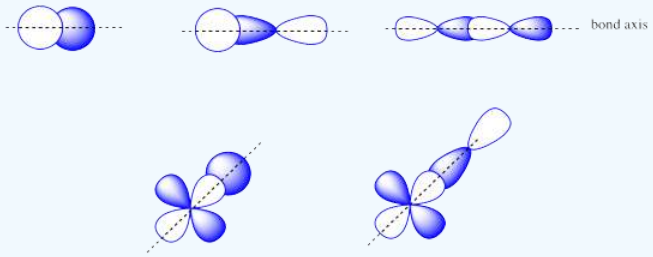
? Exercise *Section*4.1.2.4

The combinations of _____ atomic orbitals leads to σ orbitals.

Draw pictures.

Answer

The combinations of ***s*** + ***s*** OR ***s*** + ***p*** OR ***p*** + ***p*** OR ***s*** + ***d*** OR ***p*** + ***d*** atomic orbitals can lead to σ orbitals.



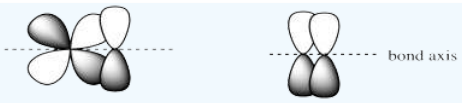
? Exercise *Section*4.1.2.5

The combinations of _____ atomic orbitals leads to π orbitals.

Draw pictures.

Answer

The combinations of side by side p + p or p + d atomic orbitals leads to π orbitals.



Exercise *Section*4.1.2.6

Which molecular orbital is typically the highest in energy?

a. p
b. σ
c. π*
d. π
e. σ*

Answer

e) σ*

Exercise *Section*4.1.2.7

Why would a *core* 1s orbital not interact with a *valence* 2s orbital?

Hint: Why is a Li_2O bond stronger than a K_2O bond?

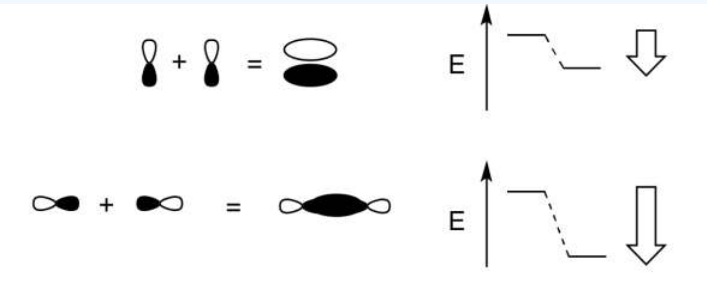
Answer

Li^+ and O^{2-} are more similar in size than K^+ and O^{2-}, so the bond between Li^+ and O^{2-} is stronger.

The energy difference between any core orbitals and valence orbitals is too large, so they cannot interact. In order for orbitals to interact, the orbitals need to have the same symmetry, be in the same plane, and be similar in energy.

Exercise *Section*4.1.2.8

Add a few words to explain the ideas conveyed in these drawings.



Answer

When two parallel p orbitals combine out-of-phase, destructive interference occurs.

There is a node between the atoms.

The energy of the electrons increases.

When two parallel p orbitals combine in-phase, constructive interference occurs.

There is no node between the atoms; the electrons are found above and below the axis connecting the atoms.

The energy of the electrons decreases.

Attribution

Chris P Schaller, Ph.D., (College of Saint Benedict / Saint John's University)

Curated or created by Kathryn Haas

This page titled Section 4.1.2: Molecular Orbitals from p Orbitals is shared under a CC BY-NC-SA 3.0 license and was authored, remixed, and/or curated by Chris Schaller.

- **5.1.2: Molecular Orbitals from p Orbitals** by Chris Schaller is licensed CC BY-NC 3.0.

Section 4.1.3: Molecular orbitals from d orbitals

In transition metals and other heavier elements, the d orbitals may combine with other orbitals of compatible symmetry (and energy) to form molecular orbitals. Generally, there are three types of bonding and antibonding interactions that may occur with d orbitals: sigma (σ), pi (π), and delta (δ) bonds.

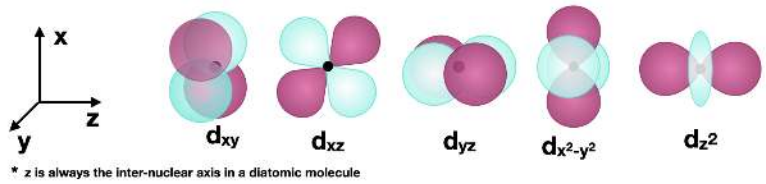


Figure *Section*4.1.3.1: The five 3d orbitals are shown. The orientation of the axes is consistent and the z axis is horizontal for convenience in drawing bonding along the z axis (see examples below). (CC-BY-SA; Kathryn Haas)

Sigma (σ) bonding with d orbitals

σ bonds are symmetric with respect to the inter-nuclear axis (in a diatomic molecule, this is the z axis). An example of a σ bond formed by d orbitals is that of two d_{z^2} orbitals (see Figure *Section*4.1.3.2). If a bonded atom is in a position other than on the z axis (in an octahedral geometry, for example), σ bonds can also form. For example, two $d_{x^2-y^2}$ orbitals on atoms bonded along the x or y axes could also form a σ bond.

d orbitals can also form σ bonds with other types of orbitals with the appropriate symmetry. Examples of orbitals with appropriate symmetry are the s orbital and certain p orbitals on another atom, as shown below in Figure *Section*4.1.3.2.

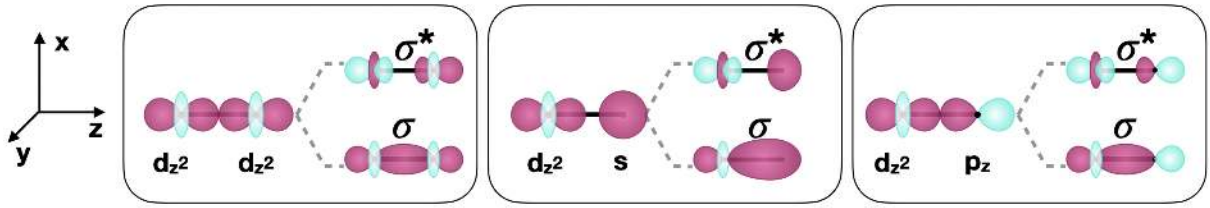


Figure *Section*4.1.3.2: Selected examples of σ bonds involving d orbitals along the z internuclear axis (shown as a bold horizontal line) between two atoms. (CC-BY-SA; Kathryn Haas)

Pi (π) bonding with d orbitals

π bonds are those with one node that is in-plane with the internuclear axis. A π bond can form between two d orbitals or between d orbitals and other types of orbitals with comparable symmetry. An example of a π bond between two d orbitals is that formed by two d_{xz} orbitals along the z axis (shown in Figure *Section*4.1.3.3). d orbitals can also form π bonds using p orbitals with compatible symmetry, as shown in Figure *Section*4.1.3.3.

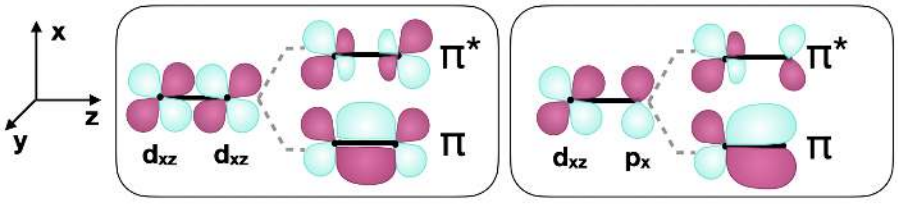


Figure *Section*4.1.3.3: Selected examples of π bonds involving d orbitals along the z internuclear axis (shown as a bold horizontal line) between two atoms. (CC-BY-SA; Kathryn Haas)

Delta (δ) bonding with d orbitals

δ bonds are those with two nodes that are in-plane with the internuclear axis. δ bonds can form between two d orbitals with appropriate symmetry. For example, when two atoms bond along the z axis, the d_{xy} orbitals and the two $d_{x^2-y^2}$ orbitals can form δ bonds (Figure *Section*4.1.3.4).

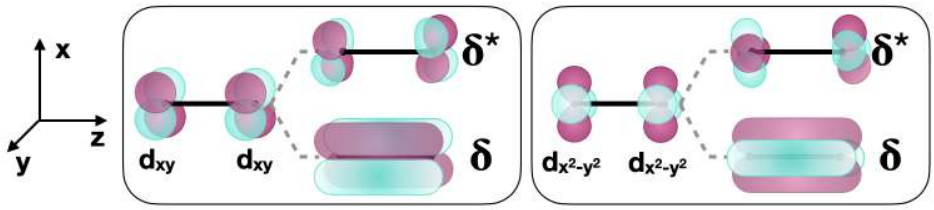


Figure *Section*4.1.3.4: Selected examples of δ bonds involving d orbitals along the z internuclear axis (shown in bold horizontal line) between two atoms. (CC-BY-SA; Kathryn Haas)

Incompatible orbitals

In the descriptions above, we focused on how bonds (and antibonds) can be formed with d orbitals. All bonding and non-bonding interactions require that orbitals have compatible symmetry to form productive interactions. It is worth mentioning that orbitals with symmetry that is incompatible with the d orbitals will not have bonding or antibonding interactions with d orbitals. The figure below shows several sets of orbitals that are incompatible for bonding.

Curated or created by Kathryn Haas

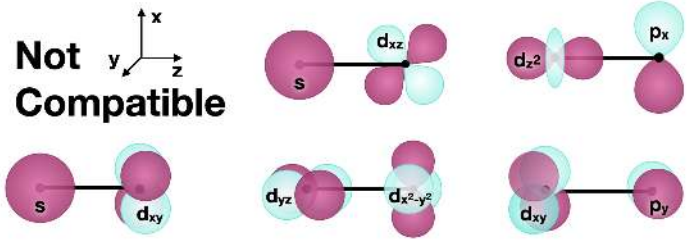


Figure *Section*4.1.3.5: Several incompatible pairs of orbitals. (CC-BY-SA; Kathryn Haas)

This page titled Section 4.1.3: Molecular orbitals from d orbitals is shared under a CC BY-NC-SA 4.0 license and was authored, remixed, and/or curated by Kathryn Haas.

- **5.1.3: Molecular orbitals from d orbitals** by Kathryn Haas is licensed CC BY-SA 4.0.

Section 4.1.4: Nonbonding Orbitals and Other Factors

The simplest case is when there is an even number of atomic orbitals that all combine to form strong bonding and antibonding orbitals. But what if there is an uneven number of atomic orbitals? Or what if there are some orbitals that don't meet the criteria for bonding? Or what if the bonding interactions are weak? In these cases, there will be molecular orbitals on the molecule that have non-bonding character.

It is important to note that the bonding, non-bonding, and antibonding nature of orbitals exist on a spectrum. Some bonding and anti-bonding orbitals may have some non-bonding character depending on where their energies lie with respect to the original atomic orbital energies. When molecular orbitals have energies similar to their original atomic orbitals, they will have some non-bonding character. The closer the energies of atomic and molecular orbitals, the more non-bonding the molecular orbitals.

Two major factors to consider

Uneven number of atomic orbitals: In the case that there is an uneven number of atomic orbitals with compatible symmetry, orbitals with non-bonding character will form. For example, in the case where three atomic orbitals combine, the most common result is formation of a low-energy bonding orbital, a high energy antibonding orbital, and a non-bonding orbital of intermediate energy (Figure *Section*4.1.4.1).

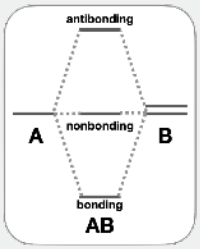


Figure *Section*4.1.4.1. This figure illustrates the most common case for three atomic orbitals that combine to form three molecular orbitals; formation of one low-energy bonding, one high-energy antibonding, and one intermediate energy non-bonding molecular orbital. (CC-BY-NC-SA, Kathryn Haas)

Differences in energy: Combination of orbitals with different energies may lead to orbitals with non-bonding character. Atomic orbitals that have similar energies will have the strongest interactions, and result in bonding molecular orbitals with much lower energies than the component atomic orbitals. On the other hand, atomic orbitals with very unequal energies have a weaker interaction because the molecular orbitals are closer in energy to the atomic orbital energies, thus there is less energy benefit to putting electrons in the bonding molecular orbitals (Figure *Section*4.1.4.2). When bonding or antibonding orbitals are close to the energies of the contributing atomic orbitals, those molecular orbitals may have some non-bonding character.

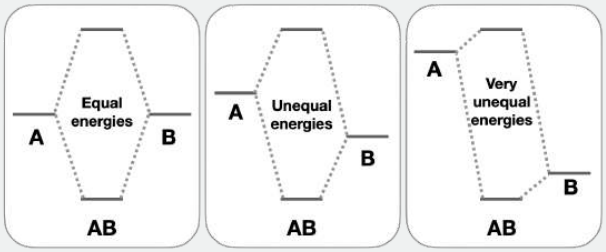


Figure *Section*4.1.4.2. This figure illustrates how relative energies of atomic orbitals result in molecular orbitals that are more or less favorable. The greater the energy difference between atomic orbitals and the bonding molecular orbital, the more eneretically favorable it is for bonding to occur. (CC-BY-NC-SA, Kathryn Haas)

This page titled Section 4.1.4: Nonbonding Orbitals and Other Factors is shared under a CC BY-NC-SA 4.0 license and was authored, remixed, and/or curated by Kathryn Haas.

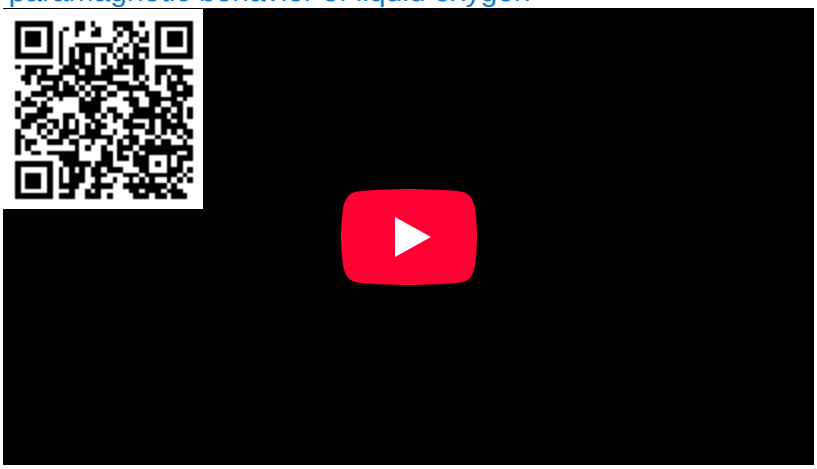
- **5.1.4: Nonbonding Orbitals and Other Factors** by Kathryn Haas is licensed CC BY-SA 4.0.

SECTION OVERVIEW

Section 4.2: Molecular Orbital Theory of Diatomic Molecules

VSPER and valence bond theory have their advantages. They are easily applied using atomic properties like valence electron configuration and electronegativity. They can easily and accurate predict many molecular properties such as molecular shape and bond angles, bond lengths and strengths, polarity, and chirality. Like any theory, there are disadvantages and places where VSPER and valence bond theory fail to explain experimental data. For example, diatomic oxygen (O_2) is a very simple molecule. Both the Lewis structure and valence bond theory would predict that O_2 has a double bond and each O atom has two lone pairs of electrons, and is a diamagnetic molecule (all the electrons are paired). Experiment shows that O_2 is in fact paramagnetic (has unpaired electrons). VSEPR and valence bond theory are not always useful at predicting reactivity. For example, those theories can predict that CO has a triple bond and one lone pair on both O and C. However those theories can't predict if C or the O of CO would react with a Lewis acid.

A video showing the paramagnetic behavior of liquid oxygen



Molecular orbital theory is another bonding theory that can work in places where VSEPR and valence bond fail. Similar to valence bond theory, molecular orbital theory involves the mixing of atomic orbitals, but rather than mixing multiple atomic orbitals on the central atom to form hybrid orbitals atomic orbitals from multiple atoms are mixed together to form molecular orbitals.

Topic hierarchy

Section 4.2.1: Orbital Overlap

Section 4.2.2: Homonuclear Diatomic Molecules

Section 4.2.3: Heteronuclear Diatomic Molecules

Section 4.2.4: Orbital Mixing

Section 4.2.5: Diatomic Molecules of the First and Second Periods

Section 4.2.6: Photoelectron Spectroscopy

Section 4.2: Molecular Orbital Theory of Diatomic Molecules is shared under a CC BY-NC-SA 4.0 license and was authored, remixed, and/or curated by LibreTexts.

Section 4.2.1: Orbital Overlap

Molecular orbital theory is based on the overlap of atomic orbitals, linear combinations of atomic orbitals are taken to form atomic orbitals. At a research level this involves computationally solving the overlap integral between the two or more contributing atomic orbital wavefunctions. In this course we will qualitatively assess orbital overlap primarily through visual inspection.

Sigma (σ) Molecular Orbitals

s orbitals

Similar to valence bond theory, the number of atomic orbitals combines is equal to the number of molecular orbitals formed. Therefore there are two types of molecular orbitals that can form from the overlap of two atomic *s* orbitals. The two types are illustrated in Figure ***Section*4.2.1.1**. The in-phase combination produces a lower energy bonding σ_s molecular orbital in which most of the electron density is directly between the nuclei. The out-of-phase addition (which can also be thought of as subtracting the wave functions) produces a higher energy antibonding σ_s^* molecular orbital in which there is a node between the nuclei. The asterisk signifies that the orbital is an antibonding orbital. Electrons in a σ_s orbital are attracted by both nuclei at the same time and are more stable (of lower energy) than they would be in the isolated atoms. Adding electrons to these orbitals creates a force that holds the two nuclei together, so we call these orbitals bonding orbitals. Electrons in the σ_s^* orbitals are located well away from the region between the two nuclei. The attractive force between the nuclei and these electrons pulls the two nuclei apart. Hence, these orbitals are called antibonding orbitals.

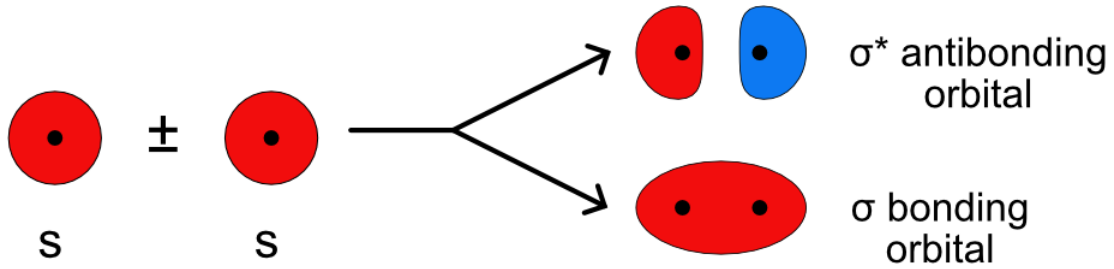


Figure ***Section*4.2.1.1**: Sigma (σ) and sigma antibonding (σ*) molecular orbitals are formed by the combination of two s atomic orbitals. (CC BY-NC-SA; Catherine McCusker)

p orbitals

Unlike s orbitals, *p* orbitals have two lobes with opposite phases, indicated by shading the orbital lobes different colors. When orbital lobes of the same phase overlap, constructive wave interference increases the electron density between the two nuclei. When regions of opposite phase overlap, the destructive wave interference decreases electron density and creates nodes between the two nucei. When *p* orbitals overlap end to end, they create σ and σ* orbitals. If the two *p* orbitals are located along the bond axis (assumed to be the *z*-axis unless otherwise stated), they overlap end to end and form σ_p (bonding) and σ_p^* (antibonding) as illustrated in (Figure ***Section*4.2.1.2**. Just as with *s*-orbital overlap, the asterisk indicates the orbital with a node between the nuclei, which is a higher-energy, antibonding orbital.

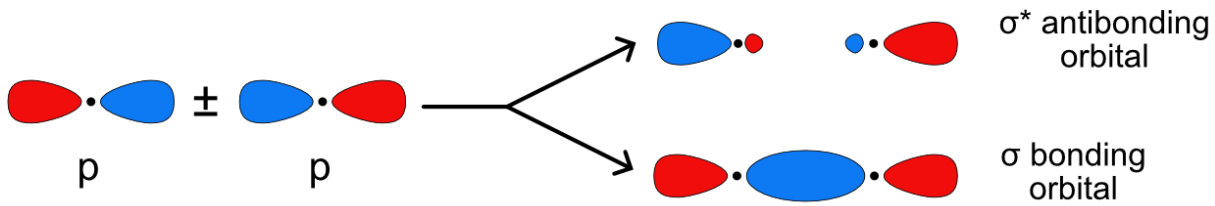


Figure ***Section*4.2.1.2**: Sigma (σ) and sigma antibonding (σ*) molecular orbitals are formed by the combination of two p atomic orbitals. (CC BY-NC-SA; Catherine McCusker)

d orbitals

Recall the shapes and orientations of the five d orbitals from chapter 2. Three of the d orbitals (d_{xy}, d_{xz}, and d_{yz}) have electron density between the axes and nodes along the axes. Two of the d orbitals (d_{z^2} and $d_{x^2-y^2}$) have electron density along the axes. Only the latter two d orbitals can possibly form sigma bonds. These will be similar to sigma bonds formed from p orbitals, when two lobes of the same phase overlap the electron density between the two nuclei increases and sigma bond is formed as shown in Figure ***Section*4.2.1.3**

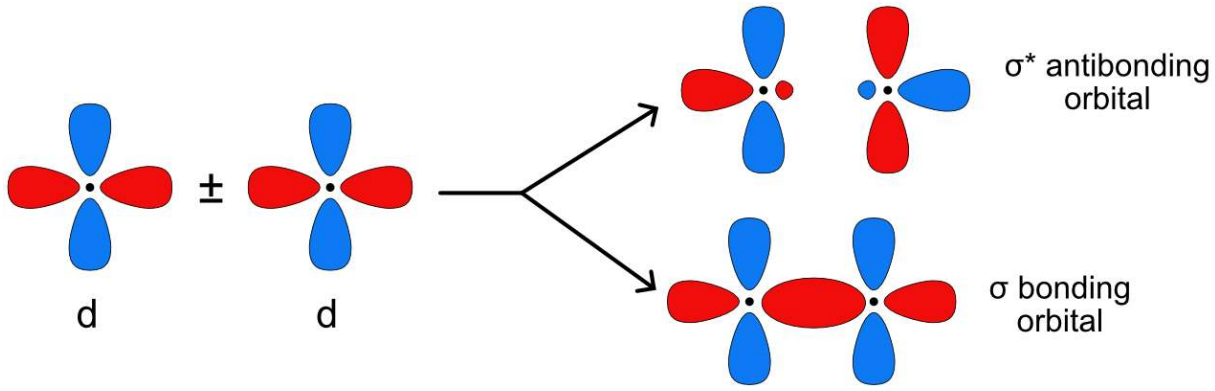


Figure ***Section*4.2.1.3**: Sigma (σ) and sigma antibonding (σ*) molecular orbitals formed from two $d_{x^2-y^2}$ orbitals. (CC BY-NC-SA; Catherine McCusker)

Pi (π) Molecular Orbitals

If two p orbitals are orientated perpendicular to the bond axis they give rise to a pi (π) bonding molecular orbital and a (π^*) antibonding molecular orbital, as shown in Figure ***Section*4.2.1.4**. The in phase overlap forms a pi bonding orbital, which has increased electron density between the nuclei above and below the internuclear bond axis, with a single node along the bond axis. For the out-of-phase combination, an antibonding orbital is formed with two nodal planes created, one along the internuclear axis and a perpendicular one between the nuclei.

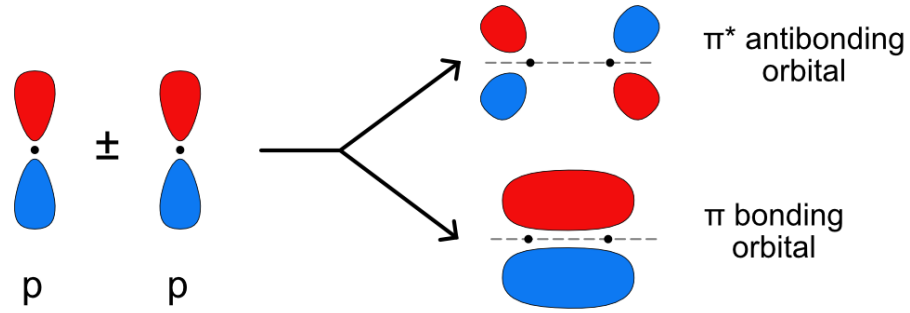


Figure ***Section*4.2.1.4**: Pi (π) and pi antibonding (π*) molecular orbitals are formed by the combination of two perpendicular p atomic orbitals. The grey dashed line indicates the one node containing the internuclear bond axis. (CC BY-NC-SA; Catherine McCusker)

The d orbitals with electron density between the axes (d_{xy}, d_{xz}, and d_{yz}) can also form pi bonds in the same way that p orbitals can, but an s orbital doesn't have the correct geometry to form pi bonds.

Delta (δ) Molecular Orbitals

In main group chemistry only sigma and pi bonds are possible. When two metal atoms are bonded together, a third type of bond, a delta bond, is possible. Two d orbitals orientated face-to-face along the internuclear bond axis ((d_{xy} or $d_{x^2-y^2}$ if the bond is on the z axis) will overlap to form delta bonding and antibonding orbitals as shown in Figure ***Section*4.2.1.5**. The in-phase bonding combination has four areas of electron density above and below the two nuclei, with a vertical and a horizontal node along the internuclear bond axis. In the out-of-phase combination there is a third node bisecting the internuclear axis. With delta bonding it it possible to have quadruple or even quintuple bonds between two metal centers, although in practice quintuple bonds are exceedingly rare and have only been observed in a few chromium and molybdenum dimers.

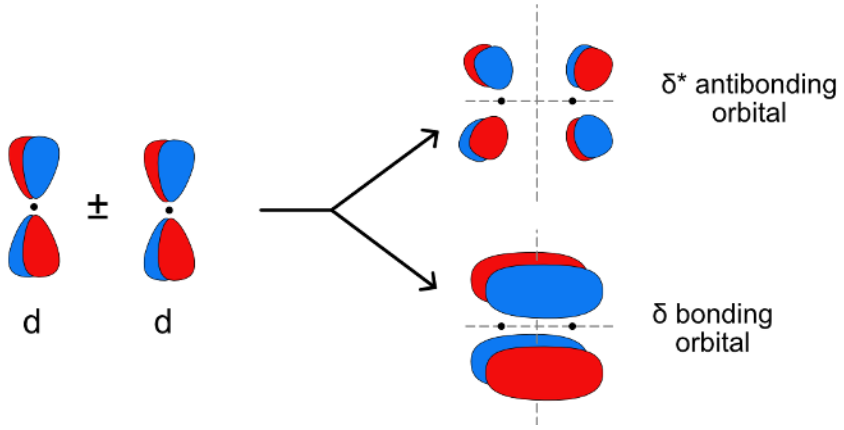


Figure *Section*4.2.1.5: Delta (δ) and delta antibonding (δ*) molecular orbitals are formed by the combination of two face-to-face d atomic orbitals. The grey dashed lines indicate the two nodes containing the internuclear bond axis. (CC BY-NC-SA; Catherine McCusker)

Summary

Bonding orbitals are ones that increase the amount of electron density between the two nuclei relative to the atomic orbitals. Antibonding orbitals are ones that decrease the amount of electron density between the two nuclei relative to the atomic orbitals. Bonding orbitals will have fewer nodes and be lower in energy than antibonding orbitals.A sigma (σ) orbital is one that has **no nodes** along the internuclear bond axis. Any two orbitals (s, p, or d) that are oriented along the bonding axis can form a sigma bond. A pi (π) orbital is one that has **one node** containing the internuclear bond axis. A pi bond can be formed from p or d orbitals orientated perpendicular to the bond axis. A delta (δ) orbital is one that has **two nodes** containing the internuclear bond axis. Only d (or f) orbitals can form delta bonds so they are only possible between two metal atoms.

Multiple Bonds

- Single bonds are formed from **1** sigma bond
- Double bonds are formed from **1** sigma bond and **1** pi bond
- Triple bonds are formed from **1** sigma bond and **2** pi bonds
- Quadruple bonds (only found between two metal atoms) are formed from **1** sigma bond, **2** pi bonds and **1** delta bond
- Quintuple bonds (only found between two metal atoms) are formed from **1** sigma bond, **2** pi bonds and **2** delta bonds

Factors That Influence Covalent Interaction

Now let us refine our understanding of molecular orbitals and molecular orbitals diagrams. Not all atomic orbitals can be combined to form molecular orbitals, and the degree of overlap or covalent interaction between two atomic orbitals can vary lot. What are the criteria according to which we can decide if covalent interaction between two atomic orbitals is possible, and if so how much? There are three criteria to consider; the symmetry criterion, the overlap criterion, and the energy criterion. The symmetry criterion says that If there is a combination of atomic orbitals with bonding and the antibonding interactions that do not cancel out then there is a bonding interaction. The overlap criterion states that the better the atomic orbitals (of appropriate symmetry!) overlap the stronger the covalent interaction. The energy criterion states that the closer the orbitals are in energy the more covalent interaction between them. We will discuss all three criteria in greater detail below.

Criteria for Covalent Interactions

- **Symmetry Criterion:** If there is a combination of atomic orbitals with bonding and the antibonding interactions that do not cancel out then there is a bonding interaction.
- **Overlap Criterion:** The better the atomic orbitals overlap the stronger the covalent interaction.
- **Energy Criterion:** The closer the atomic orbitals in energy the stronger the covalent interaction.

The Overlap Criterion

Let us now look at each criterion in more detail. Let us start with the one we can probably most easily understand, the overlap criterion. The greater the overlap the greater the covalent interaction. The overlap can be estimated according to three rules.

Rule 1: Distance

The first rule says that the overlap is the greater the smaller the distance between the two orbitals. This means that a small distance between the orbital leads to a strongly bonding and a strongly anti-bonding orbital, respectively while a large distance leads to a weakly bonding and a weakly anti-bonding orbital. When the distance is small then there is a large energy difference between the bonding and the anti-bonding molecular orbital, when the distance is large then the energy difference is small (Figure ***Section*4.2.1.6**).

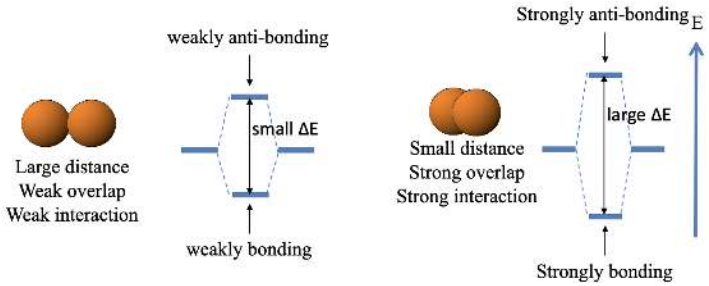


Figure ***Section*4.2.1.6** The effect of the distance between atomic orbitals on the energy difference of the resulting molecular orbitals.

Rule 2: Size

Rule 2 states that a large diffuse orbital tends to overlap better (interact more strongly) with another orbital when this orbital is also a large diffuse orbital. A small, less diffuse orbital tends to interact more strongly with another small orbital. If we combine a large orbital with a small orbital however, then this typically does not lead to good overlap and thus weak interaction. We can qualitatively understand this by looking at the image below (Figure ***Section*4.2.1.7**).

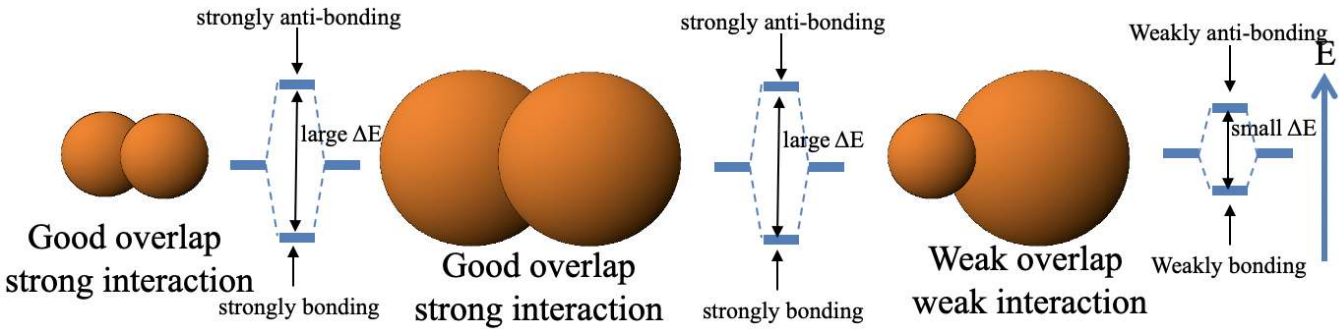


Figure ***Section*4.2.1.7** Relationships between orbital size and covalent interactions.

Only a small volume fraction of the large orbital can overlap with the small orbital due to the small size of the small orbital. Due that small overlap the bonding orbital is only weakly bonding, and the anti-bonding is only weakly anti-bonding. The energy difference between the bonding and the anti-bonding MO is small. In the other two cases, the bonding orbitals tend to be strongly bonding, and the anti-bonding ones strongly anti-bonding. The energy differences between the MOs tend to be large.

Rule 3: Orientation

Rule 3 says that that orbitals that overlap in σ-fashion tend to interact more strongly than orbitals that overlap in π-fashion, which interact more strongly than overlap in δ-fashion. One can see easily from the image below that two p orbitals that have the same distance *d* from each other overlap much more when they overlap in σ-fashion compared to π-fashion (Figure ***Section*4.2.1.8**).

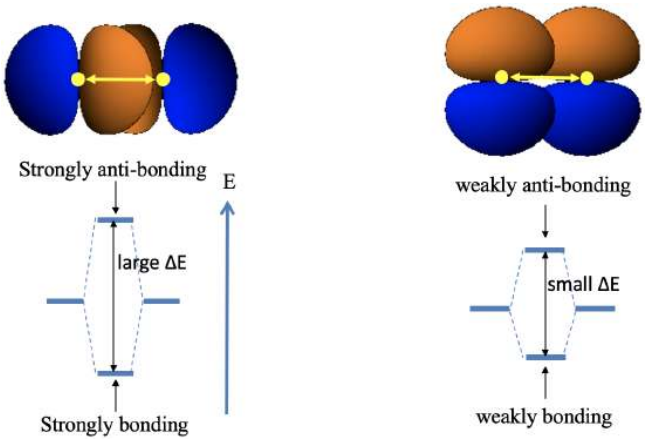


Figure *Section*4.2.1.8 Visual representation of orbitals overlapping in σ-fashion vs orbitals overlapping in π-fashion

This is because in the first case they point toward each other, and the orbital overlap is on the bond axis, while in the latter case they are oriented parallel to each other, and the orbital overlap is above and below the bond axis. This implies that σ-overlap leads to more strongly bonding and anti-bonding orbitals with a larger energy gap between them compared to π-overlap and π-overlap leads to more strongly bonding and anti-bonding orbitals compared to δ-overlap.

The Energy Criterion

The energy criterion states that the covalent interaction between atomic orbitals is larger the smaller the energy difference is between the atomic orbitals. We can understand this qualitatively when considering that orbitals are waves, and waves of similar energy interfere more significantly with each other than waves with different energies. Just imagine two waves with very different wavelengths associated with very different energies. Would they interfere effectively? No, they wouldn't. Rather, two waves with very similar wavelengths would interfere better. Because greater energy difference means less interaction, molecular orbitals that result from the interaction of two atomic orbitals with large energy difference are much more similar in shape, size, and location compared to molecular orbitals that result from atomic orbitals with similar energy.

The greatest covalent interaction is expected when the energy between the two orbitals is exactly the same. This is only possible when two, same orbitals A of the two same atoms overlap. In this case we form a perfect covalent bond with electrons exactly equally shared between the orbitals. The maximum of the amplitude of the bonding molecular orbital is exactly in the middle between the two atoms. In the molecular orbital diagram the energy difference between the bonding MO and the atomic orbitals is about the same as the energy difference between the anti-bonding MO and the atomic orbitals. Electrons the bonding (or antibonding) MO are equally shared between the atoms (Figure *Section*4.2.1.9)

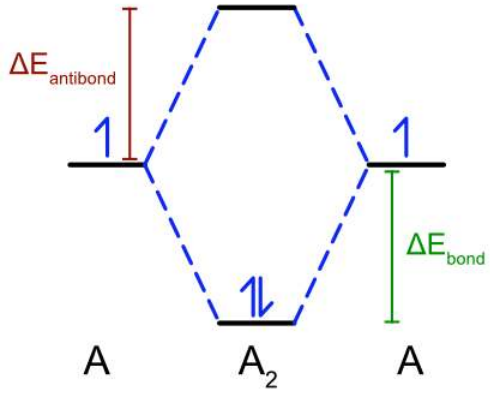


Figure *Section*4.2.1.9 Covalent interaction occurring when the energy between the two atomic orbitals is exactly the same.

Now let us make the energy of the two atomic orbitals somewhat different. Because they are different we denote the atomic orbitals A and B now, whereby we choose the energy of orbital A to be somewhat higher than that of orbital B. Overlap between the atomic orbital still produces covalent interaction yielding a bonding and an anti-bonding molecular orbital. However, the energy difference of the molecular orbitals to the two atomic orbitals is no longer the same. The antibonding MO is now closer to the atomic orbital

with the higher energy, and the bonding MO is now closer in energy to the atomic orbital with the lower energy. This has another consequence. The bonding molecular orbital is now localized primarily at atom A, and the anti-bonding orbital is located primarily at atom B. An electron in the bonding MO is now primarily localized at atom B. This means the bond is a polar covalent bond which is polarized toward atom B (Figure *Section*4.2.1.10).

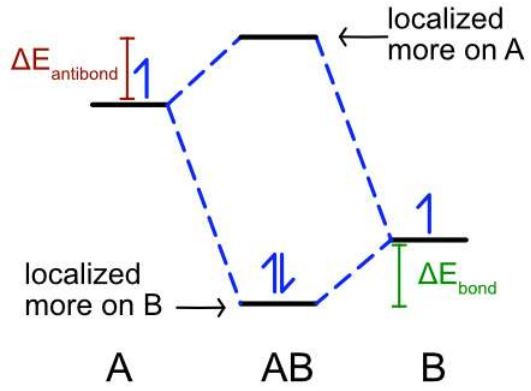


Figure *Section*4.2.1.10 An example of covalent interaction occurring when the energy between the two atomic orbitals is somewhat different

Now let us make the energy difference between the two atomic orbitals of the atoms A and B very large (Figure *Section*4.2.1.11). In this case, the bonding MO is energetically very close to the atomic orbital of atom B, and is localized almost exclusively at atom B. Actually, the bonding MO closely resembles the atomic orbital of atom B in shape, size and localization. In other words, the atomic orbital of B has hardly changed due to the very weak covalent interaction resulting from the large energy difference between the atomic orbitals. Vice versa, the antibonding orbital is energetically very close to the atomic orbital of atom A, and is localized almost completely at atom A. The antibonding MO is very close to the atomic orbital in shape, size, and location. Due to the weak covalent interaction, there is almost no change to the atomic orbital of A.

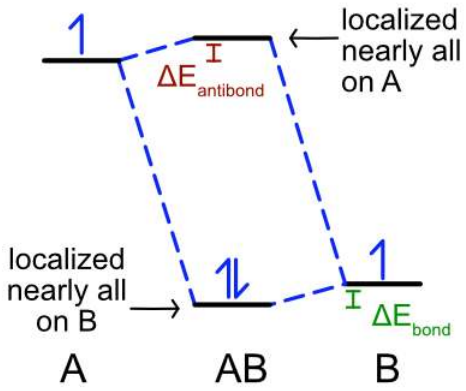


Figure *Section*4.2.1.11 Covalent interaction occurring when the energy difference between two atomic orbitals is very large.

Another conclusion that we can draw is that bonding electrons are located closer to the atom with the atomic orbital of lower energy, and antibonding electrons are located closer to the atoms with the atomic orbital of higher energy. Orbital energy is correlated with electronegativity. For orbitals of the same type and the same elements, orbitals with higher electronegativity have lower energy. For example, a 2s orbital of fluorine has a lower energy than a 2s orbital of oxygen because the electronegativity of fluorine is higher. Bonding electrons are therefore located primarily at the more electronegative atom, while anti-bonding electrons are located primarily at the less electronegative atom. When there are enough anti-bonding orbitals occupied it is possible that the overall polarity in the molecule is such that the dipole moment points toward the more electro-positive atom. An example is carbon monoxide which is slightly polarized toward the carbon atom. We will discuss the MO diagram of the carbon monoxide in detail later.

The Symmetry Criterion

Lastly, let us look at the symmetry criterion. The symmetry criterion tells us if a covalent interaction between orbitals is possible based on the relative orientation of the orbitals. Only if the bonding and antibonding interactions do not cancel out, a bonding interaction is possible, and we can construct molecular orbitals from atomic orbitals. Bonding and antibonding interactions cancel out when positive and negative interferences due to orbital overlap are exactly equal. This can be determined by inspection of orbital overlap.

For example, let us look at the orbital overlap between the 1s orbitals of hydrogen and the $2p_z$ orbital of oxygen in the water molecule (Figure ***Section*4.2.1.12**).

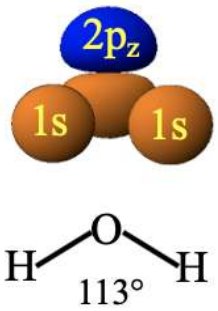


Figure ***Section*4.2.1.12** The orbital overlap between the 1s orbitals of hydrogen and the $2p_z$ orbital of oxygen in the water molecule

In the water molecule the orbitals are oriented to each other in a specific way because of the bent structure of the water molecule. Due to the bent structure of the water molecule the 1s orbitals overlap differently with the two lobes of the $2p_z$ molecule. The lobe that points downward overlaps more strongly than the lobe that points upward and the two lobes have different phases. Now we choose the phases of 1s orbitals so that bonding is maximized. We can see that the overlap of the 1s with the $2p_z$ orbital produces more constructive than destructive interferences. This is equivalent to saying that bonding and anti-bonding interactions do not cancel out. Therefore, the symmetry is “right”, we can construct molecular orbitals from this combination of atomic orbitals.

Can the $2p_x$ orbital of oxygen also combined with the 1s orbitals of the hydrogen atom to form molecular orbitals? The $2p_x$ orbital is oriented differently relative to the 1s orbitals in the H_2O molecule (Figure ***Section*4.2.1.13**).

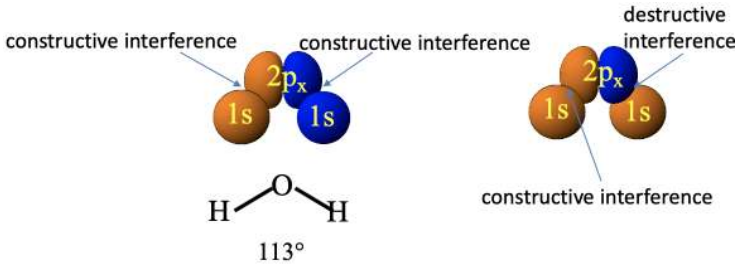


Figure ***Section*4.2.1.13** The orbital overlap between the 1s orbitals of hydrogen and the $2p_x$ orbital of oxygen in the water molecule shown in two different orientations

In this case, we must choose the phases of the two 1s orbitals to be different so that bonding interactions are possible. The bonding and the antibonding interactions only do not cancel out if the left 1s orbital has the same phanse as the left lobe of the $2p_x$ orbital and the right 1s orbital has the same phase as the right lobe of the $2p_x$ orbital. If, for instance, we chose both 1s orbitals to be the same phase then the bonding interactions between the left lobe and the left 1s orbital would be canceled out by the equally strong anti-bonding interactions between the right lobe and the right 1s orbital. Overall, we see however, that if we select the phase of the 1s orbitals appropriately then the symmetry is “right” and we can create molecular orbitals from the atomic orbitals.

What about the interactions between the 1s orbitals and the $2p_y$ orbital (Figure ***Section*4.2.1.14**)?

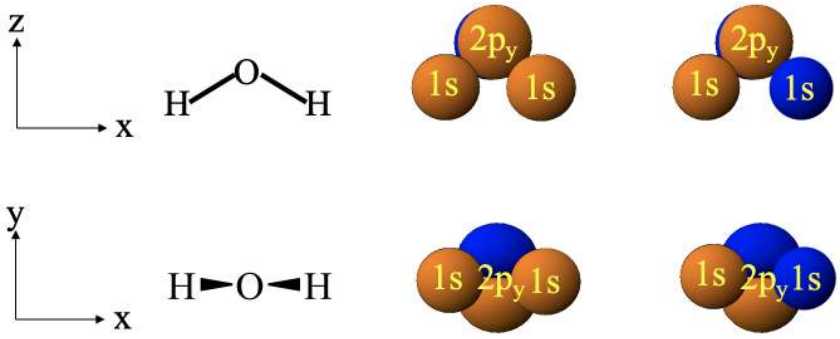


Figure *Section*4.2.1.14 The orbital overlap between the 1s orbitals of hydrogen and the $2p_y$ orbital of oxygen in the water molecule shown in two different orientations

In this case, the two 1s orbitals are in the plane of the page and the $2p_y$ orbital stands perpendicular to it. That makes the 1s orbitals overlap equally with both lobes of the $2p_y$ orbital. Because the two lobes of a $2p_y$ orbital must have different phases, the constructive and the destructive interferences will cancel out, no matter how we chose the phases of our 1s orbitals. That means there is no possibility to create orbital overlap in which bonding an anti-bonding interactions do not cancel out. Therefore, we cannot produce molecular orbitals from a combination of 1s and $2p_y$ orbitals. The $2p_y$ must remain non-bonding. You may be able to see the cancelation of the bonding and antibonding orbital overlap better if you choose your coordination system differently. Let us have the y-axis point up, and the x-axis point right (Figure *Section*4.2.1.9, bottom). Now we look at the H_2O molecule from the bird perspective, and the $2p_y$ orbital is oriented vertically. The 1s orbitals are still on the x-axis. You can see the overlap between the 1s orbitals and the $2p_y$ orbital more clearly now. No matter how we choose the phase of our orbitals, the bonding and the anti-bonding interactions cancel out.

We have seen thus far that is is possible to decide about “right” and “wrong” symmetries by inspection, but we have noticed that this is not trivial. Generally, the more complex a molecule gets the more difficult it is to decide about “right” and “wrong” symmetry. In this course we will limit our discussion of molecular orbital theory to cases where we can determine symmetry by visual inspection only. In Advanced Inorganic we will use group theory as a tool to help us decide about “right” and “wrong” symmetry for orbital overlap in more complex molecules.

Example *Section*4.2.1.1: Molecular Orbitals

Predict what type (if any) of molecular orbital would result from the overlap of each pair of orbitals shown. The orbitals are all similar in energy. Assume the z axis is the bonding axis in all cases.

a. $s + p_z$
b. $p_x + p_z$
c. $d_{xz} + d_{xz}$
d. (d_{xy} + (d_{xy}

Solution

a. These both have electron density along the bond axis, so they would form a sigma bonding molecular orbital
b. This would be a non-bonding interaction. The p_x orbital has a node at z axis where it would overlap with the p_z orbital. This means there is no net overlap and on bond of any kind is formed.
c. These d orbitals are perpendicular to the bond axis, and would therefore form a pi bond.
d. These d orbitals are oriented face-to-face along the bond axis, so they would form a delta bonding orbital.

Exercise *Section*4.2.1.1

Label the molecular orbital shown as σ,π, or δ, bonding or antibonding, and indicate where any nodes occur.



Answer

The orbital is located along the internuclear axis, so it is a σ orbital. There is a node bisecting the internuclear axis, so it is an antibonding orbital.



Contributors and Attributions

- Adapted from

  Dr. Kai Landskron (Lehigh University). If you like this textbook, please consider to make a donation to support the author's research at Lehigh University: Click Here to Donate.

  Paul Flowers (University of North Carolina - Pembroke), Klaus Theopold (University of Delaware) and Richard Langley (Stephen F. Austin State University) with contributing authors. Textbook content produced by OpenStax College is licensed under a Creative Commons Attribution License 4.0 license. Download for free at http://cnx.org/contents/85abf193-2bd...a7ac8df6@9.110).

- Modified by Catherine McCusker (East Tennessee State University)

Section 4.2.1: Orbital Overlap is shared under a CC BY-NC-SA license and was authored, remixed, and/or curated by LibreTexts.

- **3.7A: Orbital Overlap** has no license indicated.
- **8.5: Molecular Orbital Theory** by OpenStax is licensed CC BY 4.0. Original source: https://openstax.org/details/books/chemistry-2e.
- **3.1: Introduction into Molecular Orbital Theory** by Kai Landskron is licensed CC BY 4.0.

Section 4.2.2: Homonuclear Diatomic Molecules

Introduction

Using our knowledge of how the different types of atomic orbitals can overlap and form molecular orbitals (MOs), we can now construct molecular orbital diagrams for simple diatomic molecules. In these cases we can draw and visualize all the possible ways the valence atomic orbitals on both atoms can overlap.

Creating molecular orbital diagrams

- Include all the valence atomic orbitals on both atoms, whether they are empty or filled.
- The total number of atomic orbitals **MUST ALWAYS** equal the total number of molecular orbitals.
- Bonding molecular orbitals are more stable than the atomic orbitals and increase the electron density between the nuclei.
- Antibonding molecular orbitals are less stable than the atomic orbitals and decrease the electron density between the nuclei.
- Fill the completed diagram with electrons according to the Aufbau principle.

First Period Diatomic Molecules

Dihydrogen (H_2)

To generate the molecular orbital diagram for H_2, begin with the valence atomic orbitals. In the case of H_2, each H atom has a single 1s valence orbital. As seen previously, then two s orbitals overlap they form a σ bonding combination and a σ* antibonding combination. The σ bonding molecular orbital increases the electron density between the two H atoms and has no nodes, which makes this combination lower in energy than the H 1s atomic orbitals. The σ* antibonding molecular orbital has a node between the two H atoms and decreases the amount of electron density between the two H atoms, which makes this combination higher energy than the H 1s atomic orbitals. This is illustrated in Figure *Section*4.2.2.1. Notice that combining **two** 1s atomic orbitals has given **two** MOs. Each H atom has one valence electron, so two electrons are placed in the σ bonding MO.

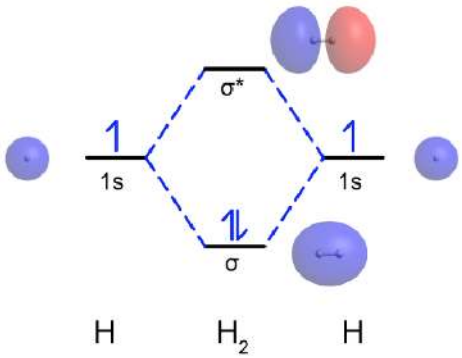


Figure *Section*4.2.2.1: Molecular orbital diagram for H_2. Atomic and molecular orbitals calculated and visualized using WebMO. (CC BY-NC-SA; Catherine McCusker)

Bond order

Once filled with electrons, molecular orbital diagrams can be used to determine bond order in a molecule. Bond order is defined as the difference between the number of electron pairs occupying bonding and antibonding orbitals in the molecule. A bond order of 1 is equivalent to a single bond, a bond order of two is equivalent to a double bond, etc.

$$bond\ order = \frac{(bonding\ electrons) - (antibonding\ electrons)}{2} \qquad \text{(Section 4.2.2.1)}$$

Equation Section 4.2.2.1 can be used to calculate the bond order of a molecule from its molecular orbital diagram. In the H_2 example in Figure *Section*4.2.2.1 There are two electrons in the sigma bonding MO and no electrons in the sigma antibonding MO. Therefore the bond order is $\frac{2-0}{2} = 1$. This agrees with the picture of H_2 from the Lewis structure where the two H atoms are bonded by a single bond.

Other first period diatomics

Qualitatively, the molecular orbital diagrams He_2 and any ions of H_2 and He_2 will be the same because they all will involve the overlap of two 1s atomic orbitals. What will change is the number of electrons in the diagram, and therefore the bond order. Consider the two hydrogen ions, H_2^+ and H_2^- (Figure ***Section*4.2.2.2**). The H_2^+ ion has one fewer electron than H_2, meaning the sigma bonding MO has one single electron in it and the sigma antibonding MO is still unoccupied. This results in H_2^+ having a bond order of 0.5. Non-integer bond order doesn't have a direct equivalent in Lewis theory. A bond order of 0.5 tell you that the molecule is (somewhat) stable relative to the two free atoms, but the bond will be weaker than a single bond. From this we can predict that H_2^+ will have a longer bond and a lower bond dissociation energy than H_2. H_2^- has one more electron than H_2, meaning the sigma bonding MO is filled and the additional electron occupies the sigma antibonding MO. This arrangement of electrons also results in a bond order of 0.5, so H_2^- is expected to have a bond strength and length similar to H_2^+. In the case of He_2, each He atom has two valence electrons so the completed MO diagram has two electrons in the sigma bonding MO and 2 electrons in the sigma antibonding MO. With both the bonding an antibonding MOs completely filled, He_2 has a bond order of 0. This means that He_2 isn't energetically favorable relative to two He atoms, and should not exist. In practice, He_2 can be observed at very low temperatures, but the "bond" between the He atoms is better described as van der Waals forces than a covalent bond.

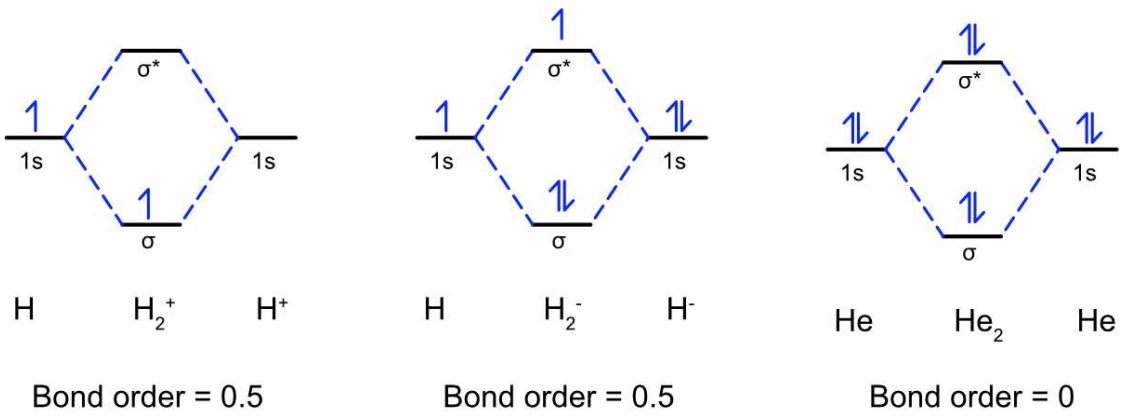
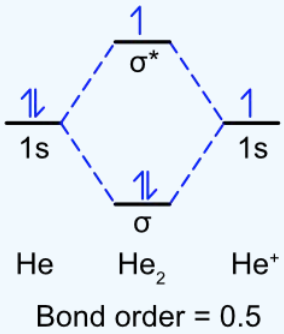


Figure ***Section*4.2.2.2**: Molecular orbital diagrams for H_2^+ (left), H_2^- (center), and He_2 (right). (CC BY-NC-SA; Catherine McCusker)

Exercise *Section*4.2.2.1

Draw the molecular orbital diagram for He_2^+ and calculate its bond order.

Answer



He_2^+ has three valence electrons, two in the sigma bonding and 1 in the sigma antibonding. This makes the bond order 0.5.

Second Period Diatomic Molecules

The four simplest molecules we have examined so far involve molecular orbitals that derived from two 1*s* atomic orbitals. If we wish to extend our model to larger atoms, we will have to contend with higher atomic orbitals as well. One greatly simplifying principle here is that only the *valence* orbitals need to be considered. Core atomic orbitals such as 1*s* are deep within the atom and

well-shielded from the electric field of a neighboring nucleus, so that these orbitals largely retain their atomic character when bonds are formed. For second period molecules that means we need to consider the overlap of the 2s and the 2p atomic orbitals.

Dioxygen (O_2)

One major failing of Lewis and valence bond theories is their inability to explain why O_2 is paramagnetic. To construct a molecular orbital diagram for O_2 we have to consider the interactions between both the 2s and 2p atomic orbitals on each oxygen atom. Because of oxygen's high effective nuclear charge and the penetration of the 2s orbital there is a large energy difference between the 2s and the 2p atomic orbitals. This means the 2s and 2p atomic orbitals do not meet the energy criterion for overlap and cannot mix together. We will consider the overlap of the 2s and 2p orbitals separately.

The energy of the 2s atomic orbitals in oxygen are lower and the radius is larger when compared to the 1s orbitals of hydrogen, but qualitatively when two 2s orbitals overlap the will also form σ bonding and antibonding molecular orbitals as seen in Figure ***Section*4.2.2.3**. As seen previously, the 2p orbitals can overlap to form both σ and π bonds. If we assume the O-O bond is on the z axis, this means the p_z orbitals on each O atom will lie along the bond axis and overlap to form σ_p bonding and σ_p* antibonding molecular orbitals. The p_x and p_y atomic orbitals both lie parallel to the bond axis and overlap to form a degenerate (same energy) pair of π_p bonding and π_p* antibonding molecular orbitals. As there is less orbital overlap in π bonds compared to σ bonds, the π_p bonding MO is stabilized less than the σ_p bonding MO and the π_p* antibonding MO is destabilized less than the σ_p* antibonding MO as shown in Figure ***Section*4.2.2.3**. Each oxygen atom has six valence electrons, and so the center MO diagram is filled with 12 electrons. This leaves two electrons in the pair of π_p* antibonding MOs, and to maximize spin multiplicity according to Hund's rule one is placed in each of the MOs. Unlike the Lewis structure, the molecular orbital diagram for O_2 shows that oxygen is paramagnetic, having two unpaired electrons, in agreement with experimental observations. The MO diagram also predicts that O_2 has a bond order of 2 ($\frac{8-4}{2} = 2$) which agrees with Lewis and valence bond theories as well as experimental bond length.

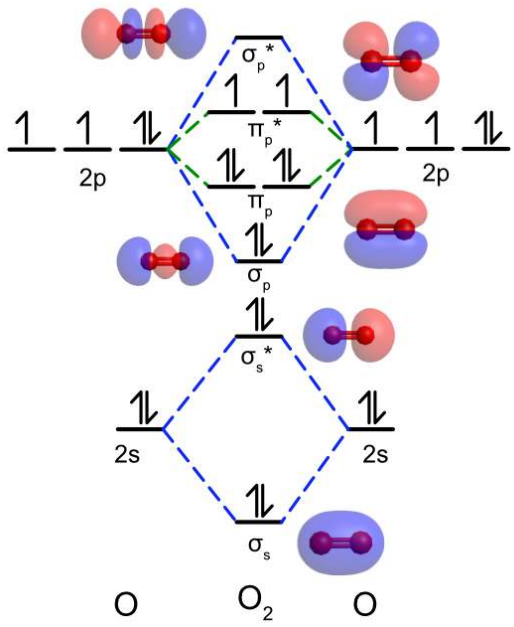


Figure ***Section*4.2.2.3**: Qualitative molecular orbital diagram for O_2. Note that the energies of the atomic orbitals are not drawn to scale. Molecular orbitals calculated and visualized using WebMO. (CC BY-NC-SA; Catherine McCusker)

s-p mixing

In the molecular orbital diagram of O_2 we made the assumption that the 2s orbitals would only interact with other 2s orbitals and that 2p orbitals would only interact with other 2p orbitals because the energy difference between the 2s and 2p is large. However, in less electronegative atoms we can't make that same assumption. As Figure ***Section*4.2.2.4** illustrates, in less electronegative elements, the energies of the 2s and 2p orbitals are closer in energy and meet the energy criterion for overlap. Therefore to construct molecular orbital diagrams for most of the second period elements (except O, F, and Ne) we need to consider how the s and p orbitals can possibly overlap.

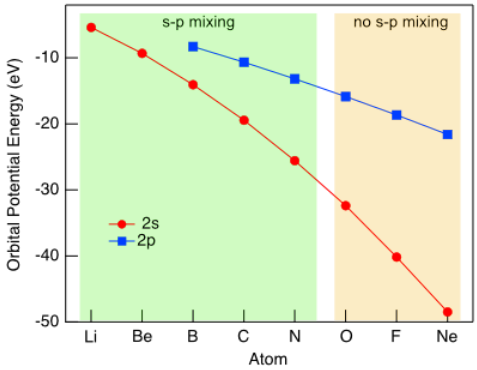


Figure *Section*4.2.2.4: Trends in the 2s (red circle) and 2p (blue square) atomic orbital potential energies for second period elements. Energies from Meissler, G. L.; Fischer, P. J.; Tarr, D. A. *Inorganic Chemistry*, 5th Ed. (CC BY-NC-SA; Catherine McCusker)

The p orbital which lies along the bond axis (p_z if we assume z is the bond axis) can overlap with the s orbital and form a sigma bonding (and antibonding) molecular orbital. The remaining two p orbitals are perpendicular to the bond axis, which means the s orbital would overlap with the node of the p orbital resulting in no net overlap and no bonding (or antibonding) MO is formed (Figure *Section*4.2.2.5). The s and p orbitals mixing together also means we have to consider what happens when more than two non-degenerate orbitals mix together. Based on the rules for forming molecular orbitals, the number of atomic orbitals that mix together is always equal to the number of molecular orbitals formed, as shown in Figure *Section*4.2.2.6. When two atomic orbitals mix they form one bonding and one antibonding MO. When three atomic orbitals mix they form one bonding and one antibonding molecular orbital plus one intermediate molecular orbital that is approximately nonbonding, meaning it is neither stabilized nor destabilized relative to the atomic orbitals. When four atomic orbitals mix two bonding MOs, one strongly stabilized and one weakly stabilized, and two antibonding MOs, one strongly destabilized and one weakly destabilized, are formed.

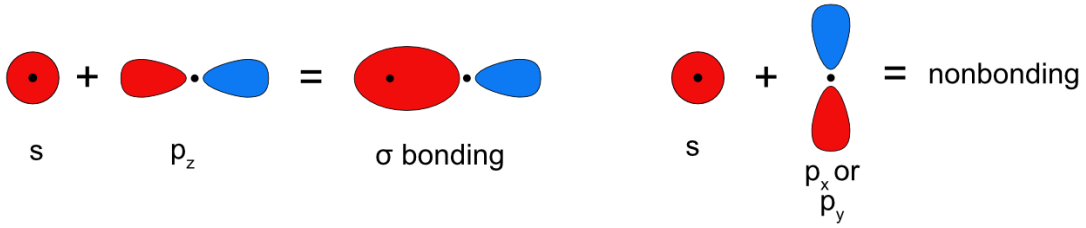


Figure *Section*4.2.2.5: Assuming the bond axis is the z axis, the s and p_z will overlap to form a sigma bond (left) and the s and p_x or p_y do not have the correct orientation to overlap (right). (CC BY-NC-SA; Catherine McCusker)

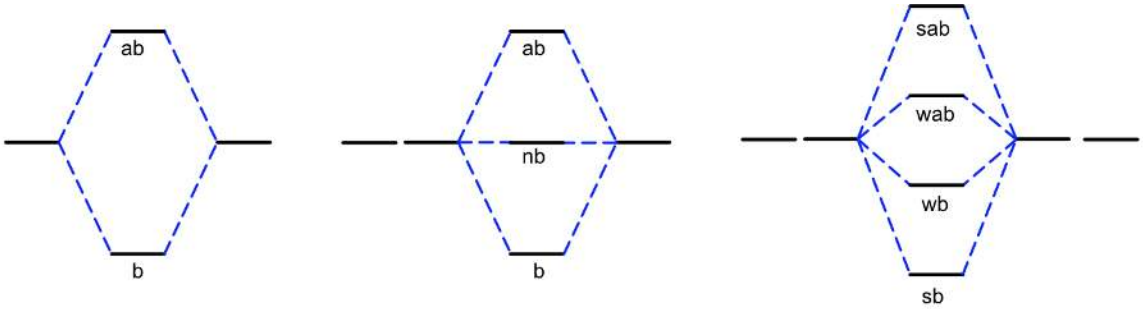


Figure *Section*4.2.2.6: Two atomic orbitals (left) will overlap to form bonding (b) and antibonding (ab) molecular orbitals. Three atomic orbitals (center) will overlap to form bonding, nonbonding (nb), and antibonding molecular orbitals. Four atomic orbitals (right) will overlap to form strongly bonding (sb), weakly bonding (wb), weakly antibonding (wab) and strongly antibonding (sab) molecular orbitals. (CC BY-NC-SA; Catherine McCusker)

Dinitrogen (N_2)

Just like in O_2 the valence orbitals used to create the molecular orbital diagram of N_2 are the 2s and 2p orbitals on each N atom. Unlike the O_2 example above we cannot make the assumption that the 2s and 2p orbitals are too far apart in energy to mix together.

In the case of N_2 there are four total atomic orbitals that can overlap in a sigma fashion, the 2s and $2p_z$ orbitals from each N atom. As shown above, when four atomic orbitals overlap the result is two bonding MOs, labeled σ_s and σ_s* in Figure *Section*4.2.2.7 to be consistent with Figure *Section*4.2.2.3, and two antibonding MOs, labeled σ_p and σ_p*. As the $2p_x$ and $2p_y$ cannot overlap with the 2s, they form a degenerate pair of pi bonding and antibonding MOs. Each N atom has 5 valence electrons, so the N_2 molecular orbital diagram is filled with 10 total electrons, giving a bond order of 3 ($\frac{8-2}{2}=3$). The biggest difference between the MO diagram of O_2 above and N_2 is the position of the σ_p MO. In O_2 it is a bonding orbital and is lower in energy than the π_p MOs. In N_2 this MO is weakly antibonding and is now higher than the π_p MOs. This change in molecular orbital ordering is the hallmark experimental observable showing s-p mixing occurs in N_2.

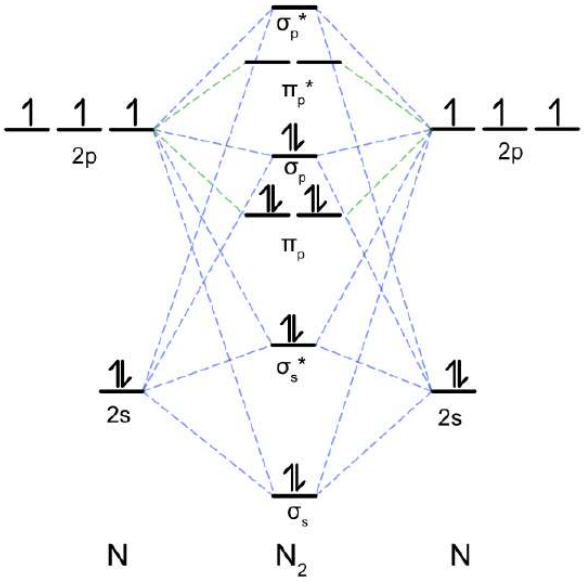


Figure *Section*4.2.2.7: Qualitative molecular orbital diagram for N_2. Blue dashed lines indicate the mixing of 2s and $2p_z$ to form sigma bonding and antibonding MO's . The green dashed lines indicate the mixing of $2p_x$ and $2p_y$ to form pi bonding and antibonding MOs. Note that the energies of the atomic orbitals are not drawn to scale. (CC BY-NC-SA; Catherine McCusker)

Exercise *Section*4.2.2.2

Draw the complete molecular orbital diagram for B_2. Calculate the bond order and indicate whether it is diamagnetic or paramagnetic.

Answer

B_2 is paramagnetic with a bond order of 1. Bond order $=\frac{4-2}{2}=1$

https://chem.libretexts.org/@go/page/440785

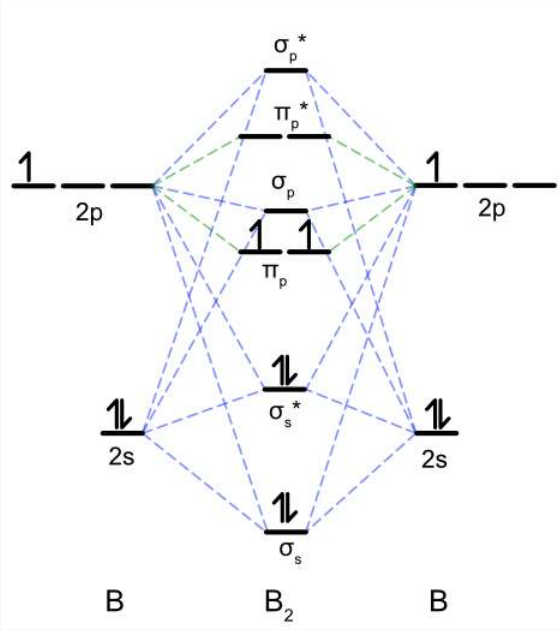
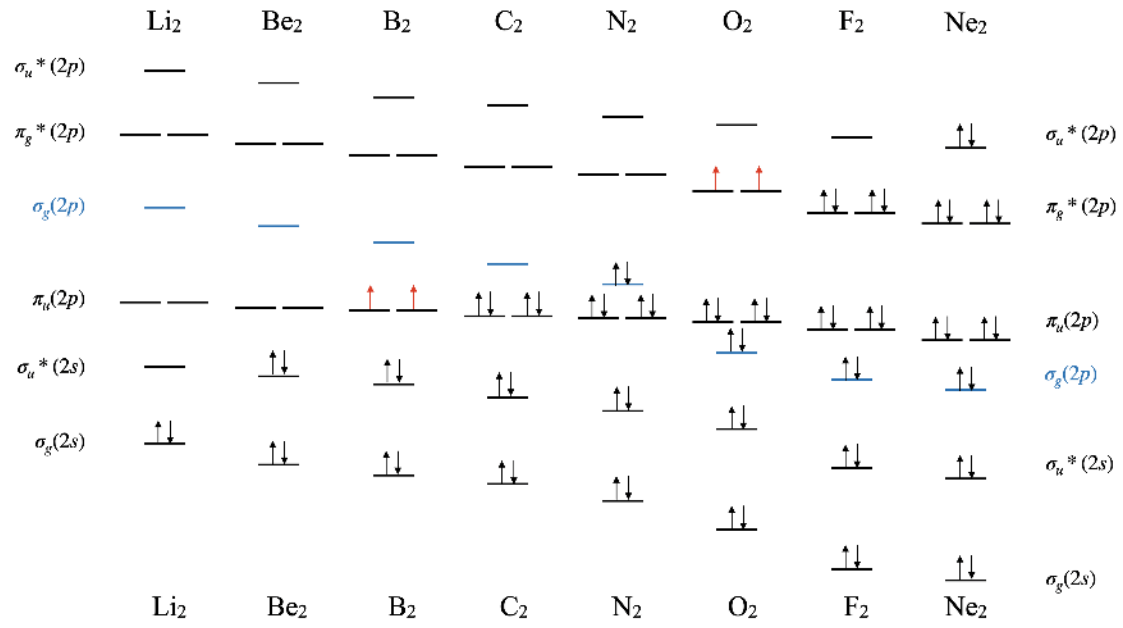


Figure for Exercise *Section*4.2.2.2. Molecular orbital diagram of B_2. (CC-BY-NC-SA, Catherine McCusker)

Overview of Second Period Homonuclear Diatomic Molecules

Orbital mixing has significant consequences for the magnetic and spectroscopic properties of second period homonuclear diatomic molecules because it affects the order of filling of the $\sigma(2p)$ and $\pi(2p)$ orbitals. Early in period 2 (up to and including nitrogen), the $\pi(2p)$ orbitals are lower in energy than the $\sigma(2p)$ (see Figure *Section*4.2.2.1). However, later in period 2, the $\sigma(2p)$ orbitals are pulled to a lower energy. This lowering in energy of $\sigma(2p)$ is not unique; all of the σ orbitals in the molecule are pulled to lower energy due to the increasing positive charge of the nucleus. The π orbitals in the molecule are also effected, but to a much lesser extent than σ orbitals. The reason has to do with the high penetration of s atomic orbitals compared to p atomic orbitals (recall our previous discussion on penetration and shielding, and its effect on periodic trends). The σ molecular orbitals have more s character and are thus their energy is more influence by increasing nuclear charge.



	Li_2	Be_2	B_2	C_2	N_2	O_2	F_2	Ne_2
Unpaired e⁻	0	0	2	0	0	2	0	0
Bond Order	1	0	1	2	3	2	1	0
Experimental* Bond Length (pm)	267.3	246.0	159.0	124.3	109.8	120.8	141.2	310.0

*Experimental bond lengths from "List of Experimental Diatomic Bond Lengths", NIST, https://cccbdb.nist.gov/diatomicexpbondx.asp

Figure ***Section*4.2.2.8**: Molecular Orbital Energy-Level Diagrams for the Diatomic Molecules of the Period 2 Elements. In these diagrams, *only the valence molecular orbital energy levels for the* ***molecules*** *are shown here (atomic orbitals not shown for simplicity).* For Li_2 through N_2, the $\sigma(2p)$ orbital is higher in energy than the $\pi(2p)$ orbitals. In contrast, from O_2 onward, the $\sigma(2p)$ orbital is *lower* in energy than the $\pi(2p)$ orbitals due to the increase in the nuclear charge increases across the row. The experimental bond lengths correlate with calculated bond order. (CC-BY-NC-SA, Kathryn Haas)

Dilithium, Li_2 $[\sigma(2s)^2]$: This molecule has a bond order of one and is observed experimentally in the gas phase to have one Li-Li bond.

Diberylium, Be_2 $[\sigma(2s)^2\sigma(2s)^{*2}]$: This molecule has a bond order of zero due to equal number of electrons in bonding and antibonding orbitals. Although Be does not exist under ordinary conditions, it can be produced in a laboratory and its bond length measured (Figure ***Section*4.2.2.9**). Although the bond is very weak, its bond length is surprisingly ordinary for a covalent bond of the second period elements.

Diboron, B_2 $[\sigma(2s)^2\sigma(2s)^{*2}\pi(2p)^2]$: The case of diboron is one that is much better described by molecular orbital theory than by Lewis structures or valence bond theory. This molecule has a bond order of one. The molecular orbital description of diboron also predicts, accurately, that dibornon is paramagnetic. The paramagnetism is a consequence of sp mixing, resulting in the $\sigma(2p)$ orbital at a higher energy than two degenerate $\pi(2p)$ orbitals.

Dicarbon, C_2 $[\sigma(2s)^2\sigma(2s)^{*2}\pi(2p)^4]$: This molecule has a bond order of two. Molecular orbital theory predicts two bonds with π symmetry, and no σ bonding. C_2 is rare in nature because its allotrope, diamond, is much more stable.

Dinitrogen, N_2 $[\sigma(2s)^2\sigma(2s)^{*2}\pi(2p)^4\sigma(2p)^2]$: This molecule is predicted to have a triple bond. This prediction is consistent with its short bond length and bond dissociation energy. The energies of the $\sigma(2p)$ and $\pi(2p)$ orbitals is very close, and their relative energy levels has been a subject of some debate.

Dioxygen, O_2 $[\sigma(2s)^2\sigma(2s)^{*2}\sigma(2p)^2\pi(2p)^4\pi(2p)^{*2}]$: This is another case where valence bond theory fails to predict actual properties. Molecular orbital theory correctly predicts that dioxygen is paramagnetic, with a bond order of two. Here, the molecular orbital

diagram returns to its "normal" order of orbitals where orbital mixing could be somewhat ignored, and where $\sigma_g(2p)$ is lower in energy than $\pi_u(2p)$.

Difluorine, F_2 $[\sigma(2s)^2\sigma(2s)^{*2}\sigma(2p)^2\pi(2p)^4\pi(2p)^{*4}]$: This molecule has a bond order of one and like oxygen, the $\sigma(2p)$ is lower in energy than $\pi(2p)$.

Dineon, Ne_2 $[\sigma(2s)^2\sigma(2s)^{*2}\sigma(2p)^2\pi(2p)^4\pi(2p)^{*4}\sigma(2p)^{*2}]$: Like other noble gases, Ne exists in the atomic form and does not form bonds at ordinary temperatures and pressures. Like Be_2, Ne_2 is an unstable species that has been created in extreme laboratory conditions and its bond length has been measured (Figure ***Section*4.2.2.9**)

Bond Lengths

The trends in experimental bond lengths are predicted by molecular orbital theory, specifically by the calculated bond order. The values of bond order and experimental bond lengths for the second period diatomic molecules are given in Figure ***Section*4.2.2.8**, and shown in graphical format on the plot in Figure ***Section*4.2.2.9**. From the plot, we can see that bond length correlates well with bond order, with a minimum bond length occurring where bond order is greatest ($\mathbf{N_2}$). The shortest bond distance is at $\mathbf{N_2}$ due to its high bond order of 3. From $\mathbf{N_2}$ to $\mathbf{F_2}$ the bond distance increases despite the fact that atomic radius decreases.

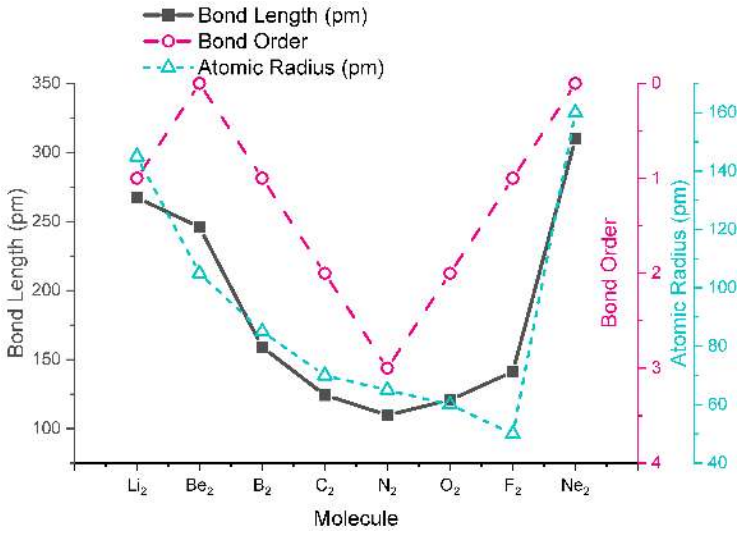


Figure ***Section*4.2.2.9**: Overlayed plots of bond length (black squares), bond order (pink circles), and atomic radius (teal triangels) versus atomic number for second period homonuclear diatomic molecules. (CC-BY-NC-SA; Kathryn Haas)

References

1. Schöllkopf, W.; Toennies, J. P. Nondestructive Mass Selection of Small van der Waals Clusters. *Science* **1994**, *266* (5189), 1345–1348.
2. NIST, Calculated Geometries available for H_2^+ (Hydrogen cation) 2Σg+ D∞h, available at https://cccbdb.nist.gov/diatomicexpbondx.asp
3. Merritt, J. M.; Bondybey, V. E.; Heaven, M. C., Beryllium Dimer-Caught in the Act of Bonding. *Science* **2009,** *324* (5934), 1548-1551.
4. Meissler, G. L.; Fischer, P. J.; Tarr, D. A. *Inorganic Chemistry*, 5th Ed; Pearson, 2014.

Contributors and Attributions

- Stephen Lower, Professor Emeritus (Simon Fraser U.) Chem1 Virtual Textbook
- Curated or created by Kathryn Haas
- Modified by Catherine McCusker, ETSU

Section 4.2.2: Homonuclear Diatomic Molecules is shared under a CC BY-NC-SA 4.0 license and was authored, remixed, and/or curated by LibreTexts.

- **3.7B: Homonuclear Diatomic Molecules** is licensed CC BY-NC-SA 4.0.

- **5.2.3: Diatomic Molecules of the First and Second Periods** by Kathryn Haas is licensed CC BY-SA 4.0.

Section 4.2.3: Heteronuclear Diatomic Molecules

Atomic Orbital Energies

Diatomic molecules with two non-identical atoms are called heteronuclear diatomic molecules. When atoms are not identical, the molecule forms by combining atomic orbitals of unequal energies. The result is a polar bond in which atomic orbitals contribute unevenly to each molecular orbital.

The application of molecular orbital theory to heteronuclear diatomic molecules is similar to the case of homonuclear diatomics, except that the atomic orbitals from each atom have different energies and contribute unequally to molecular orbitals. Recall that atomic orbitals must have compatible symmetry and similar energy to combine into molecular orbitals. In the case where atomic orbitals of like symmetry have different energies, they combine less favorably than orbitals that are closer to one another in energy. As a general rule, orbitals that have energy differences of greater than 10-14 eV do not combine favorably. In the molecular orbital diagram, the closer a molecular orbital is to an atomic orbital, the more that atomic orbital contributes to the molecular orbital. This last point is helpful for back-of-the napkin estimations of what the molecular orbitals "look" like.

In this section, you should learn how to generate molecular orbital diagrams of heteronuclear diatomic molecules. To approach such a problem, we must start with a knowledge of the relative energies of electrons in different atomic orbitals. In other words, we need knowledge of the orbital potential energies (or orbital ionization energies).

Orbital Ionization Energies

There are two approaches you can use to "know" or estimate the atomic orbital energy levels.

1. Use a table of atomic orbital ionization energies, like those found in Table ***Section*4.2.3.1**.
2. When you do not have access to a table of values like the one below, use periodic trends in electronegativity and/or ionization energies as your guide to approximate relative values for different atoms.

Table ***Section*4.2.3.1**: These are one-electron ionization energies of the valence orbitals calculated by average energies of both the ground-state and ionized-state configurations in eV. (From Harry Gray, “Electrons and Chemical Bonding,” Benjamin, 1964, Appendix)

Atom	1s	2s	2p	3s	3p
H	-13.64				
He	-24.55				
Li		-5.46			
Be		-9.30			
B		-14.01	-8.31		
C		-19.47	-10.66		
N		-25.54	-13.14		
O		-32.36	-15.87		
F		-46.37	-18.72		
Ne		-48.48	-21.57		
Na				-5.21	
Mg				-7.69	
Al				-11.28	-5.95
Si				-15.00	-7.81
P				-18.72	-10.17
S				-20.71	-11.65
Cl				-25.29	-13.76
Ar				-29.26	-15.87

MO Diagrams for Heteronuclear Diatomic Molecules

The molecular orbital diagram of a heteronuclear diatomic molecule is approached in a similar way to that of homonuclear diatomic molecule. The orbital diagrams may also look similar. A major difference is that the more electronegative atom will have orbitals at a lower energy level. Two examples of heteronuclear diatomic molecules will be explored below as illustrative examples.

Carbon monoxide MO diagram

Carbon monoxide is an example of a heteronuclear diatomic molecule where both atoms are second-row elements. The valence molecular orbitals in both atoms are the $2s$ and $2p$ orbitals. The molecular orbital diagram for carbon monoxide (Figure $Section 4.2.3.1$) is constructed similarly to how you would construct dicarbon or dioxygen, except that the oxygen orbitals have a lower potential energy than analogous carbon orbitals. The labeling of molecular orbitals in this diagram follows a convention by which orbitals are given serial labels according to type of orbital (σ, π, etc). The lowest energy orbitals of any type are assigned a value of 1 and higher energy orbitals of the same type are assigned by increasing intervals (..2, 3, 4...).

A consequence of unequal atomic orbital energy levels is that orbital mixing is significant. Notice the order of the molecular orbitals labeled 1π and 3σ in Figure $Section 4.2.3.1$. This is a similar order of π and σ orbitals as we saw in the case of N_2 and lighter diatomics of the second period. Because the oxygen $2p_z$ orbital is close in energy to both the carbon $2p_z$ and carbon $2s$, these three orbitals will have significant interaction (overlap). The result is an increase in the energy of the 3σ orbital and a decrease in energy of the $2\sigma^*$ orbital, resulting in the diagram shown in Figure $Section 4.2.3.1$.

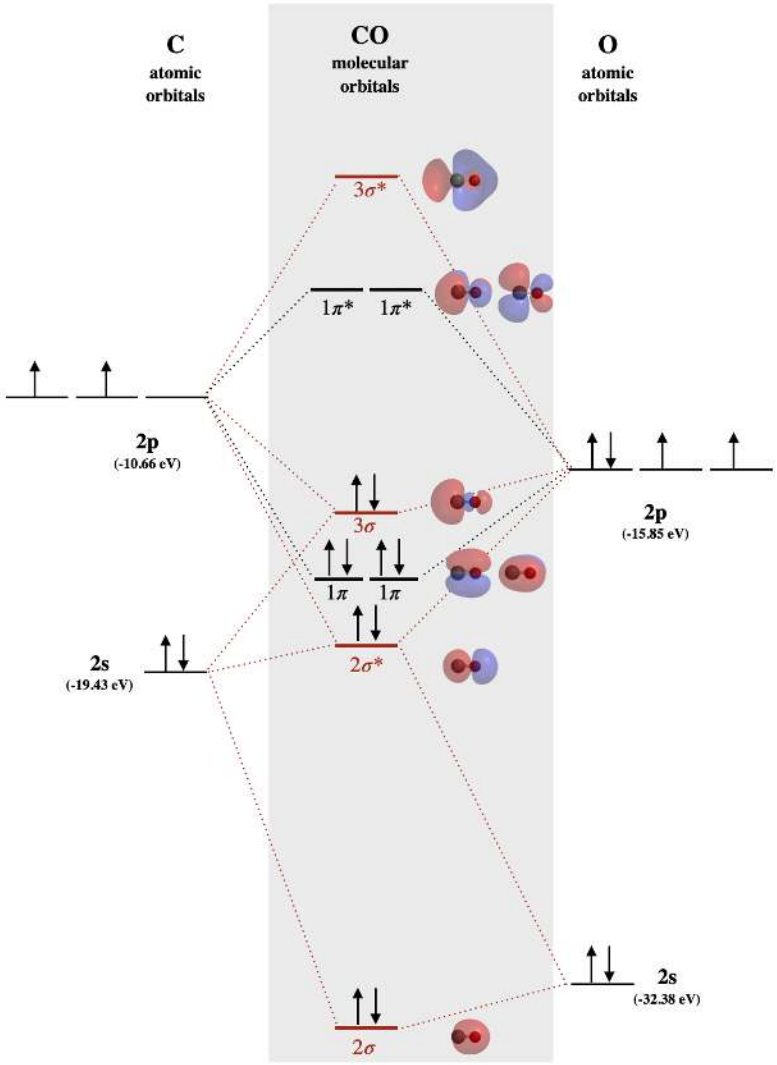
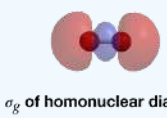


Figure *Section*4.2.3.1: Molecular orbital diagram of carbon monoxide. The labeling of molecular orbitals in this diagram follows a convention by which orbitals are given serial names according to type of orbital (σ, π, etc). The lowest energy orbitals of any type are assigned a value of 1 and higher energy orbitals of the same type are assigned by increasing intervals (..2, 3, 4...). Molecular orbital surfaces were calculated using Spartan software. (Kathryn Haas, CC-BY-NC-SA)

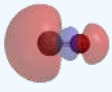
In the case of carbon monoxide (Figure *Section*4.2.3.1), atomic orbitals contribute unequally to each molecular orbital. For example, because the $2s$ orbital of oxygen is very close in energy to the 2σ molecular orbital, it contributes to that molecular orbital more than the $2s$ orbital from carbon. Notice the shape of this 2σ orbital and how it is unevenly distributed over the two atoms; it is more heavily distributed on the oxygen because it is most like the oxygen $2s$. This is in-line with the assumption that electron density is distributed more on oxygen because it is a more electronegative than carbon. Likewise, the 1π orbitals are unevenly distributed, with more distribution close to the oxygen.

Exercise *Section*4.2.3.1

Examine the shape of the 3σ orbital of carbon monoxide in Figure (*Section*4.2.3.1). Describe what ways this shape is different from the shape of the σ_g orbitals from second period homonuclear diatomic molecules. Rationalize these differences. Both orbitals are re-created below for convenience.



σ_g of homonuclear diatomic



3σ of CO

Answer

The 3σ orbital is like the σ_g in that it has three lobes and two nodes distributed along the internuclear bond. They are different in their distribution. The two external lobes of σ_g are evenly distributed because the are an equal combination of two p_z orbitals (one from each atom). The 3σ orbital is more heavily distributed toward the carbon atom, the less electronegative atom, than toward the oxygen. The unequal distribution of 3σ is apparent in the unequal sizes of its exterior lobes, and the uneven shape of the interior lobe. The heavier distribution within the exterior lobe on carbon caused by the mixing of the carbon $2s$ orbital with carbon and oxygen $2p_z$ orbitals. The uneven shape of the interior lobe, where it leans toward oxygen, is best explained by the fact that the 3σ orbital is closer in energy to the oxygen $2p_z$ than the carbon $2p_z$.

Hydrogen fluoride MO diagram

Hydrogen fluoride is an example of a heteronuclear diatomic molecule in which the two atoms are from different periods. In this case, the valence orbital of H is $1s$ while those of F are $2s$ and $2p$. The molecular orbital diagram for HF is shown in Figure *Section*4.2.3.2.

Three of these orbitals have compatible symmetry for mixing; these are the hydrogen $1s$, fluorine $2s$, and fluorine $2p$. However, the extent to which they will interact depends on their relative energies. Fluorine is more electronegative than H, and the fluorine atom has a higher first ionization energy than does hydrogen. From these trends, we can expect that the fluorine valence orbitals are lower in energy than that of hydrogen. From Table *Section*4.2.3.1, we find that the 1s orbital of H (-13.6 eV) is higher in energy than both fluorine orbitals (-18.7 and -40.2 eV, respectively for $2p$ and $2s$). The energies of hydrogen $1s$ and fluorine $2p$ are a good match for combination, however, the $2s$ orbital is much too different to create a productive interaction. Therefore, we expect that the fluorine $2s$ will create a non-bonding molecular orbital, while the $1s$ and $2p_z$ orbital combine to make σ bonding and σ^* antibonding molecular orbitals. The remaining $2p_x$ and $2p_y$ orbitals do not have compatible symmetry for bonding with hydrogen, and they will form non-bonding π molecular orbitals. The non-bonding orbitals will have the same energy and character as their component atomic orbitals.

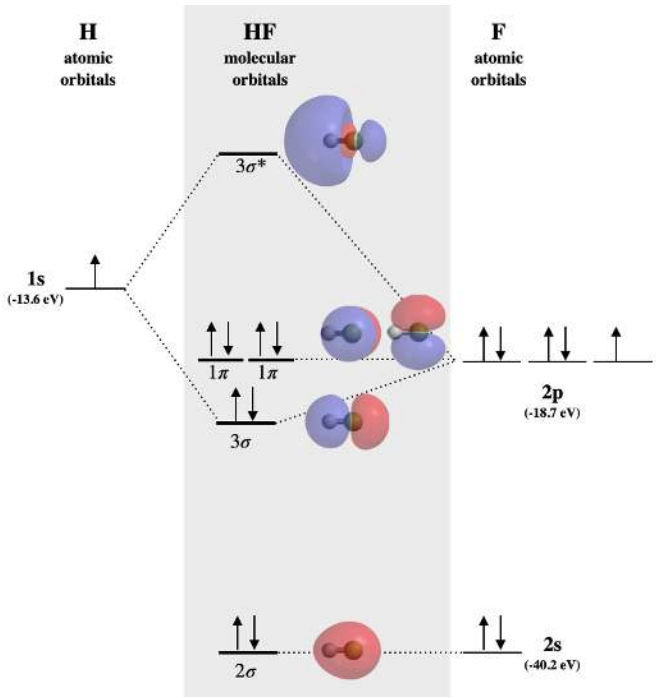


Figure *Section*4.2.3.2: Molecular Orbital diagram of hydrogen fluoride. Molecular orbitals calculated using Spartan software. (Kathryn Haas, CC-BY-NC-SA)

Chemical Reactivity

Knowledge of molecular orbital diagrams, and the shapes of molecular orbitals, can be used to accurately explain and predict chemical reactivity. Chemical reactions take place using the highest occupied molecular orbitals (HOMO) of a nucleophile or

Lewis base, and the lowest unoccupied molecular orbital (LUMO) of an electrophile or Lewis acid.

> *Lewis bases react using electrons in the HOMO, while Lewis acids react using the empty LUMO.*

Example: Reactivity of CO with metal ions

CO is an excellent ligand for many metal ions. In fact, the strong affinity between CO and the heme iron (Fe) ions in hemoglobin can explain the mechanism of carbon monoxide poisoning. When CO binds in place of O_2 to hemoglobin, that hemoglobin can no longer carry O_2 to tissue cells. CO binding to hemoglobin is strong and practically irreversible. When CO binds to metal ions, it does so through the carbon atom. This is contrary to expectations based on the Lewis structure and the known bond polarity, where electron density is polarized toward oxygen. The distribution of the electron density of the HOMO of CO can explain this observation!

Exercise *Section*4.2.3.2

Refer to the MO diagram for CO. Identify the HOMO and explain why CO bonds to metal ions through the carbon atom rather than through the oxygen atom.

Answer

The HOMO of CO is the 3σ MO. That MO is closer in energy to both the C 2s and 2p than the contributing O atomic orbitals. This means the MO has more C character and is localized more on the C than the O. When CO acts as a Lewis base and bonds to a metal (a Lewis acid) it donates electrons from the HOMO orbital

---

Sources:

- Gray, Harry. *Electrons and Chemical Bonding*, Benjamin, 1964.
- Miessler, Gary L, and Donald A. Tarr. *Inorganic Chemistry*. Upper Saddle River, N.J: Pearson Education, 2014. Print.

Curated or created by Kathryn Haas

Section 4.2.3: Heteronuclear Diatomic Molecules is shared under a CC BY-NC-SA license and was authored, remixed, and/or curated by LibreTexts.

- **3.7C: Heteronuclear Diatomic Molecules** has no license indicated.
- **5.3: Heteronuclear Diatomic Molecules** by Kathryn Haas is licensed CC BY-SA 4.0.
- **5.3.2: Polar bonds** by Kathryn Haas is licensed CC BY-SA 4.0.

Section 4.2.4: Orbital Mixing

In the previous section, we introduced a simplified molecular orbital (MO) diagram, assuming that interactions were limited to degenerate orbitals of compatible symmetry. A version of that *simplified* diagram for second-row homonuclear diatomics is shown on the left side of Figure ***Section*4.2.4.1** (only valence orbitals shown).

In reality, orbitals of compatible symmetry can combine, or mix, even when they have different energies. When sets of orbitals mix, it has the effect of decreasing the energy of the lower-energy set and increasing the energy of the higher-energy set. There are two ways to explain mixing, described in the points below. The diagram on the right of side of Figure ***Section*4.2.4.1** shows how energy levels are affected by orbital mixing.

- **Starting from the simplified MO diagram and mixing molecular orbitals of like symmetry**: If we start with the "no mixing" simplified diagram shown on the left, we can pick out the orbitals with like symmetry and consider what will happen if these molecular orbitals mix. For example, starting from the MO diagram on the left side of Figure ***Section*4.2.4.1**, we see that there are two σ_g orbitals that have identical symmetry (hence they have identical symmetry labels). Upon mixing, the lower-energy $\sigma_g(2s)$ will decrease in energy while the higher-energy $\sigma_g(2p)$ will increase in energy. Likewise, there are two σ_u^* orbitals that will mix, decreasing the energy of $\sigma_u^*(2s)$ while increasing the energy of $\sigma_u^*(2p)$.
- **Starting from and mixing atomic orbitals of compatible symmetry**: Starting from the atomic orbitals, we can select the orbitals that have compatible symmetry to make productive interactions, and combine them as a set to make molecular orbitals. From the two sets of atomic orbitals on the right panel in Figure ***Section*4.2.4.1**, there are two sets of four orbitals with compatable symmetry; one is the set of two $2s$ and two $2p_z$ orbitals. These four orbitals can combine to form molecular orbitals with σ symmetry. They combine to form one lowest-energy bonding σ_g, a highest-energy σ_u^*, and two orbitals with intermediate energy (σ_g, and σ_u^*). This treatment can be expressed as the linear combination of four atomic orbitals:

  $$\Psi = c_1\psi(2s_a) \pm c_2\psi(2s_b) \pm c_3\psi(2p_a) \pm c_4\psi(2p_b)$$

  where the coefficients $c_1 = c_2$ and $c_3 = c_4$ for homonuclear diatomic molecules.

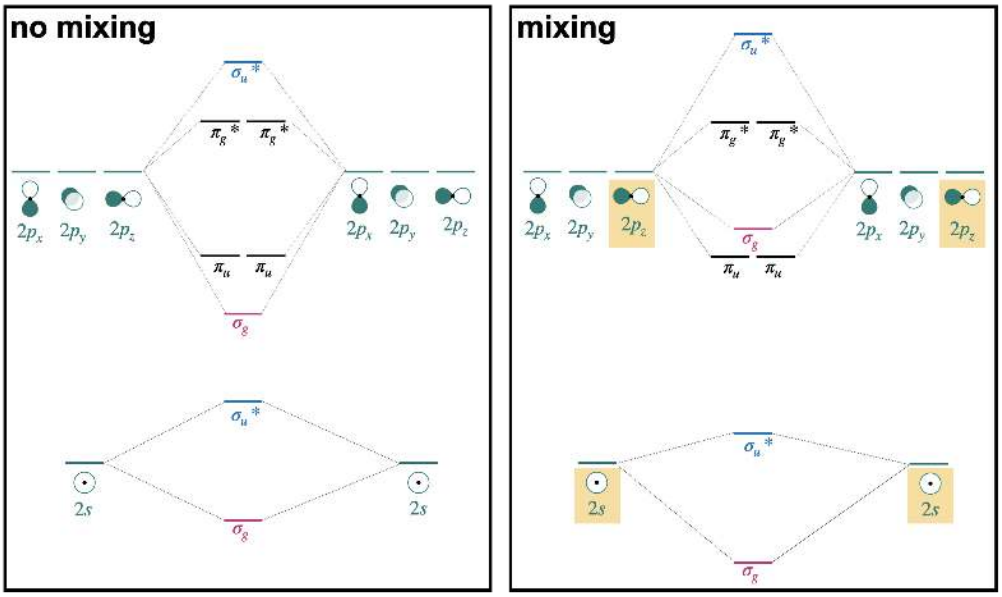


Figure ***Section*4.2.4.1**: Mixing of orbitals with like symmetry affects the energies of molecular orbitals. The simplified case where no mixing occurs is shown on the left. The effects of mixing are shown on the right. The σ_g orbitals of like symmetry are highlighted in fuschia and the σ_u^* orbitals of like symmetry are highlighted in blue. A group of atomic orbitals of similar symmetry are highlighted in yellow boxes; these atomic orbitals combine to give all σ molecular orbitals. (CC-BY-SA, Kathryn Haas)

In the case of homonuclear diatomic molecules of the second row, orbital mixing has important consequences for the energetic order of the $\sigma_g(2p)$ and $\pi_u(2p)$ orbitals. This will be discussed in the next section.

This page titled Section 4.2.4: Orbital Mixing is shared under a CC BY-NC-SA 4.0 license and was authored, remixed, and/or curated by Kathryn Haas.

- **5.2.2: Orbital Mixing** by Kathryn Haas is licensed CC BY-SA 4.0.

Section 4.2.5: Diatomic Molecules of the First and Second Periods

First Period Homonuclear Diatomic Molecules

In the first row of the periodic table, the valence atomic orbitals are $1s$. There are two possible homonuclear diatomic molecules of the first period:

Dihydrogen, H_2 [$\sigma_g^2(1s)$]: This is the simplest diatomic molecule. It has only two molecular orbitals (σ_g and σ_u^*), two electrons, a bond order of 1, and is diamagnetic. Its bond length is 74 pm. MO theory would lead us to expect bond order to decrease and bond length to increase if we either add or subtract one electron. The calculated bond length for the H_2^+ ion is approximately 105 pm.[1]

Dihelium, He_2 [$\sigma_g^2\sigma_u^{*2}(1s)$]: This molecule has a bond order of zero due to equal number of electrons in bonding and antibonding orbitals. Like other nobel gases, He exists in the atomic form and does not form bonds at ordinary temperatures and pressures.

? Exercise *Section*4.2.5.1

Draw the complete molecular orbital diagrams for H_2 and for He_2. Include sketches of the atomic and molecular orbitals.

Answer

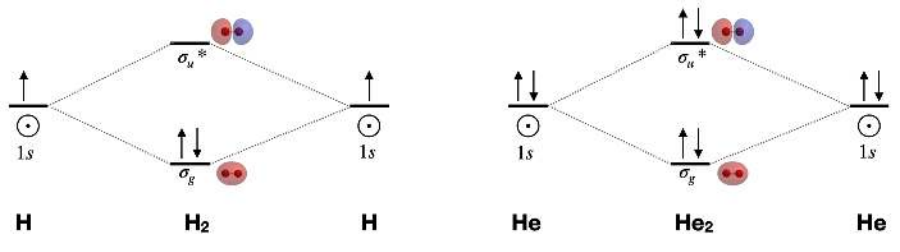


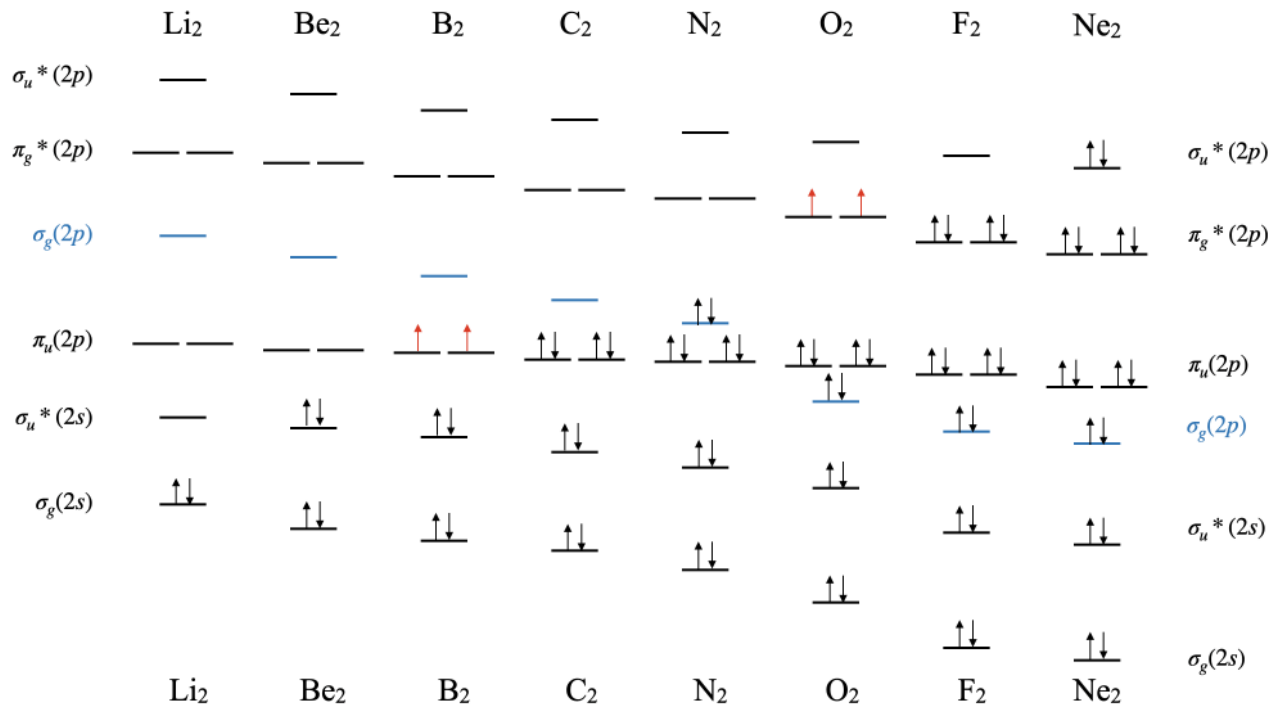
Figure for Exercise *Section*4.2.5.1: Molecular orbital diagrams for dihydrogen and dihelium. Molecular orbital surfaces calculated using Spartan software. (CC-BY-NC-SA; Kathryn Haas)

A complete molecular orbital diagram includes all atomic orbitals and molecular orbitals, their symmetry labels, and electron filling.

Second Period Homonuclear Diatomic Molecules

The second period elements span from Li to Ne. The valence orbitals are 2s and 2p. In their molecular orbital diagrams, non-valence orbitals (1s in this case) are often disregarded in molecular orbital diagrams.

Orbital mixing has significant consequences for the magnetic and spectroscopic properties of second period homonuclear diatomic molecules because it affects the order of filling of the $\sigma_g(2p)$ and $\pi_u(2p)$ orbitals. Early in period 2 (up to and including nitrogen), the $\pi_u(2p)$ orbitals are lower in energy than the $\sigma_g(2p)$ (see Figure *Section*4.2.5.1). However, later in period 2, the $\sigma_g(2p)$ orbitals are pulled to a lower energy. This lowering in energy of $\sigma_g(2p)$ is not unique; all of the σ orbitals in the molecule are pulled to lower energy due to the increasing positive charge of the nucleus. The π orbitals in the molecule are also affected, but to a much lesser extent than σ orbitals. The reason has to do with the high penetration of s atomic orbitals compared to p atomic orbitals (recall our previous discussion on penetration and shielding, and its effect on periodic trends). The σ molecular orbitals have more s character and thus their energy is more influenced by increasing nuclear charge. As nuclear charge increases, the energy of the $\sigma_g(2p)$ orbital is lowered significantly more than the energy of the $\pi_u(2p)$ orbitals (Figure *Section*4.2.5.1).



	Li_2	Be_2	B_2	C_2	N_2	O_2	F_2	Ne_2
Unpaired e⁻	0	0	2	0	0	2	0	0
Bond Order	1	0	1	2	3	2	1	0
Experimental* Bond Length (pm)	267.3	246.0	159.0	124.3	109.8	120.8	141.2	310.0

*Experimental bond lengths from "List of Experimental Diatomic Bond Lengths", NIST, https://cccbdb.nist.gov/diatomicexpbondx.asp

Figure *Section*4.2.5.1: Molecular orbital energy-level diagrams for the diatomic molecules of the period 2 elements. Unlike earlier diagrams, *only the valence molecular orbital energy levels for the* ***molecules*** *are shown here (atomic orbitals not shown for simplicity).* For Li_2 through N_2, the $\sigma_g(2p)$ orbital is higher in energy than the $\pi_u(2p)$ orbitals. In contrast, from O_2 onward, the $\sigma_g(2p)$ orbital is *lower* in energy than the $\pi_u(2p)$ orbitals because the nuclear charge increases across the row. The experimental bond lengths correlate with the calculated bond order. (CC-BY-NC-SA, Kathryn Haas)

Dilithium, Li_2 $[\sigma_g^2(2s)]$: This molecule has a bond order of one and is observed experimentally in the gas phase to have one Li-Li bond.

Diberylium, Be_2 $[\sigma_g^2\sigma_u^{*2}(2s)]$: This molecule has a bond order of zero due to the equal number of electrons in bonding and antibonding orbitals. Although Be_2 does not exist under ordinary conditions, it can be produced in a laboratory and its bond length measured (Figure *Section*4.2.5.2). Although the bond is very weak, its bond length is surprisingly ordinary for a covalent bond of the second period elements.[2]

Diboron, B_2 $[\sigma_g^2\sigma_u^{*2}(2s)\pi_u^1\pi_u^1(2p)]$: The case of diboron is one that is much better described by molecular orbital theory than by Lewis structures or valence bond theory. This molecule has a bond order of one. The molecular orbital description of diboron also predicts, accurately, that diboron is paramagnetic. The paramagnetism is a consequence of orbital mixing, resulting in the σ_g orbital's being at a higher energy than the two degenerate π_u^* orbitals.

Dicarbon, C_2 $[\sigma_g^2\sigma_u^{*2}(2s)\pi_u^2\pi_u^2(2p)]$: This molecule has a bond order of two. Molecular orbital theory predicts two bonds with π symmetry, and no σ bonding. C_2 is rare in nature because its allotrope, diamond, is much more stable.

Dinitrogen, N_2 $[\sigma_g^2\sigma_u^{*2}(2s)\pi_u^2\pi_u^2\sigma_g^2(2p)]$: This molecule is predicted to have a triple bond. This prediction is consistent with its short bond length and bond dissociation energy. The energies of the $\sigma_g(2p)$ and $\pi_u(2p)$ orbitals are very close, and their relative energy levels have been a subject of some debate (see next section for discussion).

Dioxygen, O_2 $[\sigma_g^2\sigma_u^{*2}(2s)\sigma_g^2\pi_u^2\pi_u^2\pi_g^{*1}\pi_g^{*1}(2p)]$: This is another case where valence bond theory fails to predict actual properties. Molecular orbital theory correctly predicts that dioxygen is paramagnetic, with a bond order of two. Here, the molecular orbital diagram returns to its "normal" order of orbitals where orbital mixing could be somewhat ignored, and where $\sigma_g(2p)$ is lower in energy than $\pi_u(2p)$.

Difluorine, F_2 $[\sigma_g^2\sigma_u^{*2}(2s)\sigma_g^2\pi_u^2\pi_u^2\pi_g^{*2}\pi_g^{*2}(2p)]$: This molecule has a bond order of one and like oxygen, the $\sigma_g(2p)$ is lower in energy than $\pi_u(2p)$.

Dineon, Ne_2 $[\sigma_g^2\sigma_u^{*2}(2s)\sigma_g^2\pi_u^2\pi_u^2\pi_g^{*2}\pi_g^{*2}\sigma_u^{*2}(2p)]$: Like other noble gases, Ne exists in the atomic form and does not form bonds at ordinary temperatures and pressures. Like Be_2, Ne_2 is an unstable species that has been created in extreme laboratory conditions and its bond length has been measured (Figure ***Section*4.2.5.2**)

? Exercise *Section*4.2.5.2

Draw the complete molecular orbital diagram for O_2. Show calculation of its bond order and tell whether it is diamagnetic or paramagnetic.

Answer

O_2 is paramagnetic with a bond order of 2. Its $\sigma_g(2p)$ molecular orbital is lower in energy that the set of $\pi_u(2p)$ orbitals.

$$\text{Bond order} = \frac{1}{2}\left[\left(\begin{array}{c}\textbf{8 electrons in}\\ \textbf{valence bonding orbitals}\end{array}\right) - \left(\begin{array}{c}\textbf{4 electrons in}\\ \textbf{valence antibonding orbitals}\end{array}\right)\right]$$

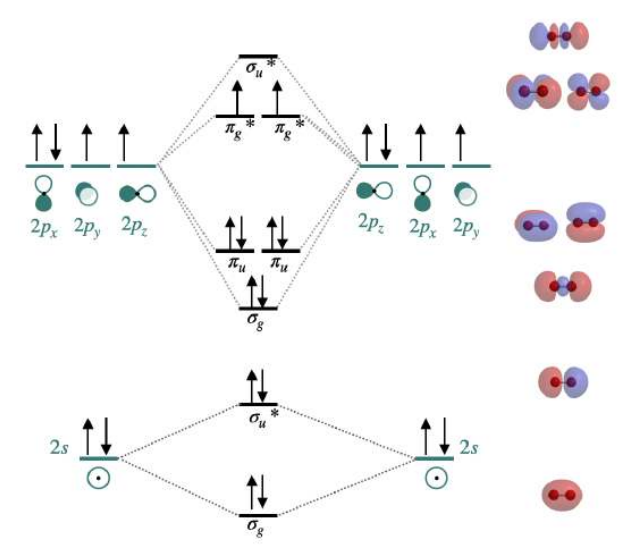


Figure for Exercise ***Section*4.2.5.2**. Molecular orbital diagram of O_2. (CC-BY-NC-SA, Kathryn Haas)

? Exercise *Section*4.2.5.3: The Peroxide Ion

Use a qualitative molecular orbital energy-level diagram to predict the electron configuration, the bond order, and the number of unpaired electrons in the peroxide ion (O_2^{2-}).

Answer

This diagram looks similar to that of $\mathbf{O_2}$, except that there are two additional electrons.
$(\sigma_g(2s))^2\,(\sigma_u^*(2s))^2\,(\sigma_g(2p))^2\,(\pi_u(2p))^4\,(\pi_g(2p))^4$; bond order of 1; no unpaired electrons.

Bond Lengths in Homonuclear Diatomic Molecules

The trends in experimental bond lengths are predicted by molecular orbital theory, specifically by the calculated bond order. The values of bond order and experimental bond lengths for the second period diatomic molecules are given in Figure ***Section*4.2.5.1**,

and shown in graphical format on the plot in Figure ***Section*4.2.5.2**. From the plot, we can see that bond length correlates well with bond order, with a minimum bond length occurring where the bond order is greatest ($\mathbf{N_2}$). The shortest bond distance is at $\mathbf{N_2}$ due to its high bond order of 3. From $\mathbf{N_2}$ to $\mathbf{F_2}$ the bond distance increases despite the fact that atomic radius decreases.

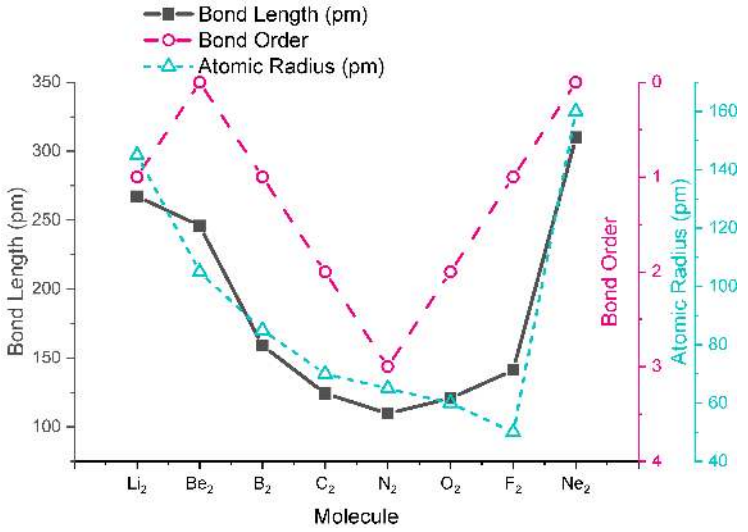


Figure ***Section*4.2.5.2**: Overlayed plots of bond length (black squares), bond order (pink circles), and atomic radius (teal triangles) versus atomic number for second period homonuclear diatomic molecules. (CC-BY-NC-SA; Kathryn Haas)

References

1. NIST, Calculated Geometries available for H_2^+ (Hydrogen cation) 2Σg+ D∞h, available at https://cccbdb.nist.gov/diatomicexpbondx.asp
2. Merritt, J. M.; Bondybey, V. E.; Heaven, M. C., Beryllium Dimer-Caught in the Act of Bonding. *Science* **2009,** *324* (5934), 1548-1551.

This page titled Section 4.2.5: Diatomic Molecules of the First and Second Periods is shared under a CC BY-NC-SA 4.0 license and was authored, remixed, and/or curated by Kathryn Haas.

- **5.2.3: Diatomic Molecules of the First and Second Periods** by Kathryn Haas is licensed CC BY-SA 4.0.
- **5.P: Problems** is licensed CC BY-SA 4.0.

Section 4.2.6: Photoelectron Spectroscopy

A photoelectron spectrum can show the relative energies of occupied molecular orbitals by ionization. The *ionization energy* is a direct measure of the energy required to just remove the electron concerned from its initial level to the vacuum level (free electron). Photoelectron spectroscopy measures the relative energies of the ground and excited positive ion states that are obtained by removal of single electrons from the neutral molecule.

$$A + \text{photon} \rightarrow A^+ + e^-$$

The information obtained from photoelectron spectroscopy is typically discussed in terms of the electronic structure and bonding in the ground states of neutral molecules, with ionization of electrons occurring from bonding molecular orbitals, lone pairs, antibonding molecular orbitals, or atomic cores. These descriptions reflect the relationship of ionization energies to the molecular orbital model of electronic structure.

Ionization energies are directly related to the energies of molecular orbitals (by Koopmans' theorem).

Example: Photoelectron spectrum of dihydrogen

The molecular orbital description of dihydrogen involves two $1s$ atomic orbitals generating two molecular orbitals: a bonding σ_g and an antibonding σ_u^*. The two electrons occupy the σ_g bonding orbital, leaving the molecule with a bond order of one (Figure ***Section*4.2.6.1**). The PES spectrum of dihydrogen (Figure ***Section*4.2.6.1**) has a single band that corresponds to the ionization of one electron from the σ_g. The multiple peaks are due to electrons ejecting from a range of stimulated vibrational energy levels. When extensive vibrational structure is resolved in a PES molecular orbital, then the removal of an electron from that molecular orbital induces a significant change in the bonding (in this case an increase in the bond length due to decrease in bond order).

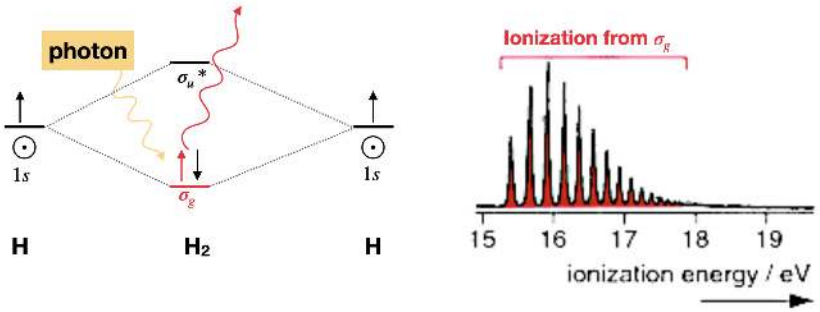


Figure ***Section*4.2.6.1**: The molecular orbital diagram and photoelectron spectrum of dihydrogen. (CC-BY-NC-SA; Libretexts)

Example: Photoelectron spectrum of dinitrogen

Diatomic nitrogen is more complex than hydrogen since multiple molecular orbitals are occupied. Five molecular orbitals are occupied; two of them are degenerate. Three bands in the photoelectron spectrum correspond to ionization of an electron in $\sigma_g(2p)$, $\pi_u(2p)$ and $\sigma_u^*(2s)$ molecular orbitals. Ionization of the fourth type of orbital, $\sigma_g(2s)$, does not appear in Figure ***Section*4.2.6.2** because it is either off scale or because the incident light $h\nu$ used did not have sufficient energy to ionize electrons in that deeply stabilized molecular orbital. Note that extensive vibrational structure for the $\pi_u(2p)$ band indicates that the removal of an electron from this molecular orbital causes a significant change in the bonding.

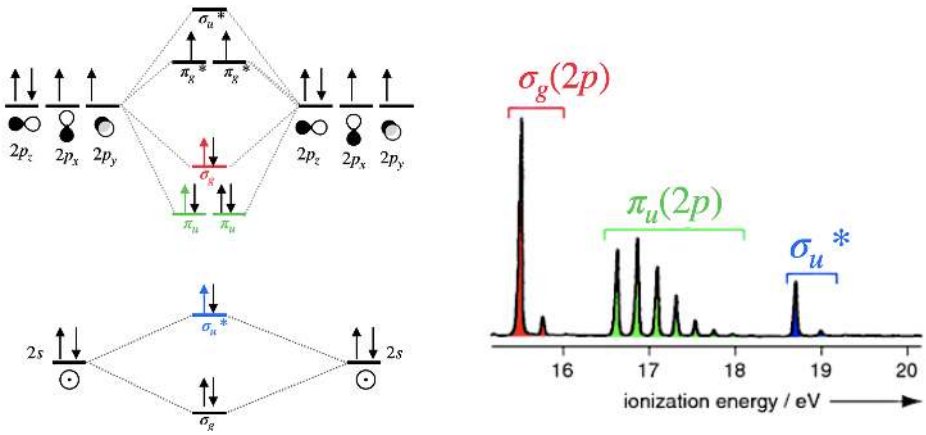


Figure *Section*4.2.6.2: The molecular orbital diagram and photoelectron spectrum of dinitrogen. (CC-BY-NC-SA; Libretexts)

From the photoelectron spectrum of dinitrogen, we can see that the electrons in the $\sigma_g(2p)$ orbital can be ionized using less energy than required to ionize electrons in the $\pi_u(2p)$ orbital. This is evidence for $\sigma_g(2p)$ existing at a higher energy than the $\pi_u(2p)$ orbitals.

This page titled Section 4.2.6: Photoelectron Spectroscopy is shared under a CC BY-NC-SA 4.0 license and was authored, remixed, and/or curated by Kathryn Haas.

- **10.4: Photoelectron Spectroscopy** by Roger Nix is licensed CC BY 4.0.

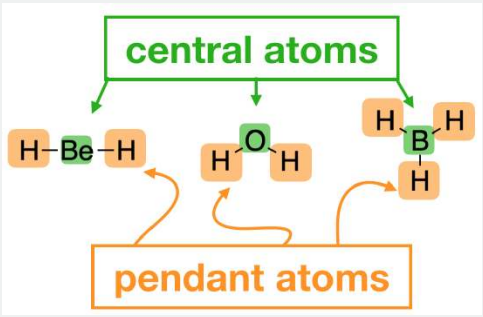
SECTION OVERVIEW

Section 4.3: Larger (Polyatomic) Molecules

We can extend the method we used for diatomic molecules to draw the molecular orbitals of more complicated, polyatomic molecules (molecules with more than two atoms). To combine several different atoms in a molecular orbital diagram, we will group orbitals from different atoms into sets that match the symmetry of a central atom. These **group orbitals** are also referred to as **symmetry adapted linear combinations (SALCs)**. We'll use a stepwise approach to do this as summarized below.

Symmetry adapted linear combinations (SALCs)

We need SALCs (aka group orbitals) to draw molecular orbital (MO) diagrams of *polyatomic* molecules. SALCs are groups of orbitals on **pendant atoms**. These groups of orbitals much match the symmetry of valence orbitals on the **central atom** in order to create a productive interaction. When we combine SALCs with the atomic orbitals on the central atom, we can generate an MO diagram that gives us information about the molecule's bonding and electronic states.



Below is a set of steps you can follow to find SALCs and draw an MO Diagram. Each step will be illustrated in detail through the examples in the subsections that follow this page.

1. Find the **point group** of the molecule and assign Cartesian coordinates so that z is the principal axis.
   Sometimes we can simplify things by looking only at the point group of the relevant orbitals. Only simplify when instructed to do so.*
2. Identify and count the pendant atoms' valence orbitals.
   Is there more than 1 type for each atom (ex. just s, or s and p?) We expect 1 SALC for each ligand orbital.
3. Generate a **reducible representation (Γ)** for the group of pendant atom orbitals using the appropriate character table.
   You have to do this for each set of orbital types. If you only have s orbitals for each ligand, you only need to generate 1 reducible representation. If you have p orbitals, you would generate additional Γ*'s for p_x, p_y, and p_z.*
4. Break the Γ into its component **irreducible representations** from the character table. Note the symmetry of each irreducible representation, its associated orbitals, and their degeneracy.
5. If you are asked to sketch the shapes of SALCs, determine what they "look like" using one of the following strategies.
   (a) Shortcut: if the reducible representations are listed with s, p, or d orbitals in the character table, just draw them (… and skip steps b-c)
   (b) Systematic (Projection Operator) method: Draw an expanded character table and draw your molecule with each ligand identified by letters or numbers (*a,b,c...* or *i,j,k...* or *1,2,3...*) Determine where each pendant atom/orbital ends up under each of the operations of your expanded table. Project the values for each irreducible representation onto the chart you created and then add up the values. Positive and negative values are opposite signed orbitals.
6. Draw the MO diagram by combining SALCs with AO's of like symmetry. When drawing SALC energy levels, remember that the more nodal planes in your SALC orbital drawing, the higher the energy for that SALC orbital.

** When we are focused on orbitals, as in the case for finding group orbitals and drawing molecular orbital diagrams, the symmetry of the orbitals is what we are interested in. In the case of high-symmetry point groups, like $D_{\infty h}$ and $C_{\infty v}$, even though the molecule may have a C_∞ axis, the orbitals do not necessarily retain this symmetry element. For example, the p_x orbital would not have a C_∞ axis, but rather a C_2 axis. It is sufficient and useful to substitute D_{2h} for $D_{\infty h}$ and C_{2v} for $C_{\infty v}$ to simplify the problem.*

Section 4.3.1: Bifluoride anion

Section 4.3.2: Carbon Dioxide

Section 4.3.3: H_2O

Section 4.3.4: NH_3

Section 4.3.5: CO_2 (Revisted with Projection Operators)

Section 4.3.6: BF_3

Section 4.3: Larger (Polyatomic) Molecules is shared under a CC BY-NC-SA 4.0 license and was authored, remixed, and/or curated by LibreTexts.

Section 4.3.1: Bifluoride anion

Finding SALCs and drawing the MO diagram for [F-H-F]⁻

The linear anion [F-H-F]⁻ is a good place to start as an example to illustrate the process of generating pendant atom SALCs and then constructing a molecular orbital diagram for a polyatomic molecule. We will proceed using the steps outlined on the previous page for generating SALCs and a molecular orbital diagram.

Step 1. Find the point group of the molecule and assign Cartesian coordinates so that z is the principal axis.

We begin by assigning the appropriate point group for this molecule: $D_{\infty h}$ (Figure *Section*4.3.1.1). As mentioned in the previous page, it is useful to substitute D_{2h} for $D_{\infty h}$ when generating SALCs and molecular orbital diagrams. The z axis is assigned to be colinear with the principal axis, and in this case is the same as the C_∞ axis (Figure *Section*4.3.1.1).

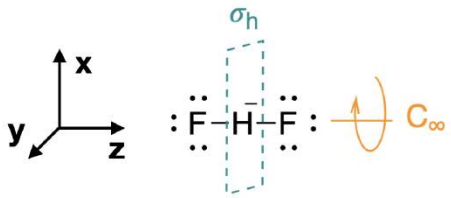


Figure *Section*4.3.1.1: The [FHF]⁻ anion belongs to the $D\infty_h$ point group. (CC-BY-NC-SA; Kathryn Haas)

Step 2. Identify and count the pendant atoms' valence orbitals.

The next step is to identify the valence orbitals on the pendant F atoms that will form SALCs. In most cases, you should consider all of the valence orbitals. In this case, each of the fluorine atoms has four valence orbitals ($2s$, $2p_x$, $2p_y$, and $2p_z$). From these eight fluorine valence orbitals, we should expect eight group orbitals (SALCs).

3. - 5. Generate SALCS (shortcut)

To draw these SALCs for this molecule is rather simple, and we don't need to follow all the steps of finding the **Γ**'s and reducing them. Rather, you can proceed as if you are creating bonding and antibonding molecular orbitals between the two F atoms, except that the F orbitals are separated by the H atom. Approximate sketches of the eight SALCs from F valence orbitals are shown in Figure *Section*4.3.1.2.

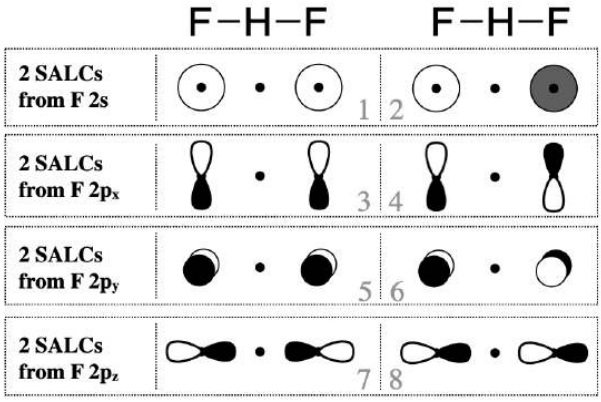


Figure *Section*4.3.1.2: Eight SALCs from the valence orbitals of two fluorine atoms. (CC-BY-NC-SA; Kathryn Haas)

6. Draw the MO diagram by combining SALCs with AO's of like symmetry.

SALCs can productively interact with the central atom only when symmetry is compatible. Just some of the groups of orbitals in Figure *Section*4.3.1.2 possess appropriate symmetry to combine with the hydrogen atom valence orbital (the H $1s$). In this simple case, you can decide whether orbitals have compatible symmetry by visually inspecting the shapes of the group orbitals. The F $2p_y$ and $2p_x$ orbitals do not have appropriate symmetry to bond to the H $1s$ orbital because the nodes of these orbitals run through the center of the H $1s$ orbital, thus we can eliminate all SALCs composed from F $2p_x$ and $2p_y$ (*these are SALCs numbered 3-6 in Figure* *Section*4.3.1.2). On the other hand, the F $2s$ and $2p_z$ orbitals individually do have appropriate shape and direction in space for

productive interaction with an H $1s$ orbital. However only SALCs where the *entire group* has appropriate symmetry will combine with H $1s$ to produce bonding or antibonding molecular orbitals. Only the SALCs labeled with numbers 1 and 7 can combine with an s orbital in the center of the group. The ways in which these SALCs are able to combine with H $1s$ are illustrated in Figure *Section*4.3.1.3.

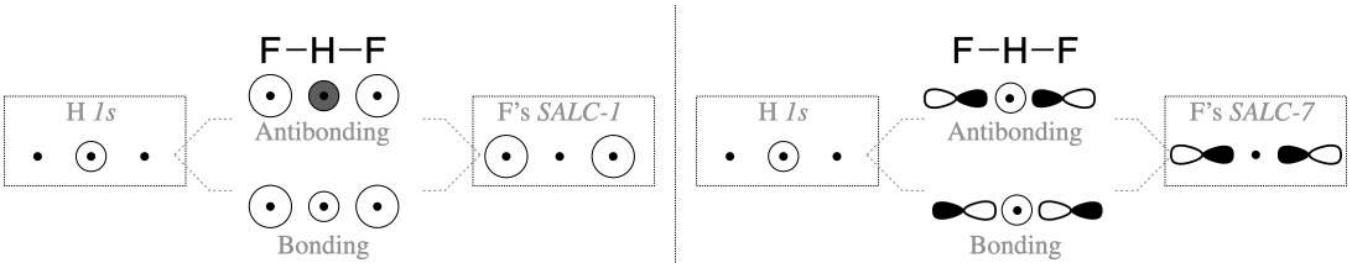


Figure *Section*4.3.1.3: Combinations of a central H $1s$ orbital with the group orbitals, SALC-1 and SALC-7 from Figure *Section*4.3.1.2, to create bonding and antibonding interactions. (CC-BY-NC-SA; Kathryn Haas)

Before we assume that both SALC-1 and SALC-7 will combine with the H $1s$ orbital, we must consider the energies of all atomic orbitals. The F $2p_z$ orbital has a potential energy of -18.7 eV (see Table 5.3.1). This is a good match for the H $1s$ orbital (-13.6 eV). However, the F $2s$ orbital has a much lower energy of -46.37 eV and would have weak interaction with the H $1s$.

The molecular orbital diagram for $[F\text{-}H\text{-}F]^-$ is shown in Figure *Section*4.3.1.4. Notice that all atomic orbitals, group orbitals (SALCs), and molecular orbitals in Figure *Section*4.3.1.4 are assigned a symmetry label that corresponds to each element's symmetry under the D_{2h} point group. The molecular orbital labels correspond to **lower-case Mulliken Labels** of individual reducible representations from the D_{2h} character table. Upper-case symbols are used to indicate symmetry and irreducible representations, while lower-case symbols are used to indicate the identity of an orbital with that symmetry. The labeling methods described for simple diatomic linear molecules (σ, π) are not sufficient to indicate the more complex symmetries of the molecular orbitals in polyatomic molecules. The use of lower-case Mulliken symbols is the most rigorous way to label the orbitals. Refer to your instructor for how you should label orbitals for any graded work.

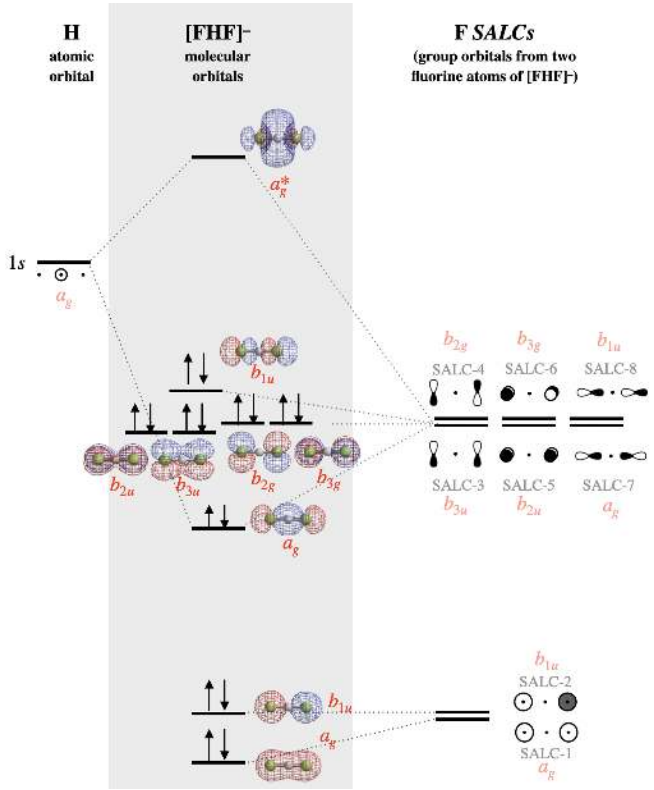
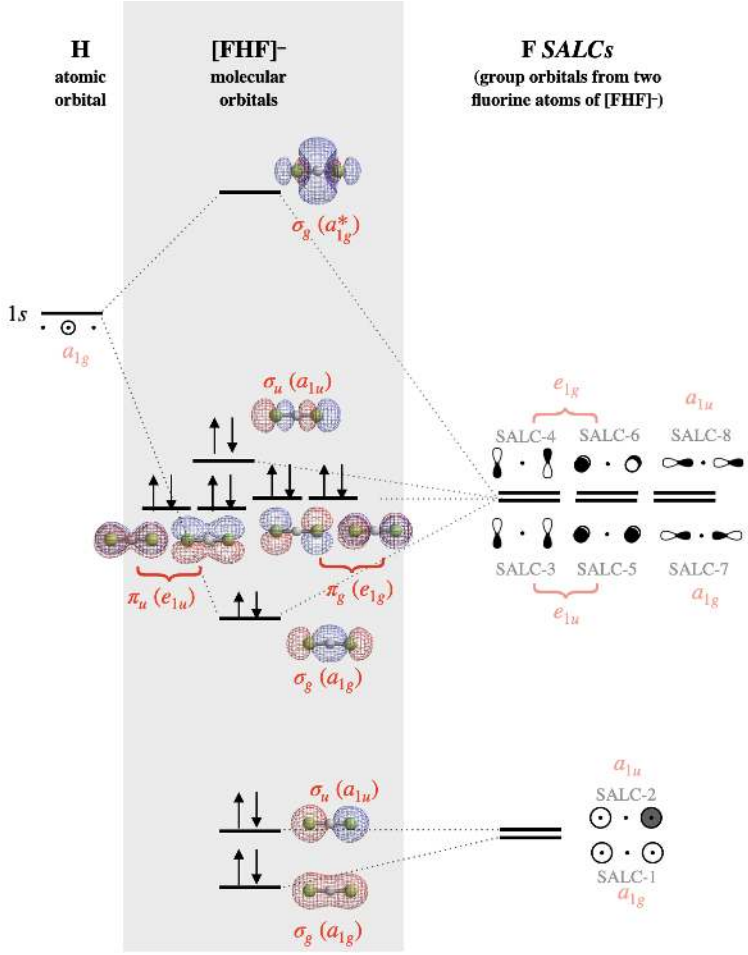

H
atomic
orbital
[FHF]⁻
molecular
orbitals
F SALCs
(group orbitals from two
fluorine atoms of [FHF]⁻)
1s
a_g
a_g^*
b_{1u}
b_{2u}
b_{3u}
b_{2g}
b_{3g}
a_g
b_{2g}
b_{3g}
b_{1u}
SALC-4
SALC-6
SALC-8
SALC-3
SALC-5
SALC-7
b_{3u}
b_{2u}
a_g
b_{1u}
a_g
b_{1u}
SALC-2
SALC-1
a_g

Figure *Section*4.3.1.4:The molecular orbital diagram for [F-H-F]⁻. The molecular orbital surfaces and relative energy levels were calculated using Spartan software. SALCs are labeled according to numbers assigned in Figure *Section*4.3.1.2. The symmetry of each SALC and orbital under the D_{2h} **point group** is shown in red font. (CC-BY-NC-SA; Kathryn Haas)

Click here for a version of Figure *Section*4.3.1.4 using $D_{\infty h}$ labeling:

For high-symmetry groups, a shortcut is to use a lower-symmetry group that maintains the critical symmetry elements. In the case of the $D_{\infty h}$ point group, it is often sufficient to use the approximation of the D_{2h} point group and character table. This is the same MO diagram as shown above, but using the symmetry labels appropriate for the D_{2h} approximation.



Alternate Figure *Section*4.3.1.4: The molecular orbital diagram for [F-H-F]⁻. The molecular orbital surfaces and relative energy levels were calculated using Spartan software. SALCs are labeled according to numbers assigned in Figure *Section*4.3.1.2. The symmetry of each SALC and orbital under the D_{2h} **point group** is shown in red font. (CC-BY-NC-SA; Kathryn Haas)

Constructing the MO diagram

After identifying the atomic orbitals and constructing SALCs, place the atomic orbitals of H on one side of the diagram and all SALCs from F on the other side. Molecular orbitals are in the center.

The lowest-energy fluorine SALCs will be those composed of the lowest-energy atomic orbitals of fluorine; these would be SALC-1 (a_{1g}) and SALC-2 (a_{1u}) that are constructed from fluorine s atomic orbitals. Of these two orbitals, the one with zero nodes would be slightly lower in energy than the one with one node. When these two orbitals form molecular orbitals, the completely symmetric SALC-1 will be mostly non-bonding with slight bonding character from minor combination with the hydrogen $1s$ orbital. SALC-2, however is symmetrically incompatible with hydrogen $1s$ and will be a truly non-bonding orbital distributed over both F atoms.

The six SALCs constructed of fluorine p orbitals will have higher energy since the fluorine p atomic orbitals are higher in energy than the s orbitals (SALC-3 through SALC-8). Again, we expect SALCs with more nodes (SALC-4, -6, -8) to have slightly higher

energy than those with fewer nodes (SALC-3, -5, -7). SALC-7 will form a bonding and antibonding interaction with the hydrogen **1*s*** orbital. All other SALCS are truly non-bonding, but are non-degenerate non-bonding orbitals.

In bifluoride, there is an important distinction between the Lewis structure and molecular orbital description of lone pairs. In Lewis theory, the lone pairs are localized to individual fluorine atoms, while in the molecular orbital description each lone pair is distributed over both fluorine atoms at once (see surface depiction of each molecular orbital in Figure ***Section*4.3.1.4**).

Section 4.3.1: Bifluoride anion is shared under a CC BY-NC-SA 4.0 license and was authored, remixed, and/or curated by LibreTexts.

- **5.4.1: Bifluoride anion** is licensed CC BY-SA 4.0.

Section 4.3.2: Carbon Dioxide

Construct SALCs and the molecular orbital diagram for CO_2

Carbon dioxide is another linear molecule. This example is slightly more complex than the previous example of the bifluoride anion. While bifluoride had only one valence orbital to consider in its central H atom (the $1s$ orbital), carbon dioxide has a larger central atom, and thus more valence orbitals that will interact with SALCs.

Preliminary Steps

Step 1. Find the point group of the molecule and assign Cartesian coordinates so that z is the principal axis.

The CO_2 molecule is linear and its point group is $D_{\infty h}$. The z axis is collinear with the C_∞ axis. We will use the D_{2h} point group as a substitute since the orbital symmetries are retained in the D_{2h} point group.

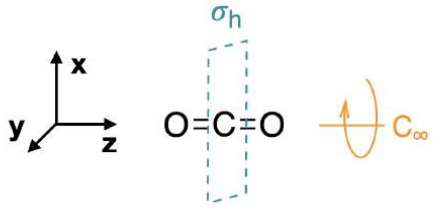


Figure *Section*4.3.2.1: CO_2 belongs to the $D_{\infty h}$ point group. (CC_BY-NC-SA; Kathryn Haas)

Step 2. Identify and count the pendant atoms' valence orbitals.

Each of the two pendant oxygen atoms has four valence orbitals; $2s$, $2p_x$, $2p_y$, and $2p_z$. Thus, we can expect a total of eight SALCs.

Generate SALCs

The SALCs for CO_2 are identical in shape and symmetry to those described in the previous example for the bifluoride anion. But instead of cutting to the shortcut, we will systematically derive the SALCs here to demonstrate the process.

Step 3. Generate the Γ's

Use the D_{2h} character table to generate four reducible representations ($\Gamma's$); one for each of the four types of pendant atom orbitals (s, p_x, p_y, p_z). For each s orbital, assign a value of 1 if it remains in place during the operation or zero if it moves out of its original place. For each p orbital, assign 1 if there is no change, -1 if it remains in place but is inverted, and 0 if it moves out of its original position. The four Γ's are given below:

D_{2h}	E	$C_2(z)$	$C_2(y)$	$C_2(x)$	i	$\sigma(xy)$	$\sigma(xz)$	$\sigma(yz)$
Γ_{2s}	2	2	0	0	0	0	2	2
Γ_{2p_x}	2	−2	0	0	0	0	2	−2
Γ_{2p_y}	2	−2	0	0	0	0	−2	2
Γ_{2p_z}	2	2	0	0	0	0	2	2

Step 4. Break Γ's into irreducible representations for individual SALCs

Reduce each Γ into its component irreducible representations. There are two strategies that can be used to do this. The quick and easy way is to do it "by inspection", but this only works well for simple cases. The other is by using the systematic approach for breaking a Γ into reducible representations described previously in section 4.4.2 using the following formula:

$$\text{number of } i = \frac{1}{h}\sum(\text{number of operations in class}) \times (\chi_\Gamma) \times (\chi_i) \qquad \text{(Section 4.3.2.1)}$$

In other words, the number of irreducible representations of type i is equal to the sum of the number of operations in the class × the character of the Γ_{modes} × the character of i, and that sum is divided by the order of the group (h).

Using either approach results in the following eight irreducible representations ($2A_g + 2B_{1u} + B_{2g} + B_{3u} + B_{3g} + B_{2u}$):

$\mathbf{D_{2h}}$	E	$C_2(z)$	$C_2(y)$	$C_2(x)$	i	$\sigma(xy)$	$\sigma(xz)$	$\sigma(yz)$	
$\mathbf{\Gamma_{2s} = A_g + B_{1u}}$	$\mathbf{\Gamma_{2s}}$	**2**	**2**	**0**	**0**	**0**	**0**	**2**	**2**
	A_g	1	1	1	1	1	1	1	1
	B_{1u}	1	1	−1	−1	−1	−1	1	1
$\mathbf{\Gamma_{2p_x} = B_{2g} + B_{3u}}$	$\mathbf{\Gamma_{2p_x}}$	**2**	**−2**	**0**	**0**	**0**	**0**	**2**	**−2**
	B_{2g}	1	−1	1	−1	1	−1	1	−1
	B_{3u}	1	−1	−1	1	−1	1	1	−1
$\mathbf{\Gamma_{2p_y} = B_{3g} + B_{2u}}$	$\mathbf{\Gamma_{2p_y}}$	**2**	**−2**	**0**	**0**	**0**	**0**	**−2**	**2**
	B_{3g}	1	−1	−1	1	1	−1	−1	1
	B_{2u}	1	−1	1	−1	−1	1	−1	1
$\mathbf{\Gamma_{2p_z} = A_g + B_{1u}}$	$\mathbf{\Gamma_{2p_z}}$	**2**	**2**	**0**	**0**	**0**	**0**	**2**	**2**
	A_g	1	1	1	1	1	1	1	1
	B_{1u}	1	1	−1	−1	−1	−1	1	1

Step 5. Sketch the SALCs

From the systematic process above, you have found the symmetries (the irreducible representations) of all eight SALCs under the D_{2h} point group. To sketch the SALC that corresponds to each irreducible representation, again we use the D_{2h} character table, and specifically the functions listed on the right side columns of the table.

Two A_g SALCs (one from s and one from p_z): The A_g SALCs are each singly degenerate and symmetric with respect to both the principal axis (z) and the inversion center (i) (based on its Mulliken Label). We can look at the functions in the D_{2h} character table that correspond to A_g and see that it is completely symmetric under the group (because the combination of x^2, y^2, z^2 shows that it is totally symmetric). This would be the same symmetry as an s orbital on the central atom. From this information, we know that these SALCs must have symmetry compatible with an s orbital on the central atom, and we can draw the two A_g SALCs shown in Figure *Section*4.3.2.2.

Two B_{1u} SALCs (one from s and one from p_z): The Mulliken Label tells us that the B_{1u} SALCs are each antisymmetric with respect to both the principal axis and the inversion center. The function, z, appearing with B_{1u} in the character table tells us that these SALCs have the same symmetry as the z axis, or a p_z orbital on the central atom. From this information, we know that these two SALCs should be compatible with a p_z orbital on the central atom, and we can draw the two B_{1u} SALCs shown in Figure *Section*4.3.2.2.

All other SALCs shown below are derived using a strategy similar to the one in the two cases described above.

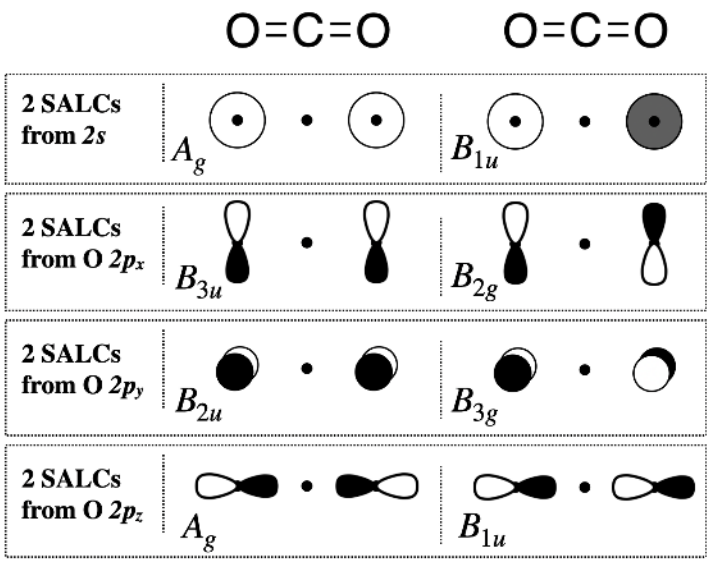


Figure *Section*4.3.2.2: SALCs from the valence orbitals of oxygen atoms in CO_2. (CC-BY-NC-SA; Kathryn Haas)

Draw the MO diagram for CO_2

Step 6. Combine SALCs with AO's of like symmetry.

First we identify the valence orbitals on carbon: there are four including $2s$, $2p_x$, $2p_y$, and $2p_z$. Now we identify the symmetry of each using the D_{2h} character table. The symmetry of a central s orbital corresponds to the combination of functions x^2, y^2, and z^2 in the character table; this is A_g. The p_z orbital corresponds to the symmetry of the linear function z in the character table; this is B_{1u}. And so on... The symmetries of the C valence orbitals are listed below.

$$2s = A_g$$
$$2p_x = B_{3u}$$
$$2p_y = B_{2u}$$
$$2p_z = B_{1u}$$

Now that we have identified the symmetries of the eight oxygen SALCs and the four valence orbitals on carbon, we know which atomic orbitals and SALCs may combine based on compatible symmetries. We also need to know the relative orbital energy levels so that we can predict the relative strength of orbital interactions. The orbital ionization energies are listed in Section 5.3.

With knowledge of both orbital symmetries and energies, we can construct the molecular orbital diagram. The carbon atom goes on one side of the diagram while the oxygen SALCs are drawn on the opposite side. Molecular orbitals are drawn in the center column of the diagram:

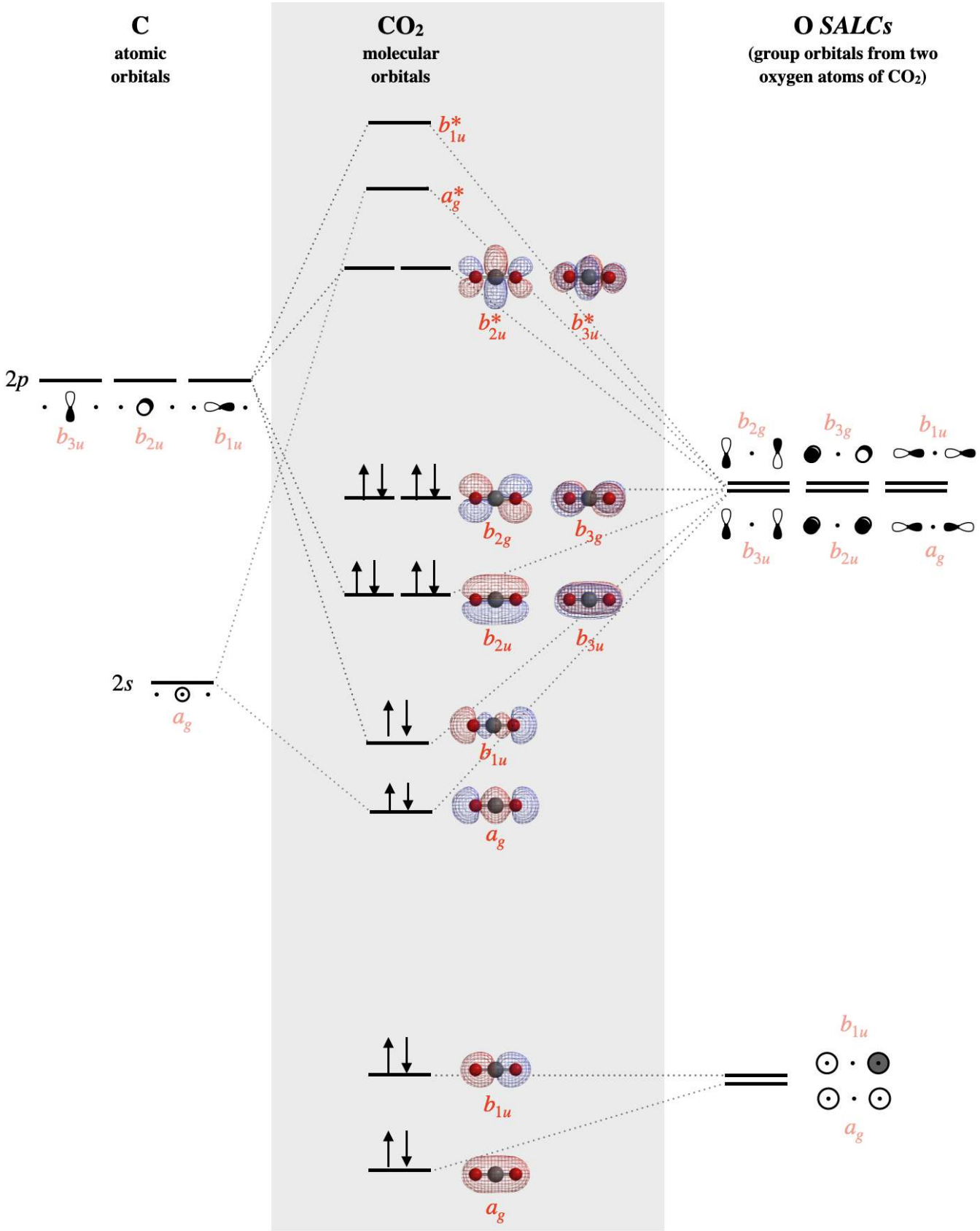


Figure *Section*4.3.2.3: Molecular orbital diagram for carbon dioxide. (CC-BY-NC-SA; Kathryn Haas)

The SALCs on the right side of the diagram above are constructed from groups of either the $2s$ atomic orbitals of oxygen, or the $2p$ atomic orbitals of oxygen. Each SALC will combine with the atomic orbitals of carbon that have compatible symmetry; but the strength of the interaction depends on their relative energies. The individual valence atomic orbitals of oxygen have energies of $-32.36eV$ ($2s$) and $-15.87eV$ ($2p$), while the valence orbitals of carbon have energies of $-19.47eV$ ($2s$) and $-10.66eV$ ($2p$). The $2s$ orbitals of the oxygen are far lower in energy ($-32.36eV$) than all other valence orbitals, and so we should expect that molecular orbitals that are constructed from these oxygen $2s$ will be mostly non-bonding. These mostly non-bonding orbitals are the a_{1g} and b_{1g} orbitals shown at the bottom of Figure $Section 4.3.2.3$. The a_g orbital is lower in energy than the b_{1u} due to slight mixing with other orbitals of a_g symmetry.

The bonding orbitals of CO_2 include two $sigma$ molecular orbitals of a_g and b_{1u} symmetry and two π molecular orbitals of b_{2u} and b_{3u} symmetry. Each of these bonding molecular orbitals possesses a higher-energy antibonding partner. The b_{2g} and b_{3g} SALCs that are formed from oxygen $2p_x$ and $2p_y$ orbitals have no compatible match with carbon valence orbitals; thus they form two b_{2g} and b_{3g} molecular orbitals, which are truly non-bonding and mostly oxygen in character. Still, notice that each orbital is spread across both oxygen atoms at once, and again we see that each non-bonding electron pair in the HOMO is very different in molecular orbital theory compared to Lewis theory. Each non-bonding pair is distributed over both oxygen atoms at once in molecular orbital theory, while in Lewis theory each lone pair is isolated to one atom or to localized bonds attached to that atom.

This page titled Section 4.3.2: Carbon Dioxide is shared under a CC BY-NC-SA 4.0 license and was authored, remixed, and/or curated by Kathryn Haas.

- **5.4.2: Carbon Dioxide** by Kathryn Haas is licensed CC BY-SA 4.0.

Section 4.3.3: H_2O

Construct SALCs and the molecular orbital diagram for H_2O.

This is the first example so far that is not a linear molecule. Water is a bent molecule, and so it is important to remember that interactions of pendant ligands are dependent on their positions in space. You should consider the positions of the three atoms in water to be essentially fixed in relation to each other. The process for constructing the molecular orbital diagram *for a non-linear molecule*, like water, is similar to the process for linear molecules. We will walk through the steps below to construct the molecular orbital diagram of water.

Preliminary Steps

Step 1. Find the point group of the molecule and assign Cartesian coordinates so that z is the principal axis.

The H_2O molecule is bent and its point group is C_{2v}. The z axis is collinear with the principal axis, the C_2 axis. There is no need to simplify this problem, as we had done for previous examples. The C_{2v} point group is simple enough.

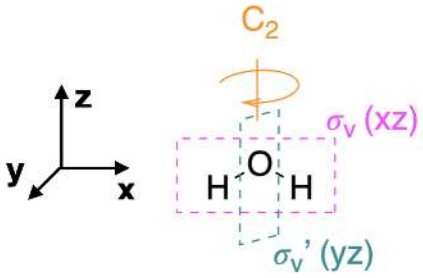


Figure ***Section*4.3.3.1**: The water molecular is in the C_{2v} point group. (CC-BY-NC-SA; Kathryn Haas)

Step 2. Identify and count the pendant atoms' valence orbitals.

Each of the two pendant hydrogen atoms has one valence orbital, the $1s$. Thus, we can expect a total of two SALCs from these two atoms.

Generate SALCs

The SALCs for H_2O are quite simple, yet we will systematically derive the SALCs here to demonstrate the process.

Step 3. Generate the Γ's

Use the C_{2v} character table to generate one reducible representation (Γ); in this case we need only one Γ because there is only one type of valence orbital (the $1s$). For each s orbital, assign a value of 1 if it remains in place during the operation or zero if it moves out of its original place. The Γ is given below:

$\mathbf{C_{2v}}$	E	C_2	$\sigma_v(xz)$	$\sigma_v'(yz)$
$\mathbf{\Gamma_{1s}}$	2	0	2	0

Step 4. Break Γ's into irreducible representations for individual SALCs

Reduce each Γ into its component irreducible representations. Using either of the processes described previously, we find that the Γ reduces to the two irreducible representations A_1 and B_1 under the C_{2v} point group.

$\mathbf{C_{2v}}$	E	C_2	$\sigma_v(xz)$	$\sigma_v'(yz)$
$\mathbf{\Gamma_{1s}}$	**2**	**0**	**2**	**0**
A_1	1	1	1	1
B_1	1	−1	1	−1

Step 5. Sketch the SALCs

From the systematic process above, you have found the symmetries (the irreducible representations) of both SALCs under the C_{2v} point group. To sketch the SALC that corresponds to each irreducible representation, again we use the C_{2v} character table, and

specifically the functions listed on the right side columns of the table.

One A_1 SALC: The A_1 SALC is singly degenerate and symmetric with respect to both the principle axis (z) and the inversion center (i) (based on its Mulliken Label). We can look at the functions in the C_{2v} character table that correspond to A_1 and see that it is completely symmetric under the group (because the combination of x^2, y^2, z^2 shows that it is totally symmetric). This would be the same symmetry as an s orbital on the central oxygen atom. From this information, we know that this SALC must have symmetry compatible with an s orbital on the central atom. We can also see from the character table that the z axis, and thus a p_z orbital on oxygen, also possesses A_1 symmetry. This tells us that in addition to being compatible with the oxygen s orbital, it should also be compatible with the oxygen p_z orbital. From this information we can draw the A_1 SALC shown in Figure *Section*4.3.3.2. *If it is not obvious how the A_1 sketch in Fig. Section*4.3.3.2 *is compatible with the s and p_z orbitals of oxygen, inspect the drawings corresponding to molecular orbitals $2a_1$ and $3a_1$ in Fig. Section*4.3.3.3.

One B_1 SALC: The Mulliken Label tells us that the B_1 SALC is singly degenerate and antisymmetric with respect to both the principal axis and the inversion center. The function, x, appearing with B_1 in the character table tells us that this SALC has the same symmetry as the x axis, or a p_x orbital on the central oxygen atom. From this information, we know that this SALC should be compatible with a p_x orbital on the central atom, and we can draw the B_1 SALCs shown in Figure *Section*4.3.3.2. *If it is not obvious how the B_1 sketch in Fig. Section*4.3.3.2 *is compatible with the p_x orbital of oxygen, inspect the drawing corresponding to molecular orbital $1b_1$ in Fig. Section*4.3.3.3.

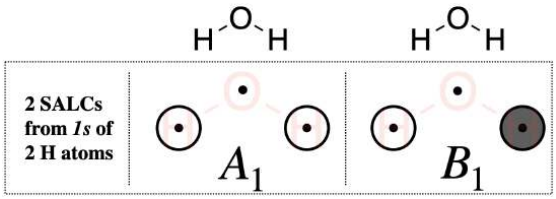


Figure *Section*4.3.3.2: Sketch of the A_1 and B_1 hydrogen SALCs of water. (CC-BY-NC-SA; Kathryn Haas)

Not convinced about the sketches of these SALCs? You can convince yourself by putting them to the test. Try the exercise below.

? Exercise *Section*4.3.3.1

Perform all operations of the C_{2v} point group on the two sketches of H SALCs shown in Figure *Section*4.3.3.2, and convince yourself that each sketch does possess the A_1 and B_1 symmetries assigned to them, respectively, under the C_{2v} point group.

Answer

Add texts here. Do not delete this text first.

Draw the MO diagram for H_2O

Step 6. Combine SALCs with AO's of like symmetry.

First we must identify the valence orbitals on the central oxygen: there are four including $2s$, $2p_x$, $2p_y$, and $2p_z$. Now we identify the symmetry of each using the C_{2v} character table. The symmetry of a central $2s$ orbital corresponds to the combination of functions x^2, y^2, and z^2 in the character table; this is A_1. The p_z orbital also corresponds to A_1. And so on... The symmetries of oxygen valence orbitals are listed below.

$$2s = A_1$$
$$2p_x = B_1$$
$$2p_y = B_2$$
$$2p_z = A_1$$

Now that we have identified the symmetries of the two hydrogen SALCs and the four valence orbitals on oxygen, we know which atomic orbitals and SALCs may combine based on compatible symmetries. We also need to know the relative orbital energy levels so that we can predict the relative strength of orbital interactions. The orbital ionization energies are listed in Section 5.3.1.

With knowledge of both orbital symmetries and energies, we can construct the molecular orbital diagram. The valence orbitals of oxygen go on one side of the diagram while the hydrogen group orbitals are drawn on the opposite side. Molecular orbitals are

drawn in the center column of the diagram, as shown in Figure *Section*4.3.3.3:

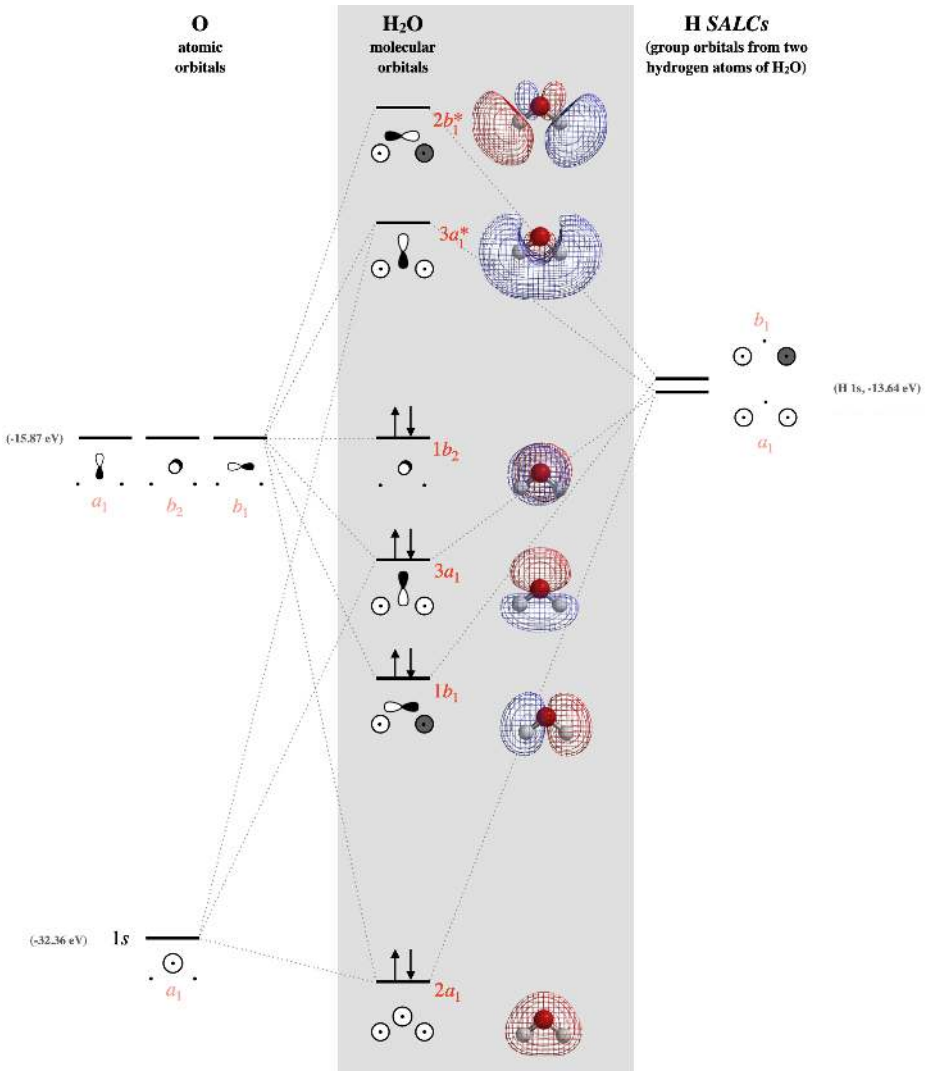


Figure *Section*4.3.3.3: The molecular orbital diagram of water. Molecular orbital surfaces calculated using Spartan software. The surface of the $3a_1^*$ orbital has been trimmed. (CC-BY-NC-SA; Kathryn Haas)

✔ Example *Section*4.3.3.1

In the previous examples shown for the molecular orbital diagrams of the bifluoride anion and carbon dioxide, we discussed differences in the understanding of those molecules from molecular orbital theory compared to Lewis structures. Water contains two lone pairs in its Lewis structure. Compare the predictions about water's lone pairs of electrons and its reactivity based on (1) the combination of elementary models (Lewis, Valence Bond, and Hybridized Orbital theories) and (2) Molecular Orbital theory. Specifically address and explain how the elementary models differ from molecular orbital theory in the following respects:

a. Where are the lone pairs in water?
b. Are the two lone pairs equivalent or are they different?
c. Where are sites on the molecule that will undergo reaction with electrophiles and nucleophiles?

Solution

1) Elementary models: The Lewis structure predicts that two lone pairs are (a) localized on the oxygen atom of water and that (b) both lone pairs are equivalent. The Lewis structure, combined with Valence Bond Theory, would predict that lone pairs occupy two equivalent hybridized sp^3 atomic orbitals on oxygen. (c) Lewis theory would predict that the oxygen lone pairs are

nucleophiles; thus an electrophile would react with the oxygen atom lone pairs. The polarized O-H bond leaves the H atoms as the most electrophilic locations on the water molecule; thus nucleophiles would react at the H atoms of water.

2) Molecular orbital theory: The molecular orbitals predict that (a) the two lone pairs of water are not equivalent, and that (b) each is distributed over the entire molecule. One lone pair is in the truly non-bonding $1b_2$ orbital (Figure *Section*4.3.3.3), which is also the HOMO. There is not another truly non-bonding orbital in the molecule, but the lowest-energy $2a_1$ orbital could be considered mostly non-bonding due to the large energy difference between it and other valence orbitals. (c) Although the $2a_1$ orbital can be considered mostly non-bonding, we cannot expect the electrons in $2a_1$ to react readily, as they are in the lowest-energy molecular orbital. Molecular orbital theory predicts that reactions occur at the HOMO and LUMO orbitals. The HOMO reacts with electrophiles, and in this case, the HOMO is distributed over the top and bottom faces of the molecule, and is centered on the oxygen atom. The LUMO would react with nucleophiles. The LUMO is the orbital labeled $3a_1^*$ in Figure *Section*4.3.3.3, and has a major lobe that is distributed more heavily over the H atoms, and from this we should predict H atoms to be the preferred site of reaction for nucleophiles.

Expressing molecular orbitals in terms of Ψ

The general expression for a molecular orbital, or the linear combination of atomic orbitals (LCAO), was given previously as $\Psi = c_a\psi_a + c_b\psi_b$. In this expression, the wavefunction of two atoms (ψ_a and ψ_b) is combined to form the wavefunction of the molecular orbital. The coefficients c_a and c_b quantify the contribution of each atomic ψ to the molecular Ψ.

$$\Psi = c_a\psi_a + c_b\psi_b$$

In the case of polyatomic orbitals, each LCAO is constructed of atomic orbitals from a central atom and group orbitals (SALCs) from the pendent atoms. In the case of water, the expression above could be modified to give the expression below.

$$\Psi = c_{oxygen}\,(\psi_{oxygen}) + c_{SALCs}\,(N(\psi_{H_a} \pm \psi_{H_b}))$$

N represents the normalizing requirement that was mentioned previously in reference to the requirements for electron wavefunctions and probability functions. The normalizing requirement simply stated is the requirement that the probability of finding the electron in any orbital, including group orbitals, is 1. In general, the value of N for a group orbital is...

$$N = \frac{1}{\sum c_i^2}$$

...where c_i is the coefficient of each unique atomic orbital that contributes to the group. For the hydrogen SALCs of water, there are two atomic orbitals that contribute to equally to each SALC, and so the coefficient on each of the two orbitals is 1. This gives $N = \left(\frac{1}{\sqrt{1^2+1^2}}\right) = \frac{1}{\sqrt{2}}$ for the H SALCs of water.

There are only two hydrogen SALCs: the one in which the hydrogen wavefunctions are added ($N(\psi_{H_a} + \psi_{H_b})$) has A_1 symmetry, and the one in which the hydrogen wavefunctions are subtracted ($N(\psi_{H_a} - \psi_{H_b})$) has B_1 symmetry.

The molecular orbitals from Figure *Section*4.3.3.3 are expressed below in terms of their LCAO of individual wavefunctions. Yet, note that these expressions are simplifications that ignore orbital mixing. For example, as expressed below, they ignore contributions of oxygen $2s$ to the higher energy moelcular orbitals with A_1 symmetry (the $3a_1$ and $3a_1^*$ in Figure *Section*4.3.3.3).

MO		*OxygenAO*		*HydrogenSALC*	*Description*
Ψ_{2a_1}	=	$c_{(ox1)}\psi_{(2s)}$	+	$c_{(hy1)}[N(\psi_{H_a} + \psi_{H_b})]$	$c_{(hy1)}$ is positive; bonding, slightly nonbonding
Ψ_{1b_1}	=	$c_{(ox2)}\psi_{(2p_x)}$	+	$c_{(hy2)}[N(\psi_{H_a} - \psi_{H_b})]$	$c_{(hy2)}$ is positive; bonding
Ψ_{3a_1}	=	$c_{(ox3)}\psi_{(2p_z)}$	+	$c_{(hy3)}[N(\psi_{H_a} + \psi_{H_b})]$	$c_{(hy3)}$ is positive; bonding
Ψ_{1b_2}	=	$\psi_{(2p_y)}$			nonbonding
$\Psi^*_{3a_1}$	=	$c_{(ox4)}\psi_{(2p_z)}$	+	$c_{(hy4)}[N(\psi_{H_a} + \psi_{H_b})]$	$c_{(hy4)}$ is negative; antibonding
$\Psi^*_{1b_1}$	=	$c_{(ox5)}\psi_{(2p_x)}$	+	$c_{(hy5)}[N(\psi_{H_a} - \psi_{H_b})]$	$c_{(hy5)}$ is negative; antibonding

Section 4.3.3: H_2O is shared under a CC BY-NC-SA 4.0 license and was authored, remixed, and/or curated by LibreTexts.

- **5.4.3: H_2O** is licensed CC BY-SA 4.0.

Section 4.3.4: NH_3

Construct SALCs and the molecular orbital diagram for NH_3

This is the first example so far that has more than two pendant atoms and the first example in which the molecule has atoms that lie in three dimensions (i.e., it is not flat). Ammonia is a trigonal pyramidal molecule, with three pendant hydrogen atoms. The three-dimensional shape and the odd number of pendant atoms makes this example more complicated than the previous cases of water, carbon dioxide, and bifluoride. In this case, sketching the shapes (step 5) of pendant atom SALCs is less straightforward; rather, an alternative method, the **projection operator method**, is preferred for generating pictorial representations of the SALCs.

As in previous examples, it is important to remember that interactions of pendant ligands are dependent on their positions in three-dimensional space. You should consider the positions of the four atoms in ammonia to be essentially fixed in relation to each other. We will walk through the steps used to construct the molecular orbital diagram of ammonia. The first few steps are the same as you've seen before:

Step 1. Find the point group of the molecule and assign Cartesian coordinates so that z is the principal axis.

The NH_3 molecule is trigonal pyramidal and its point group is C_{3v}. The z axis is collinear with the principal axis, the C_3 axis.

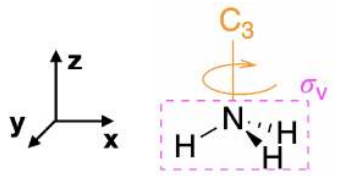


Figure *Section*4.3.4.1: The ammonia molecule is in the C_{3v} point group. (CC-BY-NC-SA; Kathryn Haas)

Step 2. Identify and count the pendant atoms' valence orbitals.

Each of the three pendant hydrogen atoms has one valence orbital; the $1s$. Thus, we can expect a total of three SALCs from these three atoms.

Step 3. Generate the Γ's

Use the C_{3v} character table to generate one reducible representation (Γ); in this case we need only one Γ because there is only one type of valence orbital (the $1s$). For each s orbital, assign a value of 1 if it remains in place during the operation or zero if it moves out of its original place. The Γ is given below:

C_{3v}	E	$2C_3$	$3\sigma_v$
Γ_{1s}	3	0	1

Step 4. Break Γ's into irreducible representations for individual SALCs

Reduce each Γ into its component irreducible representations. Using either of the processes described previously, we find that the Γ reduces to the two irreducible representations A_1 and E under the C_{3v} point group.

C_{3v}	E	$2C_3$	$3\sigma_v$
Γ_{1s}	3	0	2
A_1	1	1	1
E	2	−1	0

Notice that we only found TWO irreducible representations. But, in fact we have THREE different SALCs. The E irreducible representation is doubly degenerate, which in this context means that it corresponds to two degenerate SALCs. Thus, we have already found the symmetries of the three SALCs for ammonia: Two of the SALCs are degenerate with E symmetry under the C_{3v} point group, while the third SALC has A_1 symmetry.

Step 5. Sketch the SALCs using the PROJECTION OPERATOR METHOD

From the first four steps (described above), you have found the symmetries (the irreducible representations) of all three SALCs under the C_{3v} point group. To sketch the SALC that corresponds to each irreducible representation, again we use the C_{3v} character

table. But now we will introduce the **projection operator method** to derive the surface representation of each SALC.

Step 5.1: Label the pendent atoms

In the projection operator method, first **label each of the pendant atoms so that we can distinguish identical atoms from one another**; for example, identify the three hydrogen atoms on ammonia as H_a, H_b, and H_c (Figure *Section*4.3.4.2).

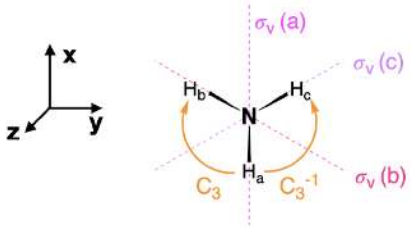


Figure *Section*4.3.4.2: The three H's in $\mathbf{NH_3}$ are chemically identical, but we can distinguish them using labels for the purpose of applying the projection operator method. In this figure, we have placed the z axis along the principal C_3 axis and placed the x axis colinear with one H. Each of the three H atoms has been labeled as H_a, H_b, or H_c. The σ_v that is coplanar with each H is labeled similarly (a, b, c) to keep account of each individual plane of symmetry. (CC-BY-NC-SA; Kathryn Haas)

Step 5.2: Create an expanded character table with one pendant atom's projected position after each operation

We will **perform each operation of the C_{3v} point group on this labeled molecule** and follow where one of the atoms is projected after the operation is complete. We will arbitrarily choose H_a. For example, upon performing the identity operation, E, the H_a atom is projected onto itself. On the other hand, H_a is projected onto H_b upon a clockwise C_3 rotation (as drawn in Figure *Section*4.3.4.2). We take into account the result of each operation using an expanded character table (refer to the table below, Section 4.3.4.1). In the expanded character table, each operation within each class is written separately (i.e., $2C_3$ is accounted for separately as C_3 and C_3^{-1}).

Table Section 4.3.4.1: The expanded character table, and the projection of H_a by each operation is shown below.

$\mathbf{C_{3v}}$	E	C_3	C_3^{-1}	$\sigma_v(a)$	$\sigma_v(b)$	$\sigma_v(c)$
Projection of $\mathbf{H_a}$	H_a	H_b	H_c	H_a	H_c	H_b

(Section 4.3.4.1)

Step 5.3: Find the contribution of each pendant atom to each SALC

Next, **create a linear combination of the projections for each of the SALCs** (the irreducible representations found in step 4). For each of the irreducible representations, multiply the projection by the respective character of the operation.

$$\text{Contribution of each atom to the SALC } = \sum(\text{Projection of } H_a \times \chi)$$

The linear combination for all irreducible representations of C_3v is shown below.

Table Section 4.3.4.2: The symmetry adapted linear combination (SALC) for each irreducible representation of C_3v is shown.

$\mathbf{C_{3v}}$	E	C_3	C_3^{-1}	$\sigma_v(a)$	$\sigma_v(b)$	$\sigma_v(c)$	Linear Combination
Projection of $\mathbf{H_a}$	$\mathbf{H_a}$	$\mathbf{H_b}$	$\mathbf{H_c}$	$\mathbf{H_a}$	$\mathbf{H_c}$	$\mathbf{H_b}$	
A_1	1	1	1	1	1	1	$= \mathbf{2H_a + 2H_b + 2H_c}$
A_2	1	1	1	−1	−1	−1	$= \mathbf{0}$
E	2	−1	−1	0	0	0	$= \mathbf{2H_a - H_b - H_c}$

(Section 4.3.4.2)

Notice that there are only two irreducible representations that produce SALCs, and these are the same that were found in Step 4, above. This illustrates the fact that only the irreducible representations found through the reduction of the Γ will produce SALCs. We can ignore any irreducible representations that were not found in Step 4. Or, you can check your work in Step 4 by applying the projection operator to any irreducible representations not found in Step 4, and finding that they produce a sum of zero.

Step 5.4: Sketch the SALCs

The meaning of the linear combinations found in Table Section 4.3.4.2 is as follows:

- **Sketch the SALC with A_1 symmetry:** The linear combination $2H_a + 2H_b + 2H_c$ indicates all contributions to this SALC are of the same sign (of the wavefunction). Qualitatively, this means there is no node in this SALC. We can take this SALC almost literally to assume that all three H 1s wavefunctions contribute equally to the SALC. We can also use the fact that the A_1 representation possesses the full symmetry of the C_3v point group, is compatible with an s orbital on N, and thus is a totally symmetric SALC.

  Quantitatively, we can apply the normalizing factor, N, for this SALC. The linear combination for the A_1 SALC in Table Section 4.3.4.2 shows us that the coefficient for each orbital is 1. Thus, the normalizing factor for the A_1 SALC is $N = \left(\frac{1}{\sqrt{1^2+1^2+1^2}}\right) = \frac{1}{\sqrt{3}}$. This tells us that H_a, H_b, and H_c each contribute $\frac{1}{\sqrt{3}}$ to the normalized A_1 group orbital:

  $$A_1 \text{ group orbital } = \frac{1}{\sqrt{3}}[\psi_{H_a} + \psi_{H_b} + \psi_{H_c}]$$

  This is shown visually in Figure *Section*4.3.4.3.
- **Sketch two SALCs with E symmetry:** The linear combination $2H_a - H_b - H_c$ indicates that there are contributions with both positive and negative sign to the wavefunction for each of the E group orbitals. Qualitatively, this tells us that there is a node within each of these two SALCs, and that the total contribution of the positive portion of the wavefunction is equal to the contribution of the negative portion.
  - **Finding the first E SALC:**
    For one of the SALCs, we can take the linear combination from Table Section 4.3.4.2 almost literally: The contribution from H_a is equal and opposite to the sum of the contributions from $H_b + H_c$. This would result in a SALC as shown in Figure *Section*4.3.4.3 (E, left), that would have symmetry of the x axis and that would be compatible with the p_x orbital on N. The node exists in the yz plane and there is an equal contribution of positive and negative parts of the total wavefunction.

    We can also apply the normalizing factor, N, to find this SALC. The linear combination for the E SALC in Table Section 4.3.4.2 shows us that the coefficients for orbital contributions are 2, -1, and -1. Thus, the normalizing factor for the first E SALC is $N = \left(\frac{1}{\sqrt{2^2+(-1)^2+(-1)^2}}\right) = \frac{1}{\sqrt{6}}$. This normalized E group orbital is:

    $$\text{First } E \text{ group orbital } = \frac{1}{\sqrt{6}}[2\psi_{H_a} - \psi_{H_b} - \psi_{H_c}]$$

    This is shown visually in Figure *Section*4.3.4.3 (E, left).
  - **Finding the second E SALC:**
    The second SALC is less obvious at first glance. We must use clues from the character table to help us determine what it should "look like". Since the E representation transforms as the group, (x, y), we know that one of the SALCs will have the symmetry of the x axis and p_x orbital on the central nitrogen atom, while the other should possess the symmetry of the y axis and be compatible with the p_y orbital on nitrogen. This alone could lead you to the sketch of the second SALC with E symmetry shown in Figure *Section*4.3.4.3 (E, right). This second E SALC must have a node in the xz plane, and because H_a lies in this node, H_a cannot contribute to this group orbital. Retaining the fact that the positive and negative contributions of the linear combination must be equal, we can arrive at a SALC that has equal but opposite contributions of H_b and H_c, and no contribution by H_c (Figure *Section*4.3.4.3, right).

    We can also apply the normalizing factor, N, to find this SALC. But we must apply the fact that H_a cannot contribute to the SALC with "y" symmetry. We remove the contribution of H_a, leaving us with coefficients of 0 for H_a and 1 for H_b and H_c. Thus, the normalizing factor for the second E SALC is $N = \left(\frac{1}{\sqrt{0^2+1^2+1^2}}\right) = \frac{1}{\sqrt{2}}$. To this, we must add positive and negative coefficients so that the entire wavefunction of this SALC is normalized. The result for this normalized E group orbital is:

    $$\text{Second } E \text{ group orbital } = \frac{1}{\sqrt{2}}[\psi_{H_b} - \psi_{H_c}]$$

    This is shown visually in Figure *Section*4.3.4.3.

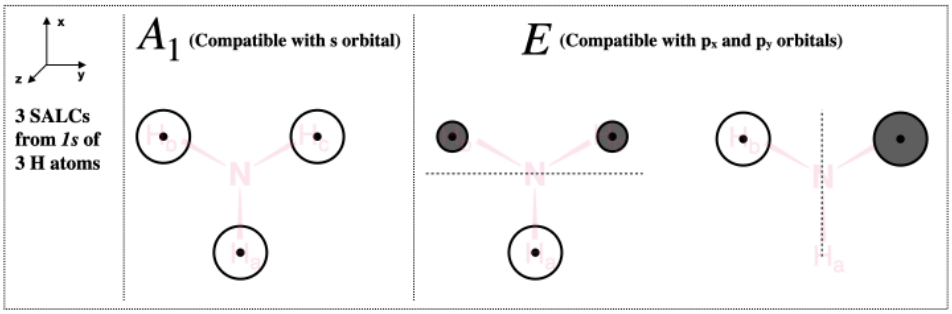


Figure **Section4.3.4.3**: Sketches of H SALCs of ammonia from the perspective of the C_3 axiz (z axis). The A_1 SALC is shown at the left, while two degenerate SALCs with E symmetry are shown on the right. Nodes for E group orbitals are shown as dashed lines. (CC-BY-NC-SA; Kathryn Haas)

Step 6. Combine SALCs with AO's of like symmetry to draw the MO diagram for NH_3

First we must identify the valence orbitals on the central nitrogen: there are four including $2s$, $2p_x$, $2p_y$, and $2p_z$. Now we identify the symmetry of each using the C_{3v} character table. The symmetry of a central $2s$ orbital corresponds to the combination of functions x^2, y^2, and z^2 in the character table; this is A_1. The p_z orbital also corresponds to A_1. And so on... The symmetries of nitrogen valence orbitals are listed below.

$$2s = A_1$$
$$(2p_x,\ 2p_y) = E$$
$$2p_z = A_1$$

The next step is to get a sense of the relative energies of valence atomic orbitals for nitrogen and hydrogen, and then construct the molecular orbital diagram. The nitrogen $2s$ orbital is about 12 eV lower in energy than a H $1s$. This difference is an acceptable energy-match for the H orbitals to interact, but would not usually result in a strong interaction. On the other hand, the nitrogen 2p orbitals have an energy very close to the hydrogen 1s, different by only 0.5 eV. Knowledge of the relative energies of the atomic orbitals tells us that, when constructing a diagram, we can place the H SALCs at an energy similar to that of the N $2p$ orbitals, while the N $2s$ is much lower (Figure **Section4.3.4.4**).

The $2s$ and $2p_z$ orbitals have A_1 symmetry and can combine with the A_1 SALC. These orbitals will give three molecular orbitals. The $2s$ orbital will not have strong interactions with the other orbitals of A_1 symmetry due to the large energy difference. The $2p_z$ orbital will not have good overlap with the wavefunctions for the three hydrogen orbitals due to their positions in space: The $2p_z$ orbital has half of its angular distribution pointed away from the hydrogen orbitals, and half pointed toward the center of a triangle formed by the three hydrogen atoms. The nitrogen $2s$ and $2p_z$ will combine with the hydrogen SALC of A_1 symmetry to give three molecular orbitals; one low-energy bonding orbital, one mid-energy non-bonding orbital, and one high-energy antibonding orbital. The mid-level non-bonding a_1 molecular orbital is close in energy to, and resembles, the nitrogen $2p_z$ orbital. The lowest energy a_1 molecular orbital will be lower in energy, but be similar to the nitrogen $2s$.

The remaining two $2p$ orbitals are degenerate and possess E symmetry under the C_{3v} point group. Although these orbitals are a good energy match, again, their orientation and positions in space do not allow for good orbital overlap, and their bonding and antibonding interactions are relatively weak compared to what we might otherwise expect from such a good energy match. The e atomic orbitals of nitrogen will combine with the e SALCs to give a set of two degenerate bonding molecular orbitals and a set of two degenerate antibonding orbitals (four total molecular orbitals of e symmetry). The MO diagram for NH_3 is shown in Figure **Section4.3.4.4**, with calculated electron density surfaces of each MO shown.

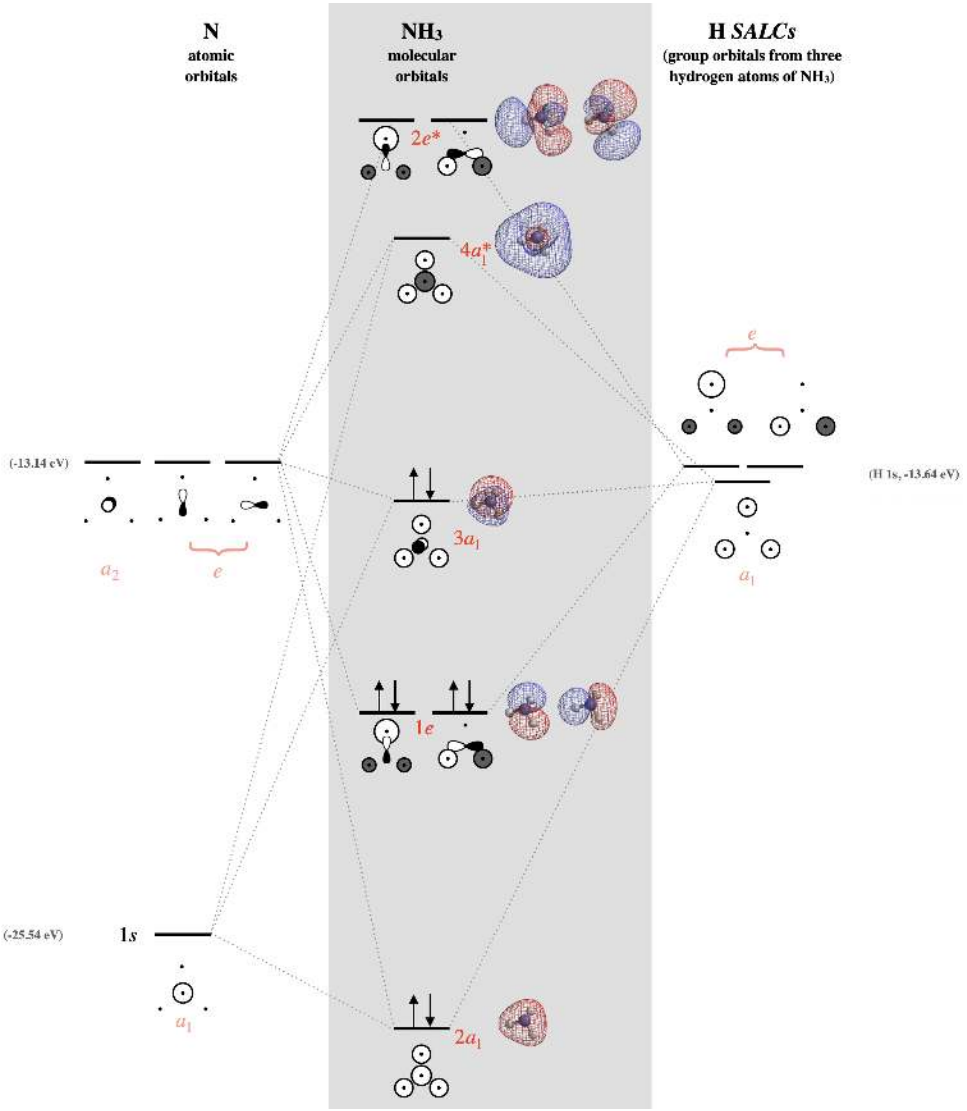


Figure ***Section*4.3.4.4**: The molecular orbital diagram of ammonia. Molecular orbitals surfaces calculated using Spartan software. (CC-BY-NC-SA; Kathryn Haas)

This page titled Section 4.3.4: NH_3 is shared under a CC BY-NC-SA 4.0 license and was authored, remixed, and/or curated by Kathryn Haas.

- **5.4.4: NH_3** by Kathryn Haas is licensed CC BY-SA 4.0.

Section 4.3.5: CO_2 (Revisted with Projection Operators)

The process for finding SALCs and constructing the molecular orbital diagram for carbon dioxide was described in a previous section (Section 5.4.2). However, we also just presented an alternative strategy, the projection operator method, to finding the shapes of SALCs in Section 5.4.4. Let's revisit carbon dioxide and demonstrate how you can use the projection operator method to find SALCs for carbon dioxide.

Just as before, we can simplify the problem by approximating the $D_{\infty h}$point group using D_{2h}. The first four steps for constructing the MO diagram would be the same as described in Section 5.4.2. and we will pick up from that point (with Step 5) to find what the SALCs look like using the projection operator method.

The projection operator method applied to CO_2

Step 5.1: Label the pendent atoms.

We can label the pendant atoms as O_a and O_b, as in Figure *Section*4.3.5.1.

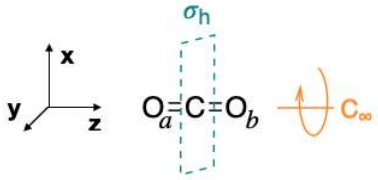


Figure *Section*4.3.5.1: The structure of carbon dioxide with pendant oxygen atoms distinguished with labels *a* and *b*. Note that we will approximate the C_∞ axis as a C_2 axis to simplify the process of finding the SALCs. (CC-BY-SA; Kathryn Haas)

Step 5.2: Create an expanded character table with one pendant atom's projected position for each operation

The D_{2h} character table needs no expansion because each operation is in its own class. We will arbitrarily choose to determine the new position of O_a after each operation.

D_{2h}	E	$C_2(z)$	$C_2(y)$	$C_2(x)$	i	$\sigma(xy)$	$\sigma(xz)$	$\sigma(yz)$
Projection of O_a	O_a	O_a	O_b	O_b	O_b	O_b	O_a	O_a

Step 5.3: Find the contribution of each pendant atom to each SALC

Create a linear combination of the projections for each or the SALCs. The irreducible representations were found in step 4 in Section 5.4.2. Eight irreducible representations were found to be: $2A_g + 2B_{1u} + B_{2g} + B_{3u} + B_{3g} + B_{2u}$. For each of the irreducible representations, multiply the projection by the respective character of the operation.

$$\text{Contribution of each atom to the SALC } = \sum(\text{Projection of } H_a \times \chi)$$

The linear combination for all irreducible representations of D_{2h} are shown below.

Table Section 4.3.5.1: The symmetry adapted linear combination (SALC) for each irreducible representations of C_3v are shown.

D_{2h}	E	$C_2(z)$	$C_2(y)$	$C_2(x)$	i	$\sigma(xy)$	$\sigma(xz)$	$\sigma(yz)$	Linear Combination
Projection of O_a	O_a	O_a	O_b	O_b	O_b	O_b	O_a	O_a	
A_g	1	1	1	1	1	1	1	1	$= 4O_a + 4O_b$
B_{1u}	1	1	−1	−1	−1	−1	1	1	$= 4O_a - 4O_b$
B_{2g}	1	−1	1	−1	1	−1	1	−1	$= 0$
B_{3u}	1	−1	−1	1	−1	1	1	−1	$= 0$
B_{3g}	1	−1	−1	1	1	−1	−1	1	$= 0$
B_{2u}	1	−1	1	−1	−1	1	−1	1	$= 0$

(Section 4.3.5.1)

Notice that there are only two irreducible representations that produce SALCs, the A_g and the B_{1u}. Since we found two of each ($2A_g + 2B_{1u}$) when we found the irreducible representations, we know that there will be two SALCs of A_g symmetry and two of B_{1u}

symmetry; that is four total SALCs from the pendant oxygens. This is the same as what we found in Section 5.4.2 using a different method.

Step 5.4: Sketch the SALCs

The SALCs with A_g symmetry: Quantitatively, we can apply the normalizing factor, N, for these SALCs. Each atom contributes equally to the SALCs, thus the normalizing factor for the A_g SALC is $N = \left(\frac{1}{\sqrt{1^2+1^2}}\right) = \frac{1}{\sqrt{2}}$. This tells us that each oxygen contributes $\frac{1}{\sqrt{2}}$ to each of the normalized A_g group orbitals:

$$A_g \text{ group orbital } = \frac{1}{\sqrt{2}}\left[\psi_{O_a} + \psi_{O_b}\right]$$

The linear combination $4O_a + 4O_b$ indicates that wavefunctions from each oxygen atom contribute equally to each of the two SALCs, with the same sign of the wavefunction for each. Because we know that A_g is totally symmetric (all 1's in the characters), we can assume that the SALC's will look like a symmetric arrangement of oxygen orbitals. But which orbitals contribute? We could peek at the character table to get a hint. But we'll treat this problem systematically.

The SALCs with B_{1u} symmetry: The linear combination $4O_a - 4O_b$ indicates that each oxygen atom contributes equally, but that they have opposite wavefunctions. Application of the normalizing factor would give us:

$$B_{1u} \text{ group orbital } = \frac{1}{\sqrt{2}}\left[\psi_{O_a} + \psi_{O_b}\right]$$

But how do we know what the SALCs look like? Again, the character table can give us some hints, but we'll use a systematic process, below.

What do the SALCs look like? One way to systematically derive the SALC shapes is to perform the projection (Step 5.3) on specific groups of orbitals on the oxygen atom. For example, if we replicate Table Section 4.3.5.1 using just the group of oxygen 2s orbitals and the A_g and B_{1u} representations, we get the following:

D_{2h}	E	$C_2(z)$	$C_2(y)$	$C_2(x)$	i	$\sigma(xy)$	$\sigma(xz)$	$\sigma(yz)$	Linear Combination
Projection of 2s orbital of O_a	$O1s_a$	$O1s_a$	$O1s_b$	$O1s_b$	$O1s_b$	$O1s_b$	$O1s_a$	$O1s_a$	
A_g	1	1	1	1	1	1	1	1	$= 4O1s_a + 4O1s_b$
B_{1u}	1	1	−1	−1	−1	−1	1	1	$= 4O1s_a - 4O1s_b$

(Section 4.3.5.2)

This tells us that one of the A_g SALCs looks like two oxygen 1s orbitals with equal signs and contributions. It also tells us that one of the B_{1u} SALCs looks like two s orbitals with opposite signs and equal magnitudes. These two SALCs are shown in Figure *Section*4.3.5.2.

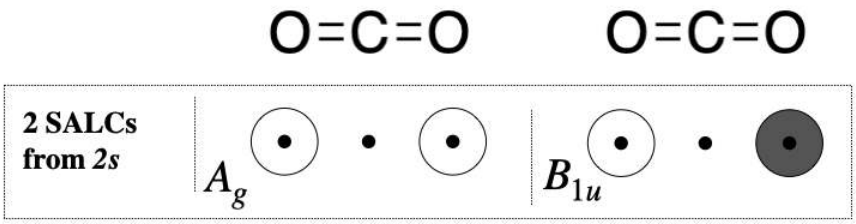


Figure *Section*4.3.5.2: SALCs derived from two oxygen $2s$ orbitals from carbon dioxide. Compare to Section 5.4.2. (CC-BY-SA; Kathryn Haas)

If we do the same for the $2p_z$ orbitals, we need to pay attention to the orientation of the p orbital lobes. If the orbital is moved into the opposite orientation, it would get a negative sign in the projection (see below).

D_{2h}	E	C_2 (z)	C_2 (y)	C_2 (x)	i	$\sigma(x$ $y)$	$\sigma(x$ $z)$	$\sigma(yz)$	Linear Combination
Projection of 2px orbital of O_a	$+O2$ pz_a	$+O2$ pz_a	$-O2$ pz_b	$+O2$ pz_b	$-O2$ pz_b	$-O2$ pz_b	$+O2$ pz_a	$+O2$ pz_a	
A_g	1	1	1	1	1	1	1	1	$= 4O2pz_a$ $- 4O2pz_b$
B_{1u}	1	1	−1	−1	−1	−1	1	1	$= 4O2pz_a$ $+ 4O2pz_b$

(Section 4.3.5.3)

This tells us that one of the A_g SALCs is derived from two $2p_z$ orbitals of opposite sign but equal magnitude. In other words, the two p orbitals are pointing in opposite directions, but the lobes that are facing one another are of the same sign (see Figure *Section*4.3.5.3, left). This also tells us that one of the B_{1u} orbitals is derived from two p_z orbitals of equal magnitude and equal sign (pointing in the same directions, with lobes facing one another of opposite sign!) (see Figure *Section*4.3.5.3, right).

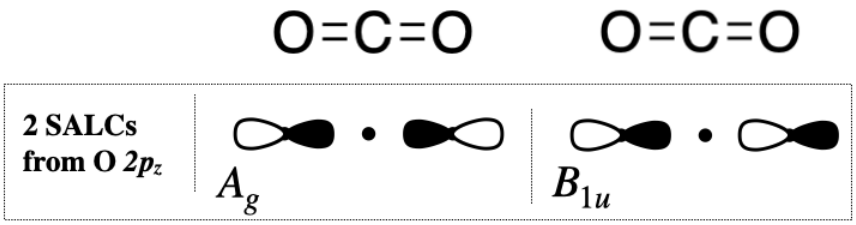


Figure *Section*4.3.5.3: SALCs derived from two oxygen $2p_z$ orbitals from carbon dioxide. Compare to Section 5.4.2. (CC-BY-SA; Kathryn Haas)

Now we have reached the same SALCs that we found previously in Section 5.4.2, but by an alternate method.

Section 4.3.5: CO_2 (Revisted with Projection Operators) is shared under a CC BY-NC-SA 4.0 license and was authored, remixed, and/or curated by LibreTexts.

- **5.4.4: NH_3** by Kathryn Haas is licensed CC BY-SA 4.0.

Section 4.3.6: BF_3

The case of boron trifluoride (BF_3) is an example of a molecule with one more layer of complexity than the other examples we have seen in previous sections in this chapter. (BF_3) is more complex than previous examples because it is the first case in which there are multiple types of valence orbitals on the pendant atoms. (BF_3) possesses s and p orbitals on *both* the central atom and all of the pendant atoms. We can follow the same steps that we have previously to derive other molecular orbital diagrams; however, there is one important difference: we will treat each type of pendant orbital as an individual set of SALCs.

Step 1. Find the point group of the molecule and assign Cartesian coordinates so that z is the principal axis.

The BH_3 molecule is trigonal planar, and its point group is D_{3h}. The z axis is colinear with the principle axis, the C_3 axis.

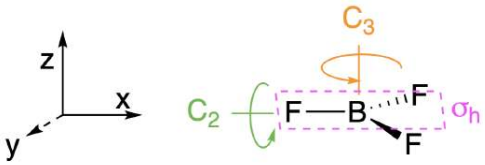


Figure *Section*4.3.6.1: The molecule is in the D_{3h} point group. (CC-BY-NC-SA; Kathryn Haas)

Step 2. Identify and count the pendant atoms' valence orbitals.

Each of the three pendant fluorine atoms has four valence orbitals: one $2s$ and three $2p$ orbitals. Thus, we can expect a total of twelve SALCs from the three atoms. However, we will treat each type of orbital from the F atoms as its own set; each will have its own set of coordinates, with the y axis along the M-L bond. Thus we expect the following:

- One set of $2s$ SALCs: there is one 2s orbital on each of three atoms. This set will have three SALCs.
- One set of $2p_x$ SALCs: there is one $2p_x$ orbital on each of three atoms. Each of these individual orbitals is perpendicular to the M-L bond and coplanar with the molecule. This set will have three SALCs.
- One set of $2p_y$ SALCs: there is one $2p_y$ orbital on each of three atoms. Each of these individual orbitals is colinear with the M-L bond. This set will have three SALCs.
- One set of $2p_z$ SALCs: there is one $2p_z$ orbital on each of three atoms. Each of these individual orbitals is perpendicular to the M-L bond and parallel with the principal axis of the molecule. This set will have three SALCs.

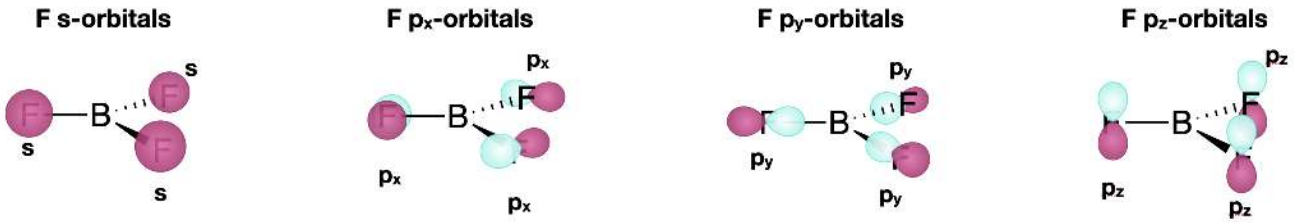


Figure *Section*4.3.6.2: Individual sets of pendant fluorine atomic orbitals will create separate sets of SALCs. (CC-BY-SA; Kathryn Haas)

Step 3. Generate the Γ's for each set of SALCs

Use the D_{3h} character table to generate one reducible representation (Γ) for each of the four sets of pendant atomic orbitals shown in Figure *Section*4.3.6.2; in this case we need four Γ because there are four types of valence orbital (the s, p_x, p_y, p_z).

- For the set of s orbitals: perform the operation for each class in the character table. Each s orbital is assigned a value depending on whether it moves or not: assign a value of 1 if it remains in place during the operation, or 0 (zero) if it moves out of its original place.
- for each set of p orbitals: Now there are phases (signs of the wavefunction), so a negative value is possible. Assign a value of 1 to each p orbital if it remains in place and in phase during the operation; assign a -1 if the atom's position remains, while the phase of the orbital is inverted (the positive lobe moves to the position of the negative lobe and vice versa); assign a 0 if it moves out of its original position.

The Γ for each type is given below:

The Γ for each type is given below:

$\mathbf{D_{3h}}$	E	$2C_3$	$3C_2$	σ_h	$2S_3$	$3\sigma_v$
$\mathbf{\Gamma_{2s}}$	3	0	1	3	0	1
$\mathbf{\Gamma_{2p_x}}$	3	0	−1	3	0	−1
$\mathbf{\Gamma_{2p_y}}$	3	0	1	3	0	1
$\mathbf{\Gamma_{2p_z}}$	3	0	−1	−3	0	1

Step 4. Break Γ's into irreducible representations for individual SALCs

Reduce each Γ into its component irreducible representations. Using either of the processes described previously, we find that each of the Γ reduces to two irreducible representations under the D_{3h} point group; in each case one is singly degenerate (A) and the other doubly degenerate (E). This equates to three SALCs for each Γ (orbital type) and a total of twelve SALCs. This should give us confidence! We were in fact expecting 12 SALCs because we found that there were twelve pendant atomic orbitals to start with.

D_{3h}	E	$2C_3$	$3C_2$	σ_h	$2S_3$	$3\sigma_v$
$\mathbf{\Gamma_{2s}}$	**3**	**0**	**1**	**3**	**0**	**1**
A_1'	1	1	1	1	1	1
E'	2	−1	0	2	−1	0

D_{3h}	E	$2C_3$	$3C_2$	σ_h	$2S_3$	$3\sigma_v$
$\mathbf{\Gamma_{2p_x}}$	**3**	**0**	**−1**	**3**	**0**	**−1**
A_2'	1	1	−1	1	1	−1
E'	2	−1	0	2	−1	0

D_{3h}	E	$2C_3$	$3C_2$	σ_h	$2S_3$	$3\sigma_v$
$\mathbf{\Gamma_{2p_y}}$	**3**	**0**	**1**	**3**	**0**	**1**
A_1'	1	1	1	1	1	1
E'	2	−1	0	2	−1	0

D_{3h}	E	$2C_3$	$3C_2$	σ_h	$2S_3$	$3\sigma_v$
$\mathbf{\Gamma_{2p_z}}$	**3**	**0**	**−1**	**−3**	**0**	**1**
A_2''	1	1	−1	−1	−1	1
E''	2	−1	0	−2	1	0

Step 5: Sketch the SALCs

We'll skip this step for now to make this problem simpler.

Step 6: Draw the MO diagram by combining SALCs with AO's of like symmetry.

We now know the symmetries of different pendant orbital SALCs - and it is helpful if we also know their relative energies, and the energies of the valence orbitals on the central boron atom. We can make predictions based on periodic trends, or we can use a table of ionization energies as a guide. The symmetries of the boron $2s$ and $2p$ orbitals can be found from the D_{3h} character table.

Section 4.3.6: BF_3 is shared under a CC BY-NC-SA 4.0 license and was authored, remixed, and/or curated by LibreTexts.

- **5.4.4: NH_3** by Kathryn Haas is licensed CC BY-SA 4.0.

Section 4.4: Problems

Concept Review Questions

1. What are the assumptions (axioms) of molecular orbital (MO) theory?

2. Explain qualitatively why the vectorial addition of atomic orbitals creates molecular orbitals (which underlying physical phenomenon is described by the vectorial addition?).

3. Explain qualitatively why molecular orbital theory is suitable to describe covalent bonding.

4. What are the three criteria that determine the degree of covalent interaction in MO theory?

5. Which three rules determine the degree of orbital overlap in MO theory?

6. Explain why the combination of a large, diffuse orbital and a small orbital produces only weak covalent interaction.

7. Explain why sigma interactions between atomic orbitals typically produce larger orbital overlaps than pi interactions.

8. Explain why the combination of orbitals of the same energy leads to the largest degree of covalent interaction.

9. What can be said about energy and location of a bonding and an anti-bonding molecular orbital that are made from atomic orbitals of large energy difference?

10. MO theory – even though designed for covalent bonding – can also make statements about ionic bonding. Explain why.

11. Explain the principles of SALC.

Dr. Kai Landskron (Lehigh University). If you like this textbook, please consider to make a donation to support the author's research at Lehigh University: Click Here to Donate.

Homework Problems

Section 1

Exercise 1

What will most likely lead to the smallest covalent interaction?

a) Overlap of a small and a large orbital.

b) Overlap of two small orbitals.

c) Overlap of two large orbitals.

Answer

a) Overlap of a small and a large orbital.

Exercise 2

What will most likely lead to the largest covalent interaction?

a) orbital overlap in sigma-fashion

b) orbital overlap in pi-fashion

c) orbital overlap in delta-fashion

Answer

a) orbital overlap in sigma-fashion

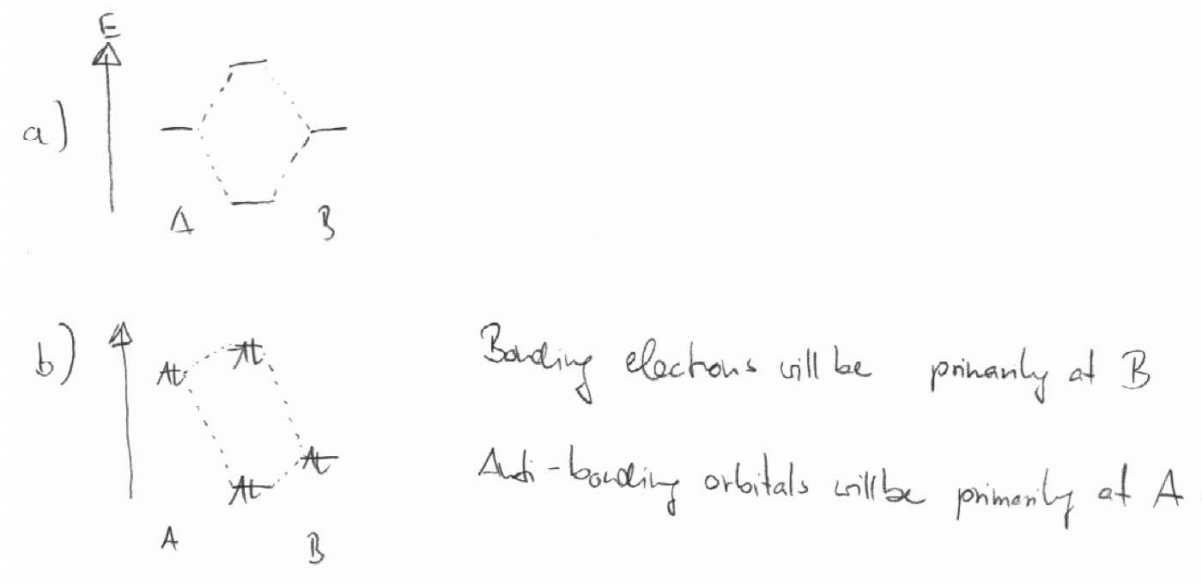
Exercise 3

Qualitatively construct the MO diagrams composed of

a) two 2s atom orbitals A and B of equal energy.

b) two 2s atom orbitals where the orbital energy of atom A is significantly higher than that of B. If both the bonding and the antibonding MO are filled with electrons, where will bonding and antibonding electrons primarily be located? Briefly explain your decision.

Answer



Exercise 4

Decide by "inspection" which of the following combinations of orbitals have the "right" symmetries to form molecular orbitals.

a) The $2p_x$ orbital of the first N atom and the $2p_y$ orbital of the second N atom in the molecule N_2. The z axis is defined as the bond axis in N_2.

b) The F $2p_x$ and the H 1s orbital in the HF molecule. The z axis is defined as the bond axis.

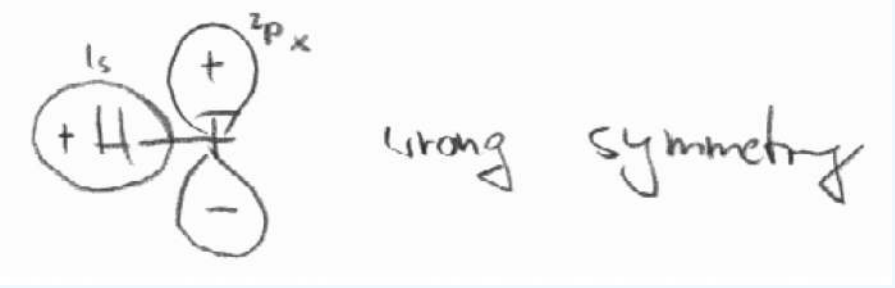
c) The $2p_z$ orbital of F and the 1s orbital in the HF molecule. The z axis is defined as the bond axis.

Answer

a)



b)



c)



Exercise 5

The CH_4 molecule belongs to the point group T_d. You can find the character table of the point group in the internet.

a) Calculate the reducible representation for the ligand group orbitals (LGOs).

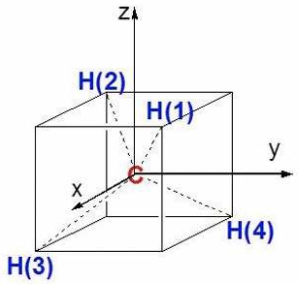
b) Calculate the irreducible representations of the ligand group orbitals (LGOs).

c) Draw a qualitative molecular orbital diagram for CH_4.

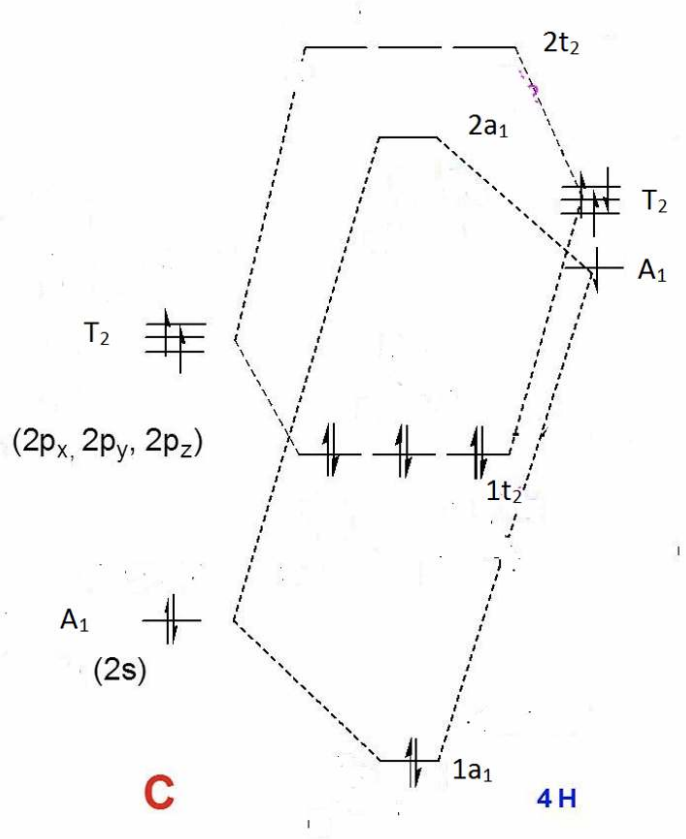
Answer

The symmetry of 4H group orbitals:

$\Gamma_r = 4E+1C_3+0C_2+0S_4+2\sigma_d = A_1 + T_2$



T_d		
A_1		$x^2+y^2+z^2$
A_2		
E		$(2z^2-x^2-y^2, x^2-y^2)$
T_1	(R_x,R_y,R_z)	
T_2	(x,y,z)	(xz, yz, xy)



Exercise 6

Which are the symmetry types of the central atom orbitals in the PCl_5 molecule?

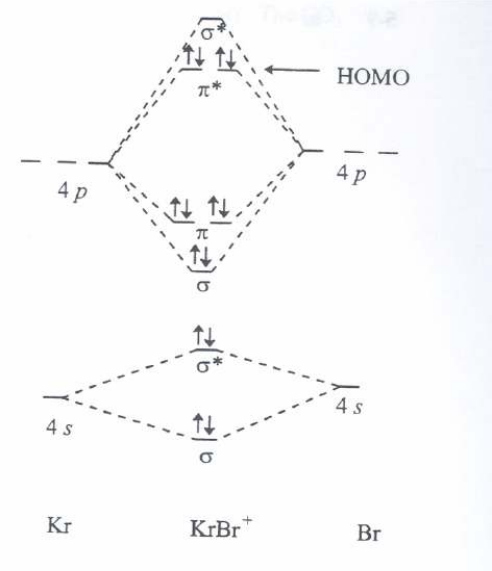
Answer

1. Determine point group of PCl_5. --> D_{3h}.
2. Decide what are the valence orbitals of the central atom: 3s, 3p
3. Look up the character table of D_{3h}, e.g., in the internet. You will find their symmetries to be: A_1' (3s), A_2'' ($3p_z$), E'($3p_x$, $3p_y$)

Exercise 7

For the hypothetical $BrKr^+$ molecule: Toward which atom is the HOMO polarized? Explain briefly why.

Answer



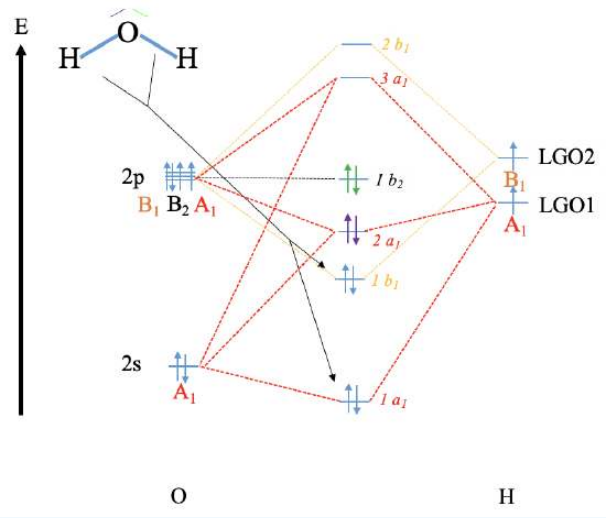
Orbital energies of Kr must be somewhat lower than the ones of Br because the electrons experience higher effective nuclear charge (Z_{eff} increases within a period). This means that the antibonding HOMO is polarized towards Br (HOMO energetically closer to 4p(Br) than 4p(Kr)).

Exercise 8

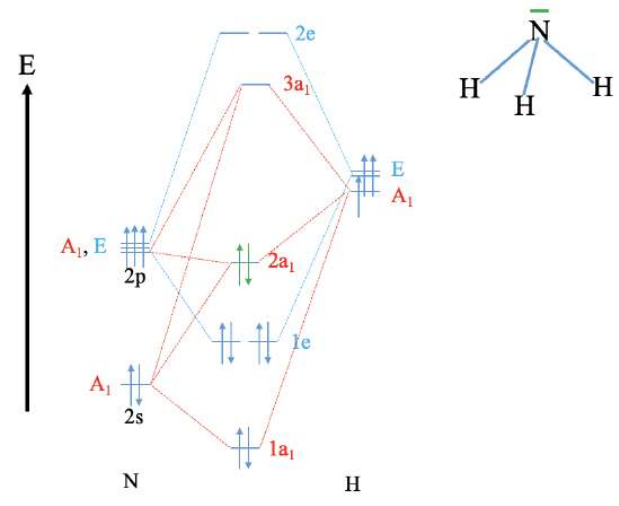
Reconstruct the MO diagram for water and NH_3 (repeat what we did in class without looking at your notes (only use the respective character tables).

Answer

Water



NH_3



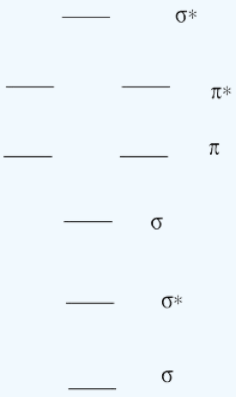
Dr. Kai Landskron (Lehigh University). If you like this textbook, please consider to make a donation to support the author's research at Lehigh University: Click Here to Donate.

Exercise *Section*4.4.1

A Molecular Orbital Diagram for a diatomic molecule (two atoms) always has the same basic pattern.

- Draw a picture of the levels.
- Label each level with σ, σ*, π, π*

Answer



Exercise *Section*4.4.2

A Molecular Orbital Diagram for a diatomic molecule (two atoms) varies in the number of electrons. How do you populate the electrons?

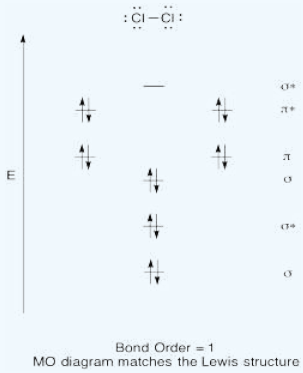
Answer

• Count the valence electrons on the molecule. That's the number of valence electrons on each atom, adjusted for any charge on the molecule. (eg C_2^{2-} has 10 valence electrons: 4 from each carbon -- that's 8 -- and two more for the 2- charge).
• Fill electrons into the lowest energy orbitals first.
• Pair electrons after all orbitals at the same energy level have one electron.

Exercise *Section*4.4.3

Construct a qualitative molecular orbital diagram for chlorine, Cl_2. Compare the bond order to that seen in the Lewis structure (remember that an electron in an antibonding orbital cancels the stabilization due to bonding of an electron in a bonding orbital).

Answer

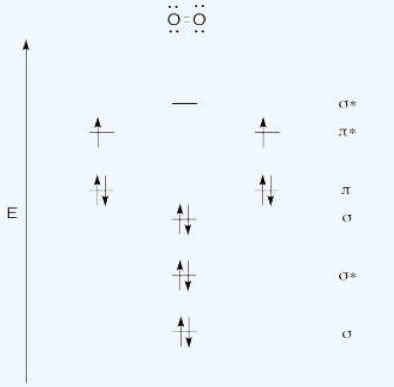


Bond Order = 1
MO diagram matches the Lewis structure

Exercise *Section*4.4.4

a. Construct a qualitative molecular orbital diagram for oxygen, O_2.
b. Compare the bond order to that seen in the Lewis structure.
c. How else does this MO picture of oxygen compare to the Lewis structure? What do the two structures tell you about electron pairing?
d. Compounds that have all of their electrons paired are referred to as diamagnetic. Those with unpaired electrons are referred to as paramagnetic. Paramagnetic materials are attracted by a magnetic field, but diamagnetic things are not. How would you expect molecular oxygen to behave?

Answer



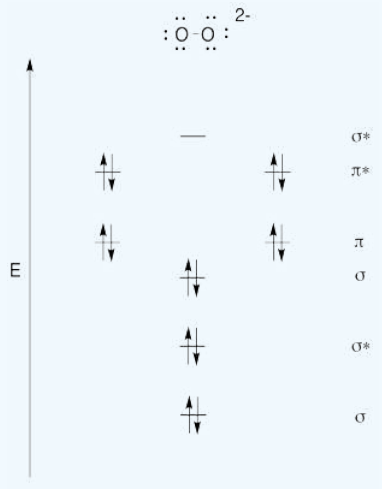
Bond Order = 2
MO diagram indicates two unpaired electrons and therefore does not match the Lewis structure. Based on the MO diagram oxygen would be paramagnetic and would be attracted to a magnetic field

Exercise *Section*4.4.5

a. Construct a qualitative molecular orbital diagram for peroxide anion, O_2^{2-}.
b. Compare the bond order to that seen in the Lewis structure.
c. How else does this MO picture of oxygen compare to the Lewis structure? What do the two structures tell you about electron pairing?

d. Based on molecular orbital pictures, how easily do you think dioxygen could be reduced to peroxide (through the addition of two electrons)?

Answer

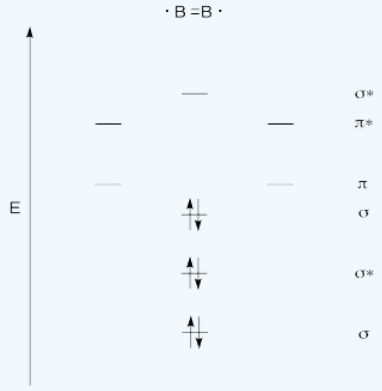


Bond Order = 1
MO diagram matches the Lewis structure. Both predict a Bond Order of 1 and 6 lone pairs of electrons. The addition of two electrons to O_2 to O_2^{2-} would be possible.

Exercise *Section*4.4.6

Construct a qualitative molecular orbital diagram for diboron, B_2. Do you think boron-boron bonds could form easily, based on this picture?

Answer

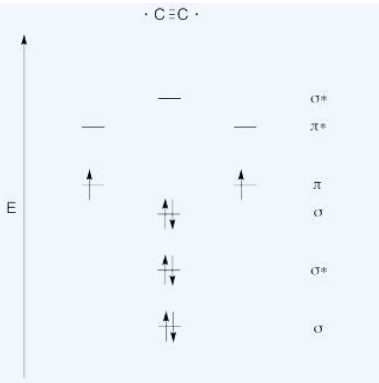


Bond Order = 1
Boron-Boron bonding should be possible

Exercise *Section*4.4.7

a. Construct a qualitative molecular orbital diagram for dicarbon, C_2.
b. Compare the bond order to that seen in the Lewis structure.
c. How else does this MO picture of oxygen compare to the Lewis structure? What do the two structures tell you about electron pairing?

Answer

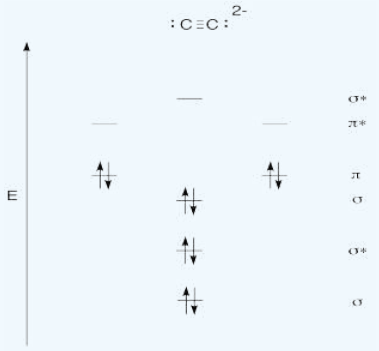


Bond Order = 2
MO diagram does not match the Lewis structure.
However, the MO diagram does concur about the
2 unpaired electrons.

Exercise *Section*4.4.8

a. Construct a qualitative molecular orbital diagram for acetylide anion, C_2^{2-}.
b. Compare the bond order to that seen in the Lewis structure.
c. How else does this MO picture of oxygen compare to the Lewis structure? What do the two structures tell you about electron pairing?
d. Based on molecular orbital pictures, how easily do you think dicarbon could be reduced to acetylide (through the addition of two electrons)?

Answer

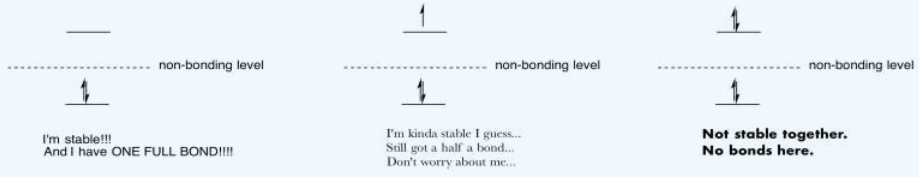


Bond Order = 3
MO diagram matches the Lewis structure.
Both predict a Bond Order of 3 and 2 lone
pairs of electrons. The addition of two
electrons to C_2 to C_2^{2-} would be possible.

Exercise *Section*4.4.9

Make drawings and notes to summarize the effect of populating antibonding orbitals.

Answer



Exercise *Section*4.4.10

Researchers at Johns Hopkins recently reported the formation of Na_4Al_2 in a pulsed arc discharge (they put a lot of electric current through a sample of sodium and aluminum; Xinxing Zhang, Ivan A. Popov, Katie A. Lundell, Haopeng Wang, Chaonan Mu, Wei Wang, Hansgeorg Schnöckel, Alexander I. Boldyrev, Kit H. Bowen, *Angewandte Chemie International Edition*, **2018**, *57*(43), 14060-14064. Copyright 2018, John Wiley & Sons. Used with permission.).

a. The compound is ionic. Explain which atoms form the cations, based on periodic trends.
b. Therefore, what atoms form the anion?
c. The anion is one molecule. What is the charge on this molecule?
d. Show how to calculate the total valence electrons in this molecular anion.
e. Draw a Lewis structure for this molecular anion.
f. Construct a diatomic molecular orbital energy level diagram for this molecule. Label the energy levels (sigma, pi, etc.) and add in the correct number of electrons.
g. Show how to calculate the bond order in the molecule.

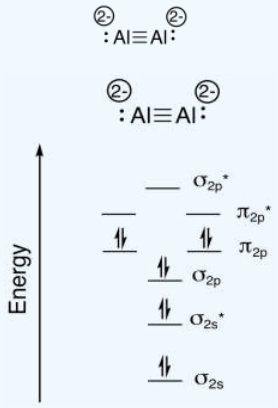
Answer

a) Na, because Na has a lower ionization potential (and a lower electronegativity) than Al.

b) Al

c) 4-, because there are four Na^+

d) total e^- = 2 x 3 e^- (per Al) + 4 e^- (for the negative charge) = 10 e-



g) bond order= $\frac{(\#bonding\ e^- - \#antibonding\ 3^-)}{2} = \frac{8-2}{2} = 3$

Exercise *Section*4.4.1

Draw the molecular orbital diagram for (NO^-).

Answer

Add texts here. Do not delete this text first.

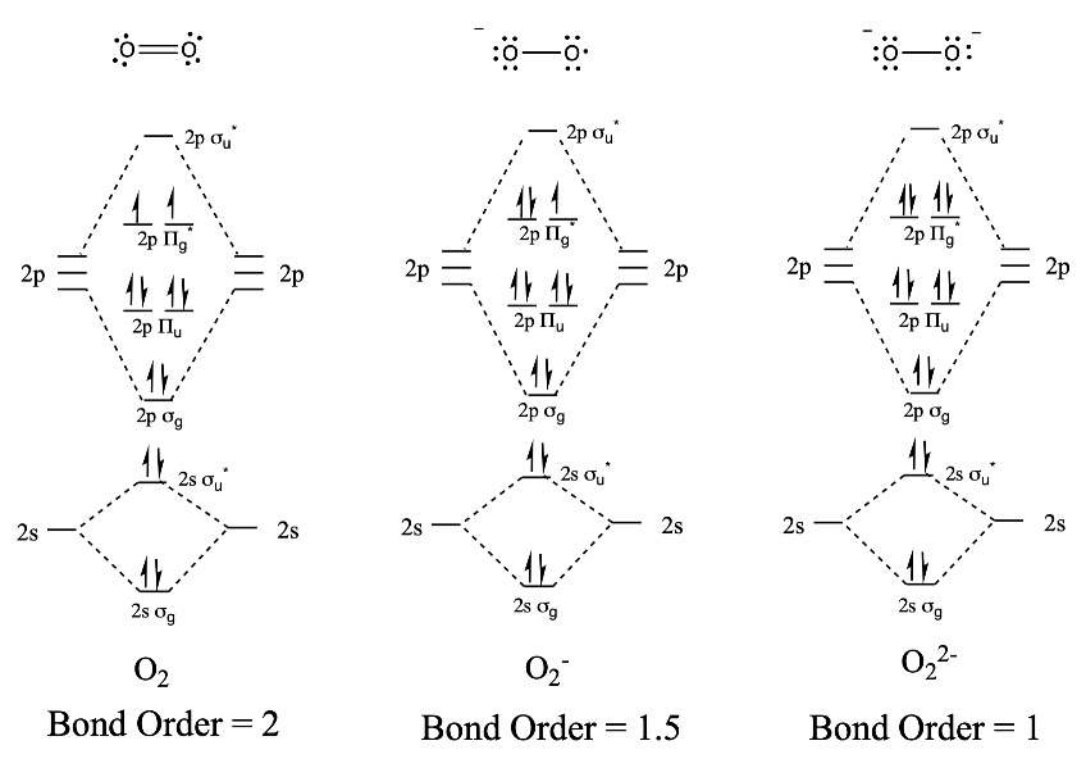
Exercise *Section*4.4.1

Draw and compare the molecular orbital diagrams to the Lewis structure diagrams for O_2, O_2^-, and O_2^{2-}.

Answer

The Lewis structures and MO diagrams are shown below. In general, the bond order derived from the MO diagram agrees with the Lewis structure for each species. In the case of the two ions, the number of unpaired electrons from MO theory and the Lewis structure also agrees. In the case of dioxygen, however, there is an inconsistency between the Lewis

representation and the MO diagram. While the Lewis structure would lead us to believe that all electrons are paired, the MO diagram indicates paramagnetism, with two unpaired electrons. The MO diagram explains the magnetic behaviour of dioxygen.



Exercise *Section*4.4.1

Draw the molecular orbital diagram for hydroxide ion (OH^-).

Answer

Add texts here. Do not delete this text first.

Exercise *Section*4.4.1

Draw the molecular orbital diagram for hydroxide fluoride (**HF**).

Answer

Add texts here. Do not delete this text first.

Exercise *Section*4.4.1

Draw the molecular orbital diagram for borane (**BN**).

Answer

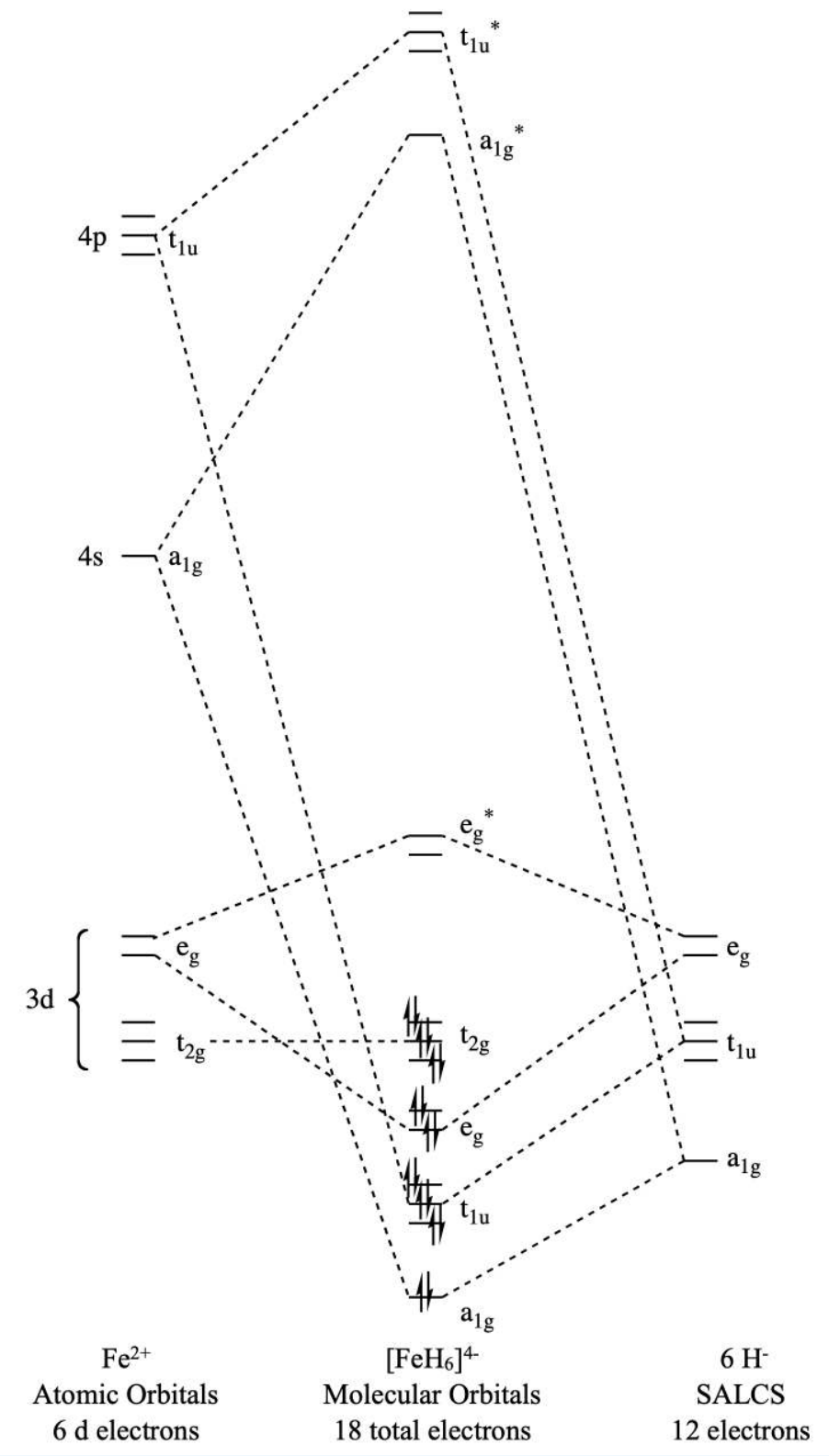
Add texts here. Do not delete this text first.

BH3

Exercise *Section*4.4.1

Draw the molecular orbital diagram for (FeH_6).

Answer



Exercise *Section*4.4.1

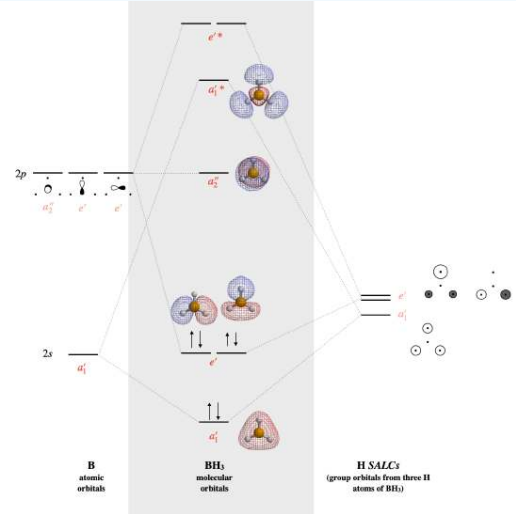
Draw the molecular orbital diagram for boron trifluoride ($\mathbf{BF_3}$).

- What is the non-bonding orbital?
- What are the HOMO and LUMO orbitals?
- Why does e' have 2 lines of energy levels compared to a1', which has only a 1-line energy level?
- What is the bond order of $\mathbf{BH_3}$ in this MO diagram?

Answer

The calculated MO diagram is shown below.

- a_2'' is the lone non-bonding orbital.
- The HOMO is the a_2'' nonbonding orbital, the LUMO is a bonding e' set of two degenerate orbitals/
- e' is doubly degenerate
- The bond order is 3



Section 4.4: Problems is shared under a CC BY-NC-SA 4.0 license and was authored, remixed, and/or curated by LibreTexts.

- **Concept Review Questions Chapter 3** by Kai Landskron is licensed CC BY 4.0.
- **Homework Problems Chapter 3** by Kai Landskron is licensed CC BY 4.0.
- **13.6: Assembling the Complete Diagram and Electron Population** by Chris Schaller is licensed CC BY-NC 3.0. Original source: https://employees.csbsju.edu/cschaller/structure.htm.

CHAPTER OVERVIEW

Chapter 5: Coordination Chemistry- Structure and Isomers

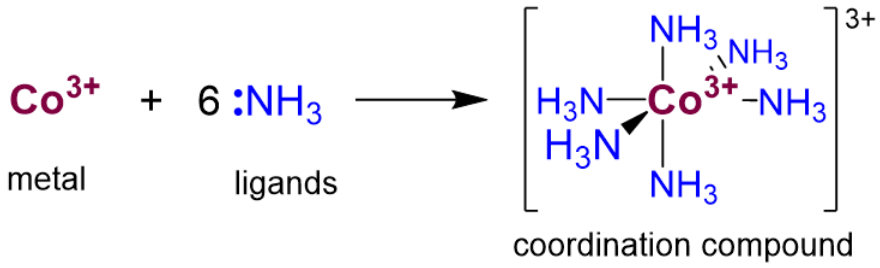
Introduction

Coordination compounds are important to all areas of chemistry, engineering, the life and environmental sciences, and beyond. In the synthetic laboratory catalytic amounts of coordination compounds enable organic chemists to synthesize new compounds selectively and in high yield under mild condition. Applied industrially, coordination compound catalysts serve as vital catalysts that facilitate the conversion of raw petrochemical or bio-derived feedstocks into useful industrial and consumer products. Without them life as we know it would be impossible as many biochemical systems are coordination complexes. Examples include the hemoglobin which transports oxygen around our bodies and the myoglobin which stores it, the photosystems which harvest light and use light energy in photosynthesis, the constituents of the respiratory chain, and many of the enzymes involved in the expression and transmission of genetic information. In studying coordination chemistry you are about to take your first steps into a vast and exciting world.

What is a Coordination Compound?

Coordination compounds consist of one or more metals bound to one or more Lewis base ligands. For example, hexaminechromium(III) ion is a coordination complex in which six ammonia ligands coordinate a Co^{3+} ion, as shown in Scheme ***Chapter*5.1**.

Scheme ***Chapter*5.1**: Formation of hexaminechromium(III) ion from Co^{3+} and NH_3.



(Chapter 5.1)

Such complexes are called coordination compounds or complexes because the ligand-metal bond may be thought of as a coordinate covalent bond in which both of the bonding electrons come from the ligand, which is then said to coordinate the metal. This coordinate covalent model is a very useful formalism for understanding the basic features of coordination chemistry, although it does not always accurately reflect the actual details of the bonding in every coordination complex. Nevertheless, even in those cases where the simple coordinate covalent bond model breaks down the coordinate covalent bond concept supplies the language sophisticated models employ to describe the more complex bonding involved.

Additional Important Terms

Some of the common widely terms that follow from the coordinate covalent model of bonding in coordination complexes include

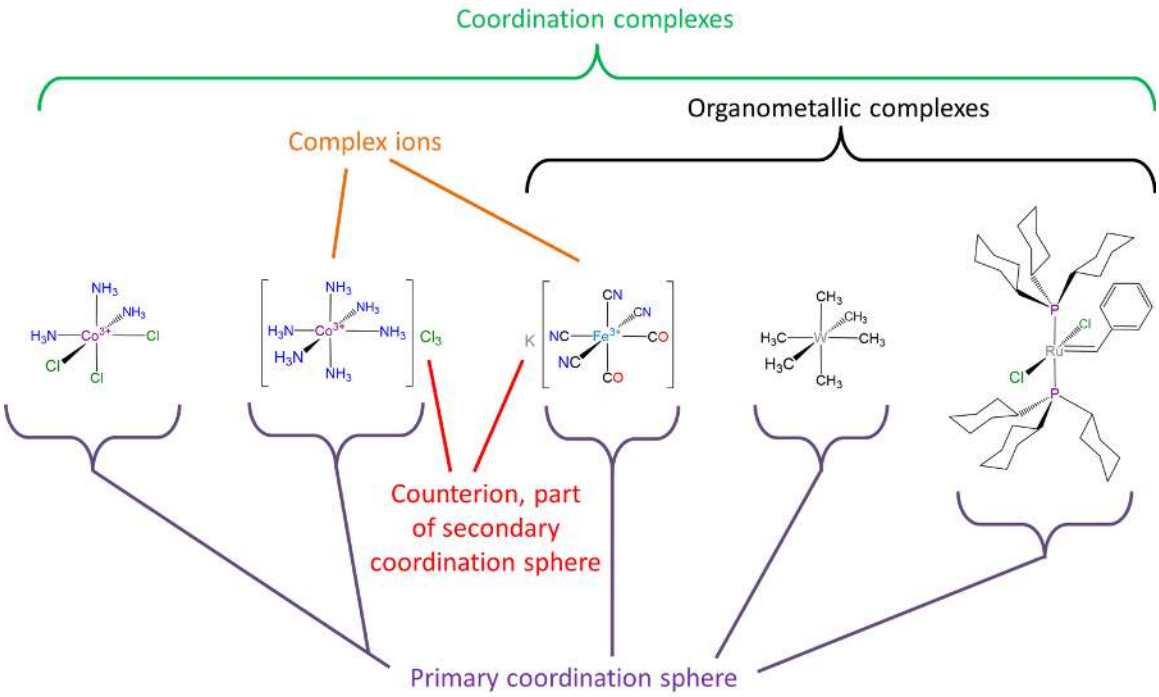
- Coordination compounds are also called **coordination complexes**, **metal complexes**, or just **complexes**. The term **complex** refers to coordination compounds' composite nature, in that they may be thought of as comprised of multiple ligand and metal ion parts that can be restored by breaking the coordinate covalent bonds holding the complex together. This is in contrast to inorganic or organic molecules which are more commonly thought about as whole molecules held together by the sharing of electrons contributed by all the atoms.
- Coordination complexes that are ions are called **complex ions.**
- Ligands bound to the coordination complex are said to reside in the **primary** or **inner coordination sphere**. These bound ligands are not readily exchangeable, in contrast to nearby counterions and solvent molecules, which are said to reside in the

secondary or **outer coordination sphere**.

- The portion of the complex contributing the electron pairs is said to be the **donor** and the portion which receives them the **acceptor**. In conventional coordination compounds the ligand is the donor and the metal the acceptor. In these cases it would be equally convenient to refer to the ligand donor as the Lewis base and the metal acceptor as the Lewis acid. However, in more complex bonding scenarios there may be multiple electron pair donation and acceptance interactions taking place between each pair of atoms and donor-acceptor language will be more convenient.
- The number of ligand sites donating lone pairs to the central atom is referred to as the **coordination number**. For most complexes this will just be equal to the number of ligand atoms bound to the metal. In simple complexes it is just equal to the number of ligands. For instance, the cobalt in Scheme **Chapter5.1** has a coordination number of six.
- Although technically compounds with metal-carbon bonds are coordination complexes term coordination complex is sometimes used to refer to complexes which do not possess metal-carbon bonds in their primary coordination sphere. Complexes which possess metal-carbon bonds are called organometallic compounds instead. The use of the terms organometallic and coordination to distinguish organometallic compounds from other types of coordination compounds is often convenient since many organometallic ligands engage in more than simple σ donor acceptor coordinate covalent bond formation with the metal center. However, this is true of some wholly inorganic ligands too so it should always be kept in mind that organometallic compounds are just a type of coordination compound and that inorganic ligands can in principle be tuned in interact with a metal center in much the same way an organic ligand does.

A summary of some of the concepts and terms used to describe coordination compounds is given in Scheme ***Chapter5.2***.

Scheme ***Chapter5.2***: Some terms used to describe coordination compounds. This work by Stephen Contakes is licensed under a Creative Commons Attribution 4.0 International License.



Contributors and Attributions

Stephen Contakes, Westmont College

Unless otherwise noted, all line drawings on this page are by Stephen Contakes and licensed under a Creative Commons Attribution 4.0 International License.

Learning Objectives

- Determine the correct name and chemical formula for a metal complex from its structure
- Identify the denticity of a ligand from its structure
- Recognize and name the different types of isomers in metal complexes

Section 5.1: History

Section 5.2: Nomenclature and Ligands

Section 5.3: Acid-Base and Donor-Acceptor Chemistry

Section 5.3.1: Acid-Base Models as Organizing Concepts

Section 5.3.2: Lewis Concept and Frontier Orbitals

Section 5.3.2.1: The frontier orbital approach considers Lewis acid-base reactions in terms of the donation of electrons from the base's highest occupied orbital into the acid's lowest unoccupied orbital.

Section 5.3.2.2: All other things being equal, electron withdrawing groups tend to make Lewis acids stronger and bases weaker while electron donating groups tend to make Lewis bases stronger and acids weaker

Section 5.3.2.3: The electronic spectra of charge transfer complexes illustrate the impact of frontier orbital interactions on the electronic structure of Lewis acid-base adducts

Section 5.3.2.4: Substances' solution phase Lewis basicity towards a given acid may be estimated using the enthalphy change for dissociation of its adduct with a reference acid of similar hardness.

Section 5.3.2.5: In the boron trifluoride affinity scale, the enthalphy change on formation of an adduct between the base and boron trifluoride is taken as a measure of Lewis basicity.

Section 5.3.2.6: Lewis base strength may also be estimated by measuring structural or energy changes upon formation of a Lewis acid-base complex, as illustrated by efforts to spectroscopically assess the strengths of halogen bonds

Section 5.3.2.7: Bulky groups weaken the strength of Lewis acids and bases because they introduce steric strain into the resulting acid-base adduct.

Section 5.3.2.8: Frustrated Lewis pair chemistry uses Lewis acid and base sites within a molecule that are sterically restricted from forming an adduct with each other.

Section 5.3.3: Hard and Soft Acids and Bases

Section 5.3.3.1: Hard-Hard and Soft-Soft preferences may be explained and quantified in terms of electrostatic and covalent and electronic stabilization on the stability of Lewis acid-base adducts

Section 5.3.3.2: Quantitative Measures of Hardness, Softness, and Acid-Base Interactions from a Hard Soft Acid-Base Principle Perspective Involve Orbital Energies and/or Apportioning Acid-Base Bonding in Terms of Electrostatic and Covalent Factors

Section 5.3.4: Problems

Section 5.4: Coordination Numbers and Structures

Section 5.5: Isomerism

Chapter 5: Coordination Chemistry- Structure and Isomers is shared under a CC BY-NC-SA 4.0 license and was authored, remixed, and/or curated by LibreTexts.

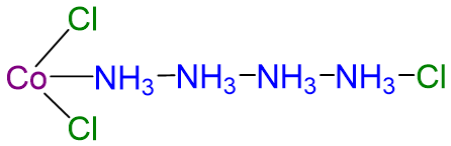
Section 5.1: History

History of the Coordination Compounds

Coordination compounds have been known and used since antiquity; one of the oldest synthetic pigments is the blue pigment Egyptian blue, a copper complex of formula $CaCuSi_4O_{10}$ used by the Egyptians since the third Millenium B.C. (in ancient China the Ba analogue, Han blue, was discovered independently). The blue color of Egyptian blue is due to interlocked $Cu(Si_2O_7)_4$ units in which each copper is coordinated by four O atoms in a square planar arrangement. Later, in 1706, the Berlin painter Diesbach would discover another deep blue pigment, Prussian blue: $KFe_2(CN)_6$.

Despite their long use, the chemical nature of coordination compounds was unclear for a number of reasons. For example, many compounds called "double salts" were known, such as $AlF_3 \cdot 3\,KF$, $Fe(CN)_2 \cdot 4\,KCN$, and $ZnCl_2 \cdot 2\,CsCl$, which were combinations of simple salts in fixed and apparently arbitrary ratios. Why should $AlF_3 \cdot 3\,KF$ exist but not $AlF_3 \cdot 4\,KF$ or $AlF_3 \cdot 2\,KF$? And why should a 3:1 KF:AlF_3 mixture have different chemical and physical properties than either of its components? Similarly, adducts of metal salts with neutral molecules such as ammonia were also known—for example, $CoCl_3 \cdot 6\,NH_3$, which was first prepared sometime before 1798. Like the double salts, the compositions of these adducts exhibited fixed and apparently arbitrary ratios of the components. For example, $CoCl_3 \cdot 6\,NH_3$, $CoCl_3 \cdot 5\,NH_3$, $CoCl_3 \cdot 4\,NH_3$, and $CoCl_3 \cdot 3\,NH_3$ were all known and had very different properties, but despite all attempts, chemists could not prepare $CoCl_3 \cdot 2\,NH_3$ or $CoCl_3 \cdot NH_3$.

Although the chemical composition of such compounds was readily established by existing analytical methods, their chemical nature was puzzling and highly controversial. The major problem was that what we now call valence (i.e., the oxidation state) and coordination number were thought to be identical. As a result, highly implausible (to modern eyes at least) structures were proposed for such compounds. Of these the most influential was the Blomstrand-Jørgensen chain theory of bonding in coordination compounds, which predicted the "Chattanooga choo-choo" model for $CoCl_3 \cdot 4NH_3$ shown in Scheme **Section5.1.I**.



Scheme **Section5.1.I**. Blomstrand-Jørgensen chain theory model of bonding in $CoCl_3 \cdot 4NH_3$.

Nevertheless, this theory was not wholly illogical and, in fact, explained much of the analytical data on coordination compounds available to chemists of the time. This data included the electrical conductivity of aqueous solutions of these compounds, which was roughly proportional to the number of ions formed per mole, and the number of free chloride ions present, which could be determined by precipitating them gravimetrically as AgCl. In the case of $CoCl_3 \cdot 4NH_3$, two ions and one chloride were produced when the compound was dissolved in water, which Jørgensen was able to explain using the chain structure shown above by postulating that chlorides attached to NH_3 could dissociate while those attached to Co could not. The modern theory of coordination chemistry, which overthrew the chain theory, is based largely on the work of Alfred Werner (1866–1919; Nobel Prize in Chemistry in 1913). In a series of careful experiments carried out in the late 1880s and early 1890s, he examined the properties of several series of metal halide complexes with ammonia. For example, five different "adducts" of ammonia with $PtCl_4$ were known at the time: $PtCl_4 \cdot nNH_3$ (n = 2–6). Some of Werner's original data on these compounds are shown in Table ***Section*5.1.1**. Werner's data on $PtCl_4 \cdot 6NH_3$ in Table ***Section*5.1.1** showed that all the chloride ions were present as free chloride. In contrast, $PtCl_4 \cdot 2NH_3$, was a neutral molecule that did not give free chloride ions when dissolved in water.

Alfred Werner (1866–1919)

Werner, the son of a factory worker, was born in Alsace. He developed an interest in chemistry at an early age, and he did his first independent research experiments at age 18. While doing his military service in southern Germany, he attended a series of chemistry lectures, and he subsequently received his PhD at the University of Zurich in Switzerland, where he was appointed professor of chemistry at age 29. He won the Nobel Prize in Chemistry in 1913 for his work on coordination compounds, which he performed as a graduate student and first presented at age 26. Apparently, Werner was so obsessed with solving the riddle of the structure of coordination compounds that his brain continued to work on the problem even while he was asleep. In

1891, when he was only 25, he woke up in the middle of the night and, in only a few hours, had laid the foundation for modern coordination chemistry.

Table *Section*5.1.1: Werner's Data on Complexes of Ammonia with $PtCl_4$

Complex	Conductivity (ohm^{-1})	Number of Ions per Formula Unit	Number of Cl^- Ions Precipitated by Ag^+
$PtCl_4 \cdot 6NH_3$	523	5	4
$PtCl_4 \cdot 5NH_3$	404	4	3
$PtCl_4 \cdot 4NH_3$	299	3	2
$PtCl_4 \cdot 3NH_3$	97	2	1
$PtCl_4 \cdot 2NH_3$	0	0	0

These data led Werner to postulate that metal ions have two different kinds of valence: (1) a primary valence (oxidation state) that corresponds to the positive charge on the metal ion and (2) a secondary valence (coordination number) that is the total number of ligands bound to the metal ion. If Pt had a primary valence of 4 and a secondary valence of 6, Werner could explain the properties of the $PtCl_4 \cdot NH_3$ adducts by the following reactions, where the metal complex is enclosed in square brackets:

$$[Pt(NH_3)_6]Cl_4 \rightarrow [Pt(NH_3)_6]^{4+}(aq) + 4Cl^-(aq) \quad \text{(Section 5.1.1)}$$

$$[Pt(NH_3)_5Cl]Cl_3 \rightarrow [Pt(NH_3)_5Cl]^{3+}(aq) + 3Cl^-(aq) \quad \text{(Section 5.1.2)}$$

$$[Pt(NH_3)_4Cl_2]Cl_2 \rightarrow [Pt(NH_3)_4Cl_2]^{2+}(aq) + 2Cl^-(aq) \quad \text{(Section 5.1.3)}$$

$$[Pt(NH_3)_3Cl_3]Cl \rightarrow [Pt(NH_3)_3Cl_3]^{+}(aq) + Cl^-(aq) \quad \text{(Section 5.1.4)}$$

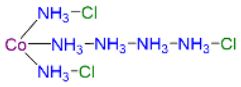
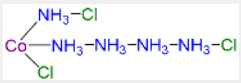
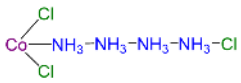
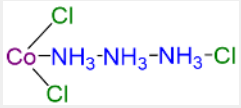
$$[Pt(NH_3)_2Cl_4] \rightarrow [Pt(NH_3)_2Cl_4]^{0}(aq) \quad \text{(Section 5.1.5)}$$

Further work showed that the two missing members of the series—$[Pt(NH_3)Cl_5]^-$ and $[PtCl_6]^{2-}$—could be prepared as their mono- and dipotassium salts, respectively. Similar studies established coordination numbers of 6 for Co^{3+} and Cr^{3+} and 4 for Pt^{2+} and Pd^{2+}.

? Exercise *Section*5.1.1. The $CoCl_3xNH_3$ series.

The series $CoCl_3 \cdot xNH_3$ was particularly important in establishing the correctness of Werner's coordination theory over the rival chain theory. By ~1900 conductivity measurements suggested that the members of the series gave the number of ions shown in Table **Section5.1.1**.

Table **Section5.1.1**. The CoCl3·xNH3 series according to coordination theory, chain theory, and experiment.

Compound	Color	Werner formulation	Blomstrand-Jørgensen chain theory formulation	Number of ions in solution
$CoCl_3 \cdot 6NH_3$	yellow	$[Co(NH_3)_6]Cl_3$		4
$CoCl_3 \cdot 5NH_3$	violet	$[Co(NH_3)_5Cl]Cl_2$		3
$CoCl_3 \cdot 4NH_3$	green	$[Co(NH_3)_4Cl_2]Cl$		2
$CoCl_3 \cdot 3NH_3$	orange	$[Co(NH_3)_4Cl_3]$		0

What does this data suggest about the relative explanatory power of Werner's coordination theory and chain theory? Explain.

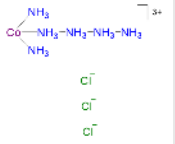
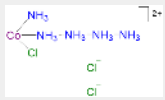
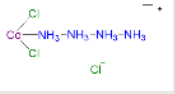
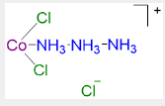
Answer

Remember that

- chain theory predicts that the number of ions is the number formed when the Cl atoms bound in a chain with NH_3 dissociate.
- coordination theory predicts the number of ions based on the number of complex ions and their counterions.

Based on this the predictions of coordination theory and chain theory can be compared with the experimental data, as is done in Table **Section5.1.2**.

Table **Section5.1.2**: Comparison of ions predicted for the $CoCl_3 \cdot xNH_3$ series by coordination theory and chain theory with the number observed experimentally.

Compound	Color	Ions predicted by Werner's coordination theory	Number of ions predicted by coordination theory	Ions predicted by Blomstrand-Jørgensen chain theory	Number of ions predicted by chain theory	Observed Number of ions in solution
$CoCl_3 \cdot 6NH_3$	yellow	$[Co(NH_3)_6]^{3+}$ Cl^- Cl^- Cl^-	4		4	4
$CoCl_3 \cdot 5NH_3$	violet	$[Co(NH_3)_5Cl]^{2+}$ Cl^- Cl^-	3		3	3
$CoCl_3 \cdot 4NH_3$	green	$[Co(NH_3)_4Cl_2]^+$ Cl^-	2		2	2
$CoCl_3 \cdot 3NH_3$	orange	None	0		2	0

As can be seen by comparing the number of ions predicted by coordination and chain theory in Table **Section5.1.2**, coordination theory successfully explains all the observed ion counts, while chain theory fails to explain the lack of ions observed for $CoCl_3 \cdot 3NH_3$.

Nevertheless, as is often the case when developing theoretical models using data from real experimental investigations, these observations did not convince Jørgensen, who could point to the experimental difficulty of determining the number of ions present from solution conductivity data.

What ultimately convinced Jørgensen of the correctness of Werner's coordination model over his own chain theory was how Werner's explanation of the structure of cobalt coordination complexes using an octahedral coordination geometry explained the existence of isomers in Co complexes containing Cl and NH_3 ligands. In the case of $[Co(NH_3)_4Cl_2]Cl$ two isomers were known: one red and the other green. Because both compounds had the same chemical composition and the same number of groups of the same kind attached to the same metal, there had to be something different about the arrangement of the ligands around the metal ion. Werner's key insight was that the six ligands in $[Co(NH_3)_4Cl_2]Cl$ had to be arranged at the vertices of an octahedron because that was the only structure consistent with the existence of two, and only two, stereoisomers (Figure ***Section*5.1.1**). His conclusion was also corroborated by the existence of two and only two stereoisomers of the next compound in the series: $Co(NH_3)_3Cl_3$.

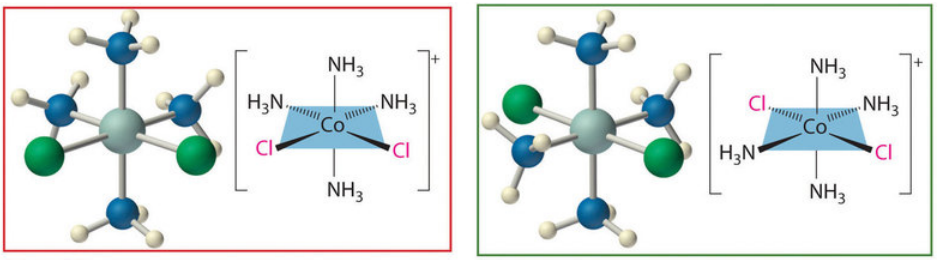


Figure ***Section*5.1.1**. The $[Co(NH_3)_4Cl_2]^+$ ion can have two different arrangements of the ligands, which results in different colors: if the two Cl^- ligands are next to each other (*cis*), the complex is red (a), but if they are opposite each other (*trans*), the complex is green (b).

✔ Example *Section*5.1.1: Why did Werner propose an octahedral geometry for 6-coordinate complexes?

In Werner's time, many complexes of the general formula MA_4B_2 were known, but no more than two different compounds with the same composition had been prepared for any metal. To confirm Werner's reasoning that this suggests these complexes possess an octahedral geometry, calculate the maximum number of different structures possible for six-coordinate MA_4B_2 complexes with each of the three most symmetrical possible structures the ligands will form about the central metal - a hexagon, a trigonal prism, and an octahedron.

Assuming that the absence of evidence for additional compounds in this case serves as reasonable circumstantial evidence for their absence, what does the fact that no more than two forms of any MA_4B_2 complex were known suggest about the three-dimensional structures of these complexes?

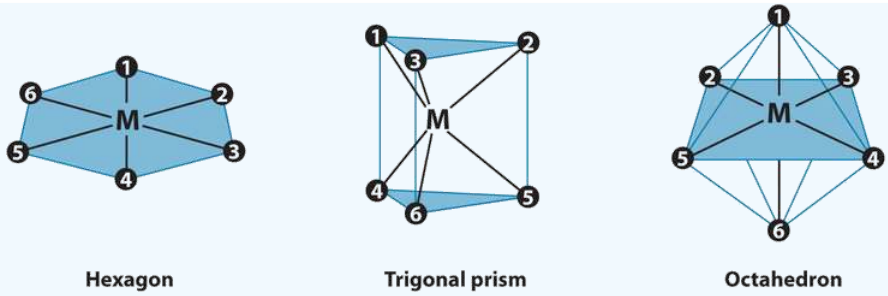
Solution

In this problem you are given

- the stochiometry of the complexes, MA_4B_2
- three possible coordination geometries - hexagonal, trigonal prismatic, and octahedral.

In order to calculate the number of isomers that could be present for each geometry it is best to follow a systematic approach. Since there are fewer B type ligands than A type ligands, the easiest way to do this for each geometry is to start by placing a B ligand at one vertex and then to determine how many different positions are available for the second B ligand.

The three regular six-coordinate structures are shown here, with each coordination position numbered so that we can keep track of the different arrangements of ligands. For each structure, all vertices are equivalent. We begin with a symmetrical MA_6 complex and simply replace two of the A ligands in each structure to give an MA_4B_2 complex:



Hexagon Trigonal prism Octahedron

For the hexagon, we place the first B ligand at position 1. There are now **three** possible places for the second B ligand:

- position 2 (or 6)
- position 3 (or 5)
- position 4

The (1, 2) and (1, 6) arrangements are chemically identical because the two B ligands are adjacent to each other. The (1, 3) and (1, 5) arrangements are also identical because in both cases the two B ligands are separated by an A ligand. Those of you who remember your ogranic chemistry might recognize that this situation is formally analogous to the *ortho-*, *meta-*, and *para-* isomerism in disubstituted benzenes.

Turning to the trigonal prism, we place the first B ligand at position 1. Again, there are three possible choices for the second B ligand:

- at position 2 or 3 on the same triangular face
- position 4 (on the other triangular face but adjacent to 1)
- position 5 or 6 (on the other triangular face but not adjacent to 1).

The (1, 2) and (1, 3) arrangements are chemically identical, as are the (1, 5) and (1, 6) arrangements.

In the octahedron, however, if we place the first B ligand at position 1, then we have only two choices for the second B ligand:

- position 2 (or 3 or 4 or 5)
- position 6.

In the latter, the two B ligands are at opposite vertices of the octahedron, with the metal lying directly between them. Although there are four possible arrangements for the former, they are chemically identical because in all cases the two B ligands are adjacent to each other.

The number of possible MA_4B_2 arrangements for the three geometries is thus: hexagon, 3; trigonal prism, 3; and octahedron, 2. The fact that only two different forms were known for all MA_4B_2 complexes that had been prepared suggested that the correct structure was the octahedron but did not prove it. For some reason one of the three arrangements possible for the other two structures could have been less stable or harder to prepare and had simply not yet been synthesized. When combined with analogous results for other types of complexes (e.g., MA_3B_3), however, the data were best explained by an octahedral structure for six-coordinate metal complexes.

? Exercise *Section*5.1.1

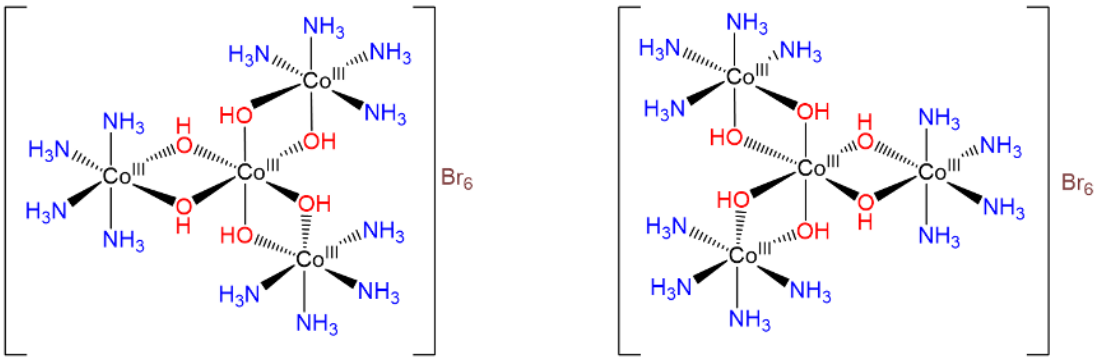
Determine the maximum number of structures that are possible for a four-coordinate MA_2B_2 complex with either a square planar or a tetrahedral symmetrical structure.

Answer

square planar, 2; tetrahedral, 1

Even Werner's explanation of isomerism in coordination complexes in terms of octahedral and other recognized coordination geometries did not convince all chemists until he was able to resolve a racemic mixture of *d*- and *l*-[Co{Co(NH3)$_4$(OH)$_2$}$_3$] into its

enantiomers, which are shown in Scheme **Section5.1.II**. By doing so Werner demonstrated to chemists of his time (virtually none of whom knew group theory) that tetrahedral carbon atoms were not required for chirality; D_3 octahedral complexes were also chiral.



Scheme **Section5.1.II**: d- and l-enantiomers of $[Co\{Co(NH3)_4(OH)_2\}_3]$, colloquially referred to as hexol. This work by Stephen Contakes is licensed under a Creative Commons Attribution 4.0 International License.

Section 5.1: History is shared under a CC BY-NC-SA 4.0 license and was authored, remixed, and/or curated by LibreTexts.

- **24.1: Werner's Theory of Coordination Compounds** by Anonymous is licensed CC BY-NC-SA 4.0.

Section 5.2: Nomenclature and Ligands

Introduction

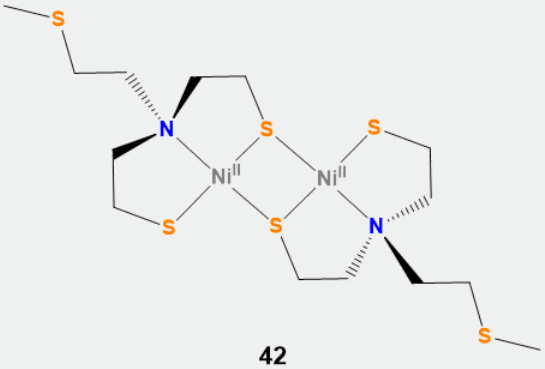
There are well-established rules for both naming and writing the formulae of coordination compounds. The purpose of these rules is to facilitate clear and precise communication among chemists. As with all such rules some are more burdensome than others to employ and some serve more crucial roles in the communication process while others are more peripheral - and all are poorly used in the service of pedantic tyranny, especially when against those who are otherwise doing good work. For this reason, you are urged to approach the rules in a spirit of generosity towards others in

- naming and writing formulas as reasonably accurately as you can so that ligands and metals are where readers expect them and thus can understand what you mean more easily.
- being gracious towards the many professional inorganic chemists who adhere loosely to some of the rules you are about to learn.
- recognizing that in cases when a structure is particularly complex and a picture may make be particularly useful you should supply one (See the note below).

Note Section5.2.1: Sometimes the most helpful name to give a compound is 42.

Even though the IUPAC nomenclature rules permit specification of even the most complex structures, it is often much easier and more effective to supply a numbered structure that can be referred to instead of the IUPAC name. Consider bis{[(μ-2-mercaptoethyl)(2-mercaptoethyl)-methylthioethylaminato (2-)]Nickel(II)}. Which is easier, to expect readers and hearers to work out the structure from that name or to just refer them to compound **42** in Scheme**Section5.2.I**?

Scheme Section5.2.I. Structure of bis{[(μ-2-mercaptoethyl)(2-mercaptoethyl)-methylthioethylaminato (2-)]Nickel(II)}. The authors of the synthesis of this compound in *Inorganic syntheses*[1] may have had to figure out an IUPAC name for this compound but if you have this scheme in your paper and your instructor is OK with it you can just call it **42**.



42

Coordination Complex Nomenclature

A variety of systems have been used for naming coordination compounds since the development of the discipline in the time of Alfred Werner. In this section the most common approaches as they are currently used by practicing chemists will be described. Those who need a more thorough and accurate acquaintance with the full IUPAC nomenclature rules are encouraged to consult the IUPAC brief guide to inorganic nomenclature followed by complete guidelines, commonly known as the IUPAC red book. If those are still not enough a careful read of note **Section5.2.1** is suggested.

The systems for naming coordination compounds used at present are additive, meaning that they consider coordination compounds as comprised of a central metal to which are added ligands. To specify the structure and bonding in this metal-ligand complex then involves

1. When there are several different ways of attaching the metal and ligands, specifying the structural or stereoisomer

2. systematically listing the ligands in a way that, as necessary, conveys information about how they are linked to the metal and their stereochemistry

3. providing the identity of the metal and its oxidation state, or if the oxidation state is unclear, at least the overall charge on the complex

4. specifying any counterions present

Since the stereochemistry of coordination compounds forms the subject of the next section, in this section it will be addressed in this section by simply giving the prefixes that designate stereochemistry as if they were self-evident. Do not worry about these for now. They will make sense after you have learned more about stereochemistry in the next section. At that time, you can go back over the examples in that section to solidify your understanding of how to name coordination compounds.

However, in order to name coordination compounds accurately you will need to learn about how to think about and name ligands first.

Ligands

Ligands are classified based on whether they bind to the metal center through a single site on the ligand or whether they bind at multiple sites. Ligands which bind through only a single site are called **monodentate** at the Latin word for tooth; in contrast those those which bind through multiple sites are called **chelating** after the Greek $\chi\alpha\lambda\epsilon$ for "claw". These relationships are summarized in Figure Section5.2.1.

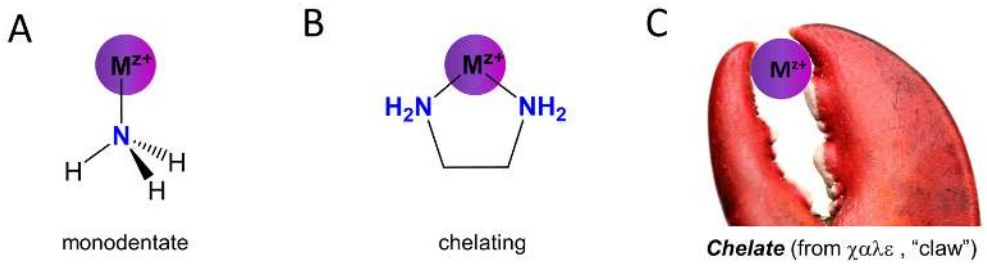
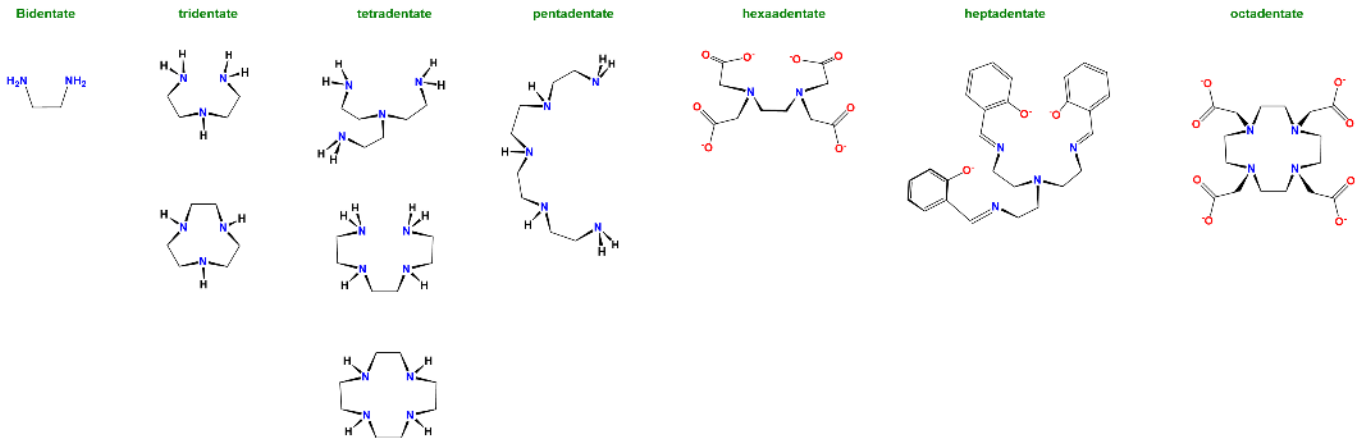


Figure Section5.2.1. (A) Ammonia is monodentate ligand while (B) ethylene diamine is a chelating ligand owing to its capacity to bind metals via its two amine functional groups. (C) Chelating ligands act like a Lobster claw in attaching to the metal via multiple sites. The lobster claw image is adapted from https://www.clipart.email/download/1127636.html. Otherwise this work by Stephen Contakes is licensed under a Creative Commons Attribution 4.0 International License.

Following naturally from the classification of non-chelating ligands as monodentate, chelating ligands are further classified according to the number of sites which they can use to bind a metal center. This number of binding sites is called the denticity and ligands are referred to as monodentate (non chelating), bidentate, tridentate, etc. based on the number of sites available. Ligands with two binding sites have a denticity of two and are said to be bidentate; those with three are tridentate, four tetradentate, and so on. To illustrate this classification system examples of chelating ligands classified according to denticity are given in Scheme Section5.2.I.

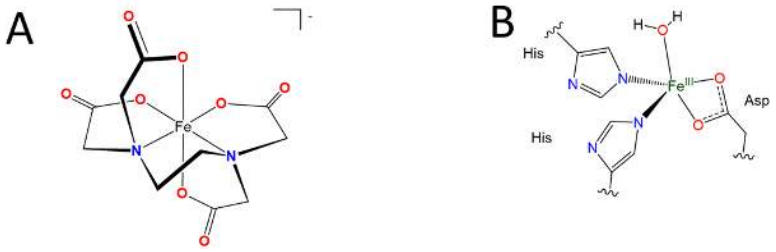
Scheme Section5.2.I. A selection of chelating ligands classified according to denticity. this work by Stephen Contakes is licensed under a Creative Commons Attribution 4.0 International License.



The classification of several of the ligands in Scheme **Section5.2.I** requires a bit of explanation, specifically as to why the dentificity of the carboxylate-containing ligands is less than the total number of lone-pair bearing oxygen and nitrogens present. This is because only one of the carboxylate oxygens is counted. Only one is counted because in most cases only one oxygen binds to a metal at any given time. When that oxygen is bound the other oxygen faces away from the metal, as depicted for the iron complex shown in Scheme **Section5.2.IIA**. Because only one oxygen per carboxylate *typically* binds only one is counted when assigning a ligand's denticity.

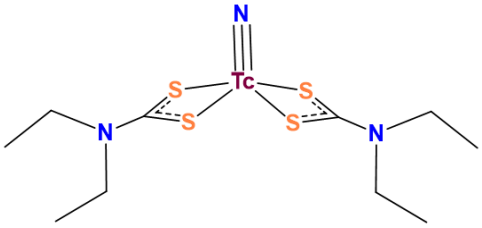
Although only one carboxylate oxygen usually binds to a metal it is still possible to bind a metal using both oxygens. As shown in Scheme **Section5.2.IIB** complexes in which both carboxylates bind to a metal are known, and in fact are common in the active sites of some enzymes. It is just that the binding of both oxygens gives a strained four-membered ring that is usually unstable.

Scheme Section5.2.II. (A) Only one oxygen per carboxylate counts towards the denticity of EDTA since on binding the other oxygen generally points away from the metal center, as in the structure of $Fe(EDTA)^-$. This does not mean that both oxygens of a carboxylate can *never* both bind to metal centers in a complex. (B) Structures in which both oxygens of a carboxylate side chain bind to a metal are sometimes found in the active sites of some of the nonheme iron enzymes your body uses to break down amino acids. this work by Stephen Contakes is licensed under a Creative Commons Attribution 4.0 International License.



As was the case for carboxylate groups above, sometimes the classification of a group's denticity is based on experimental knowledge of their common binding modes. Carboxylates might commonly act as monodentate ligands but dithiocarbamates more commonly bind metals through both sulfur atoms (Scheme **Section5.2.III**) and are classified as bidentate.

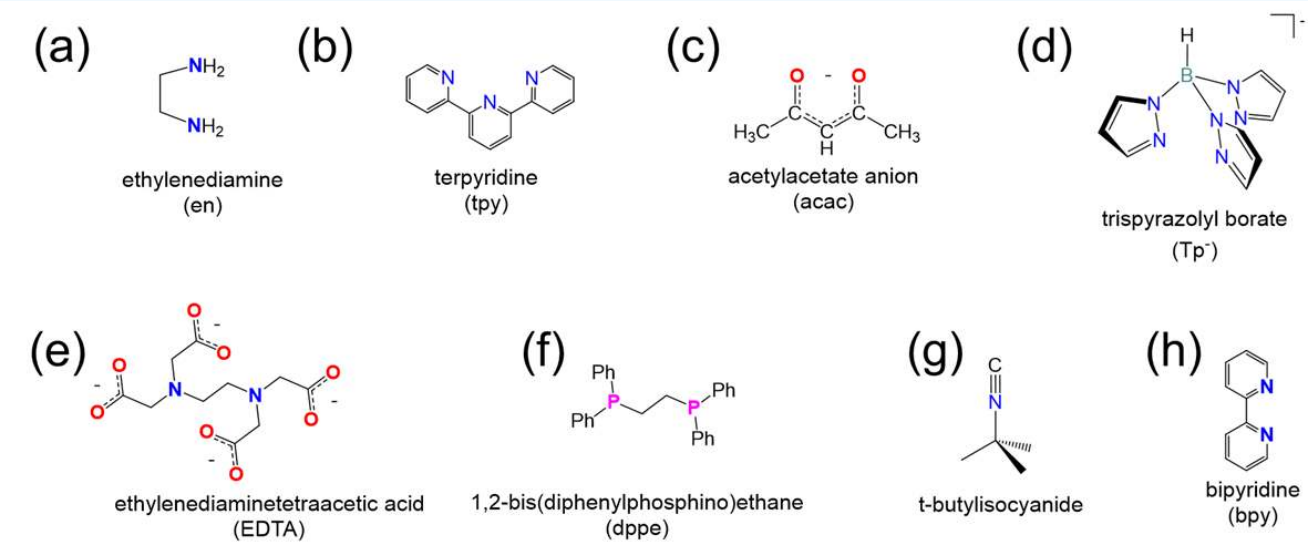
Scheme Section5.2.III. As in this complex, dithiocarbamates commonly bind metals through both sulfur atoms. Consequently, dithiocarbamates are classified as bidentate. this work by Stephen Contakes is licensed under a Creative Commons Attribution 4.0 International License.



Because of these factors it is technically more correct to say that carboxylates *usually act as* monodentate ligands and dithiocarbamates bidentate ones than it is to say that carboxylates *are* monodentate ligands and dithiocarbamates bidentate ones. So in other words the ligand classifications presented here are just represent common binding modes.

Exercise *Section*5.2.1

Determine the denticity of each ligand in the list below and classify them as monodentate, tridentate, etc.



Answer

(a) bidentate

(b) tridentate

(c) bidentate

(d) tridentate (only the lower N on each ring has a lone pair that can be used to bind the metal)

(e) hexadentate (remember that each carboxylate only counts as one point of attachment)

(f) bidentate

(g) monodentate (through the lone pair on the isocyanide C)

(h) bidentate

This experimentally-based classification of dithiocarbamates as bidentate and carboxylates as monodentate can be confusing to a beginner. Fortunately, such experimentally based classifications are embedded in the lists of common monodentate ligands are given in Table **Section5.2.1** and common chelating ligands in Table **Section5.2.2.**

A perusal of the ligands in Table **Section5.2.1** reveals that several can bind to a metal in multiple ways. For example, thiocyanate, SCN^- can bind metal's through its S or N atoms. Such ligands are called **ambidentate ligands**. When naming an ambidentate ligand the atom through which it attaches to the metal is commonly specified after the ligand name using the italicized element symbol or, more formally a κ followed by the italicized element symbol. An example is given in Scheme **Section5.2.I.**[2]

Scheme Section5.2.I. Two possible binding modes of nitrite acting as a ligand.[3]

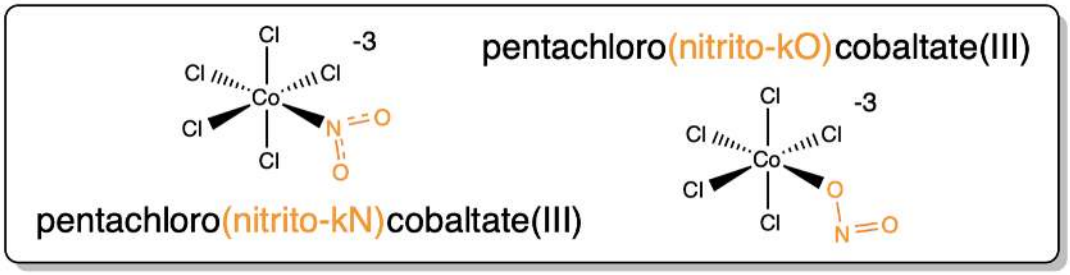
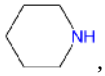

-3
pentachloro(nitrito-kO)cobaltate(III)
-3
pentachloro(nitrito-kN)cobaltate(III)

Table Section5.2.1. Common monodentate ligands. Most chemists still prefer common names over the IUPAC ones.

Ligand	Common name	IUPAC name
H^- (H ligands are always considered anions for naming purposes)	hydrido	hydrido
F^-	fluoro	fluorido
Cl^-	chloro	chlorido
Br^-	bromo	bromido
I^-	iodo	iodido
CN^-, M-CN	cyano	cyanido or cyanido-κC or cyanido-*C*
CN^-, as M-NC	isocyano	isocyanido or cyanido-κN or cyanido-*N*
CH_3NC	methylisocanide	methylisocyanide
N_3^-	azido	azido
SCN^-, *e.g.* thiocyanate as M-SCN	thiocyanato	thiocyanato-κS or thiocyanato-*S*
NCS^-, *e.g.* thiocyanate as M-NCS	isothiocyanato	thiocyanato-κN or thiocyanato-*N*
$CH_3CO_2^-$	acetato	ethanoato
N^{3-}	nitrido	nitrido
NH^{2-}	imido	azanediido
NH_2^-	amido	azanido
NH_3	ammine	ammine
RNH_2, R_2NH, R_3N	alkylamine, dialkylamine, trialkalyamine (*e.g.* methylamine for CH_3NH_2)	alkylamine, dialkylamine, trialkalyamine (*e.g.* methylamine for CH_3NH_2)
 , piperidine, abbreviated pip	piperidine	piperidine
 , pyridine, abbreviated py	pyridine	pyridine
CH_3CN, acetonitrile, abbreviated MeCN	acetonitrile	acetonitrile
P^{3-}	phosphido	phosphido
PH_3	phosphine	phosphane
PR_3	trialkylphosphine (*e.g.* trimethylphosphine for Me_3P)	trialkylphosphane (*e.g.* trimethylphosphane for Me_3P)
PAr_3	triarylphosphine (*e.g.* triphenylphosphine for Ph_3P)	triarylphosphine (*e.g.* triphenylphosphane for Ph_3P)
 , dimethylsulfoxide or DMSO or dmso	dimethylsulfoxide (sometimes called dimethylsulfoxo but this usage is rare and violates the nomenclature rules for neutral ligands)	(methanesulfinyl)methane or dimethyl(oxido)sulfur

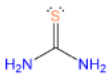
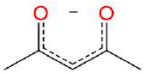
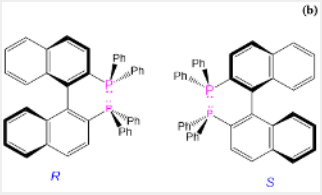
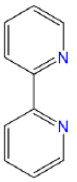
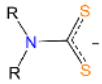
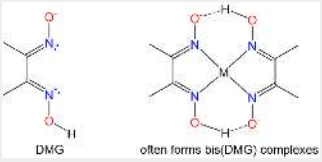
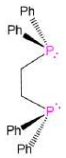
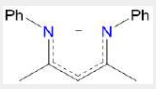
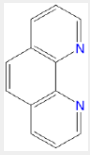
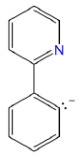
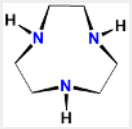
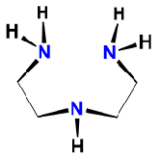
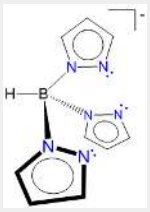
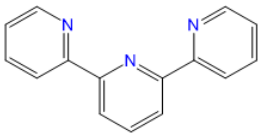
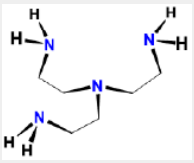
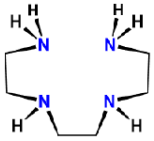
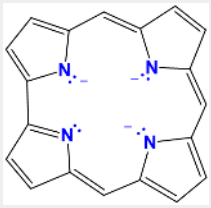
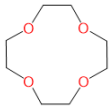
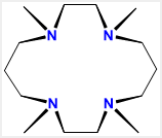
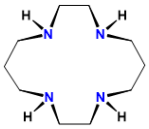
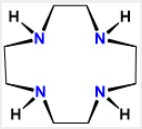
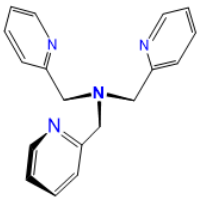
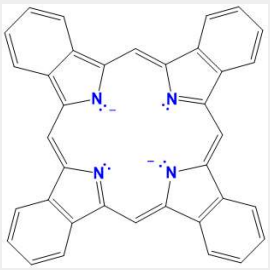
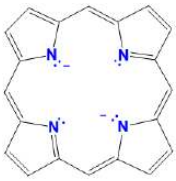
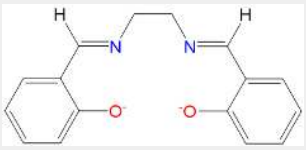
 , thiourea or tu	thiourea	thiourea
O^{2-}	oxo	oxido
OH^-	hydroxo	hydroxido
H_2O	aqua	aqua
S^{2-}	sulfo	sulfo
HS^-	hydrosulfido	hydrosulfido
RS^-	alkanethiolate (*e.g.* ethanthiolate for EtS^-)	thioalkanoate
H_2S	hydrogen sulfide	hydrogen sulfide
R_2S	alkylsulfanylalkane (*e.g.* ethylsulfanylethane for Et_2S)	dialkyl sulfide
O_2	dioxygen	dioxygen
O_2^-, superoxide	superoxido	dioxido(1-) or superoxido
O_2^{2-}, peroxide	peroxido	dioxido(2-) or peroxido
N_2	dinitrogen	dinitrogen
NO (are always considered neutral for naming purposes)	nitrosyl	nitrosyl
CO	carbonyl	carbonyl
CS	thiocarbonyl	thiocarbonyl
SO, as M-SO	sulfino	sulfur monoxide-κ*S* or sulfur monoxide-*S*
NO_2, as M-NO_2	nitryl	nitrogen dioxide-κN or nitrogen dioxide-*N*
CO_3^{2-}	carbonato	carbonato
NO_2^-, as M-NO_2	nitro or nitrito-*N*	nitrito-κ*N* or nitrito-*N*
NO_2^-, as M-ONO	nitrito or nitrito-*O*	nitrito-κ*O* or nitrito-*O*
NO_3^-	nitrato	nitrato
SO_3^{2-}	sulfito	sulfito
SO_4^{2-}	sulfato	sulfato
$S_2O_3^{2-}$, as M-S-SO_2-O^-	thiosulfato-*S*	thiosulfato-κ*S* or thiosulfato-*S*
$S_2O_3^{2-}$, as M-O-SO_2-S^-	thiosulfato-*O*	thiosulfato-κ*O* or thiosulfato-*O*

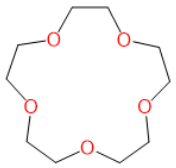
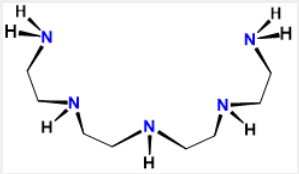
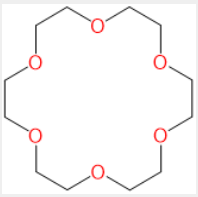
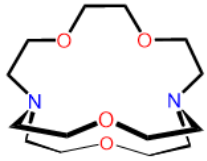
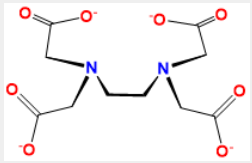
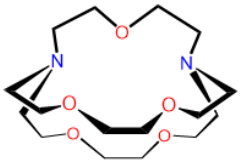
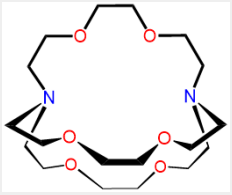
Table Section5.2.2. Common chelating ligands organized by denticity. Most chemists use the common names and abbreviations to

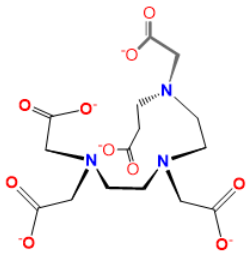
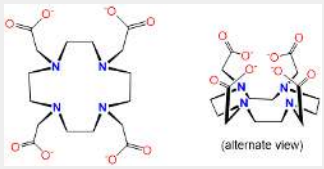
describe these ligands.

Common Ligand name	IUPAC ligand name	abbreviation (if applicable)	structure or representative/parent structure (shown in the ionization state in which they bind to a metal)
bidentate ligands			
acetylacetonato	2,4-pentanediono	acac	
R-BINAP and *S*-BINAP	*R*- or *S*-2,2'-bis(diphenylphosphino)-1,1'-binapthyl	BINAP	
2,2'-bipyridine	2,2'-bipyridine	bpy or bipy	
cyclooctadiene	1,5-cyclooctadiene	COD	 (binding to the metal occurs through the alkene π cloud)
dialkyldithiocarbamato	dialkylcarbamodithiolato	$R_2NCS_2^-$ or dtc	
dimethylgloximato	butanedienedioxime	Hdmg or DMG	
diphenylphosphinoethane or 1,2-(diphenylphosphino)ethane	Ethane-1,2-diylbis(diphenylphosphane)	dppe	
ethylenediamine	Ethane-1,2-diamine	en	
ethylenedithiolato	Ethane-1,2-dithiolato	$C_2H_2S_2^{2-}$	
nacnac	*N*,*N*'-diphenyl-2,4-pentanediiminato	nacnac	

oxalato	oxalato	ox	
1,10-phenanthroline or *o*-phenanthroline	1,10-phenanthroline	phen or *o*-phen	
phenylpyridinato	2-phenylpyridinato-C^2,*N* or 2-phenylpyridinato-κC^2,*N*	ppy	
tridentate ligands			
triazacyclononane	1,3,7-triazacyclononane	tacn	
diethylenetriamine	1,4,7-triazaheptane	dien	
pyrazoylborato (scorpionate)	hydrotris(pyrazo-1-yl)borato	Tp	
terpyridine or 2,2';6',2''-terpyridine	1^2,2^2:2^6,3^2-terpyridine or 2,6-bis(2-pyridyl)pyridine, tripyridyl, 2,2′:6′,2″-terpyridine	tpy or terpy	
tetradentate ligands			
β, *β*', *β*''-triaminotriethylamine	*β*, *β*', *β*''-tris(2-aminoethyl)amine	tren	
triethylenetetramine	1,4,7,10-tetraazadecane	trien	

corroles	variable and generally not used	cor or Cor	
12-crown-4	1,4,7,10-tetraoxacyclododecane	12-crown-4	
tetramethylcyclam	1,4,8,11-tetramethyl-1,4,8,11-tetraazacyclotetradecane	TMC or cyclam	
cyclam	1,4,8,11-tetraazacyclotetradecane	cyclam	
cyclen	1,4,7,10-tetraazacyclododecane	cyclen	
tris(2-pyridylmethyl)amine	1-pyridin-2-yl-*N*,*N*-bis(pyridin-2-ylmethyl)methanamine	tpa or TPA	
phthalocyanines	variable and generally not used	variable, usually a modified Pc	
porphyrins	variable and generally not used	variable, usually a modified por, Por, or P (e.g. TPP = tetraphenylporphyrin)	
salen	2,2'-ethylenebis(nitrilomethylidene) diphenoxido	salen	
pentadentate ligands			

15-crown-5	1,4,7,10,13-Pentaoxacyclopentadecane	15-crown-5	
tetraethylenepentamine	1,4,7,10,13-pentaazatridecane	tepa or TEPA	
hexadentate ligands			
18-crown-6	1,4,7,10,13,16-hexaoxacyclooctadecane	18-crown-6	
2,1,1-cryptand	4,7,13,18-Tetraoxa-1,10-diazabicyclo[8.5.5]icosane	2,1,1-crypt or [2.1.1]-cryptand kryptofix 211 and variations thereof	
ethylenediaminetetraaceto	2,2′,2″,2‴-(Ethane-1,2-diyldinitrilo)tetraaceto	EDTA, edta, Y^{4-}	
heptadentate ligands			
2,2,1-cryptand	4,7,13,16,21-pentaoxa-1,10-diazabicyclo[8.8.5]icosane	2,2,1-crypt or [2.2.1]-cryptand kryptofix 221 and variations thereof	
octadentate ligands			
2,2,2-cryptand	4,7,13,16,21,24-Hexaoxa-1,10-diazabicyclo[8.8.8]hexacosan	2,2,2-crypt or [2.2.2]-cryptand kryptofix 222 and variations thereof	

pentetato acid or diethylenetriaminepentaacetato or DTPA	2-[bis[2-[bis(carboxylatomethyl)amino]ethyl]amino]acetato	DTPA	
DOTA or tetraxetan	1,4,7,10-Tetraazacyclododecane-1,4,7,10-tetraacetic acid	Dota, DOTA	

Rules for Naming Coordination Compounds

As explained above, the name of a coordination compound communicates

- As appropriate, information about isomerism
- systematically listing the ligands in a way that as necessary conveys information about their oxidation state and how they are linked to the metal
- the identity of the metal and its oxidation state
- any counterions present

Before going into these rules it is worth pointing out a few things.

1. It is easiest to learn these rules by starting with one or two of the rules, learning how to apply them, and then adding additional rules one at a time. To that end, instructors who wish to use a more programmed approach may find it convenient to first direct their students to this page which focuses on getting the names of the ligands and metal right, without working about isomerism or stereochemistry.

2. The rules also assume some familiarity with common coordination geometries and patterns of isomerism in metal complexes. Thus it might be easiest to learn about common coordination geometries first, followed by common patterns of isomerism in metal complexes before beginning this section. If you decide to dive right in to this section you might find it helpful to know that when applying nomenclature and formula rules most textbooks *assume*

- complexes in which the metal has a coordination number of six are octahedral
- complexes in which the metal has a coordination number of five are trigonal bipyramidal
- complexes in which Pt^{II} , Pd^{II} , or Rh^{I}, or Ir^{I} have a coordination number of four are square planar
- other complexes in which the metal has a coordination number of four are tetrahedral

Like all assumptions these don't always work in real life but they should be good enough to get you through your first inorganic chemistry course.

For the pedants among you, note that the complexes given as examples and in exercises on this page have been selected for pedagogical utility. Although many are well-known compounds, others are hypothetical.

Now on to the rules.

Name the cation first, followed by the anion.

Examples:

$K_2[Pt^{II}Cl_4]$ potassium tetrachloroplatinate(2-)

$[Co^{III}(NH_3)_6](NO_3)_3$ hexaamminecobalt(3+) nitrate

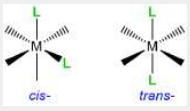
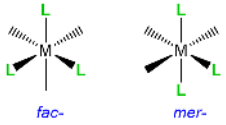
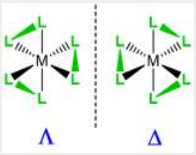
$[Co^{III}(NH_3)_6][Cr^{III}(C_2O_4)_3]$ hexaamminecobalt(3+) tris(oxalato)chromium(3-)

Designate the isomer in italics in front of the name

If you have not yet learned about isomerism in coordination compounds skip this rule for now and return to it after you have.

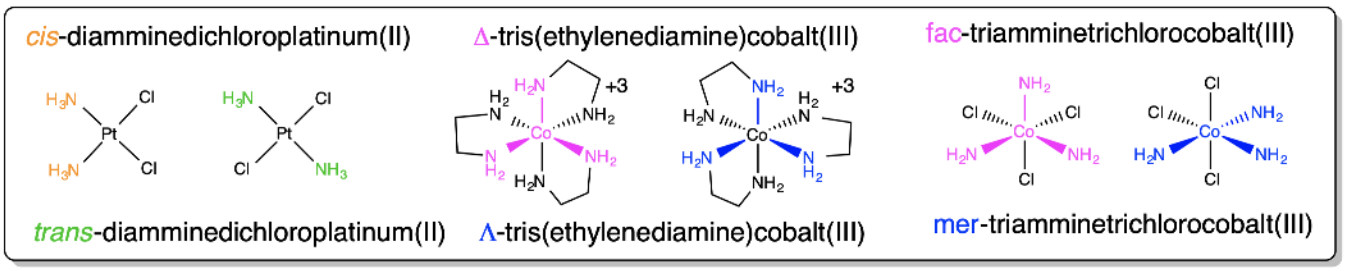
When a complex might exist as one of two stereosisomers prefixes are commonly used to designate which isomer is present. The most common cases are listed in Table Section5.2.3.

Table Section5.2.3. Prefixes used to specify isomerism about a metal center when naming and writing coordination compounds' formulae.

Type of isomerism	Graphical reminder	Prefixes
Geometric, *cis-* , *trans-*		*cis-* or *trans-*
Geometric, *fac- /mer-*		*fac-* or *mer-*
Enantiomers, Λ-, Δ-		Λ- or Δ-

Examples of how isomerism about a metal center is designated are given in Scheme Section5.2.II.

Scheme Section5.2.II. Application of nomenclature rules for stereosimerism about a metal.[3]



There are a number of other cases where it might be advisable to specify the stereochemistry of a complex. These cases involve specifying

- the coordination geometry about a metal center (octahedral, trigonal prismatic, tetrahedral, square planar, etc.)
- the geometry cannot be unambigouously described by a single *cis/trans* or *fac/mer* relaionship of ligands

These cases may also be handled by using a designator to specify the coordination geometry and, as necessary, giving the position of ligated atoms in terms of designated numbered positions for that geometry. See the IUPAC red book for details as such cases fall outside the scope of what is normally advisable for an undergraduate course.

Specify the identity and number of the ligands in alphabetical order by ligand name.

Before specifying the metal, the ligands are written as prefixes of the metal.

In specifying the ligands several rules are followed.

1. The ligands are written in alphabetical order by the ligand name only; symbols are not considered and prefixes do not count in determining alphabetical order.

Example: In the name of the complex ion $[Co(NH)_3Cl]^{2+}$, pentamminechlorocobalt(II), the ammine ligand is named before the chloro ligand because the order is alphabetical by the ligand name by virtue of which ammine comes before chloro.

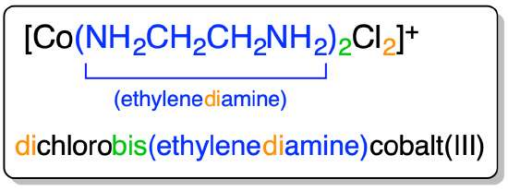
2. Prefixes are used to indicate the number of each ligand present. Specifically, *di-*, *tri-*, *tetra-* , *penta-*, *hexa-*, *etc.* prefixes are used to indicate multiple ligands of the same type EXCEPT when the ligand is polydentate or its name already has a *di-*, *tri-*, *tetra-* etc. In that case *bis-*,*tris-*, *tetrakis-*, etc. are used instead. These prefix rules are summarized in Table **Section5.2.3**.

Table Section5.2.3. Prefixes used to specify the number of a given ligand present.

Number of identical ligands	prefix used when the ligand name is simple	prefix used when the ligand is polydentate or its name already has a *di-*, *tri-*, *tetra-* etc.
2	di-	bis-
3	tri-	tris-
4	tetra-	tetrakis-
5	penta-	pentakis-
6	hexa-	hexakis-
7	hepta-	heptakis-
8	octa-	octakis-
9	nona-	nonakis-
10	deca-	decakis-

An example of the application of the prefix rule is given in Scheme **Section5.2.III**.

Scheme Section5.2.III. Example of the use of prefixes to specify the number of ligands of each type in a complex.[3]



3. Ligand names are based on their charge

- Neutral and cationic ligand names are the same as the names of their neutral compounds with two caveats

  i. names that involve spaces should either be put in parentheses or the spaces should be eliminated (preferred)

  Example: cis-dichlorobis(**dimethyl sulfoxide**)platinum(II) or *cis*-dichlorobis(**dimethylsulfoxide**)platinum(II)

  ii. A few ligands are given common names.

  - H_2O = aqua
  - NH_3 = ammine (notice that there are two m's)
  - CO = carbonyl
  - CS = thiocarbonyl
  - NO = nitrosyl

- For anionic ligands, the vowel at the end of their anion names is changed to an -"o"

  Examples: Cl^- = chlorido, NH_2^- = amido, N_3^- = azido

  Caveat: some anionic ligands have common names that may also be used

  Examples:

I^- = iodo or iodino

CN^- = cyano or cyanido

O^{2-} = oxo or oxido

The IUPAC and common names of many ligands are given in Tables Section5.2.1. and Section5.2.2.

4. When an ambidentate ligand is present the atom through which it is bound to the metal is indicated by giving either its element symbol or a κ and its element symbol in italics after the ligand name

   Example:

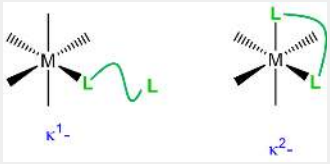
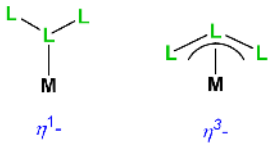
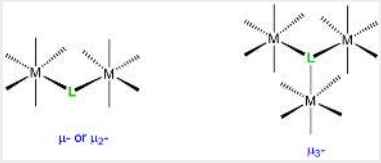
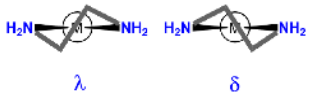
   M-SCN is thiocyanato-*S* or thiocyanato-κ*S*

   M-NCS = thiocyanato-*N or* thiocyanato-κ*N*

   The use of κ and an element symbol to indicate how a ligand and metal are linked is called a **k-term**. More complex k-terms might also involve specifying the atoms by number, though their use is outside the scope of this text.

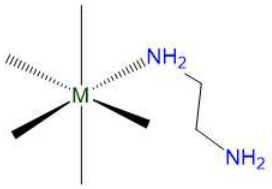
5. As appropriate, additional information about the way a ligand is bound to the metal center and/or its stereochemistry is specified using a prefix. The prefixes to provide linkage and stereochemistry for ligands are given in TableSection5.2.4.

TableSection5.2.4. Prefixes used to specify ligands' isomerism when naming and writing coordination compounds' formulae. Some of these types of isomerism will be discussed in later pages.

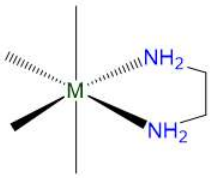
Type of isomerism	Graphical reminder	Prefixes
when a multidentate ligand binds through less than the full number of atoms		κ^n where n is the number of attached atoms; used when the attached atoms are not directly connected by a chemical bond. The metal-ligand bonding usually involves σ-type coordination.
hapticity		η^n where n is the number of attached atoms; used when the coordinated atoms are all connected by bonds. Usually the metal-ligand bonding involves for π-type coordination. In speech, η^1=monohapto; η^2=dihapto; η^3 =trihapto, etc.
bridging ligands		μ_n where n is the number of atoms bridged. The number n is usually omitted when n =2.
chelating ligand ring twist		λ- or δ-

A example showing how the nomenclature rule is applied to a ligand that can have two coordination modes is given in Scheme Section5.2.IV.

Scheme Section5.2.IV. Use of the κ notation to specify the number of attached groups in a multidentate ligand.



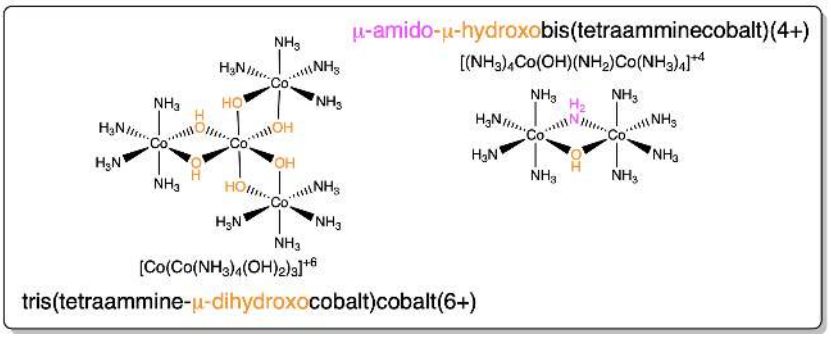
κ1-ethylenediamine



κ2-ethylenediamine

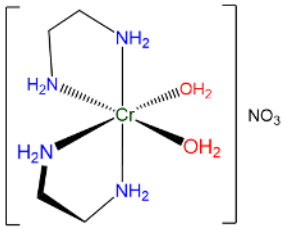
Two examples showing how the nomenclature rule is applied to bridging ligands are given in Scheme Section5.2.V. The names of the complexes follow the rules described in 9.2.6: multinuclear coordination complexes.

Scheme Section5.2.V. Use of the μ notation to specify bridging ligands in metal complexes.[3]



6. If desired, parentheses *may* be used to delineate a ligand name to make it easier to identify in the name. This can be particularly helpful when the name contains a lot of information to keep track of. An example is given in Scheme Section5.2.VI.

   Scheme Section5.2.VI. When naming the complex shown *cis*-diaquabis(ethylenediamine)chromium(III) nitrate is easier to read than *cis*-diaquabisethylenediaminechromium(III) nitrate.



Specify the metal

- In neutral and cationic complexes the metal's name is used directly

  - *e.g.* as in hexammineruthenium(III) for $[Ru(NH_3)_6]^{3+}$

- In anionic complexes, *-ate* replaces *-ium*, *-en*, or *–ese* or adds to the metal name.

  e.g. as in hexachloromanganate(IV) for $MnCl_6^{2-}$

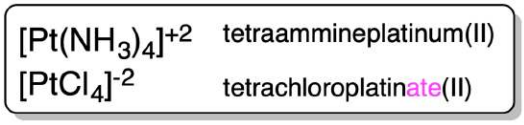
- In anionic complexes of some metals a Latin-derived name is used instead of the element's English name. These names are given in Table Section5.2.5.

  Table Section5.2.5. Latin terms for Select Metal Ions. Redrawn from this page describing the nomenclature of coordination complexes.

Transition Metal	Latin
Copper	Cuprate
Gold	Aurate
Iron	Ferrate
Lead	Plumbate
Silver	Argentate
Tin	Stannate

An example of the application of the metal naming rules is given in Scheme \sf{\PageIndex{VII}}\).

Scheme Section5.2.VII. Example of the application of the metal specification rules to a cationic and anionic platinum complexes.[3]



Specify the oxidation state of the metal.

Two different systems are used to specify the oxidation state of the metal.

1. In the **Stock system** the metal's oxidation state is indicated in Roman numerals after the metal name.

   Examples:

   $[CoCl(NH_3)_5]Cl_2$ = pentamminechlorocobalt(III) chloride

   $[PtBr_2(bpy)]$ = bipyridinedibromoplatinium(II)

   $K[Ag(SCN)_2]$ = potassium di-*S*-thiocyanatoargentate(I)

2. In the **Ewing-Bassett system** the charge on the complex is specified in Arabic numerals after the complex name. This provides a way of specifying a complex even when the oxidation state of the metal isn't known and, in cases where it is known, the value of the metal's oxidation state may be inferred from the complex ion's charge.

   $[CoCl(NH_3)_5]Cl_2$ = pentamminechlorocobalt(2+) chloride

   $[PtBr_2(bpy)]$ = bipyridinedibromoplatinium(0)

   $K[Ag(SCN)_2]$ = potassium di-*S*-thiocyanatoargentate(1-)

Summary

A graphical summary of the **rules for naming complexes** along with a few examples that you can use to review the nomenclature rules is given in Figure **Section5.2.1**. This work by Stephen Contakes is licensed under a Creative Commons Attribution 4.0 International License.

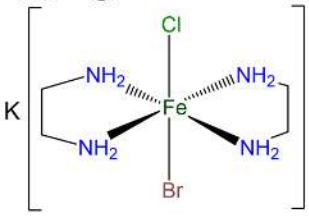
stereochemical prefix-	**Specify Ligands**	**Indicate Metal**	**Charge on the complex or metal oxidation state**
As appropriate use *cis-*, *trans-*, *fac-*, *mer-*, Λ-, Δ-, to indicate stereochemistry.	What ligands and how many? – List alphabetically by ligand name • Neutral – ligand name • Carionic – ligand name • Anionic – change last vowel to "o" – Indicate # by di-, tri-, tetra-, etc. (or bis-, tris-, tetrakis-, etc. if there is a di-, tri-, tetra, etc. in the ligand name) As appropriate, how are the ligands arranged? – Ambidentate – indicate linkage point by κ & italicized element symbol - other structure – use κ^n, η^n, μ_n, λ-, δ- For clarity, parentheses may be used to delineate ligands	Neutral, cationic: English name Anionic – change ending to "ate" - Latin names for Ag, Au, Cu, Fe, Pb, Sn; English for others	Stock system: Metal Oxidation state in capital Roman numerals Ewing-Bassett system: Complex's charge in Arabic numerals

Examples:

$[Ru(NH_3)_6](NO_3)_3$ hexammineruthenium(3+) nitrate or hexammineruthenium(III) nitrate

$K_2[PtCl_4]$ potassium tetrachloroplatinate(2-) or potassium tetrachloroplatinate(II)

$K[Ag(CN)_2]$ potassium dicyanoargentate(1-) or potassium dicyanoargentate(I)



potassium *trans*- bromochlorobis(ethylenediamine)iron(1+) (Ewing-Bassett)

-or-

potassium *trans*-bromochlorobis(ethylenediamine)iron(III) (Stock)

Figure **Section5.2.1**. Summary of nomenclature rules for coordination complexes along with a few examples of their application.

When learning chemical nomenclature practice makes perfect. The following examples and exercises are provided to give you this practice. Additional examples and exercises on the https://chem.libretexts.org/ site include a set of simple examples with explained solutions, a set of simple exercises with solutions, and a set of more challenging exercises without solutions.

Exercise *Section*5.2.2. Assigning metal oxidation states in a complex

In order to name a complex in the Stock system it is necessary to assign a formal oxidation state to the metal.

For this reason it is important to be able to assign the oxidation state of a metal in a complex. Fortunately, this is easy to do if you remember

1. The sum of all atom's oxidation states will equal the overall charge on the complex
2. When determining the metal's oxidation state the ligands can be treated as having an oxidation state equal to their charge - *i.e.* the charge they possess in the form they coordinate the metal so if they need to lose a proton to bind don't forget to account for that.

Given the above, assign the oxidation state of the metal in the following real and hypothetical complexes.

a. $K_3[Fe(CN)_6]$
b. $[CoCl(NH_3)_5](NO_3)_2$
c. $K_2[PtCl_4]$
d. [MnCl(por)]
e. $[Ru(bpy)_3]Cl_2$
f. $[PdCl_2(dppe)]$
g. $[Mn(en)_2(SCN)_2]$

Answer for $K_3[Fe(CN)_6]^{3-}$.

This contains $[Fe(CN)_6]^{3-}$; so O.S.$_{Fe}$ + 6 x (-1) (for CN^-) = -3 (the complexes' charge) so O.S.$_{Fe}$ = +3 or Fe^{3+}.

Answer for $[CoCl(NH_3)_5](NO_3)_2$.

This contains $[CoCl(NH_3)_5]^{2+}$; so O.S.$_{Co}$ + 1 x (-1) (for Cl^-) + 0 x 5 (for NH_3) = +2 (the complexes' charge) so O.S.$_{Co}$ = +3 or Co^{3+}.

Answer for $K_2[PtCl_4]$.

This contains $2K^+$ and $[PtCl_4]^{2-}$; so O.S.$_{Pt}$ + 4 x (-1) (for Cl^-) = -2 (the complexes' charge) so O.S.$_{Pt}$ = +2 or Pt^{2+}.

Answer for [MnCl(por)].

O.S.$_{Pt}$ + 1 x (-2) (for por; see table 9.2.2) + 1 x (-1) (for Cl^-) = +0 (the complexes' charge) so O.S.$_{Mn}$ = +3 or Mn^{3+}.

Answer $[Ru(bpy)_3]Cl_2$.

The complex is $[Ru(bpy)3]^{2+}$ so O.S.$_{Ru}$ + 0 x 3 (for bpy) = +2 (the complexes' charge) so O.S.$_{Ru}$ = +2 or Ru^{2+}.

Answer $[PdCl_2(dppe)]$.

O.S.$_{Pd}$ + 2 x (-1) (for Cl^-) + 0 x 3 (for dppe) = +0 (the complexes' charge) so O.S.$_{Pd}$ = +2 or Pd^{2+}.

Answer $[Mn(en)_2(SCN)_2]$.

O.S.$_{Mn}$ + (2 x 0) (for en) + 2 x (-1) (for SCN^-) = +0 (the complexes' charge) so O.S.$_{Mn}$ = +2 or Mn^{2+}.

Exercise *Section*5.2.3: Simple Nomenclature Problems.

Name the following compounds in both the Stock and Ewing-Bassett systems:

a. $[Ru(NH_3)_6](NO_3)_3$
b. $K_2[PtCl_4]$
c. $K[Ag(CN)_2]$
d. $Cs[CuBrCl_2F]$
e. $[Cu(acac)_2]$

Answer

	Complex	Stock system name	Ewing-Bassett System name
a	$[Ru(NH_3)_6](NO_3)_3$	hexammineruthenium(III) nitrate	hexammineruthenium(3+) nitrate
b	$K_2[PtCl_4]$	potassium tetrachloroplatinate(II)	potassium tetrachloroplatinate(2-)
c	$K[Ag(CN)_2]$	potassium dicyanoargentate(I)	potassium dicyanoargentate(1-)
d	$Cs_2[CuBrCl_2F]$	cesium bromodichloroflourocuprate(II)	cesium bromodichloroflourocuprate(2-)
e	$[Cu(acac)_2]$	bis(acetylacetonato)copper(II)	bis(acetylacetonato)copper(0)

Exercise *Section*5.2.4: More simple nomenclature problems.

Name the following compounds and ions in both the Stock and Ewing-Bassett systems.

a. $Cu(OH)_4^-$
b. $[AuXe_4]^{2+}$
c. $AuCl_4^-$
d. $Fe(CN)_6^{3-}$
e. $K_4[Fe(CN)_6]$
f. *trans*-$[Cu(en)_2(NO_2)_2]$ (the N is bound to Cu)
g. cis-$IrCl_2(CO)(PPh_3)$ (ignore stereochemistry)
h. $IrCl(PPh_3)$

Answer

	Compound	Stock System Name	Ewing-Bassett System Name
a	$Cu(OH)_4^-$	tetrahydroxocuprate(III) or tetrahydroxidocuprate(III)	tetrahydroxidocuprate(1-) or tetrahydroxidocuprate(1-)
b	$[AuXe_4]^{2+}$	tetraxenongold(II)	tetraxenongold(2+)
c	$AuCl_4^-$	tetrachloroaurate(III)	tetrachloroaurate(1-)
d	$Fe(CN)_6^{3-}$	hexacyanoferrate(III) or hexacyanidoferrrate(III)	hexacyanoferrate(3-) or hexacyanidoferrate(3-)
e	$K_4[Fe(CN)_6]$	potassium hexacyanoferrate(II) or potassium hexacyanidoferrrate(II)	potassium hexacyanoferrate(4-) or potassium hexacyanidoferrrate(4-)
f	*trans*-$[Cu(en)_2(NO_2)_2]$ (the N is bound to Cu)	bis(ethylenediamine)bisnitrocopper(II) or bis(ethylenediamine)bis(nitrito-*κN*)copper(II)	bis(ethylenediamine)bisnitrocopper(0) or bis(ethylenediamine)bis(nitrito-*κN*)copper(0)
g	*cis*-$IrCl_2(CO)(PPh_3)$	*cis*-dichlorocarbonyltriphenylphosphineiridium(I) or *cis*-dichloro(carbonyl)(triphenylphosphine)iridium(I)	*cis*-dichlorocarbonyltriphenylphosphineiridium(0) or *cis*-dichloro(carbonyl)(triphenylphosphine)iridium(0)
h	$IrCl(PPh_3)$	chlorotris(triphenylphosphine)iridium(I)	chlorotris(triphenylphosphine)iridium(0)

Exercise *Section*5.2.5: Even more simple nomenclature problems.

Name the following compounds and ions in both the Stock and Ewing-Bassett systems. Ignore prefixes for designating isomers if you haven't learned about those.

a. $Fe(acac)_3$
b. $K_2[CuBr_4]$
c. ReH_9
d. $[Ag(NH_3)_2]BF_4$
e. $[Ag(NH_3)_2][Ag(CN)_2]$

f. $[Ni(CN)_4]^{2-}$
g. $[Co(N_3)(NH_3)_5]SO_4$
h. $[CoBrCl(H_2O)(NH_3)]I$ (ignore stereochemistry)

Sample Answers

	Complex	Stock system name	Ewing-Bassett System name
a	$Fe(acac)_3$	tris(acetoacetato)iron(III)	tris(acetoacetato)iron(0)
b	$Na_2[CuBr_4]$	sodium tetrabromocuprate(II)	sodium tetrabromocuprate(2-)
c	$[Co(NH_3)_6][Co(ox)_3]$	hexamminecobalt(III) tris(oxalato)cobalt(III)	hexamminecobalt(3+) tris(oxalato)cobalt(3-)
d	$[Ag(NH_3)_2]BF_4$	diamminesilver(I) tetrafluoroborate	diamminesilver(1+) tetrafluoroborate
e	$[Ag(NH_3)_2][Ag(CN)_2]$	diamminesilver(I) dicyanoargentate(I) or diamminesilver(I) dicyanidoargentate(I)	diamminesilver(1+) dicyanoargentate(1-) or diamminesilver(1+) dicyanidoargentate(1-)
f	$[Ni(CN)_4]^{2-}$	tetracyanonickelate(II) or tetracyanonickelate(II) ion	tetracyanonickelate(2-) or tetracyanonickelate(2-) ion
g	$[Co(N_3)(NH_3)_5]SO_4$	pentammineazidocobalt(III) sulfate	pentammineazidocobalt(2+) sulfate
h	$[CoBrCl(H_2O)(NH_3)]I$ (ignore stereochemistry)	ammineaquabromochlorocobalt(III) iodide	ammineaquabromochlorocobalt(1+) iodide

Exercise *Section*5.2.6: Nomenclature problems, some of which involve consideration of isomerism.

Name the following compounds and ions in both the Stock and Ewing-Bassett systems. Ignore prefixes for designating isomers if you haven't learned about those.

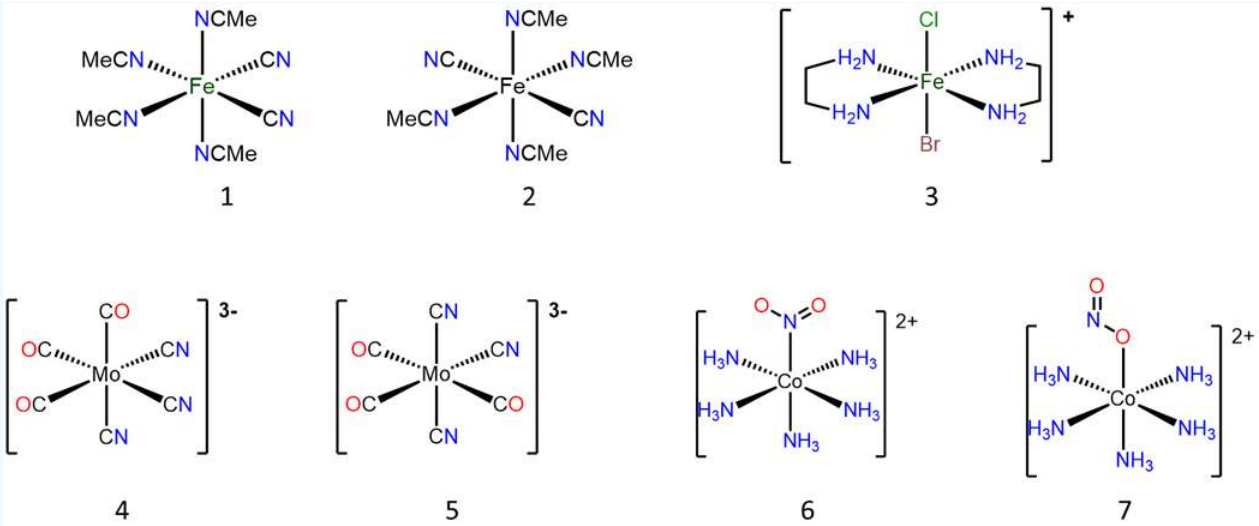
a. *trans*-$[Cu(dppe)_2(NO_2)_2]$ (the N is bound to Cu)
b. $[Pd(en)_2(SCN)_2]$, with the thiocyanates bound Pd-SCN
c. $[Mn(CO)_6]BPh_4$ (BPh_4 = tetraphenylborate)
d. $Rb[AgF_4]$
e. K_2ReH_9
f. K_3CrCl_6
g. $[Ru(H_2O)_6]Cl_2$
h. [*cis*-$Fe(CO)_4I_2$]
i. K_2[*trans*-$Fe(CN)_4(CO)_2$]
j. [*cis*-$MnCl(H_2O)_4(NH_3)](NO_3)$
k. K_3[*fac*-$RuCl_3(PMe_3)_3$]

Answer

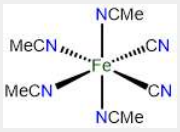
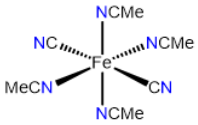
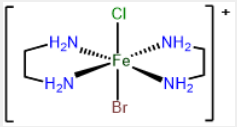
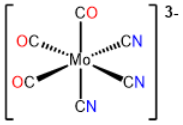
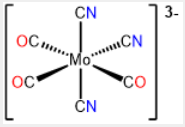
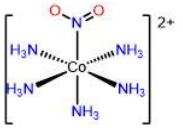
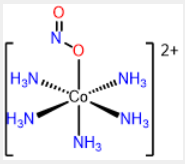
	Complex	Stock system name	Ewing-Bassett System name
a	*trans*-$[Cu(dppe)_2(NO_2)_2]$	*trans*-bis(diphenylphosphinoethane)bisnitrocopper(II) or *trans*-bis(diphenylphosphinoethane)bis(nitrito-κN)copper(II)	*trans*-bis(diphenylphosphinoethane)bisnitrocopper(0) or *trans*-bis(diphenylphosphino)ethane bis(nitrito-κN)copper(0)
b	$[Pd(en)_2(SCN)_2]$, with the thiocyanates bound Pd-SCN	bis(ethylenediamine)bisthiocyanatopalladium(II) or bis(ethylenediamine)bis(thiocyanato-*S*)palladium(II) or bis(ethylenediamine)bis(thiocyanato-κS)palladium(II)	bis(ethylenediamine)bisthiocyanatopalladium(0) or bis(ethylenediamine)bis(thiocyanato-*S*)palladium(0) or bis(ethylenediamine)bis(thiocyanato-κS)palladium(0)
c	$[Mn(CO)_6]BPh_4$	hexacarbonylmanganese(I) tetraphenylborate	hexacarbonylmanganese(I) tetraphenylborate
d	$Rb[AgF_4]$	rubidium tetraflouroargentate(III)	rubidium tetraflouroargentate(1-)
e	K_2ReH_9	potassium nonahydridorhenium(VII)	potassium nonahydridorhenium(2-)
f	K_3CrCl_6 or $K_3[CrCl_6]$	potassium hexachlorochromium(III) or potassium hexachloridochromium(III)	potassium hexachlorochromium(3-) or potassium hexachloridochromium(3-)
g	$[Ru(H_2O)_6]Cl_2$	hexaaquaruthenium(II) chloride	hexaaquaruthenium(2+) chloride
h	[*cis*-$Fe(CO)_4I_2$]	*cis*-tetracarbonyldiiodoiron(II)	*cis*-tetracarbonyldiiodoiron(0)
i	K_2[*trans*-$Fe(CN)_4(CO)_2$]	potassium *trans*-dicarbonyltetracyanoferrate(II)	potassium *trans*-dicarbonyltetracyanoferrate(2-)
j	[*cis*-$MnCl(H_2O)_4(NH_3)$] (NO_3)	*cis*-amminetetraaquachloromanganese(0) nitrate	*cis*-amminetetraaquachloromanganese(1+) nitrate
k	K[*fac*-$RuCl_3(PMe_3)_3$]	potassium *fac*-trichlorotris(triphenylphosphine)ruthenium(II)	potassium *fac*-trichlorotris(triphenylphosphine)ruthenium(1-)

Exercise *Section*5.2.7

Name the compounds and ions belowusing both the Stock and Ewing-Bassett systems. Ignore prefixes for designating isomers if you haven't learned about those.


NCMe
MeCN
CN
Fe
MeCN
CN
NCMe
1
NCMe
NC
NCMe
Fe
MeCN
CN
NCMe
2
Cl
+
H2N
NH2
Fe
H2N
NH2
Br
3
CO
3-
OC
CN
Mo
OC
CN
CN
4
CN
3-
OC
CN
Mo
OC
CO
CN
5
O
N
O
2+
H3N
NH3
Co
H3N
NH3
NH3
6
O
N
O
2+
H3N
NH3
Co
H3N
NH3
NH3
7

Answer

#	Structure	Stock system name	Ewing-Bassett system name
1		*cis*-tetraacetonitriledicyanoiron(II) or *cis*-tetraacetonitriledicyanidoiron(II)	*cis*-tetraacetonitriledicyanoiron(0) or *cis*-tetraacetonitriledicyanoiron(0)
2		*trans*-tetraacetonitriledicyanoiron(II) or *trans*-tetraacetonitriledicyanidoiron(II)	*trans*-tetraacetonitriledicyanoiron(0) or *trans*-tetraacetonitriledicyanidoiron(0)
3		*trans*-bromochlorobis(ethylenediamine)iron(III) or *trans*-bromidochloridobis(ethylenediamine)iron(III)	*trans*-bromochlorobis(ethylenediamine)iron(1+) or *trans*-bromidochloridobis(ethylenediamine)iron(1+)
4		*fac*-tricarbonyltricyanomolybdate(0) or *fac*-tricarbonyltricyanidomolybdate(0)	*fac*-tricarbonyltricyanomolybdate(3-) or *fac*-tricarbonyltricyanidomolybdate(3-)
5		*mer*-tricarbonyltricyanomolybdate(0) or *mer*-tricarbonyltricyanidomolybdate(0)	*mer*-tricarbonyltricyanomolybdate(3-) or *mer*-tricarbonyltricyanidomolybdate(3-)
6		pentamminenitrito-*N*-cobalt(III), pentamminenitrito-κ*N*-cobalt(III), or pentamminenitrocobalt(III)	pentamminenitrito-*N*-cobalt(2+), pentamminenitrito-κ*N*-cobalt(2+), or pentamminenitrocobalt(2+)
7		pentamminenitrito-*O*-cobalt(2+), pentamminenitrito-κ*O*-cobalt(2+), or pentamminenitritocobalt(2+)	pentamminenitrito-*O*-cobalt(2+), pentamminenitrito-κ*O*-cobalt(2+), or pentamminenitritocobalt(2+)

Exercise *Section*5.2.8

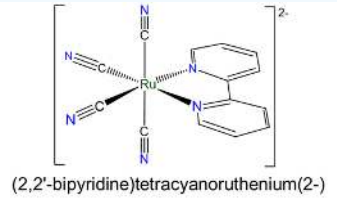
Draw structural formulae for the following compounds and ions. You may assume that

- complexes in which the metal has a coordination number of six are octahedral
- complexes in which the metal has a coordination number of five are trigonal bipyramidal
- complexes in which Pt^{II} , Pd^{II} , or Rh^{I}, or Ir^{I} have a coordination number of four are square planar
- other complexes in which the metal has a coordination number of four will be tetrahedral

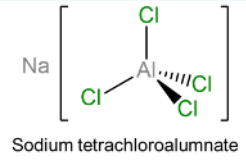
a. (2,2'-bipyridine)tetracyanoruthenium(2-)
b. sodium tetrachloroalumnate (note that since Al is a main group metal with a generally fixed oxidation state no oxidation state is given)
c. pentaamminechlorocobalt(2+) sulfate
d. carbonylhydridotris(triphenylphosphine)rhodium(I) (the ligands in this complex occupy sterically preferred positions)
e. bromotrichlorocobaltate(III)
f. hexaaquacopper(2+) sulfate
g. sodium tris(oxalato)cobalt(III)
h. *fac*-(1,10-phenanthroline)tricarbonylchlororhenium(I)
i. *mer*-triaquatrichlorochromium(III)
j. *trans*-dichlorobis(ethylenediamine)platinum(IV)

Answers

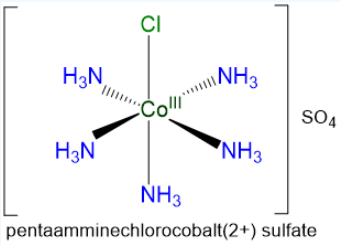
a



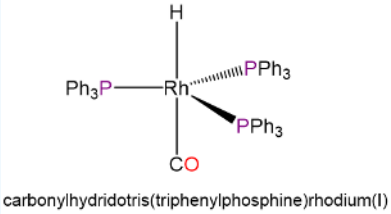
b



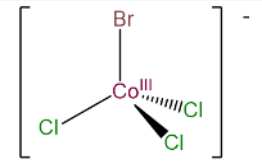
c



d

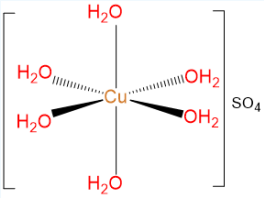


e



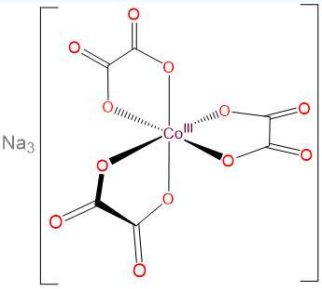
bromotrichlorocobaltate(III)

f



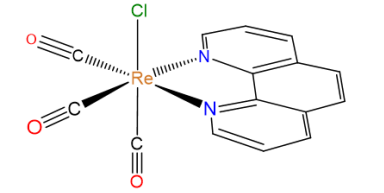
hexaaquacopper(2+) sulfate

g



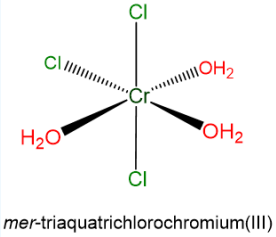
sodium tris(oxalato)cobalt(III)
Λ-enantiomer shown

h



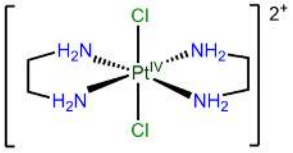
fac-(1,10-phenanthroline)tricarbonylchlororhenium(I)

i



mer-triaquatrichlorochromium(III)

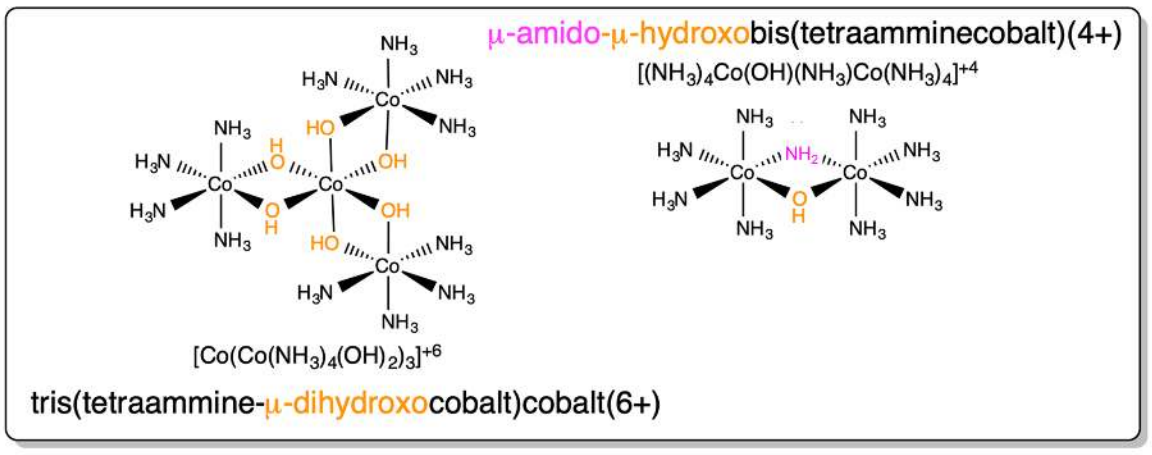
j



trans-dichlorobis(ethylenediamine)platinum(IV)

Exercise *Section*5.2.9.

The name of the structure named tris(tetraammine-μ-dihydroxocobalt)cobalt(6+) in Scheme **Section5.2.III** (reproduced below) is incomplete. Give the complete name of the structure in both the Stock and Ewing-Basset systems.



Answer

Δ-tris(tetraammine-μ-dihydroxocobalt)cobalt(6+) or **Δ**-tris(tetraammine-μ-dihydroxocobalt(III)cobalt(III)

Rules for Writing Chemical Formulas

The rules for writing the formulas of coordination compounds follow the same general convention used to specify their names, but are not always adhered to in the chemical literature. Organized predictable formulae can be easier to read and understand than haphazardly written ones the rules for writing the formulae of coordination compounds have value. The rules as given here are adapted from a summary by Robert Lancashire.

1.If there are multiple ions present list the cations before anions.

2.Enclose all the constituents of each complex ion in square brackets.

3.For each complex ion,

- Give the **central metal** atom first.
- Then **ligands** next, listed in alphabetical order, ignoring prefixes according to the first letters in the ligand's symbol as written. This is true regardless of whether the symbol is an element symbol (like C, N, O, etc.) or a symbol for the ligand name (bpy, en, MeCN, etc.). Contrary to widely-circulated myths, the ligand's charge does not matter.[4]
- The formulae or abbreviations (*e.g.* en) for all polyatomic ligands should be enclosed in ordinary parentheses.
- As appropriate, use italicized atom symbols to indicate linkage isomerism and prefixes such as *cis*-, *trans*-, *fac*-, *mer*-, **Λ**-, **Δ**-, κ^n, η^n , μ_n, **λ**-, \or (\delta\)- to indicate stereochemistry.
- When a ligand is bound to a metal through a particular atom, preferably place that atom closest the metal - *e.g.* $[Fe(CN)_6]^{3-}$ not $[Fe(NC)_6]^{3-}$ (Note: this rule primarily is used for ambidentate ligands; although IUPAC reccomends that aqua ligands be written as OH_2 when the O would be closest to its coordinated metal they are still usually written as H_2O).

These rules are graphically summarized in Figure **Section5.2.2**.

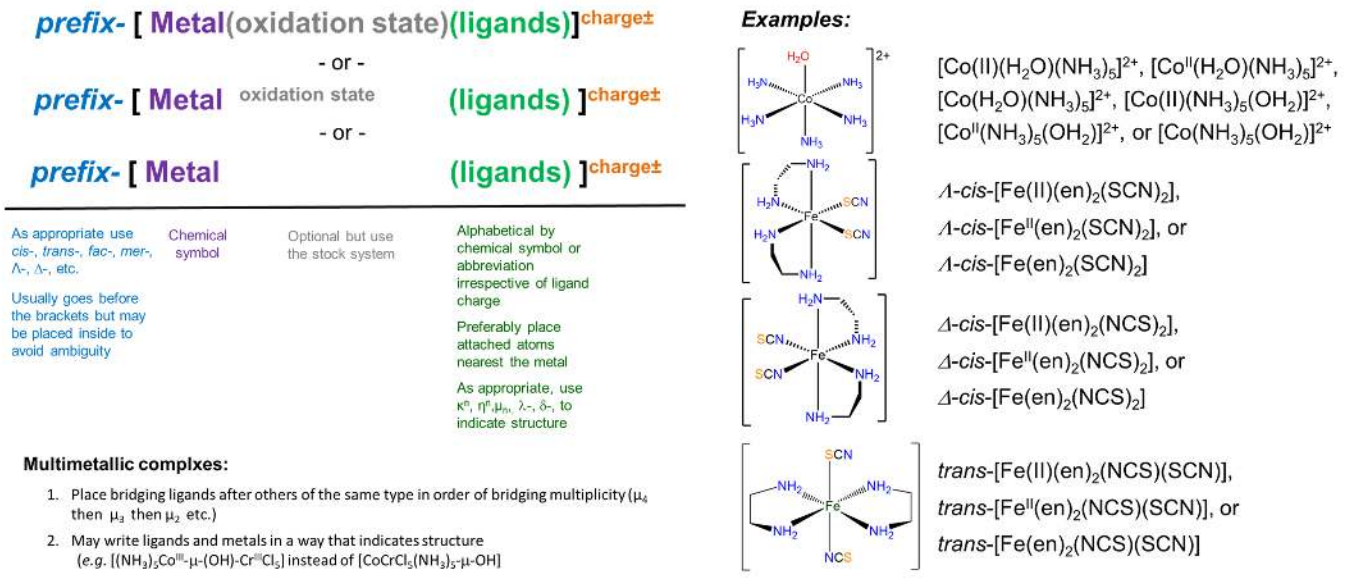
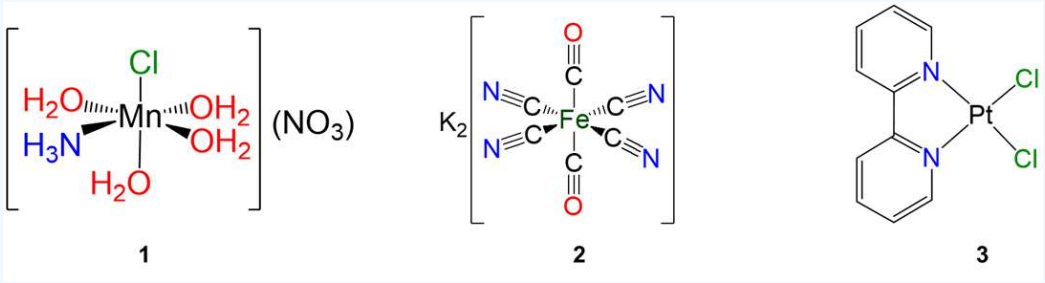


Figure **Section5.2.2**. Summary of the rules for writing the formula of a coordination complexes along with a few examples of their application. This work by Stephen Contakes is licensed under a Creative Commons Attribution 4.0 International License.

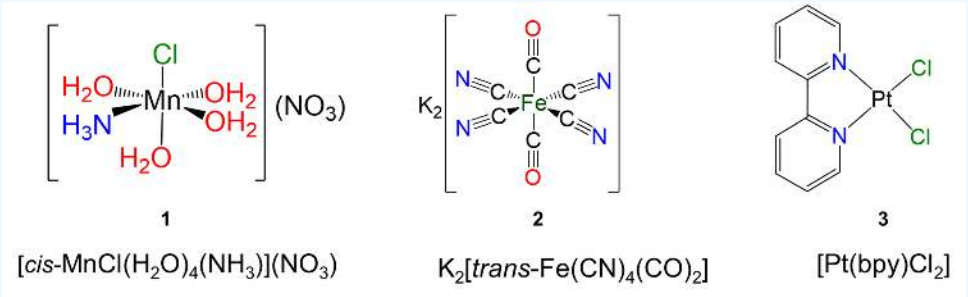
Exercise *Section*5.2.10

Give the formulae of the following complexes.



.

Answer



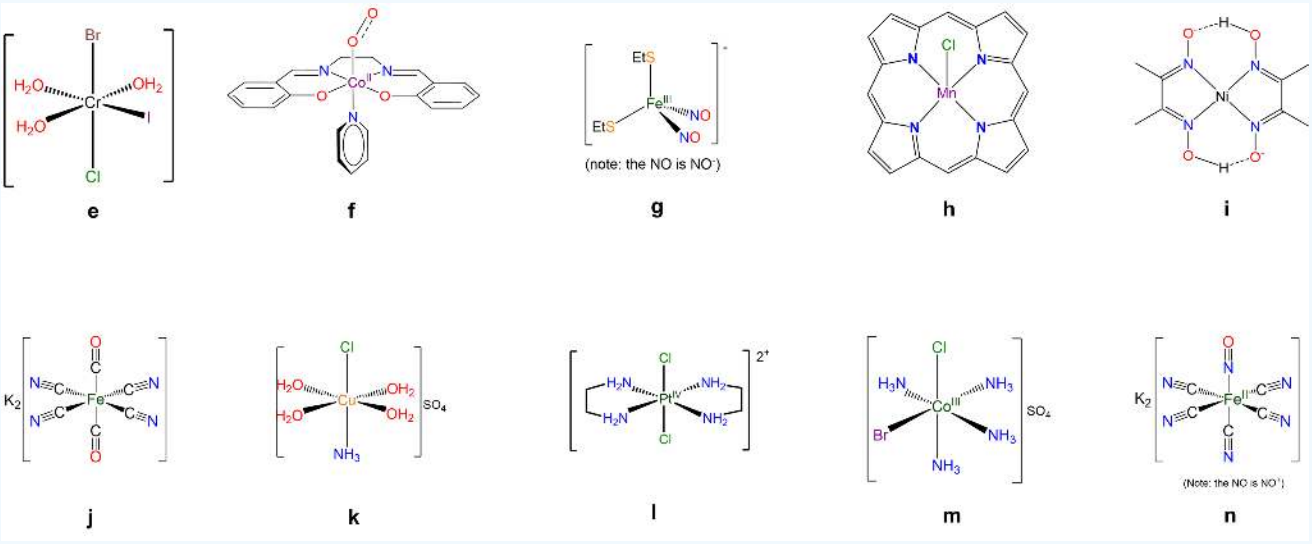
Exercise *Section*5.2.11

Write formulae for each of the following compounds and ions. When multidentate ligands are present use suitable abbreviations.

a. pentaamminechlorocobalt(2+) sulfate
b. Δ-diamminebis(oxalato)manganate(III)

c. *trans*-tetraacetonitriledicyanoiron(II)

d. tricarbonyldichlorobis(triphenylphosphine)molybdenum



Answers

a.

$[CoCl(NH_3)_5](SO_4)$

b.

Δ-$[Mn(NH_3)_2(ox)_2]^-$

c.

trans-$[Fe(CN)_2(NCMe)_4]$

d.

$[MoCl_2(CO)_3(PPh_3)]$ or $MoCl_2(CO)_3(PPh_3)$

e.

mer-$[CrBrCl(H_2O)_3I]$

f.

$[Co(O_2)py(salen)]$

g.

$[Fe(NO)_2(SEt)_2]^-$

h.

[NiCl(por)] or $[MnCl(porphyrin)]^-$

i.

$[Ni(DMG)_2]$ or $[Ni(Hdmg)_2]$

j.

potassium *trans*-$[Fe(CN)_2(CO)_4]$

k.

trans-$[CuCl(H_2O)_4(NH_3)]SO_4$

l.

trans-$[PtCl_2(en)_2]^{2+}$

m.

cis-$[CoBrCl(NH_3)_4]SO_4$

n.

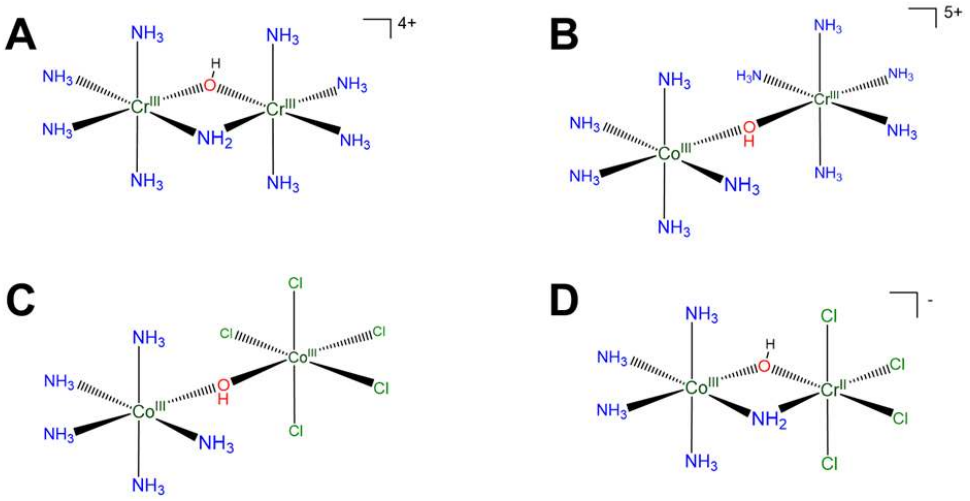
$K_2[Fe(CN)_5NO]$

Multinuclear Coordination Complexes

Multinuclear coordination complexes contain multiple metals connected by one or more bridging ligands. The structures of bridging complexes can usually be inferred from their μ-tagged ligands in their names and formulae. For the benefit of instructors who wish to have their students name multinuclear complexes.

Multinuclear complexes are named differently depending on whether the groups on either side of the bridging ligands are identical or different, as shown in Scheme **Section5.2.VIII**.

Scheme Section5.2.VIII. Multinuclear coordination complexes may be named differently depending on whether the groups on either side of the bridging ligands are the same or different. The groups are the same if the metal, ligands, and ligand arrangement are identical. This is true in A but in B the metals differ, in C the ligands differ, and in D both the metal and ligands differ.



Naming multinuclear complexes

Let's look at the rules for naming symmetric and asymmetric multinuclear complexes.

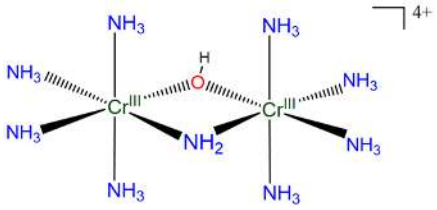
Symmetric complexes

The IUPAC naming system helpfully avoids the sort of ambiguities and *ad hoc* choices involved in most textbook-level nomenclature systems for multimetallic complexes. Unfortunately, it is correspondingly difficult for beginners to employ. Thus it will only be applied in depth to the case of symmetric complexes. Symmetric complexes are particularly easy to name in the IUPAC system and several of its variants that find common use. In these

1. The ligands are given in alphabetical order. When there are bridging and non-bridging ligands of the same type the bridging ligands are given first. When there are multiple bridging ligands of the same type but which use different bridging modes (*e.g.* μ_4-, μ_3-, μ_2-) the bridging ligands are specified in decreasing order of bridging multiplicity, *e.g.* μ_3 -sulfido-di-μ-sulfido.
2. The groups bridged are given afterwards using names that follow the ordinary rules. Generally this either involves
   a. naming all the ligands followed by all the metals, in both cases using prefixes to indicate the number of each
   b. naming each group of atoms individually as in the less formal naming system, using prefixes to indicate the number of ligands (this is an unofficial variant of the IUPAC system that some textbook authors seem to prefer).

These two rules are sufficient to describe simple symmetric bridging complexes.

Example: The compound in Scheme **Section5.2.VIIIA**



may be named

[μ-amido-μ-hydroxo-octaamminedichromium(4+)] ion

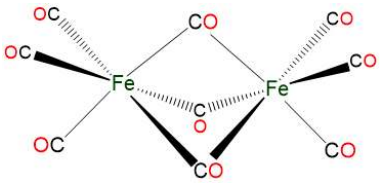
or

[μ-amido-μ-hydroxo-bis(tetraamminechromium(III))] ion

or

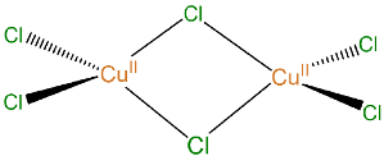
[μ-amido-μ-hydroxo-bis(tetraamminechromium)(4+)] ion

Example: The complex[5]



may be named [tri-μ-carbonyl-bis(tricarbonyliron)(0)], [tri-μ-carbonyl-bis(tricarbonyliron(0))], or [tri-μ-carbonyl-hexacarbonyldiiron)(0)]

Example: The complex



may be named di-μ-chlorido-tetrachloridodicopper(II), di-μ-chlorido-bis(dichlorocopper(II)), or di-μ-chlorido-bis(dichlorocopper)(0)

Asymmetric complexes

For a symmetrical complex like the $[Cu_2Cl_4(\mu\text{-}Cl)_2]$ considered above it is enough to specify the existence of the two bridging and four terminal chloro ligands; there is no need to number the chloro ligands or to specify exactly which ones are involved in bridging or to clarify that the bridging involves κ^2 coordination of the chloro ligands. In cases where the two metal centers or the chloro ligands differ it is necessary to specify the exact ligands and metals involved and how they are connected.

For example, a more extensive IUPAC name for $[Cu_2Cl_4(\mu\text{-}Cl)_2]$ in which the chloro ligands are individually and more completely specified would read di-μ_2-chlorido-tetrachlorido-1κ^2Cl,2κ^2Cl-dicopper(II).

Even more extensive systems would involve numbering the metals and specifying how they are connected together too. The details of how this is done are typically beyond the level of most undergraduate and graduate courses in inorganic chemistry. Those who want to know the details should consult the red book. In many cases it is sufficient to reserve the use of formal IUPAC names for use in publications and to employ a comvenient shorthand naming system for everyday use. An example of one type of system that is sometimes employed is given next.

Unofficial methods

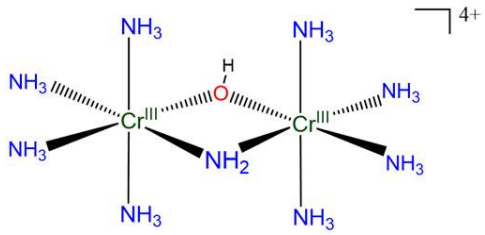
It can be quite complicated to use the IUPAC system to name asymmetric multinuclear coordination complexes. Fortunately it is rarely necessary and there are a variety of simpler somewhat *ad hoc* methods that work well for such cases. Since these methods

are commonly used by textbooks and inorganic instructors it is likely worth your while to learn about their general features. In these methods

1. A multinuclear complex is named as a derivative of one of the metal centers and the other metal centers and their ligands are treated as ligands to the prioritized metal center.
2. Unfortunately, most of the time the choice of which metals are part of the ligands and which one is central is made haphazardly. In other words, there is no agreed upon system for assigning which metal center is the central metal and which should be regarded as part of the ligands around it. One way to be more systematic about the selection of the central and ligand-embedded metals is to assign the central metal as the metal of highest priority in the IUPAC priority rules. In the IUPAC priority rules he central metal is the highest priority metal alphabetically by name; then if there is a tie the ligands on each tied metal center are ranked alphabetically and the tied metal center with the highest priority (or most highest priority) ligands wins.
3. The metal centers not chosen as the primary metal center and all ligands around them, including those bridging to the winning metal center, are then treated as a single ligand that coordinates the winning metal center.
4. When naming the ligands and the overall complex, again there is much that is haphazard. However, in the best systems each coordination sphere is named using the same rules as for mononuclear complexes - *i.e.* the ligands are given in alphabetical order, etc.
    - This is true of any metal center-containing ligands.
    - When there is a bridging and non-bridging ligand of the same type the bridging ligands are given first. When there are multiple bridging ligands of the same type but which use different bridging modes (*e.g.* μ_4-, μ_3-, μ_2-) the ligands are specified in decreasing order of bridging multiplicity, *e.g.* μ_3 -sulfido-di-μ-sulfido.

Let's apply these rules to the examples in Scheme Section5.2.VIII.

Compound A:



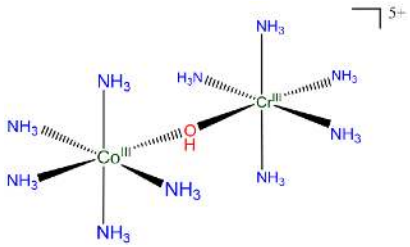
Using hydroxo for the OH^- it may be named

[(μ-amido-tetraammine-μ-hydroxochromium(III))tetraamminechromium(III)] ion

or

[(μ-amido-tetraammine-μ-hydroxochromium)chromium(4+)] ion

Compound B:



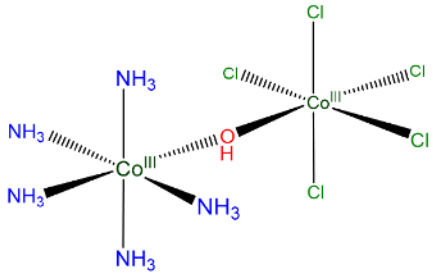
Using hydroxo for OH^- it may be named

[(pentaammine-μ-hydroxocobalt(III))tetraamminechromium(III)] ion

or

[(pentaammine-μ-hydroxocobalt)tetraamminechromium(5+)] ion

Compound C:



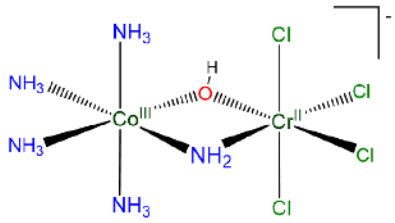
Using hydroxo for OH^- it may be named

[pentaammine(pentachloro-μ-hydroxocobalt(III))cobalt(III)]

or

[pentaammine(pentachloro-μ-hydroxocobalt)cobalt](0)]

Compound D:



Using hydroxo for OH^- and chloro for Cl^- it may be named

[pentaammine(pentachloro-μ-hydroxocobalt(III))chromate(III)] ion

or

[(tetrammine-μ-ammine-μ-hydroxocobalt)tetrachlorochromate](1-)] ion

As can be seen from the examples above this system gives serviceable names for multimetallic complexes but those names are not the IUPAC names and so should not be used to describe complexes outside of pedagogical and informal settings.

Writing and interpreting formulas for multinuclear complexes

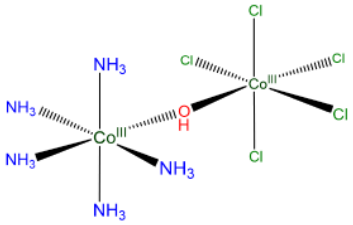
The rules for writing formulae for multinuclear complexes are the same as form mononuclear ones with two added details

1. Write bridging ligands after nonbridging ligands of the same type. For example, Cu_2Cl_6 should be written as $[Cu_2Cl_4$-μ-$Cl)_2]$
2. Although you may ignore that and other rules if you find it helpful to keep groups of metals and ligands together in a way that better convey how the atoms are connected. Just as the structure of ethane may be more clearly conveyed as H_3CCH_3 instead of CH_3CH_3 the complex $[Cu_2Cl_4\mu$-$Cl)_2]$ may be written as $[(Cl_2Cu)(\mu$-$Cl)_2(CuCl_2)]$

Other Examples:

For dichromate write, $[Cr_2O_6(\mu$-$O)]^{2-}$ or $[O_5Cr$-μ-O-$CrO_5]^{2-}$

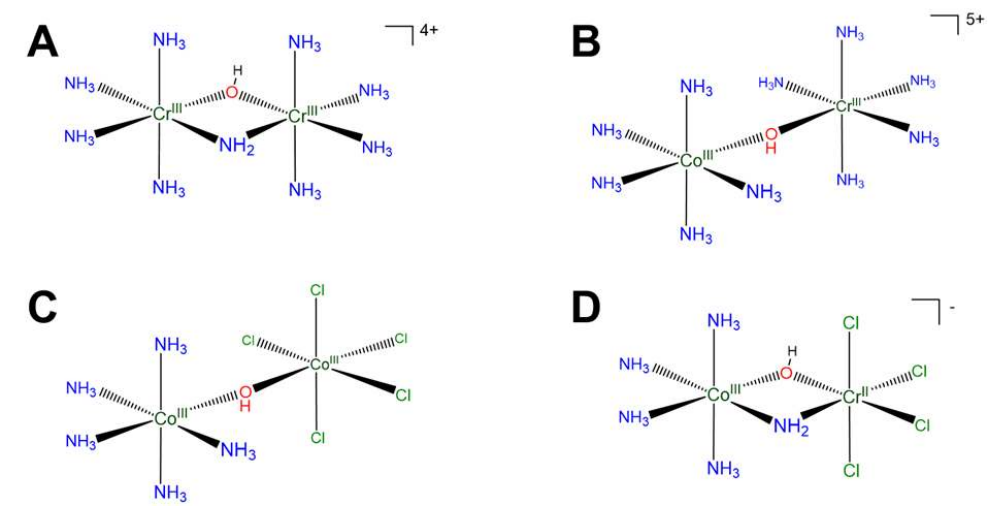
For compound C of Scheme **Section5.2.VIII**.



write $[Co_2Cl_5(NH_3)_5(\mu$-$OH)]$ or, even better, $[(H_3N)_5Co(\mu$-$OH)CoCl_5]$.

Exercise *Section*5.2.10

Write reasonable formulae for complexes A, B, and D in Scheme **Section5.2.VIII**, which for convenience is reproduced below.



Sample answers for A

$[Cr_2(NH_3)_8\text{-}\mu(NH_2)\text{-}\mu(OH)]^{4+}$ or $[(H_3N)_4Cr^{III}\text{-}\mu(NH_2)\text{-}\mu(OH)\text{-}Cr^{II}(NH_3)_4]$ and variants thereof involving writing the H_3N as NH_3, μ as μ_2, etc.

Sample answers for B

$[CoCr(NH_3)_{10}\text{-}\mu(OH)]^{5+}$ or, better, $[(H_3N)_5Co^{III}\text{-}\mu(OH)\text{-}Cr^{III}(NH_3)_5]^{5+}$

Sample answers for C

This was already done as an example above, $[Co_2Cl_5(NH_3)_5\text{-}\mu(OH)]$ or, better, $[(NH_3)_5Co^{III}\text{-}\mu(OH)\text{-}Co^{III}Cl_5]$ and variants thereof

Sample answers for D

$[CoCrCl_4(NH_3)_4\text{-}\mu(NH_2)\text{-}\mu(OH)]$ or, better, $[(H_3N)_4Co^{III}\text{-}\mu(NH_2)\text{-}\mu(OH)\text{-}Cr^{II}Cl_4]$

References

1. International Union of Pure and Applied Chemistry *Nomenclature of Inorganic Chemistry* Cambridge, UK, 2005.

2. The structure and name is taken from Choudhury, S. B.; Allan, C. B.; Maroney, M.; Wodward, A. D.; Lucas, C. R. *Inorg. Synth.* **1998**, *32*, 98-107.

3. Haas, K. Naming Transition Metal Complexes. https://chem.libretexts.org/Courses/Saint_Mary's_College%2C_Notre_Dame%2C_IN/CHEM_342%3A_Bio-inorganic_Chemistry/Readings/Week_2%3A_Introduction_to_Metal-Ligand_Interactions_and_Biomolecules/2.1_Transition_metal_complexes/2.1.6%3A_Naming_Transition_Metal_Complexes

4. There is a widely-circulated myth that anionic ligands should be names before neutral ones. This myth is false. According to the IUPAC red book (bolding mine):

IR-2.15.3.4: Ordering ligands in formulae and names In formulae of coordination compounds,

The formulae or abbreviations representing the ligands **are cited in alphabetical order as the general rule**. Bridging ligands are cited immediately after terminal ligands of the same kind, if any, and in increasing order of bridging multiplicity. (See also Sections IR-9.2.3 and IR-9.2.5.)

IR-9.2.3.1 Sequence of symbols within the coordination formula

(i) The central atom symbol(s) is (are) listed first.

(ii) The **ligand symbols (line formulae, abbreviations or acronyms) are then listed in alphabetical order** (see Section IR-4.4.2.2).5 Thus, CH_3CN, MeCN and NCMe would be ordered under C, M and N respectively, and CO precedes Cl because single letter symbols precede two letter symbols. **The placement of the ligand in the list does not depend on the charge of the ligand.**

(iii) More information is conveyed by formulae that show ligands with the donor atom nearest the central atom; this procedure is recommended wherever possible, even for coordinated water.

5. Technically organometallic complexes are named according to slightly different rules but the coordination compound naming system works here. Note that this complex was once thought to possess an Fe-Fe bond, in accordance with the predictions of the 18 electron rule. Consequently, older sources often give an [*Fe-Fe*] after the name to reflect the presence of that bond. However, as the complex is no longer though to possess an Fe-Fe bond it is omitted here.

Contributors and Attributions

Stephen Contakes, Westmont College, to whom comments, corrections, and criticisms should be addressed.

with some examples taken from Naming Transition Metal Complexes by Kathryn Haas.

Consistent with the policy for original artwork made as part of this project, all unlabeled drawings of chemical structures are by Stephen Contakes and licensed under a Creative Commons Attribution 4.0 International License.

Section 5.2: Nomenclature and Ligands is shared under a CC BY-NC-SA 4.0 license and was authored, remixed, and/or curated by LibreTexts.

- **9.3: Nomenclature and Ligands** by Stephen M. Contakes has no license indicated.
- **8.2: Nomenclature and Ligands** is licensed CC BY-NC-SA 4.0.

SECTION OVERVIEW

Section 5.3: Acid-Base and Donor-Acceptor Chemistry

Section 5.3.1: Acid-Base Models as Organizing Concepts

Section 5.3.2: Lewis Concept and Frontier Orbitals

Section 5.3.2.1: The frontier orbital approach considers Lewis acid-base reactions in terms of the donation of electrons from the base's highest occupied orbital into the acid's lowest unoccupied orbital.

Section 5.3.2.2: All other things being equal, electron withdrawing groups tend to make Lewis acids stronger and bases weaker while electron donating groups tend to make Lewis bases stronger and acids weaker

Section 5.3.2.3: The electronic spectra of charge transfer complexes illustrate the impact of frontier orbital interactions on the electronic structure of Lewis acid-base adducts

Section 5.3.2.4: Substances' solution phase Lewis basicity towards a given acid may be estimated using the enthalphy change for dissociation of its adduct with a reference acid of similar hardness.

Section 5.3.2.5: In the boron trifluoride affinity scale, the enthalphy change on formation of an adduct between the base and boron trifluoride is taken as a measure of Lewis basicity.

Section 5.3.2.6: Lewis base strength may also be estimated by measuring structural or energy changes upon formation of a Lewis acid-base complex, as illustrated by efforts to spectroscopically assess the strengths of halogen bonds

Section 5.3.2.7: Bulky groups weaken the strength of Lewis acids and bases because they introduce steric strain into the resulting acid-base adduct.

Section 5.3.2.8: Frustrated Lewis pair chemistry uses Lewis acid and base sites within a molecule that are sterically restricted from forming an adduct with each other.

Section 5.3.3: Hard and Soft Acids and Bases

Section 5.3.3.1: Hard-Hard and Soft-Soft preferences may be explained and quantified in terms of electrostatic and covalent and electronic stabilization on the stability of Lewis acid-base adducts

Section 5.3.3.2: Quantitative Measures of Hardness, Softness, and Acid-Base Interactions from a Hard Soft Acid-Base Principle Perspective Involve Orbital Energies and/or Apportioning Acid-Base Bonding in Terms of Electrostatic and Covalent Factors

Section 5.3.4: Problems

Section 5.3: Acid-Base and Donor-Acceptor Chemistry is shared under a CC BY-NC-SA 4.0 license and was authored, remixed, and/or curated by LibreTexts.

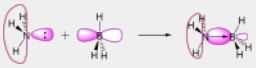
Section 5.3.1: Acid-Base Models as Organizing Concepts

> *In a very real sense, we can make an acid anything we wish. The differences between the various acid-base concepts are not concerned with which is 'right', but which is most convenient to use in a particular situation.*
>
> *James E. Huheey, Ellen A. Keiter, and Richard L. Keiter*

The concept of acids and bases is often associated with the movement of hydrogen ions from one molecule or ion to another. However, a host of acid-base concepts have been developed to help chemists organize and make sense of a wide range of reactions (Table 6.1).

Table 6.1. Summary of major acid-base models.

Definition	Theoretical paradigm and notable features.	Acid	Base	Illustrative sample reactions
Arrhenius (1894)	Interested in what the substance does to the state of an aqueous solution. In particular it assesses proton donation to & removal from water using [H_3O^+] as a proxy. Readily accommodates the pH concept as a measure of the state of a solution.	Increases [H_3O^+]	Decreases [H_3O^+]	$\underset{acid}{HCl} + H_2O \rightarrow H_3O^+ + Cl^-$ $\underset{base}{NH_3} + H_2O \rightarrow NH_4^+ + OH^-$
Brønsted-Lowry (1923)	Envisions acid-base reactivity in terms of the transfer of an H^+ from one substance to another. Allows for conjugate acids and bases and solvent autoionization.	Donates H^+	Accepts H^+	$\underset{acid}{HCl} + \underset{base}{NH_3} \rightarrow \underset{conj.\ acid}{NH_4^+} + \underset{conj.\ base}{Cl^-}$ $\underset{acid}{HOAc} + \underset{base}{NH_3} \rightarrow \underset{conj.\ acid}{NH_4^+} + \underset{conj.\ base}{OAc^-}$ $\underset{amphoteric}{2\ H_2O} \rightarrow \underset{conj.\ acid}{H_3O^+} + \underset{conj.\ base}{OH^-}$
Lux-Flood (1939-~47)	Describes reactions involving oxides and oxyanions in terms of the transfer of oxide ion (O^{2-}). Mainly used in geochemistry, although it also can be used to describe some redox reactions.	Oxide acceptor	Oxide donor	$\underset{acid}{SiO_2} + \underset{base}{CaO} \rightarrow CaSiO_3$ $\underset{base}{H_2O} + \underset{acid}{CO} \rightarrow H_2 + CO_2$
Solvent System	Applies aspects of the Arrhenius , Brønsted-Lowry, and Lux-Flood acid base concepts to solvent cation & anion formation in a generalized reaction. Can be used to describe solution chemistry in nonaqueous solvent systems like BrF_3.	Is a solvent cation or increases the solvent cation concentration, often by receiving a lone pair- bearing group	Is a solvent anion or increases the solvent anion concentration, often by donating a lone pair- bearing group	$\underset{acid}{SbF_5} + \underset{base}{BrF_3} \rightarrow \underset{conj.\ base}{SbF_6^-} + \underset{conj.\ acid}{BrF_2^+}$ $\underset{amphoteric}{2\ BrF_3} \rightarrow \underset{conj.\ acid}{BrF_2^+} + \underset{conj.\ base}{BrF_4^-}$
Lewis (1923)	Envisions acid-base reactivity in terms of electron pair donation. Encompasses the Arrhenius , Brønsted-Lowry, Lux-Flood, and Solvent System definitions and readily	Accepts an electron pair	Donates an electron pair	$\underset{base}{:NH_3} + \underset{acid}{BF_3} \rightarrow H_3N + BF_3$

Definition	Theoretical paradigm and notable features.	Acid	Base	Illustrative sample reactions
	integrates with molecular orbital descriptions of chemical reactivity in Frontier orbital theory.			
Nucleophile-Electrophile	Applies the Lewis concept to organic reactivity. Nucleophiles are Lewis bases which tend to react to form a bond with Lewis acid sites called electrophilic centers.	(The electrophile) Tends to react by receiving an electron pair from a nucleophile, forming a bond in the process	(The nucleophile) Donates an electron pair to form a bond to an electrophile	$\underset{base}{Br^-} + \underset{acid}{CH_3-Cl} \rightarrow Br-CH_3 + Cl^-$
Usanovich (1939)	Extends Lewis theory to include the donation and acceptance of any number of electrons, whether through the formation of an adduct or electron transfer.	Accepts electrons	Donates electrons	$\underset{base}{:NH_3} + \underset{acid}{BH_3} \rightarrow \underset{adduct}{H_3N-BH_3}$ $\underset{acid}{Fe^{2+}} + \underset{base}{Zn^0} \rightarrow Fe^0 + Zn^{2+}$
Frontier Orbital (1960s)	Envisions Lewis Acid-base/Electrophile-nucleophile reactions in terms of the donation and acceptance of electrons between the reactant's frontier orbitals. Specifically, the reaction is envisioned in terms of donation of the base's HOMO electrons into the acid's LUMO level.	Possesses a LUMO capable of forming an occupied bonding MO on mixing with a base's HOMO.	Possesses an electron-bearing HOMO capable of forming a filled bonding MO on mixing with an acid's LUMO.	 base acid adduct

Some concepts involve defining acids and bases in particular ways that allow for the understanding of particular types of chemical systems. For example, the familiar Arrhenius and Brønsted acid and base concepts used in general chemistry help chemists make sense of the behavior of compounds which can transfer H^+ ions among themselves, often in aqueous solution. However, the solvent system acid-base concept defines acids and bases in terms of the transfer of a lone-pair bearing group and is particularly useful for conceptualizing the reactivity of main group halides, oxides, and related compounds. Some acid-base definitions seek to encompass an extremely wide range of chemical reactions. For instance, the Lewis acid-base definition encompasses the Arrhenius , Brønsted, and solvent system definitions and has also found wide use in inorganic chemistry owing to the ease with which Lewis acid-base interactions may be described by the Frontier Orbital approach in terms of interacting molecular orbitals on the acid and base.

References

Huheey, J. E.; Keiter, E. A.; Keiter, R. L., *Inorganic Chemistry: Principles of Structure and Reactivity. 4th ed.*; HarperCollins: New York, NY, 1993, pg. 318.

Section 5.3.1: Acid-Base Models as Organizing Concepts is shared under a CC BY-NC-SA 4.0 license and was authored, remixed, and/or curated by Stephen M. Contakes.

- **6.1: Acid-Base Models as Organizing Concepts** by Stephen M. Contakes is licensed CC BY 4.0.

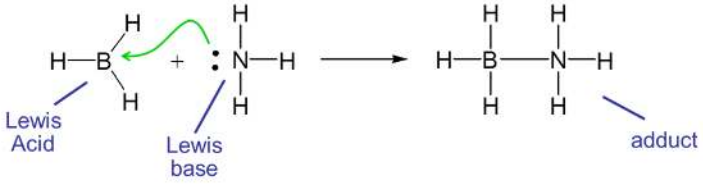
Section 5.3.2: Lewis Concept and Frontier Orbitals

The Lewis acid-base concept generalizes the Brønsted and solvent system acid base concepts by describing acid-base reactions in terms of the donation and acceptance of an electron pair.

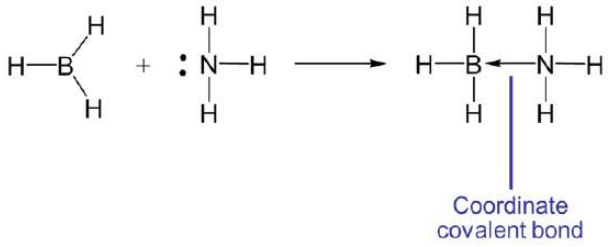
Under the Lewis definition

- **Lewis acids** are electron pair acceptors
- **Lewis bases** are electron pair donors

and in Lewis acid-base reactions, a Lewis base donates an electron pair to the Lewis acid, which accepts it. The reaction between borane, BH_3, and NH_3 is the classic example:

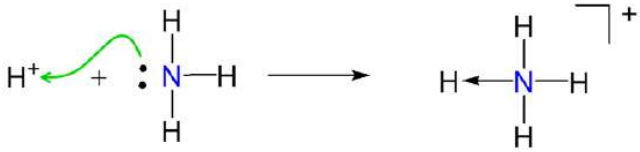


In this case the Lewis acid-base reaction results in the formation of a bond between BH_3, and NH_3. When the acid and base combine to form a larger unit, that unit is said to be an adduct, and the resulting bond is said to be a coordinate covalent or dative bond. Such coordinate covalent bonds are often represented by an arrow that indicates the direction of electron donation from the base to the acid. For instance, the reaction between BH_3 and NH_3 could also have been written as

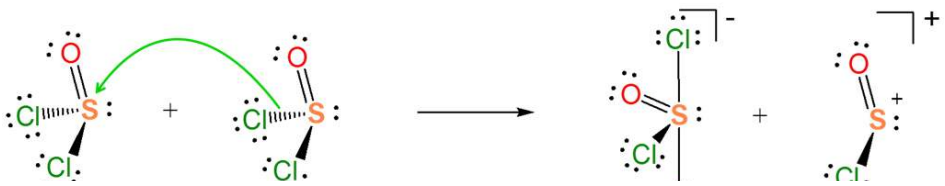


The arrow notation for the coordinate covalent bond is really just a convenient formalism - a bookkeeping tool to help keep track of where the electrons came from and where they might return if the reverse reaction occurs. In actuality a coordinate covalent bond is just an ordinary covalent bond like any other.

For example, in Brønsted acid-base reactions, the hydrogen ion is an acid because it accepts an electron pair from the Brønsted base. Consequently, under the Lewis acid-base concept, Brønsted acid-base reactions involve the formation of an adduct between H^+ and a base.



The Lewis acid-base concept nicely explains ionization reactions involving nonaqueous solvents. For instance, the autoionization of $SOCl_2$ is an acid-base reaction between two $SOCl_2$ molecules.



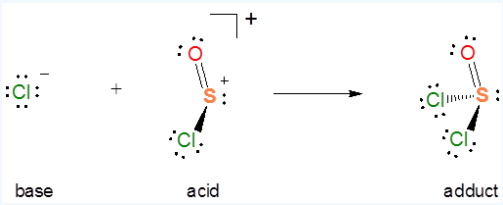
:Cl:

Example *Section*5.3.2.1

Explain how the autoionization of $SOCl_2$ is a Lewis acid-base displacement reaction.

Solution

In the autoionization of $SOCl_2$ the pair of electrons donated comes from the S-Cl bond, and the S-Cl bond is broken to give a lone pair bearing a Cl^- base and an $SOCl^+$ Lewis acid fragment. If you are having trouble seeing how this works, it can be instructive to consider the reverse of this process. It is a Lewis acid-base reaction to give a Lewis acid-base adduct:

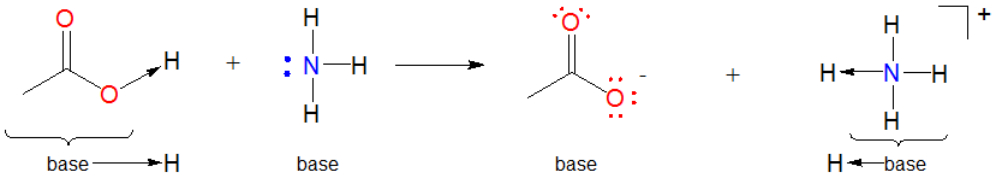


From the autoionization reaction it is also apparent that $SOCl_2$ itself acts as a Lewis acid towards the liberated Cl^-. So the autoionization reaction involves a transfer of the Cl^- base between the two Lewis acids - a Lewis acid-base displacement reaction.



It can be helpful to keep several distinctions in mind when using the Lewis acid-base concept to describe chemical reactions.

1. Many Lewis-Acid base reactions are displacement reactions. This is because the hydrogen ion is usually bound to something at the start of the reaction. In such cases the Lewis acid H^+ unit is transferred from one Lewis base to another :



Such acid-base reactions are sometimes called displacement reactions since the base group in the initial Lewis acid-base complex is displaced by the incoming Lewis base to generate another complex.

2. Substances are sometimes considered amphoteric because they exhibit Lewis acidity and basicity at different types of atomic centers. The classic example is aluminum hydroxide, $Al(OH)_3$. In water $Al(OH)_3$ can act as a Lewis acid towards OH^- ion. The reaction occurs by formation of an adduct at $Al(OH)_3$'s Al^{3+} center:

$$Al(OH)_3 + OH^- \rightarrow Al(OH)_4^-$$

Notice that in addition to acting as a Lewis acid, in this reaction $Al(OH)_3$

- does not act as a Brønsted acid or base since no H^+ ion transfer occurs
- but does act as an Arrhenius acid since OH^- ion is consumed from solution, decreasing $[OH^-]$ and increasing $[H^+]$

In water $Al(OH)_3$ also acts as a Lewis base towards H^+ through the lone pairs on its hydroxide ligands.

$$Al(OH)_3 + 3H^+ + 3H_2O \rightarrow Al(H_2O)_6^{3+}$$

Notice that in addition to acting as a Lewis base, in this reaction $Al(OH)_3$ also acts as a

- Brønsted base, since a H^+ ion is transferred onto the OH^- ligand
- Arrhenius base, since H^+ ion is consumed from solution, decreasing $[H^+]$
- Lewis acid at its Al^{3+} center, since Al-O metal-ligand bonds are formed

Substances that rapidly undergo Lewis acid-base reactions are called nucleophiles and electrophiles.

Two factors govern the course of chemical reactions - thermodynamics and kinetics. Thermodyamics determines what possible fates of the reaction can take place while kinetics determines which among those possible fates will take place quickly under a particular set of reaction conditions. Because of this, it can be helpful to distinguish Lewis acids and bases that tend to undergo reaction quickly with one another from those which do so more slowly. For this reason, synthetic chemists use the terms electrophile and nucleophile to refer to Lewis acids and bases that react quickly:

- electrophile - Lewis acids that rapidly react with a given Lewis base or class of Lewis bases are said to be good electrophiles
- nucleophile - Lewis bases that rapidly react with a given Lewis acid or class of Lewis acids are said to be good nucleophiles

The electrophile-nucleophile concept is sometimes referred to as the Ingold-Robinson acid-base concept after two organic chemists who did much to illustrate the utility of thinking about Lewis acid-base reactions in kinetic terms.

Several distinctions that should be kept in mind when using the electrophile-nucleophile/Ingold-Robinson concept to think about chemical reactivity:

1. Whether a given Lewis acid or base is able to react rapidly depends on the reaction conditions and the substrate (substance it is reacting with). This means that in principle, the terms nucleophile and electrophile should not be used without appropriately qualifying what the substances act as a nucleophile or electrophile towards and under what conditions. Unfortunately this is rarely done. In such cases, the conditions and substrate must be inferred from the context. For instance, when you learned that the chloride ion is a good nucleophile when studying organic chemistry, what was meant is that chloride is a good nucleophile towards electrophilic carbon atoms in organic molecules.

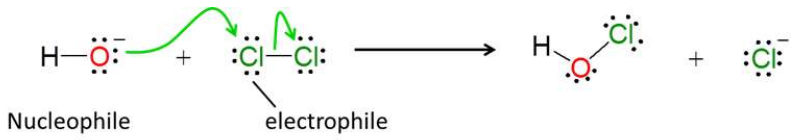
2. Acid and base strength and electrophilicity-nucleophilicity are not exactly the same thing. In many contexts where Lewis acids and bases are classified as electrophilic and nucleophilic substances, it is common to also refer to substances as being good acids or bases on the basis of their Brønsted acidity and basicity. In these contexts, the terms acid and base typically refer to the thermodynamic propensity of a substance to give and accept hydrogen ions while the terms nucleophile and electrophile refer to a substance's kinetic propensity to react with carbon-based Lewis acids and bases, respectively.

A substance may be both a good nucleophile and a strong Brønsted base. For instance, alkyllithium carbanion reagents and alkali metal hydrides are strong bases and good nucleophiles towards electrophilic carbon atoms in organic solvents at moderate temperatures. However, this is not always the case. Under such conditions iodide ion, I^-, is a good nucleophile towards electrophilic carbon atoms but is a poor Brønsted base (it is the conjugate of the strong acid HI). In fact, for the halide ions the order of Brønsted basicity is the opposite of the order of nucleophilicity towards electrophilic carbon:

stronger Brønsted base: F^-, Cl^-, Br^-, I^-: weaker Brønsted base

better nucleophlie: I^-, Br^-, Cl^-, F^-: poorer nucleophile

3. Although the nucleophile-electrophile concept is most often used to describe organic reactions, it is also useful for describing inorganic reactions as well. For instance, the formation of hypochlorite ion in chlorine water possibly involves nucleophilic attack of hydroxide on an electrophilic chlorine atom in an S_N2 type process:



The Usanovich Acid-base Concept

The Usanovich Acid-base concept encompasses a wider range of reactions than the Lewis acid-base concept but is perhaps too general to serve as a convenient framework for understanding reaction chemistry. The Usanovich acid-base concept was developed by the Russian chemist Mikhail Usanovich and extends the Lewis acid-base concept's definition of acids and bases as electron pair donors and acceptors even further. Within the Usanovich definition:

- Acids are anything that accepts electrons, increases cation concentrations, decreases anion concentrations, or reacts with bases
- Bases are anything that donates electrons, increases anion concentrations, decreases cation concentrations, or reacts with acids

These definitions essentially expand the Lewis definition by removing the requirement that the electrons donated or accepted be a pair and practically mean that Usanovich acid-base reactions include Lewis acid-base reactions plus oxidation-reduction reactions. In other words:

- Usanovich acids are Lewis acids plus oxidants
- Usanovich bases are Lewis bases plus reductants

Under this definition BF_3, Fe^{3+}, and $[Fe(CN)_6]^{3-}$ all act as acids, and : NH_3, CN^-, and Zn are all bases:

$$\underset{acid}{BF_3} + \underset{base}{NH_3} \rightarrow F_3B-NH_3$$

$$\underset{acid}{Fe^{3+}} + 6\underset{base}{CN:^-} \rightarrow [Fe(CN)_6]^{3-}$$

$$2\underset{acid}{[Fe(CN)_6]^{3-}} + \underset{base}{Zn} \rightarrow 2[Fe(CN)_6]^{3-} + Zn^{2+}$$

However, notice that while it is easy to think about how any acids might interchangeably react with a given base (and vice versa), under the other acid-base concepts chemists have found it more difficult to think about reactions between oxidants/reductants and Lewis acids and bases. For example, it is difficult to think about how a reaction between BF_3 and Zn metal might occur. Would two Zn donate a pair of electrons to the BF_3? For this reason, most chemists find it more convenient to think about Lewis acid-base and redox reactions under separate categories rather than unite them under the Usanovich definition.

$$2\underset{oxidant}{[Fe(CN)_6]^{3-}} + \underset{reductant}{Zn} \rightarrow 2[Fe(CN)_6]^{3-} + Zn^{2+}$$

Again, it can be helpful to remember Huheey's dictum that deciding between acid-base concepts is not a matter of which concept is the most correct but rather of which is more convenient for a given application.

Section 5.3.2: Lewis Concept and Frontier Orbitals is shared under a CC BY-NC-SA 4.0 license and was authored, remixed, and/or curated by Stephen M. Contakes.

- **6.4: Lewis Concept and Frontier Orbitals** by Stephen M. Contakes is licensed CC BY 4.0.

Section 5.3.2.1: The frontier orbital approach considers Lewis acid-base reactions in terms of the donation of electrons from the base's highest occupied orbital into the acid's lowest unoccupied orbital.

Another way the Lewis-Acid base concept is widely employed for understanding chemical reactivity is through the frontier orbital approach to chemical reactions. The frontier orbital concept conceptualizes chemical bonding and reactivity in terms of the interactions between frontier orbitals on the chemical species undergoing an interaction (*e.g.* molecules, atoms, ions, or groups as they interact to form a bond or undergo a reaction). Frontier orbitals are those at the frontier between occupied and unoccupied. They are often taken to be the highest energy occupied and lowest energy unoccupied molecular orbitals, called the HOMO and LUMO levels. However, it can sometimes be more convenient to think about them as atomic orbitals or Valence Bond approach-derived orbitals. When developing rough qualitative frontier orbital descriptions of the orbital interactions involved in a given system, the choice of what types of orbitals to use is often a matter of what is the most informative and convenient.

In particular, the frontier orbital concept envisions a Lewis acid-base interaction as involving an interaction between some of the frontier orbitals of the Lewis acid and base, specifically the donation of electrons from the base's HOMO level into the acid's LUMO level. For example, in the frontier orbital approach, adduct formation between $\boldsymbol{NH_3}$ and $\boldsymbol{BH_3}$ involves the donation of electrons from ammonia's a_1 HOMO into BH_3's a_2'' LUMO level.

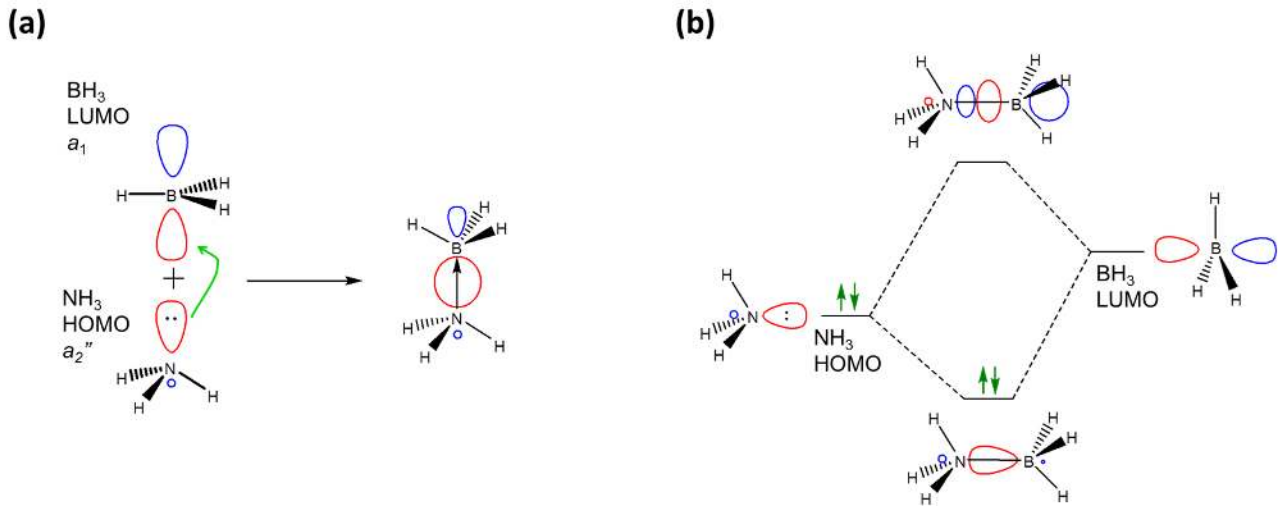


Figure ***Section*5.3.2.1.1**. Frontier orbital picture of adduct formation between ammonia and borane. (a) As $\boldsymbol{NH_3}$ and $\boldsymbol{BH_3}$ approach one another, interaction between the $\boldsymbol{NH_3}$ HOMO and $\boldsymbol{BH_3}$ LUMO gives a bonding MO. (b) Partial molecular orbital diagram for $\boldsymbol{NH_3 \rightarrow BH_3}$ showing the stabilization of the base ($\boldsymbol{NH_3}$) lone pair in a sigma bonding MO upon adduct formation.

As expected when two orbitals of the appropriate symmetry combine, the result of the interaction is the formation of a lower energy bonding orbital between the acid and base (Figure ***Section*5.3.2.1.1**). Since it is occupied by an electron, the net result of the interaction is the lowering of the base's lone pair energy as it interacts with the Lewis acid. In this case the interaction just follows the general pattern for Lewis-Acid base adduct formation, which is:

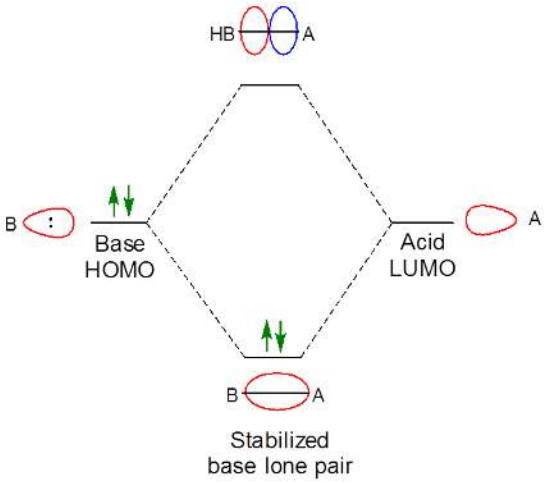
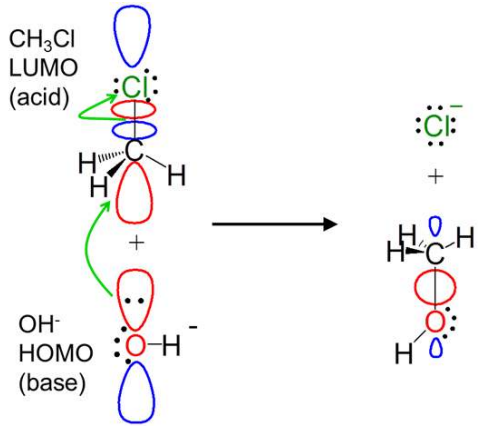


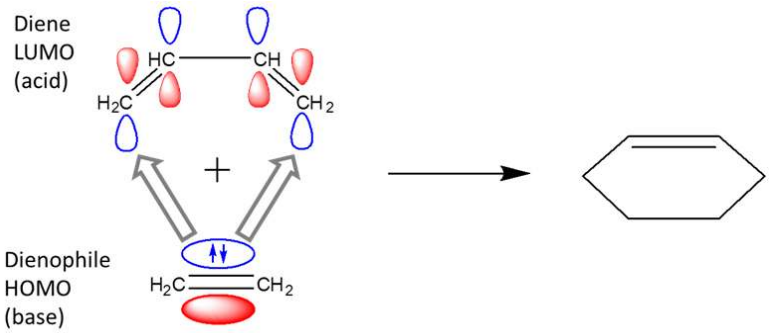
Figure *Section*5.3.2.1.2. Generalized frontier orbital picture for adduct formation between a Lewis base (B) and a Lewis acid (A) involving stabilization of the lone pair of the base HOMO by formation of a bonding orbital with the acid LUMO. The relative energies of the acid LUMO and base HOMO affect the character of the bonding and antibonding MOs but are otherwise unimportant in determining the general features of the interaction. In some cases the base HOMO is higher in energy; in others the acid LUMO is higher in energy; in still others they are equal in energy. In any case the net result is the stabilization of the base lone pair.

The frontier orbital concept illuminates the orbital interactions involved in reactions. For instance, from a frontier orbital perspective the alkyl halide substitution reaction between hydroxide and CH_3Cl via the S_N2 mechanism involves a Lewis acid-base interaction:

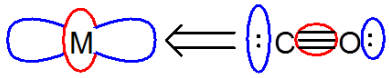


Notice how the frontier orbital approach even explains the displacement of the chloride leaving group. The donation of electrons from the hydroxide HOMO populates the antibonding CH_3Cl LUMO, breaking the C-Cl bond.

With the frontier orbital approach, it becomes apparent that pericyclic reactions are Lewis acid-base reactions. For example, in the Diels-Alder reaction, the dienophile acts as a Lewis base and the diene as a Lewis acid.



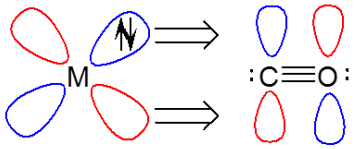
The orbital interactions involved in a given reaction can include both reactants acting as both an acid and base. In these cases the HOMO of each reactant interacts with the LUMO of the other. A good example of this involves **Π**-type interactions between a metal ion with occupied *d* orbitals and a pi-acceptor ligand. The ligand acts as a base and the metal as an acid to give a M-CO single bond:



Metal LUMO (d_{z^2}) acts as an acid

Carbon monoxide HOMO acts as a base

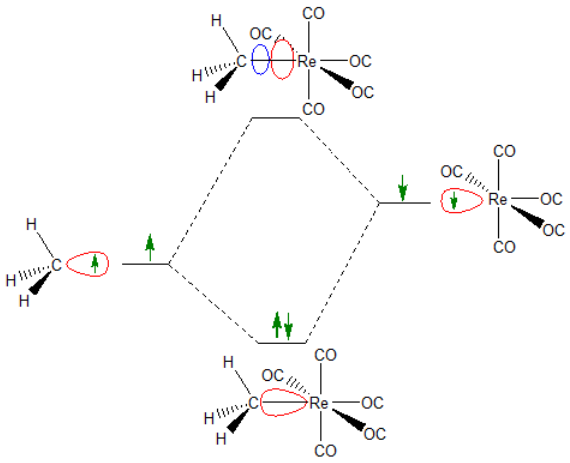
However, the metal can also act as a base towards the ligand LUMO (π^*) orbitals.



Metal HOMO (d_{xz}, d_{xz}) acts as a base

Carbon monoxide LUMO (π^*) acts as an acid

The frontier orbital concept can also be used to describe interactions between one or more singly occupied frontier orbitals. In fact, when approximate molecular orbital diagrams are being constructed, it can often be helpful to focus on one or two particularly instructive interactions. In these cases, it is sometimes convenient to think about a chemical bond as involving the formation of bonding and antibonding interactions between singly occupied frontier orbitals on different molecular fragments. For instance, when thinking about the chemistry of $CH_3Re(CO)_5$ it can sometimes be helpful to think about the C-Re bond as arising from the interaction between a singly-occupied sp^3 type orbital on a CH_3 group and a singly occupied d^2sp^3 orbital on the Re.



In introducing singly occupied orbitals, the frontier orbital concept formally handles interactions that the Lewis acid-base concept does not, since Lewis acid-base behavior is formally confined to the acceptance and donation of electron *pairs*.

Section 5.3.2.1: The frontier orbital approach considers Lewis acid-base reactions in terms of the donation of electrons from the base's highest occupied orbital into the acid's lowest unoccupied orbital. is shared under a CC BY-NC-SA 4.0 license and was authored, remixed, and/or curated by Stephen M. Contakes.

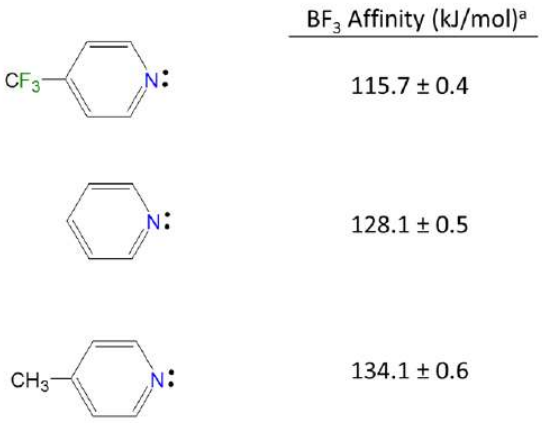
- **6.4.1: The frontier orbital approach considers Lewis acid-base reactions in terms of the donation of electrons from the base's highest occupied orbital into the acid's lowest unoccupied orbital.** by Stephen M. Contakes is licensed CC BY 4.0.

Section 5.3.2.2: All other things being equal, electron withdrawing groups tend to make Lewis acids stronger and bases weaker while electron donating groups tend to make Lewis bases stronger and acids weaker

The electrons donated from a Lewis base to a Lewis acid in a Lewis acid-base reaction are donated and accepted at particular atomic centers. For instance, the formation of an adduct between ammonia and BF_3 involves the donation of the lone pair on the ammonia nitrogen atom to the Lewis acid site on BF_3.



Because Lewis acid-base reactions involve electron donation and acceptance at particular sites, substituent groups which alter the electron density at a site through inductively donating or withdrawing electron density will affect the Lewis acid-base properties of that site. For instance, the BF_3 affinities of 4-substituted pyridines increase slightly as the substituent on the aromatic ring is changed from electron donating Me to electron withdrawing CF_3.



a) Data from Laurence, C.; Gal, J.-F. o., *Lewis basicity and Affinity Scales: Data and Measurement. John Wiley: Chichester, West Sussex, U.K., 2010; pp. 91-101.*

Substituent inductive effects are much as one might predict. Since Lewis bases donate electron pairs and Lewis acids accept them:

- electron withdrawing substituents tend to decrease the Lewis basicity of basic sites while electron donating substituents increase site Lewis basicity by making them more electron rich.
- electron withdrawing substituents increase the Lewis acidity of acidic sites by making those sites more electron deficient while electron donating substituents tend to decrease Lewis acidity by making sites less electron deficient.

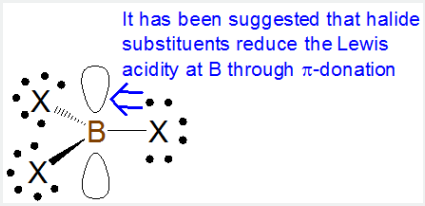
Nevertheless it can be difficult to predict substituent-based trends in Lewis acidity and basicity by inductive effects alone. This is because inductive effects are modest and often exists in competition with other substituent effects, such as

- Steric effects, discussed in section 6.4.7
- Hardness effects, discussed in section 6.6
- π-donation and acceptance effects, which can increase or decrease electron density at a given site as well as create an energy barrier for any structural distortions that might occur upon adduct formation.

Avoid misconceptions about the impact of π donation and acceptance on Lewis acid-base affinity

As with σ-based induction effects, π-donation tends to increase Lewis basicity and decrease Lewis acidity while π-withdrawal tends to decrease Lewis basicity and increase Lewis acidity. However, care needs to be taken in assessing the effect of π-

donation effects on Lewis acidity and basicity. For example, some textbooks claim that the Lewis acidity of boron trihalides is dominated by the reduction of boron acidity through π-donation from the halide substituents:

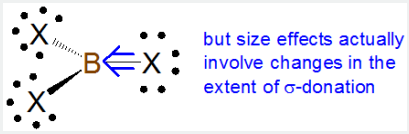


According to this explanation, the extent of this π-donation decreases down the halogen group as the boron-halogen bond distance decreases. This is consistent with the observed trend in Lewis acidity of the boron trihalides towards most bases, which runs counter to that suggested by inductive effects alone:

$$BI_3 > BBr_3 > BCl_3 >> BF_3$$

However, computational work suggests that this explanation is incorrect, since

- atomic size effects are important mainly for substituents in which the connected atom is in row 3+ or higher;
- atomic size effects mainly involve changes in the extent of σ-overlap. In other words, the larger halogens are less able to reduce the electron deficiency at the boron center through σ interactions while π-interactions play little or no role.



References:

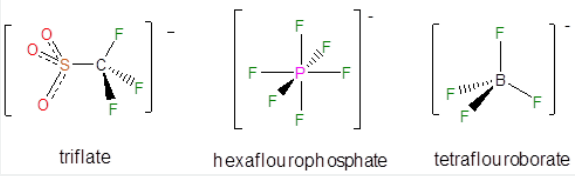
1. Plumley, J. A.; Evanseck, J. D., Periodic Trends and Index of Boron Lewis Acidity. *The Journal of Physical Chemistry A* 2009, 113 (20), 5985-5992.

2. Jupp, A. R.; Johnstone, T. C.; Stephan, D. W., Improving the Global Electrophilicity Index (GEI) as a Measure of Lewis Acidity. *Inorganic Chemistry* 2018, 57 (23), 14764-14771.

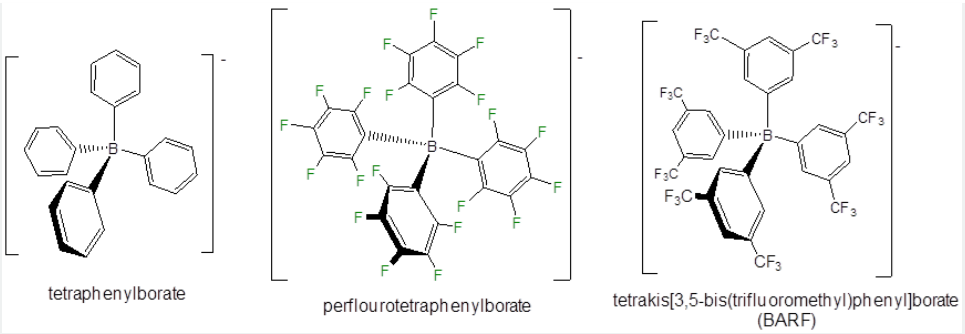
The conjugate bases of many Brønsted superacids have electron-withdrawing substituents that make them such poor Lewis bases that they are useful as noncoordinating anions.

The nonreactivity of Brønsted superacids' conjugate bases towards hydrogen ions is often mirrored in nonreactivity towards other Lewis Acids/electrophiles, most notably metals. This makes these substances useful as inert or noncoordinating ions, although since all are reactive towards suitably electrophilic centers, they are perhaps better understood as weakly coordinating.

A number of noncoordinating anions are commonly used in synthetic and other applications. The conjugate base of perchloric acid, perchlorate, was a common noncoordinating inert anion in classical coordination chemistry and continues to be used widely in electrochemistry. In contrast, the conjugate bases of triflic acid, hexafluoroboric acid, and tetrafluoroboric acid are now more commonly used as counterions for isolating reactive cations.



Even less reactive noncoordination anions include derivatives of tetraphenylborate, particularly those with electron withdrawing substituents.



Other classes of noncoordinating ions include fluoroantimonate clusters, derivatives of the carborane anion ($CB_{11}H_{11}^-$), and fluorinated aluminum tetraalkoxides.

References

Engesser, T. A.; Lichtenthaler, M. R.; Schleep, M.; Krossing, I., Reactive p-block cations stabilized by weakly coordinating anions. *Chemical Society reviews* **2016**, *45 (4)*, 789-899.

Section 5.3.2.2: All other things being equal, electron withdrawing groups tend to make Lewis acids stronger and bases weaker while electron donating groups tend to make Lewis bases stronger and acids weaker is shared under a CC BY-NC-SA 4.0 license and was authored, remixed, and/or curated by Stephen M. Contakes.

- **6.4.2: All other things being equal, electron withdrawing groups tend to make Lewis acids stronger and bases weaker while electron donating groups tend to make Lewis bases stronger and acids weaker** by Stephen M. Contakes is licensed CC BY 4.0.

Section 5.3.2.3: The electronic spectra of charge transfer complexes illustrate the impact of frontier orbital interactions on the electronic structure of Lewis acid-base adducts

When a Lewis acid-base adduct is formed, electron density and negative charge are transferred from the Lewis base to the acid.

The formation of a Lewis-acid base complex involves the transfer of electron density from the base to the acid.



Figure 6.4.2.*Section*5.3.2.3.1.

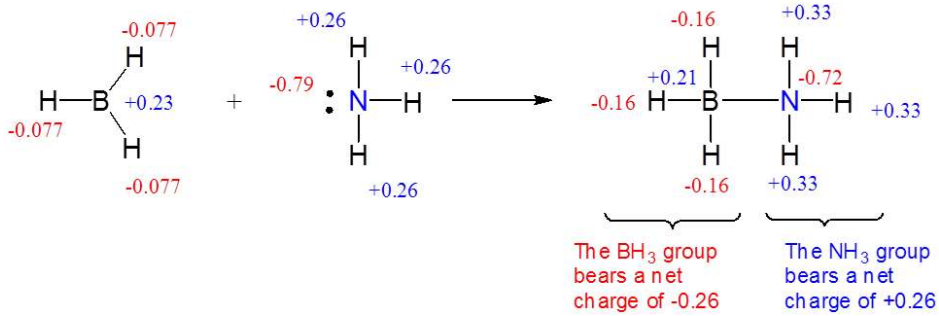


Figure 6.4.2.*Section*5.3.2.3.1. Calculated change in atomic charge distribution upon formation of an adduct between BH_3 and NH_3 in the gas phase. All partial charges were calculated for geometry-optimized molecules at the 6-31G** level.

Weakly bound Lewis acid-base adducts in which charge is incompletely transferred are called charge transfer complexes.

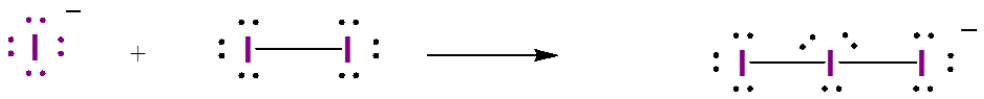
In many weakly bound Lewis acid-base complexes, the transfer of electron density and, consequently, charge from the base group to the acid group is only partial:

$$A + B \rightleftharpoons A^{\delta-}B^{\delta+}$$

Such Lewis acid-base adducts are commonly called **charge transfer complexes (CT complexes)** or **donor-acceptor complexes (DA complexes)**. In these

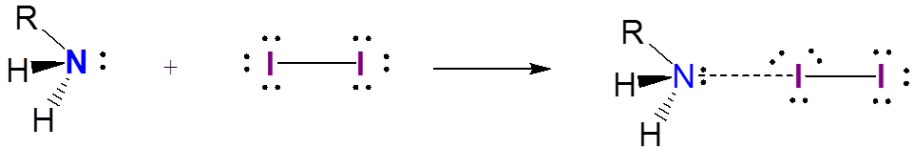
- the base is called the **donor (D)** since it is a net donor of electrons and, consequently, their negative charge
- the acid is called the **acceptor (A)** since it is a net acceptor of electrons and, consequently, their negative charge

A particularly well-known class of charge transfer complexes is the iodine charge transfer complexes. In iodine charge transfer complexes the I_2 acts as a Lewis acid. This is possible since iodine is a Row 3+ element and so is capable of forming hypervalent complexes on reaction with a Lewis base. For example, I_2 reacts with I^- to give the triiodide ion.

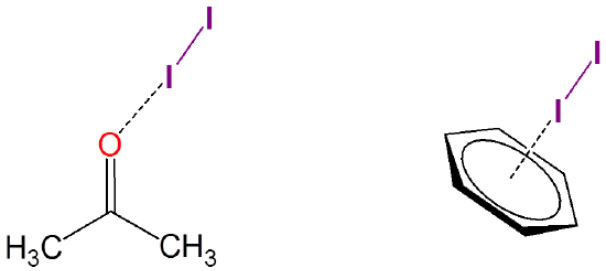


Triiodide is well-known from introductory chemistry from the bright blue color that appears when the triiodide complexes with starch to give the dark blue starch-iodide complex.

In contrast to the stable triiodide anion, iodine charge transfer complexes are only weakly associated. Complexes between iodine and amines are a well known example:

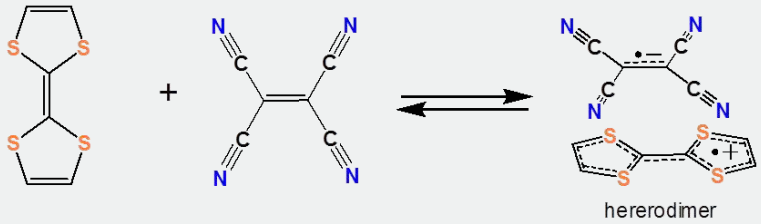


Iodine also forms weakly-associated charge transfer complexes with many solvents. For instance, iodine can weakly associate with both acetone and benzene:

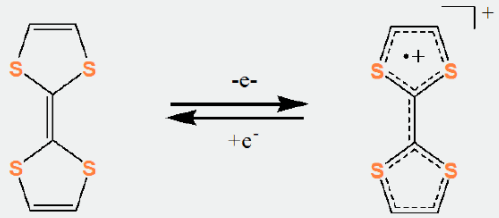


Organic Charge Transfer Complexes

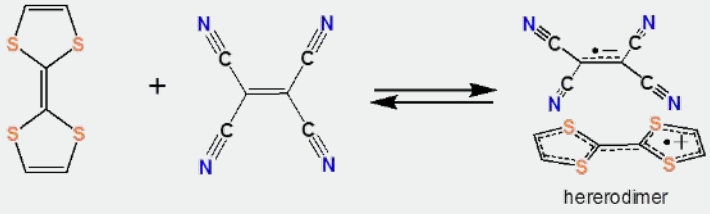
It is worth noting in passing that several organic charge transfer complex systems have been developed in which organic electron donors and acceptors weakly associate with each other. These are of considerable interest for use in molecular electronics applications, and as a result, a large variety of organic electron donors and acceptors have been developed. An example of an organic electron acceptor is tetracyanoethylene (TCNE):



and an example of an organic electron acceptor is tetrathiofulvalene (TTF).



Together they form a charge transfer complex:



Similar organic charge transfer systems have been investigated for use in organic photovoltaic cells. There is considerable interest in developing such organic photovoltaic devices owing to the ease with which organic materials may be fabricated from organic solutions and suspensions.

Charge transfer complexes exhibit charge transfer transitions in which absorption triggers the transfer of an electron from the donor to the acceptor.

When iodine is dissolved in solutions of donor solvents, the striking purple color of molecular iodine is replaced by a yellow-brown color. This is because charge transfer complexes like those formed by I_2 can absorb light in ways that neither the donor nor the acceptor can on their own. Specifically, charge transfer complexes exhibit **charge transfer bands (CT bands)** in their absorption spectra. In the charge transfer transition the initial partial transfer of charge from the donor Lewis base to the acceptor Lewis acid in the charge transfer complex is pushed further by photoexcitation.

$$D^{\delta+} - A^{\delta-} \xrightarrow{h\nu_{CT}} D^{+} - A^{-}$$

The nature of these charge transfer transitions is seen from the orbital description of binding for iodine charge transfer complexes. When a donor-I_2 complex forms, the formation of donor-I_2 bonding and antibonding orbitals results in a shift in the $I2\sigma \rightarrow \sigma*$ transition to higher energy, as a new charge transfer band is formed, associated with the excitation of an electron from the largely amine-centered amine-I_2 σ orbital to the largely I_2-centered amine-I_2 $\sigma*$ orbital.

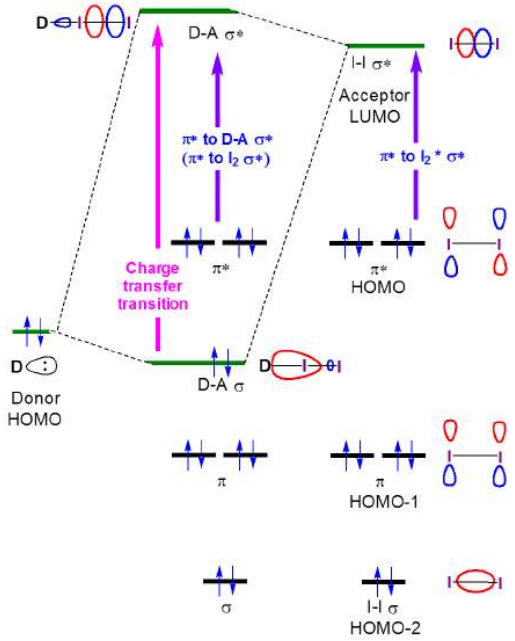


Figure 6.4.2.*Section*5.3.2.3.2. Frontier orbital interactions that give rise to changes in the absorption spectra of iodine when it forms a charge transfer complex with a Lewis base donor.

Solutions of I_2 as mixtures with Lewis bases such as amines and in donor solvents clearly have charge transfer bands in their absorption spectra. Several such spectra are given in Figure 6.4.2.3.

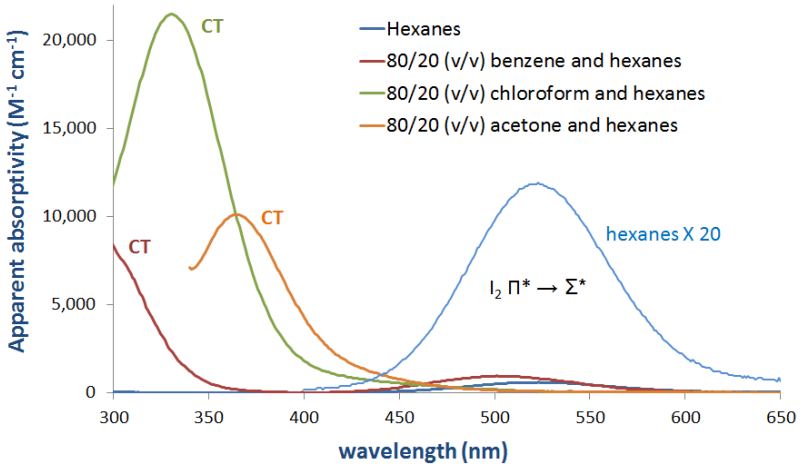


Figure ***Section*5.3.2.3.3**. Absorption spectrum of molecular iodine (I_2) in various solvents showing the appearance of a CT band in donor solvents.*

In principle, the energies of both the charge transfer and $I_2\ \pi*\ \rightarrow\ D-A\ \sigma*$ transitions both increase with donor strength, as shown in Figure 6.4.2.4.

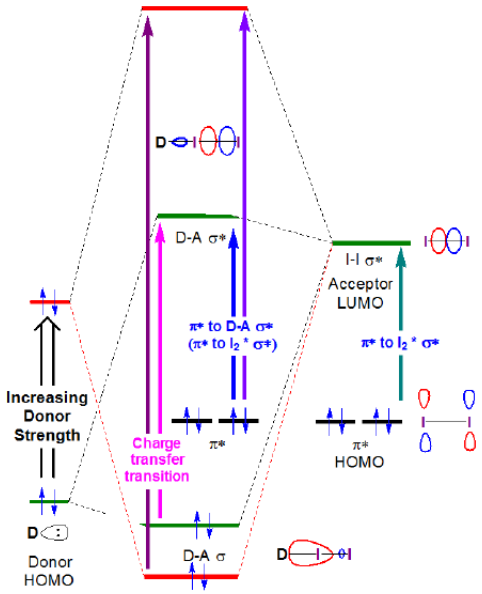


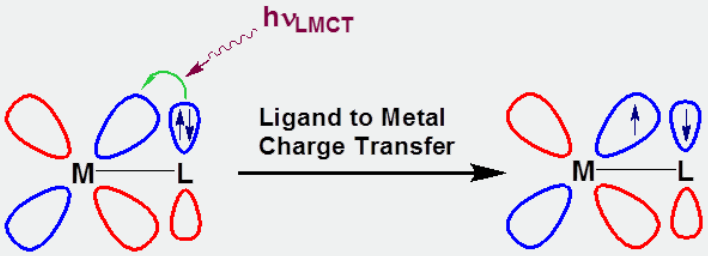
Figure ***Section*5.3.2.3.4**. Expected change in the frontier orbital energies associated with I_2 donor acceptor complex formation when the HOMO energy of the donor is increased.

As can be seen in Figure 6.4.2, the charge transfer band energy might be expected to increase as the donor HOMO increases in energy to become closer in energy to the acceptor LUMO. Although care should be taken when interpreting the solution phase spectra of I_2, this expectation is borne out by a cursory and qualitative analysis of the spectra in Figure 6.4.2.3. The CT transition energy shifts towards lower wavelengths (and thus higher energy) as the highest occupied atomic orbital energy for the donor atom increases on going from acetone (oxygen, -15.85 eV) to chloroform (chlorine, -13.67eV) and finally benzene (carbon, -10.66 eV).**

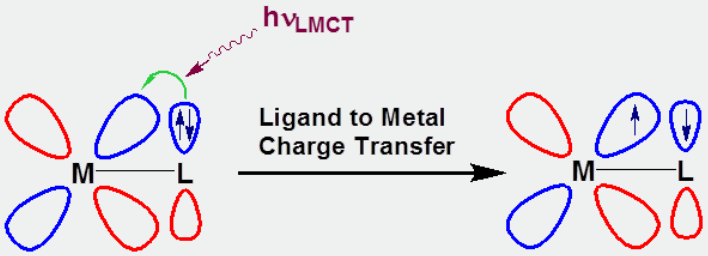
Charge Transfer Bands in Transition Metal Chemistry

Charge transfer transitions are responsible for the intense color of many transition metal complexes. In these cases, however, the weak Lewis acid-base interaction involves incomplete electron donation and acceptance in a $p\pi - d\pi$ (or $p\pi - d\pi*$)-bond between a metal and ligand. The charge transfer bands in the absorption spectra of these complexes involve the transfer of electrons between the metal and ligand. In particular,

- Metal to ligand charge transfer (MLCT or CTTL) bands involve the transfer of an electron from a filled or partly filled metal *d* orbital to a ligand $\pi*$-type orbital.



- Ligand to metal charge transfer (LMCT or CTTM) bands involve the transfer of an electron from a filled or partly filled ligand orbital to a metal *d*-orbital.



- Metal to metal charge transfer bands can be observed in some bimetallic complexes. However, these are usually thought of only as an electron transfer rather than as a shift in the status of a Lewis acid-base interaction.

Because metal-ligand charge transfer bands involve intermolecular electron transfer between the metal and ligand to generate a high energy redox state, the CT excited state is both a better oxidant and reductant than the ground state. Consequently there has been intense research into the development of metal complexes whose charge transfer excited states are powerful oxidants and reductants in the expectation that they will be able to drive the photocatalytic oxidation and reduction of substrates.

* The apparent absorptivity of I_2 in hexanes was calculated from the absorption spectrum of 215 μM I_2 in hexanes. All other apparent absorptivities were calculated from absorption spectra of solutions that were 44 μM in I_2.

** The band positions are not the CT band energies, and the HOMO energies given are atomic energy levels and do not necessarily correspond to the HOMO of the donor in solution. Because of this and other simplifications this analysis is not intended to replace a rigorous computational analysis of the factors that give rise to CT band positions.

References

1. Meyerstein, D.; Treinin, A., Charge-transfer complexes of iodine and inorganic anions in solution. Transactions of the Faraday Society 1963, 59 (0), 1114-1120.
2. Baskar, A. J. A.; Rajpurohit, A. S.; Panneerselvam, M.; Jaccobb, M.; RoopSingh, D.; Kannappan, V., Experimental and theoretical analysis of substituent effect on charge transfer complexes of iodine and some alkylbenzenes in n-hexane solution at 303K. Chemical Data Collections 2017, 7-8, 80-92.

Section 5.3.2.3: The electronic spectra of charge transfer complexes illustrate the impact of frontier orbital interactions on the electronic structure of Lewis acid-base adducts is shared under a CC BY-NC-SA 4.0 license and was authored, remixed, and/or curated by Stephen M. Contakes.

- **6.4.3: The electronic spectra of charge transfer complexes illustrate the impact of frontier orbital interactions on the electronic structure of Lewis acid-base adducts** by Stephen M. Contakes is licensed CC BY 4.0.

Section 5.3.2.4: Substances' solution phase Lewis basicity towards a given acid may be estimated using the enthalphy change for dissociation of its adduct with a reference acid of similar hardness.

A number of spectroscopic and thermodynamic scales have been developed to quantify the strength of Lewis acids and bases.[1,2] For the sake of simplicity only thermodynamic scales will be described. Thermodynamic scales are based on the energetics of Lewis acid-base reactions. When substances act as a Lewis base (**B**) they form adducts with a Lewis acid (**A**):

$$B: + A \rightleftharpoons B-A$$

Various thermodynamic parameters for this process may be taken as a measure of the strength of the Lewis base towards that acid. For instance, in the case of iodine charge transfer complexes, the equilibrium constant for adduct formation is sometimes used as an informal measure of Lewis base strength.

The thermodynamic parameters used to define Lewis acid and base strength are similar to those used to define Brønsted acidity and basicity. Just as Brønsted acidity and basicity were defined in terms of the free energy change for the dissociation and association of a hydrogen ion, Lewis acidities and basicities are defined in terms of the free energy change for adduct formation:

$$B: + A_{reference} \rightleftharpoons B-A \qquad -\Delta G = Lewis\ basicity\ of\ B\ towards\ A$$

$$B:_{reference} + A \rightleftharpoons B-A \qquad -\Delta G = Lewis\ acidity\ of\ A\ towards\ B$$

The physical meaning of Lewis acidities and basicities may be easier to grasp by considering that Lewis acidities and basicities correspond to the free energy for dissociation of acid-base adducts:

$$B-A \rightleftharpoons B: + A_{reference} \qquad \Delta G = Lewis\ basicity\ of\ B\ towards\ A$$

$$B-A \rightleftharpoons B:_{reference} + A \qquad \Delta G = Lewis\ acidity\ of\ A\ towards\ B$$

Since in practice it is much easier to measure the reaction enthalpies for these processes, many scales use the enthalpy change instead of the free energies. To distinguish these enthalpy changes from Lewis *acidities* and *basicities*, the enthalpy changes are called Lewis acid and base *affinities*. Of these, however, Lewis acid affinities are poorly characterized at present (perhaps one of you readers will help redress this). Thus the remainder of this section will focus on Lewis base affinities.

Before discussing Lewis base affinities it is worth noting that there is no universal reference scale of Lewis base strength. That is because the thermodynamics of a given Lewis acid-base interaction is contingent on a number of factors, including:

- The relative hardness of the acid and base according to Pearson's hard-soft acid base principle. Roughly, Lewis acids tend to associate more strongly with Lewis bases with similar charge densities and polarizabilities. This means that the affinity of a given base for Lewis acids is not a static parameter. Rather it differs markedly with the acid's hardness.
- Steric effects. Sterically hindered Lewis acid-base interactions will be weaker than sterically accessible ones.
- Solvent effects. In solutions, the adduct and the free acid and base pair will in general be differentially stabilized. To avoid solvent effects, some scales quantify Lewis acid and base strength in terms of gas phase adduct formation. However, it is not always possible or desirable to quantify a Lewis acid or base's strength in the gas phase, since gas phase affinities do not always allow for adequate prediction of the strength of a Lewis acid-base interaction in solution.

Because Lewis base affinity depends on hardness, steric effects, and solvent effects care should be taken when acid-base parameters are used to predict the strength of a given interaction. In particular, steric effects should be considered separately, and if predictions are made using scales that employ reference acids or bases that differ markedly in hardness from the interaction to be predicted or which correspond to unrealistic solvent conditions, they should always be taken as tentative.

References

1. Laurence, C.; Graton, J.; Gal, J.-F., An Overview of Lewis Basicity and Affinity Scales. Journal of Chemical Education 2011, 88 (12), 1651-1657.
2. Laurence, C.; Gal, J.-F. o., Lewis basicity and affinity scales: data and measurement. John Wiley: Chichester, West Sussex, U.K., 2010.

Section 5.3.2.4: Substances' solution phase Lewis basicity towards a given acid may be estimated using the enthalphy change for dissociation of its adduct with a reference acid of similar hardness. is shared under a CC BY-NC-SA 4.0 license and was authored, remixed, and/or curated by Stephen M. Contakes.

- **6.4.4: Substances' solution phase Lewis basicity towards a given acid may be estimated using the enthalphy change for dissociation of its adduct with a reference acid of similar hardness.** by Stephen M. Contakes is licensed CC BY 4.0.

Section 5.3.2.5: In the boron trifluoride affinity scale, the enthalphy change on formation of an adduct between the base and boron trifluoride is taken as a measure of Lewis basicity.

The physical meaning of Lewis acid and base affinities are defined as the negative of the enthalphy for formation of an adduct with a reference base and acid, respectively:

$$B + A_{reference} \rightleftharpoons B-A \qquad -\Delta H = \text{Lewis basicity of B towards A}$$

$$B_{reference} + A \rightleftharpoons B-A \qquad -\Delta H = \text{Lewis acidity of A towards B}$$

Two common scales of Lewis base affinity involve the use of $SbCl_5$ and BF_3 as the reference base. Specifically,

- In the **Guttman donor-acceptor scale,** Lewis bases' **donor numbers** are equal to the negative enthalpy change for formation of the base's $SBCl_5$ adduct in dilute 1,2-dichloroethane (EDC*):

$$Base(EDC\ solution) + SbCl_5(EDC\ solution) \rightarrow Base-SbCl_5(EDC\ solution) \qquad -\Delta H = \text{Guttman Donor Number}$$

- The **BF_3 affinity scale** has largely supplanted the Guttman scale owing to the ease with which its results may be correlated with computational data (it is easier to calculate energies for adducts of BF_3 than of SbF_5). In the BF_3 affinity scale, Lewis bases' **BF_3 affinities** are equal to the negative enthalpy change for formation of a solution phase adduct between the base and gaseous BF_3. The reaction is:

$$Base(solution) + BF_3(g) \rightarrow Base-BF_3(solution) \qquad -\Delta H = BF_3\ \text{Affinity}$$

BF_3 affinity values for a wide range of organic bases were compiled by Laurence, Graton, and Gal in reference 2 and salient trends in this data will be discussed in subsequent sections.

References

1. Laurence, C.; Graton, J.; Gal, J.-F., An Overview of Lewis Basicity and Affinity Scales. Journal of Chemical Education 2011, 88 (12), 1651-1657.
2. Laurence, C.; Gal, J.-F. o., Lewis basicity and affinity scales: data and measurement. John Wiley: Chichester, West Sussex, U.K., 2010.

Notes

* EDC stands for ethylene dichloride, the common name of 1,2-dichloroethane.

Section 5.3.2.5: In the boron trifluoride affinity scale, the enthalphy change on formation of an adduct between the base and boron trifluoride is taken as a measure of Lewis basicity. is shared under a CC BY-NC-SA 4.0 license and was authored, remixed, and/or curated by Stephen M. Contakes.

- **6.4.5: In the boron trifluoride affinity scale, the enthalphy change on formation of an adduct between the base and boron trifluoride is taken as a measure of Lewis basicity.** by Stephen M. Contakes is licensed CC BY 4.0.

Section 5.3.2.6: Lewis base strength may also be estimated by measuring structural or energy changes upon formation of a Lewis acid-base complex, as illustrated by efforts to spectroscopically assess the strengths of halogen bonds

When a Lewis acid and base form an adduct, it shifts the bond lengths, and strengths in the acid and base also shift.

According to the frontier orbital description of Lewis acid-base interactions, adduct formation results in a net transfer of electron density from the base HOMO to the acid LUMO. This transfer

- increases the electron density between the acid (A) and base (D)
- alters the strength of the bonding within the base as the base LUMO becomes partially populated.

These changes result in structural and spectroscopic shifts on adduct formation that can be taken as a measure of the strength of the Lewis acid-base interaction. Since these shifts depend on the nature of the bonding in the acid and base, in practice structural and spectroscopic measurements of Lewis basicity are applied to a few classes of Lewis acid-base interactions, most notably hydrogen bonding and halogen bonding. Since hydrogen bonds will be discussed in section 6.5.1. the remainder of this subsection will focus on halogen bonds.

Halogen bonds are coordinate covalent bonds formed between a Lewis base and an organohalogen.

The halogens in compounds containing a singly-bonded halogen can engage in a special type of intermolecular interaction called halogen bonding, since the bonded halogens are electrophilic on the opposite side of the bond. This electrophilicity is apparent from the charge distribution in CF_5I shown in Figure 4.5.1, in which the charge is distributed on the I such that the I is Lewis basic perpendicular to the C-I bond and Lewis acidic opposite to it. This region of diminished electron density on the halogen opposite the existing sigma bond is called a σ-hole.*

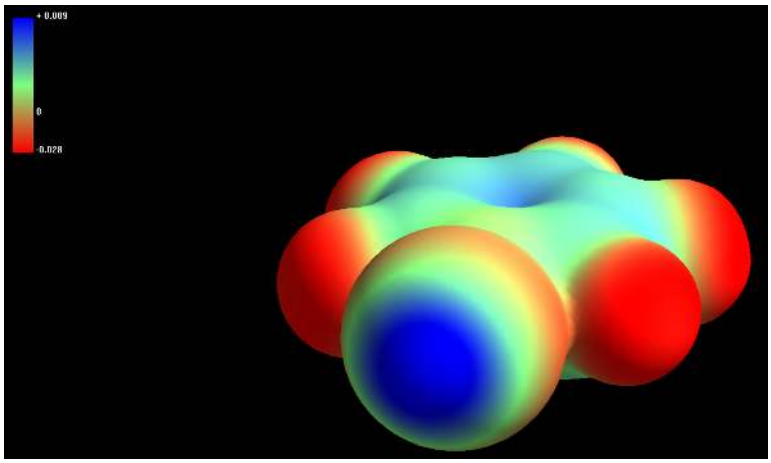
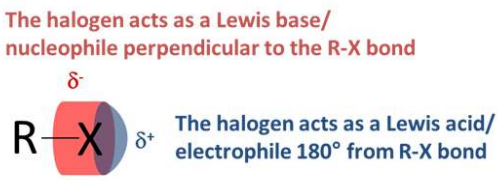
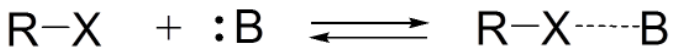


Figure **Section5.3.2.6.1**. Electrostatic surface calculated for CF_5I at the STO-3-21G level oriented so that the C-I bond is facing toward the viewer. The sigma hole shown is the region of positive electron density on the I atom at the front of the image. This work by Stephen Contakes is licensed under a Creative Commons Attribution 4.0 International License.

Schematically,



Since the halogen can act as a Lewis acid in the direction opposite the R-X bond it can form adducts with Lewis bases in that direction.



The bonds holding these adducts together are called **halogen bonds**, often abbreviated XB.

The halogen is said to act as a halogen bond donor when it forms a halogen bond with a base along that direction, with the base acting as the halogen bond acceptor. Consequently, the two previous schemes may also be given as:



The ability of singly-bonded halogen atoms to form halogen bonds forms the basis of many efforts to engineer structures in which halogen-containing compounds are held together into chains, sheets, or 3D structures using halogen bonds. One easy-to-see example involves 1D chains formed between *p*-diiodotetrafluorobenzene and *p*-bis(dimethylamino)benzene.[3]

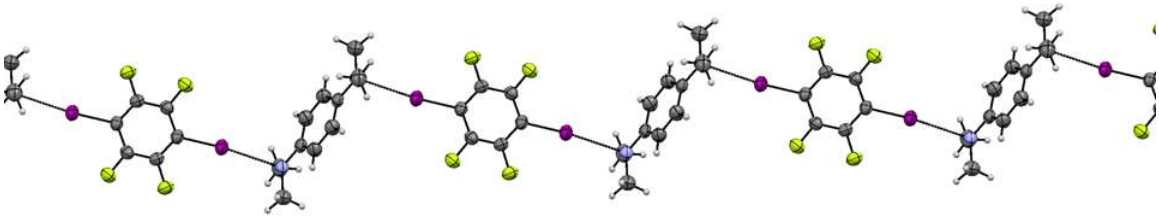
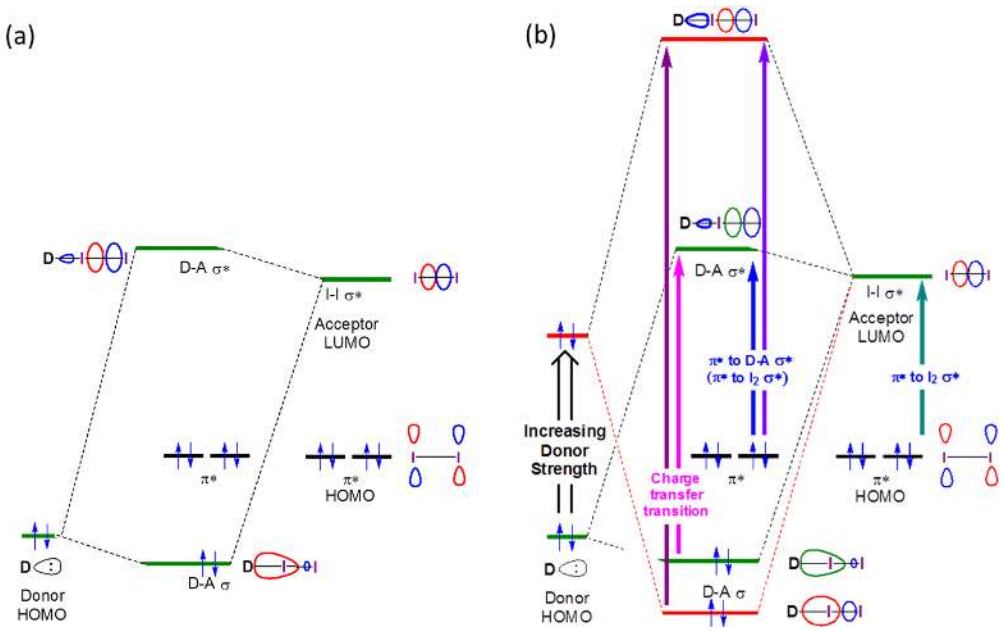


Figure **Section5.3.2.6.2**. 1D chains of *p*-tetrafluorodiiodobenzene and *p*-bis(dimethylamino)benzene molecules in which I is shown in purple, N in blue, F in yellow, and C in grey. The chains are held together by C-I---N halogen bonds with a contact angle of 174 degrees. The figure was produced using Mercury 3.5.1 based on Cambridge crystallographic database entry 172272. This work by Stephen Contakes is licensed under a Creative Commons Attribution 4.0 International License.

Trends in halogen bond strength in a closely-related series of compounds may be assessed by examining how the vibrational stretching frequency of I_2 and the I_2 π^* to σ^* transition energy change upon formation of the adduct.

From the description of halogen bonding above it should be apparent that the iodine charge transfer complexes described in section 6.4.2 are held together by halogen bonds. This means that the description of the bonding in I_2 charge transfer complexes given in that section illustrate how vibrational and electronic transitions shift when a halogen-bonded adduct is formed between a halogen bond donor and acceptor.

The orbital interactions involved in halogen bond formation are shown in Figure 6.4.5.3. As can be seen from that figure, the formation of an adduct between I_2 and a Lewis base is expected to result in weakening of the I-I bond and a shift in the I_2 $\pi^* \rightarrow \sigma^*$ transition energy to higher energy/shorter wavelengths (*i.e.*, a blueshift). Further, both the weakening of the I-I bond and the I_2 $\pi^* \rightarrow \sigma^*$ blueshift are expected to increase with the HOMO energy of the Lewis base.



Figures 6.4.2.2 and 6.4.2.4. This work by Stephen Contakes is licensed under a Creative Commons Attribution 4.0 International License.

Because the I-I bond strength and $I_2\ \pi^* \rightarrow \sigma^*$ blueshift increase with the Lewis basicity of the donor, the blueshift and the I-I vibrational stretching frequency are sometimes used as measures of donor's halogen bond affinity. However, the data obtained from such spectroscopic measurements should be interpreted with a degree of caution. As seen in Table 6.4.5.1, the extent to which the I-I bond is weakened (indicated by $\Delta\nu_{I-I}$) and the $I_2's\ \pi^* \rightarrow \sigma^*$ band is blue shifted are imperfectly correlated overall. However, a careful comparison of the data in 6.4.5.1. reveals that the I-I bond weakening and $I_2's\ \pi^* \rightarrow \sigma^*$ blue shift correlate well for Lewis bases of a given type. Consequently, shifts in the I-I stretching frequency and $I_2\ \pi^* \rightarrow \sigma^*$ absorption band are not useful as an absolute measure of Lewis basicity but can be used to rank the halogen bond affinity of a closely-related set of donors.**

Table **Section5.3.2.6.1**. Spectroscopic measures of Lewis basicity for I_2 adducts of selected bases arranged in order of extent of blue shift. The data are excerpted from the extensive compilation given in reference 4.

Base (type)	$\Delta\nu_{I-I}\ cm^{-1}$	Blue shift of $I_2's\ \pi* \rightarrow \sigma*$
4-methylpyridine (pyridines)	29.1	4730
pyridine (pyridines)	27.4	4560
tetrahydrothiophene (thioethers)	44.5	3640
tetrahydrofuran, THF (ethers)	6.4	2280
diethyl ether (ethers)	5.5	1950
acetone (ketone)	5.0	1850
acetophenone (ketone)	4.6	1650
acetonitrile (nitrile)	4.1	1610
hexamethylbenzene (aromatic)	10.4	1070
benzene (aromatic)	4.3	450

References and Further Reading

1. Cavallo, G.; Metrangolo, P.; Milani, R.; Pilati, T.; Priimagi, A.; Resnati, G.; Terraneo, G., The Halogen Bond. *Chemical Reviews* 2016, *116 (4)*, 2478-2601.
2. Politzer, P.; Murray, J.S. σ-Hole Interactions: Perspectives and Misconceptions. *Crystals* **2017**, *7*, 212.

3. R.Liantonio, S.Luzzati, P.Metrangolo, T.Pilati, G.Resnati, *Tetrahedron*, 2002, 58, 4023, DOI: 10.1016/S0040-4020(02)00264-8
4. Laurence, C.; Gal, J.-F. o., *Lewis Basicity and Affinity scales: Data and Measurement*. John Wiley: Chichester, West Sussex, U.K., 2010.

Notes

* Other compounds also exhibit σ-holes (and π-holes) that can be used in crystal engineering. For details see reference 2.

** for more details consult reference 4, pp. 286-309.

Contributors and Attributions

Consistent with the policy for original artwork made as part of this project, all unlabeled drawings of chemical structures are by Stephen Contakes and licensed under a Creative Commons Attribution 4.0 International License.

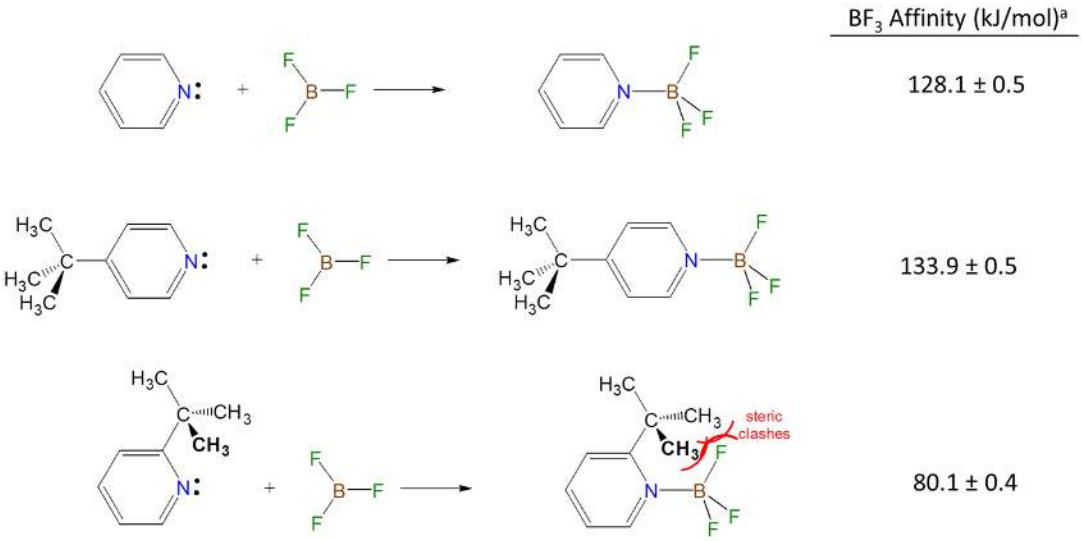
Section 5.3.2.6: Lewis base strength may also be estimated by measuring structural or energy changes upon formation of a Lewis acid-base complex, as illustrated by efforts to spectroscopically assess the strengths of halogen bonds is shared under a CC BY-NC-SA 4.0 license and was authored, remixed, and/or curated by Stephen M. Contakes.

- **6.4.6: Lewis base strength may also be estimated by measuring structural or energy changes upon formation of a Lewis acid-base complex, as illustrated by efforts to spectroscopically assess the strengths of halogen bonds** by Stephen M. Contakes is licensed CC BY 4.0.

Section 5.3.2.7: Bulky groups weaken the strength of Lewis acids and bases because they introduce steric strain into the resulting acid-base adduct.

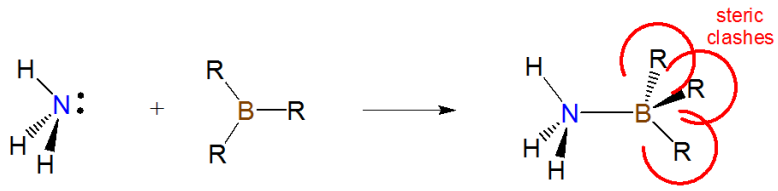
Steric effects can influence the ability of a Lewis acid or base to form adducts by introducing:

- **front strain (F-strain)** whereby bulky groups make it difficult for the Lewis acid and Lewis base centers to approach and interact.



a) Data from Laurence, C.; Gal, J.-F. o., *Lewis basicity and Affinity Scales: Data and Measurement. John Wiley: Chichester, West Sussex, U.K., 2010; pp. 91-101.*

- **back strain (B-strain)** associated with steric interactions that do not directly impede the Lewis acid and base centers from interacting but instead occur as the acid and base rearrange upon adduct formation. For instance, when trivalent boron compounds form adducts with amines, the boron center changes from a more open trigonal geometry to a more hindered tetrahedral one:



- **internal strain (I-strain)** is also associated with the geometry changes incident on adduct formation. However, while B-strain involves direct steric clashes that occur on adduct formation, I-strain is the strain involved in deforming bond and torsional angles away from more stable local geometries. Thus it is more important for Lewis base centers embedded in rings or clusters.

References

1. Alder, R. W., Strain effects on amine basicities. *Chemical Reviews* 1989, 89 (5), 1215-1223.

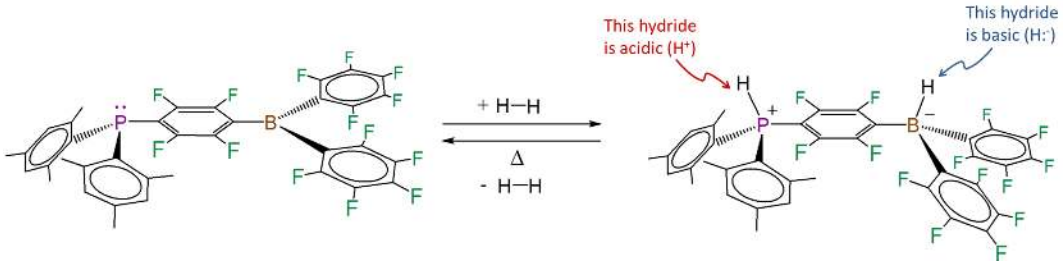
Section 5.3.2.7: Bulky groups weaken the strength of Lewis acids and bases because they introduce steric strain into the resulting acid-base adduct. is shared under a CC BY-NC-SA 4.0 license and was authored, remixed, and/or curated by Stephen M. Contakes.

- **6.4.7: Bulky groups weaken the strength of Lewis acids and bases because they introduce steric strain into the resulting acid-base adduct.** by Stephen M. Contakes is licensed CC BY 4.0.

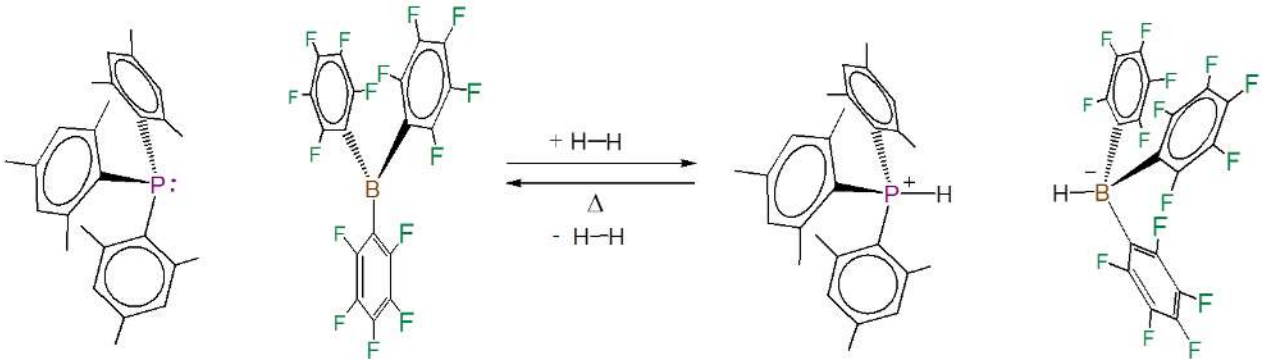
Section 5.3.2.8: Frustrated Lewis pair chemistry uses Lewis acid and base sites within a molecule that are sterically restricted from forming an adduct with each other.

In certain cases when a Lewis acid-base adduct is sterically hindered from quantitatively forming an adduct (and perhaps even when they are so able), the Lewis acid and Lewis base can act together to heterolytically cleave chemical bonds. In such cases the pair of electrons that would otherwise be donated by the base is said to be a **frustrated Lewis pair (FLP)** and in performing the heterolytic cleavage the Lewis acid and base are said to exhibit **frustrated Lewis pair chemistry**.

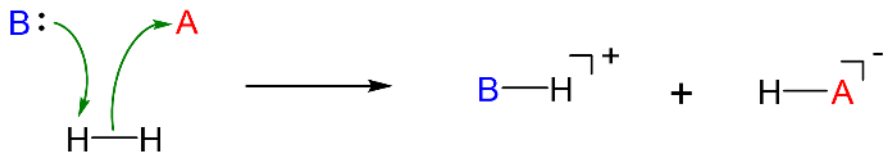
The **Stephan's phosphinoborane** illustrates how FLP chemistry works. It reversibly cleaves dihydrogen to give a zwitterionic species containing both acidic and basic element hydride bonds.



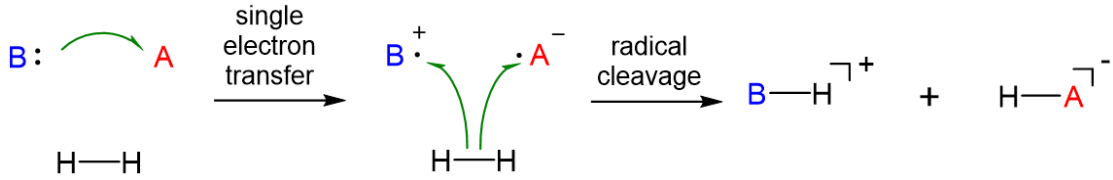
Note that the Lewis acid and base do not need to be part of the same molecule. Hydrogen is also heterolytically cleaved by mixtures of sterically encumbered triarylphosphines and triarylboranes. This time the reaction gives phosphonium and hydroborate ions:



Given the description of FLP systems as frustrated Lewis acid-base adducts, it is natural to think about the cleavage of substrates like H_2 as involving nucleophilic attack by the Lewis base while the Lewis acid acts like an electrophile in a heterolytic cleavage mechanism.



However, only some FLP systems cleave substrates through this mechanism. In others the mechanism involves homolytic cleavage by a diradical intermediate.



In either case, when substrates like H_2 are cleaved by FLPs, they are generally separated into more reactive fragments (e.g., in the case of H_2, H^+ and H^-). Because of this the substrates are said to be activated to undergo further reactions. Because FLP systems can cleave and activate substrates, there is considerable interest in the development of FLP systems that can facilitate reactions of economic or environmental interest. So far FLP systems have been developed that can catalyze various hydrogenations and activate numerous substrates, including CO, SO_2, and N_2.

References

1. Stephan, D. W., Frustrated Lewis Pairs: From Concept to Catalysis. *Accounts of Chemical Research* 2015, 48 (2), 306-316.
2. Fontaine, F.-G.; Stephan D. W., On the concept of frustrated Lewis pairs. *Philosophical Transactions of the Royal Society A: Mathematical, Physical and Engineering Sciences* 2017, 375 (2101), 20170004.
3. Jupp, A. R.; Stephan, D. W., New Directions for Frustrated Lewis Pair Chemistry. *Trends in Chemistry* 2019, 1 (1), 35-48.

Section 5.3.2.8: Frustrated Lewis pair chemistry uses Lewis acid and base sites within a molecule that are sterically restricted from forming an adduct with each other. is shared under a CC BY-NC-SA 4.0 license and was authored, remixed, and/or curated by Stephen M. Contakes.

- **6.4.8: Frustrated Lewis pair chemistry uses Lewis acid and base sites within a molecule that are sterically restricted from forming an adduct with each other.** by Stephen M. Contakes is licensed CC BY 4.0.

Section 5.3.3: Hard and Soft Acids and Bases

Origin of the Hard-Soft Acid-Base Principle

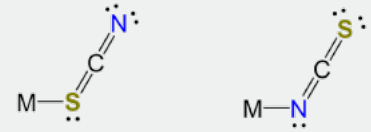
One of the strengths of the Lewis acid-base concept is the readiness with which it illuminates the role that covalent and electrostatic interactions in acid base behavior, specifically through its ability to explain chemical interactions in terms of frontier orbitals and the interactions between charged groups as electrons are donated from a base to an acid. However, simply acknowledging the presence of such interactions does little to illuminate the degree to which each mode of explanation best explains the bonding in a given system? To what extent is a given adduct better described as held together by covalent bonds as opposed to ionic ones - *e.g.* better described as a molecule rather than an ion pair? Moreover, does it even matter, given that the orbitals of quantum mechanics result from the combination of electrons' wavelike behavior with their electrostatic attraction to nuclei in either case?[1] These questions and more are addressed by one of the most important conceptual tools in contemporary inorganic chemistry, the Hard-Soft acid-base principle.

The **Hard-Soft acid-base principle (HSAB principle)** stems from the recognition that some Lewis acids and bases seem to have a natural affinity for one another.* Consider the following:

- Some metals are commonly found in nature as salts of chloride or as oxide ores while others are found in combination with sulfur. Geochemists even use the Goldschmidtt classification scheme to classify the halide and oxide formers as lithophiles and the sulfide formers as chalcophiles.
- In living systems small highly charged metals ions like Fe^{3+} are usually found bound to N and O atoms while larger metals with lower charges such as Zn^{2+} are often found attached to at least one S atom. Similarly, metals prefer to bind to one coordination site over the other when forming complexes with ambidentate ligands. The most well-known instances involve complexes of cyanate and thiocyanate, which can coordinate metals through either the N or chalcogen atom. For instance, Cu^{2+} and Zn^{2+} form *N*-thiocyanato complexes in species like $[Cu(NCS)_2(py)_2]$ and $[Zn(NCS)_4]^{2-}$ while their larger cogeners Au^{3+} and Hg^{2+} preferentially forms *S*-thiocyanato complexes, giving species like $[Hg(SCN)_4]^{2-}$.

Ambidentate ligands

Ambidentate ligands possess multiple coordination sites through which a metal may bind. For instance, thiocyanate may coordinate metals (M) at either the S or N to give *S*-thiocyanato or *N*-thiocyanato complexes.



S-thiocyanato *N*-thiocyanato

- The solubility trends for the alklai metal halides and silver halides are opposite, even though both involve salts of formula M^+X^- (salts can be thought of as involving Lewis acid-base adduct formation between the anions and cations). Specifically, although the silver halides are all relatively insoluble in water, the very modest solubility they possess follows the order:

$$X = F >> Cl > Br > I \text{ (for the solubility of AgX)}$$

In contrast, the much more ample solubility of the alkali metal halides** follows the opposite order. For example, the order for the lithium halides is

$$X = F << Cl < Br << I \text{ (for the solubility of LiX)}$$

Notes

1. Albeit suitably fudged through such niceties as the Aufbau principle and other approximations.

* Despite the fruitfulness of this observation, in general it is important to reduce the potential for observer bias by checking observations like these against compounds reported in the chemical literature and databases like the Inorganic Crystal Structure and Cambridge Crystallographic Databases.

** These are very soluble in water, to the point where some solutions are perhaps better described as solutions of water in the halide.

† This can be predicted based on the relative hardness of BF_3, BR_3, and BH_3 in the list of hard and soft acids. However, for those of you who may be confused as to why H is considered a better electron donor for the purposes of softening a Lewis acid center while alkyl groups are better electron donors for the purposes of stabilizing carbocations in organic chemistry, the dominant effect is the lower electronegativity of H relative to carbon (in CH_3). The effect of electron donation due to hyperconjugation isn't as great for thermodynamically stable bases like BX_3/BR_3.

Section 5.3.3: Hard and Soft Acids and Bases is shared under a CC BY-NC-SA 4.0 license and was authored, remixed, and/or curated by Stephen M. Contakes.

- **6.6: Hard and Soft Acids and Bases** by Stephen M. Contakes is licensed CC BY 4.0.

Section 5.3.3.1: Hard-Hard and Soft-Soft preferences may be explained and quantified in terms of electrostatic and covalent and electronic stabilization on the stability of Lewis acid-base adducts

The Hard Soft Acid Base Principle is a Conceptual Tool for Thinking About Patterns of Lewis Acid-Base Reactivity

The explanation of the trends in metal distribution, halide salt solubility, and preferred metal coordination patterns is rooted in Arland, Chatt, and Davies' observation that *Lewis acids and bases could be classified into two groups based on their propensity to form stable compounds with one another* (*e.g.* acids in a class tend to form more stable adducts with bases in the same class than they did with bases in the other).[1] Arland, Chatt, and Davies somewhat boringly termed these groups class a and class b but today they are known by Ralph Pearson's name for them. Pearson called the class a acids and bases hard and class b acids and bases soft. These terms reflect how "soft" these substance's electron clouds are towards distortion or, in other words, their polarizability (Figure ***Section*5.3.3.1.1**). Pearson terms acids and bases which are relatively polarizable **soft** and those which are difficult to polarize **hard.**

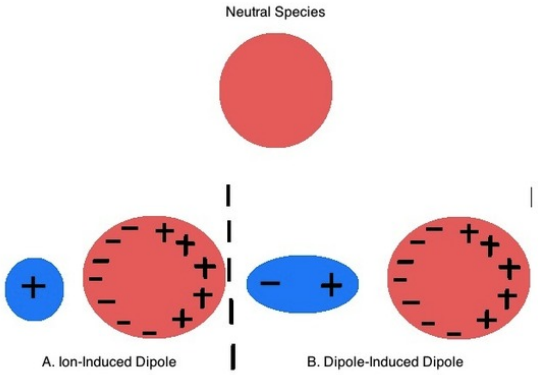


Figure ***Section*5.3.3.1.1**: Polarizability refers to the ease with which a substance's electron cloud may be distorted under the action of an electric field. A fragment's polarizability determines the degree to which its electron cloud is distorted by A.) an Ion and B.) a polar molecule to induce a dipole moment. The figure is taken from (and the caption expanded from) Cox, Kelly and Dana Reusser "Polarizability"

Recognizing Hard and Soft Acids and Bases

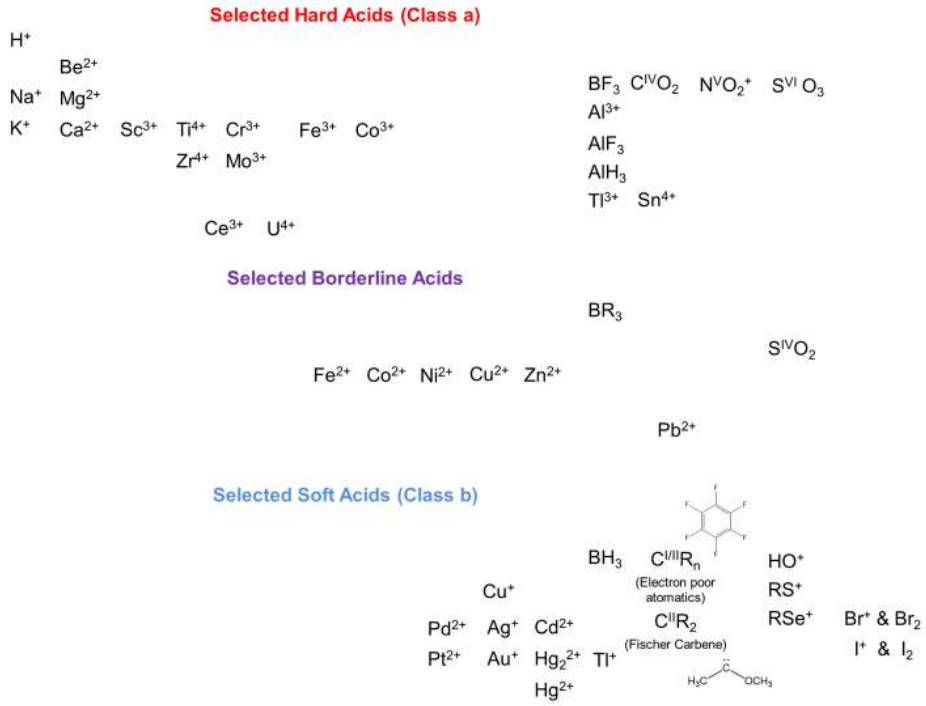
Hard acids and bases come in two varieties:

1. hard acid and base sites that possess few valence electrons and for which polarization therefore involves distorting core electrons, which are difficult to distort because they are close to the nucleus and experience a high nuclear charge. The most common examples of such substances are Lewis acid hard acids towards the left of the periodic table.
2. hard acid and base sites with a high charge density (highly charged relative to size) and/or which are electron deficient. In these cases polarization involves distorting electrons that already experience strong unshielded electrostatic interactions.

Soft acids and bases also come in two varieties

1. soft acids and bases which posses many valence electrons and so are more readily polarized. In consequence, all other things being equal, soft acids and bases are more likely to be found towards the middle or right of the periodic table.
2. soft acids and bases with little charge density and/or which are relatively electron rich.

Note that the hard-soft classification should not be thought of as if all hard acids and bases are equally hard and all soft acids and bases equally soft. There is a graduation in hardness and softness and a number of intermediate acids and bases which do not fit neatly in either category. With this caveat in mind, representative **hard, soft, and borderline acids** are given below. Notice how they illustrate the trends just outlined.



As expected, hard acids tend to be found towards the left side of the periodic table and involve higher oxidation states and/or electron donating substituents while soft acids are more common to the right of the periodic table and involve lower oxidation states and/or electron donating substituents.

Illustrative hard, soft, and borderline bases are given below. Again, notice how these substances illustrate the general trends.

Selected Hard Bases (Class a)

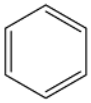
Nitrogen bases	Oxygen bases		small halides
NH_2^-	OH^-	CO_3^{2-}	F^-
NH_3	H_2O	RCO_2^-	Cl^-
RNH_2	ROH	NO_3^-	
NH_2NH_2	ROR	PO_4^{3-}	
		SO_4^{2-}	

Selected Borderline Bases

electron-poor Nitrogen bases		low oxidation state element oxyanions	intermediate halides
N_3^-		NO_2^-	
NO_2^-			Br^-
SCN^-		SO_3^{2-}	
N_2			

Selected Soft Bases (Class b)

Carbon bases	P and As bases	Sulfur bases	large halides & pseudohalides
R^-	PR_3	RS^-	H^-
CO	$P(OR)_3$	RSH	I^-
CN^-	AsR_3	RSR	
RNC		SCN^-	
$R_2C{=}CR_2$ (alkenes)			



(electron-rich aromatics)

Qualitative Estimation of the Relative Hardness and Softness of Lewis Acids and Bases

As can be seen from the examples above, **hard acids are relatively electron-poor and hard bases electron-rich** since they have comparatively

- small frontier orbitals, reflective of their relatively small atom/ion/fragment sizes
- high (for acids) or low (for bases) oxidation states on the base atom, reflected in a large positive formal charge (for acids) or negative formal charge (for bases)
- low polarizability, due to loss or gain of substantial numbers of electrons, or the localization of
  - positive charge on an electropositive element or an atom bearing electron-withdrawing substituents
  - negative charge on an electronegative element or an atom bearing electron-donating substituents

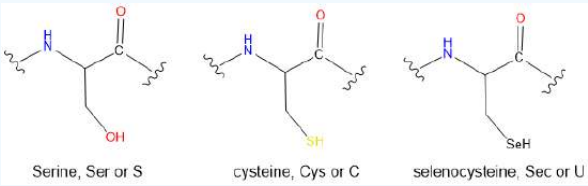
In contrast to hard acids and bases, **soft acids are relatively electron-rich and soft bases larger and more electron poor** since they have comparatively

- large frontier orbitals, reflective of their relatively large atom/ion/fragment sizes
- low oxidation states, often resulting in small or nonexistent atomic charges
- high polarizability, as might be expected of species in which electron-electron repulsions are lower and electrons are spread over a large volume. Sometimes this is indicated by
  - positive charge on an electronegative element or an atom bearing electron-donating substituents
  - negative charge on an electropositive element or an atom bearing electron-withdrawing substituents

Exercise *Section*5.3.3.1.1

Rank the acids or bases in each set in increasing order of expected hardness.

a. Cr^{2+} and Cr^{3+}
b. H^+, Cs^+, and Tl^+
c. SCN^- (acting as a base at N) and SCN^- (acting as a base at S)
d. AlF_3, AlH_3, $AlMe_3$
e. The side chains of the following proteinogenic amino acids

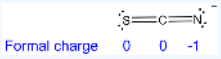


Answer

(a) $Cr^{2+} < Cr^{3+}$ All other things being equal, hardness increases with oxidation state.

(b) $Tl^+ < Cs^+ < H^+$ The order reflects Cs^+ and Tl^+'s larger size relative to H^+ (which doesn't possess any electrons that can be polarized anyway) and that Tl^+ still possesses two valence electrons while Cs^+ possesses none.

(c) SCN^- (acting as a base at S) < SCN^- (acting as a base at N). The order reflects the greater electronegativity of N than S and N's possession of a more negative formal charge of -1.



(d) $AlH_3 < AlMe_3 < AlF_3$. The hardness increases as the substituents on the Lewis acid Al center become less electron donating and more electron withdrawing (and, incidentally, harder bases) as their electronegativity increases in the order $H^- < CH_3^- < F^-$. Note that the order of electron donating ability for H^- and CH_3^- is the opposite observed for carbocations, for which hyperconjugation plays a larger role.

(e) Sec < Cys < Ser. The hardness increases as the electronegativity of the Lewis base chalcogen increases on going from a selenol to a thiol to an alcohol.

The Hard-Soft Acid-Base Principle (HSAB Principle)

The **Hard-Soft acid-base principle (HSAB Principle) explains patterns in Lewis acid-base reactivity in terms of a *like reacts with like preference***. Both thermodynamically and kinetically, hard acids prefer hard bases and soft acids soft bases. Specifically,

- Thermodynamically, hard acids form stronger acid-base complexes with hard bases while soft acids form stronger complexes with soft bases.
- Kinetically, hard acids/electrophiles react more quickly with hard bases/nucleophiles while soft acids/electrophiles react more quickly with soft bases/neucleophiles.

Applications of the HSAB principle include

1. Predicting the equilibrium or speed of *Lewis acid-base metathesis and displacement reactions.* In a Lewis acid-base **metathesis reaction** the acids and bases swap partners

$$\mathbf{A_1 : B_1 + A_2 : B_2 \overset{k_1,\, K_{eq_1}}{\rightleftharpoons} A_1 : B_2 + A_2 : B_1}$$

For example, the equilibrium position of the metathesis reaction between **TlF** and $\mathbf{K_2S}$ favors the products:

$$\mathbf{2\,TlF + H_2S \rightleftharpoons Tl_2S + 2\,KF}$$

consistent with the HSAB's hard-hard and soft-soft preference.



The HSAB principle also allows for prediction of the position of displacement reactions, in which a Lewis acid or base forms an adduct using a base or acid from an existing Lewis acid-base complex. In these reactions, the displacement of acid or base from the reactant complex may be thought of as a sort of metathesis reaction, one in which in the unbound acid or base switches places with one in the complex. For example, the reaction between **HI** and methylmercury cation

$$\mathbf{HI + HgSCH_3^+ \rightleftharpoons CH_3SHgI + H^+}$$

involves displacement of an iodide from **HI** to give $\mathbf{CH_3HgI}$. The position of the equilibrium favors $\mathbf{CH_3HgI}$ since both $\mathbf{CH_3Hg^+}$ and $\mathbf{I^-}$ are soft, while $\mathbf{H^+}$ is a hard acid.



Exercise *Section*5.3.3.1.2

Predict the position of equilibrium for the following reaction.

$$\mathbf{Fe_2O_3 + 3\,Ag_2S \rightleftharpoons Fe_2S_3 + 3\,Ag_2O}$$

Answer

The equilibrium will favor the reactants (K<1) since the hard-hard and soft-soft interactions in the reactants are more stable than the hard-soft interactions in the products.



Exercise *Section*5.3.3.1.3

Predict whether K for the following equilibria will be <<1, ~1, or >>1.

a. $\mathbf{2\,HF + (CH_3Hg)_2S \rightleftharpoons 2\,CH_3HgF + H_2S}$
b. $\mathbf{Ag(NH_3)_2^+ + 2\,PH_3 \rightleftharpoons Ag(PH_3)_2^+ + 2\,NH_3}$
c. $\mathbf{Ag(PH_3)_2^+ + 2\,H_3B{-}SH_2 \rightleftharpoons 2\,H_3B{-}PH_3 + Ag(SH_2)_2^+}$
d. $\mathbf{H_3B{-}NH_3 + F_3B{-}SH_2 \rightleftharpoons H_3B{-}SH_2 + F_3B{-}NH_3}$

Answer

a. K< < 1 since the reactant adducts are hard-hard and soft-soft while the products involve hard-soft interactions.

b. K>>1 since the reactant complex, diamine silver(I), is a complex of a hard base, NH_3, with the soft acid, Ag^+, while the product is a complex of the same soft acid with the soft base phosphine.

c. K~1 since all the adducts amongst the reactants and products involve soft acids and bases.

d. K>>1 since BH_3 is a softer acid than BF_3, so it will form a stronger complex with the softer base H_2S while the harder BF_3 forms a stronger complex with the harder base NH_3.

2. Predicting the relative strengths of a given set of *Lewis acids or bases towards a particular substrate*. Consider, for example, the relative strengths of a BH_3, BMe_3, and BF_3 towards group 15 hydrides like NH_3, PH_3, and AsH_3. Of the

boranes listed, the hardest acid BF_3 is the strongest acid towards the hard base NH_3 while BH_3 is the strongest towards AsH_3.[†]

? Exercise *Section*5.3.3.1.4

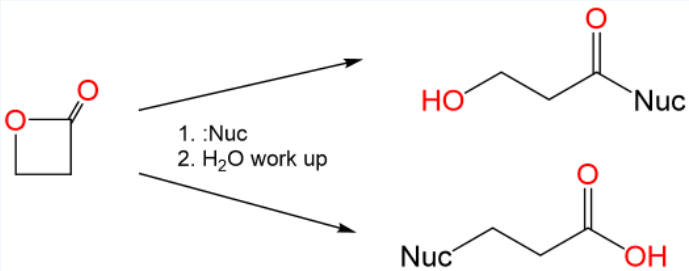
Which acid will form the most stable complex with **CO**: $\mathbf{BH_3}$, $\mathbf{BF_3}$, or $\mathbf{BMe_3}$?

Answer

$\mathbf{BH_3}$. Since **CO** forms complexes primarily through its carbon lone pair, it is a soft base and so will form the strongest complex with the softest Lewis acid.

? Exercise *Section*5.3.3.1.5

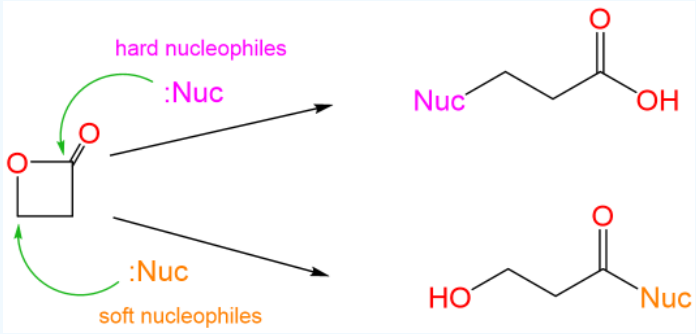
When lactones react with nucleophiles, they can undergo ring opening reactions to give either an alcohol or a carboxylic acid, as shown for propiolactone below:



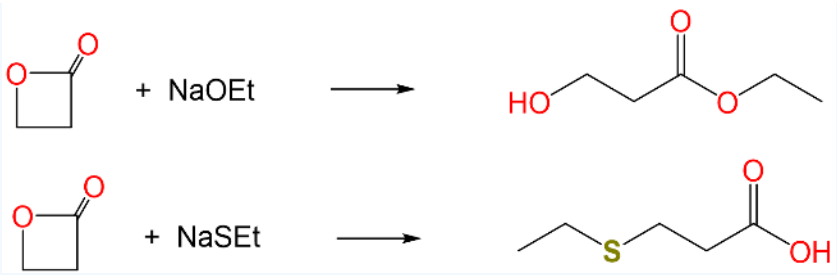
In the reaction above, sterically unhindered alkoxides give one product and sterically unhindered thioalkoxides the other. Explain why this is the case and predict the products of the reaction between propiolactone and the sodium salts of ethoxide and thioethoxide.

Answer

The two reaction products correspond to nucleophilic attack at the lactones' two electrophilic carbon centers. Specifically, the acid is produced by attack at the softer C^{I} center of the CH_2 directly attached to the ester oxygen and the alcohol by nucleophilic attack at the harder C^{III} center of the ester carbonyl.



Consequently, it is reasonable to expect that the harder base ethoxide will nucleophilically attack the harder carbonyl carbon while the softer thioethoxide will attack the softer methylene carbon.



The theoretical interpretation of the hard-soft acid-base principle is that hard-hard preferences reflect superior electrostatic stabilization while soft-soft preferences reflect superior covalent stabilization.

The hard-hard and soft-soft preferences in Lewis acid-base interactions reflect that

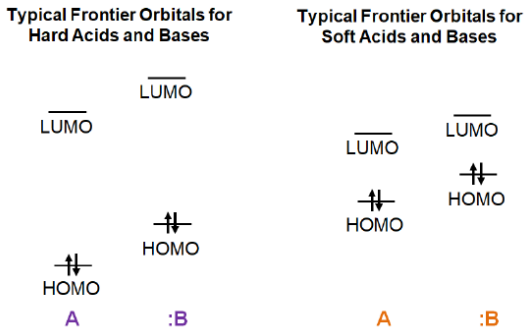
- The lone pair of a hard base is strongly stabilized electrostatically by a hard acid.
- The lone pair of a soft base is strongly stabilized by forming a covalent bond with a soft acid.
- The lone pair of a hard or soft base is comparatively weakly stabilized by an acid opposite to it in hardness or softness since the overall electrostatic and covalent stabilization of the adduct is comparatively weak.

To see why this is the case it is helpful to divide the contributions to the interaction energy between an acid and a base as follows:

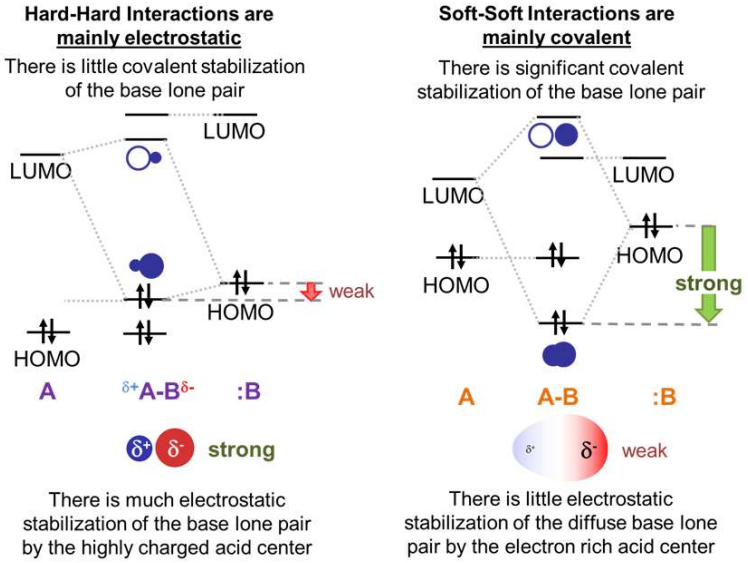
$$\text{Interaction Energy} = \underbrace{\text{Electrostatic attractions and repulsions of partial atomic charges}}_{\text{Ionic term}} + \underbrace{\text{Interactions between filled orbitals on one fragment and unfilled orbitals on the other}}_{\text{Covalent term}} + \underbrace{\text{Electrostatic repulsions between filled orbitals on the two fragments}}_{\text{Steric term}}$$

Of the three contributions to the interaction energy, only the ionic and covalent terms directly relate to the hardness of the interacting acid and base. One approach to thinking about how hardness influences the ionic and covalent contributions is to consider the frontier orbitals involved in the acid-base interaction. This is sometimes done through the use of the Salem-Klopman equation,[1,*] although in the treatment which follows a more qualitative approach will be employed.

Both hard acids and bases will have comparatively low energy HOMO levels and high energy LUMO levels, with a correspondingly high HOMO-LUMO gap. In contrast, soft acids and bases will have comparatively high-energy HOMO levels and low-energy LUMO levels, giving a comparatively smaller HOMO-LUMO gap.



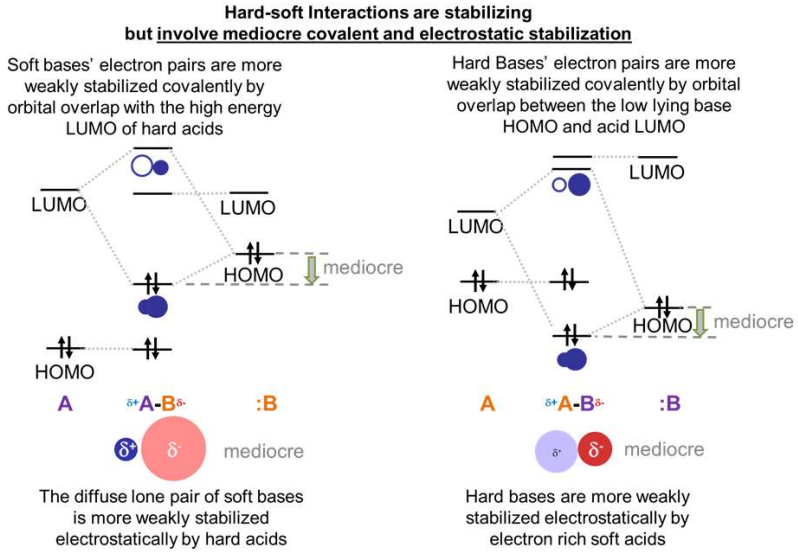
Given this, consider the frontier orbital interactions involved in the formation of an acid-base complex for the possible cases, as illustrated schematically below.



The large gap in energy between hard bases' highly stabilized HOMO lone pairs and the high energy LUMO of hard acids ensures that in **hard acid-hard base adducts the dominant stabilizing interaction will involve electrostatic attraction between the base lone pair and the electropositive Lewis acid center**. Fortunately, since the electron clouds in hard bases are relatively dense and electron rich while hard Lewis acids are highly charged and small, these electrostatic interactions are strong.

In contrast, in **soft acid-soft base adducts, the dominant stabilizing interaction will be covalent.** This is because the small gap in energy between a soft base HOMO and soft acid LUMO enables the formation of a well-stabilized bonding orbital with significant electron density between the acid and base.

The orbitals' interactions between hard acids and soft bases and soft acids and hard bases are intermediate between the hard acid-hard base and soft acid-soft base cases.



This means that the adducts are stable relative to free acid and base – just not as well stabilized as in the hard acid and hard base case. In the case of hard acids and soft bases the hard acids are less able to stabilize the soft bases' relatively diffuse electron pair electrostatically and there isn't as much covalent stabilization as in adducts of soft acids and bases due to the hard acid's high energy.

References

1. Ahrland, S.; Chatt, J.; Davies, N. R., The relative affinities of ligand atoms for acceptor molecules and ions. Quarterly Reviews, Chemical Society 1958, 12 (3), 265-276.

2. Pearson, R. G., Hard and Soft Acids and Bases. Journal of the American Chemical Society 1963, 85 (22), 3533-3539.

3. Fleming, I., Molecular orbitals and organic chemical reactions. Reference ed.; Wiley: Hoboken, N.J., 2010.

Notes

* Despite the fruitfulness of this observation, in general it is important to reduce the potential for observer bias by checking observations like these against compounds reported in the chemical literature and databases like the Inorganic Crystal Structure and Cambridge Crystallographic Databases.

** These are very soluble in water, to the point where some solutions are perhaps better described as solutions of water in the halide.

† This can be predicted based on the relative hardness of BF_3, BR_3, and BH_3 in the list of hard and soft acids. However, for those of you who may be confused as to why H is considered a better electron donor for the purposes of softening a Lewis acid center while alkyl groups are better electron donors for the purposes of stabilizing carbocations in organic chemistry, the dominant effect is the lower electronegativity of H relative to carbon (in CH_3). The effect of electron donation due to hyperconjugation isn't as great for thermodynamically stable bases like BX_3/BR_3.

†† For more on the Salem-Klopman equation see Fleming, I., Molecular orbitals and organic chemical reactions. Reference ed.; Wiley: Hoboken, N.J., 2010; pp. 138-143.

Section 5.3.3.1: Hard-Hard and Soft-Soft preferences may be explained and quantified in terms of electrostatic and covalent and electronic stabilization on the stability of Lewis acid-base adducts is shared under a CC BY-NC-SA 4.0 license and was authored, remixed, and/or curated by Stephen M. Contakes.

- **6.6.2: Hard-Hard and Soft-Soft preferences may be explained and quantified in terms of electrostatic and covalent and electronic stabilization on the stability of Lewis acid-base adducts** by Stephen M. Contakes is licensed CC BY 4.0.

Section 5.3.3.2: Quantitative Measures of Hardness, Softness, and Acid-Base Interactions from a Hard Soft Acid-Base Principle Perspective Involve Orbital Energies and/or Apportioning Acid-Base Bonding in Terms of Electrostatic and Covalent Factors

Pearson Absolute Hardness is a useful metric of hardness based on orbital energies

The recognition that hard acids and bases possess a large HOMO-LUMO gap suggests that the gap size itself might serve as a useful index of hardness. The basis for this idea may be found by considering Pearson's definition of absolute hardness, η.[1] **Pearson's absolute hardness, η**, is half the second derivative of a species' energy with respect to changes in total number of electrons, N_{e^-}.

$$\text{Pearson's absolute hardness} = \eta = \frac{1}{2}\frac{d^2E}{dN_{e^-}^2}$$

$$(in \;\; eV)$$

and, since acids' and bases' hardness and softness are inversely related, Pearson's absolute softness, σ, is just the inverse of hardness.

$$\text{Pearson's softness} = \frac{1}{\eta}$$

Of these, Pearson's absolute hardness is related to the **Mulliken definition of electronegativity** as the first derivative of a species' energy with respect to changes in total number of electrons.

$$\text{Mulliken electronegativity} = \chi = \frac{dE}{dN_{e^-}}$$

$$(in \;\; eV)$$

Operationally, both the Pearson hardness and Mulliken electronegativity are approximated in terms of the energies associated with unit changes in the number of electrons – *i.e.*, in terms of ionization energies and electronegativities. Specifically,

$$\text{Pearson's absolute hardness} = \eta \approx \frac{IE - EA}{2}$$

$$\text{Mulliken electronegativity} = \chi \approx \frac{IE + EA}{2}$$

where IE and EA are in eV.

The connection between Pearson's absolute hardness/softness and the HOMO-LUMO gap then follows from Koopman's theorem, in which the ionization energy (IE) is just the opposite of the HOMO energy.

$$IE = -E_{HOMO}$$

Similarly, the electron affinity (EA), defined as the opposite of the energy released on absorption of an electron, may be taken as an approximation of the LUMO energy.

$$E_{LUMO} \approx -EA$$

So Pearson's absolute hardness is just half the HOMO-LUMO gap (band gap) size in electron volts:

$$\text{Pearson's absolute hardness} = \eta \approx \frac{E_{LUMO} - E_{HOMO}}{2}$$

where all values are given in eV,

and the Mulliken electronegativity is just the average of the HOMO and LUMO energies (~Fermi energy):

$$Mulliken\ electronegativity, \chi \approx -\frac{E_{LUMO} + E_{HOMO}}{2}$$

where all values are given in eV

The relationships between the Pearson absolute hardness, Mulliken electronegativity, and HOMO and LUMO energies are depicted schematically for the group 1A monocations in Figure ***Section*5.3.3.2.1**.

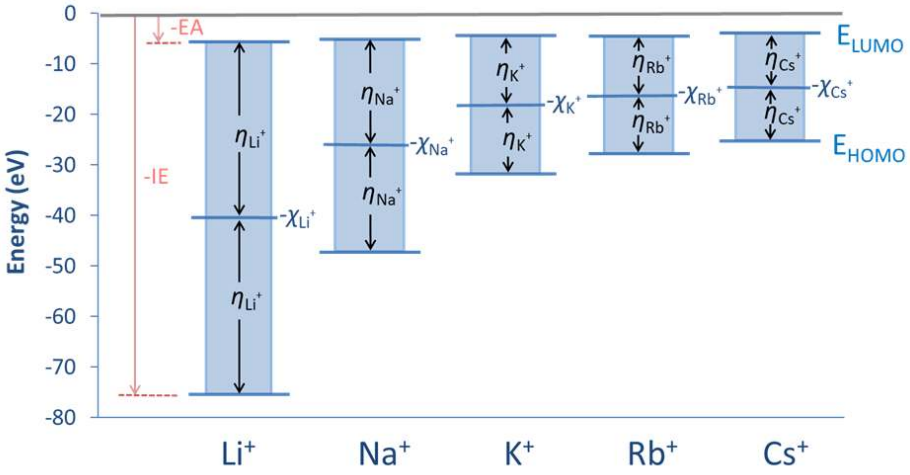


Figure ***Section*5.3.3.2.1**. Relationships between Pearson absolute hardness, Mulliken electronegativity, and HOMO and LUMO energies for the group 1A monocations.

Values of the Pearson hardness and Mulliken electronegativity for several acids and bases are given in Table ***Section*5.3.3.2.1**. The values in the table confirm the expected trends, showing an increase in hardness with size (down a group), with increasing charge, and as substituent electronegativity increases for a series of isolobal ions.

Table ***Section*5.3.3.2.1**: Pearson Absolute Hardness and Related Parameters for Selected Acids and Bases.[2] Taken from Pearson, R. G., Absolute electronegativity and hardness: application to inorganic chemistry. Inorganic Chemistry 1988, 27 (4), 734-740.

Species	Ionization Energy, IE or I (eV)	Electron Affinity, EA or A (eV)	Mulliken Electronegativity, χ (eV)	Pearson Absolute Hardness, η (eV)
Selected Acids				
Group 1A monocations				
Li^+	75.64	5.39	40.52	35.12
Na^+	47.29	5.14	26.21	21.08
K^+	31.63	4.34	17.99	13.64
Rb^+	27.28	4.18	15.77	11.55
Cs^+	25.1	3.89	14.5	10.6
Group 11 monocations				
Cu^+	20.29	7.73	14.01	6.28
Ag^+	21.49	7.58	14.53	6.96
Au^+	20.5	9.23	14.9	5.6
Isoelectronic Row 3 Metal Cations				
Na^+	47.29	5.14	26.21	21.08
Mg^{2+}	80.14	15.04	47.59	32.55
Al^{3+}	119.99	28.45	74.22	45.77
Changes with Transition Metal Ion Charge				
Fe^{2+}	30.65	16.18	23.42	7.24
Fe^{3+}	54.8	30.65	42.73	12.08
Co^{2+}	33.50	17.06	25.28	8.22
Co^{3+}	51.3	22.5	42.4	8.9
Boron trihalides				
BF_3	15.81	-3.5	6.2	9.7
BCl_3	11.60	0.33	5.97	5.64
BBr_3	10.51	0.82	5.67	4.85
CO_2	13.8	-3.8	5.0	8.8
CS_2	10.08	0.62	5.35	5.56
Selected Bases				
Group 17 monoanions (taken to be identical to the free atom values; for arguments as to why this is reasonable see Pearson, R. G., Inorg. Chem. 1988, 27 (4), 734-740.)				
F^-	17.42	3.40	10.41	7.01
Cl^-	13.01	3.62	8.31	4.70
Br^-	11.84	3.36	7.60	4.24
I^-	10.45	3.06	6.76	3.70

Species	Ionization Energy, IE or I (eV)	Electron Affinity, EA or A (eV)	Mulliken Electronegativity, χ (eV)	Pearson Absolute Hardness, η (eV)
Group 15 hydrides				
NH_3	10.7	-5.6	2.6	8.2
PH_3	10.0	-1.9	4.1	6.0
Trimethylpnictides				
NMe_3	7.8	-4.8	1.5	6.3
PMe_3	8.6	-3.1	2.8	5.9
$AsMe_3$	8.7	-2.7	3.0	5.7
Group 16 hydrides				
H_2O	12.6	-6.4	3.1	9.5
H_2S	10.5	-2.1	4.2	6.2
Phosphorous trihalides				
PF_3	12.3	-1.0	5.7	6.7
$PC1_3$	10.2	0.8	5.5	4.7
PBr_3	9.9	1.6	5.6	4.2

Drago-Wayland Acid-Base Parameters allow for estimation of the electrostatic and covalent contributions to the enthalpy of formation of a Lewis acid-base adduct.

Although Pearson hardness values are a useful metric of acids' and bases' hardness, they cannot easily be used to estimate the Lewis acid-base interaction energy. This is not the case for the EC model developed by Drago and Wayland.[3] In the **Drago and Wayland's EC Model,** the enthalpy of formation of an acid-base adduct, AB,

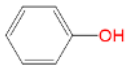
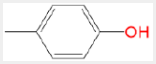
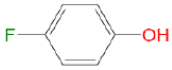
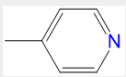
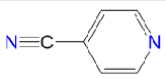
$$A + B \rightleftharpoons AB \qquad \Delta H_{AB\ adduct}$$

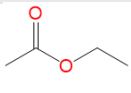
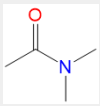
from the acid (A) and base (B) can be calculated as the sum of products of electrostatic (E) and covalent (C) factors that reflect the propensity of the acid and base to engage in strong electrostatic and covalent interactions with one another:

$$-\Delta H_{AB\ adduct} = E_A E_B + C_A C_B$$

where E_A and C_A are the electrostatic and covalent parameters for the acid and E_B and C_B the electrostatic and covalent parameters for the base given in units of $kcal^{½}\ mol^{-½}$. E and C parameters for selected acids and bases are given in Table ***Section*5.3.3.2.2** .

Table ***Section*5.3.3.2.2**: E and C Parameters for selected Lewis acids and bases according to the ECW model.[4,5] Taken from Vogel, G. C.; Drago, R. S., The ECW Model. *Journal of Chemical Education* 1996, 73 (8), 701 and Drago, R. S. A modern approach to acid-base chemistry. *Journal of Chemical Education* 1974, 51 (5), 300 (for BF_3).

Species	E (kcal^{½} mol$^{-½}$)	C (kcal^{½} mol$^{-½}$)	W (kcal mol^{-1})	C/E
Acids				
I_2	0.5†	2†	0	4
ICl	2.92	1.66	0	0.57
H_2O	1.31	0.78	0	0.59
SO_2	0.51	1.56	0	3.1
$HCCl_3$ (chloroform)	1.56	0.44	0	0.28
$(CH_3)_3COH$	1.07	0.69	0	0.65
$(CF_3)_3COH$	3.06	1.88	-0.87	0.61
	2.27	1.07	0	0.47
	2.23	1.03	0	0.46
	2.30	1.11	0	0.48
	1.38	0.68	0	0.49
BF_3	1.62	9.88		6.10
$B(CH_3)_3$	2.90	3.60	0	1.2
$Al(CH_3)_3$	8.66	3.68	0	0.43
$Ga(C_2H_5)_3$	6.95	1.48	0	0.21
$In(CH_3)_3$	6.60	2.15	0	0.33
$Zn[N(Si(CH_3)_3)]_2$	2.75	2.32	0	0.84
$Cd[N(Si(CH_3)_3)]_2$	2.50	1.83	0	0.73
Bases				
NH_3	2.31	2.04		0.88
CH_3NH_2	2.16	3.13		1.4
$(CH_3)_2NH$	1.80	4.21		2.3
$(CH_3)_3N$	1.21	5.61		4.6
	1.78	3.54		2.0
	1.81	3.73		2.0
	1.53	2.94		1.9

Species	E ($kcal^{½}\ mol^{-½}$)	C ($kcal^{½}\ mol^{-½}$)	W ($kcal\ mol^{-1}$)	C/E
CH_3CN	1.64	0.71		0.43
$ClCH_2CN$	1.67	0.33		0.20
$CH_3C(O)CH_3$	1.74	1.26		0.72
$(C_2H_5)_2O$	1.80	1.63		0.91
	1.64	2.18		1.3
 (EtOAc)	1.63	0.95		0.58
	2.35†	1.31		0.56
$(CH_3)_2S$	0.25	3.75		15
$(CH_3CH_2)_2S$	0.24	3.92†		15
	0.26	4.07		16
$(CH_3)_2Se$	0.05	4.24		83
$(CH_3)_2SO$	2.4	1.47		0.61
$(CH_3)_3P$	0.25	5.81		24
$(CH_3O)_3P$	0.13	4.83		37
$(C_6H_5)_3PO$	2.59	1.67		0.64
$(C_6H_5)_3PS$	0.35	3.65		10
C_6H_6	0.70	0.45		0.64

† These values were fixed to parameterize the rest of the E and C parameters.

Trends in the relative values of C and E for the acids and bases in Table ***Section*5.3.3.2.2** are very roughly consistent with the trends in hardness and softness outlined earlier. However, the parameters suggest that some trends in hardness reflect changes in species' ability to engage in ionic interactions while others reflect changes in species' ability to engage in strong covalent interactions. For example, C_B for the dimethylchalcogenides increases steadily from 1.5 to 4.25 $kcal^{½}\ mol^{-½}$ on going from Me_2O to Me_2Se while E_B decreases from 1.68 to 0.05 $kcal^{½}\ mol^{-½}$, suggesting that electrostatic and covalent factors are both involved in a decrease in base hardness down group 16. However, in the case of phosphines and amines it appears that electrostatic factors are primarily responsible for the decrease in hardness down group 15. On going from Me_3N to Me_3P, C_B only increases slightly from 5.61 to 5.81 $kcal^{½}\ mol^{-½}$ while E_B decreases from 1.21 to 0.25 $kcal^{½}\ mol^{-½}$ - *i.e.*, to 20% of the Me_3N value.

However, some species tend to have very high values for both E and C, reflecting their ability to engage in strong electrostatic and covalent interactions, while others have small values for both, reflecting their relative stability as free species in solution.

As can be seen by comparing the acids and bases listed in the absolute hardness table (Table ***Section*5.3.3.2.1**) and the EC parameters table (Table ***Section*5.3.3.2.2**). The EC model has primarily been applied to organic and main group organometallic acids and bases. However, a variety of extensions have been proposed that enable its wider applicability.

The simple EC model only includes electrostatic and covalent considerations and thus ignores steric, lattice energy, and other contributions to the interaction energy. Thus it is only useful for analyzing the interaction energies of sterically unhindered adducts in which solvation energy and other contributions to the overall interaction energy are insignificant. However, additional refinements of the model attempt to extend its usefulness by accomodating various factors, such as

- *Steric strain.* Specifically, Hancock and Martell[6] introduced a D parameter to account for any additional steric strain introduced upon adduct formation,* giving

$$-\Delta H_{AB\ adduct} = E_A E_B + C_A C_B - D_A D_B$$

- *Charge transfer upon adduct formation.* As discussed in section 6.4.2, the formation of a Lewis acid-base complex results in a net transfer of electron density from the electron donor (base) to the acceptor (acid). Drago and Wong[7] extended the EC model to include that charge transfer by adding what they called receptance factors that account for the acid's ability to receive electron density (R_A) and transference factors that account for the base's ability to donate electron density (T_B), giving

$$-\Delta H_{AB\ adduct} = E_A E_B + C_A C_B + R_A T_B$$

  This extension of the EC model is called the **electrostatic-covalent-transfer or ECT model**. Notably, it has been applied successfully to adducts involving ions, for which the $R_A T_B$ term can account for as much as 31% of the interaction energy.

- *Any constant energy term, such as the energy needed to cleave a dimer in order to make the Lewis acid (e.g., $Al_2Cl_6 \rightarrow 2AlCl_3$).* Drago and Vogel[4] extended the EC model to accommodate these constant energy terms, which they designated W. The resulting model is called the **ECW model,** for which

$$-\Delta H_{AB\ adduct} = E_A E_B + C_A C_B + W$$

where

$$W = W_A + W_B$$

A simple application of EC and extended EC models is that they allow the enthalpy of adduct formation to be calculated. These enthalpy calculations based on the EC model are consistent with the superior interaction energy of hard-hard and soft-soft interactions compared to hard-soft ones. Consider, for example, the transfer of I_2 between BF_3 and $InMe_3$, H_3N-BF_3, and H_3N-$InMe_3$.

$$H_3N - BF_3 + InMe_3 \rightleftharpoons BF_3 + H_3N - InMe_3$$

Since H_3N is a hard base and BF_3 and $InMe_3$ are harder and softer acids, respectively, the equilibrium is expected to favor the reactant, H_3N-BF_3. Assuming the equilbrium is enthalpically driven, this qualitative analysis is consistent with the expected endothermic enthalpy of the reaction, as may be seen from the calculated enthalpies of adduct formation for both H_3N-BF_3 and H_3N-$InMe_3$.

For H_3N-BF_3:

$$-\Delta H_{H_3N-BF_3} = E_{BF_3} E_{NH_3} + C_{BF_3} C_{NH_3}$$

$$-\Delta H_{H_3N-BF_3} = (1.62)(2.31) + (9.88)(2.04)$$

$$-\Delta H_{H_3N-BF_3} = 3.74\ kcal/mol + 20.1\ kcal/mol = 23.8\ kcal/mol$$

$$\Delta H_{H_3N-BF_3} = -23.8\ kcal/mol$$

For H_3N-$InMe_3$:

$$-\Delta H_{H_3N-InMe_3} = E_{InMe_3} E_{NH_3} + C_{InMe_3} C_{NH_3}$$

$$-\Delta H_{H_3N-InMe_3} = (6.6)(2.31) + (2.15)(2.04)$$

$$-\Delta H_{H_3N-InMe_3} = 15.25\ kcal/mol + 4.39\ kcal/mol = 19.63\ kcal/mol$$

$$\Delta H_{H_3N-InMe_3} = -19.63\ kcal/mol$$

So H_3N-BF_3 is enthalpically favored by -4.2 kcal/mol [=-23.8 kcal/mol - (-19.63 kcal/mol) according to Hess' Law].

In addition to their utility for estimating enthalpies of Lewis acid-base complex formation, EC and related models serve as a useful tool for estimating the relative importance of ionic, covalent, and steric factors in complex formation. Specifically,

- The relative contributions of ionic and covalent factors can be calculated directly, as from the E and C terms. This can provide insight into why some complexes are more stable than others. Such calculations reveal that the hard-hard adduct H_3N-BF_3 is favored over the hard-soft adduct H_3N-$InMe_3$ because of the strong covalent interaction holding together H_3N-BF_3. The covalent term accounts for 84% of the energy of the H_3N-BF_3 interaction and is largely lost upon formation of H_3N-$InMe_3$, for which it contributes only 22% of the interaction energy. When the electrostatic term is accounted for, it can be seen that the formation of H_3N-$InMe_3$ from H_3N-BF_3 is disfavored, since it would result in a loss of 15.7 kcal/mol of covalent stabilization that would be incompletely compensated for by a gain of 11.5 kcal/mol of electrostatic stabilization.
- The role of other contributions to the bonding in a Lewis acid-base complex may be estimated from the discrepancy between the experimental and EC model calculated stabilization energies. This is because the EC parameters assume sigma bonding and so any deviation between the calculated and experimental enthalpies of complex formation can be attributed to non-sigma contributions.
    - This is done explicitly in extensions of the EC model. For instance, in the case of the Hancock and Martell, ECT, and ECW extensions of the EC model, the contributions of the steric, charge transfer, and constant energy factors (like dimer dissociation) are directly computed in the model.
    - Comparisons of the difference between the energies calculated using ordinary EC parameters and the observed enthalpies has also been used as an estimate of the
        - steric strain energy in strained adducts, which exhibit a less exothermic heat of adduct formation than expected
        - π-backbonding energy in adducts which are capable of such interactions and exhibit a more exothermic heat of formation than expected.[8-10]
    - For examples see (a) Drago, R. S., The interpretation of reactivity in chemical and biological systems with the E and C model. Coordination Chemistry Reviews 1980, 33 (3), 251-277; (b) Drago, R. S.; Bilgrien, C. J., Inductive transfer and coordination of ligands in metal—metal bonded systems. Polyhedron 1988, 7 (16), 1453-1468; (c) Drago, R. S., The question of a synergistic metal-metal interaction leading to .pi.-back-bond stabilization in dirhodium tetrabutyrate adducts. Inorganic Chemistry 1982, 21 (4), 1697-1698.
- The role of electrostatic, covalent, and other contributions to the spectroscopic behavior of Lewis acid-base complexes can be assessed similarly using specialized versions of the ECW or ECT model that allow for calculation of changes in spectroscopic parameters upon adduct formation - *e.g.*, OH stretching frequencies. Details are beyond the scope of this text but may be found in the original literature,[11] for example, Drago, R. S.; Vogel, G. C. *JACS* 1992, 114 (24), 9527-9532; Vogel, G. C.; Drago, R. S., *J. Chem. Educ.* 1996, 73 (8), 701; Drago, R. S.; Wong, N. M., *J. Chem. Educ.* 1996, 73 (2), 123.).

Pearson Softness Parameters have been proposed as a means of calculating the equilibrium constant for formation of a Lewis acid-base adduct, although they are more commonly used to estimate metal toxicity

Pearson also proposed a softness parameter that can be used to estimate the thermodynamics of Lewis acid-base complex formation, this time in the form of the equilibrium constant for

$$A + B \overset{K}{\rightleftharpoons} AB$$

for which Pearson proposed

$$logK = S_A S_B + \sigma_A \sigma_B$$

where S_A and S_B are acid and base parameters related to the strength of the acid-base interaction and σ_A and σ_B are acid and base parameters related to softness. This approach hasn't found as wide an acceptance in studies of chemical reactivity as the Drago-Wayland and absolute hardness parameters. However, because the toxicity of metal ions sometimes depends on their propensity to bind soft Lewis bases in living systems, the softness parameters which Pearson and Mawby subsequently proposed based on the relative energies of metal fluorine and metal iodine bonds[12] have been widely used as a tool for predicting metal ion toxicity.[13]

References

1. Pearson, R. G., Absolute electronegativity and absolute hardness of Lewis acids and bases. *Journal of the American Chemical Society* 1985, 107 (24), 6801-6806.

2. Pearson, R. G., Absolute electronegativity and hardness: application to inorganic chemistry. *Inorganic Chemistry* 1988, 27 (4), 734-740.

3. Drago, R. S.; Wayland, B. B., A Double-Scale Equation for Correlating Enthalpies of Lewis Acid-Base Interactions. *Journal of the American Chemical Society* 1965, 87 (16), 3571-3577.

4. Vogel, G. C.; Drago, R. S., The ECW Model. *Journal of Chemical Education* 1996, 73 (8), 701.

5. Drago, R. S. A modern approach to acid-base chemistry. *Journal of Chemical Education* 1974, 51 (5), 300

6. Hancock, R. D.; Martell, A. E., Hard and Soft Acid-Base Behavior in Aqueous Solution: Steric Effects Make Some Metal Ions Hard: A Quantitative Scale of Hardness-Softness for Acids and Bases. *Journal of Chemical Education* 1996, 73 (7), 654.

7. Drago, R. S.; Wong, N. M., The Role of Electron-Density Transfer and Electronegativity in Understanding Chemical Reactivity and Bonding. *Journal of Chemical Education* 1996, 73 (2), 123.

8. Drago, R. S., The interpretation of reactivity in chemical and biological systems with the E and C model. Coordination Chemistry Reviews 1980, 33 (3), 251-277.

9. Drago, R. S.; Bilgrien, C. J., Inductive transfer and coordination of ligands in metal—metal bonded systems. Polyhedron 1988, 7 (16), 1453-1468.

10. Drago, R. S., The question of a synergistic metal-metal interaction leading to .pi.-back-bond stabilization in dirhodium tetrabutyrate adducts. Inorganic Chemistry 1982, 21 (4), 1697-1698.

11. Drago, R. S.; Vogel, G. C., Interpretation of spectroscopic changes upon adduct formation and their use to determine electrostatic and covalent (E and C) parameters. *Journal of the American Chemical Society* 1992, 114 (24), 9527-9532.

12. Pearson, R. G.; Mawby, R. J. The Nature of Metal-Halogen Bonds in Gutmann, V. *Halogen Chemistry, vol. 3.* Academic Press: London, 1967, pp. 55-84.

13. Kinraide, T. B. Improved Scales for Metal Ion Softness and Toxicity *Environmental Toxicology and Chemistry* 2009, 28 (3), 525-533.

Notes

* More precisely, the D parameters account for the difference in steric strain in the adduct relative to a water adduct of the Lewis acid.

Section 5.3.3.2: Quantitative Measures of Hardness, Softness, and Acid-Base Interactions from a Hard Soft Acid-Base Principle Perspective Involve Orbital Energies and/or Apportioning Acid-Base Bonding in Terms of Electrostatic and Covalent Factors is shared under a CC BY-NC-SA 4.0 license and was authored, remixed, and/or curated by Stephen M. Contakes.

- **6.6.1: Quantitative Measures of Hardness, Softness, and Acid-Base Interactions from a Hard Soft Acid-Base Principle Perspective Involve Orbital Energies and/or Apportioning Acid-Base Bonding in Terms of Electrostatic and Covalent Factors** by Stephen M. Contakes is licensed CC BY 4.0.

Section 5.3.4: Problems

6.07: Problems

Section 5.3.4: Problems is shared under a CC BY-NC-SA 4.0 license and was authored, remixed, and/or curated by LibreTexts.

Section 5.4: Coordination Numbers and Structures

Why Do Coordination Complexes Form the Structures They Do?

As with all chemical structure, coordination complexes form the structures they do so as to best stabilize the metal center and ligands through the formation of metal-ligand bonds. while avoiding destabilizing interactions like steric repulsions. The issue then is how many metal-ligand bonds should be formed and how those bonds should be arranged spatially to give the largest net stabilization possible. This question will eventually be considered in detail in connection with the nature of bonding in coordination compounds. For now, it will be helpful to think about it in terms of seven factors:

The stabilizing effect of metal-ligand bond formation

The driving force for complex formation is the stabilization of electrons in covalent chemical bonds. In the vast majority of cases this largely involves stabilization of the ligand lone pair is as it experiences the effective nuclear charge of the metal, although in a few involves stabilization of metal electrons by ligand nuclei (inverse ligand fields). Regardless, metal-ligand bond formation is stabilizing and classified in the way its effect is to preference the addition of ligands to the complex.

Steric effects

One reason coordination numbers do not increase indefinitely is that only so many ligands can fit around a metal. Exactly how many can fit depends on:

- **Size of metal center:** This is one of the more important factors and many metals tend to exhibit preferred coordination numbers, which depend on their oxidation state and size as shown in Figure ***Section*5.4.1**. Larger inner transition metals like the lanthanides and actinides can accommodate 9-12 sterically undemanding ligands while the smaller transition metals tend to accommodate up to six, although larger coordination numbers are more common for larger low valent metals. Thus molybdenum forms seven and eight coordinate $[Mo^{III}(CN)_7]^{4-}$ and $[Mo^{IV}(CN)_8]^{4-}$ with the sterically undemanding cyano ligand.
- **Size and shape of ligands:** As long as ligands are not excessively rigid and bulky their size is less important than the size of the metal in determining the number of ligands that coordinate. Ligands' ability to donate electrons to the metal center also tends to influence coordination number more than ligand size. However, all other things being equal for a given metal and ligand donor ability, small ligands allow higher coordination numbers while fewer bulky ligands will fit around the metal center. Ligands that are more sterically demanding in the vicinity of the metal center tend to limit the ability of other ligands to bind than those which bind through a small extended group. For example, a bulky isocyanide like tBuCN will sterically crowd the metal less than a bulky phosphine like $^{t}BuH_2P$ would. For this reason the effective size of a ligand is sometimes rated in terms of either a cone angle of space they are estimated to occupy around the metal (called the Tolman cone angle, it is commonly used to evaluate phosphines' steric bulk) or the in terms of the percentage of the metal's coordination sphere the ligand occupies (called the percent buried volume, it is used to estimate the steric impact of *N*-heterocyclic carbenes).

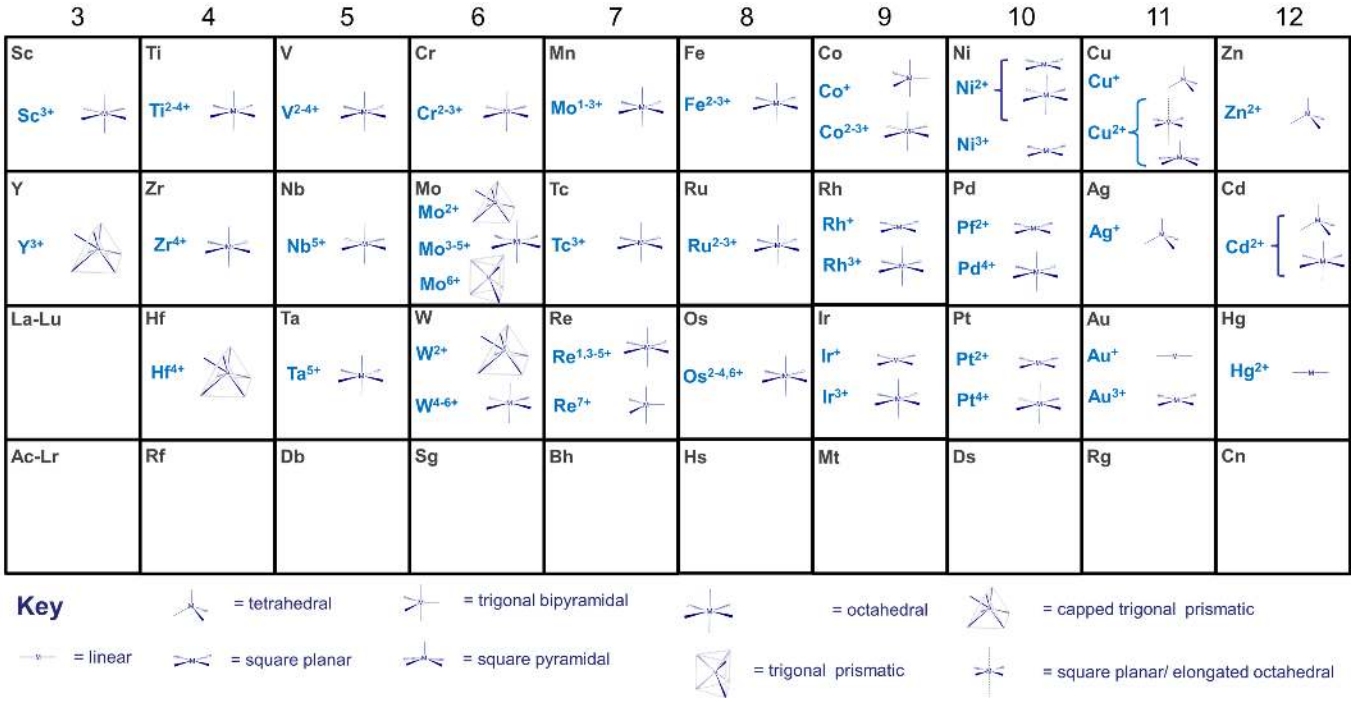


Figure ***Section*5.4.1**. Preferred coordination geometries of the transition elements. Assignments are as reported in reference 1 except for Cu^{2+}, which is assigned above as square planar/elongated octahedral instead of the square planar assignment given in that work.
This work by Stephen Contakes is licensed under a Creative Commons Attribution 4.0 International License.

Repulsion between M-L bonding electrons

For many complexes steric effects are neither the only effects nor the most important. Among the additional factors that should be considered are the repulsions that occur between the electrons that different ligands donate to the metal-ligand bonding. These electron-electron repulsions affect the

- **Coordination number:** When a ligand donates its electrons to a metal center to form a new metal-ligand bond, the electron density around the metal increases, raising the overall energy of the other M-L bonding electrons. This increased repulsion often limits the number of coordinated ligands. As more ligands are added the electron-electron repulsions keep increasing until the lowering of energy of the ligand electrons in the new bond is insufficient to compensate for the raising of energy of the existing M-L bonding electrons. Based on this effect alone:
  - larger metals tend to achieve higher coordination numbers than smaller ones because the electron-electron repulsions are spread across a larger coordiantion sphere.
  - With a given metal, more electron donating ligands have a greater tendency to form complexes with lower coordination numbers than similar neutral ones do. This is why anionic ligands (which tend to be better electron donors) tend to give lower coordination numbers than comparable neutral ligands (which tend to be weaker donors). Thus Co^{2+} forms $CoCl_4^{2-}$ with chloro ligands but $[Co(H_2O)_6]^{2+}$ with aqua ligands.
- **Coordination geometry:** In the Kepert model for the shapes of coordination complexes, this intraligand repulsion determines the most stable coordination geometry by causing the ligands to move as far apart form one another on the metal's coordination sphere as possible.

Formally, according to the Kepert model:

- any of the metal's valence electrons not involved in metal-ligand bonds occupy (n-1)*d* orbitals and function as core electrons. As core electrons they do not influence the molecular shape
- electrons involved in bonding to a given ligand constitute an electron group that repels all other electron groups around the metal.
- all other things being equal the complex will form the geometry that minimizes the repulsions between electron groups.

Notice the similarities of these postulates to those of VSEPR theory. In predicting coordination geometries in terms of electron-electron repulsions, the Kepert model is just an extension of VSEPR theory to coordination compounds. The difference between VSEPR theory and the Kepert model is that in the Kepert model only electrons involved in metal-ligand bonds count.

Coordination geometries predicted by the Kepert model for coordination numbers two through nine are given in Figure ***Section*5.4.2**. As may be seen from the geoemtries listed in Figure ***Section*5.4.2**, these are just equivalent to VSEPR geometries for cases in which the number of electron groups is equal to the coordination number.

The difference between optimal and suboptimal coordination geometries is greater with few ligands and becomes smaller and ligands become increasingly dispersed across the metal's coordination sphere. In complexes containing five, seven, eight, or higher coordinate metals a number of geometries that are similar in energy to the preferred geometry. These geometries, which should be regarded as accessible, are also listed in Figure ***Section*5.4.2**.

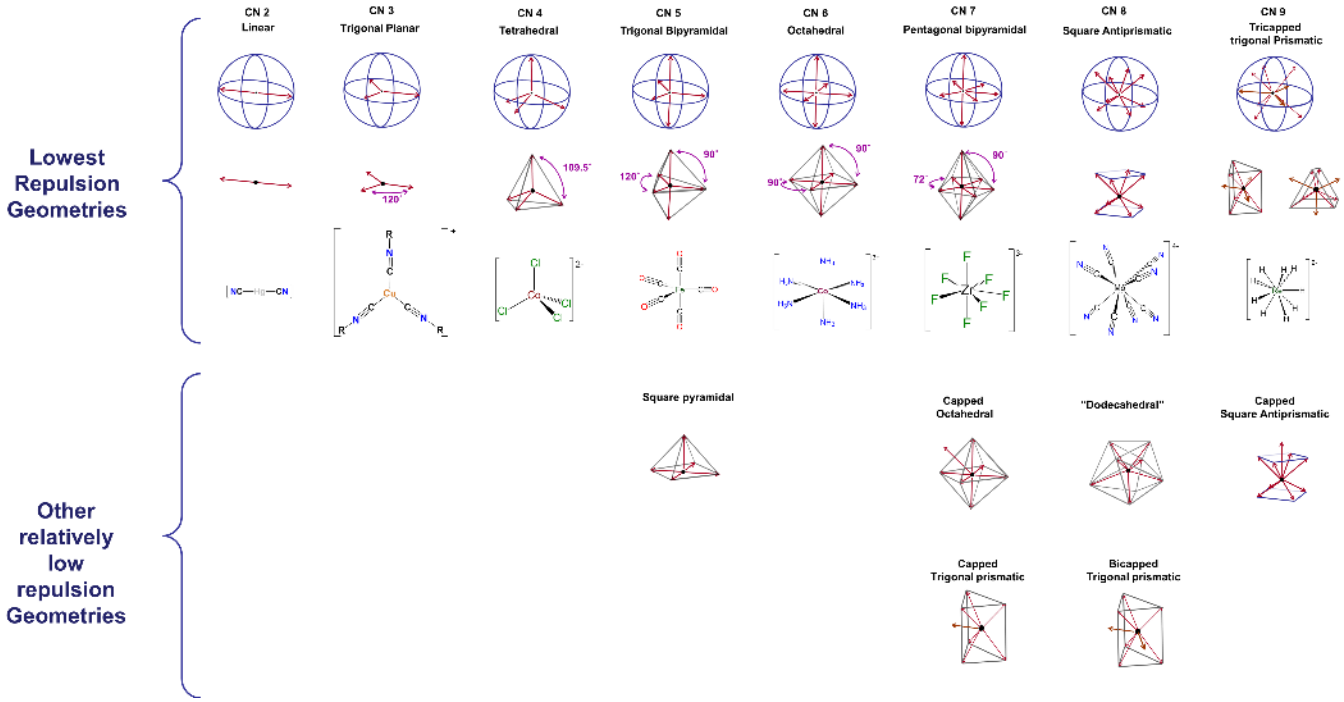


Figure ***Section*5.4.2**. Coordination geometries predicted by the Kepert model for coordination numbers two through nine along with other coordination geometries similar in energy to the lowest repulsion geometry. This work by Stephen Contakes is licensed under a Creative Commons Attribution 4.0 International License.

Ligand field effects

A few coordination geometries are noticeably absent from the Kepert-preferred and Kepert-accessible geometries in Figure ***Section*5.4.2**. These include the trigonal prismatic geometries formed by compounds like $W(CH_3)_6$ and the very common square planar geometry illustrated by complexes like $[PtCl_4]^{2-}$ and $[IrClH(PPh_3)_2]$. One of the reasons the Kepert model fails to predict the existence of such structures is its neglect of directional interactions involving *d* electrons on the metal center. Metal *d* electrons exert on profound influence on almost all properties of transition metal complexes, including their structures. The way in which this occurs will be explored at length in the next chapter. For now, it is enough to note that both the ligand-donated electrons surrounding a metal center and the electrons occupying particular *d* orbitals on that metal are oriented in specific directions relative to one another. Because of this the strength of the interactions between the ligand and metal *d* electrons depend on both the number of *d* electrons present, how strongly metal-ligand binding affects their energy, and how the ligands are arranged about the metal center. The impact of these effects, here termed ligand field effects, differ from case to case and can include

- distortions of the complex's geometry. For instance, an ideal octahedral coordination geometry might be tetragonally distorted by flattening or elongating it.
- imparting a strong preference for a non-Kepert coordination geometries. This is why, for example, 2nd and 3rd row complexes in which the metal has a d^8 electron configuration are almost always square planar.

- stabilizing non-Kepert geometries enough to permit complexes to adopt them in the presence of a rigid or semirigid ligand that prefers to coordinate the metal in that geometry.[3]

Because of these effects square planar and trigonal prismatic geometries are also observed and the list of coordination geometries given in Figure ***Section*5.4.2** may be extended to that shown in Figure ***Section*5.4.3**.

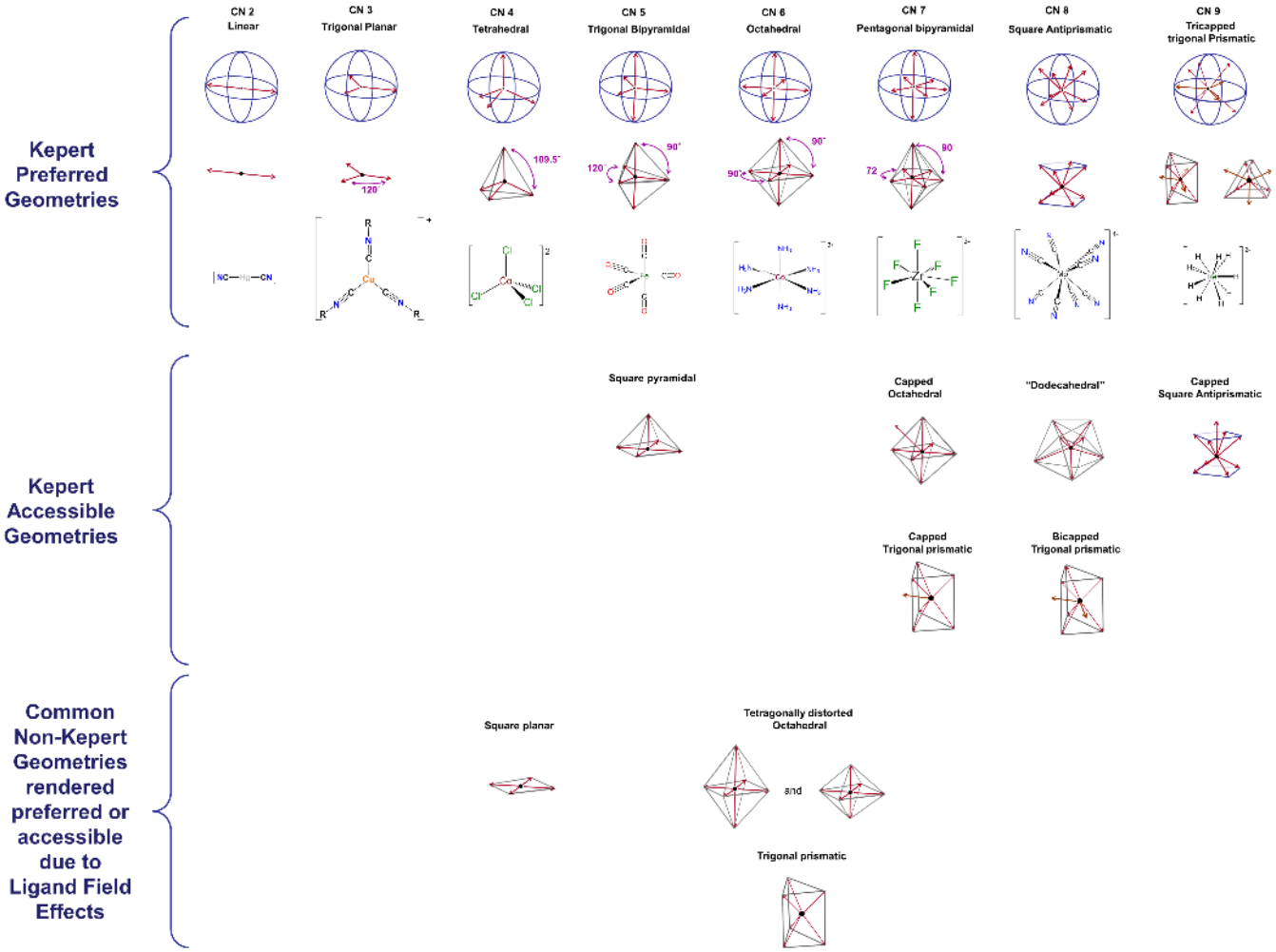


Figure ***Section*5.4.3**. Coordination geometries accessible in for 2-9 coordinate complexes even without constraint by rigid or semirigid ligands. This work by Stephen Contakes is licensed under a Creative Commons Attribution 4.0 International License.

Ligand geometry constraints

Rigid or semirigid ligands influence the coordination geometry of metal complexes in two main ways:

- Bulky rigid ligands that crowd the metal center prevent other ligands from binding. Such ligands are useful for preparing low-coordinate complexes.
- Rigid and semirigid ligands can impose their preferred coordination geometry on a metal center. This is because these ligands energetically prefer to adopt a particular conformation when they bind a metal center. In doing so they shift the coordination geometry energy landscape toward that preferred geometry. If the shift is large enough relative to the native preference due to ligand repulsion and ligand field effects the complex will either adopt the ligand-preferred geometry or be distorted in the direction of the ligand-preferred geometry. Examples are given in Figure ***Section*5.4.4**.

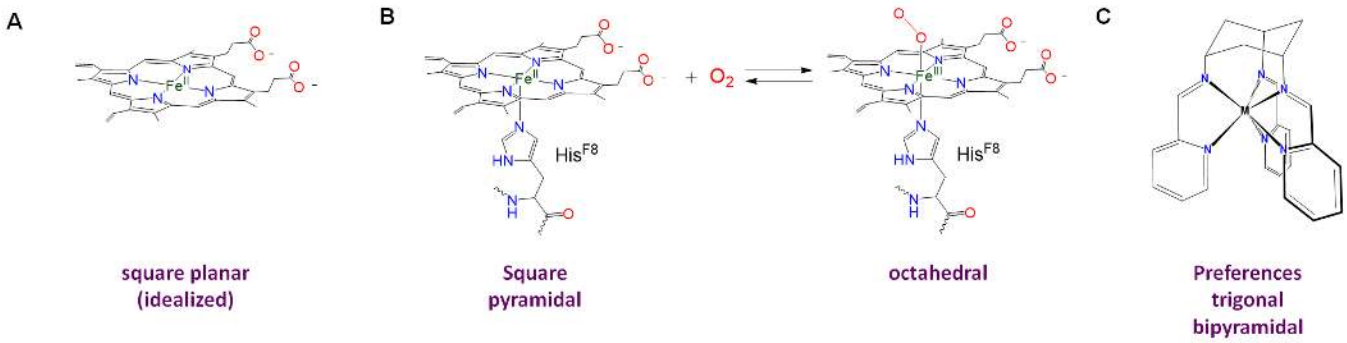


Figure *Section*5.4.4. Examples of rigid or semirigid ligands that can impose their preferred coordination geometry on a metal center. Porphyrins, phyhalocyanines and related macrocycles tend to impose a slightly bent square planar coordination geometry, although (B) many such complexes, including the iron of myoglobin's heme cofactor coordinate additional ligands to give square pyramidal or octahedral complexes. (C) Synthetic multidentate ligands have been developed to preference trigonal prismatic coordination geometries, including the one shown here. It forms roughly trigonal prismatic complexes with Co^{II} and $Zn^{II,}$ albeit imperfect ones.[3] This work by Stephen Contakes is licensed under a Creative Commons Attribution 4.0 International License.

The influence of ligands on coordination geometry is important in living systems in which proteins and nucleic acids can act as rigid or semirigid ligands. The ability of these ligands to distort the coordination geometries of metal atoms in ways that enable them to perform specific functions is so common that the resulting distorted geometries are termed entactic states. A particulary spectacular case of an entactic state involves the blue copper proteins azurin and plastocyanin, the structure of which is given in Figure *Section*5.4.5.

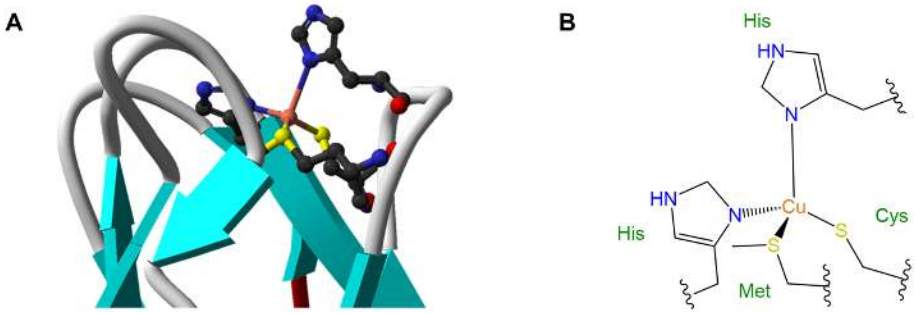


Figure *Section*5.4.5. (A) Structure and (B) schematic of the plastocyanin active site showing the distorted tetrahedral coordination environment that the protein imposes on the copper center (tan), which is most evident from the long vertically oriented Cu-Histidine bond. The image in part A is cropped from an original image by Ben Mills - Own work, Public Domain, https://commons.wikimedia.org/w/inde...?curid=6202620. The image in part B is by Stephen Contakes and licensed under a Creative Commons Attribution 4.0 International License.

As may be seen from the structure in Figure *Section*5.4.5, the copper in plastocyanin exibits a distorted tetrahedral coordination geometry. The protein is said to act like a medieval torture device called a rack in stretching the metal into its distorted geometry. This distortion makes its easier for the copper center to undergo facile redox reactions, enabling it to better function as an electron carrier.

Crystal packing effects

This effect is similar to that of ligand constraints except that in this case arise not from the structure internal to a ligand but out of the forces involves in maximizing the stabilization energy of a crystal. With lower coordination number complexes packing effects can shift the conformations of flexible ligands but only give rise to very small distortions of the overall coordination geometry. Packing effects can drive a shift in the overall coordination geometry of higher coordination number complexes, for which packing effects are significant relative to the small difference in energy between geometries. Thus while $[Mo(CN)_8]^{4-}$ has a square antiprismatic coordination geometry in solution it exhibits a docecahedral coordination geometry in the crystals of many of its salts.

Relatavistic effects on orbital energies

The proximity of fast moving electrons to massive nuclei in the heavier transition elements results in relatavistic expansion and contraction of orbitals. The net results are that

- heavier elements tend to be smaller than expected. This effect preferences lower coordination numbers.
- the relative energies of orbitals shift. Orbitals which become contracted are lowered in energy while those which are expanded increase in energy, as shown for the case of gold in Figure ***Section*5.4.6*A***.

The combination of smaller sizes and altered orbital energies affect coordination preferences. Relatavistic effects contribute to the greater tendency of Au(I) relative to other group 11 metals to form linear two coordinate complexes. As shown in Figure ***Section*5.4.6*B***, the relative closeness in energy of the 6*s* and 5*d* orbitals of gold makes mixing of these orbitals more favorable, facilitating the ability of gold to form two coordinate complexes with strong sigma bonds oriented 180° from one another.

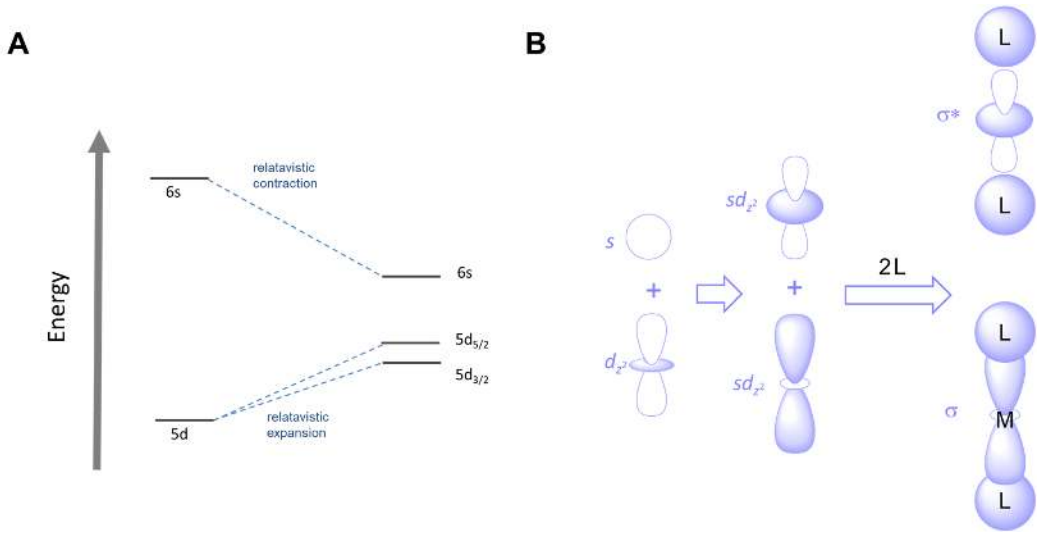


Figure ***Section*5.4.6**. (A) Gold experiences relatavistic expansion and contraction of its 5*d* and 6*s* orbitals, resulting in shifts to their relative energies. (B) This makes mixing of these orbitals more favorable, facilitating the ability of gold to form two coordinate complexes with strong sigma bonds that involve considerable sd_{z^2} character. This work by Stephen Contakes is licensed under a Creative Commons Attribution 4.0 International License.

What Structures do Coordination Complexes Form?

Metal complexes with coordination numbers ranging from one to 16 are known, although values greater than seven are rare for the transition metals. In this section examples of common coordination geometries will be presented in order of coordination number.

Coordination Number 1

Condensed phase monocoordinate complexes are unknown for the transition metals, although the post transition metals Tl and In form monocoordinate complexes with the bulky ligands triazapentadienyl and 2,6-tris(2,4,6-triisoprophylphenyl)benzene as shown in Figure ***Section*5.4.7**.

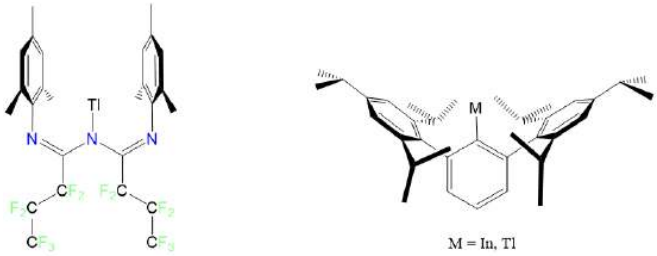
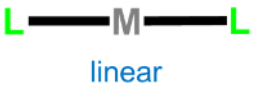


Figure ***Section*5.4.7**. No monocoordiante transition metal complexes are known but Tl^+ and In^+ form monocoordinate complexes with extremely bulky ligands. This work by Stephen Contakes is licensed under a Creative Commons Attribution 4.0 International License.

Coordination Number 2

This coordination number is rare outside of d^{10} complexes of the group 11 metals and mercury, specifically, Cu^+, Ag^+, Au^+, and Hg^{2+}. In accordance with the predictions of the Kepert model these give linear complexes.



linear

Among these:

- Cu^+ more commonly gives tetrahedral complexes but can be coaxed to give linear ones. The most prominent example is $[CuCl_2]^-$, which forms when CuCl is treated with concentrated HCl under anerobic conditions.
- Ag^+ also commonly forms tetrahedral or trigonal planar complexes but can give linear ones. The most prominent example is $[Ag(NH_3)_2]^+$, which can be formed by treating silver salts with concentrated aqueous or liquid ammonia.
- Au^+ almost always forms linear complexes but many of these formally two coordinate complexes associate as depicted in Figure ***Section*5.4.8**. The ability of Au^+ to form linear complexes with cyanide is even used to selectively extract metallic gold from low grade ores. The stability of $[Au(CN)_2]^-$ means that the dissolution of metallic gold in aqueous cyanide is thermodynamically favorable under aerobic conditions.

$$4\ Au + 8\ CN^- + O_2 + 2\ H_2O \longrightarrow 4\ [Au(CN)_2]^- + 4\ OH^- \qquad \text{(Section 5.4.1)}$$

- Hg^{2+}, like Au^+, benefits from relativistic effects and more commonly forms two-coordinate complexes with a linear geometry. Among these is $[Hg(CN)_2]$. However, its preference for linearity is not as rigid as for Au^+ and so complexes with a variety of coordination geometries are known.

An by means of honorary mention the mercury(I),Hg_2^{2+}, forms linear complexes of the type L-Hg-Hg-L, although since Hg_2^{2+} is often considered as a single unit these aren't always considered to be two coordinate complexes.

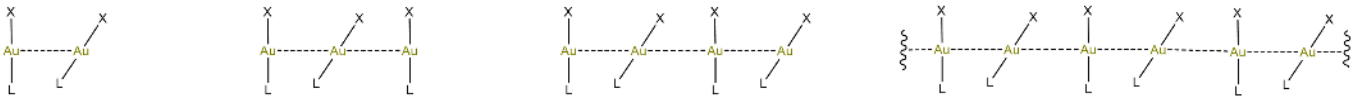
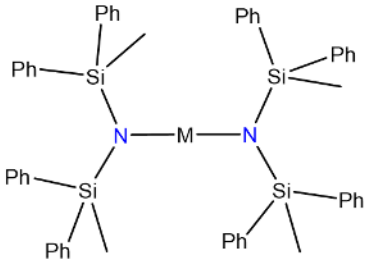


Figure ***Section*5.4.8**. Many "linear" gold complexes associate side-on to form dimers, trimers, tetramers, and chains. Although in this chapter L is usually taken to represent a generic ligand, in this scheme L represents a neutral ligand that donates two electrons to the metal (py, PR_3, CO etc.) and X an anionic one (*e.g.* Cl^-, CN^-, etc.). Exactly which structure forms depends on the identity of L and X. Redrawn from reference 5. This work by Stephen Contakes is licensed under a Creative Commons Attribution 4.0 International License.

Two coordinate complexes may also be formed through the use of bulky ligands that only allow for the binding of two to the metal center. Classic examples are given in Figure ***Section*5.4.9**.



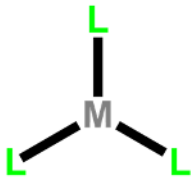
M = Mn, Fe, Co

Figure ***Section*5.4.9**. Two coordinate complexes form between Mn^{2+}, Fe^{2+}, and Co^{2+} and $N(SiMePh_2)_2$.[6] This work by Stephen Contakes is licensed under a Creative Commons Attribution 4.0 International License.

Coordination Number 3

Three coordinate complexes are similar to two coordinate ones in that they are rare and, aside from the constraining influence of ligands, usually limited to d^{10} metal ions such as Cu^+, Ag^+, Au^+, Hg^{2+}, and Pt^0. As expected from the Kepert model, in the absence

of constraining ligands three coordinate complexes are trigonal planar.



Trigonal planar

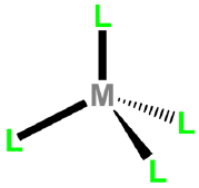
Many of the examples involve soft ligands. They include $[Cu(SPMe_3)_3]^+$, $[Ag(PPh_3)_3]^+$, $[Au(PPhCy_2)_3]^+$, HgI_3^-, and $[Pt(PPh_3)_3]$. Non-d^{10} metal centers have successfully been constrained to adopt a three coordinate trigonal planar geometry using bulky and semirigid ligands. Examples of such three-coordinate complexes are given in Figure ***Section*5.4.10**.



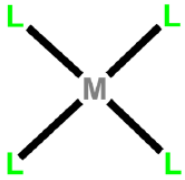
Figure ***Section*5.4.10**: Three coordinate complexes prepared using bulky and semirigid ligands. This work by Stephen Contakes is licensed under a Creative Commons Attribution 4.0 International License.

Coordination Number 4

Four is one of the most common coordination numbers found in transition metal complexes. The two common four coordinate geometries are tetrahedral and square planar.



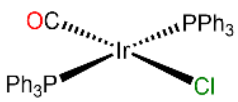
tetrahedral



Square planar

Tetrahedral complexes are commonly formed by metals possessing either a d^0 or d^{10} electron configuration. Monometallic examples of the former include $TiCl_4$, VO_4^{3-}, WS_4^{2-}, MnO_4^-, CrO_4^{2-}, and OsO_4 while d^{10} examples are $[Ni(CO)_4]$, $[HgBr_4]^{2-}$, $[ZnCl_4]^{2-}$, $[CdI_4]^{2-}$. Otherwise tetrahedral complexes are known but much less common. Examples usually involve good donor ligands and include $[FeCl_4]^-$ (d^5), $[CoCl_4^{2-}]$ (d^6), and $[NiCl_4]^{2-}$ (d^7).

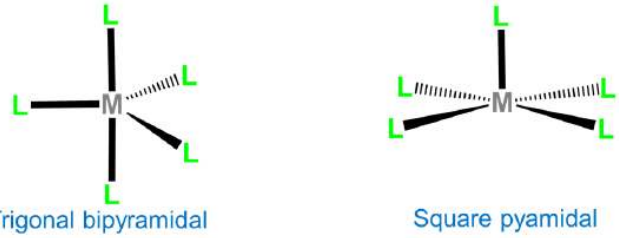
Second and third row transition metal centers with d^8 electron configurations like Rh^+, Ir^+, Pd^{2+}, and Pt^{2+}, Au^{3+} almost exclusively exhibit square planar geometries. Beyond this, square planar geometries are often formed by Ni^{2+} (d^8), Ni^{3+} (d^7), and Cu^{2+} (d^9). Examples of square planar complexes include $[Cu(acac)_2]$; $[PtCl_4]^{2-}$;Wilkinson's catalyst, $[RhCl(PPh_3)_3]$; and Vaska's complex, *trans*-$[Ir(CO)Cl(PPh_3)_2]$. Porphyrins, phthalocyanines, and other rigid macrocycles can also impose a square planar geometry on coordinated metals.



Vaska's Complex

Coordination Number 5

The two common coordination geometries for five coordinate complexes are trigonal bipyramidal and square pyramidal.



Five coordinate complexes are rare. Complexes that exhibit trigonal bipyramidal geometry include $[Fe(CO)_5]$ and $[CuCl_5]^{3-}$ and complexes containing tripodal ligands that preference formation of a trigonal pyramidal structure with an open coordination site, as shown in Figure ***Section*5.4.11**.

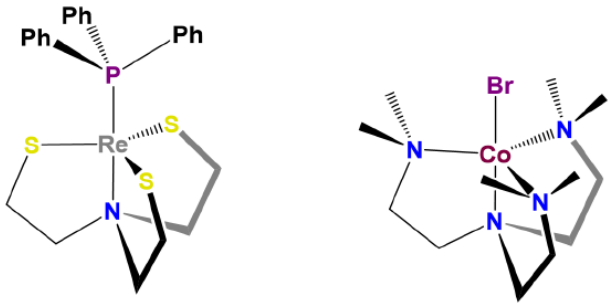


Figure ***Section*5.4.11**: Some tripodal ligands preference the formation of trigonal bipyramidal complexes. This work by Stephen Contakes is licensed under a Creative Commons Attribution 4.0 International License.

Homoleptic $[Ni(CN)_5]^{3-}$ possesses a square pyramidal structure, although the geometry is more common for macrocyclic complexes like the iron protoporphyrin of deoxymyoglobin shown in Figure ***Section*5.4.4** and for complexes containing oxo and nitrido ligands, examples of which are shown in Figure ***Section*5.4.12**.

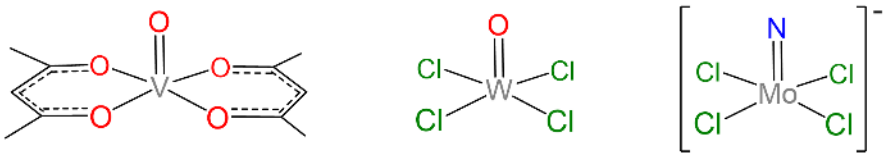


Figure ***Section*5.4.12**: Some square pyramidal oxo and nitrido complexes. This work by Stephen Contakes is licensed under a Creative Commons Attribution 4.0 International License.

In the absence of rigid constraining ligands the relatively low energy difference between the trigonal bipyramidal and square pyramidal coordination geometries provides a mechanism for interconversion of the axial and equatorial ligands in a trigonal planar complex. For example, pentacarbonyliron(0) exhibits fluxionality involving a square pyramidal intermediate via a Berry pseudorotation mechanism, as shown in Figure ***Section*5.4.13**

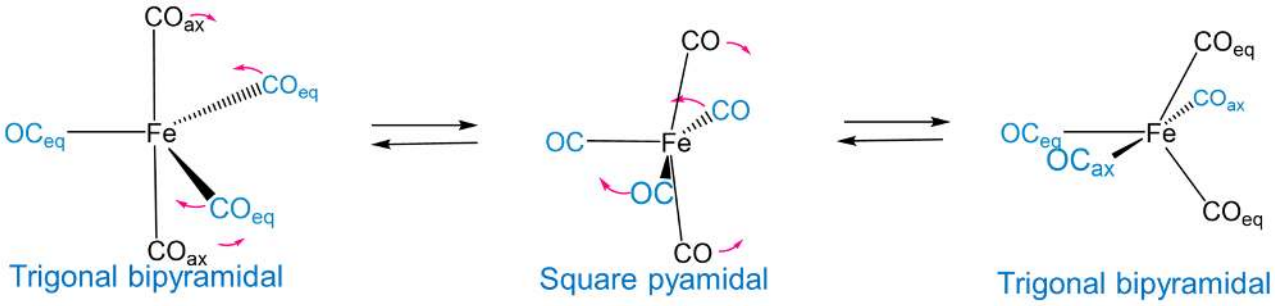
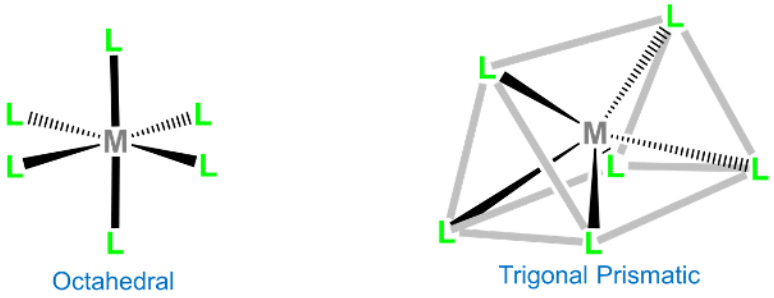


Figure ***Section*5.4.13**: Fluxionality in pentacarbonyliron(0) involves exchange of axial and equatorial carbonyl ligands via Berry pseudorotation. Interconversion of the axial and equatorial carbonyl groups occurs faster than the NMR timescale at room temperature. As a result the ^{13}C NMR spectrum of $Fe(CO)_5$ exhibits a single signal rather than two separate signals for the axial and equatorial carbonyl carbons. This work by Stephen Contakes is licensed under a Creative Commons Attribution 4.0 International License.

Coordination Number 6

The two common octahedral coordination geometries are octahedral and trigonal prismatic.



Octahedral

Of these octahedral is by far the most common mode of coordination exhibited by transition metals. Most metals can be induced to form octahedral complexes and examples exist for every d electron configuration ranging from d^0 to d^{10}. Among these are the 28 metal oxidation states listed in Figure ***Section*5.4.1** for which octahedral is the most common coordination geometry. Because of this it is worth pointing out that octahedral complexes possessing d^4, d^7 , or d^9 electron configurations commonly exhibit tetragonal distortions depicted in Figure ***Section*5.4.14**.

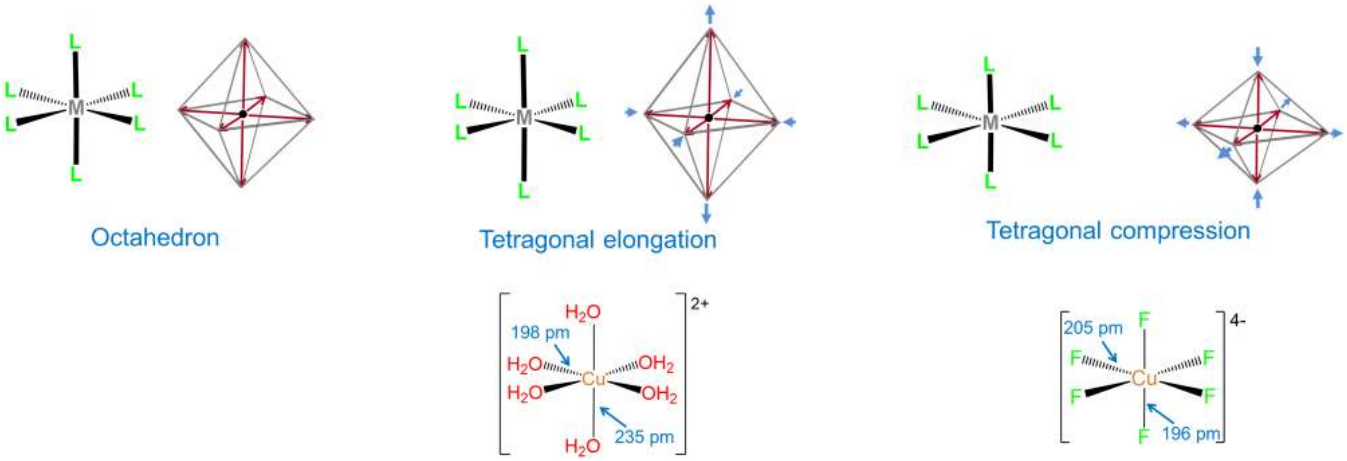


Figure ***Section*5.4.14**: Tetragonal distortions commonly occur for d^4, d^7 , and d^9 octahedral complexes. The most common type involves axial elongation in which the octahedron is stretched along a single *trans*-L-M-L axis but axial compressions in which the octahedron is compressed along such an axis instead are sometimes observed. An example of an axial elongated complex is $[Cu(H_2O)_6]^{2+}$ in solution while $[CuF_6]^{4-}$ is axially compressed when doped into a Ba_2ZrF_6 lattice (it is elongated when doped into a Bond distances are taken from references 7 and 8. This work by Stephen Contakes is licensed under a Creative Commons Attribution 4.0 International License.

Trigonal prismatic

Trigonal prismatic coordination is related to octahedral coordination as shown in Figure ***Section*5.4.15**. As may be seen in Figure ***Section*5.4.15**, an octahedral coordination sphere is just a trigonal antiprism in which all edge lengths are identical. Rotation of one triangular face relative to its opposite until the two are eclipsed gives a triganal prismatic geometry. In fact, since continuation of this rotation gives another octahedral complex the trigonal prismatic geometry is an intermediate in isomerization reactions involving octahedral complexes.

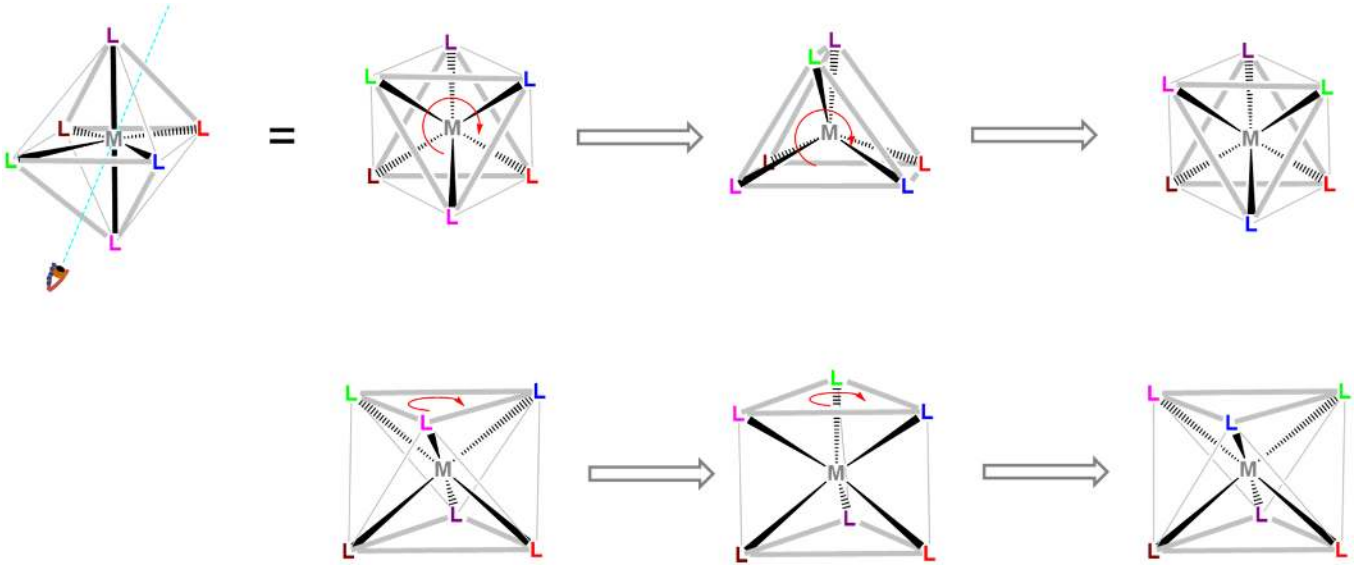


Figure *Section*5.4.15: Since an octahedron is a trigonal antiprism a trigonal prism may be produced by rotating or "twisting" one face of the octahedron relative to its opposite. Since continuation of the rotation gives an isomer of the original octahedron, when the energy landscape for twists like these is thermally or photochemically accessible twists like these provide one pathway for isomerisation reactions involving octahedral complexes. In tris- and bis-chelates such isomerizations are said to occur by Bailar and Ray-Dutt twists, which differ only in the relationship between the chelate rings and the faces twisted. Top: View down looking down an axis bisecting a pair of opposing faces. Bottom: View perpendicular to that shown at top. This work by Stephen Contakes is licensed under a Creative Commons Attribution 4.0 International License.

In contrast to octahedral coordination geometries, trigonal prismatic coordination (and distorted versions thereof) are rare and occur mostly for d^0, d^1, and d^2 configurations. Examples of trigonal prismatic metal centers include the d^2 Mo^{4+} centers in MoS_2, d^1 $[Re(S_2C_2Ph_2)_3]^-$, and d^0 $[Ta(CH_3)_6]^-$, of which the latter two structures are given in Figure **Section**5.4.16. Semirigid ligands like that shown in Figure *Section*5.4.4*C* may be used to encourage the adoption of a trigonal prismatic geometry, although once the number of *d* electrons present the preference for octahedral coordination is too great for a trigonal prismatic geometry to occur.

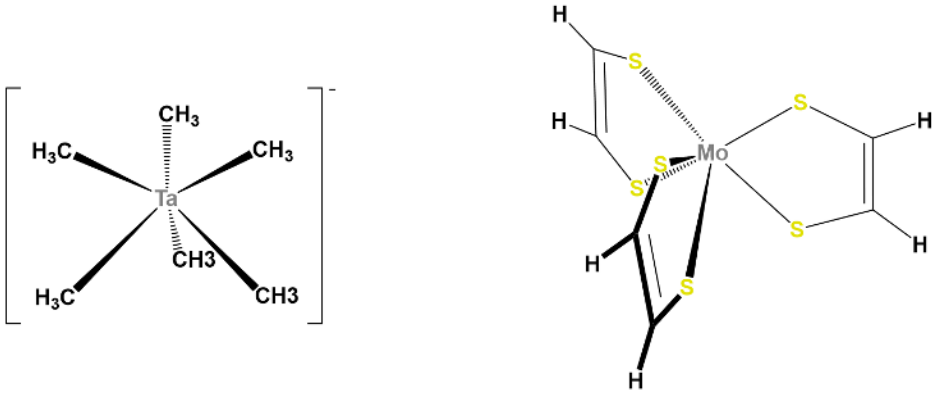
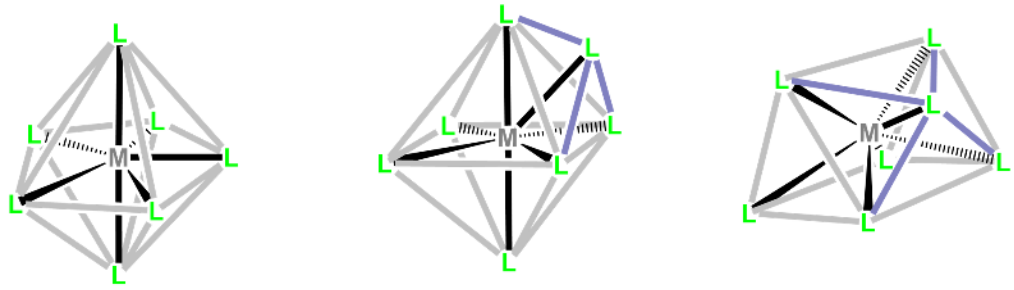


Figure *Section*5.4.16: The complexes $[Ta(CH_3)_6]^-$ and $[Mo(S_2C_2H_2)_3]$ adopt a trignal prismatic geometry. Trigonal primatic coordination is common for d^0 and d^1 complexes with alkyl and dithiolene ligands. It is also typical for the dithiolene ligands to coordinate along the rectangular edges of the trigonal prism instead of the triangular ones. This work by Stephen Contakes is licensed under a Creative Commons Attribution 4.0 International License.

Coordination Number 7

Seven coordinate complexes are rare outside of the relatively large early transition metals, lanthanides, and actinides. The three common seven coordinate geometries are pentagonal bipyramidal, monocapped octahedral, and monocapped trigonal prismatic. The latter two are often called capped octahedral, and capped trigonal prismatic, with the mono- prefix being understood.



Although intraligand repulsions are smaller in the pentagonal bipyramidal coordination geometry than the capped octahedral and capped trigonal prismatic geometries the difference is small and the three structures are often close in energy. As a result the structure observed is often dependent on ligand-based constraints, crystal packing, and solvent effects that preference one geometry over the others.

Heptacyano complexes are often pentagonal bipyramidal. Examples include $[Mo(CN)_7]^{3-}$, $[W(CN)_7]^{3-}$, and $[Os(CN)_7]^{3-}$. Seven coordinate complexes containing oxo ligands commonly are pentagonal bipyramidal with the oxo ligand(s) in the less sterically hindered axial position. Examples include $[NbOF_6]^{3-}$ and, for the inner transition metals, $[UO_2F_5]^{3-}$. Ligands that have been used to promote formation of seven-coordinate species include 15-crown-5 and 2,2':6',2":6",2"'-quaterpyridine and 15-crown-5. Representative complexes are given in (Figure **Section5.4.17**.

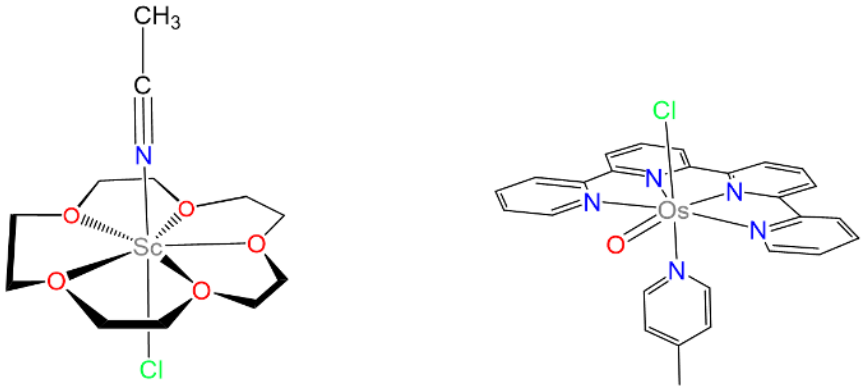


Figure ***Section*5.4.17**: Seven coordinate complexes containing ligands that encourage the formation of seven-coordinate geometries. Note that while in $[NbOF_6]^{3-}$ and $[UO_2F_5]^{3-}$ the oxo ligands occupy axial positions the Osmium complex shown possesses an oxo ligand in an equatorial position. This is likely because the parent octahedral complex, in which the oxo ligand is not present, possesses an expanded outer N-Os-N angle of 121.655° that opens to 154.161° to accommodate the oxo group. Drawn based on the structures reported in references 9 and 10. This work by Stephen Contakes is licensed under a Creative Commons Attribution 4.0 International License.

Capped trigonal prismatic geometries are common for complexes of the early transition metals. Examples include $[NbF_7]^{2-}$, $[TaF_7]^{2-}$, and $[ZrF_7]^{3-}$ in $(NH_4)_3[ZrF_7]$.

Capped octahedral geometries are found in $[MoMe_7]^-$, $[WMe_7]^-$, and $[WBr_3(CO)_4]$, which contains three pairs of *trans*-Br and CO with the final CO capping the octahedron's $(CO)_3$ face, as shown in Figure ***Section*5.4.18**.

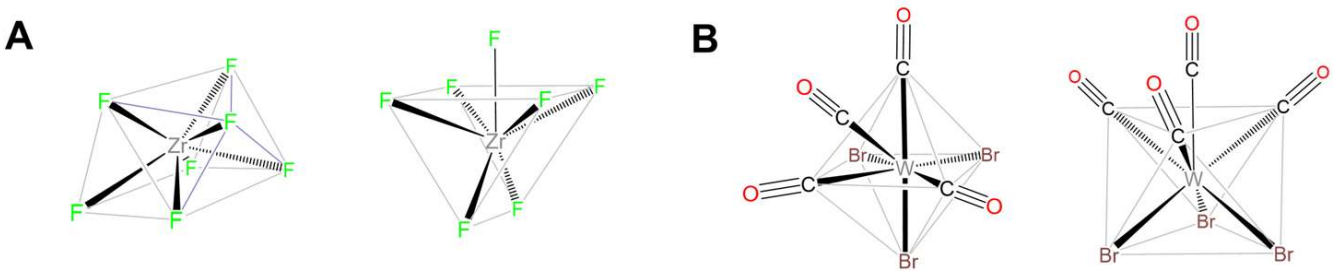


Figure *Section*5.4.18: Examples of complexes that adopt monocapped triconal prismatic and monocapped octahedral geometries.(A) Two views of the structure of (A) capped trigonalprismatic $[ZrF_7]^{3-}$ and (B) capped octahedral $[WBr_3(CO)_4]$. This work by Stephen Contakes is licensed under a Creative Commons Attribution 4.0 International License.

In seven and higher coordinate complexes ligand and crystal packing effects frequently give distorted coordination geometries. These geometries are intermediate between two or more of the idealized seven coordinate geometries, making it difficult to tell exactly which structure they are a distortion of (Figure Section5.4.19.

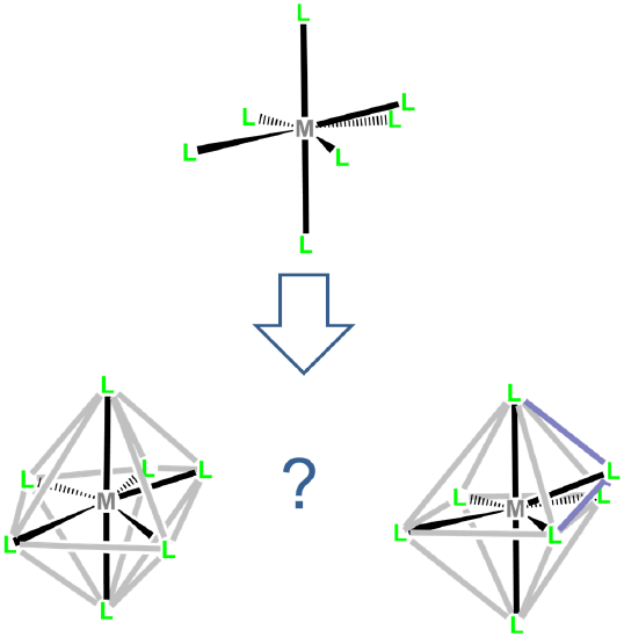
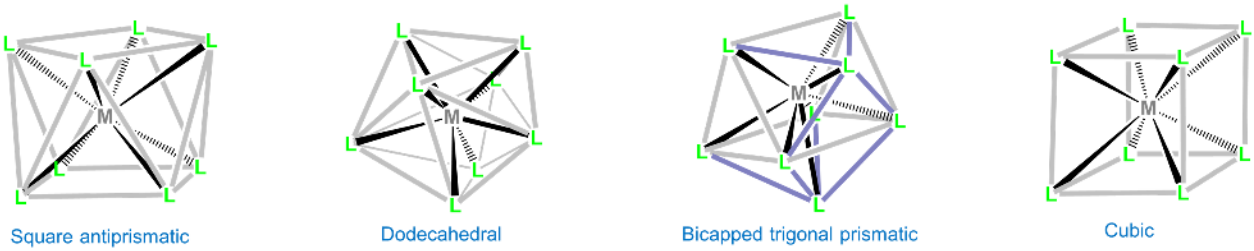


Figure *Section*5.4.19: Many seven-coordinate structures are distorted and can be difficult to classify. For example, how should the geometry of this complex be described - as distorted trigonal bipyramidal or distorted monocapped octahedral? This work by Stephen Contakes is licensed under a Creative Commons Attribution 4.0 International License.

Coordination Number 8

Eight coordinate complexes are rare and occurs in discrete molecules and ions only for the relatively large early transition metals, lanthanides, actinides. The three common eight coordinate geometries are square antiprismatic, dodecahedral, and bicapped trigonal prismatic. In contrast, the cubic coordination geometry is only found in ionic lattices like that of CsCl and in complexes of the inner transition metals such as $Na_3[UF_8]$.



The simplest structure is the cube, which is rare because it does not minimize interligand repulsive interactions. Square antiprismatic, dodecahedral, and bicapped trogonal prismatic coordination are more common. Of these the square antirpismatic and dodecahedral geometries can both be considered as distorted cubic structures. As shown in Figure *Section*5.4.20, the square antiprism may be made by twisting one face of a cube relative to one another and the dodecahedron by folding opposing faces towards one another.

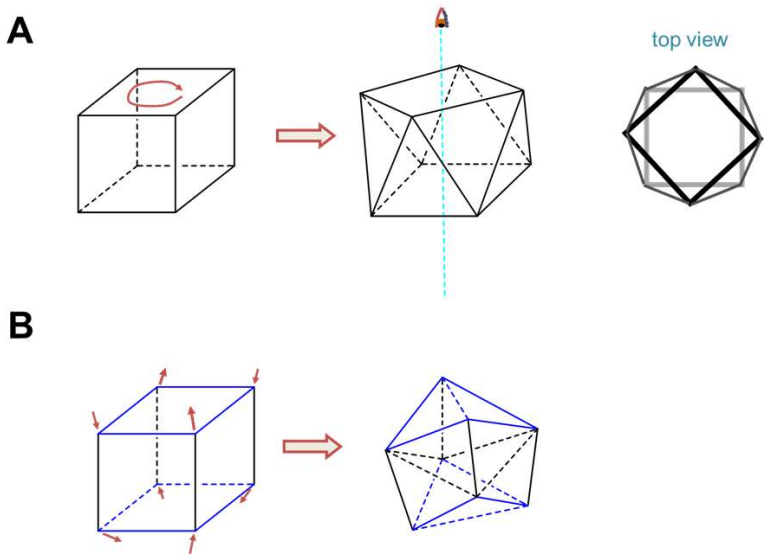


Figure *Section*5.4.20: The (A) square antiprismatic and (B) dodecahedral coordination geometries are distorted cubic geometries. (A) The square antiprismaric coordination geometry is just a cubic coordination geometry in which one face has been rotated 45° relative to its opposite (and for which the distance between those faces need not be equal to the distance between adjacent atoms within a face) (B) The dodecahedral geometry may be thought of as a cube in which opposing faces are folded up and down relative to one another as shown. This work by Stephen Contakes is licensed under a Creative Commons Attribution 4.0 International License.

As with other high-coordinate structures the energy difference between these eightfold coordination geometries is small enough that packing effects can significantly influnece the observed structure. For example, octacyanomolybdates commonly adopt a square antiprismatic coordination geometry but depending on the counterions present can give dodecahedral or bicapped trigonal prismatic complexes. Examples are given in Figure Section5.4.21.

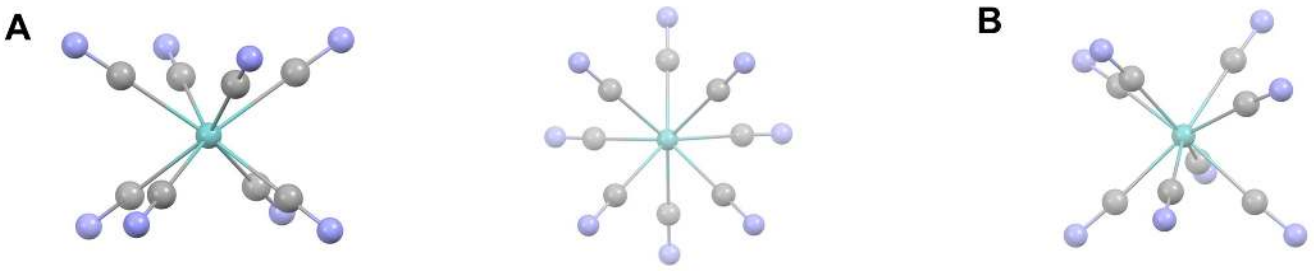
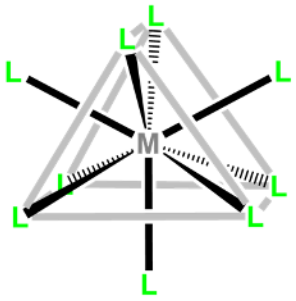


Figure *Section*5.4.21: Structures reported for (A) square antiprismatic $[Mo(CN)_8]^{3-}$ as a solid 4,4'-Diazenediyldipyridinium salt and (B) dodecahedral $[Mo(CN)_8]^{4-}$ as a solid tetra-n-butylammonium salt.

Coordination Number 9

Again, nine coordinate complexes typically require larger transition metals, lanthanides, and actinides. Coordination geometries are typically either tricapped trigonal prismatic or idosynchraitcally determined by the ligands. Simpleexamples include the aqua complexes $[Sc(H_2O)_9]^{3+}$, $[Y(H_2O)_9]^{3+}$, and $[La(H_2O)_9]^{3+}$ as well as $[TcH_9]^{2-}$ and $[ReH_9]^{2-}$.



Tricapped trigonal Antiprism

The classic example of a nine-coordinate complex, $[ReH_9]^{2-}$, is shown in Figure ***Section*5.4.22**.

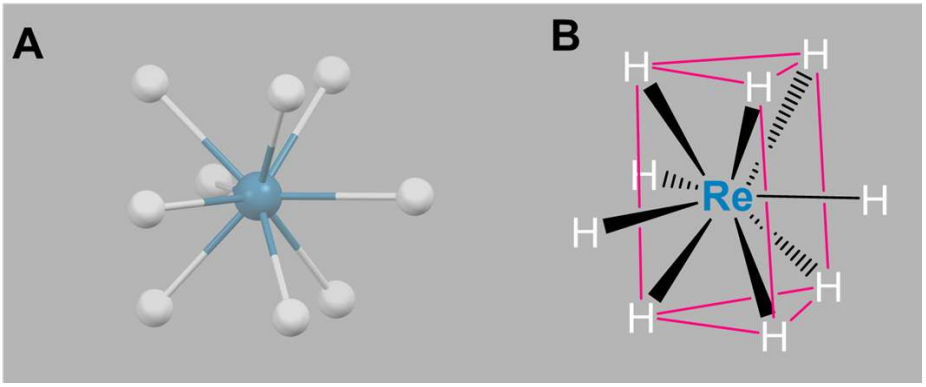


Figure ***Section*5.4.22**: (A) Structure of $[ReH_9]^{2-}$ in $K_2[ReH_9]$ and (B) schematic showing how the structure maps onto a tricapped trigonal pyramidal coordination geometry. This work by Stephen Contakes is licensed under a Creative Commons Attribution 4.0 International License.

Coordination Numbers 10-16

Coordination numbers higher than nine are extremely rare for compounds that bind in κ fashion (form conventional metal-ligand bonds)[14] and usually involve some combination of large metals, sterically undemanding ligands, and special ligand structures that promote higher coordination. Noteworthy examples include

1. Twelve-coordinate $[Hf(BH_4)_4]$, which illustrates how small multidentate ligands promote higher coordination numbers. As shown in Figure ***Section*5.4.23**, $[Hf(BH_4)_4]$ has a cubooctahedral structure in which BH_4^- acts as a tridentate ligand, with BH_3 units occupying triangular faces of the cubooctahedron to give a tetrahedron of BH_4^- ligands around the Hf.

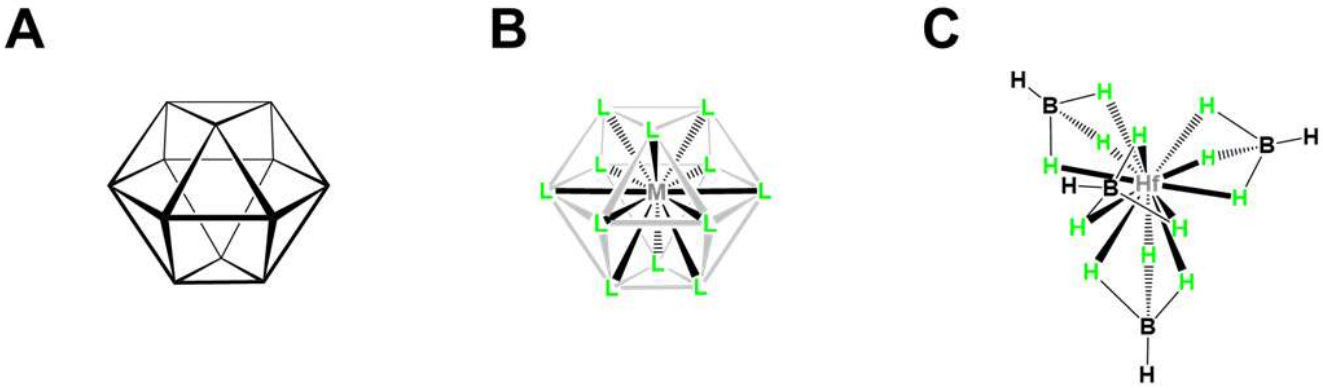


Figure ***Section*5.4.23**: The anticubooctahedral coordination geometry is observed for $[Hf(BH_4)_4]$. (A) An anticubooctahedron consists of a hexagonal ring capped with antiparallel triangles above and below the ring. (B) Idealized anticubooctahedral complex. (C) Structure of $[Hf(BH_4)_4]$. This work by Stephen Contakes is licensed under a Creative Commons Attribution 4.0 International License.

2. Twelve coordinate $[Ce(NO_3)_6]^{2-}$, in which the nitrate oxygens define an icosahedral coordination geometry as shown in Figure **Section5.4.24**. The nitrates in the structure bind the Ce center in bidentate fashion in an octahedral array.

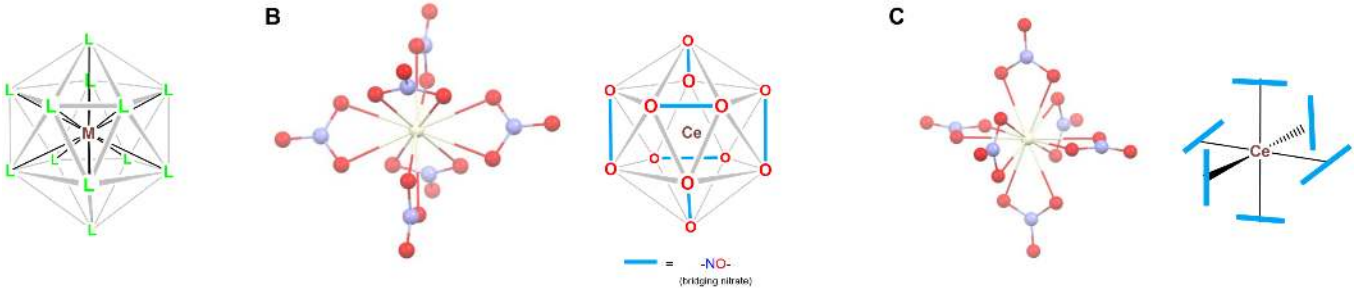


Figure ***Section5.4.24***: Coordination geometry of $[Ce(NO_3)_6]^{2-}$ in $[Mg(H_2O)_6][Ce(NO_3)_6]\cdot H_2O$. (A) Idealized icosahedral coordination. (B) View of the structure of $[Ce(NO_3)_6]^{2-}$ showing how it maps onto the icosahedral coordination geometry. (C) The structure may also be thought of as comprising an octahedral geometry in which each vertex of the octahedron is occupied by a κ^2-NO_3^-. The structure of $[Ce(NO_3)_6]^{2-}$ is rendered in Mercury from the cif data in reference 15. This work by Stephen Contakes is licensed under a Creative Commons Attribution 4.0 International License.

3. Fifteen-coordinate, $[Th(H_3BNMe_2BH_3)_4]$, which also uses bridging H-B-H units that occupy little of the coordination sphere. In $[Th(H_3BNMe_2BH_3)_4]$ three of the four $H_3BNMe_2BH_3$ bind in κ^4 fashion and one binds κ^3, giving the fifteen fold coordination.[16]

4. Sixteen-coordinate $[CoB_{16}]^-$, which possesses the highest coordination number yet observed. Its structure is given in Figure **Section5.4.25** The coordination geometry is an octahedral antiprism and the complex should be considered as involving a Co center in the midst of a B_{16}^- "molecular drum" held together by cluster bonds.

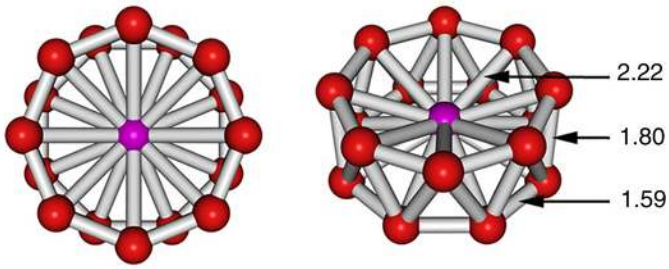


Figure ***Section5.4.25***: Structure of the D_{8d} isomer of the 16 coordinate complex $[CoB_{16}]^-$, with distances shown in Ångstroms. The image is Figure 2A from from Popov, I., Jian, T., Lopez, G. *et al.* Cobalt-centred boron molecular drums with the highest coordination number in the CoB_{16}^- cluster. *Nat Commun* **6,** 8654 (2015). https://doi.org/10.1038/ncomms9654, which is is licensed in that publication under a Creative Commons Attribution 4.0 International License.

References

1. Dudev, M.; Wang, J.; Dudev, T.; Lim, C., Factors Governing the Metal Coordination Number in Metal Complexes from Cambridge Structural Database Analyses. *The Journal of Physical Chemistry B* **2006**, *110(4)*, 1889-1895.

2. Kuppuraj, G.; Dudev, M.; Lim, C., Factors Governing Metal−Ligand Distances and Coordination Geometries of Metal Complexes. *The Journal of Physical Chemistry B* 2009, 113 (9), 2952-2960.

3. Cremades, E.; Echeverría, J.; Alvarez, S., The Trigonal Prism in Coordination Chemistry. *Chemistry – A European Journal* 2010, 16 (34), 10380-10396.

4. Xiong, X.-G.; Wang, Y.-L.; Xu, C.-Q.; Qiu, Y.-H.; Wang, L.-S.; Li, J., On the gold–ligand covalency in linear $[AuX_2]^-$ complexes. *Dalton Transactions* 2015, 44 (12), 5535-5546.

5. Concepción Gimeno, M. The Chemistry of Gold in Laguna, Antonio (ed.) *Modern Supramolecular Gold Chemistry: Gold-Metal Interactions and Applications*. Wiley, 2008.

6. Andersen, R. A.; Faegri, K.; Green, J. C.; Haaland, A.; Lappert, M. F.; Leung, W. P.; Rypdal, K., Synthesis of bis[bis(trimethylsilyl)amido]iron(II). Structure and bonding in M[N(SiMe3)2]2 (M = manganese, iron, cobalt): two-coordinate transition-metal amides. *Inorganic Chemistry* 1988, 27 (10), 1782-1786.

7. Persson, I., Hydrated metal ions in aqueous solution: How regular are their structures? Pure and Applied Chemistry 2010, 8*2(10)*, 1901.

8. Aramburu, J. A.; García-Fernández, P.; García-Lastra, J. M.; Moreno, M., Jahn–Teller and Non-Jahn–Teller Systems Involving CuF_6^{4-} Units: Role of the Internal Electric Field in Ba2ZnF6:Cu2+ and Other Insulating Systems. *The Journal of Physical Chemistry C* 2017, *121(9)*, 5215-5224.

9. Brown, M. D.; Levason, W.; Murray, D. C.; Popham, M. C.; Reid, G.; Webster, M., Primary and secondary coordination of crown ethers to scandium(iii). Synthesis, properties and structures of the reaction products of ScCl3(thf)3, ScCl3·6H2O and Sc(NO3)3·5H2O with crown ethers. Dalton Transactions 2003, (5), 857-865.

10. Liu, Y.; Ng, S.-M.; Lam, W. W. Y.; Yiu, S.-M.; Lau, T.-C., A Highly Reactive Seven-Coordinate Osmium(V) Oxo Complex: [OsV(O)(qpy)(pic)Cl]2+. Angewandte Chemie International Edition 2016, 55 (1), 288-291.

11. Popov, I., Jian, T., Lopez, G. *et al.* Cobalt-centred boron molecular drums with the highest coordination number in the CoB_{16}^- cluster. *Nat Commun* **6,** 8654 (2015). https://doi.org/10.1038/ncomms9654

12. The structures are rendered from cif data reported in the following publications (A) square antiprismatic $[Mo(CN)_8]^{3-}$: Wen-Yan Liu, Hu Zhou, Ai-Hua Yuan, *Acta Crystallographica Section E: Structure Reports Online*, 2008, 64, m1151, (B) dodecahedral $[Mo(CN)_8]^{4-}$: B.J.Corden, J.A.Cunningham, R.Eisenberg, *Inorganic Chemistry*, 1970, 9, 356.

13. The structure of ReH_9^{2-} is rendered from the structure reported in Abrahams, S.C.; Ginsberg, A.P.; Knox, K. Transition metal-hydrogen compounds. II. The crystal and molecular structure of potassium rhenium hydride, K_2ReH_9 *Inorganic Chemistry*, **1964**, *3*, 558-567.

14. There are other complexes in which a metal may be said to interact with more than sixteen "ligand atoms" but these are not usually considered to possess a higher coordination number. For example in some π complexes like η^5-Cp_4U technically there are 20 C atoms fastened to the U but these complexes are better considered as 12 coordinate than twenty (since each cyclopentadienl ring is isolobal with a *fac* coordinated set of 3 L ligands) while the metal centers in endohedral fullerene species like $La@C_{60}$ do not interact with all sixty carbon atoms at once are so are better thought of as a metal trapped in a spacious sixty-carbon cage.

15. Zalkin, A.; Forrester, J.D.; Templeton, D.H. Crystal structure of cerium magnesium nitrate hydrate *Journal of Chemical Physics*, **1963**, *39*, 2881-2891.

16. Daly, S. R.; Piccoli, P. M. B.; Schultz, A. J.; Todorova, T. K.; Gagliardi, L.; Girolami, G. S., Synthesis and Properties of a Fifteen-Coordinate Complex: The Thorium Aminodiboranate [Th(H3BNMe2BH3)4]. Angewandte Chemie International Edition 2010, 49 (19), 3379-3381.

17. Popov, I., Jian, T., Lopez, G., Boldyrev, A. I.; Wang, L-S. Cobalt-centred boron molecular drums with the highest coordination number in the CoB_{16}^- cluster. *Nat Commun* **6,** 8654 (2015).

Contributors

Stephen Contakes, Westmont College, to whom comments, corrections, and criticisms should be addressed.

Consistent with the policy for original artwork made as part of this project, all unlabeled drawings of chemical structures are by Stephen Contakes and licensed under a Creative Commons Attribution 4.0 International License.

Section 5.4: Coordination Numbers and Structures is shared under a CC BY-NC-SA 4.0 license and was authored, remixed, and/or curated by LibreTexts.

- **9.5: Coordination Numbers and Structures** by Stephen M. Contakes is licensed CC BY 4.0.
- **8.3: Coordination Numbers and Structures** is licensed CC BY-NC-SA 4.0.

Section 5.5: Isomerism

Metal complexes present a rich, interesting, and diverse structural chemistry. Major points of variation in the structural chemistry of metal complexes include

1. **coordination number** and **coordination geometry**, which involve differences in how many ligands surround a central metal and their overall geometric arrangement. Examples of the latter include the tetrahedral and square planar geometries commonly observed for four-coordinate metal centers. Tetrahedral, square planar, and octahedral coordination serve as a backdrop to the discussion of isomerism on this page. Readers who are unfamiliar with these structures might consider reading the section on coordination geometries before this one.
2. **structural iosmerism** involves differences in how potential ligand atoms are bound to metals in a complex. Possibilities for structural isomerism include
   - linkage or ambidentate isomerism
   - hydrate/solvate isomerism
   - ionization isomerism
   - coordination isomerism.

   Of these, linkage isomerism should always be considered when working with ambidentate ligands. As classifications, the last three forms of structural isomerism are mainly of academic interest since they represent permutations of ordinary structure patterns for solvates, salts, and coordination complexes, respectively.
3. **stereochemistry**, which includes
   - which coordination geometry is adopted for a metal with a given set of ligands in a particular oxidation state. For instance, $[Ni^{II}Cl_4]^{2-}$ is tetrahedral while $[Pt^{II}Cl_4]^{2-}$ is square planar. Since this geometry is usually fixed by the metal and ligands it is typically not a source of stereoisomeric varierty.
   - metal-centric stereoisomerism involving possible variations in where ligands are located relative to one another around the metal. The possibilities depend on the coordination number, geometry, and number of different types of ligands. For instance, square planar complexes can exhibit *cis-/trans-* isomerism while tetrahedral ones cannot. Tetrahedral complexes with four different ligands exhibit *R* and *S* chirality but complexes of that type are relatively rare. The more common cases include *cis* and *trans* isomerism in square planar complexes and *cis* & *trans-*, *mer* & *fac-*, and Λ & Δ isomerism in octahedral ones, although some multidentate ligands present additional possibilities for stereochemical variation
   - Stereoisomerism centered on the ligands bound to a metal center. Possibilities include
     - stereoisomerism inherent to a ligand. This would include cases where the ligand itself is chiral or, as in the case of amines, exists as a rapidly interconverting mixture of isomers. Thus this sort of stereoisomerism is an extension of the isomerism encountered in ordinary organic and other main group compounds. The main new issues introduced by binding of such ligands to a metal center involve the creation of new possibilities for diastereoisomerism based on the stereochemistry of the metal center and the freezing out of stereocenter inversion on binding to a metal. The latter is particularly important for amines, which as free amines racemize rapidly by nitrogen inversion.
     - or conformational isomerism involving five-membered **chelate rings** created when a multidentate ligand binds to a metal. This isomerism is often called chelate ring twist since individual rings can exhibit one of two conformations depending on how they twist on binding.

A summary of these forms of isomerism is given in Figure **Section5.5.1**.

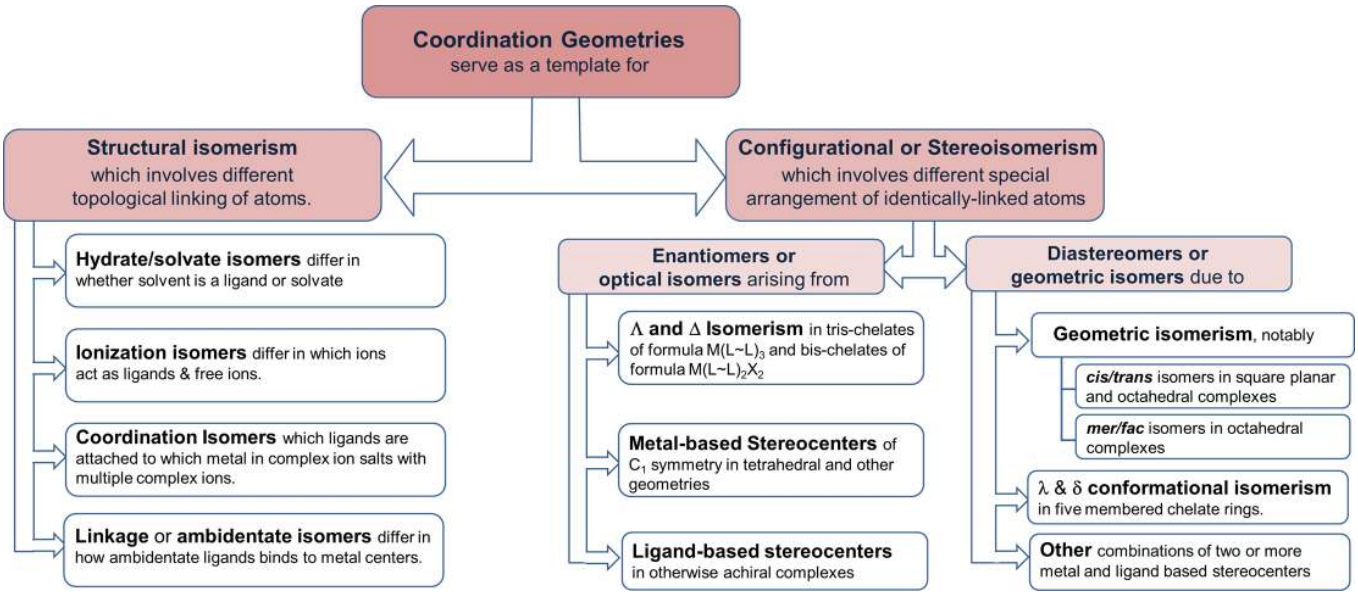


Figure **Section5.5.1**. Relationship among the common types of isomerism in metal complexes. This work by Stephen Contakes is licensed under a Creative Commons Attribution 4.0 International License.

Structural isomers

Structural isomerism involves different topological linkages of atoms. Differences in atomic linkages distinctive to coordination chemistry involve the linkages between metals and ligands. The main variations are:

1. Hydrate/solvate isomerism

Solvate isomers differ in terms of whether a molecule acts as a ligand or whether it acts as a solvate by occupying a lattice site in the crystal. Among solvate isomers, the case in which water is the ligand or solvate is the best known. The resulting isomers are called **hydrate isomers** after the term for water acting as a solvate, hydrate. A well-known example that illustrates how solvate isomerism works is the series $[CrCl_x(H_2O)_{6-x}]Cl_{3-x}{\cdot}xH_2O$, for which x = 0-2. The structures of the complex ions involved in this series are shown in Figure **Section5.5.2**.[1]

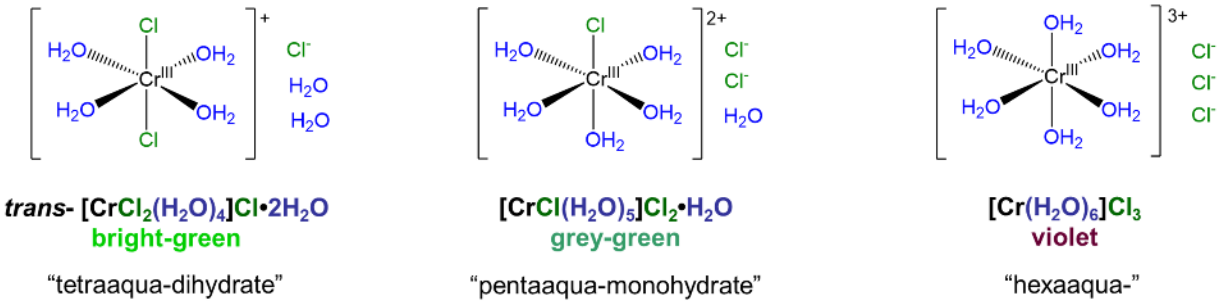


Figure **Section5.5.2**. Complexes of the hydrate isomer series $[CrCl_x(H_2O)_{6-x}]Cl_{3-x}{\cdot}xH_2O$ (x = 0-2). This work by Stephen Contakes is licensed under a Creative Commons Attribution 4.0 International License.

As can be seen from the compounds in Figure **Section5.5.2**, hydrate isomers differ both in terms of whether water acts as a ligand or hydrate *and* in terms of whether a potential counterion acts as a counterion or ligand. Thus, in *trans*-$[CrCl_2(H_2O)_4]Cl{\cdot}2H_2O$ two chlorides act as chloro ligands and four waters as aqua ligands while in $[CrCl(H_2O)_5]Cl_2{\cdot}H_2O$ five water molecules act as aqua ligands while only one chloride acts as a chloro ligand. In this way, solvate isomers simply represent cases in which two or more of the possible permutations for metal ligand binding among a set of solvent and counterion molecules are stable.

2. Ionization isomerism

In **ionization isomerism** there are two or more potential ions that can act as ligands. The ionization isomers differ in terms of which of these ions act as counterions and which act as ligands. Consider, for instance, the complexes shown in Figure **Section5.5.3**. These complexes differ in terms of whether the chloride or sulfate acts as a ligand, with the other acting as a counterion.

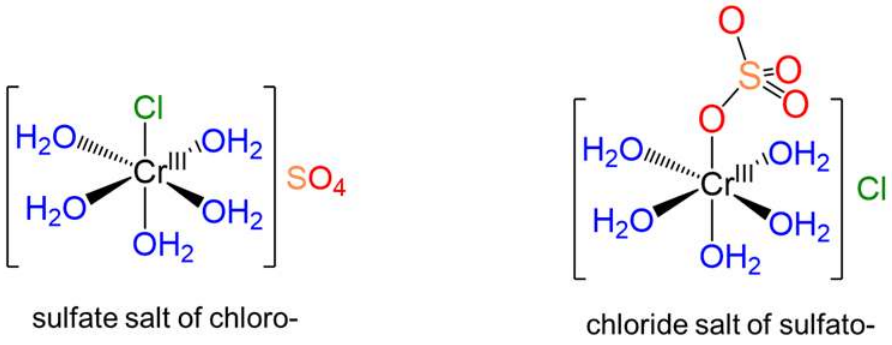


Figure Section5.5.3. Ionization isomers comprising a pentaaquachromium(III) fragment and the anions chloride and sulfate. As with all ionization isomers, the isomers differ in terms of which anion acts as a ligand and which a counterion. This work by Stephen Contakes is licensed under a Creative Commons Attribution 4.0 International License.

3. Coordination isomerism

Coordination isomers exist in compounds containing two or more complexes, each of which possesses a different set of ligands that can in principle be swapped with a ligand of the other complex. An example involves $[Co^{III}(NH_3)_6][Cr^{III}(ox)_3]$, depicted in Figure Section5.5.4A.[1] Coordination isomers of this complex involve swapping the ammine ligands around the Co^{3+} center for oxalato ligands surrounding the Cr^{3+} center. For instance, swapping all the ammine and oxalato ligands between the metal centers gives the coordination isomer $[Cr^{III}(NH_3)_6][Co^{III}(ox)_3]$ shown in Figure Section5.5.4B.

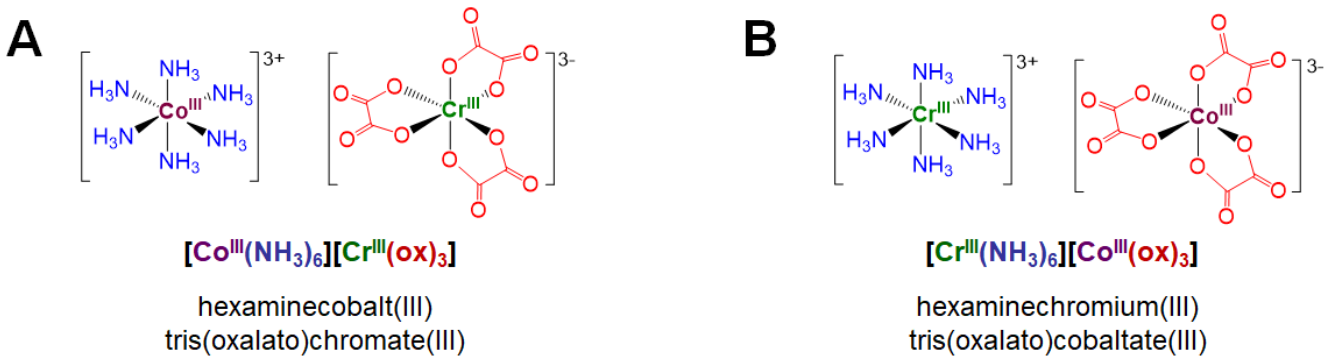
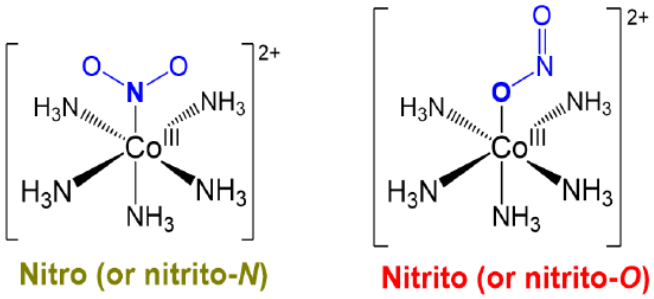


Figure Section5.5.4. Two coordination isomers comprising a Co^{3+} ,Cr^{3+}, six NH_3. and three oxalato ligands. The isomers differ in terms of which ligand type is bound to which metal. This work by Stephen Contakes is licensed under a Creative Commons Attribution 4.0 International License.

As classifications, hydrate/solvate, ionization, and coordination isomerism represent permutations of ordinary structure patterns for solvates, salts, and coordination complexes, respectively. As a result these forms of isomerism are rarely used as independent conceptual frameworks when thinking and talking about the structure of coordination compounds. Not so the final type of structural isomerism, linkage isomerism. That is because linkage isomerism has to do with the special *capacity* of ambidentate ligands to bind metals in multiple ways.

4. Linkage or ambidentate isomerism

Linkage or ambidentate isomers differ in how one or more ambidentate ligands bind to metal centers in a complex. The classic example dating from the work of Jørgensen and Werner is given in Scheme Section5.5.I.



Scheme **Section5.5.I**. Linkage isomers of penaamminenitritocobalt(III) ion. This work by Stephen Contakes is licensed under a Creative Commons Attribution 4.0 International License.

Just as alkenes exist as *E* and *Z* isomers, compounds possessing ambidentate ligands exist as one among the possible linkage isomers. As such, when working with ambidentate ligands the particular linkage isomer formed should be determined experimentally and considered when interpreting the complex's chemical and physical behavior.

The main ambidentate ligands which give rise to linkage isomerism are

- cyanide, CN^-
- thiocyanate, SCN^-, and the O and Se analogues, OCN^- and $SeCN^-$
- nitrite, NO_2^-
- sulfite, SO_3^-
- nitrosyl, NO

Although ambidentate ligands can bind metals in multiple ways, most exhibit a preferred binding mode (*i.e.*, prefer to bind metal centers in one of the possible ways). For instance, cyanide almost always binds through its carbon atom and thiocyanate almost always binds through its nitrogen (*μ-N*). However, the other binding mode can sometimes be formed kinetically or by using conditions that particularly favor its formation. Thus thiocyanate forms M-SCN^- linkages in the presence of exceptionally soft metal centers or in hard polar solvents (in which Lewis acid groups can stablize the terminal nitrogen of a bound thiocyanate ligand).

Ambidentate ligands are of significant research interest because many don't just bind to metal centers in two ways; the linkage isomers sometimes have significantly different physical properties. In addition, the possibility of two binding modes introduces the possibility of exploiting linkage isomerism to take advantage of some of these ligands:

a. different structural chemistry in different coordination modes. In mononuclear complexes the coordination mode influences which side of the ligand faces away from the complex and might be susceptible to stabilization by interaction with solvent. Additionally, the orientation of the ligand relative to the metal center might differ between one coordination mode and another. For instance, as predicted from the minor contributor to its resonance structure, thiocyanate binds nonlinearly via its S atom and linearly via its N (Figure **Section5.5.5**). Because of this the apparent steric bulk of the ligand around the metal center might differ between forms.

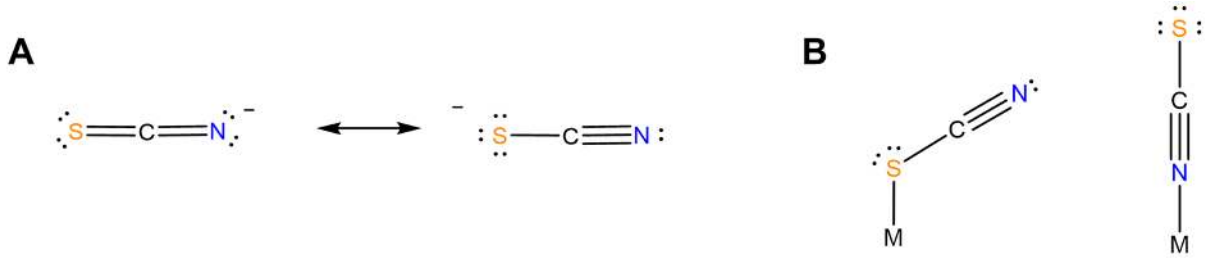


Figure **Section5.5.5**. Thiocyanate generally prefers to bind metals nonlinearly but in some cases forms linear M-SCN bonds. This work by Stephen Contakes is licensed under a Creative Commons Attribution 4.0 International License.

b. bind two different metal centers at the same time, linking them together. Perhaps the best-known examples involve thiocyanate and cyanide. The latter forms linkages of the type M-C≡N-M'. In the dye Prussian blue these take the form Fe^{II}-C≡N-Fe^{III}. An example from the author's graduate research involved tetrahedral clusters containing four metal atoms linked by six cyano ligands, as shown in Figure **Section5.5.6**.

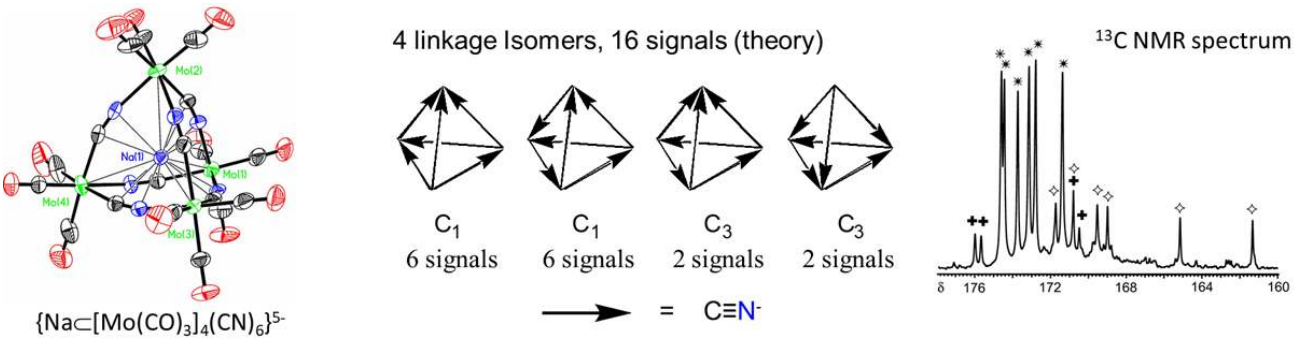


Figure **Section5.5.6**. (A) Structure of {Na@[Mo(CO)$_3$]$_4$(CN)$_6$} showing the linking of four Mo centers by six CN ligands. Thermal ellipsoids for the C atoms are shown in black; those of the N atoms in blue. (B) The complex exists as a mixture of four linkage isomers in which the bridging CN$^-$ ligands are oriented in different ways, as may be seen from the presence of the expected sixteen signals in its ^{13}C NMR spectrum. Based on work reported in reference 2.

c. can be induced to change from one binding mode to another in response to a stimulus. The classic example involves the light-driven transformation of the thermodynamically more stable yellow nitro complex of pentamminecobalt(III), $[Co(NH_3)_5NO_2]^{2+}$ to the less stable red *O*-nitrito complex, $[Co(NH_3)_5ONO]^{2+}$. Less stable cyanometallate coordination networks like those in the red K{Fe^{II}[Cr^{III}(CN)$_6$]} transform into the more stable green K{Fe^{II}[Cr^{III}(NC)$_6$]} form on heating, as shown in Figure **Section5.5.7**.[3]

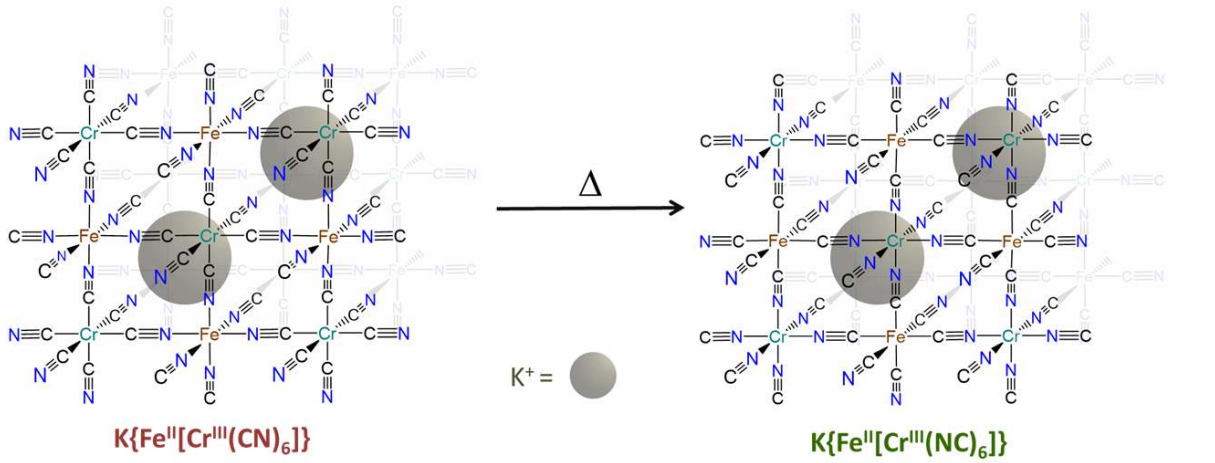


Figure **Section5.5.7**. Thermally-induced transformation of one K{Fe^{II}[Cr^{III}(CN)$_6$]} into its more stable green linkage isomer K{Fe^{II}[Cr^{III}(NC)$_6$]} involves "flipping" the cyano ligands. This work by Stephen Contakes is licensed under a Creative Commons Attribution 4.0 International License.

? Exercise *Section*5.5.1: Bridging ambidentate ligands and the Hard-Soft Acid- Base Principle.

The hard-soft acid-base principle helps explain the preference of bridging ambidentate ligands for particular binding modes. How might the greater stability of the green K{Fe^{II}[Cr^{III}(NC)$_6$]} over red K{Fe^{II}[Cr^{III}(CN)$_6$]} be explained in terms of the hard and soft acid-base concept?

Answer

The greater stability of K{Fe^{II}[Cr^{III}(NC)$_6$]} over K{Fe^{II}[Cr^{III}(CN)$_6$]} reflects the greater stability of the Fe^{II}-CN-Cr^{III} linkages in the former over the Fe^{II}-NC-Cr^{III} linkages in the latter. This is consistent with the preference for hard-hard and soft-soft Lewis acid-base interactions of the Hard-Soft Acid-Base Principle.

The Fe^{II}-CN-Cr^{III} linkages are more stable because they possess bonds between

- the softer Lewis acid (Fe^{II}) and Lewis base (the C end of CN$^-$)
- the harder Lewis acid (Cr^{III}) and Lewis base (the N end of CN$^-$)

In contrast, the Fe^{II}-NC-Cr^{III} linkages in the less stable linkage isomer involve bonds between

- the softer base (the C end of CN^-) and harder acid (Cr^{III})
- the harder base (the N end of CN^-) and softer acid (Fe^{II})

Stereoisomerism

Optical Isomerism/Chirality

Molecules of D_n, C_n, or C_1 symmetry with only proper rotation axes (including $E = C_1$) are chiral and exhibit optical isomerism. As described in Figure **Section5.5.1**, the main sources of such optical isomerism in coordination chemistry are:

1. Chirality inherent to an organic or main group ligand.

   This type of isomerism is just an extension of the sort described in undergraduate organic texts and consequently does not merit separate discussion here, other than to note that some forms of optical isomerism which are of little importance in organic chemistry lead to optical activity in coordination compounds. In particular, the nitrogen inversion process which serves to rapidly racemize chiral amines is frozen out on formation of a metal-ligand bond. Because of this chiral amine, ligands bound to a metal form non-interconvertible *R* and *S* enantiomers, as shown in Figure **Section5.5.8**.

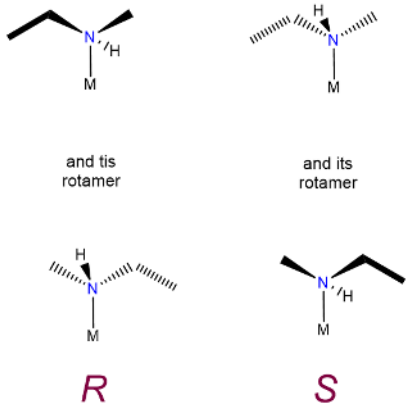


Figure **Section5.5.8**. Two views of *R* and *S* enantiomers formed when the chiral amine ethylmethylamine binds a metal that are commonly used to represent chiral amines in complexes. This work by Stephen Contakes is licensed under a Creative Commons Attribution 4.0 International License.

2. Chirality arising from the symmetry of ligands about a metal center.

   The two common situations through which such chirality arises involve:

   i. Chirality at a tetrahedral metal center surrounded by four different ligand attachment points.

   Such cases are often referred to as MABCD or Mabcd where M stands for the metal and a, b, c, and d the four different ligand attachment points. An example of such a complex is given in Figure **Section5.5.9A**. The chirality of such complexes is analogous to the chirality arising from a tetrahedral carbon stereocenter. There are two caveats, though. First, it is not enough to have a four-coordinate complex; the metal must possess tetrahedral symmetry since, as shown in Figure **Section5.5.9B**, square planar M complexes with four different ligands are identical to their mirror images. Second, such chirality is most easily realized using macrocyclic ligands like proteins. Metal ligand bonds involving sterically unhindered monodentate complexes like that in the example of Figure **Section5.5.9A** are in general weaker and more flexible than analogous carbon-carbon bonds. Consequently, in such cases it is likely that the enantiomers would interconvert through a fluxional process, making their resolution difficult if not impossible.

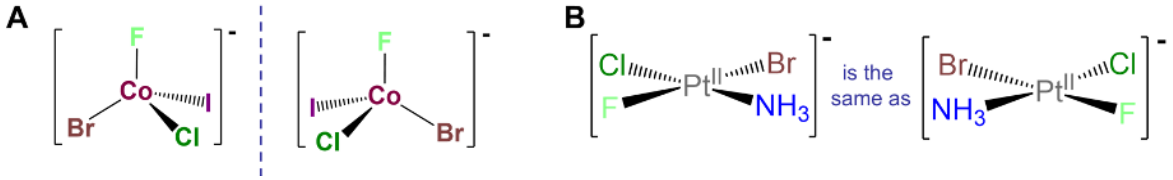


Figure **Section5.5.9**. (A) In principle tetrahedral metal centers surrounded by four different ligands (Mabcd) exhibit chirality analogous to the chirality of tetrahedral carbon stereocenters; (B) in contrast, square planar Macbd complexes like $[PtBrClF(NH_3)]^-$ are not chiral since they are the same as their mirror images. (It is easiest to see this by either working out its point group (C_s) or by rotating the left $[PtBrClF(NH_3)]^-$ structure clockwise 180 degrees to give its mirror image. This work by Stephen Contakes is licensed under a Creative Commons Attribution 4.0 International License.

ii. **Λ** and **Δ** isomerism at octahedral metal centers surrounded by two or three chelating ligands.

Specifically,

a. Octahedral tris-chelates of formula $M(L\sim L)_3$ exhibit D_3 symmetry.
b. cis-octahedral bis-chelates of formula $M(L\sim L)_2XY$ exhibit C_2 or C_1 symmetry: C_2 if X = Y and C_1 if $X \neq Y$.

As shown in Figure **Section5.5.10A**, octahedral tris-chelates like $[V(ox)_3]^{3-}$ are chiral and can exist as nonsuperimposable **Λ** and **Δ** enantiomers. The chirality of these tris-chelates is analogous to that of pinwheels. As shown in Figure **Section5.5.10B**, when looking directly at the head of any individual pinwheel from above, the blades will be angled from back to front going around the pinwheel in either the clockwise or counterclockwise direction. As shown in Figure **Section5.5.10C**, the case for which the blades are angled in the clockwise direction is analogous to the **Λ** enantiomer and the case when they are angled in the counterclockwise direction the **Δ**.

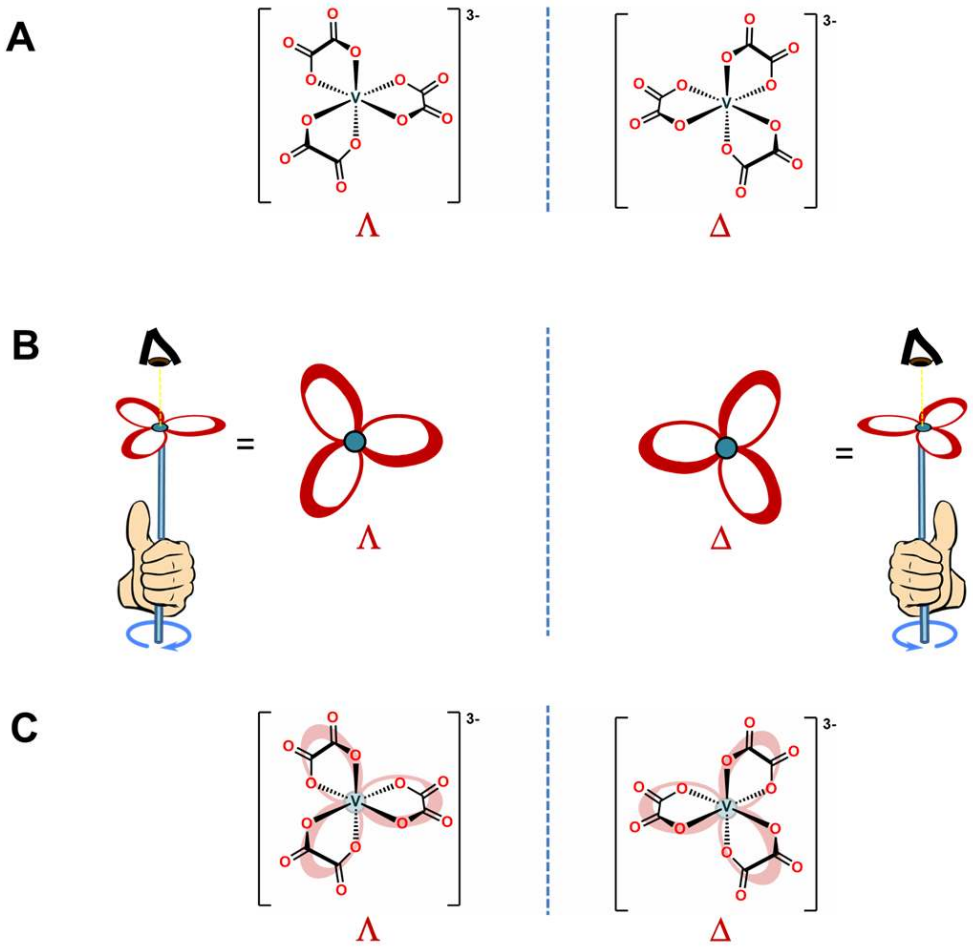


Figure **Section5.5.10**. (A) Octahedral tris-chelates like $[V(ox)_3]^{3-}$ are chiral and can exist as **Λ** and **Δ** enantiomers. (B) The chirality in these systems is analogous to that of a pinwheel, with the **Λ** enantiomer exhibiting the symmetry of a left-handed pinwheel and the **Δ** enantiomer that of a right handed one. (C) The pinwheel-like nature of **Λ** and **Δ** enantiomers is easiest to see by overlaying the structures of $[V(ox)_3]^{3-}$ from A with the pinwheel structures of B. One way to recognize **Λ** and **Δ** enantiomers is to draw them in these projections. If a left hand is curled around the **Λ** enantiomer with the thumb facing up the curl of the fingers will flow from the back of each ligand towards the front. The same will be true if the right hand is curled around the **Δ** enantiomer. Credits: Although the image is largely an original drawing, the hand images used in part B are adapted from an image by SVGguru / CC BY-SA (https://creativecommons.org/licenses/by-sa/4.0). Otherwise this work by Stephen Contakes is licensed under a Creative Commons Attribution 4.0 International License.

The **Λ** and **Δ** chirality in octahedral bis-chelates is analogous to that in the tris-chelates except this time the third chelating ligand is replaced by an arbitrary pair of ligands. This lowers the symmetry of the complex to either C_2 or C_1, as shown for the C_2 complex $[CoCl_2(en)_2]^+$ in Figure **Section5.5.11A**. In either case the result is that such complexes exist as **Λ** and **Δ** enantiomers analogous to those in the metal tris-chelates, as shown in Figure **Section5.5.11B**.

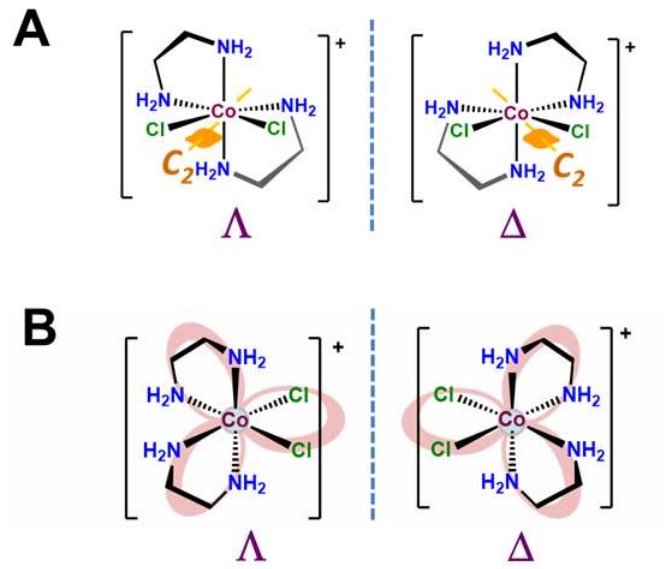


Figure **Section5.5.9C**. This work by Stephen Contakes is licensed under a Creative Commons Attribution 4.0 International License.

Octahedral complexes containing ligands with denticities of four or more also exhibit **Λ** and **Δ** chirality; it is just that in such cases the bound ligand defines multiple rings within the complex that can be defined as existing in either **Λ** or **Δ** orientations relative to each other. The procedure for making these assignments is beyond the scope of most introductory inorganic courses but the result is that such complexes are designated as **ΛΛ**, **ΔΔ**, **ΔΛ**, **ΔΔΔ**, etc., depending on the number of relationships involving the rings defined by the bound ligand. Interested readers should consult reference 4 for more details.

Circular dichroism may be used to characterize optically active metal complexes.

At the present the most definitive way to determine the absolute configuration of an optically active coordination compound is to determine its 3D molecular structure using single crystal X-ray crystallography.[5] However, as that is not always possible or convenient, the optical activity of coordination complexes is also commonly studied using circular dichroism (CD) spectroscopy. CD spectroscopy is used because, unlike most chiral organics, optically active coordination complexes possess low-energy electronic transitions that occur in the far UV and visible range. This means that it is often convenient to use the ability of a complex to refract and absorb different circular polarizations of light to derive information about both the configuration of an optically active complex and its electronic structure. The focus of this section will be to explain how the determination of absolute configuration by circular dichroism and optical rotatory dispersion work, as well as the relationship of these techniques to the more ordinary sort of polarimetry used to measure optical rotation in organic systems. Only brief notes will be made about the instrumental and electronic structure applications of these techniques since the electronic spectra of metal complexes will be discussed in Chapter 11: Coordination Chemistry III - Electronic Spectra and the instrumental aspects of CD are well-treated elsewhere.

Both polarimetry and circular dichroism spectroscopy are grounded in the recognition that plane polarized light is equivalent to a superposition of left and right circularly polarized light, as shown in Figure **Section5.5.12**.

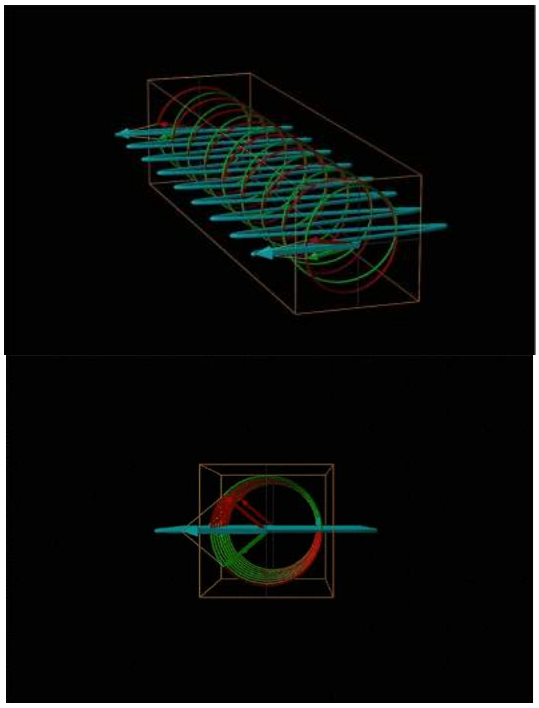


Figure **Section5.5.12**. Angled and front view of plane polarized light (light blue) as the vector sum of left circularly polarized light (red) and right circularly polarized light (green). Created using EMANIM Version 1.2 (2011 July) by Andras Szilagyi (www.enzim.hu/~szia/emanim). This work by Stephen Contakes is licensed under a Creative Commons Attribution 4.0 International License.

When plane polarized light passes through a chiral medium, its left and right circularly polarized components move at different rates (*i.e.*, have different indices of refraction). This causes the plane of polarization to rotate in the direction of the faster component according to the relationship

$$\alpha = \frac{n_l - n_r}{\lambda}$$

where α is the angle of rotation, λ the light's wavelength, and n_l and n_r the refractive indices experienced by left and right circularly polarized light.

An example of such a rotation is shown in Figure **Section5.5.13**.

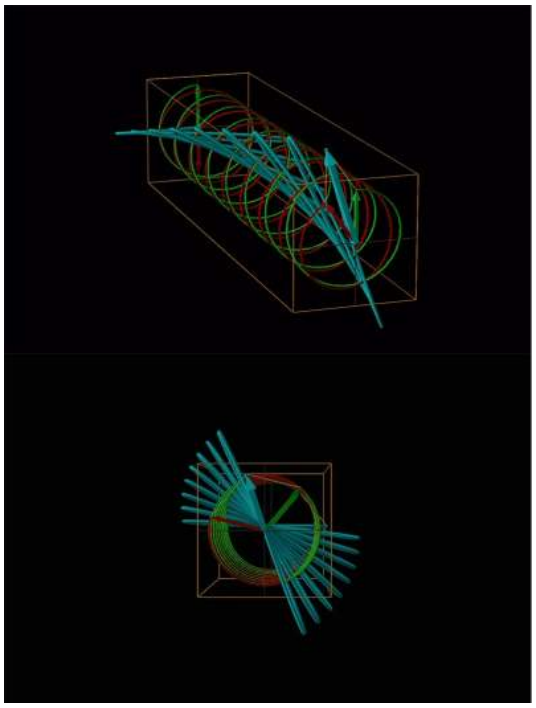


Figure Section5.5.13. Angled and front view of plane polarized light (light blue) as it passes through a medium (represented by the orange box) in which left circularly polarized light (red) experiences a higher refractive index (and so moves slower) than right circularly polarized light (green). Created using EMANIM Version 1.2 (2011 July) by Andras Szilagyi (www.enzim.hu/~szia/emanim) with a refractive index of 1.05 for left circularly polarized light and 1.00 for right circularly polarized light. This work by Stephen Contakes is licensed under a Creative Commons Attribution 4.0 International License.

Chemists typically call this rotation of light by a chiral medium optical rotation. In organic chemistry it is common to measure the optical rotation at the sodium D wavelength of 589.29 nm, a much longer wavelength than most organics are able to absorb. Because of this the optical rotations commonly measured by organic chemists are largely independent of absorption and mainly serve as a characteristic physical property similar to melting points or are used to establish the purity of a mixture of enantiomers. The sort of spectroscopic data used to characterize chiral coordination compounds more commonly makes use of the relationship between absorption and optical rotation.

In coordination chemistry the wavelength-dependence of optical rotation is used to discern information about compounds' electronic spectra. This measurement of the wavelength dependence of optical rotation is called **optical rotatory dispersion (ORD)** and the resulting plots are called optical rotatory dispersion or ORD spectra or curves. Such ORD curves are useful for characterizing the chiral environment in a coordination complex because the ORD curves exhibit a characteristic shape. This characteristic shape is because according to the **Cotton Effect,** the optical rotation changes sign at the absorption maximum of a chromophore in the compound. For one configuration the rotation will go from negative to positive with increasing wavelength and is called a **positive cotton effect**; for the other configuration the rotation will go from positive to negative or exhibit a **negative cotton effect**. This behavior is summarized in the top two curves of Figure Section5.5.14.

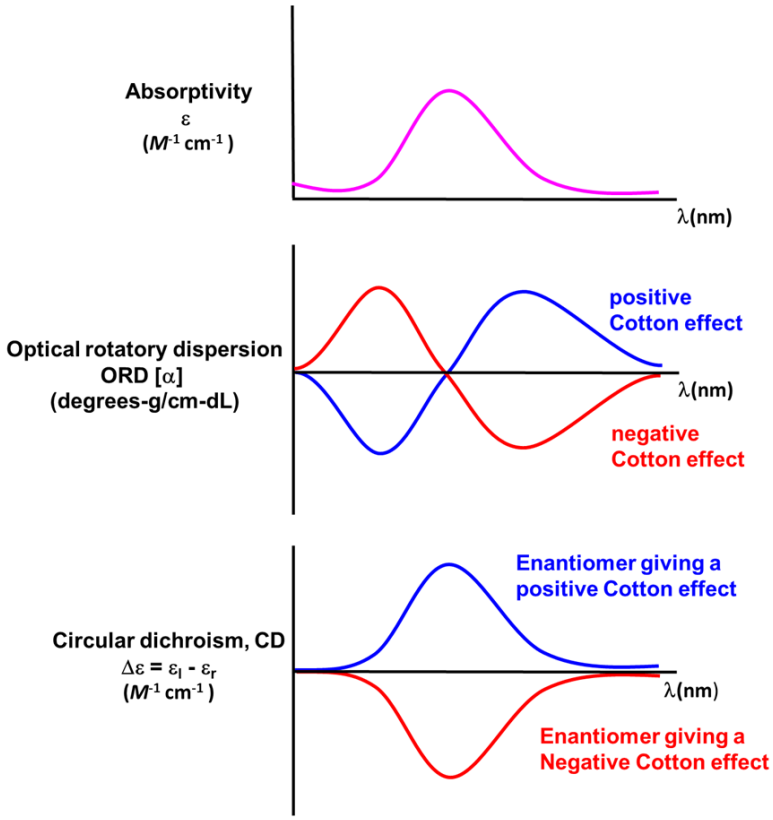


Figure Section5.5.14. Idealized relationship between absorbance, ORD, and CD spectra for enantiomers exhibiting a positive and negative Cotton effect. This work by Stephen Contakes is licensed under a Creative Commons Attribution 4.0 International License.

A technique used even more often than ORD is **circular dichroism (CD)**, represented by the lowest spectrum in Figure Section5.5.14. Circular dichroism arises from the differential absorption of left and right circularly polarized light by a chiral compound. This gives elliptically polarized light as shown in Figure Section5.5.15.

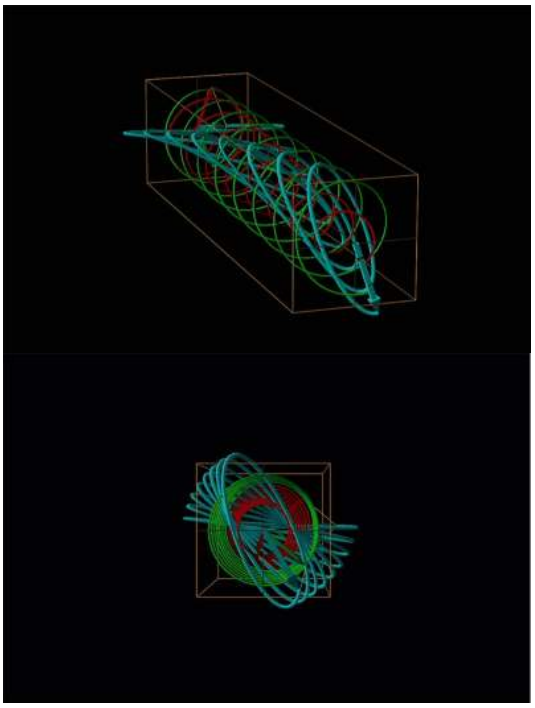


Figure **Section5.5.15**. Angled and front view of plane polarized light (light blue) as it passes through a medium (represented by the orange box) in which left circularly polarized light (red) both experiences a higher refractive index and greater absorption than right circularly polarized light (green). Created using EMANIM Version 1.2 (2011 July) by Andras Szilagyi (www.enzim.hu/~szia/emanim) with a refractive index of 1.05 and an extinction coefficient of 0.05 for left circularly polarized light and a refractive index of 1.00 and extinction coefficient of 0 for right circularly polarized light. This work by Stephen Contakes is licensed under a Creative Commons Attribution 4.0 International License.

In circular dichroism (CD) spectroscopy a sample is irradiated with polarized light resulting in the transmission of elliptically polarized light due to differential refraction and absorption of the polarized light's left and right circularly polarized components. For achiral molecules the handedness doesn't affect absorbance, but for chiral molecules, which chiral ground and excited states the handedness of an EM wave affects can determine how readily that wave can distort the chiral ground state into the chiral excited one. For this reason chiral molecules absorb left and right circularly polarized light differently.

In CD spectroscopy the magnitudes of the left and right circularly polarized components of light that is transmitted by the sample are measured and used to determine how much light of each was absorbed (just as in regular absorbance spectroscopy). The difference in absorption between left and right circularly polarized light constitutes the primary signal in CD spectroscopy. More specifically, circular dichroism spectra (CD spectra) show the difference in extinction coefficients for left and right circularly polarized light, $\Delta\epsilon$, as a function of wavelength, where

$$\Delta\epsilon = \epsilon_l - \epsilon_r$$

where Missing open brace for subscript and Missing open brace for subscript are the extinction coefficients observed with left and right circularly polarized light, respectively.

As with ORD spectra, the signs of the features in CD spectra like that of Δ–$[Co(en)_3]Cl_3$ given in Figure **Section5.5.16** are enantiomer-dependent. As illustrated in the lower spectrum in Figure **Section5.5.14** , the CD spectra of enantiomers mirror one another. Because of this difference in behavior it is possible in principle to determine the absolute configuration of a complex from its CD spectrum.

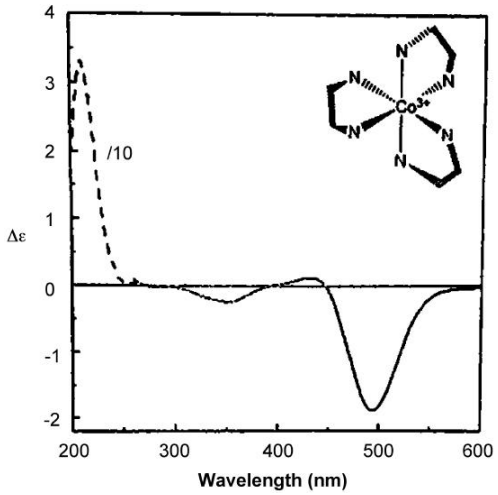


Figure Section5.5.16. CD spectrum of Δ–$[Co(en)_3]Cl_3$. Taken from reference 6.

There are several ways that ORD and CD spectra can be useful for determining the absolute configuration of a chiral complex.

1. First, the sign of the Cotton effect and peaks in CD spectra exhibited by a given absolute configuration is often consistent across a series of compounds. Thus if a new member of the series is isolated, its configuration can be determined based on which enantiomer has the same Cotton effect. For instance, if both the **Λ** isomer of a metal diimine complex like $[Ru(bpy)_3]^{2+}$ exhibit a positive Cotton effect and a newly resolved metal diimine exhibits a negative Cotton effect it might reasonably be inferred that the newly-resolved complex is in the opposite or **Δ** configuration.
2. Second, for some systems the expected sign of the Cotton effect and CD peaks for each enantiomer may be predicted semi-empirically based on the spatial locations of substituents relative to the chromophore (the part of the molecule that changes electronic structure during the transition), although the details are beyond the scope of the present discussion.
3. Consideration of interactions between multiple chromophores in a compound can be used to infer absolute configuration. Again, the details are beyond the scope of the present discussion. Interested readers are referred to reference 7 for details.

Common patterns of Diastereomerism

Geometric isomerism

Geometric isomerism involves differences in the geometric placement of atoms in a compound. In coordination chemistry, geometric isomerism involves differences in the relative placement of a set of ligands about a metal center. There are two main types:

cis and *trans* isomerism

This type of isomerism has to do with how two ligands are oriented relative to one another in a square planar or octahedral complex. As shown in Figure Section5.5.17, ligands that are next to one another with a L-M-L bond angle of 90° are said to be *cis*; those on opposite sides of the metal with a L-M-L bond angle of 180° are in the *trans* arrangement.



Figure Section5.5.17. *cis* and *trans* arrangement of ligands around (A) square planar and (B) octahedral metal centers. Since both types of complexes feature 90° L-M-L bond angles, the arrangements are fundamentally the same in both cases. This work by Stephen Contakes is licensed under a Creative Commons Attribution 4.0 International License.

Simple *cis* and *trans* geometric isomers can be identified when there are two identical ligands (A) or chelating ligands with distinguishable attachment points (A~B) oriented about either a square planar or octahedral center. Examples are given in Figure

Section5.5.18. Notice from the example given in Figure Section5.5.18C that multidentate ligands have the potential to constrain complexes to adopt a particular geometry.

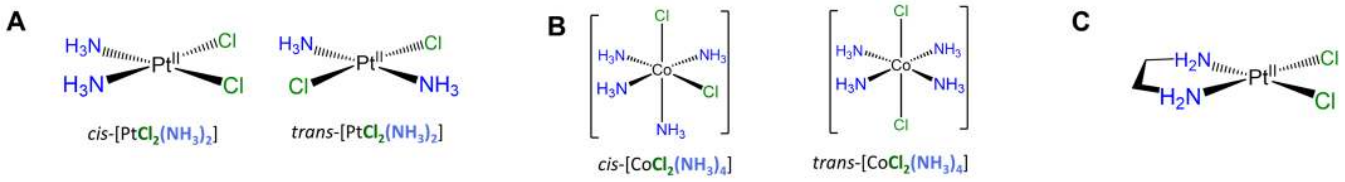


Figure Section5.5.18. Examples of square planar and octahedral *cis* and *trans* isomers. (A) *cis* and *trans* isomers of $[PtCl_2(NH_3)_2]$; the former is medicinally important. Sold under the name cisplatin, the *cis* isomer is used as a chemotheraphy against various forms of cancer. (B) *cis* and *trans* isomers of $[CoCl_2(NH_3)_4]$, a compound of more academic interest. (C) $PtCl_2$(en) only exists as the *cis* isomer because the chelating en ligand can only bind in a *cis* arrangement. This work by Stephen Contakes is licensed under a Creative Commons Attribution 4.0 International License.

Slightly more involved examples involve perturbations of the simple cases above in which there are multiple distinguishable *cis* and/or *trans* relationships. Two square planar examples are given in Figure Section5.5.19.

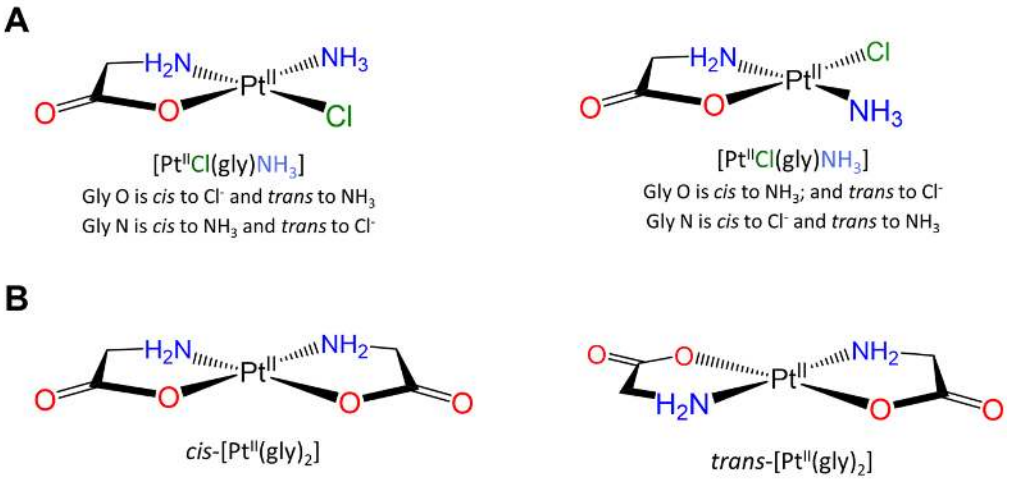


Figure Section5.5.19. Examples of more complex square planar systems. (A) Geometric isomers of $[PtCl(gly)NH_3]$, a MA_2BC system for which A = gly^-, B = Cl^-, and C = NH_3. Swapping of the ammine and chloro ligands changes both the *cis* and *trans* relationships involving the Gly ligand. (B) Geometric isomers of $[Pt(gly)_2]$, an $M(A{\sim}B)_2$ system for which A = the κO glycine carboxy group and B its κN amine. The only possible geometric isomerism involves swapping the orientation of one glycine relative to the other. For this reason the two complexes shown can be designated as *cis* and *trans* isomers based on whether the κO and κN ends of the glycine are *cis* or *trans* to one another. This work by Stephen Contakes is licensed under a Creative Commons Attribution 4.0 International License.

More complex examples of *cis* and *trans* relationships between ligands in octahedral complexes are given in the exercises that conclude this page, which also demonstrates how a systematic approach may be used to identify isomers.

mer and *fac* isomerism

This type of isomerism has to do with how three ligands are oriented relative to one another in an octahedral complex. The arrangements are represented in Figure Section5.5.20.

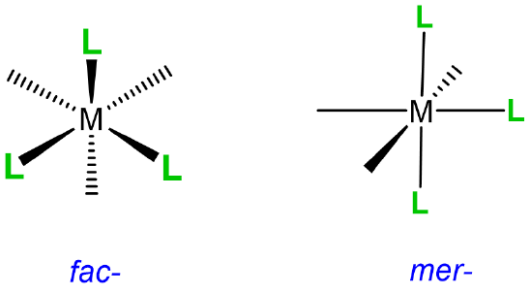


Figure **Section5.5.20**. Simple representation of the *fac* and *mer* arrangements of ligands around an octahedral metal center. This work by Stephen Contakes is licensed under a Creative Commons Attribution 4.0 International License.

Since it can help to visualize the *mer* and *fac* geometry from multiple points of view, several representations are given in Figure **Section5.5.21**. As shown in Figure **Section5.5.21**, in ***fac*** or **facial arrangements**, the ligands occupy the same "face" of the octahedral coordination sphere, while in the ***mer*** or **meridional geometry** the ligands form a T shape in the same plane or its "meridian."[8]

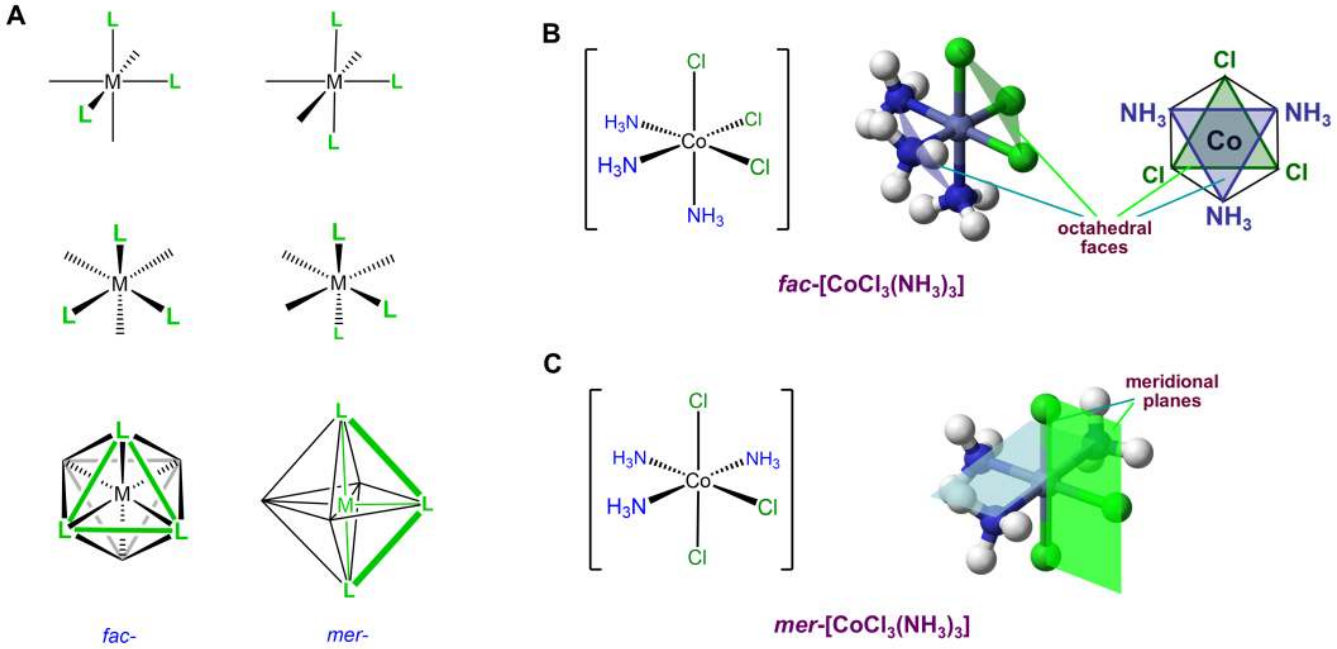
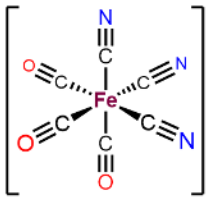
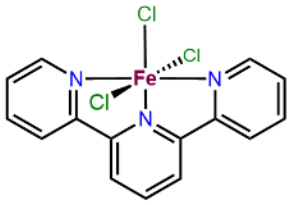
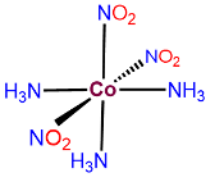


Figure **Section5.5.21**. (A) Three projections of *fac* and *mer* arrangements of ligands around an octahedral metal center emphasizing that in the *fac* arrangement the ligands are oriented along a face of the octahedron while in the *mer* arrangement they are oriented in a plane. (B) Structure of *fac*-$[CoCl_3(NH_3)_3]$ showing the octahedral faces occupied by the chloro and amine ligands. (C) Structure of *mer*-$[CoCl_3(NH_3)_3]$ showing the planar arrangement of the chloro and ammine ligands. The ball and stick models are modified from images by Benjah-bmm27 - Own work, Public Domain, https://commons.wikimedia.org/w/inde...?curid=1874872 and curid=1874873. Otherwise this work by Stephen Contakes is licensed under a Creative Commons Attribution 4.0 International License.

Octahedral complexes with three identical ligands oriented about an octahedral center can only exist in *mer* and *fac* arrangements. Consequently, such complexes can be designated as *mer* and *fac* isomers. Examples are given in Figure **Section5.5.22**.







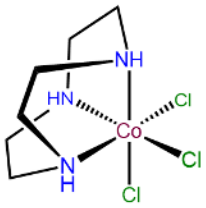


Figure **Section5.5.22**. Examples of *fac* and *mer* octahedral complexes. Note how some chelating ligands preferentially bind to the metal in a *fac* or *mer* arrangement and, in so doing, force the other ligands to also form a *mer* or *fac* arrangement. This work by Stephen Contakes is licensed under a Creative Commons Attribution 4.0 International License.

Diastereomerism arising from multiple ligand-associated chiral centers

Diastereomerism can also arise when two or more chiral ligands bind to a metal center. Such cases typically give rise to a complex mixture of isomers, as shown by the example in Figure **Section5.5.23**. As may be seen from Figure **Section5.5.23**, the differences between these isomers can arise from both changes in the stereochemical configuration of the ligand and the relationship of particular ligand centers relative to one another. For instance, the leftmost two structures in Figure **Section5.5.23** possess one *R* and *S* nitrogen center each but differ in whether the centers are oriented so that the *R* and *S* centers on the two ligands are *trans* or *cis* to one another.

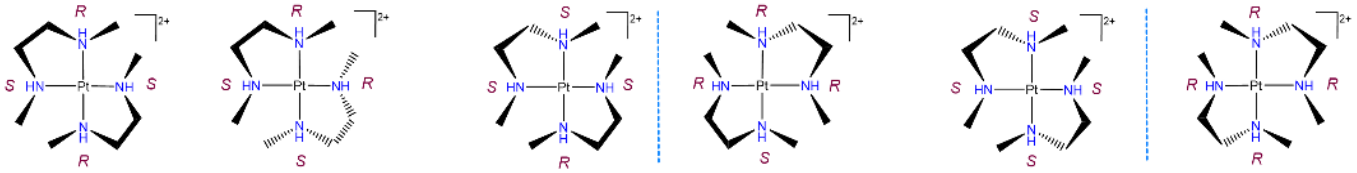


Figure **Section5.5.23**. Diastereomers that can in principle be formed when two *N*,*N*′-dimethylethylenediamine ligands coordinate a Pt^{2+} center. This work by Stephen Contakes is licensed under a Creative Commons Attribution 4.0 International License.

Diastereomerism arising from λ and δ ring conformation isomerism.

Chelate rings are formed when a chelating ligand binds a metal

As may also be seen from the structures in Figure **Section5.5.23**, when a multidentate ligand coordinates a metal, the ligand and metal center comprise one or more **chelate rings**. Examples of such chelate rings are shown in Figure **Section5.5.24**.

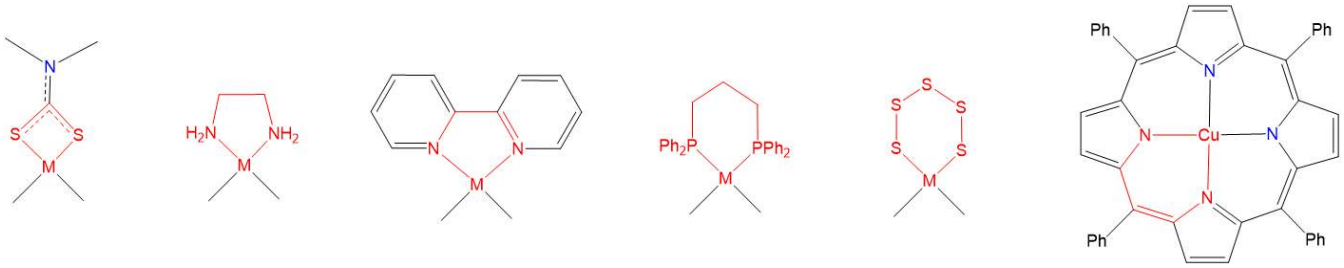


Figure **Section5.5.24**. Four, five, and six-membered chelate rings (shown in red) formed by coordination of selected bidentate ligands to a metal center. This work by Stephen Contakes is licensed under a Creative Commons Attribution 4.0 International License.

As may be inferred from the examples in Figure Section5.5.24, chelate rings may be of different sizes, although four, six, and especially five-membered rings are particularly common. Exactly which ring sizes will be more stable for a given system depends on the coordination geometry and, due to differences in M-L bond lengths, to a lesser degree on the metal. As a result, for octahedral and square planar complexes with 90° L-M-L bond angles between *cis* ligands, *five-membered rings tend to be especially stable* (Figure Section5.5.25).

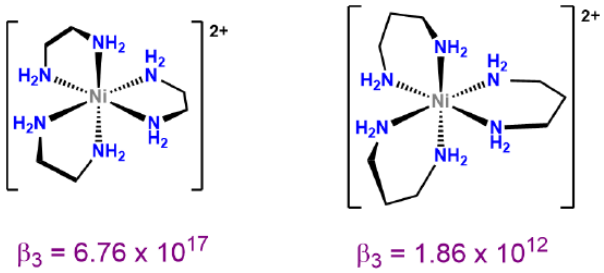


Figure Section5.5.25. The greater stability of five-membered chelate rings involving Ni^{2+} and organic ligands is reflected in the higher overall formation constant (β_3) for the five-membered chelate rings contained in $[Ni(en)_3]^{2+}$ compared to that of $[Ni(et)_3]^{2+}$, which has six-membered rings. The data in this figure is taken from Stability of Metal Complexes and Chelation by Robert Lancashire. This work by Stephen Contakes is licensed under a Creative Commons Attribution 4.0 International License.

Not all metal chelates prefer to form five-membered rings. The steric requirements of chelate rings depend on both the preferred coordination geometry of the metal center and the stereochemistry of the ligand. Both of these effects are typically considered in terms of preferred L-M-L bond angles. From the perspective of the metal center, the preferred bond angle is determined by the coordination geometry. Octahedral and square planar metals prefer 90° L-M-L bond amgles, trigonal bipyramidal systems 90 and 120° L-M-L bond angles, and tetrahedral complexes 109.5° L-M-L angles. The larger preferred bond angles in tetrahedral and trigonal bipyramidal systems often require the formation of larger six or seven-membered chelate rings for maximum stability. The size of the chelate ring actually formed between a metal and ligand is determined by the ligand's structure. As the contributor of all the atoms in the chelate ring but one, the ligand directly determines the chelate ring size. More subtly, ligands naturally prefer to coordinate metals at a particular L-M-L angle, called the **bite angle**, as shown in Figure Section5.5.26A. Ligands with bite angles corresponding to the ideal L-M-L angle for a metal's preferred geometry tend to form more stable complexes, although in turn ligand bite angles can cause metals with a weak coordination geometry preference to adopt the ligand's preferred geometry instead.[10] As may be seen from the values in Figure Section5.5.26B, bite angles roughly increase with the size of the chelate ring formed but are also influenced by the types of structures used to connect the ligand's Lewis base sites. This facilitates the use of diphosphine ligands to tailor the structure and reactivity of phosphine-containing organometallic catalysts.



Figure Section5.5.26. (A) Definition of the bite angle as the angle at which the ligand's preferred L-M-L angle when coordinating a metal center. (B) Bite angles of selected diphosphines.[9] The bite angles of many such diphosphines have been determined to facilitate the design of phosphine-containing organometallic catalysts. This work by Stephen Contakes is licensed under a Creative Commons Attribution 4.0 International License.

λ and δ isomerism involves differences in the conformation of nonplanar five-membered chelate rings

As shown in Figure Section5.5.27, some chelate ring systems are planar while others are not.

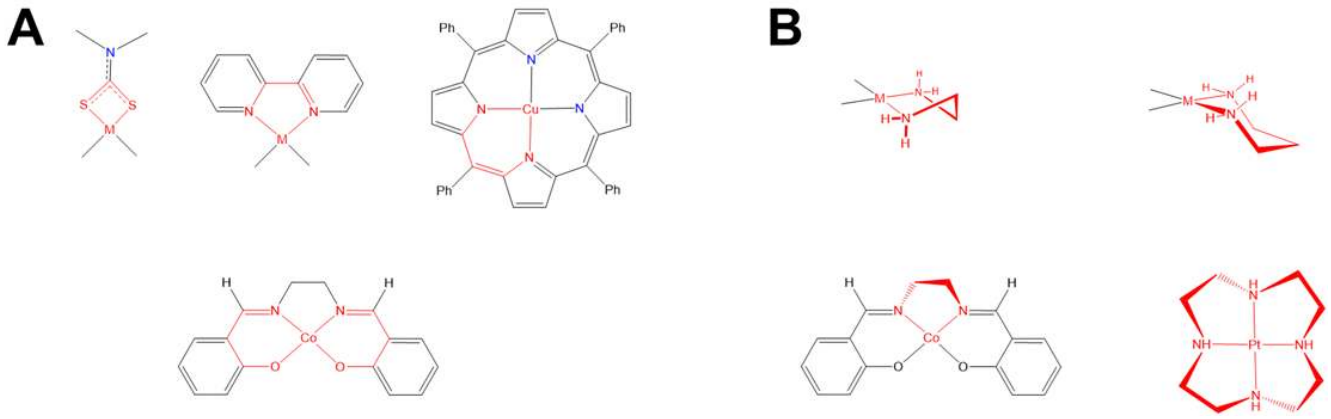


Figure Section5.5.27. (A) Planar and (B) Nonplanar chelate rings shown highlighted in red. Notice how [Co(salen)] possesses a nonplanar chelate ring and two planar ones. This work by Stephen Contakes is licensed under a Creative Commons Attribution 4.0 International License.

Among the nonplanar chelate ring systems are ligands like en and dppe, which contain tetrahedral C, N, O, P, and S atoms. Because these atoms create kinks in the chelate ring they introduce additional opportunities for diastereomerism due to differences in the chelate ring conformation, called **ring twist**. Ring twist in nonplanar systems has been most extensively explored for five-membered chelates like those formed by dppe and by en and other chelating amines. Unlike the more rigid four-membered chelate rings, five-membered chelates tend to be conformationally flexible, but not so conformationally flexible that their conformers are rapidly interconverting at room temperature (at least not when the rings are substituted to introduce additional steric strain). This balance between flexibility and rigidity enables some five-membered chelate rings to exist as mixtures of distinguishable conformational isomers at room temperature.

To understand the two most stable conformers that five-membered chelates rings tend to form, it is helpful to think of five-membered chelate rings as involving two components (Figure Section5.5.28):

- a planar L-M-L group, where L are the atoms directly attached to the metal, M, and
- the remaining two ring atoms, E, which form a rigid E-E bar across the back of the chelate ring.

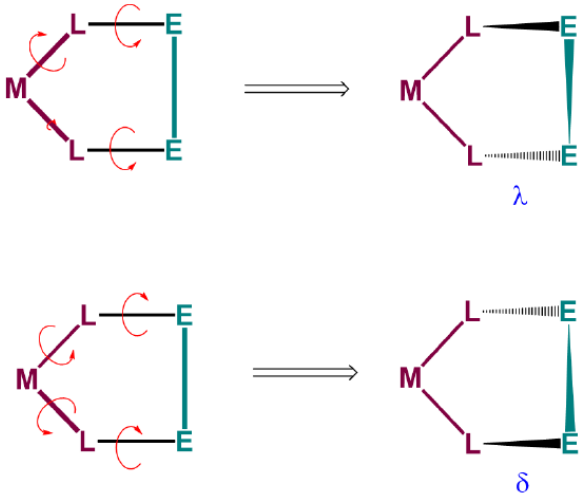


Figure Section5.5.28. Five-membered chelate rings consist of a planar L-M-L group connected to a rigid E-E bar. Conformers arise as rotation about the M-L and L-E bonds causes twisting of the E-E bar relative to the L-M-L plane. This work by Stephen Contakes is licensed under a Creative Commons Attribution 4.0 International License.

As can be seen from Figure Section5.5.28 , rotation about the M-L and L-E bonds causes twisting of the E-E bar relative to the L-M-L plane. The two most stable conformers produced by these motions are the λ or δ conformations as shown in Figures Section5.5.29 and Section5.5.29.

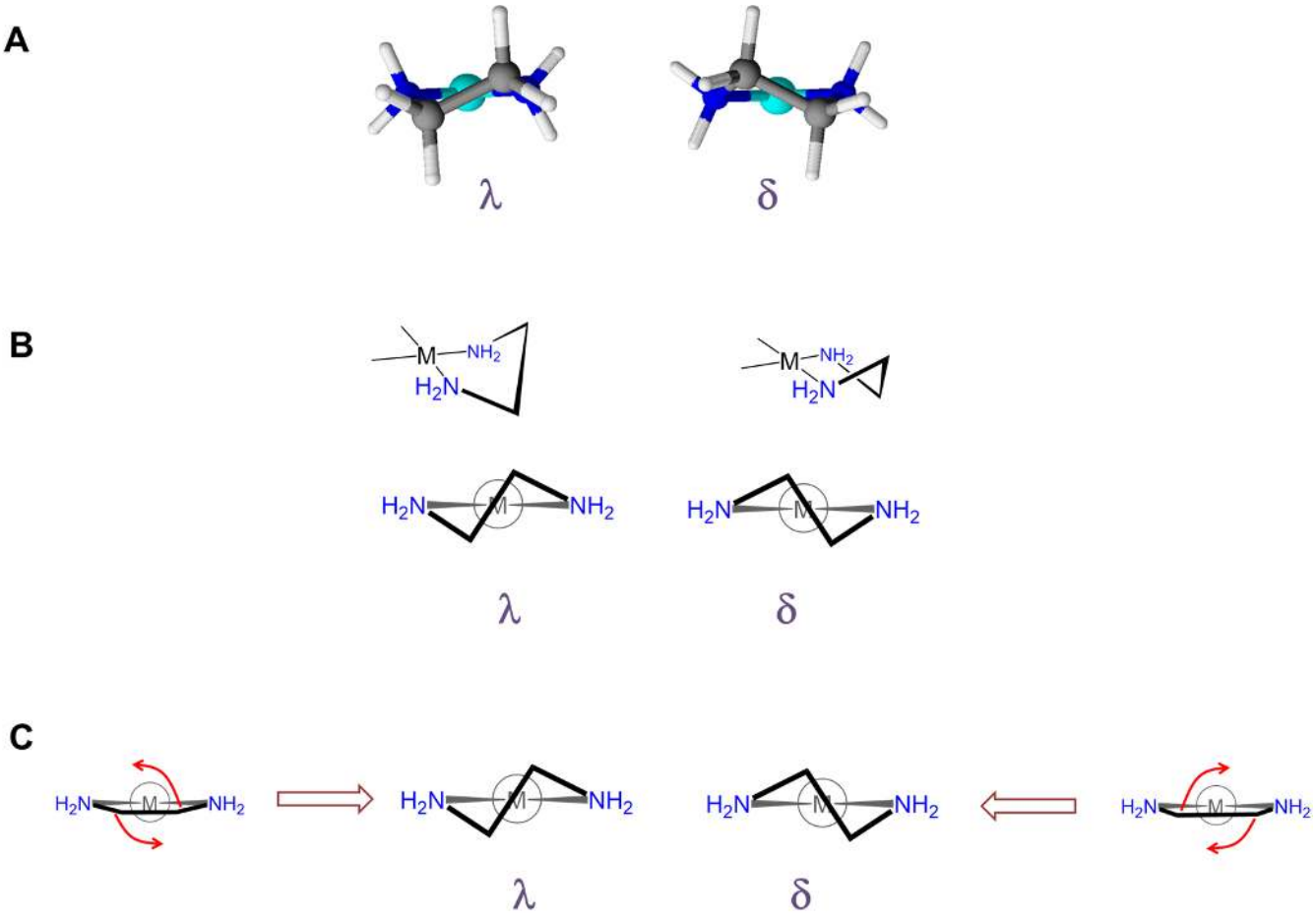


Figure **Section5.5.29**. (A) **λ** and **δ** ring twist in a square planar metal ethylenediamine complex (B) along with several ways to represent it in line drawing form. (C) Of these, the projection looking down an axis bisecting the chelate ring makes it easiest to see that, starting with a planar chelate ring the **λ** conformer corresponds to a counterclockwise twist of the CH_2CH_2 bond relative to the N-M-N plane and the **δ** conformer a clockwise twist relative to the N-M-N plane. This work by Stephen Contakes is licensed under a Creative Commons Attribution 4.0 International License.

The relative stability of the **λ** and **δ** conformers will depend on the configuration of any stereocenters present and steric factors. As with organic ring systems, steric effects tend to favor conformers in which bulky groups are placed in the less sterically strained equatorial positions while the configuration of the stereocenters present can serve to restrict the allowable ring twist conformations, as illustrated in Figure **Section5.5.30**. A detailed treatment of such systems is beyond the scope of this page. Interested readers are referred to reference 12 for more details.

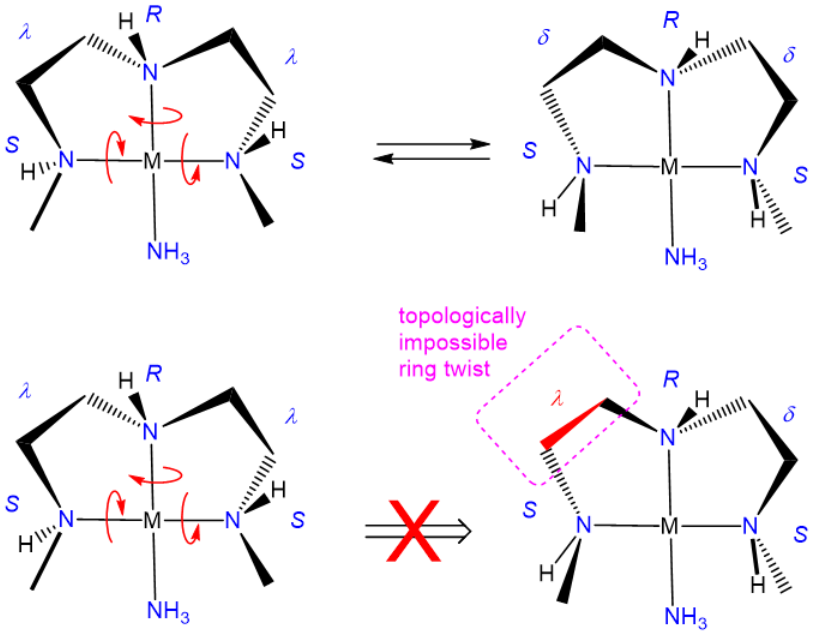


Figure Section5.5.30. The configurations at nitrogen in the complex shown restrict the chelate ring conformations to either a λλ or δδ conformation because the rotations needed to enable a λδ configuration are topologically impossible. This work by Stephen Contakes is licensed under a Creative Commons Attribution 4.0 International License.

In closing, it should be noted that it might seem to be making much of small effects in pointing out that one source of diastereomerism in metal complexes involves the freezing out of chelate ring conformations. However, that would be to mistake the impacts that ring conformations can have on the steric accessibility of a coordination site and shaping the course of processes that might occur there. As illustrated in Figure Section5.5.31, a simple shift in the conformation of one ring in a square planar, pyramidal, or octahedral complex containing coplanar ethylene diamine ligands can exert a significant effect on the steric profile of the complex perpendicular to the MN_4 square plane. Because of effects like these, ring conformation isomerism plays a role in the design of stereoselective transition metal catalysts.

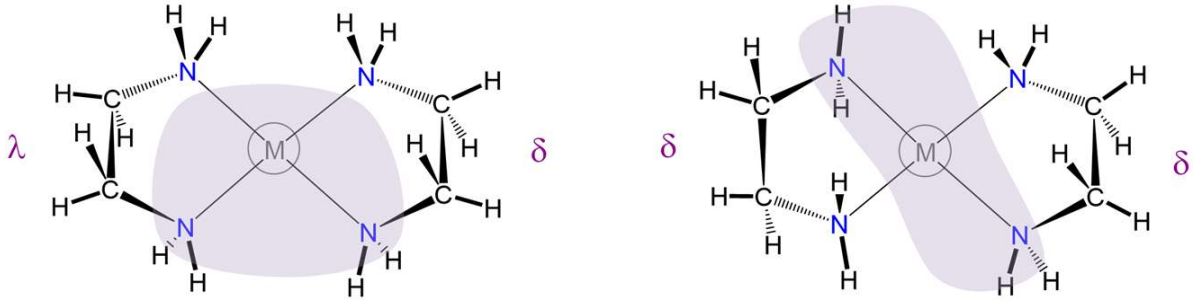


Figure Section5.5.31. Schematic illustrating how the conformation of ethlyenediamine ligands bound to a metal center affects the steric accessibility of the metal (shown shaded in violet) to potential ligands attempting to bind from above the MN_4 plane. This work by Stephen Contakes is licensed under a Creative Commons Attribution 4.0 International License.

Exercises

? Exercise *Section*5.5.1. Identify the type of isomerism

What type of isomers are

a. $[CoCl(NH_3)_5](NO_3)$ and $[Co(NH_3)_5(N\text{-}NO_2)]Cl$?
b. $[Co(NH_3)_5\text{-}CN\text{-}Ru(NH_3)_5]^{4+}$ and $[Co(NH_3)_5\text{-}NC\text{-}Ru(NH_3)_5]^{4+}$
c. $[Cr(CN)_5\text{-}CN\text{-}Co(NH_3)_5]$ and $[Co(CN)_5\text{-}CN\text{-}Cr(NH_3)_5]$
d. *cis*-$[Mn(en)_2(CN)_2]$ and *trans*-$[Mn(en)_2(CN)_2]$

Answer a.

Ionization isomers.

Answer b.

Linkage isomers.

Answer c.

Coordination isomers.

Answer d.

Geometric isomers, specifically *cis*/*trans* isomers.

? Exercise *Section*5.5.2. Assigning metal oxidation states in a complex

Many properties of transition metal complexes depend on the metal's oxidation state. For instance,

- octahedral complexes of Co^{II} lose and gain ligands rapidly
- octahedral complexes of Co^{III} lose and gain ligands very slowly
- four-coordinate complexes are generally tetrahedral
- EXCEPT four-coordinate complexes of metals like Pt^{II} , Pd^{II} , Rh^{I}, and Ir^{I}, among others, are square planar

For this reason it is important to be able to estimate the formal oxidation state of a metal in a complex. Fortunately, this is easy to do if you remember

1. The sum of all atoms' oxidation states will equal the overall charge on the complex
2. When determining the metal's oxidation state, the ligands can be treated as having an oxidation state equal to their charge - *i.e.*, the charge they possess in the form in which they coordinate the metal - so if they need to lose a proton to bind, don't forget to account for that.

Given the above, estimate the oxidation state of the metal in the following real and hypothetical complexes.

a. $Na_4[Fe(CN)_6]$
b. $[Cu(phen)_2]BF_4$
c. $[PtF_4(NH_3)_2]$
d. $[Ni(en)_2]SO_4$
e. $Co(acac)_3$
f. [MnCl(O)(salen)]

Answer for $Na_4[Fe(CN)_6]$.

This contains $[Fe(CN)_6]^{4-}$; so $O.S._{Fe}$ + 6 x (-1) (for CN^-) = -4 (the complex's charge) so $O.S._{Fe}$ = +2 or Fe^{2+}.

Answer for $[Cu(phen)_2]BF_4$.

Since tetrafluoroborate is a monoanion, the complex is $[Cu(phen)_2]^+$ so $O.S._{Cu}$ + 0 x 2 (for phen) = +1 (the complex's charge) so $O.S._{Cu}$ = +1 or Cu^+.

Answer for $[PtF_4(NH_3)_2]$.

$O.S._{Pt}$ + 4 x (-1) (for F^-) + 0 x 2 (for NH_3) = +0 (the complex's charge) so $O.S._{Pt}$ = +4 or Pt^{4+}.

Answer $[Ni(en)_2]SO_4$.

The complex is $[Ni(en)_2]^+$ so $O.S._{Ni}$ + 0 x 2 (for en) = +2 (the complex's charge) so $O.S._{Ni}$ = +2 or Ni^{2+}.

Answer $Co(acac)_3$.

$O.S._{Co}$ + 3 x (-1) (for acac; see table 9.2.2) = +0 (the complex's charge) so $O.S._{Co}$ = +3 or Co^{3+}.

Answer [MnCl(O)(salen)].

$O.S._{Mn}$ + 1 x (-1) (for Cl^-) + 1 x (-2)(for oxo) + 1 x (-2) (for salen; see table 9.2.2) = +0 (the complex's charge) so $O.S._{Mn}$ = +5 or Mn^{5+}.

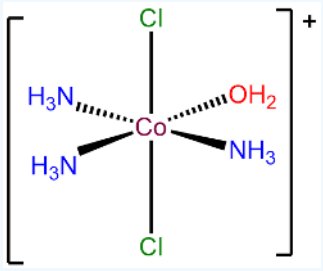
Exercise *Section*5.5.3. Drawing isomers from descriptions

Draw structures that match the descriptions given, assuming that

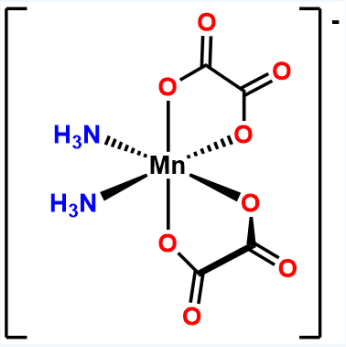
- complexes in which the metal has a coordination number of six are octahedral
- complexes in which the metal has a coordination number of five are trigonal bipyramidal
- complexes in which Pt^{II} , Pd^{II} , or Rh^{I}, or Ir^{I} have a coordination number of four are square planar
- other complexes in which the metal has a coordination number of four will be tetrahedral

a. *mer*-triammineaqua-*trans*-dichlorocobalt(III) ion
b. **Δ**-diaminebis(oxalato)manganate(III)
c. $[CoCl_4]^{2-}$
d. *trans*-diamminebis(ethylenediamine)Nickel(2+) tetracyanopalladate(2-)
e. **Λ**-bis(ethylenediamine)cobalt(III)- μ-amido μ-hydroxo-**Δ**-bis(ethylenediamine)cobalt(III)

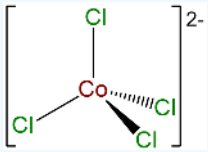
Answer a. *mer*-triammineaqua-*trans*-dichlorocobalt(III) ion.



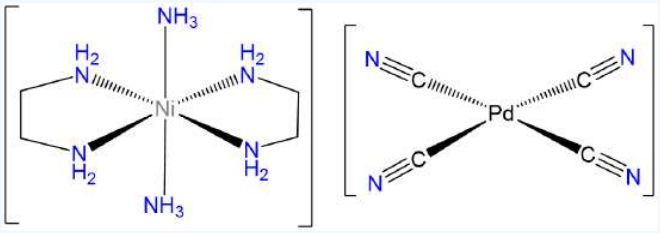
Answer b. Δ-diaminebis(oxalato)manganate(III).



Answer c. $[CoCl_4]^{2-}$.



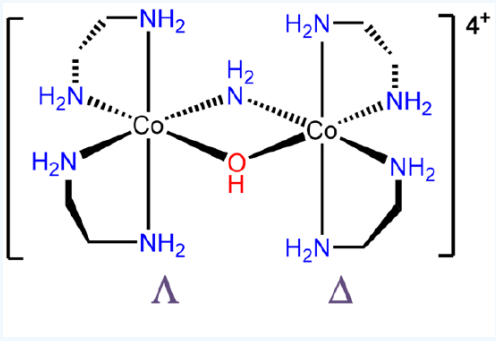
Answer d. *trans*-diamminebis(ethylenediamine)Nickel(2+) tetracyanopalladate(2-).



Note that since the Pd in $[Pd(CN)_4]^{2-}$ is Pd^{2+} it will be square planar.

https://chem.libretexts.org/@go/page/440819

Answer e. Λ-bis(ethylenediamine)cobalt(III)- μ-amido μ-hydroxo-Δ-bis(ethylenediamine)cobalt(III).



? Exercise *Section*5.5.4. Stereoisomers of complexes containing only monodentate ligands.

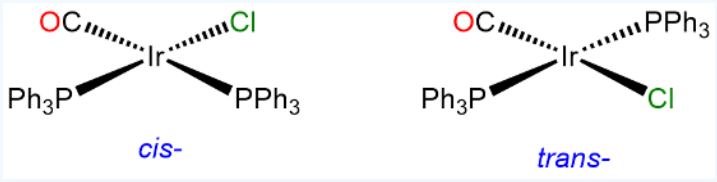
Draw all the stereoisomers of the following real and hypothetical complexes. You may assume that

- complexes in which the metal has a coordination number of six are octahedral
- complexes in which the metal has a coordination number of five are trigonal bipyramidal
- complexes in which Pt^{II} , Pd^{II} , or Rh^{I}, or Ir^{I} have a coordination number of four are square planar
- other complexes in which the metal has a coordination number of four will be tetrahedral

a. $[IrCl(CO)(PPh_3)_2]$
b. $[CoCl_3(NH_3)_3]$
c. $[CoCl_2(H_2O)_2(NH_3)_2]^+$
d. $[CoBrCl(H_2O)_2(NH_3)_2]^+$
e. $[CoBrClI(NH_3)_3]$

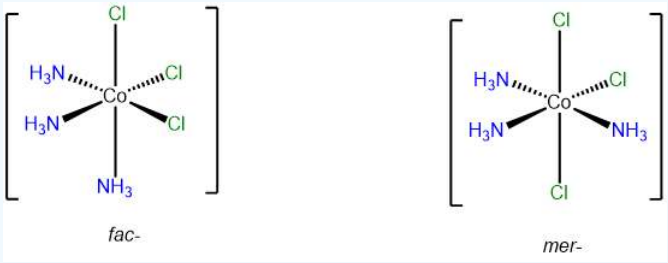
Answer a. $[IrCl(CO)(PPh_3)_2]$

This is a 4-coordinate Ir^{I} complex and, as such will be square planar. Since two of the ligands are identical, it will have *cis* and *trans* isomers. The *trans* isomer is famous for its ability to form adducts and is called Vaska's complex.



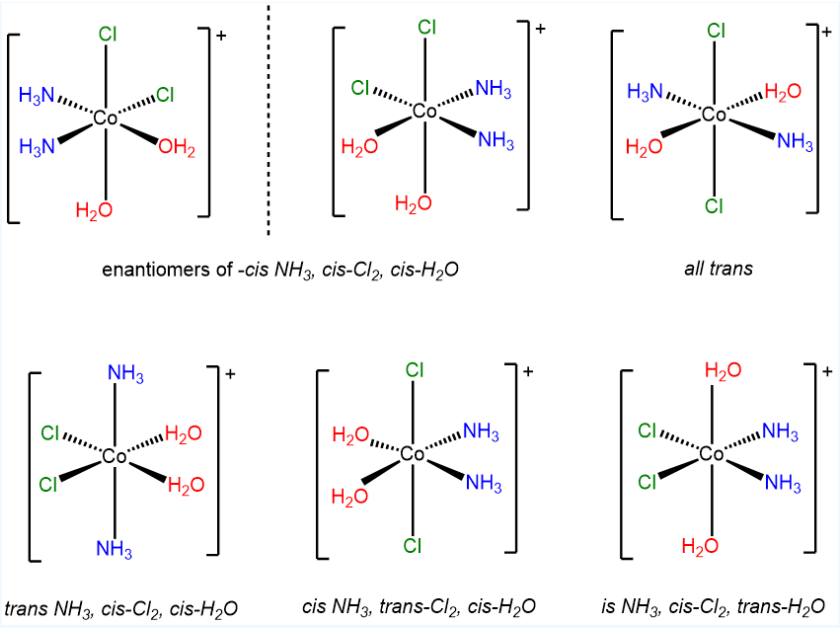
Answer b. $[CoCl_3(NH_3)_3]$

This complex contains three ammine and three chloro ligands and so will have *fac* and *mer* isomers.



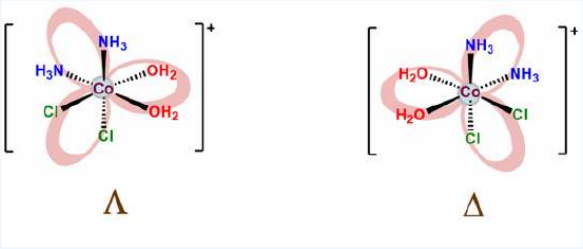
Answer c. $[CoCl_2(H_2O)_2(NH_3)_2]^+$

This is a case of an $MA_2B_2C_2$ system (A = Cl^-, B = H_2O, C = NH_3) involving multiple *cis* and *trans* relationships. The six stereoisomers are shown below.



Since it may not be obvious how to arrive at a set of isomers like the ones above, it is worth considering how one might work through the possibilities for a system of ligands like this one. Several systems may be used to systematically identify isomers. Once approach is the Macbdef system described in Note **Section5.5.1** at the end of these exercises. The solutions presented here and in subsequent problems employ a variant of that approach.

- Start by fixing one set of ligands. In this case the chloro ligands were first fixed as *cis* to one another. Then the remaining ligands might be *cis* or *trans* to one another, although since the *chloro* ligands are already *cis*, the ammine and aqua ligands cannot both be *trans* at the same time. Thus for *cis* chloro ligands the possibilities for the others are:
  - *cis*-H_2O ,*cis*-NH_3,
  - *cis*--H_2O, *trans*-NH_3
  - *trans*-H_2O, *cis*-NH_3
- Swap the configuration of the ligand set you started with. In this case it means placing the chloro ligands *trans* to one another. From that configuration, the possibilities for the ammine and aqua ligands are
  - *cis*-H_2O ,*cis*-NH_3,
  - *trans*-H_2O, *trans*-NH_3
- Check for enantiomers and create mirror images of any chiral complexes you drew. The easiest way to do this is to assign point groups. However, it turns out that the octahedral all-*cis* case is D_3 and formally equivalent to the symmetry of a tris chelate, as shown below.

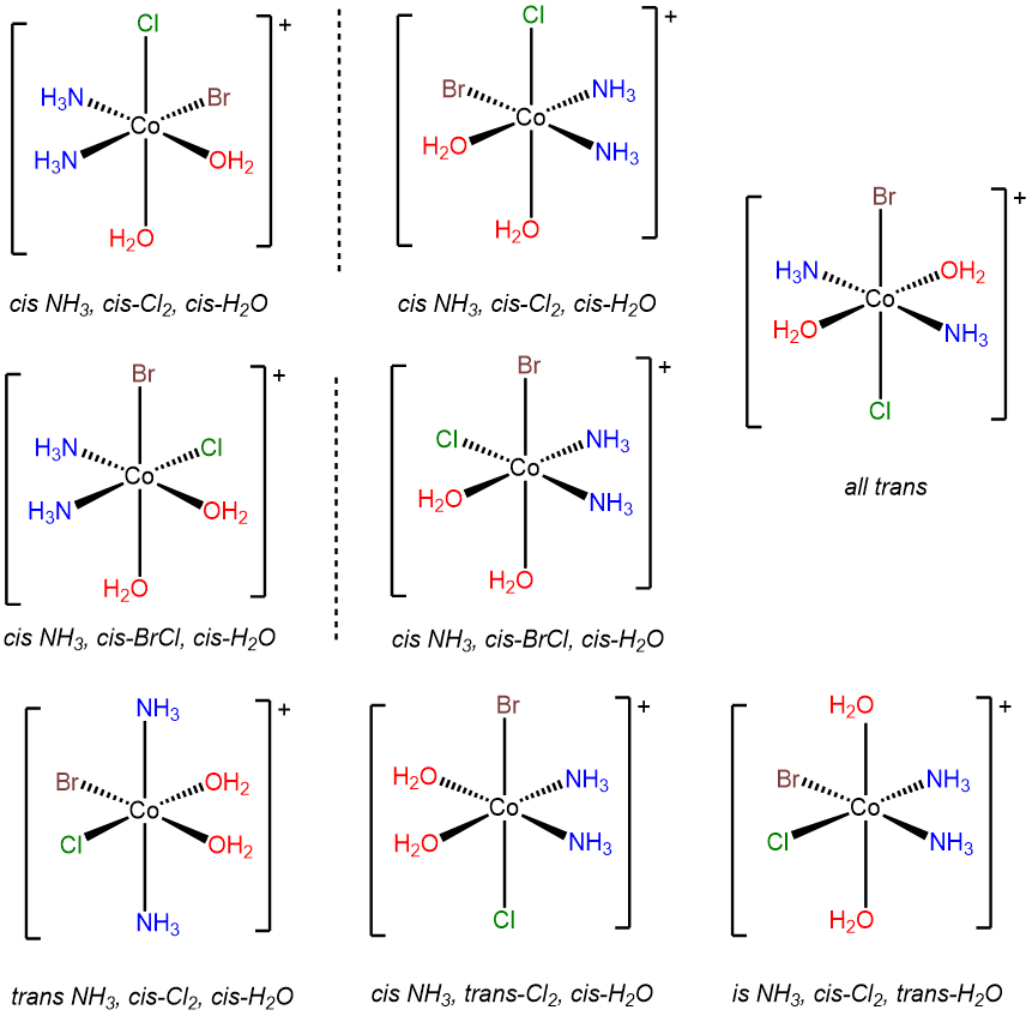


- finally, check to make sure you didn't include the same complex twice. Humans do make mistakes after all.

Answer d. $[CoBrCl(H_2O)_2(NH_3)_2]^+$

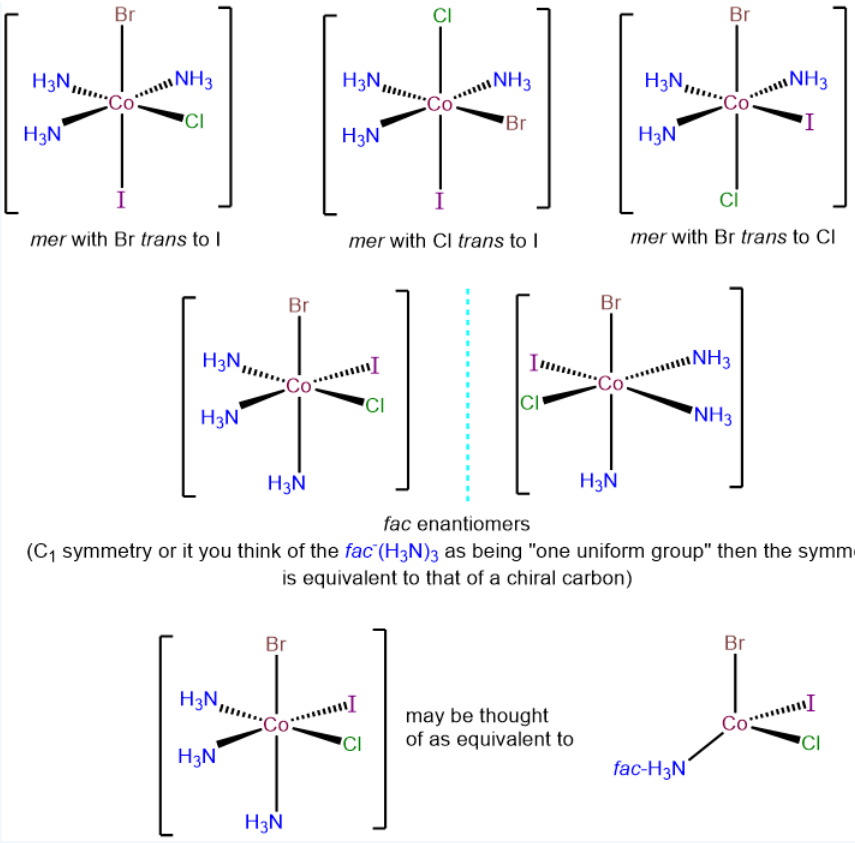
This problem is analogous to the one above except that this complex contains a bromo and chloro ligand in place of the two chloro ligands in $[CoCl_2(H_2O)_2(NH_3)_2]^+$. Consequently, when the bromo and chloro ligands are *cis* to one

another, additional possibilities for isomers arise based on whether ammine or aqua ligands are *trans* to the chloro and bromo. The result is eight isomers.



Answer e. [CoBrClI(NH_3)$_3$]

There are two possibilities for this complex - a *fac*-(NH_3)$_3$ and a *mer*-(NH_3)$_3$ arrangement. These may be taken as starting points for examining the possible permutations for the Cl^-, Br^-, and I^- ligands. The top row presents the three possibilities within the *mer*-(NH_3)$_3$ arrangement; each corresponds to a different ligand *trans* to an ammine ligand. The bottom row presents the two possible isomers with a *fac*-(NH_3)$_3$ arrangement. In each, the Cl^-, Br^-, and I^- ligands are *trans* to ammine ligands. However, the complexes possess C_1 symmetry and so are chiral and exist as enantiomers.



? Exercise *Section*5.5.5. Stereoisomers of complexes with bidentate ligands (ignoring ring twist).

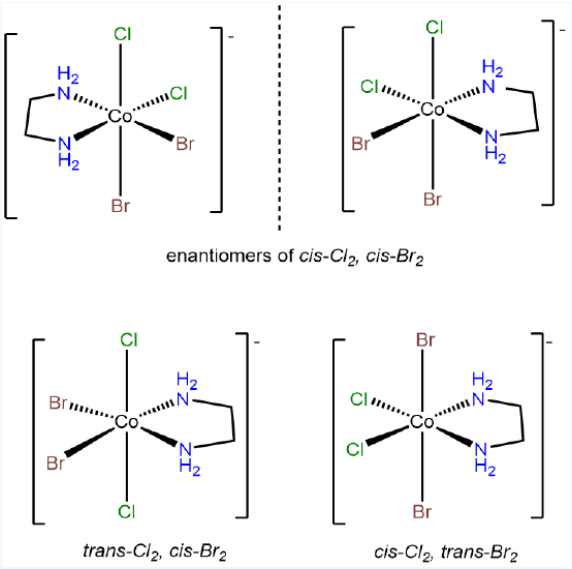
Ignoring ring twist, draw all the stereoisomers of the following real and hypothetical octahedral complexes.

a. $[CoBr_2Cl_2(en)]^-$
b. $[CoBrCl(en)_2]^+$
c. $[CoBrCl(gly)_2]^-$
d. $[Co(en)_3]^{3+}$
e. $[Co(gly)_3]$

Answer a. $[CoBr_2Cl_2(en)]^-$

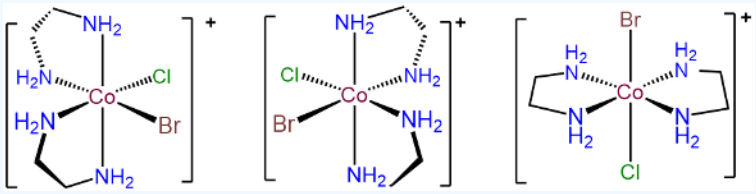
This complex is analogous to $[CoCl_2(H_2O)_2(NH_3)_2]^+$ in possessing pairs of identical ligating groups. The main difference is that in $[CoBr_2Cl_2(en)]^-$ the two amine ligating group of the en ligand are restricted to a *cis* arrangement. Under the MABCDEF system explained in Note *Section*5.5.1, $[CoCl_2(H_2O)_2(NH_3)_2]^+$ may be $MA_2B_2C_2$, but this complex, $[CoBr_2Cl_2(en)]^-$, is $M(AA)B_2C_2$. The isomers are:

https://chem.libretexts.org/@go/page/440819



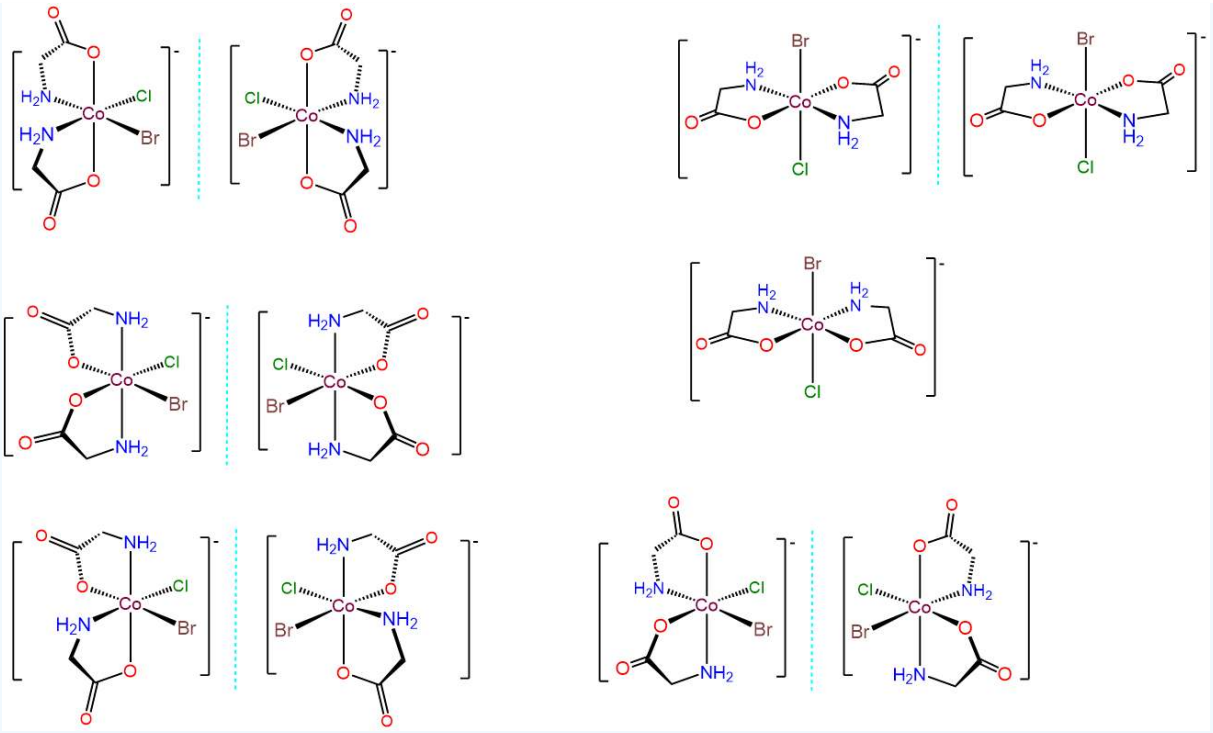
Answer b. $[CoBrCl(en)_2]^+$

The key to problems like this is to focus on the unique ligands, in this case Br^- and Cl^-. These can exist in either a *cis* or *trans* arrangement. The *trans* form is achiral, but in the case where Br^- and Cl^- are *cis*, **Λ** and **Δ** enantiomers are possible. The result is three isomers.



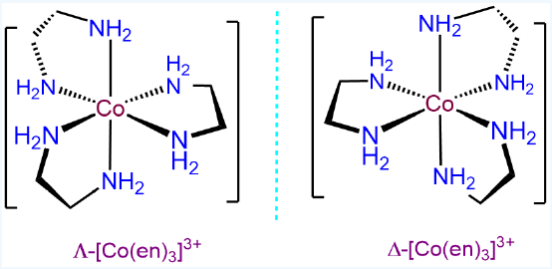
Answer c. $[CoBrCl(gly)_2]^-$

This case is analogous to the one above, but this time the bidentate ligand, gly, possesses distinguishable binding sites. Thus there are additional permutations involving how the gly ligands are bound relative to one another and/or whether the O or N end of the gly is bound *trans* to Br or Cl. The result is 11 different isomers, which are given below.



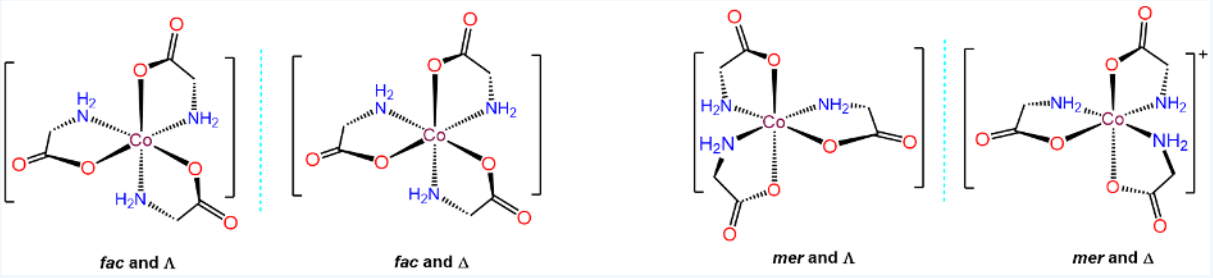
Answer d. $[Co(en)_3]^{3+}$

As a tris-chelate of symmetric bidentate ligands, ignoring ring twist, $[Co(en)_3]^{3+}$ will only exhibit **Λ** and **Δ** isomerism.



Answer e. $[Co(gly)_3]$

Since there are three gly ligands, each of which have carboxy and amine ends, the allowable arrangements involve whether the resulting three carboxy and three amine ends are oriented in a *mer* or *fac* arrangement. This gives two possibilities, each of which can exist as either the **Λ** or **Δ** enantiomer, for a total of four isomers, which are given below.



? Exercise *Section*5.5.6. More stereoisomers: Now featuring linkage isomerism

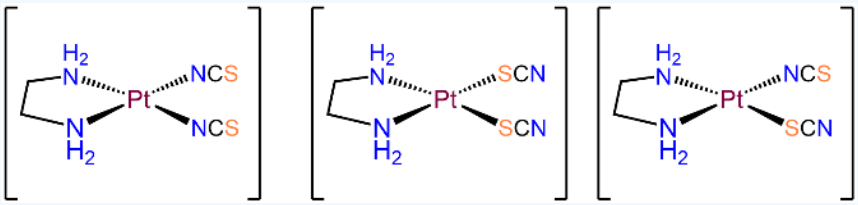
Ignoring ring twist, draw all chemically reasonable stereoisomers for the following real and hypothetical complexes. You may assume that

- complexes in which the metal has a coordination number of six are octahedral
- complexes in which the metal has a coordination number of five are trigonal bipyramidal
- complexes in which Pt^{II} , Pd^{II} , or Rh^{I}, or Ir^{I} have a coordination number of four are square planar
- other complexes in which the metal has a coordination number of four will be tetrahedral

a. $[Pt(en)(SCN)_2]$
b. $[Pt(NH_3)_2(SCN)_2]$
c. $[Co(en)_2(SCN)_2]^+$

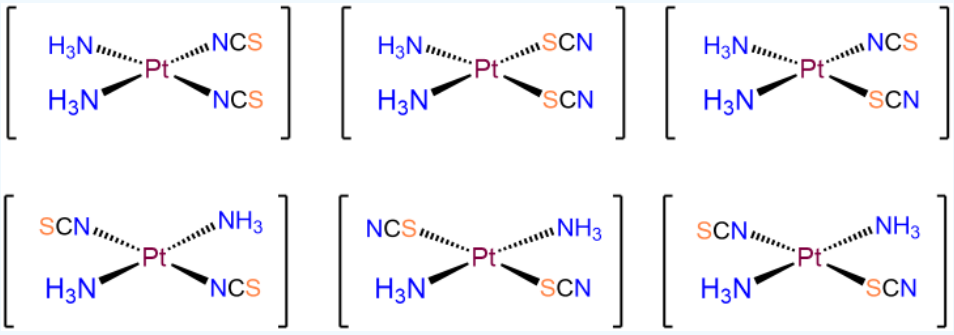
Answer a. $[Pt(en)(SCN)_2]$

The Pt in this neutral complex must be Pt^{2+} to balance the negative charges of the two SCN^- ligands. Complexes of Pt^{2+} are square planar and four coordinate, consistent with the bidentate en and two thiocyanato ligands. Of the ligands, the en ligand must bind in a *cis* arrangement. Consequently, the two SCN^- ligands will be in a *cis* arrangement as well. The isomers will therefore only differ in whether the two SCN^- bind κN or κS. The possibilities are:

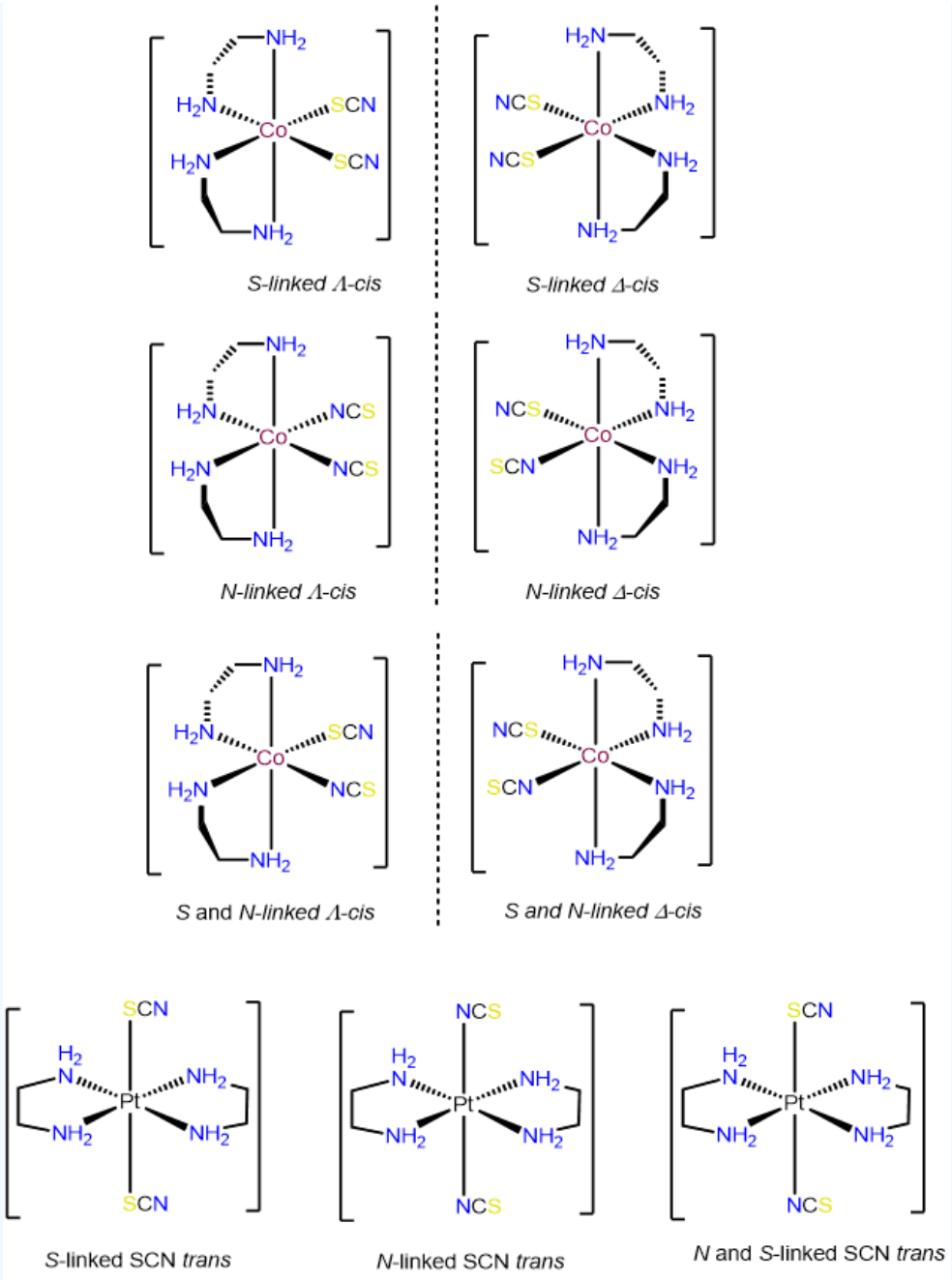


Answer b. $[Pt(NH_3)_2(SCN)_2]$

As with the preceding example, this will be a square planar Pt^{2+} complex. The main difference is that this time the coordinated nitrogens are not constrained to adopt a *cis* arrangement so there will be both *cis* and *trans* isomers.



Answer c. $[Co(en)_2(SCN)_2]^+$



? Exercise *Section*5.5.7. Stereoisomer free for all.

Ignoring ring twist, draw all chemically reasonable stereoisomers for the following real and hypothetical complexes. You may assume that

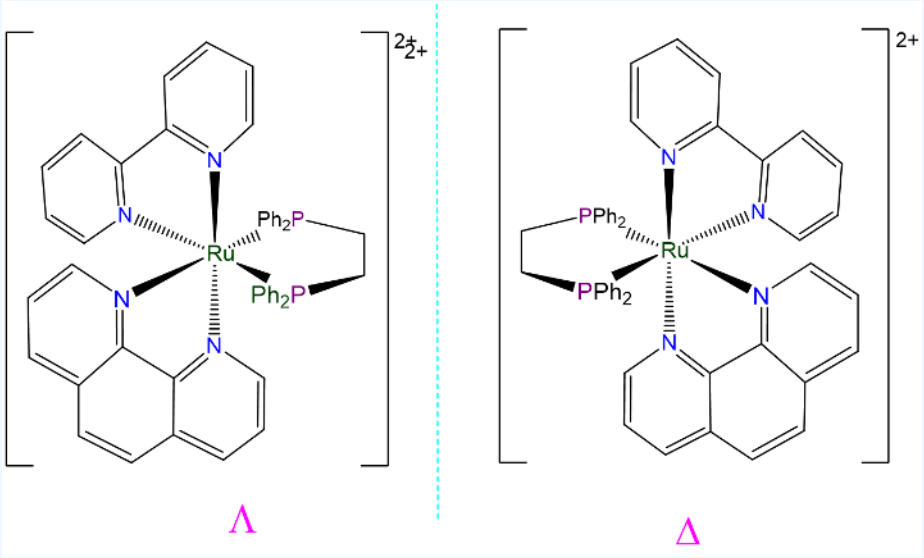
- complexes in which the metal has a coordination number of six are octahedral
- complexes in which the metal has a coordination number of five are trigonal bipyramidal
- complexes in which Pt^{II} , Pd^{II} , or Rh^{I}, or Ir^{I} have a coordination number of four are square planar
- other complexes in which the metal has a coordination number of four will be tetrahedral

a. $[Ru(bpy)(phen)(dppe)]^{2+}$
b. $[CoClF(PPh_3)(py)]^{-}$
c. $[Ni(en)_2(NO_2)_2]$

d. $[Fe(H_2O)_3(SCN)_3]$
e. $[PtClF(PPh_3)(py)]$
f. $[CoBr_2Cl(NH_3)_3]$

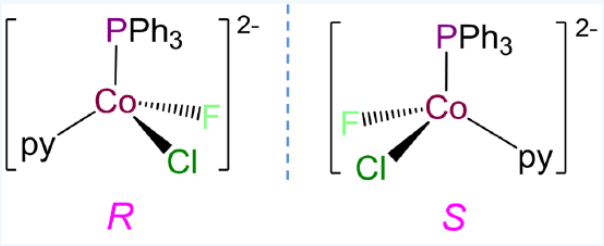
Answer a. $[Ru(bpy)(phen)(dppe)]^{2+}$

This complex is an octahedral tris-chelate containing symmetric ligands. As such it will exhibit **Λ** and **Δ** isomers:



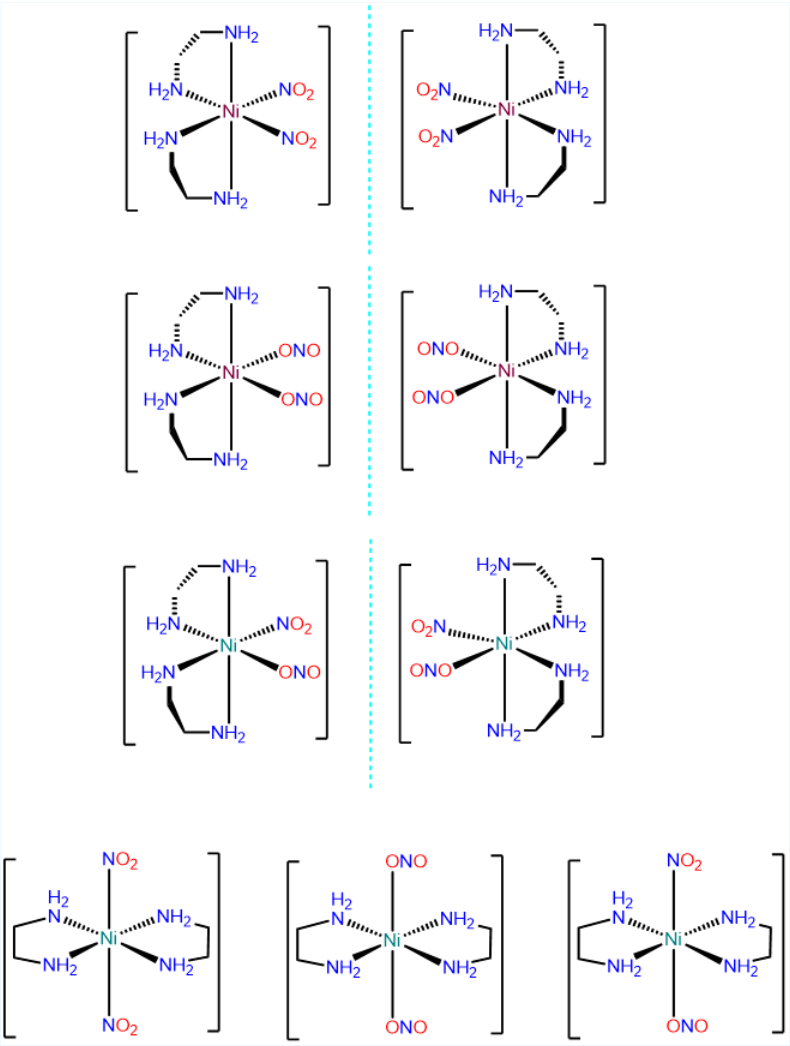
Answer b. $[CoClF(PPh_3)(py)]^-$

This complex has a coordination number of 4 and contains a Co^{2+} ion with a d^7 electron configuration, so a tetrahedral geometry is expected. Tetrahedral complexes like this one with four different ligands are chiral and can form *R* and *S* enantiomers.



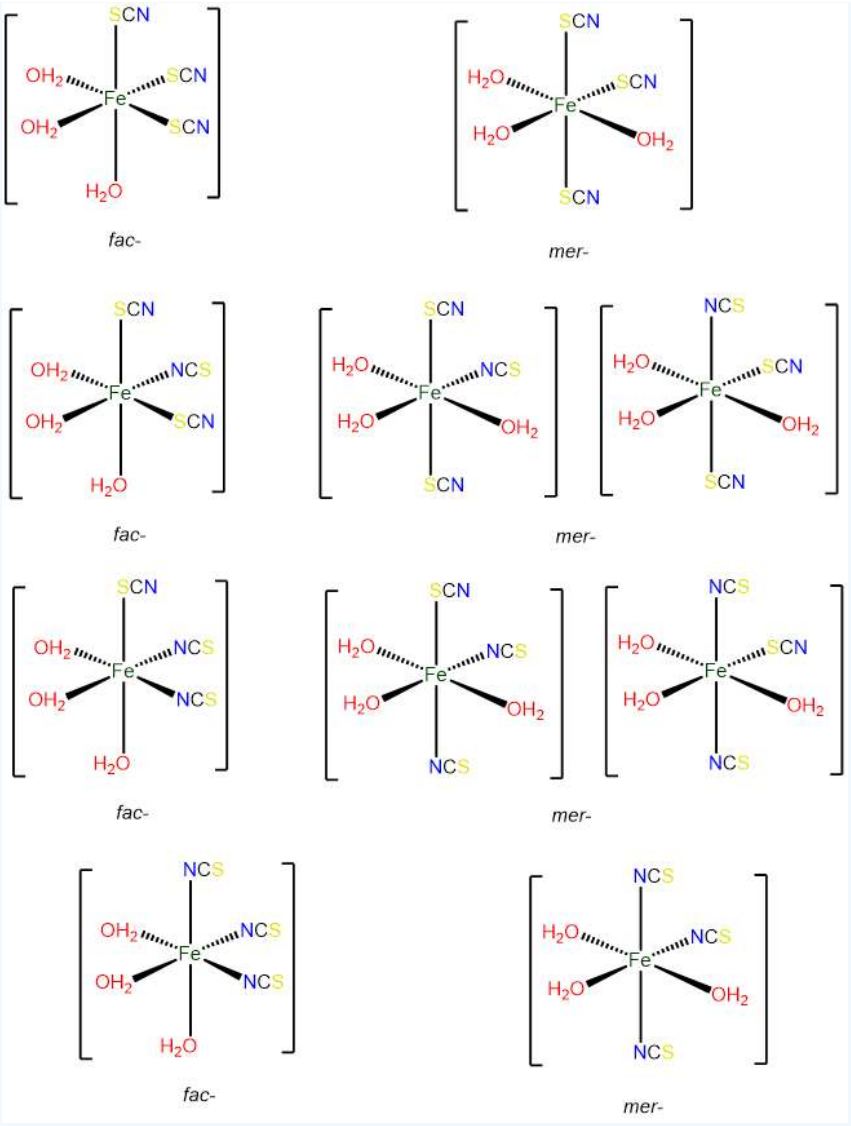
Answer c. $[Ni(en)_2(NO_2)_2]$

This is an octahedral bis-chelate and will exist in **Λ** and **Δ** configurations. Within each configuration the NO_2^- ligands can exist as ***κN*** and ***κO***, leading to the following possibilities:



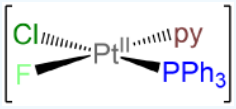
Answer d. $[Fe(H_2O)_3(SCN)_3]$

As an octahedral complex with three identical ligands it can exist in *mer* and *fac* configurations, with the ambidentate SCN ligand providing additional possibilities for isomerism.



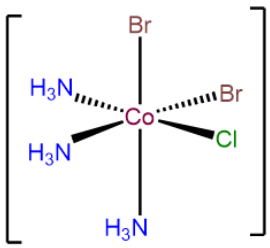
Answer e. [PtClF(PPh$_3$)(py)]

As a square planar complex with four nonidentical ligands, this complex exists as a single isomer.

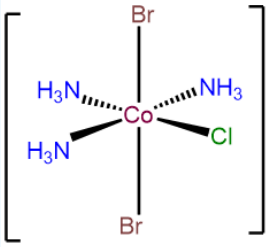


Answer f. [CoBr$_2$Cl(NH$_3$)$_3$]

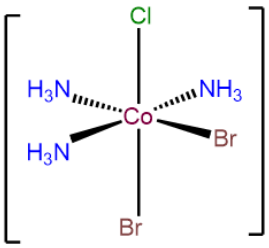
As an octahedral complex with three identical ligands it will exhibit *mer* and *fac* isomerism. In addition, it will have two *mer* configurations that differ in terms of the cis and trans relationships between the bromo and chloro ligands.



fac



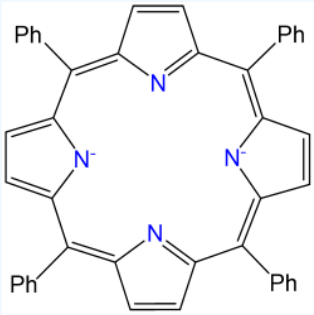
mer with Br *trans* to Br



mer with Cl *trans* to Br

Exercise *Section*5.5.8

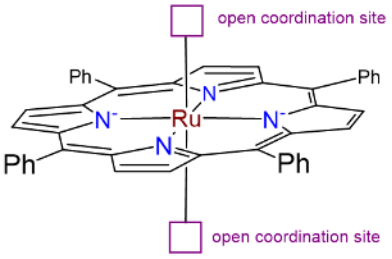
Complexes of formula Ru(TPP)py_2 have been prepared, in which TPP is tetraphenylporphyrin, which binds metals in the form given below. Draw all isomers of Ru(TPP)py_2.

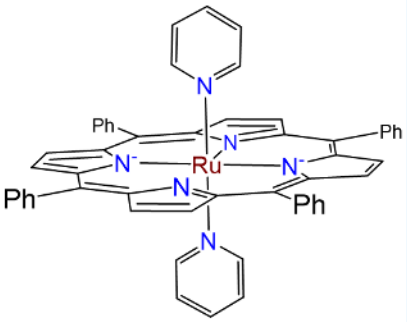


Answer

There is only one isomer. While normally complexes containing two identical ligands (in this case py) can exhibit *cis* and *trans* isomerism, in this case the planar tetraphenylporphyrin ring ligates the Ru^{2+} ion in a square planar arrangement, as shown at left in the image below. This leaves only a pair of *trans* coordination sites for the chloro ligands to occupy, giving the isomer shown at right below.

When TPP ligates Ru^{2+} it leaves only *trans* open coordination sites so only the *trans* isomer can form.

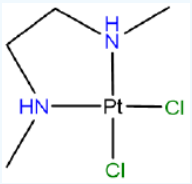




trans-[Ru(py)$_2$(TPP)]

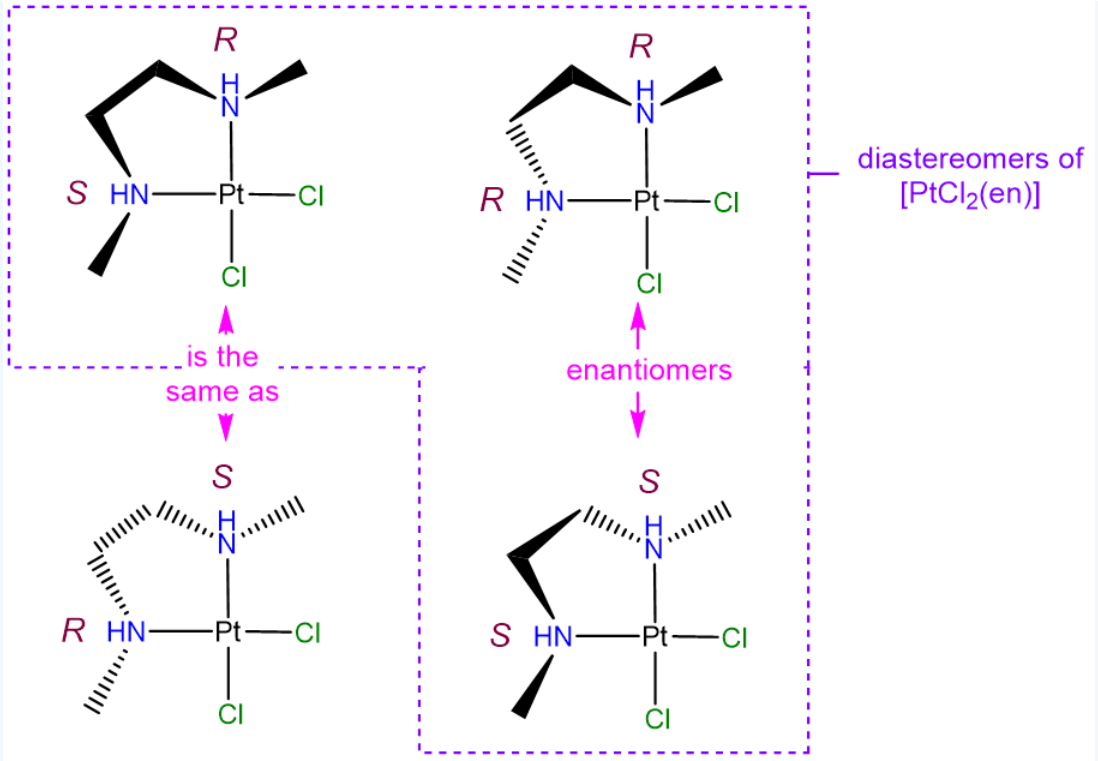
? Exercise *Section*5.5.9

Draw the diastereomers formed due to the chirality of the amine nitrogen atoms in [$PtCl_2$(*N*,*N*'-dimethylethane-1,2-diamine)] which has the atomic connectivity represented below



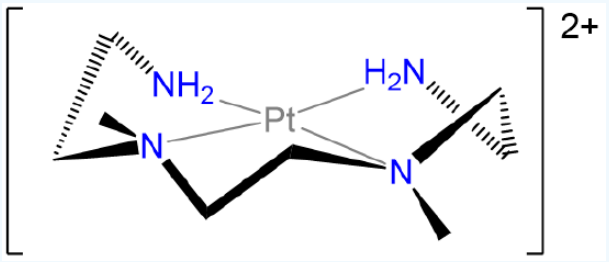
Answer

The diastereomers will differ in whether the N atoms adopt an *R* or *S* configuration at the nitrogen atoms. The possible permutations are (*R*,*R*), (S,*S*), (*R*,*S*), and (S,*R*). However, as may be seen from the image below, the (*R*,*S*) and (S,*R*) configurations are identical (the two projections shown can be interconverted through a C_2 rotation along an axis bisecting the Cl-Pt-Cl unit). As a result there are only three unique isomers. Of these, the (*R*,*R*) and (S,*S*) configurations are enantiomers (they are mirror images by reflection in the $PtCl_2N_2$ plane). Note that in solving problems like this one it can be helpful to keep track of possible isomers by assigning the stereochemistry at each chiral center as *R* or *S* using the Cahn-Ingold-Prelog-convention, though it is not strictly necessary to do so.

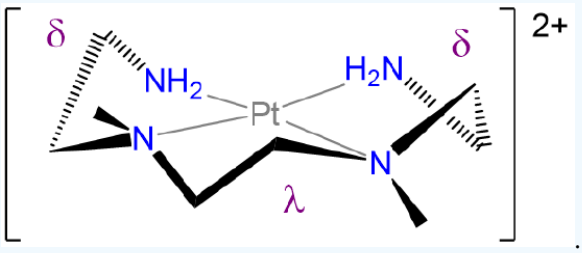


? Exercise *Section*5.5.10

Label the conformations of all chelate rings in the structure below.



Answer



Appendix: The MABCDEF bookkeeping system for identifying isomers

The Mabcdef or MABCDEF system is one method for identifying the number of isomers in an octahedral complex, although since it is really just a bookkeeping and organizational system it can easily be extended to other geometries as well. The M in Mabcdef stands for metal and the other letters are used to stand in for ligands. The basic approach involves

- classifying the ligands as A, B, C, D, E, or F in order of multiplicity. Thus for

$[Cr(NH_3)_6]^{3+}$ A = NH_3; there are no B, C, D,E, or F ligands; and the complex is classified as MA_6

$[CoCl(NH_3)_5]^{2+}$ A = NH_3, B = Cl^-, and the complex is MA_5B

$[CrCl_2(H_2O)_2(NH_3)_2]^+$ A = Cl^-, B = H_2O, C = NH_3, and the complex is $MA_2B_2C_2$

- in the classification above, multidentate ligands are typically classified before monodentate ones and are designated AA, AB, ABC, ABA, etc. based on the symmetry of the attachment points. Thus

  en has identical attachment amine points and is AA

  gly has a carboxy and amine attachment points and is AB

  trien is ABA

  $CoCl_2(en)_2^+$ is $M(AA)_2B_2$

  $CoCl_2(gly)_2^-$ is $M(AB)_2C_2$

  $CoCl_2(en)(gly)$ is $M(AA)(AB)C_2$

- Systematically list out the possible *trans* arrangements of ligands by
  1. assigning one pair of ligands to be *trans* to one another.
  2. Then systematically list out the other possible *trans* pairs by permuting the remaining trans arrangements. It can help to organize the permutations in a table, such as that shown below for an MABCDEF complex where A and B are assigned *trans*. In looking at the table notice how the second set of trans permutations is systematically varied. This helps ensure that no possibility is skipped.
  3. Go through the list of isomers and remove any duplicates you generated so far. For instance, notice in the table below that the last three stereoisomers are identical with the first three (*e.g.*, stereoisomer 4 is identical to stereoisomer 3, 5 with 2, and 6 with 1).

Stereoisomer 1	Stereoisomer 2	Stereoisomer 3	Stereoisomer 4 (same as isomer 3)	Stereoisomer 5 (same as isomer 2)	Stereoisomer 6 (same as isomer 1)
trans AB (fixed)	*trans* AB (fixed)	*trans* AB (fixed)	*trans* AB (fixed)	*trans* AB (fixed)	*trans* AB (fixed)
trans CD	*trans* CE	*trans* CF	*trans* DE	*trans* DF	*trans* EF
trans EF	*trans* DF	*trans* DE	*trans* CF	*trans* CE	*trans* CD

  4. If the complex possesses multidentate ligands that demand that certain groups exist and *cis* pairs, then also remove any configurations which do not agree with the known binding capability of the ligand (*e.g.*, the two amine groups of ethylenediamine cannot be *trans* to one another, so if you have an en ligand, remove configurations like that from the list).

5. Next, swap or permute the original *trans* pair and repeat the process you just followed. In the case of Mabcdef this gives the following results:

Isomer	"fixed" trans pair	Additional trans pairs	
1	AB	CD	EF
2	AB	CE	DF
3	AB	CF	DE
4	AC	BD	EF
5	AC	BE	BF
6	AC	BF	DE
7	AD	BC	EF
8	AD	BE	CF
9	AD	BF	CE
10	AE	BC	DF
11	AE	BD	CF
12	AE	BF	CD
13	AF	BC	DE
14	AF	BD	CE
15	AF	BE	CD

- Since the procedure explained above only identifies isomers based on unique *trans* pairings, **it does not identify when a configuration is chiral and corresponds to a pair of enantiomers.** Any enantiomers can be identified by drawing out the complexes and either classifying their point groups or by drawing their mirror images and checking if they are superimposable. In the MABCDEF case - *i.e.*, where all the ligands are different - all of the isomers identified have C_1 symmetry so are chiral. This means there will be a pair of enantiomers for each, giving 15 x 2 = 30 different stereoisomers.

References

1. These examples are taken from http://wwwchem.uwimona.edu.jm/courses/inorgnom.html

2. Contakes S. M.; Rauchfuss, T.B. *Chem. Commun.* 2001, 553-554.

3. Shriver, D. F.; Shriver, S. A.; Anderson, S. E., *Inorg. Chem.* 1965, *4(5)*, 725-730.

4. Zelewsky, A. v., *Stereochemistry of Coordination Compounds* Wiley, 1996.

5. In the past it was difficult to determine absolute configurations from X-ray data alone, but recent advances have made it easier to do so.

6. Pavan M. V. Raja & Andrew R. Barron "Circular Dichroism Spectroscopy and its Application for Determination of Secondary Structure of Optically Active Species" in *Physical Methods in Chemistry and Nano Science* https://chem.libretexts.org/Bookshelves/Analytical_Chemistry/Book%3A_Physical_Methods_in_Chemistry_and_Nano_Science_(Barron)/07%3A_Molecular_and_Solid_State_Structure/7.07%3A_Circular_Dichroism_Spectroscopy_and_its_Application_for_Determination_of_Secondary_Structure_of_Optically_Active_Species

7. Berova, N.; Bari, L. D.; Pescitelli, G., *Chemical Society Reviews* 2007, 36 (6), 914-931.

8. Of course, if one set of ligands occupies a meridional plane, then the other three ligands will be oriented in an equatorial one. The reason they may both be considered meridional is because if the complex were rotated, the equatorial plane would be meridional and vice versa. From that point of view both might be considered meridional planes - albeit not at the same time.

9. Bite angles are taken from Mansell, S. M., Catalytic applications of small bite-angle diphosphorus ligands with single-atom linkers. Dalton Transactions 2017, 46 (44), 15157-15174.

10. Hancock, R. D., The pyridyl group in ligand design for selective metal ion complexation and sensing. Chemical Society Reviews 2013, 42 (4), 1500-1524.

11. Sasi, D.; Ramkumar, V.; Murthy, N. N., Bite-Angle-Regulated Coordination Geometries: Tetrahedral and Trigonal Bipyramidal in Ni(II) with Biphenyl-Appended (2-Pyridyl)alkylamine N,N'-Bidentate Ligands. ACS Omega 2017, 2 (6), 2474-2481.

12. Ehnbom, A.; Ghosh, S. K.; Lewis, K. G.; Gladysz, J. A., Octahedral Werner complexes with substituted ethylenediamine ligands: a stereochemical primer for a historic series of compounds now emerging as a modern family of catalysts. Chemical Society Reviews 2016, 45 (24), 6799-6811.

Section 5.5: Isomerism is shared under a CC BY-NC-SA 4.0 license and was authored, remixed, and/or curated by LibreTexts.

- **9.4: Isomerism** by Stephen M. Contakes is licensed CC BY 4.0.

CHAPTER OVERVIEW

Chapter 6: Coordination Chemistry- Bonding

With the exception of molecular orbital theory, the bonding models discussed in previous courses for main group complexes are not easily applied to transition metal complexes. This chapter describes bonding models that are used to explain the bonding and electronic structures of coordination complexes. As with many theories, the crystal field and ligand field theories discussed in this chapter were developed because existing bonding theories couldn't explain the observed properties of some transition metal complexes.

As an example let us consider the following two transition metal complexes, $[Fe(NH_3)_6]^{2+}$ and $[Co(NH_3)_6]^{3+}$. The Fe^{2+} and the Co^{3+} centers both have a valence electron configuration of $3d^6$ and have the same ligands coordinated. Lewis, VSEPR, and valence bond theories predict that two isoelectronic molecules should have very similar properties, but in the case of $[Fe(NH_3)_6]^{2+}$ and $[Co(NH_3)_6]^{3+}$ that is not true. The light absorption properties (and colors) of the two are quite different. The iron complex absorbs very little visible light and therefore appears a very pale yellow color and the cobalt complex strongly absorbs visible light and has a dark red-orange color. Also, the iron complex is paramagnetic (having unpaired electrons) and the cobalt complex is diamagnetic (having no unpaired electrons). Crystal field theory, and later ligand field theory were developed in part to explain the spectroscopic and magnetic properties of transition metal complexes.

Complex	**$[Fe(NH_3)_6]^{2+}$**	**$[Co(NH_3)_6]^{3+}$**
Valence electron configuration	[Ar] $3d^6$	[Ar] $3d^6$
Color	pale yellow	Red-orange
Magnetic properties	paramagnetic	diamagnetic

Learning Objectives

- Draw a crystal field diagram for a given metal complex and use to identify the number of unpaired electrons
- Identify whether a given metal complex will be high or low spin
- Calculate the crystal field stabilization energy for a given metal complex
- Use ligand field theory to explain the spectrochemical series

Section 6.1: Crystal Field Theory
Section 6.2: Crystal Field Stabilization Energy
Section 6.3: Factors That Affect Crystal Field Splitting
Section 6.4: Ligand Field Theory
Section 6.5: Metal-Metal Bonds
Section 6.5.1: Metal-Metal Multiple Bonds
Section 6.6: Jahn-Teller Distortions

Chapter 6: Coordination Chemistry- Bonding is shared under a CC BY-NC-SA 4.0 license and was authored, remixed, and/or curated by LibreTexts.

Section 6.1: Crystal Field Theory

Crystal Field Theory

Crystal field theory (CFT) describes the breaking of orbital degeneracy in transition metal complexes due to the presence of ligands. CFT qualitatively describes the strength of the metal-ligand bonds. Based on the strength of the metal-ligand bonds, the energy of the system is altered. This may lead to a change in magnetic properties as well as color. This theory was developed by Hans Bethe and John Hasbrouck van Vleck in the late 1920's. Crystal field theory is a purely electrostatic theory and uses classical potential energy equations that take into account the attractive and repulsive interactions between charged particles (that is, Coulomb's Law interactions).

$$E \propto \frac{q_1 q_2}{r} \qquad \text{(Section 6.1.1)}$$

with

- E the bond energy between the charges and
- q_1 and q_2 are the charges of the interacting ions and
- r is the distance separating them.

For this simple approach to work, CFT makes some assumptions and simplifications. All ligands are modeled as negative point charges with no orbitals and the metal orbitals are modeled as clouds of negative charge. This approach leads to the correct prediction that large cations of low charge, such as K^+ and Na^+, should form few coordination compounds. For transition metal cations that contain varying numbers of d electrons in orbitals that are NOT spherically symmetric, however, the situation is quite different. The shape and occupation of these d-orbitals then becomes important in an accurate description of the bond energy and properties of the transition metal compound.

Orientation of *d*-Orbitals

To understand CFT, one must first understand the shape and orientation of the d orbitals:

- d_{xy}: lobes lie in-between the x and the y axes.
- d_{xz}: lobes lie in-between the x and the z axes.
- d_{yz}: lobes lie in-between the y and the z axes.
- $d_{x^2-y^2}$: lobes lie on the x and y axes.
- d_{z^2}: there are two lobes on the z axes and there is a donut shape ring that lies on the xy plane around the other two lobes.

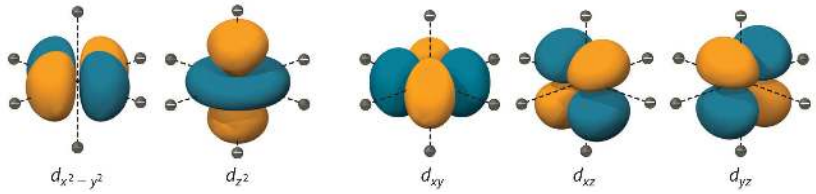


Figure *Section*6.1.1: Spatial arrangement of ligands in the an octahedral ligand field with respect to the five d-orbitals.

Octahedral Crystal Field

When examining a single transition metal ion in free space, the five d-orbitals have the same energy (Figure *Section*6.1.2). When ligands approach the metal ion, the ligand negative point charges destabilize the metal d-orbital based on the geometric structure of the molecule. Since ligands approach from different directions, not all d-orbitals interact equally. These interactions, however, create a splitting due to the electrostatic environment, orbitals with more interaction are higher in energy and orbitals with less interaction are lower in energy.

Definition: Barycenter

In crystal field theory the barycenter is the energy of the d orbitals in a spherical crystal field, where the negative lignad charges are evenly distributed around the metal ion in a sphere. The splitting of the d orbitals in other crystal fields will be symmetric around the barycenter (i.e. the total amount of stabalization will always be equal to the total amount of destabalization)

For example, consider a molecule with octahedral geometry. Ligands approach the metal ion along the x, y, and z axes. Therefore, the electrons in the d_{z^2} and $d_{x^2-y^2}$ orbitals (which lie along these axes) experience greater repulsion and are therefore at higher energy. Compared to a spherical field, where ligands are evenly distributed around the metal center, the d orbitals that lie between the axes (d_{xy}, d_{xz}, and d_{yz} experience less repulsion when the ligands are in an octahedral arrangement and are stabilized. This causes a splitting in the energy levels of the d-orbitals, known as crystal field splitting. For octahedral complexes, crystal field splitting is denoted by Δ_o (or Δ_{oct}) (in older texts and papers it may also be labeled as 10Dq). Any orbital that has a lobe on the axes moves to a higher energy level. The energies of the e_g symmetry orbitals (d_{z^2} and $d_{x^2-y^2}$) increase due to greater interactions with the ligands. The t_{2g} symmetry orbitals (d_{xy}, d_{xz}, and d_{yz}) decrease in energy with respect to the spherical energy level and become

more stable. This splitting is symmetric around the barycenter (the theoretical energy of the d orbitals with spherical charge distribution) which means that the energy levels of e_g are higher (by $0.6\Delta_o$) while t_{2g} are lower (by $0.4\Delta_o$). It should be noted that the labels t_{2g} and e_g come from group theory and the octahedral point group. The energy difference between the t_{2g} and e_g orbitals dictates the energy that the complex will absorb causing electrons to move from one level to the next. For transition metal complexes, the absorbed energy is typically in the visible part of the spectrum and thus this will determine the color of the complex. Whether the complex is paramagnetic or diamagnetic will be determined by the spin state. If there are unpaired electrons, the complex is paramagnetic; if all electrons are paired, the complex is diamagnetic.

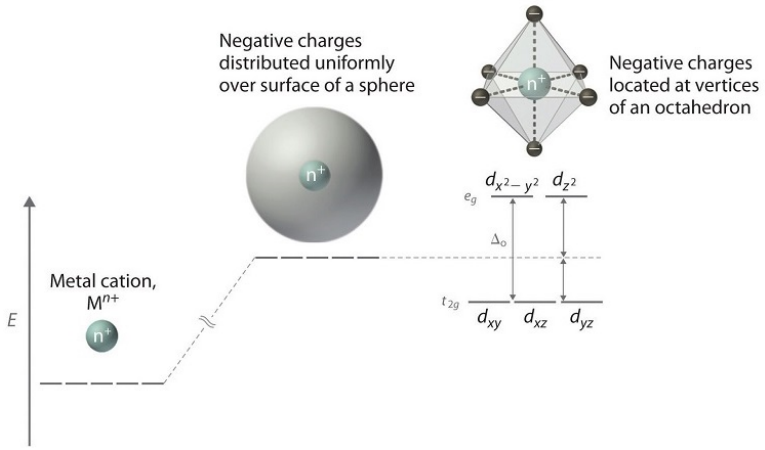


Figure ***Section*6.1.2**: (a) Distributing a charge of −6 uniformly over a spherical surface surrounding a metal ion causes the energy of all five d orbitals to increase due to electrostatic repulsions, but the five d orbitals remain degenerate. Placing a charge of −1 at each vertex of an octahedron causes the d orbitals to split into two groups with different energies: the $d_{x^2-y^2}$ and d_{z^2} orbitals increase in energy, while the, d_{xy}, d_{xz}, and d_{yz} orbitals decrease in energy. The average energy of the five d orbitals is the same as for a spherical distribution of a −6 charge, however. Attractive electrostatic interactions between the negatively charged ligands and the positively charged metal ion (far right) cause all five d orbitals to decrease in energy but does not affect the splittings of the orbitals. (b) The two e_g orbitals (left) point directly at the six negatively charged ligands, which increases their energy compared with a spherical distribution of negative charge. In contrast, the three t_{2g} orbitals (right) point between the negatively charged ligands, which decreases their energy compared with a spherical distribution of charge.

Filling Electrons in Orbitals

d^1 - d^3

For one, two, or three d electrons the filling is straightforward. According to the Aufbau principle, electrons are filled from lower to higher energy orbitals. In an octahedral crystal field, this corresponds to the d_{xy}, d_{xz}, and d_{yz}) orbitals. Following Hund's rule, electrons are filled in order to have the highest number of unpaired electrons. Therefore, each electron occupies one of the t_{2g} symmetry orbitals d_{xy}, d_{xz}, or d_{yz}) and all the electrons are orientated in the same direction to maximize spin multiplicity as shown in Figure ***Section*6.1.3**.

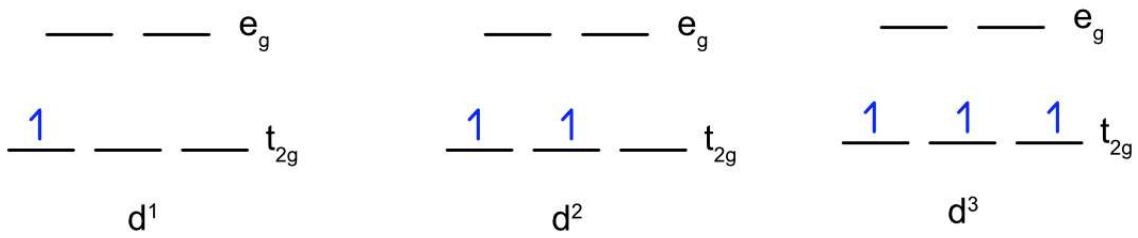


Figure ***Section*6.1.3**: Arrangement of the d electrons in a octahedral crystal field for 1, 2, and 3 d electrons. (CC-BY-NC-SA; Catherine McCusker)

d^4 - d^7

When a complex has between 4 and 7 d electrons there are two ways the electrons can be arranged into the d orbitals. As an example, in d^4 the first three electrons are placed one in each of the t_{2g} symmetry orbitals. The fourth electron can either be placed in one of the empty e_g symmetry orbitals or it can be paired in one or the t_{2g} symmetry orbitals, as shown in Figure ***Section*6.1.4**. The first configuration is called high spin because it maximizes the number of unpaired electrons and the second is called low spin. Whether a complex will have the high spin or low configuration depends on the relative magnitude of the spin pairing energy (the energy required to place two negatively charged electrons in the same orbital) and the crystal field splitting (Δ_o). In cases where the spin pairing energy is larger than Δ_o the complex will adopt the high spin configuration because it requires less energy to place an electron in a higher energy e_g orbital than is does to pair two electrons in the same t_{2g} orbital. In cases where Δ_o is larger than the spin pairing energy the complex will adopt a low spin configuration because it requires less energy to place a second electron in a t_{2g} orbital than it does to place one in the higher energy e_g orbitals.

Definition: Spin Pairing Energy

The spin pairing energy is the energy required to pair two electrons in an orbital. It is based on the Coulombic repulsion between the two negative charges. Larger, more diffuse orbitals will have lower spin pairing energy because the two electrons can be further apart

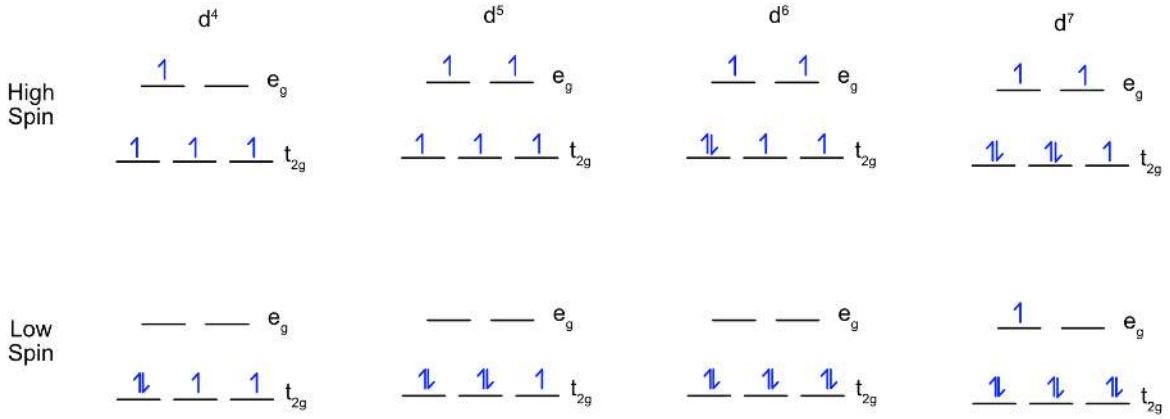


Figure ***Section*6.1.4**: High spin and low spin arrangements of electrons for d^4 - d^7. (CC-BY-NC-SA; Catherine McCusker)

d^8 - d^{10}

For complexes with 8 - 10 d electrons there is again only one way to arrange the electrons. Whether or not the e_g orbitals are filled before electrons are paired in the t_{2g} orbitals the final electron configurations are as shown in Figure ***Section*6.1.5**.

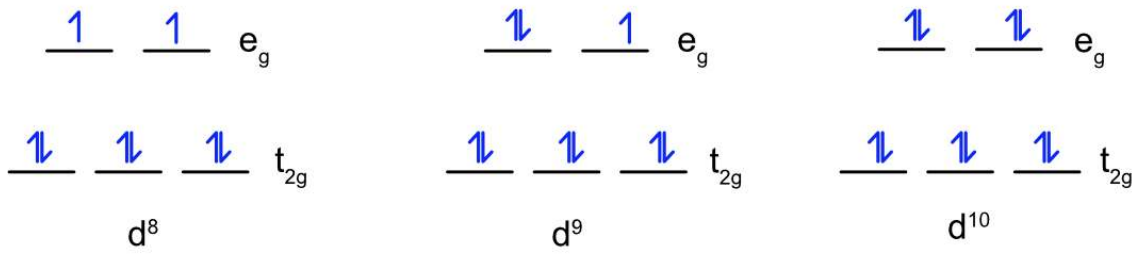


Figure ***Section*6.1.5**: Arrangement of the d electrons in a octahedral crystal field for 8, 9, and 10 d electrons. (CC-BY-NC-SA; Catherine McCusker)

Tetrahedral Crystal Field

In a tetrahedral complex, the four ligands are orientated at opposite corners of a cube as shown in Figure ***Section*6.1.6*a*** rather than along the axes. With the ligands between the axes, the three d orbitals which lie between the axes, d_{xy}, d_{xz}, and d_{yz} (t_2 symmetry in tetrahedral), now interact more with the ligands and are destabilized relative to the spherical crystal field. Conversely, the two d orbitals that lie along the axes, $d_{x^2-y^2}$ and d_{z^2} (e symmetry in tetrahedral), now interact less with the d orbitals and are stabilized relative to the spherical crystal field. As shown in Figure ***Section*6.1.6*b*** the splitting of the d orbitals in a tetrahedral crystal field is essentially the inverse of the octahedral crystal field. The crystal field splitting energy in a tetrahedral crystal field is Δ_t. Because a tetrahedral complex has fewer ligands than an octahedral complex, and those ligands are not ideally orientated to overlap with the d orbitals Δ_t is less than Δ_o for the same metal and ligands:

$$\Delta_t \approx \frac{4}{9}\Delta_o \qquad \textbf{(Section 6.1.2)}$$

Consequentially, Δ_t is typically smaller than the spin pairing energy, so tetrahedral complexes are usually high spin. As seen with octahedral compounds, the labels for the groups of orbitals, t_2 and e in this case, come from group theory and the tetrahedral point group.

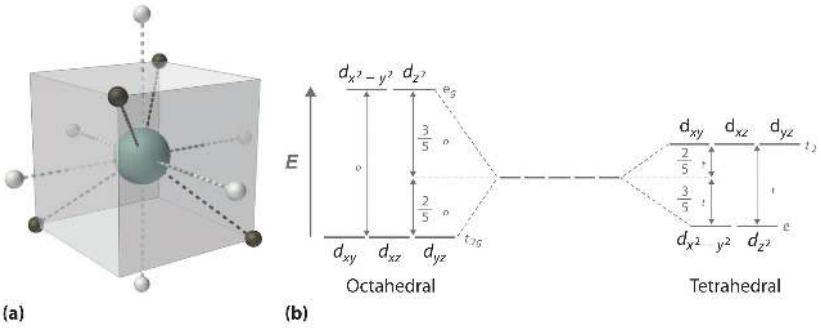


Figure ***Section*6.1.6**: (a) Tetrahedral ligand field surrounding a central transition metal (teal sphere). (b) Splitting of the degenerate d-orbitals (without a ligand field) due to an octahedral ligand field (left diagram) and the tetrahedral field (right diagram).

Square Planar Crystal Field

In a complex with four ligands, the other possible arrangement of ligands is square planar. The easiest way to visualize the square planar geometry is to start with an octahedral complex and remove the two ligands that are along the z axis. The four remaining ligands are in the xy plane, along the x and y axes. From a crystal field splitting perspective, when the z ligands are removed the d orbitals split further. In an octahedral crystal field both $d_{x^2-y^2}$ and d_{z^2} are destabilized. When the z ligands are removed the d_{z^2} orbital is stabilized because it no longer interacts with ligands on the z axis. Conversely the $d_{x^2-y^2}$ orbital is further destabilized because all of the ligand negative charges are concentrated in the xy plane. Removing the z ligand has a similar effect on the d_{xy}, d_{xz}, and d_{yz} orbitals, although the magnitude of the stabilization and destabilization is less because those orbitals do not directly interact with the ligands. The d_{xy} orbital is destabilized because it also lies in the xy plane and the d_{xz} and d_{yz} orbitals are stabilized because they have lost the (indirect) interaction with the ligands on the z axis. Overall the $d_{x^2-y^2}$ orbital is significantly more destabilized than the other d orbitals, meaning the square planar geometry is most favored in complexes with 8 electrons where the $d_{x^2-y^2}$ is empty and the other more stabilized d orbitals are filled.

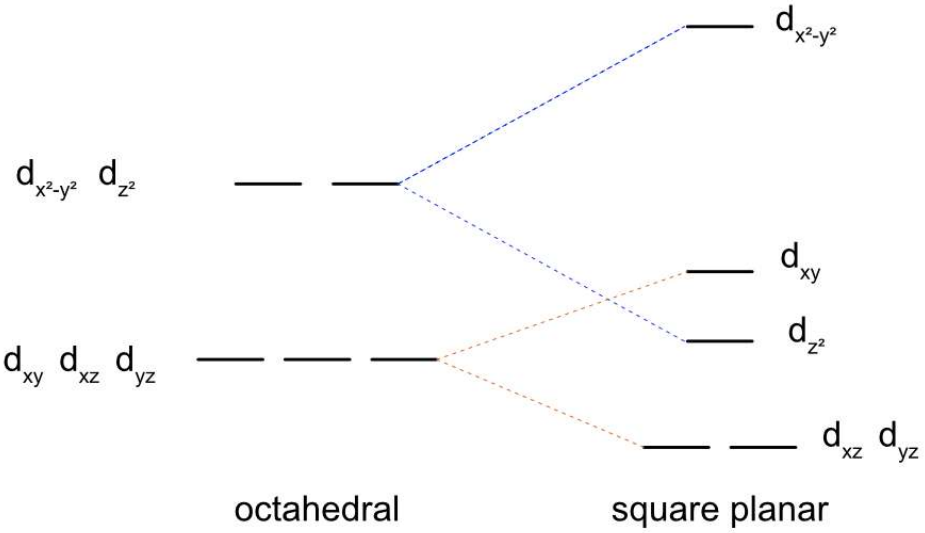
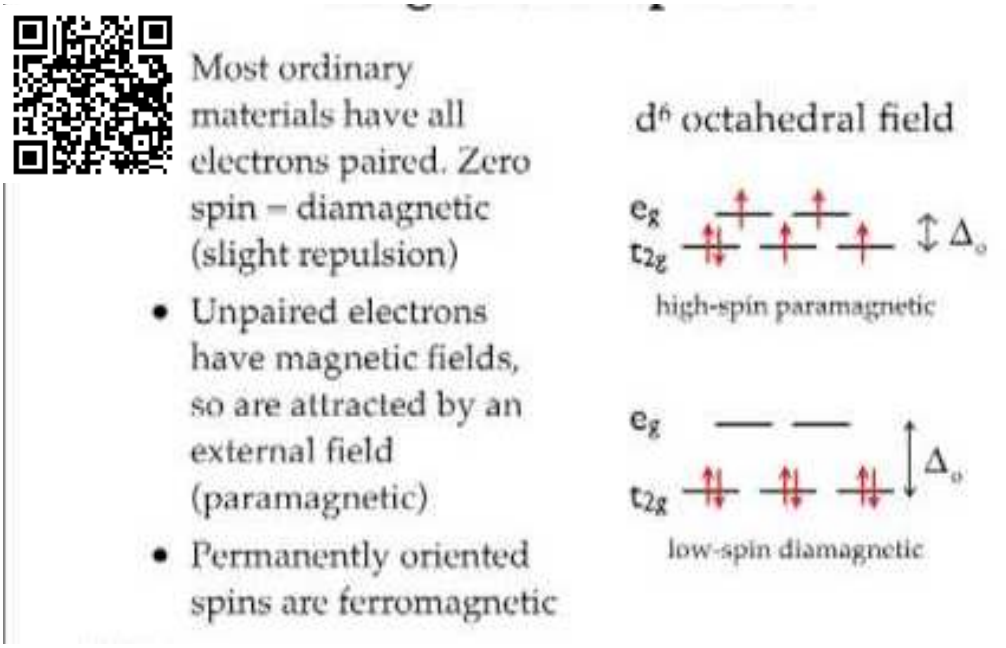


Figure ***Section*6.1.7**: Comparison between octahedral and square planar crystal field splittings, showing how the energies of the d orbitals change when the two z ligands are removed from an octahedral complex to form a square planar complex. (CC-BY-NC-SA; Catherine McCusker)

Video:



Tetrahedral vs Square Planar

From VSEPR theory we know that sterically the most favorable way to arrange four ligands around a metal ion is in the tetrahedral arrangement. That puts the most possible space between the four ligands. Because of this, a four coordinate metal complex will prefer a tetrahedral geometry UNLESS there is a larger crystal field stabilization energy (CFSE) for the square planar arrangement. As discussed above, this means square planar is the preferred geometry for most metal complexes with 8 d electrons, especially when the crystal field splitting (Δ) is large. While not every d^8 complex is square planar, almost all square planar complexes are d^8 (there are examples of d^7 and d^9 square planar complexes but they are less common)

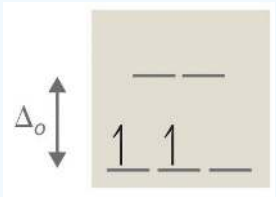
Exercise *Section*6.1.3

For each of the following, sketch the d-orbital splitting diagram, fill the diagram with the correct number of d-electrons, list the number of unpaired electrons, and label whether they are paramagnetic or diamagnetic:

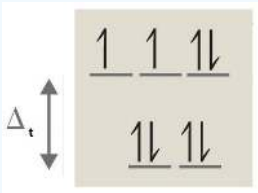
1. $[Ti(H_2O)_6]^{2+}$
2. $[NiCl_4]^{2-}$ (tetrahedral)
3. $[CoF_6]^{3-}$ (high spin)
4. $[Co(NH_3)_6]^{3+}$ (low spin)

Answer

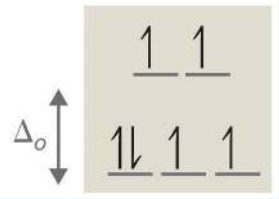
1. 2 unpaired electrons, paramagnetic



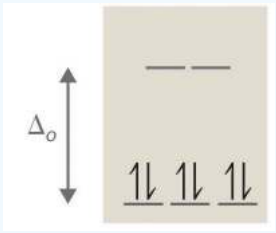
2. 2 unpaired electrons, paramagnetic



3. 4 unpaired electrons, paramagnetic



4. 0 unpaired electrons, diamagnetic



Contributors and Attributions

- Asadullah Awan (UCD), Hong Truong (UCD)
- Prof. Robert J. Lancashire (The Department of Chemistry, University of the West Indies)
- Modified by Catherine McCusker (East Tennessee State University)

Section 6.1: Crystal Field Theory is shared under a CC BY-NC-SA 4.0 license and was authored, remixed, and/or curated by LibreTexts.

- **9.1: Crystal Field Theory** is licensed CC BY-NC-SA 4.0.

Section 6.2: Crystal Field Stabilization Energy

Crystal Field Stabilization Energy

A consequence of crystal field theory is that the distribution of electrons in the d orbitals may lead to net stabilization (decrease in energy) of some complexes depending on the specific ligand geometry and metal d-electron configurations. It is a simple matter to calculate this stabilization since all that is needed is the electron configuration and knowledge of the splitting patterns.

Definition: Crystal Field Stabilization Energy (CFSE)

The crystal field stabilization energy is defined as the energy of the electron configuration in the crystal field minus the energy of the electronic configuration in the spherical field.

$$CFSE = \Delta E = E_{\text{crystal field}} - E_{\text{spherical field}} \quad \text{(Section 6.2.1)}$$

The CSFE will depend on multiple factors including:

- Geometry (crystal field splitting pattern)
- Number of d-electrons
- Spin Pairing Energy (the contribution of spin pairing energy is often negligible in comparison to other contributions and is omitted at times)

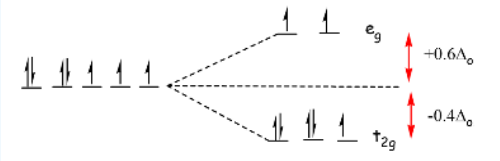
For an octahedral complex, each of the more stable t_{2g} orbitals are stabilized by $-0.4\Delta_o$ relative to spherical field whereas the higher energy e_g orbitals are destabilized by $+0.6\Delta_o$. For a complex the stabilization or destabilization of each electron is summed. Any electrons that are paired within a single orbital, also contribute spin pairing energy (+P). The overall CFSE for a complex is expressed as a multiple of the crystal field splitting parameter Δ_o.

Example *Section*6.2.1: CFSE for a high Spin d^7 complex

What is the CFSE for a high spin d^7 octahedral complex?

Solution

The splitting pattern and electron configuration for both spherical and octahedral ligand fields are compared below.



The energy of the spherical field ($E_{\text{spherical field}}$) is

$$E_{\text{spherical field}} = 7 \times 0 + 2P = 2P$$

The energy of the octahedral crystal field $E_{\text{oct field}}$ is

$$E_{\text{oct field}} = (5 \times -0.4\Delta_o) + (2 \times 0.6\Delta_o) + 2P = -0.8\Delta_o + 2P$$

So via Equation Section 6.2.1, the CFSE is

$$\begin{aligned} CFSE &= E_{\text{oct field}} - E_{\text{spherical field}} \\ &= (-0.8\Delta_o + 2P) - 2P \\ &= -0.8\Delta_o \end{aligned}$$

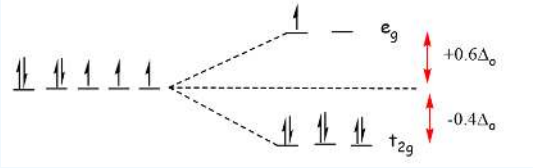
Notice that the spin pairing energy cancels out in this case (and will when calculating the CFSE of high spin complexes) since the number of paired electrons in the octahedral field is the same as that in spherical field of the free metal ion.

Exercise *Section*6.2.1

What is the CFSE for a low spin d^7 octahedral complex?

Answer

The splitting pattern and electron configuration for both spherical and octahedral ligand fields are compared below.



The energy of the spherical field is the same as calculated for the high spin configuration in Example 1:

$$E_{\text{spherical}} = 7 \times 0 + 2P = 2P$$

The energy of the octahedral ligand\) field $E_{\text{oct field}}$ is

$$\begin{aligned} E_{\text{oct field}} &= (6 \times -0.4\Delta_o) + (1 \times 0.6\Delta_o) + 3P \\ &= -1.8\Delta_o + 3P \end{aligned}$$

So via Equation Section 6.2.1, the CFSE is

$$\begin{aligned} CFSE &= E_{\text{oct field}} - E_{\text{spherical field}} \\ &= (-9/5\Delta_o + 3P) - 2P \\ &= -9/5\Delta_o + P \end{aligned}$$

This appears more a more stable configuration than the high spin d^7 configuration in Example *Section*6.2.1, but we have then to take into consideration the pairing energy P to know definitely, which varies between $200 - 400\ kJ\ mol^{-1}$ depending on the metal.

Table *Section*6.2.1: Crystal field stabilization energies (CFSE) for high and low spin octahedral complexes

Total d-electrons	Spherical Field	Octahedral Field				Crystal Field Stabilization Energy	
		High Spin		Low Spin			
	$E_{\text{spherical field}}$	Configuration	$E_{\text{crystal field}}$	Configuration	$E_{\text{crystal field}}$	High Spin	Low Spin
d^0	0	$t_{2g}^0\ e_g^0$	0	$t_{2g}^0 e_g^0$	0	0	0
d^1	0	$t_{2g}^1\ e_g^0$	-2/5 Δ_o	$t_{2g}^1 e_g^0$	-2/5 Δ_o	-2/5 Δ_o	-2/5 Δ_o
d^2	0	$t_{2g}^2\ e_g^0$	-4/5 Δ_o	$t_{2g}^2 e_g^0$	-4/5 Δ_o	-4/5 Δ_o	-4/5 Δ_o
d^3	0	$t_{2g}^3\ e_g^0$	-6/5 Δ_o	$t_{2g}^3 e_g^0$	-6/5 Δ_o	-6/5 Δ_o	-6/5 Δ_o
d^4	0	$t_{2g}^3\ e_g^1$	-3/5 Δ_o	$t_{2g}^4 e_g^0$	-8/5 Δ_o + P	-3/5 Δ_o	-8/5 Δ_o + P
d^5	0	$t_{2g}^3\ e_g^2$	0 Δ_o	$t_{2g}^5 e_g^0$	-10/5 Δ_o + 2P	0 Δ_o	-10/5 Δ_o + 2P
d^6	P	$t_{2g}^4\ e_g^2$	-2/5 Δ_o + P	$t_{2g}^6 e_g^0$	-12/5 Δ_o + 3P	-2/5 Δ_o	-12/5 Δ_o + P
d^7	2P	$t_{2g}^5\ e_g^2$	-4/5 Δ_o + 2P	$t_{2g}^6 e_g^1$	-9/5 Δ_o + 3P	-4/5 Δ_o	-9/5 Δ_o + P
d^8	3P	$t_{2g}^6\ e_g^2$	-6/5 Δ_o + 3P	$t_{2g}^6 e_g^2$	-6/5 Δ_o + 3P	-6/5 Δ_o	-6/5 Δ_o
d^9	4P	$t_{2g}^6\ e_g^3$	-3/5 Δ_o + 4P	$t_{2g}^6 e_g^3$	-3/5 Δ_o + 4P	-3/5 Δ_o	-3/5 Δ_o
d^{10}	5P	$t_{2g}^6\ e_g^4$	0 Δ_o + 5P	$t_{2g}^6 e_g^4$	0 Δ_o + 5P	0	0

P is the spin pairing energy and represents the energy required to pair up electrons within the same orbital. For a given metal ion P (pairing energy) is constant, but it does not vary with ligand and oxidation state of the metal ion).

Octahedral Preference

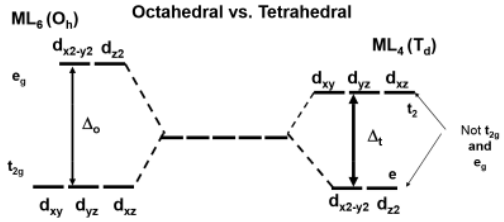
Similar CFSE values can be constructed for non-octahedral ligand field geometries once the knowledge of the d-orbital splitting is known and the electron configuration within those orbitals known, e.g., the tetrahedral complexes in Table *Section*6.2.2. These energies geoemtries can then be contrasted to the octahedral CFSE to calculate a thermodynamic preference for a metal-ligand combination to favor the octahedral geometry. This is quantified via an octahedral site preference energy defined below.

Definition: Octahedral Site Preference Energies (OSPE)

The octahedral site preference energy (OSPE) is defined as the difference of CFSE energies for a non-octahedral complex and the octahedral complex. For comparing the preference of forming an octahedral ligand field vs. a tetrahedral ligand field, the OSPE is thus:

$$OSPE = CFSE_{(oct)} - CFSE_{(tet)} \qquad \text{(Section 6.2.2)}$$

The OSPE quantifies the preference of a complex to exhibit an octahedral geometry vs. another geometry. The OSPE for octahedral vs tetrahedral geometries is illustrated below.



Note: the conversion between Δ_o and Δ_t used for these calculations is:

$$\Delta_t \approx \frac{4}{9}\Delta_o \qquad \text{(Section 6.2.3)}$$

which is applicable for comparing octahedral and tetrahedral complexes that involve same ligands only.

Table *Section*6.2.2: Octahedral Site Preference Energies (OSPE)

Total d-electrons	CFSE(Octahedral)	CFSE(Tetrahedral)	OSPE (for high spin complexes)**

Total d-electrons	CFSE(Octahedral)		CFSE(Tetrahedral)		OSPE (for high spin complexes)**
	High Spin	Low Spin	Configuration	**Always High Spin***	
d^0	0 Δ_o	0 Δ_o	e^0	0 Δ_t	0 Δ_o
d^1	-2/5 Δ_o	-2/5 Δ_o	e^1	-3/5 Δ_t	-6/45 Δ_o
d^2	-4/5 Δ_o	-4/5 Δ_o	e^2	-6/5 Δ_t	-12/45 Δ_o
d^3	-6/5 Δ_o	-6/5 Δ_o	$e^2t_2^1$	-4/5 Δ_t	-38/45 Δ_o
d^4	-3/5 Δ_o	-8/5 Δ_o + P	$e^2t_2^2$	-2/5 Δ_t	-19/45 Δ_o
d^5	0 Δ_o	-10/5 Δ_o + 2P	$e^2t_2^3$	0 Δ_t	0 Δ_o
d^6	-2/5 Δ_o	-12/5 Δ_o + P	$e^3t_2^3$	-3/5 Δ_t	-6/45 Δ_o
d^7	-4/5 Δ_o	-9/5 Δ_o + P	$e^4t_2^3$	-6/5 Δ_t	-12/45 Δ_o
d^8	-6/5 Δ_o	-6/5 Δ_o	$e^4t_2^4$	-4/5 Δ_t	-38/45 Δ_o
d^9	-3/5 Δ_o	-3/5 Δ_o	$e^4t_2^5$	-2/5 Δ_t	-19/45 Δ_o
d^{10}	0	0	$e^4t_2^6$	0 Δ_t	0 Δ_o

P is the spin pairing energy and represents the energy required to pair up electrons within the same orbital.

Note

Tetrahedral complexes are always high spin since the splitting is appreciably smaller than ***P*** (Equation Section 6.2.3).

After conversion with Equation Section 6.2.3. The data in Tables ***Section*6.2.1** and ***Section*6.2.2** are represented graphically by the curves in Figure ***Section*6.2.1** below for the high spin complexes only. The low spin complexes require knowledge of ***P*** to graph, which will vary depending on the identiy of the metal ion.

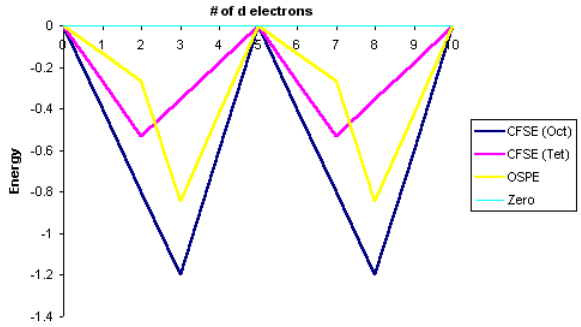


Figure ***Section*6.2.1**: Crystal Field Stabilization Energies for both high spin octahedral fields ($CFSE_{oct}$) and tetrahedral fields ($CFSE_{tet}$). Octahedral Site Preference Energies (OSPE) are in yellow. This is for high spin complexes only.

From a simple inspection of Figure ***Section*6.2.1**, the following observations can be made:

- The OSPE is *small* in d^1, d^2, d^5, d^6, d^7 high spin complexes and other factors influence the stability of the complexes including steric factors
- The OSPE is *large* in d^3 and d^8 high spin complexes which strongly favor octahedral geometries

Applications

The "double-humped" curve in Figure *Section*6.2.1 is found for various properties of the first-row transition metals, including hydration and lattice energies of the M(II) ions, ionic radii as well as the stability of M(II) complexes. This suggests that these properties are somehow related to crystal field effects.

In the case of hydration energies describing the complexation of water ligands to a bare metal ion:

$$M^{2+}(g) + H_2O \rightarrow [M(OH_2)_6]^{2+}(aq) \qquad \text{(Section 6.2.4)}$$

Table *Section*6.2.3 and Figure *Section*6.2.2 shows this type of curve. Note that in any series of this type not all the data are available since a number of ions are not very stable in the M(II) state in water.

Table *Section*6.2.3: Hydration energies of M^{2+} ions

M	ΔH°/kJmol^{-1}	M	ΔH°/kJmol^{-1}
Ca	-2469	Fe	-2840
Sc	no stable 2+ ion	Co	-2910
Ti	-2729	Ni	-2993
V	-2777	Cu	-2996
Cr	-2792	Zn	-2928
Mn	-2733		

Graphically the data in Table 2 can be represented by:

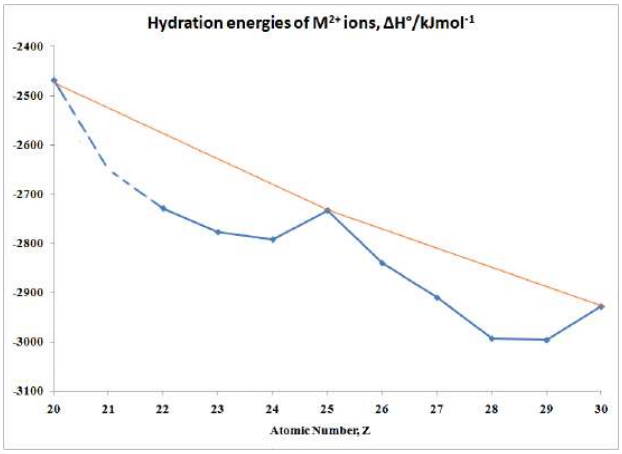


Figure *Section*6.2.2: Hydration energies of M^{2+} ions

Contributors and Attributions

- Prof. Robert J. Lancashire (The Department of Chemistry, University of the West Indies)

Section 6.2: Crystal Field Stabilization Energy is shared under a CC BY-NC-SA 4.0 license and was authored, remixed, and/or curated by LibreTexts.

- **9.2: Crystal Field Stabilization Energy** is licensed CC BY-NC-SA 4.0.

Section 6.3: Factors That Affect Crystal Field Splitting

Magnitude of Crystal Field Splitting

The magnitude of the crystal field splitting (Δ) dictates whether a complex with four, five, six, or seven d electrons (in an octahedral complex) is high spin or low spin, which affects its magnetic properties, structure, and reactivity. Large values of Δ (i.e., Δ > P) yield a low-spin complex, whereas small values of Δ (i.e., Δ < P) produce a high-spin complex. The magnitude of Δ depends on four factors: the valence of the metal, the principal quantum number of the metal (and thus its location in the periodic table), the geometry, and the nature of the ligand(s). Values of Δ for some representative transition metal complexes are given in Table *Section*6.3.1.

Table *Section*6.3.1: Crystal Field Splitting Energies for Some Octahedral (Δ_o)* and Tetrahedral (Δ_t) Transition-Metal Complexes

Octahedral Complexes	Δ_o (cm^{-1})	Octahedral Complexes	Δ_o (cm^{-1})	Tetrahedral Complexes	Δ_t (cm^{-1})
$[Ti(H_2O)_6]^{3+}$	20,300	$[Fe(CN)_6]^{4-}$	32,800	VCl_4	9010
$[V(H_2O)_6]^{2+}$	12,600	$[Fe(CN)_6]^{3-}$	35,000	$[CoCl_4]^{2-}$	3300
$[V(H_2O)_6]^{3+}$	18,900	$[CoF_6]^{3-}$	13,000	$[CoBr_4]^{2-}$	2900
$[CrCl_6]^{3-}$	13,000	$[Co(H_2O)_6]^{2+}$	9300	$[CoI_4]^{2-}$	2700
$[Cr(H_2O)_6]^{2+}$	13,900	$[Co(H_2O)_6]^{3+}$	27,000		
$[Cr(H_2O)_6]^{3+}$	17,400	$[Co(NH_3)_6]^{3+}$	22,900		
$[Cr(NH_3)_6]^{3+}$	21,500	$[Co(CN)_6]^{3-}$	34,800		
$[Cr(CN)_6]^{3-}$	26,600	$[Ni(H_2O)_6]^{2+}$	8500		
$Cr(CO)_6$	34,150	$[Ni(NH_3)_6]^{2+}$	10,800		
$[MnCl_6]^{4-}$	7500	$[RhCl_6]^{3-}$	20,400		
$[Mn(H_2O)_6]^{2+}$	8500	$[Rh(H_2O)_6]^{3+}$	27,000		
$[MnCl_6]^{3-}$	20,000	$[Rh(NH_3)_6]^{3+}$	34,000		
$[Mn(H_2O)_6]^{3+}$	21,000	$[Rh(CN)_6]^{3-}$	45,500		
$[Fe(H_2O)_6]^{2+}$	10,400	$[IrCl_6]^{3-}$	25,000		
$[Fe(H_2O)_6]^{3+}$	14,300	$[Ir(NH_3)_6]^{3+}$	41,000		

*Energies obtained by spectroscopic measurements are often given in units of wave numbers (cm^{-1}); the wave number is the reciprocal of the wavelength of the corresponding electromagnetic radiation expressed in centimeters: 1 cm^{-1} = 11.96 J/mol.

Source of data: Duward F. Shriver, Peter W. Atkins, and Cooper H. Langford, Inorganic Chemistry, 2nd ed. (New York: W. H. Freeman and Company, 1994).

Valence of the metal

Increasing the valence of a metal ion has two effects: the radius of the metal decreases and ligands are more strongly attracted to it due to Coulombic attraction. Both factors decrease the metal–ligand distance, which in turn causes the ligands to interact more strongly with the d-orbitals. Consequently, the magnitude of Δ_o increases as the valence of the metal increases. Typically, Δ_o for a M(III) is about 50% greater than for the M(II) of the same metal; for example, for $[V(H_2O)_6]^{2+}$, Δ_o = 11,800 cm^{-1}; for $[V(H_2O)_6]^{3+}$, Δ_o = 17,850 cm^{-1}.

Principal quantum number of the metal

For a series of complexes of metals from the same group in the periodic table with the same charge and the same ligands, the magnitude of Δ_o increases with increasing principal quantum number: Δ (3d) < Δ (4d) < Δ (5d). The data for hexaammine complexes of the trivalent Group 9 metals illustrate this point:

$$[Co(NH_3)_6]^{3+}: \Delta_o = 22{,}900\ cm^{-1}$$

$$[Rh(NH_3)_6]^{3+}: \Delta_o = 34{,}100\ cm^{-1}$$

$$[Ir(NH_3)_6]^{3+}: \Delta_o = 40{,}000\ cm^{-1}$$

The increase in Δ with increasing principal quantum number is due to the larger radial extension of the d orbitals as n increases. In addition, repulsive ligand–ligand interactions are most important for smaller metal ions. Relatively speaking, this results in shorter M–L distances and stronger d orbital–ligand interactions. The increase in Δ going from 3d to 4d and 5d is so large that all 4d and 5d metals will form low spin complexes.

Geometry of the complex

The number of ligands in a complex as well as how well the ligand geometry overlaps with the d orbitals is also a factor in the magnitude of the crystal field splitting. For example, comparing octahedral and tetrahedral geometries the octahedral geometry has 6 ligands, and those 6 ligands overlap directly with the two d orbitals that lie along the axes, $d_{x^2-y^2}$ and d_{z^2}. The tetrahedral geometry has fewer ligands than octahedral, and those ligands overlap less ideally with the ligands that lie between the axes, d_{xy}, d_{xz}, and d_{yz}. Because of this the crystal field splitting of a tetrahedral complex is generally less than half ($\frac{4}{9}$ than an octahedral complex with the same metal and ligands. For example $[FeCl_4]^-$ has a $\Delta_t = 5{,}200\ cm^{-1}$ and $[FeCl_6]^{3-}$ has a $\Delta_o = 11{,}600\ cm^{-1}$.

Nature of the ligands

In crystal field theory ligands are all modeled as negative point charges, which means that all ligands should behave identically. Experimentally, it is found that the Δ_o observed for a series of complexes of the same metal ion depends strongly on the nature of the ligands. For a series of chemically similar ligands, the magnitude of Δ_o decreases as the size of the donor atom increases. For example, Δ_o values for halide complexes generally decrease in the order F > Cl > Br > I because smaller, more localized charges, such as we see for F, interact more strongly with the d-orbitals of the metal. In addition, a small neutral ligand with a highly localized lone pair, such as NH_3, results in significantly larger Δ_o values than might be expected. Because the lone pair points directly at the metal ion, the electron density along the M–L axis is greater than for a spherical anion such as F. The experimentally observed order of the crystal field splitting energies produced by different ligands is called the spectrochemical series.

Ligands are classified as strong field or weak field based on the spectrochemical series:

weak field $I^- < Br^- < Cl^- < \underline{S}CN^- < F^- < OH^- < ox^{-2} < \underline{O}NO < H_2O < SC\underline{N}^- < NH_3 <$ en $< \underline{N}O_2 < CN^-$, CO strong field

Note that SCN and NO_2 ligands are represented twice in the above spectrochemical series since there are two different Lewis base sites (e.g., free electron pairs to share) on each ligand (e.g., for the SCN ligand, the electron pair on the sulfur or the nitrogen can form the bond to a metal). The specific atom that binds in such ligands is underlined. Ligands on the weak field end of the series (halogens, OH, H_2O) will tend to form high spin complexes and ligands on the strong field end of the series (CN, CO, NO_2) will tend to form low spin complexes. Intermediate ligands in the midle of the series could form high or low spin complexes depending on other factors.

How to determine if a complex is high or low spin

1. How many d electrons does the complex have?
   - Only complexes with 4-7 d electrons have high spin and low spin configurations
2. What period is the metal?
   - 3d metals could either be high or low spin
   - 4d and 5d metals will ALWAYS be low spin
3. What is the geometry of the complex?
   - Tetrahedral complexes with 3d metals will almost always be high spin because Δt is generally less than spin pairing energy

- Square planar complexes will almost always be low spin because they are favored over tetrahedral when crystal field splitting is large
- Octahedral complexes could be either high or low spin

4. What are the ligands?
   - Strong field ligands will form low spin complexes
   - Weak field ligands will form high spin complexes
   - Intermediate field ligands could form high or low spin complexes. Additional information (like number of unpaired electrons) is needed

- Adapted by Catherine McCusker (East Tennessee State University)

Section 6.3: Factors That Affect Crystal Field Splitting is shared under a CC BY-NC-SA 4.0 license and was authored, remixed, and/or curated by LibreTexts.

- **9.4: Factors That Affect Crystal Field Splitting** is licensed CC BY-NC-SA 4.0.

Section 6.4: Ligand Field Theory

Extension of Crystal Field Theory

Experimentally it is known that the nature of the ligand plays an important role in the magnitude of the crystal field splitting in metal complexes and can determine whether a complex is high or low spin. Empirically ligands can be ordered in the spectrochemical series, but using crystal field theory we cannot rationalize where ligands fall in the series. For example, why is the neutral CO one of the strongest field ligands in the series while the anionic halogens are weak field ligands? To understand why ligands behave differently we have to consider how ligand orbitals interact with the metal d orbitals. Ligand field theory is essentially a combination between crystal field theory and molecular orbital theory where we focus only on the orbital overlap between the metal d orbitals and select ligand orbitals (rather than considering all of the valence orbitals on both the metal and ligand)

Metal-Ligand σ Bonding

The bond between a metal and a ligand is primarily a Lewis acid-base interaction where the ligand is a Lewis base and donates a pair of electron to the metal, the Lewis acid. This interaction forms a coordinate covalent bond. As with molecular orbital theory we have to decide how (or if) the ligand lone pairs will overlap with each of the d orbitals, and what type of bonding will be formed In an octahedral complex the ligands and their lone pairs lie along the x, y, and z axes. As shown in Figure *Section*6.4.1, the two on axis d orbitals ($d_{x^2-y^2}$ and d_{z^2}) have to correct orientation to form sigma bonds with the ligands. With the three off axis d orbitals (d_{xy}, d_{xz}, and d_{yz}) the ligand lone pair overlaps with a node in these orbitals (Figure *Section*6.4.1c). This means there is no net overlap and no bonding (or antibonding) molecular orbital can be formed.

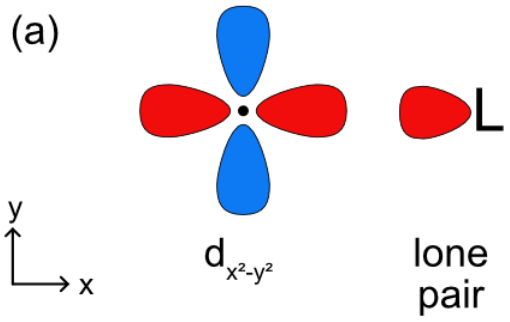


Figure ***Section*6.4.1*a***: Overlap between a ligand lone pair orbital and the metal $d_{x^2-y^2}$ orbital to form a sigma bond (CC BY-NC-SA, Catherine McCusker)

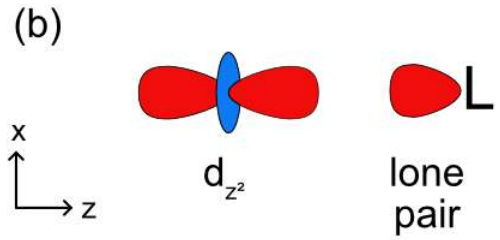


Figure ***Section*6.4.1*b***: Overlap between a ligand lone pair orbital and the metal d_{z^2} orbital to form a sigma bond (CC BY-NC-SA, Catherine McCusker)

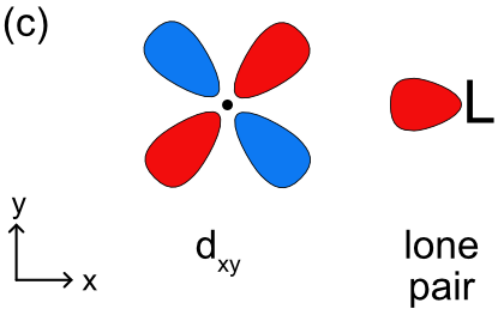


Figure ***Section*6.4.1*c***: There is no net overlap between the ligand lone pair orbital and the d_{xy} metal orbital, so this is a non bonding interaction (CC BY-NC-SA, Catherine McCusker)

Knowing this, we can construct a ligand field splitting diagram (a simplified molecular orbital diagram) (Figure ***Section*6.4.2**). In the free metal ion all 5 of the d orbitals are degenerate and before they interact with the metal all 6 of the ligand lone pair orbitals are at the same energy as well. Generally, based on electronegativity the ligand lone pair orbitals will be lower in energy than the metal d orbitals. When the ligand lone pairs interact with metal d orbitals the on axis set of d orbitals ($d_{x^2-y^2}$ and d_{z^2}) will form sigma bonding (e_g) and sigma antibonding (e_g*) molecular orbitals. The off axis set of d orbitals are nonbonding and are not stabilized or destabilized by the ligand lone pairs. Unlike a complete molecular orbital diagrams, a ligand field diagram won't necessarily have the same number of molecular orbitals as atomic orbitals becuse not every possible bonding interaction is included (for example, any overlap between the ligand orbitals and the metal s and p orbitals are not included). As in crystal field theory we can define an octahedral ligand field splitting energy (Δ_o), which will be the difference between the two molecular orbitals with the most metal d orbital character. In Figure ***Section*6.4.2** the t_{2g} set of d orbitals are nonbonding and therefore 100% metal character. The e_g bonding orbital is closer in energy to the ligand lone pairs and will have a higher % contribution from the ligands, and the e_g* antibonding orbital is closer in energy to the metal d orbitals and will have a higher % contribution from the metal. The relevant energy difference is between the t_{2g} and e_g* orbitals, as highlighted in green in Figure ***Section*6.4.2**. The splitting energy will increase as there is a stronger interaction between the metal and ligand orbitals (based on the criteria discussed previously) and the e_g* is more destabilized.

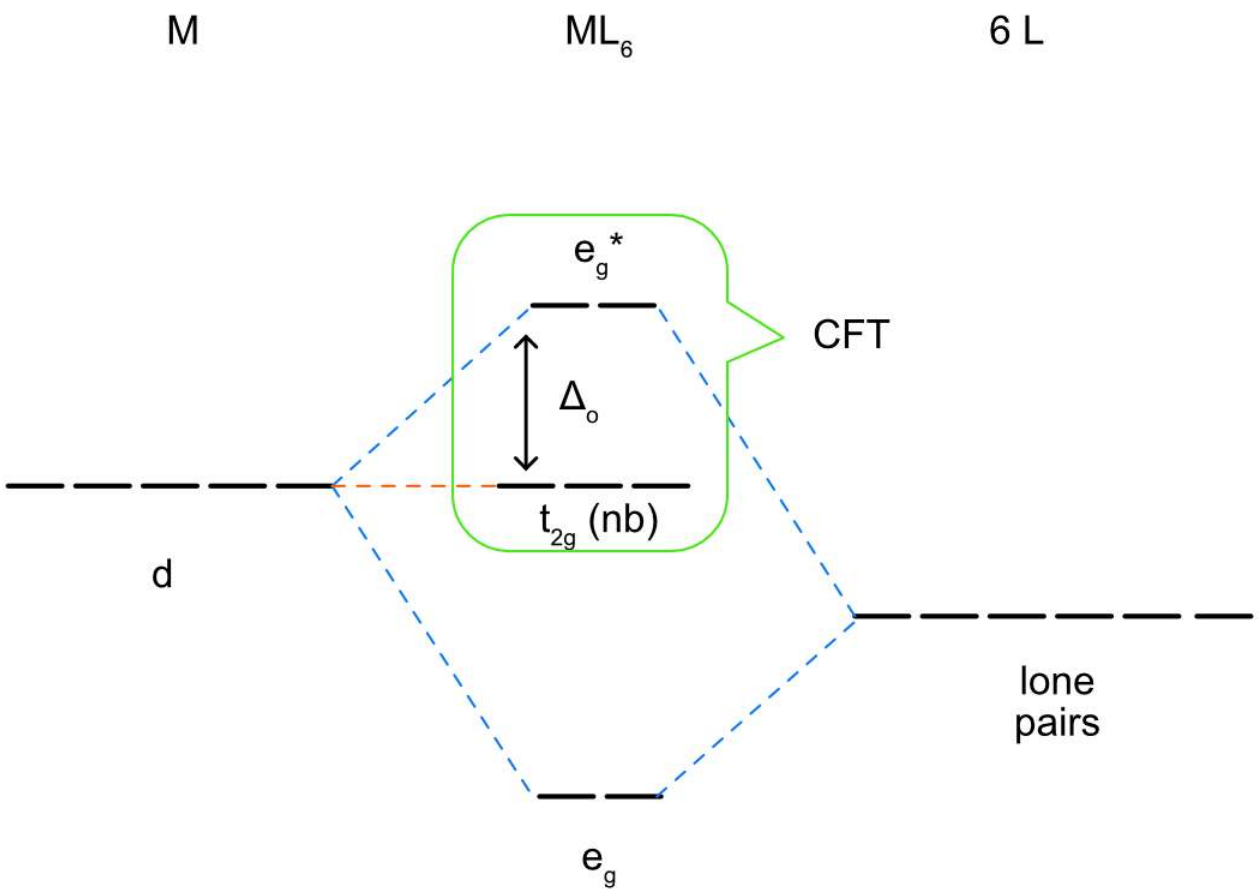


Figure *Section*6.4.2: Octahedral ligand field splitting diagram for only sigma bonding. The $d_{x^2-y^2}$ and d_{z^2} metal orbitals form sigma bonding (e_g) and antibonding molecular orbitals (e_g*). The d_{xy}, d_{xz}, and d_{yz} orbital are nonbonding (t_{2g} (nb)). The green outline highlights the portion of the diagram that is equivalent to the crystal field splitting diagram. (CC BY-NC-SA; Catherine McCusker)

Metal-Ligand π Bonding

In addition to sigma bonding, some ligands have orbitals available which can form π bonds with metals as well. These could include p orbitals on a single donor atom such as a halogen ion or π bonding or antibonding molecular orbitals on a molecular ligand. To determine how π bonding will change the ligand field splitting picture in Figure *Section*6.4.2, we will visualize how a ligand p orbital will interact with the metal d orbitals. The $d_{x^2-y^2}$ and d_{z^2} orbitals do not have the correct symmetry to form any type of bond with a ligand p orbital as shown in Figures *Section*6.4.3*a* – *b* The d_{xy}, d_{xz}, and d_{yz} orbitals all have the correct symmetry to form π bonds with a ligand p orbital (Figure *Section*6.4.3*c*).

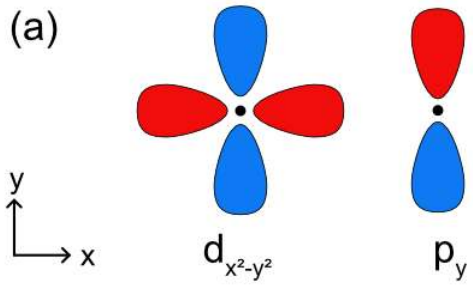


Figure *Section*6.4.3*a*: There is no net overlap between the ligand p orbital and the $d_{x^2-y^2}$ metal orbital, so this is a non bonding interaction (CC BY-NC-SA, Catherine McCusker)

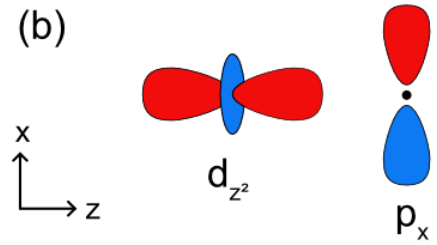


Figure *Section*6.4.3*b*: There is no net overlap between the ligand p orbital and the d_{z^2} metal orbital, so this is a non bonding interaction (CC BY-NC-SA, Catherine McCusker)

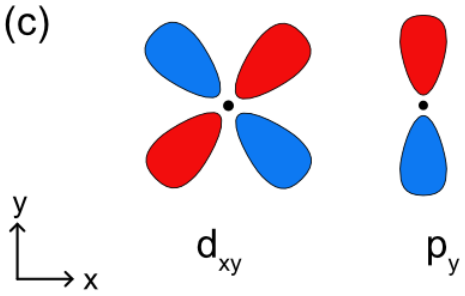


Figure *Section*6.4.3*c*: Overlap between a ligand p orbital and the metal d_{xy} orbital to form a π bond (CC BY-NC-SA, Catherine McCusker)

Unlike metal-ligand σ bonding, where electrons are always donated from the ligand to the metal, electrons in metal-ligand π bonding can be donated from either the metal or the ligand depending on the nature of the orbitals involved. In cases where ligands have empty p or π symmetry orbitals that are close in energy to the metal d orbitals, they can accept electrons from a filled metal orbital. This is also known as π backbonding because the direction of electron donation is opposite of that found in sigma metal ligand bonding. These ligands are called π acceptor ligands. In cases where ligands have filled p or π symmetry orbitals that are close in energy to the metal d orbitals, they can donate electrons to an empty metal orbital. These ligands are called π donor ligands.

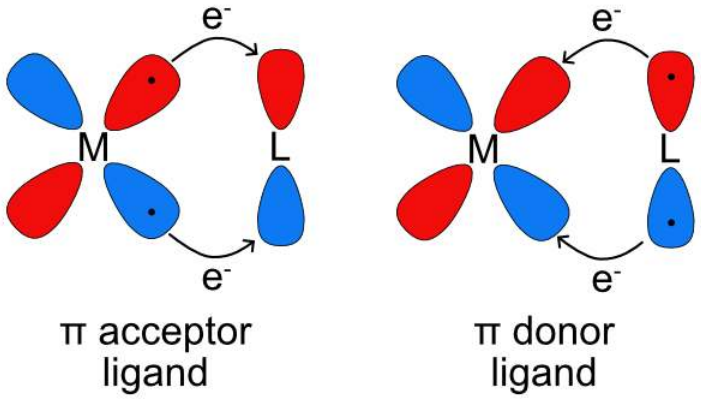


Figure *Section*6.4.4: Illustration of metal-ligand π bonding with π acceptor and donor ligands. Filled orbitals are represented with black dots. (CC BY-NC-SA, Catherine McCusker)

π Acceptors

Ligands that are π acceptors have empty, low energy π symmetry orbitals available to accept electrons from the metal center. Most often this is a π^* antibonding molecular orbital but it could also be an empty p orbital. Due to the aufbau principle, these empty orbitals will be higher in energy than any filled lone pairs on the ligands and will also generally be higher energy than the metal d orbitals. Similar to multiple bonding in main group compounds π bonding always occurs in combination with sigma bonding so in the ligand field splitting diagram of metal-ligand bonding with a π acceptor ligand the lone pairs for sigma bonding must be included as well as the empty orbitals for π bonding. As seen in Figure *Section*6.4.3, the $d_{x^2-y^2}$ and d_{z^2} orbitals do not overlap with the ligand p orbitals. The on axis d orbitals will form sigma bonding (e_g) and sigma antibonding (e_g*) molecular orbitals. Unlike the sigma bonding only diagram, the off axis d orbitals (d_{xy}, d_{xz}, and d_{yz}) overlap with the ligand p orbitals to form π bonding (t_{2g}) and π antibonding (t_{2g}*) molecular orbitals as seen in Figure *Section*6.4.5. Rather than being nonbonding, like in the sigma bonding only picture, the metal based t_{2g} molecular orbital is bonding. This increases the energy difference between the t_{2g} and e_g* and therefore increases Δ_o.

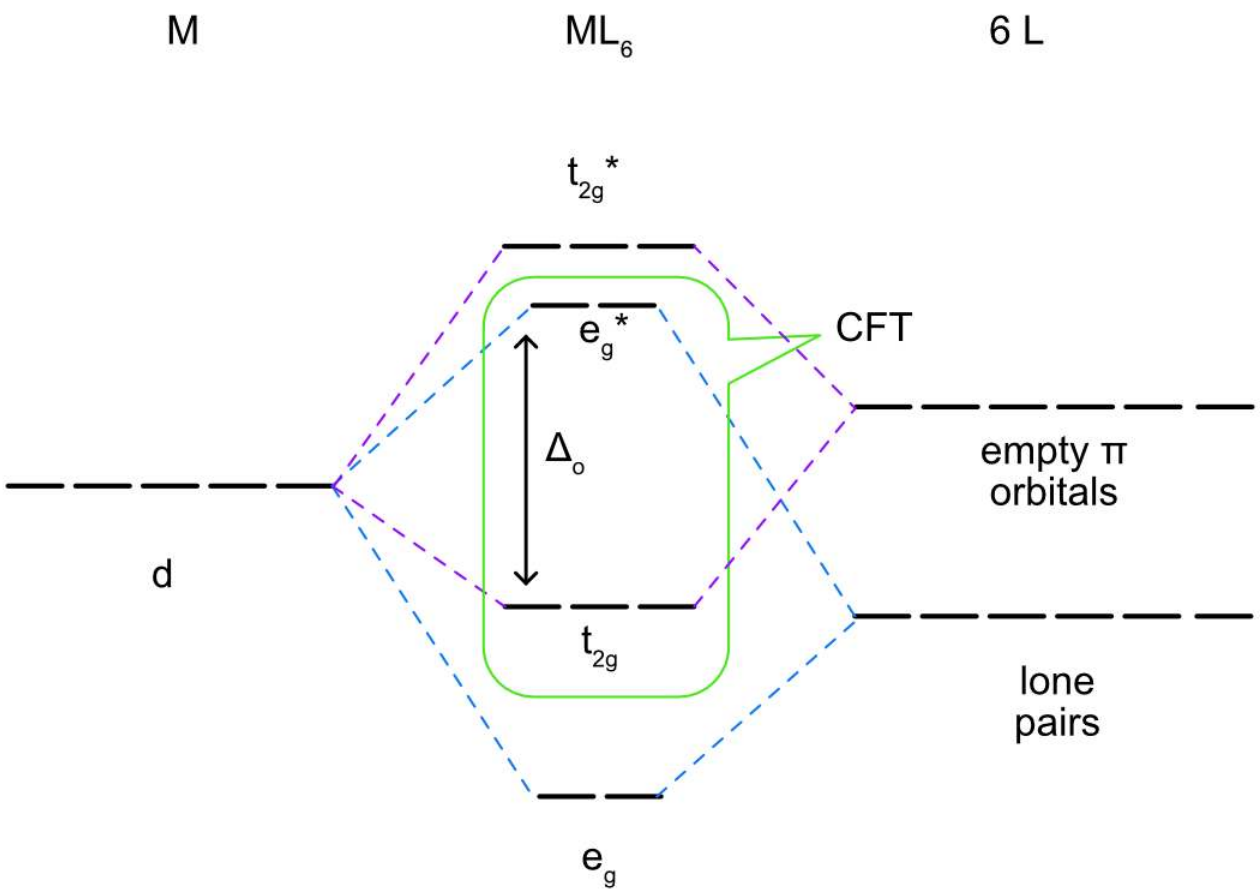


Figure *Section*6.4.5: Octahedral ligand field splitting diagram with a π acceptor ligand. The $d_{x^2-y^2}$ and d_{z^2} metal orbitals form sigma bonding (e_g) and antibonding molecular orbitals (e_g*) with the ligand lone pairs. The d_{xy}, d_{xz}, and d_{yz} orbital form pi bonding (t_{2g}) and pi antibonding molecular orbitals (t_{2g}*) with the empty π symmetry orbitals. The green outline highlights the portion of the diagram that is equivalent to the crystal field splitting diagram. (CC BY-NC-SA; Catherine McCusker)

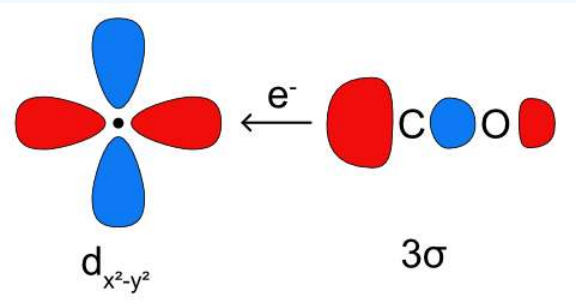
Exercise *Section*6.4.1

Carbon monoxide is one of the most common, and strongest π acceptor ligands in inorganic chemistry. Refer to the molecular orbital diagram of CO and sketch likely metal-ligand orbital interactions for both sigma and pi bonding in a metal-CO complex. Indicate the direction of electron donation in both cases.

Answer

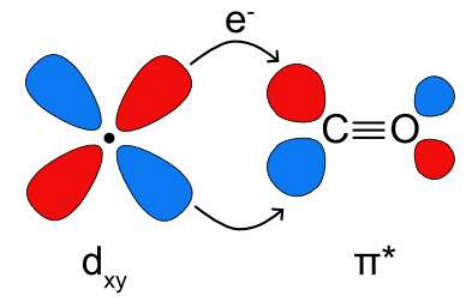
Sigma bonding:

Sigma bonding between a metal ion and a CO ligand involves overlap between the HOMO of CO (3σ) and the metal $d_{x^2-y^2}$ or d_{z^2} orbitals. Electrons are donated from the ligand to the metal.



Pi bonding:

Pi bonding between a metal ion and CO ligand involves overlap between the LUMO of CO (π^*) and the metal d_{xy}, d_{xz}, or d_{yz} orbitals. Electrons are donated from the metal to the ligand.



π Donor Ligands

Ligands that are π donors have filled π symmetry orbitals that are high enough in energy to donate electrons to the metal center. Most often this is a filled p orbital, but it could also be a π bonding molecular orbital. As lone pairs are generally the highest occupied orbitals is a molecule, the filled π orbitals will be lower in energy as seen in Figure ***Section*6.4.6**. The sigma interaction between the ligand lone pairs and the metal $d_{x^2-y^2}$ and d_{z^2} remain the same as previously described, forming the e_g bonding and e_g* antibonding molecular orbitals. The d_{xy}, d_{xz}, and d_{yz} overlap with the filled π orbitals to form π bonding (t_{2g}) and π antibonding (t_{2g}*) molecular orbitals. The difference between the ***pi*** acceptor and donor ligands is the energy and character of the t_{2g} and t_{2g}* molecular orbitals. In the π acceptor case above, the t_{2g} orbital is above the e_g and has a higher contribution from the metal and the t_{2g}* is above the e_g* and has a higher contribution from the ligand. In the π donor case the opposite is true. The t_{2g} orbital is below the e_g and has a higher contribution from the ligand and the t_{2g}* is below the e_g* and has a higher contribution from the metal. In this case Δ_o is smaller than in the sigma only picture because the t_{2g} symmetry molecular orbital has gone from nonbonding to antibonding and the energy difference between t_{2g}* and e_g* is smaller.

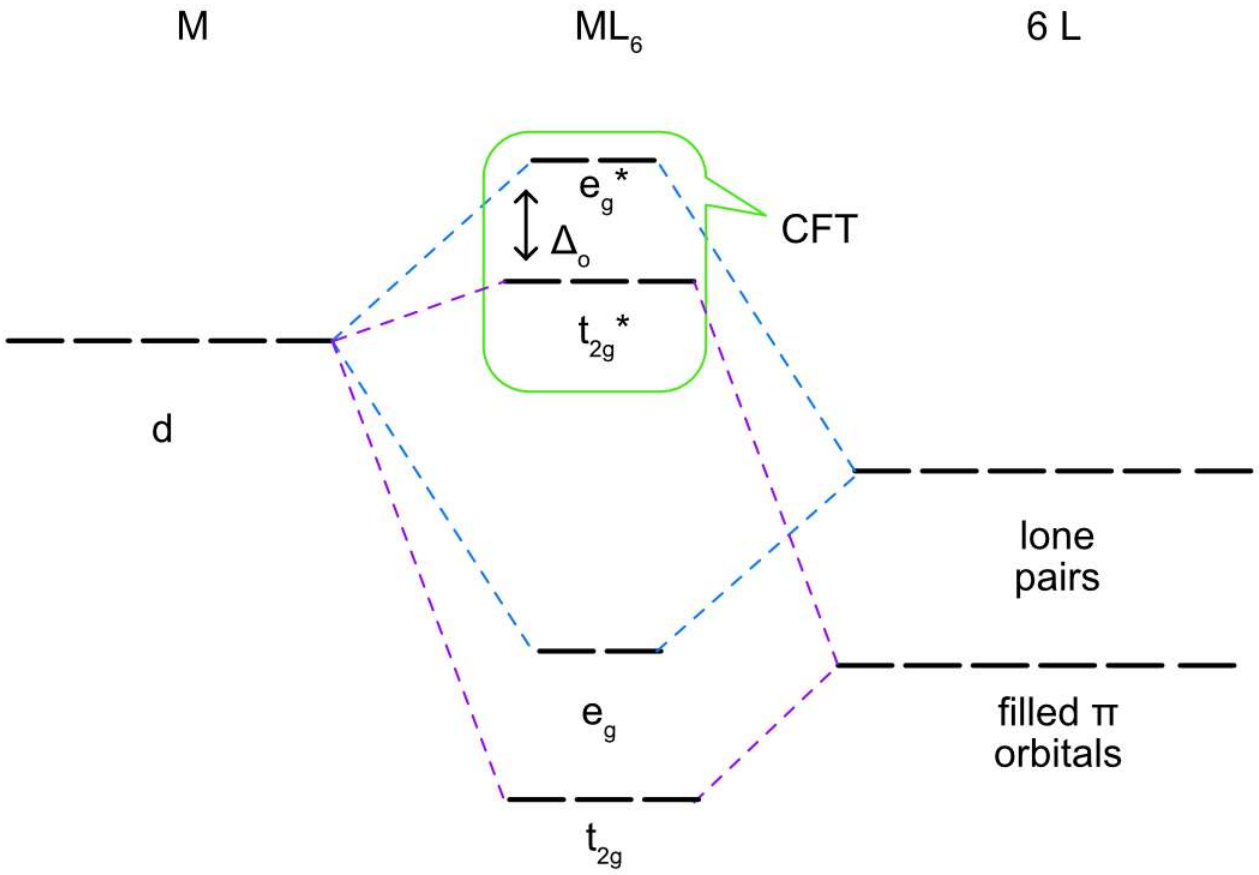


Figure ***Section*6.4.6**: Octahedral ligand field splitting diagram with a π donor ligand. The $d_{x^2-y^2}$ and d_{z^2} metal orbitals form sigma bonding (e_g) and antibonding molecular orbitals (e_g*) with the ligand lone pairs. The d_{xy}, d_{xz}, and d_{yz} orbital form pi bonding (t_{2g}) and pi antibonding molecular orbitals (t_{2g}*) with the filled π symmetry orbitals. The green outline highlights the portion of the diagram that is equivalent to the crystal field splitting diagram. (CC BY-NC-SA; Catherine McCusker)

The Spectrochemical Series

As discussed above, crystal field theory alone can't distinguish the behaviors of different ligands or explain why some ligands inherently produce larger splittings than others. Armed with ligand field theory we can now revisit the spectrochemical series and explain why ligands fall where they do within the series.

Strong field ligands

Strong field ligands are ones that produce large splittings between the d orbitals and form low spin complexes. Examples of strong field ligands include CO, CN^-, and NO_2. From a ligand field theory perspective all three of these ligands have strong π bonds (either double or triple bonds) and have empty π* molecular orbitals available for backbonding. Strong field ligands are both sigma donors (all ligands are sigma donors) and π acceptors. π backbonding between a metal and a ligand stabilizes the metal based t_{2g} molecular orbital and increases Δ_o.

Weak field ligands

Weak field ligands are ones that produce small splittings between the d orbitals and form high spin complexes. Examples of weak field ligands include the halogens, OH^- and H_2O. From a ligand field perspective these ions or molecules all have filled orbitals

which can π bond with the metal d orbitals. In the case of the halogens these are filled p orbitals and in the case of OH^- and H_2O these are lone pairs which are perpendicular to the metal-ligand bond. Weak field ligands are both sigma donors and π donors. The π donation from the ligand to the metal destabilizes the metal based t_{2g} molecular orbital and decreases Δ_o.

Intermediate field ligands

Intermediate field ligands produce intermediate splittings between the d orbitals and could form high or low spin complexes. Examples of intermediate field ligands include NH_3 or ethylenediamine (en). From a ligand field perspective these ligands only have a single lone pair available for sigma bonding. All of the other orbitals on nitrogen are used for sigma bonding to the H or C atoms within the molecule. Intermediate ligands are those which are only sigma donors, and are not π donors or π acceptors. In this case the t_{2g} symmetry d orbitals are nonbonding and the Δ_o is determined by the strength of the metal ligand sigma interaction (and amount of destabilization of the e_g* molecular orbital)

This page titled Section 6.4: Ligand Field Theory is shared under a CC BY-NC-SA 4.0 license and was authored, remixed, and/or curated by Catherine McCusker.

- **9.5: Ligand Field Theory** by Catherine McCusker is licensed CC BY-NC-SA 4.0.

Section 6.5: Metal-Metal Bonds

Molecular orbital considerations in Dinuclear Metal Complexes with Multiple M-M Bonds

Let us begin a new chapter and think about dinuclear transition metal complexes with multiple metal-metal bonds. What is the maximum bond order that we could expect? The transition metals have five d-orbitals available, and in order to determine the maximum possible bond order we need to see how they overlap to form molecular orbitals (Fig. 11.1.1).

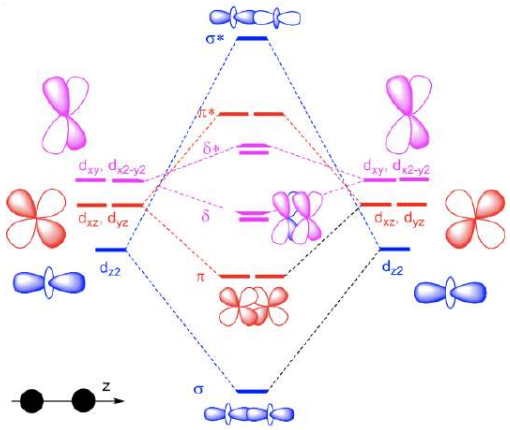


Figure 11.1.1 Molecular orbital overlap of metal d-orbitals forming M-M bonds

If we define the M-M bond axis as the z-axis, then two d_{z^2}-orbitals can overlap in σ-fashion to form a bonding and an anti-bonding σ-molecular orbital. A d_{xz}, and a d_{yz} can overlap with another d_{xz} and another d_{yz} in π-fashion to form two degenerated bonding π and two degenerated anti-bonding π*-orbitals. π-overlap is smaller than σ-overlap, therefore the split in energy between the bonding and the anti-bonding π-orbitals is smaller than the split between the bonding and the anti-bonding σ-orbitals. The d_{xy} orbital can overlap with another d_{xy} orbital in ***δ***-fashion, and so can the $d_{x^2-y^2}$ with another $d_{x^2-y^2}$. This gives two bonding ***δ***-orbitals and two anti-bonding ***δ***-orbitals. The ***δ***-overlap is even smaller than the π-overlap, therefore the energy split between the bonding and the anti-bonding ***δ***-orbitals is even smaller than those for the π and π*-orbitals. So what would be the maximum bond order that could be achieved? The maximum bond order would be achieved when all bonding MOs were full, and all anti-bonding MOs were empty. We have overall five bonding MOs that we could fill with ten electrons from two metal atoms with d^5-electron configuration. The maximum bond order BO would therefore be BO=5. However, in practice only bond orders up to 4 are well known. This is because the $d_{x^2-y^2}$ orbital is usually too involved in the bonding with the ligands thereby becoming unavailable for metal-metal interactions. The $d_{x^2-y^2}$ orbital makes the strongest interactions with the ligands because most ligands approach on or near the x and the y-axes.

Electron Configurations and Multiple M-M Bonds

We can easily predict now which electron configuration leads to which metal-metal bond order. The bond order increases from 1 to 4 with the electron configuration changing from d^1 to d^4. At d^4 all bonding MOs are full with eight electrons.

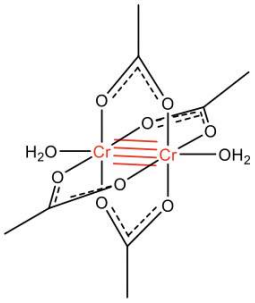


Figure 11.1.2 Tetraacetatodiaquadichromium complex

An example of a complex with a bond order of 4 is the tetraacetatodiaquadichromium complex shown (Fig. 11.1.2). Cr is in the oxidation state +2, which makes the chromium a d^4 species. We can quickly show this by counting the valence electrons. A neutral

Cr atom has 6 VE, and an electron configuration $3d^5 4s^1$. There are four acetate ligands having a 1- charge each which gives four negative charges overall. The complex is overall neutral which means that each Cr must have formally a 2+ charge, and the electron configuration is $3d^4$.

d^1	d^2	d^3	d^4	d^5	d^6	d^7	d^8
1	2	3	4	3	2	1	0

Figure 11.1.3 Relationship between metal-metal bond order and electron configuration

With even more electrons in the metal d-orbitals the bond order begins to decrease again as anti-bonding MOs need to be filled (Fig. 11.1.3). The combination of two metals with d^5 electron configuration leads to a triple bond, two d^6-metals give a double bond, and two d^7 metals give a single bond. A metal-metal bond should not exist for two d^8-metals because then the bond order is zero.

Evidence for M-M Multiple Bonds

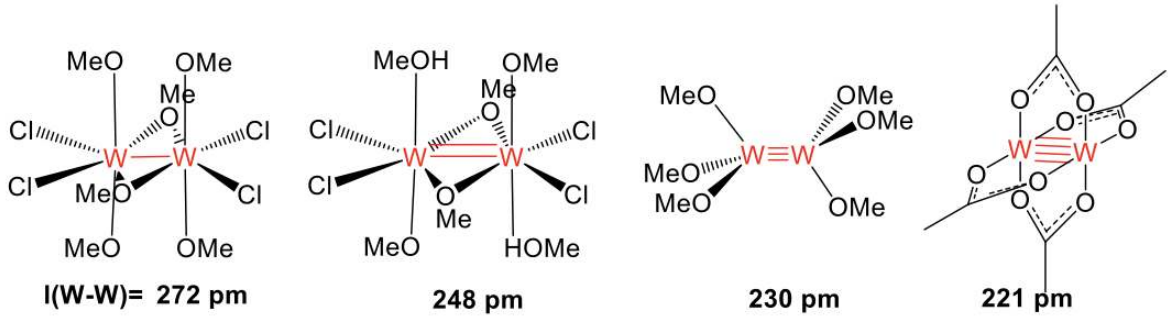


Figure 11.1.4 M-M bond length in four tungsten complexes

What experimental evidence can support the existence of a particular bond order (Fig. 11.1.4)? One argument is the bond length which can be obtained through the crystal structure determination of the complex. The shorter the bond, the higher the bond order. For instance, in the four tungsten complexes shown the bond lengths decrease from 272 pm, to 248 pm, to 230 pm to 221 pm corresponding to a single, double, triple, and quadruple bond, respectively.

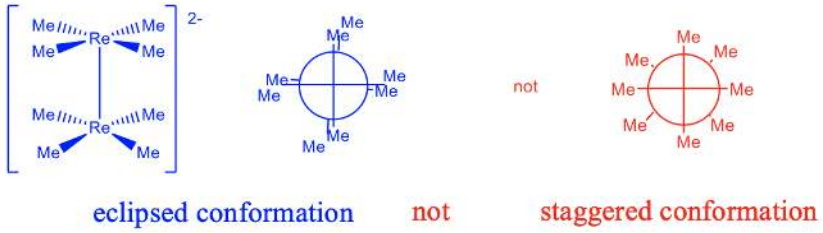


Figure 11.1.5 $ReMe_4$ confirmations

Another hint can be the conformation of a molecule (Fig. 11.1.5). For instance, the two square-planar units of the $Re_2Me_8^{2-}$ complex anion show eclipsed conformation. Steric repulsion arguments would favor the staggered conformation, so there must be a reason why the two $ReMe_4$ units are eclipsed. The rhenium is in the oxidation state +3, thus it is a d^4 species, and we would argue that there may be a Re-Re quadruple bond. This quadruple bond can only form when the d_{xy} orbitals are in eclipsed conformation, and this is only possible when the two $ReMe_4$ fragments are in eclipsed conformation. The very short bond length of 218 pm further supports the existence of the quadruple bond.

Dr. Kai Landskron (Lehigh University). If you like this textbook, please consider to make a donation to support the author's research at Lehigh University: Click Here to Donate.

Section 6.5: Metal-Metal Bonds is shared under a CC BY-NC-SA 4.0 license and was authored, remixed, and/or curated by LibreTexts.

- **11.1: Complexes with Multiple Metal-Metal Bonds** by Kai Landskron is licensed CC BY 4.0.

Section 6.5.1: Metal-Metal Multiple Bonds

Molecular orbital considerations in Dinuclear Metal Complexes with Multiple M-M Bonds

Let us begin a new chapter and think about dinuclear transition metal complexes with multiple metal-metal bonds. What is the maximum bond order that we could expect? The transition metals have five d-orbitals available, and in order to determine the maximum possible bond order we need to see how they overlap to form molecular orbitals (Fig. 11.1.1).

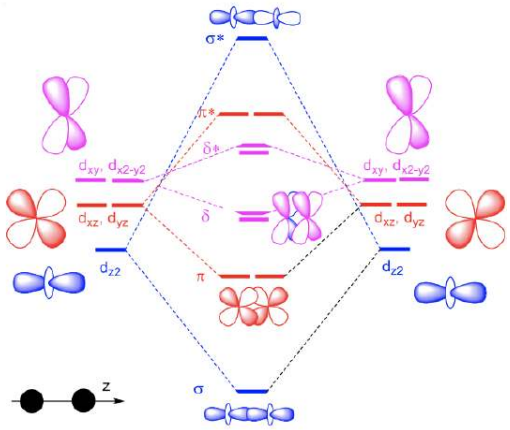


Figure 11.1.1 Molecular orbital overlap of metal d-orbitals forming M-M bonds

If we define the M-M bond axis as the z-axis, then two d_{z^2}-orbitals can overlap in σ-fashion to form a bonding and an anti-bonding σ-molecular orbital. A d_{xz}, and a d_{yz} can overlap with another d_{xz} and another d_{yz} in π-fashion to form two degenerated bonding π and two degenerated anti-bonding π*-orbitals. π-overlap is smaller than σ-overlap, therefore the split in energy between the bonding and the anti-bonding π-orbitals is smaller than the split between the bonding and the anti-bonding σ-orbitals. The d_{xy} orbital can overlap with another d_{xy} orbital in ***δ***-fashion, and so can the $d_{x^2-y^2}$ with another $d_{x^2-y^2}$. This gives two bonding ***δ***-orbitals and two anti-bonding ***δ***-orbitals. The ***δ***-overlap is even smaller than the π-overlap, therefore the energy split between the bonding and the anti-bonding ***δ***-orbitals is even smaller than those for the π and π*-orbitals. So what would be the maximum bond order that could be achieved? The maximum bond order would be achieved when all bonding MOs were full, and all anti-bonding MOs were empty. We have overall five bonding MOs that we could fill with ten electrons from two metal atoms with d^5-electron configuration. The maximum bond order BO would therefore be BO=5. However, in practice only bond orders up to 4 are well known. This is because the $d_{x^2-y^2}$ orbital is usually too involved in the bonding with the ligands thereby becoming unavailable for metal-metal interactions. The $d_{x^2-y^2}$ orbital makes the strongest interactions with the ligands because most ligands approach on or near the x and the y-axes.

Electron Configurations and Multiple M-M Bonds

We can easily predict now which electron configuration leads to which metal-metal bond order. The bond order increases from 1 to 4 with the electron configuration changing from d^1 to d^4. At d^4 all bonding MOs are full with eight electrons.

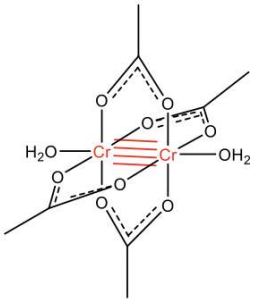


Figure 11.1.2 Tetraacetatodiaquadichromium complex

An example of a complex with a bond order of 4 is the tetraacetatodiaquadichromium complex shown (Fig. 11.1.2). Cr is in the oxidation state +2, which makes the chromium a d^4 species. We can quickly show this by counting the valence electrons. A neutral

Cr atom has 6 VE, and an electron configuration $3d^5 4s^1$. There are four acetate ligands having a 1- charge each which gives four negative charges overall. The complex is overall neutral which means that each Cr must have formally a 2+ charge, and the electron configuration is $3d^4$.

d^1	d^2	d^3	d^4	d^5	d^6	d^7	d^8
1	2	3	4	3	2	1	0

Figure 11.1.3 Relationship between metal-metal bond order and electron configuration

With even more electrons in the metal d-orbitals the bond order begins to decrease again as anti-bonding MOs need to be filled (Fig. 11.1.3). The combination of two metals with d^5 electron configuration leads to a triple bond, two d^6-metals give a double bond, and two d^7 metals give a single bond. A metal-metal bond should not exist for two d^8-metals because then the bond order is zero.

Evidence for M-M Multiple Bonds

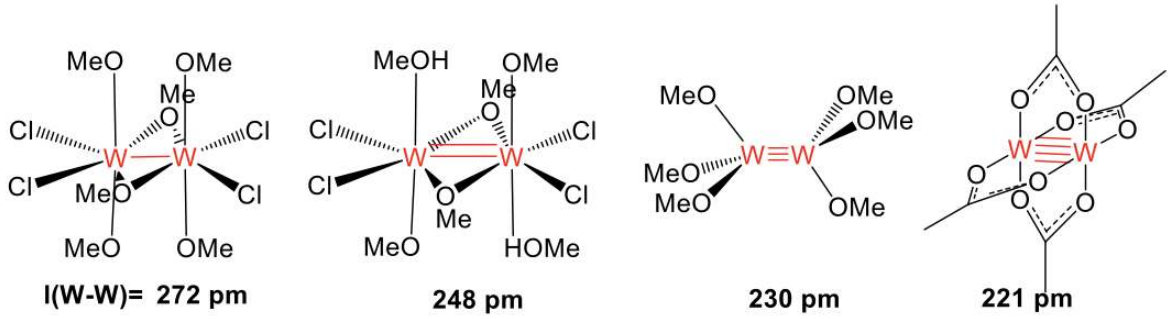


Figure 11.1.4 M-M bond length in four tungsten complexes

What experimental evidence can support the existence of a particular bond order (Fig. 11.1.4)? One argument is the bond length which can be obtained through the crystal structure determination of the complex. The shorter the bond, the higher the bond order. For instance, in the four tungsten complexes shown the bond lengths decrease from 272 pm, to 248 pm, to 230 pm to 221 pm corresponding to a single, double, triple, and quadruple bond, respectively.

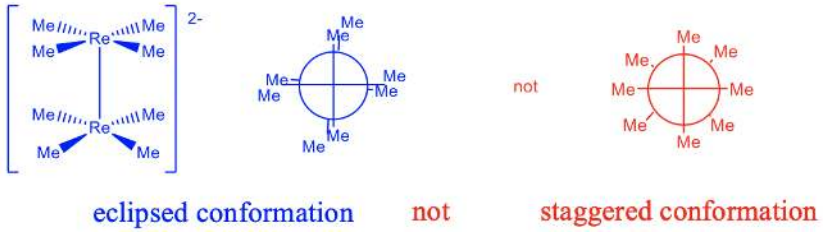


Figure 11.1.5 $ReMe_4$ confirmations

Another hint can be the conformation of a molecule (Fig. 11.1.5). For instance, the two square-planar units of the $Re_2Me_8^{2-}$ complex anion show eclipsed conformation. Steric repulsion arguments would favor the staggered conformation, so there must be a reason why the two $ReMe_4$ units are eclipsed. The rhenium is in the oxidation state +3, thus it is a d^4 species, and we would argue that there may be a Re-Re quadruple bond. This quadruple bond can only form when the d_{xy} orbitals are in eclipsed conformation, and this is only possible when the two $ReMe_4$ fragments are in eclipsed conformation. The very short bond length of 218 pm further supports the existence of the quadruple bond.

Dr. Kai Landskron (Lehigh University). If you like this textbook, please consider to make a donation to support the author's research at Lehigh University: Click Here to Donate.

Section 6.5.1: Metal-Metal Multiple Bonds is shared under a CC BY-NC-SA 4.0 license and was authored, remixed, and/or curated by LibreTexts.

- **11.1: Complexes with Multiple Metal-Metal Bonds** by Kai Landskron is licensed CC BY 4.0.

Section 6.6: Jahn-Teller Distortions

The Jahn-Teller effect is a geometric distortion of a non-linear molecular system that reduces its symmetry and energy. This distortion is typically observed among octahedral complexes where the two axial bonds can be shorter or longer than those of the equatorial bonds. This effect can also be observed in tetrahedral compounds. This effect is dependent on the electronic state of the system.

Introduction

In 1937, Hermann Jahn and Edward Teller postulated a theorem stating that "stability and degeneracy are not possible simultaneously unless the molecule is a linear one," in regards to its electronic state.[1] This leads to a break in degeneracy which stabilizes the molecule and by consequence, reduces its symmetry. Since 1937, the theorem has been revised which Housecroft and Sharpe have eloquently phrased as "any non-linear molecular system in a degenerate electronic state will be unstable and will undergo distortion to form a system of lower symmetry and lower energy, thereby removing the degeneracy."[2] This is most commonly observed with transition metal octahedral complexes, however, it can be observed in tetrahedral compounds as well.

For a given octahedral complex, the five d atomic orbitals are split into two degenerate sets when constructing a molecular orbital diagram. These are represented by the sets' symmetry labels: t_{2g} (d_{xz}, d_{yz}, d_{xy}) and e_g (d_{z^2} and $d_{x^2-y^2}$). When a molecule possesses a degenerate electronic ground state, it will distort to remove the degeneracy and form a lower energy (and by consequence, lower symmetry) system. The octahedral complex will either elongate or compress the z ligand bonds as shown in Figure ***Section*6.6.1** below:

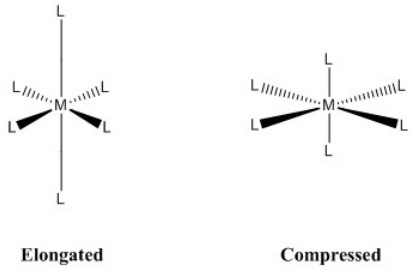


Figure ***Section*6.6.1**: Jahn-Teller distortions for an octahedral complex.

When an octahedral complex exhibits elongation, the axial bonds are longer than the equatorial bonds. For a compression, it is the reverse; the equatorial bonds are longer than the axial bonds. Elongation and compression effects are dictated by the amount of overlap between the metal and ligand orbitals. Thus, this distortion varies greatly depending on the type of metal and ligands. In general, the stronger the metal-ligand orbital interactions are, the greater the chance for a Jahn-Teller effect to be observed.

Elongation

Elongation Jahn-Teller distortions occur when the degeneracy is broken by the stabilization (lowering in energy) of the d orbitals with a z component, while the orbitals without a z component are destabilized (higher in energy) as shown in Figure ***Section*6.6.2** below:

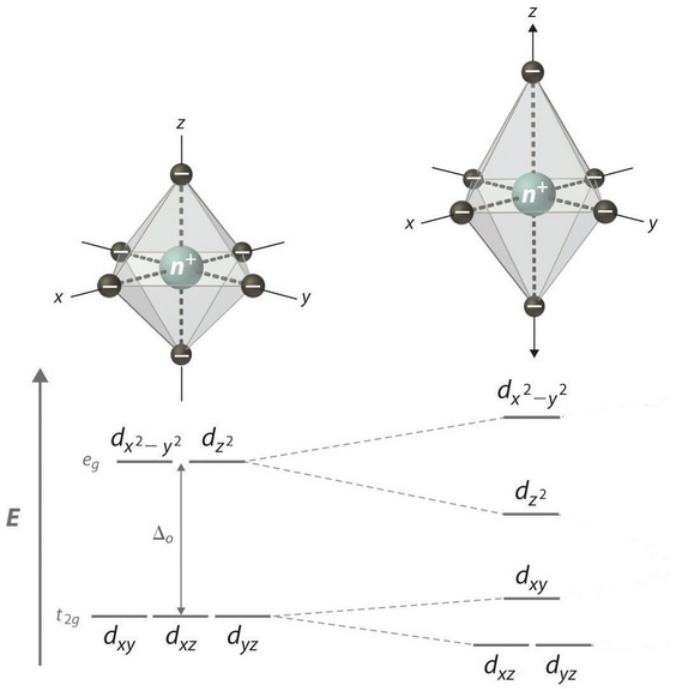


Figure ***Section*6.6.2**: Illustration of tetragonal distortion (elongation) for an octahedral complex.

This is due to the d_{xy} and $d_{x^2-y^2}$ orbitals having greater overlap with the ligand orbitals, resulting in the orbitals being higher in energy. Since the $d_{x^2-y^2}$ orbital is antibonding, it is expected to increase in energy due to elongation. The d_{xy} orbital is still nonbonding, but is destabilized due to the interactions. Jahn-Teller elongations are well-documented for copper(II) octahedral compounds. A classic example is that of copper(II) fluoride as shown in Figure ***Section*6.6.3**.

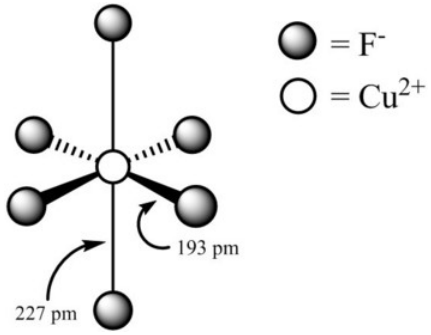


Figure ***Section*6.6.3**: Structure of octahedral copper(II) fluoride.[3]

Notice that the two axial bonds are both elongated and the four shorter equatorial bonds are the same length as each other. According the theorem, the orbital degeneracy is eliminated by distortion, making the molecule more stable based on the model presented in Figure ***Section*6.6.2**.

Compression

Compression Jahn-Teller distortions occur when the degeneracy is broken by the stabilization (lowering in energy) of the d orbitals *without* a *z* component, while the orbitals with a *z* component are destabilized (higher in energy) as shown in Figure ***Section*6.6.4** below:

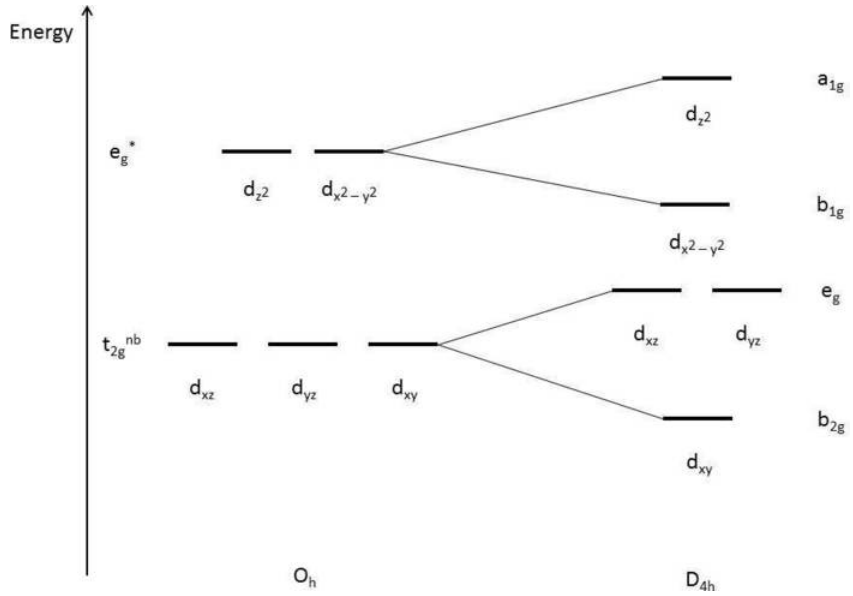


Figure *Section*6.6.4: Illustration of tetragonal distortion (compression) for an octahedral complex.

This is due to the *z*-component d orbitals having greater overlap with the ligand orbitals, resulting in the orbitals being higher in energy. Since the d_{z^2} orbital is antibonding, it is expected to increase in energy due to compression. The d_{xz} and d_{yz} orbitals are still nonbonding, but are destabilized due to the interactions.

Electronic Configurations

For Jahn-Teller effects to occur in transition metals there must be degeneracy in either the t_{2g} or e_g orbitals. The electronic states of octahedral complexes depend on the number of d-electrons and the splitting energy, **Δ**. When **Δ** is large and is greater than the energy required to pair electrons, electrons pair in t_{2g} before occupying e_g. On the other hand, when **Δ** small and is less than the pairing energy, electrons will occupy e_g before pairing in t_{2g}. The **Δ** of an octahedral complex is dictated by the chemical environment (ligand identity), and the identity and charge of the metal ion. If there electron configurations for any d-electron count is different depending on **Δ**, the configuration with more paired electrons is called low spin while the one with more unpaired electrons is called high spin.

The electron configurations diagrams for d1 through d10 with large and small **Δ** are illustrated in the figures below. Notice that the electron configurations for d^1, d^2, d^3, d^8, d^9, and d^{10} are the same no matter what the magnitude of **Δ**. Low spin and high spin configurations exist only for the electron counts d^4, d^5, d^6, and d^7.

Large Δ

Figure *Section*6.6.5 (below) shows the various electronic configurations for octahedral complexes with large **Δ**, including the low-spin configurations of d^4, d^5, d^6, and d^7:

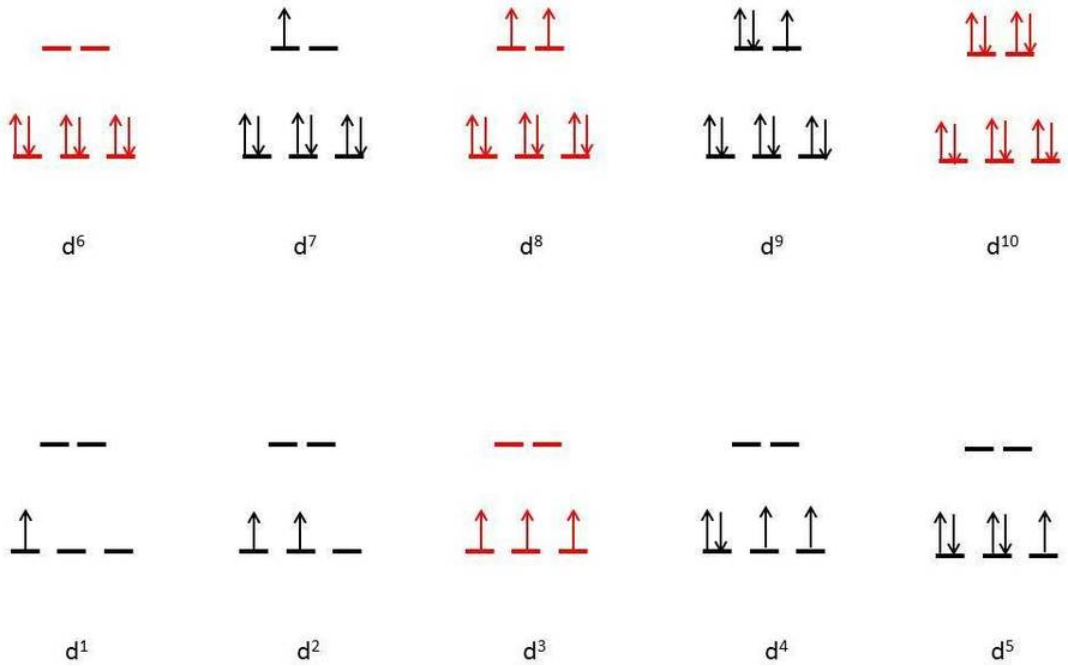


Figure *Section*6.6.5: Electron configuration diagram of octahedral complexes (red indicates no degeneracies possible, thus no Jahn-Teller effects).

The figure illustrates the electron configurations in the case of large **Δ**. The electron configurations highlighted in red (d^3, low spin d^6, d^8, and d^{10}) **do not** exhibit Jahn-Teller distortions. On the other hand d^1, d^2, low spin d^4, low spin d^5, low spin d^7, and d^9, would be expected to exhibit Jhan-Teller distortion. These electronic configurations correspond to a variety of transition metals. Some common examples include Cr^{3+}, Co^{3+}, and Ni^{2+}.

Small Δ

Figure *Section*6.6.6 (below) shows the various electronic configurations for octahedral complexes with small **Δ**, including the high-spin configurations of d^4, d^5, d^6, and d^7::

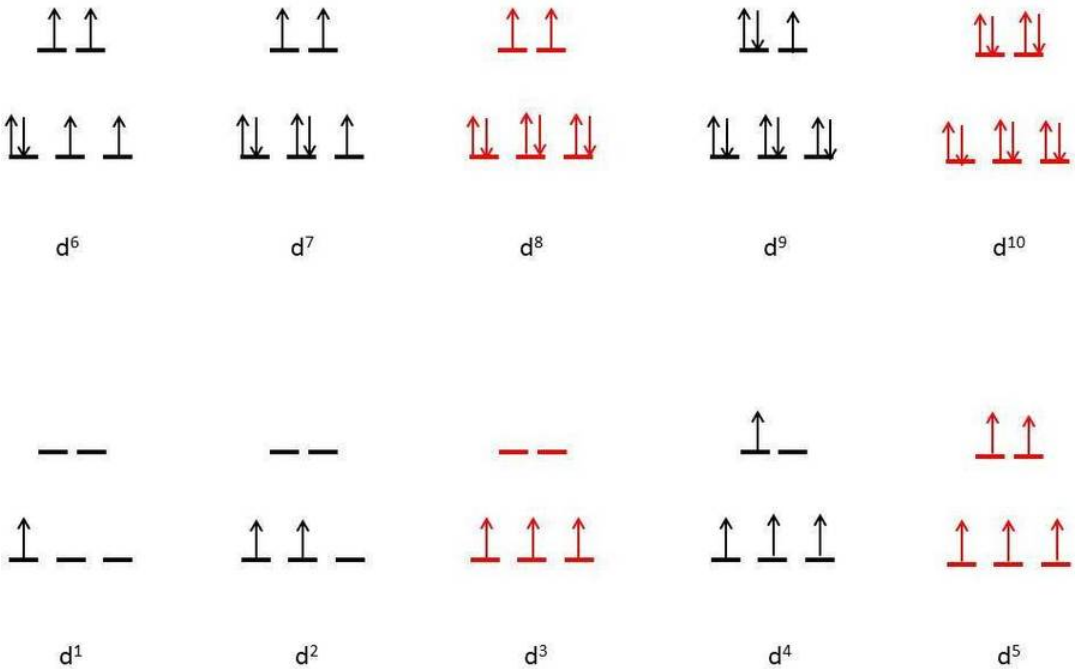


Figure *Section*6.6.6: High spin octahedral coordination diagram (red indicates no degeneracies possible, thus no Jahn-Teller effects).

The figure illustrates the electron configurations in the case of small Δ. The electron configurations highlighted in red (d^3, high spin d^5, d^8, and d^{10}) **do not** exhibit Jahn-Teller distortions. In general, degenerate electronic states occupying the e_g orbital set tend to show stronger Jahn-Teller effects. This is primarily caused by the occupation of these high energy orbitals. Since the system is more stable with a lower energy configuration, the degeneracy of the e_g set is broken, the symmetry is reduced, and occupations at lower energy orbitals occur.

Spectroscopic Observation

Jahn-Teller distortions can be observed using a variety of spectroscopic techniques. In UV-VIS absorption spectroscopy, distortion causes splitting of bands in the spectrum due to a reduction in symmetry (O_h to D_{4h}). Consider a hypothetical molecule with octahedral symmetry showing a single absorption band. If the molecule were to undergo Jahn-Teller distortion, the number of bands would increase as shown in Figure ***Section*6.6.7** below:

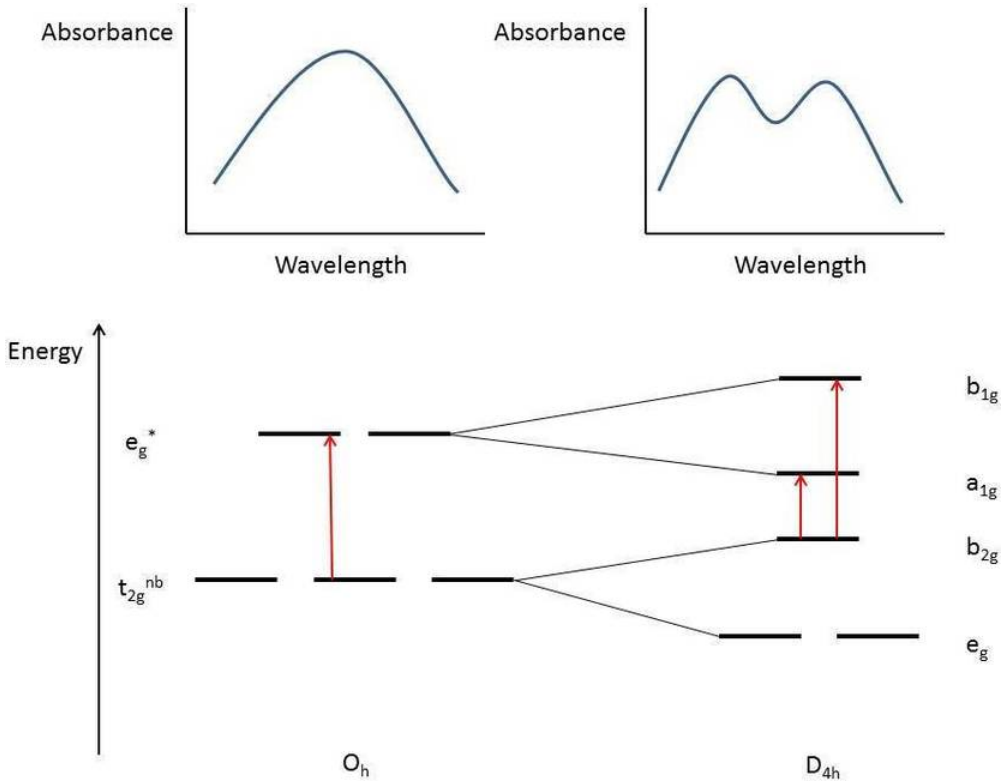


Figure ***Section*6.6.7**: Hypothetical absorption spectra of an octahedral molecule (left) and the same molecule with Jahn-Teller elongation (right). The red arrows indicate electronic transitions.

A similar phenomenon can be seen with IR and Raman vibrational spectroscopy. The number of vibrational modes for a molecule can be calculated using the 3n - 6 rule (or 3n - 5 for linear geometry) rule. If a molecule exhibits an O_h symmetry point group, it will have fewer bands than that of a Jahn-Teller distorted molecule with D_{4h} symmetry. Thus, one could observe Jahn-Teller effects through either IR or Raman techniques. This effect can also be observed in EPR experiments as long as there is at least one unpaired electron.

Table *Section*6.6.1: Examples of Jahn-Teller distorted complexes

$CuBr_2$	4 Br at 240 pm 2 Br at 318 pm
$CuCl_2$	4 Cl at 230 pm 2 Cl at 295 pm
$CuCl_2.2H_2O$	2 O at 193 pm 2 Cl at 228 pm 2 Cl at 295 pm
$CsCuCl_3$	4 Cl at 230 pm 2 Cl at 265 pm
CuF_2	4 F at 193 pm 2 F at 227 pm
$CuSO_4.4NH_3.H_2O$	4 N at 205 pm 1 O at 259 pm 1 O at 337 pm
K_2CuF_4	4 F at 191 pm 2 F at 237 pm
$KCuAlF_6$	2 F at 188 pm 4 F at 220 pm
CrF_2	4 F at 200 pm 2 F at 243 pm
$KCrF_3$	4 F at 214 pm 2 F at 200 pm
MnF_3	2 F at 209 pm 2 F at 191 pm 2 F at 179 pm

The Jahn-Teller Theorem predicts that distortions should occur for *any degenerate state*, including degeneracy of the t_{2g} level, however distortions in bond lengths are much more distinctive when the degenerate electrons are in the e_g level.

References

1. Jahn, H. A.; Teller, E. *Proc. R. Soc. London A*, **1937**, *161*, 220-235. DOI: 10.1098/rspa.1937.0142
2. Housecroft, C.; Sharpe, A. G. *Inorganic Chemistry*. Prentice Hall, 3rd Ed., 2008, p. 644. ISBN: 978-0-13-175553-6
3. Billy, C.; Haendler, H. A. *J. Am. Chem. Soc.*, **1957**, *79*, 1049–1051. DOI: 10.1021/ja01562a011

References

- Janes, R.; Moore, E. A. *Metal-ligand bonding*. The Open University, 2004, p. 23. ISBN 0-85404-979-7
- P.T.Miller, P.G.Lenhert and M.D.Joesten, *Inorg. Chem.*, 11, 2221, 1972.
- J.S.Wood, C.P.Keijzers and R.O.Day, *Acta Crystallogr., Sect.C (Cr. Str. Comm.)*, 40, 404, 1984.
- M.D.Joesten, M.S.Hussain and P.G.Lenhert, *Inorg. Chem.*, 9, 151, 1970.

Practice Questions

1. Why do d^3 complexes not show Jahn-Teller distortions?
2. Does the spin system (high spin v. low spin) of a molecule play a role in Jahn-Teller effects?
3. What spectroscopic method would one utilize in order to observe Jahn-Teller distortions in a diamagnetic molecule?
4. What spectroscopic method(s) would one utilize in order to observe Jahn-Teller distortions in a paramagnetic molecule?
5. Why are Jahn-Teller effects most prevalent in inorganic (transition metal) compounds?

Answers

1. Complexes with d^3 electron configurations do not show Jahn-Teller distortions because there is no ground state degeneracy.
2. Yes. Examining the d^5 electron configuration, one finds that the high spin scenario contains all singly occupied d orbitals (no degeneracy). However, the low spin d^5 electron configuration shows degeneracy, which then leads to possible Jahn-Teller effects.
3. UV-VIS absorption spectroscopy is one of the most common techniques for observing these effects. In general, it is independent of magnetism (diamagnetic v. paramagnetic). Thus, one would see the effect in the spectrum of UV-VIS absorption analysis. Note that EPR requires at least one unpaired electron, and therefore not EPR active.
4. Inorganic, specifically transition metal, complexes are most prevalent in showing Jahn-Teller distortions due to the availability of d orbitals. The most common geometry that the Jahn-Teller effect is observed is in octahedral complexes (see **Figures 2, 4, 5** and **6** above) due to the splitting of d orbitals into two degenerate sets. Due to stabilization, the degeneracies are removed, making a lower symmetry and lower energy molecule.

5. In addition to UV-VIS absorption, one can also employ EPR spectroscopy if a molecule possesses and unpaired electron.

Section 6.6: Jahn-Teller Distortions is shared under a CC BY-NC-SA 4.0 license and was authored, remixed, and/or curated by LibreTexts.

- **9.3: Jahn-Teller Distortions** by Kamran Ghiassi, Robert Lancashire is licensed CC BY-NC-SA 4.0.

CHAPTER OVERVIEW

Chapter 7: Coordination Chemistry- Reactions and Mechanisms

Learning Objectives

- Determine whether an metal ion will be labile or inert.
- Use kinetic data to determine if a ligand substitution occurs by an associative or dissociative mechanism
- Predict the product of a square planar ligand substitution reaction based on the trans effect and trans influence
- Explain the difference between and inner sphere and outer sphere electron transfer reaction

Section 7.1: Thermodynamic Stability of Metal Complexes

Section 7.2: Trends in Kinetic Lability

Section 7.3: Ligand Substitution Mechanisms

Section 7.4: The Trans Effect Observation

Section 7.5: The Trans Effect Explanation

Section 7.6: Electron Transfer Reactions

Chapter 7: Coordination Chemistry- Reactions and Mechanisms is shared under a CC BY-NC-SA 4.0 license and was authored, remixed, and/or curated by LibreTexts.

Section 7.1: Thermodynamic Stability of Metal Complexes

Chelate Complexes

As seen in Chapter 8, ligands like chloride, water, and ammonia are monodentate More complex ligands can, however, be bidentate, tridentate, or, in general, polydentate Ethylenediamine ($H_2NCH_2CH_2NH_2$, often abbreviated as en) and diethylenetriamine ($H_2NCH_2CH_2NHCH_2CH_2NH_2$, often abbreviated as dien) are examples of a bidentate and a tridentate ligand, respectively, because each nitrogen atom has a lone pair that can be shared with a metal ion. When a bidentate ligand such as ethylenediamine binds to a metal such as Ni^{2+}, a five-membered ring is formed. A metal-containing ring like that shown is called a chelate ring. Correspondingly, a polydentate ligand is a chelating agent, and complexes that contain polydentate ligands are called chelate complexes.



A chelate complex

Experimentally, it is observed that metal complexes of polydentate ligands are significantly more stable than the corresponding complexes of chemically similar monodentate ligands; this increase in stability is called the chelate effect. For example, the complex of Ni^{2+} with three ethylenediamine ligands, $[Ni(en)_3]^{2+}$, should be chemically similar to the Ni^{2+} complex with six ammonia ligands, $[Ni(NH_3)_6]^{2+}$. In fact, the equilibrium constant for the formation of $[Ni(en)_3]^{2+}$ is almost 10 orders of magnitude larger than the equilibrium constant for the formation of $[Ni(NH_3)_6]^{2+}$ (Table E4):

$$[Ni(H_2O)_6]^{2+} + 6NH_3 \rightleftharpoons [Ni(NH_3)_6]^{2+} + 6H_2O(l) \quad K_f = 4 \times 10^8 \qquad \text{(Section 7.1.1)}$$

$$[Ni(H_2O)_6]^{2+} + 3en \rightleftharpoons [Ni(en)_3]^{2+} + 6H_2O(l) \quad K_f = 2 \times 10^{18} \qquad \text{(Section 7.1.2)}$$

The formation constants are formulated as ligand exchange reactions with aqua ligands being displaced by new ligands (NH_3 or en) in the examples above.

> *Chelate complexes are more stable than the analogous complexes with monodentate ligands.*

The stability of a chelate complex depends on the size of the chelate rings. For ligands with a flexible organic backbone like ethylenediamine, complexes that contain five-membered chelate rings, which have almost no strain, are significantly more stable than complexes with six-membered chelate rings, which are in turn much more stable than complexes with four- or seven-membered rings. For example, the complex of nickel (II) with three ethylenediamine ligands is about 363,000 times more stable than the corresponding nickel (II) complex with trimethylenediamine ($H_2NCH_2CH_2CH_2NH_2$, abbreviated as tn):

$$[Ni(H_2O)_6]^{2+} + 3en \rightleftharpoons [Ni(en)_3]^{2+} + 6H_2O(l) \quad K_f = 6.76 \times 10^{17} \qquad \text{(Section 7.1.3)}$$

$$[Ni(H_2O)_6]^{2+} + 3tn \rightleftharpoons [Ni(tn)_3]^{2+} + 6H_2O(l) \quad K_f = 1.86 \times 10^{12} \qquad \text{(Section 7.1.4)}$$

*The above measurements were done in a solution of ionic strength 0.15 at 25° C.

Example *Section*7.1.1

Arrange $[Cr(en)_3]^{3+}$, $[CrCl_6]^{3-}$, $[CrF_6]^{3-}$, and $[Cr(NH_3)_6]^{3+}$ in order of increasing stability.

Given: four Cr(III) complexes

Asked for: relative stabilities

Strategy:

A Determine the relative basicity of the ligands to identify the most stable complexes.

B Decide whether any complexes are further stabilized by a chelate effect and arrange the complexes in order of increasing stability.

Solution

A The metal ion is the same in each case: Cr^{3+}. Consequently, we must focus on the properties of the ligands to determine the stabilities of the complexes. Because the stability of a metal complex increases as the basicity of the ligands increases, we need to determine the relative basicity of the four ligands. Our earlier discussion of acid–base properties suggests that ammonia and ethylenediamine, with nitrogen donor atoms, are the most basic ligands. The fluoride ion is a stronger base (it has a higher charge-to-radius ratio) than chloride, so the order of stability expected due to ligand basicity is

$$[CrCl_6]^{3-} < [CrF_6]^{3-} < [Cr(NH_3)_6]^{3+} \approx [Cr(en)_3]^{3+}.$$

B Because of the chelate effect, we expect ethylenediamine to form a stronger complex with Cr^{3+} than ammonia. Consequently, the likely order of increasing stability is

$$[CrCl_6]^{3-} < [CrF_6]^{3-} < [Cr(NH_3)_6]^{3+} < [Cr(en)_3]^{3+}.$$

Exercise *Section*7.1.1

Arrange $[Co(NH_3)_6]^{3+}$, $[CoF_6]^{3-}$, and $[Co(en)_3]^{3+}$ in order of decreasing stability.

Answer: $[Co(en)_3]^{3+} > [Co(NH_3)_6]^{3+} > [CoF_6]^{3-}$

The Chelate Effect

The chelate effect can be seen by comparing the reaction of a chelating ligand and a metal ion with the corresponding reaction involving comparable monodentate ligands. For example, comparison of the binding of 2,2'-bipyridine with pyridine or 1,2-diaminoethane (ethylenediamine=en) with ammonia. It has been known for many years that a comparison of this type always shows that the complex resulting from coordination with the chelating ligand is **much more thermodynamically stable**. This can be seen by looking at the values for adding two monodentates compared with adding one bidentate, or adding four monodentates compared to two bidentates, or adding six monodentates compared to three bidentates.

> *The Chelate Effect is that complexes resulting from coordination with the chelating ligand is much more thermodynamically stable than complexes with non-chelating ligands.*

A number of points should be highlighted from the formation constants in Table E4. In Table ***Section*7.1.1**, it can be seen that the ΔH° values for the formation steps are almost identical, that is, heat is evolved to about the same extent whether forming a complex involving monodentate ligands or bidentate ligands. What is seen to vary significantly is the ΔS° term which changes from negative (unfavorable) to positive (favorable). Note as well that there is a dramatic increase in the size of the ΔS° term for adding two compared to adding four monodentate ligands. (-5 to -35 $JK^{-1}mol^{-1}$). What does this imply, if we consider ΔS° to give a measure of disorder?

In the case of complex formation of Ni^{2+} with ammonia or 1,2-diaminoethane, by rewriting the equilibria, the following equations are produced.

$$\begin{array}{lcl} [Ni(H_2O)_6]^{2+} + 6\,NH_3 \overset{\beta_6}{\Leftrightarrow} [Ni(NH_3)_6]^{2+} & & \textbf{1f} \\ [Ni(NH_3)_6]^{2+} \Leftrightarrow [Ni(H_2O)_6]^{2+} + 6\,NH_3 & & \textbf{1d} \\ [Ni(H_2O)_6]^{2+} + 3\,en \overset{\beta_3}{\Leftrightarrow} [Ni(en)_3]^{2+} & & \textbf{2f} \\ \hline [Ni(NH_3)_6]^{2+} + 3\,en \Leftrightarrow [Ni(en)_3]^{2+} + 6NH_3 & & \textbf{3} \end{array}$$

Using the equilibrium constant for the reaction (3 above) where the *three* bidentate ligands replace the *six* monodentateligands, we find that at a temperature of 25° C:

$$\Delta G° = -2.303\,RT\,\log_{10} K \qquad \text{(Section 7.1.5)}$$

$$= -2.303\,RT\,(18.28 - 8.61) \qquad \text{(Section 7.1.6)}$$

$$= -54\ \text{kJ mol}^{-1} \qquad \text{(Section 7.1.7)}$$

Based on measurements made over a range of temperatures, it is possible to break down the $\Delta G°$ term into the enthalpy and entropy components.

$$\Delta G° = \Delta H° - T\Delta S° \quad \text{(Section 7.1.8)}$$

The result is that: $\Delta H° = -29 kJ mol^{-1}$

$$- T\Delta S° = -25 \text{ kJ mol}^{-1}$$
and at 25C (298K)
$$\Delta S° = +88 \text{ J K}^{-1} \text{ mol}^{-1}$$

Caution

For many years, these numbers have been **incorrectly recorded** in textbooks. For example, the third edition of "Basic Inorganic Chemistry" by F.A. Cotton, G. Wilkinson and P.L. Gaus, John Wiley & Sons, Inc, 1995, on page 186 gives the values as:

$$\Delta G° = -67 \text{ kJ mol}^{-1}$$
$$\Delta H° = -12 \text{ kJ mol}^{-1}$$
$$-T\Delta S° = -55 \text{ kJ mol}^{-1}$$

The conclusion they drew from these incorrect numbers was that the chelate effect was essentially an entropy effect, since the $T\Delta S°$ contribution was nearly 5 times bigger than $\Delta H°$.

In fact, the breakdown of the $\Delta G°$ into $\Delta H°$ and $T\Delta S°$ shows that the two terms are nearly equal (-29 and -25 kJ mol^{-1}, respectively) with the $\Delta H°$ term a little bigger! The entropy term found is still much larger than for reactions involving a non-chelating ligand substitution at a metal ion. How can we explain this enhanced contribution from entropy? One explanation is to count the number of species on the left and right hand side of the equation above.

It will be seen that on the left-hand-side there are 4 species, whereas on the right-hand-side there are 7 species, that is a net gain of 3 species occurs as the reaction proceeds. This can account for the increase in entropy since it represents an increase in the disorder of the system. An alternative view comes from trying to understand how the reactions might proceed. To form a complex with 6 monodentates requires 6 separate favorable collisions between the metal ion and the ligand molecules. To form the tris-bidentate metal complex requires an initial collision for the first ligand to attach by one arm but remember that the other arm is always going to be nearby and only requires a rotation of the other end to enable the ligand to form the chelate ring.

If you consider dissociation steps, then when a monodentate group is displaced, it is lost into the bulk of the solution. On the other hand, if one end of a bidentate group is displaced the other arm is still attached and it is only a matter of the arm rotating around and it can be reattached again. **Both** conditions favor the formation of the complex with bidentate groups rather than monodentate groups.

This page titled Section 7.1: Thermodynamic Stability of Metal Complexes is shared under a CC BY-NC-SA 4.0 license and was authored, remixed, and/or curated by Robert J. Lancashire.

- **10.1: Thermodynamic Stability of Metal Complexes** by Robert J. Lancashire is licensed CC BY-NC-SA 4.0.

Section 7.2: Trends in Kinetic Lability

Introduction

Kinetics is a branch of chemistry that is concerned with the rates of chemical reactions. In this section, we will discuss the rates of metal-ligand (M-L) substitution reactions.

Let's start with some examples. In the table below are three examples of ligand substitution reactions of hexaaquo metal complexes to form hexaammine complexes. These reactions are nearly identical with the exception of the metal ion. The products are thermodynamically favored in all cases.

Reaction	Rate constant (k)	Labile or Inert
$[Ni(OH_2)]^{2+} + 6NH_3 \rightleftharpoons [Ni(NH_3)_6]^{2+}$	$k = 10^4 s^{-1}$	Labile (happens in < 1 min)
$[Cr(OH_2)]^{3+} + 6NH_3 \rightleftharpoons [Cr(NH_3)_6]^{3+}$	$k = 10^{-3} s^{-1}$	Inert (slow, takes hours)
$[Cu(OH_2)]^{2+} + 6NH_3 \rightleftharpoons [Cu(NH_3)_6]^{2+}$	$k = 10^8 s^{-1}$	Very Labile (happens in seconds)

Definitions

- **Labile** - Metal complexes that undergo "kinetically fast" substitution reactions are **labile**. These reactions usually happen in less than one minute.
- **Inert** - Metal complexes that undergo "kinetically slow" substitution reactions are **inert** or **non-labile**. These reactions usually take hours.
- **Intermediate** - Metal complexes that undergo "kinetically intermediate" substitution reactions are **intermediate**.

A common pitfall is to confuse the meaning of kinetic terms, like *labile* and *inert*, with thermodynamic terms, like *stable* and *unstable*. It is important to distinguish between kinetics and thermodynamics. For example, the complex $[Fe(H_2O)Cl]^{2+}$ has a large formation constant and is thermodynamically stable; yet it is also labile. On the other hand, the complex $[Co(NH_3)_6]^{3+}$ is unstable in acidic aqueous solution and decomposes spontaneously to $[Co(H_2O)_6]^{3+}$; yet it decomposes slowly because it is inert. It is good practice to distinguish between meanings by using terms such as "kinetically labile" or "kinetically inert" and "thermodynamically stable" and "thermodynamically unstable".

Reaction Coordinate Diagrams

One way to visualize chemical reactions is through reaction coordinate diagrams (Figure ***Section*7.2.1**). These diagrams illustrate the relative free energy of the reactants and products, when the free energy of the products is lower than the reactants ΔG_{rxn} is negative and the reaction is spontaneous. This is what determines thermodynamic stability. These diagrams also illustrate the changes in free energy as the reaction progresses from reactants to products. In the case of a single step, concerted reaction the reactants go through a higher energy transition state before (potentially) forming products. The free energy difference between the reactants and the transition state is the free energy of activation ($\Delta G^{\ddagger}$), which determines the rate of the reaction. A larger $\Delta G^{\ddagger}$ yields a slower reaction rate because fewer reactants have sufficient energy to form products. In cases where the reaction occurs in 2 steps an intermediate is formed. The step with the largest $\Delta G^{\ddagger}$ will be the slowest, rate determining step. The magnitude of $\Delta G^{\ddagger}$ is what determines kinetic lability.

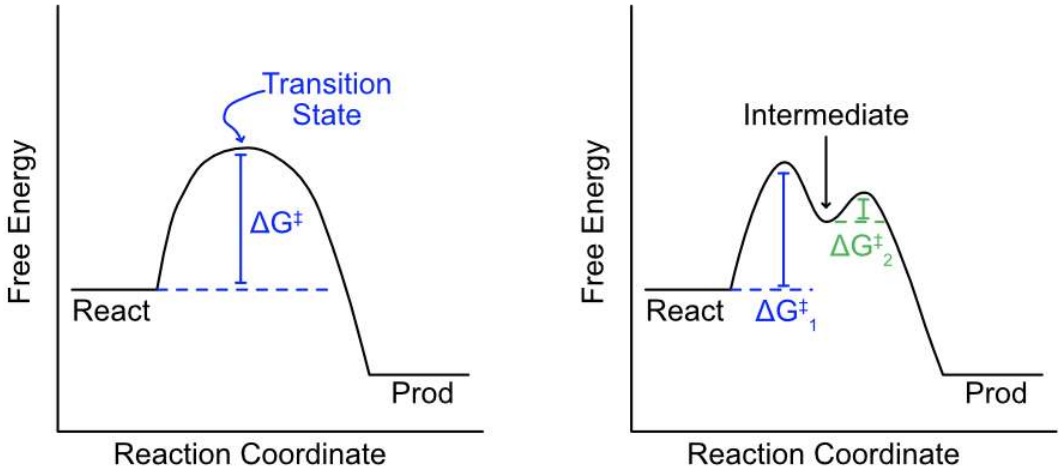


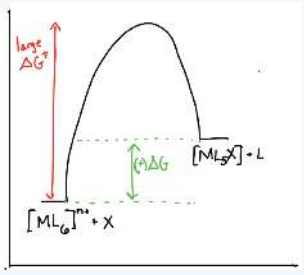
Figure *Section*7.2.1: Example reaction coordinate diagrams for a single step reaction (left) and a reaction with an intermediate (right). $\Delta G^{\ddagger}$ is the free energy of activation. (CC BY-NC-SA; Catherine McCusker)

Exercise *Section*7.2.1

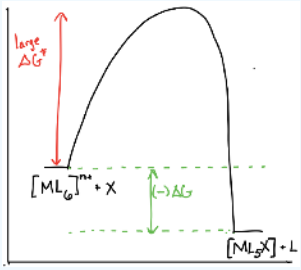
Draw the reaction coordinate diagrams for a reaction of the form $[ML_6]^{n+} + X \rightleftharpoons [ML_5X]^{n+} + L$ in the following scenarios:

a. $[ML_6]^{n+}$ is thermodynamically stable and kinetically inert.
b. $[ML_6]^{n+}$ is thermodynamically unstable and kinetically inert.
c. $[ML_6]^{n+}$ is thermodynamically stable and kinetically labile.
d. $[ML_6]^{n+}$ is thermodynamically unstable and kinetically labile.

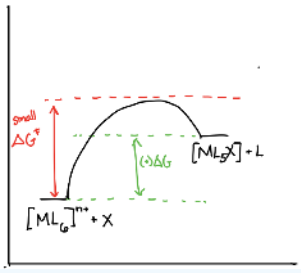
Answer a)



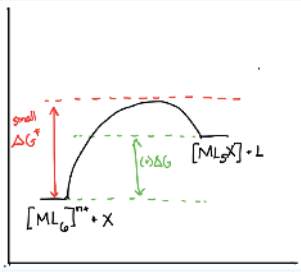
Answer b)



Answer c)



Answer d)



Self Exchange Reactions

$$[ML_5L]^{n+} + L \rightleftharpoons [ML_5L]^{n+} + L \qquad \text{(Section 7.2.1)}$$

The rate of a chemical reaction depends on both thermodynamic and kinetic factors. One way to isolate the kinetic factors is to study self exchange reactions. In a self exchange reaction the incoming and outgoing ligand are the same and the ΔG_{rxn} of the reaction is 0. In practice this is often done by dissolving hexaaqua metal complexes in isotopically labeled water and monitoring the ligand exchange reaction by NMR. These experiments have found reaction rates for different metals that span more than 12 orders of magnitude as shown in Figure *Section*7.2.2.

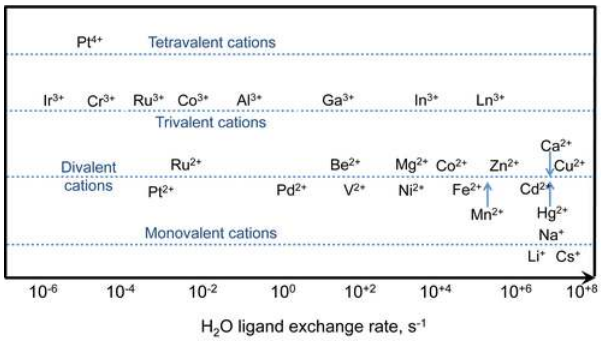


Figure *Section*7.2.2: Water exchange rates measured by NMR for a series of metal ions. (CC BY-SA; Tem5psu via Wikimedia)

Factors that Affect Rates of Substitution Reactions

Some of the factors that affect rates of ligand substitution reactions are those that also affect thermodynamic stability. It is important to remember that kinetic and thermodynamic factors are related, yet separate. The same factors that make a complex stable can also make it more inert. However, it is incorrect to assume that stability is always correlated with reaction rates.

Why are kinetic factors related to thermodynamic stability? For a complex to react or exchange one ligand for another, it must change its geometry to form an intermediate or transition state. For example, inert octahedral complexes often have stable electron configurations. When the reactant electron configuration is particularly stable, it can result in a higher activation energy associated with moving away from the stable configuration.

Factors to consider

1. Electron configuration and LFSE: Electron configurations that place electrons in higher-energy orbitals (particularly antibonding orbitals) result in more labile complexes. As long as there are not electrons in higher-energy orbitals, the lability correlates roughly with LFSE. The more negative the LFSE, the more inert.
2. Size and charge of the metal ion: In general, higher charge density on the metal ion leads to stronger electrostatic attraction between metal and ligand; higher charge density generally correlates with slower rates of ligand substitution.

Taube's Observations of Substitution Rates

Henry Taube (Nobel Prize, 1983) tried to understand lability by comparing the factors that govern bond strengths in ionic complexes to observations about the rates of reaction of coordination complexes. He saw some things that were unsurprising. He also drew some new conclusions based on ligand field theory. Taube observed that many M^{+1} ions are more labile than many M^{+3} ions, in general. That isn't too surprising, since metal ions function as electrophiles or Lewis acids and ligands function as nucleophiles or Lewis bases in forming coordination complexes. In other words, metals with higher charges ought to be stronger Lewis acids, and so they should bind ligands more tightly. However, there were exceptions to that general rule. For example, Taube also observed that Mo^{+5} compounds are more labile than Mo^{+3} compounds. So, there must be more going on here than just the effects of electrostatic attraction.

Another factor that governs ionic bond strengths is the size of the ion. Typically, ions with smaller atomic radii form stronger bonds than ions with larger radii. Taube observed that Al^{3+}, V^{3+}, Fe^{3+} and Ga^{3+} ions are all about the same size. All these ions exchange ligands at about the same rate. That isn't surprising, because they have the same charge and the same radius. However, Cr^{3+} is also about the same size as those ions and it also has the same charge, but it is much less labile. Once again, there are exceptions to our regular expectations based on simple electrostatic considerations. Furthermore, 4d and 5d transition metals (Y→Cd, and Ac→Hg) are much more inert than 3d transition metals (Sc→Zn). This is unexpected when we consider size; the 4d and 5d metals are much larger than the 3d metals. This unexpected behavior tells us that electrostatics alone cannot predict lability.

Exercise *Section*7.2.2

In which compound from each pair would you expect the strongest ionic bonds? Why?

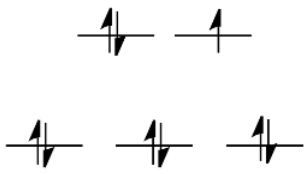
a) LiF vs KBr
b) $CaCl_2$ vs. KCl

Answer a

The ions in LiF are both smaller than in KBr, so the force of attraction between the ions in LiF is greater because of the smaller separation between the charges.

Answer b

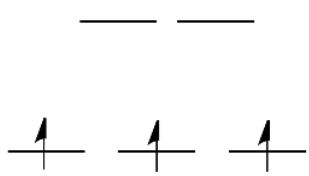
Calcium has a 2+ charge in $CaCl_2$, whereas potassium has only a + charge, so the chloride ions are more strongly attracted to the calcium than to the potassium.



Cu^{2+}

Taube came up with a hypothesis that could explain the seeming contradictory observations described above: *kinetic lability must be affected by d-electron configuration*. This idea forms the basis of Taube's rules about lability. For example, metals like Ni^{2+} and Cu^{2+} are very labile. The d orbital splitting diagrams for those compounds would have d electrons in the e_g set. Remember, the e_g

set arises from interaction with the ligand donor orbitals; this set corresponds to a σ antibonding level. By comparison, V^{2+} is rather inert. The d orbital splitting diagram in this case has electrons in the t_{2g} set, but none in the e_g set. So, having electrons in the higher energy, antibonding e_g level weakens the bond to the ligand, so the ligand can be replaced more easily. In the absence of those higher energy electrons, the bond to the ligand is stronger, and the ligand isn't replaced as easily.



V^{2+}

On the other hand, metals like Ca^{2+}, Sc^{3+} and Ti^{4+} are pretty labile. The d orbital splitting diagrams in those cases are pretty simple: there are no d-electrons at all in these ions. That means having no electrons in these mostly non-bonding levels leaves the complex susceptible to ligand replacement. But it's hard to see why population of an orbital that is mostly non-bonding would have an effect on ligand bond strength. Instead, this factor probably has something to do with the part of ligand substitution that we have ignored so far. Not only does one ligand need to leave, but a second one needs to bond in its place. So, having an empty orbital for the ligand to donate electrons into (or, put another way, not having electrons in the way that may complicate donation from the ligand) makes that part of the reaction easier.

Electron configurations can be generally classified as inert or labile based on crystal field stabilization energy. Configurations with high CFSE will be inert and configurations with low CFSE will be labile. Configurations that are most susceptible to Jahn-Teller distortions will be exceptionally labile, as the elongated bonds will be weaker and those ligands more easily exchanged.

Labile and inert electron configurations

Inert	Labile	Very labile
d^3, ls d^4, ls d^5, ls d^6,	d^1, d^2, hs d^5, hs d^6, hs d^7, d^{10}	hs d^4, d^9

Exercise *Section*7.2.3

Put the metal ions in order of decreasing reaction rate (from labile to inert):

a) Al^{3+}, Na^{+}, Mg^{2+}

b) $Ca^{2+}, Mg^{2+}, Sr^{2+}$

Answer (a)

Most labile to most inert: $Na^{+} > Mg^{2+} > Al^{3+}$

These are metal ions with similar size and varying charge. They are in order of increasing charge and increasing density from left to right.

Answer (b)

Most labile to most inert: $Sr^{2+} > Ca^{2+} > Mg^{2+}$

These metal ions have the same charge, and vary in size. They are in order of decreasing charge and increasing charge density from left to right.

Exercise *Section*7.2.4

Predict whether octahedral complexes of the following metals are labile or inert

a) Co^{3+} (high spin)

b) Co^{3+} (low spin)

c) Fe^{2+} (low spin)

d) Fe^{2+} (high spin)

e) Zn^{2+}

Answer a

hs d^6 labile (electrons in higher energy d orbital set)

Answer b

ls d^6 inert (all electrons in lower energy d orbitals)

Answer c

ls d^6 inert (all electrons in lower energy d orbitals)

Answer d

hs d^5 labile (electrons in higher energy d orbital set, CFSE = 0)

Answer e

d^{10} labile (electrons in higher energy d orbital set, CFSE = 0)

Overall Generalizations for Kinetics

1. s-block metals are very labile, except for those with very high charge density (eg. Mg^{2+} *is inert*)
2. d^{10} metals are labile (eg: Zn^{2+}, Cu^{+}, Hg^{2+})
3. Other ions with a full shell are labile (eg: La^{3+} of f-block)
4. 3d M^{2+}, *when high spin*, are generally labile (eg. Cu^{2+}*is very labile*)
5. 4d and 5d are usually inert due to higher CFSE (low spin, high CFSE)
6. M^{2+} is more labile than the same metal as M^{3+}
7. d^3 and low spin d^6 are inert (eg. Cr^{3+}, Co^{3+}, low spin Fe^{2+})

Attribution

Chris P Schaller, Ph.D., (College of Saint Benedict / Saint John's University)

Curated or created by Kathryn Haas

- Modified by Catherine McCusker (East Tennessee State University)

Section 7.2: Trends in Kinetic Lability is shared under a CC BY-NC-SA license and was authored, remixed, and/or curated by LibreTexts.

- **10.2: Trends in Kinetic Lability** has no license indicated.

Section 7.3: Ligand Substitution Mechanisms

Ligand Substitution Reactions

Ligand substitution is one of the simplest reactions a metal complex may undergo. In general, ligand substitution involves the exchange of one ligand for another, with no change in oxidation state at the metal center. The incoming and outgoing ligands may be neutral or ionic but the charge of the complex changes if the ligand charge changes. Keep charge conservation in mind when writing out ligand substitutions.

How do we know when a ligand substitution reaction is favorable? The thermodynamics of the reaction depend on the relative strength of the two metal-ligand bonds, and the stability of the departing and incoming ligands (or salts of the ligand, if they're ionic). It's often useful to think of X-for-X substitutions like acid-base reactions, with the metal and spectator ligands serving as a "glorified proton." Like acid-base equilibria in organic chemistry, we look to the relative stability of the two charged species (the free ligands) to draw conclusions. Of course, we don't necessarily need to rely just on thermodynamics to drive ligand substitution reactions. Photochemistry, neighboring-group participation, relative concentrations, and other tools can facilitate otherwise difficult substitutions.

Ligand substitution is characterized by a continuum of mechanisms bound by associative (A) and dissociative (D) extremes. At the associative extreme, the incoming ligand first forms a bond to the metal, then the departing ligand takes its lone pair and leaves. At the dissociative extreme, the order of events is opposite—the departing ligand leaves, then the incoming ligand comes in. Associative substitution is common for square planar (like d8 complexes of Ni, Pd, and Pt), while dissociative substitution is more common for octahedral complexes. Then again, reality is often more complicated than these extremes. In some cases, evidence is available for simultaneous dissociation and association, and this mechanism has been given the name interchange (IA or ID).

Associative Substitution

The associative substitution reaction is the inorganic analog of an S_{N2} reaction. In associative ligand substitution, the incoming ligand (Y) forms a new bond with the metal (M) before the bond to the leaving ligand (X) breaks. The first step, formation of the new M-Y bond is generally rate-determining. A typical mechanism for associative ligand substitution in both octahedral and square planar complexes is shown in Figure $\mathit{Section}7.3.1$.

$$ML_nX \xrightarrow{Y} ML_nXY \rightarrow ML_nY + X \qquad \text{(Section 7.3.1)}$$

In an octahedral complex the intermediate is 7 coordinate, so associative ligand exchange in octahedral complexes is rare and only favored with larger metal ions and ligands that are not sterically demanding. In contrast, ligand substitution in square planar complexes almost always occurs via an associative mechanism, involving approach of the incoming ligand to the open coordination sites above or below the plane. Let's begin with the kinetics of the reaction. How can we spot an associative mechanism in experimental data, and what are some of the consequences of this mechanism?

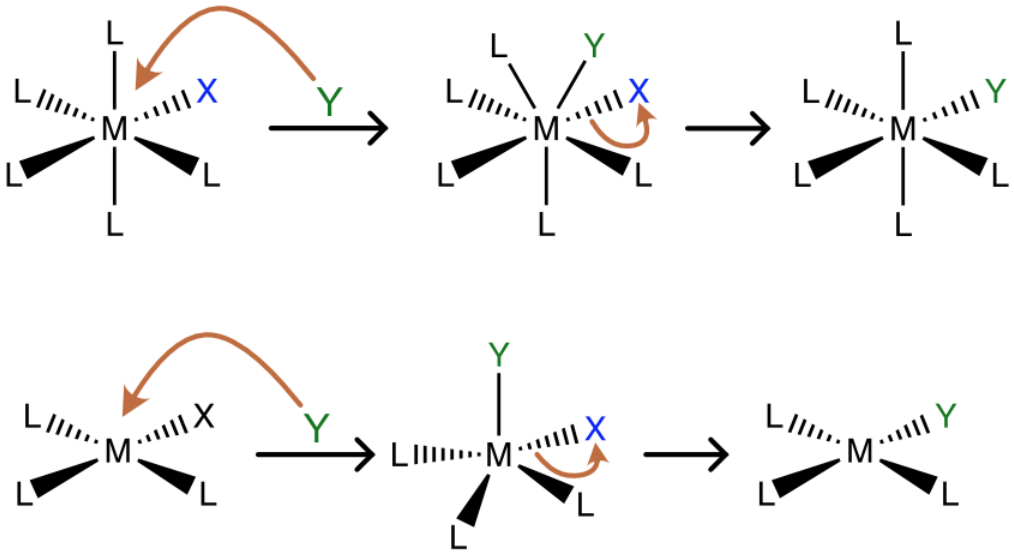


Figure *Section*7.3.1: Scheme of associative ligand substitution in an octahedral (top) and square planar (bottom) metal complex. (CC BY-NC-SA; Catherine McCusker)

Reaction Kinetics

$$L_nM\text{–}X + Y \xrightarrow{k_1} L_nM\text{–}Y + X \qquad \text{(Section 7.3.2)}$$

$$\frac{d[L_nM\text{–}Y]}{dt} = rate = k_1[L_nM\text{–}X][Y] \qquad \text{(Section 7.3.3)}$$

Reaction kinetics are commonly used to elucidate reaction mechanisms, and ligand substitution is no exception. Different mechanisms of substitution may follow different rate laws, so plotting the dependence of reaction rate on concentration often allows us to distinguish mechanisms. In the associative mechanism, the rate law is second order overall, first order in both L_nMX and Y. (Figure *Section*7.3.2). If a large excess of Y is used in the reaction is will become pseudo first order, where the reaction appears first order because the [Y] doesn't change significantly over the course of the reaction.

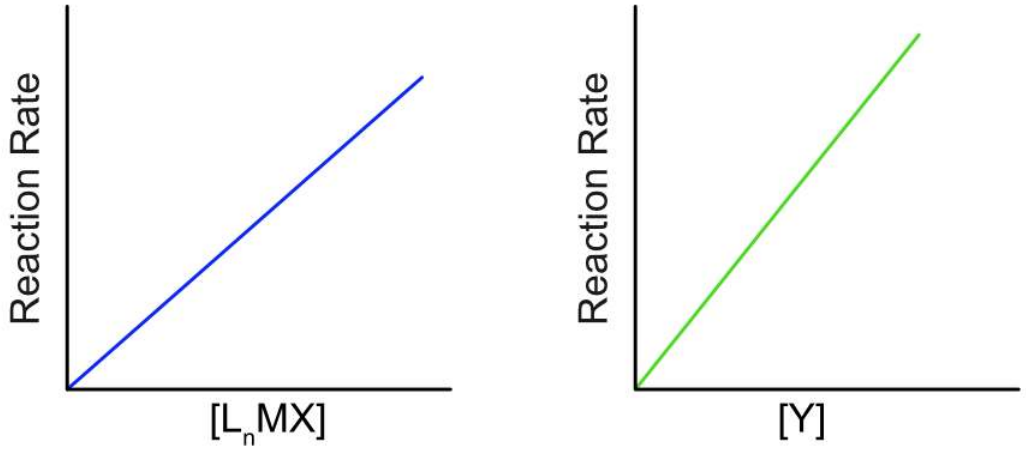


Figure *Section*7.3.2: Dependence of associative reaction rate on concentration of the starting metal complex $[ML_nX]$ and the incoming ligand [Y]. (CC BY-NC-SA; Catherine McCusker)

Dissociative Substitution

The associative substitution mechanism is unlikely for 6 coordinate complexes. For octahedral complexes dissociative substitution mechanisms involving 5 coordinate intermediates are more likely. In

a slow step, the departing ligand leaves, generating a coordinatively unsaturated 5 coordinate intermediate. The incoming ligand then enters the coordination sphere of the metal to generate the product. We'll focus on the kinetics of the reaction and the nature of the unsaturated intermediate (which influences the stereochemistry of the reaction). The reverse of the first step, re-coordination of the departing ligand (rate constant k_{-1}), is often competitive with dissociation.

$$ML_nX \rightarrow ML_n + X + Y \rightarrow ML_nY + X \quad \text{(Section 7.3.4)}$$

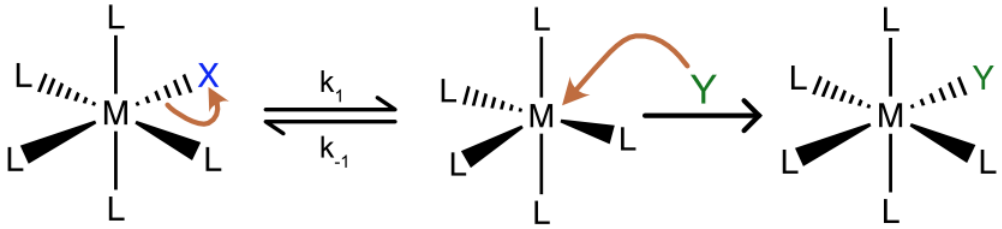


Figure *Section*7.3.3: A general scheme for dissociative ligand substitution in an octahedral complex. (CC BY-NC-SA; Catherine McCusker)

Reaction Kinetics

Let's begin with the general situation in which k_1 and k_{-1} are similar in magnitude. Since k_1 is rate limiting, k_2, the rate of the second step is assumed to be much larger than k_1 and k_{-1}. Most importantly, we need to assume that variation in the concentration of the unsaturated intermediate is essentially zero. This is called the steady state approximation, and it allows us to set up an equation that relates reaction rate to observable concentrations.

$$\text{rate} = k_2[L_nM][Y] \quad \text{(Section 7.3.5)}$$

Of course, the unsaturated complex is present in very small concentration and is unmeasurable, so this equation doesn't help us much. We need to remove the concentration of the unmeasurable intermediate from (1), and the steady state approximation helps us do this. We can express variation in the concentration of the unsaturated intermediate as (processes that make it) minus (processes that destroy it), multiplying by an arbitrary time length to make the units work out. All of that equals zero, according to the steady state approximation.

$$\Delta[L_nM] = 0 = (k_1[L_nM\text{–}X] - k_{-}1[L_nM][X] - k_2[L_nM][Y])\Delta t \quad \text{(Section 7.3.6)}$$

$$0 = k_1[L_nM\text{–}X] - k_{-1}[L_nM][X] - k_2[L_nM][Y] \quad \text{(Section 7.3.7)}$$

Rearranging to solve for [L_nM], we arrive at the following.

$$[L_nM] = k_1\frac{[L_nM\text{–}X]}{(k_{-1}[X] + k_2[Y]} \quad \text{(Section 7.3.8)}$$

Finally, substituting into Equation Section 7.3.5 we reach a verifiable rate equation.

$$\text{rate} = k_2k_1\frac{[L_nM\text{–}X][Y]}{(k_{-1}[X] + k_2[Y])} \quad \text{(Section 7.3.9)}$$

When k_{-1} is negligibly small, Equation Section 7.3.9 reduces to the familiar Equation Section 7.3.10, typical of dissociative reactions like S_N1.

$$\text{rate} = k_1[L_nM\text{–}X] \quad \text{(Section 7.3.10)}$$

This rate does not depend on the concentration of incoming ligand. For reactions that are better described by Equation Section 7.3.9, we can use a large excess of Y to make $k_2[Y]$ far greater than $k_{-1}[X]$, essentially forcing the reaction to fit Equation Section 7.3.10.

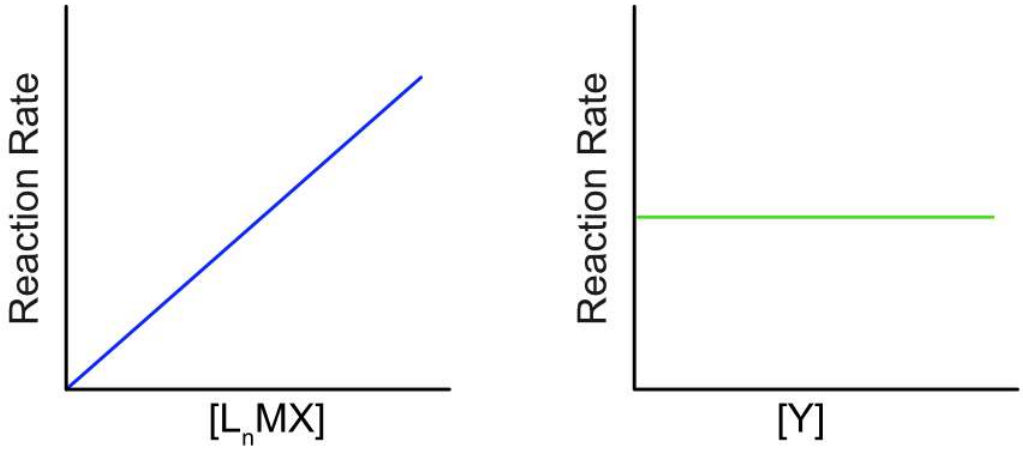


Figure ***Section*7.3.4**: Dependence of dissociative reaction rate on concentration of the starting metal complex [ML_nX] and the incoming ligand [Y]. (CC BY-NC-SA; Catherine McCusker)

Stereochemistry

Dissociation of a ligand from an octahedral complex generates an unsaturated ML_5 intermediate. The five coordinate intermediate could adopt either a trigonal bipyramidal (TBP) geometry or a square pyramidal geometry (SP). Both steric and electronic factors combine to determine which geometry is most favorable. For example, with 6 d electrons an issue arises with the TBP geometry. With 6 d electrons, the TBP geometry has two unpaired electrons in degenerate orbitals. Unpaired electrons in degenerate orbitals lead to Jahn-Teller distortion. For a TBP geometry, distortion to a SP or a distorted TBP geometry removes the degeneracy, and so five-coordinate d6 complexes typically have square pyramidal or distorted TBP geometries.

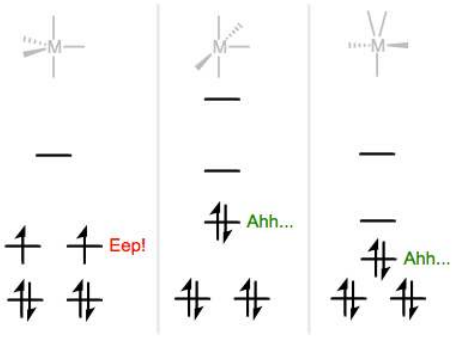


Figure ***Section*7.3.5**: TBP geometry (left) is electronically disfavored for d6 metals. Distorted TBP (right) and SP (center) geometries are favored.

When the intermediate adopts square pyramidal geometry, the incoming ligand can simply approach where the departing ligand left, resulting in retention of stereochemistry. Inversion is more likely when the intermediate is a distorted trigonal bipyramid.

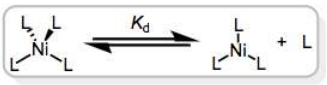
Factors That Favor Dissociative Substitution

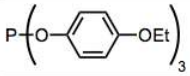
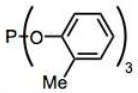
In general, introducing structural features that either stabilize the unsaturated intermediate or destabilize the starting complex can encourage dissociative substitution. Both of these strategies lower the activation barrier for the reaction.

Let's begin with features that stabilize the unsaturated intermediate. Electronically, the intermediate loves it when its d electron count is nicely matched to its crystal field orbitals. As you study inorganic chemistry, you'll learn that there are certain "natural" d electron counts for particular geometries that fit well with the metal-centered orbitals predicted by crystal field theory. Octahedral geometry is great for six d electrons, for example, and square planar geometry loves eight d electrons. Complexes with "natural" d electron counts—but bearing one extra ligand—are ripe for dissociative substitution. The classic examples are d^8 TBP complexes, which become d^8 square planar complexes (think Pt(II) and Pd(II)) upon dissociation. Similar factors actually can also stabilize the

starting complexes, making them less reactive in dissociative substitution reactions. Fro example, low spin d^6 octahedral complexes are particularly happy, and react most slowly in dissociative substitutions.

Destabilization of the starting complex is commonly accomplished by adding steric bulk to its ligands. Naturally, dissociation relieves steric congestion in the starting complex. Chelation has the opposite effect, and tends to steel the starting complex against dissociation.



L	Cone Angle	K_d
$P(OEt)_3$	109	$< 10^{-10}$
	128	$6 * 10^{-10}$
$P(Oi\text{-}Pr)_3$	130	$2.7 * 10^{-5}$
	141	$4 * 10^{-2}$
PPh_3	145	huge

As steric bulk on the ligand increases, dissociation becomes more favorable.

Interchange Substitution

Real life chemical reactions don't always fall neatly into one of the categories above. In some cases the M-X bond can break and the M-Y bond can form simultaneously. An interchange reaction is a concerted reaction without an intermediate. The transition state is a species where the bond to Y is partially formed and the bond to X is partially broken as seen in Figure ***Section*7.3.6**. If the new M-Y bond forms faster than the M-X bond breaks tat is an associative interchange (IA) reaction and if the M-X bond breaks faster than the new M-Y bond forms that is a dissociative interchange reaction (ID)

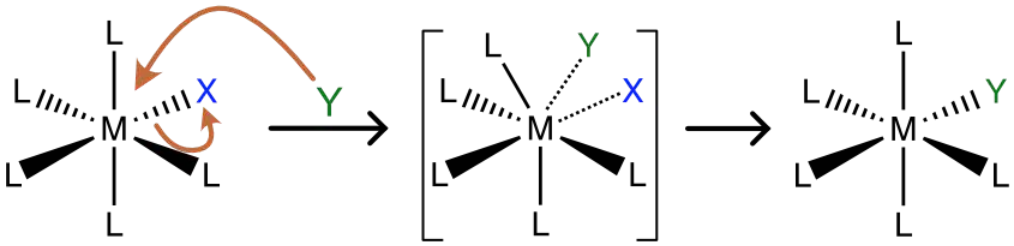


Figure ***Section*7.3.6**: A general scheme for an interchange ligand substitution reaction. Species in brackets is the transition state, not an intermediate. (CC BY-NC-SA; Catherine McCusker)

Contributors and Attributions

- Dr. Michael Evans (Georgia Tech)
- Modified by Catherine McCusker (East Tennessee State University)

This page titled Section 7.3: Ligand Substitution Mechanisms is shared under a CC BY-NC-SA 4.0 license and was authored, remixed, and/or curated by Michael Evans.

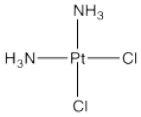
- **10.3: Ligand Substitution Mechanisms** by Michael Evans is licensed CC BY-NC-SA 4.0.
- **4.2: Associative Ligand Substitution** by Michael Evans is licensed CC BY-NC-SA 4.0.
- **4.3: Dissociative Ligand Substitution Reactions** by Michael Evans is licensed CC BY-NC-SA 4.0.
- **4.4: Ligand substitution** by Michael Evans is licensed CC BY-NC-SA 4.0.

Section 7.4: The Trans Effect Observation

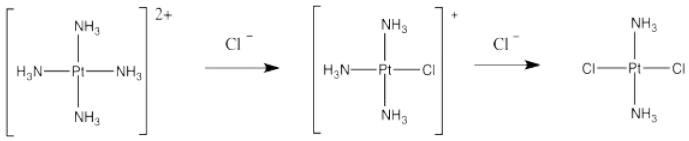
Occasionally in ligand substitution there is a situation in which there are two identical ligands that could be replaced, but two different products would result depending on which ligand left. This situation often happens in square planar complexes, for example. Replacement of one ligand would lead to a *cis* product. Replacement of the other one would lead to a *trans* product.



An important example of this issue is in the synthesis of cis-platin, an antitumour medication frequently used to treat ovarian and testicular cancer.

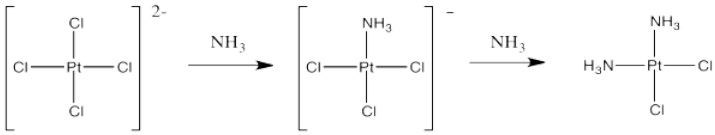


Cis-platin could be made from treatment of tetraammineplatinum(II) with chloride salts. The chloride ion could replace two of the ammonia ligands.



But that doesn't work. That synthesis results in the formation of *trans*-platin, a compound that has all of the nasty side effects of the *cis* isomer but with none of the therapeautic benefit.

If instead you were to start with tetrachloroplatinate salts and treat them with ammonia, you could replace two of the chloride ligands. That works really well, and it provides *cis*-platin, not *trans*-platin.



? Exercise *Section*7.4.1

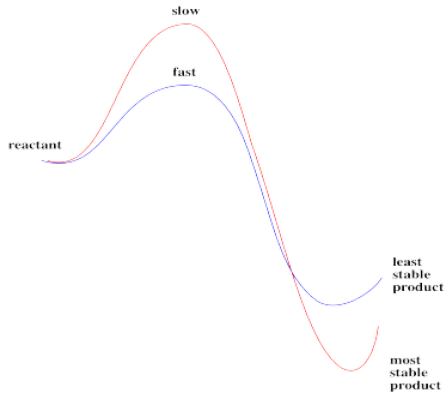
What do you think is the mechanism of substitution of the two reactions above? Why?

Answer

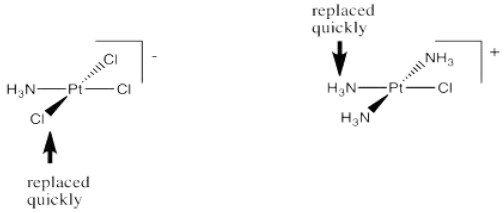
This is probably an associative mechanism because of the square planar geometry.

This reaction, if run under these conditions, is clearly not always under thermodynamic control. Two different products result, depending on how the reaction is done. One of those isomers is probably more stable than the other; if thermodynamics were in charge, it would form the same thing both times.

Instead, there may be an element of kinetic control for at least one of the pathways. A given product might be made, not because it is more stable, but simply because it forms more quickly than the other one.



Take another look at those two reactions. One of the things that they have in common is that the ligand that gets replaced is *trans* to a chloride. It is not *trans* to an ammonia. Maybe the other ligands in the complex can influence how quickly one ligand can leave.



Specifically, the "*trans* effect" is the role of *trans*-ligands in influencing substitution rates in square planar complexes.

The following kinetic data were obtained for substitutions on square planar platinum complexes, in the reaction:

$$trans-(PEt_3)_2PtLCl + py \rightarrow trans-(PEt_3)_2PtLpy^+ + Cl^-$$

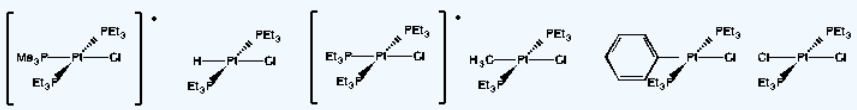
L	k_{obs} (s^{-1})	T, °C
PMe_3	0.20	0
H^-	0.047	0
PEt_3	0.041	0
CH_3^-	6.0×10^{-4}	25
$C_6H_5^-$	1.2×10^{-4}	25
Cl^-	3.5×10^{-6}	25

Ref: Cooper Langford & Harry Gray, *Ligand Substitution Processes*, W.A. Benjamin, NY, 1965, p. 25.

? Exercise *Section*7.4.2

Draw structures for each of the complexes listed in the table.

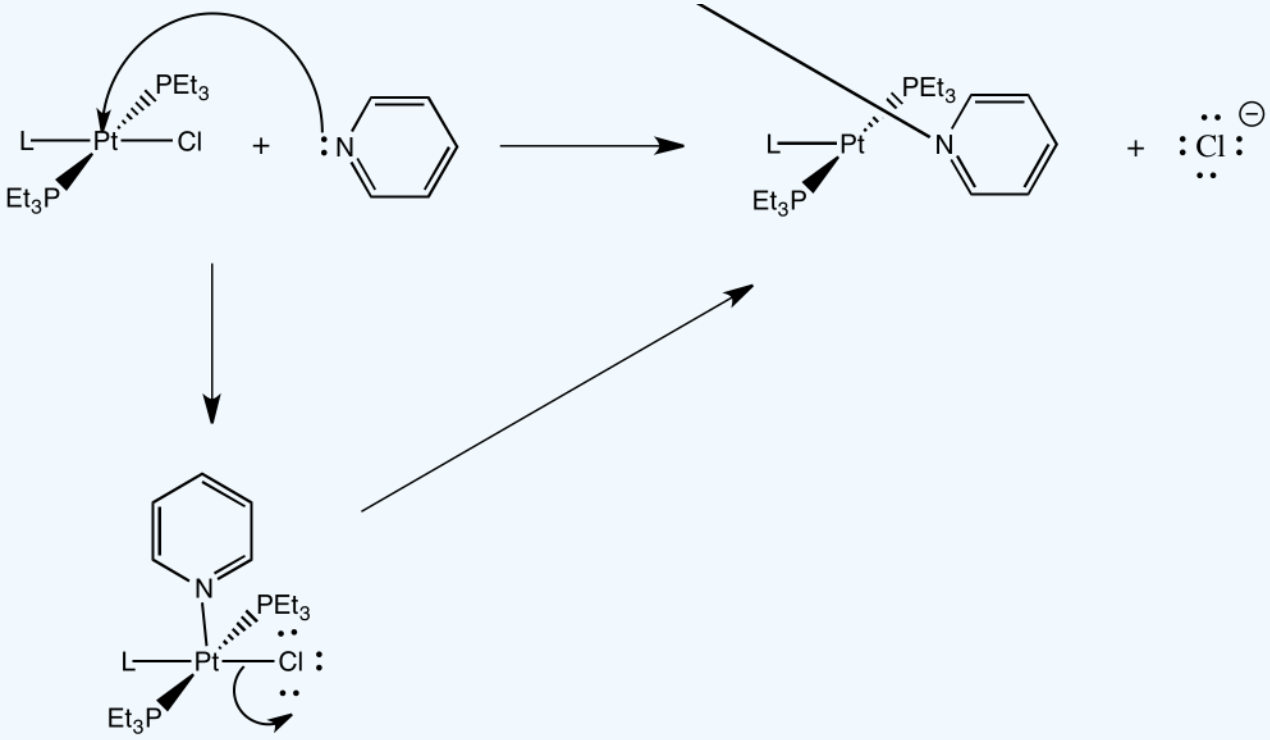
Answer



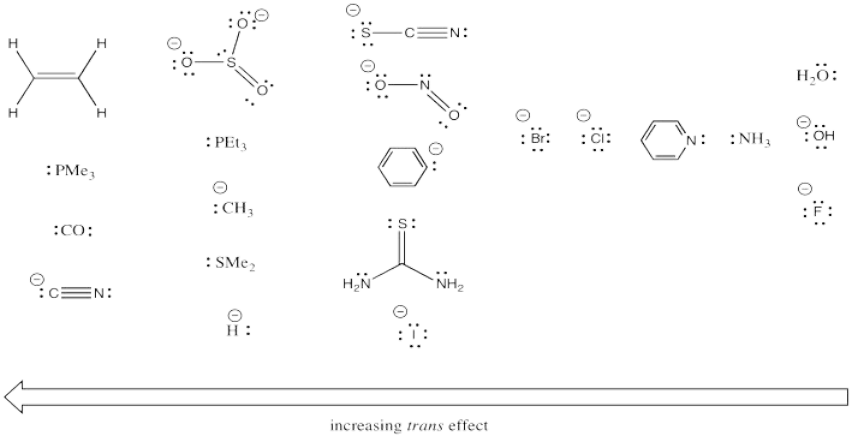
Exercise *Section7.4.3*

Provide a mechanism with arrows for the reaction studied in the table.

Answer



Clearly that *trans* ligand has a dramatic effect on how quickly the chloride can be substituted in the above study. Additional studies like this one have led to some general trends. Below, the ligands on the left have strong *trans*-effects. Ligands *trans* to them are substituted very quickly. The ligands on the right have very modest *trans* effects. Ligands *trans* to them are substituted only slowly.



Exercise *Section7.4.4*

Look for empirical trends in the series of ligands above. Without trying to explain exactly why, find chemically relevant factors that may be responsible for these reactivity trends.

Answer

There is an electronegativity trend: the less electronegative, the greater the *trans* effect (see the halogens, as well as the series O,N,C and also the orders within several pairings: S,P; O,S and N,P).

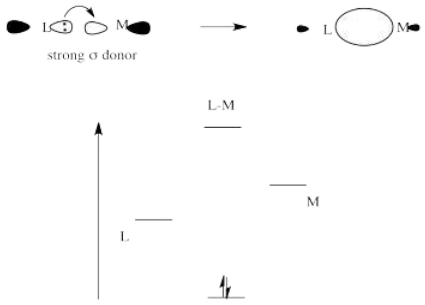
Alternatively, some of the above could be described by a polarizability trend: more polarizable atom, greater *trans* effect (for example, the halogens).

Most of the ligands containing π-bonds have strong *trans* influence (but not all).

Most of the π-donors have a weaker *trans* influence. However, these ligand cover a very broad range in this series.

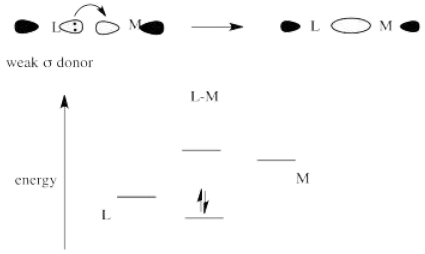
In general, explanations of the trans effect have focused on two separate types of ligands. These are strong sigma donors and strong pi acceptors.

Strong sigma donors donate electrons very effectively to the metal via a sigma bond. Because the ligand trans to this donor would be bonding via donation to the same metal p orbital, there is a competition. The metal p orbital bonds more favorably with the strong sigma donor, and the ligand trans to it is left with a weaker bond.



The strong sigma donor gets good overlap with the metal orbital and the resulting interaction goes down low in energy.

The weak sigma donor gets poorer overlap with the metal orbital and only weak stabilization of the donor electrons.



Place these two choices together, and the metal orbital will engage in a strong bonding interaction with the strong σ-donor. Doing so lowers the electronic energy significantly. It won't interact very much with the weak σ-donor, because doing that won't result in as much lowering of electronic energy. The result is a strong bond on one side of the metal and a weak bond on the other. That weak bond will break easily and that ligand will be replaced easily.



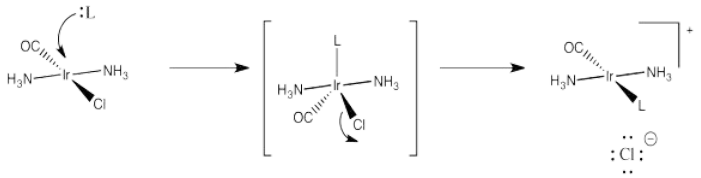
? Exercise *Section*7.4.5

Which of the ligands in the *trans* effect series are probably strong σ-donors? Why?

Answer

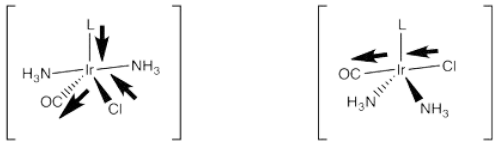
The strongest σ-donors are typically those with more polarizable donor atoms (such as S, P, I) as well as those with less electronegative donor ions such as C^- and H^-.

Strong pi acceptors exert their trans effect in a different way. They are thought to stabilize a particular geometry of the five-coordinate intermediate in substitution of square planar complexes. We haven't worried too much about the geometry of that intermediate, but it is probably trigonal bipyramidal. It would have three ligands in an equatorial plane and two more directly opposite each other, in the axial positions.



Essentially, the incoming ligand pushes two of the ligands down from the square plane to form this trigonal bipyramid. When it comes time for a ligand to leave, it is probably going to be one of these ligands that is already on the move. They are already on a trajectory out of the square plane, anyway.

A strong pi acceptor like CO exerts its *trans* effect by making sure it, along with the ligand opposite it, gets into that equatorial plane. It does that by a stabilizing delocalization that happens when the π-acceptor is in the electron-rich equatorial plane. In that position, it can draw electron density via π-donation from two different donors. If it were in an axial position, it could still delocalize electrons this way, but it would draw most effectively from just one donor rather than two.



favoured

So which of those two ligands is going to keep moving and leave the complex? It certainly won't be the one that is exerting a stabilizing, delocalizing effect on the complex via its strong bonding interactions. It will be the unlucky *trans* ligand that got dragged along with it.

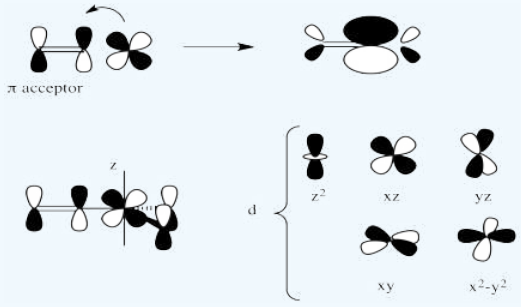
? Exercise *Section*7.4.6

Which of the ligands in the *trans*-effect series are probably strong π-acceptors? Show why.

? Exercise *Section*7.4.7

Draw an orbital picture showing the -delocalization described in the trigonal bipyramidal intermediate. Label the orbitals, assuming the z axis is along the axis of the trigonal bipyramid (i.e. the equatorial plane is the xy plane).

Answer



? Exercise *Section*7.4.8

Substitution of trans ligands in μ-oxo-bis(μ-acetato)diruthenium complexes: Synthesis and kinetic studies. Hussain, Bhatt, Kumar, Thorat, Padhiyar and Shukla, *Inorganica Chemica Acta*, **2009**, *362*, 1101-1108.

Given the structure $[Ru_2O(L)_6(acetate)_2](PF_6)_2$, in which L is a neutral donor,

a) Draw the structure of the counterion, PF_6^-.

b) Provide an account of the valence electron count in the ruthenium coordination complex.

Valence electrons on metal	
Total charge on ligands	
Charge on the metal	
Revised count on metal	
Electrons donated by ligands	
Total electrons on metal in complex	

Data shows that the ligands L are *trans* to the bridging oxo ligand are labile.

c) Use orbital cartoons and words to provide an explanation for this effect.

When water is added to an acetone solution of $[Ru_2O(pyridine)_4(L)_2(acetate)_2](PF_6)_2$, then $[Ru_2O(pyridine)_4(H_2O)_2(acetate)_2](PF_6)_2$ is formed.

d) Draw the product of this reaction.

When pyridine is added to $[Ru_2O(pyridine)_4(H_2O)_2(acetate)_2](PF_6)_2$, then $[Ru_2O(pyridine)_6(acetate)_2](PF_6)_2$ is formed. The following rate constants were observed for this reaction.

[pyridine] mol L^{-1}	k_{obs} s^{-1} (x 10^{-3})
0.005	1.75
0.012	2.53
0.025	9.7
0.049	16.7
0.100	35.2

e) Use the data from this table to determine the order in pyridine. Provide an explanation for your conclusion.

f) Draw a mechanism for the reaction, consistent with the data.

g) Write a rate law for the reaction.

h) The authors studies the same reaction with different ligands instead of pyridine. They observed an increase in rate constants with increasing basicity of the incoming ligands. Provide an explanation for this observation.

Answer a



5 valence electrons - 6 bonds - 0 nonbonding = -1

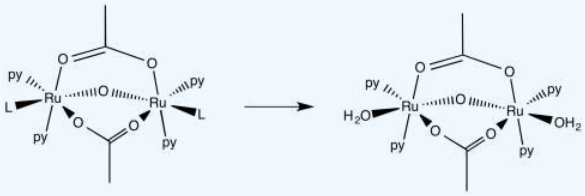
Answer b

Valence electrons on metal	8
Total charge on ligands	-4 (-2 per Ru)
Charge on the metal	+2
Revised count on metal	6
Electrons donated by ligands	12
Total electrons on metal in complex	18

Answer c

The oxo is a strong sigma donor and hogs the orbital with the metal thus leaving very little room for orbital bonding trans to the sigma donor.

Answer d



Answer e

First order. Although there is some amount of error in the data, doubling the pyridine concentration generally results in a doubling of the rate.

Answer f

The mechanism you draw would have to involve a first associative step; because the complex is already 18 electrons, associative interchange is likely.

Answer g

$$Rate = k[ML_n][py]$$

Answer h

Basic ligands have stronger attraction to the metal thus accelerating the reaction.

This page titled Section 7.4: The Trans Effect Observation is shared under a CC BY-NC 3.0 license and was authored, remixed, and/or curated by Kathryn Haas.

- **3.7: The Trans Effect** by Chris Schaller is licensed CC BY-NC 3.0. Original source: https://employees.csbsju.edu/cschaller/ROBI2.htm.

Section 7.5: The Trans Effect Explanation

The trans effect is an ancient but venerable observation. First noted by Chernyaev in 1926, the trans effect and its conceptual siblings (the trans influence, cis influence, and cis effect) are easy enough to comprehend. That is, it's simple enough to know what they are. To understand why they are, on the other hand, is much more difficult.

Definitions & Examples

Let's begin with definitions: what is the trans effect? There's some confusion on this point, so we need to be careful. The trans effect proper, which is often called the kinetic trans effect, refers to the observation that certain ligands increase the rate of ligand substitution when positioned trans to the departing ligand. The key word in that last sentence is "rate"—the trans effect proper is a kinetic effect. The trans influence refers to the impact of a ligand on the length of the bond trans to it in the ground state of a complex. The key phrase there is "ground state"—this is a thermodynamic effect, so it's sometimes called the thermodynamic trans effect. Adding to the insanity, cis effects and cis influences have also been observed. Evidently, ligands may also influence the kinetics or thermodynamics of their cis neighbors. All of these phenomena are independent of the metal center, but do depend profoundly on the geometry of the metal (more on that shortly).

Kinetic trans and cis effects are shown in the figure below. In both cases, we see that X1 exhibits a stronger effect than X2. The geometries shown are those for which each effect is most commonly observed. The metals and oxidation states shown are prototypical.

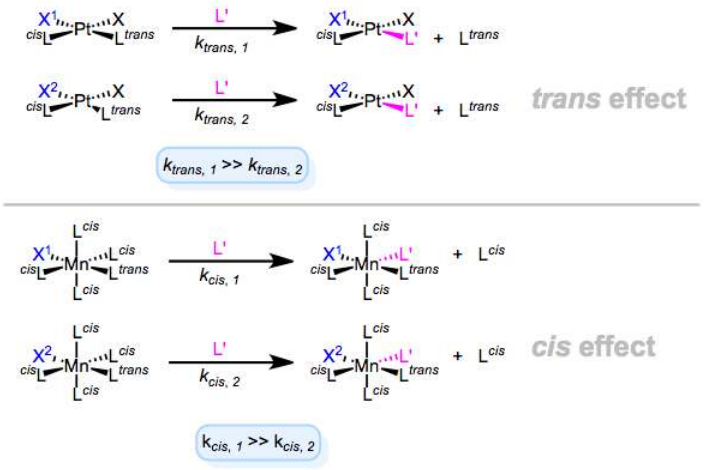


Figure 1: *The kinetic trans and cis effects in action. X^1 is the stronger (trans/cis)-effect ligand in these examples.*

On to the influences, which are simpler to illustrate since they're concerned with ground states, not reactions. The lengthened bonds below are exaggerated.

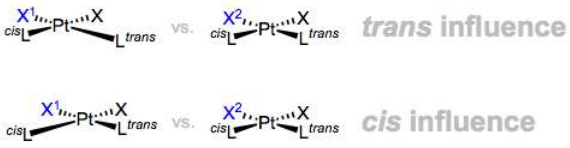


Figure 2: *The trans and cis influences in action. Note the elongated bond lengths.*

And there we have it folks, the thermodynamic and kinetic cis/trans effects. It's worth keeping in mind that the kinetic trans effect is most common for d8 square planar complexes, and the kinetic cis effect is most common for d6 octahedral complexes (particularly when the departing L is CO). But a lingering question remains: what makes for a strong trans effect ligand?

Origins of Effects & Influences

The trans effect and its cousins are all electronic, not steric effects. So, the electronic properties of the ligand dictate the strength of its trans effect. Let's finally dig into the trans effect series:

(weak) F^-, HO^-, H_2O <NH_3 < py < Cl^- < Br– < I–, SCN^-, NO_2^-, $SC(NH_2)_2$, Ph^- < SO_3^{2-} < PR_3 < AsR_3, SR_2, H_3C^- < H^-, NO, CO, NC^-, C_2H_4 (strong)

What's the electronic progression here? It's clear that electronegativity decreases across the series: F^- < Cl^- < Br^- < I^- < H_3C^-. From a bonding perspective, we can say that ligands with strong trans effects are strong σ-donors (or σ-bases). Yet σ-donation doesn't tell the whole story. What about ethylene and carbon monoxide, which both appear at the top of the heap? Neither of these ligands are strong σ-donors, but their π systems do interact with the metal center through backbonding. Consider the following sub-series: S=C=N– < PR_3 < CO. Backbonding increases across this series, along with the strength of the trans effect. Strong backbonders—better known as π-acceptors or π-acids—exhibit strong trans effects.

Strong trans effect = strong σ-donor + strong π-acceptor

Wonderful! Using these ideas we can identify ligands with strong trans effects. But we can dive deeper down the rabbit hole: why does this particular combination of electronic factors lead to a strong trans effect? To understand this, we need to know the mechanism of the ligand substitution reaction that's sped up by strong trans effect ligands. For 16-electron Pt(II) complexes, associative substitution is par for the course. The incoming ligand binds to the metal first, forming an 18-electron complex (yay!), which jettisons a ligand to yield a new 16-electron product. The mechanism in all its glory is shown in the figure below.

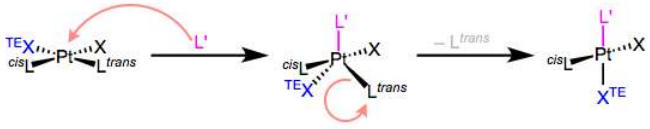


Figure 3: *The mechanism of associative ligand substitution of Pt(II) complexes.*

Some very important points about this mechanism:

- The incoming ligand always sits at an equatorial site in the trigonal bipyramidal intermediate. More on this another day, but I think of this result as governed by the principle of least motion. Consider the molecular gymnastics that would have to happen to place the incoming ligand in an axial position.
- Two ligands in the square plane are "pushed down" and become the other two equatorial ligands.
- Owing to microscopic reversibility, the leaving group must be one of the equatorial ligands.

The third point reveals that once L' has "pushed down" XTE and Ltrans, Ltrans has no choice but to leave (assuming XTE stays put). Thus, the trans effect has nothing to do with the second step of the mechanism, which is not rate determining anyway. The key is the first step—in particular, the "pushing down" event. Apparently, ligands with strong trans effects like to be pushed down. They like to occupy the equatorial plane of the TBP intermediate. Now here's the kicker: the equatorial sites of the TBP geometry are more π basic than the axial sites. The equatorial plane is just the xy-plane of the metal center, and the d orbitals in that plane (when occupied) are great electron sources for π-acidic ligands. Thus, π-acidic ligands want to occupy those equatorial sites, to receive the benefits of strong backbonding! Boom; strong π-acids encourage loss of the ligand trans to themselves.



Figure 4: *The equatorial sites of TBP metals are rich in electrons that can π bond.*

What about those pesky σ donors? Well, we can imagine that in a square planar complex, a ligand and its trans partner are competing for donation into the same d orbital. Strong σ donation from a ligand should thus weaken the bond trans to it. Although this is the thermodynamic trans effect (trans influence) in action, the resulting destabilization of the ground state relative to the transition state is a kinetic effect. On the whole, the barrier to substitution of the trans ligand goes down as σ-donating strength goes up.

This idea of "competition for the metal center" is a nice heuristic to use when thinking about the trans and cis influences. The type of metallic orbital involved in M–L bonding determines the strength of L's trans and cis influences on neighboring ligands that also need that metallic orbital for bonding. For example: both influences are large if the metal's s orbital is a significant contributor to

M–L bonding, since it's non-directional; the trans influence is much greater than the cis influence when metallic p orbitals are primarily involved in M–L. For a deeper explanation of these ideas, see this paper.

Summing up

Perhaps the most valuable lesson from a study of the trans effect is that many concepts from organometallic chemistry involve more than meets the eye. Geometric effects and influences are real icebergs, in the sense that the observations and trends are easy to grasp, but difficult to explain. We had to dig all the way into the mechanism of associative ligand substitution before a satisfactory explanation emerged!

Contributors

Dr. Michael Evans (Georgia Tech)

Section 7.5: The Trans Effect Explanation is shared under a CC BY-NC-SA 4.0 license and was authored, remixed, and/or curated by LibreTexts.

Section 7.6: Electron Transfer Reactions

Test Tube Experiments

Easy chemical or biological reactions performed in test tubes are sometimes called test tube experiments. Solutions in test tubes are mixed at room temperature in air and the mixture is shaken to observe a color change or formation of precipitates and the results of the reactions are speculated on. University professors occasionally attempt these sorts of experiments. Although easy, these simple experiments show only the effects of visible light absorption and solubility. However, since even great discoveries can be born from such experiments, they should not be dismissed.

Henry Taube wrote that he found a hint of the inner-sphere electron transfer mechanism from test tube experiments. He mixed Cr^{2+} (aq) and I_2 in a test tube in order to clarify the oxidation of Cr^{2+}(aq) and observed the change of color to the one characteristic of $[Cr(H_2O)_6]^{3+}$ via green. The green color is due to $[(H_2O)_5CrI]^{2+}$ which is unstable and changes to $[Cr(H_2O)_6]^{3+}$ + I^-. He assumed that this was due to the formation of a Cr-I bond before Cr(II) was oxidized by I_2. Subsequently, he performed another test tube experiment using $[(NH_3)_5CoCl]^{2+}$ as an oxidant and found that Cr^{2+}(aq) was converted into $[Cr(H_2O)_6]^{3+}$ via green $[(H_2O)_5CrCl]_{2+}$. This reaction established the inner-sphere electron transfer mechanism in which a Co-Cl-Cr bridge forms between Co^{3+} and Cr^{2+} and led to the Nobel Prize in a later year.

Redox reactions

The oxidation number of the central metal in a transition-metal compound can vary in a few steps from low to high. Namely, the oxidation state of a compound is changeable by redox reactions. As a consequence of this, the bond distance and the bond angle between the metal and coordinating elements, or between metals, change, and at times the whole structure of a complex can be distorted remarkably or the compound may even decompose. The reactions of a metal compound with various reducing or oxidizing agents are also very important from the viewpoint of synthetic chemistry. Especially, reduction reactions are used in the preparation of organometallic compounds, such as metal carbonyls or cluster compounds.

Meanwhile, the study of electron transfer between complexes, especially the redox reactions of transition metal complexes, has developed. Taube won the Nobel Prize (1983) for the study of electron transfer reactions in transition metal complexes, classifying such reactions into two mechanisms. The mechanism of electron transfer in which a bridging ligand is shared between two metals is called the **inner-sphere mechanism**, and the one involving a direct transfer of electrons between two metals without a bridging ligand is called the **outer-sphere mechanism**.

Inner Sphere Electron Transfer

In some cases, electron transfers occur much more quickly in the presence of certain ligands. For example, compare the rate constants for the following two electron transfer reactions, involving almost exactly the same complexes:

$$Co(NH_3)_6^{3+} + Cr^{2+} \longrightarrow Co^{2+} + Cr^{3+} + 6\,NH_3 \quad k = 10^{-4} M^{-1} s^{-1}$$

$$Co(NH_3)_5Cl^{2+} + Cr^{2+} \longrightarrow Co^{2+} + CrCl^{2+} + 6\,NH_3 \quad k = 6 \times 10^{5} M^{-1} s^{-1}$$

(Note: aqua ligands are omitted for simplicity. Ions, unless noted otherwise, are aqua complexes.)

Notice two things: first, when there is a chloride ligand involved, the reaction is much faster. Second, after the reaction, the chloride ligand has been transferred to the chromium ion. Possibly, those two events are part of the same phenomenon.

Similar rate enhancements have been reported for reactions in which other halide ligands are involved in the coordination sphere of one of the metals.

In the 1960's, Henry Taube of Stanford University proposed that halides (and other ligands) may promote electron transfer via bridging effects. What he meant was that the chloride ion could use one of its additional lone pairs to bind to the chromium ion. It would then be bound to both metals at the same time, forming a bridge between them. Perhaps the chloride could act as a conduit for electron transfer. The chloride might then remain attached to the chromium, to which it had already formed a bond, leaving the cobalt behind.

Electron transfers that occur via ligands shared by the two metals undergoing oxidation and reduction are termed "inner sphere" electron transfers. Taube was awarded the Nobel Prize in chemistry in 1983; the award was based on his work on the mechanism of electron transfer reactions.

Exercise *Section*7.6.1

Take another look at the two electron transfer reactions involving the cobalt and chromium ion, above.

a. What geometry is adopted by these complexes?
b. Are these species high spin or low spin?
c. Draw d orbital splitting diagrams for each complex.
d. Explain why electron transfer is accompanied by loss of the ammonia ligands from the cobalt complex.
e. The chloride is lost from the cobalt complex after electron transfer. Why does it remain on the chromium?

Answer a

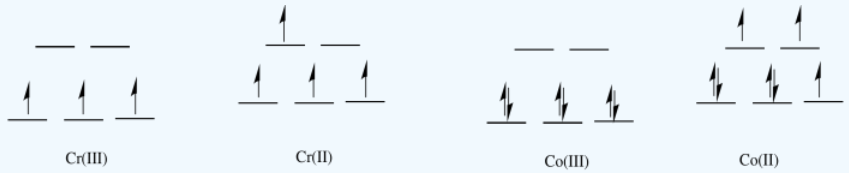
a) octahedral

Answer b

b) In the first row, 2^+ complexes are almost always high spin. However, 3^+ complexes are sometimes low spin.

Answer c

c)



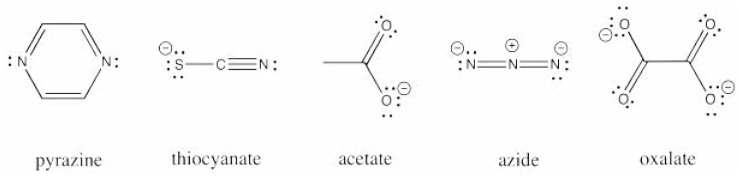
Answer d

d) The Co(II) complex is high spin and labile. The ligands are easily replaced by water.

Answer e

e) The Cr(III) complex is only d^3; it is inert.

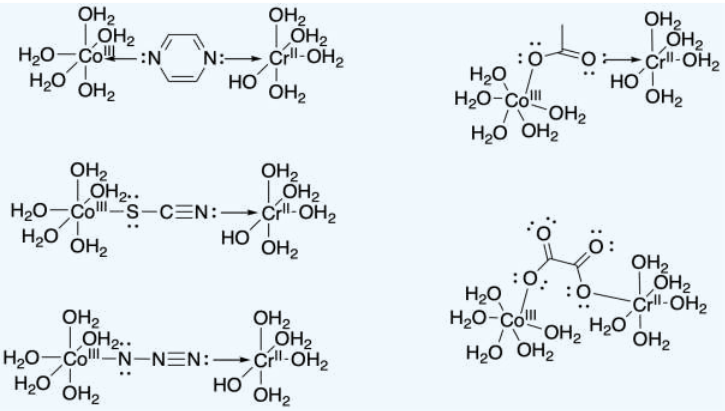
Other ligands can be involved in inner sphere electron transfers. These ligands include carboxylates, oxalate, azide, thiocyanate, and pyrazine ligands. All of these ligands have additional lone pairs with which to bind a second metal ion.



Exercise *Section*7.6.2

Draw an example of each of the ligands listed above bridging between a cobalt(III) and chromium(II) aqua complex.

Answer

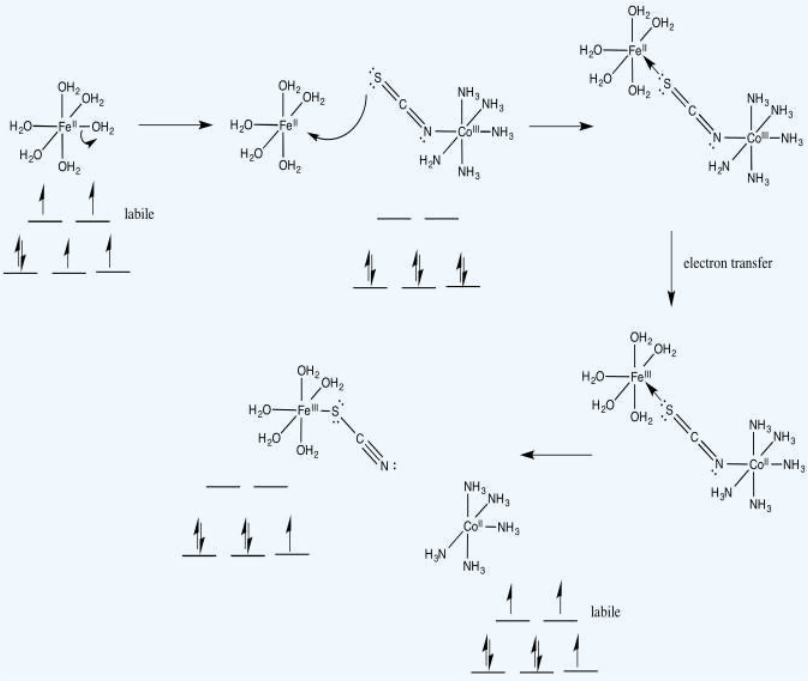


Exercise *Section*7.6.3

Explain, with structures and d orbital splitting diagrams, how the products are formed in the following reaction, in aqueous solution.

$$Fe(OH_2)_6^{2+} + (SCN)Co(NH_3)_5^{2+} \longrightarrow (NCS)Fe(OH_2)_5^{2+} + Co(OH_2)_6^{2+} + 5\,NH_3$$

Answer



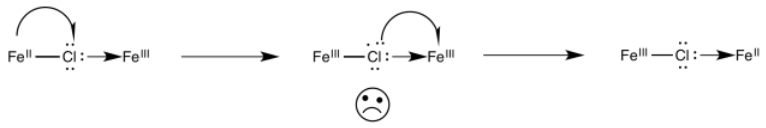
How does the electron travel over the bridge?

Once the bridge is in place, the electron transfer may take place via either of two mechanisms. Suppose the bridging ligand is a chloride. The first step might actually involve an electron transfer from chlorine to the metal; that is, the chloride could donate one electron from one of its idle lone pairs. This electron could subsequently be replaced by an electron transfer from metal to chlorine.



Sometimes, we talk about the place where an electron *used to be*, describing it as a "hole". In this mechanism, the electron donated from the bridging chloride ligand leaves behind a hole. The hole is then filled with an electron donated from the other metal.

Alternatively, an electron might first be transferred from metal to chlorine, which subsequently passes an electron along to the other metal. In the case of chlorine, this idea may be unsatisfactory, because chlorine already has a full octet. Nevertheless, some of the other bridging ligands may have low-lying unoccupied molecular orbitals that could be populated by this extra electron, temporarily.

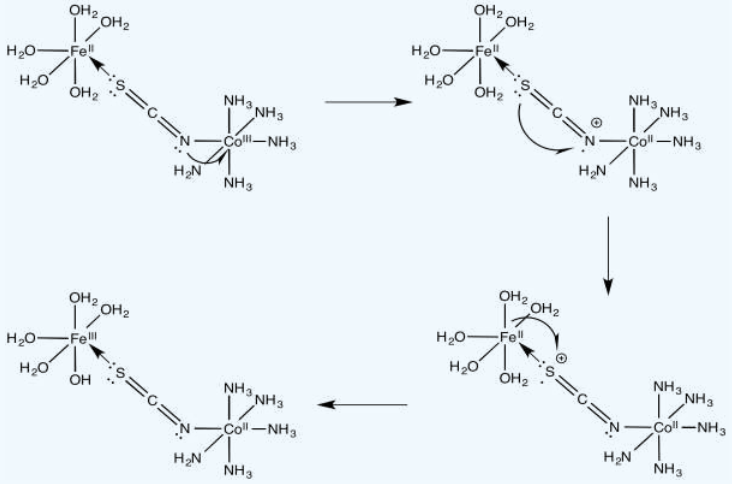


Exercise *Section*7.6.4

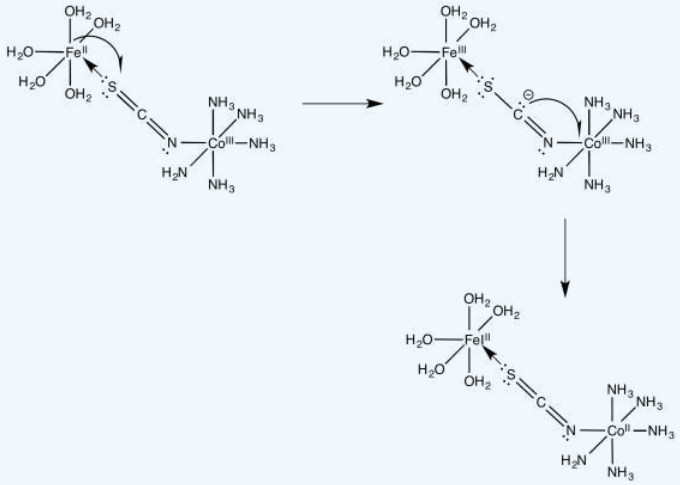
For the iron / cobalt electron transfer in problem Exercise ***Section*7.6.3** (RO9.3.), show

a. an electron transfer mechanism via a hole migration along the bridge
b. an electron transfer mechanism via an electron migration along the bridge

Answer a



Answer b



Exercise *Section*7.6.5

One of the many contributions to the barrier for electron transfer between metal ions is internal electronic reorganization.

a) Draw d orbital splitting diagrams for each of the following metal ions in an octahedral environment.

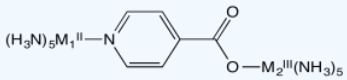
Ru(II) or Os(II)

Ru(III) or Os(III)

Co(II)

Co(III)

Flash photolysis is a method in which an electron can be moved instantly "uphill" from one metal to another (e.g. from M_2^{II} to M_1^{III}, below); the electron transfer rate can then be measured as the electron "drops" back from M_1^{II} to M_2^{III}.



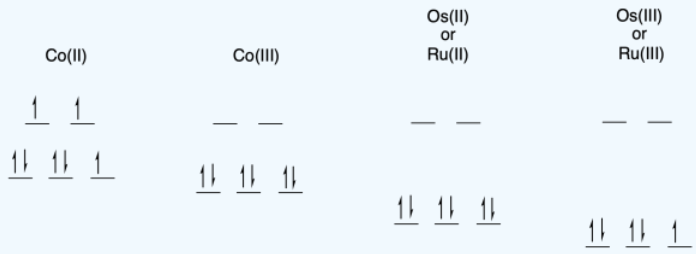
b) Explain the relative rates of electron transfer reaction in this system, as measured by flash photolysis in the table below.

M_1^{II}	M_2^{III}	k_{obs} s^{-1}
Os	Ru	$> 5 \times 10^9$
Os	Co	1.9×10^5

c) Does the reaction above probably occur via an inner sphere or by an outer sphere pathway? Why?

Answer a

a)



Answer b

b) The electron transfer between Os(II) and Ru(III) will not involve any electron reorganization because both are low spin to begin with. However, the electron transfer between Os(II) and Co(III) will result in cobalt changing from low spin to high spin. The need to move electrons between different d orbitals on the cobalt will add to the barrier, slowing down the reaction.

Answer c

c) The pathway is probably inner sphere because of the bridging ligand. Furthermore, the conjugation in the bridging ligand would help in conducting an electron from one end of the ligand to the other, either through an electron mechanism or a hole mechanism.

Exercise *Section*7.6.6

Outer sphere electron transfer rates depend on the free energy change of the reaction (ΔG°) and the distance between oxidant and reductant (d) according to the relation

Rate constant = $k = Ae^{(-\Delta G)}e^{-d}$

a) What happens to the rate of the reaction as distance increases between reactants?

One potential problem in measuring rates of intramolecular electron transfer (i.e. *within* a molecule) is competition from intermolecular electron transfer (*between* molecules).

b) What would you do in the flash photolysis experiment above to discourage intermolecular electron transfer?

c) How could you confirm whether you were successful in discouraging intermolecular reaction?

Answer a

a) The rate decreases exponentially as distance increases.

Answer b

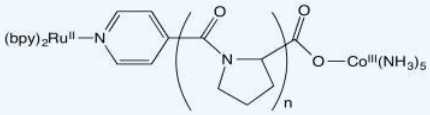
b) You might keep the concentration low in order to increase the distance between molecules, reducing the likely hood of an outer-sphere electron transfer.

Answer c

c) If you ran the experiment at a series of dilutions, intramolecular electron transfer would be unaffected but outer sphere electron transfer would not. If the rates were the same across a number of different concentrations, the reaction would probably be intramolecular.

Exercise *Section* 7.6.7

Stephan Isied and coworkers at Rutgers measured the following electron transfer rates between metal centers separated by a peptide. (*Chem Rev* **1992**, *92*, 381-394)



a. The proline repeating unit is crucial in ensuring a steady increase in distance between metal centers with increased repeat units, n. Why?
b. An inner sphere pathway in this case is expected to be somewhat slow because of the lack of conjugation in the polyproline bridge. Explain why.
c. Plot the data below, with log*k* on the y axis (range from 4-9) and d on the x axis (12-24 Angstroms).

n	d (Å)	k_{obs} (s^{-1})
1	12.2	5×10^8
2	14.8	1.6×10^7
3	18.1	2.3×10^5
4	21.3	5.1×10^4
5	24.1	1.8×10^4

d) A linear relationship is in agreement with Marcus theory; log*k* = - c x d. Is your plot linear?

Isied offers a number of possible explanations for the data, all of which involve two competing reaction pathways.

e) Suggest one explanation for the data.

Answer a

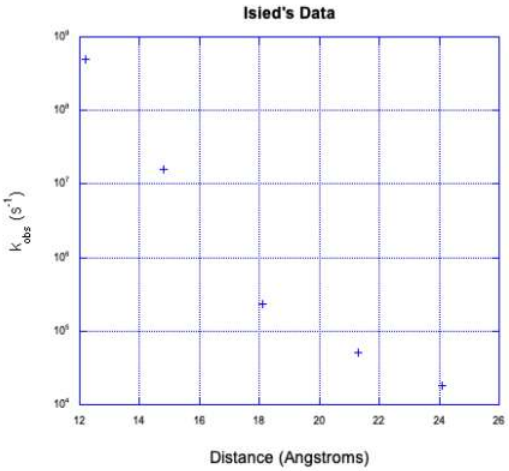
a) Rings are frequently used to introduce conformational rigidity (or decrease conformational flexibility), limiting the range of potential shapes a molecule could adopt. If the molecule can't wiggle around as much, then the distance between the ends of the molecule should be more constant.

Answer b

b) Although the ligand is bridging, it would be difficult to picture either an electron or hole mechanism of inner sphere electron transfer. There are few pi bonds or lone pairs to use as places to put electrons or temporarily remove electrons from, shuttling the electrons from place to place along the ligand. A conjugated system would be much more likely to carry out inner sphere electron transfer.

Answer c

c)



Answer d

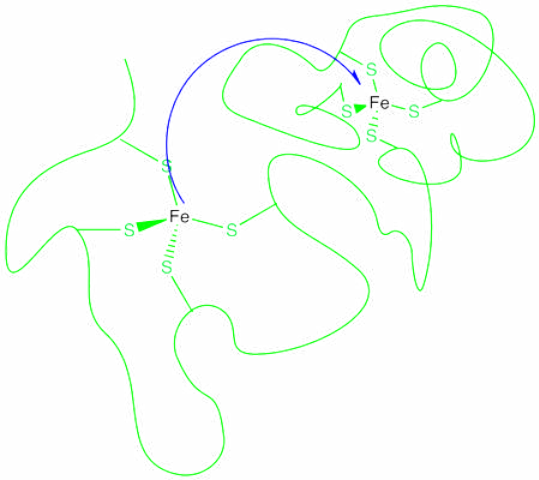
d) The data is not linear.

Answer e

e) The data appear to show two lines that cross. That's a classic symptom of two competing mechanisms. The faster mechanism, to the left, is probably an intramolecular electron transfer. The slower mechanism, to the right, may be an intermolecular electron transfer.

Outer Sphere Electron Transfer

Without a bridging ligand, how does an electron get from one metal to another? This might be a more difficult task than it seems. In biochemistry, an electron may need to be transferred a considerable distance. Often, when the transfer occurs between two metals, the metal ions may be constrained in particular binding sites within a protein, or even in two different proteins.



That means the electron must travel through space to reach its destination. Its ability to do so is generally limited to just a few Angstroms (remember, an Angstrom is roughly the distance of a bond). Still, it can react with something a few bond lengths away. Most things need to actually bump into a partner before they can react with it.

This long distance hop is called an outer sphere electron transfer. The two metals react without ever contacting each other, without getting into each others' coordination spheres. Of course, there are limitations to the distance involved, and the further away the metals, the less likely the reaction. But an outer sphere electron transfer seems a little magical.

Barrier to Reaction: A Qualitative Picture of Marcus Theory

So, what holds the electron back? What is the barrier to the reaction? Rudy Marcus at Caltech has developed a mathematical approach to understanding the kinetics of electron transfer, in work he did beginning in the late 1950's. We will take a very qualitative look at some of the ideas in what is referred to as "Marcus Theory". An electron is small and very fast. All those big, heavy atoms involved in the picture are lumbering and slow. The barrier to the reaction has little to do with the electron's ability to whiz around, although even that is limited by distance. Instead, it has everything to do with all of those things that are barely moving compared to the electron.

Imagine an iron(II) ion is passing an electron to an iron(III) ion. After the electron transfer, they have switched identities; the first has become an iron(III) and the second has become an iron(II) ion.

Nothing could be simpler. The trouble is, there are big differences between an iron(II) ion and an iron(III) ion. For example, in a coordination complex, they have very different bond distances. Why is that a problem? Because when the electron hops, the two iron atoms find themselves in sub-optimal coordination environments.

Exercise *Section*7.6.1

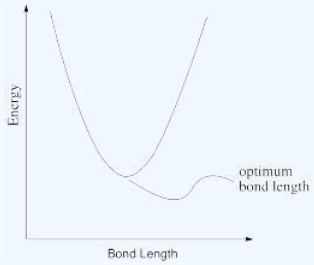
Suppose an electron is transferred from an Fe(II) to a Cu(II) ion. Describe how the bond lengths might change in each case, and why. Don't worry about what the specific ligands are.

Answer

The bonds to iron would contract because the increased charge on the iron would attract the ligand donor electrons more strongly. The bonds to copper would lengthen because of the lower charge on the copper.

Exercise *Section*7.6.2

In reality, a bond length is not static. If there is a little energy around, the bond can lengthen and shorten a little bit, or vibrate. A typical graph of molecular energy vs. bond length is shown below.



a. Why do you think energy increases when the bond gets shorter than optimal?
b. Why do you think energy increases when the bond gets longer than optimal?
c. In the following drawings, energy is being added as we go from left to right. Describe what is happening to the bond length as available energy increases.

Answer a

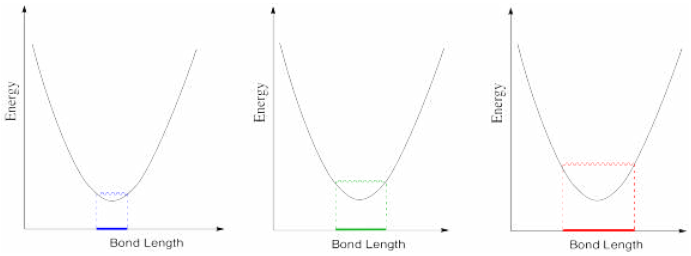
a) Most likely there are repulsive forces between ligands if the bonds get too short.

Answer b

b) Insufficient overlap between metal and ligand orbitals would weaken the bond and raise the energy.

Answer c

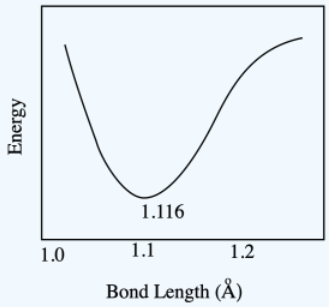
c) The range of possible bond lengths gets broader as energy is increased. The bond has more latitude, with both longer and shorter bonds allowed at higher energy.



Exercise *Section*7.6.3

The optimum C-O bond length in a carbon dioxide molecule is 1.116 Å. Draw a graph of what happens to internal energy when this bond length varies between 1.10 Å and 1.20 Å. Don't worry about quantitative labels on the energy axis.

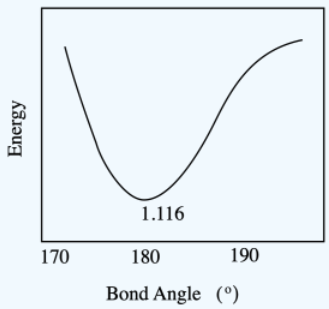
Answer



Exercise *Section*7.6.4

The optimum O-C-O bond angle in a carbon dioxide molecule is 180 °. Draw a graph of what happens to internal energy when this bond angle varies between 170 ° and 190 °. Don't worry about quantitative labels on the energy axis.

Answer



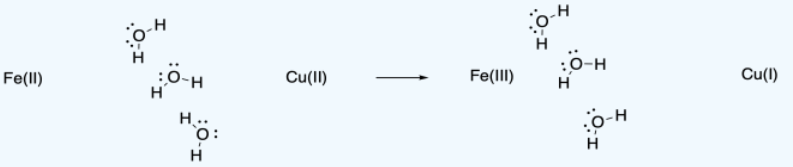
The barrier to electron transfer has to do with reorganizations of all those big atoms before the electron makes the jump. In terms of the coordination sphere, those reorganizations involve bond vibrations, and bond vibrations cost energy. Outside the coordination sphere, solvent molecules have to reorganize, too. Remember, ion stability is highly influenced by the surrounding medium.

Exercise *Section*7.6.5

Draw a Fe(II) ion and a Cu(II) ion with three water molecules located somewhere in between them. Don't worry about the ligands on the iron or copper. Show how the water molecules might change position or orientation if an electron is transferred from iron to copper.

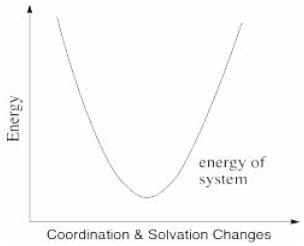
Answer

The water molecules may pivot toward the more highly charged Fe(III), or they may shift closer to it because of the attraction between the ion and the dipole of the water molecule.



Keep in mind that such adjustments would happen in non-polar solvents, too, although they would involve weaker IMFs such as ion - induced dipole interactions.

Thus, the energetic changes needed before electron transfer can occur involve a variety of changes, including bond lengths of several ligands, bond angles, solvent molecules, and so on. The whole system, involving both metals, has some optimum set of positions of minimum energy. Any deviations from those positions requires added energy. In the following energy diagram, the x axis no longer defines one particular parameter. Now it lumps all changes in the system onto one axis. This picture is a little more abstract than when we are just looking at one bond length or one bond angle, but the concept is similar: there is an optimum set of positions for the atoms in this system, and it would require an input of energy in order to move any of them move away from their optimum position.

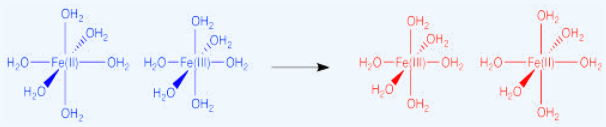


It is thought that these kinds of reorganizations -- involving solvent molecules, bond lengths, coordination geometry and so on -- actually occur prior to electron transfer. They happen via random motions of the molecules involved. However, once they have happened, there is nothing to hold the electron back. Its motion is so rapid that it can immediately find itself on the other atom before anything has a chance to move again.

Consequently, the barrier to electron transfer is just the amount of energy needed for all of those heavy atoms to get to some set of coordinates that would be accessible in the first state, before the electron is transferred, but that would also be accessible in the second state, after the electron is transfered.

Exercise *Section*7.6.6

Describe some of the changes that contribute to the barrier to electron transfer in the following case.

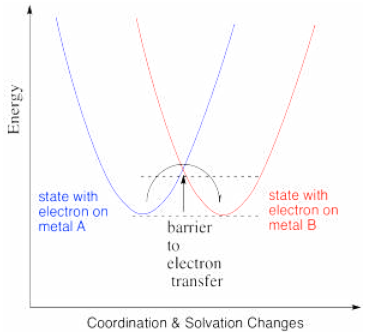


Answer

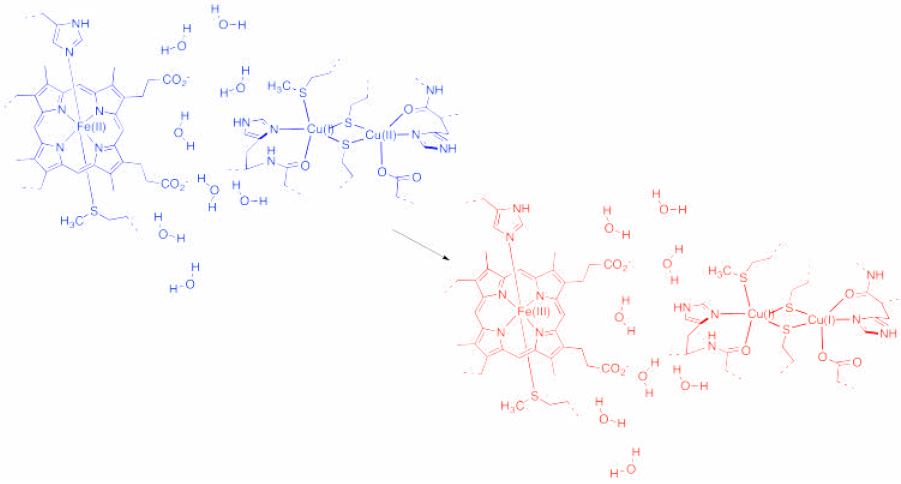
The reactants and products are very similar in this case. However, the Fe(III) complex has shorter bonds than the Fe(II) complex because of greater electrostatic interaction between the metal ion and the ligands. These changes in bond length

needed in order to get ready to change from Fe(III) to Fe(II) (or the reverse) pose a major barrier to the reaction.

In the drawing below, an electron is transferred from one metal to another metal of the same kind, so the two are just switching oxidation states. For example, it could be an iron(II) and an iron(III), as pictured in the problem above. In the blue state, one iron has the extra electron, and in the red state it is the other iron that has the extra electron. The energy of the two states are the same, and the reduction potential involved in this transfer is zero. However, there would be some atomic reorganizations needed to get the coordination and solvation environments adjusted to the electron transfer. The ligand atoms and solvent molecules have shifted in the change from one state to another, and so our energy surfaces have shifted along the x axis to reflect that reorganization.



That example isn't very interesting, because we don't form anything new on the product side. Instead, let's picture an electron transfer from one metal to a very different one. For example, maybe the electron is transferred from cytochrome c to the "copper A" center in cytochrome c oxidase, an important protein involved in respiratory electron transfer.



Exercise *Section*7.6.7

In the drawing above, some water molecules are included between the two metal centres.

a. Explain what happens to the water molecules in order to allow electron transfer to occur, and why.
b. Suppose there were a different solvent, other than water, between the complexes. How might that affect the barrier to the reaction?

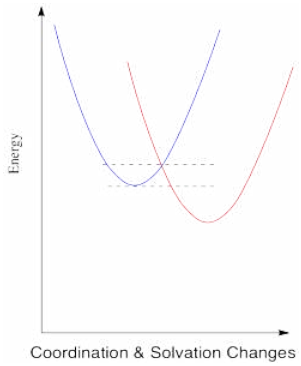
Answer a

a) The drawing is an oversimplification, but in general the water molecules are shown reorienting after the electron transfer because of ion-dipole interactions. In this case, the waters are shown orienting to present their negative ends to the more positive iron atom after the electron transfer. In reality, in a protein there are lots of other charges (including charges on the ligand) that may take part in additional ion-dipole interactions.

Answer b

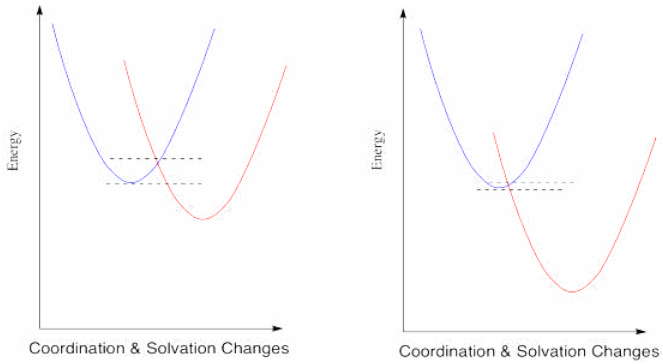
b) Because electron transfer is so fast, atomic and molecular reorganisations are actually thought to happen before the electron transfer. The water molecules would happen to shift into a position that would provide the greatest possible stabilisation for the ions and then the electron would be transferred. A less polar solvent than water would be less able to stabilize ions and the electron would be slower to transfer as a result. In addition, a less polar solvent than water would be a poor medium to transmit an electron, which is charged and therefore stabilized by interactions with polar solvents.

The energy diagram for the case involving two different metals is very similar, except that now there is a difference in energy between the two states. The reduction potential is no longer zero. We'll assume the reduction potential is positive, and so the free energy change is negative. Energy goes down upon electron transfer.



Compare this picture to the one for the degenerate case, when the electron is just transferred to a new metal of the same type. A positive reduction potential (or a negative free energy change) has the effect of sliding the energy surface for the red state downwards. As a result, the intersection point between the two surfaces also slides downwards. Since that is the point at which the electron can slide from one state to the other, the barrier to the reaction decreases.

What would happen if the reduction potential were even more positive? Let's see in the picture below.



The trend continues. According to this interpretation of the kinetics of electron transfer, the more exothermic the reaction, the lower its barrier will be. It isn't always the case that kinetics tracks along with thermodynamics, but this might be one of them.

But is all of this really true? We should take a look at some experimental data and see whether it truly works this way.

Oxidant	E°	k ($M^{-1}s^{-1}$) (margin of error shown in parentheses)
$Co(diene)(NH_3)_2^{3+}$	0.12	3.0(4)
$Co(diene)H_2O)NCS^{2+}$	0.38	11(1)
$Co(diene)(H_2O)_2^{3+}$	0.53	800(100)
Co(EDTA)	0.60	6000(1000)

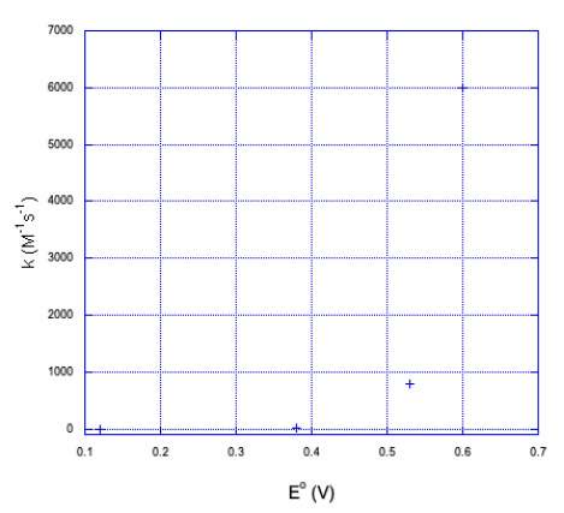
As the reduction potential becomes more positive, free energy gets more negative, and the rate of the reaction dramatically increases. So far, Marcus theory seems to get things right.

Exercise *Section*7.6.8

a. Plot the data in the above table.
b. How would you describe the relationship? Is it linear? Is it exponential? Is it direct? Is it inverse?
c. Plot rate constant versus free energy change. How does this graph compare to the first one?

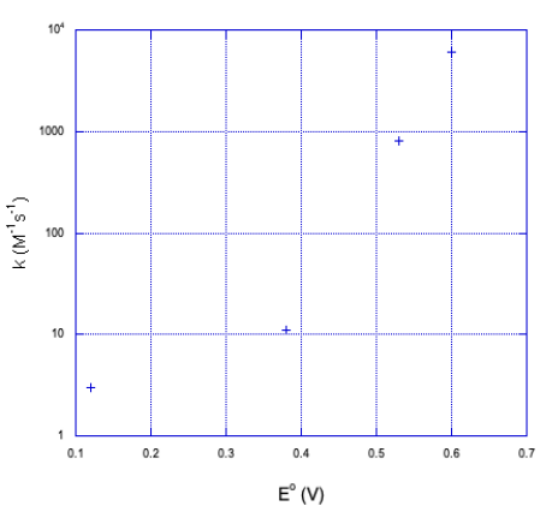
Answer a

a) Here is a plot of the data.



Answer b

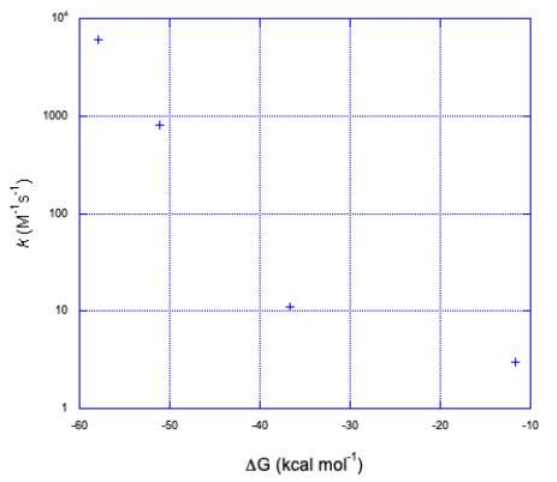
b) It doesn't look linear. If we plot the y axis on a log scale, things become a little more linear.



It looks closer to a logarithmic relationship than a linear one.

Answer c

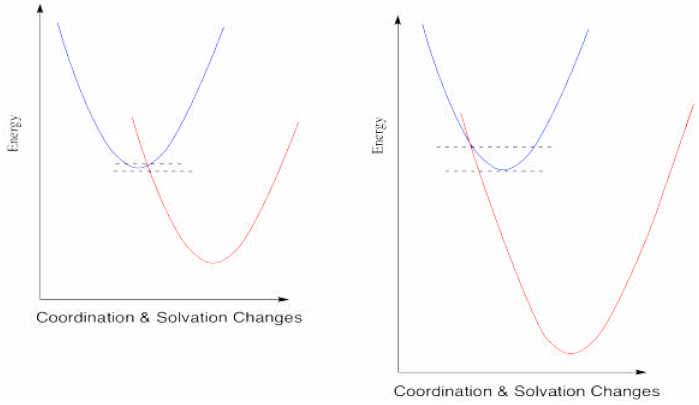
c) Assuming one electron transfer:



The graph takes the same form but in the opposite direction along the x axis.

Marcus Inverted Region

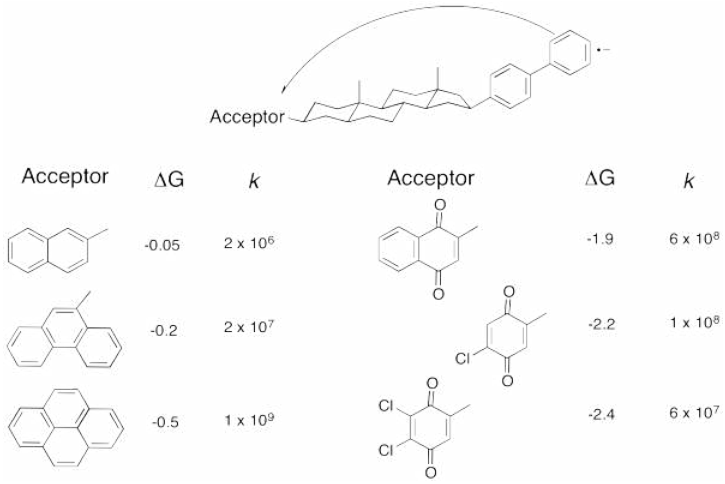
When you look a little closer at Marcus theory, though, things get a little strange. Suppose we make one more change and see what happens when the reduction potential becomes *even more* positive.



So, if Marcus is correct, at some point as the reduction potential continues to get more positive, reactions start to slow down again. They don't just reach a maximum rate and hold steady at that plateau; the barrier gets higher and higher and the reactions get slower and slower. If you feel a little skeptical about that, you're in good company.

Marcus always maintained that this phenomenon was a valid aspect of the theory, and not just some aberration that should be ignored. The fact that nobody had ever actually observed such a trend didn't bother him. The reason we didn't see this kind of thing, he said, was that we just hadn't developed technology that was good enough to measure these kind of rates accurately.

But technology did catch up. Just take a look at the following data (from Miller, *J. Am.Chem. Soc.* **1984**, *3047*).



Don't worry that there are no metals involved anymore. An electron transfer is an electron transfer. Here, an electron is sent from the aromatic substructure on the right to the substructure on the left. By varying the part on the left, we can adjust the reduction potential (or the free energy change, as reported here.

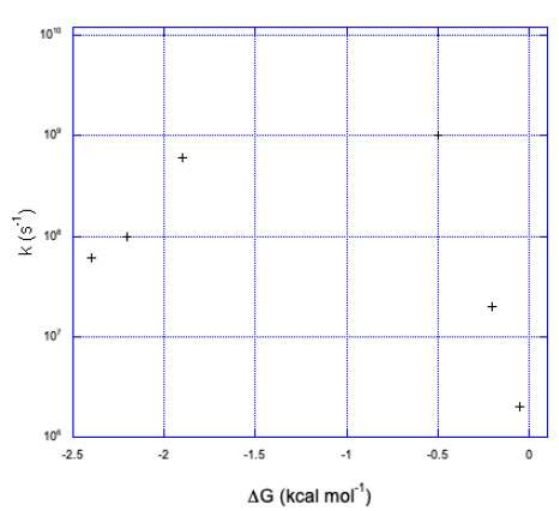
Exercise *Section*7.6.9

a. Plot the data in the above table.

b. How would you describe the relationship?

Answer a

a)



Answer b

b) We can see two sides of an inverted curve. The reaction gets much faster as the free energy becomes more negative, but at some point the rate begins to decrease again.

As the reaction becomes more exergonic, the rate increases, but then it hits a maximum and decreases again. Data like this means that the "Marcus Inverted Region" is a real phenomenon. Are you convinced? So were other people. In 1992, Marcus was awarded the Nobel Prize in Chemistry for this work.

Exercise *Section*7.6.10

Take a look at the donor/acceptor molecule used in Williams' study, above. a) Why do you suppose the free energy change is pretty small for the first three compounds in the table? b) Why does the free energy change continue to get bigger over the last three compounds in the table?

Answer

The acceptor compound becomes an anion when it accepts an electron. The first three compounds do not appear to be strongly electrophilic; they can accept electrons simply because of resonance stability of the resulting anion. The last three have electron withdrawing groups (chlorines and oxygens) that would stabilize the anion even further.

Exercise *Section*7.6.11

The rates of electron transfer between cobalt complexes of the bidentate bipyridyl ligand, $Co(bipy)_3^{n+}$, are strongly dependent upon oxidation state in the redox pair. Electron transfer between Co(I)/Co(II) occurs with a rate constant of about 10^9 $M^{-1}s^{-1}$, whereas the reaction between Co(II)/Co(III) species proceeds with k = 18 $M^{-1}s^{-1}$.

a. What geometry is adopted by these complexes?
b. Are these species high spin or low spin?
c. Draw d orbital splitting diagrams for each complex.
d. Explain why electron transfer is so much more facile for the Co(I)/Co(II) pair than for the Co(II)/Co(III) pair.

Answer a

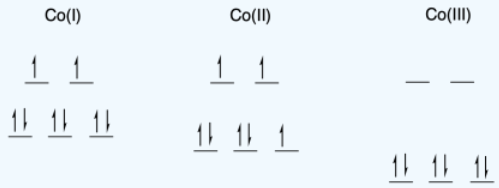
a) octahedral; bpy is a bidentate ligand.

Answer b

b) Co is first row; Co(I) and Co(II) have relatively low charge. Usually we would expect them to be high spin. Co(III) is at a cut-off point in the first row; it is just electronegative enough that it is usually low spin.

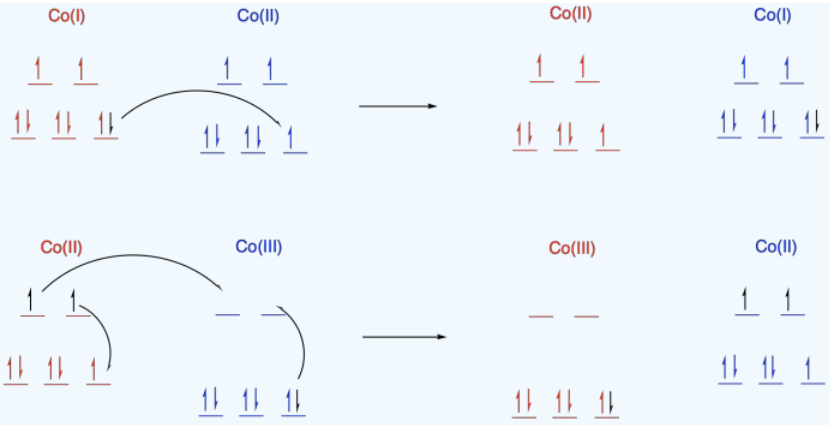
Answer c

c)



Answer d

d) In a transfer from Co(II) to Co(III), there is additional reorganization needed because the metal changes between high and low spin. Not only does one electron have to move from one metal to another metal, but additional electrons have to shuffle from one orbital to another on the same metal to accommodate the change. These reorganizations have a barrier, slowing the reaction.



Attribution

Chris P Schaller, Ph.D., (College of Saint Benedict / Saint John's University)

Section 7.6: Electron Transfer Reactions is shared under a CC BY-NC-SA 4.0 license and was authored, remixed, and/or curated by LibreTexts.

- **10.5: Electron Transfer Reactions** is licensed CC BY-NC-SA 4.0.

CHAPTER OVERVIEW

Chapter 8: Coordination Chemistry - Electronic Spectra

- Section 8.1: Absorption of Light
  - Section 8.1.1: Beer-Lambert Absorption Law
- Section 8.2: Quantum Numbers of Multielectron Atoms
  - Section 8.2.1: Finding Microstates and Term Symbols
  - Section 8.2.2: Spin-Orbit Coupling
- Section 8.3: Electronic Spectra of Coordination Compounds
  - Section 8.3.1: Tanabe-Sugano Diagrams
  - Section 8.3.2: Symmetry labels for split terms
  - Section 8.3.3: Selection Rules
  - Section 8.3.4: Correlation Diagrams
  - Section 8.3.5: Applications of Tanabe-Sugano Diagrams
  - Section 8.3.6: Tetrahedral Complexes
  - Section 8.3.7: Charge-Transfer Spectra
  - Section 8.3.8: Applications of Charge-Transfer

Chapter 8: Coordination Chemistry - Electronic Spectra is shared under a CC BY-NC-SA 4.0 license and was authored, remixed, and/or curated by LibreTexts.

Section 8.1: Absorption of Light

Introduction

The d-orbital splitting in coordination complexes results in a gap (Δ) that happens to be just the right magnitude to absorb visible light. Because metal complexes can absorb visible light, they display an array of colors. Not only is the color attractive to the eye, it is an indication of the chemical and physical properties of the metal complex. The color (like the magnitude of Δ) depends on the identity of the metal ion, the coordination geometry, and the ligand identity. Chemists don't just "look" at color, though - we measure it using electronic absorption spectroscopy. This is usually done in a lab using a UV-visible spectrophotometer.

An example of such a measurement is shown below in Figure ***Section*8.1.1** for a Cu(II) complex. The sample appears a pink color to the eye, and when it is measured using a UV-visible spectrometer, it is shown to absorb visible light at approximately 530 nm. The absorption spectrum can indicate the oxidation state of Cu, the ligands bound to the Cu(II) ion, and the coordination geometry. The color of the solution in Figure ***Section*8.1.1** is a shade of pink.

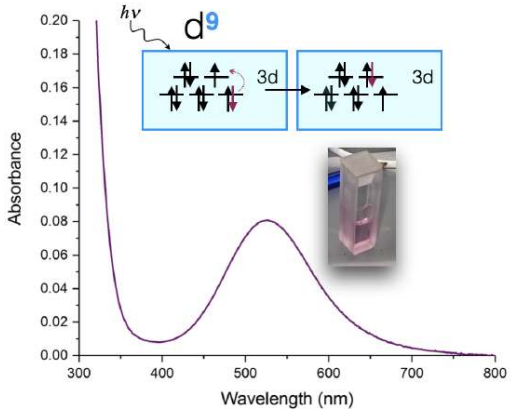


Figure ***Section*8.1.1**: A UV-visible spectrum of a Cu(II)-peptide complex. A photo of the sample shows its pink color. The splitting diagram for its approximation as an octahdral complex is shown, where an electronic transition from t_{2g} to e_g is shown. (CC-BY-NC-SA; Kathryn Haas)

We observe the complementary color of light absorbed

The absorption spectrum shown above in Figure ***Section*8.1.1** is a simple case in which only one absorption band is observed in the visible region of the spectrum. In a simple case like this, the color of a complex can be predicted as the complementary color of the light absorbed by the solution. When a solution or object absorbs a certain wavelength, we see the complementary color; or the color opposite to the absorbed wavelength on the color wheel in Figure ***Section*8.1.2**. In the case of the Cu(II) complex spectrum shown in Figure ***Section*8.1.1**, the color of the light absorbed at 530 nm is green, and the predicted color observed is pink.

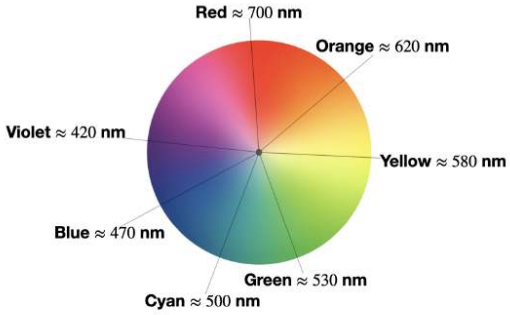


Figure ***Section*8.1.2**: Color wheel with approximate wavelengths of colors. (CC-BY-NC-SA; Kathryn Haas)

The table below lists the approximate colors of absorption corresponding to wavelengths of light absorbed, and gives similar information to that deduced from Figure ***Section*8.1.2**.

Table ***Section*8.1.1**: Approximate wavelengths of absorption and their complementary colors observed. * This prediction is limited to simple cases where there is only one absorption band in the visible spectrum.

λ absorbed	E (cm^{-1})	E (eV)	Approximate color absorbed	Predicted color observed (by eye)
> 700 nm	$< 14,000 \frac{1}{cm}$	< 1.77 eV	Infrared	not observable
$\approx 700 - 635$ nm	$\approx 14,300 - 16,000 \frac{1}{cm}$	$\approx 1.77 - 1.95$ eV	Red	Green
$\approx 635 - 590$ nm	$\approx 15,700 - 16,900 \frac{1}{cm}$	$\approx 1.95 - 2.10$ eV	Orange	Blue
$\approx 590 - 560$ nm	$\approx 16,900 - 17,900 \frac{1}{cm}$	$\approx 2.10 - 2.21$ eV	Yellow	Violet
$\approx 560 - 520$ nm	$\approx 17,900 - 19,200 \frac{1}{cm}$	$\approx 2.21 - 2.38$ eV	Green	Red
$\approx 520 - 490$ nm	$\approx 19,200 - 20,400 \frac{1}{cm}$	$\approx 2.38 - 2.53$ eV	Cyan	Red-Orange
$\approx 490 - 450$ nm	$\approx 20,400 - 22,200 \frac{1}{cm}$	$\approx 2.53 - 2.76$ eV	Blue	Orange
$400 - 450$ nm	$\approx 22,200 - 25,000 \frac{1}{cm}$	$\approx 2.76 - 3.10$ eV	Violet	Yellow
<400 nm	$> 25,000 \frac{1}{cm}$	> 3.10 eV	Ultraviolet (UV)	not observable

Energy of electronic absorption

The absorption spectrum of a metal complex can be used to calculate the splitting energy, Δ, when the absorption corresponds to a $d \rightarrow d$ transition. Let's use the d^9 Cu(II) complex (discussed above) as an example. A d^9 metal ion has only one visible-light $d \rightarrow d$ transition. Let's assume that the coordination geometry is *approximately* octahedral (although it is actually a Jahn-Teller distorted octahedron, and more like a square plane). If we assume it's octahedral, then the d-orbital splitting diagram (see Figure *Section*8.1.1) leads us to expect one electronic transition: an electron is excited from the t_{2g} to e_g. The energy absorbed is equal to the energy of the Δ.

Many cases are not as simple as a d^9 octahedral case because there are multiple possible electronic transitions, and also multiple absorption bands in the UV-vis spectrum. In these more complex cases, the actual energy of the transition are affected by differences in electron-electron repulsion energies in the ground state and the excited states. We will learn how to account for multiple possible excited states and electron-electron repulsions using Tanabe-Sugano diagrams later in this chapter.

This page titled Section 8.1: Absorption of Light is shared under a CC BY-NC-SA 4.0 license and was authored, remixed, and/or curated by Kathryn Haas.

- **11.1: Absorption of Light** by Kathryn Haas has no license indicated.

Section 8.1.1: Beer-Lambert Absorption Law

When light passes through a solution that absorbs light, it enters the solution with an initial intensity (I_o) at a given wavelength, and it emerges with an intensity, I.

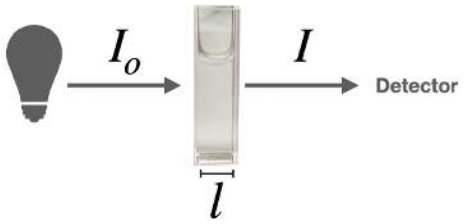


Figure *Section*8.1.1.1: Initial intensity (I_o) of light passes through a solution and emerges as intensity, I. The path length is l. (CC-BY; Kathryn Haas)

The Beer-Lambert Law defines the relationship between absorbance at a given wavelength and the concentration of the solution.

$$\log\left(\frac{I_o}{I}\right) = A = \varepsilon l c \qquad \text{(Section 8.1.1.1)}$$

The absorbance (A) is a unitless number because $\frac{I_o}{I}$ is unitless. The absorbance depends on the concentration (c) and the path length (l). The concentration of the sample solution is measured in molarity (M) and the length of the light path in centimeters (cm). The Greek letter epsilon (ε) in these equations is called the **molar absorptivity** (also called the **molar absorption coefficient**). The units of ε are $\frac{L}{mol \times cm}$ or $L \times mol^{-1} \times cm^{-1}$.

Chemists most often measure and report absorbed light in terms of wavelength (λ) in units of nanometers (nm). But the wavelength scale is inconvenient for measuring energy because it is inversely proportional to both frequency and energy. In other disciplines, like physics for example, absorption spectra are more often reported in terms of frequency (ν) using units of inverse centimeters (cm^{-1}). The relationships between energy (E), ν, and λ are given by the equation below:

$$E = h\nu = \frac{hc}{\lambda} = hc\left(\frac{1}{\lambda}\right) = hc\bar{\nu} \qquad \text{(Section 8.1.1.2)}$$

This page titled Section 8.1.1: Beer-Lambert Absorption Law is shared under a CC BY-NC-SA 4.0 license and was authored, remixed, and/or curated by Kathryn Haas.

- **11.1.1: Beer-Lambert Absorption Law** by Kathryn Haas has no license indicated.

Section 8.2: Quantum Numbers of Multielectron Atoms

Note

The quantum numbers of atoms (and ions) correspond to quantized energy states, called microstates, that depend on the electron configuration. Electrons within a subshell or orbital can adopt different configurations of their electrons, with different individual quantum numbers. These different electron configurations are **microstates**, and they can be grouped into **terms** and ordered according to their relative energies. Since electronic transitions occur between terms of different energies, knowledge of the terms for a given atom or ion can aid in the interpretation of electronic spectra.

Introduction

Transition metal ions can give rise to a spectrum of beautifully colored colored complexes. The colors are often caused by absorption of visible light due to electronic transitions involving metal d-orbitals. These electronic transitions are not only attractive to the eye, they are useful spectroscopic signals because the transitions occur between quantized electronic energy states, called microstates. Spectroscopy, coupled with knowledge of the possible microstates and their energies can yield clues about molecular structure.

To learn what a microstate is, let's use the simple example of a carbon atom with a $1s^2 2s^2 2p^2$ electron configuration. The s subshell is full, and there is only one way to put two electrons into an s subshell. Both electrons must occupy the orbital having $m_l = 0$, and each must have opposite spins, ($m_s = +\frac{1}{2}$), and ($m_s = -\frac{1}{2}$). On the other hand, the p subshell of carbon has two electrons that can occupy any of three orbitals (Figure *Section*8.2.1). This leaves room for different orientations of the electrons within the p subshell. Each different electron configuration is a **microstate**, and each has an energy that can be distinguished using electronic spectroscopy (UV-vis for example). In the case of a carbon atom with a two p electrons, there are 15 different possible microstates, as illustrated in Figure *Section*8.2.1.

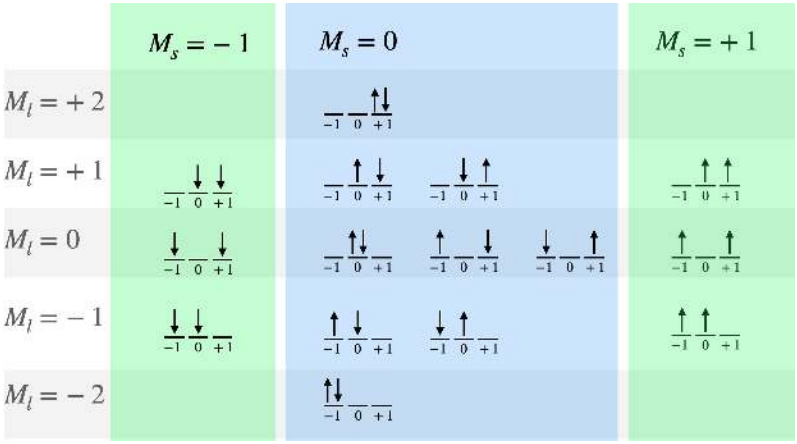


Figure *Section*8.2.1: Fifteen possible microstates for two electrons in a p subshell. These microstates are organized according to their total spin (M_s) and total magnetic (M_l) quantum numbers. Arrows pointing upward represent electrons with $m_s = +\frac{1}{2}$, and those pointing downward represnt $m_s = -\frac{1}{2}$. Each horizontal line represents a p orbital, and m_l values are indicated under each orbital. (CC-BY-NC; Kathryn Haas)

Just as individual electrons have quantum numbers (n, l, m_l, m_s), the electronic states of atoms have quantum numbers (L, M_l, M_s, S, J). Each individual microstate in Figure *Section*8.2.1 can be described by quantum numbers M_l and M_s. The values of total angular momentum (L), and total intrinsic spin (S) arise from sets of microstates, and are related to quantum numbers M_l and M_s for individual microstates. The relative energies of the terms for 3d metals and other light atoms can be predicted (roughly) by Hund's Rules, according to values of S and L. These atomic quantum numbers and Hund's rules are described below.

A closer look at electronic spectra

Let us take a closer look at optical absorption spectra, also called electronic spectra, of coordination compounds. We have previously argued that ligand field theory can predict and explain the electronic spectra. However, ligand field theory (LFT) is sufficient to explain the spectra in only a few cases. For example the $[Ni(H_2O)_6]^{2+}$ ion is an octahedral d^8-complex ion. According

to LFT, the metal d-orbitals in an octahedral field are the t_{2g} and the e_g–orbitals (Figure *Section*8.2.2). Six electrons are in the t_{2g} orbitals, and two electrons are in the e_g orbitals (Figure *Section*8.2.2). Ligand field theory (LFT) would predict that there is one electron transition possible, namely the promotion of an electron from a t_{2g} into an e_g orbital. This process would be triggered by the absorption of light whereby the wavelength of the light would depend on the Δ_o between the t_{2g} and the e_g orbitals. Overall, this should lead to a single absorption band in the absorption spectrum of the complex. We can check this prediction by experimentally recording the absorption spectrum of the complex (Figure *Section*8.2.2).

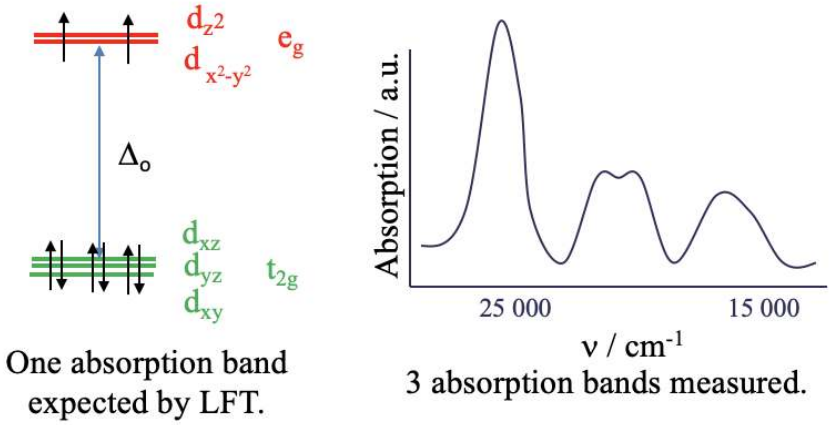


Figure *Section*8.2.2. Electron transition according to LFT and actual absorption spectrum of the $[Ni(H_2O)_6]^{2+}$ complex ion. Attribution: E.R. Schofield.

What we find is that the absorption spectrum is far more complex than expected. Instead of just a single absorption band there are multiple ones. Obviously, LFT is unable to explain this spectrum. The question is: why? The answer is: LFT assumes that there are no electron-electron interactions. However, in reality there is repulsion between electron in d-orbitals and this has an effect on their energy. And, electrons within the d-subshell, for example, repel each other to different extents depending on the relative orientations of their orbitals in space.

To illustrate how electrons in different orbitals might have different interactions, let's consider the case of a d^2 excited state in an octahedral ligand field (Figure *Section*8.2.3).

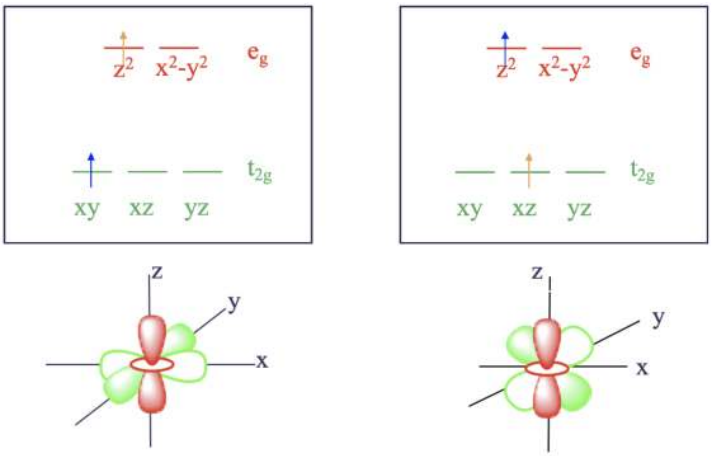


Figure *Section*8.2.3: Two microstates with different energies for a d^2 ion in an octahedral ligand field. Electron configurations of two different microstates are shown on the top, and the orbitals associated with each shown underneath each configuration. Left: An excited microstate with one electron in the d_{xy} orbital (shown in green) and one electron in the d_{z^2} (shown in red). Right: An excited microstate with one electron in the d_{xz} orbital (shown in green) and one electron in the d_{z^2} (shown in red).

According to LFT, both electrons would be in the t_{2g} orbitals in the ground state. For instance, they could be in the microstate where one electron is in d_{xy}, and the other is in the d_{xz} orbital (not pictured). This configuration is called a microstate of a state because there are other combinations of orbitals possible. For example, the ground state would also be realized by a microstate in which the electrons were in the d_{xz} and the d_{yz} orbitals. Upon absorption of light, the electron in the d_{xy} orbital could be excited into one of the higher-energy e_g orbitals. That excited electron could occupy either the d_{z^2} or the $d_{x^2-y^2}$ orbitals. Those two possibilities

reflect two different microstates associated with the excited state. For a moment, let's assume that the excited electron goes into the d_{z^2} orbital. In this microstate one electron would be in the d_{xz} orbital and the other one in the d_{z^2} orbital (Figure *Section*8.2.3, right). There is another possibility for how to excite an electron from the ground state. We could assume that instead of the d_{xy} electron being promoted, the d_{xz} electron gets promoted. In this case, we would realize a microstate in which one electron in the d_{xy} orbital and the other one in the d_{z^2} orbital (Figure *Section*8.2.3, left).

Now let us compare the two cases shown in Figure *Section*8.2.3. Ligand field theory would argue that both excited microstates have the same energy. However, in fact they do not. Why? It is because the electrons in the first excited microstate interact differently than those of the second excited microstate. This difference becomes plausible when considering the orbital shapes and orientations (Figure *Section*8.2.3, bottom). The d_{xz} orbital has electron density on the z-axis, while the d_{xy} orbital is perpendicular to d_{z^2}. The different relative orientations of d_{xy} and d_{xz} with respect to d_{z^2} cause electrons in the d_{z^2} orbital to interact differently with an electron in a d_{xy} than in a d_{xz}. As a result, the two excited microstates do not have the same energy. In other words, to achieve either of these different excited microstates from the ground state, we need different amounts of energy. Thus, the complex would absorb light with different energies (or wavelengths). This is in contrast to what LFT predicts.

If LFT cannot predict the number of electronic transitions, then how can we correctly predict how many absorption bands we get? The answer is, we must find all possible microstates for the d^2 electron configuration and group together those with the same energy. A group of microstates with the same energy is called a **term**. *The number of electron transitions can then be predicted from the number of terms.*

Quantum Numbers

The table below summarizes the quantum numbers of atoms (individual microstates and sets of microstates). You may wish to review the quantum numbers for individual electrons and then refer to this table as you read this and the next sections. Recall the meanings of the quantum numbers for individual electrons (n, l, m_l, m_s that were described in a previous section (Section 2.2.2).

Symbol	Name	Allowed Range	Comment
L	Total Orbital Angular Momentum	$\lvert l_1 + l_2\rvert, \lvert l_1 + l_2\text{-}1\rvert, \ldots, \lvert l_1\text{-}l_2\rvert$	Total *orbital* angular momentum of a *collection of microstates*, designated as S, P, D, F..etc
S	Total Intrinsic Spin	$\lvert m_{s1} + m_{s2}\rvert, \lvert m_{s1} + m_{s2}\text{-}1\rvert, \ldots, \lvert m_{s1}\text{-}m_{s2}\rvert$	Total spin of a *collection of microstates*
M_l	Magnetic Quantum Number	$L, L-1, L-2, \ldots, -L$	Direction of total angular momentum for an individual microstate
M_s	Spin Magnetic Quantum Number	$S, S-1, S-2, \ldots -S$	Total spin of electrons for an individual microstate
J	Total Angular Momentum	$L+S, \ldots, \lvert L-S\rvert$	Total angular momentum

Quantum Numbers S and L for sets of microstates

The quantum numbers S and L represent sets of microstates. Once these values are found, they can be ordered in terms of relative energies, first according to the value of S, then L.

Total Orbital Angular Momentum Quantum Number: L

L gives the total sum of orbital angular momentum vectors in a multielectron atom. The possible values of L can be found from the values of l for individual electrons in the system. For example, in a system with two electrons with values of m_{l_1} and m_{l_2}, the possible values of L are:

$$L = \sum_i^n m_{l_i} = \lvert m_{l_1} + m_{l_2}\rvert, \lvert m_{l_1} + m_{l_2}\text{-}1\rvert, \ldots, \lvert m_{l_1}\text{-}m_{l_2}\rvert \qquad \text{(Section 8.2.1)}$$

The absolute value symbols indicate that L cannot be a negative value. The values of L correspond to different energy levels for groups of microstates. Microstates with values of $L = 0, 1, 2, 3...$ correspond to symbols $S, P, D, F...$ respectively. This is analogous to the relationship between the electron quantum number, l, and the $s, p, d, f..$ orbital subshells. However, the capital letters used for microstates do not indicate orbital or subshell assignments for the electrons.

The Total Intrinsic Spin Quantum Number: S

The sum total of the spin vectors of all of the electrons is called S. The values of S are computed from m_s in a manner very similar to how L is computed from m_l. Because S measures the magnitude of a vector, it cannot be negative. For a system with two electrons, each with spin m_{s1}, and m_{s2}, the possible values of S are given below.

$$S = \sum_{i}^{n} m_{si} = |m_{s1} + m_{s2}|, |m_{s1} + m_{s2}\text{-}1|, ..., |m_{s1}\text{-}m_{s2}| \qquad \text{(Section 8.2.2)}$$

The possible values of S fall into a series that depend on whether there are an odd or even number of electrons.

- Odd number of electrons: $S = \frac{1}{2}, \frac{3}{2}, \frac{5}{2}, ...$
- Even number of electrons: $S = 0, 1, 2, 3, ...$

Example 11.2.1 : Total Orbital Angular Momentum of Carbon

What are the possible L values for the electrons in the $1s^2 2s^2 2p^2$ configuration of carbon?

Solution

Both electrons (i.e., the 2p electrons) are $l = 1$. The possible combinations are 0, 1, and 2 corresponding to symbols S, P, and D, respectively.

Example 11.2.2 : Total Orbital Angular Momentum of Unknown Species

What are the possible L values for the electrons in the $[Xe]6s^2 4f^1 5d^1$?

Solution

We can ignore the electrons in the $[Xe]$ core and the electrons in the $6s$ block. So all we have to consider is the lone f electron ($l = 3$) and the lone d electron ($l = 2$).

The two extremes for possible L values are $3 + 2 = 5$ and $3\text{-}2 = 1$.

Thus, possible values of L for this Xe atom are 5(H), 4(G), 3(F), 2(D), and 1(P).

Example 11.2.5 : The Hydrogen Ground State

Find S for $1s^1$.

Solution

S must be $\frac{1}{2}$, since that's the spin of a single electron and there's only one electron.

Example 11.2.6 : The Beryllium Excited State

Find S for $1s^2 2s^1 2p^1$.

Solution

$S = 1, 0$

Example 11.2.7 : The Carbon Ground State

Find S for carbon atoms with the $1s^2 2s^2 2p^2$ electron configuration.

Solution

$S = 1, 0$ This is the same as the previous problem. Notice that S is not affected by which orbitals are occupied by electrons. S depends only on the number of unpaired electrons. These are usually the electrons in partially-filled subshells (i.e., unpaired electrons in open shells).

Example 11.2.8 : The Nitrogen Ground State

Find S for nitrogen atoms with the $1s^2 2s^2 2p^3$ electron configuration.

Solution

S can be $S = \frac{3}{2}, \frac{1}{2}$.

Quantum numbers M_l and M_s for individual microstates

Once S and L are found, the allowed values of M_l and M_s can be calculated.

The Total Magnetic Quantum Number: M_l

The Total Magnetic Quantum Number M_l is the total z-component of all of the relevant electrons' orbital momentum. While L describes the total angular momentum in the system, M_l tells you which direction it is pointing. L can be assigned to a collection of microstates, but M_l is unique to a specific microstate in that group. Unlike L, M_l is allowed to have negative values. The possible values of M_l are integer values ranging from the largest positive sum to the most negative sum of possible m_l values:

$$M_l = L, L-1, L-2, ..., -L \qquad \text{(Section 8.2.3)}$$

For the p^2 case, the m_l values of p orbitals are $-1, 0, +1$. The largest value of M_l would come from a state where both electrons occupy $m_l = +1$, thus the maximum is $M_l = L = 2$. Likewise, the minimum value of M_l comes from both electrons occupying $m_l = -1$ to give $M_l = -L = -2$. The possible M_l values for p^2 are the series of integer values $+2, +1, 0, -1, -2$.

It is worth noting that there are values of M_l that are forbidden due to the Pauli exclusion principle. For example, the value of $M_l = +3$ could only come from three electrons occupying the $m_l = +1$ orbital. That is impossible because more than one electron would possess the same set of electron quantum numbers.

The Total Spin Magnetic Quantum Number: M_s

M_s is the sum total of the z-components of the electrons' inherent spin in an individual microstate. The difference between S and M_s is subtle, but important. M_s indicates the total z-component of the electrons' spins, while S indicates the entire resultant vector. It is also distinct from M_l, which is the sum total of the z-component of the *orbital angular momentum*. M_s can be computed from S, as shown below. Note that while S must be positive, M_s can have negative values.

$$M_s = S, S-1, S-2, ... -S \qquad \text{(Section 8.2.4)}$$

For the p^2 case, the possible values of M_s are $M_s = +1, 0, -1$. The value $M_s = +1$ comes from the sum of two electrons with spin "up", $m_s = +\frac{1}{2}$. The value $M_s = -1$ comes from the sum of two electrons with spin "down", $m_s = -\frac{1}{2}$. And the value $M_s = 0$ comes from the sum of one electron with $m_s = +\frac{1}{2}$ and the other with $m_s = -\frac{1}{2}$.

There are some values of M_s that will be forbidden, but not in the case of p^2. However in the case of a p^4, for example, the value M_s =2 is forbidden because there is no way to put four "up" electrons in three orbitals without violating the Pauli exclusion principle.

Example 11.2.3 : Total Magnetic Quantum Number of the Zirconium Ground State

What are the possible values M_l of a zirconium atom with the $[Kr]5s^2 4d^2$ electron configuration?

Solution

Both open-shell electrons (i.e., the 4d electrons) are $l = 2$, so the values are 4, 3, 2, 1, 0, -1, -2, -3, -4.

Example 11.2.4 : Total Spin Magnetic Quantum Number of the Carbon Ground State

What are the M_s values for $1s^2 2s^2 2p^2$?

Solution

This system is paramagnetic, with two unpaired electrons in the $2p$ orbital. The three p orbitals have values of $m_s = -1, 0, 1$. The maximum value of $M_s = +1$ would come from the two electrons occupying $m_{s_1} = +1$ and $m_{s_2} = 0$. The minimum value, $M_s = -1$ would come from the two electrons occupying $m_{s_1} = -1$ and $m_{s_2} = 0$. Thus, the possible values for the total spin magnetic quantum number are $M_s = 1, 0, -1$, where the value of $M_s = 0$ comes from a configuration where, for example, $m_{s_1} = +1$ and $m_{s_2} = -1$.

Example 11.2.4 : Total Spin Magnetic Quantum Number of the Nitrogen Ground State

What are the M_s values for $1s^2 2s^2 2p^3$?

Solution

$M_s = +\frac{3}{2}, +\frac{1}{2}, -\frac{1}{2}, -\frac{3}{2}$

This page titled Section 8.2: Quantum Numbers of Multielectron Atoms is shared under a CC BY-NC-SA 4.0 license and was authored, remixed, and/or curated by Kathryn Haas.

- **8.8: Term Symbols Gives a Detailed Description of an Electron Configuration** by Mattanjah de Vries is licensed CC BY 4.0.
- **8.1: Microstates and Terms** by Kai Landskron is licensed CC BY 4.0.

Section 8.2.1: Finding Microstates and Term Symbols

Constructing "Free Ion" Term Symbols and their Relative Energies

The different electronic states of an atom or ion are described by L and S in the form of a **term symbol** (Figure *Section*8.2.1.1). Keep in mind that M_l is related to L, and M_s is related to S, and in some cases their values are equal.

One term symbol can describe one or more microstates with the same energy. The free ion terms are useful in the interpretation of electronic spectra. These term symbols are also commonly called *free ion terms (*or *Russell-Saunders terms*) because they describe the atomic or ionic state, free of any ligands. The term symbol indicates the total orbital angular momentum of the atom, (L), and the multiplicity, ($2S+1$), of the state. The multiplicity can be found with the formula, ($2S+1$), but it is also equal to the number of unpaired electrons plus one.

Misplaced '#'

The generic form of a free ion term symbol is shown in Figure *Section*8.2.1.1. Recall that $L = 0, 1, 2, 3...$ is denoted by a capital letter $S, P, D, F...$, respectively. The latter designation for L is used in the term symbol.

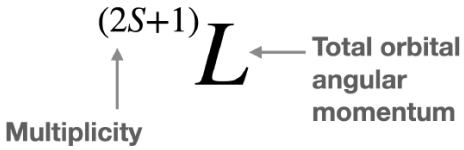


Figure *Section*8.2.1.1: A term symbol of the free ion takes the form ${}^{(2S+1)}L$, where L is the total orbital angular momentum quantum number, and S is the total intrinsic spin quantum number. The value $2S+1$ is called the multiplicity. (CC-BY-NC; Kathryn Haas)

Example 11.2.1.1 : Hydrogen Ground State

What is the free ion term symbol of an H atom in the ground state ($1s^1$)? How many microstates are there for the ground state hydrogen atom? Comment on the degeneracy and multiplicity of the state.

Solution

There is only one electron in a s orbital. That electron must have $l = 0$, and s could be either $+\frac{1}{2}$ or $-\frac{1}{2}$. This is two possible microstates, one with spin "up" and one with spin "down". In either case there is only one value of the total intrinsic spin quantum number, $S = +\frac{1}{2}$. Therefore, the only possible value of spin multiplicity is Multiplicity $= 2 \times (+\frac{1}{2}) + 1 = 2$. The s orbital corresponds to $l = 0$, so $L = 0$, or S. Thus the term symbol is ${}^2S$.

There are two possible microstates of the ground state (both represented by the ground state term). One microstate has $m_s = +\frac{1}{2}$ and the other has $m_s = -\frac{1}{2}$.

The question about degeneracy specifically asks about degeneracy of *the state*. Let's give the most complete answer possible. In terms of energy levels (the ground state in this case), there are two microstates with approximately equal (degenerate) energy, thus the degeneracy of the state is two (2) and is the same as the multiplicity ($2S+1 = 2$). However, sometimes we also refer to the "degeneracy" of electron configurations. It is important to recognize that ground state electron configuration with $M_s = m_s = +\frac{1}{2}$ is singly degenerate, and the same is true for $M_s = m_s = -\frac{1}{2}$. Recognising degeneracy of electron configurations will be useful later in this chapter because the degeneracy of an electron configuration can be helpful for interpreting term symbols in an octahedral field.

Exercise *Section*8.2.1.1

Find the term symbols for the following cases:

a. $L = 0,\ S = 0$
b. $L = 0,\ S = \frac{1}{2}$
c. $L = 1,\ S = 1$
d. $L = 2,\ S = \frac{3}{2}$

e. $L = 3,\ S = 2$

Answer

(a) ^1S
(b) ^2S
(c) ^3P
(d) ^4D
(e) ^5F

Finding all possible microstates for an atom or ion

What are the possible microstates and the overall number of microstates for a free ion with d^2-electron configuration? We can express this in a so-called microstate table (*Section* 8.2.1.2).

M_S \ M_L	-4	-3	-2	-1	0	+1	+2	+3	+4
-1	Not possible (Pauli principle)	$-2^-\ -1^-$	$-2^-\ 0^-$	$-2^-\ 1^-$ $-1^-\ 0^-$	$-2^-\ 2^-$ $-1^-\ 1^-$	$-1^-\ 2^-$ $0^-\ 1^-$	$0^-\ 2^-$	1^-2^-	Not possible (Pauli principle)
0	$-2^-\ -2^+$	$-2^-\ -1^+$ $-2^+\ -1^-$	$-2^-\ 0^+$ $-2^+\ 0^-$ $-1^-\ -1^+$	$-2^-\ 1^+$ $-2^+\ 1^-$ $-1^-\ 0^+$ $-1^+\ 0^-$	$-2^-\ 2^+$ $-2^+\ 2^-$ $-1^-\ 1^+$ $-1^+\ 1^-$ $0^-\ 0^+$	$-1^-\ 2^+$ $-1^+\ 2^-$ $0^-\ 1^+$ $0^+\ 1^-$	$0^-\ 2^+$ $0^+\ 2^-$ $1^-\ 1^+$	1^-2^+ 1^+2^-	$2^-\ 2^+$
+1	Not possible (Pauli principle)	$-2^+\ -1^+$	$-2^+\ 0^+$	$-2^+\ 1^+$ $-1^+\ 0^+$	$-2^+\ 2^+$ $-1^+\ 1^+$	$-1^+\ 2^+$ $0^+\ 1^+$	$0^+\ 2^+$	1^+2^+	Not possible (Pauli principle)

Figure *Section* 8.2.1.2. d^2 electron configuration microstate table. This table is organized with M_l values increasing horizontally and M_s values decreasing vertically. You may see different ways to organize a microstate table, and there is no wrong orientation to use, as long as you can use it to correctly find and organize microstates. Each microstate is indicating using notion $(m_l)^{m_s}$, where only the sign of m_s is indicated for simplicity. For example, an electron in $m_l = -2$ with $m_s = +\frac{1}{2}$ is notated -2^+.

You can see the microstate table for the d^2 electron configuration depicted above. Each column represents a possible value M_l. For the d^2 configuration, M_l can adopt values from -4 to +4, hence there there are 9 columns. Each row represents possible M_s value. For the d^2 electron configuration, M_s can vary between +1 and -1. $M_s = +1$ means both electrons have the spin $+\frac{1}{2}$, $M_s = 0$ means one electron has the spin $+\frac{1}{2}$ and the other one has the spin $-\frac{1}{2}$. The $M_s = -1$ value is adopted when both electrons have the spin $-\frac{1}{2}$. Now we can combine each M_s value with each M_l value, which defines a particular field in the table. You can see that some fields are empty due to the Pauli principle. For example, the field for $M_l = -4$ and $M_s = -1$ is not filled because in this case both electrons would have the same quantum numbers, namely $m_l = 2$, and $m_s = -\frac{1}{2}$. We can further see that for some fields only one combination of electrons is possible, while for others there are multiple possible microstates. For example, for the field with $M_l = 4$ and $M_s = 0$ there is only one combination of electrons possible. You can see the notation "2^-2^+" in this field. This means that the first electron has an m_l value of 2 and a spin of $-\frac{1}{2}$ and the second electron also has an m_l value of 2 and an m_s value of $+\frac{1}{2}$. The most populated field is the field for $M_l = 0$ and $M_s = 0$; there are overall five microstates with that combination of M_l and M_s values. If we count the overall number of microstates in the table then we arrive at the number 45. This is consistent with what we would expect according to the following formula.

Misplaced '#'

In our example L=4 and S = 1, and thus the number of microstates is: $((2x4) + 1)((2x1) + 1) = 45$. **In general for a d^n electron configuration with n d-electrons, the number of microstates is** $(10!)/((10 - n)!n!)$**.**

One useful property of a microstate table is that we can derive all possible terms and term symbols for a particular electron configuration from it. For simplification's sake, we indicate a possible microstate in the table in Figure *Section*8.2.1.5 just by an "x". Then we draw the largest possible rectangular box into the microstate table that contains only fields with at least one possible electron combination (Figure *Section*8.2.1.5).

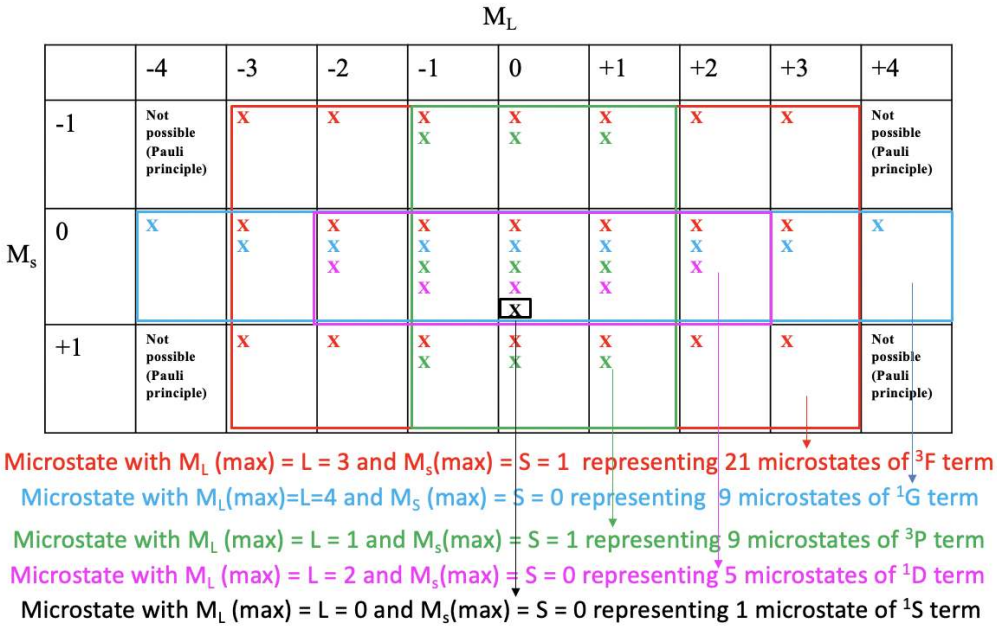


Figure *Section*8.2.1.5. Deriving the terms and term symbols for the d^2 electron configuration from the microstate table

You can see that the largest possible box is the red box drawn (Figure *Section*8.2.1.5). This box contains the microstates that belong to the first term of the electron configuration d^2. The number of microstates is equal to the number of fields within the red box. That makes $7 \times 3 = 21$ microstates. What is the term symbol for this term? In order to answer this question we need to find the microstate in the red box that has the highest M_l and the highest M_s value. You can see that it is the one with $M_l = 3$ and $M_s = 2$. Thus, L=3 and S=1. This defines the term as a ^{3}F term because 2S+1 = 3, and L=3 corresponds to the term symbol F. This term is a triplet term. Note that a triplet term also includes microstates with opposite spins. Overall seven of the 21 microstates have $M_s = 0$.

Next, we look what is the next-largest rectangular box we can draw, and which contains microstates we did not consider yet. We can see that the blue box contains nine fields equaling nine microstates. The microstate within this box that has the highest M_l and M_s values is the one with $M_l = 4$ and $M_s = 0$. This defines a ^{1}G term. This is a singlet term. Note that a singlet term ONLY has microstates with paired spins (M_s=0).

There is another rectangular box which also contains nine microstates. It is the green one. The microstate with the highest M_l and M_s values is the one with $M_l = 1$ and $M_s = 1$. Thus, $L = 1$, and $2S + 1 = 3$, which defines a ^3P term. Note that despite this being a triplet term, which indicates two unpaired electrons (\S=1\), the term also contains three microstates that have opposite spins with a total $M_s = 0$.

The next-largest box is the purple one containing five fields and five microstates. What is the term with the highest M_l and M_s values? It is the one with $M_l = 2$ and $M_s = 0$. This means that L=2 and S=0, which defines a ^{1}D term, a singlet term with only microstates with paired spins. There is one microstate left that we did not consider thus far, the one with $M_l = 0$ and $M_s = 0$. These are the highest M_l and M_s values because there is no other microstate. Thus, this term contains only one microstate and the term symbol is ^1S. Now we have found all the terms and term symbols.

✔ Example 11.2.1.2 : Boron

What are the possible term symbols for $1s^2 2s^2 2p^1$ electronic configuration of boron? Which is the ground state?

Solution

We only need to consider the one electron in the $2p$ orbital, since that is the only open shell electron. For one electron, there is only one value of $S = ½$, so multiplicity must be $2S + 1 = 2$. The possible values of L for one electron in a p orbital are $L = 0, 1$ (or S, and P terms). This gives the free ion term symbols ^2P and ^2S. Both of these terms have multiplicity of 2, so the ground state would be the one with the highest value for L. The ground state term is ^2P.

Example 11.2.1.3 : Beryllium Excited State

What are the term symbols for the $1s^2 2s^1 2p^1$ excited-state electronic configuration of Beryllium?

Solution

The term symbols will be of the form ^1P and ^3P. For the ^1P state, $L = 1$ and $S = 0$, so the total angular momentum $J = 1$. For the second state, $L = 1$ and $S = 1$, so the possible values of $J = 2, 1, 0$. There are four microstates for this configuration with term symbols of $^1P_1$ and $^3P_2$, $^3P_1$, and $^3P_0$.

Finding The Ground State Term

...from a list of microstates

Each term symbol represents an atomic state with an associated energy level. If you have found all the possible microstates using a microstate table, and have identified their terms, then the term with the lowest energy (ie the ground state) can be found using Hund's first two rules. In abbreviated form, Hund's rules state...

1. The lowest energy electron configuration has the maximum multiplicity (the maximum number of unpaired electrons).
2. For a given multiplicity, the configuration with the largest total orbital angular momentum (L) value has the lowest energy.

In the case of the p^2 carbon atom (see Figure $Section 8.2.1.1$), the lowest energy state would have a multiplicity of 3 (two unpaired electrons). Of the states with a multiplicity of 3, the largest value of L is 1 (and thus, P). Thus, the ground state term for carbon is ^3P. These rules are reliable for identifying the ground state term for any atom, but have limited use for ordering relative energies outside of the ground state for 3d metal ions and other light atoms. For heavier atoms (e.g., 4d metals) another type of interaction, called jj coupling must be considered, but this is outside the scope of this discussion. **Tip:** There is a deep symmetry that connects different electronic configurations. It turns out that a p^1 configuration has the same term symbols as a p^5. Similarly, $p^2 = p^4$. A similar relationship can be used to figure out high electron number term symbols for the d and f orbitals.

...if you just want the find Ground State term

To assign transitions in an electronic spectrum, we should know the ground state term, as well as all other terms and their relative energies for a given atom or ion. However, the identification of all possible terms becomes tedious with more than one or two electrons in the d orbitals. Fortunately, there are tools (like correlation diagrams) that can help us find all terms for an atom or ion, as long as the ground state term can be identified. Here is a quick shortcut for finding the ground state term for transition metal complex with partially-filled d shell.

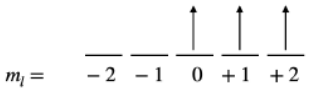
Quickly find the ground state free ion tern

In this case, we'll focus on transition metal d-orbitals. To begin, you'll need to know the metal ion identity and its oxidation state. These instructions assume that the d orbital is the only shell that is partially filled.

1. Determine the number of d-electrons.
2. Then fill these electrons into an electron orbital diagram of five degenerate orbitals, putting electrons into the highest value of m_l first, and filling orbitals with single electrons before pairing them (just as you may have done in an introductory chemistry course).
3. Calcuate the total intrinsic spin (\S\) and spin multiplicity using the diagram drawn in #2.
4. Calculate L using the diagram drawn from #2.
5. Write the term symbol for the ground state.

Let's use the example of the $[Cr(NH_3)_6]^{3+}$ complex ion, and determine its ground state term following the shortcut described above.

1. Determine the number of d-electrons.
   $[Cr(NH_3)_6]^{3+}$ contains Cr^{3+}, which is a d^3 metal ion. There are three d electrons.
2. Draw a diagram of five degenerate d orbitals, with m_l values labeled. Fill in the electrons to maximize m_s and m_l.



3. Calculate spin multiplicity (should be the maximum possible value!).
   $S = m_{s_1} + m_{s_2} + m_{s_3} = +\frac{1}{2} + +\frac{1}{2} + +\frac{1}{2} = \frac{3}{2}$
   Spin multiplicity = $2S + 1 = 2\frac{3}{2} + 1 = 4$
4. Calculate L (should be the maximum possible value after spin is maximized.
   $L = m_{l_1} + m_{l_2} + m_{l_3} = 2 + 1 + 0 = 3$
5. Write the ground state free ion term:
   ${}^{(2S+1)}L = {}^4F$

? Exercise *Section*8.2.1.2

Earlier on this page, you found all the terms for a d^2 metal ion. Use both of the methods (Hund's rule, and the shortcut method) described here to identify the ground state term for d^2.

Answer

Using Hund's rule: The terms identified for d^2 are ${}^3F$, ${}^1G$, ${}^3P$, ${}^1D$, and ${}^1S$. Hund's first rule tells us that either ${}^3F$ or ${}^3P$ could be the ground state because these two terms have the highest multiplicity. Hund's second rule tells us that ${}^3F$ must be the ground state because it has the largest value of L.

Using the shortcut: The drawing is shown below, with one electron in $m_l = +2$ and the second electron in $m_l = +1$. Both electrons are unpaired with $m_s = +\frac{1}{2}$. This gives $L = 3$ or an F term. And, $S = 1$ with a multiplicity of 3. The ground state term is ${}^3F$.

? Exercise *Section*8.2.1.3

Find the ground state free ion terms for the metal ions in the following cases:

(a) $[Ti(H_2O)_6]Cl_2$

(b) $[Ti(NH_3)_6]Cl_3$

(c) $[Cu(H_2O)_6]Cl_2$

Answer

(a) Ti^{2+} is a d^2 metal ion, ${}^3F$

(b) Ti^{3+} is a d^1 metal ion, ${}^2D$

(c) Cu^{1+} is a d^9 metal ion, ${}^2D$. Note that d^9 and d^1 are related by the symmetry of their electronic states.

This page titled Section 8.2.1: Finding Microstates and Term Symbols is shared under a CC BY-NC-SA license and was authored, remixed, and/or curated by Kathryn Haas.

- **8.8: Term Symbols Gives a Detailed Description of an Electron Configuration** by Mattanjah de Vries is licensed CC BY 4.0.
- **8.1: Microstates and Terms** by Kai Landskron is licensed CC BY 4.0.

Section 8.2.2: Spin-Orbit Coupling

The magnetic fields created by S and L are not isolated from one another; they interact through **spin-orbit coupling** *(aka Russell-Saunders coupling)*. We will consider only this simple form of coupling in this text. Its application is limited to the elements with $z < 40$, including the first row of the transition elements. In the case of heavier elements, we must also consider jj coupling; however, we will not discuss the latter here.

In the Russell-Saunders spin-orbit coupling scheme, the interaction between S and L is expressed by an additional quantum number, the total angular momentum quantum number (J). The possible values of J are values between $L+S$ and $|L-S|$.

$$J = L+S,\ L+S-1,\ L+S-2,\ ...,\ |L-S| \qquad \text{(Section 8.2.2.1)}$$

A value of J must be positive or zero for a multielectron system. J values can fall into series $\frac{1}{2}, \frac{3}{2}, \frac{5}{2}, ...$ or $0, 1, 2, ...$ The quantum number J is added to the term symbol as a subscript to the right of the letter describing the term. A full term symbol is as follows:

$$^{(2S+1)}L_J \qquad \text{(Section 8.2.2.2)}$$

The result of spin-orbit coupling is that a term for the free ion is split into states of different energies. For example, a ^3P state of a carbon atom with a p^2 electron configuration would be split into three different energy states (according to the three possible J values 0, 1, and 2): $^3P_0$,$^3P_1$,$^3P_2$.

The relative energies of the states can be predicted from Hund's Third Rule.

Hund's third Rule:

- For subshells that are less than half-filled, the lowest energy state has the lowest J value.
- For subshells that are exactly half-filled, there is only one J value, thus it is the lowest energy.
- For subshells that are more than half-filled, the lowest energy state has the largest J value.

Thus, in this case where the p subshell is less than half full, the lowest energy state from the ^3P free ion term would be that with $J = 0$, $^3P_0$, followed by $J = 1$ and $J = 2$. The splitting and relative energies are depicted in Figure *Section*8.2.2.1. Spin-orbit coupling and the splitting of the free ion terms have important implications for electronic spectra because they affect the energies of electronic transitions.

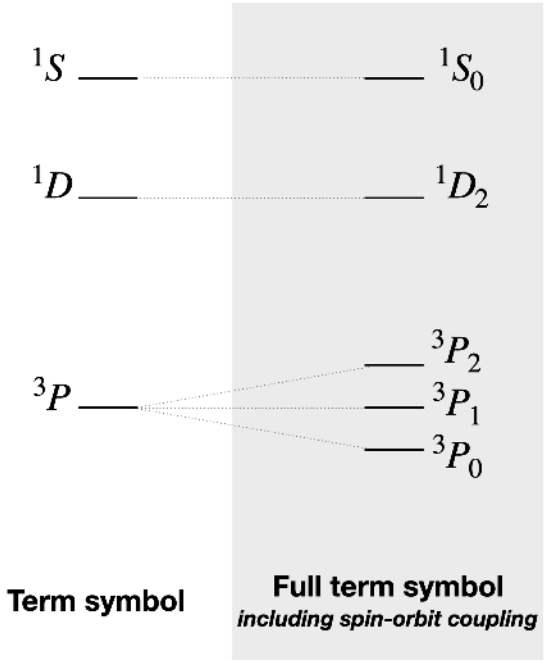


Figure *Section*8.2.2.1: The effects of spin-orbit (Russell-Sauders) coupling on the "free ion" term symbols for. Energy splitting not shown to scale. (CC-BY-NC; Kathryn Haas)

Section 8.2.2: Spin-Orbit Coupling is shared under a CC BY-NC-SA 4.0 license and was authored, remixed, and/or curated by LibreTexts.

- **8.1: Microstates and Terms** by Kai Landskron is licensed CC BY 4.0.
- **11.2.2: Spin-Orbit Coupling** has no license indicated.

SECTION OVERVIEW

Section 8.3: Electronic Spectra of Coordination Compounds

Types of transitions related to the metal ion:

1. **d-d transitions**: d-d transitions are electronic transitions that occur between the molecular orbitals (MOs) that are mostly metal in character: specifically, the orbitals that we think of as the d-orbitals of a transition metal complex. These transitions are useful in determining the energy of splitting and can be used to indicate coordination chemistry (geometry and ligand sets). In octahedral complexes, d-d transitions occur between the t_{2g} and e_g orbitals (across Δ). These transitions cannot occur in metal complexes where the d-orbital is completely empty (d^0) or completely full (d^{10}). In other words, a d-d transition is only possible in $d^1 - d^9$ metal ions. In a UV-visible absorption spectrum, d-d transitions appear as relatively weak absorptions with extinction coefficients (ε) less than 1,000.
2. **Charge transfer (CT) transitions**: Charge transfer transitions occur between MOs that are mostly metal in character and those that are mostly ligand in character. These transitions depend on the type of ligand: they occur only when the metal is bound to ligands that are π-donors or π-acceptors. And there are two types of CT transitions. If the metal is bound to a π-donor ligand, electrons from lower-energy MO's that are mostly ligand in character can become excited to MO's that are mostly metal in character. These are **ligand to metal charge transfers (LMCT) transitions** (Figure *Section*8.3.1, left diagram). If the the metal is bound to ligands that are π-acceptors, electrons from the MO's that are mostly metal in character can become excited to higher-energy orbitals that are mostly ligand in character. These are **metal to ligand charge transfer (MLCT)** transitions (Figure *Section*8.3.1, right diagram). In a UV-visible absorption spectrum, CT transitions appear as relatively intense absorptions with extinction coefficients (ε) much greater than 1,000.

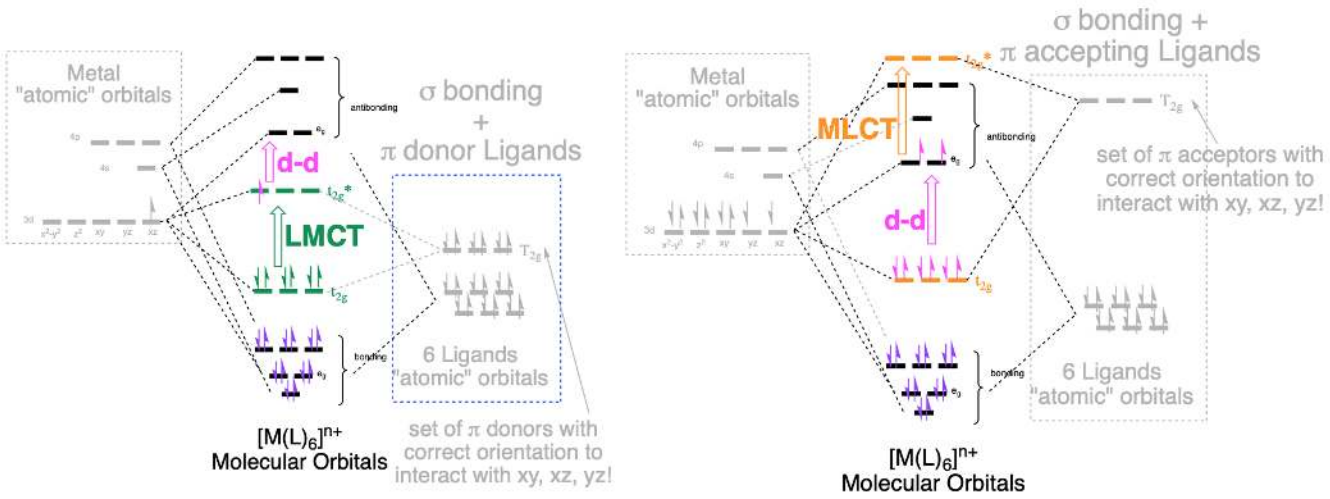


Figure *Section*8.3.1: Abbreviated and annotated MO diagrams for example cases of metal ions in octahdral geometry with sets of π-donor and π-acceptor lignads. In both example MO diagrams, d-d transitions are shown (pink, open arrow from t_{2g} to e_g). **Left:** LMCT transitions are possible with π-donor ligands when electrons are excited from MOs that are mostly ligand in character to MOs that are mostly metal in character. An example of LMCT is shown (green, open arrow from t_{2g} to $t*_{2g}$). **Right:** MLCT transitions are possible with π-acceptor ligands when electrons from MOs that are mostly metal in character are excited to orbitals that are mostly ligand in character (the π^* orbitals from ligands). An example MLCT is shown ((orange, open arrow from e_g to $t*_{2g}$).

Section 8.3.1: Tanabe-Sugano Diagrams

Section 8.3.2: Symmetry labels for split terms

Section 8.3.3: Selection Rules

Section 8.3.4: Correlation Diagrams

Section 8.3.5: Applications of Tanabe-Sugano Diagrams

Section 8.3.6: Tetrahedral Complexes

Section 8.3.7: Charge-Transfer Spectra

Section 8.3.8: Applications of Charge-Transfer

This page titled Section 8.3: Electronic Spectra of Coordination Compounds is shared under a CC BY-NC-SA 4.0 license and was authored, remixed, and/or curated by Kathryn Haas.

Section 8.3.1: Tanabe-Sugano Diagrams

Tanabe-Sugano diagrams are modified forms of correlation diagrams. The modification is simply that the energies of terms are plotted in terms of transition energy and Δ divided by a constant, B, called the Racha parameter. Terms are plotted relative to the lowest-energy term; in other words, the ground state term is plotted as the horizontal axis (x-axis). The Tanabe-Sugano diagram of a d^2 transition metal complex is shown below in Figure ***Section*8.3.1.1**. Tanabe-Sugano diagrams for other d-electron counts are available in the Reference Section of LibreTexts.

Tanabe-Sugano diagram of a d^2 octahedral complex

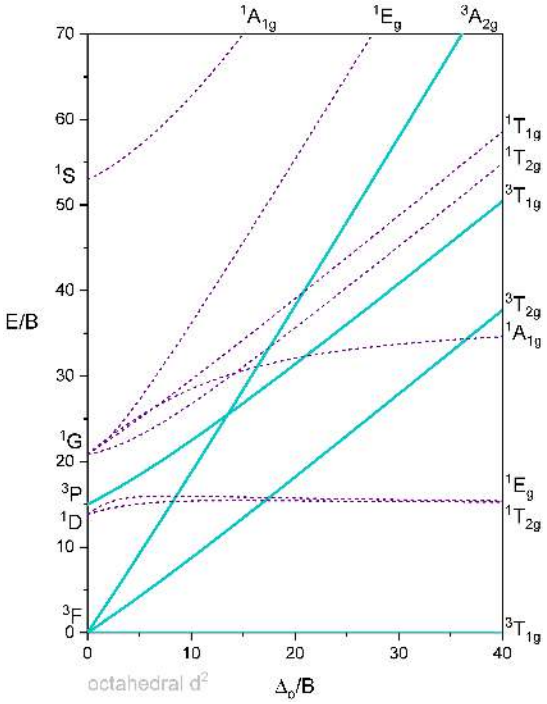


Figure ***Section*8.3.1.2**: d^3: Tanabe-Sugano Diagram for octahedral metal complex with two d electrons. For convenience, terms that can accommodate spin-allowed transitions from the ground state are indicated by solid lines. Terms that have different multiplicity than the ground state are shown in dashed lines. (CC-BY-SA; Kathryn Haas)

The difference between the diagram shown in Figure ***Section*8.3.1.1** and the previously-discussed correlation diagram for a d^2 metal ion is that the energy of the ground state is plotted horizontally, and the energy of all other terms are plotted relative to that. In the case of the d^2 electron configuration, the $^3T_{1g}$ term is the ground term and is plotted as a horizontal line. We can see that the ligand field strength on the x-axis is given in units of B (specifically as $\frac{\Delta}{B}$), and the energy of the terms is also given in units of B (specifically $\frac{E}{B}$. B is a so-called Racah parameter, which is a quantum-mechanical energy unit for the electromagnetic interactions between the electrons. It is chosen because it provides “handy” numbers.

You can see that some lines in Figure ***Section*8.3.1.1** are bent (eg the two $^1A_{1g}$ terms), and some are straight. Bending of lines occurs when two terms interact with each other because they are close in energy and have the same symmetry. This is again an analogy to orbitals. Just as orbitals interact when they have the same symmetry type and similar energy, terms also interact when they have the same symmetry and similar energy. Without taking their interactions into account, their energies can cross when the energy of term A declines and the energy of term B increases with increasing field strength (Figure ***Section*8.3.1.2**). The closer the terms come to the point where they cross, the stronger their interactions, because their energies become more and more similar. These interactions lead to the "bending away" of the terms from each other, leading to bent curves. This means that curves for two terms of the same symmetry type will bend away in a Tanabe-Sugano diagram and never cross. For example the terms for the two $^1A_{1g}$ terms bend away from each other and do not cross.

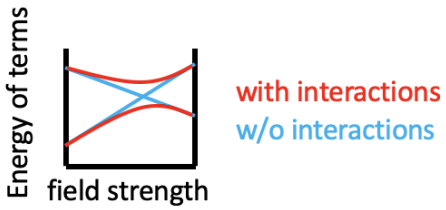


Figure *Section*8.3.1.2: Origin of line-bending in Tanabe-Sugano diagrams.

Next, let us think about which electron transitions would be allowed by considering spin selection and the Laporte rule. First, notice that all the terms in Figure *Section*8.3.1.1 have "gerade" symmetry and are labeled with a "g" subscript. In fact, this is the case for the terms of any octahedral complex. What does this mean for the allowance of electron transitions? It means that no electron transition would be allowed by the Laporte Rule, and that would imply that the complex could not absorb light. The Laporte selection rule, however, does not hold strictly. It only says that the probability of the electron-transition is reduced - but not forbidden. This means that an absorption band that disobeys the Laporte rule will have lower intensity compared to one that follows the Laporte rule, but it can still be observed. The spin-selection rule, however, holds strictly, and transitions between terms of different spin multiplicity are strictly forbidden, meaning that they have near zero probability to occur. Overall, we can therefore excite an electron from the $^3T_1$ ground state to other triplet terms, namely the $^3T_2$ term, and the $^3A_2$ term (Figure *Section*8.3.1.1).

Tanabe-Sugano diagram of d^3 octahedral complexes

Now, let us have a look at the Tanabe-Sugano diagram of a d^3 ion in an octahedral ligand field (Figure *Section*8.3.1.3). What is the ground term? We can see that the term designation on the horizontal line reads "$^4A_{2g}$", therefore this term is the ground term. How many electron transitions from the ground state should we expect? To answer this question we need to count the number of other quartet terms. There is the $^4T_{2g}$, the $^4T_{1g}$, and another $^4T_{1g}$. Thus, there are overall three electron transitions possible.

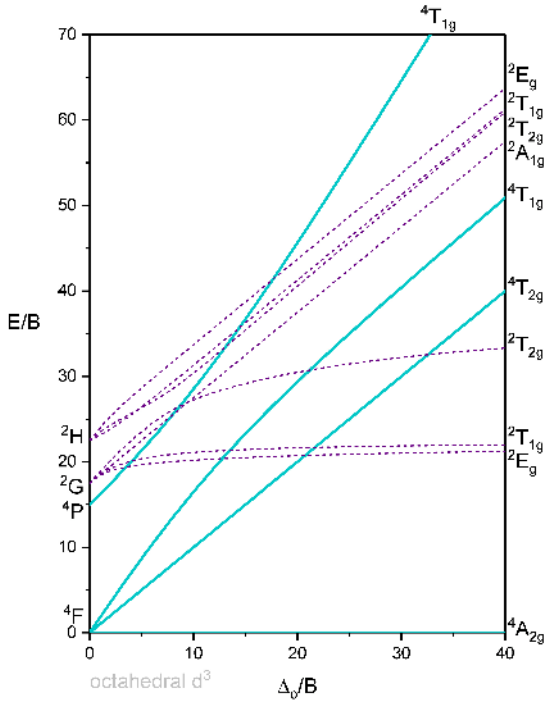


Figure *Section*8.3.1.3: d^3: Tanabe-Sugano Diagram for octahedral metal complex with three *d* electrons. For convenience, terms that can accommodate spin-allowed transitions from the ground state are indicated by solid lines. Terms that have different multiplicity than the ground state are shown in dashed lines. (CC-BY-SA; Kathryn Haas)

Can we understand why the ground state is a quartet term? It helps to consider how we would fill the electrons into the d-orbitals for the electron configuration d^3. All three electrons would be filled spin-up in the t_{2g} orbital following Hund's rule (Figure *Section*8.3.1.4). Because each electron has the spin +1/2 the total spin of all three electrons is 3x1/2=3/2. Thus, the spin multiplicity is ((2x3/2)+1)=4. Note that the microstate we have drawn is actually only one of the (2L+1)(2S+1) microstates. S=3x1/2=3/2, but

what is L? You can see on the left side of the diagram that the $^4A_2$ term originated from a ^4F term. This means L=3, and (2L+1)((2S+1)=7x4=28. This means that there are actually 27 other microstates that have the same energy as the microstate that we drew. Why did we draw this microstate in favor of the others? This is because this microstate is the state with the maximum M_L (=L) and M_s (=S) values determining the term symbol.

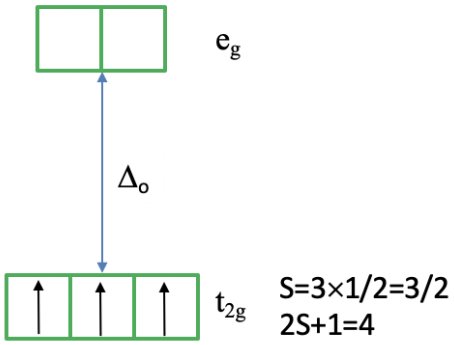


Figure ***Section*8.3.1.4**: d-orbitals in an octahedral ligand field for the electron configuration d^3

Tanabe-Sugano diagram of d^4 octahedral complexes

Now let us look at the Tanabe-Sugano diagram of a d^4 octahedral complex (Figure ***Section*8.3.1.5**). You can see that this diagram is separated into two parts separated by a vertical line. The line indicates the ligand field strength at which the complex changes from a high spin complex to a low spin complex. At lower ligand field strengths, the ground term is a ^5E_g term (solid turquoise line). At higher field strength the ground term is a $^3T_{1g}$ term (dashed purple line).

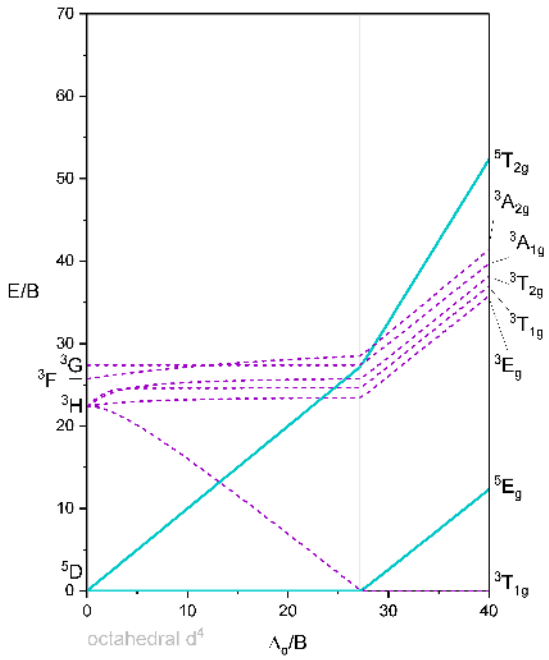
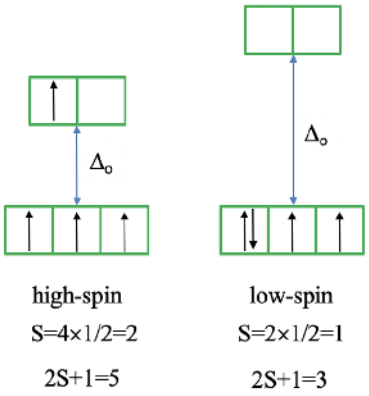


Figure ***Section*8.3.1.5**: d^4, simplified: Tanabe-Sugano Diagram for octahedral metal complex with four d electrons. A grey vertical line at 27.2 $\frac{\Delta_o}{B}$ divides high spin from low spin cases. For convenience, terms that can accommodate spin-allowed transitions from the pentet ground state in high spin (left of grey line) are indicated by heavy solid lines. Terms that can accommodate spin-allowed transitions from the low spin triplet ground state are shown in heavy dashed lines. This version of the d^4 Tanabe Sugano Diagram is abbreviated in that it shows only the spin-allowed terms that are most relevant for interpreting UV-visible spectra. For the full version of a d^4 diagram, see the Resources section. (CC-BY-SA; Kathryn Haas)

We can rationalize this again by drawing the orbital box representation of the d-orbitals in the octahedral ligand field. In the high spin state, there are four unpaired electrons, thus S=4x1/2=2, and 2S+1=5. In the low spin state, there are two unpaired electrons, and thus S=2x1/2=1, and 2S+1=3. This explains the quintet and the triplet nature of the high and low spin ground terms. Note

again, that the two microstates represented by the orbital box diagrams (*Section*8.3.1.6) are not the only microstates that have the respective energy. They are only the "representative" microstates because they have the maximum M_L and M_S values.



*Section*8.3.1.6: d-orbitals in the octahedral ligand field for the electron configuration d^4.

How many electron transitions are possible from the ground term? For a high spin complex there is only one because the is only one other quintet term, namely the $^5T_{2g}$ term. For the low spin complex, there are five transitions because there are five other triplet terms.

Tananbe-Sugano diagram of d^5 octahedral complexes

The Tanabe-Sugano diagram of a d^5 octahedral complex is also divided into two parts separated by a vertical line (Figure *Section*8.3.1.7). The left part reflects the high spin and the right part the low spin complex.

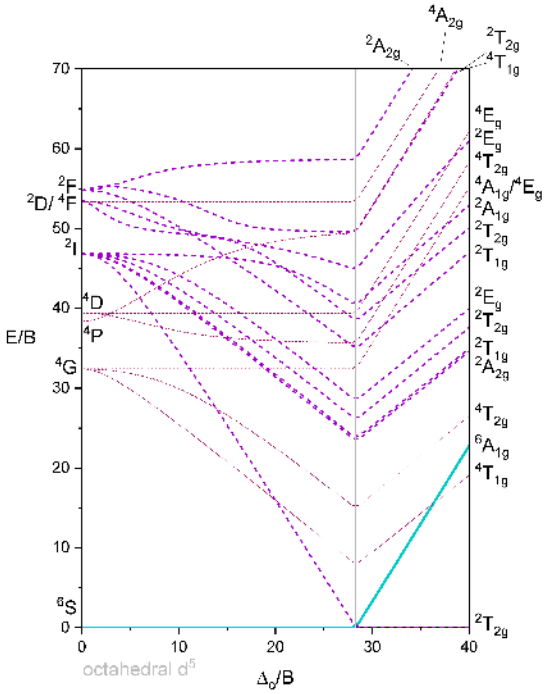


Figure *Section*8.3.1.7: d^5, simple: Tanabe-Sugano Diagram for octahedral metal complex with five d electrons. A grey vertical line at 27.3 $\frac{\Delta_o}{B}$ divides high spin from low spin cases. For convenience, terms that can accommodate spin-allowed transitions from the sextet ground state in low spin (right of grey line) are indicated by heavy solid lines. Terms that can accommodate spin-allowed transitions from the low spin doublet ground state are shown in heavy dashed lines. Terms that have different multiplicity than ground states are shown in lighter dotted lines. This version of the d^5 Tanabe Sugano Diagram is abbreviated for simplicity and for the purpose of interpreting UV-visible spectra. For the full version of a d^5 diagram, see the Resources section. (CC-BY-SA; Kathryn Haas)

The high spin ground state is a sextet term, and the low spin ground state is a doublet term. We can understand the sextet and doublet nature of the terms when considering that the associated electron box diagrams have five and one unpaired electrons

respectively. S=5x1/2=5/2 and 2S+1=6 for the high spin term, and S=1x1/2=1/2 and 2S+1=2 for the low spin term. What are the possible electron transitions from the ground state? For the high-spin complex there is no other sextet term, meaning that there is no electron transition possible. Hence, high-spin octahedral d^5-complexes are colorless. An example is the hexaaqua manganese (2+) complex. A solution of this complex is near colorless, only very slightly pinkish. The slight color is because also spin-forbidden transitions can occur, albeit at a very low probability. For a d^5-low spin complex there are three additional doublet states, and thus there are three electron transitions possible.

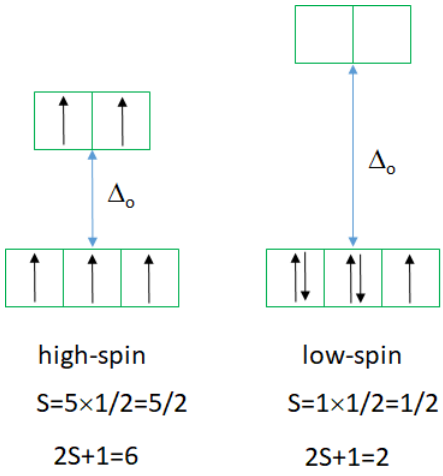


Figure *Section*8.3.1.8: d-orbitals in the octahedral ligand field for the electron configuration d^5

Tanabe-Sugano diagram of d^6 octahedral complexes

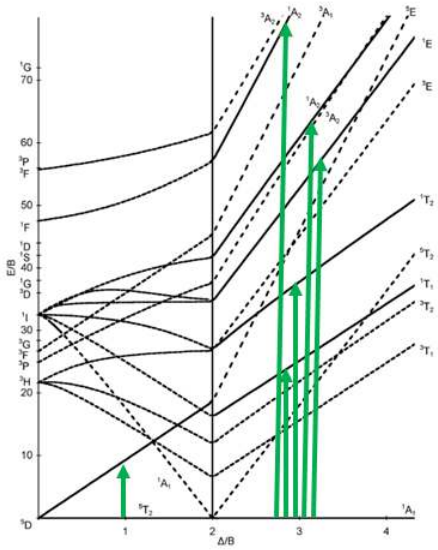


Figure 8.2.13 Tanabe-Sugano diagram of the d^6 octahedral complex (Chem507f091 / Public domain https://commons.wikimedia.org/wiki/F...no_diagram.png)

The next diagram is the one for the d^6 electron configuration (Fig. 8.2.13). Again, the diagram is separated into parts for high and low spin complexes. The dashed lines in the diagram indicate the terms that have a different spin multiplicity than the ground term. This way we can more easily see how many electron transitions are allowed.

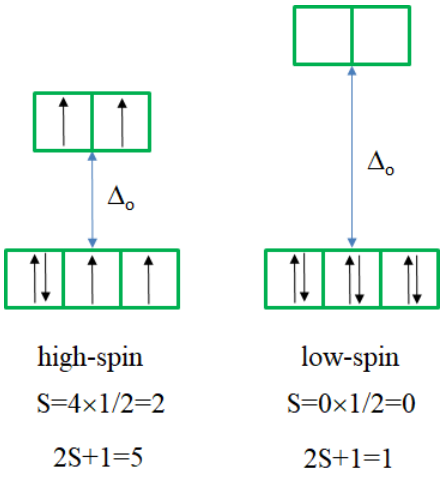


Figure 8.2.14 d-orbitals in the octahedral ligand field for the electron configuration d^6

The ground term for the high-spin complex is the quintet $^5T_2$ term. It is a quintet term because four electrons in the d-orbitals are unpaired, and two are paired. The value for S is thus 4x1/2=2, and the spin multiplicity is 2S+1=5. The ground term for the low spin complex is a $^1A_1$ term. It is a singlet term because all electrons are paired, and thus S=0, and 2S+1=1. How many electron transitions are there for the high-spin complex? There is only one because the ^5E term is the only other quintet term. There are five transitions possible for the low-spin case because there are five additional singlet terms.

Tanabe-Sugano diagram of d^7 octahedral complexes

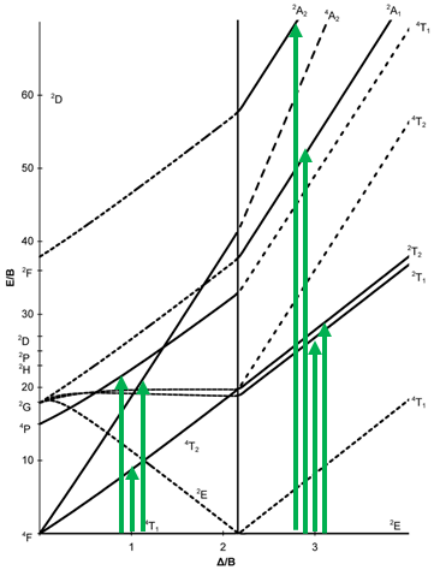


Figure 8.2.15 Tanabe-Sugano diagram of the d^7 octahedral complex (Attribution: Chem507f091 / Public domain https://commons.wikimedia.org/wiki/F...no_diagram.png)

Next, let us look at the Tanabe-Sugano diagram of a d^7 octahedral complex (Fig. 8.2.15). In this case, the high spin complex has a $^4T_1$ ground term, and the low spin complex has a ^2E ground term.

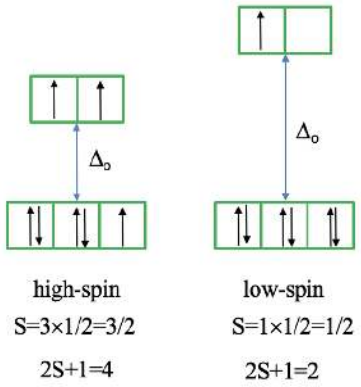


Figure 8.2.16 d-orbitals in the octahedral ligand field for the electron configuration d^7

The microstate that "represents" the high spin ground term has three unpaired electrons, hence the spin quantum number S=3/2 and the spin multiplicity is 2S+1=4. The microstate that represents the low spin ground term has one unpaired electron, an S value of ½, and a spin multiplicity of 2. There are three other quartet terms, and four other doublet terms, hence there are three electron transitions for the high-spin complex, and four for the low spin complex.

Tanabe-Sugano diagram of d^8 octahedral complexes

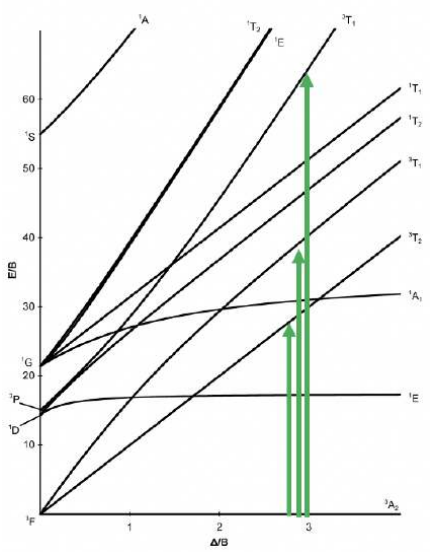


Figure 8.2.17 Tanabe-Sugano diagram of the d^8 octahedral complex (Attribution: Chem507f091 / Public domain https://commons.wikimedia.org/wiki/F...no_diagram.png)

Now let us look at an octahedral complex with d^8 electron configuration. For this electron configuration, there are no high and low spin complexes possible, therefore, the Tanabe-Sugano diagram is no longer divided into two parts (Fig. 8.2.17).

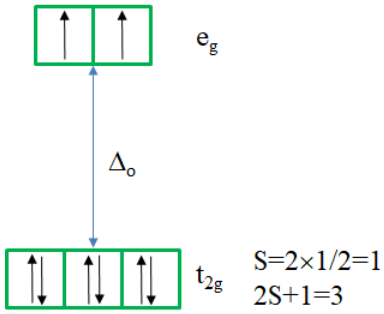


Figure 8.2.18 d-orbitals in the octahedral ligand field for the electron configuration d^8

There is a single ground term of the type $^3A_2$. It is a triplet state because the microstate representing the term has two unpaired electrons in the e_g orbitals (Fig. 8.2.18). Thus, S=2x1/2=1, and the spin multiplicity is 2S+1=2. How many electron transitions would you expect? There are three other triplet states, namely the $^3T_2$ and two $^3T_1$ terms. Therefore, there are three electron transitions possible.

Unnecessary diagrams for d^1, d^9, d^10

We could also ask: Are there Tanabe-Sugano diagrams for d^1, d^9, and d^{10}? For, d^1 there are no electron-electron interactions, thus the simple orbital picture is sufficient. The ^2D term splits into T_{2g} and E_g terms, and there is only one electron transition possible. The d^9 electron configuration is the "hole-analog" of the d^1 electron configuration. It has also just one ^2D term which splits into a T_{2g} and an E_g term in the octahedral ligand field. Therefore, also in this case there is only one electron transition from the T_{2g} into the E_g term possible. In the case of d^{10} all microstates are filled with orbitals, and there is only the ^1S term which does not split in an octahedral ligand field. Therefore, there are no electron transitions in this case.

Jahn-Teller distortions and other geometries

Some of the electron configurations discussed above are ones that are particularly susceptible to Jahn-Teller distortion. The Jahn-Teller theorem predicts that electron configurations with asymmetrically populated orbitals (i.e., those that have spin multiplicity of a doublet or greater), will distort. Distortions affect the electronic spectra of coordination complexes, and in practice Jahn-Teller distortions are significant only in the cases where the e_g orbitals are asymmetrically populated (e.g., octahedral d^9 and high spin d^4).

Finally, it should be mentioned that it is also possible to construct Tanabe-Sugano diagrams for other shapes such as the tetrahedral shape, but we will not discuss these further here.

Dr. Kai Landskron (Lehigh University). If you like this textbook, please consider to make a donation to support the author's research at Lehigh University: Click Here to Donate.

This page titled Section 8.3.1: Tanabe-Sugano Diagrams is shared under a CC BY-NC-SA license and was authored, remixed, and/or curated by Kai Landskron.

- **8.2: Term splitting in ligand fields, selection rules, Tanabe-Sugano diagrams. Metal to ligand, and ligand to metal transitions** by Kai Landskron is licensed CC BY 4.0.

Section 8.3.2: Symmetry labels for split terms

While the free ion terms symbols are derived using Russell-Saunders terms, we only briefly discussed how the term symbols may be found from a character table upon ligand-field splitting. The symmetry labels (called Mulliken Labels) that are used in character tables to describe the symmetry of wavefunctions were described in a previous section (Section 4.3.3). Just as orbitals are wavefunctions that are described by the irreducible representations that are part of a character table, so are the terms. When we are discussing the terms of an octahedral complex, we can apply what we already know about octahedral symmetry and symmetry labels to understand how the terms labels are assigned.

Upon close inspection of any of the Tanabe-Sugano diagrams shown previously, or in the Resources Section, you may notice that each free ion term (listed at the right of the diagram) splits into a term or set of terms that retain the same multiplicity (the left superscript). Under an octahedral field, all terms have symbols A, B, E or T because they are singly, doubly, or triply degenerate. While some of these terms have subscripts "1" or "2", all the terms also have "g" subscripts due to the symmetry of the d orbitals. Some of the symbols might also look familiar, as they are similar to the labels you know for splitting of d orbitals, like E_g and T_{2g}.

It is useful to know that under an octahedral field, the D, F, G, H, I terms split, but the terms S, P do not split. From inspection of the O_h character table, we find that free ion terms will split as follows:

Free Ion Term	Terms under O_h
S	A_{1g}
P	T_{1g}
D	$T_{2g} + E_g$
F	$A_{2g} + T_{2g} + T_{1g}$
G	$A_{1g} + E_g + T_{2g} + T_{1g}$
H	$E_g + T_{1g} + T_{1g} + T_{2g}$
I	$A_{1g} + A_{2g} + E_g + T_{1g} + T_{2g} + T_{2g}$

The term symbols under an octahedral field have symmetry that matches symmetry of other elements within the molecule, including the d-orbitals. A reminder of their symmetry meanings is below (see also Section 4.3.3).

Review of Mulliken Labels

Each wavefunction (including terms) can be described by a Mulliken label (symmetry label). The labels used for terms in an octahedral ligand field are listed in the table below.

Mulliken Labels	meaning
A or B	singly degenerate
E	doubly degenerate
T	triply degenerate
Subscripts	**meaning**
1	symmetric to σ_v or perpendicular C_2
2	anti-symmetric to σ_v or perpendicular C_2
g	symmetric to inversion center
u	anti-symmetric to inversion center

We can use our knowledge of symmetry to derive the term labels for a given electron configuration under an octahedral field. Let's focus only on the capital letter that is assigned as the term symbol. Assignment of the octahedral term subscripts will not be described here, but are similar to assignment of these same subscripts to orbitals with matching symmetry.

For example, the d^1 electron configuration has a free ion ground state term of ^2D. According to the table shown above, these terms will split into E_g and T_{2g} terms. Which would be its ground state term under an octahedral field? And which is the excited state term? To answer these questions we need to look at the electron configurations of the ground and excited states in an octahedral field. It is convenient to know that the term symbol under an octahedral field indicates the *degeneracies of the related electron configurations*.

Let's take a look at the electron configurations of the split d-orbitals to determine which term is the ground state. In the ground state of a d^1 under an octahedral ligand field, there would be one electron in the t_{2g} orbitals, thus the electron configuration is $t_{2g}^1 e_g^0$. For simplicity we can consider only the cases where m_s values are $+\frac{1}{2}$. There are three ways to put the electron in t_{2g} therefore, the ground state is triply degenerate, with a symbol "T". This is illustrated in the left panel of Figure *Section*8.3.2.1.

In the excited state of a d^1 under an octahedral ligand field, there would be one electron in the e_g orbitals, or a configuration of $t_2g^0 e_g^1$. There are two ways to arrange the electron with $m_s = +\frac{1}{2}$ in the e_g orbitals (Figure *Section*8.3.2.1, left). Therefore, the excited state is doubly degenerate, with a symbol "E".

In summary, the ^2D free ion term for d^1 splits into a lower-energy $^2T_{2g}$ and a higher-energy ^2E_g term under an octahedral field (Figure *Section*8.3.2.1, left).

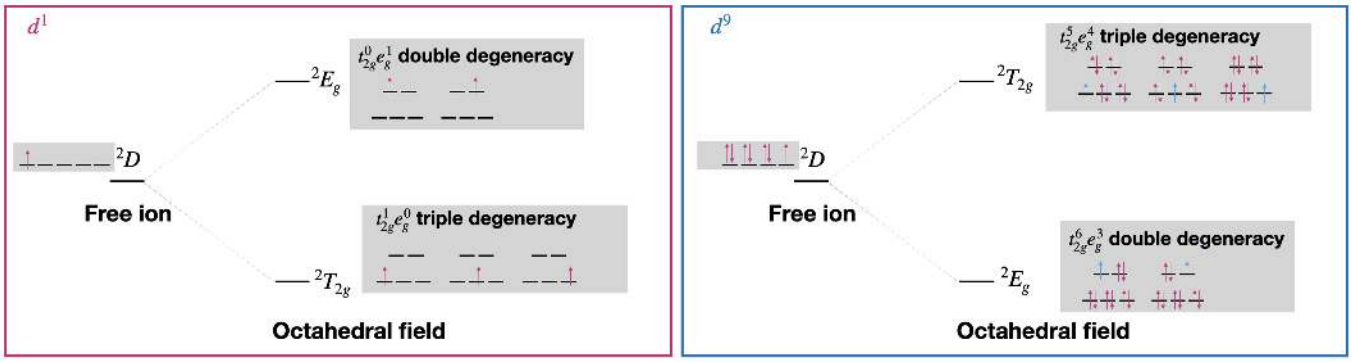


Figure *Section*8.3.2.1: Term splitting of d^1 and d^9 free ion terms in an octahedral field. The symbols of the octahedral terms match the degeneracies of the electron configurations. (CC-BY-SA; Kathryn Haas)

We could use a similar treatment to derive the relative energies and terms of a d^9 ion in an octahedral field. The ground state term of d^9 is the same as for d^1: it is ^2D. If we look at the ground state and excited state electron configurations of a d^9 ion, we find that the ground state configuration is $t_{2g}^6 e_g^3$, which is doubly degenerate. On the other hand, the excited state has an electron configuration of $t_{2g}^5 e_g^4$, and has triple degeneracy. In summary, in the case of d^9, the ^2D free ion term splits into a lower energy ^2E_g term and a higher-energy $^2T_{2g}$ term. *This is exactly the opposite of* d^1*!*

The d^1 and d^9 cases are opposite because they are related by what is said to be a "positive hole" concept. The d^9 configuration could be derived from a d^{10} configuration with one positive "hole" (an electron removed). The positive hole is similar to the lone electron in d^1 except that in the ground state, the hole is in e_g, while the electron in d^1 is in t_{2g}; thus the two situations are exact opposites.

Just as d^1 and d^9 are related by the hole concept, so are d^4 and d^6. If you consider that d^1 is the addition of one electron to the totally symmetric d^0 case, then perhaps you can see how d^6 is similar in that it is the addition of one electron to the totally symmetric d^5 case. Thus, d^1 and d^6 have similar splittings under the octahedral field. Similarly, d^9 is created by removing one electron from the totally symmetric case of d^{10} and d^4 is created by removing one electron from d^5. Thus d^4 and d^9 have identical splittings for their ground state free ion terms, which in these cases are a D term.

Due to the relationships between d^1, d^4, d^6, and d^9, the same Orgel Diagram is used to show term splitting for these cases (Figure *Section*8.3.2.2). Orgel diagrams are yet another form of correlation diagrams.

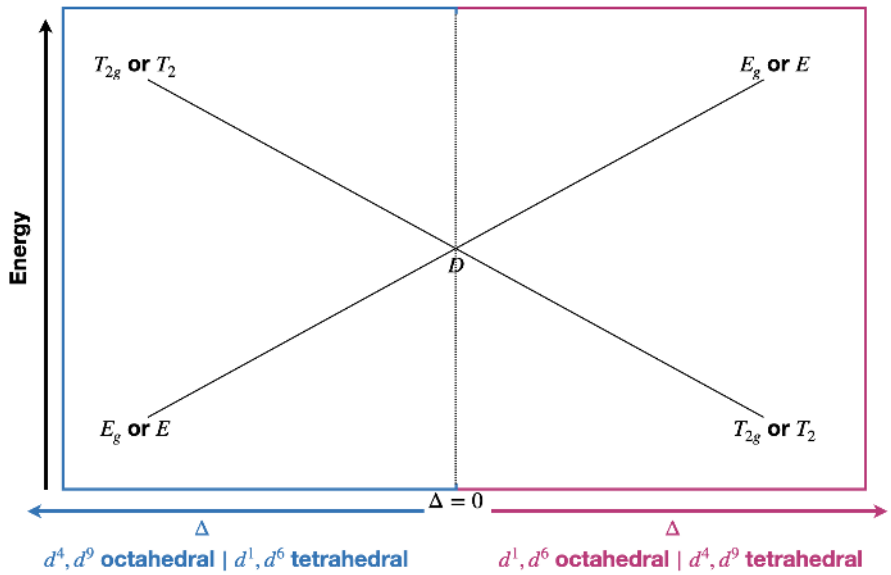


Figure *Section*8.3.2.2: Orgel diagram for splitting of the ground state D term of d^1, d^4, d^6, and d^9 ions in an tetrahedral or octahedral field. (CC-BY-SA; Kathryn Haas)

Just as there are relationships between d^1, d^4, d^6, and d^9, there are similar relationships between d^2, d^3, d^7, and d^8, and there is an Orgel diagram that can represent the splitting of their relevant free-ion terms.

Tetrahedral splitting

Because tetrahedral field splitting has the opposite pattern to octahedral field splitting of the d-orbitals, there are relationships between tetrahedral and octahedral terms. In general, for a tetrahedral field with d^n electrons, the Tanabe-Sugano diagram of an octahedral diagram for d^{10-n} can be used to interpret the tetrahedral case. The Orgel diagrams are labeled in general terms for this reason. They can be applied to both tetrahedral and octahedral cases.

Jahn-Teller distortions

We can also see what would happen to the terms in the case of Jahn-Teller distortion. In the case of a Jahn-Teller distortion (most common for d^9 and high-spin d^4 where the e_g orbitals are asymmetrically occupied), we can use the degeneracy of orbital electron configurations to identify term labels. Let's walk through an example using the most simple case: a d^1 metal ion (Figure *Section*8.3.2.3).

Jahn-teller usually causes a tetragonal distortion of an octahedron. This would be a change from O_h to D_{4h} symmetry.

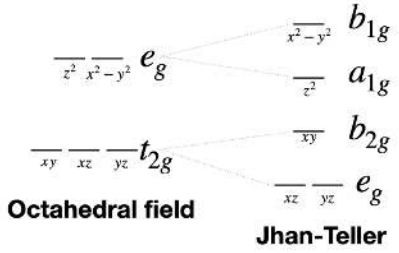


Figure *Section*8.3.2.3: Splitting of d-orbitals from O_h to D_{4h} symmetry by Jahn-Teller distortion. (CC-BY-SA; Kathryn Haas)

The t_{2g} orbitals (the set d_{xy}, d_{xz}, d_{yz} are split into e_g (d_{xz}, d_{yz}) and b_{2g} (d_{xy}) by this symmetry change. Thus, we can expect any T_{2g} terms to be split similarly into E_g and B_{2g} terms by Jahn-Teller distortion. The e_g orbitals under O_h are split into a_1g (d^{z^2}) and b_1g ($d_{x^2-y^2}$) under D_{4h}. Thus, we can expect E_g terms to be split into B_{1g} and A_{1g} terms by Jahn-Teller distortion (Figure *Section*8.3.2.4).

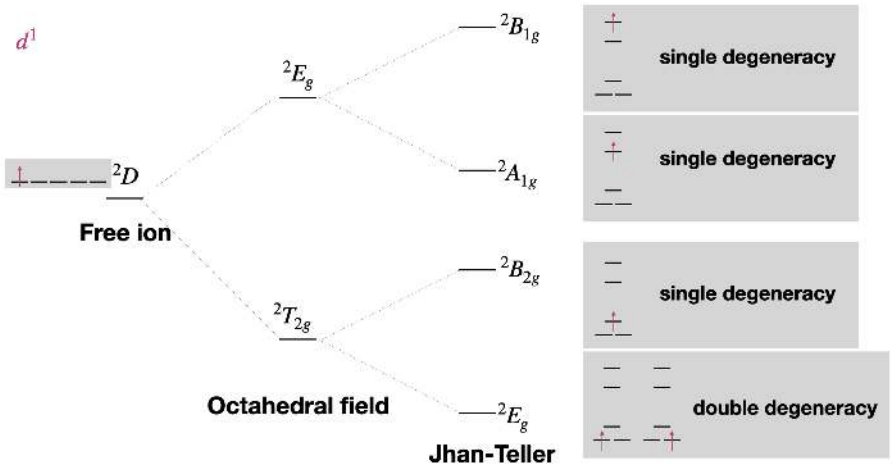


Figure *Section*8.3.2.4: Splitting of d^1 from an octahedral field to D_{4h} by Jhan-Teller tetragonal distortion. (CC-BY-SA; Kathryn Haas)

Just as d^1 and d^9 gave opposite order of their terms under an octahedral field, they also give opposite order of terms in the Jahn-Teller distortion.

This page titled Section 8.3.2: Symmetry labels for split terms is shared under a CC BY-NC-SA license and was authored, remixed, and/or curated by Kathryn Haas.

- **4.3.3: Character Tables** by Kathryn Haas is licensed CC BY-NC-SA 4.0.

Section 8.3.3: Selection Rules

Electronic transitions between states of different energies give rise to electronic spectra. However, some transitions are more probable, and thus more intense, than others. In UV-vis spectroscopy, for example, the transitions that are "allowed" can give rise to absorption bands that are much more intense than transitions that are "forbidden". To be clear, "forbidden" transitions are still possible, and are sometimes observable, but are less intense because they happen less frequently than "allowed" transition when the molecules are exposed to electromagnetic radiation.

Selection Rules that govern Electronic Transitions

The Selection Rules governing transitions between electronic energy levels (including microstates and terms) are:

1. **The Spin Selection Rule**, $\Delta S = 0$.
2. **The Laporte (or orbital) Selection Rule**, for centrosymmetric molecules $g \rightarrow u$ or $u \rightarrow g$, or $\Delta l = \pm 1$.

Selection rules that govern electronic transitions

Spin selection rule

The Spin Selection Rule forbids transitions between states with different total spin, and thus different spin multiplicity. This rule allows transitions only between states with the same total intrinsic spin ($\Delta S = 0$), and thus the same spin multiplicity value in the term symbol. In other words, the direction of the promoted electron's spin should not change. Just in case it is not obvious yet, the spin multiplicity is the left superscript in the term symbol, so this rule allows transitions between terms with the same superscript. For example, this rule would allow a transition from a ^3T term to a ^3A term, but not from ^3T to ^2D.

Laporte (orbital) Selection Rule

The Laporte Selection Rule applies to molecules that have a center of symmetry (aka center of inversion, centrosymmetric). This rule forbids transitions between states with the same parity (symmetry) with respect to an inversion center (i). Parity is indicated on molecular orbitals and on term symbols with subscripts g (gerade, or even) and u (ungerade, or uneven). Transitions between u and g terms are allowed (eg $T_{2g} \rightarrow T_{1u}$ is allowed), but those between two g or two u terms are forbidden (eg $T_{2g} \rightarrow T_{1g}$ is forbidden). Because different types of orbitals have different symmetries with respect to i, this rule is sometimes referred to as the "orbital selection rule". It forbids transitions within one type of orbital subshell. For example, p orbitals are antisymmetric with respect to i, while both s and d orbitals are symmetric with respect to i. This rule forbids $s \rightarrow s$, $p \rightarrow p$, $d \rightarrow d$, and $d \rightarrow s$ transitions, but allows transition between $d \rightarrow p$ and $d \rightarrow s$ orbitals. This rule is important in transition metal complexes because it fobids $d - d$ transitions in centrosymmetric geometries, including octahedral and linear coordination geometries.

Despite these selection rules, $d \rightarrow d$ transitions are a hallmark feature of octahedral transition metal complexes, and are often responsible for their brilliant colors. These $d \rightarrow d$ transtions, and other forbidden transitions may still occur, primarily through relaxation of these rules in specific cases.

Breaking the rules!

Relaxation of the Laporte and Spin Selection Rules rules can occur through:

- **Vibronic coupling:** the bonds of metal complexes vibrate and may cause temporary distortions in molecular symmetry. These distortions can cause temporary loss in symmetry (as well as some orbital mixing), and thus allow $d \rightarrow d$ transitions in those moments of distortion. Despite being forbidden by the Laporte Selection rule, the $d \rightarrow d$ transitions in octahedral complexes appear, but are weak (of low intensity) with molar absorptivities $\leq 100\ M^{-1}cm^{-1}$.
- **Orbital Mixing**: In the case of octahedral complexes, π-acceptor and π-donor ligands can mix with the d-orbitals so that transitions are no longer purely $d \rightarrow d$ (but these are usually considered "charge transfer" transitions, not $d \rightarrow d$). In the case of tetrahedral complexes, the molecule has no center of symmetry (thus no u or g subscripts on the terms). In the valence orbital model, a tetrahedral molecule is said to have sp^3 and sd^3 hybridized orbitals, while MO theory predicts MO's with mixtures of some s, p, and d character - this mixing of orbital types can allow transitions between "mixed" orbitals that

would otherwise be forbidden in "pure" orbitals. A similar phenomenon would occur in octahedrons with significant distortion, or in other coordination geometries that provide potential for orbital mixing.

- **Spin-Orbit coupling**: This gives rise to spin-forbidden bands of low intensity, usually with very weak molar absorptivities approximately $\leq 1 M^{-1} cm^{-1}$. This phenomenon is usually more important for transition metals of the second row $4d$ and beyond.

? Exercise *Section*8.3.3.1

Consider the d^2 case presented in a previous section. The free ion terms for d^2 were found to be ^3F, ^1G, ^3P, ^1D, ^1S. First, identify the ground state term. Then identify the Spin-Allowed excitations starting from the ground state.

Answer

The ground state is ^3F. There is only one spin-allowed transition: $^3F \rightarrow ^3 P$.

The spin-forbidden transitions from ^3F include $^3F \rightarrow ^1 D$, $^3F \rightarrow ^1 G$, and $^3F \rightarrow ^1 S$.

This page titled Section 8.3.3: Selection Rules is shared under a CC BY-NC-SA license and was authored, remixed, and/or curated by Kathryn Haas.

- **Selection Rules for Electronic Spectra of Transition Metal Complexes** by Robert J. Lancashire is licensed CC BY 4.0.

Section 8.3.4: Correlation Diagrams

Splitting of Terms in an Octahedral Field

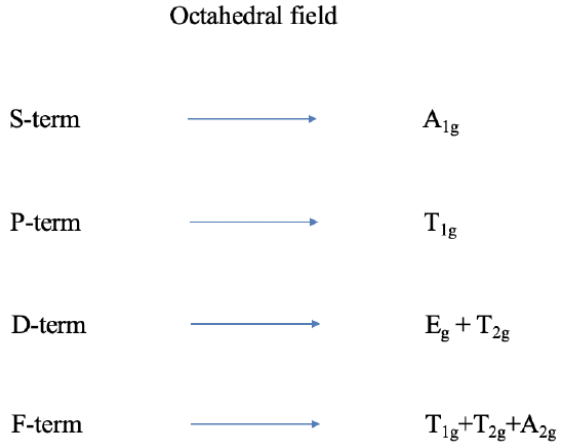


Figure *Section*8.3.4.1: Octahedral field term splitting

Thus far we have only considered free ion terms, which means terms without the presence of a ligand field. Let us think next about the influence of an octahedral field on a term. Terms are wavefunctions, just like orbitals, and therefore they behave like orbitals in a ligand field. For example, the d-orbitals split into $t_{2g}$and e_g orbitals in an octahedral ligand field. A D-term behaves similarly. It splits into T_{2g} and E_g terms (note the capital letters that describe term, and the lower-case letters that describe orbitals!). \The p-orbitals are triple-degenerate, having T_{1g} symmetry in the O_h (octahedral) point group, and do not split in energy: they give the t_{1g} orbitals under an octahedral field. Similarly, the P-terms have the same symmetry and also do not split. The P-term becomes a T_{1g} term in an octahedral field.

Following analogous arguments, S terms become A_{1g} terms. F terms do split in energy like f-orbitals and become T_{1g}, T_{2g}, and A_{2g} terms. Overall, the presence of the octahedral field increases the number of terms from four to seven (Figure *Section*8.3.4.1). It is easy to see that the ligand field leads to many states, and many potential electron transitions. Thus, we would expect quite complicated spectra. For other ligand fields, the terms also behave analogously to orbitals. For, instance in a tetrahedral field D-terms split into E and T_2 terms, and so forth.

Term Splitting for octahedral d^2 metal complexes

Now let us think about how the term energies of our free d^2-ion changes when placed in an octahedral ligand field, depending on the ligand field strength. We can express this by a correlation diagram (Figure *Section*8.3.4.2). In a correlation diagram, we plot the energies of the terms relative to the field strength.

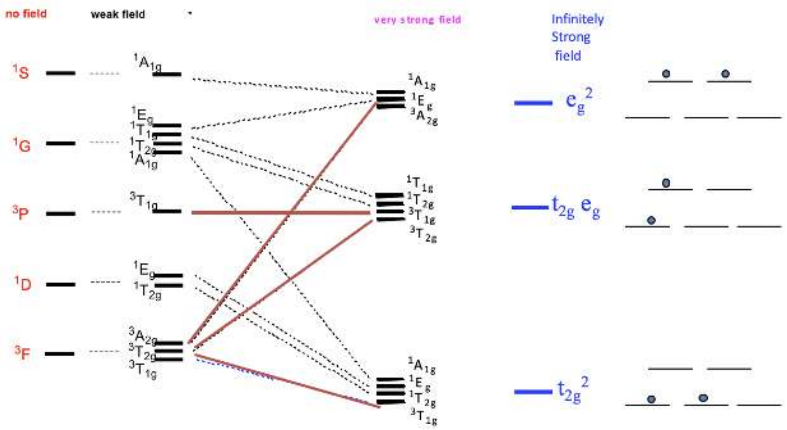


Figure *Section*8.3.4.2: Correlation diagram

On the left side we plot the terms without any field according to their energies. In the case of a d^2 ion, the energies are

$^3F^1D^3P^1G^1S <<<< .$

Next, we plot the relative energies in a weak octahedral ligand field, and label the terms according to their symmetry. We can see that the D, F, and G terms split in energy, while the S and P terms do not. Because of the weak field, energy differences are very small. Now let us increase the ligand field strength continuously, until we have reached a very strong ligand field. We see that some of the terms move up in energy, while other terms move down as the ligand field increases. For example, two of the three terms resulting from the F-terms increase in energy while one decreases. It is also possible that a term does not change its energy. For example, the $^3T_{1g}$ term from the ^3P term does not change its energy. In very strong ligand field there are three groups of terms that have similar energy. In the hypothetical case of an infinitely strong ligand field, the terms that belong to a particular group become identical in energy. In this case, there are only three states for the electrons possible. The field is considered so strong that the energy associated with electron-electron interactions become negligible compared to the energy of the field. The electrons behave as though there were no electron-electron interactions. Therefore, we can call the lowest energy state the t_{2g}^2 state. It is equivalent to the state of the two electrons being in the t_{2g} orbitals. The second state is called the $t_{2g}e_g$ state. It is equivalent to the state of one electron being in the t_{2g} and one electron being in the e_g orbitals. The third state is called the e_g^2 state, which is equivalent to the state with both electrons in the e_g^2-orbitals.

This page titled Section 8.3.4: Correlation Diagrams is shared under a CC BY-NC-SA license and was authored, remixed, and/or curated by Kai Landskron.

- **8.2: Term splitting in ligand fields, selection rules, Tanabe-Sugano diagrams. Metal to ligand, and ligand to metal transitions** by Kai Landskron is licensed CC BY 4.0.

Section 8.3.5: Applications of Tanabe-Sugano Diagrams

The Tanabe-Sugano diagrams can be used to interpret absorption spectra and gain insight into the properties of a coordination complex. For example, you could use the appropriate diagram to predict the number of transitions, assign the identity of a specific transition, or calculate the value of Δ for a specific metal complex.

How to use the Tanabe-Sugano Diagrams

1. Determine the d-electron count of the metal ion of interest.
2. Choose the appropriate Tanabe-Sugano diagram: this is the one matching the d-electron count of the metal ion. There is a full list of Tanabe-Sugano diagrams in the Resources Section.
3. Acquire an electronic spectrum of the metal complex and identify λ_{max} for spin-allowed (strong intensity) and spin forbidden (weak intensity) transitions.
4. Convert wavelength (λ_{max}) to energy (E) in wavenumbers (cm^{-1}) and generate energy ratios relative to the lowest-energy allowed transition. (i.e. $\frac{E_2}{E_1}$ and $\frac{E_3}{E_1}$).
5. Using a ruler, slide it across the printed Tanabe-Sugano diagram until the E/B ratios between lines is equivalent to the ratios found in step 4.
6. Solve for B using the E/B values (y-axis, step 4) and Δ_{oct}/B (x-axis, step 5) to yield the ligand field splitting energy, $Delta$ (Sometimes this is labeled as $10D_q$, and it is useful to know that $\Delta = 10D_q$).

Example *Section*8.3.5.1: Chromium Splitting

A Cr^{3+} metal complex has strong transitions and λ_{max} at

- 431.03 nm,
- 781.25 nm, and
- 1,250 nm.

Determine the Δ_{oct} for this complex.

Solution

1. Cr has 6 electrons. Cr^{3+} has three electrons, so it has a d-configuration of d^3
2. Locate the d^3 Tanabe-Sugano diagram
3. Convert to wavenumbers:

$$\frac{10^7(nm/cm)}{1250\ nm} = 8,000\ cm^{-1} \quad \text{(Section 8.3.5.1)}$$

$$\frac{10^7(nm/cm)}{781.25\ nm} = 13,600\ cm^{-1} \quad \text{(Section 8.3.5.2)}$$

$$\frac{10^7(nm/cm)}{431.03\ nm} = 23,200\ cm^{-1} \quad \text{(Section 8.3.5.3)}$$

4. Allowed transitions are $^4T_{1g} \leftarrow {}^4A_{2g}$, $T \leftarrow {}^4{}_{1g}{}^4A_{2g}$ and $^4T_{2g} \leftarrow {}^4A_{2g}$.

Transition	Energy cm^{-1}	Ratios to lowest
$^4T_{1g} \leftarrow {}^4A_{2g}$	23,200	2.9
$T \leftarrow {}^4{}_{1g}{}^4A_{2g}$	13,600	1.7
$^4T_{2g} \leftarrow {}^4A_{2g}$	8,000	1

5. Sliding the ruler perpendicular to the x-axis of the d^3 diagram yields the following values:

Δ_{oct}/B	10	20	30	40
Height E(ν_3)/B	29	45	64	84
Height E(ν_2)/B	17	30	40	51
Height E(ν_1)/B	10	20	30	40
Ratio E(ν_3)/E(ν_1)	2.9	2.25	2.13	2.1
Ratio E(ν_2)/E(ν_1)	1.7	1.5	1.33	1.275

6. Based on the two tables above it should be assessed that the Δ_{oct}/B value is 10. B is found by dividing E by the height.

Energy cm^{-1}	Height	B
23,200	29	800
13,600	17	800
8,000	10	800

7. Next multiply Δ_{oct}/B by B to yield the Δ_{oct} energy.

$$10 \times 800 = 8000\ cm^{-1} = \Delta_{oct} \qquad \text{(Section 8.3.5.4)}$$

Each problem is of varying complexity as several steps may be needed to find the correct Δ_{oct}/B values that yield the proper energy ratios.

This page titled Section 8.3.5: Applications of Tanabe-Sugano Diagrams is shared under a CC BY-NC-SA license and was authored, remixed, and/or curated by Kathryn Haas.

Section 8.3.6: Tetrahedral Complexes

Transitions in tetrahedral complexes are Laporte-allowed

Tetrahedral metal complexes often have more intense electronic transitions than their octahedral counterparts. This is due to the fact that the $d-d$ transitions in a tetrahedron are allowed by the Laporte selection rule, while $d-d$ transitions in an octahedral complex are Laporte-forbidden. Recall that the Laporte selection rule applies to centrosymmetric complexes only. The Laporte rule applies to octahedral complexes but not to tetrahedral complexes because a tetrahedron does not have a center of inversion. Notice that the terms (and orbital labels) in a tetrahedron do not include the g subscripts that are present under octahedral symmetry (Figure *Section*8.3.6.1). The splitting pattern of a tetrahedral complex is exactly opposite to the octahedral case. In the case of a tetrahedron, however, the "g" subscripts are inappropriate because of the tetrahedron's lack of a center of inversion, and transitions between the terms in a tetrahedron do not violate the Laporte Rule.

Another way to explain this in terms of electron transitions between orbitals is through the orbital mixing required to form a tetrahedral complex. Orbital types (i.e., s, p, d) must mix to form the moleculare orbitals of a tetrahedral transition metal complex. The mixing of s and p orbitals with the d orbitals allows transitions that are forbidden in the case of pure d-orbitals.

It is also worth noting that $\Delta_t = \frac{4}{9}\Delta_o$. The smaller Δ for transition metals means that the tetrahedral complexes can absorb at a lower energy and longer wavelength relative to an analogous octahedron.

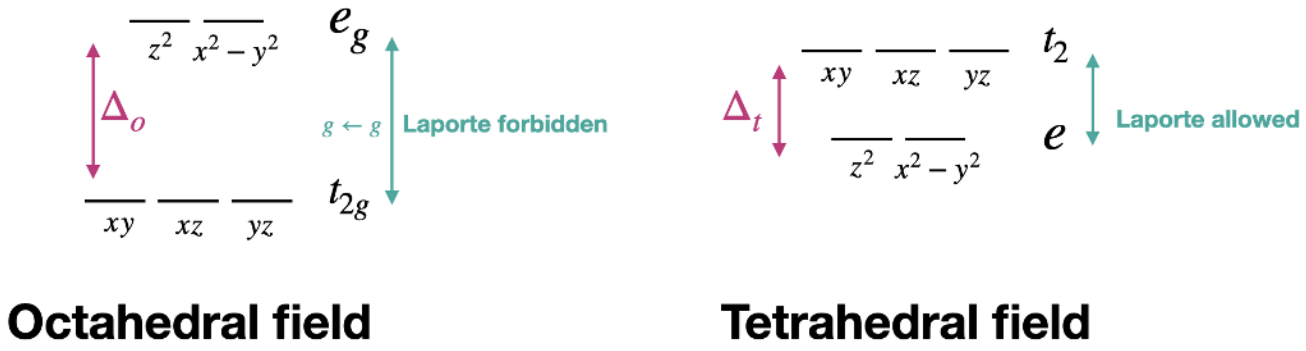


Figure *Section*8.3.6.1: $d-d$ transitions in octahedral complexes are Laporte-forbidden, while those in tetrahedral complexes are Laporte-allowed. (CC_BY_SA; Kathryn Haas)

Tanabe-Sugano diagrams for tetrahedral complexes

Due to the opposite splitting pattern, the transitions for a d^n tetrahedral complex are sufficiently represented by the d^{10-n} Tanabe-Sugano diagram (just drop the g subscripts from the diagrams). For example, the electronic spectrum of a d^8 tetrahedral complex (e.g., $[Ni(H_2O)_6]^{2+}$) can be interpreted using the d^2 Tanabe-Sugano diagram.

This page titled Section 8.3.6: Tetrahedral Complexes is shared under a CC BY-NC-SA license and was authored, remixed, and/or curated by Kathryn Haas.

Section 8.3.7: Charge-Transfer Spectra

Charge Transfer Transitions

Zn^{2+}		d^{10} ion	white
$[Cu(MeCN)_4]^+$	Cu(I)	d^{10} ion	colourless
$[Cu(phen)_2]^+$	Cu(I)	d^{10} ion	dark orange
TiF_4		d^0 ion	white
$TiCl_4$		d^0 ion	white
$TiBr_4$		d^0 ion	orange
TiI_4		d^0 ion	dark brown
$[MnO_4]^-$	Mn(VII)	d^0 ion	extremely purple
$[Cr_2O_7]^-$	Cr(VI)	d^0 ion	bright orange

Figure ***Section*8.3.7.1**: Some examples of complexes with d^0 and d^{10} electron configurations, and their colors. Attribution: E.R. Schofield.

We are still not done with our electronic spectra. Thus far, we have only considered transitions of d-electrons between d-orbitals, and their terms. These are called d-d transitions. However, there are also so-called charge transfer transitions possible, which are not d-d transitions. We can easily see that there must be transitions other than d-d transitions when we look at the colors of d^{10} and d^0 ions. For those, there are no d-d transitions possible. Therefore, they all should be colorless. However, that is not always true. Some of these ions are indeed colorless, but some are not (Figure ***Section*8.3.7.2**). For example, Zn^{2+}, a d^{10} ion, is colorless in complexes, but not Cu(I), which is also d^{10}. While tetrakis(acetonitrile)copper(+) is colorless, bis(phenanthrene) copper(+) is dark orange. d^0 ions have similar properties: While TiF_4 and $TiCl_4$ are colorless, $TiBr_4$ is orange, and TiI_4 is brown. Some d^0 species are even extremely colorful, for example, permanganate with Mn^{7+}, which is extremely purple, and dichromate with Cr(VI), which is bright orange.

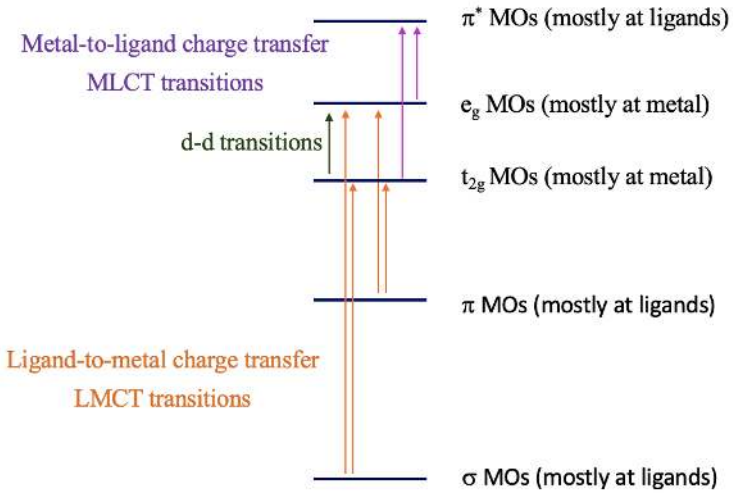


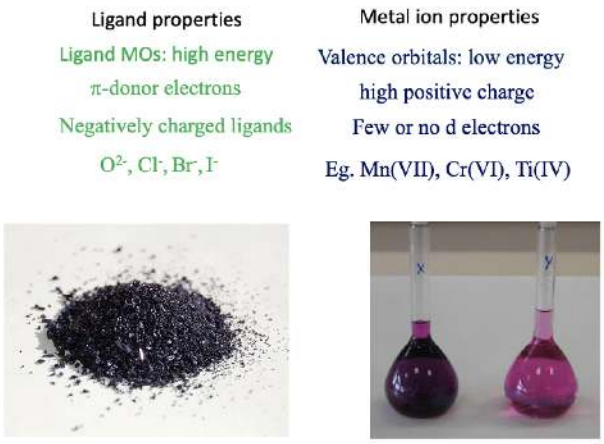
Figure ***Section*8.3.7.2**: Charge-transfer transitions. Attribution: E.R. Schofield.

The explanation for these phenomena is charge-transfer transitions (***Section*8.3.7.2**). There are two types of charge-transfer transitions: ligand-to-metal (LMCT) and metal-to-ligand (MLCT) charge transfer transitions. For the ligand-to-metal transitions, electrons from bonding σ and π-orbitals get excited into metal d-orbitals in the ligand field, for example the t_{2g} and the e_g orbitals in an octahedral complex. If the energy difference between the σ/π-orbitals and the d-orbitals is small enough, then this electron transition is associated with the absorption of visible light. The transition is called a ligand-to-metal transition because the ligand σ/

π-orbitals are mostly located at the ligands, while the metal-d-orbitals in a ligand field are mostly located at the metal. Vice versa, the metal-to-ligand transition involves the transition of an electron from metal d-orbitals in a ligand field to ligand π*-orbitals. This essentially moves electron density from the metal to the ligand, hence the name ligand-to-metal-charge transfer transition. If the energy-difference between the ligand π* and the metal orbitals is small enough, then the absorption occurs in the visible range. Charge-transfer transitions are usually both spin- and Laporte allowed; hence, if they occur, the color is often very intense. How can we distinguish between d-d and charge transfer transitions? Charge transfer transitions often change in energy as the solvent polarity is varied (solvatochromic), as there is a change in polarity of the complex associated with the charge transfer transition. This can be used to distinguish between d-d transitions and charge-transfer bands.

LMCT Transitions

Can we predict when the energy windows between the bonding molecular orbitals and the metal d-orbitals are small enough for LMCT transitions in the visible to take place? Generally, it would be desirable if the energy of the metal orbitals were as low as possible and the energy of the bonding ligand orbitals were as high as possible. The energy of metal d-orbitals decreases with increasing positive charge at the metal because the effective nuclear charge on the metal increases. This means that very high metal oxidation states favor LMCT transitions. The d-orbitals should have few or no electrons, so that electrons can be promoted into the orbitals, and orbital energy decreases because electron-electron repulsion is minimized. Examples are Mn(VII), Cr(VI), and Ti(IV). The energy of MOs from bonding ligand orbitals increases when the ligand orbitals have high energy; this is typically the case for π-donor ligands with a negative charge (Fig. 8.2.21).



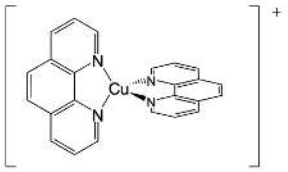
***Section*8.3.7.1**: The properties of the metal ions and ligands suitable for LMCT transitions. MnO_4^- is deep purple due to LMCT transitions (Attribution: Benjah-bmm27 / Public domain https://commons.wikimedia.org/wiki/F...ate-sample.jpg) and (Attribution: Pradana Aumars / CC0 https://commons.wikimedia.org/wiki/F...entrations.jpg), respectively.

Examples of ligands are oxo- and halo ligands. This explains, for example, the LMCT transitions in permanganate. The Mn is in the very high oxidation state +7, and the ligands are oxo-ligands, which are π-donors with a 2- negative charge. The transitions are both Laporte and spin-allowed, leading to a very high intensity of light absorption, and thus color (Fig. 8.2.21).

MLCT Transitions

What are favorable metal ion and ligand properties for a metal-to-ligand transition, then? In this case we would like to keep the energy of the metal orbitals as high as possible so that the energy difference between a metal d-orbital and a π*-orbital is minimized. This is accomplished when the positive charge at the metal ion is small, and there are many d-electrons that can repel each other, thereby increasing orbital energies, for example Cu(I), Fig. 8.2.22.

Metal ion properties	Ligand properties
low metal ion charge	π-acceptor ligand with low-lying π* orbitals
many electrons	
Cu(I), d^{10} ion	1,10-phenanthroline, CN^-, CO, SCN^-



$[Cu(phen)_2]^+$, dark orange

***Section*8.3.7.3**: bis(phenanthroline) copper(+). Attribution: E.R. Schofield.

The ligand should be a π-acceptor with low-lying π*-orbitals - for example, phenanthroline, CN^-, SCN^-, and CO. The bis(phenanthroline) copper(+) ion, for instance, is dark orange and has an MLCT absorption band at 458 nm. This MLCT transfer is both spin and Laporte-allowed.

It should be mentioned that some complexes allow for both metal-to-ligand and ligand-to-metal transitions. For example, in the $Cr(CO)_6$ complex, the σ-orbitals are high enough and the π*-orbitals are low enough in energy to allow for light absorption in the visible range. Finally, intraligand bands are also possible when the ligand is a chromophore.

Dr. Kai Landskron (Lehigh University). If you like this textbook, please consider to make a donation to support the author's research at Lehigh University: Click Here to Donate.

This page titled Section 8.3.7: Charge-Transfer Spectra is shared under a CC BY-NC-SA license and was authored, remixed, and/or curated by Kathryn Haas.

- **8.2: Term splitting in ligand fields, selection rules, Tanabe-Sugano diagrams. Metal to ligand, and ligand to metal transitions** by Kai Landskron is licensed CC BY 4.0.

Section 8.3.8: Applications of Charge-Transfer

Transition metal complexes with strong π-accepting ligands have proven quite useful across many applications in industry, materials science, and medicine due to their intense absorption of light, photostability, and unique geometric, redox, and photodynamic properties. These complexes usually have low-valent metal ions (low oxidation state) with π-accepting ligands constructed of conjugated poly-aromatic rings. Intense light absorption occurs through metal-to-ligand charge transfer (MLCT), causing a formal oxidation of the metal ion and reduction of the ligand. These compounds are used as sensors, and their excited states can be used as indispensable reactants. Some examples of their applications are discussed briefly below.

Ruthenium bypyridine derivatives

Let's use the example of a simple and interesting metal complex: tris(bypyridine)ruthenium(II), or $[Ru(bpy)_3]^{2+}$. This molecule is the most generic form of a family of derivatives that have this core structure in common. $[Ru(bpy)_3]^{2+}$ absorbs ultraviolet light at 452 nm due to an intense MLCT. It also absorbs light at shorter wavelenghts due to ligand-centered $\pi* \leftarrow \pi$, metal-centered $d \leftarrow d$, and LMCT transitions. The ground state is a singlet state (all paired electrons), and the spin-selection rule allows formation of a singlet excited state. However, in the case of high-atomic-number d^6 metal ions, like Ru, there is intense spin-orbit coupling that favors intersystem crossing. **Intersystem crossing** is the phenomenon by which a system's spin multiplicity can change by the transition of an electron's spin without energy cost. In the case of $[Ru(bpy)_3]^{2+}$, the excited singlet state transitions to an isoenergetic (or degenerate) triplet excited state. $[Ru(bpy)_3]^{2+}$ has a long-lived excited state due to the fact that the transition between the triplet excited state and the singlet ground state is spin-forbidden. The excited state can relax to the singlet ground state radiatively (releasing a photon) or non-radiatively (as phonons/heat).

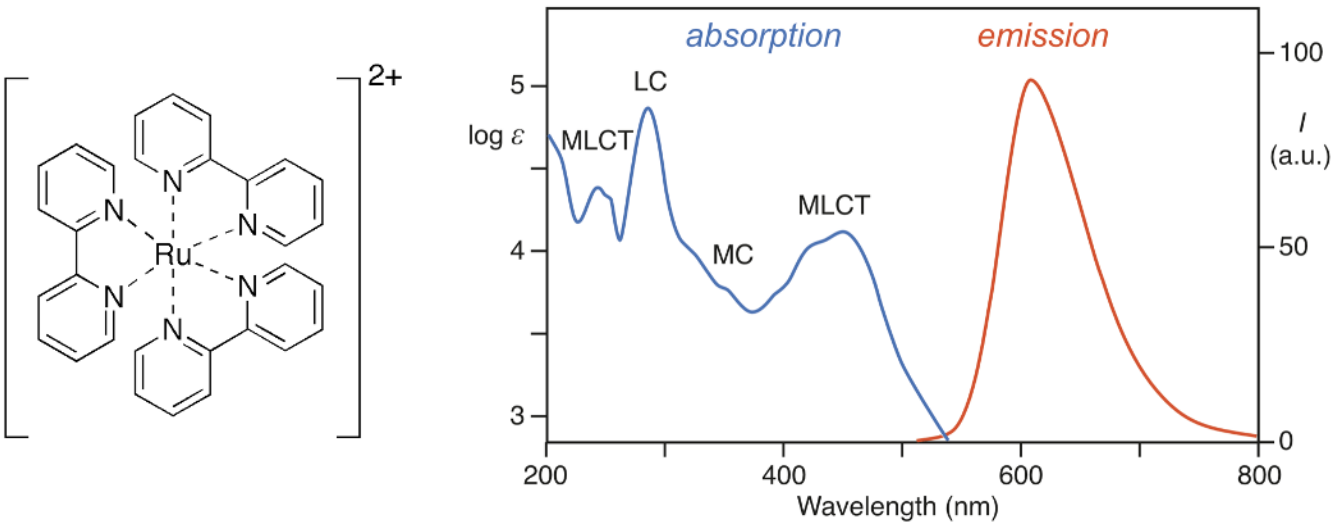


Figure *Section*8.3.8.1: Structure of $[Ru(bpy)_3]^{2+}$ (left) and its absorption and emission spectrum (right). (CC-BY-SA: Albris, Ru(bpy)32+ absorption&emission, Added structure of Ru(bpy)3 by Kathryn Haas)

Bioimaging

The $[Ru(bpy)_3]^{2+}$ complex is fluorescent, with a quantum yeld of approximately 2%. Derivatives of this core structure offer a variety of interesting properties, including a tunable color of emission. Other modifications have been made to make Ru bipyridine derivatives more functional for cellular imaging. For example, these metal complexes have been modified to bind to carbohydrates, specific organelles, or specific organs for targeted biological imaging applications.

Energy and catalysis

Due to the long lifetime of the $[Ru(bpy)_3]^{2+}*$ excited triplet state, this molecule has potential as a photosensitizer for the oxidation and reduction of water (water splitting) for energy production. The MLCT excitation is essentially a removal of an electron from Ru (an oxidation of Ru) and a placement of an electron onto a bpy ligand (a reduction of the ligand). The resultant $[Ru^{3+}]$ center is a powerful oxidant, capable of oxidizing water, while the unpaired electron on reduced bpy is a powerful reductant. The power of

this complex for catalyzing the splitting of water has been demonstrated using an electron mediator, methyl viologin, a Pt catalyst, and a sacrificial reductant. Once the excited $[Ru(bpy)_3]^{2+*}$ has formed, the excited electron can be captured by methyl viologen and passed to a Pt catalyst which reduces hydrogen ion (H^+) to H_2. The oxidized $[Ru(bpy)_3]^{3+}$ complex is then reduced by reaction with a sacrificial reductant like EDTA or triethanolamine to re-form $[Ru(bpy)_3]^{2+}$.

$[Ru(bpy)_3]^{2+}$ is also used as a photosensitizer for organic synthesis. Many analogues of $[Ru(bpy)_3]^{2+}$ are employed as well. These transformations exploit the redox properties of excited $[Ru(bpy)_3]^{2+*}$ and its reductively quenched derivative $[Ru(bpy)_3]^{+}$. (from Wikipedia)

Other applications

Derivatives of $[Ru(bpy)_3]^{2+}$ are numerous. Such complexes are widely discussed for applications in biodiagnostics, photovoltaics, and organic light-emitting diodes, but no derivative has been commercialized. Application of $[Ru(bpy)_3]^{2+}$ and its derivatives to fabrication of optical chemical sensors is arguably one of the most successful areas so far. (from Wikipedia)

This page titled Section 8.3.8: Applications of Charge-Transfer is shared under a CC BY-NC-SA license and was authored, remixed, and/or curated by Kathryn Haas.

CHAPTER OVERVIEW

Chapter 9: Structure and Energetics of Solids

In the chemistry of molecular compounds, we are accustomed to the idea that properties depend strongly on structure. For example we can rationalize the polarity of the water molecule based on its shape. We also know that two molecules with the same composition (e.g., ethanol and dimethyl ether) have very different properties based on the bonding arrangements of atoms. It should come as no surprise that the properties of extended solids are also connected to their structures, and so to understand what they do we should begin with their crystal structures. Most of the metals in the periodic table have relatively simple structures and so this is a good place to begin.

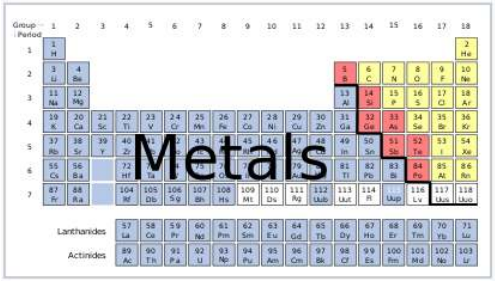


Figure *Chapter*9.1: Over $\frac{2}{3}$ of the elements in the periodic table are metals. All elemental metals (except the three - Cs, Ga, Hg - that are liquid at or near room temperature) are crystalline solids at room temperature, and most have one of three simple crystal structures.

With ionic solids we "graduate" from simple metal structures based on sphere packings to more complex structures where there are both anions and cations. In this chapter we will try to systematize the structures of inorganic solids - metal oxides, halides, sulfides, and related compounds - and develop some rules for which structures to expect based on electronegativity differences, hard-soft acid-base rules, and other periodic trends. We will see that many of these structures are based on the simple packing of spheres.



Figure *Chapter*9.2: The morphology of twinned crystals of iron pyrite (FeS_2) is related to the underlying cubic symmetry of the unit cell. Like NaCl, the pyrite crystal structure can be thought of as a face-centered cubic array of anions (S_2^{2-}) with cations (Fe^{2+}) occupying all the octahedral holes.

Inorganic solids often have simple crystal structures, and some of these structures are adopted by large families of ionic or covalent compounds. Examples of the most common structures include NaCl, CsCl, NiAs, zincblende, wurtzite, fluorite, perovskite, rutile, and spinel. We will develop these structures systematically from the close packed and non-close packed lattices.

Learning Objectives

- Determine the formula of an ionic solid based on the unit cell
- Predict relative lattice energies based on ion sizes and charges
- Understand how lattice energy plays a role in solubility
- Explain how particle size affects the material properties in nanomaterials

Section 9.1: Crystal Structures and Unit Cells
Section 9.2: Energetics of Ionic Solids- Lattice Energy
Section 9.3: Lattice Enthalpies and Born Haber Cycles

Section 9.4: Lattice Energy and Solubility
Section 9.5: Bonding in Metals and Semicondoctors
Section 9.6: Nanomaterials
Section 9.1b: Ionic Radii and Radius Ratios

Chapter 9: Structure and Energetics of Solids is shared under a CC BY-NC-SA license and was authored, remixed, and/or curated by LibreTexts.

Section 9.1: Crystal Structures and Unit Cells

Introduction

The term "closest packed structures" refers to the most tightly packed or space-efficient composition of crystal structures (lattices). Imagine an atom in a crystal lattice as a sphere. While cubes may easily be stacked to fill up all empty space, unfilled space will always exist in the packing of spheres. To maximize the efficiency of packing and minimize the volume of unfilled space, the spheres must be arranged as close as possible to each other. These arrangements are called **closest packed structures**. The packing of spheres can describe the solid structures of crystals. In a crystal structure, the centers of atoms, ions, or molecules lie on the lattice points. Atoms are assumed to be spherical to explain the bonding and structures of metallic crystals. These spherical particles can be packed into different arrangements. In closest packed structures, the arrangement of the spheres are densely packed in order to take up the greatest amount of space possible.

Close-Packing of Identical Spheres

Crystals are of course three-dimensional objects, but we will begin by exploring the properties of arrays in two-dimensional space. This will make it easier to develop some of the basic ideas without the added complication of getting you to visualize in 3-D — something that often requires a bit of practice. Suppose you have a dozen or so marbles. How can you arrange them in a single compact layer on a table top? Obviously, they must be in contact with each other in order to minimize the area they cover. It turns out that there are two efficient ways of achieving this:



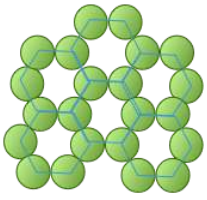
The essential difference here is that any marble within the interior of the square-packed array is in contact with four other marbles, while this number rises to six in the hexagonal-packed arrangement. It should also be apparent that the latter scheme covers a smaller area (contains less empty space) and is therefore a more efficient packing arrangement. If you are good at geometry, you can show that square packing covers 78 percent of the area, while hexagonal packing yields 91 percent coverage.

If we go from the world of marbles to that of atoms, which kind of packing would the atoms of a given element prefer?



If the atoms are identical and are bound together mainly by dispersion forces which are completely non-directional, they will favor a structure in which as many atoms can be in direct contact as possible. This will, of course, be the hexagonal arrangement.

Directed chemical bonds between atoms have a major effect on the packing. The version of hexagonal packing shown at the right occurs in the form of carbon known as *graphite* which forms 2-dimensional sheets. Each carbon atom within a sheet is bonded to three other carbon atoms. The result is just the basic hexagonal structure with some atoms missing.



The coordination number of 3 reflects the sp^2-hybridization of carbon in graphite, resulting in plane-trigonal bonding and thus the sheet structure. Adjacent sheets are bound by weak dispersion forces, allowing the sheets to slip over one another and giving rise to the lubricating and flaking properties of graphite.

Types of Holes From Close-Packing of Spheres

When a single layer of spheres is arranged into the shape of a hexagon, gaps are left uncovered. The hole formed between three spheres is called a **trigonal hole** because it resembles a triangle. In Figure *Section*9.1.1, two out of the the six trigonal holes have been highlighted green.

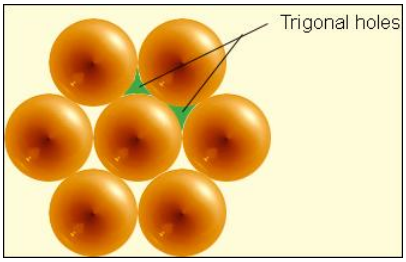


Figure *Section*9.1.1: Trigonal holes (green) between close packed spheres in a single layer

Once the first layer of spheres is laid down, a second layer may be placed on top of it. The second layer of spheres may be placed to cover the trigonal holes from the first layer. Holes now exist between the first layer (the orange spheres) and the second (the lime spheres), but this time the holes are different (Figure *Section*9.1.2). The triangular-shaped hole created over a orange sphere from the first layer is known as a **tetrahedral hole** because the surrounding spheres are in a tetrahedral arrangement. A hole from the second layer that also falls directly over a hole in the first layer is called an **octahedral hole** because the surrounding spheres are in an octahedral arrangement.

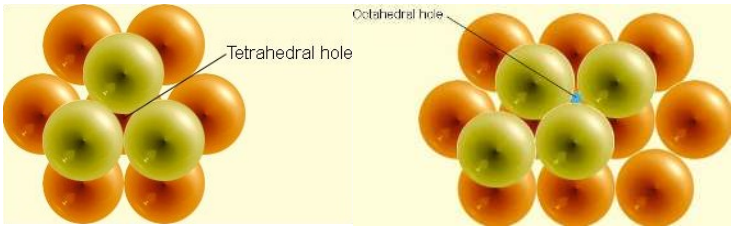


Figure *Section*9.1.2: Illustrations of tetrahedral (left) and octahedral (right) holes formed between two close packed layers

Close Packed Crystal Structures

Hexagonal Close-Packed (hcp)

In a hexagonal close-packed structure, the third layer has the same arrangement of spheres as the first layer and covers all the tetrahedral holes. Since the structure repeats itself after every two layers, the stacking for hcp may be described as "a-b-a-b-a-b." The atoms in a hexagonal close-packed structure efficiently occupy 74% of space while 26% is empty space.

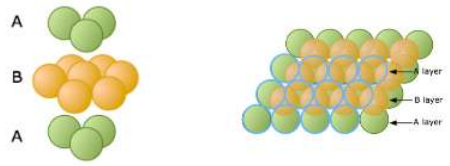


Figure *Section*9.1.3: Side and top views of the layers in the hexagonal close-packed (hpc) structure.

Cubic Close-Packed (ccp)

The arrangement in a cubic closest packing also efficiently fills up 74% of space. Similar to hexagonal closest packing, the second layer of spheres is placed on to of half of the depressions of the first layer. The third layer is completely different than that first two layers and is stacked in the depressions of the second layer, thus covering all of the octahedral holes. The spheres in the third layer are not in line with those in layer A, and the structure does not repeat until a fourth layer is added. The fourth layer is the same as the first layer, so the arrangement of layers is "a-b-c-a-b-c."

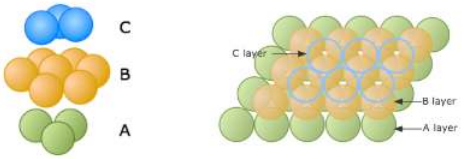


Figure *Section*9.1.4: Side and top views of the layers in cubic close-packed (ccp) structure.

Coordination Number and Number of Atoms Per Unit Cell

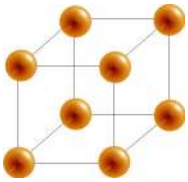
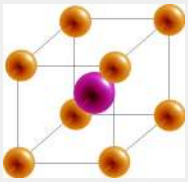
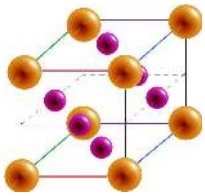
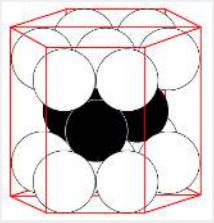
A unit cell is the smallest representation of an entire crystal. All crystal lattices are built of repeating unit cells. In a unit cell, an atom's coordination number is the number of atoms it is touching.

- The simple cubic has a sphere at each corner of a cube. Each sphere has a coordination number of 6 and there is 1 atom per unit cell.
- The body-centered cubic (bcc) has a sphere at each corner of a cube and one in the center. Each sphere has a coordination number 8 and there are 2 atoms per unit cell.
- The cubic closest packed, also called face-centered cubic (fcc) has has a sphere at each corner and each face of a cube. Each sphere has a coordination number of 12 and there are 4 atoms per unit cell.
- The hexagonal closest packed has spheres arranged in hexagons with one in the center. each sphere has a coordination number of 12 and there are 6 atoms per unit cell.

Atoms Per Unit Cell

The amount that an atom contributes to a unit cell depends on its position in the unit cell

- Each corner atom contributes $\frac{1}{8}$ to the unit cell in the cubic cells and $\frac{1}{6}$ to the unit cell in hcp
- Each edge atom contributes $\frac{1}{4}$ to the unit cell
- Each face atom contributes $\frac{1}{2}$ to the unit cell
- Each center atom contributes 1 to the unit cell

Unit Cell	Coordination Number	# of Atoms Per Unit Cell	% space
Simple Cubic 	**6**	**1**	**52%**
Body-Centered Cubic 	**8**	**2**	**68%**
Face-centered Cubic 	**12**	**4**	**74.04%**
Hexagonal Closest Packed 	**12**	**6**	**74.04%**

Inorganic Crystals

Many common inorganic crystals have structures that are related to cubic close packed (face-centered cubic) or hexagonal close packed sphere packings. One component of the material will pack in one of the arrangements above. The remaining component(s) will fill some or all of the holes between the layers. An interstitial atom filling a tetrahedral hole is coordinated to four packing atoms, and an atom filling an octahedral hole is coordinated to six packing atoms. In both the hexagonal close packed and cubic close packed lattices, there is one octahedral hole and two tetrahedral holes per packing atom.

Are Anions or Cations Better Packing Atoms?

We might expect that anions, which are often larger than cations, would be better suited to the positions of packing atoms. While this is often true, there are many examples of structures in which cations are the packing atoms, and others in which the distinction is arbitrary. The NaCl structure is a good example of the latter.

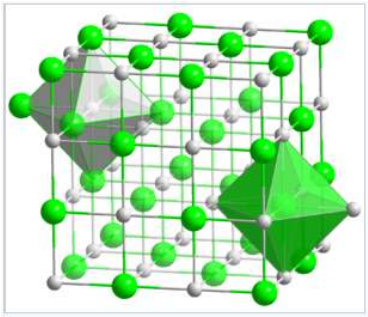


Figure *Section*9.1.5: Crystal structure of NaCl. Both the Na^+ (grey) and Cl^- (green) ions are octahedrally coordinated.

In the rock salt or NaCl structure, shown in Figure *Section*9.1.5, the green spheres are the Cl^- ions and the gray spheres are the Na^+ ions. The packing atoms (Na^+) are in a face centered cubic arrangement. The octahedral holes in a face-centered cubic lattice can be found at the edges and in the center of the unit cell, and they are filled by the chloride ions. Alternatively the structure can be described as the Cl^- ions in a fcc arrangement with the Na^+ ions occupying the octrahedral holes. Another way of stating this is that the structure consists of **two interpenetrating fcc lattices**, which are related to each other by a translation of half the unit cell along any of the three Cartesian axes. Thus the distinction between packing and interstitial atoms in this case is arbitrary.

NaCl is interesting in that it is a three-dimensional checkerboard, and thus there are no NaCl "molecules" that exist in the structure. When this structure was originally solved (in 1913 by using X-ray diffraction) by W. L. Bragg, his interpretation met resistance by chemists who thought that precise integer stoichiometries were a consequence of the valency of atoms in molecules. The German chemist Pfeiffer noted in 1915 that ‘the ordinary notion of valency didn’t seem to apply’, and fourteen years later, the influential chemist Armstrong still found Bragg’s proposed structure of sodium chloride ‘more than repugnant to the common sense, not chemical cricket’! Nevertheless, Bragg and his father, W. H. Bragg, persevered and used the then-new technique of X-ray diffraction to determine the structures of a number of other compounds, including diamond, zincblende, calcium fluoride, and other alkali halides. These experiments gave chemists their first real look at the atomic structure of solids, and laid the groundwork for X-ray diffraction experiments that later elucidated the structures of DNA, proteins, and many other compounds. For their work on X-ray diffraction the Braggs received the Nobel prize in Physics in 1915.

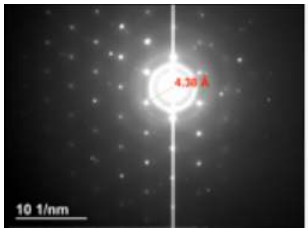


Figure *Section*9.1.6: X-ray difffraction pattern for a NaCl crystal. The lattice dimensions and positions of atoms in crystals such as NaCl are inferred from diffraction patterns.

Since each type of atom in the NaCl structure forms a face-centered cubic lattice, there are four Na and four Cl atoms per NaCl unit cell. It is because of this ratio that NaCl has a 1:1 stoichiometry. The shaded green and gray octahedra in the NaCl lattice (Figure *Section*9.1.5) show that the Na^+ ions are coordinated to six Cl^- ions, and vice versa.

Other materials with the NaCl structure

- Alkali Halides (except CsCl, CsBr, and CsI)
- Transition Metal Monoxides (TiO, VO,..., NiO)
- Alkali Earth Oxides and Sulfides (MgO, CaO, BaS... except BeO and MgTe)
- Carbides and Nitrides (TiC, TiN, ZrC, NbC) -these are very stable refractory, interstitial alloys (metallic)

Other Unit Cell Types

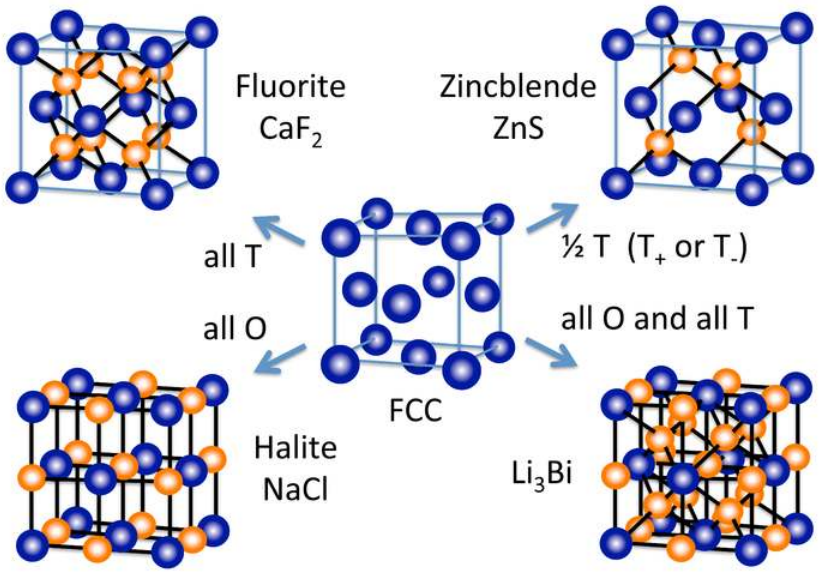


Figure *Section*9.1.7: Illustration of how different unit cell types are formed by filling holes in the fcc lattice

A number of other inorganic crystal structures are formed (at least conceptually) by filling octahedral and/or tetrahedral holes in close-packed lattices. Figure *Section*9.1.7 shows some of the most common structures (fluorite, NaCl, and zincblende) as well as a rather rare one (Li_3Bi) that derive from the fcc lattice. From the hcp lattice, we can make the NiAs and wurzite structures, which are the hexagonal relatives of NaCl and zincblende, respectively.

An alternative and very convenient way to represent inorganic crystal structures (especially complex structures such as Li_3Bi) is to draw the unit cell in slices along one of the unit cell axes. This kind of representation is shown at the left for the fcc lattice and the NaCl structure. Since all atoms in these structures have z-coordinates of either 0 or 1/2, only those sections need to be drawn in order to describe the contents of the unit cell. It is a useful exercise to draw some of the fcc compound structures (above) in sections.

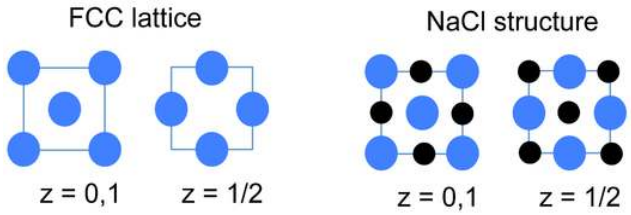


Figure *Section*9.1.8: Alternative representation of the fcc lattice (left) and the NaCl structure (right). The z = 0,1 represent the bottom and top faces of the unit cell. The z = $\frac{1}{2}$ represents a slice through the center of the unit cell

Fluorite

In ccp and hcp lattices, there are two tetrahedral holes per packing atom. A stoichiometry of either M_2X or MX_2 gives a structure that fills all tetrahedral sites, while an MX structure fills only half of the sites. An example of an MX_2 structure is fluorite, CaF_2, whose structure is shown in the figure at the left. The packing atom in fluorite is Ca^{2+} and the structure is composed of three interpenetrating fcc lattices. It should be noted that the Ca^{2+} ion (gray spheres) as a packing atom defies our "rule" that anions are larger than cations and therefore must be the packing atoms. The fluorite structure is common for ionic MX_2 (MgF_2, ZrO_2, etc.) and M_2X compounds (Li_2O). In contrast, the hcp relative of the fluorite structure is quite rare because of unfavorable close contacts between like-charged ions.

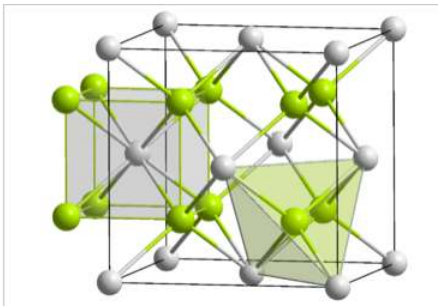


Figure *Section*9.1.9: The fluorite (CaF_2) crystal structure showing the coordination environments of the Ca (grey) and F (green) atoms

In terms of geometry, Ca^{2+} is in cubic coordination with eight F^- neighbors, and the fluoride ions are tetrahedrally coordinated by four Ca^{2+} ions. The 8:4 coordination geometry is consistent with the 1:2 Ca:F stoichiometry; in all crystal structures the ratio of the coordination numbers is the inverse of the stoichiometric ratio. Looking more closely at the tetrahedral sites in fluorite, we see that they fall into two distinct groups: T_+ and T_-. If a tetrahedron is oriented with a vertex pointing upwards along the stacking axis, the site is T_+. Likewise, a tetrahedron with a vertex oriented downward is T_-. The alternation of T_+ and T_- sites allows for efficient packing of ions in the structure.

Zincblende and wurtzite

Tetrahedrally bonded compounds with a 1:1 stoichiometry (MX compounds) have only half of the tetrahedral sites (either the T_+ or T_- sites) filled. In this case, both the M and the X atoms are tetrahedrally coordinated. The zincblende and wurtzite structures of ZnS are 1:1 tetrahedral structures based on fcc and hcp lattices, respectively. Both structures are favored by p-block compounds that follow the octet rule, and these compounds are usually semiconductors or insulators. The zincblende structure, Figure *Section*9.1.10, can be thought of as two interpenetrating fcc lattices, one of anions and one of cations, offset from each other by a translation of 1/4 along the body diagonal of the unit cell. Examples of compounds with the zincblende structure include CuCl, CuI, ZnSe, HgS, BeS, CdTe, AlP, GaP, SnSb, CSi, and diamond. Using ZnS as a representative of zincblende, the coordination of both Zn and S atoms is tetrahedral.

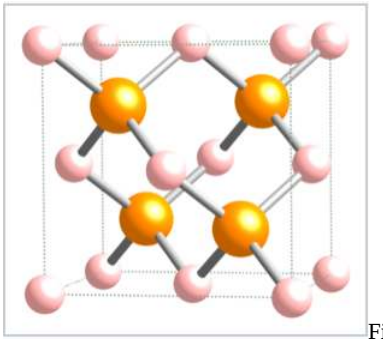


Figure *Section*9.1.10: The zincblende structure of ZnS. The Zn^{2+} ions are in pink and the S^{2-} ions are in orange.

The wurtzite structure is a close relative of zincblende, based on filling half the tetrahedral holes in the hcp lattice. Like zincblende, wurtzite contains planes of fused six-membered rings in the chair conformation. Unlike zincblende, however, the rings joining these planes contain non-planar, six-membered rings. The structure aligns the anions so that they are directly above the cations in the structure, a less favorable situation sterically but a more favorable one in terms of electrostatics. As a result, the wurtzite structure tends to favor more polar or ionic compounds (e.g., ZnO, $NH_4^+F^-$) than the zincblende structure. As with zincblende, both ions are in tetrahedral (4:4) coordination and there are typically eight valence electrons in the MX compound. Examples of compounds with this structure include: BeO, ZnO, MnS, CdSe, MgTe, AlN, and NH_4F.

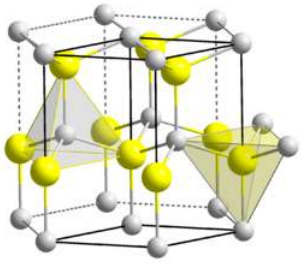


Figure *Section*9.1.11: The wurtzite structure of ZnS with the tetrahedral coordination of anion and cation highlighted. The Zn^{2+} ions are in grey and the S^{2-} ions are in yellow. (Public domain; Solid State via Wikimedia Commons)

An interesting consequence of the layer stacking in the wurtzite structure is that the crystals are polar. When cleaved along the c-axis (the stacking axis), crystals of ZnO, ZnS, and GaN have one negatively charged face and an opposite positively charged face. An applied electric field interacts with the crystal dipole, resulting in compression or elongation of the lattice along this direction. For this reason crystals of compounds in the wurtzite structure are typically piezoelectric (increasing the pressure on the material generates a voltage in the material).

Some compounds are diamorphic and can have either the zincblende or wurtzite structure. Examples of these compounds that have intermediate polarities include CdS and ZnS. SiO_2 exists in polymorphs (crystobalite and tridymite) that resemble zincblende and wurtzite with O atoms midway between each of the Si atoms. The zincblende and wurtzite structures have efficient packing arrangements for tetrahedrally bonded networks and are commonly found in compounds that have tetrahedral bonding. Water, for example, has a tetrahedral hydrogen bonding network and is wurtzite-type. The undistorted wurtzite and zincblende structures are typically found for AX compounds with eight valence electrons, which follow the octet rule. AX compounds with nine or ten electrons such as GaSe and GaAs crystallize in distorted variants of the wurtzite structure. In GaSe, the extra electrons form lone pairs and this creates layers in the structure, as can be seen in the figure below. To the right of GaSe, the structures of As, Sb, and SbAs show an ever further breakdown of the structure into layers as more valence electrons are added.

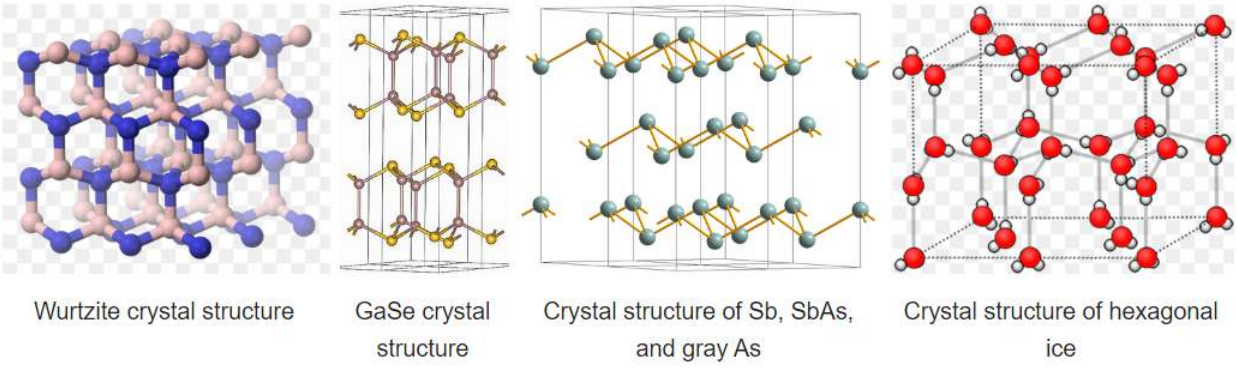


Figure *Section*9.1.12: Different variations of the wurtzite crystal structure (Copyright; author via source)

Hexagonal ice is the most stable polymorph of ice, which is obtained upon freezing at 1 atmosphere pressure. This polymorph (ice-I) has a hcp wurtzite-type structure. Looking at the structure shown at the right, we see that there are irregular arrangements of the O-H---O bonds. In the structure, hydrogen bonding enforces the tetrahedral coordination of each water molecule, resulting in a relatively open structure that is less dense than liquid water. For this reason, ice floats in water.

References

1. Conway, J. H. and Sloane, N. J. A. *Sphere Packings, Lattices, and Groups, 2nd ed.* New York: Springer-Verlag, 1993.
2. Krishna, P. and Verma, A. R. Closed Packed Structures, Chester, UK: International Union of Crystallography, 1981.
3. Petrucci, Ralph H., William S. Harwood, F. Geoffrey Herring, and Jeffry D. Madura. "Crystal Structures" General Chemistry: Principles & Modern Applications, ninth Edition. New Jersey: Pearson Education, Inc., 2007. 501-508.

Contributors and Attributions

- Stephen Lower, Professor Emeritus (Simon Fraser U.) Chem1 Virtual Textbook
- Brittanie Harbick, Laura Suh, Jenny Fong

Section 9.1: Crystal Structures and Unit Cells is shared under a CC BY-NC-SA 4.0 license and was authored, remixed, and/or curated by LibreTexts.

- **5.1: Crystal Structures and Unit Cells** is licensed CC BY-NC-SA 4.0.
- **7.8: Cubic Lattices and Close Packing** by Stephen Lower is licensed CC BY 3.0. Original source: http://www.chem1.com/acad/webtext/virtualtextbook.html.
- **8.2: Close-packing and Interstitial Sites** by Chemistry 310 is licensed CC BY-SA 4.0. Original source: https://en.wikibooks.org/wiki/Introduction_to_Inorganic_Chemistry.
- **8.4: Tetrahedral Structures** by Chemistry 310 is licensed CC BY-SA 4.0. Original source: https://en.wikibooks.org/wiki/Introduction_to_Inorganic_Chemistry.

Section 9.2: Energetics of Ionic Solids- Lattice Energy

Lattice Energy

Many ionic compounds have simple structures. Because the forces holding the atoms together are primarily electrostatic, we can calculate the cohesive energy of the crystal lattice with good accuracy. Interesting questions to ask about these lattice energy calculations are:

- How accurate are lattice energy calculations?
- What do they teach us about the chemical bonds in ionic crystals?
- Can we use lattice energies to predict properties such as solubility, stability, and reactivity?
- Can we use lattice energies to predict the crystal structures of ionic compounds?

Let's start by looking at the forces that hold ionic lattices together. There are mainly two kinds of force that determine the energy of an ionic bond.

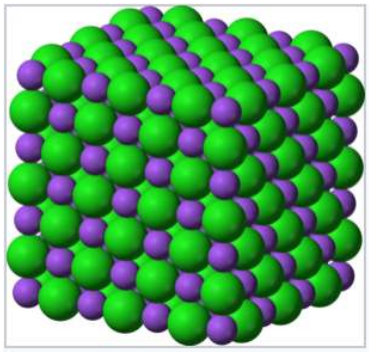


Figure ***Section*9.2.1**: The NaCl crystal structure is the archetype for calculating lattice energies and computing enthalpies of formation from Born-Haber cycles.

Electrostatic force

Electrostatic force is the attraction and repulsion between ions described by Coulomb's Law. Two ions with charges z_+ and z_-, separated by a distance r, experience a force F:

$$\mathbf{F} = -\frac{e^2}{4\pi\varepsilon_0}\frac{z_+ z_-}{r^2} \qquad \text{(Section 9.2.1)}$$

where

e = 1.6022×10^{-19} C

$4\,\pi\,\varepsilon_0$ = 1.112×10^{-10} $C^2/(J\ m)$

This force is attractive for ions of opposite charge and repulsive for ions of the same charge.

Closed-shell repulsion

When electrons in the core shells of one ion overlap with those of another ion, there is a repulsive force due to the Pauli exclusion principle. A third electron cannot enter an orbital that already contains two electrons. This force is short range, and is typically modeled as falling off exponentially or with a high power of the distance r between atoms. For example, in the Born approximation, B is a constant and ρ is a number with units of length, which is usually empirically determined from compressibility data. A typical value of ρ is 0.345 Å.

$$\mathbf{E}_{repulsion} = Bexp(\frac{-r}{\rho}) \qquad \text{(Section 9.2.2)}$$

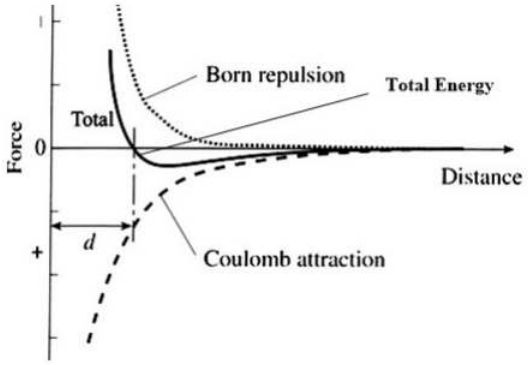


Figure *Section*9.2.2: Total energy of an ionic bond (solid) determined by the combination of Coulombic attraction (dashed) and Born (closed-shell) repulsion (dotted).

The energy of the ionic bond between two atoms is then calculated as the combination of net electrostatic and the closed-shell repulsion energies, as shown in Figure *Section*9.2.2. Note that for the moment we are ignoring the attractive van der Waals forces between ions. For a pair of ions, the equilibrium distance between ions is determined by the minimum in the total energy curve.

Madelung Constant

We can use the above equations to calculate the lattice energy of a crystal by summing up the interactions between all pairs of ions. Because the closed-shell repulsion force is short range, this term is typically calculated only for interactions between neighboring ions. However, the Coulomb force is long range, and must be calculated over the entire crystal. This problem was first solved in 1918 by Erwin Madelung, a German physicist.

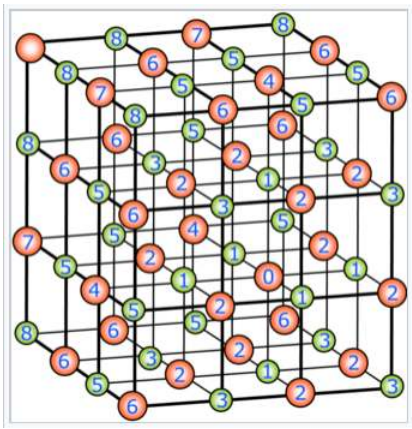


Figure *Section*9.2.3: The Madelung constant is calculated by summing up electrostatic interactions with ion labeled 0 in the expanding spheres method. Each number designates the order in which it is summed. For example, ions labeled 1 represent the six nearest neighbors (attractive interaction), ions labeled 2 are the 12 next nearest neighbors (repulsive interaction) and so on.

Consider an ion in the NaCl structure labeled "0" in Figure *Section*9.2.3. We can see that the nearest neighbor interactions (+ -) with ions labeled "1" are attractive, the next nearest neighbor interactions (- - and + +) are repulsive, and so on. In the NaCl structure, counting from the ion in the center of the unit cell, there are 6 nearest neighbors (on the faces of the cube), 12 next nearest neighbors (on the edges of the cube), 8 in the next shell (at the vertices of the cube), and so on. Their distances from ion "0" increase progressively: r_o, $\sqrt{2}\ r_o$, $\sqrt{3}\ r_o$, and so on, where r_o is the nearest neighbor distance.

We can now write the electrostatic energy at ion "0" as:

$$\mathbf{E}_{elec} = -6\frac{e^2}{4\pi\varepsilon_0}\frac{z_+z_-}{r_o} + 12\frac{e^2}{4\pi\varepsilon_0}\frac{z_+z_-}{\sqrt{2}r_o} - 8\frac{e^2}{4\pi\varepsilon_0}\frac{z_+z_-}{\sqrt{3}r_o} + \ldots \qquad \textbf{(Section 9.2.3)}$$

Factoring out constants and the nearest-neighbor bond distance r_o we obtain:

$$\mathbf{E}_{elec} = \frac{e^2}{4\pi\varepsilon_0}\frac{z_+z_-}{r_o}\left(6 - \frac{12}{\sqrt{2}} + \frac{8}{\sqrt{3}} - \frac{6}{\sqrt{4}} + \ldots\right) \qquad \textbf{(Section 9.2.4)}$$

Where the sum in parentheses, which is unitless, slowly converges to a value of A = 1.74756. Generalizing this formula for any three-dimensional ionic crystal we get a function:

$$\mathbf{E}_{elec} = \frac{e^2}{4\pi\varepsilon_0}\frac{z_+z_-}{r_o}NA \qquad \text{(Section 9.2.5)}$$

where N is Avogadro's number (because we are calculating energy per mole of ions) and A is called the *Madelung constant*. The **Madelung constant** depends only on the geometrical arrangement of the ions and so it varies between different types of crystal structures, but within a given structure type it does not change. Thus MgO and NaCl have the same Madelung constant because they both have the NaCl structure.

Table *Section*9.2.1: Madelung Constants

Compound	*Crystal Lattice*	*M*	*A : C*	*Type*
NaCl	NaCl	1.74756	6 : 6	Rock salt
CsCl	CsCl	1.76267	6 : 6	CsCl type
CaF_2	Cubic	2.51939	8 : 4	Fluorite
$CdCl_2$	Hexagonal	2.244	6 : 3	
MgF_2	Tetragonal	2.381		
ZnS (wurtzite)	Hexagonal	1.64132	4 : 4	Wurtzite
TiO_2 (rutile)	Tetragonal	2.408	6 : 3	Rutile
$bSiO_2$	Hexagonal	2.2197		
Al_2O_3	Rhombohedral	4.1719	6 : 4	Corundum
A is the number of anions coordinated to cation and *C* is the numbers of cations coordinated to anion.				

Born–Landé Equation

There are other factors to consider for the evaluation of lattice energy and the treatment by Max Born and Alfred Lande led to the formula for the evaluation of lattice energy for a mole of **crystalline solid**. The Born–Landé equation (Equation Section 9.2.6) is a means of calculating the lattice energy of a crystalline ionic compound and derived from the electrostatic potential of the ionic lattice and a repulsive potential energy term

$$U = \frac{N_A M Z^2 e^2}{4\pi\epsilon_o r}\left(1 - \frac{1}{n}\right) \qquad \text{(Section 9.2.6)}$$

where

- N_A is Avogadro constant;
- M is the Madelung constant for the lattice
- z^+ is the charge number of cation
- z^- is the charge number of anion
- e is elementary charge, 1.6022×10^{-19} C
- ε_0 is the permittivity of free space
- r_0 is the distance to closest ion
- n is the **Born exponent** that is typically between 5 and 12 and is determined experimentally. n is a number related to the electronic configurations of the ions involved (Table *Section*9.2.3).

Table *Section*9.2.2: n values for select solids

Atom/Molecule	*n*
He	5
Ne	7
Ar	9
Kr	10
Xe	12
LiF	5.9
LiCl	8.0
LiBr	8.7
NaCl	9.1
NaBr	9.5

Example *Section*9.2.1: NaCl

Estimate the lattice energy for **NaCl**.

Solution

Using the values giving in the discussion above, the estimation is given by

$$U_{NaCl} = \frac{(6.022 \times 10^{23}/mol)(1.74756)(1.6022 \times 10^{-19})^2(1.747558)}{4\pi\,(8.854 \times 10^{-12}C^2/m)(282 \times 10^{-12}\,m)}\left(1 - \frac{1}{9.1}\right)$$
$$= -756\,kJ/mol$$

Much more should be considered in order to evaluate the lattice energy accurately, but the above calculation leads you to a good start. When methods to evaluate the energy of crystallization or lattice energy lead to reliable values, these values can be used in the Born-Hable cycle to evaluate other chemical properties, for example the electron affinity, which is really difficult to determine directly by experiment.



Figure *Section*9.2.4: Lithium fluoride (shown here as a large single crystal in a beaker of water) is the only alkali halide that is not freely soluble in water. The lattice energy of LiF is the most negative of the alkali fluorides because Li^+ and F^- are both small ions and lattice energy is proportional to $1/r_0$.

Section 9.2: Energetics of Ionic Solids- Lattice Energy is shared under a CC BY-NC-SA 4.0 license and was authored, remixed, and/or curated by LibreTexts.

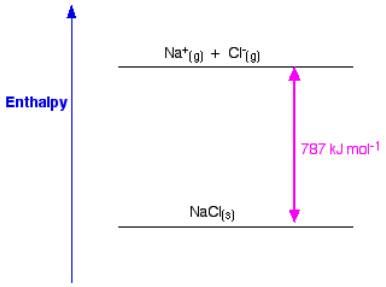
- **5.2: Energetics of Ionic Solids- Lattice Energy** is licensed CC BY-NC-SA 4.0.
- **9.3: Energetics of Crystalline Solids- The Ionic Model** by Chemistry 310 is licensed CC BY-SA 4.0. Original source: https://en.wikibooks.org/wiki/Introduction_to_Inorganic_Chemistry.
- **6.13E: Madelung Constants** is licensed CC BY-NC-SA 4.0.

Section 9.3: Lattice Enthalpies and Born Haber Cycles

Lattice enthalpy is a measure of the strength of the forces between the ions in an ionic solid. The greater the **lattice enthalpy**, the stronger the forces. This page introduces lattice enthalpies (lattice energies) and Born-Haber cycles.

Defining Lattice Enthalpy

There are two different ways of defining lattice enthalpy which directly contradict each other, and you will find both in common use. In fact, there is a simple way of sorting this out, but many sources do not use it. Lattice enthalpy is a measure of the strength of the forces between the ions in an ionic solid. The greater the lattice enthalpy, the stronger the forces. Those forces are only completely broken when the ions are present as gaseous ions, scattered so far apart that there is negligible attraction between them. You can show this on a simple enthalpy diagram.



For sodium chloride, the solid is more stable than the gaseous ions by 787 kJ mol^{-1}, and that is a measure of the strength of the attractions between the ions in the solid. Remember that energy (in this case heat energy) is released when bonds are made, and is required to break bonds.

So lattice enthalpy could be described in either of two ways.

- It could be described as the enthalpy change when 1 mole of sodium chloride (or whatever) was formed from its scattered gaseous ions. In other words, you are looking at a downward arrow on the diagram.
- Or, it could be described as the enthalpy change when 1 mole of sodium chloride (or whatever) is broken up to form its scattered gaseous ions. In other words, you are looking at an upward arrow on the diagram.

Both refer to the same enthalpy diagram, but one looks at it from the point of view of making the lattice, and the other from the point of view of breaking it up. Unfortunately, both of these are often described as "lattice enthalpy".

Definitions

- The *lattice dissociation enthalpy* is the enthalpy change needed to convert 1 mole of solid crystal into its scattered gaseous ions. Lattice dissociation enthalpies are **always positive**.
- The *lattice formation enthalpy* is the enthalpy change when 1 mole of solid crystal is formed from its separated gaseous ions. Lattice formation enthalpies are **always negative**.

This is an absurdly confusing situation which is easily resolved by never using the term "lattice enthalpy" without qualifying it.

- You should talk about "lattice dissociation enthalpy" if you want to talk about the amount of energy needed to split up a lattice into its scattered gaseous ions. For NaCl, the lattice dissociation enthalpy is +787 kJ mol^{-1}.
- You should talk about "lattice formation enthalpy" if you want to talk about the amount of energy released when a lattice is formed from its scattered gaseous ions. For NaCl, the lattice formation enthalpy is -787 kJ mol^{-1}.

That immediately removes any possibility of confusion.

Factors affecting Lattice Enthalpy

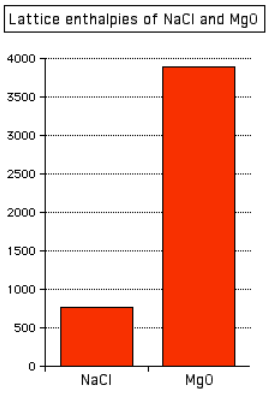
The two main factors affecting lattice enthalpy are

- The charges on the ions and

- The ionic radii (which affects the distance between the ions).

The charges on the ions

Sodium chloride and magnesium oxide have exactly the same arrangements of ions in the crystal lattice, but the lattice enthalpies are very different.

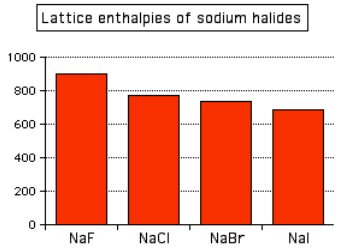


You can see that the lattice enthalpy of magnesium oxide is much greater than that of sodium chloride. That's because in magnesium oxide, 2+ ions are attracting 2- ions; in sodium chloride, the attraction is only between 1+ and 1- ions.

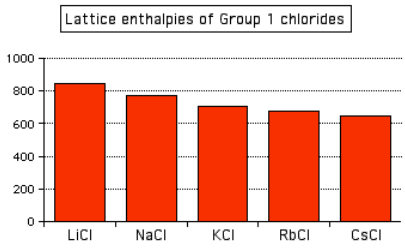
The Radius of the Ions

The lattice enthalpy of magnesium oxide is also increased relative to sodium chloride because magnesium ions are smaller than sodium ions, and oxide ions are smaller than chloride ions. That means that the ions are closer together in the lattice, and that increases the strength of the attractions.

This effect of ion size on lattice enthalpy is clearly observed as you go down a Group in the Periodic Table. For example, as you go down Group 7 of the Periodic Table from fluorine to iodine, you would expect the lattice enthalpies of their sodium salts to fall as the negative ions get bigger - and that is the case:



Attractions are governed by the distances between the centers of the oppositely charged ions, and that distance is obviously greater as the negative ion gets bigger. And you can see exactly the same effect if as you go down Group 1. The next bar chart shows the lattice enthalpies of the Group 1 chlorides.



Calculating Lattice Enthalpy

It is impossible to measure the enthalpy change starting from a solid crystal and converting it into its scattered gaseous ions. It is even more difficult to imagine how you could do the reverse - start with scattered gaseous ions and measure the enthalpy change when these convert to a solid crystal. Instead, lattice enthalpies always have to be calculated, and there are two entirely different ways in which this can be done.

1. You can can use a Hess's Law cycle (in this case called a Born-Haber cycle) involving enthalpy changes which can be measured. Lattice enthalpies calculated in this way are described as experimental values.
2. Or you can do physics-style calculations working out how much energy would be released, for example, when ions considered as point charges come together to make a lattice. These are described as theoretical values. In fact, in this case, what you are actually calculating are properly described as lattice energies.

Born-Haber Cycles

Standard Atomization Enthalpies

Before we start talking about Born-Haber cycles, we need to define the **atomization enthalpy**, ΔH_a^o. The standard atomization enthalpy is the enthalpy change when 1 mole of gaseous atoms is formed from the element in its standard state. Enthalpy change of atomization is always positive. You are always going to have to supply energy to break an element into its separate gaseous atoms. All of the following equations represent changes involving atomization enthalpy:

$$\frac{1}{2}Cl_2(g) \rightarrow Cl(g) \quad \Delta H_a^o = +122\,kJ\,mol^{-1}$$

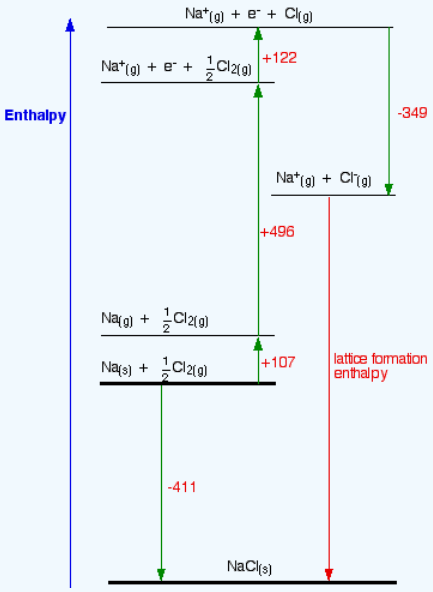
$$\frac{1}{2}Br_2(l) \rightarrow Br(g) \quad \Delta H_a^o = +122\,kJ\,mol^{-1}$$

$$Na(s) \rightarrow Na(g) \quad \Delta H_a^o = +107\,kJ\,mol^{-1}$$

Notice particularly that the "mol^{-1}" is per mole of atoms **formed** - NOT per mole of element that you start with. You will quite commonly have to write fractions into the left-hand side of the equation. Getting this wrong is a common mistake.

Example *Section*9.3.1: Born-Haber Cycle for NaCl

Consider a Born-Haber cycle for sodium chloride, and then talk it through carefully afterwards. You will see that I have arbitrarily decided to draw this for lattice formation enthalpy. If you wanted to draw it for lattice dissociation enthalpy, the red arrow would be reversed - pointing upwards.



Focus to start with on the higher of the two thicker horizontal lines. We are starting here with the elements sodium and chlorine in their standard states. Notice that we only need half a mole of chlorine gas in order to end up with 1 mole of NaCl. The arrow pointing down from this to the lower thick line represents the enthalpy change of formation of sodium chloride.

The Born-Haber cycle now imagines this formation of sodium chloride as happening in a whole set of small changes, most of which we know the enthalpy changes for - except, of course, for the lattice enthalpy that we want to calculate.

- The +107 is the atomization enthalpy of sodium. We have to produce gaseous atoms so that we can use the next stage in the cycle.
- The +496 is the first ionization energy of sodium. Remember that first ionization energies go from gaseous atoms to gaseous singly charged positive ions.
- The +122 is the atomization enthalpy of chlorine. Again, we have to produce gaseous atoms so that we can use the next stage in the cycle.
- The -349 is the first electron affinity of chlorine. Remember that first electron affinities go from gaseous atoms to gaseous singly charged negative ions.
- And finally, we have the positive and negative gaseous ions that we can convert into the solid sodium chloride using the lattice formation enthalpy.

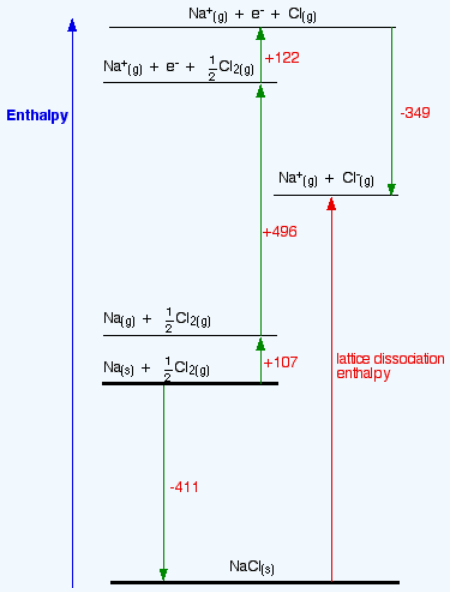
Now we can use Hess' Law and find two different routes around the diagram which we can equate. As drawn, the two routes are obvious. The diagram is set up to provide two different routes between the thick lines. So, from the cycle we get the calculations directly underneath it . . .

$$-411 = +107 + 496 + 122 - 349 + LE$$

$$LE = -411 - 107 - 496 - 122 + 349$$

$$LE = -787 \text{ kJ mol}^{-1}$$

How would this be different if you had drawn a lattice dissociation enthalpy in your diagram? Your diagram would now look like this:



The only difference in the diagram is the direction the lattice enthalpy arrow is pointing. It does, of course, mean that you have to find two new routes. You cannot use the original one, because that would go against the flow of the lattice enthalpy arrow. This time both routes would start from the elements in their standard states, and finish at the gaseous ions.

$$-411 + LE = +107 + 496 + 122 - 349$$

$$LE = +107 + 496 + 122 - 349 + 411$$

$$LE = +787 \text{ kJ mol}^{-1}$$

Once again, the cycle sorts out the sign of the lattice enthalpy.

Theoretical Estimates of Lattice Energies

Let's assume that a compound is fully ionic. Let's also assume that the ions are point charges - in other words that the charge is concentrated at the center of the ion. By doing physics-style calculations, it is possible to calculate a theoretical value for what you would expect the lattice energy to be. Calculations of this sort end up with values of *lattice energy*, and not *lattice enthalpy*. If you know how to do it, you can then fairly easily convert between the two.

There are several different equations, of various degrees of complication, for calculating lattice energy in this way. There are two possibilities:

- There is reasonable agreement between the experimental value (calculated from a Born-Haber cycle) and the theoretical value. Sodium chloride is a case like this - the theoretical and experimental values agree to within a few percent. That means that for sodium chloride, the assumptions about the solid being ionic are fairly good.
- The experimental and theoretical values do not agree. A commonly quoted example of this is silver chloride, AgCl. Depending on where you get your data from, the theoretical value for lattice enthalpy for AgCl is anywhere from about 50 to 150 kJ mol^{-1} less than the value that comes from a Born-Haber cycle. In other words, treating the AgCl as 100% ionic underestimates its lattice enthalpy by quite a lot.

The explanation is that silver chloride actually has a significant amount of covalent bonding between the silver and the chlorine, because there is not enough electronegativity difference between the two to allow for complete transfer of an electron from the silver to the chlorine. Comparing experimental (Born-Haber cycle) and theoretical values for lattice enthalpy is a good way of judging how purely ionic a crystal is.

Example *Section*9.3.2: Born-Haber Cycle for $MgCl_2$

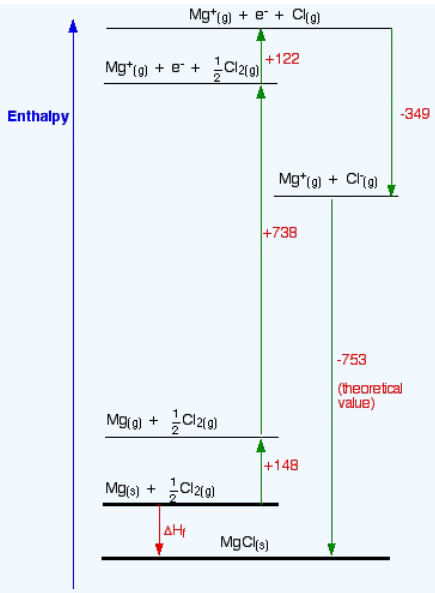
The question arises as to why, from an energetics point of view, magnesium chloride is $MgCl_2$ rather than MgCl or $MgCl_3$ (or any other formula you might like to choose). It turns out that $MgCl_2$ is the formula of the compound which has the most negative enthalpy change of formation - in other words, it is the most stable one relative to the elements magnesium and chlorine.

Let's look at this in terms of Born-Haber cycles of and contrast the enthalpy change of formation for the imaginary compounds MgCl and $MgCl_3$. That means that we will have to use theoretical values of their lattice enthalpies. We ca not use experimental ones, because these compounds obviously do not exist! I'm taking theoretical values for lattice enthalpies for these compounds that I found on the web. I can't confirm these, but all the other values used by that source were accurate. The exact values do not matter too much anyway, because the results are so dramatically clear-cut.

1. The Born-Haber cycle for MgCl

We will start with the compound MgCl, because that cycle is just like the NaCl one we have already looked at.

$$Mg(s) + \tfrac{1}{2} Cl_2(g) \rightarrow MgCl(s)$$



Find two routes around this without going against the flow of any arrows. That's easy:

$$\Delta H_f = +148 + 738 + 122 - 349 - 753$$

$$\Delta H_f = -94 \text{ kJ mol}^{-1}$$

So the compound MgCl is definitely energetically **more stable** than its elements. I have drawn this cycle very roughly to scale, but that is going to become more and more difficult as we look at the other two possible formulae. So I am going to rewrite it as a table. You can see from the diagram that the enthalpy change of formation can be found just by adding up all the other numbers in the cycle, and we can do this just as well in a table.

	kJ
atomization enthalpy of Mg	+148
1st IE of Mg	+738
atomization enthalpy of Cl	+122
electron affinity of Cl	-349
lattice enthalpy	-753
calculated ΔH_f	-94

2. The Born-Haber cycle for $MgCl_2$

The equation for the enthalpy change of formation this time is

$$Mg\,(s) + Cl_2\,(g) \rightarrow MgCl_2\,(s)$$

So how does that change the numbers in the Born-Haber cycle?

- You need to add in the second ionization energy of magnesium, because you are making a 2+ ion.
- You need to multiply the atomization enthalpy of chlorine by 2, because you need 2 moles of gaseous chlorine atoms.
- You need to multiply the electron affinity of chlorine by 2, because you are making 2 moles of chloride ions.
- You obviously need a different value for lattice enthalpy.

	kJ
atomization enthalpy of Mg	+148
1st IE of Mg	+738
2nd IE of Mg	+1451
atomization enthalpy of Cl (x 2)	+244
electron affinity of Cl (x 2)	-698
lattice enthalpy	-2526
calculated ΔH_f	-643

You can see that much more energy is released when you make $MgCl_2$ than when you make MgCl. Why is that? You need to put in more energy to ionize the magnesium to give a 2+ ion, but a lot more energy is released as lattice enthalpy. That is because there are stronger ionic attractions between 1- ions and 2+ ions than between the 1- and 1+ ions in MgCl. So what about $MgCl_3$? The lattice energy here would be even greater.

3. The Born-Haber cycle for $MgCl_3$

The equation for the enthalpy change of formation this time is

$$\mathrm{Mg\,(s) + \tfrac{3}{2}\,Cl_2\,(g) \rightarrow MgCl_3\,(s)}$$

So how does that change the numbers in the Born-Haber cycle this time?

- You need to add in the third ionization energy of magnesium, because you are making a 3+ ion.
- You need to multiply the atomization enthalpy of chlorine by 3, because you need 3 moles of gaseous chlorine atoms.
- You need to multiply the electron affinity of chlorine by 3, because you are making 3 moles of chloride ions.
- You again need a different value for lattice enthalpy.

	kJ
atomization enthalpy of Mg	+148
1st IE of Mg	+738
2nd IE of Mg	+1451
3rd IE of Mg	+7733
atomization enthalpy of Cl (x 3)	+366
electron affinity of Cl (x 3)	-1047
lattice enthalpy	-5440
calculated ΔH_f	+3949

This time, the compound is hugely energetically unstable, both with respect to its elements, and also to other compounds that could be formed. You would need to supply nearly 4000 kJ to get 1 mole of $MgCl_3$ to form!

Look carefully at the reason for this. The lattice enthalpy is the **highest** for all these possible compounds, but it is not high enough to make up for the very large third ionization energy of magnesium.

Why is the third ionization energy so big? The first two electrons to be removed from magnesium come from the 3s level. The third one comes from the 2p. That is closer to the nucleus, and lacks a layer of screening as well - and so

much more energy is needed to remove it. The 3s electrons are screened from the nucleus by the 1 level and 2 level electrons. The 2p electrons are only screened by the 1 level (plus a bit of help from the 2s electrons).

Conclusion

Magnesium chloride is $MgCl_2$ because this is the combination of magnesium and chlorine which produces the most energetically stable compound - the one with the most negative enthalpy change of formation.

Contributors and Attributions

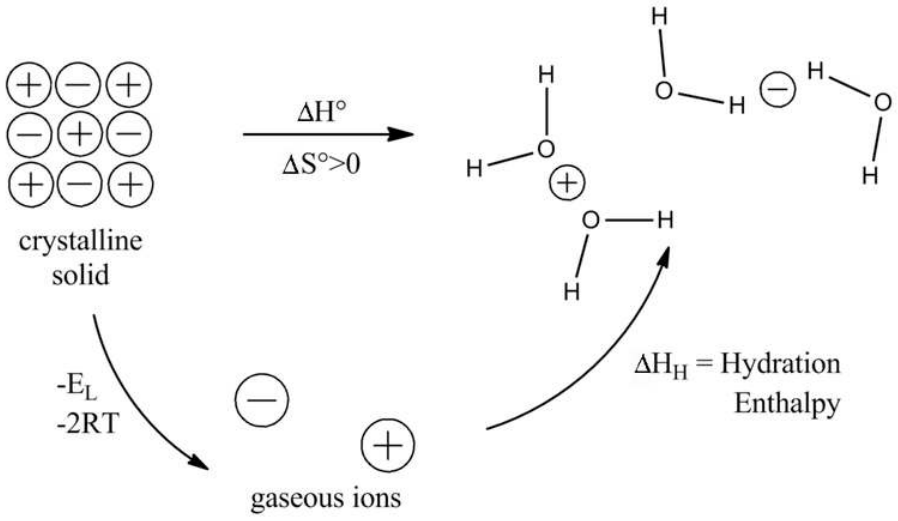
- Jim Clark (Chemguide.co.uk)

This page titled Section 9.3: Lattice Enthalpies and Born Haber Cycles is shared under a CC BY-NC-SA 4.0 license and was authored, remixed, and/or curated by Jim Clark.

- **Lattice Enthalpies and Born Haber Cycles** by Jim Clark is licensed CC BY-NC 4.0.

Section 9.4: Lattice Energy and Solubility

Lattice energies can also help predict compound solubilities. Let's consider a Born-Haber cycle for dissolving a salt in water. We can imagine this as the sum of two processes: (1) the vaporization of the salt to produce gaseous ions, characterized by the lattice enthalpy, and (2) the hydration of those ions to produce the solution. The enthalpy change for the overall process is the sum of those two steps. We know that the entropy change for dissolution of a solid is positive, so the solubility depends on the enthalpy change for the overall process.



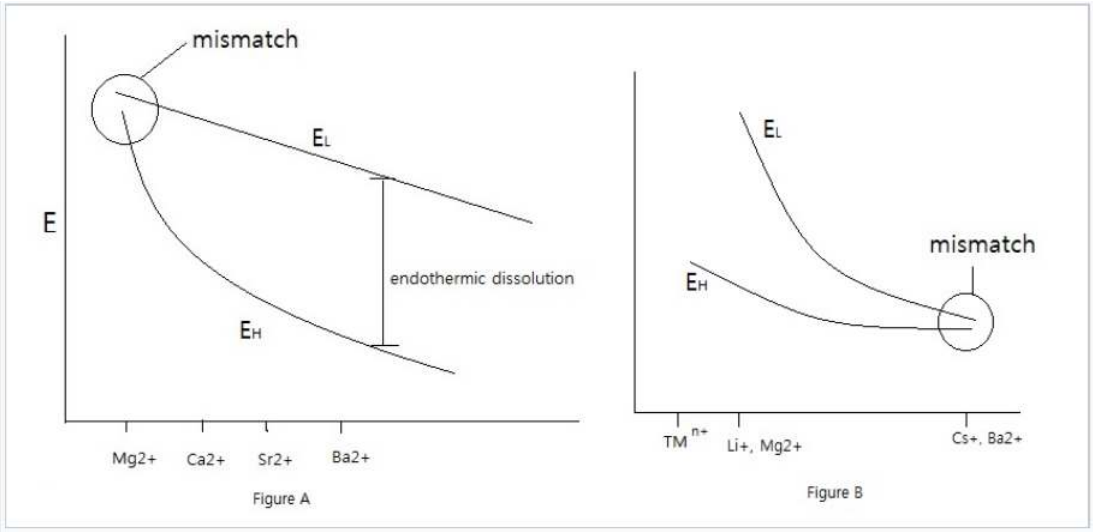
Here we need to consider the trends in both the lattice energy E_L and the hydration energy E_H. The lattice energy depends on the sum of the anion and cation radii ($r_+ + r_-$), whereas the hydration energy has separate anion and cation terms. Generally the solvation of small ions (typically cations) dominates the hydration energy because of the $1/r^2$ dependence.

$$E_L \alpha \frac{1}{r_+ + r_-} \quad \text{(Section 9.4.1)}$$

$$E_H \alpha \frac{1}{r_+^2} + \frac{1}{r_-^2} \quad \text{(Section 9.4.2)}$$

For salts that contain large anions, E_L doesn't change much as r_+ changes. That is because the anion dominates the $r_+ + r_-$ term in the denominator of the formula for E_L. On the other hand, E_H changes substantially with r_+, especially for small cations.

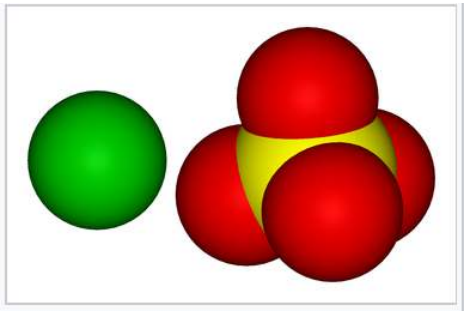
As a result, sulfate salts of small divalent cations, such as $MgSO_4$ (epsom salts), are soluble, whereas the lower hydration energy of Ba^{2+} in $BaSO_4$ makes that salt insoluble ($K_{sp} = 10^{-10}$).



Left: E_L diagram for sulfate salts. The large SO_4^{2-} ion is size-mismatched to small cations such as Mg^{2+}, which have large hydration energies, resulting soluble salts. With larger cations such as Ba^{2+}, which have lower E_H, the lattice energy exceeds the solvation enthalpy and the salts are insoluble.. Right: In the case of small anions such as F^- and OH^-, the lattice energy dominates with small cations such as transition metal ions (TM^{n+}), Mg^{2+}, and Li^+. Anion-cation size mismatch occurs with larger cations, such as Cs^+ and Ba^{2+}, which make soluble fluoride salts.

For small anions, E_L is more sensitive to r_+, whereas E_H does not depend on r_+ as strongly. For fluorides and hydroxides, LiF is slightly soluble whereas CsF is very soluble, and $Mg(OH)_2$ is insoluble whereas $Ba(OH)_2$ is very soluble.

Putting both trends together, we see that **low solubility** is most often encountered when the **anion and cation match well in their sizes**, especially when one or both are **multiply charged**.



Space-filling models showing the van der Waals surfaces of Ba^{2+} and SO_4^{2-}. The similarity in size of the two ions contributes to the low solubility of $BaSO_4$ in water.

Combining all our conclusions about solubility, we note the following trends:

1) Increasing **size mismatch** between the anion and cation leads to greater solubility, so CsF and LiI are the most soluble alkali halides.

2) Increasing **covalency** leads to lower solubility in the salts (due to larger E_L. For example, AgF, AgCl, AgBr, and AgI exhibit progressively lower solubility because of increasing covalency.

AgF > AgCl > AgBr > AgI

3) Increasing the **charge on the anion** lowers the solubility because the increase in E_L is large relative to the increase in E_H.

4) Small, polyvalent cations (having large E_H) make **soluble salts with large, univalent anions** such as I^-, NO_3^-, ClO_4^-, PF_6^-, and acetate.

Examples: Salts of transition metal and lanthanide ions

- Ln^{3+}: Nitrate salts are soluble, but oxides and hydroxides are insoluble.
- Fe^{3+}: Perchlorate is soluble, but sulfate is insoluble.

5) Multiple charged anions such as O^{2-}, S^{2-}, PO_4^{3-}, and SO_4^{2-} make insoluble salts with most M^{2+}, M^{3+}, and M^{4+} metals.

Section 9.4: Lattice Energy and Solubility is shared under a CC BY-NC-SA license and was authored, remixed, and/or curated by LibreTexts.

- **9.12: Lattice Energies and Solubility** by Chemistry 310 is licensed CC BY-SA 4.0. Original source: https://en.wikibooks.org/wiki/Introduction_to_Inorganic_Chemistry.
- **5.4: Lattice Energy and Solubility** is licensed CC BY-SA 4.0.

Section 9.5: Bonding in Metals and Semicondoctors

Band Theory

Band theory was developed with some help from the knowledge gained during the quantum revolution in science. In 1928, Felix Bloch had the idea to take the quantum theory and apply it to solids. In 1927, Walter Heitler and Fritz London discovered bands- very closely spaced orbitals with not much difference in energy. One way to conceptualize band theory is to view is as an extension of molecular orbital theory where the number of atomic orbitals mixed is increased to an infinite number and the energy difference between the molecular orbitals formed approaches 0 (Figure *Section*9.5.1).

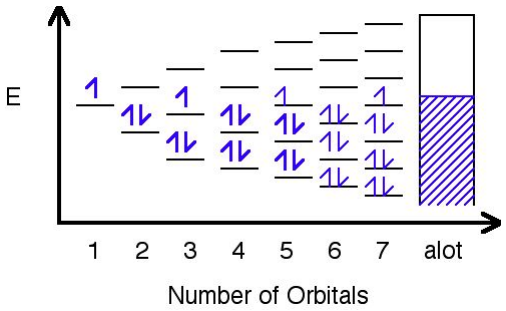


Figure *Section*9.5.1: In this image, orbitals are represented by the black horizontal lines, and they are being filled with an increasing number of electrons as their amount increases. Eventually, as more orbitals are added, the space in between them decreases to hardly anything, and as a result, a band is formed where the orbitals have been filled.

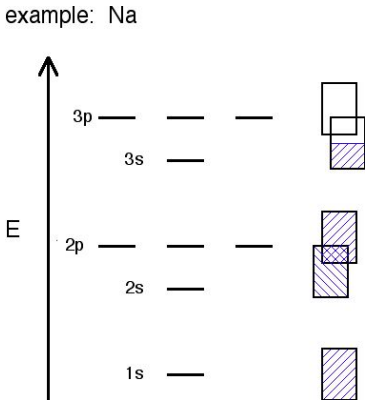


Figure *Section*9.5.2: Bands diagram of sodium metal. Filled bands are blue and empty bands are white. Because the 3s orbital is half filled in Na, the band formed form the 3s orbitals is also half filled.

Different metals will produce different combinations of filled and half filled bands depending on their valence electron configuration. Sodium's bands are shown in Figure *Section*9.5.2. As you can see, bands may overlap each other (the bands are shown askew to be able to tell the difference between different bands). The lowest unoccupied band is called the conduction band, and the highest occupied band is called the valence band.

Bands will follow a trend as you go across a period:

- In Na, the 3s band is 1/2 full.
- In Mg, the 3s band is full.
- In Al, the 3s band is full and the 3p band is 1/2 full... and so on.

In order for the material to conduct electricity, electrons should be in the conduction band where they are able to move freely through the material. The probability of finding an electron in the conduction band is shown by the equation:

$$P = \frac{1}{e^{\frac{\Delta E}{k_b T}} + 1} \qquad \text{(Section 9.5.1)}$$

The ΔE in the equation stands for the energy gap between the valence and conduction bands. k_b is the Boltzmann constant and T is temperature in K. That equation and the table below show that the larger the band gap between the valence band and the conduction band, the less likely electrons are to be found in the conduction band. This is because they don't have sufficient energy to make the jump up to the conduction band.

Table *Section*9.5.1: Band Gaps and Conduction Band Electron Densities for Group 4 Elements

ELEMENT	ΔE(kJ/mol) of energy gap	# of electrons/cm^3 in conduction band	material type
C (diamond)	524	10^{-27}	insulator
Si	117	10^{9}	semiconductor
Ge	66	10^{13}	semiconductor

Conductors, Insulators and Semiconductors

The conductivity of materials is directly related to the band gap and the probability of having electrons in the conduction band. Materials can be divided into three classes based on their band gaps (Figure *Section*9.5.3).

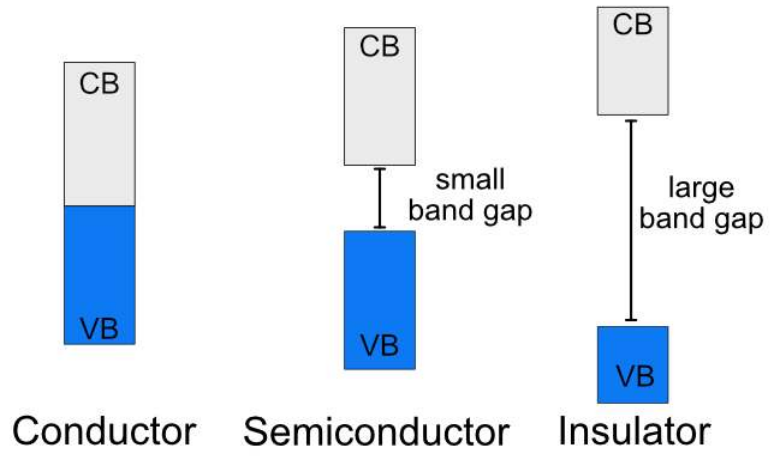


Figure *Section*9.5.3: Illustration of the energy difference between the valence band (VB) and conduction band (CB) in conductors, semiconductors and insulators. (CC BY-NC-SA; Catherine McCusker)

Conductors

Conductors have no band gap between their valence and conduction bands, since they overlap. There is no barrier for electrons to move from the valence to conduction band. Electrons can move freely through the material, which makes it able to conduct electricity. When the temperature of a conductor increases, the resistivity increases (and the conductivity decreases). Conductivity and resistivity are inversely proportional to each other. When conductivity is low, resistivity is high. When resistivity is low, conductivity is high. Since conductivity is the measure of how easily electricity flows, electrical resistivity measures how much a material resists the flow of electricity. As electrons move through a material, they come into contact with nuclei in the material. Collisions slow the electrons down. Each collision increases the resistivity of the material, and as temperature increases the electron are more likely to have collisions.

Insulators

Insulators have a large band gap between the valence and conduction bands. In insulators electrons do not have sufficient energy to jump from the valence band to the conduction band and the probability of finding an electron in the conduction band approaches 0. An insulator material won't conduct any electricity at any temperature.

Semiconductors

Semiconductors are an intermediate between conductors and insulators. They have a small energy gap between the valence band and the conduction band. Some electrons have sufficient energy that they can make the jump up to the conduction band. Semiconductors can conduct electricity, but not as easily as conductors. The probability of finding electrons in the conduction band of a semiconductor, and therefore it's ability to conduct electricity, will vary with the band gap and the temperature. Unlike conductors, semiconductors are more conductive at higher temperatures because more electrons have the energy to jump into the conduction band. There are two types of semiconductors: **intrinsic** and **extrinsic**.

Intrinsic Semiconductors

An intrinsic semiconductor is a pure material with a small band gap. For every electron that jumps into the conduction band, the missing electron will generate a hole that can move freely in the valence band. Both conduction band electrons and valence band holes can contribute to conducting electricity. The number of holes will equal the number of electrons that have jumped.

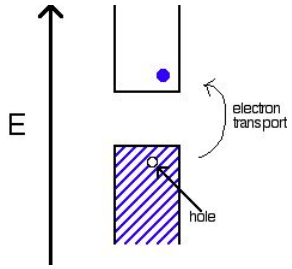


Figure *Section*9.5.4: Illustration of an intrinsic semiconductor. The electron in the conduction band (blue dot) leaves behind a vacancy (hole) in the valence band (white dot).

Extrinsic Semiconductors

Extrinsic semiconductors are not good conductors in their pure forms, they have larger band gaps than intrinsic semiconductors. In extrinsic semiconductors, the conductivity is controlled by purposefully adding small amounts of impurities to the material. This process is called doping. Doping, or adding impurities to the lattice can change the electrical conductivity of the lattice and therefore vary the efficiency of the semiconductor. In extrinsic semiconductors, the number of valence band holes will not equal the number of conduction band electrons. Silicon is one of the most common extrinsic semiconductors. If silicon is doped with an atom with fewer electron, such as boron, electron from the silicon valence band can hop to the boron atoms, leaving holes in the valence band to conduct electricity. If silicon is doped with an atom with more electrons, such as phosphorus, the extra electron from the phosphorus atoms can jump into the silicon conduction band.

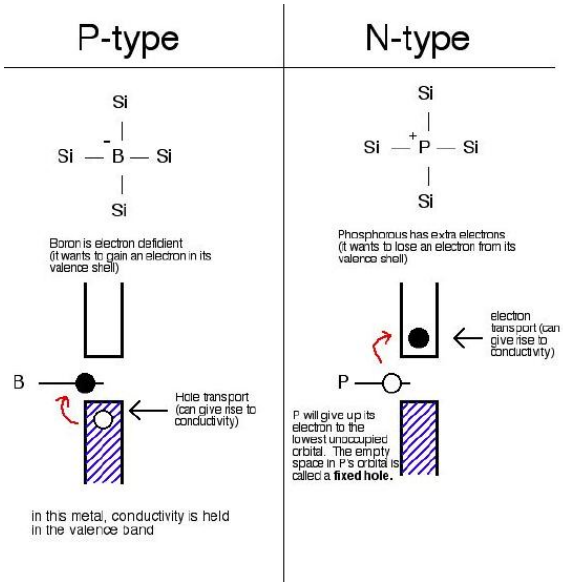


Figure *Section*9.5.5: P-type (left) n-type (right) silicon semiconductors. In the p-type an electron from the valence band can jump to a vacancy on boron, leaving a hole in the valence band. In the n-type an electron from the phosphorus dopant can jump into the conduction band.

Exercise *Section*9.5.1

Describe the difference between a valence band and a conduction band

Answer

The valence band is the highest band with electrons in it, the equivalent of the HOMO in MO theory. The conduction band is the highest band with no electrons in it, the equivalent of the LUMO in MO theory.

Exercise *Section*9.5.2

A conductor material and a semiconductor material have the same conductivity at 100 K. Which will be more conductive when the temperature is increased to 200 K?

Answer

The conductivity of conductors will decrease as the temperature increases and the conductivity of semiconductors will increase as the temperature increases. Therefore at higher temperature the semiconductor material will have higher conductivity.

References

1. Electrical Conductivity and Resistivity, Heaney, Michael, Electrical Measurement, Signal Processing, and Displays. Jul 2003
2. Levy, Peter M., and Shufeng Zhang. "Electrical Conductivity of Magnetic Multilayered Structures." *Physical Review Letters* 65.13 (1990): 1643-646. Print.
3. Petrucci, Harwood, Herring, Madura. GENERAL CHEMISTRY Principles and Modern Applications 9th Edition. Macmillan Publishing Co: New Jersey. 1989.
4. Moore, John T. Chemistry Made Simple. Random House Inc: New York. 2004.

Contributors and Attributions

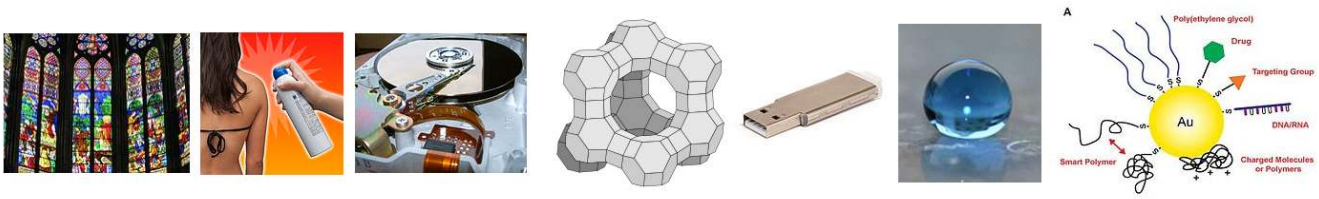
- Michael Ford (UCD) and Alexandra Christman (UCD)
- Sierra Blair (UCD)
- Jim Clark (Chemguide.co.uk)

Section 9.5: Bonding in Metals and Semicondoctors is shared under a CC BY-NC-SA 4.0 license and was authored, remixed, and/or curated by LibreTexts.

- **5.5: Bonding in Metals and Semicondoctors** is licensed CC BY-NC-SA 4.0.
- **6.8A: Electrical Conductivity and Resistivity** is licensed CC BY-NC-SA 4.0.

Section 9.6: Nanomaterials

What do stained glass, sunscreen, magnetic hard drives, heterogeneous catalysts, consumer electronics, stain-resistant clothing, self-cleaning glass, and medical diagnostics all have in common? All of them derive some special property and utility from nanoscale materials: ordinary elements and inorganic compounds such as gold, silver, TiO_2, chromium, SiO_2, and silicon that acquire different properties when their characteristic dimensions are somewhere between 1 and 100 nm. In this section we will learn about the basic science of nanomaterials, i.e., what it is about their size that makes them different.



Surface Area

Nanoparticles have a substantial fraction of their atoms on the surface, as shown in Figure ***Section*9.6.1**. This high surface area to volume ratio is an important factor in many of the physical properties of nanoparticles, such as their melting point and vapor pressure, and also in their reactivity. In some cases, such as TiO_2, it can change which polymorph is most stable. The most stable form of bulk TiO_2 is rutile, but in TiO_2 nanoparticles, the most stable polymorph is anatase. Heterogeneous catalysts, for example, are often based on nanoparticles because the catalytically reactive atoms are those that are on the surface of the particle, and this allows for the most reactive surface sites with the smallest amount of material.

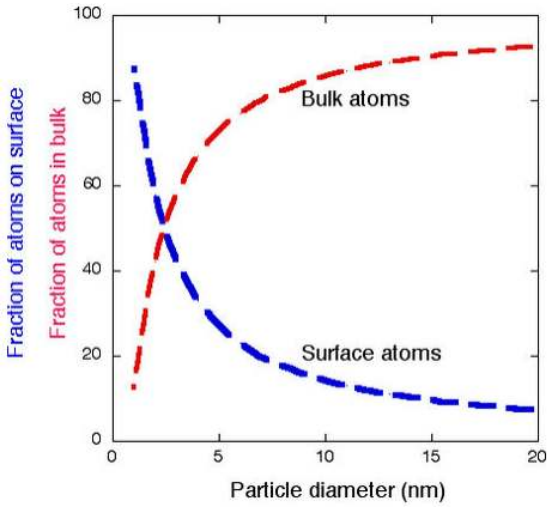


Figure ***Section*9.6.1**: Plot of how the ratio of surface to bulk atoms changes with particle size.

Surface Energy

The surface energy is always positive. A key quantity that is connected with the chemistry of all surfaces is the **surface energy**. This is the (thermodynamically unfavorable) energy of making "dangling bonds" at the surface. Atoms at the surface are under-coordinated, and because breaking bonds costs energy, surface atoms always have higher energy than atoms in the bulk. This happens regardless of whether the bonding is covalent (as in a metal), ionic (in a salt), or non-covalent (in a liquid such as water). We see this effect, for example, in water droplets that bead up on a waxy surface. The droplet contracts into a sphere (against the force of gravity that works to flatten it) in order to minimize the number of dangling hydrogen bonds at the surface.

In the case of metal or semiconductor particles, strong covalent bonds are broken at the surface. For example, a gold atom in bulk face-centered cubic Au has 12 nearest neighbors, but a gold atom on the surface of the crystal has six nearest neighbors in-plane and three underneath, for a total of 9. We might expect the surface energy of this crystal face to be a little less (because the remaining bonds will become slightly stronger) than 3/12 = 1/4 of the bonding energy of bulk Au, and this is in fact a fairly good

rule of thumb for many materials. When translated into energy per unit area, the surface energy of metals and inorganic salts is usually in the range of 1-2 J/m^2.

Example *Section*9.6.1

The sublimation energy of bulk gold is 334 kJ/mol, and the surface energy is 1.5 J/m^2. What percentage of the bulk bonding energy is lost by atoms at the surface of a gold crystal?.

Solution

To solve this problem, we need to know the surface area per Au atom. Gold has the face-centered cubic structure, and the unit cell edge length is 4.08 Å. From this we can determine that the Au-Au distance is 4.08/1.414 = 2.88 Å. In a hexagonal array of gold atoms with this interatomic spacing, the surface area per atom is (2.88 Å)^2 x 0.866 = 7.2 Å^2. Multiplying by Avogadro's number, we find that the area per mole of Au surface atoms on the crystal face is 4.3 x 10^4 m^2.

Now we multiply this area by the surface energy:

$(4.3 \times 10^4 \frac{m^2}{mol}) \times (1.5 \frac{J}{mol}) \times (\frac{1kJ}{1000J}) = +65\text{kJ}$ per mole of Au surface atoms.

$\frac{65kJ}{334kJ} \times 100\% = 19\%$ of the bulk bonding energy is lost by atoms at the surface.

It is clear from the above example that the surface energy of nanoparticles can have a major effect on their physical properties, since a large fraction of the atoms in a nanoparticle are on the surface. A good example of this is the dramatic depression of the melting point. Solid nanocrystals are in general faceted, whereas liquid droplets made by melting nanocrystals adopt a spherical shape to minimize the surface area.

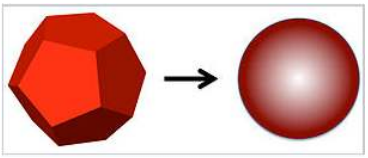


Figure *Section*9.6.2: A faceted solid nanocrystal melts into a spherical droplet in order to minimize its surface energy.

Let's consider melting a silver nanocrystal that is 2 nm in diameter, meaning that about $\frac{1}{2}$ of the atoms are on the surface. The spherical liquid droplet has lower surface area than the faceted crystal. For example, a cube has 1.24 times the surface area of a sphere of the same volume. If the decrease in surface area is about 20% upon melting, and the surface energy is about 1/4 of the bulk bonding energy of the atoms, then for a 2 nm diameter nanocrystal we would estimate that:

$$\begin{aligned} \Delta H^o_{fusion} &\approx \Delta H^o_{fusion,\ bulk} - (\frac{1}{2})(0.25)(\frac{1}{4})\Delta H^o_{vap} \\ &= \Delta H^o_{fusion,\ bulk} - 0.025\Delta H^o_{vap,\ bulk} \end{aligned} \qquad \text{(Section 9.6.1)}$$

where $\Delta H°_{vap,\ bulk}$, the heat of vaporization, is the total bonding energy of atoms in a bulk crystal. For silver, $\Delta H°_{fusion,\ bulk}$ = 11.3 kJ/mol and $\Delta H°_{vap,\ bulk}$ = 250 kJ/mol. From this we can calculate the heat of fusion of a 2 nm Ag nanocrystal:

$$\Delta H^o_{fusion} \approx 11.3 - (0.025)(25) = 5.1 \frac{kJ}{mol} \qquad \text{(Section 9.6.2)}$$

The melting point of bulk silver is 962 °C = 1235 K. Assuming that the entropy of fusion is the same in the bulk and in the nanocrystal, the melting point of the nanocrystal should be $1234K \times (\frac{5.1}{11.3}) = 557K = 284°C$, a drop of almost 700 degrees from the bulk value. Experimentally, the melting point of a 2 nm diameter silver nanocrystal drops about 800 degrees below that of the bulk, to 127 °C. This is a whopping big change in the melting point, which is in reasonable agreement with our rough estimate. The same effect - energetic destabilization of the surface atoms relative to bulk atoms - results in the lower boiling point, higher vapor pressure, higher solubility, and higher reactivity of nanocrystals relative to larger crystals of the same material.

Quantum Dots

One of the most fascinating and well-studied mesoscopic effects occurs with semiconductor particles of various shapes when one or more of their dimensions is in the range of a few nanometers. These so-called "quantum dots" (0D), "quantum rods" (1D) and "nanosheets" (2D) acquire striking new electronic and optical properties.

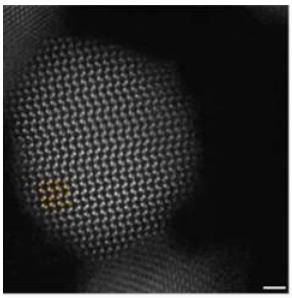


Figure *Section*9.6.3: Atomic resolution image of a CdSe nanoparticle.

The synthesis of semiconductor quantum dots, which is discussed in more detail below, is sufficiently well controlled to give essentially perfect crystals of a few thousand atoms, something that is statistically impossible in a macroscopic crystal. An image of such a crystal is shown in Figure *Section*9.6.3. The band gap in many of these quantum dots is in a range where absorption of visible light can promote an electron from the valence band to the conduction band as shown in Figure *Section*9.6.4. Relaxation of that electron back into the valence band results in emission. The quantum yield for band gap emission of semiconductor quantum dots is typically high, giving rise to the bright emission colors shown in (Figure *Section*9.6.5) for CdSe particles of different sizes. Because of their strong and narrow emission bands, quantum dots are of interest as luminescent tags for biological imaging applications, and also as light absorbers and emitters in solar cells and LEDs.

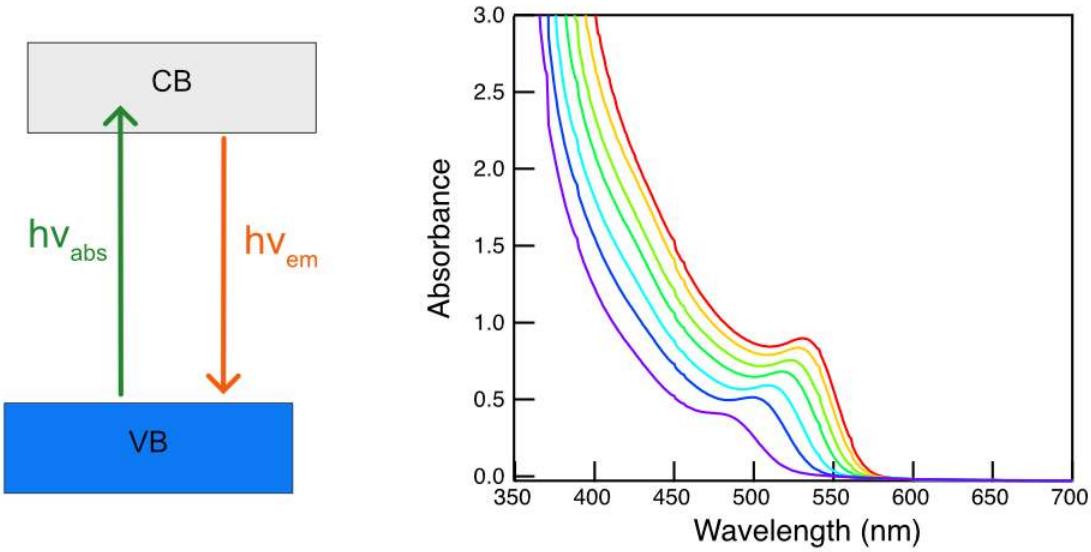


Figure *Section*9.6.4: Diagram (left) showing the band gap absorption and emission of visible light in quantum dots. UV-visible spectrum (right) of a series of CdSe quantum dots. (CC BY-NC-SA, Catherine McCusker)

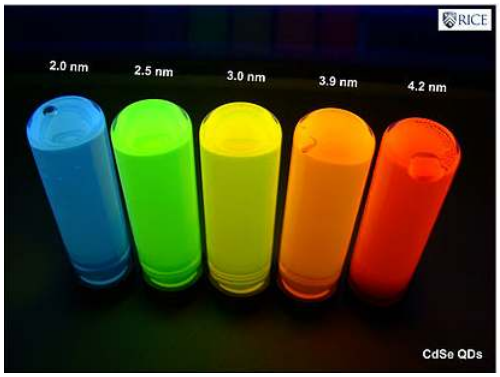


Figure *Section*9.6.5: Emission colors of CdSe nanoparticles of different sizes. Smaller particles emit blue light because the exciton energy increases as the size decreases.

Size dependence

The size-dependence of the emission color comes primarily from a particle-in-a-box effect. The electron and hole that are created when the quantum dot absorbs light are bound together as an exciton by the confines of the "box". Louis Brus used first-order perturbation theory to determine that the band gap of a semiconductor quantum dot is given approximately by:

$$E_{gap} = E_{gap,bulk} + \frac{h^2}{8\mu R^2} - \frac{1.8e^2}{4R\pi\varepsilon\varepsilon_0} + \ldots \qquad \text{(Section 9.6.3)}$$

where R is the particle radius, μ is the electron-hole reduced mass ($1/\mu = 1/m_e^* + 1/m_h^*$), m_e^* and m_h^* are the electron and hole effective masses, and ε is the dielectric constant of the semiconductor. In this equation, the first term after the bulk bandgap is the kinetic energy due to confinement of the exciton, and the second term represents the electrostatic attractive energy between the confined electron and hole. Because the energy is a function of R^2, it can be widely tuned across the visible spectrum by changing the size of the quantum dot.

Definition: Exciton

A conduction band electron and its valence band hole together form an exciton. Excitons are formed when an electron is promoted from the valence band to the conduction band of a material.

Synthesis

Early work on the quantum size effect in semiconductor nanoparticles used simple metathesis reactions in the synthesis. For example, CdSe and PbS can be precipitated at ambient temperature by the reactions:

$$CdCl_{2\,(aq)} + H_2Se_{(g)} = CdSe_{(s)} + 2\,HCl_{(aq)}$$

$$Pb(NO_3)_2 + H_2S_{(g)} = PbS_{(s)} + 2\,HNO_{3\,(aq)}$$

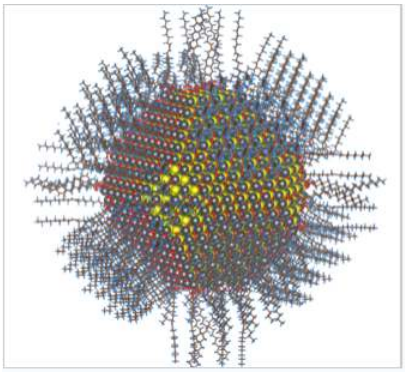


Figure *Section*9.6.6: Complete atomistic model of a 5 nm diameter colloidal lead sulfide nanoparticle with surface passivation by oleic acid, oleyl and hydroxyl groups.

The growth of the particles was restricted by carrying out these reactions in different matrices, such as in polymer films or the silicate cages of zeolites, and capping ligands were also sometimes used to limit particle growth. While these reactions did produce nanoparticles, in general a broad distribution of particle sizes was obtained. The particles were also unstable to **Ostwald ripening** - in which large particles grow at the expense of smaller ones in order to minimize the total surface energy - because of the reversibility of the acid-forming synthetic reactions in aqueous media. The lack of good samples prevented detailed studies and the development of applications for semiconductor quantum dots.

A very important development in nanoparticle synthesis came in the early 1990's, when Murray, Norris, and Bawendi introduced the first non-aqueous, controlled growth process for II-VI semiconductor quantum dots. The keys to this synthesis were (1) to use non-aqueous solvents and capping ligands to stabilize the products against ripening, (2) to carry out the reaction at high temperature to ensure good crystallinity, and (3) to separate the steps of particle **nucleation** and **growth**, and thereby obtain particles of uniform size. This procedure is illustrated below in Figure *Section*9.6.7.

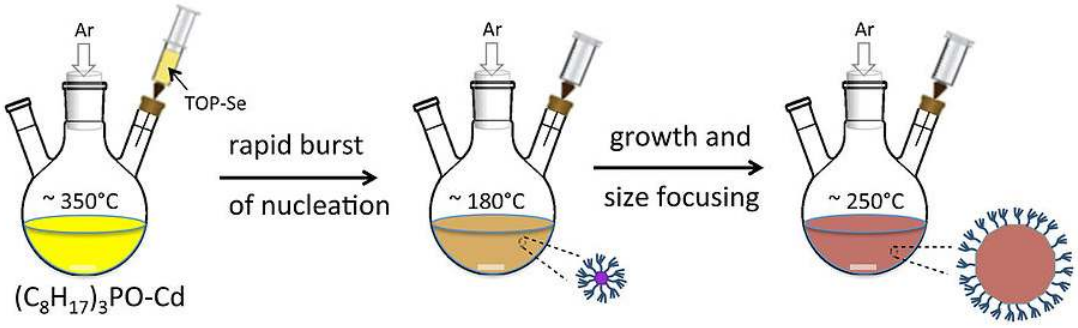


Figure *Section*9.6.7: Illustration of the steps of CdSe nanoparticle synthesis

The synthesis is carried out in a coordinating, high boiling solvent that is a mixture of trioctylphosphine (TOP) and trioctylphosphine oxide (TOPO). IAt the start of the reaction, a selenium source is rapidly injected into the hot (350 °C) reaction mixture containing Cd. The reaction causes a rapid burst of nanoparticle nucleation, but the temperature also drops as the cold solvent is injected and so the nucleation event ends quickly. The cooled solution now contains nanocrystal seeds. It is supersaturated in TOPO-Cd and TOP-Se, but particle growth proceeds slowly until the solution is heated again to the growth temperature, ca. 250°C. Particle growth and size-focusing occurs because small particles require less added material to grow by an amount ΔR than larger particles. This is because the volume of an added shell around a spherical seed is $4\pi R^2\Delta R$, so for larger R, ΔR is smaller. Very narrow particle size distributions can be obtained under conditions of high supersaturation, where the rate of nanoparticle growth is fast relative to particle dissolution and Ostwald ripening. Because the nanoparticles are capped with a ligand shell of TOP, they can be precipitated and re-suspended in organic solvents.

The high temperature synthesis of semiconductor quantum dots has been applied to a broad variety of materials. Monodisperse nanoparticles of controlled shapes can be made by variants of this method. For example, it is possible to adjust the conditions so that CdSe nucleates in the zincblende polymorph as tetrahedrally shaped seeds, and then grow polar wurtzite "arms" onto each triangular face, resulting in nanocrystal tetrapods. Numerous other nanocrystal shapes such as rods, arrowheads, rice (tapered rods), and polar structures such as Janus rods can be made by variants of this technique. These shape-control strategies often involve the use of ligands that adsorb specifically to certain crystal faces and inhibit their growth. For example, hexylphosphonic acid ligands adsorb selectively to Cd-rich crystal faces and thus lead to the growth of prismatic wurtzite-phase CdSe nanocrytals.

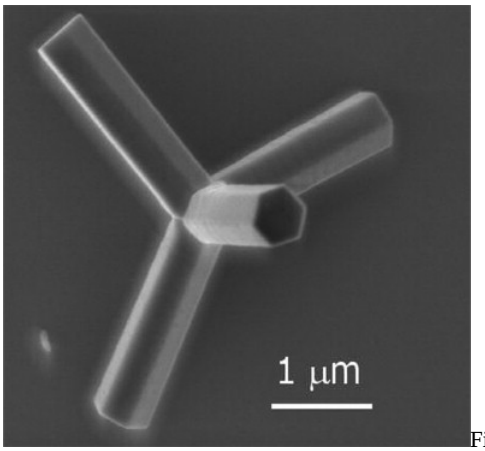
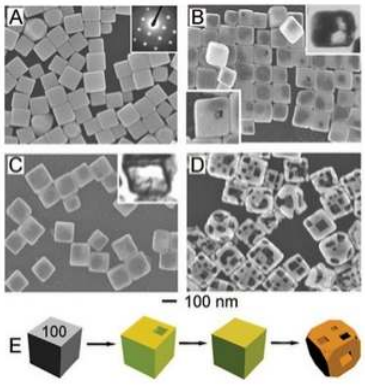
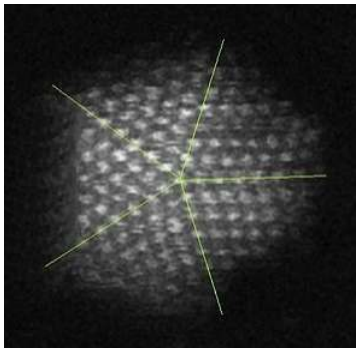


Figure *Section*9.6.1: Scanning electron microscope (SEM) image of a ZnO tetrapod nanocrystal. (CC BY-NC-ND 3.0; ScienceDirect via https://doi.org/10.1016/S1369-7021(07)70079-2)



Nanoscale metal particles have been the subject of intense research over the past 20 years, especially because of their unusual **optical**, **magnetic**, and **catalytic** properties. The synthesis of metal nanocrystals in various shapes has become increasingly sophisticated and rational, like the synthesis of semiconductor nanocrystals described above. By controlling the separate phases of nucleation and growth, and by using ligands that cap specific crystal faces during growth, it is possible to make metal nanocrystals of uniform size in a variety of interesting and useful shapes including cubes, truncated cubes, octahedra, triangular prisms, and high aspect ratio rods. By exploiting displacement reactions that replace one metal with another, complex hollow shapes such as nanocages (as shown at the left) can be made starting with other shapes. In this case, solid silver nanocubes are transformed to gold nanocages.



Five-fold twinning in a gold nanoparticle

The interesting optical properties of nanocrystalline Au, Ag, Cu, and a number of other metals, derive from the collective oscillation of their valence electrons, a phenomenon known as **plasmon resonance**. Remember that in these metals, the electron mean free path is long (about 100 times larger than the size of the atoms), so the valence electrons feel only the average positive charge of the atomic cores as they zoom around the crystal. Light impinging on the metal acts as an oscillating electric field, pushing and pulling on the valence electrons at the characteristic frequency of the light wave. The situation is very much like a pendulum or a weight on a spring. The electrons, pushed away from their equilibrium positions, feel a restoring force that is proportional to their displacement. Their motion can be described by **Hooke's Law**:

$$F = kx \qquad \text{(Section 9.6.4)}$$

where the spring constant k determines the "stiffness" of the spring. In the case of the plasmon resonance, k is proportional to the number density of valence electrons n, and the square of the electronic charge e:

$$k = \frac{ne^2}{\varepsilon_0} \qquad \text{(Section 9.6.5)}$$

The **resonant frequency** of the plasma oscillation is given by:

$$\omega_p = (\frac{k}{m})^{\frac{1}{2}} = (\frac{ne^2}{m_e \varepsilon_0}^{\frac{1}{2}} \quad \text{(Section 9.6.6)}$$

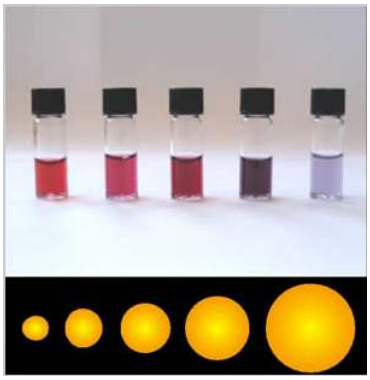
where m_e is the electron mass. For most metals, the plasmon resonance is in the ultraviolet part of the spectrum, but for a few metals like Au, Ag, and Cu it is in the visible.



The Lycurgus cup (4th century Roman glass) derives its unique coloration from noble metal nanoparticles. The cup is red in transmitted light and green in scattered (reflected) light.

For metal particles that are much smaller than the wavelength of light, this effect is called the **localized surface plasmon resonance**, or LSPR. There are three important consequences of the LSPR effect:

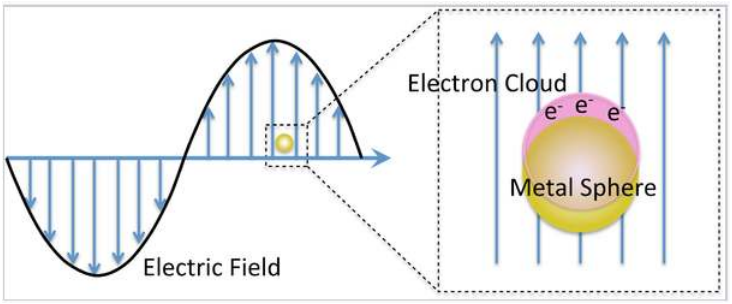
- The **local electric field** of the incoming light wave is greatly **enhanced** at the particle surface. This gives rise to huge enhancement factors in optical processes such as **Raman scattering** and **fluorescence**. Thus, certain analytical spectroscopic techniques are greatly enhanced by LSPR.
- Near the plasmon resonance frequency, metal nanocrystals **absorb** and **scatter light** very strongly. This makes them brightly reflective, and the strong light absorption can be exploited for light-induced local heating. These properties are being applied in medical diagnostics and therapy, e.g., for detection and photothermal destruction of cancer cells. By adjusting the size and shape of the gold nanoparticles, which are more stable than Ag and Cu in biological media, the plasmon frequency can be tuned to the tissue-transparent near-IR region of the spectrum between 700 and 900 nm. Small quantities of plasmonic Ag and Au particles also make brightly colored and strongly scattering pigments, e.g. in stained glass as shown above at the right.
- The plasmon frequency is sensitive to the refractive index of the particle's surroundings, i.e., its chemical environment. This makes metal nanoparticles of special interest for **sensing and biosensing** applications.



The colors of plasmonic gold nanoparticles depend on their size and shape.

Theory of light scattering and absorption by metal nanoparticles

The valence electrons in metal nanoparticles oscillate in the electric field of a light wave. While the nature of these oscillations is somewhat complex in metal particles that are non-spherical, the theory for spherical particles is relatively simple and in fact was worked out over 100 years ago by German physicist Gustav Mie.



Mie considered the interaction of a spherical particle with a **uniform electric field, E,** oscillating at angular frequency ω (= 2π f). This is a good approximation when the particle diameter is much smaller than the wavelength of light, as shown on the left. The particle is embedded in a uniform, insulating material (e.g. a solvent) that has a dielectric constant ε_{diel}. For insulators, ε_{diel} is a positive real number.

The dielectric constant ε of a metal is actually a complex number:

$$\varepsilon = \varepsilon' + i\varepsilon'' \qquad \text{(Section 9.6.7)}$$

Here the real part, ε', is related to the refraction of light, and the imaginary part, ε", is related to light absorption. Both ε' and ε" are dependent on the frequency of the light. For metals near the plasmon resonance frequency, ε' is typically a *negative number.*

The **cross-section for absorption** of the light wave by the particle is:

$$\sigma_{absorption} = \frac{9\omega}{c}\epsilon_{diel}^{\frac{3}{2}} V \frac{\epsilon''_{metal}}{(\epsilon'_{metal} + 2\epsilon_{diel})^2 + (\epsilon''_{metal})^2} \qquad \text{(Section 9.6.8)}$$

and the **cross-section for scattering** is:

$$\sigma_{scattering} = \frac{3}{2\pi}\left(\frac{\omega^4}{c}\right)\epsilon_{diel}^2 V^2 \frac{(\epsilon'_{metal} - \epsilon_{diel})^2 + (\epsilon''_{metal})^2}{(\epsilon'_{metal} + 2\epsilon_{diel})^2 + (\epsilon''_{metal})^2} \qquad \text{(Section 9.6.9)}$$

The sum of these two is the **cross-section for extinction**:

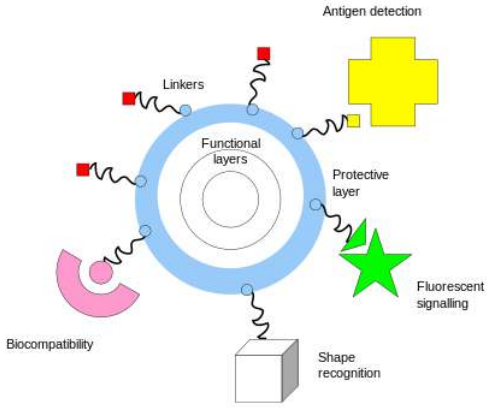
$$\sigma_{extinction} = \sigma_{absorption} + \sigma_{scattering} \qquad \text{(Section 9.6.10)}$$

These cross-sections become large when the (ε'_{metal} + $2\varepsilon_{diel}$) term in the denominator becomes small. This occurs when

$$\epsilon'_{metal} \simeq -2\epsilon_{diel} \qquad \text{(Section 9.6.11)}$$

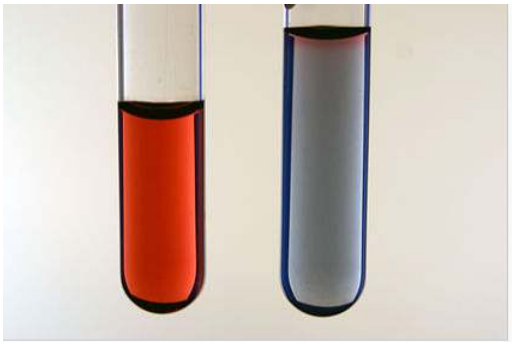
For 15 nm diameter gold nanoparticles in water, this happens at about 580 nm, resulting in the characteristic wine-red color of colloidal gold solutions. Changing the solution environment (e.g., by adsorbing a molecule onto the gold surface) changes ε_{diel} and thus alters the color slightly.

It is important to note that the cross-section for **scattering** is proportional to the **square of the volume** of the particle, V^2, whereas the absorption is proportional to V. This means that very small gold particles (< 5 nm) are strongly absorbing but not strongly scattering. Larger particles (>30 nm) scatter light very strongly. Depending on the application, therefore, we choose larger or smaller particles.



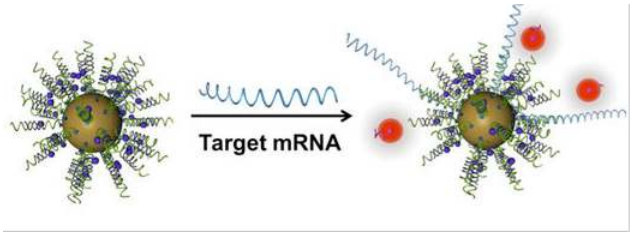
One of the key complementary properties of noble metal nanoparticles that is important to their use in biomedicine is the ease with which they can be **covalently conjugated** with polymers or small molecules, typically via thiol or amine bonds at their surface. This imparts biological recognition properties to the particles that enables them to bind to specific biomolecular targets. The figure at the left illustrates some of the functionality that can be imparted to nanoparticles through surface functionalization.

Functionalization of gold nanoparticles with thiol-terminated single-stranded DNA was the basis of one of the first nanoparticle sensors, developed by the Mirkin group at Northwestern University. **DNA-coated nanoparticles** have the characterstic wine-red plasmonic color of spherical nano-gold. However, when these particles are linked together by a complementary DNA strand, the resonance frequency shifs, resulting in a blue color. This color change, illustrated in the figure at the right, provides a "litmus test" for the presence of the target DNA sequence.[10] "Melting" of the DNA - heating it to the temperature at which double stranded DNA dissociates to make single strands - reverses the color change. The DNA hybridization/melting transition is highly **cooperative** because of the aggregation of many gold particles, so the transition temperature is very sharp. With proper temperature control, the color change can be sensitive to a **single base mismatch** in the target DNA that is detected by this method.



Aggregation of Au nanoparticles (in this case by adding salt to a colloidal solution) causes a color change from wine red (left) to blue (right). Photo credit: George Lisensky, Beloit College

Subsequent research has developed sophisticated diagnostic and therapeutic ("theranostic") applications for these **spherical nucleic acid**[11] particles. These particles easily penetrate cell membranes and can report on the chemistry happening inside living cells.



General schematic of nanoflare-based detection.

An important property of gold nanoparticles in these applications is their ability to **quench** the **fluorescence** of reporter molecules that are near their surface. Nucleic acid strands that contain a hairpin loop can position fluorescent molecules near the gold surface, where their fluorescence is turned off by nanoparticle quenching. Hybridization of these sequences to target RNA or DNA causes the fluorescence to turn on by moving the fluorescent molecule away from the nanoparticle surface. These so called "nanoflares" can thus signal the up- or down-regulation of specific genes inside cells. Nanoflares are the basis of the Verigene System, developed and commercialized by Nanosphere, Inc. to detect markers for infectious diseases and cancers.

References

1. K. J. Klabunde, J. Stark, O. Koper, C. Mohs, D. G. Park, S. Decker, Y. Jiang, I. Lagadic, and D. Zhang, "Nanocrystals as Stoichiometric Reagents with Unique Surface Chemistry," J. Phys. Chem. 1996, 100, 12142–12153. DOI: 10.1021/jp960224x.
2. Brus, Louis E. (1984). "Electron–electron and electron-hole interactions in small semiconductor crystallites: The size dependence of the lowest excited electronic state". J. Chem. Phys. 80, 4403. DOI: 10.1063/1.447218.
3. C. B. Murray, D. J. Norris, and M. G. Bawendi, "Synthesis and characterization of nearly monodisperse CdE (E = sulfur, selenium, tellurium) semiconductor nanocrystallites," J. Am. Chem. Soc. 1993, 115, 8706–8715. DOI: 10.1021/ja00072a025.
4. Y. Yin and A. P. Alivisatos, "Colloidal nanocrystal synthesis and the organic–inorganic interface," Nature 2005, 437, 664-670. DOI: 10.1038/nature04165
5. G. Zheng, F. Patolsky, Y. Cui, W. U. Wang and C. M. Lieber, "Multiplexed electrical detection of cancer markers with nanowire sensor arrays," Nature Biotechnol. 2005, 23, 1294 - 1301. DOi:10.1038/nbt1138.
6. Mirkin, C. A., et al., A DNA-based method for rationally assembling nanoparticles into macroscopic materials. *Nature* 1996, 382 (6592), 607-609.
7. Cutler, J. I., et al., Spherical Nucleic Acids. *J Am Chem Soc* 2012, 134 (3), 1376-1391.

Section 9.6: Nanomaterials is shared under a CC BY-NC-SA license and was authored, remixed, and/or curated by LibreTexts.

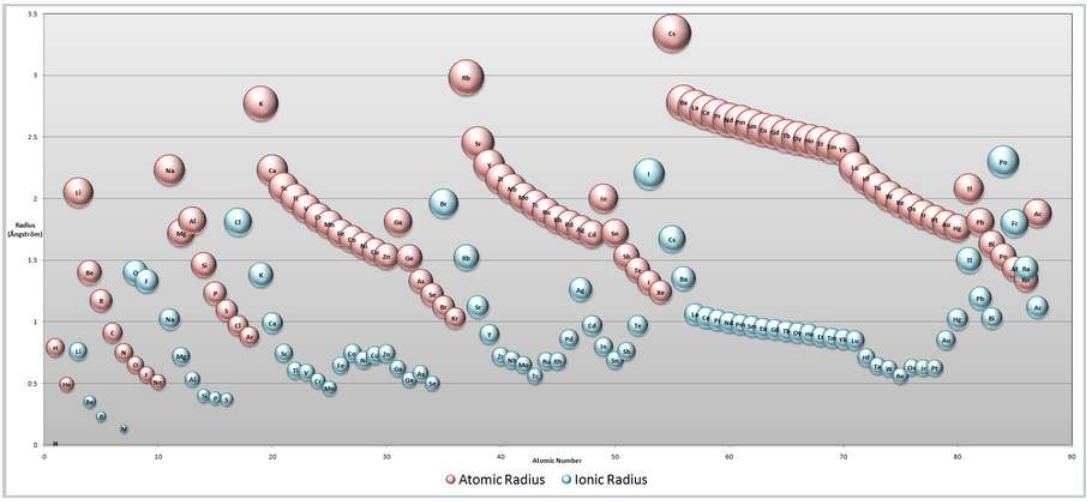
- **11.1: Prelude to Basic Science of Nanomaterials** by Chemistry 310 is licensed CC BY-SA 4.0. Original source: https://en.wikibooks.org/wiki/Introduction_to_Inorganic_Chemistry.
- **5.6: Nanomaterials** is licensed CC BY-SA 4.0.
- **11.5: Surface Energy** by Chemistry 310 is licensed CC BY-SA 4.0. Original source: https://en.wikibooks.org/wiki/Introduction_to_Inorganic_Chemistry.
- **11.3: Semiconductor Quantum Dots** by Chemistry 310 is licensed CC BY-SA 4.0. Original source: https://en.wikibooks.org/wiki/Introduction_to_Inorganic_Chemistry.
- **11.4: Synthesis of Semiconductor Nanocrystals** by Chemistry 310 is licensed CC BY-SA 4.0. Original source: https://en.wikibooks.org/wiki/Introduction_to_Inorganic_Chemistry.
- **11.6: Nanoscale Metal Particles** by Chemistry 310 is licensed CC BY-SA 4.0. Original source: https://en.wikibooks.org/wiki/Introduction_to_Inorganic_Chemistry.

Section 9.1b: Ionic Radii and Radius Ratios

Atoms in crystals are held together by electrostatic forces, van der Waals interactions, and covalent bonding. It follows that arrangements of atoms that can maximize the strength of these attractive interactions should be most favorable and lead to the most commonly observed crystal structures.

Radius ratio rules

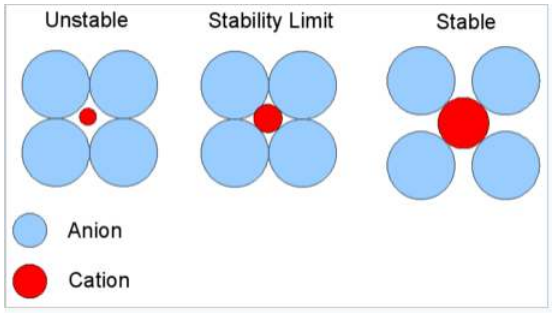
Early crystallographers had trouble solving the structures of inorganic solids using X-ray diffraction because some of the mathematical tools for analyzing the data had not yet been developed. Once a trial structure was proposed, it was relatively easy to calculate the diffraction pattern, but it was difficult to go the other way (from the diffraction pattern to the structure) if nothing was known *a priori* about the arrangement of atoms in the unit cell. It was (and still is!) important to develop some guidelines for guessing the coordination numbers and bonding geometries of atoms in crystals. The first such rules were proposed by Linus Pauling, who considered how one might pack together oppositely charged spheres of different radii. Pauling proposed from geometric considerations that the quality of the "fit" depended on the **radius ratio** of the anion and the cation.



Atomic and Ionic Radii. Note that cations are always smaller than the neutral atom (pink) of the same element, whereas anions are larger. Going from left to right across any row of the periodic table, neutral atoms and cations contract in size because of increasing nuclear charge. (click for larger image)

The basic idea of radius ratio rules is illustrated at the right. We consider that the anion is the packing atom in the crystal and the smaller cation fills interstitial sites ("holes"). Cations will find arrangements in which they can contact the largest number of anions. If the cation can touch all of its nearest neighbor anions, as shown at the right for a small cation in contact with larger anions, then the fit is good. If the cation is too small for a given site, that coordination number will be unstable and it will prefer a

lower coordination structure. The table below gives the ranges of cation/anion radius ratios that give the best fit for a given coordination geometry.



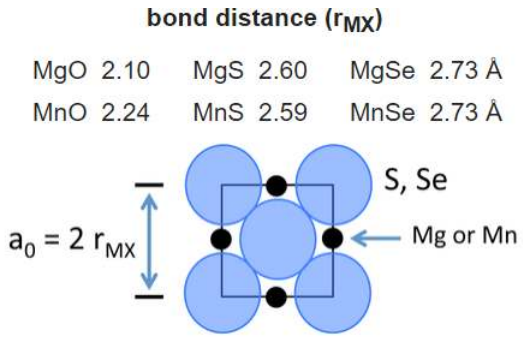
Critical Radius Ratio. This diagram is for coordination number six: 4 anions in the plane are shown, 1 is above the plane and 1 is below. The stability limit is at $r_C/r_A = 0.414$

Coordination number	Geometry	$\rho = r_{cation}/r_{anion}$
2	linear	0 - 0.155
3	triangular	0.155 - 0.225
4	tetrahedral	0.225 - 0.414
4	square planar	0.414 - 0.732
6	octahedral	0.414 - 0.732
8	cubic	0.732 - 1.0
12	cuboctahedral	1.0

There are unfortunately several challenges with using this idea to predict crystal structures:

- We don't know the radii of individual ions
- Atoms in crystals are not really ions - there is a varying degree of covalency depending electronegativity differences
- Bond distances (and therefore ionic radii) depend on bond strength and coordination number (remember Pauling's rule D(n) = D(1) - 0.6 log n)
- Ionic radii depend on oxidation state (higher charge => smaller cation size, larger anion size)

We can build up a table of ionic radii by assuming that the bond length is the sum of the radii ($r_+ + r_-$) if the ions are in contact in the crystal. Consider for example the compounds MgX and MnX, where X = O, S, Se. All of these compounds crystallize in the NaCl structure:



For the two larger anions (S^{2-} and Se^{2-}), the unit cell dimensions are the same for both cations. This suggests that the anions are in contact in these structures. From geometric considerations, the anion radius in this case is given by:

Extra close brace or missing open brace

and thus the radii of the S^{2-} and Se^{2-} ions are 1.84 and 1.93 Å, respectively. Once the sizes of these anions are fixed, we can obtain a self-consistent set of cation and anion radii from the lattice constants of many MX compounds.

How well does this model work? Let's consider the structures of tetravalent metal oxides (MO_2), using Pauling radii and the predictions of the radius ratio model:

Oxide MO_2	Radius ratio	Predicted coord. no.	Observed coord no. (structure)
CO_2	~0.1	2	2 (linear molecule)
SiO_2	0.32	4	4 (various tetrahedral structures)
GeO_2	0.43	4	4 (silica-like structures)
"	0.54	6	6 (rutile)
TiO_2	0.59	6	6 (rutile)
ZrO_2	0.68	6	7 (baddleyite)
"	0.77	8	8 (fluorite)
ThO_2	0.95	8	8 (fluorite)

Note that cations have different radii depending on their coordination numbers, and thus different radius ratios are calculated for Ge^{4+} with coordination numbers 4 and 6, and for Zr^{4+} with coordination numbers 6 and 8.

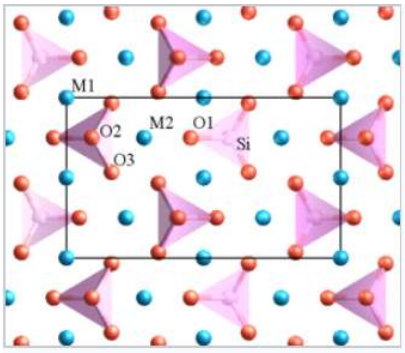
For this series of oxides, the model appears to work quite well. The correct coordination number is predicted in all cases, and borderline cases such as GeO_2 and ZrO_2 are found in structures with different coordination numbers. The model also correctly predicts the structures of BeF_2 (SiO_2 type), MgF_2 (rutile), and CaF_2 (fluorite).

What about the alkali halides NaCl, KBr, LiI, CsF, etc.? All of them have the NaCl structure except for CsCl, CsBr, and CsI, which have the CsCl (8-8) structure. In this case the radius ratio model fails rather badly. The Li^+ salts LiBr and LiI are predicted to have tetrahedral structures, and KF is predicted to have an 8-8 structure like CsCl. We can try adjusting the radii (e.g., making the cations larger and anions smaller), but the best we can do with the alkali halides is predict about half of their structures correctly. Since the alkali halides are clearly ionic compounds, this failure suggests that there is something very wrong with the radius ratio model, and its success with MO_2 compounds was coincidental.

In addition to the radius ratio rule, Linus Pauling developed other useful rules that are helpful in rationalizing and also predicting the structures of inorganic compounds. Pauling's rules[1] state that:

- Stable structures are **locally electroneutral**. For example, in the structure of the double perovskite Sr_2FeMoO_6, MO_6 (M = Fe^{2+}, Mo^{6+}) octahedra share all their vertices, and Sr^{2+} ions fill the cubooctahedral cavities that are flanked by eight MO_6 octahedra.[2] Each O^{2-} ion is coordinated to one Fe^{2+} and one Mo^{6+} ion in order to achieve local electroneutrality, and thus the FeO_6 and MoO_6 octahedra alternate in the structure.
- **Cation-cation repulsion** should be minimized. Anion polyhedra can share vertices (as in the perovskite structure) without any energetic penalty. Shared polyhedral edges, and especially shared faces, cause cation-cation repulsion and should be avoided. For example, in rutile, the most stable polymorph of TiO_2, the TiO_6 octahedra share vertices and two opposite edges, forming ribbons in the structure. In anatase TiO_2, each octahedron shares four edges so the anatase polymorph is less thermodynamically stable.

- **Highly charged cations** in anion polyhedra tend not to share edges or even vertices, especially when the coordination number is low. For example, in orthosilicates such as olivine (M_2SiO_4), there are isolated SiO_4^{4-} tetrahedra.



Structure of olivine. M (Mg or Fe) = blue spheres, Si = pink tetrahedra, O = red spheres.

As we will soon see, all of Pauling's rules are justified on the basis of lattice energy considerations. In ionic compounds, the arrangement of atoms that maximizes anion-cation interactions while minimizing cation-cation and anion-anion contacts is energetically the best.

This page titled Section 9.1b: Ionic Radii and Radius Ratios is shared under a CC BY-SA 4.0 license and was authored, remixed, and/or curated by Chemistry 310 (Wikibook) via source content that was edited to the style and standards of the LibreTexts platform.

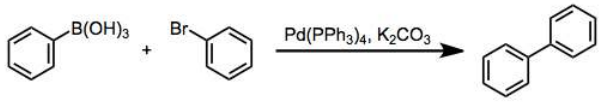
- **9.1: Ionic Radii and Radius Ratios** by Chemistry 310 is licensed CC BY-SA 4.0. Original source: https://en.wikibooks.org/wiki/Introduction_to_Inorganic_Chemistry.

CHAPTER OVERVIEW

Chapter 10: Organometallic Chemistry

Organometallic chemistry is a subfield of inorganic chemistry involving the study of compounds containing, and reactions involving, metal-carbon bonds. The metal-carbon bond may be transient or temporary, but if one exists during a reaction or in a compound of interest, we're squarely in the domain of organometallic chemistry. In addition to M-C bond, bonds between metals and the other common elements of organic chemistry also appear in organometallic chemistry: metal-nitrogen, metal-oxygen, metal-halogen, and even metal-hydrogen bonds all play a role. Metals cover a vast swath of the periodic table and include the alkali metals, alkali earth metals, transition metals, the main group metals, and the lanthanides and actinides. We will focus most prominently on the transition metals in this chapter.

Why is the subject worth studying? Organometallic complexes are catalysts for a wide range of industrially important chemical reactions from polymers to pharmaceuticals. There's a reason the "organo" comes first in "organometallic chemistry"—These catalysts usually the aid in the creation of new bonds in organic compounds, building up complex products from simple starting materials. The fact is that you can do things with organometallic chemistry that you cannot do using straight-up organic chemistry. Case in point:



The venerable Suzuki reaction...unthinkable without palladium!

The establishment of a bond between two phenyl rings seems unthinkable to the pure organic chemist, but with a palladium catalyst it si a commonplace reaction. Bromobenzene looks like a potential electrophile at the bromine-bearing carbon, and if you're familiar with hydroboration you might see phenylboronic acid as a potential nucleophile at the boron-bearing carbon. Catalytic palladium makes it all happen. Organometallic chemistry is full of these mind-bending transformations, and can expand the synthetic toolbox of the organic chemist considerably.

Contributors and Attributions

- Dr. Michael Evans (Georgia Tech)

Learning Objectives

- Illustrate the orbital overlap involved in metal-ligand bonding for different classes of organometallic ligands
- Determine the metal electron count and use that to predict reactivity of the metal complex
- Recognize the different classes of reactions important to organometallic catalysis

Section 10.1: The 18 Electron Rule
Section 10.2: Organometallic Ligands
Section 10.3: Characterization of Organometallic Complexes

This page titled Chapter 10: Organometallic Chemistry is shared under a CC BY-NC-SA 4.0 license and was authored, remixed, and/or curated by Michael Evans.

SECTION OVERVIEW

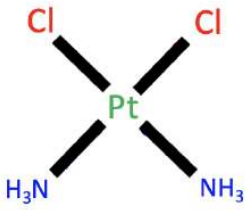
Section 10.1: The 18 Electron Rule

Electron Counting In Transition Metal Complexes

In this chapter we will learn how to count valence electrons in coordination compounds. Electron counting is important because the number of electrons in a complex can tell us a lot about the stability and reactivity in a coordination compound. In addition, it allows us to predict and understand structures to a certain extent. Electron counting sounds trivial, but it is not as trivial as it seems, actually there are even two different methods for electron counting. Each method leads to the same result. Which method you prefer is “personal taste”, but each method is about equally common in the literature, so you need to know both of them.

The Neutral Atom Method

The first method is called the “neutral atom method”. As the name suggests, we will break up the complex into neutral fragments, and count the electrons that contribute to the bonding in each of the fragments. The neutral atom method is carried out according to the following three steps. First, we count the number of the valence electron of the metal. We consider the metal as neutral atom. The number valence electrons is the same as the group number of the transition metal in the periodic table. For transition metals the group number varies from 3 to 12. In the second step, we account for the ionic charge of the complex, if the complex is not neutral. This will reduce the number of electrons for a complex cation, and increase the number of valence electrons for a complex anion. In the third step, we need to determine how many electrons are contributed by each ligand. This is the most complicated step. To determine the number of electrons must cleave each metal-ligand bond so that a ligand fragment results that is neutral. We then count the number of electrons at the ligand that contributed to the bond. The number of electrons contributed by each ligand is then summed up. This is sum is then added to the number of electrons determined by the previous steps. This is gives the overall number of valence electrons.



	Number of e's
Pt	10
charge	0
2 Cl	2 · 1 = 2
2 N	2 · 2 = 4
Total	= 16

Figure 6.1.1 Example of neutral atom method

Let us apply these rules by an example, the cis-platinum complex. We first need to count the number of electrons of the metal. The metal is platinum which is located in group 10 of the periodic table. Therefore, a neutral platinum atom has ten valence electrons.

Next, we look at the charge of the complex. In this case, there is no charge, and therefore no electrons are added or subtracted.

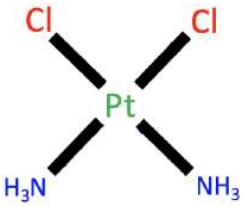
Lastly, we count the electrons of the ligands. There are two types of ligands, the chloro-ligands and the ammine ligands. Now, our task is to cleave the Pt-ligand bond so that neutral ligand fragments result. We can see that for the chloro-ligands we must cleave the Pt-Cl bond, homoleptically, meaning in the middle, assigning one electron to the Pt and one electron to Cl, because doing so creates a neutral chlorine atom. The fact that we cleaved the bond homoleptically, means that the chloro ligand contributed one electron. Because we have two chloro ligands, there are overall two electrons.

Now, let us think about how many electrons the ammine ligands contribute. In this case we need to cleave the metal-ligand bond heteroleptically to produce a neutral ligand fragment. Both bonding electrons are assigned to the ligand. This produces a neutral NH3 molecule. This means that each ammine ligand contributes two electrons. Overall, that makes four electrons, because we have two ammine ligands.

Finally, we need to sum up the electrons from all three steps. That is ten electrons from Pt, zero electrons due to charge, two electrons from the chloro ligands, and four electrons from the ammine ligands equaling 16 valence electrons total. This is the final result.

"Oxidation State" Method

The oxidation state method is also comprised of three steps. The first step is the same as in the neutral atom method. We determine the number of electrons of the neutral metal which the same as its group number in the periodic table. The next step is different though. It requires the determination of the oxidation state of the metal. How can we determine it? First, we cleave the metal-ligand bonds heteroleptically so that all bonding electrons are assigned to the ligands. Then we determine what is the charge of the ligands? Ligands can either be neutral of negatively charged. We determine the overall number of charges at the ligands. The difference between that number and the charge of the complex is the oxidation state of the metal. We either add or subtract electrons depending on the oxidation state of the metal. If the oxidation state is positive we subtract electrons, if it is negative, which is rare, then we add electrons. The third step counts the number of the electrons contributed by the ligands. Because we cleaved all bonds homoleptically, all bonding electrons are considered to be contributed by the ligands, and we count them accordingly. Finally, we sum up the electrons of all three steps which gives the total number of electrons.



	Number of electrons
Pd	10
Oxid. state	-(+2)
2 Cl^-	$+2 \cdot 2 = 4$
2 N	$+2 \cdot 2 = 4$
Total	**= 16**

Figure 6.1.2 Example of oxidation state method

Let us apply the method to the previous example cis-platinum. Applying the first step gives us 10 valence electrons for the platinum.

Next, we need to determine the oxidation state of Pt. To do so, we must now cleave all metal-ligands heteroleptically, so that all bonding electrons are assigned to the ligand. By the way, this is equivalent to saying that we treat all the bonds as dative bonds with all electrons coming from the ligands as the donors. When we do this for the chloro ligands we see that this created chloride anions with a 1- charge. Cleaving the Pt-N bonds heteroleptically leads to neutral NH_3 molecules. Therefore the overall number of charges at the ligands is 2x(-1)+2x0=-2. The charge at the complex is zero, therefore the oxidation state of Pt is 0-(-2)=+2. We must therefore subtract two electrons from the 10 electrons of the platinum.

Now we must determine the number electrons coming from the ligands. Because all bonds are considered as dative bonds, the chloro ligands contribute two electrons each, and the ammine ligands contribute two electrons each. That makes overall four electrons.

In sum, 10 electrons from the neutral Pt atom minus two electrons due to the +2 oxidation state of Pt plus 2x2=4 electrons from Cl plus 2x2=4 electrons from NH_3 gives 16 electrons total. We can see that we have arrived at the same results as in the case of the oxidation state method.

We can discuss the advantages and disadvantages of both methods, also. They neutral atom method has the advantage that we do not have to think about charges at ligands and oxidation states. However, we have to think about how to cleave bonds to create neutral fragments. We may need ot cleave bonds in an way that is not reflecting the donor-acceptor nature of a coordination compound. The oxidation method does account for the donor-acceptor nature of a coordination compound because the bonds are considered dative bonds, and the electrons are assigned to the ligands and metal accordingly. We not not need to think how to cleave bonds, because we cleave the bonds always heteroleptically. However, it requires us to think about charges at the ligands to determine oxidation states which is an additional, non-trivial step.

Counting Electrons: Ligand Contributions

The most difficult step in electron counting is mostly the determination of the number of electrons a ligand provides. Therefore, let us practice this by a few example.

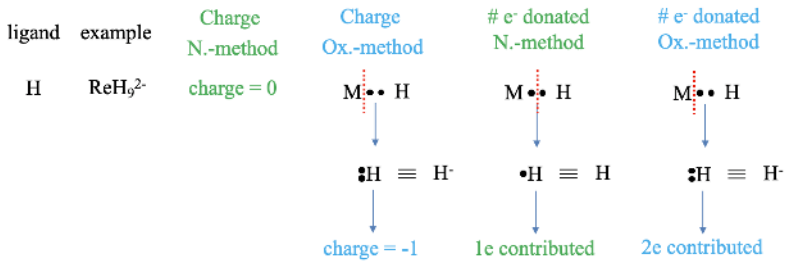


Figure 6.1.3 Example of counting electrons with a hydrido ligand

Let us first look at an hydrido ligand which for example occurs in the nonohydridorhentate(2-) complex. What is the charge of the ligand in the two methods? In the neutral atom method the charge is always zero, this is a no-brainer. In the case of the oxidation statement method, we need to treat the bond as a dative bond, and that means that we must cleave the bond heteroleptically, so that both bonding electrons can be assigned to the ligand. An H atom with two electrons is a hydride anion with a -1 charge. Next, let us think about the number of electrons donated. In the neutral atom method we need to produce neutral ligand fragments. To do so we must cleave the M-H bond homoleptically, because this will create a neutral hydrogen atom. How many electron will it contribute. It will contribute one electron, because we cleaved the bond homoleptically assigning only one of the two bonding electrons to H. In the oxidation state method, the hydrido ligand contributes two electrons because the bond was considered dative and therefore cleaved heteroleptically. Both bonding electrons were assigned to the ligand, therefore the ligand contributes two electrons.

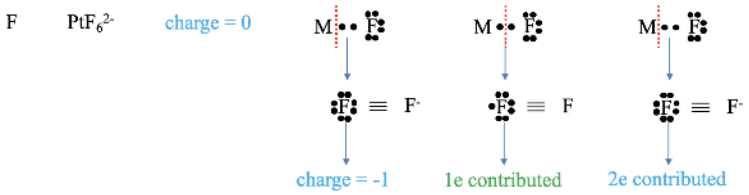


Figure 6.1.4 Example of counting electrons with a halogenide ligand

Next, let us consider a halogenide ligand. What is the charge at the ligand. For the neutral atom method, the answer is trivial, the charge is always zero. In the oxidation state method both bonding electrons in the M-L bond get assigned to the ligand. This gives the ligand a -1 charge. What is the number of electrons contributed? In the neutral atom method we need to think again how to cleave the M-L bond to create a neutral ligand fragment. We need to see that we must cleave the bond homoleptically to produce that fragment. Cleaving the bond homolopetically means that that ligand has contributed one electron. In the oxidation state method, we cleave the bond always heteroleptically so that all bonding electrons are assigned to the ligand. Thus, the ligand contributes two electrons.

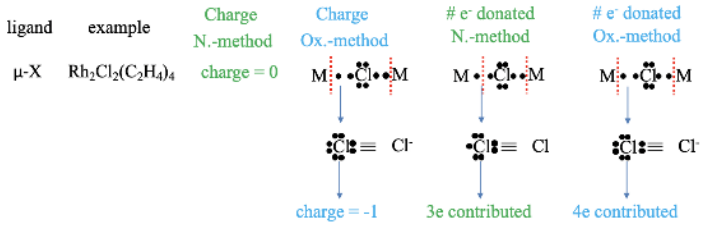


Figure 6.1.5 Example of counting electrons with a bridging halogenide ligand

A halogenide anion as a ligand cannot only be terminal, but bridging. An example is the μ-dichloro bis(tetraethylene rhodium(I)) complex in which two chloro-ligands bridge two rhodium atoms. What is the charge in the neutral atom method. Of course, it is zero. What is the charge in the oxidation state method? We can see that if we consider both metal-ligand bonds dative bonds, and cleave the bonds heteroleptically, that the Cl atom is surrounded by eight unshared electrons, which give it a -1 charge. How, many electrons are contributed in the neutral atom method? To answer this question, we need to decide if we have to cleave the bonds homo- or heteroleptically to produce a neutral Cl atom. Can you see it? The answer is: We must cleave one bond homoleptically, and the other one heteroleptically. How many electrons are then contributed by the chloro ligan? It is the two electrons from the heteroleptically cleaved bond, and one electron from the homoleptically cleaved bond. So overall it is three electrons. What about

the oxidation state method? In this case both bonds very cleaved heteroleptically, and this means that overall four electrons have been contributed.

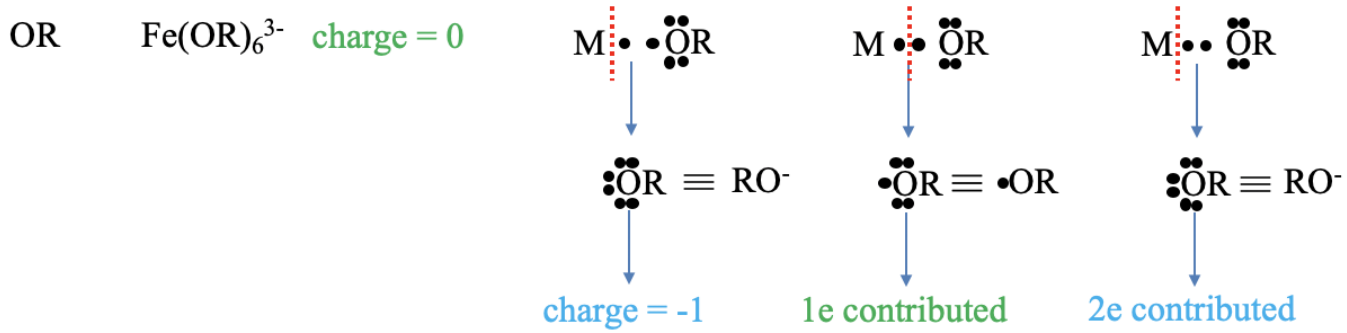


Figure 6.1.6 Example of counting electrons with an OR ligand

What are the charges and electrons contributed by an alkoxy ligand? An example for a complex with such as ligand is pentaphenoxy ferrate (3-). The charge according to the neutral atom method is zero. In the oxidation state method we cleave the bonds heteroleptically, and our ligand becomes an alkoxide anion. This anion has a 1- charge. How many electrons does the ligand contribute? To get a neutral fragment we must cleave the bond homoleptically. This actually produces an alkoxy radical. This radical contributes its radical electron, thus there is one contributed electron. In the oxidation state method we treated the bond as a dative bond and cleaved the bond heteroleptically. Therefore two electrons are contributed according to the oxidation state method.

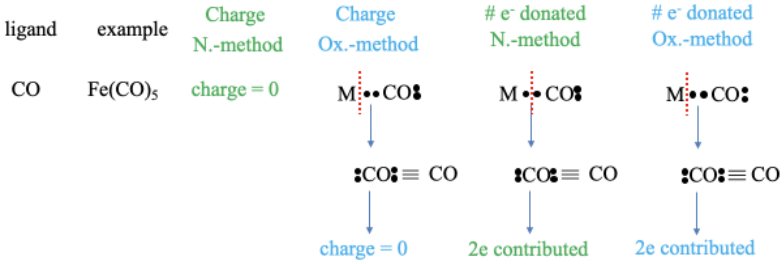


Figure 6.1.7 Example of counting electrons with a carbonyl ligand

Next, let us apply electron counting to the carbonyl ligand. For example four carbon monoxide molecules form an iron pentacarbonyl complex with iron. The charge at the ligand in the neutral atom method is zero. In the oxidation state method, we assign both bonding electrons to the ligand, and that produces a neutral carbon monoxide molecule. Note that the carbon atom is formally negatively charged, because it is surrounded by 5 electrons, but the oxygen atom is positively charged because it is surrounded by five electrons. So overall, the molecule is neutral. What is the number of electrons contributed in the neutral atom method? To produce a neutral ligand we must cleave the bond heteroleptically. This produces a neutral carbon monoxide molecule. Because we cleaved the bond heteroleptically, the ligand contributes two electrons. In the oxidation state method we always cleave the bonds heteroleptically, and thus two electrons come from the ligand.

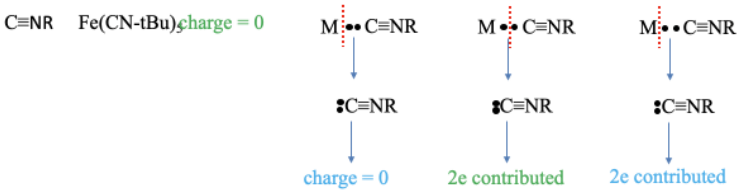


Figure 6.1.8 Example of counting electrons with

The last ligand we discuss here is the isonitrile ligand. An example is the pentakis-(tert-butyl isonitrile) iron molecule. The charge of the ligand is zero in the neutral atom method, but what is it in the oxidation state method? Let us see what happens as we assign both bonding electrons to the ligand. We we see that the carbon is now surrounded by five electrons. Three are in the carbon-nitrogen triple bond and they other two come from the electron lone pair at the carbon atom. This means that the carbon atom has a -1 charge. Now, let us look at the N atom. We see that it is surrounded by four electrons, three coming from the C-N triple bond, and one from the C-R bond. That means that the N atom has a +1 charge. Overall, the molecule is neutral and does not carry a

charge. What about the number of electrons contributed? We can see that we must cleave the bond heteroleptically to produce a neutral isoitrile, there are two electrons are contributed in the neutral atom method. The oxidation state method must cleave the bond heteroleptically, therefore, the number of electrons is also two.

18 Electron Rule

Electron counting is important in the context of an important rule in coordination chemistry: The 18 electron rule. The 18 electron rule states that for d-block elements *normally* complexes with 18 electrons in the shell ($ns^2(n-1)d^{10}np^6$ configuration) are most stable. If this number is not reached, the species is **coordinatively unsaturated** and tend to add more ligands. It also tends to be reduced because adding electrons brings the complex to or at least closer to 18 electrons. Coordinatively unsaturated complexes therefore tend to have a higher reactivity.

Definition: Coordinatively Unsaturated

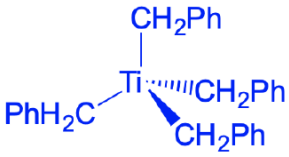
A species is coordinatively unsaturated when the 18 electrons are not reached in the ($ns^2(n-1)d^{10}np^6$ configuration) shell. They tend to add more ligands, and to be reduced. They are associated with higher reactivity.

If a species has more than 18 electrons it is coordinatively oversaturated and tends to lose ligands. It is usually easily oxidized. Both loss of ligands and oxidation reduces to the number of electrons to or at least closer to 18.

Definition: Coordinatively Oversaturated

A species is coordinatively oversaturated when it has more than 18 electrons in the shell ($ns^2(n-1)d^{10}np^6$ configuration) shell. They tend to lose ligands and are easily oxidized.

The 18 electron rule has many exceptions, and therefore needs to be applied with caution. In particular group 3, 4, and 10 complexes deviate often from the 18 electron rule.



Contribution metal:	4e
Oxidation state: +4	-4e
Electrons contributed by ligands:	4x2e=8e
Sum:	**8e**

Figure 6.1.9 Example of counting electrons in the tetrahedral tetrabenzyltitanium(0) complex

For illustration purposes, let count the number of electrons of the tetrahedral tetrabenzyltitanium(0) complex by the oxidation state method. We could also use the neutral atom method, which would give the same results. This complex is a group 4 complex because titanium is in group 4. How many electrons will the titanium contribute? Because number of electrons is always the same as the group number, it will contribute four electrons. Next, what is oxidation state of Ti? To determine it we must determine the charge at the ligands. To do that we cleave the bonds heteroleptically. This will give benzylate anions with -1 charge. There are four of these ions, and therefore there will be four negative charges overall. The complex is charge-neutral, and thus the oxidation state is +4 because -4+4=0. Therefore, we need to subtract four electrons. Because we cleaved the bond heteroleptically, each ligand contributed two electrons, giving overall eight electrons coming from the four ligands. This means that we have overall eight electrons, or an 8-electron complex. This is far, far away from 18 electrons. Nonetheless, the complex is quite stable, does not have a tendency to get reduced, or to add ligands. How can we explain this. The answer is that in order to achieve 18 electrons it would need to add five additional ligands if each ligand is considered a 2-electron donor. This would increase the coordination number to 9 which is too high to produce a stable complex. In order to reduce the complex to an 18 electron complex, 10 electrons would need to be added. This would produce a complex with a -10 charge which is way to high to be stable. The arguments are

generalizable for group 3 and group 4 complexes. Because these elements only have a few d electrons, the ligands would contribute a lot of electrons to produce an 18 electrons complex. This would require just too many ligands to add. The coordination numbers would get too high. If electrons are added instead to ligands, the negative charge at the complex would be to high to be stable based on electron-electron repulsion arguments.



Contribution metal:	10e
Charge:	0e
Electrons contributed by Cl ligands:	2x1e=2e
Electrons contributed by NH_3 ligands:	2x2e=4e
Sum:	**16e**

Figure 6.1.10 Example of counting electrons in the dichlorodiammine palladium complex

These arguments cannot be applied for group 10 elements, because these elements have many d electrons. The explanation in this case is that these elements like to make square planar complexes when in the common oxidation state +2. Square planar complexes prefer 16 instead of electrons. You can see that the square planar dichlorodiammine palladium complex shown is square planar and has sixteen electrons. There are 10 electrons coming from Pd. If we use the neutral atom method, no electrons need to be added or subtracted due to the charge at complex. The complex is charge-neutral. To assess how many electrons come from the ligands we need to cleave the bonds so that neutral ligands are produced. The Pd-Cl bonds need to be cleave homoleptically, the Pd-N bonds need to be cleave heteroleptically. Therefore, the two chloro ligands are 1e donors, and the two ammine ligands are 2e donors. This gives 10+4+2=16 electrons

---

This page titled Section 10.1: The 18 Electron Rule is shared under a CC BY-NC-SA 4.0 license and was authored, remixed, and/or curated by Kai Landskron.

Section 10.2: Organometallic Ligands

There are some classes of ligands and modes of bonding that are important and in some cases unique to organometallic complexes and reactions. Before discussing reactions of organometallic complexes we will start with an overview of ligands common to organometallic complexes. In organometallic reactions, ligands can be either spectators, not chemically involved or changed during the reaction, or actors, chemically changed during the reaction. Similar to enzymes, a substrate will often bond to an organometallic catalyst as a ligands undergo a chemical transformation, and leave as a product.

Carbon Monoxide

Carbon monoxide is a neutral strong field ligand that we have discussed previously. We've seen that there are two bonding interactions at play in the metal carbonyl bond: a ligand-to-metal $n \rightarrow d_\sigma$ interaction (σ donation) and a metal-to-ligand $d_\pi \rightarrow \pi^*$ interaction (π accepting). The latter interaction is called backbonding because the metal donates electron density back to the ligand.

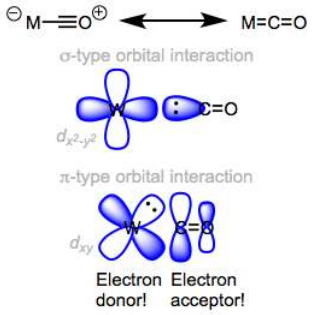


Figure ***NaN.2.1***: Orbital interactions in M=C=O. (Copyright; Michael Evans)

CO is a fair σ-donor (or σ-base) and a good π-acceptor (or π-acid). The properties of ligated CO depend profoundly upon the identity of the metal center. More specifically, the electronic properties of the metal center dictate the importance of backbonding in metal carbonyl complexes. Most bluntly, *more electron-rich metal centers are better at backbonding to CO.* Why is it important to ascertain the strength of backbonding?

Backbonding and CO vibrational frequency

Infrared spectroscopy has famously been used to empirically support the idea of backbonding. The table below arranges some metal carbonyl complexes in "periodic" order and provides the frequency corresponding to the C=O stretching mode. Notice that without exception, every complexed CO has a stretching frequency lower than that of free CO. Backbonding is to blame! When a metal donates electrons into a π* antibonding MO on CO, the C-O bond order is lowered and the bond strength is weakened. According to Hooke's law, assuming all other things are equal, when the force constant (bond strength) decreases the vibrational frequency also decreases. Complexes with the strongest metal-CO backbonding will have the lowest frequency CO bond vibration(s).

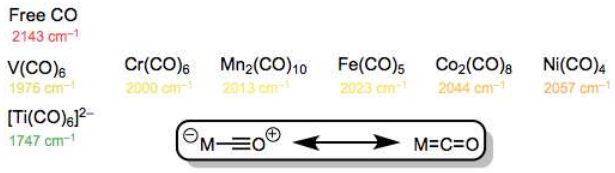


Figure ***NaN.2.2***: CO stretching frequencies in metal-carbonyl complexes. (Copyright; Michael Evans)

The figure above depicts a clear increase in frequency (an increase in C–O bond order) as we move left to right across the periodic table. This finding may seem odd if we consider that the number of *d* electrons in the neutral metal increases as we move left to right. Shouldn't metal centers with more *d* electrons be better at backbonding (and more "electron rich")? What's going on here? Recall the periodic trend in *orbital energy*. As we move left to right, the *d* orbital energies decrease and the energies of the d_π and π* orbitals separate. As a result, the backbonding orbital interaction becomes worse (remember that strong orbital interactions require well-matched orbital energies) as we move toward the more electronegative late transition metals. We can draw an analogy

to enamines and enols from organic chemistry. The more electronegative oxygen atom in the enol is a worse electron donor than the enamine's nitrogen atom.

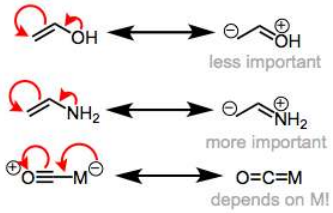


Figure ***NaN*.2.3**: The importance of backbonding depends on the electronegativity of the metal and its electron density. (Copyright; Michael Evans)

Of course, the contribution of other ligands on the metal center to backbonding cannot be forgotten, either. Logically, electron-donating ligands will tend to make the backbond stronger (they make the metal a better electron donor), while electron-withdrawing ligands will worsen backbonding. Adding electron-rich phosphine ligands to a metal center, for instance, *decreases* the CO stretching frequency due to *improved* backbonding.

CO as a bridging ligand

Carbonyl ligands are famously able to bridge multiple metal centers. Bonding in bridged carbonyl complexes may be either "traditional" or delocalized, depending on the structure of the complex and the bridging mode. The variety of bridging modes stems from the different electron donors and acceptors present on the CO ligand (and the possibility of delocalized bonding). Known bridging modes are shown in the figure below.

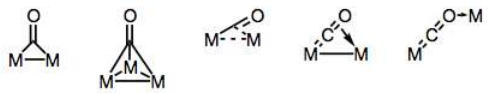
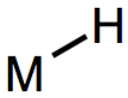


Figure ***NaN*.2.4**: Building bridges with carbonyl ligands. (Copyright; Michael Evans)

Metal Hydrides

Metal hydrides occupy an important place in transition metal organometallic chemistry as the M−H bonds can undergo insertion reactions with a variety of unsaturated organic substrates yielding numerous organometallic compounds with M−C bonds. Not only the metal hydrides are needed as synthetic reagents for preparing the transition metal organometallic compounds but they also are required for important hydride insertion steps in many catalytic processes. The first transition metal hydride compound was reported by W. Heiber in 1931 when he synthesized $Fe(CO)_4H_2$. Though he claimed that the $Fe(CO)_4H_2$ contained Fe−H bond, it was not accepted until 1950s, when the concept of normal covalent M−H bond was widely recognized.



Spectroscopic identification

The metal hydride moieties are easily detectable in ^{1}H NMR as they appear upfield of TMS in the region between 0 to -60 ppm, where no other H resonances appear. The hydride moieties usually couple with metal centers possessing nuclear spins. Similarly, the hydride moieties also couple with the adjacent metal bound phosphine ligands, if present in the complex, exhibiting characteristic *cis* (J = 15 − 30 Hz) and *trans* (J = 90 − 150 Hz) coupling constants. In the IR spectroscopy, the M−H frequencies appear between (1500 − 2200) cm^{-1} but their intensities are mostly weak. Crystallographic detection of metal hydride moiety is difficult as hydrogen atoms in general are poor scatterer of X−rays. Located adjacent to a metal atom in a M−H bond, the detection of hydrogen atom thus becomes challenging and as a consequence the X−ray crystallographic method systematically underestimates the M−H internuclear distance by ~ 0.1 Å. However, better data could be obtained by performing the X−ray diffraction studies at a low temperature in which the thermal motion of the atoms are significantly reduced. In light of these facts, the neutron diffraction becomes a powerful method for detection of the metal hydride moieties as hydrogen scatters neutrons more

effectively and hence the M−H bond distances can be measured more accurately. A limitation of neutron diffraction method is that large sized crystals are required for the study.

Bridging hydrides

Bridging hydrides are an intriguing class of ligands. A question to ponder: how can a ligand associated with only two electrons possibly bridge two metal centers? How can two electrons hold three atoms together? Enter the magic of three-center, two-electron bonding. We can envision the M–H sigma bond as an electron donor itself! With this in mind, we can imagine that hydrides are able to bind end-on to one metal and side-on to another. Consistent with the idea that bridging is the result of “end-on + side-on” bonding, bond angles of bridging hydrides are never 180°.

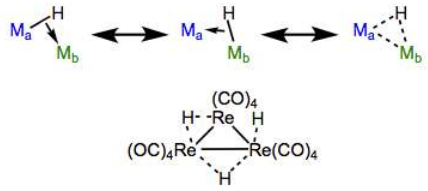
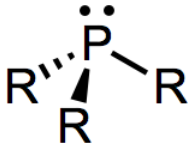


Figure ***NaN*.2.5**: Resonance forms of bridging hydrides, with an example. Sigma complexes like these show up in other contexts

Phosphines

Phosphines are most notable for their remarkable electronic and steric tunability and their “innocence”—they tend to avoid participating directly in reactions, but have the ability to profoundly modulate the electronic properties of the metal center to which they’re bound. Furthermore, because the energy barrier to inversion is quite high, “chiral-at-phosphorus” ligands can be isolated in enantioenriched form and introduced to metal centers, bringing asymmetry just about as close to the metal as it can get in chiral complexes. The one stable isotope of P (^{31}P) is NMR active so ^{31}P NMR is often used to cahrecterize complexes and reactions involving phosphine ligands . Soft phosphines match up very well with the soft low-valent transition metals. Electron-poor phosphines are even good π-acids.



Bonding

Like CO, phosphines are neutral σ donors and π acceptors that formally contribute two electrons to the metal center. Unlike CO, most phosphines are not small enough for more than four to bond to a single metal center (and for large R, the number is even smaller). Steric hindrance becomes a problem when five or more PR_3 ligands try to make their way into the space around the metal. Bridging by phosphines is extremely rare, but ligands containing multiple phosphine donors such as diphenylphosphinoethane metal center are common. For entropic reasons, chelating ligands like these bind to a single metal center at multiple points if possible, instead of attaching to two different metal centers (the aptly named chelate effect). An important characteristic of chelating phosphines is bite angle, defined as the predominant P–M–P angle in known complexes of the ligand. When the preferred bite angle of the ligand doesn't match the ideal bond angles of the geometry (i.e. 90° for octahedral) that introduces strain, and potentially reactivity into the complex.

The predominant orbital interaction contributing to phosphine binding is the one we expect, a lone pair on phosphorus donating to an empty metal d orbital. The electronic nature of the R groups influences the electron-donating ability of the phosphorus atom. For instance, alkylphosphines, which possess P–Csp^3 bonds, tend to be better electron donors than arylphosphines, which possess P–Csp^2 bonds. The rationale here is the greater electronegativity of the sp^2 hybrid orbital versus the sp3 hybrid, which causes the phosphorus atom to hold more tightly to its lone pair when bound to an sp^2 carbon. The same idea applies when electron-withdrawing and -donating groups are incorporated into R: the electron density on P is low when R contains electron-withdrawing groups and high when R contains electron-donating groups.

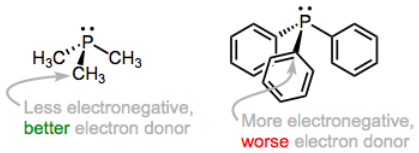
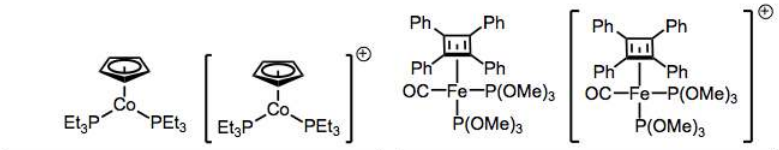


Figure ***NaN*.2.6**: As we add electronegative R groups, the phosphorus atom (and the metal to which it's bound) become more electron poor.

Like CO, phosphines participate in backbonding to a certain degree; however, the phenomenon here is of a fundamentally different nature than CO backbonding. For one thing, phosphines lack a π* orbital. In the days of yore, chemists attributed backbonding in phosphine complexes to an interaction between a metallic dπ orbital and an empty 3d orbital on phosphorus. However, this idea has elegantly been proven bogus, and a much more organic-friendly explanation has taken its place (no d orbitals on P required). In an illuminating series of experiments, M–P and P–R bond lengths were measured via crystallography for several redox pairs of complexes.



M–P	2.218 Å	2.230 Å	**M–P**	2.146 Å	2.261 Å
P–R	1.846 Å	1.829 Å	**P–R**	1.598 Å	1.578 Å

Figure ***NaN*.2.7**: Upon oxidation, M–P bond lengths increase and and P–R bond lengths decrease.

Oxidation decreases the ability of the metal to backbond, because it removes electron density from the metal. This explains the increases in M–P bond length—just imagine a decrease the M–P bond order due to decreased backbonding. And the decrease in P–R bond length? It's important to see that invoking only the phosphorus 3d orbitals would not explain changes in the P–R bond lengths, as the 3d atomic orbitals are most definitely localized on phosphorus. Instead, we must invoke the participation of σ*P–R orbitals in phosphine backbonding to account for the P–R length decreases. The figure below depicts one of the interactions involved in M–P backbonding, a dπ → σ* interaction (an orthogonal dπ → σ* interaction also plays a role). As with CO, a resonance structure depicting an M=P double bond is a useful heuristic! Naturally, R groups that are better able to stabilize negative charge—that is, electron-withdrawing groups—facilitate backbonding in phosphines. Electron-rich metals help too.

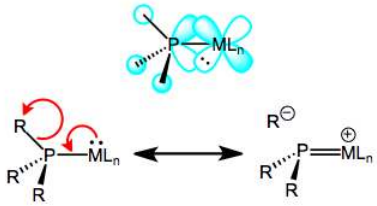


Figure ***NaN*.2.8**: Backbonding in phosphines, a sigma-bond-breaking affair.

Cone Angle

The steric and electronic properties of phosphines vary enormously. Tolman devised some intriguing parameters that characterize the steric and electronic properties of this class of ligands. To address sterics, he developed the idea of cone angle—the apex angle of a cone formed by a point 2.28 Å from the phosphorus atom (an idealized M–P bond length), and the outermost edges of atoms in the R groups, when the R groups are folded back as much as possible. Wider cone angles, Tolman reasoned, indicate greater steric congestion around the phosphorus atom. To address electronics, Tolman used the CO stretching frequency (νCO) of mixed phosphine-carbonyl complexes. Specifically, he used Ni(CO)3L complexes, where L is a tertiary phosphine, as his standard.

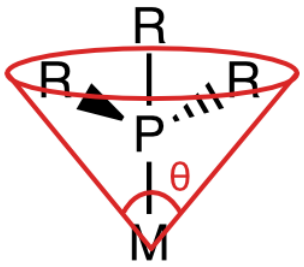
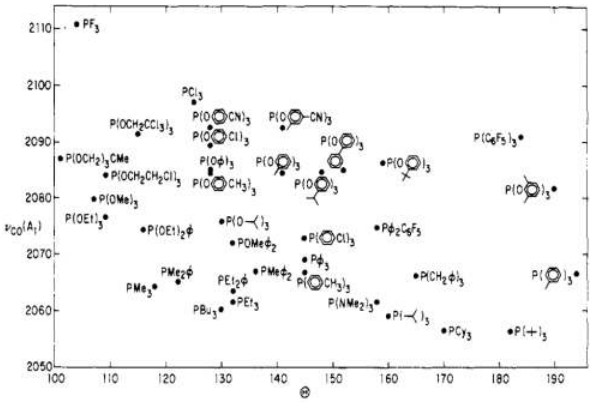


Figure ***NaN*.2.9** : Illustration of the cone angle in phosphines. (CC BY-NC-SA; Catherine McCusker)

Tolman's logic went as follows: more strongly electron-donating phosphines are associated with more electron-rich metals, which are better at CO backbonding (due fundamentally to higher orbital energies). Better CO backbonding corresponds to a lower νCO due to decreased C–O bond order. Thus, better donor ligands should be associated with lower νCO values (and vice versa for electron-withdrawing ligands). Was he correct? Exhibit A…



Tolman's map of the steric and electronic properties of phosphine ligands.

Notice the trifluorophosphine stuck in the "very small, very withdrawing" corner, and its utter opposite, the gargantuan tri(tert-butyl)phosphine in the "extremely bulky, very donating" corner.

σ Complexes

General Properties

Previously our discussion of metal-ligand σ bonding was limited to ligand lone pairs acting as donors. Ligands can also use a filled σ bonding molecular orbital to donate to a metal as shown in Figure ***NaN*.2.10**. This binding mode results in side-on η^2 bonding. If the backbonding interaction is too strong the single L-L ligands can become two L^- ligands by breaking the L-L sigma bond.

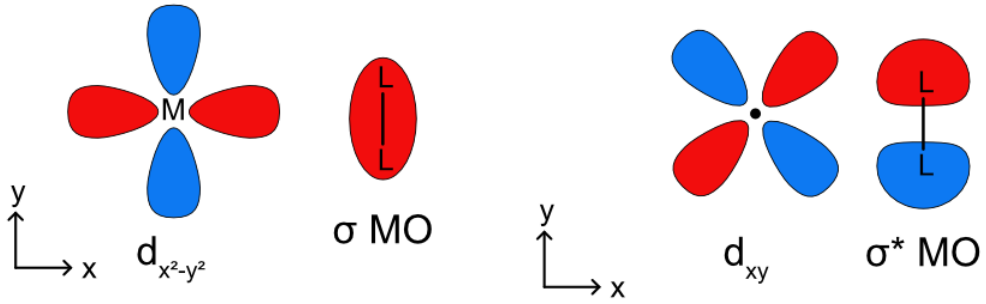


Figure ***NaN*.2.10**: Sigma bonding (left) and pi backbonding (right) orbital interaction in metal σ complexes (CC BY-NC-SA; Catherine McCusker)

The first thing to realize about σ complexes is that they are highly sensitive to steric bulk. Any old σ bond won't do; hydrogen at one end of the binding bond or the other (or both) is necessary. The best studied σ complexes involve dihydrogen (H2), so let's start there.

Dihydrogen complexes

Mildly backbonding metals may bind dihydrogen "side on." Like side-on binding in π complexes, there are two important orbital interactions at play here: σH–H → dσ and dπ → σ*H–H. Dihydrogen complexes can "tautomerize" to $(H)_2$ isomers through oxidative addition of the H–H bond to the metal. We should expect more electron-rich metal centers to favor the X2 isomer, since these should donate more strongly into the σ*H–H orbital. This idea was masterfully demonstrated in a study by Morris, in which he showed that H_2 complexes of π-basic metal centers show all the signs of dihydride complexes, rather than hydrogen complexes. More generally, metal centers in σ complexes need a good balance of π basicity and σ acidity (I like to call this the "Goldilocks effect"). Because of the need for balance, σ complexes are most common for centrally located metals (groups 6-9).

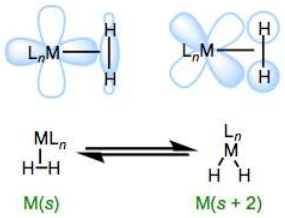


Figure ***NaN*.2.11**: Orbital interactions and L-X_2 equilibrium in σ complexes.

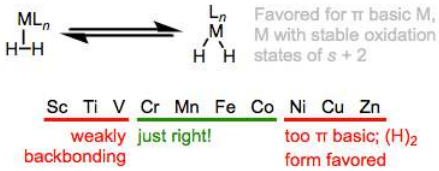
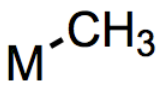


Figure ***NaN*.2.12**: Oxidative addition of H_2 is important for electron-rich, π-basic metal centers. Groups 6-9 hit the "Goldilocks" spot.

Metal Alkyls

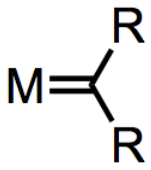


Alkyl or aryl transition metal compounds have M-C single bonds. In spite of many attempts over most of the course of chemical history, their isolation was unsuccessful and it was long considered that all M-C bonds were essentially unstable. Stable alkyl complexes began to be prepared gradually only from the 1950s. $Cp_2ZrCl(Pr)$,WMe_6, $CpFeMe(CO)_2$, $CoMe(py)(dmg)_2$, (dmg = dimethylglyoximato), $IrCl(X)(Et)(CO)(PPh_3)_2$, $NiEt_2(bipy)$, $PtCl(Et)(PEt_3)_2$ are some representative compounds. Among various synthetic processes so far developed, the reactions of compounds containing M-halogen bonds with main-group metal-alkyl compounds, such as a Grignard reagent or an organolithium compound, are common synthetic routes. Especially vitamin B_{12}, of which Dorothy Hodgkin (1964 Nobel Prize) determined the structure, is known to have a very stable Co-C bond. Metal alkyl compounds which have only alkyl ligand, such as WMe_6, are called homoleptic alkyls.

It is gradually accepted that a major cause of the instability of alkyl complexes is the low activation energy of their decomposition rather than a low M-C bond energy. The most general decomposition path is β elimination. Namely, the bonding interaction of a hydrocarbon ligand with the central transition metal tends to result in the formation of a metal hydride and an olefin. Such an interaction is called an **agostic interaction**. Although an alkyl and an aryl ligand are 1-electron ligands, they are regarded as anions when the oxidation number of the metal is counted. The hydride ligand, H, resembles the alkyl ligand in this aspect.

Carbenes

In this section we'll investigate two classes of carbenes, which are characterized by a metal-carbon double bond. Fischer carbenes and Shrock carbenes are usually actor ligands, but they may be either nucleophilic or electrophilic, depending on the nature of the R groups and metal. In addition, these ligands present some interesting synthetic problems: because free carbenes are quite unstable, ligand substitution reactons can't be used for metal carbene synthesis.



Fisher vs Schrock carbenes

Metal carbenes all possess a metal-carbon double bond. What's interesting for us about this double bond is that there are multiple ways to deconstruct it to determine the metal's oxidation state and number of d electrons. We could give one pair of electrons to the metal center and one to the ligand. This procedure nicely illustrates why compounds containing M=C bonds are called "metal carbenoids"—the deconstructed ligand is a neutral carbenoid. Alternatively, we could give both pairs of electrons to the ligand and think of it as a dianionic ligand. The appropriate procedure depends on the ligand's substituents and the electronic nature of the metal. The figure below summarizes the two deconstruction procedures.

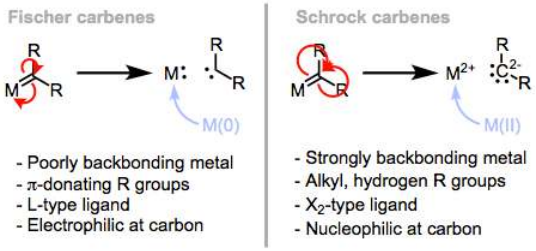


Figure ***NaN*.2.13**: The proper method of deconstruction depends on the electronic nature of the ligand and metal.

When the metal possesses π-acidic ligands and the R groups are π-basic, the complex is best described as an L-type Fischer carbene and the oxidation state of the metal is unaffected by the carbene ligand. When the ligands are "neutral" (R = H, alkyl) and the metal is a good backbonder—that is, in the absence of π-acidic ligands and electronegative late metals—the complex is best described as an anionic X_2-type Schrock carbene. Notice that the oxidation state of the metal depends on our deconstruction method. In organometallic complexes it isn't uncommon for the oxidation state of the metal and ligand to be ambiguous.

Deconstruction reveals the typical behavior of the methylene carbon in each class of complex. The methylene carbon of Schrock carbenes, on which electron density is piled through backbonding, is nucleophilic. On the other hand, the methylene carbon of Fischer carbons is electrophilic, because backbonding is weak and does not compensate for σ-donation from the ligand to the metal. To spot a Fischer carbene, be on the lookout for reasonable zwitterionic resonance structures like the one at right below.

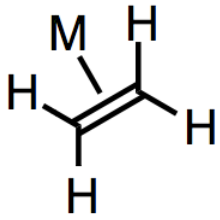


Thanks to the pi-accepting CO ligands, the metal handles the negative charge well. This is a Fischer carbene.

The clever reader may notice that we haven't mentioned π-acidic R groups, such as carbonyls. Complexes of this type are best described as Fischer carbenes as well, as the ligand is still electrophilic. However, complexes of this type are difficult to handle and crazy reactive (see below) without a π-basic substituent to hold them in check. Take care when diagnosing the behavior of metal carbenes. In these complexes, there is often a subtle interplay between the R groups on the carbene and other ligands on the metal. In practice, many carbenes are intermediate between the Fischer and Schrock ideals.

π Systems

In contrast to neutral spectator ligands, π systems most often play an important role in the reactivity of the organometallic complexes of which they are a part (since they act in reactions, they're called "actors"). π systems do useful chemistry, not just with the metal center, but also with other ligands and external reagents. Thus, in addition to thinking about how π systems affect the steric and electronic properties of the metal center, we need to start considering the metal's effect on the ligand and how we might expect the ligand to behave as an active participant in reactions. To the extent that structure determines reactivity—a commonly repeated, and extremely powerful maxim in organic chemistry—we can think about possibilities for chemical change without knowing the elementary steps of organometallic chemistry in detail yet.



General Properties

Similar to σ complexes, the π bonding orbitals of alkenes, alkynes, carbonyls, and other unsaturated compounds may overlap with dσ orbitals on metal centers. This is the classic ligand HOMO → metal LUMO interaction that we've seen many times. Because of this electron donation from the π system to the metal center, coordinated π systems often act electrophilic, even if the starting alkene was nucleophilic. The π → dσ orbital interaction is central to the structure and reactivity of π-system complexes. π systems are also often subject to important backbonding interactions. We'll focus on alkenes here, but these same ideas apply to carbonyls, alkynes, and other unsaturated ligands bound through their π clouds. For alkene ligands, the relative importance of "normal" bonding and backbonding is nicely captured by the relative importance of the two resonance structures in Figure ***NaN*.2.14**.

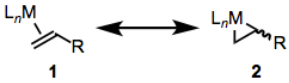


Figure ***NaN*.2.14**: Resonance forms of alkene ligands. In 1 backbonding is weak and in 2 the backbonding is strong.

Complexes of weakly backbonding metals, such as the electronegative late metals, are best represented by the traditional dative resonance structure **1**. But complexes of strong backbonders, such as electropositive Ti(II), are often best drawn in the metallacyclopropane form **2**. Bond lengths and angles in the alkene change substantially upon coordination to a strongly backbonding metal. We see an elongation of the C=C bond (consistent with decreased bond order) and some pyramidalization of the alkene carbons (consistent with a change in hybridization from sp^2 to sp^3). A complete orbital picture of sigma bonding and pi backbonding in alkenes is shown in Figure ***NaN*.2.15**.

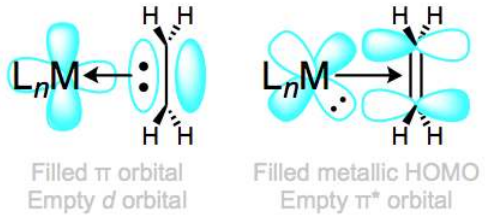
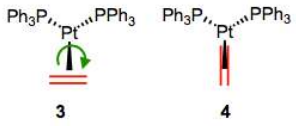


Figure ***NaN*.2.15**: Normal sigma bonding and pi backbonding in alkene complexes.

Here's an interesting question with stereochemical implications: what is the orientation of the alkene relative to the other ligands? From what we've discussed so far, we can surmise that one face of the alkene must point toward the metal center. Put differently, the bonding axis must be normal to the plane of the alkene. However, this restriction says nothing about rotation about the bonding axis, which spins the alkene ligand like a pinwheel. Is a particular orientation preferred, or can we think about the alkene as a circular smudge over time? The figure below depicts two possible orientations of the alkene ligand in a trigonal planar complex. Other orientations make less sense because they would involve inefficient orbital overlap with the metal's orthogonal d orbitals. Which one is favored?

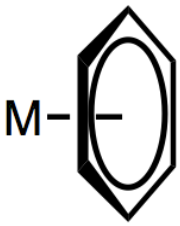


Two limiting cases for alkene orientation in a trigonal planar complex.

First of all, we need to notice that these two complexes are diastereomeric. They have different energies as a result, so one must be favored over the other. Steric considerations suggest that complex **4** ought to be more stable (in most complexes, steric factors dictate alkene orientation). To dig a little deeper, let's consider any electronic factors that may influence the preferred geometry. We've already seen that electronic factors can overcome steric considerations when it comes to complex geometry. To begin, we need to consider the crystal field orbitals of the complex as a whole. Verify on your own that in this d^{10}, Pt(0) complex, the crystal-field HOMOs are the d_{xy} and \(d-{x^2–y^2\) orbitals. Where are these orbitals located in space? In the xy-plane! Only the alkene in **3** can engage in efficient backbonding with the metal center. In cases when the metal is electron rich and/or the alkene is electron poor, complexes like **3** can sometimes be favored in spite of sterics.

Arenes

Arenes or aromatic ligands are neutral ligands that may serve either as actors or spectators. Arenes commonly bind to metals through more than two atoms, although η^2-arene ligands are known. Structurally, most η^6-arenes tend to remain planar after binding to metals. Both sigma bonding and pi backbonding are possible for arene ligands; however, arenes are stronger sigma donors than CO and backbonding is less important for these ligands. The reactivity of arenes changes dramatically upon metal binding, along lines that we would expect for strongly electron-donating ligands. After coordinating to a transition metal, the arene usually becomes a better electrophile (particularly when the metal is electron poor). Thus, metal coordination can enable otherwise difficult nucleophilic aromatic substitution reactions.



General Properties

The coordination of an aromatic compound to a metal center through its aromatic π MOs removes electron density from the ring. π → dσ (sigma bonding) and dπ → π* (backbonding) orbital interactions are possible for arene ligands, with the former being much more important, typically. To simplify drawings, you often see chemists draw arenes involving a circle and single central line to represent the π → dσ orbital interaction. Despite the single line these are not simple 2 electron donors. For instance, η^6-arenes are best describes as six-electron donors.

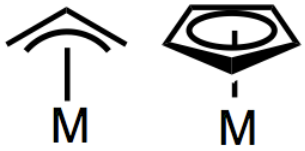
Multiple coordination modes are possible for arene ligands. When all six atoms of a benzene ring are bound to the metal (η^6-mode), the ring is flat and C–C bond lengths are slightly longer than those in free benzene. The ring is bent and non-aromatic in η^4-mode, so that the four atoms bound to the metal are coplanar while the other π bond is out of the plane. Even η^2-arene ligands bound through one double bond are known. Coordination of one π bond results in dearomatization and makes η^2-benzene behave more like butadiene, and furan act more like a vinyl ether. With naphthalene as ligand, there are multiple η^2 isomers that could form; the isomer observed is the one that retains aromaticity in the free portion of the ligand. In fact, this result is general for polycyclic aromatic hydrocarbons: binding maximizes aromaticity in the free portion of the ligand. Arene ligands are usually hydrocarbons, not heterocycles. Why? Aromatic heterocycles, such as pyridine, more commonly bind using their basic lone pairs. That said, a few heterocycles form important π complexes. Thiophene is perhaps the most heavily studied, as the desulfurization of thiophene from fossil fuels is an industrially useful process.



Figure ***NaN.2.16***: Arene ligands exhibit multiple coordination modes.

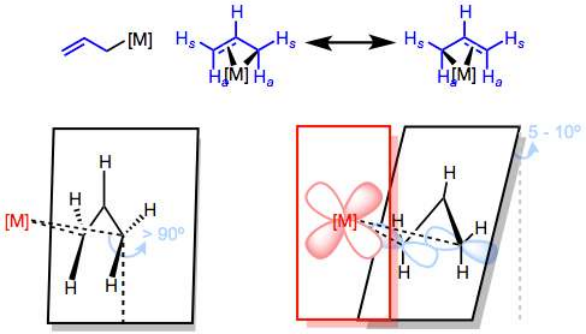
Odd Numbered π Systems

Odd-numbered π systems—most notably, the allyl and cyclopentadienyl ligands—are formally monoanionic ligands which donate n+1 electrons (i.e. η^5 cyclopentadienyl ligand is a 6 electron donor). To illustrate the plurality of equally important resonance structures for this class of ligands, we often just draw a curved line from one end of the π system to the other. Yet, even this form is not perfect, as it obscures the possibility that the datively bound atoms may dissociate from the metal center, forming σ-allyl or ring-slipped ligands. What do the odd-numbered π systems really look like, and how do they really behave?



Metal Allyls

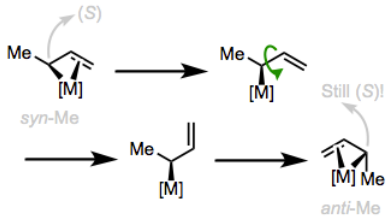
Allyls are often actor ligands, most famously in allylic substitution reactions. The allyl ligand is an interesting beast because it may bind to metals in two ways. When its double bond does not become involved in binding to the metal, allyl is a simple anionic ligand bound covalently through one carbon—basically, a monodentate alkyl! Alternatively, allyl can act as a bidentate LX-type ligand, bound to the metal through all three conjugated atoms. The LX or "trihapto" form can be represented using one of two resonance forms, or (more common) the "aromatic" form seen in the illustration above.



Can we use FMO theory to explain the wonky geometry of the allyl ligand?

The lower half of the figure above illustrates the slightly weird character of the geometry of allyl ligands. In a previous post on even-numbered π systems, we investigated the orientation of the ligand with respect to the metal and came to some logical conclusions by invoking FMO theory and backbonding. A similar treatment of the allyl ligand leads us to similar conclusions: the plane of the allyl ligand should be parallel to the xy-plane of the metal center and normal to the z-axis. In reality, the allyl plane is slightly canted to optimize orbital overlap—but we can see at the right of the figure above that π2–dxy orbital overlap is key. Also note the rotation of the anti hydrogens (anti to the central C–H, that is) toward the metal center to improve orbital overlap.

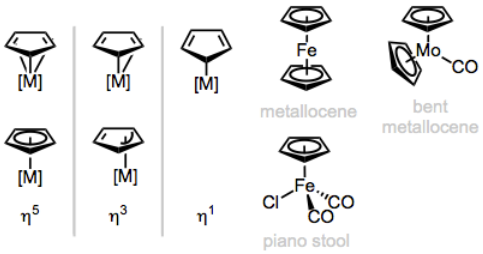
Exchange of the syn and anti substituents can occur through σ,π-isomerization followed by bond rotation and formation of the isomerized trihapto form. Notice that the configuration of the stereocenter bearing the methyl group is unaffected by the isomerization! It should be noted that 1,3-disubstituted allyl complexes almost exclusively adopt a syn,syn configuration without danger of isomerization.



The methylene and central C–H simply change places!

Metal Cyclopentadienyls

Upon deconstruction, the cyclopentadienyl (Cp) ligand yields the aromatic cyclopentadienyl anion, an L2X-type ligand. Cp is normally an η^5-ligand, but η^3 (LX) and η^1 (X) forms are known in cases where the other ligands on the metal center are tightly bound. η^1-Cyclopentadienyl ligands can sometimes be fluxional—the metal has the ability to "jump" from atom to atom. Variations on the Cp lignad include Cp* (C_5Me_5) and the monomethyl version (C_5H_4Me). A single Cp may bond alongside other ligands (in "half-sandwich" or "piano-stool" complexes), or paired up with a second Cp ligand in metallocenes. The piano-stool and bent metallocene complexes are most interesting for us, since these have potential for open coordination sites—metallocenes tend to be relatively stable and boring.



Binding modes of Cp and general classes of Cp complexes.

Contributors and Attributions

- Dr. Michael Evans (Georgia Tech)
- Modified by Catherine McCusker (East Tennessee State University)

This page titled Section 10.2: Organometallic Ligands is shared under a CC BY-NC-SA 4.0 license and was authored, remixed, and/or curated by Michael Evans.

- **2: Organometallic Ligands** by Michael Evans is licensed CC BY-NC-SA 4.0.
- **11.1: Organometallic Ligands** by Michael Evans is licensed CC BY-NC-SA 4.0.
- **2.2: Carbon Monoxide** by Michael Evans has no license indicated.
- **2.6: Metal Hydrides** by Michael Evans is licensed CC BY-NC-SA 4.0.
- **2.9: Phosphines** by Michael Evans is licensed CC BY-NC-SA 4.0.
- **2.3: σ Complexes** by Michael Evans is licensed CC BY-NC-SA 4.0.
- **2.5: Metal Alkyls** by Michael Evans is licensed CC BY-NC-SA 4.0.
- **2.1: Carbenes** by Michael Evans is licensed CC BY-NC-SA 4.0.
- **2.10: π Systems** by Michael Evans is licensed CC BY-NC-SA 4.0.
- **2.8: Odd-numbered π Systems** by Michael Evans is licensed CC BY-NC-SA 4.0.

Section 10.3: Characterization of Organometallic Complexes

Learning Objectives

In this lecture you will learn the following

- The characterization techniques of organometallic compounds.
- The NMR analysis of these compounds.
- The IR analysis of these compounds.
- The X-ray single crystal diffraction studies of these compounds.

The characterization of an organometallic complex involves obtaining a complete understanding of the same right from its identification to the assessment of its purity content, to even elucidation of its stereochemical features. Detailed structural understanding of the organometallic compounds is critical for obtaining an insight on its properties and which is achieved based on the structure-property paradigm.

Synthesis and isolation

Synthesis and isolation are two very important experimental protocols in the overall scheme of things of organometallic chemistry and thus these needs to be performed carefully. The isolation of the organometallic compounds is essential for their characterization and reactivity studies. Fortunately, many of the methods of organic chemistry can be used in organometallic chemistry as the organometallic compounds are mostly nonvolatile crystalline solids at room temperature and atmospheric pressure though a few examples of these compounds are known to exist in the liquid [$(CH_3C_5H_4Mn(CO)_3$] and even in the vapor [$Ni(CO)_4$] states. The organometallic compounds are comparatively more sensitive to aerial oxygen and moisture, and because of which the manipulation of these compounds requires stringent experimental skills to constantly provide them with anaerobic environment for their protection. All of these necessities led to the development of the so-called special Schlenk techniques, requiring special glasswares and which in conjunction with a high vacuum line and a dry box allow the lab bench-top manipulation of these compounds. Successful isolation of organometallic compounds naturally points to the need for various spectroscopic techniques for their characterizations and some of the important ones are discussed below.

1H NMR spectroscopy

The ^1H NMR spectroscopy is among the extensively used techniques for the characterization of organometallic compounds. Of particular interest is the application of ^1H NMR spectroscopy in the characterization of the metal hydride complexes, for which the metal hydride moiety appear at a distinct chemical shift range between 0 ppm to −40 ppm to the high field of tetramethyl silane (TMS). This upfield shift of the metal hydride moiety is attributed to a shielding by metal *d*−electrons and the extent of the upfield shift increases with higher the d^n configuration. Chemical shifts, peak intensities as well as coupling constants from the through-bond couplings between adjacent nuclei like that of the observation of $J_{P\text{-}H}$, if a phosphorous nucleus is present within the coupling range of a proton nucleus, are often used for the analysis of these compounds. The ^1H NMR spectroscopy is often successfully employed in studying more complex issues like fluxionality and diastereotopy in organometallic molecules (Figure ***NaN***.3.1).

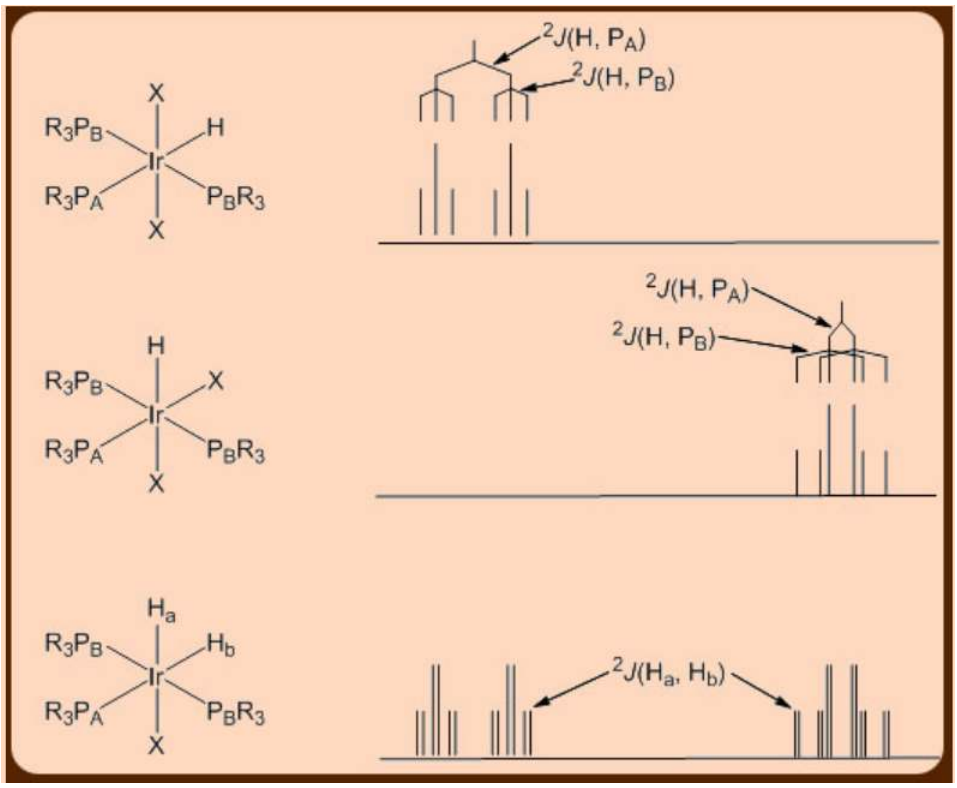


Figure ***NaN*.3.1**: Different phosphorous-proton coupling patterns in various iridium hydride complexes.

The paramagnetic organometallic complexes show a large range of chemical shifts, for example, $(\eta^6{-}C_6H_6)_2V$ exhibits proton resonances that extend even up to 290 ppm.

13C NMR spectroscopy

Although the natural abundance of NMR active ^{13}C (I = ½) nuclei is only 1 %, it is possible to obtain a proton decoupled $^{13}C\{^1H\}$ NMR spectra for most of the organometallic complexes. In addition, the off−resonance ^1H decoupled ^{13}C experiments yield $^1J_{C\text{-}H}$ coupling constants, which contain vital structural information, and hence are very critical to the ^{13}C NMR spectral analysis. For example, the $^1J_{C\text{-}H}$ coupling constants directly correlate with the hybridization of the C−H bonds with *sp* center exhibiting a $^1J_{C\text{-}H}$ coupling constant of ~250 Hz, a sp^2 center of 160 Hz and a sp^3 center of 125 Hz. Similar to what is seen in ^1H NMR, a phosphorous−carbon coupling is also observed in a ^{13}C NMR spectrum with the *trans* coupling (~100 Hz) being larger than the *cis* coupling (~10 Hz).

^{31}P NMR spectroscopy

The ^{31}P NMR spectroscopy, which in conjunction with ^1H and ^{13}C NMR spectroscopies, is a useful technique in studying the phosphine containing organometallic complexes. The ^{31}P NMR experiments are routinely run under ^1H decoupled conditions for simplification of the spectral features that allow convenience in spectral analysis. Thus, for this very reason, many mechanistic studies on catalytic cycle are conveniently undertaken by ^{31}P NMR spectroscopy whenever applicable.

IR spectroscopy

Qualitative to semi-quantitative analysis of organometallic compounds using IR spectroscopy are performed whenever possible. In general the signature stretching vibrations for chemical bonds are more conveniently looked at in these studies. The frequency (ν) of a stretching vibration of a covalent bond is directly proportional to the strength of the bond, usually given by the force constant (k) and inversely proportional to the reduced mass of the system, which relates to the masses of the individual atoms.

$$\nu = \frac{1}{2\pi C}\sqrt{\frac{k}{m_r}}$$

$$m_r = \frac{m_1 m_2}{m_1 + m_2}$$

The organometallic compounds containing carbonyl groups are regularly studied using IR spectroscopy, and in which the **CO** peaks appear in the range between 2100−1700 cm^{-1} as distinctly intense peaks.

Crystallography

The solid state structure elucidation using single crystal diffraction studies are extremely useful techniques for the characterization of the organometallic compounds and for which the X-ray diffraction and neutron diffraction studies are often undertaken. As these methods give a three dimensional structural rendition at a molecular level, they are of significant importance among the various available characterization methods. The X-ray diffraction technique is founded on Bragg's law that explains the diffraction pattern arising out of a repetitive arrangement of the atoms located at the crystal lattices.

$$2d \sin\theta = n\lambda$$

A major limitation of the X-ray diffraction is that the technique is not sensitive enough to detect the hydrogen atoms, which appear as weak peaks as opposed to intense peaks arising out of the more electron rich metal atoms, and hence are not very useful for metal hydride compounds. Neutron diffraction studies can detect hydrogens more accurately and thus are good for the analysis of the metal hydride complexes.

Summary

Along with the synthesis, the isolation and the characterization protocols are also integral part of the experimental organometallic chemistry. Because of their air and moisture sensitivities, specialized experimental techniques that succeed in performing the synthesis, isolation and storage of these compounds in an air and moisture-free environment are often used. The organometallic compounds are characterized by various spectroscopic techniques including the ^{1}H NMR, ^{13}C NMR and IR spectroscopies and the X-ray and the neutron diffraction studies.

This page titled Section 10.3: Characterization of Organometallic Complexes is shared under a CC BY-NC-SA 4.0 license and was authored, remixed, and/or curated by M. S. Balakrishna & Prasenjit Ghosh via source content that was edited to the style and standards of the LibreTexts platform.

- **12.1: Characterization of Organometallic Complexes** by M. S. Balakrishna & Prasenjit Ghosh is licensed CC BY-NC-SA 4.0. Original source: https://nptel.ac.in/courses/104101006.

CHAPTER OVERVIEW

Chapter 11: Organometallic Reactions and Catalysis

Introduction

This chapter is a survey of common organometallic reactions and catalytic cycles. The reactions of organometallic complexes are divided into two main categories: (1) Reactions that involve gain or loss of ligands, and (2) Reactions involving modification of ligands.

- Section 11.1: Reactions Involving Gain or Loss of Ligands
  - Section 11.1.1: Ligand Dissociation and Substitution
  - Section 11.1.2: Oxidative Addition
  - Section 11.1.3: Reductive Elimination
  - Section 11.1.4: Sigma Bond Metathasis
  - Section 11.1.5: Application of Pincer Ligands
- Section 11.2: Reactions Invloving Modification of Unsaturated Ligands
  - Section 11.2.1: Introduction to Insertion
  - Section 11.2.2: CO Insertions (Alkyl Migration)
  - Section 11.2.3: Migratory Insertion-1,2-Insertions
  - Section 11.2.4: β-Elimination Reactions
  - Section 11.2.5: Abstraction and Addition
- Section 11.3: Organometallic Catalysts
  - Section 11.3.1: Catalytic Deuteration
  - Section 11.3.2: Hydroformylation
  - Section 11.3.3: Monsanto Acetic Acid Process
  - Section 11.3.4: Wacker (Smidt) Process
  - Section 11.3.5: Hydrogenation by Wilkinson's Catalyst
  - Section 11.3.6: Olefin Metathesis
- Section 11.4: Heterogeneous Catalysts
  - Section 11.4.1: Ziegler-Natta Polymerizations
  - Section 11.4.2: Water-Gas Shift Reaction
- Section 11.5: Problems
  - Section 11.5.1: Concept Review Questions Chapter 12
  - Section 11.5.2: Homework Problems Chapter 12

This page titled Chapter 11: Organometallic Reactions and Catalysis is shared under a CC BY-NC-SA license and was authored, remixed, and/or curated by Kathryn Haas.

SECTION OVERVIEW

Section 11.1: Reactions Involving Gain or Loss of Ligands

Many reactions of organometallic complexes involve change in coordination number. In a dissociation reaction, one or more ligands are eliminated from the complex and the coordination number decreases. In an association, one or more ligands are added to the complex and the coordination number increases. If the coordination number changes while the metal oxidation state remains constant, the reactions are considered **association/addition** reactions or **dissociation** reactions. Reactions can also occur where the coordination number changes while the metal oxidation state also changes. These reactions are considered **reductive eliminations** or **oxidative additions** (or a combination of these).

Types of reactions involving gain or loss of ligands

- **Association or Addition Reaction**: a reaction in which the coordination number increases; metal oxidation state is unchanged.
- **Dissociation Reaction**: a reaction in which the coordination number decreases; metal oxidation state is unchanged.
- **Oxidative Addition**: a reaction in which coordination number increases while metal oxidation state increases.
- **Reductive Elimination**: a reaction in which coordination number decreases while metal oxidation state decreases.

Section 11.1.1: Ligand Dissociation and Substitution

Section 11.1.2: Oxidative Addition

Section 11.1.3: Reductive Elimination

Section 11.1.4: Sigma Bond Metathasis

Section 11.1.5: Application of Pincer Ligands

This page titled Section 11.1: Reactions Involving Gain or Loss of Ligands is shared under a CC BY-NC-SA license and was authored, remixed, and/or curated by Kathryn Haas.

Section 11.1.1: Ligand Dissociation and Substitution

As discussed in Chapter 13, ligand substitution is characterized by a continuum of mechanisms bound by associative (A) and dissociative (D) extremes. At the associative extreme, the first step is an Associative reaction; the incoming ligand forms a bond to the metal and creates an intermediate of higher coordination number. Then the departing ligand takes its lone pair and leaves. At the dissociative extreme, the fist step is a Dissociative reaction and the order of events is opposite; a ligand departs and a new complex with lower coordination number forms. Then, a new ligand associates with the complex in the second step. Sometimes, instead of reacting, the "intermediate" is simply a stable complex with a different coordination number than the reactant.

The most common reactions that are used to create new complexes are Dissociations and Substitutions (involving both Dissociation and Association steps). Associative substitution is common for 16-electron complexes (like d^8 complexes of Ni, Pd, and Pt), while both Dissociation and Dissociative Substitution are the norm for 18-electron complexes. Then again, reality is often more complicated than these extremes. In some cases, evidence is available for interchange (I_a or I_d).

In this subsection, we'll explore ligand substitution reactions and mechanisms in the context of organometallic chemistry. We'd like to be able to (a) predict whether a mechanism is likely to be associative or dissociative; (b) propose a reasonable mechanism from given experimental data; and (c) describe the results we'd expect given a particular mechanism. Keep these goals in mind as you learn the theoretical and experimental nuts and bolts of substitution reactions.

Dissociation

Carbonyl compounds are known to undergo dissociation reactions upon heating or irradiation with light. For example, upon heating, the the cyclopentadienylmolybdenum tricarbonyl dimer ($Cp_2Mo_2(CO)_6$), where Cp is the cyclopentadienyl ligand) loses a CO ligand from each Mo ion, and a triple bond between the Mo ions is formed (Top, Figure *Section*11.1.1.1). An example of a photoactivated dissociation of CO is the case of neutral iron pentacarbonyl, $Fe(CO)_5$. Irradiation of $Fe(CO)_5$ with UV produces $Fe(CO)_4$ (Bottom, Figure *Section*11.1.1.1).

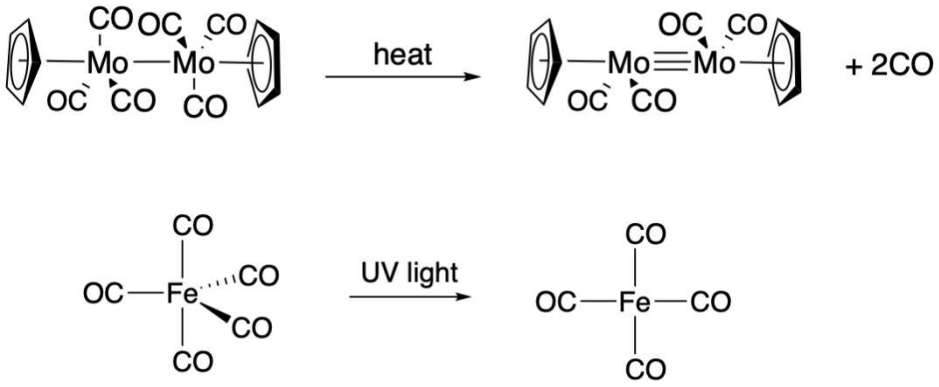


Figure *Section*11.1.1.1: Dissociation reactions: Top, the thermally-activated dissociation of CO from cyclopentadienylmolybdenum tricarbonyl dimer. Bottom, the photochemically-activated dissociation of CO from ironpentacarbonyl. (CC-BY-SA; Kathryn Haas)

However, in each of the cases shown above, the product complex is reactive toward ligand association, usually resulting in an overall substitution. The cyclopentadienylmolybdenum dicarbonyl dimer shown on the top of Figure *Section*11.1.1.1 binds a variety of substrates across the metal-metal triple bond. And the iron tetracarbonyl complex shown on the bottom in Figure *Section*11.1.1.1 readily captures a variety of ligands to result in an overall substitution (example given below); when a ligand doe not associate with it, $Fe_2(CO)_9$ is produced.

Sources: Iron Pentacarbonyl and Cyclopentadienylmolybdenum tricarbonyl dimer articles from Wikipedia.

Dissociative Substitution

Associative substitution is unlikely for saturated, 18-electron complexes—coordination of another ligand would produce a 20-electron intermediate. For 18-electron complexes, dissociative substitution mechanisms involving 16-electron intermediates are more likely. In a slow step with positive entropy of activation, the departing ligand leaves, generating a coordinatively unsaturated intermediate. The incoming ligand then enters the coordination sphere of the metal to generate the product. For the remainder of this post, we'll focus on the kinetics of the reaction and the nature of the unsaturated intermediate (which influences the stereochemistry of the reaction). The reverse of the first step, re-coordination of the departing ligand (rate constant k–1), is often competitive with dissociation.

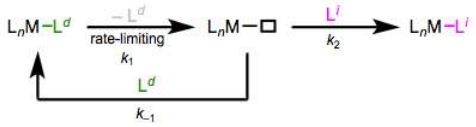


Figure *Section*11.1.1.7: A general scheme for dissociative ligand substitution. There's more to the intermediate than meets the eye! (Michael Evans)

Reaction Kinetics

Let's begin with the general situation in which k_1 and k_{-1} are similar in magnitude. Since k_1 is rate limiting, k_2 is assumed to be much larger than k_1 and k_{-1}. Most importantly, we need to assume that variation in the concentration of the unsaturated intermediate is essentially zero. This is called the steady state approximation, and it allows us to set up an equation that relates reaction rate to observable concentrations Hold onto that for a second; first, we can use step 2 to establish a preliminary rate expression.

$$\text{rate} = k_2[L_nM\text{–}\Diamond][Li] \tag{1}$$

Of course, the unsaturated complex is present in very small concentration and is unmeasurable, so this equation doesn't help us much. We need to remove the concentration of the unmeasurable intermediate from (1), and the steady state approximation helps us do this. We can express variation in the concentration of the unsaturated intermediate as (processes that make it) minus (processes that destroy it), multiplying by an arbitrary time length to make the units work out. All of that equals zero, according to the SS approximation. The painful math is almost over! Since Δt must not be zero, the other factor, the collection of terms, must equal zero.

$$\Delta[L_nM\text{–}\Diamond] = 0 = (k1[L_nM\text{–}L^d]\text{–}k\text{–}1[L_nM\text{–}\Diamond][L^d]\text{–}k_2[L_nM\text{–}\Diamond][Li])\Delta t \tag{2}$$

$$0 = k_1[L_nM\text{–}Ld]\text{–}k_{-1}[L_nM\text{–}\Diamond][Ld]\text{–}k_2[L_nM\text{–}\Diamond][Li] \tag{3}$$

Rearranging to solve for $[L_nM\text{–}\Diamond]$, we arrive at the following.

$$[L_nM\text{–}\Diamond] = k_1\frac{[L_nM\text{–}L_d]}{(k_{-1}[L_d] + k_2[Li]} \tag{4}$$

Finally, substituting into equation (1) we reach a verifiable rate equation.

$$\text{rate} = k_2k_1\frac{[L_nM\text{–}Ld][Li]}{(k_{-1}[L_d] + k_2[Li]} \tag{5}$$

When k_{-1} is negligibly small, (5) reduces to the familiar equation (6), typical of dissociative reactions like S_N1.

$$\text{rate} = k_1[L_nM\text{–}L_d] \tag{6}$$

Unlike the associative rate law, this rate does not depend on the concentration of incoming ligand. For reactions that are better described by (5), we can drown the reaction in incoming ligand to make $k_2[Li]$ far greater than $k_{-1}[Ld]$, essentially forcing the reaction to fit equation (6).

The Unsaturated Intermediate & Stereochemistry

Dissociation of a ligand from an octahedral complex generates an usaturated ML5 intermediate. When all five of the remaining ligands are L-type, as in Cr(CO)5, the metal has 6 d electrons for a total electron count of 16. The trigonal bipyramidal geometry

presents electronic problems (unpaired electrons) for 6 d electrons, as the figure below shows. The orbital energy levels come from crystal field theory. Distortion to a square pyramid or a distorted TBP geometry removes the electronic issue, and so five-coordinate d6 complexes typically have square pyramidal or distorted TBP geometries. This is just the geometry prediction process in action!

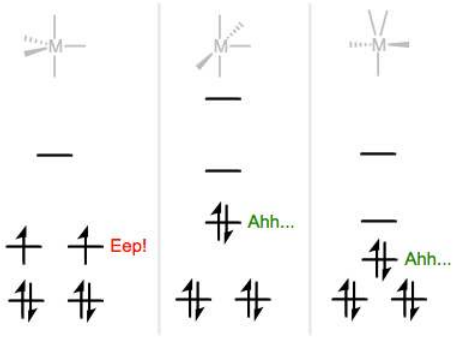


Figure *Section*11.1.1.8: TBP geometry is electronically disfavored for d6 metals. Distorted TBP and SP geometries are favored. (Michael Evans)

When the intermediate adopts square pyramidal geometry (favored for good π-acceptors and σ-donors…why?), the incoming ligand can simply approach where the departing ligand left, resulting in retention of stereochemistry. Inversion is more likely when the intermediate is a distorted trigonal bipyramid (favored for good π-donors). As we've already seen for associative substitution, fluxionality in the five-coordinate intermediate can complicate the stereochemistry of the reaction.

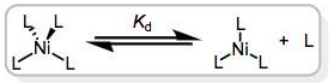
Encouraging Dissocative Substitution

In general, introducing structural features that either stabilize the unsaturated intermediate or destabilize the starting complex can encourage dissociative substitution. Both of these strategies lower the activation barrier for the reaction. Other, quirky ways to encourage dissociation include photochemical methods, oxidation/reduction, and ligand abstraction.

Let's begin with features that stabilize the unsaturated intermediate. Electronically, the intermediate loves it when its d electron count is nicely matched to its crystal field orbitals. As you study organometallic chemistry, you'll learn that there are certain "natural" d electron counts for particular geometries that fit well with the metal-centered orbitals predicted by crystal field theory. Octahedral geometry is great for six d electrons, for example, and square planar geometry loves eight d electrons. Complexes with "natural" d electron counts—but bearing one extra ligand—are ripe for dissociative substitution. The classic examples are d8 TBP complexes, which become d8 square planar complexes (think Pt(II) and Pd(II)) upon dissociation. Similar factors actually stabilize starting 18-electron complexes, making them less reactive in dissociative substitution reactions. d6 octahedral complexes are particularly happy, and react most slowly in dissociative substitutions. The three most common types of 18-electron complexes, from fastest to slowest at dissociative substitution, are:

$$d^8 \text{ TBP} > d^{10} \text{ tetrahedral} > d^6 \text{ octahedral}$$

Destabilization of the starting complex is commonly accomplished by adding steric bulk to its ligands. Naturally, dissociation relieves steric congestion in the starting complex. Chelation has the opposite effect, and tends to steel the starting complex against dissociation.



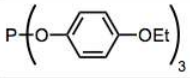
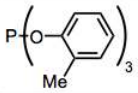
L	Cone Angle	K_d
$P(OEt)_3$	109	$< 10^{-10}$
	128	$6 * 10^{-10}$
$P(Oi\text{-}Pr)_3$	130	$2.7 * 10^{-5}$
	141	$4 * 10^{-2}$
PPh_3	145	huge

Figure ***Section***11.1.1.9: As steric bulk on the ligand increases, dissociation becomes more favorable. (Michael Evans)

I plan to cover the "quirky" methods in a post of their own, but these include strategies like N-oxides for CO removal, photochemical cleavage of the metal–departing ligand bond, and the use of silver cation to abstract halide ligands. Oxidation and reduction can also be used to encourage substitution: 17- and 19-electron complexes are much more reactive toward substitution than their 18-electron analogues.

Associative Substitutions

Despite the sanctity of the 18-electron rule in organometallic chemistry, a wide variety of stable complexes possess fewer than 18 total electrons at the metal center. Perhaps the most famous examples of these complexes are 14- and 16-electron complexes of group 10 metals (Ni, Pt, Pd). Ligand substitution in complexes of this class typically occurs via an associative mechanism, involving approach of the incoming ligand to the complex before departure of the leaving group. If we keep this principle in mind, it seems easy enough to predict when ligand substitution is likely to be associative. But how can we spot an associative mechanism in experimental data, and what are some of the consequences of this mechanism?

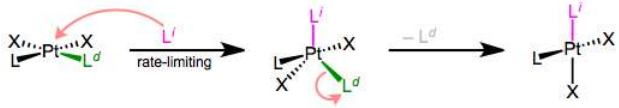


Figure ***Section***11.1.1.2: Associative substitution. (Michael Evans)

The prototypical mechanism of associative ligand substitution. The first step is rate-determining. A typical mechanism for associative ligand substitution is shown above. It should be noted that square pyramidal geometry is also possible for the intermediate, but is less common. Let's begin with the kinetics of the reaction.

Reaction Kinetics for Associative Reactions

Reaction kinetics are commonly used to elucidate organometallic reaction mechanisms, and ligand substitution is no exception. Different mechanisms of substitution may follow different rate laws, so plotting the dependence of reaction rate on concentration often allows us to distinguish mechanisms. Associative substitution's rate law is analogous to that of the S_N2 reaction—rate depends on the concentrations of both starting materials.

$$L_nM\text{–}L^d + L_i \rightarrow L_nM\text{–}L_i + L^d \qquad \textbf{(Section 11.1.1.1)}$$

$$\frac{d[L_nM\text{–}L^i]}{dt} = rate = k_1[L_nM\text{–}L^d][L^i] \qquad \textbf{(Section 11.1.1.2)}$$

The easiest way to determine this rate law is to use pseudo-first-order conditions. Although the rate law is second order overall, if we could somehow render the concentration of the incoming ligand unchanging, the reaction would appear first order. The observed rate constant under these conditions reflects the constancy of the incoming ligand's concentration ($k_{obs} = k_1[L^i]$, where both k_1 and $[Li]$ are constants). How can we make the concentration of the incoming ligand invariant, you ask? We can drown the reaction in ligand to achieve this. The teensy weensy bit actually used up in the reaction has a negligible effect on the concentration of the "sea" of starting ligand we began with. The observed rate is equal to $k_{obs}[L_nM\text{–}L^d]$, as shown by the purple trace below. By

determining k_{obs} at a variety of $[L^i]$ values, we can finally isolate k_1, the rate constant for the slow step. The red trace below at right shows the idea.

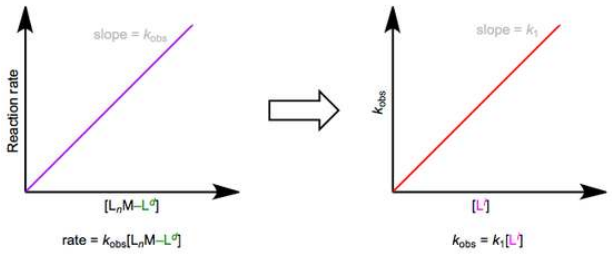


Figure *Section*11.1.1.3: Associative substitution under pseudo-first-order conditions. The reaction is "swamped out" with incoming ligand. (Michael Evans)

In many cases, the red trace ends up with a non-zero y-intercept…curious, if we limit ourselves to the simple mechanism shown in the first figure of this post. A non-zero intercept suggests a more complex mechanism. We need to add a new term (called k_s for reasons to become clear shortly) to our first set of equations:

$$rate = (k_1[L_i] + k_s)[L_nM–L^d] \quad \text{(Section 11.1.1.3)}$$

$$k_{obs} = k_1[L_i] + k_s \quad \text{(Section 11.1.1.4)}$$

The full rate law suggests that some other step (with rate ks[LnM–Ld]) independent of incoming ligand is involved in the mechanism. To explain this observation, we can invoke the solvent as a reactant. Solvent can associate with the complex first in a slow step, then incoming ligand can displace the solvent in a fast step. Solvent concentration doesn't enter the rate law because, well, it's drowning the reactants and its concentration undergoes negligible change! An example of this mechanism in the context of Pt(II) chemistry is shown below.

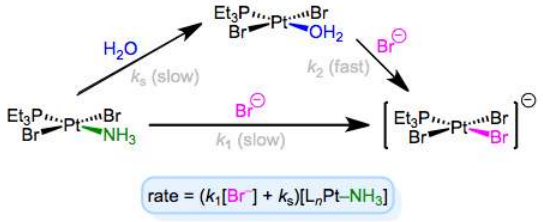


Figure *Section*11.1.1.4: Associative substitution with solvent participation—a head-scratching mechanism for many an organometallic grad student! (Michael Evans)

As an aside, it's worth mentioning that the entropy of activation of associative substitution is typically negative. Entropy decreases as the incoming ligand and complex come together in the rate-determining step. Dissociative substitution shows the opposite behavior: loss of the departing ligand in the RDS increases entropy, resulting in positive entropy of activation.

Stereochemistry of Associative Substitution

As we saw in discussions of the trans effect, the entering and departing ligands both occupy equatorial positions in the trigonal bipyramidal intermediate. Microscopic reversibility is to blame: the mechanism of the forward substitution (displacement of the leaving by the incoming ligand) must be the same as the mechanism of the reverse reaction (displacement of the incoming by the leaving ligand). This can be a confusing point, so let's examine an alternative mechanism that violates microscopic reversibility.

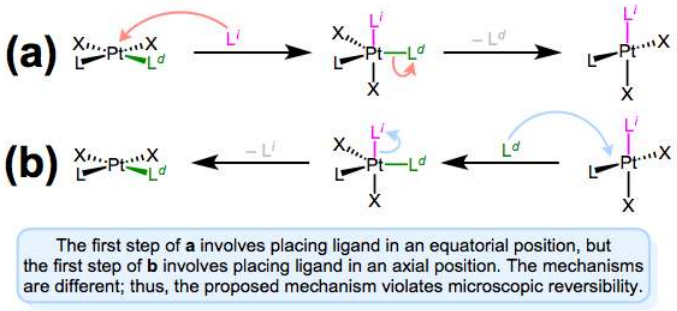


Figure *Section*11.1.1.5: A mechanism involving approach to an axial position and departure from an equatorial position violates microscopic reversibility. Forward and reverse reactions a and b differ! (Michael Evans)

The figure above shows why a mechanism involving axial approach and equatorial departure (or vice versa) is not possible. The forward and reverse reactions differ, in fact, in both steps. In forward mechanism a, the incoming ligand enters an axial site. But in the reverse reaction, the incoming ligand (viz., the departing ligand in mechanism a) sits on an equatorial site. The second steps of each mechanism differ too—a involves loss of an equatorial ligand, while b involves loss of an axial ligand. Long story short, this mechanism violates microscopic reversibility. And what about a mechanism involving axial approach and axial departure? Such a mechanism is unlikely on electronic grounds. The equatorial sites are more electron rich than the axial sites, and σ bonding to the axial d_{z^2} orbital is expected to be strong. Intuitively, then, loss of ligand from an axial site is less favorable than loss from an equatorial site.

I know what you're thinking: what the heck does all of this have to do with stereochemistry? Notice that, in the equatorial-equatorial mechanism (first figure of this post), the axial ligands don't move at all. The configuration of the starting complex is thus retained in the product. Although retention is "normal," complications often arise because five-coordinate TBP complexes—like other odd-coordinate organometallic complexes—are often fluxional. Axial and equatorial ligands can rapidly exchange through a process called Berry pseudorotation, which resembles the axial ligands "cutting through" a pair of equatorial ligands like scissors (animation!). Fluxionality means that all stereochemical bets are off, since any ligand can feasibly occupy an equatorial site. In the example below, the departing ligand starts out cis to L, but the incoming ligand ends up trans to L.

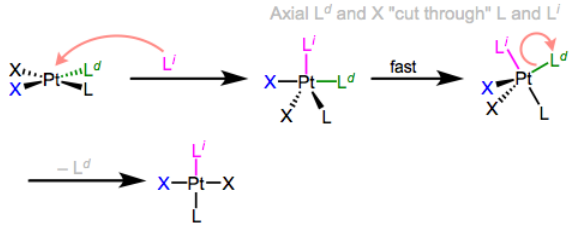


Figure *Section*11.1.1.6: Berry pseudorotation in the midst of associative ligand substitution. (Michael Evans)

Associative Substitution in 18-electron Complexes?

Associative substitution can occur in 18-electron complexes if it's preceded by the dissociation of a ligand. For example, changes in the hapticity of cyclopentadienyl or indenyl ligands may open up a coordination site, which can be occupied by a new ligand to kick off associative substitution. An allyl ligand may convert from its π to σ form, leaving an open coordination site where the π bond left. A particularly interesting case is the **nitrosyl ligand**—conversion from its linear to bent form opens up a site for coordination of an external ligand.

Summary of Associative Substitution

Associative ligand substitution is common for complexes with 16 total electrons or fewer. The reaction is characterized by a second-order rate law, the possibility of solvent participation, and a trigonal bipyramidal intermediate that is often fluxional. An open coordination site is essential for associative substitution, but such sites are often hidden in the dynamism of 18-electron complexes with labile ligands.

Dr. Michael Evans (Georgia Tech)

Quirky Substitutions

Over the years, a variety of "quirky" substitution methods have been developed. All of these have the common goal of facilitating substitution in complexes that would otherwise be inert. It's an age-old challenge: how can we turn a stable complex into something unstable enough to react? Photochemical excitation, oxidation/reduction, and radical chains all do the job, and have all been well studied. We'll look at a few examples in this post—remember these methods when simple associative or dissociative substitution won't get the job done.

Photochemical Substitution

Substitution reactions of dative ligands—most famously, CO—may be facilitated by photochemical excitation. We just discussed the photochemically-activated dissociation of CO from ironpentacarbonyl above; that reaction is often used to accomplish substitution of a CO ligand. Other CO complexes also undergo photochemically-activated CO substitution reactions. Two examples are shown below. The first reaction yields only monosubstituted product without ultraviolet light, even in the presence of a strongly donating phosphine.

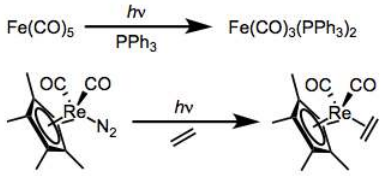


Figure *Section*11.1.1.10:Dissociative photochemical substitutions of CO and dinitrogen. (Michael Evans)

All signs point to dissociative mechanisms for these reactions (the starting complexes have 18 total electrons each). Excitation, then, must increase the M–L antibonding character of the complex's electrons; exactly how this increase in antibonding character happens has been a matter of some debate. Originally, the prevailing explanation was that the LUMO bears M–L antibonding character, and excitation kicks an electron up from the HOMO to the LUMO, encouraging cleavage of the M–L bond. A more recent, more subtle explanation backed by calculations supports the involvement of a metal-to-ligand charge-transfer state along with the "classical" ligand-field excited state.

Oxidation/Reduction

Imagine a screaming baby without her pacifier—that's a nice analogy for an odd-electron organometallic complex. Complexes bearing 17 and 19 total electrons are much more reactive toward substitution than their even-electron counterparts. Single-electron oxidation and reduction ("popping out the pacifier," if you will) can thus be used to efficiently turn on substitution. As you might expect, oxidation and reduction work best on electron-rich and electron-poor complexes, respectively. The Mn complex in the oxidative example below, for instance, includes a strongly donating MeCp group (not shown).

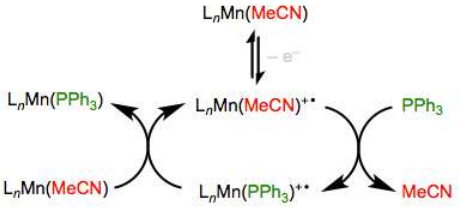


Figure *Section*11.1.1.11: Oxidation accelerates substitution in electron-rich complexes through a chain process. (Michael Evans)

Reduction works well for electron-poor metal carbonyl complexes, which are happy to accept an additional electron.

There is a two-electron oxidation method that's also worth knowing: the oxidation of CO with amine oxides. This nifty little method releases carbon dioxide, amine, and an unsaturated complex that may be quenched by a ligand hanging around. The trick is addition to the CO ligand followed by elimination of the unsaturated complex. As the oxidized CO2 and reduced amine float away, the metal complex finds another ligand.

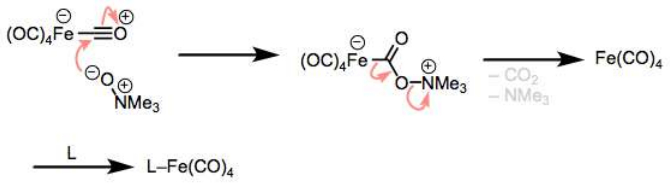


Figure *Section*11.1.1.12: Oxidation of CO with amine oxides. A fun method for dissociative substitution of metal carbonyls! (Michael Evans)

Radical Chain Processes

Atom abstraction from 18-electron complexes produces neutral 17-electron intermediates, which are susceptible to ligand substitution via radical chain mechanisms. The fact that the intermediates are neutral distinguishes these methods from oxidation-based methods. First-row metal hydrides are great for these reactions, owing to their relatively weak M–H bonds. One example is shown below.

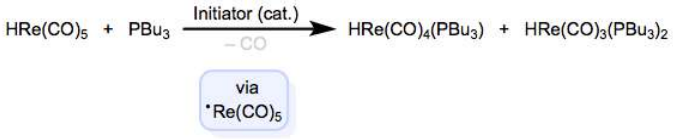


Figure *Section*11.1.1.13: Radical-chain substitution involving atom abstraction. (Michael Evans)

After abstraction of the hydrogen atom by initiator, substitution is rapid and may occur multiple times. Propagation begins anew when the substituted radical abstracts hydrogen from the starting material to regenerate the propagating radical and form the product. These quirky methods are nice to have in your back pocket when you're backed into a synthetic corner—sometimes, conventional associative and dissociative substitution just won't do the job. In the next post, we'll press on to oxidative addition.

Template:Evans

This page titled Section 11.1.1: Ligand Dissociation and Substitution is shared under a CC BY-NC-SA license and was authored, remixed, and/or curated by Kathryn Haas.

- **4.4: Ligand substitution** by Michael Evans is licensed CC BY-NC-SA 4.0.
- **4.3: Dissociative Ligand Substitution Reactions** by Michael Evans is licensed CC BY-NC-SA 4.0.
- **4.2: Associative Ligand Substitution** by Michael Evans is licensed CC BY-NC-SA 4.0.
- **4.10: Quirky Ligand Substitutions** by Michael Evans is licensed CC BY-NC-SA 4.0.

Section 11.1.2: Oxidative Addition

An **oxidative addition** is a reaction in which the coordination number and the oxidation state of the metal ion both increase by 2. In other words, the metal becomes oxidized by two electrons as the coordination number increases by 2 ligands. The microscopic reverse of oxidative addition is reductive elimination (discussed in the next section).

Oxidative addition can occur in a cis- or trans-fashion. A cis-addition means that two ligands are added so that they have cis-orientation to each other after the reaction is complete. A trans-addition implies that two new ligands are in opposite, trans-position after they have been added. We can further distinguish between mononuclear and dinuclear additions. Mononuclear addition involves a complex with a single metal. Dinuclear additions are additions to a metal-metal bond. The addition cleaves the metal-metal bond and adds one ligand to each fragment.

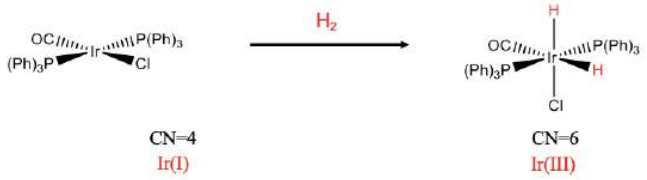


Figure ***Section*11.1.2.1**: Mononuclear oxidative cis-addition (Attribution: A. Vedernikov, U Maryland (modified))

Let's explore a few examples. The first example is a mononuclear cis-addition (Fig. ***Section*11.1.2.1**). In the reaction we add dihydrogen to a square planar iridium complex. After the reaction there are two additional hydrido ligands, and the coordination number has increased from 4 to 6. We can see that the two hydrido ligands are oriented in cis-fashion relative to each other. We can verify that the addition of the hydrido ligands oxidized the metal by determining the oxidation number of the metal before and after the reaction. There are three neutral ligands and one negatively charged chloro ligand. There is no overall charge at the complex. This means that the oxidation number of Ir is +1. After the reaction, there are the two hydrido ligands that have both a -1 charge. Remember, we get the charge at a ligand by cleaving the metal-ligand bond so that all electrons in the bond get assigned to the ligand. This means the oxidation number must be increased by +2, and is +3 after the reaction.

We can rationalize why the addition occurs in cis-fashion and not in trans-fashion. The two hydrido ligands are the smallest ligands, therefore, steric repulsion is minimized in the complex is minimized when the two hydrido ligands are in cis-position.

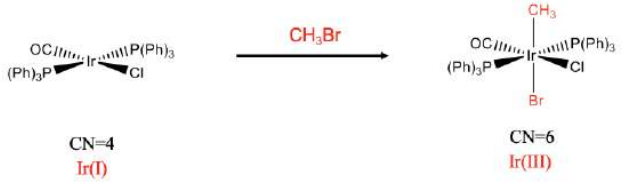


Figure ***Section*11.1.2.2**: Mononuclear oxidative trans-addition (Attribution: A. Vedernikov, U Maryland (modified))

The second example is a mononuclear trans-addition (Fig. ***Section*11.1.2.2**). In this reaction CH_3Br is added to the iridium complex. In this case the two new ligands, a CH_3 and the Br group are in opposite position. Again, the coordination number increases from four to six. We can again verify that an oxidation has occurred by analyzing the oxidation number of Ir. As previously determined, the oxidation number of iridium in the reactant complex is +1. Let us analyze the product complex. The chloro ligand and the bromo ligand have a 1- charge. In addition to that also the CH_3 ligand has a 1- charge assuming that we treat the Ir-C bond as a dative bond. Thus, the oxidation number of Ir must be +3 to give a neutral complex.

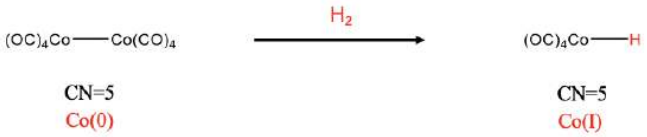


Figure ***Section*11.1.2.3**: Dinuclear addition (Attribution: A. Vedernikov, U Maryland (modified))

The third example is a dinuclear addition (Fig. ***Section*11.1.2.3**). This addition is neither cis nor trans because it cleaves a metal-metal bond, and the one new ligand is added to each fragment. In the example the Co-Co bond of the dicobalt octacarbonyl gets

cleaved upon the reaction with dihydrogen, and two $HCo(CO)_4$ complexes with Co-H bonds form. In this case the coordination number does not increase. Both the reactant and the products have the coordination number 5. We can see that an oxidation of Co has occurred by comparing the oxidation numbers. In the reactant the oxidation number of Co is zero because all CO ligands are neutral and the complex is overall neutral. In the carbonyl hydride product, Co has the oxidation number +1, because the hydrido ligand has a 1- charge.

Oxidative Additions with Intact Ligands

In the previous examples, the ligands that reacted with the complexes lost their integrity. The H-H bond in the H_2 molecule cleaved to form the hydrido ligands, and the C-Br bond in CH_3Br was cleaved to form separate Br and methyl ligands. Not all ligands lose their integrity upon their addition, in particular when they contain multiple bonds. These ligands are called intact ligands. In these cases the bond order *between two atoms in the ligand* is decreased, but the bond order is still at least 1. For example, the alkyne ligand shown belo decreases from a carbon-carbon bond order of three to a bond order of two after it binds to Pt.

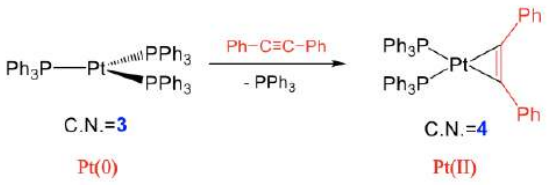


Figure ***Section*11.1.2.4**: Oxidative addition with intact ligands (Attribution: A. Vedernikov, U Maryland (modified))

Examples for intact ligands are are alkenes, alkynes, O_2, etc. In an oxidative addition with an alkyne for example, the alkyne binds side-on to the transition metal under the formation of two metal-C single bonds, and the reduction of the bond order within the alkyne from 3 to 2 (Fig. ***Section*11.1.2.4**). In the shown reaction, a diphenyl ethine molecule adds to tris(triphenyl phosphine) platinum under the formation of two Pt-C single bonds. The C-C triple bond in the ligand becomes a double bond. This reaction occurs under loss of one of the three triphenyl phosphine ligands. The coordination number at the metal increases from 3 to 4. We can again show that the reaction is oxidative by comparing the oxidation numbers of the metal. In the reactant, Pt has the oxidation number 0 because the three triphenyl phosphine ligands have no charge and the complex has overall no charge. After the reaction, the oxidation number of Pt is +2. This is because when we assign the four electrons of the two Pt-C single bonds to the ligand, the ligand becomes a $(Ph\text{-}C{=}C\text{-}Ph)^{2-}$ ligand with each C atom carrying a 1- charge. Because the product complex is overall neutral, the oxidation number of Pt is +2.

Nucleophilic Displacement Reactions

Another important reaction is the nucleophilic displacement reaction. This type of reaction can be classified as an oxidative addition although it does not strictly meet the definnition. In these reactions a metal complex (typically an anion) acts as a nucleophile. A ligand is added, but no electrons are added to the complex. The reactions can be extremely useful for the synthesis of organic compounds. The utility results mostly from the fact that an organic electrophile is turned into a nucleophile.

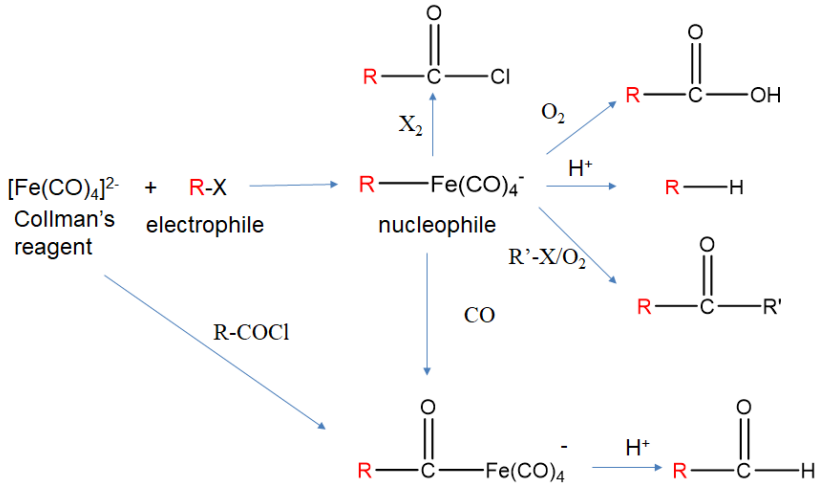


Figure *Section*11.1.2.5: Mononuclear oxidative trans-addition (Attribution: A. Vedernikov, U Maryland (modified)): Examples of nucleophilic displacement reactions

For example, tetracarbonyl ferrate (2-), also known as Collman's reagent reacts with alkyl halides to form alkyl tetracarbonyl ferrate (-) (Fig. *Section*11.1.2.5). We can check that the addition of the alkyl group did not add any electrons by counting the electrons before and after the reaction. The $Fe(CO)_4^{2-}$ anion is an 18e complex. Applying the neutral atom method to the electron counting in $[R\text{-}Fe(CO)_4]^-$ means that Fe contributes 8e, the 1- charge adds 1e, the CO ligands 4x2=8 electrons and the alkyl ligand 1e. This gives 8+1+8+1=18 electrons. Also the oxidation number of Fe has not changed upon the addition of the ligand. It is -2 before and after the reaction.

In the alkyltetracarbonyl ferrate (1-) anion, the group R which was formerly an electrophile in R-X, can now act as a nucleophile due to the fact that the Fe-C bond is polarized toward the C-atom. As a nucleophile it can for instance react with protons to form an alkane. It can also react with oxygen to form a carboxylic acid. In the presence of another alkyl halide R'-X it can form a ketone R-C(O)-R'. It can also insert CO into the Fe-C bonding in a so-called migratory insertion reaction, and the reaction product can react with acid to form an aldehyde. With dihalogens X_2 it can form acyl chloride. Collman's reagent cannot only add alkyl halides by also acyl halides to form acyl tetracarbonyl ferrates (-).

This page titled Section 11.1.2: Oxidative Addition is shared under a CC BY-NC-SA license and was authored, remixed, and/or curated by Kathryn Haas.

- **12.1: Organometallic reactions** by Kai Landskron is licensed CC BY 4.0.

Section 11.1.3: Reductive Elimination

Reductive Elimination Reactions

Reductive elimination is the microscopic reverse of oxidative addition. The reductive elimination can only occur when the two ligands to be eliminated are in cis-position.

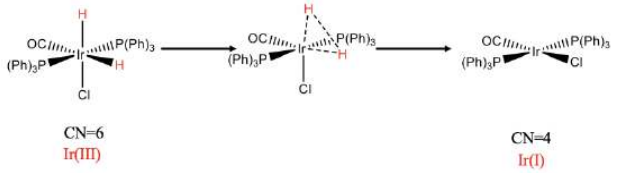


Figure ***Section*11.1.3.1**: Reductive elimination (Attribution: A. Vedernikov, U Maryland.)

For instance the previously discussed oxidative cis-addition of H_2 to the iridium complex is reversible, and the reverse is called the reductive elimination (Fig. ***Section*11.1.3.1**). The cis-orientation of the two hydrido ligands is necessary to form an H-H bond. The reaction can be thought of going along a reaction path in which the Ir-H bonds become gradually larger and and the H-H distance gradually smaller until the H_2 molecule is eliminated from the complex.

During reductive elimination, the electrons in the M–X bond head toward ligand Y, and the electrons in M–Y head to the metal. The eliminating ligands are always X-type! On the whole, the oxidation state of the metal decreases by two units, two new open coordination sites become available, and an X–Y bond forms. What does the change in oxidation state suggest about changes in electron density at the metal? As suggested by the name “reductive,” the metal gains electrons. The ligands lose electrons as the new X–Y bond cannot possibly be polarized to both X and Y, as the original M–X and M–Y bonds were. Using these ideas, you may already be thinking about reactivity trends in reductive elimination…hold that thought.

It’s been observed in a number of cases that a ligand dissociates from octahedral complexes before concerted reductive elimination occurs. Presumably, dissociation to form a distorted TBP geometry brings the eliminating groups closer to one another to facilitate elimination.

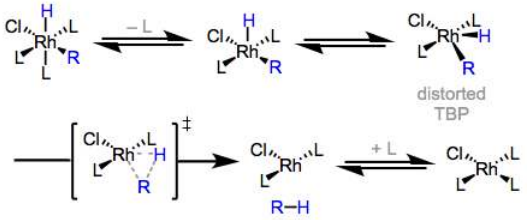


Figure ***Section*11.1.3.2**: Reductive elimination is faster from five-coordinate than six-coordinate complexes. (Michael Evans)

Square planar complexes may either take on an additional fifth ligand or lose a ligand to form an odd-coordinate complex before reductive elimination. Direct reductive elimination without dissociation or association is possible, too.

Reactivity trends in reductive elimination are opposite those of oxidative addition. More electron-rich ligands bearing electron-donating groups react more rapidly, since the ligands lose electron density as the reaction proceeds. More electron-poor metal centers—bearing π-acidic ligands and/or ligands with electron-withdrawing groups—react more rapidly, since the metal center gains electrons. Sterically bulky ancillary ligands promote reductive elimination since the release of X and Y can “ease” steric strain in the starting complex. Steric hindrance helps explain, for example, why coordination of a fifth ligand to a square planar complex promotes reductive elimination even though coordination increases electron density at the metal center. A second example: trends in rates of reductive eliminations of alkanes parallel the steric demands of the eliminating ligands: C–C > C–H > H–H.

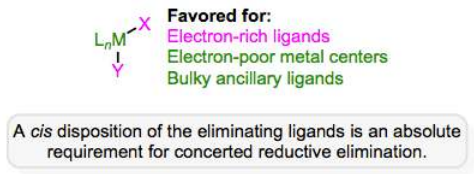


Figure ***Section*11.1.3.3**: Reactivity trends for reductive eliminations. (Michael Evans)

Mechanistic trends for reductive elimination actually parallel trends in mechanisms of oxidative addition, since these two reactions are the microscopic reverse of one another. Non-polar and moderately polar ligands react by concerted or radical mechanisms; highly polarized ligands and/or very electrophilic metal complexes react by ionic (S_N2) mechanisms. The thermodynamics of reductive elimination must be favorable in order for it to occur! Most carbon–halogen reductive eliminations, for example, are thermodynamically unfavorable (this has turned out to be a good thing, especially for cross-coupling reactions).

Reductive elimination is an important step in many catalytic cycles—it usually comes near the "end" of catalytic mechanisms, just before product formation. For some catalytic cycles it's the turnover-limiting step, making it very important to consider! Hydrocyanation is a classic example; in the mechanism of this reaction, reductive elimination of C–CN is the slow step. Electron-poor alkyl ligands, derived from electron-poor olefins like unsaturated ketones, are bad enough at reductive elimination to prevent turnover altogether! Of course, the electronegative CN ligand is not helping things either…how would you design the ancillary ligands L to speed up this step?

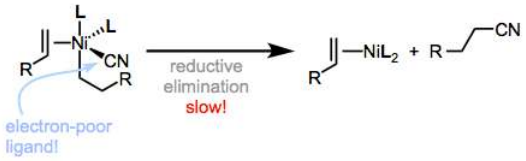


Figure ***Section*11.1.3.4**: Reductive elimination is the turnover-limiting step of hydrocyanation. How would you design L to speed it up? (Michael Evans)

Dr. Michael Evans (Georgia Tech)

Dr. Kai Landskron (Lehigh University). If you like this textbook, please consider to make a donation to support the author's research at Lehigh University: Click Here to Donate.

This page titled Section 11.1.3: Reductive Elimination is shared under a CC BY-NC-SA license and was authored, remixed, and/or curated by Kathryn Haas.

- **12.1: Organometallic reactions** by Kai Landskron is licensed CC BY 4.0.
- **4.11: Reductive Elimination- General Ideas** by Michael Evans is licensed CC BY-NC-SA 4.0.

Section 11.1.4: Sigma Bond Metathasis

Metal compounds with d^0 electron count are able to activate C-H bonds through σ bond metathesis reactions. **σ-bond metathesis** is a chemical reaction wherein a metal-ligand σ bond undergoes metathesis (exchange of parts) with the sigma bond in some other reagent. The reaction is illustrated by the exchange of lutetium(III) methyl complex with a hydrocarbon (R-H) (Figure ***Section*11.1.4.1**). The oxidation state of the metal ion does not change during the reaction. This reactivity was first observed by Patricia L. Watson, a researcher at duPont.

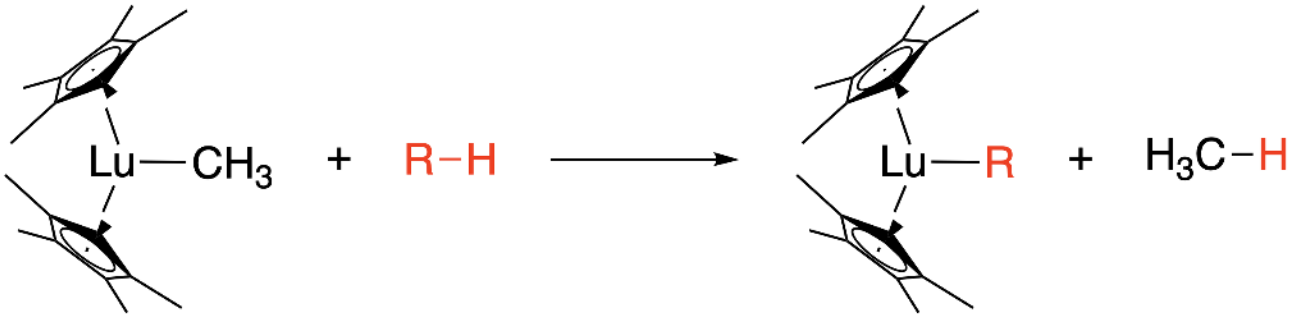


Figure ***Section*11.1.4.1**: Example of σ bond metathesis; exchange of lutetium(III) methyl complex with a hydrocarbon. The R-H bond is activated and a new C-H bond is created. (CC-BY-SA; Kathryn Haas)

The reaction is mainly observed for complexes of metals with d^0 electron configuration, e.g. complexes of Sc(III), Zr(IV), Nb(IV), Ta(V), etc. Complexes of the f-block elements also participate, regardless of the number of f-electrons. For metals unsuited for redox, sigma bond metathesis provides a pathway for introducing substituents.

The details of the reaction mechanism are somewhat a matter of debate, however a currently accepted model is that it precedes through a cycloaddition and via a "kite-shaped" transition state (Figure ***Section*11.1.4.2**). Indeed, the rate of the reaction is characterized by a highly negative entropy of activation, indicating an ordered transition state.

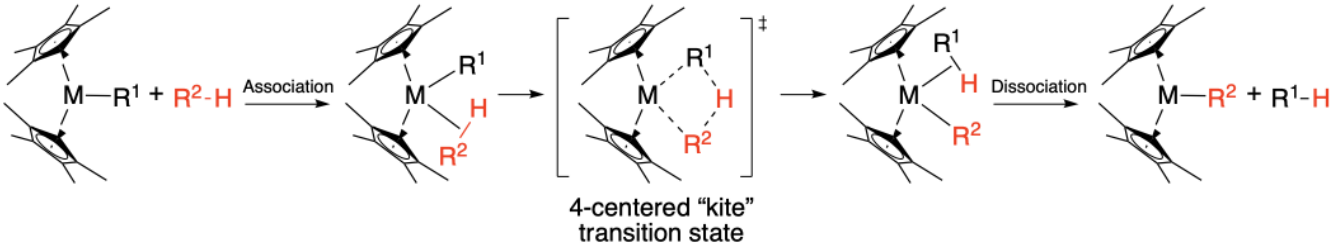


Figure ***Section*11.1.4.2**: The currently accepted mode for the mechanism of σ bond metathesis involving a kite-like transition state. (CC-BY-SA; Kathryn Haas)

The reaction attracted much attention because hydrocarbons are normally unreactive substrates, whereas some sigma-bond metatheses are facile. Unfortunately the reaction does not readily allow the introduction of functional groups. It has been suggested that dehydrocoupling reactions proceed via sigma-bond metathesis.

Sources:

- https://en.Wikipedia.org/wiki/Sigma-bond_metathesis
- *Waterman, Rory (2013). "σ-Bond Metathesis: A 30-Year Retrospective". Organometallics. **32**: 7249–7263. doi:10.1021/om400760k.*

This page titled Section 11.1.4: Sigma Bond Metathasis is shared under a CC BY-NC-SA license and was authored, remixed, and/or curated by Kathryn Haas.

Section 11.1.5: Application of Pincer Ligands

Pincer ligands are chelating agents that bind tightly to three adjacent coplanar sites of a metal complex. Stoichiometric and catalytic applications of pincer complexes have been studied at an accelerating pace since the mid-1970s.

Pincers often include one anionic, two-electron donor flanked by two neutral, two-electron donor groups. It consists of a rigid, planar backbone, usually consisting of aryl frameworks. The inflexibility of the pincer-metal interaction confers high thermal stability to the resulting complexes. This stability is in part ascribed to the constrained geometry of the pincer, which inhibits ligand exchange and cyclometallation of the pincer. In contrast, cyclometallation is often a significant deactivation process in the case of other types of chelates, in particular limiting their ability to effect C-H bond activation. The pincer ligand also creates a hydrophobic pocket around the reactive coordination site.

There are various types of pincer ligands that are used in transition metal catalysis. Often, they have the same two-electron donor flanking the metal centre, but this is not a requirement. Early examples of pincer ligands were anionic with a carbanion as the central donor site and flanking phosphine donors; these compounds are referred to as **PCP pincers**. Although the most common class of pincer ligands features PCP donor sets, variations have been developed where the phosphines are replaced by thioethers and tertiary amines. Many pincer ligands also feature nitrogenous donors at the central coordinating group position (see figure), such as pyridines. By altering the properties of the pincer ligands, it is possible to significantly alter the chemistry at the metal centre. Changing the hardness/softness of the donor, using electron-withdrawing groups (EWGs) in the backbone, and the altering the steric constraints of the ligands are all methods used to tune the reactivity at the metal centre.

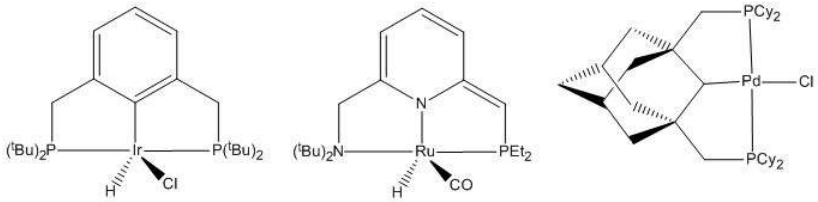


Figure ***Section*11.1.5.1**: Examples of transition metal pincer complexes. (Scott0, Examples pincer complexes, CC BY-SA 3.0)

The Role of Pincer Complexes in Catalysis

Suzuki-Miyaura coupling

Pincer complexes have been shown to catalyse Suzuki-Miyaura coupling reactions, a versatile carbon-carbon bond forming reaction. Suzuki-Miyaura coupling (or Suzuki coupling) is a metal catalyzed reaction, typically with Pd, between an alkenyl (vinyl), aryl, or alkynyl organoborane (boronic acid or boronic ester, or special cases with aryl trifluoroborane) and halide or triflate under basic conditions. This reaction is used to create carbon-carbon bonds to produce conjugated systems of alkenes, styrenes, or biaryl compounds (Scheme 1).



R^1= aryl, alkene (vinyl), alkyne **R**^{2}= H (boronic acid), alkyl (boronic ester) **R**^{3}= aryl, alkene (vinyl), alkyne

X = halide (I, Br, Cl*) triflate (-OTf) *Cl requires special conditions for activation

Scheme ***Section*11.1.5.2**: General reaction scheme of Suzuki cross coupling reaction. (Suzuki-Miyaura Coupling)

Modified conditions have demonstrated reactivity with less reactive substrates such as alkyl boranes (BR_3) or aryl or alkenyl chlorides by amending the base and ligands employed.

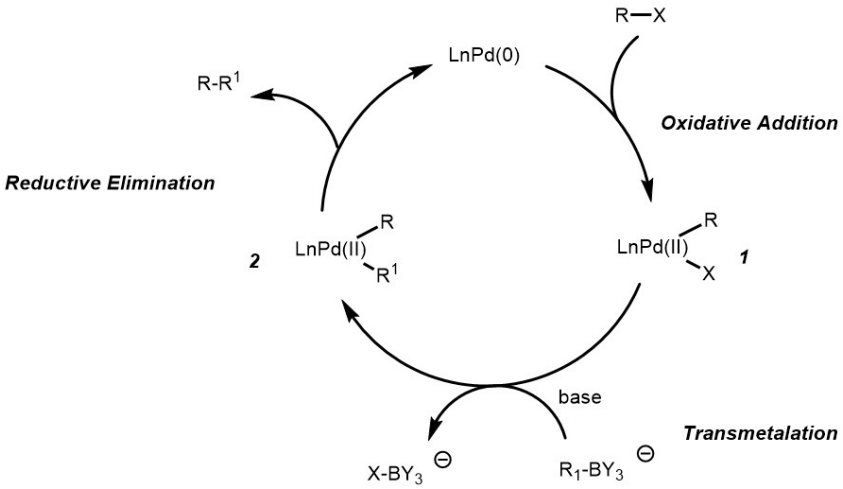
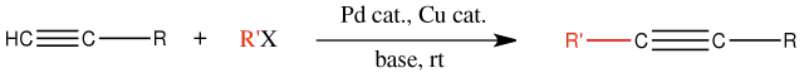


Figure ***Section*11.1.5.3**: Suzuki coupling proceeds via three basic steps: oxidative addition, transmetallation, and reductive elimination. (Suzuki-Miyaura Coupling)

Sonogashira Coupling

The Sonogashira reaction (also called the Sonogashira-Hagihara reaction) is the cross coupling of aryl or vinyl halides with terminal alkynes to generate conjugated enynes and arylalkynes (Scheme 1). The reaction typically proceeds in the presence of a palladium(0) catalyst, a copper(I) cocatalyst, and an imine base. Alternative procedures describe Sonogashira coupling reactions performed without the Cu(I) cocatalyst.



R' = Aryl, Vinyl

X = I, Br, Cl, OTf

Scheme ***Section*11.1.5.4**: *General reaction for Sonogashira Coupling*. (Jcap17, Sonogashira Cross-Coupling Reaction, CC BY-SA 3.0)

Dehydrogenation of alkanes

Alkanes undergo dehydrogenation at high temperatures. Typically this conversion is promoted heterogeneously because typically homogeneous catalysts do not survive the required temperatures (~200 °C) The corresponding conversion can be catalyzed homogeneously by pincer catalysts, which are sufficiently thermally robust. Proof of concept was established in 1996 by Jensen and co-workers. They reported that an iridium and rhodium pincer complex catalyze the dehydrogenation of cyclooctane with a turnover frequency of 12 min^{-1} at 200 °C. They found that the dehydrogenation was performed at a rate two orders of magnitude greater than those previously reported. The iridium pincer complex was also found to exhibit higher activity than the rhodium complex. This rate difference may be due to the availability of the Ir(V) oxidation state which allows stronger Ir-C and Ir-H bonds.

The homogeneously catalyzed process can be coupled to other reactions such as alkene metathesis. Such tandem reactions have not been demonstrated with heterogeneous catalysts.

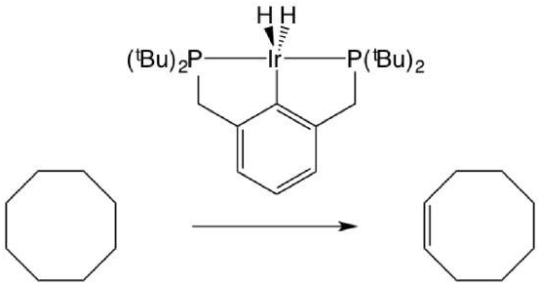


Figure *Section*11.1.5.5: Iridium pincer complex catalyzing the dehydrogenation of cyclooctane to cyclooctene. (Paul Gray, Iridium Pincer Catalysis, CC BY-SA 3.0)

Sources:

- https://en.Wikipedia.org/wiki/Transi...pincer_complex
- Sonogashira Coupling
- Suzuki-Miyaura Coupling

This page titled Section 11.1.5: Application of Pincer Ligands is shared under a CC BY-NC-SA license and was authored, remixed, and/or curated by Kathryn Haas.

SECTION OVERVIEW

Section 11.2: Reactions Invloving Modification of Unsaturated Ligands

This section will describe organometallic reactions that involve modification of unsaturated ligands.

Section 11.2.1: Introduction to Insertion

Section 11.2.2: CO Insertions (Alkyl Migration)

Section 11.2.3: Migratory Insertion-1,2-Insertions

Section 11.2.4: β-Elimination Reactions

Section 11.2.5: Abstraction and Addition

This page titled Section 11.2: Reactions Invloving Modification of Unsaturated Ligands is shared under a CC BY-NC-SA license and was authored, remixed, and/or curated by Kathryn Haas.

Section 11.2.1: Introduction to Insertion

We've seen that the metal-ligand bond is generally polarized toward the ligand, making the ligand nucleophilic. The ligand is especially nucleophilic in the case of X-type (anionic) ligands. When a nucleophilic, X-type ligand is positioned *cis* to a neutral, unsaturated ligand (L) in an organometallic complex, a migratory insertion reaction can occur. In a **migratory insertion reaction**, an anionic ligand (X^-) and a neutral unsaturated ligand (L) couple to form a new anionic ligand (^-LX) *thatisattachedtothesamemetal*(*Figure*\(*Section*11.2.1.1). The overall result is that an M-X bond is broken and M and X are added across a π bond of L. There is no change in oxidation state at the metal (unless the ligand is an alkylidene/alkylidyne), but the total electron count of the complex decreases by two during the actual insertion event.

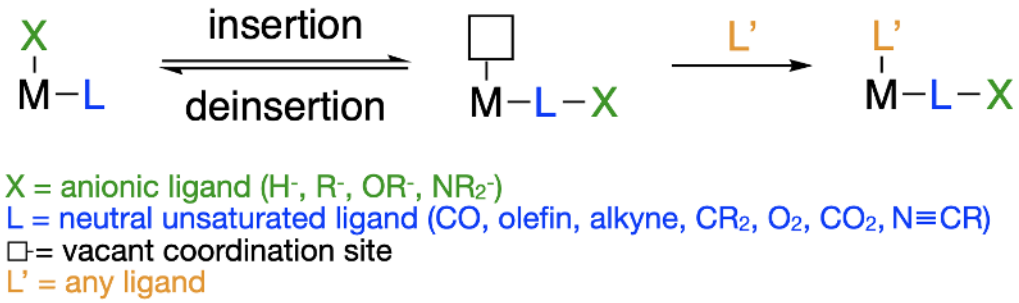


Figure *Section*11.2.1.1: Migratory insertion (CC-BY-SA; Kathryn Haas)

The migratory insertion results in a decrease in coordination number and the creation of an open coordination site on the complex. The open coordination site can be filled by an added ligand (L') (Figure *Section*11.2.1.1). The reverse of the insertion reaction is called a **deinsertion**. To drive the chemical equilibrium in the forward (insertion) direction, the reactant neutral ligand (or another neutral ligand) can be added in excess so that the neutral ligand fills the vacancy in the product complex and prevents the reverse (deinsertion) reaction. Typical neutral, unsaturated ligands are CO, olefins, alkynes, carbenes, dioxygen, carbon dioxide, and nitriles. Typical anionic ligands are hydrido, alkyl, aryl, alkoxy, and amido-ligands Figure *Section*11.2.1.1.

The open site may appear where the unsaturated ligand was *or* where the X-type ligand was, depending on which group actually moved (see below). It is more common that the anionic X ligand moves (Figure *Section*11.2.1.2).

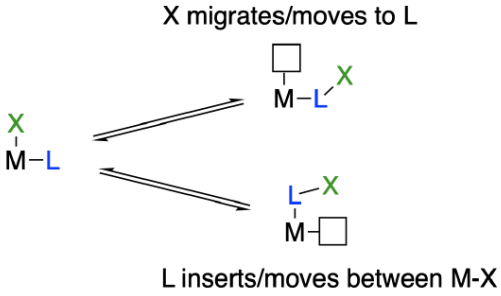


Figure *Section*11.2.1.2: X can migrate onto unsaturated ligand L, or L can move to the original position of X. The former is more common for CO insertions. (CC-BY-SA; Kathryn Haas)

We can distinguish between two types of insertions, which differ in the number of atoms in the unsaturated ligand involved in the step. Insertions of CO, carbenes, and other η^1 unsaturated ligands are called **1,1-insertions** because the X-type ligand moves from its current location on the metal to one spot over, on the atom bound to the metal. η^2 ligands like alkenes and alkynes can also participate in migratory insertion; these reactions are called **1,2-insertions** because the X-type ligand slides two atoms over, from the metal to the distal atom of the unsaturated ligand (Figure *Section*11.2.1.4).

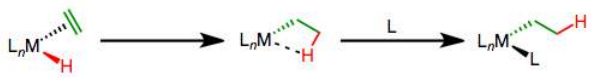


Figure *Section*11.2.1.4: 1,2-insertion of an alkene and hydride. In some cases, an agostic interaction has been observed in the unsaturated intermediate. (Michael Evans)

This is really starting to look like the addition of M and X across a π bond! However, we should take care to distinguish this completely intramolecular process from the attack of a nucleophile or electrophile on a coordinated π system, which is a different beast altogether. Confusingly, chemists often jumble up all of these processes using words like "hydrometalation," "carbometalation," "aminometalation," etc. Another case of big words being used to obscure ignorance! We'll look at nucleophilic and electrophilic attack on coordinated ligands in separate posts.

This page titled Section 11.2.1: Introduction to Insertion is shared under a CC BY-NC-SA license and was authored, remixed, and/or curated by Kathryn Haas.

- **12.1: Organometallic reactions** by Kai Landskron is licensed CC BY 4.0.

Section 11.2.2: CO Insertions (Alkyl Migration)

One of the most common types of migratory insertions is carbonyl insertion (Figure ***Section*11.2.2.3**). The carbonyl insertion produces an acyl group. Notice in the example below that the complex goes from 18 to 16 total electrons after insertion. A dative ligand comes in to fill the empty coordination site. L can be a neutral or anionic ligand, and it can even be the carbonyl oxygen itself. To drive the reaction, the reaction can be carried out in the presence of a neutral ligand like free CO, which occupies the vacant site.

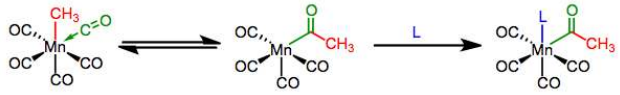


Figure ***Section*11.2.2.1**: Migratory insertion into a metal-carbon bond. (Michael Evans)

Reactivity Trends in CO Insertions

Certain conditions *must* be met for migratory insertion to occur: the two ligands undergoing the process must be *cis*, and the complex must be stable with two fewer total electrons. Thermodynamically, the formed Y–X and covalent M–Y bonds must be more stable than the broken M–X and dative M–Y bonds for insertion to be favored. When the opposite is true, the microscopic reverse (**elimination** or **deinsertion**) will occur spontaneously.

Migratory aptitudes for insertion into CO have been studied extensively, and the general conclusion here is "it's complicated." A few ligands characterized by remarkably stable metal-ligand bonds don't undergo insertion for thermodynamic reasons—the M–X bond is just too darn strong. Perfluoroalkyl complexes and metal hydrides are two notable examples. Electron-withdrawing groups on the X-type ligand, which strengthen the M–X bond, slow down insertion (likely for thermodynamic reasons though… Hammond's postulate in action).

What factors affect the relative speed (kinetics) of favorable insertions? Sterics is one important variable. Both 1,1- and 1,2-insertions can relieve steric strain at the metal center by spreading out the ligands involved in the step. In 1,2-insertions, the X-type ligand removes itself completely from the metal! Unsurprisingly, then, bulky ligands undergo insertions more rapidly than smaller ligands. Complexes of the first-row metals tend to react more rapidly than analogous second-row metal complexes, and second-row metal complexes react faster than third-row metal complexes. This trend fits in nicely with the typical trend in M–C bond strengths: first row < second row < third row. Lewis acids help accelerate insertions into CO by coordinating to CO and making the carbonyl carbon more electrophilic. For a similar reason, CO ligands bound to electron-poor metal centers undergo insertion more rapidly than CO's bound to electron-rich metals. Finally, for reasons that are still unclear, one-electron oxidation often increases the rate of CO insertion substantially.

Although the thermodynamics of alkene 1,2-insertion are more favorable for metal-carbon than metal-hydrogen bonds, M–H bonds react *much* more rapidly than M–C bonds in 1,2-insertions. This fact has been exploited for olefin hydrogenation, which would be much less useful if it had to complete with olefin polymerization (the result of repeated insertion of C=C into M–C) in the same reaction flask! More on that in the next post.

Stereochemistry in CO Insertions

Migratory insertion steps are full of stereochemistry! Configuration at the migrating alkyl group is retainedduring insertion—a nice piece of evidence supporting a concerted, intramolecular mechanism of migration.

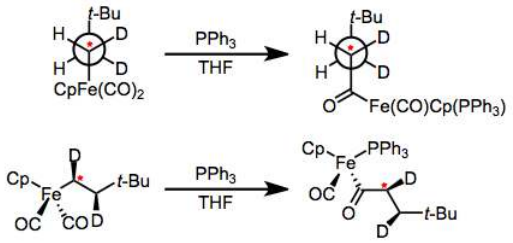


Figure ***Section*11.2.2.2**: Migratory insertion occurs with retention of configuration at the migrating alkyl group. Two different views of the same reaction are shown here. (Michael Evans)

What about stereochemistry at the metal center? Migratory insertion may create a stereogenic center at the metal—see the iron example above. Whether the X-type ligand moves onto the unsaturated ligand or *vice versa* will impact the configuration of the product complex. Calderazzo's study of this issue is one of my favorite experiments in all of organometallic chemistry! He took the simple labeled substrate in the figure below and treated it with dative ligand, encouraging insertion. Four products of insertion are possible, corresponding to reaction of the four CO ligands *cis* to the methyl ligand. Try drawing a few curved arrows to wrap your mind around the four possibilities, and consider both CO migration and Me migration as possible at this point.

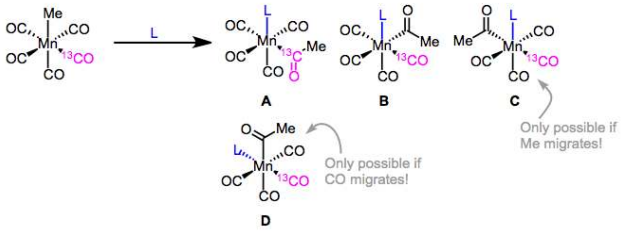


Figure ***Section*11.2.2.3**: Insertion of the labeled complex shown could produce four products. Calderazzo did not observe product **D**, supporting a mechanism involving Me migration to CO. (Michael Evans)

Note that product **D** is impossible if we only allow the Me group to migrate—the spot *trans* to the labeled CO is another CO ligand, so that spot can only pick up L if CO migrates (not if Me migrates). On the other hand, product **C** must have come from the migration of Me, since the Me group has moved from a *cis* to a *trans*position relative to the labeled CO in product **C**. Calderazzo observed products **A**, **B**, and **C**, but not **D**, supporting a mechanism involving Me migration. Other experiments since support the idea that most of the time, the alkyl group migrates onto CO. Slick, huh?

I won't address insertions into alkylidenes, alkylidynes, and other one-atom unsaturated ligands in this post, as insertions into CO are by far the most popular 1,1 insertions in organometallic chemistry. In the next post, we'll dig more deeply into 1,2-insertions of alkenes and alkynes. Thanks for reading!

This page titled Section 11.2.2: CO Insertions (Alkyl Migration) is shared under a CC BY-NC-SA license and was authored, remixed, and/or curated by Kathryn Haas.

Section 11.2.3: Migratory Insertion-1,2-Insertions

Insertions of π systems into M-X bonds are appealing in the sense that they establish two new σ bonds in one step, in a stereocontrolled manner. As we saw in the last post, however, we should take care to distinguish these fully intramolecular migratory insertions from intermolecular attack of a nucleophile or electrophile on a coordinated π-system ligand. The reverse reaction of migratory insertion, β-elimination, is not the same as the reverse of nucleophilic or electrophilic attack on a coordinated π system.

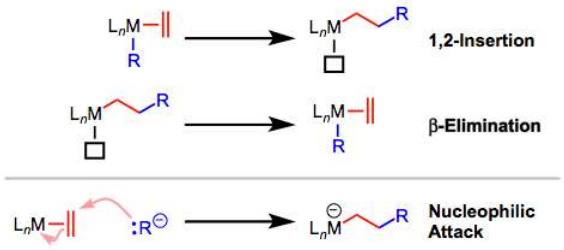


Figure *Section*11.2.3.1: 1,2-Insertion is dinstinct from nucleophilic/electrophilic attack on coordinated ligands. (Michael Evans)

Like 1,1-insertions, 1,2-insertions generate a vacant site on the metal, which is usually filled by external ligand. For unsymmetrical alkenes, it's important to think about site selectivity: which atom of the alkene will end up bound to metal, and which to the other ligand? To make predictions about site selectivity we can appeal to the classic picture of the M–X bond as M + X^-. Asymmetric, polarized π ligands contain one atom with excess partial charge; this atom hooks up with the complementary atom in the M–R bond during insertion. Resonance is our best friend here!

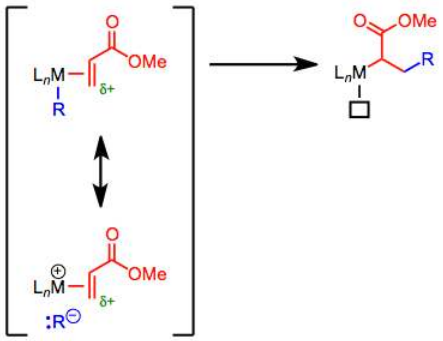


Figure *Section*11.2.3.2: The site selectivity of 1,2-insertion can be predicted using resonance forms and partial charges. (Michael Evans)

A nice study by Yu and Spencer illustrates these effects in homogeneous palladium- and rhodium-catalyzed hydrogenation reactions. Unactivated alkenes generally exhibit lower site selectivity than activated ones, although steric differences between the two ends of the double bond can promote selectivity.

Reactivity Trends in 1,2-Insertions

The thermodynamics of 1,2-insertions of alkenes depend strongly on the alkene, but we can gain great insight by examining the structure of the product alkyl. Coordinated alkenes that give strong metal-alkyl bonds after migratory insertion tend to undergo the process. Hence, electron-withdrawing groups, such as carbonyls and fluorine atoms, tend to encourage migratory insertion—remember that alkyl complexes bearing these groups tend to have stable M–C bonds.

Insertions of alkenes into both M–H and M–R (R = alkyl) are favored thermodynamically, but the kinetics of M–R insertion are much slower. This observation reflects a pervasive trend in organometallic chemistry: M–H bonds react more rapidly than M–R bonds. The same is true of the reverse, β-elimination. Even in cases when both hydride and alkyl elimination are thermodynamically favored, β-hydride elimination is much faster. Although insertion into M–R is relatively slow, this elementary step is critical for olefin polymerizations that form polyalkenes (Ziegler-Natta polymerization). This reaction deserves a post all its own!

As the strength of the M–X bond increases, the likelihood that an L-type π ligand will insert into the bond goes down. Hence, while insertions into M–H and M–C are relatively common, insertions into M–N and M–O bonds are more rare. Lanthanides and palladium are known to promote insertion into M–N in some cases, but products with identical connectivity can come from external attack of nitrogen on a coordinated π ligand. The diastereoselectivity of these reactions provides mechanistic insight—since migratory insertion is syn (see below), a syn relationship between Pd and N is to be expected in the products of migratory insertion. An anti relationship indicates external attack by nitrogen or oxygen.

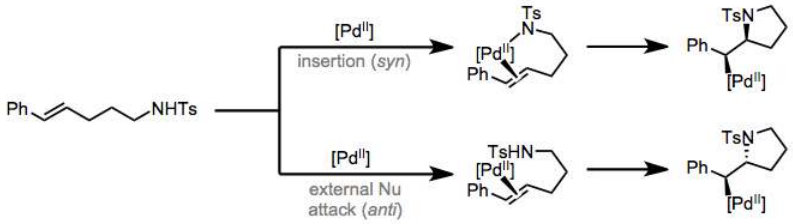


Figure *Section*11.2.3.3: The diastereoselectivity of formal insertions provides insight about their mechanisms. (Michael Evans)

Stereochemistry of 1,2-Insertions

1,2-Insertion may establish two stereocenters at once, so the stereochemistry of the process is critical! Furthermore, 1,2-insertions and β-eliminations are bound by important stereoelectronic requirements. An analogy can be made to the E2 elimination of organic chemistry, which also has strict stereoelectronic demands. For migratory insertion to proceed, the alkene and X-type ligand must be syncoplanar during insertion; as a consequence of this alignment, X and MLn end up on the same face of the alkene after insertion. In other words, insertions into alkenes take place in a syn fashion. Complexes that have difficulty achieving a coplanar arrangement of C=C and M–X undergo insertion very slowly, if at all.

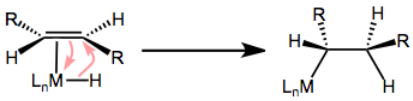


Figure *Section*11.2.3.4: 1,2-Insertions take place in a syn fashion. The metal and X end up bound to the same face of the alkene. (Michael Evans)

This observation has important implications for β-elimination, too—the eliminating X and the metal must have the ability to align syn.

Insertions of Other π Systems

To close this post, let's examine insertions into π ligands other than alkenes briefly. Insertions of alkynes into metal-hydride bonds are known, and are sometimes involved in reactions that I refer to collectively as "hydrostuffylation": hydrosilylation, hydroesterification, hydrogenation, and other net H–X additions across the π bond. Strangely, some insertions of alkynes yield trans products, even though cis products are to be expected from syn addition of M–X. The mechanisms of these processes involve initial syn addition followed by isomerization to the trans complex via an interesting resonance form. The cis complex is the kinetic product, but it isomerizes over time to the more thermodynamically stable trans complex.

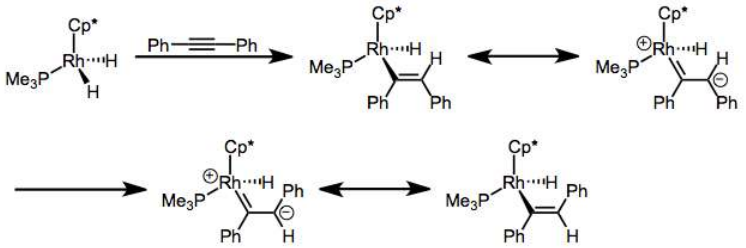


Figure *Section*11.2.3.5: Migratory insertions of alkynes into M–H produce alkenyl complexes, which have been known to isomerize. (Michael Evans)

The strongly donating Cp* ligand supports the legitimacy of the zwitterionic resonance form—and suggests that the C=C bond may be weaker than it first appears!

Polyenes can participate in migratory insertion, and insertions of polyenes are usually quite favored because stabilized π-allyl complexes result. In one mind-bending case, a coordinated arene inserts into an M–Me bond in a syn fashion!

Have you ever stopped to consider that the addition of methyllithium to an aldehyde is a formal insertion of the carbonyl group into the Li–Me bond? It's true! We can think of these as (very) early-metal "insertion" reactions. Despite this precedent, migratory insertion reactions of carbonyls and imines into late-metal hydride and alkyl bonds are surprisingly hard to come by. Rhodium is the most famous metal that can make this happen—rhodium has been used in complexes for arylation and vinylation, for example. Insertion of X=C into the M–R bond is usually followed by β-hydride elimination, which has the nifty effect of replacing H in aldehydes and aldimines with an aryl or vinyl group.

Contributors and Attributions

Dr. Michael Evans (Georgia Tech)

This page titled Section 11.2.3: Migratory Insertion-1,2-Insertions is shared under a CC BY-NC-SA license and was authored, remixed, and/or curated by Kathryn Haas.

- **4.5: Migratory Insertion- 1,2-Insertions** by Michael Evans is licensed CC BY-NC-SA 4.0.

Section 11.2.4: β-Elimination Reactions

In organic chemistry class, one learns that elimination reactions involve the cleavage of a σ bond and formation of a π bond. A nucleophilic pair of electrons (either from another bond or a lone pair) heads into a new π bond as a leaving group departs. This process is called β-elimination because the bond β to the nucleophilic pair of electrons breaks. Transition metal complexes can participate in their own version of β-elimination, and metal alkyl complexes famously do so. Almost by definition, metal alkyls contain a nucleophilic bond—the M–C bond! This bond can be so polarized toward carbon, in fact, that it can promote the elimination of some of the world's worst leaving groups, like –H and –CH3. Unlike the organic case, however, the leaving group is not lost completely in organometallic β-eliminations. As the metal donates electrons, it receives electrons from the departing leaving group. When the reaction is complete, the metal has picked up a new π-bound ligand and exchanged one X-type ligand for another.

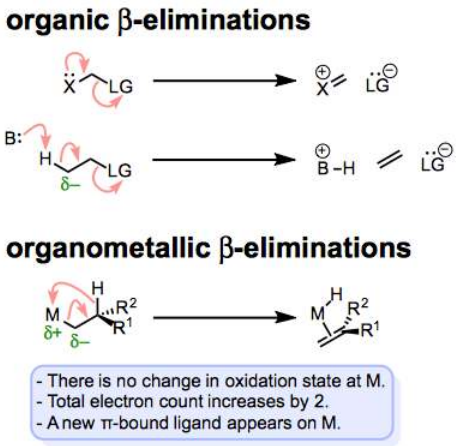


Figure *Section*11.2.4.1: Comparing organic and organometallic β-eliminations. A nucleophilic bond or lone pair promotes loss or migration of a leaving group. (Michael Evans)

In this post, we'll flesh out the mechanism of β-elimination reactions by looking at the conditions required for their occurrence and their reactivity trends. Many of the trends associated with β-eliminations are the opposite of analogous trends in 1,2-insertion reactions. A future post will address other types of elimination reactions.

β-Hydride Elimination

The most famous and ubiquitous type of β-elimination is **β-hydride elimination**, which involves the formation of a π bond and an M–H bond. Metal alkyls that contain β-hydrogens experience rapid elimination of these hydrogens, provided a few other conditions are met.

The complex must have an open coordination site and an accessible, empty orbital on the metal center. The leaving group (–H) needs a place to land. Notice that after β-elimination, the metal has picked up one more ligand—it needs an empty spot for that ligand for elimination to occur. We can envision hydride "attacking" the empty orbital on the metal center as an important orbital interaction in this process.

The M–C_α and C_β–H bonds must have the ability to align in a syn coplanar arrangement. By "syn coplanar" we mean that all four atoms are in a plane and that the M–C_α and C_β–H bonds are on the same side of the C_α–C_β bond (a dihedral angle of 0°). You can see that conformation in the figure above. In the syn coplanar arrangement, the C–H bond departing from the ligand is optimally lined up with the empty orbital on the metal center. Hindered or cyclic complexes that cannot achieve this conformation do not undergo β-hydride elimination. The need for a syn coplanar conformation has important implications for eliminations that may establish diastereomeric olefins: β-elimination is stereospecific. One diastereomer leads to the (E)-olefin, and the other leads to the (Z)-olefin.

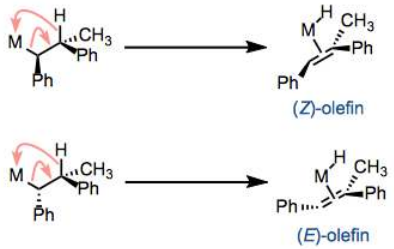


Figure *Section*11.2.4.2: β-elimination is stereospecific. One diastereomer of reactant leads to the (Z)-olefin and the other to the (E)-olefin. (Michael Evans)

The complex must possess 16 or fewer total electrons. Examine the first figure one more time—notice that the total electron count of the complex increases by 2 during β-hydride elimination. Complexes with 18 total electrons don't undergo β-elimination because the product would end up with 20 total electrons. Of course, dissociation of a loose ligand can produce a 16-electron complex pretty easily, so watch out for ligand dissociation when considering the possibility of β-elimination in a complex. Ligand dissociation may be reversible, but β-Hydride elimination is almost always irreversible.

The metal must bear at least 2 d electrons. Now this seems a bit strange, as the metal has served as nothing but an empty bin for electrons in our discussion so far. Why would the metal center need electrons for β-hydride elimination to occur? The answer lies in an old friend: backbonding. The $\sigma_{C-H} \rightarrow M$ orbital interaction mentioned above is not enough to promote elimination on its own; an $M \rightarrow \sigma^*_{C-H}$ interaction is also required! I've said it before, and I'll say it again: backbonding is everywhere in organometallic chemistry. If you can understand and articulate it, you'll blow your instructor's mind.

Other β-Elimination Reactions

The leaving group does not need to be hydrogen, of course, and a number of more electronegative groups come to mind as better candidates for leaving groups. β-Alkoxy and β-amino eliminations are usually thermodynamically favored thanks to the formation of strong M–O and M–N bonds, respectively. These reactions are so favored in β-alkoxyalkyl "complexes" of alkali and alkaline earth metals (R–Li, R–MgBr, etc.) that using these as σ-nucleophiles at carbon is untenable. Such compounds eliminate immediately upon their formation. I had an organic synthesis professor in undergrad who was obsessed with this—using a β-alkoxyalkyl lithium or β-alkoxyalkyl Grignard reagent in a synthesis was a recipe for red ink. β-Haloalkyls were naturally off limits too.

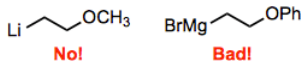


Figure *Section*11.2.4.3: Watch out…these are not stable compounds! (Michael Evans)

The atom bound to the metal doesn't have to be carbon. β-Elimination of alkoxy ligands affords ketones or aldehydes bound at oxygen or through the C=O π bond (this step is important in many transfer hydrogenations, and an analogous process occurs in the Oppenauer oxidation). Amido ligands can undergo β-elimination to afford complexes of imines; however, this process tends to be slower than β-alkoxy elimination.

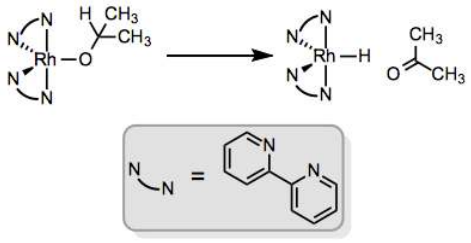


Figure *Section*11.2.4.4: β-Elimination helps transfer the elements of dihydrogen from one organic compound to another.. (Michael Evans)

Incidentally, I haven't seen any examples in which the β atom is not carbon, but would be interested if anyone knows of an example!

Applications of β-Eliminations

As with many concepts in organometallic chemistry, there are two ways to think about applications of β-elimination. One can take either the “inorganic” perspective, which focuses on the metal center, or the “organic” perspective, which focuses on the ligands.

With the metal center in focus, we can recognize that β-hydride elimination has the wonderful side effect of establishing an M–H bond—a feat generally difficult to achieve in a selective manner via oxidative addition of X–H. If the ligand from which the hydrogen came displaced something more electronegative, the whole process represents reduction at the metal center. For example, imagine rhodium(III) chloride is mixed with sodium isopropoxide, $NaOCH(CH_3)_2$. The isopropoxide easily displaces chloride, and subsequent β-hydride elimination affords a rhodium hydride, formally reduced with respect to the chloride starting material. See p. 236 of this review for more.

With the ligand in focus, we see that the organic ligand is oxidized in the course of β-hydride elimination. Notice that the metal is reduced and the ligand oxidized! A π bond replaces a σ bond in the ligand, and if the conditions are right, this represents a bona fide oxidation (as opposed to a mere elimination). For example, oxidative addition into a C–H bond followed by β-hydride elimination at a C–H bond next door sets up an alkene where two adjacent C–H bonds existed before, an oxidation process. These dehydrogenation reactions are incredibly appealing in a theoretical sense, but still at an early stage when it comes to scope and practicality.

Summary

We already encountered β-hydride elimination in an earlier series of posts on metal alkyl complexes, where we noted that it’s a very common decomposition pathway for metal alkyls. β-Hydride elimination isn’t all bad, however, as it can be an important step in catalytic reactions that result in the oxidation of organic substrates (dehydrogenations and transfer hydrogenations) and in reactions that reduce metal halides to metal hydrides. The general idea of β-elimination involves the transfer of a leaving group from a ligand to the metal center with simultaneous formation of a π bond in the ligand. β-Elimination requires an open coordination site and at least two d electrons on the metal center, and eliminations of chiral complexes are stereospecific. The leaving group is commonly hydrogen, but need not be—the more electronegative the leaving group, the more favorable the elimination. Stronger π bonds in the product also encourage β-elimination, so eliminations that form carbonyl compounds or imines are common.

In the next post, we’ll explore other types of organometallic elimination reactions, which establish π bonds at different positions in metal alkyl or other complexes. α-Eliminations, for example, establish metal-carbon, -oxygen, or -nitrogen multiple bonds, which are generally difficult to forge through other means

Contributors and Attributions

- Dr. Michael Evans (Georgia Tech)

This page titled Section 11.2.4: β-Elimination Reactions is shared under a CC BY-NC-SA license and was authored, remixed, and/or curated by Kathryn Haas.

- **4.1: β-Elimination Reactions** by Michael Evans is licensed CC BY-NC-SA 4.0.

Section 11.2.5: Abstraction and Addition

The nucleophilic and electrophilic addition and abstraction reactions can be viewed as ways of activating a ligand toward reaction with an external reagent. The external reagent reacts directly with the ligand, not with the metal center. The external reagent may be a nucleophile (Lewis Base) or an electrophile (Lewis acid).

Nucleophilic Addition and Abstraction

The reaction of an activated ligand with a nucleophilic reagent is favored if the activated ligand is electron poor. When the metal complex is either cationic and/or has spectator ligands that are are electron withdrawing, the reactive ligand becomes activated by being depleted of electron density. The attack of the nucleophile may result in the formation of a new bond between the nucleophile and the activated unsaturated substrate, in which case it is called nucleophilic addition. Alternatively, the reaction may result in an abstraction of a part or the whole of the activated ligand, in which case it is called the nucleophilic abstraction. Some examples of nucleophilic addition and the abstraction reactions are discussed below.

Nucleophilic Addition

An example of a nucleophilic addition reaction is shown in Figure *Section*11.2.5.1. The olefin is activated by its interaction with platinum. Pyridine is the nucleophile, and the result is a new C–N bond.

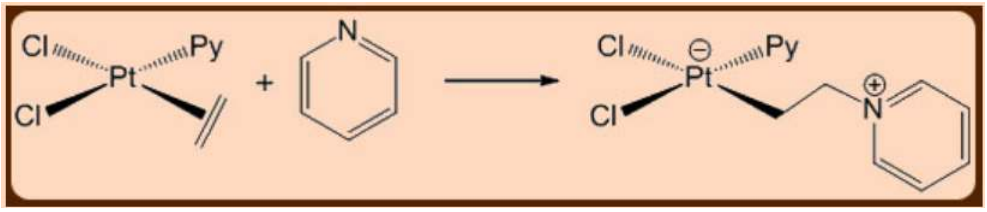


Figure *Section*11.2.5.1: An example of addition of a nucleophile to an activated ligand.

Nucleophilic Abstraction

An example of a nucleophilic abstraction reaction is shown in Figure *Section*11.2.5.2.

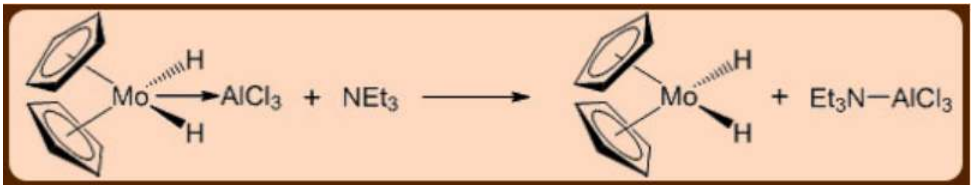


Figure *Section*11.2.5.2: An example of abstraction by a nucleophile.

Electrophilic Addition and Abstraction

Similar to the nucleophilic addition and abstraction reactions, the electrophilic counterparts of these reactions also exist. An electrophilic attack is favored if the ligand-metal fragment is more electron rich. When the complex is anionic, the metal center is at low oxidation state, and/or when the spectator ligands are electron donating, the ligand becomes activated toward reaction with an electrophile. The reaction of activated ligands with electrophilic substrates may result in the formation of a new bond between the electrophile and the activated unsaturated substrate, in which case it is called electrophilic addition, or may result in an abstraction of a part or the whole of the activated ligand, in which case it is called the electrophilic abstraction.

Electrophilic Addition

An example of an electrophile being added to an activated ligand is shown in Figure *Section*11.2.5.3. The allylic anion ligand uses its π electrons to react with hydrogen ion. This adds a hydrogen to the ligand, converting it from an anionic X-type ligand to a neutral L-type ligand .

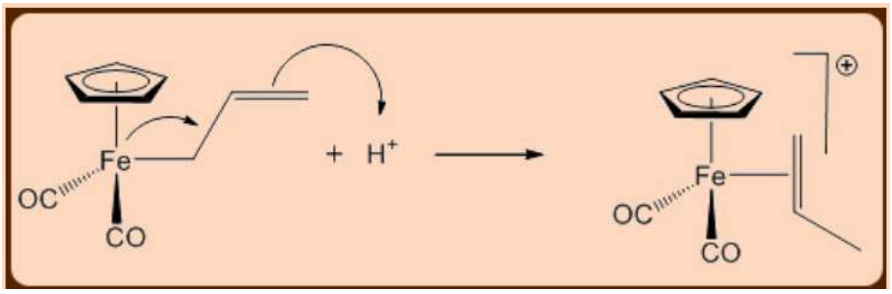


Figure *Section*11.2.5.3: An example of electrophilic addition to an activated ligand.

Electrophilic Abstraction

Depending on whether the abstraction occurs at the α or β position with respect to the metal ion, the reaction is either classified as an α-abstraction or a β-abstraction.

An example of an α electrophilic abstraction reaction is shown in Figure *Section*11.2.5.4.

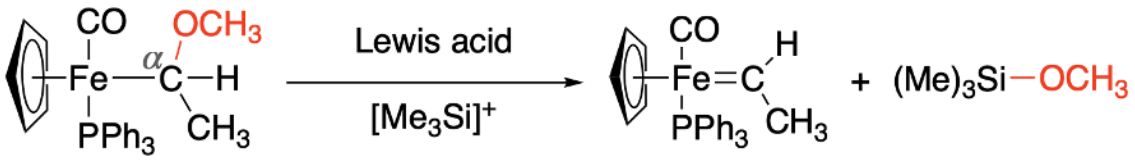


Figure *Section*11.2.5.4: An example of an electrophilic α-abstraction. (CC-BY-SA; Kathryn Haas)

Two examples of a β electrophilic abstraction are shown in Figure *Section*11.2.5.5.

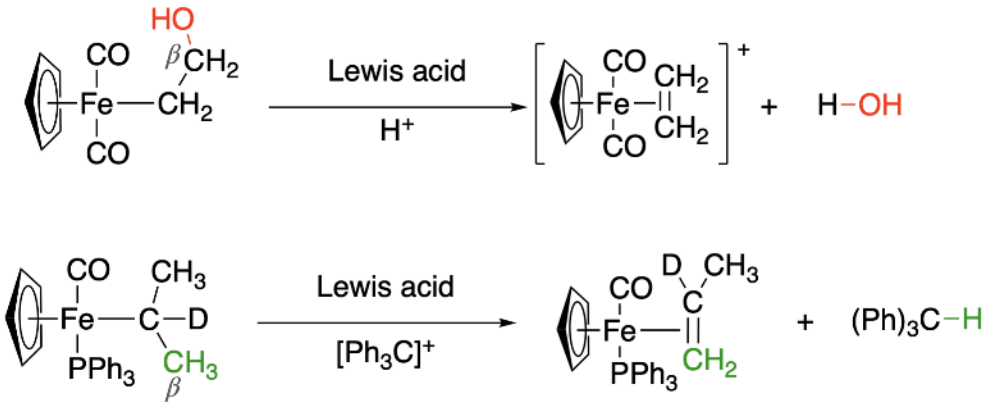


Figure *Section*11.2.5.5: Two examples of electrophilic β-abstraction. (CC-BY-SA; Kathryn Haas)

This page titled Section 11.2.5: Abstraction and Addition is shared under a CC BY-NC-SA license and was authored, remixed, and/or curated by Kathryn Haas.

- **10.3: Nucleophilic and Electrophilic Addition and Abstraction** by M. S. Balakrishna & Prasenjit Ghosh is licensed CC BY-NC-SA 4.0. Original source: https://nptel.ac.in/courses/104101006.

SECTION OVERVIEW

Section 11.3: Organometallic Catalysts

One of the most important uses of organometalic complexes is in the catalysis of chemical reactions. In this section, we will apply knowledge of reaction types and the skill of electron counting to understand organometalic catalytic cycles.

Section 11.3.1: Catalytic Deuteration

Section 11.3.2: Hydroformylation

Section 11.3.3: Monsanto Acetic Acid Process

Section 11.3.4: Wacker (Smidt) Process

Section 11.3.5: Hydrogenation by Wilkinson's Catalyst

Section 11.3.6: Olefin Metathesis

This page titled Section 11.3: Organometallic Catalysts is shared under a CC BY-NC-SA 4.0 license and was authored, remixed, and/or curated by Kathryn Haas.

Section 11.3.1: Catalytic Deuteration

Catalytic Deuteration of Benzene

Combinations of oxidative additions and reductive eliminations have many applications in the synthesis of organic molecules using an organometallic reactant.

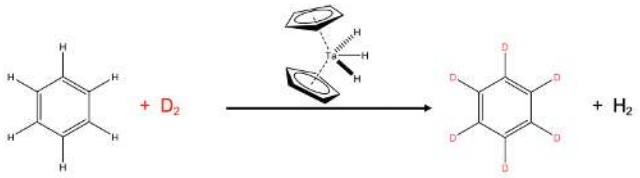


Figure ***Section*11.3.1.1** Deuteration of benzene

An example is the deuteration of benzene (Fig. ***Section*11.3.1.1**). Deuterated benzene is an important solvent in NMR spectroscopy. Industrially, the deuteration is done using a dicyclopentadienyltrihydridotantalum(V) catalyst starting out from benzene and D_2. The D_2 is provided in excess to drive the chemical equilibrium to the right side.

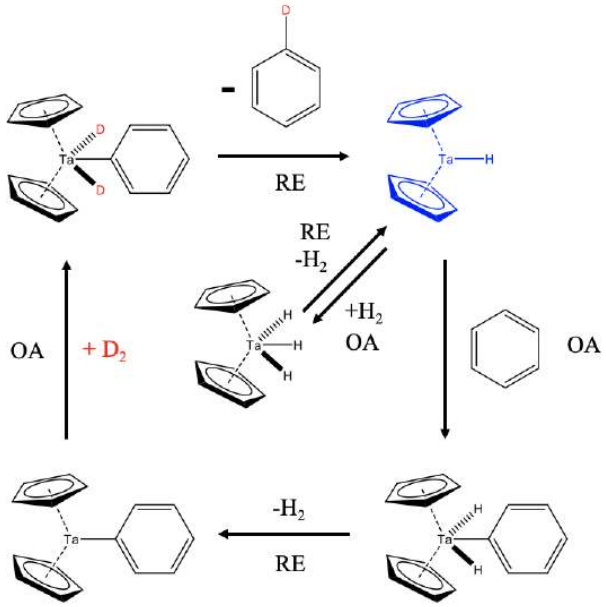


Figure ***Section*11.3.1.2** Mechanism of the catalytic deuteration of benzene

How does this reaction work mechanistically? This 18e Cp_2TaH_3 is actually a precatalyst that is in chemical equilibrium with H_2 and the 16e dicyclopentadienylhydrido tantalum(III) which is the actual catalyst (Fig. ***Section*11.3.1.2**). Elimination of H_2 from the Ta(V) catalyst is a reductive elimination (RE) and the re-addition of H_2 to the Ta(III) species an oxidative addition (OA). In the presence of benzene, the Ta(III) species can oxidatively add benzene to form an 18e Ta(V) complex. This complex can reductively eliminate H_2 to form a 16e Cp_2Ta(III)-Ph complex. In the presence of deuterium this complex can add D_2 oxidatively to form an 18e Cp_2D_2Ta(V)-Ph complex. This species can then reductively eliminate a monodeuterated benzene molecule under formation of Cp_2Ta(III)-D. In the presence of enough D_2 this monodeuterated benzene can be further deuterated in subsequent catalytic cycles.

This page titled Section 11.3.1: Catalytic Deuteration is shared under a CC BY-NC-SA license and was authored, remixed, and/or curated by Kathryn Haas.

- **12.1: Organometallic reactions** by Kai Landskron is licensed CC BY 4.0.

Section 11.3.2: Hydroformylation

Catalytic Olefin Hydroformylation

An important industrial reaction is the catalytic hydroformylation reaction, also known as oxo-process (Figure *Section*11.3.2.1). It was discovered in 1938 by Otto Roelen at BASF. In the hydroformylation reaction an H atom and a formyl group are added to an alkene to form aldehydes. The reaction can produce both branched an linear aldehydes from terminal alkenes, CO, and H_2 using a carbonyl hydrides such as $HCo(CO)_4$ as a catalyst. The reaction is performed at about 100°C at a pressure of up to 100 atm.

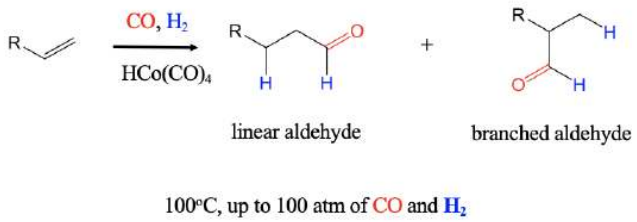


Figure *Section*11.3.2.1: Catalytic olefin hydroformylation

Mechanism of the Catalytic Olefin Hydroformylation by $HCo(CO)_4$

How does the hydroformylation work mechanistically?

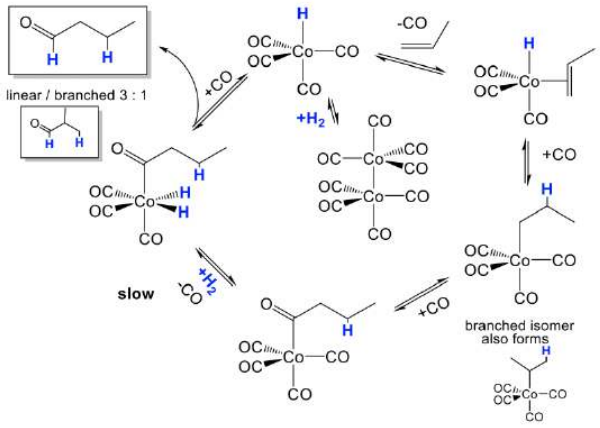


Figure *Section*11.3.2.2: Mechanism of the catalytic olefin hydroformylation by $HCo(CO)_4$ (Attribution: A. Vedernikov, U Maryland (modified).)

The mechanism is illustrated for the hydroformylation of propene (Fig. *Section*11.3.2.2:). The actual catalyst $HCo(CO)_4$ is first formed from its precatalyst $Co_2(CO)_8$ in the presence of H_2 in a dinuclear oxidative addition reaction. The catalyst can undergo a substitution reaction in which a CO ligand is replaced by the olefin that binds side-on to the cobalt. This species can then undergo a migratory olefin insertion reaction. This leads to a mixture of linear and branched alkyl groups attached to the Co. A new CO ligand can add to the vacant site. The alkyl group can then insert into a carbonyl group in another migratory insert step, and the vacant site can be reoccupied by a new CO molecule. Then, H_2 is added in an oxidative addition. This is the slowest and rate-limiting step in the catalytic cycle. From the addition product the aldehyde can then be eliminated in a reductive elimination reaction. Addition of CO regenerates the catalyst, and the catalytic cycle can begin again.

Hydrocarbonylations

After the hydroformylation, a number of other hydrocarbonylations were developed, and industrially deployed.

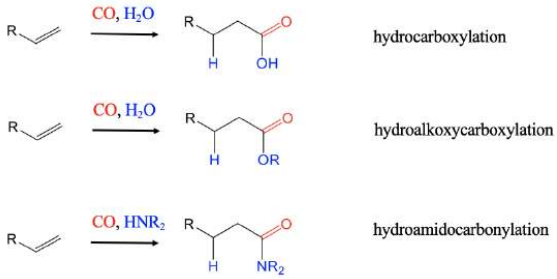


Figure *Section*11.3.2.3: Hydrocarbonylation reactions

When hydrogen is replaced by H_2O hydrocarboxylations of alkenes lead to carboxylic acids (Fig. *Section*11.3.2.3:). With an alcohol instead of H_2 hydroalkoxycarbonylcations lead to esters. The employment of amines instead of H_2 leads to amides in hydroamidocarbonylation reactions.

This page titled Section 11.3.2: Hydroformylation is shared under a CC BY-NC-SA license and was authored, remixed, and/or curated by Kathryn Haas.

- **12.2: Organometallic Catalysts** by Kai Landskron is licensed CC BY 4.0.

Section 11.3.3: Monsanto Acetic Acid Process

The Monsanto Acetic Acid Process

Another carbonylation reaction involving an organometallic catalyst is the Monsanto acetic acid process (Figure ***Section*11.3.3.1**). It has been introduced by Monsanto in the 1970s for the industrial production of acetic acid from methanol. The reaction involves dual catalysis with HI and $[RhI_2(CO)_2]^-$ as a co-catalysts. How does this reaction work?

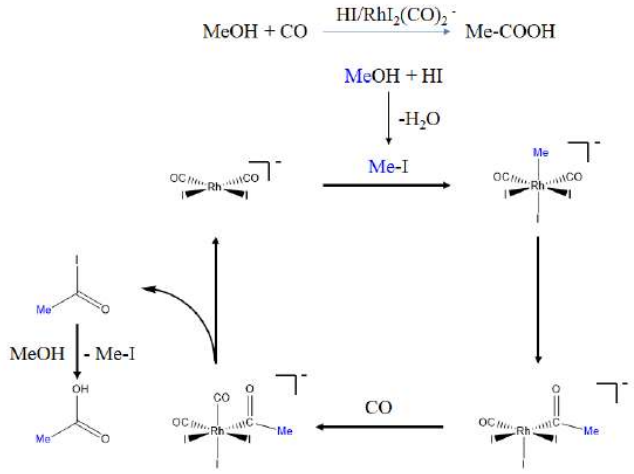


Figure ***Section*11.3.3.1**: The catalytic cycle in the Monsanto acetic acid process

In the first step methanol reacts with HI to form methyl iodide. The methyl iodide then reacts with the Rh-catalyst in an oxidative addition reaction in which a methyl and an iodo group are added in trans-fashion to the square-planar Rh-complex to give an octahedral complex. The octahedral complex then undergoes a migratory insertion reaction with CO producing an acyl group and a vacant site. A CO molecule can then add to the vacant site. The acetyl iodide can then be eliminated in a reductive elimination to reform the Rh-catalyst thereby closing the catalytic cycle. The acetyl iodide can then react with methanol to form new methyl iodide and acetic acid. The methyl iodide can start a new catalytic cycle with the Rh-catalyst.

This page titled Section 11.3.3: Monsanto Acetic Acid Process is shared under a CC BY-NC-SA license and was authored, remixed, and/or curated by Kathryn Haas.

- **12.2: Organometallic Catalysts** by Kai Landskron is licensed CC BY 4.0.

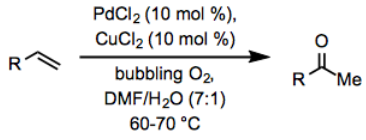
Section 11.3.4: Wacker (Smidt) Process

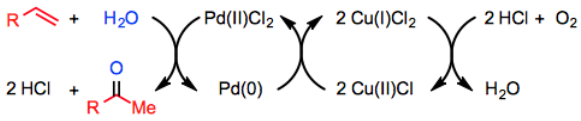
See also Wacker Oxidation (Wikipedia)

The **Wacker oxidation** refers generally to the transformation of a terminal or 1,2-disubstituted alkene to a ketone through the action of catalytic palladium(II), water, and a co-oxidant. Variants of the reaction yield aldehydes, allylic/vinylic ethers, and allylic/vinylic amines. Because of the ease with which terminal alkenes may be prepared and the versatility of the methyl ketone group installed by the reaction, the Wacker oxidation has been employed extensively in organic synthesis.[1]

Introduction

The stoichiometric conversion of ethylene to acetaldehyde by an acidic, aqueous solution of $PdCl_2$ was discovered over a century ago,[2] but fifty years passed between the discovery of this reaction and the development of a catalytic method. In 1959, researchers at Wacker Chemie reported that a similar transformation takes place in an aqueous, acidic solution of catalytic $PdCl_2$ and a stoichiometric amount of $CuCl_2$ through which oxygen is bubbled (Equ. ***Section*11.3.4.1**).[3]





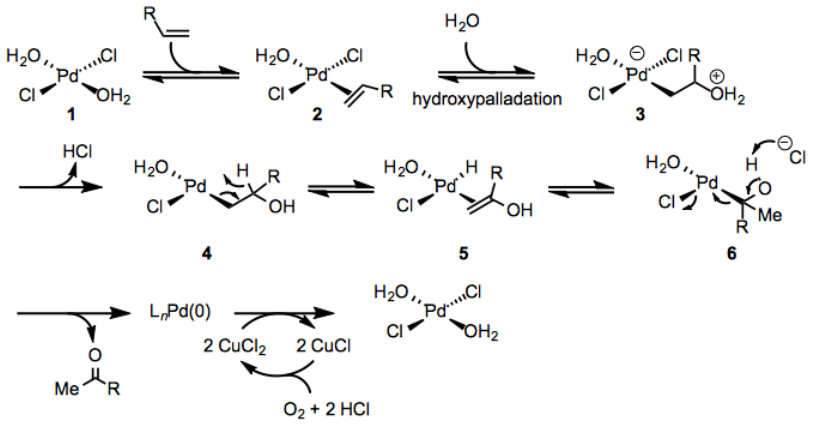
Equation ***Section*11.3.4.1**

Since this initial report, the Wacker process has been widely applied in organic synthesis and has been extended to other classes of substrates and products. To encourage mixing of the organic reactants with the aqueous phase, a co-solvent is generally employed along with water. Dimethylformamide (DMF) is a common choice; when DMF is used as a co-solvent with a stoichiometric amount of CuCl under balloon pressure of oxygen, the reaction is called the "Tsuji-Wacker oxidation."[4] Applications of the Wacker oxidation to organic synthesis typically involve the installation of a methyl ketone moiety, which may subsequently undergo nucleophilic addition or deprotonation to form an enolate.

Mechanism and Stereochemistry

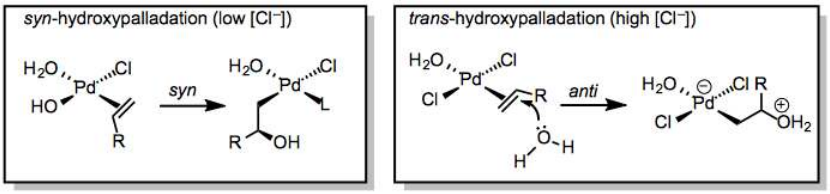
Prevailing Mechanism: Water Nucleophile

The mechanism of the Wacker oxidation has been studied both experimentally and theoretically (Eq. 2). The first step of the Wacker oxidation involves coordination of the the alkene to the palladium center to form π-complex **2**. Evidence for this step is provided by the relative sluggishness of electron-poor alkenes, which generally require higher catalyst loadings than unactivated alkenes. Hydroxypalladation then occurs to yield either zwitterionic complex **3** or neutral complex **4** depending on the mode of hydroxypalladation (see below). Studies employing deuterated substrates suggest that β-hydride elimination then occurs to afford enol complex **5**, which re-inserts into the Pd-H bond to afford complex **6**.[5] Computational studies support the involvement of chloride-assisted deprotonation in the subsequent step,[6] which affords the product and palladium(0). Oxidation of palladium(0) by copper(II) then occurs, regenerating palladium(II) species **1**. The role of copper(II) in the mechanism is poorly understood at present.



Equation *Section*11.3.4.2

The mode of hydroxypalladation is an important issue for the Wacker oxidation. Hydroxypalladation may occur either in a *syn* fashion through an inner-sphere mechanism or in an *anti* fashion via nucleophilic attack on the coordinated alkene (Eq. 3). Although the stereocenter in **4** is ultimately destroyed upon elimination, the mode of hydroxypalladation can influence the site selectivity of the reaction. Markovnikov-type addition of water to the more substituted carbon of the alkene forms a methyl ketone, while attack of water at the less substituted position ultimately yields an aldehyde. The mode of hydroxypalladation has been shown to affect the distribution of ketone and aldehyde products, and is also important in stereoselective Wacker cyclization reactions. ***(2)***

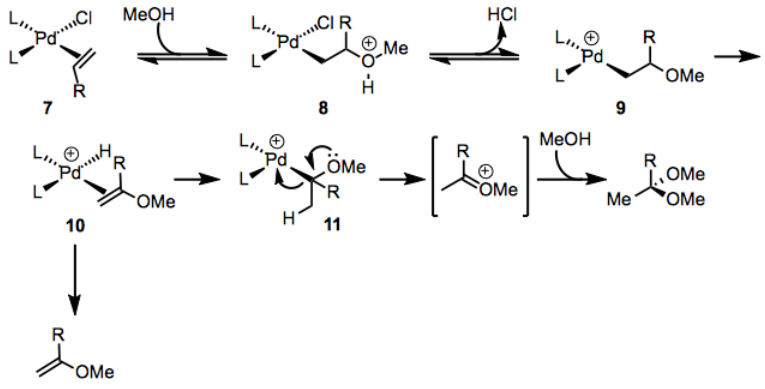


Equation *Section*11.3.4.3

At low concentrations of chloride ion, *syn*-hydroxypalladation appears to be the norm.[7] Water coordinates to the metal and migratory insertion into the Pd-OH bond occurs to generate **4** directly. At high concentrations of chloride ion, chloride competes with hydroxide for binding at palladium, and thus *anti*-hydroxypalladation may occur.[8] ***(3)***

Prevailing Mechanism: Alcohol Nucleophiles

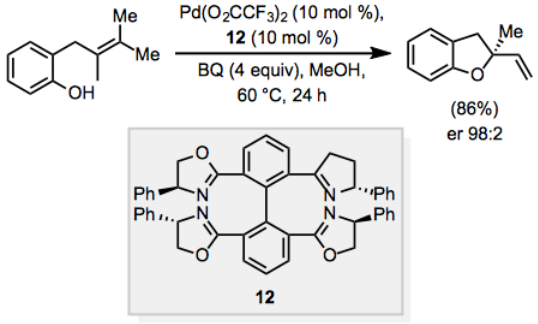
Alcohols may also be employed as nucleophiles in the Wacker process. The initial steps of the mechanism are similar to those for the Wacker oxidation with water, but the mechanisms diverge at alkoxy complex **11** (Eq. 4). Elimination of palladium occurs to generate an oxocarbenium ion, which may be captured by solvent to generate an acetal. Small amounts of vinyl ether products support the intermediacy of complex **10**.[9]



Equation *Section*11.3.4.4

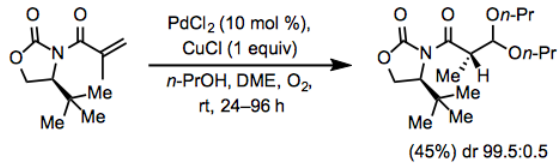
Enantioselective Variants

When the substrate contains a tethered nucleophile, such as a hydroxyl group or protected amine, the nucleophile may react to form a cyclic, allylic or vinylic ether or amine after β-hydride elimination. This process is known as the "Wacker cyclization," and when the product is allylic, a stereocenter may be established. Chiral ligands have been used to render the Wacker cyclization enantioselective. For example, use of tetra(dihydrooxazoline) ligand **12** and benzoquinone (BQ) as a co-oxidant resulted in formation of allylic ether product in an enantiomeric ratio of 98:2 (Eq. 5). [10]



Equation
***Section*11.3.4.5**

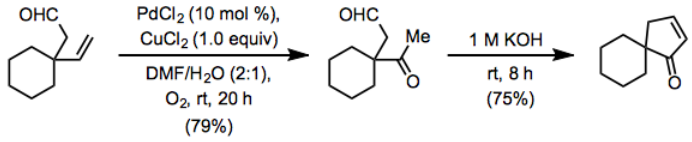
The Wacker process may also establish a stereocenter in 1,1-disubstituted alkenes via acetal formation. A chiral auxiliary in the alkene has been used successfully to generate chiral acetals with high diastereomeric ratio. The acetal forms at the more electron-deficient site of the alkene (Eq. 6).[11]



Equation ***Section*11.3.4.6**

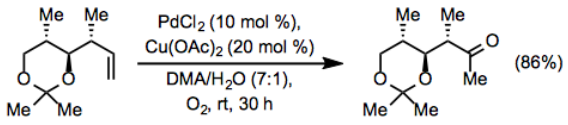
Scope and Limitations

Terminal alkenes are the most commonly employed substrates for the Wacker oxidation. Oxygen-containing functionality far from the reactive alkene is well tolerated by the reaction because palladium reacts selectively with the alkene in preference to lone pairs on oxygen. Wacker oxidation followed by intramolecular aldol condensation is a convenient method for the rapid synthesis of carbocycles (Eq. 7).[12]



Equation ***Section*11.3.4.7**

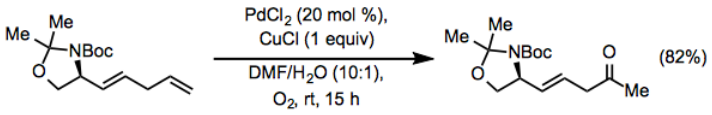
The original Wacker process and Tsuji-Wacker conditions can present problems for substrates containing acid-sensitive functionality, such as acetals and silyl ethers. Use of copper(II) chloride leads to the generation of strongly acidic hydrochloric acid. To mitigate this issue, a method employing copper(II) acetate has been developed. Some acid-sensitive groups are able to withstand the milder acetic acid generated by this method (Eq. 8).[13] Under similar conditions involving copper(I) chloride, a yield of only 56% was obtained.



Equation ***Section*11.3.4.8**

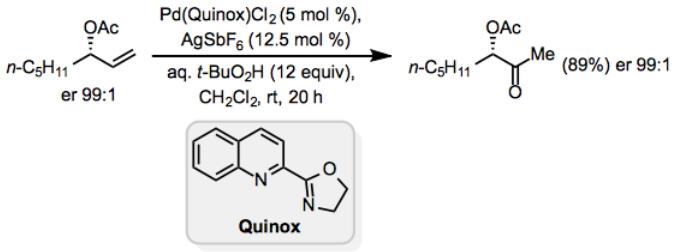
Unprotected amines coordinate strongly to palladium and thus cause problems for Wacker oxidations. Amines protected with electron-withdrawing substituents often do not interfere in Wacker oxidations,[14] although they may participate in aza-Wacker cyclizations if appropriately positioned in the substrate (see below).

Tri-substituted alkenes are completely inert to the conditions of the Wacker oxidation; only terminal and 1,1-disubstituted alkenes react. Terminal alkenes are usually oxidized selectively over internal alkenes, except under rather specialized circumstances.[15] Eq. 9 represents a typical case of selectivity for terminal alkenes.[14]



Equation ***Section*11.3.4.9**

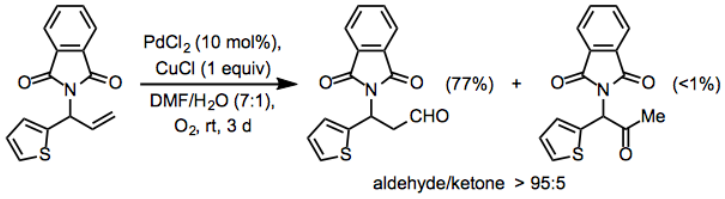
Lewis-basic functionality in the allylic or homoallylic position relative to the reactive alkene may cause unpredictable site selectivity in Wacker oxidations. Under standard Tsuji-Wacker conditions, unprotected allylic alcohols form mixtures of methyl ketone and aldehyde products.[16] The catalyst Pd(Quinox)Cl_2 was developed to address this problem; allylic alcohols react selectively in the presence of this catalyst to afford methyl ketones (Eq. 10).[17] *tert*-Butyl hydroperoxide (TBHP) is used as the oxygen source in this reaction.



Equation
***Section*11.3.4.10**

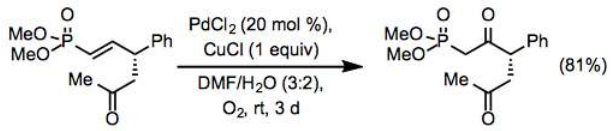
Protected, homoallylic alcohols generally form the methyl ketone selectively, but results are more unpredictable for unprotected homoallylic alcohols.[18]

Protected allylic amines generally give higher yields of aldehyde than comparable protected allylic alcohols; these results suggest that coordination of palladium to the Lewis base is responsible for the formation of aldehydes. Using a phthalimide group in the allylic position, the Wacker oxidation may be rendered completely selective for aldehydes (Eq. 11).[19]



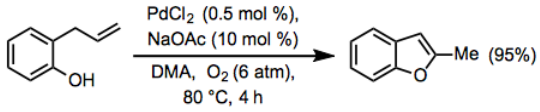
Equation
***Section*11.3.4.11**

Site selectivity in reactions of internal alkenes is low unless an allylic or homoallylic Lewis base is present in the substrate. Electron-withdrawing groups can direct oxidation to the β position of the alkene (Eq. 12), but relatively high catalyst loadings are required.[20]



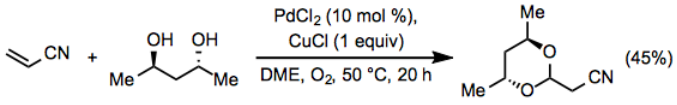
Equation
***Section*11.3.4.12**

When an appropriately situated nucleophile is present in the substrate, Wacker cyclization may occur to yield an allylic or vinylic ether (Eq. 13).[21] The aza-Wacker cyclization involves protected amino nucleophiles such as sulfonamides.[22]



Equation
*Section*11.3.4.13

When an alcohol is used in stoichiometric or solvent quantities or a diol is present in the substrate, acetal formation may occur. Acetal formation, like ketone formation, generally occurs with Markovnikov selectivity. For example, a Michael acceptor forms an acetal at the β position in the presence of (*R*,*R*)-2,4-pentanediol (Eq. 14).[23]

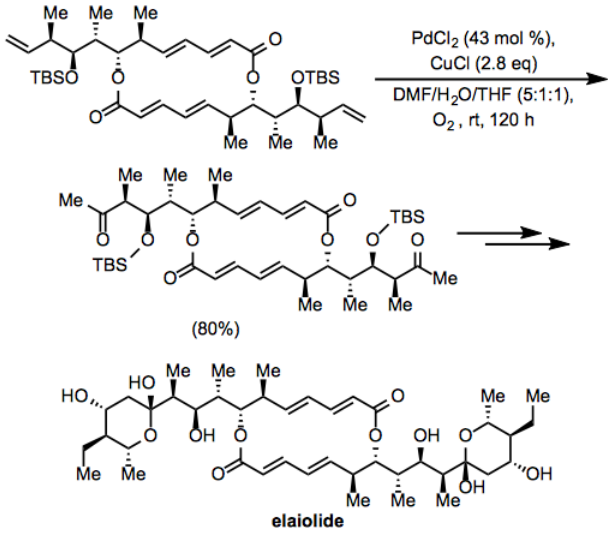


Equation
*Section*11.3.4.14

Synthetic Applications

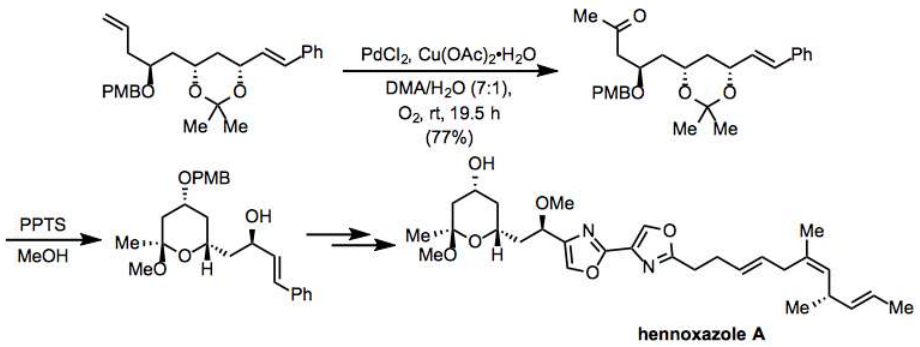
The Wacker oxidation has been used extensively in organic synthesis. A number of methods exist for the installation of terminal alkenes and the methyl ketone products of the reaction can be elaborated easily to more complex compounds. In addition, the reaction is aerobic and operationally simple.

The Wacker oxidation was employed in the course of synthesis of the macrolide elaiolide. Oxidation at two terminal alkenes in a C_2-symmetric intermediate afforded a diketone, which was subsequently elaborated to the symmetric natural product (Eq. 15).[24] Notably, the internal alkenes and esters in the intermediate appeared not to affect the oxidation.



Equation
*Section*11.3.4.15

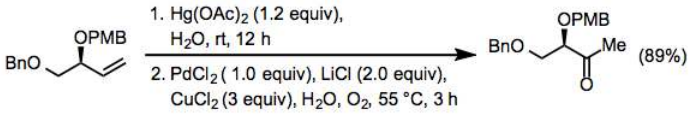
A modification of Tsuji-Wacker conditions employing copper(II) acetate was used in the course of a synthesis of hennoxazole A (Eq. 16).[25] After the oxidation, deprotection under acidic conditions led to the intramolecular formation of an acetal present in the target compound.



Equation
*Section*11.3.4.16

Comparison to Other Methods

Few true alternatives to the Wacker oxidation (that is, other hydration-oxidation reactions) are known. One rather harsh method involves oxymercuration followed by transmetalation to palladium (Eq. 17).[26]



Equation
*Section*11.3.4.17

Experimental Conditions and Procedure

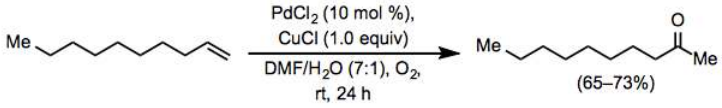
Typical Conditions

Tsuji-Wacker conditions represent a good starting point for experimental conditions for this reaction. Water is mixed with an organic co-solvent (often DMF) and 10 mol% $PdCl_2$, stoichiometric CuCl, and 1 atmosphere of oxygen gas. Copper(I) salts are generally superior to copper(II) salts because the former minimize the concentration of chloride in solution, encouraging *syn*-hydroxypalladation. Copper(I) is rapidly oxidized to copper(II) by dissolved oxygen; a period of 30 minutes prior to the introduction of the substrate is used to ensure that this oxidation is complete. For situations in which Tsuji-Wacker conditions fail, a wide variety of modifications of the reaction conditions may be employed.

Using high oxygen pressure and a judicious choice of solvent, Wacker oxidations can be carried out without the need for a co-oxidant. Certain ligands also promote direct O_2-coupled oxidations.[27]

Peroxides may also be used as the oxygen source in Wacker oxidations; these reactions do not require a co-oxidant. In the Pd(Quinox)/TBHP system, silver hexafluoroantimonate serves as a scavenger of chloride ions.

Experimental Procedure[4]



Equation
*Section*11.3.4.18

A 100-mL, 3-necked, round-bottomed flask was fitted with a magnetic stirring bar and a pressure-equalizing dropping funnel containing 1-decene (4.2 g, 30 mmol, 1.0 equiv). The flask was charged with a mixture of $PdCl_2$ (0.53 g, 3 mmol, 0.1 equiv), CuCl (2.97 g, 30 mmol, 1.0 equiv) and aqueous DMF (DMF/H_2O = 7:1, 24 mL). With the other outlets securely stoppered and wired down, an oxygen-filled balloon was placed over one neck, and the mixture was stirred at rt to allow oxygen uptake. After 1 h, the 1-decene (4.2 g, 30 mmol) was added over 10 min, and the solution was stirred vigorously at rt under an oxygen balloon. The color of the solution turned from green to black within 15 min and returned gradually to green. After 24 h, the mixture was poured into cold 3 N HCl (100 mL) and extracted with five, 50 mL portions of ether. The extracts were combined and washed successively with 50 mL of saturated aqueous $NaHCO_3$ solution, 50 mL of brine, and then dried over anhydrous magnesium sulfate. The solvent was

removed by evaporation and the residue was distilled using a 15 cm Vigreux column to give 2-decanone as a colorless oil (3.0–3.4 g, 65–73%): bp 43.5 °C (1 mm Hg); IR (neat) 1722 cm^{-1}; ^1H NMR (CCl_4) δ 2.37 (t, J = 7 Hz, 2H), 2.02 (s, 3H), 0.7–1.8 (m, 15H).

References

1. Michel, B. W.; Steffens, L. D.; Sigman, M. S. *Org. React.* **2014**, *84*, 2. (doi: 10.1002/0471264180.or084.02)
2. Phillips, F. C. *Am. Chem. J.* **1894**, *16*, 255.
3. Smidt, J.; Hafner, W.; Jira, R.; Sedlmeier, J.; Sieber, R.; Ruttinger, R.; Kojer, H. *Angew. Chem.* **1959**, *71*, 176.
4. [a] [b] Tsuji, J.; Nagashima, H.; Nemoto, H. *Org. Synth.* **1984**, *62*, 9.
5. Smidt, J.; Hafner, W.; Jira, R.; Sieber, R.; Sedlmeier, J.; Sabel, A. *Angew. Chem.* **1962**, *74*, 93.
6. Eshtiagh-Hosseini, H.; Beyramabadi, S. A.; Morsali, A.; Housaindokht, M. R. *J. Mol. Struct.: THEOCHEM* **2010**, *941*, 138.
7. Henry, P. M. *J. Am. Chem. Soc.* **1964**, *86*, 3246.
8. Bäckvall, J. E.; Akermark, B.; Ljunggren, S. O. *J. Chem. Soc., Chem. Commun.* **1977**, 264.
9. Balija, A. M.; Stowers, K. J.; Schultz, M. J.; Sigman, M. S. *Org. Lett.* **2006**, *8*, 1121.
10. Zhang, Y. J.; Wang, F.; Zhang, W. *J. Org. Chem.* **2007**, *72*, 9208.
11. Hosokawa, T.; Yamanaka, T.; Itotani, M.; Murahashi, S.-I. *J. Org. Chem.* **1995**, *60*, 6159.
12. Srikrishna, A.; Kumar, P. P. *J. Indian Chem. Soc.* **1999**, *76*, 521.
13. Smith, A. B., III; Cho, Y. S.; Friestad, G. K. *Tetrahedron Lett.* **1998**, *39*, 8765.
14. [a] [b] Reginato, G.; Mordini, A.; Verrucci, M.; Degl'Innocenti, A.; Capperucci, A. *Tetrahedron: Asymmetry* **2000**, *11*, 3759.
15. Ho, T.-L.; Chang, M. H.; Chen, C. *Tetrahedron Lett.* **2003**, *44*, 6955.
16. Muzart, J. *Tetrahedron* **2007**, *63*, 7505.
17. Michel, B. W.; Camelio, A. M.; Cornell, C. N.; Sigman, M. S. *J. Am. Chem. Soc.* **2009**, *131*, 6076.
18. Kang, S.-K.; Jung, K.-Y.; Chung, J.-U.; Namkoong, E.-Y.; Kim, T.-H. *J. Org. Chem.* **1995**, *60*, 4678.
19. Weiner, B.; Baeza, A.; Jerphagnon, T.; Feringa, B. L. *J. Am. Chem. Soc.* **2009**, *131*, 9473.
20. Yan, B.; Spilling, C. D. *J. Org. Chem.* **2008**, *73*, 5385.
21. Mitsudome, T.; Umetani, T.; Nosaka, N.; Mori, K.; Mizugaki, T.; Ebitani, K.; Kaneda, K. *Angew. Chem., Int. Ed.* **2006**, *45*, 481.
22. Hegedus, L. S.; McKearin, J. M. *J. Am. Chem. Soc.* **1982**, *104*, 2444.
23. Hosokawa, T.; Ataka, Y.; Murahashi, S. *Bull. Chem. Soc. Jpn.* **1990**, *63*, 166.
24. Barth, R.; Mulzer, J. *Tetrahedron* **2008**, *64*, 4718.
25. Yokokawa, F.; Asano, T.; Shioiri, T. *Tetrahedron* **2001**, *57*, 6311.
26. Ellis, J. M.; Crimmins, M. T. *Chem. Rev.* **2008**, *108*, 5278.
27. Cornell, C. N.; Sigman, M. S. *Org. Lett.* **2006**, *8*, 4117.

Contributors

- This page is based on *Organic Reactions*. The primary collection of full *Organic Reactions* chapters is maintained by John Wiley & Sons.

This page titled Section 11.3.4: Wacker (Smidt) Process is shared under a CC BY-NC-SA license and was authored, remixed, and/or curated by Kathryn Haas.

Section 11.3.5: Hydrogenation by Wilkinson's Catalyst

Organometallic Compounds as Hydrogenation Catalysts

Migratory insertions play an important role in catalysis.

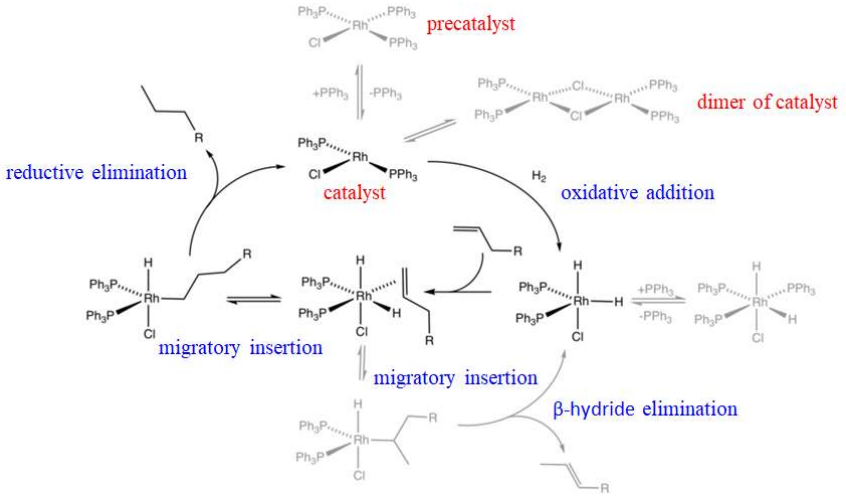


Figure ***Section*11.3.5.1**: Mechanism of the Wilkinson hydrogenation catalyst (Attribution: Smokefoot / CC BY-SA (https://creativecommons.org/licenses/by-sa/4.0) https://commons.wikimedia.org/wiki/F...cleJMBrown.png)

For example a Rh-catalyst called the Wilkinson catalyst is an effective hydrogenation catalyst for olefins. The mechanism of the hydrogenation involves a combination of oxidative additions, olefin migratory insertions, and reductive eliminations (Fig. ***Section*11.3.5.1**). Wilkinson's catalyst is the square planar chloro tris(triphenylphosphine) rhodium(I) complex. This molecule is actually a precatalyst that becomes the actual catalyst when it statistically loses a triphenylphosphine ligand producing chloro bis(triphenylphosphine) rhodium(I). The loss of this ligand is a reversible reaction, and thus the catalyst is in chemical equilibrium with the precatalyst. The actually catalyst is in a second chemical equilibrium with its dimer. The chloro bis(triphenylphosphine) rhodium(I) catalyst can undergo an oxidative addition in the presence of hydrogen to form a trigonal bipyramidal chlorodihydrido bis(triphenylphosphine) (III) rhodium complex. This species is in chemical equilibrium with an octahedral chlorodihydrido tris(triphenyl phosphine) rhodium(III) species that can form due to the presence of free triphenylphosphine ligands in the system. The trigonal bipyramidal species can then add an olefin that binds side-on to the Rh. Because the olefin is in cis-position to the hydride ligand it can undergo an olefin insertion. The Rh-C bond can either form with the first or the second carbon in the carbon chain of the olefin, giving a linear and a branched alkyl complex, respectively. The branched complex can undergo a β-hydride elimination thereby reforming the trigonal bipyramidal Rh-complex, and an olefin. This reaction is a side-reaction because the branched alkyl complex is sterically more crowded than the linear complex. The linear alkyl Rh complex can undergo a reductive elimination to form the linear alkane and the $RhCl(PPh_3)_2$ catalyst. This completes the catalytic cycle, and a new cycle can start.

This page titled Section 11.3.5: Hydrogenation by Wilkinson's Catalyst is shared under a CC BY-NC-SA license and was authored, remixed, and/or curated by Kathryn Haas.

- **12.2: Organometallic Catalysts** by Kai Landskron is licensed CC BY 4.0.

Section 11.3.6: Olefin Metathesis

Olefin Metathesis

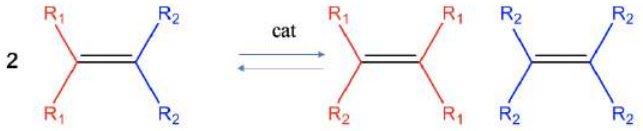


Figure ***Section*11.3.6.1**: Olefin metathesis

Olefin metathesis is a reaction which allows to cut and rearrange C=C double bonds in olefins to make new olefins (Fig. ***Section*11.3.6.1**). Formally, the carbon-carbon bond of the reactant is cleaved homoleptically and the two carbene fragments are combined in a different way. This reaction is typically an equilibrium reaction, and neither the reactants nor the products are clearly favored. This reaction is catalyzed by molybdenum arylamido carbene complexes or ruthenium carbene complexes.

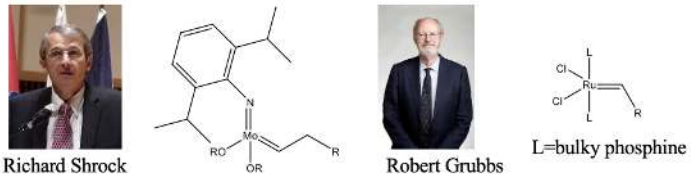


Figure ***Section*11.3.6.2**: Shrock catalyst (Attribution: R._Schrock_-_IChO_2012_Opening_Ceremony.JPG: A.mela93derivative work: Materialscientist / CC BY-SA (https://creativecommons.org/licenses/by-sa/3.0) https://commons.wikimedia.org/wiki/F...hrock_2012.jpg) and (Attribution: The Royal Society / CC BY-SA (https://creativecommons.org/licenses/by-sa/3.0) https://commons.wikimedia.org/wiki/F...al_Society.jpg)

The former are called Shrock catalysts, and the latter Grubbs catalysts named after their discoverers Richard Shrock and Robert Grubbs who received the Nobel prize for Chemistry in 2005 (Fig. ***Section*11.3.6.2**). The Schrock catalysts are more active, but also very sensitive to air and water. The Grubbs catalysts, while less active, are less sensitive to air and water.

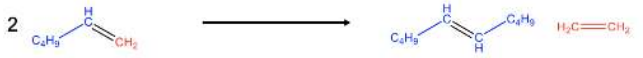


Figure ***Section*11.3.6.3**: Regular metathesis

Olefin metathesis often allows for simpler preparation of olefins compared to other methods. Olefin metathesis is particularly powerful when one olefin product is gaseous because then it can be quite easily removed from the chemical equilibrium by purging. This drives the chemical equilibrium to the right side. An example is the preparation of 5-decene from 1-hexene. Cleavage of the C=C double bond in the hexene leads to C_5 and C_1 carbene fragments (Fig. ***Section*11.3.6.3**). The two C_1 fragments can combine to form ethylene and the two C_5 fragments combine to 5-decene. The ethylene is volatile and can be purged from the reaction system thereby driving the chemical reaction to the right side.

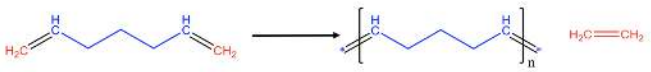


Figure ***Section*11.3.6.4**: Acylic diene metathesis (ADMET)

The same principles can also be applied to produce polymers from dienes with two terminal C=C double bonds at the chain ends. This is called acylic diene metathesis (ADMET), Fig. ***Section*11.3.6.4**. For instance the cleavage of the two terminal double bonds in a diene with seven C atoms leads to C_1 and C_5 fragments. The C_1 fragments can combine to form ethylene, and the C_5 fragments can combine to make an unsaturated polymer of the type $[CH(CH_2)_3CH]_n$. Again, the reaction can be driven to the right side by removing the gaseous ethylene from the reaction mixture through purging.

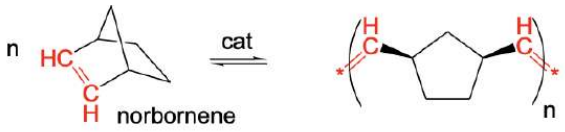


Figure *Section*11.3.6.5: Ring-opening metathesis polymerization (ROMP)

Another variation of olefin metathesis is ring-opening metathesis polymerization (ROMP). It allows to make polymers from strained cycloolefins, for example norbornene. The reaction driving force is the relief of the strain. Because the strain is removed in the polymer, the chemical equilibrium lies far on the right side. The reaction product in norbornene is a polymer with 5-membered rings that are interconnected by ethylene -CH=CH- units (Fig. *Section*11.3.6.5).

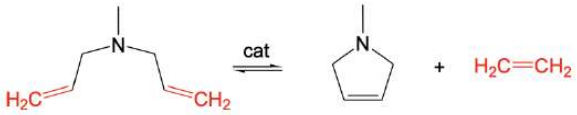


Figure *Section*11.3.6.6: Ring-closing metathesis (RCM)

The opposite of ROMP is ring-closure metathesis (RCM). RCM allows for the preparation of unstrained rings with C=C double bonds from dienes with C=C double bonds that are five or six carbon atoms apart. This distance is suitable to produce unstrained rings. In the shown example a five-membered ring with a C=C double bond is formed from a diene with terminal C=C double bonds that are five atoms apart.

The Mechanism of Olefin Metathesis

What is the mechanism of olefin metathesis?

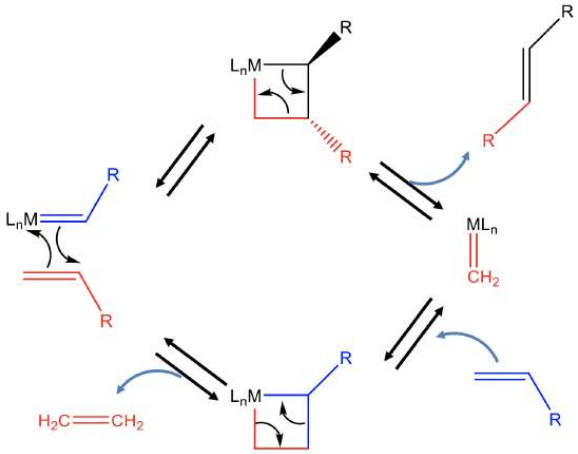


Figure *Section*11.3.6.7: The mechanism of olefin metathesis

In the first step, the alkene adds to the the carbene fragment of the catalyst in a 2+2 cycloaddition reaction to produce an unstable intermediate with a highly strained four-membered ring (Fig. *Section*11.3.6.7). This four membered ring can open to produce the first new alkene product R-CH=CH-R and a metal carbene species. This metal carbene can react with another reactant olefin to form another highly stained 4-ring intermediate via a 2+2 cycloaddition reaction. This ring can then reopen again to produce the second alkene metathesis product, in this case ethylene, and the original catalyst. The regenerated catalyst can then start a new catalytic cycle.

Dr. Kai Landskron (Lehigh University). If you like this textbook, please consider to make a donation to support the author's research at Lehigh University: Click Here to Donate.

This page titled Section 11.3.6: Olefin Metathesis is shared under a CC BY-NC-SA license and was authored, remixed, and/or curated by Kathryn Haas.

- **12.2: Organometallic Catalysts** by Kai Landskron is licensed CC BY 4.0.

Section 11.4: Heterogeneous Catalysts

Heterogeneous Catalysis

In **heterogeneous catalysis**, the catalyst is in a different phase from the reactants. At least one of the reactants interacts with the solid surface in a physical process called adsorption in such a way that a chemical bond in the reactant becomes weak and then breaks. Poisons are substances that bind irreversibly to catalysts, preventing reactants from adsorbing and thus reducing or destroying the catalyst's efficiency.

An example of heterogeneous catalysis is the interaction of hydrogen gas with the surface of a metal, such as Ni, Pd, or Pt. As shown in part (a) in Figure ***Section*11.4.2**, the hydrogen–hydrogen bonds break and produce individual adsorbed hydrogen atoms on the surface of the metal. Because the adsorbed atoms can move around on the surface, two hydrogen atoms can collide and form a molecule of hydrogen gas that can then leave the surface in the reverse process, called desorption. Adsorbed H atoms on a metal surface are substantially more reactive than a hydrogen molecule. Because the relatively strong H–H bond (dissociation energy = 432 kJ/mol) has already been broken, the energy barrier for most reactions of H_2 is substantially lower on the catalyst surface.

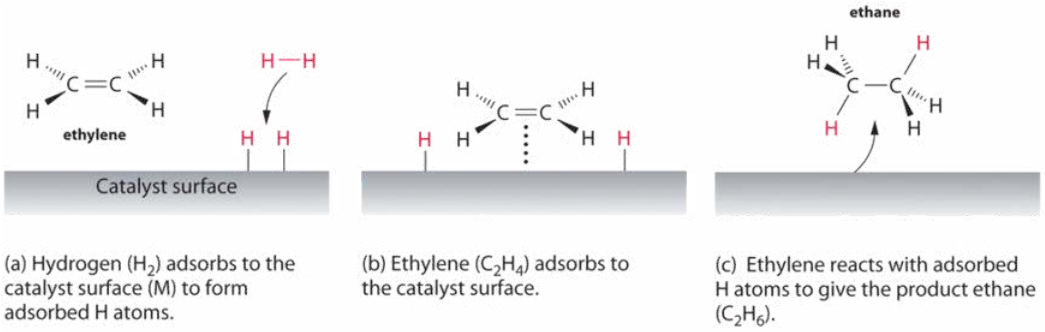


Figure ***Section*11.4.1**: Hydrogenation of Ethylene on a Heterogeneous Catalyst. When a molecule of hydrogen adsorbs to the catalyst surface, the H–H bond breaks, and new M–H bonds are formed. The individual H atoms are more reactive than gaseous H_2. When a molecule of ethylene interacts with the catalyst surface, it reacts with the H atoms in a stepwise process to eventually produce ethane, which is released. (CC BY-NC-SA; anonymous)

Figure ***Section*11.4.1** shows a process called *hydrogenation*, in which hydrogen atoms are added to the double bond of an alkene, such as ethylene, to give a product that contains C–C single bonds, in this case ethane. Hydrogenation is used in the food industry to convert vegetable oils, which consist of long chains of alkenes, to more commercially valuable solid derivatives that contain alkyl chains. Hydrogenation of some of the double bonds in polyunsaturated vegetable oils, for example, produces margarine, a product with a melting point, texture, and other physical properties similar to those of butter.

Several important examples of industrial heterogeneous catalytic reactions are in Table ***Section*11.4.1**. Although the mechanisms of these reactions are considerably more complex than the simple hydrogenation reaction described here, they all involve adsorption of the reactants onto a solid catalytic surface, chemical reaction of the adsorbed species (sometimes via a number of intermediate species), and finally desorption of the products from the surface.

Table ***Section*11.4.1**: Some Commercially Important Reactions that Employ Heterogeneous Catalysts

Commercial Process	Catalyst	Initial Reaction	Final Commercial Product
contact process	V_2O_5 or Pt	$2SO_2 + O_2 \rightarrow 2SO_3$	H_2SO_4
Haber process	Fe, K_2O, Al_2O_3	$N_2 + 3H_2 \rightarrow 2NH_3$	NH_3
Ostwald process	Pt and Rh	$4NH_3 + 5O_2 \rightarrow 4NO + 6H_2O$	HNO_3
water–gas shift reaction	Fe, Cr_2O_3, or Cu	$CO + H_2O \rightarrow CO_2 + H_2$	H_2 for NH_3, CH_3OH, and other fuels
steam reforming	Ni	$CH_4 + H_2O \rightarrow CO + 3H_2$	H_2
methanol synthesis	ZnO and Cr_2O_3	$CO + 2H_2 \rightarrow CH_3OH$	CH_3OH
Sohio process	bismuth phosphomolybdate	$\mathbf{CH_2{=}CHCH_3 + NH_3 + \frac{3}{2}O_2 \rightarrow CH_2{=}CHCN + 3H_2O}$	$\mathbf{CH_2{=}CHCN}$ acrylonitrile
catalytic hydrogenation	Ni, Pd, or Pt	RCH=CHR′ + H2 → RCH_2—CH_2R'	partially hydrogenated oils for margarine, and so forth

This page titled Section 11.4: Heterogeneous Catalysts is shared under a CC BY-NC-SA license and was authored, remixed, and/or curated by Kathryn Haas.

- **14.7: Catalysis** is licensed CC BY-NC-SA 3.0.

Section 11.4.1: Ziegler-Natta Polymerizations

Another example of an organometallic catalytic reaction is the Ziegler-Natta olefin polymerization. This reaction is of high industrial importance for the production of olefins like polyethylene. There are both heterogeneous and homogeneous Ziegler-Natta catalysts. The mechanism for the homogeneous catalysts is generally well understood. Homogeneous catalysts are typically metallocene catalysts.

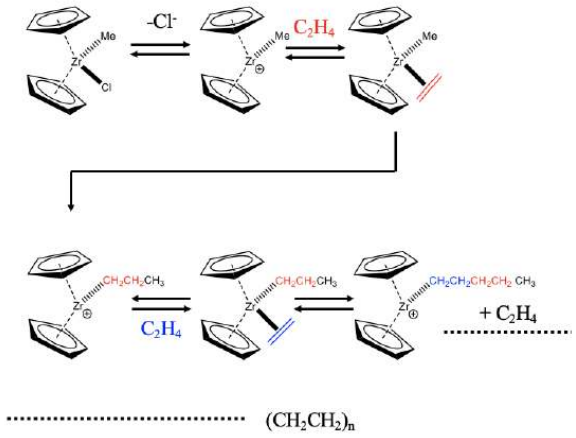


Figure ***Section*11.4.1.1**: Zirconium-based Ziegler-Natta catalyst (Attribution: A. Vedernikov, U Maryland (modified).)

An example of a zirconium-based catalyst is shown (Fig. ***Section*11.4.1.1**). The catalyst is a coordinatively unsaturated complex cation with two cyclopentadienyl rings and a methyl group. The catalyst is formed from its precatalyst, a neutral molecule with an additional chloro ligand. The catalyst oxidatively adds an olefin like an ethylene molecule to the coordinatively unsaturated site. This step is followed an olefin insertion step that produces a propyl group. The migratory insertion leads to the formation of a vacant site, that can be re-oocupied by another ethylene molecule. This molecule can insert into the propyl chain thereby prolonging the propyl chain to a pentyl chain. The olefin insertion step generates another vacant site that can be reoccupied by a new ethylene molecule. Repeating the catalytic cycle many times eventually leads to polyethylene.

The Ziegler-Natta (ZN) catalyst, named after two chemists: Karl Ziegler and Giulio Natta, is a powerful tool to polymerize α-olefins with high linearity and stereoselectivity (Figure 1). A typical ZN catalyst system usually contains two parts: a transition metal (Group IV metals, like Ti, Zr, Hf) compound and an organoaluminum compound (co-catalyst). The common examples of ZN catalyst systems include $TiCl_4$ + Et_3Al and $TiCl_3$ + $AlEt_2Cl$.

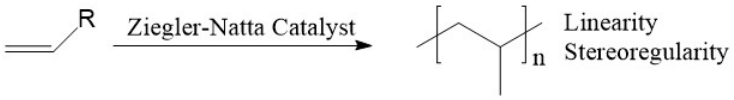


Figure ***Section*11.4.1.2**: The generic reaction equation for polymerization of -olefins.

In 1953, German chemist Karl Ziegler discovered a catalytic system able to polymerize ethylene into linear, high molecular weight polyethylene which conventional polymerization techniques could not make.[1] The system contained a transition metal halide with a main group element alkyl compound (Figure ***Section*11.4.1.3**).

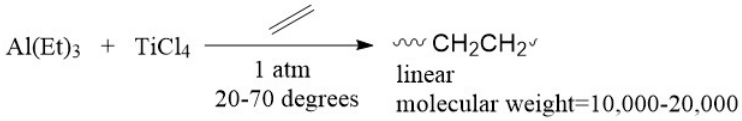


Figure ***Section*11.4.1.3**: Linear polyethylene obtained by Ziegler's catalytic system (20-70).

Following the catalytic design, Italian chemist Giulio Natta found that polymerization of α-olefins resulted in stereoregular structures,[2] either syndiotactic or isotactic, depending on the catalyst used (Figure ***Section*11.4.1.4**). Because of these important discoveries, Karl Ziegler and Giulio Natta shared the Nobel Prize in Chemistry in 1963.

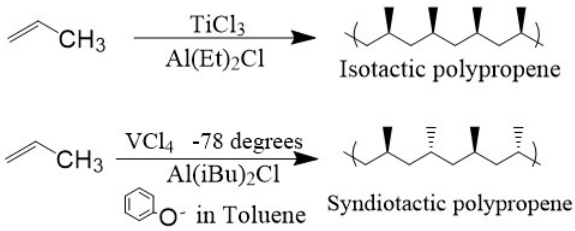


Figure ***Section*11.4.1.4**: The ZN catalytic polymerization of linear polypropene with two different stereoregular structures.

Advantages over traditional polymerization method

Traditionally, polymerization of α-olefins was done by radical polymerization (Figure ***Section*11.4.1.5**). Problem with this technique was that the formation of undesired allylic radicals leaded to branched polymers.[3] For example, radical polymerization of propene gived branched polymers with large molecular weight distribution. Also, radical polymerization had no control over stereochemistry. Linear unbranched polyethylene and stereoregulated polypropylene could not be fabricated by free radical polymerization. This technique largely limited the potential applications of these polymeric materials.

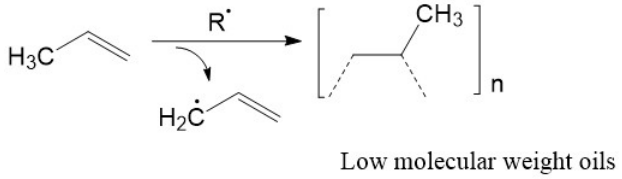


Figure ***Section*11.4.1.5**: The radical polymerization of propylene using traditional method.

The invention of ZN catalyst successfully addressed these two problems. The catalyst can give linear α-olefin polymers with high and controllable molecular weights. Moreover, it makes the fabrication of polymers with specific tacticity possible. By controlling the stereochemistry of products, either syndiotactic or isotactic polymers can be achieved.

Mechanism of Ziegler-Natta catalytic polymerization

Activation of Ziegler-Natta catalyst

It is necessary to understand the catalyst's structure before understanding how this catalyst system works. Herein, $TiCl_4$+$AlEt_3$ catalyst system is taken as an example. The titanium chloride compound has a crystal structure in which each Ti atom is coordinated to 6 chlorine atoms. On the crystal surface, a Ti atom is surrounded by 5 chlorine atoms with one empty orbital to be filled. When Et_3Al comes in, it donates an ethyl group to Ti atom and the Al atom is coordinated to one of the chlorine atoms. Meanwhile, one chlorine atom from titanium is kicked out during this process. Thus, the catalyst system still has an empty orbital (Figure ***Section*11.4.1.6**). The catalyst is activated by the coordination of $AlEt_3$ to Ti atom.

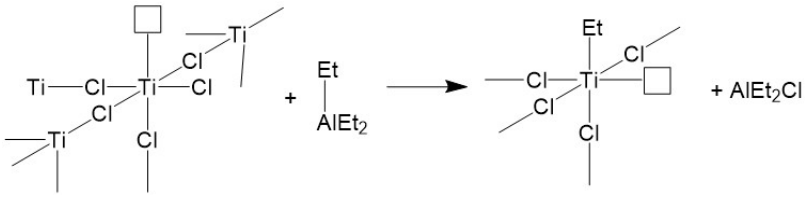


Figure ***Section*11.4.1.6**: The activation of ZN catalyst system by coordination of $AlEt_3$ to Ti atom.

Initiation step

The polymerization reaction is initiated by forming alkene-metal complex. When a vinyl monomer like propylene comes to the active metal center, it can be coordinated to Ti atom by overlapping their orbitals. As shown in Figure ***Section*11.4.1.7**, there is an empty dxy orbital and a filled dx^2-y^2 orbital in Ti's outermost shell (the other four orbitals are not shown here). The carbon-carbon double bond of alkene has a pi bond, which consists of a filled pi-bonding orbital and an empty pi-antibonding orbital. So, the alkene's pi-bonding orbital and the Ti's dxy orbital come together and share a pair of electrons. Once they're together, that Ti's dx^2-y^2 orbital comes mighty close to the pi-antibonding orbital, sharing another pair of electrons.

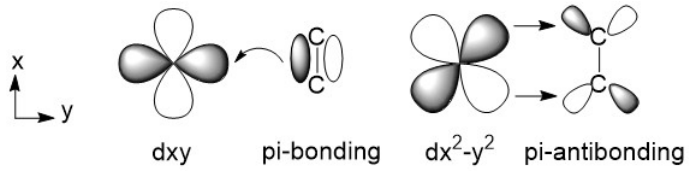


Figure *Section*11.4.1.7: Molecular orbitals representation of monomer coordinating to metal center.

The formed alkene-metal complex (1) then goes through electron shuffling, with several pairs of electrons shifting their positions: The pair of electrons from the carbon-carbon pi-bond shifts to form Ti-carbon bond, while the pair of electrons from the bond between Ti and AlEt3' ethyl group shifts to form a bond between the ethyl group and the methyl-substituted carbon of propylene (Figure *Section*11.4.1.8). After electron shuffling, Ti is back with an empty orbital again, needing electrons to fill it (2).

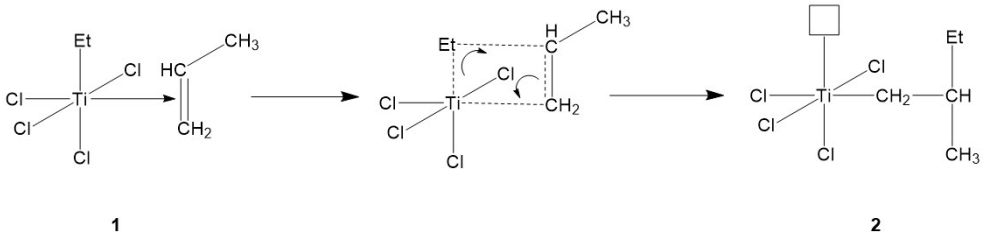


Figure *Section*11.4.1.8: The formation process of alkene-metal complex.

Propagation step

When other propylene molecules come in, this process starts over and over, giving linear polypropylene (Figure *Section*11.4.1.9).

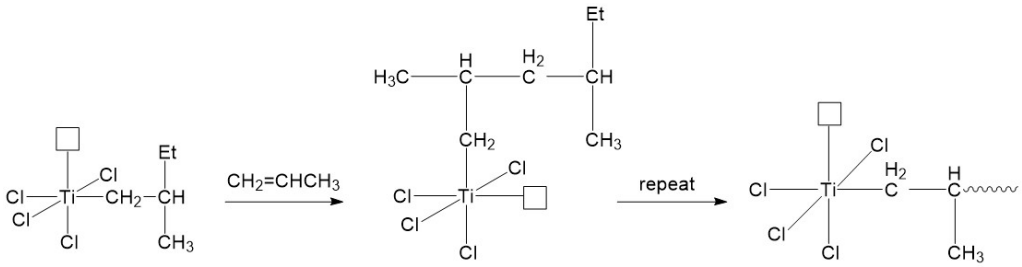


Figure *Section*11.4.1.9: Propagation towards polymeric chains.

Termination step

Termination is the final step of a chain-growth polymerization, forming "dead" polymers (desired products). Figure *Section*11.4.1.10 illustrates several termination approaches developed with the aid of co-catalyst $AlEt_3$.[4]

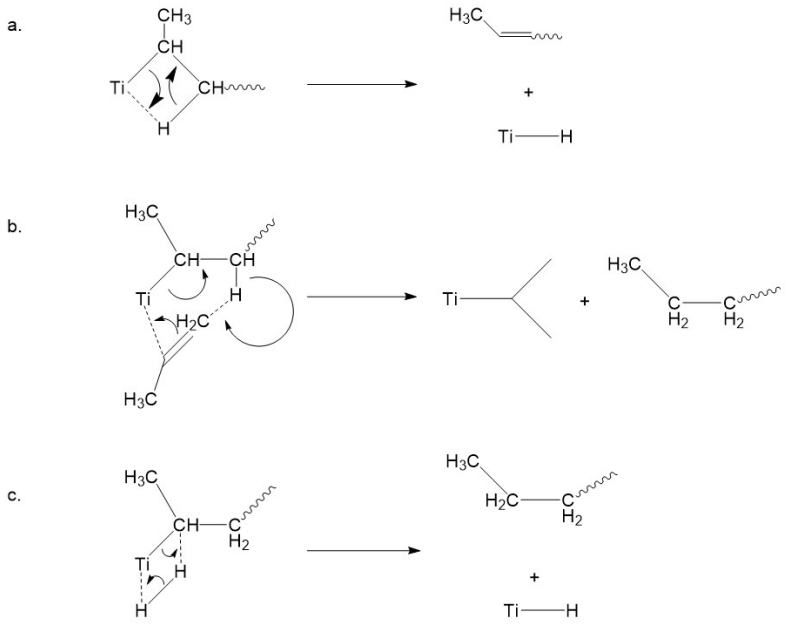


Figure *Section*11.4.1.10: Three termination approaches: (a) β-elimination from the polymer chain, forming metal hydride; (b) β-elimination with hydrogen transfer to monomer; (c)hydrogenation.

Mechanistic study: kinetic isotope effect experiments

Unlike the mechanism discussed above, there is also a competing mechanism proposed by Ivin and coworkers.[5] They proposed that a 1,2-hydrogen shift occurs prior to monomer association, giving a carbene intermediate (Figure *Section*11.4.1.11).

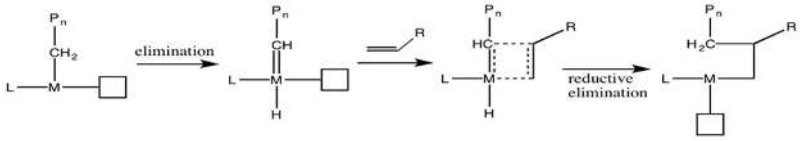


Figure *Section*11.4.1.11: Alternative propagation mechanism: hydride shift prior to monomer association.

To determine the actual mechanism, Grubbs[6] conducted kinetic isotope effect (KIE) experiments. Due to their different weights, carbon-deuterium bond reacts slower than carbon-hydrogen bond (Figure *Section*11.4.1.12). If such bonds are involved in the rate-determining step, the isotopic species should proceed in lower rate.

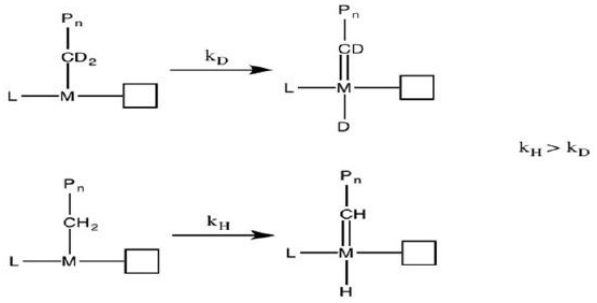


Figure *Section*11.4.1.12: Carbon-deuterium bonds react slower than carbon-hydrogen bonds.

In Grubbs's experiment, deuterated ethylene and normal ethylene were catalyzed by Ziegler-Natta catalyst with 1:1 ratio (Figure *Section*11.4.1.13). The result showed that H/D ratio in the resulting polymers was still 1:1.6 This indicated that no carbon-hydrogen bond cleavage or formation is involved in the rate determining step. Therefore, the mechanism proposed by Ivin was excluded.

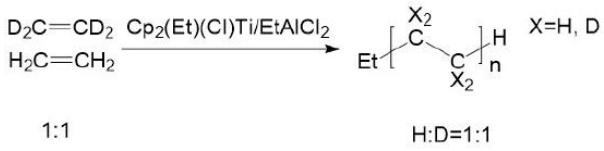


Figure ***Section*11.4.1.13**: KIE experiment excludes Ivin's mechanism.

Regio- and stero-selectivity

Regio-selectivity

For propene polymerization, most ZN catalysts are highly regioselective, favoring 1,2-primary insertion [M-R + CH2=CH(Me)=M-CH2-CH(Me)(R)] (Figure ***Section*11.4.1.14**), due to electronic and steric effects.[7]

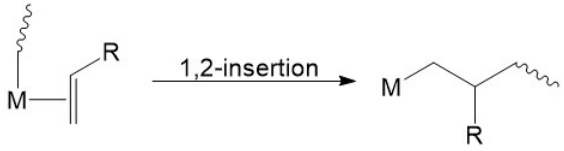


Figure ***Section*11.4.1.14**: Primary insertion occurs in ZN-catalytic system to give regioselective products.

Stereo-selectivity

Stereochemistry of polymers made from ZN-catalyst can be well regulated by rational design of ligands. By using different ligand system, either syndiotactic or isotactic polymers can be obtained (Figure ***Section*11.4.1.15**).

The relative stereochemistry of adjacent chiral centers within a macromolecule is defined as tacticity. Three kinds of stereochemistry are possible: isotactic, syndiotactic and atactic. In isotactic polymers, substituents are located on the same side of the polymer backbone, while substituents on syodiotactic polymers have alternative positions. In atactic polymers, substituents are placed randomly along the chain.

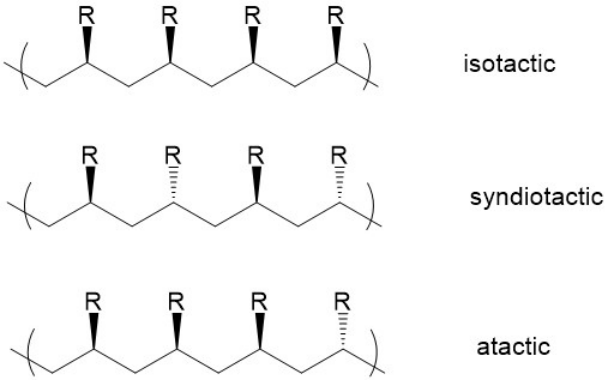


Figure ***Section*11.4.1.15**: Tacticity of macromolecules

Choice of ZN catalyst regulates the stereochemistry. We use propylene polymerization as an example here. Recall the mechanism section, a monomer approaches the metal center and forms a four-membered ring intermediate. The binding of a monomer to the reactive metal-carbon bond should occur in from the least hindered site.[8] As shown in Figure ***Section*11.4.1.16**, the trans-complex in which methyl on the growing chain is trans to the methyl group on the incoming monomer, should be energetically favored than the cis-complex, as the trans-complex experience less steric effect.

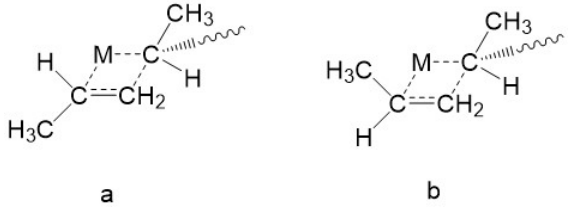


Figure ***Section*11.4.1.16**: The active state a (trans) is more stable than b (cis) due to less steric effects of methyl groups.

Following the trans- complex, the methyl group on the newly added monomer is trans to that on the previous monomer. The step repeats so that a syndiotactic polypropylene is obtained (Figure ***Section***11.4.1.17a). However, if the metal center is coordinated with bulky ligands (e.g. –iBu, -Et2 groups), as denoted by Y in Figure ***Section***11.4.1.17b, the incoming monomer will adopt a cis-conformation to avoid serious steric effect with the bulky ligand. Thus, at the presence of bulky ligand, the propylene monomer is cis to the growing chain. This results in a isotactic product.

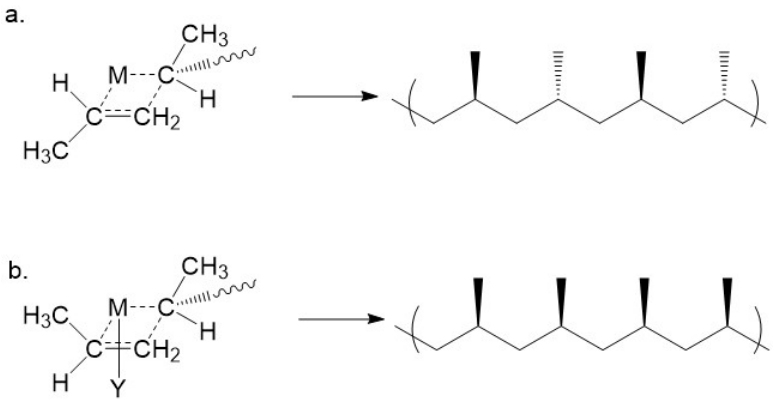


Figure ***Section***11.4.1.17: a. Trans-intermediate avoids 1,3-strain of methyl groups, producing syndiotactic polypropylene; b. at the presence of bulky ligand Y, a cis-intermediate is adopted, generating isotactic polypropylene.

Applications

ZN catalysts have provided a worldwide profitable industry with production of more than 160 billion pounds and creation of numerous positions.[9] These products have been extensively applied in different areas, largely improving the quality of people's life. They can catalyze α-olefins to produce various commercial polymers, like polyethylene, polypropylene and Polybutene-1. Polyethylene and polypropylene is reported to be the top two widely used synthetic plastic in the word.[10]

Among the polyethylene fabricated by ZN catalysts, there are three major classes: high density polyethylene (HDPE), linear low density polyethylene (LLDPE), and ultra-high molecular weight polyethylene (UHMWPE). HDPE, a linear homopolymer, is widely applied in garbage containers, detergent bottles and water pipes because of its high tensile strength. Compared with HDPE whose branching degree is quite low, LLDPE has many short branches. Its better toughness, flexibility and stress-cracking resistance makes it suitable for materials like cable coverings, bubble wrap and so on. UHMWPE is polyethylene with a molecular weight between 3.5 and 7.5 million. This material is extremely tough and chemically resistant. Therefore, it is often used to make gears and artificial joints.

Compared to polyethylene, polypropylene has enhanced mechanical properties and thermal resistance because of the additional methyl group. Moreover, isotactic polypropylene is stiffer and more resistant to creep than atactic polypropylene. Polypropylene has a wide range of applications in clothing, medical plastics, food packing, and building construction.

Substrate scope and limitations

ZN catalysts are effective for polymerization of α-Olefins (ethylene, propylene) and some dienes (butadiene, isoprene). However, they don't work for some other monomers, such as 1.2 disubstituted double bonds. Vinyl chloride cannot be polymerized by ZN catalyst either, because free radical vinyl polymerization is initiated during the reaction. Another situation that ZN catalysts don't work is when the substrate is acrylate. The reason is that ZN catalysts often initiate anionic vinyl polymerization in those monomers.[11]

References

1. Ziegler, K.; Holzkamp, E.; Breil, H.; Martin, H., Polymerisation Von Athylen Und Anderen Olefinen. Angew Chem Int Edit 1955, 67 (16), 426-426.
2. Natta, G., Une Nouvelle Classe De Polymeres D Alpha-Olefines Ayant Une Regularite De Structure Exceptionnelle. J Polym Sci 1955, 16 (82), 143-154.
3. Mulhaupt, R., Catalytic polymerization and post polymerization catalysis fifty years after the discovery of Ziegler's catalysts. Macromol Chem Phys 2003, 204 (2), 289-327.

4. Sinn, H.; Kaminsky, W., Ziegler-Natta Catalysis. In Advances in Organometallic Chemistry, Stone, F. G. A.; Robert, W., Eds. Academic Press: 1980; Vol. Volume 18, pp 99-149.
5. Ivin, K. J.; Rooney, J. J.; Stewart, C. D.; Green, M. L.; Mahtab, R., Mechanism for the stereospecific polymerization of olefins by Ziegler–Natta catalysts. Journal of the Chemical Society, Chemical Communications 1978, (14), 604-606.
6. Soto, J.; Steigerwald, M. L.; Grubbs, R. H., Concerning the Mechanism of Ziegler-Natta Polymerization - Isotope Effects on Propagation Rates. J Am Chem Soc 1982, 104 (16), 4479-4480.
7. Busico, V.; Cipullo, R.; Pellecchia, R.; Ronca, S.; Roviello, G.; Talarico, G., Design of stereoselective Ziegler-Natta propene polymerization catalysts. P Natl Acad Sci USA 2006, 103 (42), 15321-15326.
8. Zambelli, A., Stereoregulation of Propylene Polymerization. Abstr Pap Am Chem S 1974, 34-34.
9. Ittel, S. D.; Johnson, L. K.; Brookhart, M., Late-metal catalysts for ethylene homo- and copolymerization. Chem Rev 2000, 100 (4), 1169-1203.
10. Macbride, R. R., High Molecular-Weight Polyethylene Drums Show Signs of Becoming Big Business. Mod Plast 1975, 52 (12), 10-&.
11. Ivan, B., Comparison of Living Polymerization Systems. Macromol Symp 1994, 88, 201-215.

Contributors and Attributions

- Fangyuan Dong and Ru Deng

This page titled Section 11.4.1: Ziegler-Natta Polymerizations is shared under a CC BY-NC-SA 4.0 license and was authored, remixed, and/or curated by Kathryn Haas.

- **12.2: Organometallic Catalysts** by Kai Landskron is licensed CC BY 4.0.

Section 11.4.2: Water-Gas Shift Reaction

The **water-gas shift reaction** (WGSR) describes the reaction of carbon monoxide and water vapor (steam) at very high temperatures to form carbon dioxide and hydrogen:

$$\mathbf{CO + H_2O \rightleftharpoons CO_2 + H_2} \qquad \text{(Section 11.4.2.1)}$$

The WGSR is a highly valuable industrial reaction that is used in the manufacture of ammonia, hydrocarbons, methanol, and hydrogen. Its most important application is in the conversion of carbon monoxide or other hydrocarbons to produce hydrogen gas, an important source of fuel for a modern hydrogen economy. If hydrogen could be produced at low cost and using a renewable resource, it could significantly advance the movement to sustainable energy.

Most of the catalysts that are used for this process are heterogeneous catalysts. Unfortunately, the process using heterogeneous catalysts occurs only at extremely high temperatures and pressures. The high energy cost of performing the reaction limits its industrial utility, and there are efforts to produce homogeneous catalysts that catalyze the reaction at more mild conditions. Another limitation is that the reaction requires sufficient quantities of **CO**, which are primarily obtained from non-renewable coal or petroleum sources. However, there are processes that can convert methane gas, which is an abundant greenhouse gas, to .

The WGSR has been extensively studied for over a hundred years. The kinetically relevant mechanism depends on the catalyst composition and the temperature. Two mechanisms have been proposed: an associative Langmuir–Hinshelwood mechanism and a redox mechanism. The redox mechanism is generally regarded as kinetically relevant during the high-temperature WGSR (> 350 °C) over the industrial Fe-Cr catalyst. Historically, there has been much more controversy surrounding the mechanism at low temperatures. Recent experimental studies confirm that the associative carboxyl mechanism is the predominant low temperature pathway on metal-oxide-supported transition metal catalysts.

Associative mechanism

In 1920 Armstrong and Hilditch first proposed the associative mechanism. In this mechanism CO and H_2O are adsorbed onto the surface of the catalyst, followed by formation of an intermediate and the desorption of H_2 and CO_2. In general, H_2O dissociates onto the catalyst to yield adsorbed OH and H. The dissociated water reacts with CO to form a carboxyl or formate intermediate. The intermediate subsequently dehydrogenates to yield CO_2 and adsorbed H. Two adsorbed H atoms recombine to form H_2.

There has been significant controversy surrounding the kinetically relevant intermediate during the associative mechanism. Experimental studies indicate that both intermediates contribute to the reaction rate over metal oxide supported transition metal catalysts. However, the carboxyl pathway accounts for about 90% of the total rate owing to the thermodynamic stability of adsorbed formate on the oxide support. The active site for carboxyl formation consists of a metal atom adjacent to an adsorbed hydroxyl. This ensemble is readily formed at the metal-oxide interface and explains the much higher activity of oxide-supported transition metals relative to extended metal surfaces. The turn-over-frequency for the WGSR is proportional to the equilibrium constant of hydroxyl formation, which rationalizes why reducible oxide supports (e.g. CeO_2) are more active than irreducible supports (e.g. SiO_2) and extended metal surfaces (e.g. Pt). In contrast to the active site for carboxyl formation, formate formation occurs on extended metal surfaces. The formate intermediate can be eliminated during the WGSR by using oxide-supported atomically dispersed transition metal catalysts, further confirming the kinetic dominance of the carboxyl pathway.

Redox mechanism

The redox mechanism involves a change in the oxidation state of the catalytic material. In this mechanism, CO is oxidized by an O-atom intrinsically belonging to the catalytic material to form CO_2. A water molecule undergoes dissociative adsorption at the newly formed O-vacancy to yield two hydroxyls. The hydroxyls disproportionate to yield H_2 and return the catalytic surface back to its pre-reaction state.

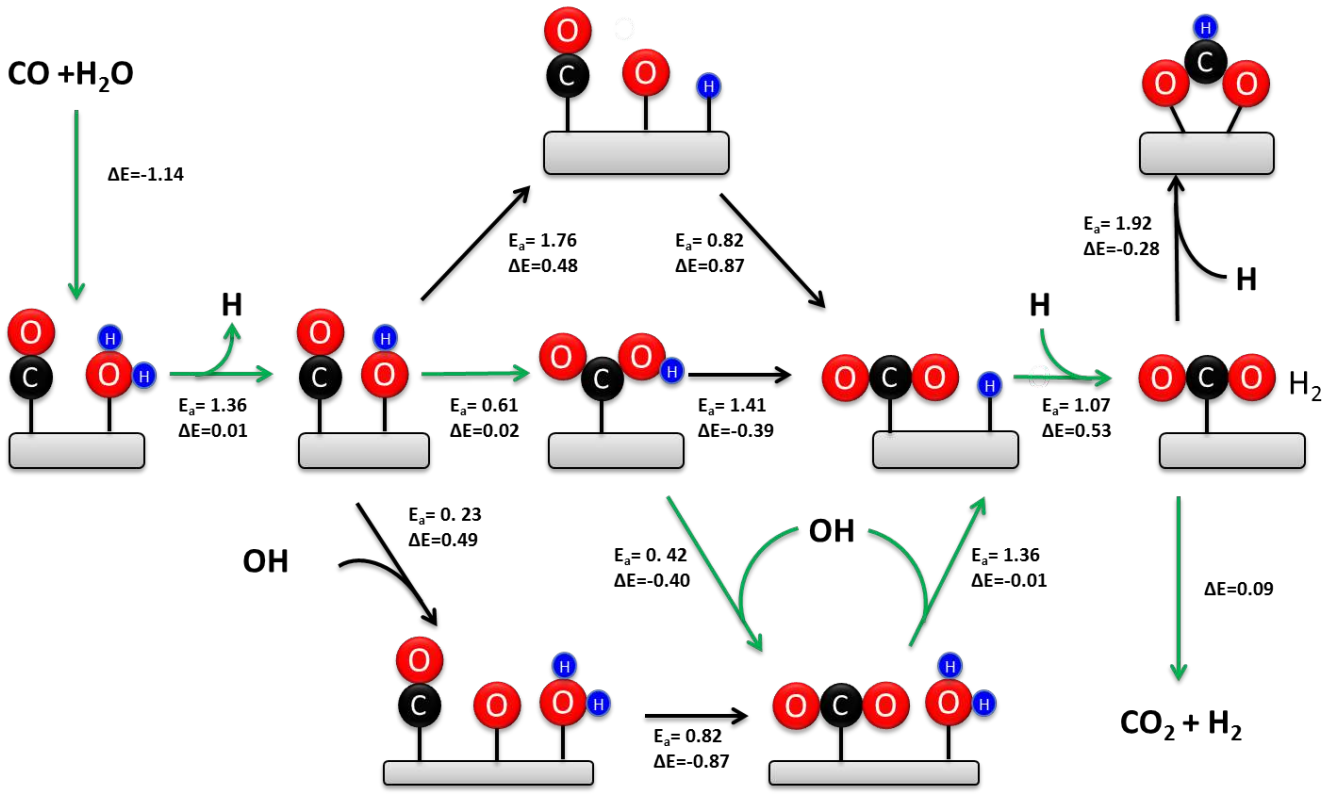


Figure *Section*11.4.2.1: Proposed associative and redox mechanisms of the water gas shift reaction. (Zwickipedia, WGS mechanism, CC BY-SA 3.0)

Source: https://en.Wikipedia.org/wiki/Water%...shift_reaction

This page titled Section 11.4.2: Water-Gas Shift Reaction is shared under a CC BY-NC-SA license and was authored, remixed, and/or curated by Kathryn Haas.

Section 11.5: Problems

This page titled Section 11.5: Problems is shared under a CC BY-NC-SA license and was authored, remixed, and/or curated by Kathryn Haas.

Section 11.5.1: Concept Review Questions Chapter 12

Concept Review Questions

Section 1

1) What is an oxidative addition?

2) What is a reductive elimination?

3) What is a cis and a trans addition, respectively?

4) Does the coordination number in oxidative additions always increase? Explain.

5) What is the reverse reaction of an oxidative addition?

6) What is a migratory insertion?

7) Are migratory insertions reversible reactions?

Section 2

1) Why are transition metal alkyl complexes that have alkyl groups longer than 1 carbon atom often unstable?

2) What is meant by beta-hydride elimination?

3) What is alpha-abstraction?

4) What is a nucleophilic displacement reaction?

5) What is meant by an oxidative addition of an intact ligand?

6) Write the catalytic cyclic for the deuteration of benzene with Cp_2TaH_3 as a catalyst. Name each reaction step.

7) What is Collman's reagent and how is it being used?

8) What is Wilkinson's catalyst, and what reactions can it be used for. Write the catalytic cycle.

9) Write done the reaction mechanism for the Ziegler-Natta olefin polymerization.

10) What is carbene migratory insertion?

11) Write down the catalytic cycle for the hydroformylation of olefins.

12) Name three hydrocarbonylation reactions. What are the reactants?

13) Write down the mechanism for the Monsanto acetic acid process.

14) What is olefin metathesis?

15) What is ring-opening olefin polymerization (ROMP)?

16) What is acyclic diene metathesis?

17) Why are olefins with terminal C=C double bonds particularly useful in olefin metathesis?

18) What is ring-closing metathesis?

19) What are the characteristics of Schrock and Grubbs catalysts, respectively?

20) Write down the catalytic cycle for olefin metathesis.

Dr. Kai Landskron (Lehigh University). If you like this textbook, please consider to make a donation to support the author's research at Lehigh University: Click Here to Donate.

This page titled Section 11.5.1: Concept Review Questions Chapter 12 is shared under a CC BY-NC-SA 4.0 license and was authored, remixed, and/or curated by Kathryn Haas.

- **Concept Review Questions Chapter 12** by Kai Landskron is licensed CC BY 4.0.

Section 11.5.2: Homework Problems Chapter 12

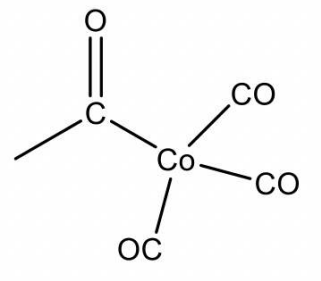
Homework Problems

Section 1

Exercise 1

The coordination compound $CH_3Co(CO)_4$ undegoes a migratory insertion. What is the reaction product?

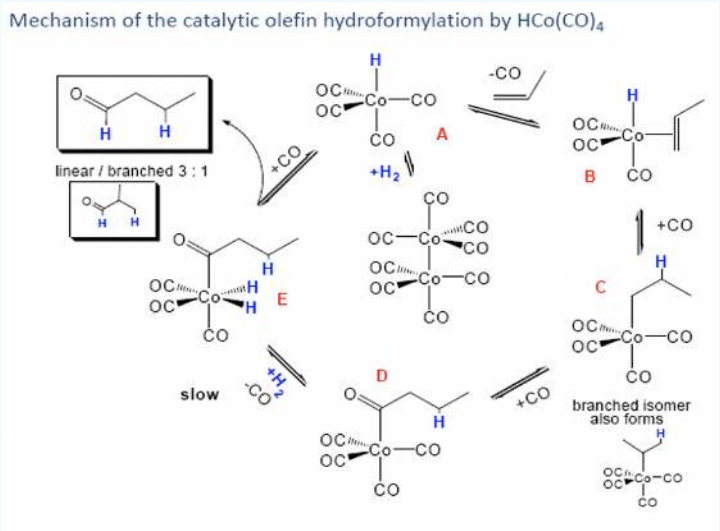
Answer



Section 2

Exercise 1

Identify all oxidative additions in the catalytic cycle of olefin hydroformylation:



Answer

Step D --> E is an oxidative addition

Formation of $HCo(CO)_4$ from $Co_2(CO)_8$ is also an oxidative addition.

Exercise 2

1. What are the reaction products of the following olefin metathesis reactions?

a) 2 CH_2=CH-Ph -->

b) n CH_2=CH-CH=CH_2 -->

Answer

a) $CH_2=CH_2$ and Ph-CH=CH-Ph

b) $CH_2=CH_2$ and $(CH=CH)_n$

Exercise 3

What reaction product would you expect would you expect from the following reaction:

$Fe(CO)_4^{2-} + CH_3CH_2I$ -->

Name the reaction.

Answer

$Fe(CO)_4CH_2CH_3^- + I^-$ Nucleophilic displacement

Exercise 4

Which of the following phosphines would you expect to be most suitable to stabilize metals in low oxidation states:

a) $P(CF_3)_3$

b) $P(CH_3)_3$

c) PH_3

Answer

a) $P(CF_3)_3$

Exercise 5

What reaction product would you expect from the following reaction?

$Pt(PPh_3)_4 + 4\ NPh_3$ -->

Answer

There would be no reaction.

Exercise 6

Which of the following complexes would likely be unstable:

a) $[PtCl_3(C_2H_5)]^{2-}$

b) $[PtCl_3(CH_3)]^{2-}$

c) $PtCl_4^{2-}$

Answer

a) $[PtCl_3(C_2H_5)]^{2-}$

Dr. Kai Landskron (Lehigh University). If you like this textbook, please consider to make a donation to support the author's research at Lehigh University: Click Here to Donate.

This page titled Section 11.5.2: Homework Problems Chapter 12 is shared under a CC BY-NC-SA 4.0 license and was authored, remixed, and/or curated by Kathryn Haas.

- **Homework Problems Chapter 12** by Kai Landskron is licensed CC BY 4.0.

CHAPTER OVERVIEW

Chapter 12: Bioinorganic Chemistry

Metals play a wide range of important roles in biological systems. This chapter will give an overview of the roles metals can play in biochemical reactions and highlight a few metal containing proteins in greater detail.

Learning Objectives

- Observe the different roles metals can play in biological systems
- Apply inorganic chemistry principles (MO theory, CFT, HSAB, etc.) to metalloproteins

Section 12.1: Biological Significance of Metals
Section 12.2: Introduction to Amino Acids and Proteins
Section 12.3: Biological Dioxygen Transport and Storage
Section 12.4: Biological Metal Storage
Section 12.5: Zinc as Lewis Acid and Template
Section 12.6: Electron Transfer

Chapter 12: Bioinorganic Chemistry is shared under a CC BY-NC-SA 4.0 license and was authored, remixed, and/or curated by LibreTexts.

Section 12.1: Biological Significance of Metals

Overview

The transition metals are among the least abundant metal ions in the sea water from which contemporary organisms are thought to have evolved (Table ***Section*12.1.1**).[1-5] For many of the metals, the concentration in human blood plasma greatly exceeds that in sea water. Such data indicate the importance of mechanisms for accumulation, storage, and transport of transition metals in living organisms.

Table ***Section*12.1.1**: Concentrations of transition metals and zinc in sea water and human plasma.*Data from References 1 - 5 and 12

Element	Sea Water (M) x 10^8	Human Plasma (M) x 10^8
Fe	0.005 - 2	2230
Zn	8.0	1720
Cu	1.0	1650
Mo	10.0	1000
Co	0.7	0.0025
Cr	0.4	5.5
V	4.0	17.7
Mn	0.7	10.9
Ni	0.5	4.4

The metals are generally found either bound directly to proteins or in cofactors such as porphyrins or cobalamins, or in clusters that are in turn bound by the protein; the ligands are usually O, N, S, or C. Proteins with which transition metals and zinc are most commonly associated catalyze the intramolecular or intermolecular rearrangement of electrons. Although the redox properties of the metals are important in many of the reactions, in others the metal appears to contribute to the structure of the active state, e.g., zinc in the Cu-Zn dismutases and some of the iron in the photosynthetic reaction center. Sometimes equivalent reactions are catalyzed by proteins with different metal centers; the metal binding sites and proteins have evolved separately for each type of metal center.

Iron

Iron is the most common transition metal in biology.[6,7] Its use has created a dependence that has survived the appearance of dioxygen in the atmosphere ca. 2.5 billion years ago, and the concomitant conversion of ferrous ion to ferric ion and insoluble rust. All plants, animals, and bacteria use iron, except for a lactobacillus that appears to maintain high concentrations of manganese instead of iron. The processes and reactions in which iron participates are crucial to the survival of terrestrial organisms, and include ribonucleotide reduction (DNA synthesis), energy production (respiration), energy conversion (photosynthesis), nitrogen reduction, oxygen transport (respiration, muscle contraction), and oxygenation (e.g., steroid synthesis, solubilization and detoxification of aromatic compounds). Among the transition metals used in living organisms, iron is the most abundant in the environment. Whether this fact alone explains the biological predominance of iron or whether specific features of iron chemistry contribute is not clear.

Many of the other transition metals participate in reactions equivalent to those involving iron, and can sometimes substitute for iron, albeit less effectively, in natural Fe-proteins. Additional biological reactions are unique to nonferrous transition metals.

Zinc

Zinc is relatively abundant in biological materials.[8,9] The major location of zinc in the body is metallothionein, which also binds copper, chromium, mercury, and other metals. Among the other well-characterized zinc proteins are the Cu-Zn superoxide

dismutases (other forms have Fe or Mn), carbonic anhydrase (an abundant protein in red blood cells responsible for maintaining the pH of the blood), alcohol dehydrogenase, and a variety of hydrolases involved in the metabolism of sugars, proteins, and nucleic acids. Zinc is a common element in nucleic-acid polymerases and transcription factors, where its role is considered to be structural rather than catalytic. Interestingly, zinc enhances the stereoselectivity of the polymerization of nucleotides under reaction conditions designed to simulate the environment for prebiotic reactions. Recently a group of nucleic-acid binding proteins, with a repeated sequence containing the amino acids cysteine and histidine, were shown to bind as many as eleven zinc atoms necessary for protein function (transcribing DNA to RNA).[10] Zinc plays a structural role, forming the peptide into multiple domains or "zinc fingers" by means of coordination to cysteine and histidine. A survey of the sequences of many nucleic-acid binding proteins shows that many of them have the common motif required to form zinc fingers. Other zinc-finger proteins called steroid receptors bind both steroids such as progesterone and the progesterone gene DNA. Much of the zinc in animals and plants has no known function, but it may be maintaining the structures of proteins that activate and deactivate genes.[11]

Copper

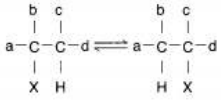
Copper and iron proteins participate in many of the same biological reactions:

1. reversible binding of dioxygen, e.g., hemocyanin (Cu), hemerythrin (Fe), and hemoglobin (Fe);
2. activation of dioxygen, e.g., dopamine hydroxylase (Cu) (important in the synthesis of the hormone epinephrine), tyrosinases (Cu), and catechol dioxygenases (Fe);
3. electron transfer, e.g., plastocyanins (Cu), ferredoxins, and c-type cytochromes (Fe);
4. dismutation of superoxide by Cu or Fe as the redox-active metal (superoxide dismutases).

The two metal ions also function in concert in proteins such as cytochrome oxidase, which catalyzes the transfer of four electrons to dioxygen to form water during respiration. Whether any types of biological reactions are unique to copper proteins is not clear. However, use of stored iron is reduced by copper deficiency, which suggests that iron metabolism may depend on copper proteins, such as the serum protein ceruloplasmin, which can function as a ferroxidase, and the cellular protein ascorbic acid oxidase, which also is a ferrireductase.

Cobalt

Cobalt is found in vitamin B_{12} , its only apparent biological site.[12] The vitamin is a cyano complex, but a methyl or methylene group replaces CN in native enzymes. Vitamin-B_{12} deficiency causes the severe disease of pernicious anemia in humans, which indicates the critical role of cobalt. The most common type of reaction in which cobalamin enzymes participate results in the reciprocal exchange of hydrogen atoms if they are on adjacent carbon atoms, yet not with hydrogen in solvent water:



(An important exception is the ribonucleotide reductase from some bacteria and lower plants, which converts ribonucleotides to the DNA precursors, deoxyribonucleotides, a reaction in which a sugar -OH is replaced by -H. Note that ribonucleotide reductases catalyzing the same reaction in higher organisms and viruses are proteins with an oxo-bridged dimeric iron center.) The cobalt in vitamin B_{12} is coordinated to five N atoms, four contributed by a tetrapyrrole (corrin); the sixth ligand is C, provided either by C5 of deoxyadenosine in enzymes such as methylmalonyl-CoA mutase (fatty acid metabolism) or by a methyl group in the enzyme that synthesizes the amino acid methionine in bacteria.

Nickel

Nickel is a component of a hydrolase (urease), of hydrogenase, of CO dehydrogenase, and of S-methyl CoM reductase, which catalyzes the terminal step in methane production by methanogenic bacteria. All the Ni-proteins known to date are from plants or bacteria.[13,14] However, about 50 years elapsed between the crystallization of jack-bean urease in 1925 and the identification of the nickel component in the plant protein. Thus it is premature to exclude the possibility of Ni-proteins in animals. Despite the small number of characterized Ni-proteins, it is clear that many different environments exist, from apparently direct coordination to protein ligands (urease) to the tetrapyrrole F430 in methylreductase and the multiple metal sites of Ni and Fe-S in a hydrogenase

from the bacterium *Desulfovibrio gigas*. Specific environments for nickel are also indicated for nucleic acids (or nucleic acid-binding proteins), since nickel activates the gene for hydrogenase.[15]

Manganese

Manganese plays a critical role in oxygen evolution catalyzed by the proteins of the photosynthetic reaction center. The superoxide dismutase of bacteria and mitochondria, as well as pyruvate carboxylase in mammals, are also manganese proteins.[16,17] How the multiple manganese atoms of the photosynthetic reaction center participate in the removal of four electrons and protons from water is the subject of intense investigation by spectroscopists, synthetic inorganic chemists, and molecular biologists.[17]

Vanadium and Chromium

Vanadium and chromium have several features in common, from a bioinorganic viewpoint.[18a] First, both metals are present in only small amounts in most organisms. Second, the biological roles of each remain largely unknown.[18] Finally, each has served as a probe to characterize the sites of other metals, such as iron and zinc. Vanadium is required for normal health, and could act *in vivo* either as a metal cation or as a phosphate analogue, depending on the oxidation state, V(lV) or V(V), respectively. Vanadium in a sea squirt (tunicate), a primitive vertebrate, is concentrated in blood cells, apparently as the major cellular transition metal, but whether it participates in the transport of dioxygen (as iron and copper do) is not known. In proteins, vanadium is a cofactor in an algal bromoperoxidase and in certain prokaryotic nitrogenases. Chromium imbalance affects sugar metabolism and has been associated with the glucose tolerance factor in animals. But little is known about the structure of the factor or of any other specific chromium complexes from plants, animals, or bacteria.

Molybdenum

Molybdenum proteins catalyze the reduction of nitrogen and nitrate, as well as the oxidation of aldehydes, purines, and sulfite.[19] Few Mo-proteins are known compared to those involving other transition metals. Nitrogenases, which also contain iron, have been the focus of intense investigations by bioinorganic chemists and biologists; the iron is found in a cluster with molybdenum (the iron-molybdenum cofactor, or FeMoCo) and in an iron-sulfur center. Interestingly, certain bacteria (*Azotobacter*) have alternative nitrogenases, which are produced when molybdenum is deficient and which contain vanadium and iron or only iron. All other known Mo-proteins are also Fe-proteins with iron centers, such as tetrapyrroles (heme and chlorins), Fe-sulfur clusters, and, apparently, non-heme/non-sulfur iron. Some Mo-proteins contain additional cofactors such as the Havins, e.g., in xanthine oxidase and aldehyde oxidase. The number of redox centers in some Mo-proteins exceeds the number of electrons transferred; reasons for this are unknown currently.

References

1. (a) J. H. Martin and R. M. Gordon, *Deep Sea Research* **35** (1988), 177; (b) F. Egami, *J. Mol. Evol.* **4** (1974), 113.
2. J. F. Sullivan *et al.*, *J. Nutr.* **109** (1979), 1432.
3. M. D. McNeely *et al.*, *Clin. Chem.* **17** (1971), 1123
4. A. R. Byrne and L. Kosta, *Sci. Total Env.* **10** (1978), 17
5. A. S. Prasad, *Trace Elements and Iron in Human Metabolism*, Plenum Medical Book Company, 1978.
6. E. C. Theil, *Adv. Inorg. Biochem.* **5** (1983), 1.
7. E. C. Theil and P. Aisen, in D. van der Helm, J. Neilands, and G. Winkelmann, eds., *Iron Transport in Microbes, Plants, and Animals*, VCH, 1987, p. 421.
8. C. F. Mills, ed., *Zinc in Human Biology*, Springer-Verlag, 1989.
9. B. L. Vallee and D. S. Auld, *Biochemistry* **29** (1990), 5647.
10. J. Miller, A. D. McLachlan, and A. Klug, *EMBO J.* **4** (1985), 1609.
11. J. M. Berg, *J. Biol. Chem.* **265** (1990), 6513.
12. C. Sennett, L. E. G. Rosenberg, and I. S. Millman, *Annu. Rev. Biochem.* **50** (1981), 1053.
13. J. J. G. Moura *et al.*, in A. V. Xavier, ed., *Frontiers in Biochemistry*, VCH, 1986, p. 1.
14. C. T. Walsh and W. H. Orme-Johnson, *Biochemistry* **26** (1987), 4901.
15. H. Kim and R. J. Maier, *J. Biol. Chem.* **265** (1990), 18729.
16. Reference 5, p. 5.
17. V. L. Schramm and F. C. Wedler, eds., *Manganese in Metabolism and Enzyme Function*, Academic Press, 1986.

18. (a) D. W. Boyd and K. Kustin, *Adv. Inorg. Biochem.* **6** (1984), 312; (b) R. C. Bruening *et al.*, *J. Nat. Products* **49** (1986), 193.
19. T. G. Spiro, ed., *Molybdenum Biochemistry*, Wiley, 1985.

Section 12.1: Biological Significance of Metals is shared under a CC BY-NC-SA 4.0 license and was authored, remixed, and/or curated by LibreTexts.

- **12.1: Biological Significance of Metals** is licensed CC BY-NC-SA 4.0.

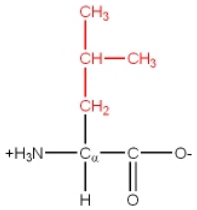
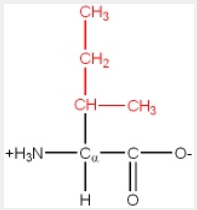
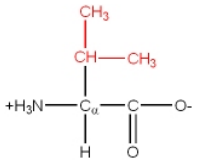
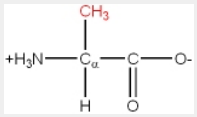
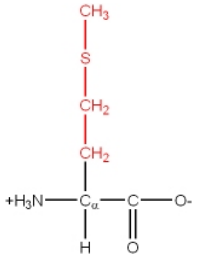
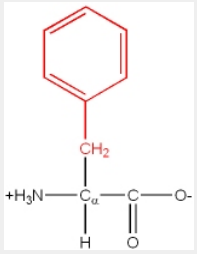
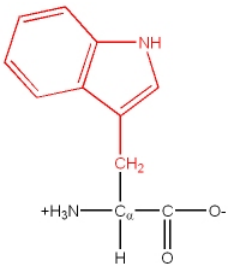
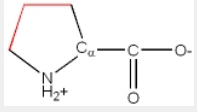
Section 12.2: Introduction to Amino Acids and Proteins

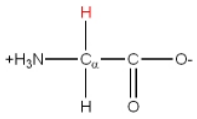
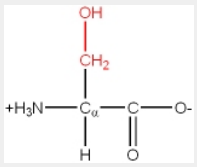
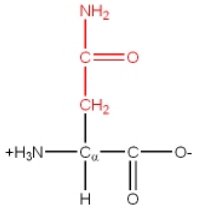
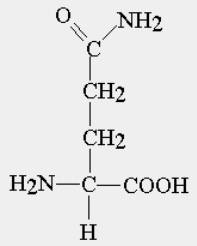
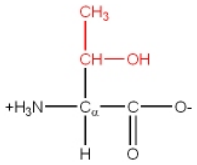
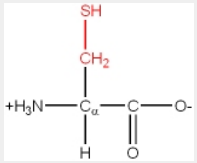
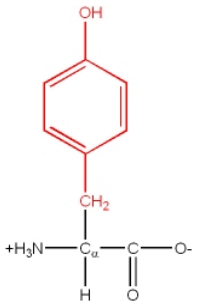
Common amino acids

There are 20 common amino acids. They are composed of C, H, O, N and S atoms. They are structurally and chemically different, and also differ in size and volume. Some are branched structures, some are linear, some have ring structures. One of the 20 common amino acids is actually an imino acid. A typical grouping of their chemical nature is as follows:

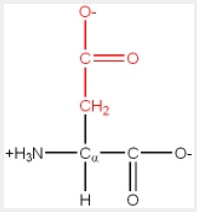
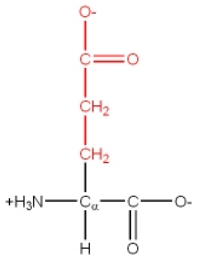
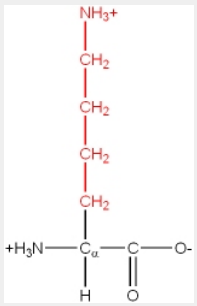
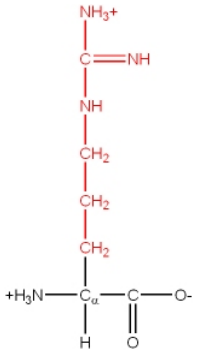
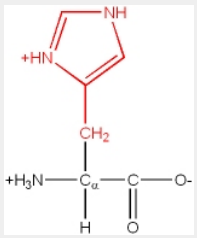
- Nonpolar (hydrocarbons and one sulfur-containing amino acid). Dispersion forces and hydrophobic effects predominate in their interactions. They cannot H-bond with water and these side chains have a characteristic hydrophobic effect in water.
- Polar uncharged. Contain functional groups that can H-bond with water and other amino acids. Include C, H, O, N and S atoms.
- Acidic. Contain a carboxylic acid functional group with a negative charge at neutral pH. Can H-bond with water, can form ionic interactions, and can also serve as nucleophiles or participate in acid-base chemistry.
- Basic. Nitrogen containing bases (e.g. guanidino, imidazole or amino groups) with a net positive charge at neutral pH. Can serve as proton donors in chemical reactions, and form ionic interactions.

The amino acids have a name, as well as a three letter or single letter mnemonic code:

Type	Name	R-group Structure
Nonpolar	Leucine Leu, L	
	Isoleucine Ile, I	
	Valine Val, V	
	Alanine Ala, A	
	Methionine Met, M	
	Phenylalanine Phe, F	
	Tryptophan Trp, W	
	Proline Pro, P	

Type	Name	R-group Structure
	Glycine Gly, G (note: sometimes included in polar group)	
Polar, uncharged	Serine Ser, S	
	Asparagine Asn, N	
	Glutamine Gln, Q	 glutamine
	Threonine Thr, T	
	Cysteine Cys, C	
	Tyrosine Tyr, Y	

https://chem.libretexts.org/@go/page/440905

Type	Name	R-group Structure
Acidic	Aspartic acid Asp, D	
	Glutamic acid Glu, E	
Basic	Lysine Lys, K	
	Arginine Arg, R	
	Histidine His, H	

Uncommon amino acids

In addition to the 20 common amino acids, there are several uncommon ones found:

- Hydroxylysine and hydroxyproline. These are found in the protein collagen. Collagen is a fibrous protein made up of three polypeptides that form a stable assembly, but only if the proline and lysine residues are hydroxylated. (requires vitamin C for reduction of these amino acids to hydroxy form)
- Thyroxine, an iodinated derivative of tyrosine, found in thyroglobulin (produced by thyroid gland; requires iodine in diet)

- g-carboxyglutamic acid (i.e. glutamic acid with two carboxyl groups) found in certain blood clotting enzymes (requires vitamin K for production)
- N-methyl arginine and n-acetyl lysine. Found in some DNA binding proteins known as histones

Amino acid derivatives not found in proteins

Some amino acids are made that are not intended for incorporation into proteins, rather they have important functionalities on their own

- Serotonin (derivative of tryptophan) and g-amino butyric acid (a derivative of glutamic acid) are both neurotransmitters
- Histamine (derivative of histidine) involved in allergic response
- Adrenaline (derivative of tyrosine) a hormone
- Various antibiotics are amino acid derivatives (penicillin)

Contributors and Attributions

- Mike Blaber (Florida State University)

Thumbnail: 3D model of L-tryptophan. (Public Domain; Benjah-bmm27).

This page titled Section 12.2: Introduction to Amino Acids and Proteins is shared under a CC BY-NC-SA 4.0 license and was authored, remixed, and/or curated by Tim Soderberg via source content that was edited to the style and standards of the LibreTexts platform.

- **Nomenclature of Amino acids** is licensed CC BY-NC-SA 4.0.

Section 12.3: Biological Dioxygen Transport and Storage

Oxygen Transport

Most organisms require molecular oxygen in order to survive. The oxygen is used in a host of biochemical transformations, although most is consumed in the reaction that is the terminal (or primary) step of oxidative phosphorylation to form ATP.

$$O_2 + 4H^+ + 4e^- \rightarrow 2H_2O \qquad \text{(Section 12.3.1)}$$

The transportation of oxygen from the air or water to the cells of an organism is vital. In the three chemically distinct dioxygen carrier proteins that have evolved and are found today, the dioxygen binding site in the protein, the active site, is an iron or copper complex. For hemoglobins, the most widely distributed family of dioxygen carriers, the active site has long been known to consist of an iron porphyrin (heme) group embedded in the protein. Almost all hemoglobins share the basic structure illustrated in Figure 4.2. Hemocyanin and hemerythrin, the other two biological dioxygen carriers, feature pairs of copper atoms and iron atoms, respectively, at the active sites.* Some basic properties of these metalloproteins are summarized in Table *Section*12.3.1.

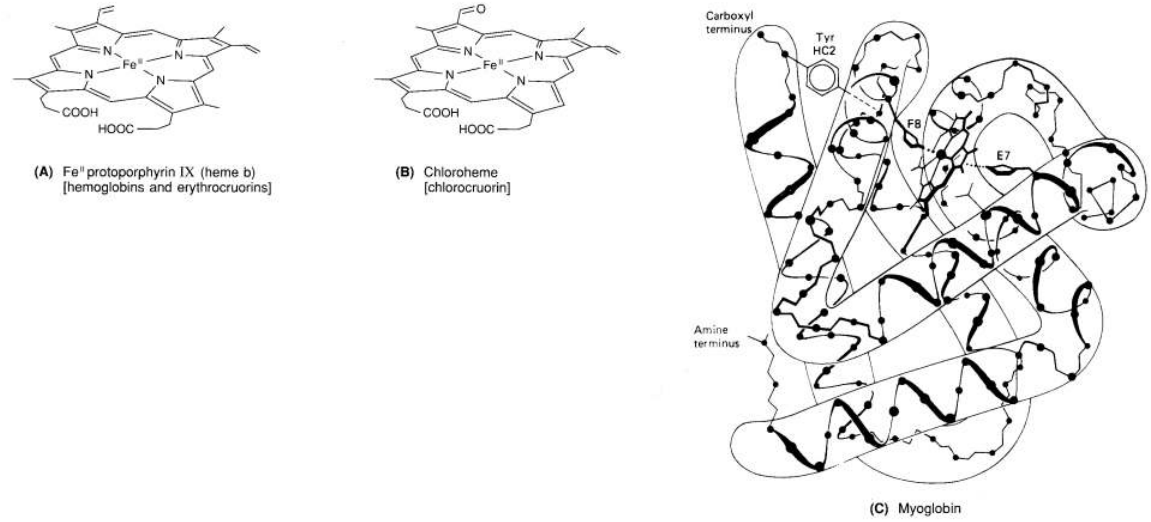


Figure *Section*12.3.1: Heme groups used in hemoglobin: (A) Protoporphyrin IX (heme b), (hemoglobins and erythrocruorins); (B) Chloroheme (chlorocruorin); (C) The encapsulation of the heme molecule in myoglobin.[11a] Reproduced with permission from M. F. Perutz, Nature **228** (1970), 726-737.

Table *Section*12.3.1: General Features of Dioxygen-carrier Proteins

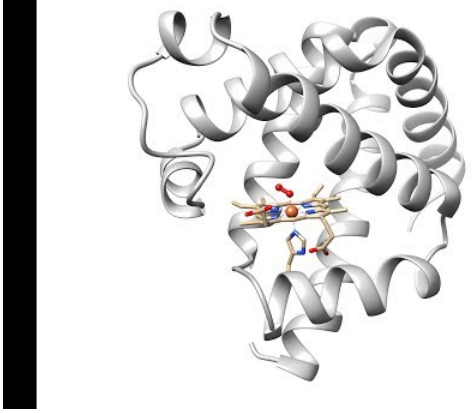
Metalloprotein	Active Site of deoxy	Color Change deoxy → oxy	MW (Dalton)	# Subunits	Average MW Subunit (Dalton)
Hemoglobins					
Vertebrate					
Human A	heme Fe^{II}	purple → red	64,000	4	16,000
Invertebrate					
Erythrocruroin (*Lumbricus terrestris*, earthworm)	heme Fe^{II}	purple → red	up to 3.3×10^6	192	17,000
Chlorocruorn *(Eudistylia vancouveri*, feather duster worm*)*	chloroheme Fe^{II}	purple → green	3.1×10^6	192	15,000
Hemocyanins					
Mollusk (*Helix pomatia*-**α**, edible snail)	$Cu^1 \ldots Cu1$	colorless → blue	-9×10^6	160	52,700
Arthropod *(Cancer magister*, crab)	$Cu^1 \ldots Cu1$	colorless → blue	-9×10^5	12	76,600
Hemerythrins *(Phascolopsis* syn. *golfingia gouldii)*	$Fe^{II} \ldots Fe^{II}$	colorless → burgundy	108,000	8	13,500

* The use of the prefix *hem-* is confusing. In this context *hem* connotes blood. Thus, since hemocyanin and hemerythrin lack a heme group [an iron(II) porphyrin], they are nonheme metalloproteins.

In many organisms an additional dioxygen-binding protein, which stores dioxygen, is located in tissues that are subject to sudden and high dioxygen demand, such as muscles. These dioxygen-storage proteins are prefixed *myo-* (from the Greek root *mys* for muscle). Thus for the dioxygen-transport protein hemerythrin there exists a chemically similar dioxygen-storage protein myohemerythrin. For the hemoglobin family the corresponding storage protein is called myoglobin. Interestingly, some organisms that use hemocyanin as the dioxygen-*transport* protein use myoglobin as the dioxygen-*storage* protein.

Introduction to Myoglobin and Hemoglobin

Myoglobin: O_2 storage



The respiratory system is an organ system in the body that functions in gas exchange with the environment. Exchange of gases like carbon dioxide (CO_2) and dioxygen (O_2) are essential for sustaining life forms. O_2 is necessary in aerobic metabolism for oxidative phosphorylation (synthesis of ATP) at the electron transport chain (ETC).[2] ATP is the energy source needed for muscular

contraction in mammals. ATP synthesis requires oxygen as an electron acceptor in the ETC, therefore oxygen must be readily available for use in metabolically active muscles. Since muscles need large quantities of O_2, it is transported by proteins in the blood and stored in muscle tissue. One of these proteins is myoglobin. Myoglobin is a hemoprotein found in the skeletal muscle of mammals that functions in oxygen storage and diffusion. The heme in myoglobin can reversibly bind a O_2 molecule to regulate the transportation of O_2 from red blood cells to mitochondria when skeletal muscles are metabolically active.

Structure of Myoglobin

The structure of myoglobin (Figure ***Section*12.3.2**) is similar to the structure of one of the β subunits of hemoglobin. Myoglobin and hemoglobin are both part of the globin family; a family of heme-containing globular polypeptides with eight α-helices in their protein fold. Myoglobin contains only one subunit of globin, while hemoglobin has four subunits.

The iron-containing heme group allows myoglobin to reversibly bind to O_2 (Figure ***Section*12.3.2**). Heme is a large, aromatic porphyrin ring with four pyrrole nitrogens bound to an Fe(II) ion at the center (Figure ***Section*12.3.2*C***).[2,3] The nitrogens from the porphyrin ring and a histidine serve as ligands for the Fe(II) metal center. The heme Fe is bound to the myoglobin polypeptide through the proximal histidine residue. The iron ion has six coordination sites: four equitorial sites are occupied by pyrole nitrogens of heme, and one axial site is occupied by a proximal histidine residue. The remaining axial coordination site is available for binding a O_2 molecule (Figure ***Section*12.3.2*A* – *C***).

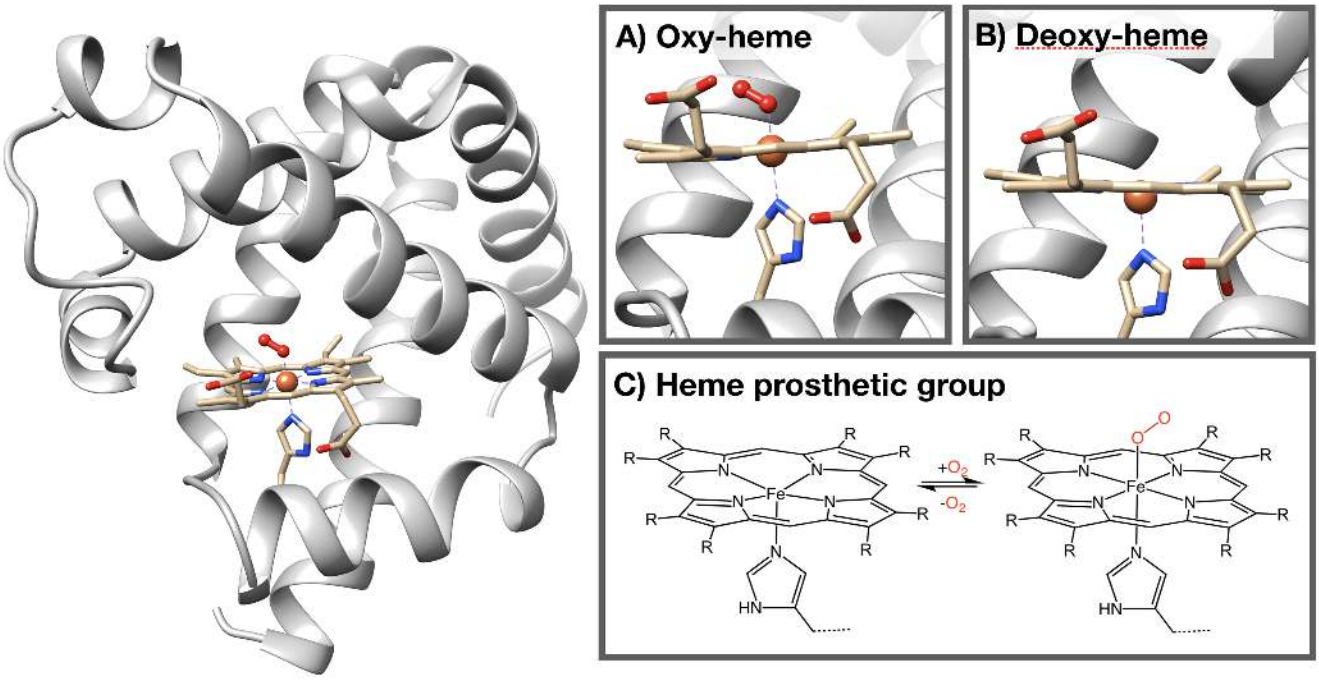


Figure ***Section*12.3.2**: Structure of myoglobin. This is a ribbon depiction of mammalian myoglobin protein (grey, PDB code 1a6m). The heme group, shown in stick depiction (tan) with Fe shown as an orange sphere, bound to a O_2 molecule (red ball-and-stick). Inset A shows enlarged view of the O_2-bound heme. Inset B illustrates the de-oxygenated heme (PDB code 1a6n). The proximal histidine imidazole bound to Fe is shown toward the bottom of insets A and B. Inset C shows reversible binding of O_2 to the skeletal structure of the heme prosthetic group. This group consists of four central nitrogen donor atoms bound to iron (II) (attribution: Smokefoot, Mboxygenation, CC BY-SA 4.0). The porphyrin ring contains four pyrrole nitrogens bound to a ferrous (Fe(II)) ion center. There are six coordination sites in the Fe(II) ion; four are occupied by the pyrrole nitrogens, one is occupied by a proximal histidine, and the final site has the ability to reversibly bond to an O_2 molecule.

Reversible binding of oxygen

Now let's move on to the function of myoglobin: oxygen storage. Myoglobin can reversibly bind a dioxygen molecule to regulate the transportation of oxygen from red blood cells to mitochondria when skeletal muscles are metabolically active. This binding occurs at the iron center of the heme group. Although the 18-electron rule was a rule developed for organometallic complexes and chemistry, we can apply it here to explain the O_2-binding behavior of myoglobin. In deoxymyoglobin, the total valence electron count around Fe is 16 electrons (See Fig. ***Section*12.3.2**, 10 electrons from ligands plus 6 electrons from Fe(II)). Under the 18-

electron rule, a predictable step for a 16-electron species is ligand addition. The binding of O_2 to Fe(II) is a ligand addition reaction. Once O_2 binds to the Fe(II) in myoglobin, the new valence electron count around Fe is 18 electron. A predictable step for an 18-electron species is a ligand dissociation reaction, as is the reaction of O_2 dissociation from the Fe center. The binding and dissociation of O_2 makes sense based on the 18-electron rule.

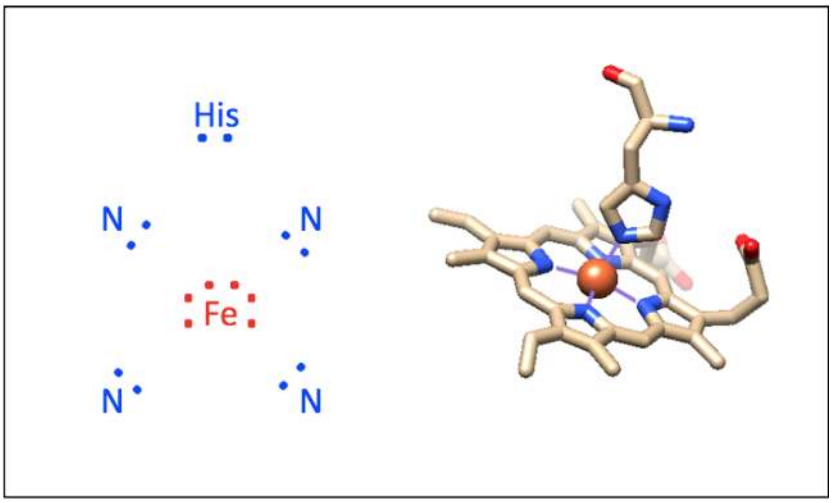


Figure *Section*12.3.3: The electron count of deoxygenated heme Fe is 16 electrons. A total of 10 electrons are donated from the ligands (8 from pyrrole nitrogens of the porphyrin ring and 2 from the imidaziole nitrogen of the proximal histidine); 6 electrons are present from the 6 d electrons of Fe(II). Thus, the deoxy-heme complex is available for another ligand to bind; this case in the form of oxygen. The image was created using PDB code 1a6n and UCSF Chimera.

Iron oxidation state

The oxidation state of Fe in oxy-myoglobin is a highly debated topic because data is inconclusive and seemingly contradictory. Data from infrared (IR) spectroscopy and magnetic measurements have lead scientists to propose two different modes of oxygen binding to the iron ion. In one model (Figure *Section*12.3.4 left), Fe(II) simply binds to O_2. A second model predicts that electrons are transfered from the Fe center to the dioxygen molecule to create Fe(III) bound to superoxide (Figure *Section*12.3.4 right). Although many debate whether the iron, after binding to oxygen, remains iron (II) or becomes iron (III), it is difficult to assign an oxidation state to the bound iron or the oxygen. The actual molecular orbitals that result from the iron-oxygen interaction have both iron and O_2 character. It is therefore not quite correct to focus on the electrons "belong" to Fe or dioxygen. The two extremes, where one is that Fe becomes an iron superoxide by donating an electron from iron to the oxygen, and the other that Fe becomes an iron oxide by sharing the electrons are probably both incorrect. The molecular orbitals contain characteristics of both iron superoxide and iron oxide.

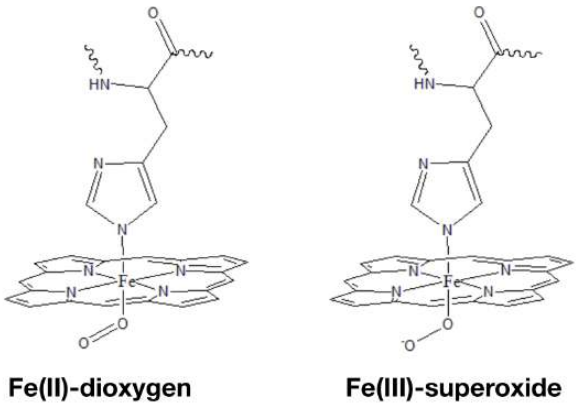


Figure *Section*12.3.4: The binding of oxygen to the metal iron ion center of heme, occupying the 6th binding site of heme. **Left:** illustrates the iron oxide binding of oxygen where there is no transfer of electrons from the oxygen to the iron ion. **Right:** illustrates the formation of the superoxide from the transfer of electrons from oxygen to iron.

Sources

1. Ordway, G. A. *Journal of Experimental Biology* 2004, *207*(20), 3441–3446.
2. Ahern, K.; Rajagopal, I.; Tan, T. *Biochemistry Free For All*; Creative Commons, 2017; Vol. 1.2.
3. Casiday, R.; Frey, R. Hemoglobin and the Heme Group: Metal Complexes in the Blood for Oxygen Transport Inorganic Synthesis Experiment
4. Penn State University. In *Chem 324: Bio-Inorganic Chemistry.*
5. Lippard, S.J., Berg, J.M. Principles of Bioinorganic Chemistry. University Science Books. 1994. 284-289.
6. Atkins, Overton, Rourke, Weller, Armstrong. Shriver and Atkins' Inorganic Chemistry. Oxford University Press. 2010. 738-79.
7. Richards, M. *Antioxidants and Redox Signaling* 2013. 2342-2351.
8. Mazumdra, S., Medhi, O.K., Mitra, S. *American Chemical Society*. 1990. 700-705.
9. Shriver, D., Atkins, P. Inorganic Chemistry, 5th ed.; W.H. Freeman and Company: New York, 2009; 739.
10. Vanholder, R., Sever, M.S., Erek, E., Lameire, N. 2000. Rhabdomyolysis. *Journal of the American Society of Nephrology* 11:1553-1561

Hemoglobin

Hemoglobin, a polypeptide found in red blood cells, allows dioxygen (O_2) to be transported within blood from the lungs to other tissues within the body. Hemoglobin is a polypeptide found in red blood cells. It allows for the transportation of O_2 from the lungs to other tissues within the body. This molecule also is also responsible for the color of blood.[1] Oxygenated blood is a bright red because hemoglobin absorbs green light of wavelengths 540-542 nm, and thus it results in a bright red colored solution.[2] Deoxygenated blood, however, is darker in color because it absorbs a more yellow/green color of wavelength 554 nm, and thus produces a darker color of red.

Hemoglobin is able to transport oxygen within the body due to its unique structure. Its structure consists of four globin subunits: two α and two β subunits. Each subunit contains a heme prosthetic group with an iron bound (Figure 1). Hemoglobin exists in high concentrations in the cytoplasm of red blood cells, so it needs to be very soluble in aqueous cytoplasm. This requirement is reflected in the protein's globular shape, and the fact that it is folded in such a way that hydrophilic residues are found on the surface of the protein exposed to water, while hydrophobic residues are found on the interior of the protein. This folding enables hemoglobin to have a stable fold in aqueous solution that also allows the protein to interact favorably with water and to be soluble in the water-filled cytoplasm of the cell.

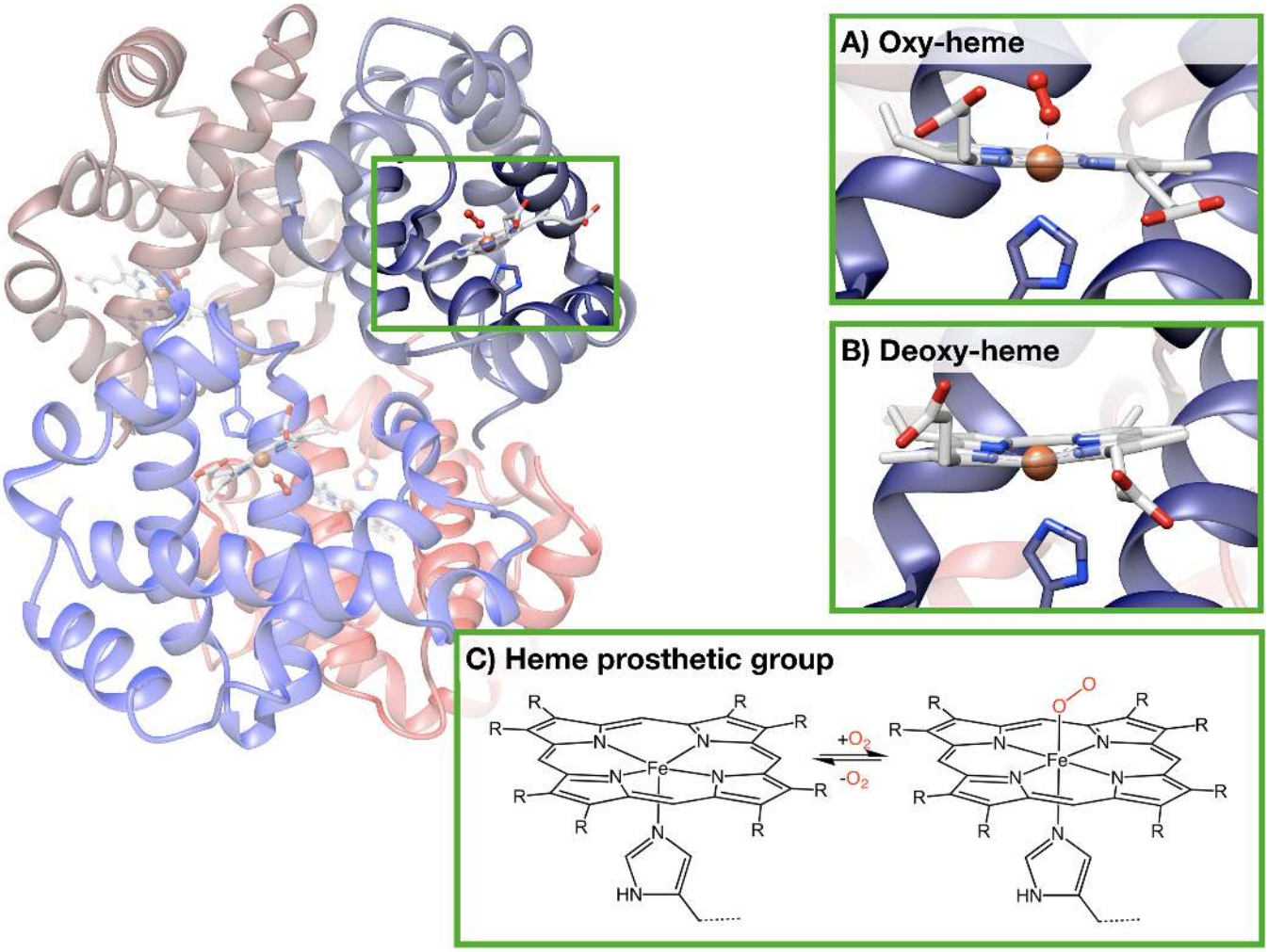


Figure ***Section*12.3.5**: On the left, the ribbon diagram of hemoglobin is displayed. Hemoglobin consists of four subunits: two α (blue) and two β subunits (red). A heme group (stick depiction) is located within each subunit, and within each heme an inorganic iron ion (orange) is located. **Inset A:** Oxy-hemoglobin has dioxygen (red) bound to the iron core of each heme group. The iron of the oxygenated hemoglobin is pulled into the porphyrin plane. **Inset B:** Deoxy-hemoglobin (no oxygen bound). The iron (II) ion lies 0.4 Å outside of the porphyrin plane. **Inset C:** Reversible binding of O_2 to the skeletal structure of the heme prosthetic group. This group consists of four central nitrogen donor atoms bound to iron (II) (attribution: Smokefoot, Mboxygenation, CC BY-SA 4.0). Iron (II) has two axial binding sites and, in hemoglobin, one is occupied by an imidazole N of the proximal histidine. The second axial coordination site has the ability to reversibly bond to an oxygen atom.

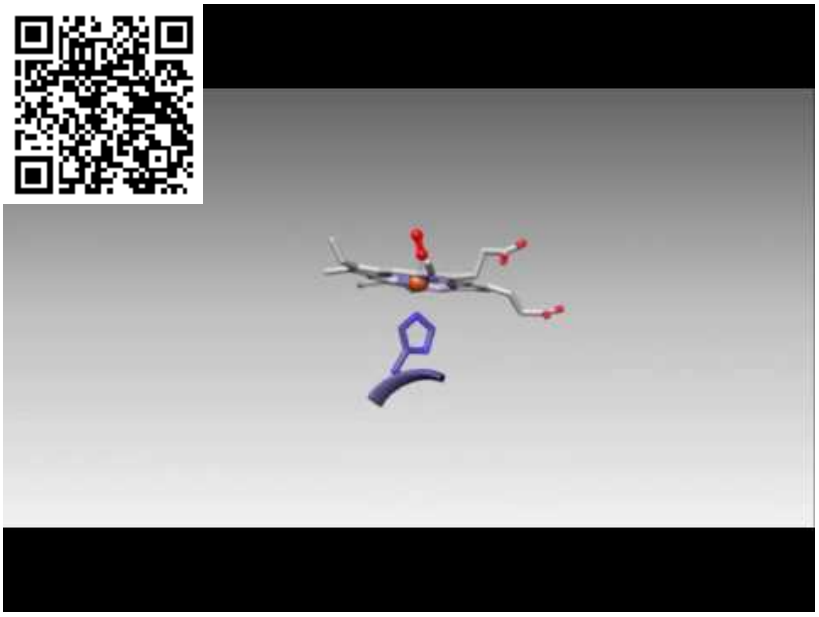
Cooperative binding of O_2

An important feature of hemoglobin is a cooperative binding of oxygen to each subunit due to conformational changes upon oxygen binding to the heme iron. Hemoglobin exists in both the T-state (tense state) and the R-state (relaxed). The T-state has lower affinity for dioxygen due to the tilting of the proximal histidine and steric hindrance of the O_2 coordination site. Steric hindrance makes it difficult for oxygen molecule to enter the site and bind to Fe. When an oxygen binds to one subunit of hemoglobin, the iron shifts into the plane of the porphoryn ring, and tugs on the proximal histidine.[3,9] This causes the proximal histidine ring to be pulled toward the plane of the prosthetic group, decreasing the tilt of the histidine, causing a shift in the tertiary structure of that subunit, and displacing residues that were providing steric hiderance of the oxygen binding site. These conformational changes in one subunit cause similar changes to the tertiary structures of adjacent subunits, in turn decreasing steric and electrostatic constraints in those adjacent units. The result is adoption of the R-state and a subsequent increase in oxygen affinity to the other subunits.

When the iron ion is bound to only five coordination sites the iron (II) lies 0.4 Å outside of the porphyrin ring.[3,9,12] When the oxygen binds to the iron core the iron becomes smaller as it becomes low-spin because electrons are pulled closer to the Fe core or

are transfered to the dioxygen molecule due to backbonding. The low spin iron and is able to fit in the plane of the porphyrin ring.[3,9]

The short video below illustrates conformational differences between fully oxygenated hemoglobin and deoxygenated hemoglobin. (Click here if the video does not load).



References

1. Casiday, R.; Frey, R. Washington University of St. Lous Chemistry. http://www.chemistry.wustl.edu/~edud...exinBlood.html (accessed 6 March).
2. Zijistra, W. G; Buursma, A.; Meeuwsen-van der Roest, W. P. Absorption Spectra of Human Fetal and Adult Oxyhemoglobin, De-Oxyhemoglobin, Carboxyhemoglobin, and Methemoglobin. Clin Chem [online] 1991, 37, 1633-1638.
3. Prahl, S. Oregon Medical Laser Center. https://omlc.org/spectra/hemoglobin/...uct/index.html (accessed 6 March).
4. Berg, J. M.; Tymoczko, J. L.; Stryer, L. *Biochemistry*, 5 ed., W. H Freeman and Company: New York, 2002; unknown.
5. Jensen, K. P.; Ryde, U.; How O2 Binds to Heme: Reasons for Rapid Binding and Spin

Inversion. *JBC* [online] **2004**, *279*, 14561-14569

6. http://chemed.chem.purdue.edu/genchem/topicreview/bp/1biochem/blood3.html iron (III) oxide also talks about cooperativity
7. http://nptel.ac.in/courses/104103069/module7/lec3/2.html iron (III) superoxide
8. https://www.ncbi.nlm.nih.gov/pmc/articles/PMC3230298/ Explains the oxygen dissociation curve
9. Shriver, D; Atkins, P. Inorganic Chemistry, 5th ed.; W.H. Freeman and Company: New York, 2009; 739.
10. Frausto da Silva J. J. R.; Williams R. J. P. The Biological Chemistry of the Elements: The Inorganic Chemistry of Life, 2nd ed.; Oxford University Press: Oxford, 2001; 370-373, 385-386.
11. Crabb, E.; Moore, E., Eds. Metals and Life; Royal Society of Chemistry: United Kingdom, 2010.
12. https://pubs.acs.org/doi/pdf/10.1021/cr00046a002 Low spin/high spin and cooperativity
13. Spin-Pairing Model of Dioxygen Binding and Its Application to Various Transition-Metal Systems as well as Hemoglobin Coopera

Hemocyanin

Hemocyanin is the oxygen transporter protein present in the hemolymph of arthropods and mollusks.[1] Hemolymph is the circulating fluid for these animals that is the invertebrate equivalent to vertebrate blood.[2] In hemocyanin, the active site contains two copper ions. Hemocyanin is a type-3 copper protein, meaning that it contains of two copper centers, each coordinated by three histidine residues, as seen in Figure ***Section*12.3.6** and Figure ***Section*12.3.7**. When deoxygenated (see Figure ***Section*12.3.6**, left), the copper exists in the colorless, reduced Cu(I) state. Molecular oxygen binds at the copper site and is reduced to peroxide (O_2^{2-}),

Cu(I) is oxidized to Cu(II), and a blue complex forms. This change in the oxidation state of copper is responsible for the blue color of oxygenated invertebrate hemolymph. The oxygen bound as peroxide bridges the two copper centers together in μ-η^2-η^2 fashion.[5]

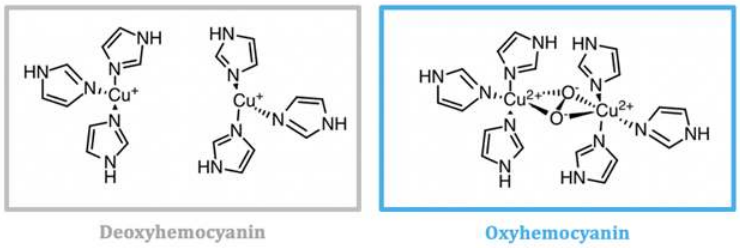


Figure ***Section*12.3.6**: Chemical Structure of Oxygen Binding Site of Hemocyanin. (Left) The deoxygenated form of the hemocyanin binding site. Each copper ion is bound to three histidine residues, however there is no oxygen bound to copper. In this state, copper is colorless and exists in the form of Cu(I). (Right) The oxygenated form of the hemocyanin binding site. Each copper is coordinated with three histidine residues, and molecular oxygen binds at the center to the copper ion as a peroxide, $\mathbf{O_2^{2-}}$, bridging the two copper centers together in a μ-η^2-η^2 fashion. Because copper is in the Cu(II) oxidation state, the oxygen-bound hemocyanin is a blue color.

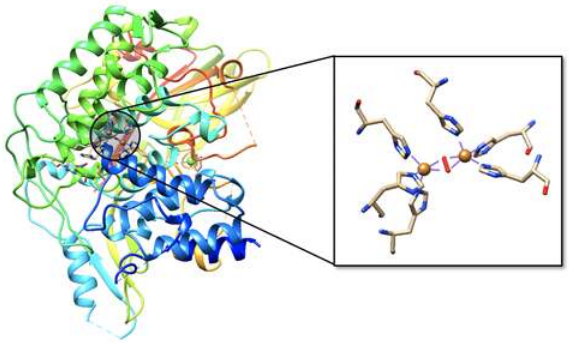


Figure ***Section*12.3.7**:[8] (Left) *Ribbon Structure of Arthropod Hemocyanin (PDB code 1NOL).* Image depicting the structure of arthropod hemocyanin (specifically from the horseshoe crab). The thin ribbons represent regions of the molecule that are unstructured. (Right) *Binding Site of Oxygen to Copper on Hemocyanin.* In the inset, three histidine residues (blue) can be seen coordinating with a copper (gold). The copper binds a molecular oxygen (red).

Mollusk and arthropod hemocyanins are structurally very different, however the active sites both contain two coppers at the center coordinated to three histidines. Arthropod hemocyanins have kidney-shaped subunits, each with an oxygen binding site, arranged into hexamers. Mollusk hemocyanin, on the other hand, is composed of about 10 subunits forming a hollow cylinder. Recently, there has been research into different therapeutic applications of hemocyanins. Studies suggest these metalloproteins have applications as viral and bacterial antigens, immune-stimulants for treatment of some cancers such as melanoma, and carrier molecules for vaccines.[9]

Note



The hemolymph of horseshoe crabs is incredibly valuable to pharmaceutical companies and biomedical researchers. It is the only known source of limulus amebocyte lysate, a substance which coagulates in the presence of bacterial endotoxin. This hemolymph extract is used to test medical devices, injectable drugs, and vaccines for bacterial contamination prior to distribution.

Learn more in this Chemistry World podcast

Image credit: CC BY; Amanda via Flickr

Structure

As seen in Figure ***Section*12.3.6** the active site of hemocyanin contains two copper ions, each bound to three histidine (His) residues. When the Cu(I) ions bind to oxygen they are oxidized to Cu(II). Cu(I) is a soft acid, Cu(II) is a borderline acid, and the imidazole ring of histidine is a borderline base. Because the copper ion alternates between a soft acid (Cu(I)) and a borderline acid (Cu(II)), it makes sense that it is bound to a borderline base. Borderline histidine is a better match for borderline Cu(II) than soft Cu(I), however His is still a better match for Cu(I) than a set of ligands that is harder. It is important to recognize, however, that there are other factors that affect metal ion selectivity, such as ionic size and ligand field stabilization energy, that must also be considered.

Hemocyanin exists in the hemolymph of invertebrates. Hemolymph is simply the invertebrate equivalent of blood that is present in vertebrates and is composed of water and organic and inorganic compounds. The inorganic metals present in hemolymph are sodium, chloride, calcium, magnesium, potassium, and manganese ions.[11,12] Na^+, Ca^{2+}, Mg^{2+}, K^+, and Mn^{2+} can all be seen as potential competitors for the copper at the active site due to the fact that they are all positively charged metal ions. They are all hard acids, indicating that they will likely not bind well with histidine, a borderline base. Based solely on HSAB, the histinines will prefer to bind to Cu(I)/Cu(II) because they are either soft/borderline acids. In addition to HSAB theory, it is also important to consider ionic size when determining if these competitors will bind in the site. These metal ions are larger than the copper ions, which may affect their ability to bind to the histidines in the pre-organized hemocyanin active site; the larger ions will not fit well into the pre-organized site, or if the site could accommodate the larger ion, it may change the protein structure to cause unfavorable steric interactions.

Kinetics and Thermodynamics

The stability of the complex is influenced by the energy of electrons in the d-orbital, as well as the geometry of the metal complexes. Because Cu(I) and Cu(II) have electrons at a higher energy, it makes them less stable and more likely to react. Additionally, Cu(II) is coordinated in a distorted tetrahedral geometry, but based on LFT, the square planar geometry is preferred. If Cu(II) was in the preferred geometry it would be more stable, and therefore reduction to Cu(I) and release of oxygen would be less favorable. Because Cu(II) is not fully stable in this environment, it allows for the cycling between the +1 and +2 oxidation states, and the transport of oxygen.

Lability is a desirable property for oxygen transport and storage proteins. The coordinated oxygen must be able to bind and unbind quickly and reversibly (carbon monoxide and cyanide gas are toxic because they will bind irreversibly with hemoglobin and displace oxygen). Cu(I) is a d^{10} metal and Cu(II) is a d^9 metal, so their higher-energy antibonding t_2 orbitals are occupied by electrons. When electrons occupy this higher-energy set of d-orbitals, the complex has a smaller CFSE and is more kinetically labile (has fast ligand substitutions reactions).

Redox Chemistry

The copper ions at the active site of hemocyanin cycle between Cu(I) and Cu(II) depending on whether or not oxygen is bound. Cu(I) is oxidized by oxygen when O_2 coordinates with the metal. For the copper oxidation half reaction, the reduction potential at pH = 7 is 0.153 V.[19] The one electron reduction of O_2 is difficult because it is spin forbidden.[20] The reduction potential of this reaction at pH = 7 is -0.33 V, which would make E_{rxn} for the one electron redox reaction -0.48 V, a non-spontaneous reaction. The two electron oxidation of O_2 to form H_2O_2 is much more favorable; the reduction potential of this reaction at pH = 7 is 0.281 V. This makes the overall which makes the overall E_{rxn} 0.128 V, which makes the binding of oxygen to hemocyanin spontaneous (Figure *Section*12.3.8).

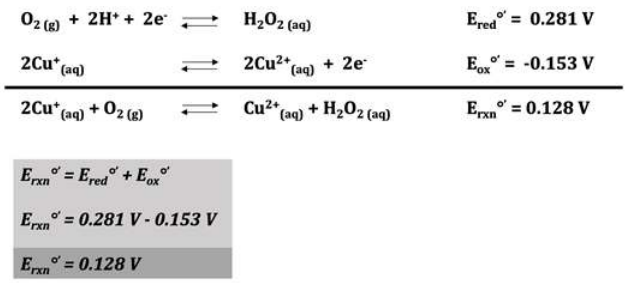


Figure *Section*12.3.8:[19] *Oxidation-Reduction Reactions for Hemocyanin.* The reduction half reaction can be seen on the first line. There are two electrons and two hydrogen ions involved in the reduction of oxygen, and the reduction potential of this reaction is 0.281 V at pH 7. On the following line, the oxidation half reaction can be seen where Cu(I) is oxidized to Cu(II) with an oxidation potential of -0.153 V at pH 7. The overall reaction appears on the third line. At pH 7, the redox potential of this reaction is 0.128 V.

Sources

1. Cook, J. D.; Penner-Hahn, J. E.; Stemmler, T. L. Structure and Dynamics of Metalloproteins in Live Cells. Methods in Cell Biology Methods in Nano Cell Biology 2008, 199–216.
2. Kanost, M. R. Hemolymph. Encyclopedia of Insects 2009, 446–449.
3. Christian, W. S.; Stefan, R. Functional morphology and diversity, Chapter 14: Circulatory System and Respiration; Oxford University Press: Oxford, 2013.
4. Hashim, O. H.; Adnan, N. A. Coenzyme, Cofactor and Prosthetic Group — Ambiguous Biochemical Jargon. Biochemical Education 1994, 22 (2), 93–94.
5. Kitajima, N.; Fujisawa, K.; Fujimoto, C.; Morooka, Y.; Hashimoto, S.; Kitagawa, T.; Toriumi, K.; Tatsumi, K.; Nakamura, A. A New Model for Dioxygen Binding in Hemocyanin. Synthesis, Characterization, and Molecular Structure of the .Mu.-.Eta.2:.Eta.2 Peroxo Dinuclear Copper(II) Complexes, [Cu(HB(3,5-R2pz)3)]2(O2) (R = Isopropyl and Ph). *Journal of the American Chemical Society* **1992**, *114* (4), 1277–1291.
6. IUPAC. Compendium of Chemical Terminology, 2nd ed. (the "Gold Book"). Compiled by A. D. McNaught and A. Wilkinson. Blackwell Scientific Publications, Oxford (1997). Online version (2019-) created by S. J. Chalk. ISBN 0-9678550-9-8. https://doi.org/10.1351/goldbook.
7. IUPAC. Compendium of Chemical Terminology, 2nd ed. (the "Gold Book"). Compiled by A. D. McNaught and A. Wilkinson. Blackwell Scientific Publications, Oxford (1997). Online version (2019-) created by S. J. Chalk. ISBN 0-9678550-9-8. https://doi.org/10.1351/goldbook.
8. Hazes, B.; Hol, W. Oxygenated Hemocyanin (Subunit Type Ii). **1996**.
9. Coates, C. J.; Decker, H. Immunological Properties of Oxygen-Transport Proteins: Hemoglobin, Hemocyanin and Hemerythrin. Cellular and Molecular Life Sciences 2016, 74 (2), 293–317.

10. Libretexts. 3.2.1: Hard and Soft Acid and Base Theory. https://chem.libretexts.org/Courses/Saint_Mary's_College,_Notre_Dame,_IN/CHEM_342:_Bio-inorganic_Chemistry/Readings/Week_3:_Metal-Ligand_Interactions_continued..../3.2:_The_identity_of_metal_ion_and_the_ligand_donor_atom(s)_affects_affinity/3.2.1:_Hard_and_Soft_Acid_and_Base_Theory (accessed Jan 28, 2020).
11. Pratoomchat, B.; Sawangwong, P.; Pakkong, P.; Machado, J. Organic and Inorganic Compound Variations in Haemolymph, Epidermal Tissue and Cuticle over the Molt Cycle in Scylla Serrata ž Decapoda/. 2002, 13.
12. Sowers, A. D.; Young, S. P.; Grosell, M.; Browdy, C. L.; Tomasso, J. R. Hemolymph Osmolality and Cation Concentrations in Litopenaeus Vannamei during Exposure to Artificial Sea Salt or a Mixed-Ion Solution: Relationship to Potassium Flux. Comparative Biochemistry and Physiology Part A: Molecular & Integrative Physiology 2006, 145 (2), 176–180. https://doi.org/10.1016/j.cbpa.2006.06.008.
13. Morris, R. H.; Lee, A.; Hadzovic, A. A Tour of Hemocyanin. https://sites.chem.utoronto.ca/chemistry/coursenotes/GTM/JM/hemocyanin/start.htm (accessed Mar 27, 2020).
14. Cirera, J.; Ruiz, E.; Alvarez, S. Stereochemistry and Spin State in Four-Coordinate Transition Metal Compounds. Inorganic Chemistry 2008, 47 (7), 2871–2889.
15. Sundberg, R. J.; Martin, R. B. Interactions of Histidine and Other Imidazole Derivatives with Transition Metal Ions in Chemical and Biological Systems. Chemical Reviews 1974, 74 (4), 471–517.
16. Nickerson, K. W.; Holde, K. E. V. A Comparison of Molluscan and Arthropod Hemocyanin—I. Circular Dichroism and Absorption Spectra. Comparative Biochemistry and Physiology Part B: Comparative Biochemistry 1971, 39 (4), 855–872.
17. Frieden, E.; Osaki, S.; Kobayashi, H. Copper Proteins And Oxygen: Correlations Between Structure And Function Of The Copper Oxidases. Journal of General Physiology 1965.
18. Tommerdahl, A. P.; Burnett, K. G.; Burnett, L. E. Respiratory Properties of Hemocyanin From Wild and Aquacultured Penaeid Shrimp and the Effects of Chronic Exposure to Hypoxia. The Biological Bulletin 2015, 228 (3), 242–252.
19. Lippard, S. J.; Berg, J. M. Principles of bioinorganic chemistry; University Science Books: Mill Valley, CA, 1994.
20. Solomon, E. I.; Heppner, D. E.; Johnston, E. M.; Ginsbach, J. W.; Cirera, J.; Qayyum, M.; Kieber-Emmons, M. T.; Kjaergaard, C. H.; Hadt, R. G.; Tian, L. Copper Active Sites in Biology. Chemical Reviews 2014, 114 (7), 3659–3853.

Contributed By:

This work was originally written by:

- ***Lydia Lorenc,*** *Spring 2018: Lydia is currently (as of 2018) a junior chemistry major at Saint Mary's College in Notre Dame, IN.*
- Margaret Benjamin, a chemistry major at Saint Mary's College, class of 2020.

This work was originally edited by Dr. Kathryn Haas, Assistant Professor and Madison Sendzik, Teaching and Research Assistant of Saint Mary's College.

Section 12.3: Biological Dioxygen Transport and Storage is shared under a CC BY-NC-SA license and was authored, remixed, and/or curated by LibreTexts.

- **12.3: Biological Dioxygen Transport and Storage** has no license indicated.

Section 12.4: Biological Metal Storage

Iron

Iron is widely used in a wide number of biological applications. Ferrous (Fe^{2+}) ion appears to have been the environmentally stable form during prebiotic times. The combination of the reactivity of ferrous ion and the relatively large amounts of iron used by cells may have necessitated the storage of ferrous ion; recent results suggest that ferrous ion may be stabilized inside ferritin long enough to be used in some types of cells. The ability of primitive organisms photosynthetically oxidize H_2O into dioxygen, probably produced the worst case of environmental pollution in terrestrial history. As a result, the composition of the atmosphere, the course of biological evolution, and the oxidation state of environmental iron all changed profoundly. Paleontologists and meteorologists estimate that there was a lag of about 200 - 300 million years between the first dioxygen production and the appearance of significant dioxygen concentrations in the atmosphere, because the dioxygen produced at first was consumed by the oxidation of ferrous ions in the oceans. The transition in the atmosphere, which occurred about 2.5 billion years ago, caused the bioavailability of iron to plummet and the need for iron storage to increase. Comparison of the solubility of Fe^{3+} at physiological conditions (about 10^{-18} M) to the iron content of cells (equivalent to 10^{-5} to 10^{-8} M) emphasizes the difficulty of acquiring sufficient iron.

Iron is stored mainly in the ferritins, a family of proteins composed of a protein coat and an iron core of hydrous ferric oxide [$Fe_2O_3(H_2O)_n$] with various amounts of phosphate.[6,7] As many as 4,500 iron atoms can be reversibly stored inside the protein coat in a complex that is soluble; iron concentrations equivalent to 0.25 M [about 10^{16}-fold more concentrated than Fe(III) ions] can be easily achieved *in vitro*. Ferritin is found in animals, plants, and even in bacteria; the role of the stored iron varies, and includes intracellular use for Fe-proteins or mineralization, long-term iron storage for other cells, and detoxification of excess iron. Iron regulates the synthesis of ferritin, with large amounts of ferritin associated with iron excess, small or undetectable amounts associated with iron deficiency.

Ferritin

Despite the importance of iron for life, excess iron can be toxic.[3] Unregulated free iron can catalyze the production of harmful reactive oxygen species (ROS) and free radicals, most commonly via Fenton chemistry. The Fenton reaction (below) is the reaction between iron(II) ions and hydrogen peroxide to produce the extremely reactive and harmful hydroxyl radical (**$^{\bullet}OH$**).[1] ROS are generally strong oxidizing agents and can cause permanent cell damage, organ failure, and death

$$\mathbf{Fe^{2+} + H_2O_2 \rightarrow Fe^{3+} + OH^- + {}^{\bullet}OH}$$

Structurally, ferritin is a hollow cage and the sequestered iron is stored as an iron(III) mineral within the protein shell (Figure ***Section*12.4.1**).[2,3]

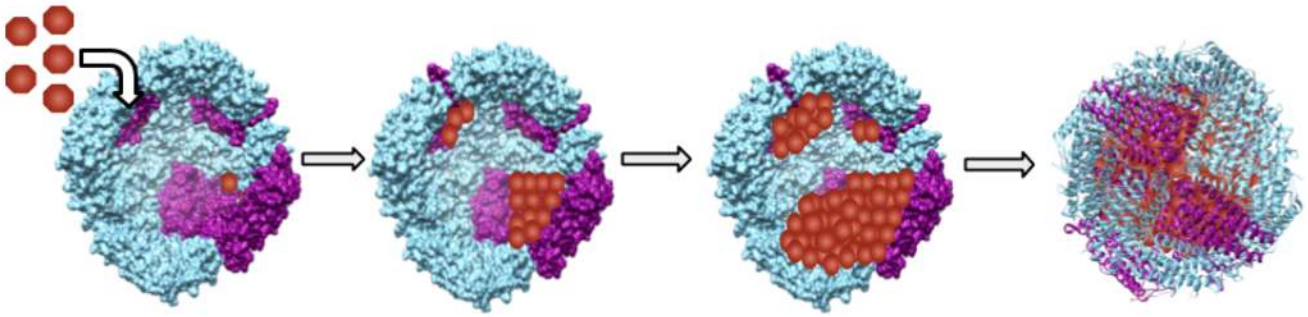


Figure *Section*12.4.1: A cartoon diagram of sequestration of iron, which has been crystallized and is stored as an iron/oxy mineral in the hollow cage of ferritin. From left to right, the diagram depicts the cross section of the ferritin protein cage and the growing nucleation in the hollow center of ferritin. Each red shape represents some crystalline, mineral combination of iron, oxygen, and hydrogen (FeOOH core). Nucleation begins on the purple surfaces of ferritin, which will be discussed in detail later, but is otherwise random. The final image in the diagram on the far right is the spherical ribbon structure of full iron-containing ferritin protein with the cartoon depiction of iron/oxy mineral (red shapes) within the center. While this diagram depicts ferritin being filled to capacity with iron, in reality, ferritin can be filled as much or as little with iron, as needed. Thus, this figure can also be interpreted as different ferritin proteins in environments of different iron concentrations and so storing different amounts of iron.

Ferritin is made of subunits. Each subunit has four polypeptide α-helices or spirals.[2] Structures of ferritin differ based on the organism which produces it. Most ferritin is made of 24 of these subunits.[6] Human ferritin is a 24-subunit, 480 kDa, 12 nm globular protein with a hollow center cavity (cavity diameter of 8 nm).[2] One 24-subunit ferritin protein can store up to 4500 iron ions in its hollow center.[2] Ferritin is a very good space-saving model for the cell because of its high iron to protein ratio (4500 iron ions/8 nm cavity).[2,9] This iron to protein ratio is 200 times that of hemoglobin.[9] Up to 24% of ferritin's weight could be stored iron ions. Meanwhile, bacterial ferritin can be either a 12- or 24-subunit globular protein.[6] However, it is thought that the 12-subunit ferritin's may play an additional role in protecting DNA from oxidative damage, while the 24-subunit bacterial ferritin may control bacterial iron metabolism.[3]

The subunits of human ferritin are classified as the heavy subunit or "H-chain" and the light subunit or "L-chain" (Figure *Section*12.4.2).[6] The two subunits, however, are not extremely different in molecular weight or amino acid sequence. The H-chain is made of 178 amino acids with a molecular weight of 21 kDa and the L-chain is made 171 amino acids and weighs 18 kDa.[4] The two types of subunits have ~53% protein sequence identity.[4] The designations of heavy and light are actually a modern recasting of designations that originally reflected the organs from which the two forms were isolated, "H" for heart and "L" for liver.[8]

The two types of subunits combine in different ratios to form the 24-subunit protein shell in humans (Figure *Section*12.4.2).[6] This ratio is dependent on the tissue where the ferritin is synthesized.[6] The H subunit is responsible for catalyzing the oxidation of iron(II).[8] The L subunit hosts the site of nucleation and storage of iron.[8] The ratio of H:L will be higher in tissues where iron oxidation activity is high and iron detoxification is needed, such as the heart or the brain.[1,4] Tissues, like those in the spleen, are used more for storage and will have a lower H:L ratio. The human liver produces ferritin that is 50% H and 50% L.

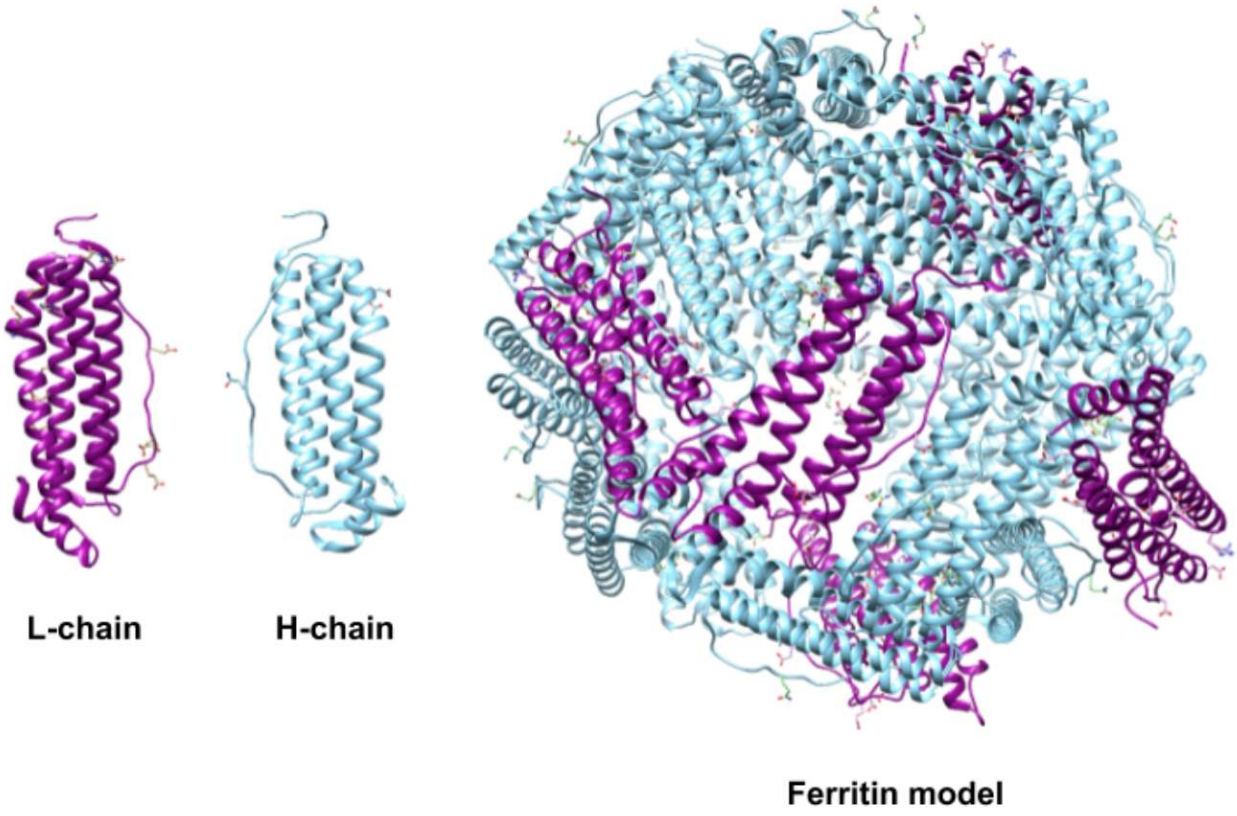


Figure *Section*12.4.2: Light (L) (PDB 2FFX) and heavy (H) (PDB 2FHA) human ferritin subunit chains combine to form the human ferritin shell in specific ratios. The H:L ratio is dependent on the tissue where the protein is synthesized. The model seen here was created from the crystal structures of individual subunits, not a biologically obtained structure. However, it is approximately 30% L-type subunit and 70% H-type subunit and would be of a similar ratio to the ferritin found in the brain.[1]

Selectivity for Iron

Fe^{2+} ions are brought to ferritin for storage by the transport protein transferrin. The ions are believed to enter through one of the eight symmetric 3-fold channels or one of the six symmetric 4-fold channels formed by the subunits in the ferritin structure highlighted in Figure *Section*12.4.3.[6]

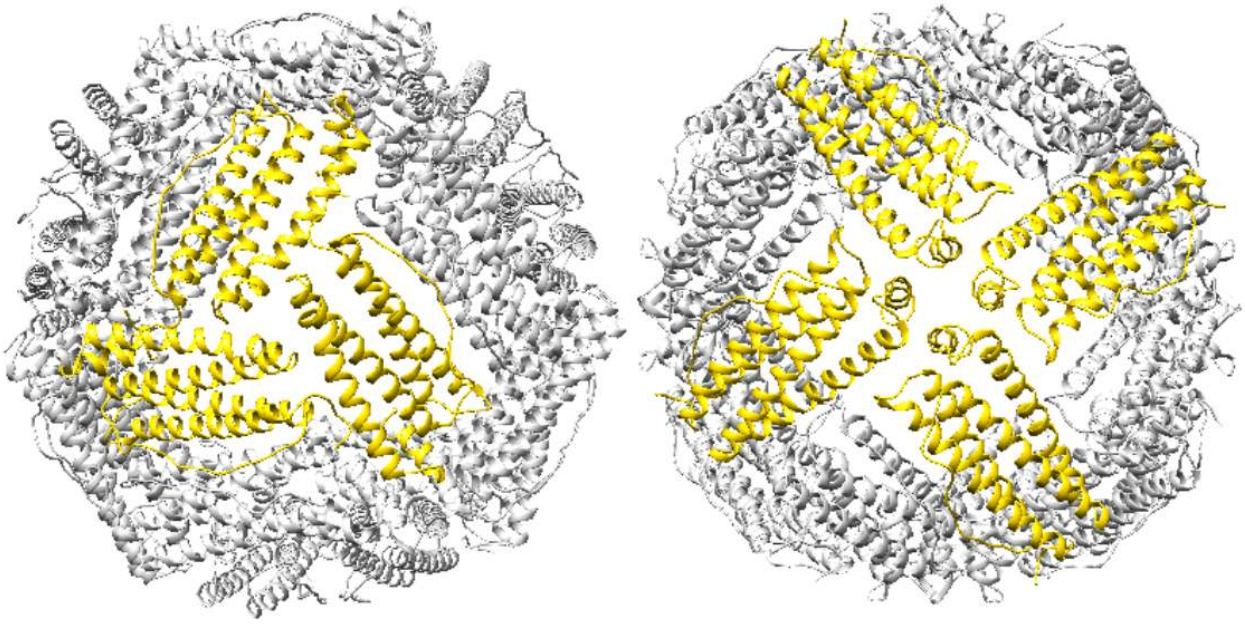


Figure *Section*12.4.3. Symmetric channels of entry and exit in Ferritin (PDB: 1FHA). The 3-fold channel on the left appears eight times in the 24 subunit ferritin protein. The 3-fold channel is formed by three subunits. The 4-fold channel on the right appears six times in the 24 subunit ferritin protein. The 4-fold channel is formed by four subunits.

The 3-fold channels are lined with the polar side chains aspartate and glutamate and make the channel hydrophilic.[2] The hydrophilicity of the channel allows for the transport of water, metal cations, and hydrophilic molecules of an appropriate size into and and out of the ferritin center.[4] Most studies indicate that the 3-fold channel is the main channel for Fe^{2+} ions both into and out of the cell.[1,3] The 4-fold channels are lined with the non-polar side chain leucine and make the channel hydrophobic. It is widely thought that the 4-fold channels are involved with the diffusion of oxygen and hydrogen peroxide into and out of the ferritin center.[1]

Iron(II) ions are oxidized at the “ferroxidase site” on the H-chain subunits (Figure ***Section*12.4.4**). After conversion to Fe^{3+}, the iron is stored as a crystalline iron/oxy mineral.[2] The mineral accumulates on the L-chain (Figure ***Section*12.4.5**).[8]

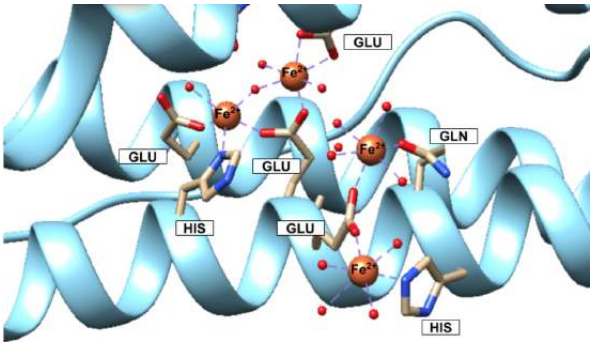


Figure ***Section*12.4.4**: Human Ferritin H-chain (PDB 4YKH). Fe2+ ions are both shown traveling on their way to the ferroxidase site and at the ferroxidase site, to be covered in detail later. Fe2+ ions can be seen binding to water molecules, oxidizing agents and residues glutamic acid (Glu or GLU), glutamine (Gln or GLN), and histidine (His or HIS). The smaller red balls connecting to the Fe2+ ions via a purple dashed line are the oxidizing agents—oxygen molecules, hydrogen peroxide, or water molecules.

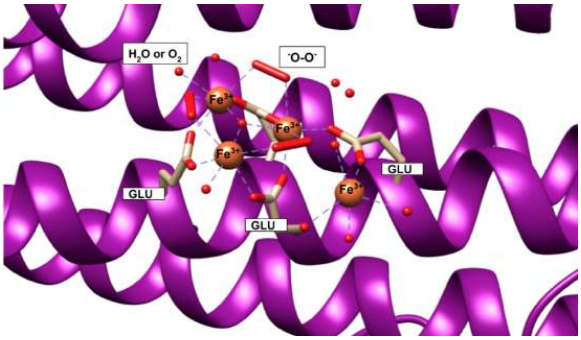


Figure ***Section*12.4.5**: Human Ferritin L-chain (PDB 5LG8). Fe3+ ions can be seen binding to water and oxygen molecules (small red balls), peroxo groups (long red cylinders), and residues of glutamic acid (Glu or GLU) from the L-chain. Fe3+ is stored as an iron/oxy mineral on the L-chain. This is the beginning of nucleation within the ferritin cavity.

Figures 4 and 5 show iron(II) at the ferroxidase site and iron/oxy mineral at the nucleation site, according to the available crystal structures. The structure of the entire iron mineral core, however, is actually inconsistent throughout the whole mineral and differs even between identical ferritin shells. Traditionally, it was believed that the iron(III)/oxy mineral that makes up the core was similar to ferrihydrite and ideally structured as 20% tetrahedral and 80% octahedral; however, as more evidence has become available this model has been replaced by a “polyphasic” or heterogeneous model of the iron core that is thought to be more accurate.[2,4] According to the polyphasic model, the mineral structure is heterogeneous in its chemical content and geometric structure.[4] X-ray absorption fine structure (EXAFS) studies concluded that the iron core of ferritin was made of iron ions that are surrounded by six or seven oxygen atoms, surrounded by another shell of iron ions.[2] This inconsistency leads to the conclusion that the mineral is a heterogeneous, hydrated iron(III)/oxy.[3] In other words, the iron core itself is not packed regularly or in a pattern within ferritin.[6]

Selectivity of iron(II) by ferritin can be explained through hard-soft acid base (HSAB) theory. Ferritin binds an Fe^{2+} ion for oxidation. Fe^{2+} is categorized as a borderline acid. The binding sites on the H-chain are glutamic acid (Glu), histidine (His), and glutamine (Gln) residues (Figure ***Section*12.4.4**).[6] Glu and Gln are categorized as hard bases, while His is categorized as borderline base. The oxidizing agents—oxygen molecules, hydrogen peroxide, or water molecules all have hard character. Fe^{2+} as a borderline acid binds well with the binding site of mixed hard and borderline character. The selection of Fe^{2+} in ferritin is further supported by experimental work where metals like zinc (which also exists in the body) were also shown to have binding abilities to ferritin.[5] But, zinc, although it is also borderline, has softer character than Fe^{2+} and so would not be as stable or favorable with the hard Glu and Gln ligands.[10]

Iron Mineralization

Iron(II) is oxidized at the ferroxidase site on the H-chain (sites A and B) by some oxidizing agent, most probably O_2 and H_2O_2.[1] Three reactions/models for Fe^{2+} oxidation and mineralization have been observed. There is a ferroxidation reaction or protein catalysis model (Reactions \PageIndex {1} -\PageIndex {4}), a mineralization reaction or crystal growth model (Reaction \PageIndex {5}), and a detoxification reaction of Fe^{2+} + H_2O_2 (Reaction \PageIndex {6}).[1] The ferroxidation reaction occurs at the ferroxidase site on the H-chain of ferritin. The ferroxidation reaction for the protein catalysis model of ferritin oxidation can be written as:

$$[2Fe^{2+} + O_2 + 4H_2O \rightarrow [Fe^{3+}-O-O-Fe^{3+}]^{2+} \quad \text{(Section 12.4.1)}$$

$$Fe^{3+}-O-O-Fe^{3+}]^{2+}] \rightarrow [Fe_2O-(OH)_2]^{2+} \quad \text{(Section 12.4.2)}$$

$$[Fe_2O-(OH)_2]^{2+} \rightarrow 2FeOOH_{core} + H_2O_2 + 4H^+ \quad \text{(Section 12.4.3)}$$

$$\text{Net: } 2Fe^{2+} + O_2 + 4H_2O \rightarrow 2FeOOH_{core} + H_2O_2 + 4H^+ \quad \text{(Section 12.4.4)}$$

The net mineralization reaction for the crystal growth model of ferritin oxidation is written as:

$$4Fe^{2+} + O_2 + 6H_2O \rightarrow 4FeOOH_{core} + 8H^+ \quad \text{(Section 12.4.5)}$$

The most recently identified of the oxidation and mineralization reactions, the Fe^{2+} + H_2O_2 detoxification reaction is written as:

2 Fe^{2+} + H_2O_2 + 2 H_2O → 2 $FeOOH_{core}$ + 4 H^+ (**3.**).[1]

Iron Release

When cells require iron, for enzyme synthesis, after blood loss, or during embryonic development, the iron stored in ferritin must be released rapidly, on demand, and under control.[8] Although, as with many aspects of ferritin function, the mechanism of iron release to the cell from ferritin is unknown. What is known inherently about the process is that over its course it must essentially reverse mineralization: the iron(III)/oxy mineral must be dissolved from its solid state to aqueous ions and the iron(III) ions must be reduced to iron(II).

Proposed models for ferritin iron release include (1) an equilibrium between the iron stored in ferritin and the iron in the cytoplasm of the cell, (2) ferritin protein degradation, (3) spontaneous, direct dissolution of iron(III) from the mineral core from scavenging by iron(III) binding proteins, and (4) the reduction of the iron(III) mineral which is then complexed iron(II) by a chelating agent and transported out of ferritin.[4,12] The last model (4) lacks confirmation, yet is considered by many to be the physiological mechanism. This model is the most efficient method and the presence of reducing agents under physiological conditions.[4]

Except the second model (2), the physiological relevance of all above models is still to be seen.[12] The ferritin degradation model (2) is the only mechanism to have been observed under physiological conditions. However, since this model would require iron release to be dependent of the turnover and synthesis of ferritin, another model is suspected to be necessary.[12]

However iron is released from ferritin, studies indicate that the physical exit of the iron from ferritin takes place via the 3-fold channels. One proposal for exit based on observations in bacterial ferritin is the localized folding/unfolding of ferritin.[4] The ferritin channels can be unfolded without affecting the overall function or structure of the protein. Unfolding the channels and thus, widening the opening, would allow for quick release of demineralized iron. The channels become highly disordered when this occurs to the effect that they do not appear in crystal structures.[8]

Much remains to be determined about human ferritin. Other functions of ferritin in the body, and the mechanisms for how Fe^{2+} enters and binds to ferritin, how Fe^{2+} is oxidized to Fe^{3+} for storage, and how iron is released remain undetermined, among others, are thought to be non-universal—even within the same organism.[3,6]

While much of the chemistry behind ferritin is, as of now, unexplained, ferritin is still an important protein for all life. Wherever iron is noted as an essential nutrient, ferritin must also be present for management and storage. The elucidation of ferritin can lead to advancements in iron metabolism and neurological disorders and new uses of ferritin chemistry in nanochemistry and catalytic industrial applications.[3,4]

Sources

[1] Bou-Abdallah, F. The Iron Redox and Hydrolysis Chemistry of the Ferritins. *Biochimica et Biophysica Acta (BBA) - General Subjects* **2010**, *1800* (8), 719–731.

[2] Crabb, E.; Moore, E. *Metals and life*; Royal Society of chemistry: Cambridge, **2010**.

[3] Theil, E. C.; Tosha, T.; Behera, R. K. Solving Biology's Iron Chemistry Problem with Ferritin Protein Nanocages. *Accounts of Chemical Research* **2016**, *49* (5), 784–791.

[4] Carmona, F.; Palacios, Ò.; Gálvez, N.; Cuesta, R.; Atrian, S.; Capdevila, M.; Domínguez-Vera, J. M. Ferritin Iron Uptake and Release in the Presence of Metals and Metalloproteins: Chemical Implications in the Brain. *Coordination Chemistry Reviews* **2013**, *257* (19–20), 2752–2764.

[5] Knovich, M. A.; Storey, J. A.; Coffman, L. G.; Torti, S. V. Ferritin for the Clinician. *Blood Rev* **2009**, *23* (3), 95–104.

[6] Bradley, J. M.; Le Brun, N. E.; Moore, G. R. Ferritins: Furnishing Proteins with Iron. *JBIC Journal of Biological Inorganic Chemistry* **2016**, *21* (1), 13–28.

[7] Watt, G. D.; Jacobs, D.; Frankel, R. B. Redox Reactivity of Bacterial and Mammalian Ferritin: Is Reductant Entry into the Ferritin Interior a Necessary Step for Iron Release? *Proceedings of the National Academy of Sciences* **1988**, *85* (20), 7457–7461.

[8] Bertini, I. *Biological Inorganic Chemistry: Structure and Reactivity*; University Science Books, **2007**.

[9] Chasteen, N. D.; Harrison, P. M. Mineralization in Ferritin: An Efficient Means of Iron Storage. *Journal of Structural Biology* **1999**, *126* (3), 182–194.

[10] Joshi, J. G.; Sczekan, S. R.; Fleming, J. T. Ferritin—A General Metal Detoxicant. *Biol Trace Elem Res* **1989**, *21* (1), 105.

[11] Bertini, I.; Lalli, D.; Mangani, S.; Pozzi, C.; Rosa, C.; Theil, E. C.; Turano, P. Structural Insights into the Ferroxidase Site of Ferritins from Higher Eukaryotes. *Journal of the American Chemical Society* **2012**, *134*(14), 6169–6176.

[12] Honarmand Ebrahimi, K.; Hagedoorn, P.-L.; Hagen, W. R. Unity in the Biochemistry of the Iron-Storage Proteins Ferritin and Bacterioferritin. *Chemical Reviews* **2015**, *115* (1), 295–326.

[13] H. Rodriguez, J.; Mccusker, J. Density Functional Theory of Spin-Coupled Models for Diiron-Oxo Proteins: Effects of Oxo and Hydroxo Bridging on Geometry, Electronic Structure, and Magnetism. *Journal of Chemical Physics* **2002**, *116*.

[14] Bertini, I., *Bioinorganic Chemistry*; Ed.; University Science Books: Mill Valley, Calif, **1994**.

Contributed By

*This work was originally written by **Anna Shadid,** Spring 2018: Anna is currently (as of 2018) a junior chemistry major at Saint Mary's College in Notre Dame, IN.*

This work was originally edited by Dr. Kathryn Haas, Associate Professor, and Madison Sendzik, Teaching and Research Assistant, of Saint Mary's College.

Zinc, Copper, Vanadium, Chromium, Molybdenum, Cobalt, Nickel, and Manganese

Ions of nonferrous transition metals require a much less complex biological storage system, because the solubilities are much higher ($\geq 10^{-8}$ M) than those for Fe^{3+}. As a result, the storage of nonferrous transition metals is less obvious, and information is more limited. In addition, investigations are more difficult than for iron, because the amounts in biological systems are so small. Essentially nothing is known yet about the storage of vanadium, chromium, molybdenum, cobalt, nickel, and manganese, with the possible exception of accumulations of vanadium in the blood cells of tunicates.

Zinc and copper, which are used in the highest concentrations of any of the non-ferrous transition metals, are specifically bound by the protein metallothionein. (see Figure ***Section*12.4.8**). Like the ferritins, the metallothioneins are a family of proteins, widespread in nature and regulated by the metals they bind. In contrast to ferritin, the amounts of metal stored in metallothioneins are smaller (up to twelve atoms per molecule) and the amount of protein in cells is less. Because the cellular concentrations of the metallothioneins are relatively low and the amount of metal needed is relatively small, it has been difficult to study the biological fate of copper and zinc in living organisms, and to discover the natural role of metallothioneins. However, the regulation of metallothionein synthesis by metals, hormones, and growth factors attests to the biological importance of the proteins. The unusual metal environments of metallothioneins have attracted the attention of bioinorganic chemists.

Metallothioneins, especially in higher animals, are small proteins rich in cysteine (20 per molecule) and devoid of the aromatic amino acids phenylalanine and tyrosine. The cysteine residues are distributed throughout the peptide chain. However, in the native form of the protein, the peptide chains fold to produce two clusters of -SH, which bind either three or four atoms of zinc, cadmium, cobalt, mercury, lead, or nickel. Copper binding is distinct from zinc, with 12 sites per molecule.

In summary, iron is stored in iron cores of a complicated protein. Ferritin, composed of a hollow protein coat, iron-protein interface, and an inorganic core, overcomes the problems of redox and hydrolysis by directing the formation of the quasi-stable mineral hydrous ferric oxide inside the protein coat. The outer surface of the protein is generally hydrophilic, making the complex highly soluble; equivalent concentrations of iron are ≤ 0.25 M. By contrast to iron, storage of zinc, copper, chromium, manganese, vanadium, and molybdenum is relatively simple, because solubility is high and abundance is lower. Little is known about the molecules that store these metals, with the possible exception of metallothionein, which binds small clusters of zinc or copper.

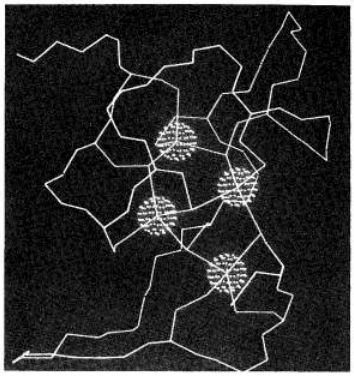


Figure ***Section*12.4.8**: - The three-dimensional structure of the a domain from rat cd_7 metallothionein-2, determined by NMR in solution, based on data in Reference 36b. The four metal atoms, bonded to the sulfur of cysteine side chains, are indicated as spherical collections of small dots. A recent description of the structure of the cd_5Zn_2 protein, determined from x-ray diffraction of crystals, agrees with the structure determined by NMR.

Section 12.4: Biological Metal Storage is shared under a CC BY-NC-SA license and was authored, remixed, and/or curated by LibreTexts.

Section 12.5: Zinc as Lewis Acid and Template

Introduction

Unlike most other biologically important metals, zinc is not redox active and does not directly participate in catalytic reaction. In biological systems zinc is primarily found as Zn^{2+}, which is a d^{10} ion, making it unfavorable to either oxidize or reduce. Zinc ions do play important biochemical roles. They can act as Lewis acids, to indirectly catalyse reactions such as the hydration of carbon dioxide in carbonic anhydrase. They can also act as templates or scaffolds for protein tertiary structure.

Zinc in Carbonic Anhydrase

Chemical Reaction

Carbon-dioxide (CO_2) hydration and its mechanism in living systems are of fundamental importance for bioinorganic chemistry. In 1932 the existence of an enzyme catalyzing CO_2 hydration in red blood cells, carbonic anhydrase, was established. In 1939 the enzyme was recognized to contain zinc. Because CO_2 is both the starting point for photosynthesis and the endpoint of substrate oxidation, carbonic anhydrases are now known to be ubiquitous, occurring in animals, plants, bacteria, and fungi. Carbonic anhydrase is a classic example of a hydrolytic enzyme, one that catalyzes addition or removal of water to a substrate molecule. More specifically, it catalyzes the reversible conversion of carbon dioxide (CO_2) to bicarbonate (HCO_3^-).



Figure ***Section*12.5.1**: Reaction catalysed by carbonic anhydrase enzymes.

Although hydration of CO_2 is spontaneous in water at pH 7, the reaction is kinetically slow ($k = 10^{-1}\ s^{-1}$), too slow to convert all CO_2 produced in respiration. Only above pH 9 does the uncatalyzed reaction become fast, due to direct attack of OH^-, which is a much better nucleophile than H_2O ($k = 10^4\ M^{-1}\ s^{-1}$, in the presence of OH^-). Figure ***Section*12.5.2** compares nucleophilic attack of water versus hydroxide (OH-) on CO_2.



Figure ***Section*12.5.2**: Nucleophilic attack on carbon in carbon dioxide (CO_2) in the formation of bicarbonate (HCO_3^-). In the top panel, H_2O is the nucleophile. The bottom panel shows the reaction with hydroxide (OH^-) as the nucleophile. Since the OH^- is a stronger nucleophile, HCO_3^- formation is faster when OH^- is the nucleophile.

Between H_2O and OH^-, formation of HCO_3^- occurs faster when OH^- is the nucleophile. A faster reaction at higher pH, when more OH^- ions are present, suggests OH^- is involved in the rate determining step. However, realistically, the pH of human blood cannot be changed to speed up hydration of CO_2. Instead, humans use carbonic anhydrase to catalyse the reaction. When carbonic anhydrase is present, the reaction is sped up to a rate of $k = 10^6\ s^{-1}$.

The ubiquity of carbonic anhydrase in different organisms reflects the importance of these enzymes in sustaining life. The speed of catalyzed CO_2 hydration is essential to meet the needs of living cells. Some physiological carbonic anhydrase functions include pH regulation, electrolyte secretion, ion transport, and CO_2 homeostasis. In the digestive tract, carbonic anhydrases plays a role in the secretion of acid and keep saliva neutral by modulating pH. Among these functions, CA most notably plays a role in transport of CO_2 and HCO_3^- related to respiration. With low blood solubility, CO_2 must be converted to a more soluble form, HCO_3^-, for

transport throughout the body. Bicarbonate ions eventually reach the lungs, get converted back to CO_2, and exit the body through exhalation.

Medical research revolving around carbonic anhydrase focuses on the Zn-containing active site as a therapeutic target for various disease treatments; both carbonic anhydrase inhibitors and activators are incorporated in drug design. Carbonic anhydrase inhibitors are used as treatment for epilepsy, ulcers, cancer, obesity, and other neurological disorders. In the eye, carbonic anhydrase produces hydrogen ions that maintain optic pressure. However, too much pressure in the eye can damage the optic nerve and cause glaucoma. Carbonic anhydrase activity can create a concentration gradient that drives the transport of water to the optical nerve. When too much water is around the optical nerve, pressure around the nerve increases causing damage. Inhibition of carbonic anhydrase has become a key treatment of glaucoma.

Role of Zinc

The zinc ion is bound to the protein via three links to separate histidine residues in the chain, shown in pink in Figure ***Section*12.5.3**. The zinc is also attached to a hydroxide ion shown in the picture using red for the oxygen and white for the hydrogen.

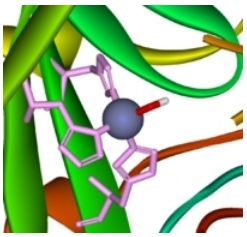
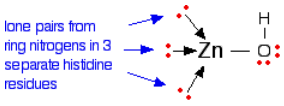


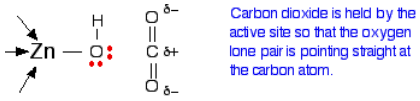
Figure ***Section*12.5.3**: Zinc active site of carbonic anhydrase showing the coordination of zinc (purple sphere) by three hisiadine residues (pink) and one hydroxide ion.

If you look at the model of the arrangement around the zinc ion in the picture above the arrangement of the four groups around the zinc is approximately tetrahedral.

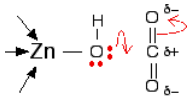


How does this catalyse the reaction between carbon dioxide and water?

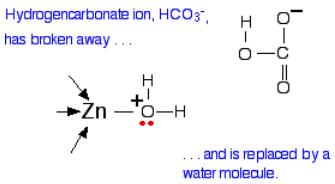
A carbon dioxide molecule is held by a nearby part of the active site so that one of the lone pairs on the oxygen is orientated towards the carbon atom of the carbon dioxide molecule. Binding the carbon dioxide in the enzyme also increases the existing polarity of the carbon-oxygen bonds.



If you have done any work on organic reaction mechanisms at all, then it is pretty obvious what is going to happen. The lone pair forms a bond with the carbon atom and part of one of the carbon-oxygen bonds breaks and leaves the oxygen atom with a negative charge on it. This results in a hydrogen carbonate ion coordinated to the zinc center.



The next step in the reaction is for the hydrogen carbonate to leave and be replaced with a water molecule from the cell solution.



All that now needs to happen to get the catalyst back to where it started is for the water to lose a hydrogen ion. This is transferred away from the zinc center and eventually out of the active site completely through the network of ordered, hydrogen bonded water molecules shown in Figure ***Section*12.5.4**. The carbonic anhydrase enzyme can do this sequence of reactions about a million times a second.

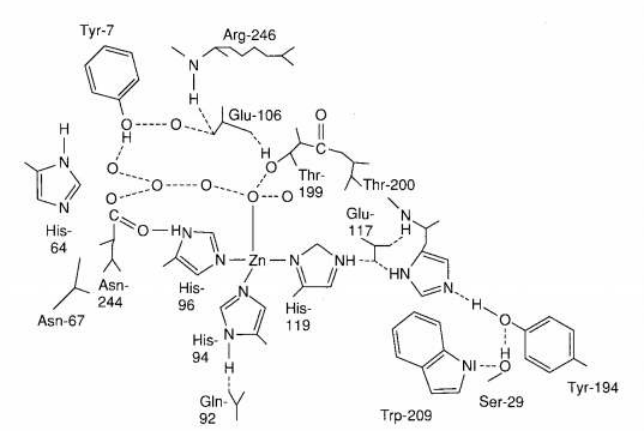


Figure ***Section*12.5.4**: Schematic representation of the active site of human carbonic anhydrase II. Hydrogen bonds (---) and ordered water molecules (o) are indicated.

Zinc as a Structural Template

Many proteins use Zn^{2+} as a structural scaffold for protein folding. These proteins employ "zinc finger" domains that bind to Zn through combinations of cysteine (Cys) and Histidine (His) side chains. Zinc binding to these domains stabilizes a specific protein fold that is critical to the protein's function. Over half of transcription factors have zinc finger domains that allow the proteins to recognize and bind to DNA. Many other proteins also have zinc-finger domains and these domains are important for a variety of functions including DNA-binding, RNA-binding, protein-protein interactions, and catalysis.

The human glioblastoma protein (GLI) family is a class of transcription factors that demonstrate sequence-specific DNA binding through "classic" Cys2His2 Zn-binding motifs. These proteins are essential during embryonic development. Dysfunction of these proteins are linked closely to glioblastoma and other aggressive cancers. The zinc finger domain of GLI1 is shown in this image (PDB 2gli),[2] where the protein surface is highlighted in yellow. GLI1 possesses five Cys2His2 zinc finger domains. When Zn is not bound to the protein, it does not have the appropriate structure to bind to recognize DNA.

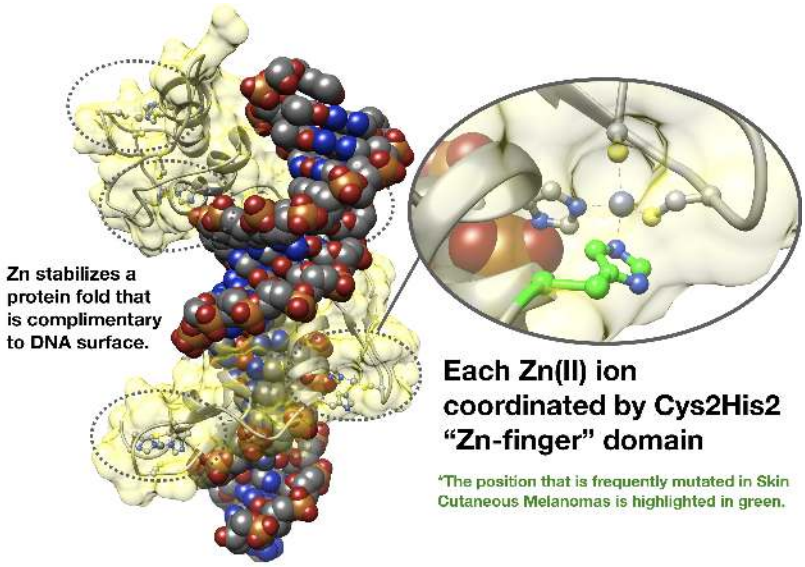


Figure *Section*12.5.5: The zinc finger domain of human glioblastoma protein GLI1 complexed with DNA. Inset shows the coordination of Zn^{2+} in the " zinc finger" domain.

The size and structure of the Zn^{2+} ion is critical to provide the correct protein fold for DNA binding. Thus, zinc fingers must bind specifically to Zn (as opposed to other biologically available metal ions). The zinc finger domains use principles of inorganic chemistry to control metal ion selectivity. While other metal ions, like Co^{2+}, Ni^{2+}, Fe^{2+}, and Mn^{2+}, can bind in the zinc finger sites, Zn^{2+} binds 1,000 to 100,000 times more strongly than any of these other metals.

Exercise *Section*12.5.1

Apply HSAB theory to explain why there is such a strong selectivity for Zn^{2+} binding in a zinc finger site as opposed to other biologically available metals, including Co^{2+}, Ni^{2+}, Fe^{2+}, and Mn^{2+}.

Answer

The zinc binding site contains two borderline histadine ligands and two soft cystine ligands. The Zn^{2+} is a softer borderline Lewis acid compared to other biologically available metal ions, especially Fe^{2+}. This is because the size of transition metal cations don't vary much across the period, giving them all similar size to charge ratios and Zn^{2+}has the highest number of valence electrons, making it the most polarizable. Because the active site has two soft base donors and two borderline base donors, softer metals will preferentially bind in the active site.

Exercise *Section*12.5.2

Cadmium (Cd^{2+}) and lead (Pb^{2+}) are toxic metal ions that bind more strongly than Zn^{2+} to zinc binding sites in proteins. Why do these toxic metals compete well with Zn^{2+}, while other metals like Co^{2+}, Ni^{2+}, Fe^{2+}, and Mn^{2+} don't?

Answer

As discussed in Exercise 1, the zinc finger binding site is biased towards coordinating softer metals. Both cadmium and lead ions are much softer than zinc and will have a stronger affinity than zinc for the zinc binding site. Under normal conditions this is not an issue because lead and cadmium are not present in significant concentrations.

Exercise *Section*12.5.1

If a toxic metal, like Cd^{2+} would bind to the Zn^{2+} binding site, how and why might this affect the protein's ability to bind to DNA?.

Answer

The proper folding and structure of these proteins is dependent on zinc coordination in the zinc finger domains. If a larger metal ion, such as Cd^{2+} were to bind in place of Zn^{2+} this would change the size and/or geometry of the zinc finger domain and therefore the entire protein. The correct shape of the protein is essential for recognition and binding of DNA.

References

1. Inspired by Zinc Finger Proteins: A Bioinorganic Example of LFSE and HSAB, a problem set created by Elizabeth R. Jamieson, Smith College (ejamieso@smith.edu) and posted on VIPEr (www.ionicviper.org) on June 24, 2013. Copyright Elizabeth R. Jamieson 2013. This work is licensed under the Creative Commons Attribution-NonCommerical-ShareAlike 3.0 Unported License. To view a copy of this license visit http://creativecommons.org/about/license/.
2. Pavletich, N. P.; Pabo, C. O., Crystal Structure of a Five-Finger Gli-DNA Complex: New Perspectives on Zinc Fingers. *Science* **1993**, *261* (5129), 1701-7.
3. Munro, D.; Ghersi, D.; Singh, M., Two Critical Positions in Zinc Finger Domains Are Heavily Mutated in Three Human Cancer Types. *PLOS Computational Biology* **2018**, *14* (6), e1006290.

Section 12.5: Zinc as Lewis Acid and Template is shared under a CC BY-NC-SA license and was authored, remixed, and/or curated by LibreTexts.

Section 12.6: Electron Transfer

Overview

Metalloproteins containing a single type of redox cofactor can be divided into two general classes: electron carriers and proteins involved in the transport or activation of small molecules. Some of the factors that seem to be characteristic of electron-transfer proteins (these proteins are sometimes called "electron transferases") are: (a) possession of a suitable cofactor to act as an electron sink (metal center with multiple stable oxidation states); (b) placement of the cofactor close enough to the protein surface to allow electrons to move in and out; (c) existence of a hydrophobic shell adjacent to, but not always entirely surrounding, the cofactor; (d) small structural changes accompanying electron transfer; and (e) an architecture that permits slight expansion or contraction in preferred directions upon electron transfer.

Metalloproteins that function as electron transferases typically place their metal coordination sites in a hydrophobic environment and may provide hydrogen bonds (in addition to ligands) to assist in stabilizing both the oxidized and the reduced forms of the cofactor. Metal-ligand bonds remain intact upon electron transfer to minimize inner-sphere reorganization energy. Many of the complex multisite metalloenzymes (e.g., cytochrome c oxidase, xanthine oxidase, the nitrogenase FeMo protein) contain redox centers that function as intramolecular electron transferases, shuttling electrons to/from other metal centers that bind exogenous ligands during enzymatic turnover.

There are three classes of metal containing electron transferases, each of which contains many members that exhibit important structural differences: blue copper proteins, iron-sulfur proteins, and cytochromes.

Blue Copper Proteins

Blue copper proteins were first isolated from bacteria in the 1950s and from plant tissues in the early 1960s. The intense blue color of these proteins is due to a strong absorption band at a wavelength of about 600 nm. Although simple Cu^{2+} complexes, such as $[Cu(H_2O)_6]^{2+}$ and $[Cu(NH_3)_4]^{2+}$, are also blue due to an absorption band at 600 nm, the intensity of the absorption band is about 100 times less than that of a blue copper protein. Moreover, the reduction potential for the Cu^{2+}/Cu^{+} couple in a blue copper protein is usually +0.3 to +0.5 V, considerably more positive than that of the aqueous Cu^{2+}/Cu^{+} couple (+0.15 V).

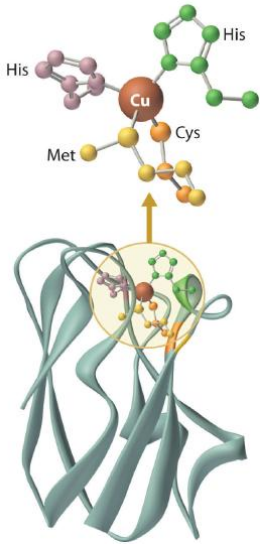


Figure ***Section*12.6.1**: A Blue Copper Protein. In both the oxidized and reduced forms of a blue copper protein, the copper is coordinated by four ligands (two histidine imidazole nitrogen atoms, a cysteine thiolate sulfur, and a thioether sulfur of a methionine) in a roughly tetrahedral arrangement.

The copper center in blue copper proteins has a distorted tetrahedral structure, in which the copper is bound to four amino acid side chains (Figure ***Section*12.6.3**). Although the most common structures for four-coordinate Cu^{2+} and Cu^{+} complexes are square planar and tetrahedral, respectively, the structures of the oxidized (Cu^{2+}) and reduced (Cu^{+}) forms of the protein are essentially identical.

Thus the protein forces the Cu^{2+} ion to adopt a higher-energy structure that is more suitable for Cu^{+}, which makes the Cu^{2+} form easier to reduce and raises its reduction potential.

Moreover, by forcing the oxidized and reduced forms of the metal complex to have essentially the same structure, the protein ensures that electron transfer to and from the copper site is rapid because only minimal structural reorganization of the metal center is required. Kinetics studies on simple metal complexes have shown that electron-transfer reactions tend to be slow when the structures of the oxidized and reduced forms of a metal complex are very different, and fast when they are similar. You will see that other metal centers used for biological electron-transfer reactions are also set up for minimal structural reorganization after electron transfer, which ensures the rapid transfer of electrons.

The blue copper proteins are characterized by intense S(Cys) → Cu chargetransfer absorption near 600 nm, an axial EPR spectrum displaying an unusually small hyperfine coupling constant, and a relatively high reduction potential.[4,8-10] With few exceptions (e.g., photosynthetic organisms), their precise roles in bacterial and plant physiology remain obscure. X-ray structures of several blue copper proteins indicate that the geometry of the copper site is approximately trigonal planar, as illustrated by the *Alcaligenes denitrificans* azurin structure (Figure 6.5).[11,12] In all these proteins, three ligands (one Cys, two His) bind tightly to the copper in a trigonal arrangement. Differences in interactions between the copper center and the axially disposed ligands may significantly contribute to variations in reduction potential that are observed[12] for the blue copper electron transferases. For example, $E^{\circ\prime}$ = 276 mV for *A. denitrificans* azurin, whereas that of *P. vulgaris* plastocyanin is 360 mV. In *A. denitrificans* azurin, the Cu-S(Met) bond is 0.2 Å longer than in poplar plastocyanin, and there is a carbonyl oxygen 3.1 Å from the copper center, compared with 3.8 Å in plastocyanin. These differences in bond lengths are expected to stabilize Cu^{II} in azurin to a greater extent than in plastocyanin, and result in a lower $E^{\circ\prime}$ value for azurin.

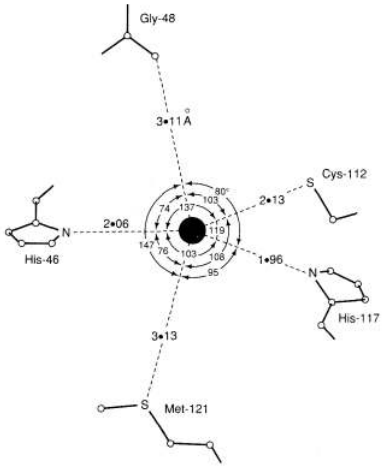


Figure 6.5 - Structure of the blue copper center in azurin.[11]

Iron Sulfur Proteins

Although all known bacteria, plants, and animals use iron–sulfur proteins to transfer electrons, the existence of these proteins was not recognized until the late 1950s. Iron–sulfur proteins transfer electrons over a wide range of reduction potentials, and their iron content can range from 1 to more than 12 Fe atoms per protein molecule. In addition, most iron–sulfur proteins contain stoichiometric amounts of sulfide (S^{2-}).

These properties are due to the presence of four different kinds of iron–sulfur units, which contain one, two, three, or four iron atoms per Fe–S complex (Figure ***Section*12.6.5**). In all cases, the Fe^{2+} and Fe^{3+} ions are coordinated to four sulfur ligands in a tetrahedral environment. Due to tetrahedral coordination by weak-field sulfur ligands, the iron is high spin in both the Fe^{3+} and Fe^{2+} oxidation states, which results in similar structures for the oxidized and reduced forms of the Fe–S complexes. Consequently, only small structural changes occur after oxidation or reduction of the Fe–S center, which results in rapid electron transfer.

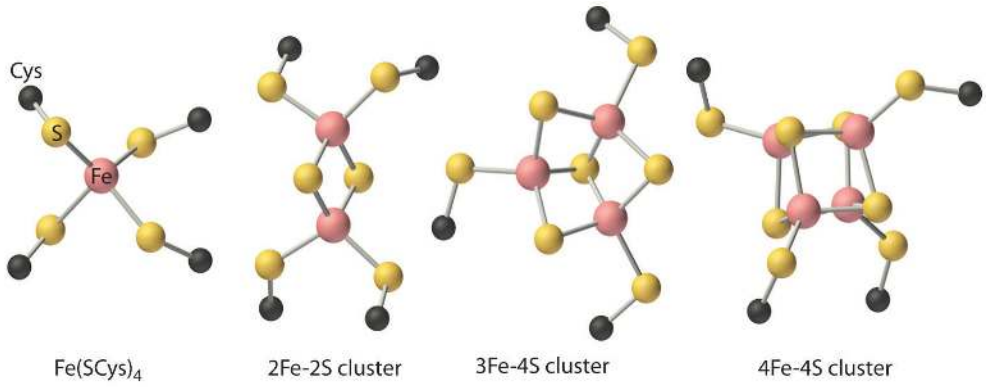


Figure *Section*12.6.5: Fe–S Centers in Proteins: Four kinds of iron–sulfur centers, containing one, two, three, and four iron atoms, respectively, are known in electron-transfer proteins. Although they differ in the number of sulfur atoms provided by cysteine thiolates versus sulfide, in all cases the iron is coordinated to four sulfur ligands in a roughly tetrahedral environment.

The iron-sulfur proteins play important roles[13,14] as electron carriers in virtually all living organisms, and participate in plant photosynthesis, nitrogen fixation, steroid metabolism, and oxidative phosphorylation, as well as many other processes (Chapter 7). The optical spectra of all iron-sulfur proteins are very broad and almost featureless, due to numerous overlapping charge-transfer transitions that impart red-brown-black colors to these proteins. On the other hand, the EPR spectra of iron-sulfur clusters are quite distinctive, and they are of great value in the study of the redox chemistry of these proteins.

The simplest iron-sulfur proteins, known as rubredoxins, are primarily found in anaerobic bacteria, where their function is unknown. Rubredoxins are small proteins (6 kDa) and contain iron ligated to four Cys sulfurs in a distorted tetrahedral arrangement. The E°' value for the $Fe^{III/II}$ couple in water is 770 mV; that of *C. pasteurianum* rubredoxin is -57 mV. The reduction potentials of iron-sulfur proteins are typically quite negative, indicating a stabilization of the oxidized form of the redox couple as a result of negatively charged sulfur ligands.

The [2Fe-2S] ferredoxins (10-20 kDa) are found in plant chloroplasts and mammalian tissue. The structure of *Spirulina platensis* ferredoxin[15] confirmed earlier suggestions, based on EPR and Mössbauer studies, that the iron atoms are present in a spin-coupled [2Fe-2S] cluster structure. One-electron reduction (E°' ~ -420 mV) of the protein results in a mixed-valence dimer (Equation 6.3):

$$[Fe_2S_2(SR)_4]^{2-} \underset{-e^-}{\overset{+e^-}{\rightleftharpoons}} [Fe_2S_2(SR)_4]^{3-} \tag{6.3}$$

$$Fd_{ox} \qquad Fd_{red} \qquad \text{(Section 12.6.1)}$$

$$2Fe(III) \qquad Fe(II) + Fe(III) \qquad \text{(Section 12.6.2)}$$

The additional electron in Fd_{red} is associated with only one of the iron sites, resulting in a so-called trapped-valence structure.[16] The $[Fe_2S_2(SR)_4]^{4-}$ cluster oxidation state, containing two ferrous ions, can be produced *in vitro* when strong reductants are used.

Four-iron clusters [4Fe-4S] are found in many strains of bacteria. In most of these bacterial iron-sulfur proteins, also termed ferredoxins, two such clusters are present in the protein. These proteins have reduction potentials in the -400 mV range and are rather small (6-10 kDa). Each of the clusters contains four iron centers and four sulfides at alternate comers of a distorted cube. Each iron is coordinated to three sulfides and one cysteine thiolate. The irons are strongly exchange-coupled, and the [4Fe-4S] cluster in bacterial ferredoxins is paramagnetic when reduced by one electron. The so-called "high-potential ironsulfur proteins" (HiPIPs) are found in photosynthetic bacteria, and exhibit anomalously high (~350 mV) reduction potentials. The *C. vinosum* HiPIP (10 kDa) structure demonstrates that HiPIPs are distinct from the [4Fe-4S] ferredoxins, and that the reduced HiPIP cluster structure is significantly distorted, as is also observed for the structure of the oxidized *P. aerogenes* ferredoxin. In addition, oxidized HiPIP is paramagnetic, whereas the reduced protein is EPR-silent.

This bewildering set of experimental observations can be rationalized in terms of a "three-state" hypothesis (i.e., $[4Fe\text{-}4S(SR)_4]^{n-}$ clusters exist in three physiological oxidation states).[17] This hypothesis nicely explains the differences in magnetic behavior and redox properties observed for these iron-sulfur proteins (Equation 6.4):

$$[4Fe-4S(SR)_4]^{-} \underset{-e^-}{\overset{+e^-}{\rightleftharpoons}} [4Fe-4S(SR)_4]^{2-} \underset{-e^-}{\overset{+e^-}{\rightleftharpoons}} [4Fe-4S(SR)_4]^{3-} \tag{6.4}$$

$HiPIP_{ox}$ $HiPIP_{red}$ $Ferredoxin_{red}$ (Section 12.6.3)

$Ferredoxing_{ox}$ (Section 12.6.4)

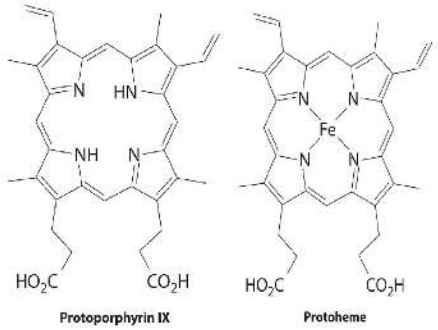
The bacterial ferredoxins and HiPIPs all possess tetracubane clusters containing thiolate ligands, yet the former utilize the -2/-3 cluster redox couple, whereas the latter utilize the -1/-2 cluster redox couple.

The protein environment thus exerts a powerful influence over the cluster reduction potentials. This observation applies to *all* classes of electron transferases—the factors that are critical determinants of cofactor reduction potentials are poorly understood at present but are thought[18] to include the low dielectric constants of protein interiors (~4 for proteins vs. ~78 for H_2O), electrostatic effects due to nearby charged amino-acid residues, hydrogen bonding, and geometric constraints imposed by the protein.

Cytochromes

The cytochromes (from the Greek cytos, meaning “cell”, and chroma, meaning “color”) were first identified in the 1920s by spectroscopic studies of cell extracts. Based on the wavelength of the maximum absorption in the visible spectrum, they were classified as cytochromes a (with the longest wavelength), cytochromes b (intermediate wavelength), and cytochromes c (shortest wavelength). It quickly became apparent that there was a correlation between their spectroscopic properties and other physical properties. For examples, cytochromes c are generally small, soluble proteins with a reduction potential of about +0.25 V, whereas cytochromes b are larger, less-soluble proteins with reduction potentials of about 0 V.

All cytochromes contain iron, and the iron atom in all cytochromes is coordinated by a planar array of four nitrogen atoms provided by a cyclic tetradentate ligand called a porphyrin. The iron–porphyrin unit is called a heme group. The structures of a typical porphyrin (protoporphyrin IX) and its iron complex (protoheme) are shown here. In addition to the four nitrogen atoms of the porphyrin, the iron in a cytochrome is usually bonded to two additional ligands provided by the protein, as shown in Figure *Section*12.6.4.



A cytochrome. Shown here is protoporphyrin IX and its iron complex, protoheme.

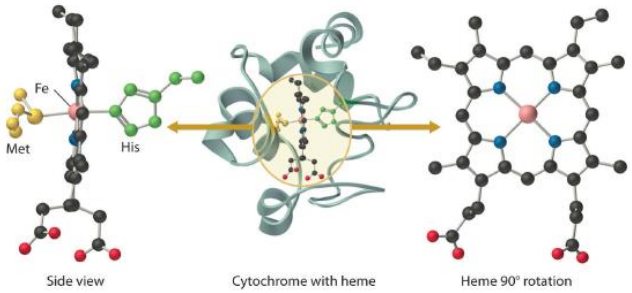


Figure *Section*12.6.4: A Cytochrome c. In a cytochrome c, the heme iron is coordinated to the nitrogen atom of a histidine imidazole and the sulfur atom of a methionine thioether, in addition to the four nitrogen atoms provided by the porphyrin.

In contrast to the blue copper proteins, two electron configurations are possible for both the oxidized and reduced forms of a cytochrome, and this has significant structural consequences. Thus Fe^{2+} is d^6 and can be either high spin (with four unpaired

electrons) or low spin (with no unpaired electrons). Similarly, Fe^{3+} is d^5 and can also be high spin (with five unpaired electrons) or low spin (with one unpaired electron). In low-spin heme complexes, both the Fe^{2+} and the Fe^{3+} ions are small enough to fit into the "hole" in the center of the porphyrin; hence the iron atom lies almost exactly in the plane of the four porphyrin nitrogen atoms in both cases. Because cytochromes b and c are low spin in both their oxidized and reduced forms, the structures of the oxidized and reduced cytochromes are essentially identical. Hence minimal structural changes occur after oxidation or reduction, which makes electron transfer to or from the heme very rapid.

> *Electron transfer reactions occur most rapidly when minimal structural changes occur during oxidation or reduction*

As a class, the cytochromes[19-22] are the most thoroughly characterized of the electron transferases. By definition, a cytochrome contains one or more heme cofactors. These proteins were among the first to be identified in cellular extracts because of their distinctive optical properties, particularly an intense absorption in the 410-430 nm region (called the Soret band). Cytochromes are typically classified on the basis of heme type. Figure 6.6 displays the three most commonly encountered types of heme: heme a possesses a long phytyl "tail" and is found in cytochrome c oxidase; heme b is found in b-type cytochromes and globins; heme c is covalently bound to c-type cytochromes via two thioether linkages. Cytochrome nomenclature presents a real challenge! Some cytochromes are designated according to the historical order of discovery, e.g., cytochrome c_2 in bacterial photosynthesis. Others are designated according to the λ_{max} of the α band in the absorption spectrum of the reduced protein (e.g., cytochrome c_{551}).

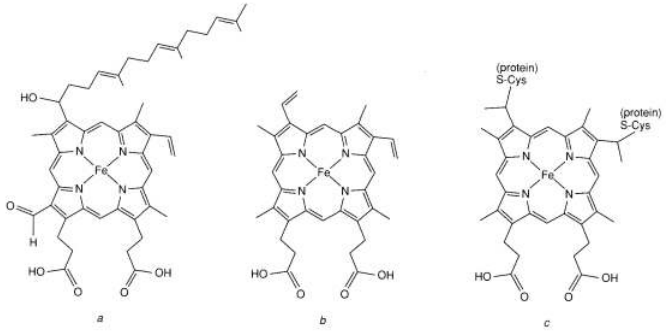


Figure 6.6 - Structures of hemes a, b, and c.

Cytochromes c are widespread in nature. Ambler[23] divided these electron carriers into three classes on structural grounds. The Class I cytochromes c contain axial His and Met ligands, with the heme located near the N-terrninus of the protein. These proteins are globular, as indicated by the ribbon drawing of tuna cytochrome c (Figure 6.7). X-ray structures of Class I cytochromes c from a variety of eukaryotes and prokaryotes clearly show an evolutionarily conserved "cytochrome fold," with the edge of the heme solvent-exposed. The reduction potentials of these cytochromes are quite positive (200 to 320 mV). Mammalian cytochrome c, because of its distinctive role in the mitochondrial electron-transfer chain, will be discussed later.

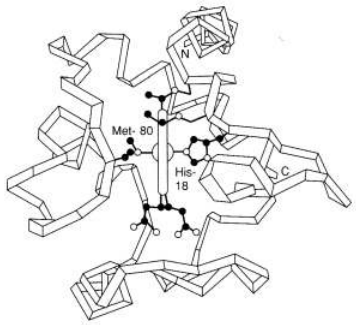


Figure 6. - Structure of tuna cytochrome c.

Class II cytochromes c ($E°' \sim -100$ mV) are found in photosynthetic bacteria, where they serve an unknown function. Unlike their Class I cousins, these c-type cytochromes are high-spin: the iron is five-coordinate, with an axial His ligand. These proteins, generally referred to as cytochromes c' , are four-α-helix bundles (Figure 6.8). The vacant axial coordination site is buried in the protein interior.

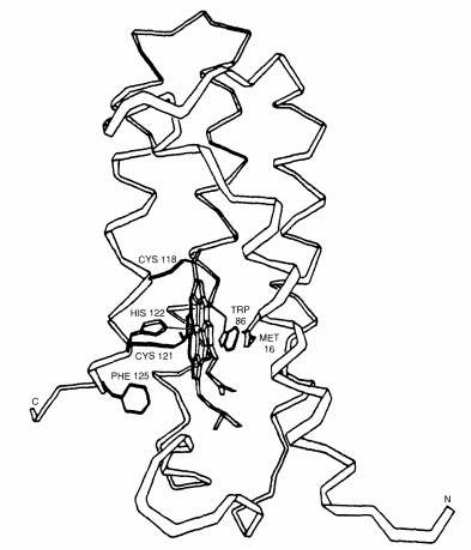


Figure 6.8 - Structure of cytochrome c'.

Finally, Class III cytochromes c, also called cytochromes c_3, contain four hemes, each ligated by two axial histidines. These proteins are found in a restricted class of sulfate-reducing bacteria and may be associated with the cytoplasmic membrane. The low molecular weights of cytochromes c_3 (~14. 7 kDa) require that the four hemes be much more exposed to the solvent than the hemes of other cytochromes (see Figure 6.9), which may be in part responsible for their unusually negative (-200 to -350 mV) reduction potentials. These proteins possess many aromatic residues and short heme-heme distances, two properties that could be responsible for their anomalously large solid-state electrical conductivity.[24]

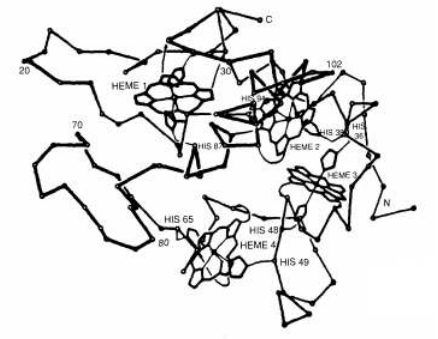


Figure 6.9 - Structure of cytochrome c_3.

Section 12.6: Electron Transfer is shared under a CC BY-NC-SA license and was authored, remixed, and/or curated by LibreTexts.

Index

A

A values
Section 7.3: Ligand Substitution Mechanisms
active site
Section 12.2: Introduction to Amino Acids and Proteins
amino acids
Section 12.2: Introduction to Amino Acids and Proteins
ammonia ligands
Section 7.1: Thermodynamic Stability of Metal Complexes
analogous complexes
Section 7.1: Thermodynamic Stability of Metal Complexes
angular nodes
Section 2.1: Quantum Numbers and Atomic Wavefunctions
antibonding molecular orbital
Section 4.2.1: Orbital Overlap
arenes
Section 10.2: Organometallic Ligands
Associative Substitution
Section 7.3: Ligand Substitution Mechanisms
atomic orbitals
Section 2.1: Quantum Numbers and Atomic Wavefunctions
Section 4.2.1: Orbital Overlap
atomic radii
Section 2.4: Periodic Properties of Atoms
atomic term symbols
Section 8.2: Quantum Numbers of Multielectron Atoms
atomization enthalpy
Section 9.3: Lattice Enthalpies and Born Haber Cycles
Aufbau principle
Section 2.2: Aufbau Principle

B

back strain
Section 5.3.2.7: Bulky groups weaken the strength of Lewis acids and bases because they introduce steric strain into the resulting acid-base adduct.
band gap
Section 9.5: Bonding in Metals and Semicondoctors
band theory
Section 9.5: Bonding in Metals and Semicondoctors
beta elmination
Section 11.2.4: β-Elimination Reactions
bidentate
Section 5.2: Nomenclature and Ligands
block diagonal
Section 3.3.1: Representations of Symmetry Operations
body centered cubic
Section 9.1: Crystal Structures and Unit Cells
bond order
Section 4.2.2: Homonuclear Diatomic Molecules
bonding molecular orbital
Section 4.2.1: Orbital Overlap
bridging ligand
Section 5.2: Nomenclature and Ligands
Section 7.6: Electron Transfer Reactions
Bromobenzene
Chapter 10: Organometallic Chemistry

C

carbene
Section 10.2: Organometallic Ligands
carbon monoxide
Section 10.2: Organometallic Ligands
carbonic anhydrase
Section 12.5: Zinc as Lewis Acid and Template
character (matrix)
Section 3.3.1: Representations of Symmetry Operations
character table
Section 3.3.4: Character Tables
charge transfer band
Section 5.3.2.3: The electronic spectra of charge transfer complexes illustrate the impact of frontier orbital interactions on the electronic structure of Lewis acid-base adducts
Chelate complexes
Section 7.1: Thermodynamic Stability of Metal Complexes
chelate effect
Section 7.1: Thermodynamic Stability of Metal Complexes
Chelation
Section 7.1: Thermodynamic Stability of Metal Complexes
chirality
Section 3.4.1: Chirality
CO Insertions
Section 11.2.1: Introduction to Insertion
Section 11.2.2: CO Insertions (Alkyl Migration)
complex ion
Chapter 5: Coordination Chemistry- Structure and Isomers
compression
Section 6.6: Jahn-Teller Distortions
conductors
Section 9.5: Bonding in Metals and Semicondoctors
coordination complex
Chapter 5: Coordination Chemistry- Structure and Isomers
coordination number
Section 5.4: Coordination Numbers and Structures
copper
Section 12.4: Biological Metal Storage
correlation diagrams
Section 8.3.4: Correlation Diagrams
crystal field splitting
Section 6.1: Crystal Field Theory
Section 6.2: Crystal Field Stabilization Energy
Section 6.3: Factors That Affect Crystal Field Splitting
crystal field stabilization energy
Section 6.2: Crystal Field Stabilization Energy
Section 7.2: Trends in Kinetic Lability
crystal field theory
Section 6.1: Crystal Field Theory
Section 6.2: Crystal Field Stabilization Energy
crystal structure
Section 9.1: Crystal Structures and Unit Cells
cubic closest packing
Section 9.1: Crystal Structures and Unit Cells
cyclopentadienyl ligands
Section 10.2: Organometallic Ligands

D

deinsertion
Section 11.2.1: Introduction to Insertion
Section 11.2.2: CO Insertions (Alkyl Migration)
delta bond
Section 4.2.1: Orbital Overlap
diamagnatic
Section 4.2.2: Homonuclear Diatomic Molecules
diamagnetic
Section 4.2: Molecular Orbital Theory of Diatomic Molecules
Section 6.1: Crystal Field Theory
diatomic molecule
Section 4.2.2: Homonuclear Diatomic Molecules
Drago and Wayland's EC Model
Section 5.3.3.2: Quantitative Measures of Hardness, Softness, and Acid-Base Interactions from a Hard Soft Acid-Base Principle Perspective Involve Orbital Energies and/or Apportioning Acid-Base Bonding in Terms of Electrostatic and Covalent Factors

E

ECW model
Section 5.3.3.2: Quantitative Measures of Hardness, Softness, and Acid-Base Interactions from a Hard Soft Acid-Base Principle Perspective Involve Orbital Energies and/or Apportioning Acid-Base Bonding in Terms of Electrostatic and Covalent Factors
effective nuclear charge
Section 2.3: Shielding
electron affinity
Section 2.4: Periodic Properties of Atoms
electronegativity (Mulliken)
Section 5.3.3.2: Quantitative Measures of Hardness, Softness, and Acid-Base Interactions from a Hard Soft Acid-Base Principle Perspective Involve Orbital Energies and/or Apportioning Acid-Base Bonding in Terms of Electrostatic and Covalent Factors
electronic configurations
Section 6.6: Jahn-Teller Distortions
electrophile
Section 5.3.2: Lewis Concept and Frontier Orbitals
Chapter 10: Organometallic Chemistry
elimination
Section 11.2.1: Introduction to Insertion
Section 11.2.2: CO Insertions (Alkyl Migration)
elongation
Section 6.6: Jahn-Teller Distortions
enantiomers
Section 3.4.1: Chirality
enzymes
Section 12.2: Introduction to Amino Acids and Proteins
ethylenediamine ligands
Section 7.1: Thermodynamic Stability of Metal Complexes

F

ferritin
Section 12.4: Biological Metal Storage

front strain
Section 5.3.2.7: Bulky groups weaken the strength of Lewis acids and bases because they introduce steric strain into the resulting acid-base adduct.

frontier orbitals
Section 5.3.2.1: The frontier orbital approach considers Lewis acid-base reactions in terms of the donation of electrons from the base's highest occupied orbital into the acid's lowest unoccupied orbital.

frustrated Lewis pair
Section 5.3.2.8: Frustrated Lewis pair chemistry uses Lewis acid and base sites within a molecule that are sterically restricted from forming an adduct with each other.

frustrated Lewis pair chemistry
Section 5.3.2.8: Frustrated Lewis pair chemistry uses Lewis acid and base sites within a molecule that are sterically restricted from forming an adduct with each other.

G

group theory
Section 3.2: Point Groups

H

halogen bond
Section 5.3.2.6: Lewis base strength may also be estimated by measuring structural or energy changes upon formation of a Lewis acid-base complex, as illustrated by efforts to spectroscopically assess the strengths of halogen bonds

Hapticity
Section 5.2: Nomenclature and Ligands

Hemocyanin
Section 12.3: Biological Dioxygen Transport and Storage

hemoglobin
Section 12.3: Biological Dioxygen Transport and Storage

Hexagonal Closest Packed
Section 9.1: Crystal Structures and Unit Cells

high spin
Section 6.1: Crystal Field Theory
Section 6.2: Crystal Field Stabilization Energy
Section 6.3: Factors That Affect Crystal Field Splitting
Section 6.6: Jahn-Teller Distortions

history
Section 1.3: History of Inorganic Chemistry

hydration
Section 6.2: Crystal Field Stabilization Energy

hydride
Section 10.2: Organometallic Ligands

hydroboration
Chapter 10: Organometallic Chemistry

Hydrocyanation
Section 11.1.3: Reductive Elimination

I

improper rotation
Section 3.1: Symmetry Operations and Elements

inert complex
Section 7.2: Trends in Kinetic Lability

inner coordination sphere
Chapter 5: Coordination Chemistry- Structure and Isomers

inner sphere
Section 7.6: Electron Transfer Reactions

Inner sphere electron transfer
Section 7.6: Electron Transfer Reactions

inorganic chemistry
Chapter 1: Introduction to Inorganic Chemistry
Section 1.1: What is Inorganic Chemistry?

Insertions
Section 11.2.3: Migratory Insertion-1,2-Insertions

insulator
Section 9.5: Bonding in Metals and Semicondoctors

Interchange
Section 7.3: Ligand Substitution Mechanisms

intermediate
Section 7.2: Trends in Kinetic Lability

inversion center
Section 3.1: Symmetry Operations and Elements

Ionic Radii
Section 2.4: Periodic Properties of Atoms

ionic solids
Chapter 9: Structure and Energetics of Solids

ionization energy
Section 2.4: Periodic Properties of Atoms

iron
Section 12.4: Biological Metal Storage

Iron storage
Section 12.4: Biological Metal Storage

L

labile complex
Section 7.2: Trends in Kinetic Lability

Lancashire
Section 6.6: Jahn-Teller Distortions

lattice enthalpy
Section 9.3: Lattice Enthalpies and Born Haber Cycles

ligand
Chapter 5: Coordination Chemistry- Structure and Isomers

ligand field theory
Section 6.4: Ligand Field Theory

ligand substitution
Section 7.3: Ligand Substitution Mechanisms
Section 11.1.1: Ligand Dissociation and Substitution

ligands
Section 5.2: Nomenclature and Ligands
Section 11.1.3: Reductive Elimination

Linear Combination of Atomic Orbitals (LCAO)
Section 4.1: Formation of Molecular Orbitals from Atomic Orbitals

low spin
Section 6.1: Crystal Field Theory
Section 6.2: Crystal Field Stabilization Energy
Section 6.3: Factors That Affect Crystal Field Splitting
Section 6.6: Jahn-Teller Distortions

M

Marcus Theory
Section 7.6: Electron Transfer Reactions

metal
Chapter 9: Structure and Energetics of Solids

metal alkyl complexes
Section 10.2: Organometallic Ligands
Section 11.2.4: β-Elimination Reactions

metal complexes
Section 7.1: Thermodynamic Stability of Metal Complexes

metallothionein
Section 12.4: Biological Metal Storage

microscopic reversibility
Section 11.1.3: Reductive Elimination

microstates
Section 8.2: Quantum Numbers of Multielectron Atoms

Migratory insertion
Section 11.2.1: Introduction to Insertion
Section 11.2.2: CO Insertions (Alkyl Migration)
Section 11.2.3: Migratory Insertion-1,2-Insertions

molecular orbital diagram
Section 4.2.2: Homonuclear Diatomic Molecules

molecular orbital theory
Section 4.2: Molecular Orbital Theory of Diatomic Molecules

monodentate
Section 5.2: Nomenclature and Ligands
Section 7.1: Thermodynamic Stability of Metal Complexes

monodentate ligands
Section 7.1: Thermodynamic Stability of Metal Complexes

Myoglobin
Section 12.3: Biological Dioxygen Transport and Storage

N

Nomenclature of Inorganic Compounds
Section 5.2: Nomenclature and Ligands

nucleophile
Section 5.3.2: Lewis Concept and Frontier Orbitals

O

octahedral
Section 6.1: Crystal Field Theory

Octahedral Complexes
Section 5.4: Coordination Numbers and Structures

Octahedral Preference
Section 6.2: Crystal Field Stabilization Energy

Octahedral Site Preference Energy
Section 6.2: Crystal Field Stabilization Energy

orbital mixing
Section 4.2.4: Orbital Mixing

orbital overlap
Section 4.2.1: Orbital Overlap

organic chemistry
Section 11.2.4: β-Elimination Reactions

organometallic
Chapter 10: Organometallic Chemistry

organometallic chemistry
Chapter 10: Organometallic Chemistry

Organometallic Ligands
Section 10.2: Organometallic Ligands

outer coordination sphere
Chapter 5: Coordination Chemistry- Structure and Isomers

Outer Sphere Electron Transfer
Section 7.6: Electron Transfer Reactions
oxidative addition
Section 11.1.2: Oxidative Addition
Section 11.1.3: Reductive Elimination
oxidative ligation
Section 11.1.2: Oxidative Addition
Oxygen Binding
Section 12.3: Biological Dioxygen Transport and Storage
oxygen transport
Section 12.3: Biological Dioxygen Transport and Storage

P

paramagnetic
Section 4.2: Molecular Orbital Theory of Diatomic Molecules
Section 4.2.2: Homonuclear Diatomic Molecules
Section 6.1: Crystal Field Theory
Pearson's absolute hardness
Section 5.3.3.2: Quantitative Measures of Hardness, Softness, and Acid-Base Interactions from a Hard Soft Acid-Base Principle Perspective Involve Orbital Energies and/or Apportioning Acid-Base Bonding in Terms of Electrostatic and Covalent Factors
peptide bond
Section 12.2: Introduction to Amino Acids and Proteins
periodic trends
Section 2.4: Periodic Properties of Atoms
philosopher's stone
Section 1.3: History of Inorganic Chemistry
phosphines
Section 10.2: Organometallic Ligands
photoelectron spectroscopy
Section 4.2.6: Photoelectron Spectroscopy
pi acceptor
Section 6.4: Ligand Field Theory
pi bond
Section 4.2.1: Orbital Overlap
pi donor
Section 6.4: Ligand Field Theory
point groups
Section 3.2: Point Groups
probability distribution function
Section 2.1: Quantum Numbers and Atomic Wavefunctions
proper rotation
Section 3.1: Symmetry Operations and Elements
proteins
Section 12.2: Introduction to Amino Acids and Proteins

Q

quantum numbers
Section 2.1: Quantum Numbers and Atomic Wavefunctions

R

radial distribution function
Section 2.1: Quantum Numbers and Atomic Wavefunctions
radial nodes
Section 2.1: Quantum Numbers and Atomic Wavefunctions
reaction coordinate diagram
Section 7.2: Trends in Kinetic Lability
reactivity trends
Section 11.2.1: Introduction to Insertion
Section 11.2.2: CO Insertions (Alkyl Migration)
Section 11.2.3: Migratory Insertion-1,2-Insertions
redox
Section 7.6: Electron Transfer Reactions
reductive elimination
Section 11.1.2: Oxidative Addition
Section 11.1.3: Reductive Elimination
reflection symmetry
Section 3.1: Symmetry Operations and Elements
representation
Section 3.3.3: Mathematical Notation of Representations
rotation axis
Section 3.3.1: Representations of Symmetry Operations

S

SALC
Section 4.3.2: Carbon Dioxide
Schrödinger equation
Section 2.1: Quantum Numbers and Atomic Wavefunctions
semiconductor
Section 9.5: Bonding in Metals and Semicondoctors
shielding constant
Section 2.3: Shielding
sigma donor
Section 6.4: Ligand Field Theory
simple cubic structure
Section 9.1: Crystal Structures and Unit Cells
Slater's rules
Section 2.3: Shielding
spectrochemical series
Section 6.3: Factors That Affect Crystal Field Splitting
spin pairing energy
Section 6.1: Crystal Field Theory
Section 6.2: Crystal Field Stabilization Energy
square planar
Section 6.1: Crystal Field Theory
Stephan's phosphinoborane
Section 5.3.2.8: Frustrated Lewis pair chemistry uses Lewis acid and base sites within a molecule that are sterically restricted from forming an adduct with each other.
stereochemistry
Section 11.2.1: Introduction to Insertion
Section 11.2.2: CO Insertions (Alkyl Migration)
Section 11.2.3: Migratory Insertion-1,2-Insertions
stereospecific
Section 11.2.4: β-Elimination Reactions
strong field
Section 6.4: Ligand Field Theory
substitutions
Section 7.3: Ligand Substitution Mechanisms
Section 11.1.1: Ligand Dissociation and Substitution
substrate
Section 12.2: Introduction to Amino Acids and Proteins
Suzuki reaction
Chapter 10: Organometallic Chemistry
symmetry
Section 3.2: Point Groups
Symmetry Adapted Linear Combinations
Section 4.3: Larger (Polyatomic) Molecules
symmetry elements
Section 3.1: Symmetry Operations and Elements
symmetry operation
Section 3.3.1: Representations of Symmetry Operations
symmetry operations
Section 3.1: Symmetry Operations and Elements

T

tetrahedral
Section 6.1: Crystal Field Theory
Tetrahedral Complexes
Section 5.4: Coordination Numbers and Structures
thermodynamically
Section 7.1: Thermodynamic Stability of Metal Complexes
thermodynamically stable
Section 7.1: Thermodynamic Stability of Metal Complexes
trans effect
Section 7.4: The Trans Effect Observation
transition state
Section 7.2: Trends in Kinetic Lability
tridentate
Section 5.2: Nomenclature and Ligands
trimethylenediamine
Section 7.1: Thermodynamic Stability of Metal Complexes

U

unsaturated ligands
Section 11.2.1: Introduction to Insertion
Section 11.2.2: CO Insertions (Alkyl Migration)
Usanovich acids
Section 5.3.2: Lewis Concept and Frontier Orbitals
Usanovich bases
Section 5.3.2: Lewis Concept and Frontier Orbitals

V

vanadium
Section 12.4: Biological Metal Storage

W

weak field
Section 6.4: Ligand Field Theory

Z

zinc
Section 12.4: Biological Metal Storage

Glossary

Sample Word 1 | Sample Definition 1

Detailed Licensing

Overview

Title: CHE 332: Inorganic Chemistry

Webpages: 146

Applicable Restrictions: Noncommercial

All licenses found:

- CC BY-NC-SA 4.0: 91.1% (133 pages)
- Undeclared: 3.4% (5 pages)
- CC BY-SA 4.0: 2.1% (3 pages)
- CC BY-NC 4.0: 1.4% (2 pages)
- CC BY-NC-SA 3.0: 1.4% (2 pages)
- CC BY-NC 3.0: 0.7% (1 page)

By Page

- CHE 332: Inorganic Chemistry - *CC BY-NC-SA 4.0*
  - Front Matter - *CC BY-NC-SA 4.0*
    - TitlePage - *CC BY-NC-SA 4.0*
    - InfoPage - *CC BY-NC-SA 4.0*
    - Table of Contents - *Undeclared*
    - Licensing - *CC BY-NC-SA 4.0*
  - Chapter 1: Introduction to Inorganic Chemistry - *CC BY-NC-SA 4.0*
    - Section 1.1: What is Inorganic Chemistry? - *CC BY-NC-SA 4.0*
    - Section 1.2: Inorganic vs Organic Chemistry - *CC BY-NC-SA 4.0*
    - Section 1.3: History of Inorganic Chemistry - *CC BY-NC-SA 4.0*
  - Chapter 2: Atomic Theory - *CC BY-NC-SA 4.0*
    - Section 2.1: Quantum Numbers and Atomic Wavefunctions - *CC BY-NC-SA 4.0*
    - Section 2.2: Aufbau Principle - *CC BY-NC-SA 4.0*
    - Section 2.3: Shielding - *CC BY-NC-SA 4.0*
    - Section 2.4: Periodic Properties of Atoms - *CC BY-NC-SA 4.0*
  - Chapter 3: Molecular Symmetry and Point Groups - *CC BY-NC-SA 4.0*
    - Section 3.1: Symmetry Operations and Elements - *CC BY-NC-SA 4.0*
    - Section 3.2: Point Groups - *CC BY-NC-SA 4.0*
    - Section 3.3: Properties and Representations of Groups - *Undeclared*
      - Section 3.3.1: Representations of Symmetry Operations - *Undeclared*
      - Section 3.3.2: Matrices - *Undeclared*
      - Section 3.3.3: Mathematical Notation of Representations - *CC BY-SA 4.0*
      - Section 3.3.4: Character Tables - *CC BY-SA 4.0*
    - Section 3.4: Examples and Applications of Symmetry - *Undeclared*
      - Section 3.4.1: Chirality - *CC BY-NC 4.0*
      - Section 3.4.2: Molecular Vibrations - *CC BY-NC 4.0*
  - Chapter 4: Molecular Orbitals - *CC BY-NC-SA 4.0*
    - Section 4.1: Formation of Molecular Orbitals from Atomic Orbitals - *CC BY-NC-SA 4.0*
      - Section 4.1.1: Molecular Orbitals from s Orbitals - *CC BY-NC-SA 3.0*
      - Section 4.1.2: Molecular Orbitals from p Orbitals - *CC BY-NC-SA 3.0*
      - Section 4.1.3: Molecular orbitals from d orbitals - *CC BY-NC-SA 4.0*
      - Section 4.1.4: Nonbonding Orbitals and Other Factors - *CC BY-NC-SA 4.0*
    - Section 4.2: Molecular Orbital Theory of Diatomic Molecules - *CC BY-NC-SA 4.0*
      - Section 4.2.1: Orbital Overlap - *CC BY-NC-SA 4.0*
      - Section 4.2.2: Homonuclear Diatomic Molecules - *CC BY-NC-SA 4.0*
      - Section 4.2.3: Heteronuclear Diatomic Molecules - *CC BY-NC-SA 4.0*
      - Section 4.2.4: Orbital Mixing - *CC BY-NC-SA 4.0*
      - Section 4.2.5: Diatomic Molecules of the First and Second Periods - *CC BY-NC-SA 4.0*

- Section 4.2.6: Photoelectron Spectroscopy - *CC BY-NC-SA 4.0*
- Section 4.3: Larger (Polyatomic) Molecules - *CC BY-NC-SA 4.0*
  - Section 4.3.1: Bifluoride anion - *CC BY-NC-SA 4.0*
  - Section 4.3.2: Carbon Dioxide - *CC BY-NC-SA 4.0*
  - Section 4.3.3: H_2O - *CC BY-NC-SA 4.0*
  - Section 4.3.4: NH_3 - *CC BY-NC-SA 4.0*
  - Section 4.3.5: CO_2 (Revisted with Projection Operators) - *CC BY-NC-SA 4.0*
  - Section 4.3.6: BF_3 - *CC BY-NC-SA 4.0*
- Section 4.4: Problems - *CC BY-NC-SA 4.0*

- Chapter 5: Coordination Chemistry- Structure and Isomers - *CC BY-NC-SA 4.0*
  - Section 5.1: History - *CC BY-NC-SA 4.0*
  - Section 5.2: Nomenclature and Ligands - *CC BY-NC-SA 4.0*
  - Section 5.3: Acid-Base and Donor-Acceptor Chemistry - *CC BY-NC-SA 4.0*
    - Section 5.3.1: Acid-Base Models as Organizing Concepts - *CC BY-NC-SA 4.0*
    - Section 5.3.2: Lewis Concept and Frontier Orbitals - *CC BY-NC-SA 4.0*
      - Section 5.3.2.1: The frontier orbital approach considers Lewis acid-base reactions in terms of the donation of electrons from the base's highest occupied orbital into the acid's lowest unoccupied orbital. - *CC BY-NC-SA 4.0*
      - Section 5.3.2.2: All other things being equal, electron withdrawing groups tend to make Lewis acids stronger and bases weaker while electron donating groups tend to make Lewis bases stronger and acids weaker - *CC BY-NC-SA 4.0*
      - Section 5.3.2.3: The electronic spectra of charge transfer complexes illustrate the impact of frontier orbital interactions on the electronic structure of Lewis acid-base adducts - *CC BY-NC-SA 4.0*
      - Section 5.3.2.4: Substances' solution phase Lewis basicity towards a given acid may be estimated using the enthalphy change for dissociation of its adduct with a reference acid of similar hardness. - *CC BY-NC-SA 4.0*
      - Section 5.3.2.5: In the boron trifluoride affinity scale, the enthalphy change on formation of an adduct between the base and boron trifluoride is taken as a measure of Lewis basicity. - *CC BY-NC-SA 4.0*
      - Section 5.3.2.6: Lewis base strength may also be estimated by measuring structural or energy changes upon formation of a Lewis acid-base complex, as illustrated by efforts to spectroscopically assess the strengths of halogen bonds - *CC BY-NC-SA 4.0*
      - Section 5.3.2.7: Bulky groups weaken the strength of Lewis acids and bases because they introduce steric strain into the resulting acid-base adduct. - *CC BY-NC-SA 4.0*
      - Section 5.3.2.8: Frustrated Lewis pair chemistry uses Lewis acid and base sites within a molecule that are sterically restricted from forming an adduct with each other. - *CC BY-NC-SA 4.0*
    - Section 5.3.3: Hard and Soft Acids and Bases - *CC BY-NC-SA 4.0*
      - Section 5.3.3.1: Hard-Hard and Soft-Soft preferences may be explained and quantified in terms of electrostatic and covalent and electronic stabilization on the stability of Lewis acid-base adducts - *CC BY-NC-SA 4.0*
      - Section 5.3.3.2: Quantitative Measures of Hardness, Softness, and Acid-Base Interactions from a Hard Soft Acid-Base Principle Perspective Involve Orbital Energies and/or Apportioning Acid-Base Bonding in Terms of Electrostatic and Covalent Factors - *CC BY-NC-SA 4.0*
    - Section 5.3.4: Problems - *CC BY-NC-SA 4.0*
  - Section 5.4: Coordination Numbers and Structures - *CC BY-NC-SA 4.0*
  - Section 5.5: Isomerism - *CC BY-NC-SA 4.0*
- Chapter 6: Coordination Chemistry- Bonding - *CC BY-NC-SA 4.0*
  - Section 6.1: Crystal Field Theory - *CC BY-NC-SA 4.0*
  - Section 6.2: Crystal Field Stabilization Energy - *CC BY-NC-SA 4.0*
  - Section 6.3: Factors That Affect Crystal Field Splitting - *CC BY-NC-SA 4.0*
  - Section 6.4: Ligand Field Theory - *CC BY-NC-SA 4.0*
  - Section 6.5: Metal-Metal Bonds - *CC BY-NC-SA 4.0*
    - Section 6.5.1: Metal-Metal Multiple Bonds - *CC BY-NC-SA 4.0*
  - Section 6.6: Jahn-Teller Distortions - *CC BY-NC-SA 4.0*

- Chapter 7: Coordination Chemistry- Reactions and Mechanisms - *CC BY-NC-SA 4.0*
  - Section 7.1: Thermodynamic Stability of Metal Complexes - *CC BY-NC-SA 4.0*
  - Section 7.2: Trends in Kinetic Lability - *CC BY-NC-SA 4.0*
  - Section 7.3: Ligand Substitution Mechanisms - *CC BY-NC-SA 4.0*
  - Section 7.4: The Trans Effect Observation - *CC BY-NC 3.0*
  - Section 7.5: The Trans Effect Explanation - *CC BY-NC-SA 4.0*
  - Section 7.6: Electron Transfer Reactions - *CC BY-NC-SA 4.0*
- Chapter 8: Coordination Chemistry - Electronic Spectra - *CC BY-NC-SA 4.0*
  - Section 8.1: Absorption of Light - *CC BY-NC-SA 4.0*
    - Section 8.1.1: Beer-Lambert Absorption Law - *CC BY-NC-SA 4.0*
  - Section 8.2: Quantum Numbers of Multielectron Atoms - *CC BY-NC-SA 4.0*
    - Section 8.2.1: Finding Microstates and Term Symbols - *CC BY-NC-SA 4.0*
    - Section 8.2.2: Spin-Orbit Coupling - *CC BY-NC-SA 4.0*
  - Section 8.3: Electronic Spectra of Coordination Compounds - *CC BY-NC-SA 4.0*
    - Section 8.3.1: Tanabe-Sugano Diagrams - *CC BY-NC-SA 4.0*
    - Section 8.3.2: Symmetry labels for split terms - *CC BY-NC-SA 4.0*
    - Section 8.3.3: Selection Rules - *CC BY-NC-SA 4.0*
    - Section 8.3.4: Correlation Diagrams - *CC BY-NC-SA 4.0*
    - Section 8.3.5: Applications of Tanabe-Sugano Diagrams - *CC BY-NC-SA 4.0*
    - Section 8.3.6: Tetrahedral Complexes - *CC BY-NC-SA 4.0*
    - Section 8.3.7: Charge-Transfer Spectra - *CC BY-NC-SA 4.0*
    - Section 8.3.8: Applications of Charge-Transfer - *CC BY-NC-SA 4.0*
- Chapter 9: Structure and Energetics of Solids - *CC BY-NC-SA 4.0*
  - Section 9.1: Crystal Structures and Unit Cells - *CC BY-NC-SA 4.0*
  - Section 9.1b: Ionic Radii and Radius Ratios - *CC BY-SA 4.0*
  - Section 9.2: Energetics of Ionic Solids- Lattice Energy - *CC BY-NC-SA 4.0*
  - Section 9.3: Lattice Enthalpies and Born Haber Cycles - *CC BY-NC-SA 4.0*
  - Section 9.4: Lattice Energy and Solubility - *CC BY-NC-SA 4.0*
  - Section 9.5: Bonding in Metals and Semicondoctors - *CC BY-NC-SA 4.0*
  - Section 9.6: Nanomaterials - *CC BY-NC-SA 4.0*
- Chapter 10: Organometallic Chemistry - *CC BY-NC-SA 4.0*
  - Section 10.1: The 18 Electron Rule - *CC BY-NC-SA 4.0*
  - Section 10.2: Organometallic Ligands - *CC BY-NC-SA 4.0*
  - Section 10.3: Characterization of Organometallic Complexes - *CC BY-NC-SA 4.0*
- Chapter 11: Organometallic Reactions and Catalysis - *CC BY-NC-SA 4.0*
  - Section 11.1: Reactions Involving Gain or Loss of Ligands - *CC BY-NC-SA 4.0*
    - Section 11.1.1: Ligand Dissociation and Substitution - *CC BY-NC-SA 4.0*
    - Section 11.1.2: Oxidative Addition - *CC BY-NC-SA 4.0*
    - Section 11.1.3: Reductive Elimination - *CC BY-NC-SA 4.0*
    - Section 11.1.4: Sigma Bond Metathasis - *CC BY-NC-SA 4.0*
    - Section 11.1.5: Application of Pincer Ligands - *CC BY-NC-SA 4.0*
  - Section 11.2: Reactions Invloving Modification of Unsaturated Ligands - *CC BY-NC-SA 4.0*
    - Section 11.2.1: Introduction to Insertion - *CC BY-NC-SA 4.0*
    - Section 11.2.2: CO Insertions (Alkyl Migration) - *CC BY-NC-SA 4.0*
    - Section 11.2.3: Migratory Insertion-1,2-Insertions - *CC BY-NC-SA 4.0*
    - Section 11.2.4: β-Elimination Reactions - *CC BY-NC-SA 4.0*
    - Section 11.2.5: Abstraction and Addition - *CC BY-NC-SA 4.0*
  - Section 11.3: Organometallic Catalysts - *CC BY-NC-SA 4.0*
    - Section 11.3.1: Catalytic Deuteration - *CC BY-NC-SA 4.0*

- Section 11.3.2: Hydroformylation - *CC BY-NC-SA 4.0*
- Section 11.3.3: Monsanto Acetic Acid Process - *CC BY-NC-SA 4.0*
- Section 11.3.4: Wacker (Smidt) Process - *CC BY-NC-SA 4.0*
- Section 11.3.5: Hydrogenation by Wilkinson's Catalyst - *CC BY-NC-SA 4.0*
- Section 11.3.6: Olefin Metathesis - *CC BY-NC-SA 4.0*

- Section 11.4: Heterogeneous Catalysts - *CC BY-NC-SA 4.0*
  - Section 11.4.1: Ziegler-Natta Polymerizations - *CC BY-NC-SA 4.0*
  - Section 11.4.2: Water-Gas Shift Reaction - *CC BY-NC-SA 4.0*
- Section 11.5: Problems - *CC BY-NC-SA 4.0*
  - Section 11.5.1: Concept Review Questions Chapter 12 - *CC BY-NC-SA 4.0*
  - Section 11.5.2: Homework Problems Chapter 12 - *CC BY-NC-SA 4.0*

- Chapter 12: Bioinorganic Chemistry - *CC BY-NC-SA 4.0*
  - Section 12.1: Biological Significance of Metals - *CC BY-NC-SA 4.0*
  - Section 12.2: Introduction to Amino Acids and Proteins - *CC BY-NC-SA 4.0*
  - Section 12.3: Biological Dioxygen Transport and Storage - *CC BY-NC-SA 4.0*
  - Section 12.4: Biological Metal Storage - *CC BY-NC-SA 4.0*
  - Section 12.5: Zinc as Lewis Acid and Template - *CC BY-NC-SA 4.0*
  - Section 12.6: Electron Transfer - *CC BY-NC-SA 4.0*
- Back Matter - *CC BY-NC-SA 4.0*
  - Index - *CC BY-NC-SA 4.0*
  - Glossary - *CC BY-NC-SA 4.0*
  - Detailed Licensing - *CC BY-NC-SA 4.0*